ANNUAL ISSUE 2006

PROGRESS IN PHYSICS

"All scientists shall have the right to present their scientific research results, in whole or in part, at relevant scientific conferences, and to publish the same in printed scientific journals, electronic archives, and any other media." — Declaration of Academic Freedom, Article 8

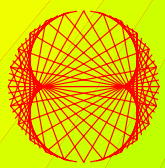

ISSN 1555-5534

The Journal on Advanced Studies in Theoretical and Experimental Physics, including Related Themes from Mathematics

PROGRESS IN PHYSICS

A quarterly issue scientific journal, registered with the Library of Congress (DC, USA). This journal is peer reviewed and included in the abstracting and indexing coverage of: Mathematical Reviews and MathSciNet (AMS, USA), DOAJ of Lund University (Sweden), Zentralblatt MATH (Germany), Referativnyi Zhurnal VINITI (Russia), etc.

Electronic version of this journal:
http://www.geocities.com/ptep_online

To order printed issues of this journal, contact the Editor in Chief.

Department of Mathematics, University of New Mexico, 200 College Road, Gallup, NM 87301, USA

This journal is powered by LaTeX

A variety of books can be downloaded free from the Digital Library of Science:
http://www.gallup.unm.edu/∼smarandache

ISSN: 1555-5534 (print)
ISSN: 1555-5615 (online)

Standard Address Number: 297-5092
Printed in the United States of America

JANUARY 2006 **VOLUME 1**

CONTENTS

Information for Authors and Subscribers

Progress in Physics has been created for publications on advanced studies in theoretical and experimental physics, including related themes from mathematics. All submitted papers should be professional, in good English, containing a brief review of a problem and obtained results.

All submissions should be designed in LaTeX format using *Progress in Physics* template. This template can be downloaded from *Progress in Physics* home page http://www.geocities.com/ptep_online. Abstract and the necessary information about author(s) should be included into the papers. To submit a paper, mail the file(s) to Chief Editor.

All submitted papers should be as brief as possible. Beginning from 2006 we accept only papers, no longer than 8 journal pages. Short articles are preferable.

All that has been accepted for the online issue of *Progress in Physics* is printed in the paper version of the journal. To order printed issues, contact Chief Editor.

This journal is non-commercial, academic edition. It is printed from private donations.

Unification of Interactions in Discrete Spacetime

Franklin Potter

Sciencegems.com, 8642 Marvale Drive, Huntington Beach, CA, USA
Formerly at Department of Physics, University of California, Irvine

E-mail: drpotter@lycos.com

I assume that both spacetime and the internal symmetry space of the Standard Model (SM) of leptons and quarks are discrete. If lepton and quark states represent specific finite binary rotational subgroups of the SM gauge group, unification with gravitation is accomplished by combining finite subgroups of the Lorentz group SO(3,1) with the specific finite SM subgroups. The unique result is a particular finite subgroup of SO(9,1) in discrete 10-D spacetime related to $E_8 \times E_8$ of superstring theory. A physical model of particles based upon the finite subgroups and the discrete geometry is proposed. Evidence for discreteness might be the appearance of a b' quark at about 80–100 GeV decaying via FCNC to a b quark plus a photon at the Large Hadron Collider.

1 Introduction

I consider both spacetime and the internal symmetry space of the Standard Model (SM) of leptons and quarks to be discrete instead of continuous. Using specific finite subgroups of the SM gauge group, a unique finite group in discrete 10-D spacetime unifies the fundamental interactions, including gravitation. This finite group is a special subgroup of the continuous group $E_8 \times E_8$ that in superstring theory (also called M-theory) is considered to be the most likely group for unifying gravitation with the SM gauge group.

This unique result follows directly from two fundamental assumptions: (1) the internal symmetry space is discrete, requiring specific finite binary rotational subgroups of the SM gauge group to dictate the physical properties of the lepton and quark states, and (2) spacetime is discrete, and therefore its discrete symmetries correspond to finite subgroups of the Lorentz group. Presumably, this discreteness must occur as one approaches the Planck scale of about 10^{-35} meters.

I suggest a particular physical model of fundamental fermions based upon these finite subgroups in the discrete geometry. Further evidence for this discreteness might be the appearance of a b' quark at about 80–100 GeV decaying via FCNC to a b quark plus a photon at the Large Hadron Collider.

2 Motivation

The Standard Model (SM) of leptons and quarks successfully describes their electromagnetic, weak and color interactions in terms of symmetries dictated by the $\mathrm{SU}(2)_L \times \mathrm{U}(1)_Y \times \mathrm{SU}(3)_C$ continuous gauge group. These fundamental fermions and their antiparticles are defined by their electroweak isospin states in two distinct but gauge equivalent unitary planes in an internal symmetry space "attached" at a spacetime point. Consequently, particle states and antiparticle states have opposite-signed physical properties but their masses are the same sign.

In an earlier 1994 paper [1] I discussed how the SM continuous gauge group could be acting like a "cover group" for its finite binary rotational subgroups, thereby hiding any important underlying discrete rotational symmetries of these fundamental particle states. From group theory, one knows that the continuous SM gauge group contains thousands of elements of finite order including, for example, all the elements of the finite binary rotational subgroups in their 3-dimensional and 4-dimensional representations. I showed that these subgroups were very important because they are connected to the j-invariant of elliptic modular functions from which one can predict the mass ratios for the lepton and quark states.

The mathematical properties of these finite subgroups of the SM dictate the same physical properties of the leptons and quarks as achieved by the SM. However, electroweak symmetry breaking to these specific finite binary rotational subgroups occurs without a Higgs particle. More importantly, some additional physical properties are dictated also, such as their mass ratios, why more than one generation is present, the important family relationships, and the dimensionalities of the particle states because they are no longer point particles.

The gravitational interaction is not included explicitly in the SM gauge group. However, because the finite binary rotational subgroup approach determined the lepton and quark mass ratios, one suspects that the gravitational interaction is included already in the discretized version of the gauge group. Or, equivalently, since mass/energy is the source of the gravitational interaction, the gravitational interaction arises from the discrete symmetries associated with the finite rotational subgroups.

Therefore, I make some conjectures. If leptons and quarks actually represent the specific discrete symmetries of the finite subgroups of the SM gauge group as proposed, the internal symmetry space may be discrete instead of being continuous. Going one step further, then not only the internal symmetry space might be discrete but also spacetime itself may be discrete, since gravitation determines the spacetime metric. Spacetime would appear to be continuous only at the low resolution scales of experimental apparatus such as the present particle colliders. Unification of the fundamental interactions then requires combining these finite groups mathematically.

3 4-D internal symmetry space?

I take the internal symmetry space of the SM to be discrete, but we need to know how many dimensions there are. Do we need two complex spatial dimensions for a unitary plane as suggested by SU(2), or do we need three as suggested by the SU(3) symmetry of the color interaction, or do we need more?

The lepton and quark particle states are defined as electroweak isospin states by the electroweak part of the SM gauge group, with particles in the normal unitary plane C^2 and antiparticles in the conjugate unitary plane C'^2. Photon, W^+, W^-, and Z^0 interactions of the electroweak $\mathrm{SU}(2)_L \times \mathrm{U}(1)_Y$ gauge group rotate the two particle states (i. e., the two complex basis spinors in the unitary plane) into one another. For example, $e^- + W^+ \rightarrow \nu_e$. These electroweak rotations can be considered to occur also in an equivalent 4-dimensional real euclidean space R^4 and in an equivalent quaternion space Q, both these spaces being useful for a better geometrical understanding of the SM.

The quark states are defined also by the color symmetries of $\mathrm{SU}(3)_C$, i. e., each quark comes in one of three possible colors, red R, green G, or blue B, while the lepton states have no color charge. Normally, one would consider $\mathrm{SU}(3)_C$ operating in a space of three complex dimensions, or its equivalent six real dimensions. In fact, $\mathrm{SU}(3)_C$ can operate successfully in the smaller unitary plane C^2, because each SU(3) operation can be written as the product of three specific SU(2) operations [2]. An alternative geometrical explanation has the gluon operations of the color interaction rotate one color state into another in a 4-dimensional real space, as discussed in my 1994 article. Briefly, real 4-dimensional space R^4 has four orthogonal coordinates (w, x, y, z), and its 4-D rotations occur simultaneously in two orthogonal planes. There being only three distinct pairs of orthogonal planes, $[wx, yz]$, $[xy, zw]$, and $[yw, xz]$, each color R, G, or B is assigned to a specific pair, thereby making color an exact geometrical symmetry. Consequently, the gluon operations of $\mathrm{SU}(3)_C$ occur in the 4-D real space R^4 that is equivalent to the unitary plane. Detailed matrix operations confirm that hadrons with quark-antiquark pairs, three quarks, or three antiquarks, are colorless combinations.

Therefore I take the internal symmetry space to be a discrete 4-dimensional real space because this space is the minimum dimensional space that allows the SM gauge group to operate completely. One does not need a larger space, e. g., a 6-dimensional real space, for its internal symmetry space.

4 Dimensions of spacetime?

I take physical spacetime to be 4-dimensional with its one time dimension. Spacetime is normally considered to be continuous and 4-dimensional, with three spatial dimensions and one time dimension. However, in the last two decades several approaches toward unifying all fundamental interactions have considered additional mathematical spatial dimensions and/or more time dimensions. For example, superstring theory [3] at the high energy regime, i. e., at the Planck scale, proposes 10 or 11 spacetime dimensions in its present mathematical formulation, including the one time dimension. These extra spatial dimensions may correspond to six or seven dimensions "curled up" into an internal symmetry space for defining fundamental particle states at each spacetime point in order to accommodate the SM in the low energy regime. The actual physical spacetime itself may still have three spatial dimensions and one time dimension.

I take 4-D spacetime to be discrete. We do not know whether spacetime is continuous or discrete. If the internal symmetry space is indeed discrete, then perhaps spacetime itself might be discrete also. Researchers in loop quantum gravity [4] at the Planck scale divide spacetime into discrete subunits, considering a discrete 4-D spacetime with its discrete Lorentz transformations to be a viable approach.

The goal now is to combine the finite subgroups of the gauge group of the SM and the finite group of discrete Lorentz boosts and discrete spacetime rotations into one unified group. All four known fundamental interactions would be unified. Although many unification schemes for the fundamental interactions have been attempted over the past three decades utilizing continuous groups, I believe this attempt is the first one that combines finite groups. Mathematically, the result must be unique, otherwise different fundamental laws could exist in different parts of the universe.

5 Discrete internal space

The most important finite symmetry groups in the 4-D discrete internal symmetry space are the 3-D binary rotational subgroups $[3, 3, 2]$, $[4, 3, 2]$, and $[5, 3, 2]$ of the SM gauge group because they are the symmetry groups I have assigned to the three lepton families. They contain discrete rotations and inversions and operate in the 3-D subspace R^3 of R^4 and C^2.

Being subgroups of $\mathrm{SU}(2)_L \times \mathrm{U}(1)_Y$, they have group operations represented by 2×2 unitary matrices or, equivalently, by unit quaternions. Quaternions provide the more obvious geometrical connection [5], because quaternions perform the dual role of being a group operation and of being a vector in R^3 and in R^4. One can think visually about the 3-D group rotations and inversions for these three subgroups as quaternions operating on the Platonic solids, with the same quaternions also defining the vertices of regular geometrical objects in R^4.

The two mathematical entities, the unit quaternion $\mathbf{q}$ and the SU(2) matrix, are related by

$$\mathbf{q} = w + x\,\boldsymbol{i} + y\,\boldsymbol{j} + z\,\boldsymbol{k} \iff \begin{pmatrix} w+iz & x+iy \\ -x+iy & w-iz \end{pmatrix} \quad (1)$$

where the $\boldsymbol{i}$, $\boldsymbol{j}$, and $\boldsymbol{k}$ are unit imaginaries, their coefficients are real, and $w^2+x^2+y^2+z^2 = 1$. The conjugate quaternion $\mathbf{q}' = w - x\,\boldsymbol{i} - y\,\boldsymbol{j} - z\,\boldsymbol{k}$ and its corresponding matrix would represent the same group operation in the conjugate unitary plane for the antiparticles. Recall that Clifford algebra and Bott periodicity dictate that only R^4, R^8, and other real spaces R^n with dimensions divisible by four have two equivalent conjugate spaces, the specific mathematical property that accommodates both particle states and antiparticle states. The group $\mathrm{U}(1)_Y$ for weak hypercharge Y then reduces the symmetry to being gauge equivalent so that particles and antiparticles have the same positive mass.

One might expect that we need to analyze each of the three binary rotational subgroups separately when the discrete internal symmetry space is combined with discrete spacetime. Fortunately, the largest binary rotational group $[5,3,2]$ of icosahedral symmetries can accommodate the two other groups, and a discussion of its 120 quaternion operations is all inclusive mathematically. The elements of this icosahedral group, rotations and inversions, can be represented by the appropriate unit quaternions.

The direct connection between the 3-D and 4-D spaces is realized when one equates the 120 group operations on the regular icosahedron (3, 5) to the vectors for the 120 vertices of the 600-cell hypericosahedron (3, 3, 5) in 4-D space in a particular way. These operations of the binary icosahedral group $[5,3,2]$ and the vertices of the hypericosahedron are defined by 120 special unit quaternions q_i known as isosians [6], which have the mathematical form

$$\begin{aligned} q_i = &\left(e_1 + e_2\sqrt{5}\right) + \left(e_3 + e_4\sqrt{5}\right) i \\ &+ \left(e_5 + e_6\sqrt{5}\right) j + \left(e_7 + e_8\sqrt{5}\right) k\,, \end{aligned} \quad (2)$$

where the eight e_j are special rational numbers. Specifically, the 120 icosians are obtained by permutations of

$$\begin{aligned} &(\pm1, 0, 0, 0)\,, (\pm1/2, \pm1/2, \pm1/2, \pm1/2)\,, \\ &(0, \pm1/2, \pm g/2, \pm G/2)\,, \end{aligned} \quad (3)$$

where $g = G^{-1} = G - 1 = (-1+\sqrt{5})/2$. Notice that in each pair, such as $(e_3 + e_4\sqrt{5})$, only one of the e_j is nonzero, reminding us that the hypericosahedron is really a 4-D object even though we can now define this object in terms of icosians that are expressed in the much larger R^8 euclidean real space.

So the quaternion's dual role allows us to identify the 120 group operations of the icosahedron with the 120 vertices of the hypericosahedron expressed both in R^4 and in R^8, essentially telescoping from 3-D rotational operations all the way to their representations in an 8-D space. These special 120 icosians are to be considered as special octonions, 8-tuples of rational numbers which, with respect to a particular norm, form part of a special lattice in R^8.

Now consider the two other subgroups. The 24 quaternions of the binary tetrahedral group $[3,3,2]$ are contained already in the above 120 icosians. So we are left with accommodating the binary octahedral group $[4,3,2]$ into the same icosian format. We need 48 special quaternions for its 48 operations, the 24 quaternions defining the vertices of the 4-D object known as the 24-cell contained already in the hypericosahedron above and another 24 quaternions for the reciprocal 24-cell. The 120 unit quaternions reciprocal to the ones above will meet this requirement as well as define an equivalent set for the reciprocal hypericosahedron, and this second set of 120 octonions also forms part of a special lattice in R^8. Together, these two lattice parts of 120 icosians in each combine to form the 240 octonions of the famous E_8 lattice in R^8, well known for being the densest lattice packing of spheres in 8-D.

Recall that the three binary rotation groups above are assigned to the lepton families because, as subgroups of the SM gauge group, they predict the correct physical properties of the lepton states, including the correct mass ratios. Therefore, the lepton states as I have defined them span only the 3-D real subspace R^3 of the unitary plane. That is why leptons are color neutral and do not participate in the color interaction, a physical property that requires the ability to undergo complete 4-D rotations.

So how do quark states fit into the icosian picture? I have the quark states in the SM spanning the whole 4-D real space, i. e., the whole unitary plane, because they are the basis states of the 4-D finite binary rotational subgroups of the SM gauge group. But free quarks in spacetime do not exist because they are confined according to QCD, forming the colorless quark-antiquark, three-quark, or three-antiquark combinations called hadrons. Mathematically, these colorless hadron states span the 3-D subspace only, so their resultant discrete symmetry group must be isomorphic to one of the three binary rotational subgroups we have just considered. Consequently, the icosians enumerated above account for all the lepton states and for all the quark states in their allowed hadronic combinations.

6 Discrete spacetime

Linear transformations in discrete spacetime are the discrete rotations and the discrete Lorentz boosts. Before considering these discrete transformations, however, I discuss the continuous transformations of the "heavenly sphere" as a useful mathematical construct before reducing the symmetry to discrete transformations in a discrete spacetime.

The continuous Lorentz group SO(3,1) contains all the rotations and Lorentz boosts, both continuous and discrete, for the 4-D continuous spacetime with the Minkowski metric. Its operations are quaternions because there exists the isomorphism

$$\mathrm{SO}(3,1) = \mathrm{PSL}(2,\mathbb{C}). \tag{4}$$

The group PSL(2,$\mathbb{C}$) consists of unit quaternions and is the quotient group $\mathrm{SL}(2,\mathbb{C})/\mathrm{Z}$ formed by its center Z, those elements of $\mathrm{SL}(2,\mathbb{C})$ which commute with all the rest of the group. Its 2×2 matrix representation has complex numbers as entries.

The continuous Lorentz transformations (including the spatial rotations) operate on the "heavenly sphere" [7], i. e., the famous Riemann sphere formed by augmenting the complex plane C by the "point at infinity". The Riemann sphere is also the space of states of a spin-1/2 particle. For the Lorentz transformations in spacetime, if you are located at the center of this "heavenly sphere" so that the light rays from stars overhead each pass through unique points on a unit celestial sphere surrounding you, then the Lorentz boost is a conformal transformation of the star locations. The constellations will look distorted because the apparent lengths of the lines connecting the stars will change but the angles between these connecting lines will remain the same.

These conformal transformations are called fractional linear transformations, or Möbius transformations, of the Riemann sphere, expressed by the general form [8]

$$w \mapsto \frac{\alpha w + \beta}{\gamma w + \delta}, \tag{5}$$

with α, β, γ, and δ complex, and $\alpha\delta - \beta\gamma \neq 0$. The 2×2 matrix representation for transformation of a spinor v as the map $v \mapsto \mathrm{M}v$ is

$$\mathrm{M} = \begin{pmatrix} \alpha & \beta \\ \gamma & \delta \end{pmatrix}. \tag{6}$$

Thus, M is the spinor representation of the Lorentz transformation. M acts on a vector $\mathrm{A} = \mathrm{vv}^\dagger$ via $\mathrm{A} \mapsto \mathrm{MAM}^\dagger$ [9]. All these relationships are tied together by the group isomorphisms in continuous 4-D spacetime

$$\mathrm{SO}(3,1) = \text{Möbius group} = \mathrm{PSL}(2,\mathbb{C}). \tag{7}$$

Discrete spacetime has discrete Lorentz transformations, not continuous ones. These discrete rotations and discrete Lorentz boosts are contained already in SO(3,1), and they tesselate the Riemann sphere. That is, they form regular polygons on its surface that correspond to the discrete symmetries of the binary tetrahedral, binary octahedral, and binary icosahedral rotation groups [3, 3, 2], [4, 3, 2], and [5, 3, 2], the same groups I used in the internal symmetry space for the discrete symmetries. Therefore, the 240 quaternions defined previously are required also for the discrete rotations and discrete Lorentz boosts in the discrete 4-D spacetime. Again, there are the same 240 icosian connections to octonions in R^8 to form a second E_8 lattice.

Thus, the Lorentz group SO(3,1) with its linear transformations in a continuous 4-D spacetime, when reduced to its discrete transformations in a 4-D discrete spacetime, is connected mathematically by icosians to the E_8 lattice in R^8, telescoping the transformations from a smaller discrete spacetime to a larger one. Hence all linear transformations for the particles in a 4-D discrete spacetime have become represented by 240 discrete transformations in the 8-D discrete spacetime.

7 Resultant spacetime

The discrete transformations in the 4-D discrete internal symmetry space and in the 4-D discrete spacetime are each represented by an E_8 lattice in the 8-D space R^8. The finite group of the discrete symmetries of the E_8 lattice is the Weyl group E_8, not to be confused with the continuous exceptional Lie group E_8. Thus, the Weyl E_8 is a finite subgroup of SO(8), the continuous group of all rotations of the unit sphere in R^8 with determinant unity. In this section I combine the two Weyl E_8 groups to form a bigger group that operates in a discrete spacetime, and then in the next section I suggest a simple physical model for fundamental fermions that would fit the geometry.

I have now two sets of 240 icosians each forming E_8 lattices in R^8, each obeying the symmetry operations of the finite group Weyl E_8. Each finite group of octonions acts as rotations and as vectors in R^8. I identify their direct product as the elements of a discrete subgroup of the continuous group PSL(2,$\mathbb{O}$), where $\mathbb{O}$ represents all the unit octonions. That is, if all the unit octonions in each were present, not just the subset of unit octonions that form the E_8 lattice, their direct product group would be the continuous group of 2×2 matrices in which all matrix entries are unit octonions. So the spinors in R^8 are octonions.

The 8-D result is analogous to the 4-D result but different. Recall that in the 4-D case, one has PSL(2,$\mathbb{C}$), the group of 2×2 matrices with complex numbers as entries, with PSL(2,$\mathbb{C}$) = SO(3,1), the Lorentz group in 4-D spacetime. Here in 8-D one has a surprise, for the final combined spacetime is bigger, being isomorphic to a 10-dimensional spacetime instead of 8-dimensional spacetime because

$$\mathrm{PSL}(2,\mathbb{O}) = \mathrm{SO}(9,1), \tag{8}$$

the Lorentz group in 10-D spacetime.

Applied to the discrete case, the combined group is the finite subgroup

$$\text{finite PSL}(2,\mathbb{O}) = \text{finite SO}(9,1)\,, \tag{9}$$

that is, the finite Lorentz group in discrete 10-D spacetime. The same results, expressed in terms of the direct product of Weyl E_8 groups, is

$$\text{Weyl } E_8 \times \text{Weyl } E_8 = \text{“Weyl” SO}(9,1)\,, \tag{10}$$

where “Weyl” SO(9,1) is defined by the direct product on the left and is a finite subgroup of SO(9,1).

Working in reverse, the discrete 10-D spacetime divides into two parts as a 4-D discrete spacetime plus a 4-D discrete internal symmetry space. There is a surprise in this result: combining a discrete 4-D internal symmetry space with a discrete 4-D spacetime creates a discrete 10-D spacetime, not a discrete 8-D spacetime. Therefore, a continuous 10-D spacetime, when “discretized”, is not required to partition into a 4-D spacetime plus a 6-D “curled up” space as proposed in superstring theory.

8 A physical particle model

In the 1994 paper I proposed originally that leptons have the symmetries of the 3-D regular polyhedral groups and that quarks have the symmetries of the 4-D regular polytope groups. Now that I have combined the discrete 4-D internal symmetry space with a discrete 4-D spacetime to achieve mathematically a discrete 10-D spacetime, the fundamental question arises: Are the leptons and quarks really 3-D and 4-D objects physically, or are they something else, perhaps 8-D or 10-D objects?

In order to answer this question I need to formulate a reasonable physical model of fundamental particles in this discrete spacetime environment. The simplest mathematical viewpoint is that discrete spacetime is composed of identical entities, call them nodes, which have no *measureable* physical properties until they collectively distort spacetime to form a fundamental particle such as the electron, for example. The collection of nodes and its distortion of the surrounding spacetime exhibit the discrete symmetry of the appropriate finite binary rotation group for the specific particle. For example, the electron family has the discrete symmetry of the binary tetrahedral group and the electron is one of its two possible orthogonal basis states. So the distortion for the collection of nodes called the electron will exhibit the discrete symmetries of its $[3,3,2]$ group as all of its physical properties emerge for this specific collection and did not exist beforehand. The positron forms in the conjugate space.

One can begin with a regular lattice of nodes in both the normal unitary plane and in its conjugate unitary plane, or one can consider the equivalent R^4 spaces, and then imagine that a spacetime distortion appears in both to form a particle-antiparticle pair. Mathematically, one begins with an isotropic vector, also called a zero length vector, which is orthogonal to itself, that gets divided into two unit spinors corresponding to the creation of the particle-antiparticle pair. No conservations laws are violated because their quantum numbers are opposite and the sum of the total mass energy plus their total potential energy is zero. The spacetime distortion that is the particle and its “field” mathematically brings the nodes closer together locally with a corresponding adjustment to the node spacing all the way out to infinite distance, all the while keeping the appropriate discrete rotational symmetry intact. The gravitational interaction associated with this discrete symmetry therefore extends to infinite distance.

This model of particle geometry must treat leptons as 3-D objects and quarks as 4-D objects in a discrete 4-D spacetime. We know that there are no isolated quarks, for they immediately form 3-D objects called hadrons. These lepton states and hadron states are described by quaternions of the form $w + x\,\boldsymbol{i} + y\,\boldsymbol{j} + z\,\boldsymbol{k}$, so these 3-D objects “live” in the three imaginary dimensions, and the 4th dimension can be called time. Therefore, leptons and hadrons each experience the “passage of time”, while indiviual quarks do not have this characteristic until they form hadrons in the 3-D subspace.

If this physical model is a reasonable approximation to describing the world of fundamental particles, why are superstring researchers working in 10-dimensions or more? Because one desires a single symmetry group that includes both the group of spacetime transformations of particles and the group of internal symmetries for the particle interactions. At the Planck scale, if one has a continuous group, then the smallest dimensional continuous spacetime one can use is 10-D in order to have a viable Lagrangian. Reducing this 10-D spacetime to the low energy regime of the SM in 4-D spacetime, the 10-D continuous spacetime has been postulated to divide into 4-D spacetime plus an additional 6-dimensional “curled up” space in which to accommodate the SM. In M-theory, one may be considering an 11-D spacetime dividing into a 4-D spacetime plus a 7-D “curled up” space. But this approach using continuous groups to connect back to the SM has proven difficult, although some significant advances have been achieved.

The analysis presented above for combining the two finite Weyl E_8 groups shows that the combined group operates in 10-D discrete spacetime with all the group operations being discrete. The particles are 3-D objects “traveling” in spacetime. No separate “curled up” space is required at the low energy limit corresponding to a distance scale of about 10^{-23} meters or larger. The discreteness at the Planck scale and the “hidden” discreteness postulated for all larger distance scales is the mathematical feature that permits the direct unique connection through icosians from the high energy world to the familiar lower energy world of the SM.

9 Mathematical connections

The mathematical connections of these binary polyhedral groups to number theory, geometry, and algebra are too numerous to list and discuss in this short article. In fact, according to B. Kostant [10], if one were to choose groups in mathematics upon which to construct the symmetries of the universe, one couldn't choose a better set, for "... in a very profound way, the finite groups of symmetries in 3-space 'see' the simple Lie groups (and hence literally Lie theory) in all dimensions." Therefore, I provide a brief survey of a few important connections here and will discuss them in more detail in future articles.

Geometrical connections are important for these groups. The continuous group PSL(2,$\mathbb{C}$) defines a torus, as does PSL(2,$\mathbb{O}$). In the discrete environment, finite PSL(2,$\mathbb{C}$) and finite PSL(2,$\mathbb{O}$) have special symmetry points on each torus corresponding to the elements of the finite binary polyhedral groups. An important mathematical property of the binary polyhedral groups is their connection to elliptic modular functions, the doubly periodic functions, and their famous j-invariant function, which has integer coefficients in its series expansion related to the largest of the finite simple groups called the Monster.

The binary tetrahedral, octahedral and icosahedral rotation groups are the finite groups of Mobius transformations PSL$(2, Z_3)$, PSL$(2, Z_4)$, and PSL$(2, Z_5)$, respectively, where Z_{n}denotes integers mod (n). PSL$(2, Z_n)$ is often called the modular group $\Gamma(\mathrm{n})$. PSL$(2, Z_{\mathrm{n}})$ = SL$(2, Z_{\mathrm{n}})/\{\pm\ \mathrm{I}\}$, so these three binary polyhedral groups (along with the cyclic and dihedral groups) are the finite modular subgroups of PSL$(2, \mathbb{C})$ and are also discrete subgroups of PSL$(2, \mathbb{R})$. PSL$(2, Z_{\mathrm{n}})$ is simple in only three cases: n = 5, 7, 11. And these three cases are the Platonic groups again: A_5 and its subgroup A_4, S_4, and A_5, respectively [11].

An important mathematical property for physics is that our binary polyhedral groups, the $\Gamma(\mathrm{n})$, are generated by the two transformations

$$X : \tau \mapsto -1/\tau \qquad Y : \tau \mapsto \tau + 1, \tag{11}$$

with τ being the lattice parameter for the plane associated with forming the tesselations of the toroidal Riemann surface. The j-invariant function $\mathrm{j}(\tau)$ of elliptic modular functions exhibits this transformation behavior. Consequently, functions describing the physical properties of the fundamental leptons and quarks will exhibit these same transformation properties. So here is where the duality theorems of M-theory, such as the S duality relating the theory at physical coupling g to coupling at $1/g$, arise naturally from mathematical properties of the finite binary polyhedral groups.

One can show also that octonions and the triality connection for spinors and vectors in R^8 are related to the fundamental interactions. In 8-D, the fundamental matrix representations both for left- and right-handed spinors and for vectors are the same dimension, 8×8 [12], leading to many interesting mathematical properties. For example, an electron represented by a left-handed octonionic spinor interacting with a W^+ boson represented by an octonionic vector becomes an electron neutrino, again an octonionic spinor. Geometrically, this interaction looks like three E_8 lattices combining momentarily to form the famous 24-dimensional Leech lattice!

By using a discrete spacetime, we have begun to suspect that Nature has established a universe based upon fundamental mathematics that dictates unique fundamental physics principles. Moreover, one might expect that all physical constants will be shown to arise from fundamental mathematical relationships, dictating one universe with unique constant values for a unique set of fundamental laws.

10 Experimental tests

There is no direct test yet devised for discrete spacetime. However, my discrete internal symmetry space approach dictates a fourth quark family with a b' quark state at about 80 GeV and a t' quark at about 2600 GeV. The production of this b' quark with the detection of its decay to a b quark and a high energy photon seems at present to be the only attainable empirical test for discreteness. Its appearance in collider decays would be an enormously important event in particle physics, strongly suggesting that the internal symmetry space and its "surrounding" spacetime are discrete.

However, the b' quark has remained hidden among the collision debris at Fermilab because its flavor changing neutral current (FCNC) decay channel has a very low probability compared to all the other particle decays in this energy regime. This b' quark decay may even be confused with the decay of the Higgs boson, should such a particle exist, until all the quantum numbers are established. The t' quark at around 2600 GeV has too great a mass to have been produced directly at Fermilab.

I expect the production of b' quarks at the Large Hadron Collider in a few years to be the acid test for discreteness and to verify the close connection of fundamental physics to the mathematical properties of the finite simple groups.

Acknowledgements

I would like to thank Sciencegems.com for generous research support via Fundamental Physics Grant — 002004-0007-0014-1 and my colleagues at the University of California, Irvine for many discussions with probing questions.

References

1. Potter F. Geometrical basis for the Standard Model. *International Journal of Theoretical Physics*, 1994, v. 33(2), 279–305.

2. Rowe D.J., Sanders B.C., de Guise H. Representations of the Weyl group and Wigner functions for SU(3). *Journal of Mathematical Physics*, 1999, v. 40(7), 3604–3615.
3. Schwarz J.H. Update on String Theory. arXiv: astro-ph/0304507.
4. Urrutia L.F. Flat space modified particle dynamics induced by Loop Quantum Gravity. arXiv: hep-ph/0402271.
5. Coxeter H.S.M. Regular complex polytopes. Cambridge University Press, Cambridge, 1974, pp. 89–97.
6. Conway J.H., Sloane N.J.A. Sphere packings, lattices and groups. 3rd ed. Springer-Verlag, New York, 1998.
7. Penrose R., Rindler W. Spinors and space-time, Volume 1, Reprint edition. Cambridge University Press, Cambridge, 1987, pp. 26–28.
8. Jones, G., Singerman, D. Complex functions: an algebraic and geometric viewpoint. Cambridge University Press, Cambridge, 1987, pp. 17–53.
9. Manogue C.A., Dray T. Octonionic Möbius transformations. *Modern Physics Letters* v.A14, 1999, 1243–1256. arXiv: math-ph/9905024.
10. Kostant B. In *Asterisque*, (Proceedings of the Conference "Homage to Elie Cartan", Lyons), 1984, p. 13.
11. Kostant B. The graph of the truncated icosahedron and the last letter of Galois. *Notices of the American Mathematical Society*, 1995, v. 42, 959–968.
12. Baez J. The octonions. arXiv: math.RA/0105155.

On Interpretations of Hubble's Law and the Bending of Light

C. Y. Lo
Applied and Pure Research Institute, 17 Newcastle Drive, Nashua, NH 03060, USA
E-mail: c_y_lo@yahoo.com; C_Y_Lo@alum.mit.edu

Currently, Hubble's law is often considered as the observational evidence of an expanding universe. It is shown that Hubble's Law need not be related to the notion of Doppler redshifts of the light from receding Galaxies. In the derivation of the receding velocity, an implicit assumption, which implies no expansion, must be used. Moreover, the notion of receding velocity is incompatible with the local light speeds used in deriving the light bending. The notion of an expanding universe is based on an unverified assumption that a local distance in a physical space is similar to that of a mathematical Riemannian space embedded in a higher dimensional flat space, and thus the physical meaning of coordinates would necessarily depend on the metric. However, this assumption has been proven as theoretically invalid. In fact, a physical space necessarily has a frame of reference, which has a Euclidean-like structure that is independent of the yet to be determined physical metric and thus cannot be such an embedded space. In conclusion, the notion of an expanding universe could be just a mathematical illusion.

1 Introduction

Currently, Hubble's law is often considered as the observational evidence of the expanding universe. This is done by considering Hubble's law essentially as a manifestation of the Doppler red shift of the light from the receding Galaxies [1]. Thus, the further a galaxies is from the Milky Way, the faster it appears to receding. However, Hubble himself rejected this interpretation and concluded in 1936 that the Galaxies are actually stationary [2]. In view of the fact that this interpretation of relating to the receding velocities is far from perfect [3], perhaps, it would be useful to reexamine how solid is such an interpretation in terms of general relativity and physics.

It will be shown that Hubble's Law need not be related to the Doppler redshifts of the light from receding Galaxies (section 2). It is pointed out, in the derivation of the receding velocity, an implicit assumption, which implies no expansion, must be used (section 3). Moreover, the receding velocity is incompatible with the light speeds used in deriving the light bending (section 4). In short, the notion of expanding universe is a production due to confusing notion of the coordinates and also due to inadequate understanding of a physical space. Thus, such a universe is unlikely related to the reality (section 5).

2 Hubble's law

Hubble discovered from light emitted by near by galaxies that the redshifts S are linearly proportion to the present distance L from the Milky Way as follows:

$$S = HL \tag{1}$$

where H is the Hubble constant although the redshifts of distant galaxies will deviate from this linear law with a slightly different constant. In terms of general relativity, it is well known that this law can be derived with the following metric [1, 3],

$$ds^2 = -d\tau^2 + a^2(\tau)(dx^2 + dy^2 + dz^2)\,, \tag{2}$$

since

$$S = \frac{\lambda_2 - \lambda_1}{\lambda_1} = \frac{\omega_1}{\omega_2} - 1 = \frac{a(\tau_2)}{a(\tau_1)} - 1\,, \tag{3}$$

where ω_1 is the frequency of a photon emitted at event P_1 at time τ_1, and ω_2 is the frequency of the photon observed at P_2 at time τ_2 [1]. Furthermore, for nearby galaxies, one has

$$a(\tau_2) \simeq a(\tau_1) + (\tau_2 - \tau_1)\,\dot{a}\,. \tag{4}$$

If

$$(\tau_2 - \tau_1) = L = \int_1^2 \sqrt{dx^2 + dy^2 + dz^2}\,, \tag{5}$$

then

$$S = \frac{\dot{a}}{a}\,L = HL, \qquad \text{and} \qquad H = \frac{\dot{a}}{a}\,. \tag{6}$$

Formula (5) is compatible with the calculation in the bending of light. Please note that Hubble's Law need not be related to the Doppler redshifts. Understandably, Hubble rejected such an interpretation himself [2]. In fact, there is actually no receding velocity since L is fixed (i. e., $dL/d\tau = 0$).

3 Hubble's law and the Doppler redshifts

On the other hand, if one chooses to define the distance between two points as

$$R = \int_1^2 a(\tau)\sqrt{dx^2 + dy^2 + dz^2} = a(\tau)L\,, \tag{7}$$

then

$$v=\frac{dR}{d\tau}=\frac{da}{d\tau}L+\frac{dL}{d\tau}a=\frac{da}{d\tau}\frac{R}{a}=HR, \quad \text{if} \quad \frac{dL}{d\tau}=0. \quad (8)$$

According to relation (7), v would be the receding velocity. Note also that according to (7), (5) would have to change into $(\tau_2-\tau_1)=R$, and (1) into $S=HR$. Thus,

$$v=S. \quad (9)$$

This means that the redshifts could be superficially considered as a Doppler effect. Thus, whether Hubble's Law represents the effects of an expanding universe is a matter of the interpretation of the local distance. From the above analysis, the crucial point is what is a valid physical velocity in a physical space.

It should be noted that $dL/dt=0$ means that the space coordinates are independent of the metric. In other words, the physical space has a Euclidean-like structure [4], which is independent of time. However, since L between any two space-points is fixed, the notion of an expanding universe, if it means anything, is just an illusion. Moreover, the validity of (7) as the physical distance has no known experimental supports since it is not really measurable (see section 5). Moreover, a problem is that the notion of velocity in (8) would be incompatible with the light speeds in the calculation of light bending experiment.

4 The coordinates of an Einstein physical space

In mathematics, the Riemannian space is often embedded in a higher dimensional flat space [5]. Then the coordinates dx^μ are determined by the metric through the metric,

$$ds^2=g_{\mu\nu}\,dx^\mu dx^\nu, \quad \text{or} \quad -g_{00}dt^2+g_{ij}\,dx^i dx^j \quad (10)$$

such as the surface of a sphere in a three-dimensional Euclidean space. For a physical space, however, there are insufficient conditions to do so. Since the metric is a variable function, it is impossible to determine the coordinates with the metric. In view of this, the coordinates must be physically independent of the metric. As shown in metric (2), a physical space has a Euclidean-like structure as a frame of reference.(1) Moreover, it has been proven from the theoretical framework of general relativity [4] that a frame of reference with the Euclidean-like structure must exist for a physical space.

For a spherical mass distribution with the center at the origin, the metric with the isotropic gauge is,

$$\begin{aligned} ds^2=&-[(1-Mk/2r)^2/(1+Mk/2r)^2]c^2dt^2+\\ &+(1+Mk/2r)^4\,(dx^2+dy^2+dz^2)\,, \end{aligned} \quad (11)$$

where $k=G/c^2$ ($G=6.67\times10^{-8}\text{erg}\times\text{cm/gm}^2$), M is the total mass, and $r=\sqrt{x^2+y^2+z^2}$. Then, if the equivalence principle is satisfied, the light speeds are determined by $ds^2=0$ [6, 7], i. e.,

$$\frac{\sqrt{dx^2+dy^2+dz^2}}{dt}=c\,\frac{1-M\kappa/2r}{[1+M\kappa/2r]^3}\,. \quad (12)$$

However, such a definition of light speeds is incompatible with the definition of velocity (8) although compatible with (5). Since this light speed is supported by observations, (8) is invalid in physics. Nevertheless, Liu [8] has defined light speeds, which is more compatible with (8), as

$$\frac{\sqrt{g_{ij}\,dx^i dx^j}}{dt}=c\,\frac{1-M\kappa/2r}{1+M\kappa/2r} \quad (13)$$

for metric (11). However, (13) implies only half of the deflection implied by (12) [6, 7].

The above analysis also explains why many current theorists insist on that the light speeds are not defined even though Einstein defined them clearly in his 1916 paper as well as in his book, *The Meaning of Relativity*. They might argued that the light speeds are not well defined since diffeomorphic metrics give different sets of light speeds for the same frame of reference. However, they should note that Einstein defines light speeds after the assumption that his equivalence principle is satisfied [6, 7]. Different metric for the same frame of reference means only that at most only one of such metrics is physically valid [4], and therefore the definition of light speeds are, in principle, uniquely well-defined.

However, since the problem of a physical valid metric has not been solved, whether a light speed is valid remains a question. Nevertheless, it has been proven that the Maxwell-Newton Approximation gives the valid first order approximation of the physical metric, the first order of the physically valid light speeds are solved [4]. Since metric (11) is compatible with the Maxwell-Newton approximation, the first order of light speed (12) is valid in physics.

Thus, the groundless speculation that local light speeds are not well defined is proven incorrect. In essence, the velocity definition (8), which leads to the notion of the Doppler redshifts, has been rejected by experiments. Nevertheless, some skeptics might prefer to accept formula (6) after light speed (12) is confirmed by the experiment of local light speeds [4].

5 Discussions and Conclusions

A major problem in Einstein's theory, as pointed out by Whitehead [9] and Fock [10], the physical meaning of coordinates is ambiguous and confusing. In view of this, it is understandable that the notion in an embedded Riemannian space is used when the physical nature of the problem is not yet clear.(2) A major difference between physics and mathematics is that the coordinates in physics must have physical meaning. Since Einstein is not a mathematician,

his natural step would be to utilize the existing theory of Riemannian space. However, as Whitehead [9] saw, this created a seemingly irreconcilable problem between coordinates of a curved space-time and physics.

Under such a circumstances, the notion of an expanding universe is created while an implicit assumption that restricts the universe as static is also used. This kind of inconsistency is expectedly inevitable because of contradictory principles, Einstein's equivalence principle that requires space-time coordinates have physical meaning and the "principle of covariance" that necessarily means that coordinates are arbitrary, are concurrently used in Einstein's theory [11]. Recently, it is proven [12] that Einstein's "principle of covariance" has no theoretical basis in physics or observational support beyond what is allowed by the principle of general relativity.(3)

This analysis demonstrates that the Hubble's Law is not necessarily related to the Doppler redshifts. It is also pointed out that the notion of an expanding universe is related to contradictory assumptions and thus is unlikely a physical possibility. Moreover, this kind notion of velocity is incompatible with the light speeds used in the calculation of light bending [6, 7].

In Einstein's theory of measurement, a local distance in a physical space is assumed to be similar to that of a mathematical Riemannian space embedded in a higher dimensional flat space, and thus the physical meaning of coordinates would necessarily depend on the metric. Recently, this unverified assumption is proven to be inconsistent with Einstein's notion of space contractions [13]. In other words, this unverified assumption contradicts Einstein's equivalence principle that the local space of a particle at free falling must be locally Minkowskian [7], from which he obtained the time dilation and space contractions.

In conclusion, the notion of an expanding universe is unlikely a physical reality, although metric (2) is only a model among other possibilities. Currently, there are three theoretical explanations for the cause to observed red shifts. They are: (1) the expanding universe; (2) Doppler redshifts; and (3) gravitational redshifts. In this paper, it has been shown that the current receding velocity of an expanding universe is only a theoretical illusion and is unrelated to the Doppler redshifts. If the notion of expanding universe cannot be explained satisfactorily, it is difficult to imagine that Doppler effects are the cause of observed Hubble's law. Moreover, this law also cannot be explained in terms of gravitational redshifts.

Then, one may ask if the observed gravitational redshifts are not due to an expanding universe, what causes such redshifts that are roughly proportional to the distances from the observer. One possibility is that the scatterings of a light ray along its path to the observer. In physics, it is known that different scatterings are common causes for losing energy of a particle, and for the case of photons it means redshifts. Since such an effect is so small, it must be the scattering of a weak field. In fact, the inelastic scattering of light by the gravitational field has been speculated [14]. Unfortunately, to test such a conjecture is not possible because no current theory of gravity is capable of handling the inelastic scatterings of lights.

At present, Einstein's equation even does not have any dynamic solution [15, 16]. Thus, to solve this puzzle rigorously seems surely in the remote future. Nevertheless, the assumption that observed redshifts could be due to inelastic scatterings may help to explain some puzzles of observed facts [17]. For instance, it is known that younger objects such as star forming galaxies have higher intrinsic redshifts, and objects with the same path length to the observer have much different redshifts while all parts of the object have about the same amount of redshifts.(4)

A noted advancement of the Euclidean-like structure [4] is that notions used in a Euclidean space could be adapted much easier in general relativity. Many things would be calculated as if in a Euclidean space. On the other hand, the speculations related to the notion of an expanding universe [1] would crease to function, and physics should return to normal. Nevertheless, when a transformation between different frames of reference is considered, the physical space is clearly Riemannian as Einstein discovered.

Acknowledgments

The author is grateful for stimulating discussions with Professors H. Arp, A. J. Coleman, A. H. Guth, and P. Morrison. This work is supported in part by the Chan Foundation, Hong Kong.

Endnotes

(1) A common problem is overlooking that the metric of a Riemannian space can actually be compatible with the space coordinates with the Euclidean-like structure. For example, the Schwarzschild solution in quasi-Minkowskian coordinates [18; p. 181] is,

$$ds^2 = -(1-2M\kappa/r)c^2dt^2 + (1-2M\kappa/r)^{-1}dr^2 + \\ + r^2(d\theta^2 + \sin^2\theta d\varphi^2), \tag{1a}$$

where (r, θ, φ) transforms to (x, y, z) by,

$$x = r\sin\theta\ \cos\varphi, \quad y = r\sin\theta\ \sin\varphi, \\ \text{and} \quad z = r\cos\theta\,. \tag{1b}$$

Coordinate transformation (1b) tells that the space coordinates satisfy the Pythagorean theorem. The Euclidean-like structure represents this fact, but avoids confusion with the notion of a Euclidean subspace determined by the metric. Metric (1a) and Euclidean-like structure (1b) are complementary to each other in the Einstein space. These space-time coordinates form not just a mathematical coordinate system

since a light speed ($ds^2 = 0$) is defined in terms of dx/dt, dy/dt, and dz/dt [19].

(2) In the initial development of Riemannian geometry, the metric was identified formally with the notion of distance in analogy as the case of the Euclidean space. Such geometry is often illustrated with the surface of a sphere, a subspace embedded in a flat space [5]. Then, the distance is determined by the flat space and can be measured with a static method. For a general case, however, the issue of measurement was not addressed before Einstein's theory. In general relativity, according to Einstein's equivalence principle, the local distance represents the space contraction [7, 19], which is actually measured in a free fall local space [13]. Thus, this is a dynamic measurement since the measuring instrument is in a free fall state under the influence of gravity, while the Euclidean-like structure determines the static distance between two points in a frame of reference. Einstein's error is that he overlooked the free fall state, and thus has mistaken this dynamic local measurement as a static measurement.

(3) If the "covariance principle" was valid, it has been shown that the "event of horizon" for a black hole could be just any arbitrary constant [20]. Zhou [21] is probably the earliest who spoke out against the "principle of covariance" and he pointed out, "The concept that coordinates don't matter in the interpretation of Einstein's theory necessarily leads to mathematical results which can hardly have a physical interpretation and are therefore a mystification of the theory." More recently, Morrison [12] commented that Einstein's "covariance principle" discontinuously separates special relativity from general relativity.

(4) These two types of puzzles would be very difficult to be explained in terms of an expanding universe alone. One might object the scattering of gravitational field on the ground that the photon flight path would be deviated and the images blurred. However, although the scattering by random objects would make blurred images, it is not clear this is the case for a scattering by a weak field. Moreover, since the scattering in the path of photons by the weak gravitational field is very weak, the deviation from the path would not be noticeable, and this is different from the gravitational lenses effects that can be directly observed.

References

1. Wald R. M. General Relativity. University of Chicago Press, Chicago, 1984.
2. Whitrow G. J. Edwin Powell Hubble. *Dictionary of Scientific Biography*, New York, Charles Scribner's Sons, v.5, 1972, p.532.
3. Ohanian H. C. and Ruffini R. Gravitation and Spacetime. Norton, New York, 1994.
4. Lo C. Y. *Chinese J. of Phys.*, 2003, v.41(4), 332.
5. Dirac P. A. M. General Theory of Relativity. John Wiley, New York, 1975.
6. Lorentz H. A. *Proc. K. Ak. Amsterdam*, 1900, v.8, 603.
7. Einstein A. The Meaning of Relativity (1921). Princeton Univ. Press, 1954.
8. Liu Liao. General Relativity. High Education Press, Shanghai, 1987, pp.26–30.
9. Whitehead A. N. The Principle of Relativity. Cambridge Univ. Press, Cambridge, 1922.
10. Fock V. A. The Theory of Space Time and Gravitation. Pergamon Press, New York, 1964.
11. Lo C. Y. *Phys. Essays*, 2002, v.15(3), 303–321.
12. Lo C. Y. *Phys. Essays*, 2005, v.18(1).
13. Lo C. Y. *Phys. Essays*, 2005, v.18(4).
14. Lo C. Y. *Phys. Essays*, 1999, v.12(2), 226–241.
15. Lo C. Y. *Astrophys. J.* 1995, v. 455, 421–428.
16. Lo C. Y. *Phys. Essays*, 2000, v.13(4), 527–539.
17. Arp H. *Progress in Physics*, 2005, v.3, 3–6.
18. Weinberg S. Gravitation and Cosmology. John Wiley Inc., New York, 1972.
19. Einstein A., Lorentz H. A., Minkowski H., and Weyl H. The Principle of Relativity. Dover, New York, 1923.
20. Lo C. Y. *Chin. Phys.*, 2004, v.13(2), 159.
21. Zhou (Chou) Peiyuan. On coordinates and coordinate transformation in Einstein's theory of gravitation. *Proc. of the Third Marcel Grossmann Meeting on Gen. Relativ.*, ed. Hu Ning, Science Press and North Holland, 1983, 1–20.

Unmatter Entities inside Nuclei, Predicted by the Brightsen Nucleon Cluster Model

Florentin Smarandache and Dmitri Rabounski

Dept. of Mathematics and Science, Univ. of New Mexico, 200 College Road, Gallup, NM 87301, USA

E-mail: fsmarandache@yahoo.com; rabounski@yahoo.com

Applying the R. A. Brightsen Nucleon Cluster Model of the atomic nucleus we discuss how unmatter entities (the conjugations of matter and antimatter) may be formed as clusters inside a nucleus. The model supports a hypothesis that antimatter nucleon clusters are present as a parton (*sensu* Feynman) superposition within the spatial confinement of the proton ($^1H_1$), the neutron, and the deuteron ($^1H_2$). If model predictions can be confirmed both mathematically and experimentally, a new physics is suggested. A proposed experiment is connected to othopositronium annihilation anomalies, which, being related to one of known unmatter entity, orthopositronium (built on electron and positron), opens a way to expand the Standard Model.

1 Introduction

According to Smarandache [1, 2, 3], following neutrosophy theory in philosophy and set theory in mathematics, the union of matter <A> and its antimatter opposite <AntiA> can form a neutral entity <NeutA> that is neither <A> nor <AntiA>. The <NeutA> entity was termed "unmatter" by Smarandache [1] in order to highlight its intermediate physical constitution between matter and antimatter. Unmatter is formed when matter and antimatter baryons intermingle, regardless of the amount of time before the conjugation undergoes decay. Already Bohr long ago predicted the possibility of unmatter with his principle of complementarity, which holds that nature can be understood in terms of concepts that come in complementary pairs of opposites that are inextricably connected by a Heisenberg-like uncertainty principle. However, not all physical union of <A> with <AntiA> must form unmatter. For instance, the charge quantum number for the electron (e^-) and its antimatter opposite positron (e^+) make impossible the formation of a charge neutral state — the quantum situation must be either (e^-) or (e^+).

Although the terminology "unmatter" is unconventional, unstable entities that contain a neutral union of matter and antimatter are well known experimentally for many years (e. g, pions, pentaquarks, positronium, etc.). Smarandache [3] presents numerous additional examples of unmatter that conform to formalism of quark quantum chromodynamics, already known since the 1970's. The basis that unmatter does exists comes from the 1970's experiments done at Brookhaven and CERN [4–8], where unstable unmatter-like entities were found. Recently "physicists suspect they have created the first molecules from atoms that meld matter with antimatter. Allen Mills of the University of California, Riverside, and his colleagues say they have seen telltale signs of positronium molecules, made from two positronium atoms" [9, 10]. A bound and quasi-stable unmatter baryonium has been verified experimentally as a weak resonance between a proton and antiproton using a Skyrme-type model potential. Further evidence that neutral entities derive from union of opposites comes from the spin induced magnetic moment of atoms, which can exist in a quantum state of both spin up and spin down at the same time, a quantum condition that follows the superposition principal of physics. In quantum physics, virtual and physical states that are mutually exclusive while simultaneously entangled, can form a unity of opposites <NeutA> via the principle of superposition.

Our motivation for this communication is to the question: would the superposition principal hold when mass symmetrical and asymmetrical matter and antimatter nucleon wavefunctions become entangled, thus allowing for possible formation of macroscopic "unmatter" nucleon entities, either stable or unstable? Here we introduce how the novel Nucleon Cluster Model of the late R. A. Brightsen [11–17] does predict formation of unmatter as the product of such a superposition between matter and antimatter nucleon clusters. The model suggests a radical hypothesis that antimatter nucleon clusters are present as a hidden parton type variable (*sensu* Feynman) superposed within the spatial confinement of the proton ($^1H_1$), the neutron, and the deuteron ($^1H_2$). Because the mathematics involving interactions between matter and antimatter nucleon clusters is not developed, theoretical work will be needed to test model predictions. If model predictions can be experimentally confirmed, a new physics is suggested.

2 The Brightsen Nucleon Cluster Model to unmatter entities inside nuclei

Of fundamental importance to the study of nuclear physics is the attempt to explain the macroscopic structural phenomena of the atomic nucleus. Classically, nuclear structure mathematically derives from two opposing views: (1) that the proton [P] and neutron [N] are independent (unbound) interacting

Matter Clusters ⟶ / Antimatter Clusters ↓	[NP] Deuteron i Stable	[NPN] Triton j Beta-unstable	[PNP] Helium-3 k Stable	[NN] Di-Neutron l	[PP] Di-Proton m	[NNN] Tri-Neutron n	[PPP] Tri-Proton o
[NˆPˆ] a Stable		[N] |NP| |NˆPˆ|	[P] |NP| |NˆPˆ|	Pions (q qˆ)	Pions (q qˆ)	[N] |NN| |NˆPˆ|	[P] |NˆPˆ| |PP|
[NˆPˆNˆ] b Beta-unstable	[Nˆ] |NP| |NˆPˆ|		Pions (q qˆ)	[Pˆ] |NN| |NˆNˆ|	[Nˆ] |NˆPˆ| |PP|	Pions (q qˆ)	Tetraquarks (q q qˆqˆ)
[PˆNˆPˆ] c Stable	[Pˆ] |NP| |NˆPˆ|	Pions (q qˆ)		[Pˆ] |NˆPˆ| |NN|	[Nˆ] |PP| |PˆPˆ|	Tetraquarks (q q qˆqˆ)	Pions (q qˆ)
[NˆNˆ] d	Pions (q qˆ)	[N] |NN| |NˆNˆ|	[P] |NP| |NˆNˆ|		Tetraquarks (q q qˆqˆ)	[N] |NN| |NˆNˆ|	[P] |PP| |NˆNˆ|
[PˆPˆ] e	Pions (q qˆ)	[N] |NP| |PˆPˆ|	[P] |NP| |PˆPˆ|	Tetraquarks (q q qˆqˆ)		[N] |PˆPˆ| |NN|	[P] |PP| |PˆPˆ|
[NˆNˆNˆ] f	[Nˆ] |NP| |NˆNˆ|	Pions (q qˆ)	Tetraquarks (q q qˆqˆ)	[Nˆ] |NN| |NˆNˆ|	[Nˆ] |NˆNˆ| |PP|		Hexaquarks (q q q qˆqˆqˆ)
[PˆPˆPˆ] g	[Pˆ] |NP| |PˆPˆ|	Tetraquarks (q q qˆqˆ)	Pions (q qˆ)	[Pˆ] |PˆPˆ| |NN|	[Pˆ] |PˆPˆ| |PP|	Hexaquarks (q q q qˆqˆqˆ)	

Table 1: Unmatter entities (stable, quasi-stable, unstable) created from union of matter and antimatter nucleon clusters as predicted by the gravity-antigravity formalism of the Brightsen Nucleon Cluster Model. Shaded cells represent interactions that result in annihilation of mirror opposite two- and three- body clusters. Top nucleons within cells show superposed state comprised of three valance quarks; bottom structures show superposed state of hidden unmatter in the form of nucleon clusters. Unstable pions, tetraquarks, and hexaquark unmatter are predicted from union of mass symmetrical clusters that are not mirror opposites. The symbol ˆ = antimatter, N = neutron, P = proton, q = quark. (Communication with R. D. Davic).

fermions within nuclear shells, or (2) that nucleons interact collectively in the form of a liquid-drop. Compromise models attempt to cluster nucleons into interacting [NP] boson pairs (e.g., Interacting Boson Model-IBM), or, as in the case of the Interacting Boson-Fermion Model (IBFM), link boson clusters [NP] with un-paired and independent nucleons [P] and [N] acting as fermions.

However, an alternative view, at least since the 1937 Resonating Group Method of Wheeler, and the 1965 Close-Packed Spheron Model of Pauling, holds that the macroscopic structure of atomic nuclei is best described as being composed of a small number of interacting boson-fermion nucleon "clusters" (e. g., helium-3 [PNP], triton [NPN], deuteron [NP]), as opposed to independent [N] and [P] nucleons acting as fermions, either independently or collectively. Mathematically, such clusters represent a spatially localized mass-charge-spin subsystem composed of strongly correlated nucleons, for which realistic two- and three body wave functions can be written. In this view, quark-gluon dynamics are confined within the formalism of 6-quark bags [NP] and 9-quark bags ([PNP] and [NPN]), as opposed to valance quarks forming free nucleons. The experimental evidence in support of nucleons interacting as boson-fermion clusters is now extensive and well reviewed.

One novel nucleon cluster model is that of R. A. Brightsen, which was derived from the identification of mass-charge symmetry systems of isotopes along the Z-N Serge plot. According to Brightsen, all beta-stable matter and antimatter isotopes are formed by potential combinations of two- and three nucleon clusters; e.g., ([NP], [PNP], [NPN], [NN], [PP], [NNN], [PPP], and/or their mirror antimatter clusters [NˆPˆ], [PˆNˆPˆ], [NˆPˆNˆ], [NˆNˆ], [PˆPˆ], [PˆPˆPˆ], [NˆNˆNˆ], where the symbol ˆ here is used to denote antimatter. A unique prediction of the Brightsen model is that a stable union must result between interaction of mass asymmetrical matter (positive mass) and antimatter (negative mass) nucleon clusters to form protons and neutrons, for example the interaction between matter [PNP] + antimatter

[NˆPˆ]. Why union and not annihilation of mass asymmetrical matter and antimatter entities? As explained by Brightsen, independent (unbound) neutron and protons do not exist in nuclear shells, and the nature of the mathematical series of cluster interactions (3 [NP] clusters = 1[NPN] cluster + 1 [PNP] cluster), makes it impossible for matter and antimatter clusters of identical mass to coexist in stable isotopes. Thus, annihilation cannot take place between mass asymmetrical two- and three matter and antimatter nucleon clusters, only strong bonding (attraction).

Here is the Table that tells how unmatter may be formed from nucleon clusters according to the Brightsen model.

3 A proposed experimental test

As known, Standard Model of Quantum Electrodynamics explains all known phenomena with high precision, aside for anomalies in orthopositronium annihilation, discovered in 1987.

The Brightsen model, like many other models (see References), is outside the Standard Model. They all pretend to expand the Standard Model in one or another way. Therefore today, in order to judge the alternative models as true or false, we should compare their predictions to orthopositronium annihilation anomalies, the solely unexplained by the Standard Model. Of those models the Brightsen model has a chance to be tested in such way, because it includes unmatter entities (the conjugations of particles and anti-particles) inside an atomic nucleus that could produce effect in the forming of orthopositronium by β^+-decay positrons and its annihilation.

In brief, the anomalies in orthopositronium annihilation are as follows.

Positronium is an atom-like orbital system that includes an electron and its anti-particle, positron, coupled by electrostatic forces. There are two kinds of that: parapositronium $^{\mathrm{S}}$Ps, in which the spins of electron and positron are oppositely directed and the summary spin is zero, and orthopositronium $^{\mathrm{T}}$Ps, in which the spins are co-directed and the summary spin is one. Because a particle-antiparticle (unmatter) system is unstable, life span of positronium is rather small. In vacuum, parapositronium decays in $\tau \simeq 1.25{\times}10^{-10}$ s, while orthopositronium is $\tau \simeq 1.4{\times}10^{-7}$ s after the birth. In a medium the life span is even shorter because positronium tends to annihilate with electrons of the media.

In laboratory environment positronium can be obtained by placing a source of free positrons into a matter, for instance, one-atom gas. The source of positrons is β^+-decay, self-triggered decays of protons in neutron-deficient atoms*

$$\mathrm{p} \rightarrow \mathrm{n} + \mathrm{e}^+ + \nu_{\mathrm{e}}.$$

Some of free positrons released from β^+-decay source into gas quite soon annihilate with free electrons and electrons in the container's walls. Other positrons capture electrons from gas atoms thus producing orthopositronium and parapositronium (in 3:1 statistical ratio). Time spectrum of positrons (number of positrons vs. life span) is the basic characteristic of their annihilation in matter.

In inert gases the time spectrum of annihilation of free positrons generally reminds of exponential curve with a plateau in its central part, known as "shoulder" [29, 30]. In 1965 Osmon published [29] pictures of observed time spectra of annihilation of positrons in inert gases (He, Ne, Ar, Kr, Xe). In his experiments he used ^{22}NaCl as a source of β^+-decay positrons. Analyzing the results of the experiments, Levin noted that the spectrum in neon was peculiar compared to those in other one-atom gases: in neon points in the curve were so widely scattered, that presence of a "shoulder" was unsure. Repeated measurements of temporal spectra of annihilation of positrons in He, Ne, and Ar, later accomplished by Levin [31, 32], have proven existence of anomaly in neon. Specific feature of the experiments done by Osmon, Levin and some other researchers in the UK, Canada, and Japan is that the source of positrons was ^{22}Na, while the moment of birth of positron was registered according to γ_{n}-quantum of decay of excited ^{22*}Ne

$$^{22*}\mathrm{Ne} \rightarrow {}^{22}\mathrm{Ne} + \gamma_{\mathrm{n}}\,,$$

from one of products of β^+-decay of ^{22*}Na.

In his experiments [33, 34] Levin discovered that the peculiarity of annihilation spectrum in neon (abnormally wide scattered points) is linked to presence in natural neon of substantial quantity of its isotope ^{22}Ne (around 9%). Levin called this effect *isotope anomaly*. Temporal spectra were measured in neon environments of two isotopic compositions: (1) natural neon (90.88% of ^{20}Ne, 0.26% of ^{21}Ne, and 8.86% of ^{22}Ne); (2) neon with reduced content of ^{22}Ne (94.83% of ^{20}Ne, 0.22% of ^{21}Ne, and 4.91% of ^{22}Ne). Comparison of temporal spectra of positron decay revealed: in natural neon (the 1st composition) the shoulder is fuzzy, while in neon poor with ^{22}Ne (the 2nd composition) the shoulder is always clearly pronounced. In the part of spectrum, to which $^{\mathrm{T}}$Ps-decay mostly contributes, the ratio between intensity of decay in poor neon and that in natural neon (with much isotope ^{22}Ne) is $1.85{\pm}0.1$ [34].

Another anomaly is substantially higher measured rate of annihilation of orthopositronium (the value reciprocal to its life span) compared to that predicted by QED.

Measurement of orthopositronium annihilation rate is among the main tests aimed to experimental verification of QED laws of conservation. In 1987 thanks to new precision technology a group of researchers based in the University of Michigan (Ann Arbor) made a breakthrough in this area. The obtained results showed substantial gap between experiment and theory. The anomaly that the Michigan group revealed

*It is also known as positron β^+-decay. During β^--decay in nucleus neutron decays $\mathrm{n} \rightarrow \mathrm{p} + \mathrm{e}^- + \tilde{\nu}_{\mathrm{e}}$.

was that measured rates of annihilation at $\lambda_{\mathrm{T(exp)}} = 7.0514 \pm \pm 0.0014\ \mu s^{-1}$ and $\lambda_{\mathrm{T(exp)}} = 7.0482 \pm 0.0016\ \mu s^{-1}$ (with unseen-before precision of 0.02% and 0.023% using vacuum and gas methods [35–38]) were much higher compared to $\lambda_{\mathrm{T(theor)}} = 7.00383 \pm 0.00005\ \mu s^{-1}$ as predicted by QED [39–42]. The effect was later called λ_{T}-anomaly [43].

Theorists foresaw possible annihilation rate anomaly not long before the first experiments were accomplished in Michigan. In 1986 Holdom [44] suggested that "mixed type" particles may exist, which being in the state of oscillation stay for some time in our world and for some time in the mirror Universe, possessing negative masses and energies. In the same year Glashow [45] gave further development to the idea and showed that in case of 3-photon annihilation $^{\mathrm{T}}$Ps will "mix up" with its mirror twin thus producing two effects: (1) higher annihilation rate due to additional mode of decay $^{\mathrm{T}}\mathrm{Ps} \rightarrow$ nothing, because products of decay passed into the mirror Universe can not be detected; (2) the ratio between orthopositronium and parapositronium numbers will decrease from $^{\mathrm{T}}\mathrm{Ps} : {}^{\mathrm{S}}\mathrm{Ps} = 3{:}1$ to $1.5 : 1$. But at that time (in 1986) Glashow concluded that no interaction is possible between our-world and mirror-world particles.

On the other hand, by the early 1990's these theoretic studies encouraged many researchers worldwide for experimental search of various "exotic" (unexplained in QED) modes of $^{\mathrm{T}}$Ps-decay, which could lit some light on abnormally high rate of decay. These were, to name just a few, search for $^{\mathrm{T}}\mathrm{Ps} \rightarrow$ nothing mode [46], check of possible contribution from 2-photon mode [47–49] or from other exotic modes [50–52]. As a result it has been shown that no exotic modes can contribute to the anomaly, while contribution of $^{\mathrm{T}}\mathrm{Ps} \rightarrow$ nothing mode is limited to 5.8×10^{-4} of the regular decay.

The absence of theoretical explanation of λ_{T}-anomaly encouraged Adkins et al. [53] to suggest experiments made in Japan [54] in 1995 as an alternative to the basic Michigan experiments. No doubt, high statistical accuracy of the Japanese measurements puts them on the same level with the basic experiments [35–38]. But all Michigan measurements possessed the property of a "full experiment", which in this particular case means no external influence could affect wave function of positronium. Such influence is inevitable due to electrodynamic nature of positronium and can be avoided only using special technique. In Japanese measurements [54] this was not taken into account and thus they do not possess property of "full experiment". Latest experiments of the Michigans [55], so-called *Resolution of Orthopositronium-Lifetime Pussle*, as well do not possess property of "full experiment", because the qualitative another statement included external influence of electromagnetic field [56, 57].

As early as in 1993 Karshenboim [58] showed that QED had actually run out of any of its theoretical capabilities to explain orthopositronium anomaly.

Electric interactions and weak interactions were joined into a common electroweak interaction in the 1960's by commonly Salam, Glashow, Weinberg, etc. Today's physicists attempt to join electroweak interaction and strong interaction (unfinished yet). They follow an intuitive idea that forces, connecting electrons and a nucleus, and forces, connecting nucleons inside a nucleus, are particular cases of a common interaction. That is the basis of our claim. If that is true, our claim is that orthopositronium atoms born in neon of different isotope contents (^{22}Ne, ^{21}Ne, ^{20}Ne) should be different from each other. There should be an effect of "inner" structure of neon nuclei if built by the Brightsen scheme, because the different proton-neutron contents built by different compositions of nucleon pairs. As soon as a free positron drags an electron from a neon atom, the potential of electro-weak interactions have changed in the atom. Accordingly, there in the nucleus itself should be re-distribution of strong interactions, than could be once as the re-building of the Brightsen pairs of nucleons there. So, lost electron of ^{22}Ne should have a different "inner" structure than that of ^{21}Ne or ^{20}Ne. Then the life span of orthopositronium built on such electrons should be as well different.

Of course, we can only qualitatively predict that difference, because we have no exact picture of what really happens inside a "structurized" nucleus. Yet only principal predictions are possible there. However even in such case we vote for continuation of "isotope anomaly" experiments with orthopositronium in neon of different isotope contents. If further experiments will be positive, it could be considered as one more auxiliary proof that the Brightsen model is true.

Acknowledgements

We very much appreciate Dr. Robert Davic, the nephew of R. A. Brightsen, for comments about the Brightsen model.

References

1. Smarandache F. Matter, antimatter, and unmatter. *Infinite Energy*, 2005, v. 11, issue 62, 50–51.
2. Smarandache F. A new form of matter — unmatter, composed of particles and anti-particles. *Progress in Physics*, 2005, v. 1, 9–11.
3. Smarandache F. Verifying unmatter by experiments, more types of unmatter, and a quantum chromodynamics formula. *Progress in Physics*, 2005, v. 2, 113–116.

UNMATTER BASIS EXPERIMENTS

4. Gray L., Hagerty P., Kalogeropoulos T. E. *Phys. Rev. Lett.*, 1971, v. 26, 1491–1494.
5. Carrol A.S., Chiang I.-H., Kucia T. F., Li K. K., Mazur P. O., Michael D. N., Mockett P., Rahm D. C., Rubinstein R. *Phys. Rev. Lett.*, 1974, v. 32, 247–250.
6. Kalogeropoulos T. E., Vayaki A., Grammatikakis G., Tsilimigras T., Simopoulou E. *Phys. Rev. Lett.*, 1974, v. 33, 1635–1637.
7. Chapiro I. S. *Physics-Uspekhi*, 1973, v. 109, 431.

8. Bogdanova L. N., Dalkarov O. D., Chapiro I. S. *Annals of Physics*, 1974, v. 84, 261–284.
9. Cassidy D. B., Deng S. H. M., Greaves R. G., Maruo T., Nishiyama N., Snyder J. B., Tanaka H. K. M., Mills A. P. Jr. *Phys. Rev. Lett.*, 2005, v. 95, No. 19, 195006.
10. Ball Ph. *News Nature*, 22 November 2005.

THE BRIGHTSEN MODEL

11. Brightsen R. A. Nucleon cluster structures in beta-stable nuclides. *Infinite Energy*, 1995, v. 1, no. 4, 55–56.
12. Brightsen R. A. Correspondence of the Nucleon Cluster Model with the Periodic Table of Elements. *Infinite Energy*, 1995/96, v. 1(5/6), 73–74.
13. Brightsen R. A. Correspondence of the Nucleon Cluster Model with the Classical Periodic Table of Elements. *J. New Energy*, 1996, v. 1(1), 75–78.
14. Brightsen R. A. The Nucleon Cluster Model and the Periodic Table of Beta-Stable Nuclides. 1996 (available online at http://www.brightsenmodel.phoenixrising-web.net).
15. Brightsen R. A. The nucleon cluster model and thermal neutron fission. *Infinite Energy*, 2000, v. 6(31), 55–63.
16. Brightsen R. A., Davis R. Appl. of the Nucleon Cluster Model to experimental results. *Infinite Energy*, 1995, v. 1(3), 13–15.
17. Bass R. W. Experimental evidence favoring Brightsen's nucleon cluster model. *Infinite Energy*, 1996, v. 2(11), 78–79.

SOME REVIEW PAPERS ON CLUSTER MODELS

18. Buck B., Merchant A. C., Perez S. M. *Phys. Rev. C*, 2005, v. 71(1), 014311–15.
19. Akimune H., Yamagata T., Nakayama S., Fujiwara M., Fushimi K., Hara K., Hara K. Y., Ichihara K., Kawase K., Matsui K., Nakanishi K., Shiokawa A., Tanaka M., Utsunomiya H., and Yosoi M. *Physics of Atomic Nuclei*, 2004, v. 67(9), 1721–1725.
20. *Clustering Aspects of Nuclear Structure and Dynamics, Cluster'99, Proc. of the 7th Intern. Conf.*, 1999, Rab (Croatia).
21. Wuosmaa A. H., Betts R. R., Freer M., and Fulton B. R. *Annual Review of Nuclear and Particle Science*. 1995, v. 45, 89–131.
22. Bromley D. A. *Clust. Aspects of Nucl. Structure, Proc. of the 4th Intern. Conf.*, Chester (UK), D. Reidel Publ., Dordrecht.
23. Horiuchi H. and Ikeda K. *Cluster Models and Other Topics, Intern. Rev. of Nucl. Physics*, 1986, v. 4, World Scientific, Singapore, 1–259.

CLUSTER MODELS THAT THE BRIGHTSEN MODEL BUILDS ON

24. Wheeler J. A. *Phys. Rev.*, 1937, v. 52, 1083.
25. Wheeler J. A. *Phys. Rev.*, 1937, v. 52, 1107.
26. Pauling L. *Proc. Natl. Acad. Sci. USA*, 1965, v. 54, no. 4, 989.
27. Pauling L. *Science*, 1965, v. 150, no. 3694, 297.
28. Pauling L. *Revue Roumain de Physique*, 1966, v. 11, no. 9/10, 825–833.

ANOMALIES OF ORTHOPOSITRONIUM ANNIHILATION

29. Osmon P. E. *Physical Review B*, 1965, v. 138, 216.
30. Tao S. J., Bell J., and Green J. H. *Proceedings of the Physical Society*, 1964, v. 83, 453.
31. Levin B. M. and Shantarovich V. P. *High Energy Chemistry*, 1977, v. 11(4), 322–323.
32. Levin B. M. *Soviet J. Nucl. Physics*, 1981, v. 34(6), 917–918.
33. Levin B. M. and Shantarovich V. P. *Soviet J. Nucl. Physics*, 1984, v. 39(6), 855–856.
34. Levin B. M., Kochenda L. M., Markov A. A., and Shantarovich V. P. *Soviet J. Nucl. Physics*, 1987, v. 45(6), 1119–1120.
35. Gidley D. W., Rich A., Sweetman E., and West D. *Physical Review Letters*, 1982, v. 49, 525–528.
36. Westbrook C. I., Gidley D. W., Conti R. S., and Rich A. *Physical Review Letters*, 1987, v. 58, 1328–1331.
37. Westbrook C. I., Gidley D. W., Conti R. S., and Rich A. *Physical Review A*, 1989, v. 40, 5489–5499.
38. Nico J. S., Gidley D. W., Rich A., and Zitzewitz P. W. *Physical Review Letters*, 1990, v. 65, 1344–1347.
39. Caswell W. E. and Lepage G. P. *Phys. Rev. A*, 1979, v. 20, 36.
40. Adkins G. S. *Ann. Phys. (N.Y.)*, 1983, v. 146, 78.
41. Adkins G. S., Salahuddin A. A., and Schalm K. E. *Physical Review A*, 1992, v. 45, 3333–3335.
42. Adkins G. S., Salahuddin A. A., and Schalm K. E. *Physical Review A*, 1992, v. 45, 7774–7780.
43. Levin B. M. *Physics of Atomic Nuclei*, 1995, v. 58(2), 332–334.
44. Holdom B. *Physics Letters B*, 1986, v. 166, 196–198.
45. Glashow S. L. *Physics Letters B*, 1986, v. 167, 35–36.
46. Atoyan G. S., Gninenko S. N., Razin V. I., and Ryabov Yu. V. *Physics Letters B*, 1989, v. 220, 317–320.
47. Asai S., Orito S., Sanuki T., Yasuda M., and Yokoi T. *Physical Review Letters*, 1991, v. 66, 1298–1301.
48. Gidley D. W., Nico J. S., and Skalsey M. *Physical Review Letters*, 1991, v. 66, 1302–1305.
49. Al-Ramadhan A. H. and Gidley D. W. *Physical Review Letters*, 1994, v. 72, 1632–1635.
50. Orito S., Yoshimura K., Haga T., Minowa M., and Tsuchiaki M. *Physical Review Letters*, 1989, v. 63, 597–600.
51. Mitsui T., Fujimoto R., Ishisaki Y., Ueda Y., Yamazaki Y., Asai S., and Orito S. *Phys. Rev. Lett.*, 1993, v. 70, 2265–2268.
52. Skalsey M. and Conti R.S. *Phys. Rev. A*, 1997, v. 55(2), 984.
53. Adkins G.S., Melnikov K., and Yelkhovsky A. *Phys. Rev. A*, 1999, v. 60(4), 3306–3307.
54. Asai S., Orito S., and Shinohara N. *Physics Letters B*, 1995, v. 357, 475–480.
55. Vallery R. S., Zitzewitz P. W., and Gidley D. W. *Phys. Rev. Lett.*, 2003, v. 90, 203402.
56. Levin B. M. arXiv: quant-ph/0303166.
57. Levin B. M. CERN EXT-2004-016.
58. Karshenboim S. G. *Yadern. Fizika*, 1993, v. 56(12), 155–171.

Fermions as Topological Objects

Vladimir N. Yershov

Mullard Space Science Laboratory (University College London),
Holmbury St. Mary (Dorking), Surrey RH5 6NT, England

E-mail: vny@mssl.ucl.ac.uk

A preon-based composite model of the fundamental fermions is discussed, in which the fermions are bound states of smaller entities — primitive charges (preons). The preon is regarded as a dislocation in a dual 3-dimensional manifold — a topological object with no properties, save its unit mass and unit charge. It is shown that the dualism of this manifold gives rise to a hierarchy of complex structures resembling by their properties three families of the fundamental fermions. Although just a scheme for building a model of elementary particles, this description yields a quantitative explanation of many observable particle properties, including their masses. PACS numbers: 12.60.Rc, 12.15.Ff, 12.10.Dm

1 Introduction

The hierarchical pattern observed in the properties of the fundamental fermions (quarks and leptons) points to their composite nature [1], which goes beyond the scope of the Standard Model of particle physics. The particles are grouped into three generations (families), each containing two quarks and two leptons with their electric charges, spins and other properties repeating from generation to generation: the electron and its neutrino, e^-, ν_e, the muon and its neutrino, μ^-, ν_μ, the tau and its neutrino, τ^-, ν_τ, the up and down quarks, $u^{+2/3}, d^{-1/3}$, charm and strange, $c^{+2/3}, s^{-1/3}$, top and bottom, $t^{+2/3}, b^{-1/3}$ (here the charges of quarks are indicated by superscripts). The composite models of quarks and leptons [2] are based on fewer fundamental particles than the Standard Model (usually two or three) and are able to reproduce the above pattern as to the electric and colour charges, spins and, in some cases, the variety of species. However, the masses of the fundamental fermions are distributed in a rather odd way [3]. They cannot be predicted from any application of first principles of the Standard Model; nor has any analysis of the observed data [4] or development of new mathematical ideas [5] yielded an explanation as to why they should have strictly the observed values instead of any others. Even there exist claims of randomness of this pattern [6]. However, the history of science shows that, whenever a regular pattern was observed in the properties of matter (e. g., the periodical table of elements or eight-fold pattern of mesons and baryons), this pattern could be explained by invoking some underlying structures. In this paper we shall follow this lead by assuming that quarks and leptons are bound states of smaller particles, which are usually called "pre-quarks" or "preons" [7]. Firstly, we shall guess at the basic symmetries of space, suggesting that space, as any other physical entity, is dual. We propose that it is this property that is responsible for the emergence of different types of interactions from a unique fundamental interaction. To be absolutely clear, we have to emphasise that our approach will be based on classical (deterministic) fields, which is opposed to the commonly-held view that quarks and leptons are quantum objects. But we shall see that by using classical fields on small scales we can avoid the problems related to the short-range energy divergences and anomalies, which is the main problem of all quantum field theories.

2 The universe

Let us begin from a few conjectures (postulates) about the basic properties of space:

- P1 Matter is structured, and the number of its structural levels is finite;
- P2 The simplest (and, at the same time, the most complex) structure in the universe is the universe itself;
- P3 The universe is self-contained (by definition);
- P4 All objects in the universe spin (including the universe itself).

The postulate P1 is based on the above mentioned historical experience with the patterns and structures behind them. These patterns are known to be simpler on lower structural levels, which suggests that matter could be structured down to the simplest possible entity with almost no properties. We shall relate this entity to the structure of the entire universe (postulate P2). This is not, of course, a novelty, since considering the universe as a simple uniform object lies in the heart of modern cosmology. The shape (topology) of this object is not derivable from Einstein's equations, but for simplicity it is usually considered as a hyper-sphere (S^3) of positive, negative or zero curvature. However, taking into account the definition of the universe as a self-contained object (postulate P3), the spherical shape becomes inappropriate, because any sphere has at least two unrelated

hyper-surfaces, which is incompatible with the definition of the uniqueness and self-containedness of the universe. More convenient would be a manifold with a unique hyper-surface, such as the Klein-bottle, K^3 [8]. Similarly to S^3, it can be of positive, negative or zero curvature. An important feature of K^3 is the unification of its inner and outer surfaces (Fig. 1). In the case of the universe, the unification might well occur on the sub-quark level, giving rise to the structures of elementary particles and, supposedly, resulting in the identification of the global cosmological scale with the local microscopic scale of elementary particles. In Fig. 1b the unification region is marked as Π (primitive particle).

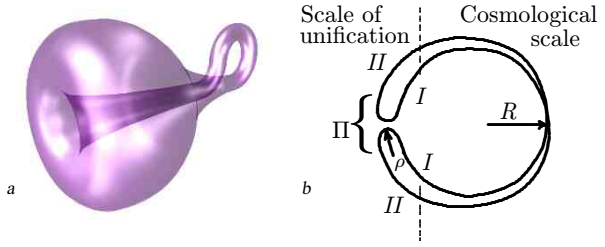

Fig. 1: (a) Klein-bottle and (b) its one-dimensional representation; the "inner" (I) and "outer" (II) hyper-surfaces are unified through the region Π (primitive particle); R and ρ are, respectively, the global and local radii of curvature.

3 The primitive particle

Let as assume that space is smooth and continuous, i.e., that its local curvature cannot exceed some finite value ε: $|\rho|^{-1} < \varepsilon$. Then, within the region Π (Fig. 1b) space will be locally curved "inside-out". In these terms, the primitive particle can be seen as a dislocation (topological defect) of the medium and, thus, cannot exist independently of this medium. Then, the postulate P4 about the spinning universe gives us an insight into the possible origin of the particle mass. This postulate is not obvious, although the idea of spinning universe was proposed many years ago by A. Zelmanov [9] and K. Gödel [10]. It comes from the common fact that so far non-rotating objects have never been observed.

The universe spinning with its angular velocity ω (of course, if considered from the embedding space) would result in the linear velocity $\pm\omega R$ of the medium in the vicinity of the primitive particle, where R is the global radius of curvature of the universe; and the sign depends on the choice of the referent direction (either inflow or outflow from the inversion region).

Due to the local curvature, ρ^{-1}, in the vicinity of the primitive particle, the spinning universe must give rise to a local acceleration, a_{g}, of the medium moving through the region Π, which is equivalent to the acceleration of the particle itself. According to Newton's second law, this acceleration can be described in terms of a force, $F_{\mathrm{g}} = m_{\mathrm{g}} a_{\mathrm{g}}$, proportional to this acceleration. The coefficient of proportionality between the acceleration and the force corresponds to the inertial mass of the particle. However, for an observer in the coordinate frame of the primitive particle this mass will be perceived as gravitational (m_{g}) because the primitive particle is at rest in this coordinate frame. Thus, the spinning universe implies the accelerated motion of the primitive particle along its world line (time-axis). If now the particle is forced to move along the spatial coordinates with an additional acceleration a_{i}, it will resist this acceleration in exactly the same way as it does when accelerating along the time-axis. A force $F_{\mathrm{i}} = m_{\mathrm{i}} a_{\mathrm{i}}$, which is required in order to accelerate the particle, is proportional to a_{i} with the coefficient of proportionality m_{i} (inertial mass). But, actually, we can see that within our framework the inertial, m_{i}, and gravitational, m_{g}, masses are generated by the same mechanism of acceleration. That is, mass in this framework is a purely inertial phenomenon ($m_{\mathrm{i}} \equiv m_{\mathrm{g}}$).

It is seen that changing the sign of ωR does not change the sign of the second derivative $a_{\mathrm{g}} = \frac{\partial^2(ict)}{\partial t^2}$, i. e., of the "gravitational" force $F_{\mathrm{g}} = m_{\mathrm{g}} a_{\mathrm{g}}$. This is obvious, because the local curvature, ρ^{-1}, is the property of the manifold and does not depend on the direction of motion. By contrast, the first derivative $\frac{\partial(ict)}{\partial t}$ can be either positive or negative, depending on the choice of the referent direction. It would be natural here to identify the corresponding force as electrostatic. For simplicity, in this paper we shall use unit values for the mass and electric charge of the primitive particle, denoting them as $m_\circ$ and $q_\circ$.

In fact, the above mass acquisition scheme has to be modified because, besides the local curvature, one must account for torsion of the manifold (corresponding to the Weyl tensor). In the three-dimensional case, torsion has three degrees of freedom, and the corresponding field can be resolved into three components (six — when both manifestations of space, I and II, are taken into account). It is reasonable to relate these three components to three polarities (colours) of the strong interaction.

Given two manifestations of space, we can resolve the field of the particle into two components, ϕ_{s} and ϕ_{e}. To avoid singularities we shall assume that infinite energies are not accessible in nature. Then, since it is an experimental fact that energy usually increases as distance decreases, we can hypothesise that the energy of both ϕ_{e} and ϕ_{s}, after reaching a maximum, decays to zero at the origin. The simplest form for the split field that incorporates the requirements above is the following:

$$\begin{aligned} F &= \phi_{\mathrm{s}} + \phi_{\mathrm{e}}\,, \\ \phi_{\mathrm{s}} &= s\exp(-\rho^{-1})\,, \quad \phi_{\mathrm{e}} = -\phi'_{\mathrm{s}}(\rho)\,. \end{aligned} \tag{1}$$

Here the signature $s = \pm 1$ indicates the sense of the interaction (attraction or repulsion); the derivative of ϕ_{s} is taken with respect to the radial coordinate ρ. Far from the

source, the second component of the split field F mimics the Coulomb gauge, whereas the first component extends to infinity being almost constant (similarly to the strong field).

In order to formalise the use of tripolar fields we have to introduce a set of auxiliary 3×3 singular matrices Π^i with the following elements:

$$^{\pm}\pi^i_{jk} = \pm\delta^i_j(-1)^{\delta^k_j}, \tag{2}$$

where δ^i_j is the Kronecker delta-function; the $(\pm)$-signs correspond to the sign of the charge; and the index i stands for the colour ($i = 1, 2, 3$ or red, green and blue). The diverging components of the field can be represented by reciprocal elements: $\tilde{\pi}_{jk} = \pi^{-1}_{jk}$. Then we can define the (unit) charges and masses of the primitive particles by summation of these matrix elements:

$$\begin{aligned} q_\Pi &= \mathbf{u}^\intercal \Pi \mathbf{u}, & \tilde{q}_\Pi &= \mathbf{u}^\intercal \tilde{\Pi} \mathbf{u} \\ m_\Pi &= \mid \mathbf{u}^\intercal \Pi \mathbf{u} \mid, & \tilde{m}_\Pi &= \mid \mathbf{u}^\intercal \tilde{\Pi} \mathbf{u} \mid \end{aligned} \tag{3}$$

($\mathbf{u}$ is the diagonal of a unit matrix; $\tilde{q}_\Pi$ and $\tilde{m}_\Pi$ diverge). Assuming that the strong and electric interactions are manifestations of the same entity and taking into account the known pattern [11] of the colour-interaction (two like-charged but unlike-coloured particles are attracted, otherwise they repel), we can write the signature s_{ij} of the chromoelectric interaction between two primitive particles, say of the colours i and j, as:

$$s_{ij} = -\mathbf{u}^\intercal \Pi^i \Pi^j \mathbf{u}\,. \tag{4}$$

4 Colour dipoles

Obviously, the simplest structures allowed by the tripolar field are the monopoles, dipoles and tripoles, unlike the conventional bipolar (electric) field, which allows only the monopoles and dipoles. Let us first consider the colour-dipole configuration. It follows from (4) that two like-charged particles with unlike-colours will combine and form a charged colour-dipole, $g^{\pm}$. Similarly, a neutral colour-dipole, g^0, can also be formed — when the constituents of the dipole have unlike-charges.

The dipoles $g^{\pm}$ and g^0 are classical oscillators with the double-well potential $V(\rho)$, Fig. 2, derived from the split field (1). The oscillations take place within the region $\rho \in (0, \rho_{\max})$, with the maximal distance between the components $\rho_{\max} \approx 1.894\rho_\circ$ (assuming the initial condition $E_0 = V(0)$ and setting this energy to zero).

Let us assume that the field $F(\rho)$ does not act instantaneously at a distance. Then, we can define the mass of a system with, say, N primitive particles as proportional to the number of these particles, wherever the field flow rate is not cancelled. For this purpose we shall regard the total field flow rate, v_N, of such a system as a superposition of the individual volume flow rates of its N constituents. Then

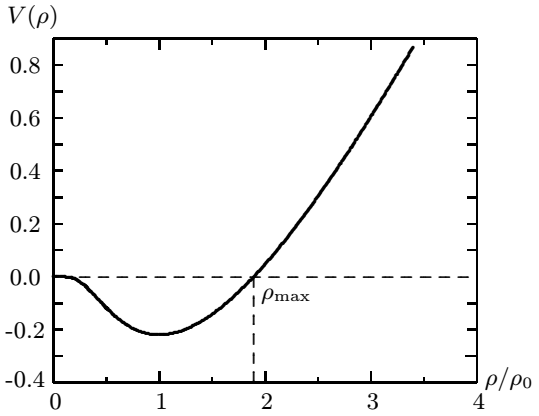

Fig. 2: Equilibrium potential based on the split field (1)

the net mass of the system can be calculated (to a first-order of approximation) as the number of particles, N, times the normalised to unity (Lorentz-additive) field flow rate v_N:

$$m_N = \mid N \mid v_N. \tag{5}$$

Here v_N is calculated recursively from

$$v_i = \frac{q_i + v_{i-1}}{1 + \mid q \mid_i v_{i-1}}, \tag{6}$$

with $i = 2, \ldots, N$ and putting $v_1 = q_1$. Then, when two unlike-charged particles combine (say red and antigreen), the magnitudes of their oppositely directed flow rates cancel each other (resulting in a neutral system). The corresponding, acceleration also vanishes, which is implicit in (5), formalising the fact that the mass of a neutral system is nullified. This formula implies the complete cancellation of masses in the systems with vanishing electric fields, but this is only an approximation because in our case the primitive particles are separated by the average distance $\rho_\circ$, whereas the complete cancellation of flows is possible only when the flow source centres coincide.

In the matrix notation, the positively charged dipole, g^+_{12}, is represented as a sum of two matrices, Π^1 and Π^2:

$$g^+_{12} = \Pi^1 + \Pi^2 = \begin{pmatrix} -1 & +1 & +1 \\ +1 & -1 & +1 \\ 0 & 0 & 0 \end{pmatrix}, \tag{7}$$

with the charge $q_{g^+_{12}} = +2$ and mass $m_{g^+_{12}} \approx 2$ and $\tilde{m}_{g^+_{12}} = \infty$, according to (3). If two components of the dipole are oppositely charged, say, $g^0_{12} = \Pi^1 + \overline{\Pi}^2$ (of whatever colour combination), then their electric fields and masses are nullified: $q_{g^0} = 0$, $m_{g^0} \approx 0$ (but still $\tilde{m}_{g^0} = \infty$ due to the null-elements in the matrix g^0). The infinities in the expressions for the reciprocal masses of the dipoles imply that neither $g^{\pm}$ nor g^0 can exist in free states (because of their infinite energies). However, in a large ensemble of neutral colour-dipoles g^0, not only electric but all the chromatic components of the field can be cancelled (statistically). Then, the mass of the neutral

dipole g^0_{ik} with an extra charged particle Π^l belonging this ensemble but coupled to the dipole, will be derived from the unit mass of Π^l:

$$\begin{aligned} m(\Pi^i, \overline{\Pi}^k, \Pi^l) &= 1\,, \\ \text{but still} \quad \widetilde{m}(\Pi^i, \overline{\Pi}^k, \Pi^l) &= \infty\,. \end{aligned} \tag{8}$$

The charge of this system will also be derived from the charge of the extra charged particle Π^l.

5 Colour tripoles

Three primitive particles with complementary colour-charges will tend to cohere and form a Y-shaped structure (tripole). For instance, by completing the set of colour-charges in the charged dipole [adding the blue-charged component to the system (7)] one would obtain a colour-neutral but electrically charged tripole:

$$\mathrm{Y} = \Pi^1 + \Pi^2 + \Pi^3 = \begin{pmatrix} -1 & +1 & +1 \\ +1 & -1 & +1 \\ +1 & +1 & -1 \end{pmatrix},$$

which is colour-neutral at infinity but colour-polarised nearby (because the centres of its constituents do not coincide). Both m and $\widetilde{m}$ of the tripole are finite, $m_{\mathrm{Y}} = \widetilde{m}_{\mathrm{Y}} = 3\ [m_\circ]$, since all the diverging components of its chromofield are mutually cancelled (converted into the binding energy of the tripole).

6 Doublets of tripoles

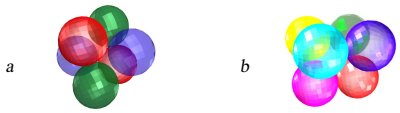

Fig. 3: The tripoles (Y-particles) can combine pairwisely, rotated by 180° (a) or 120° (b) with respect to each other.

One can show [12] that two like-charged Y-tripoles can combine pole-to-pole with each other and form a charged doublet $\delta^+ = \mathrm{Y}\lambda$ (Fig. 3a). Here the rotated symbol λ is used to indicate the rotation of the tripoles through 180° with respect to each other, which corresponds to their equilibrium position angle. The marked arm of the symbol Y indicates one of the colours, say, red, in order to visualise mutual orientations of colour-charges in the neighbouring tripoles. The charge of the doublet, $q_\delta = +6\ [q_\circ]$, is derived from the charges of its two constituent tripoles; the same is applied to its mass: $m_\delta = \widetilde{m}_\delta = 6\ [m_\circ]$. Similarly, if two unlike-charged Y-particles are combined, they will form a neutral doublet, $\gamma = \mathrm{Y}\overline{\lambda}$ (Fig. 3b) with $q_\gamma = 0$ and $m_\gamma = \widetilde{m}_\gamma = 0$. The shape of the potential well in the vicinity of the doublet allows a certain degree of freedom for its components to rotate oscillating within ±120° with respect to their equilibrium position angle (see [12] for details). We shall use the symbols ↻ and ↺ to denote the clockwise and anticlockwise rotations.

7 Triplets of tripoles

The $\frac{2}{3}\pi$-symmetry of the tripole allows up to three of them to combine if they are like-charged. Necessarily, they will combine into a loop, denoted hereafter with the symbol e. It is seen that this loop can be found in one of two possible configurations corresponding to two possible directions of rotation of the neighbouring tripoles: clockwise, $e^+_{\circlearrowright} = \mathrm{YYY}$, and anticlockwise, $e^+_{\circlearrowleft} = \mathrm{YYY}$. The vertices of the tripoles can be directed towards the centre of the structure (Fig. 4a) or outwards (Fig. 4b), but it is seen that these two orientations

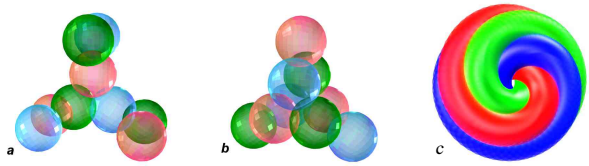

Fig. 4: Three like-charged tripoles joined with their vertices directed towards (a) and outwards (b) of the centre of the structure; (c): trajectories of colour charges in this structure.

correspond to different phases of the same structure, with its colour charges spinning around its ring-closed axis. These spinning charges will generate a toroidal (ring-closed) magnetic field which will force them to move along the torus. Their circular motion will generate a secondary (poloidal) magnetic field, contributing to their spin around the ring-axis, and so forth. The corresponding trajectories of colour-charges (currents) are shown in Fig. 4c. This mechanism, known as dynamo, is responsible for generating a self-consistent magnetic field of the triplet e.

To a first order of approximation, we shall derive the mass of the triplet from its nine constituents, suggesting that this mass is proportional to the density of the currents, neglecting the contribution to the mass of the binding and oscillatory energies of the tripoles. That is, we put $m_e = 9\ [m_\circ]$ (bearing in mind that the diverging components, $\widetilde{m}_\circ$, are almost nullified). The charge of the triplet is also derived from the number of its constituents: $q_e = \pm 9\ [q_\circ]$.

8 Hexaplets

Unlike-charged tripoles, combined pairwisely, can form chains with the following patterns:

$$\begin{aligned} \nu_{e\circlearrowright} &= \mathrm{Y}\overline{\mathrm{Y}} + \overline{\lambda}\lambda + \mathrm{Y}\overline{\mathrm{Y}} + \overline{\lambda}\lambda + \mathrm{Y}\overline{\mathrm{Y}} + \overline{\lambda}\lambda + \ldots \\ \nu_{e\circlearrowleft} &= \mathrm{Y}\overline{\mathrm{Y}} + \overline{\lambda}\lambda + \mathrm{Y}\overline{\mathrm{Y}} + \overline{\lambda}\lambda + \mathrm{Y}\overline{\mathrm{Y}} + \overline{\lambda}\lambda + \ldots \end{aligned} \tag{9}$$

corresponding to two possible directions of rotation of the neighbouring tripoles with respect to each other. The cycle of rotations repeats after each six consecutive links, making the orientation of the sixth link compatible with (attractive to) the first link by the configuration of their colour-charges.

This allows the closure of the chain in a loop (which we shall call hexaplet and denote as ν_e). The pattern (9) is visualised in Fig. 5a where the antipreons are coded with lighter colours. The corresponding trajectories of charges (currents) are shown in Fig. 5b. They are clockwise or anticlockwise helices, similar to those of the triplet e^-. The hexaplet consists of $n_{\nu_e} = 36$ preons (twelve tripoles); it is electrically neutral and, therefore, almost massless, according to Eq. (3).

Some properties of the simple preon-based structures are summarised in Table 1.

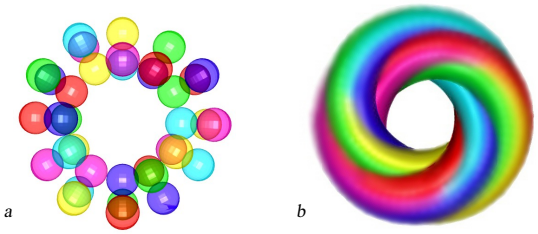

Fig. 5: (a) Structure of the hexaplet $\nu_e = 6\mathsf{Y}\overline{\mathsf{Y}}$ and (b) the corresponding helical trajectories (currents) formed by the motions of the hexaplet's colour-charges.

9 Combinations of triplets and hexaplets

The looped structures $e = 3\mathsf{Y}$ and $\nu_e = 6\mathsf{Y}\overline{\mathsf{Y}}$ can combine with each other, as well as with the simple tripole Y, because of their $\frac{2}{3}\pi$-symmetry and residual chromaticism. That is, separated from other particles, the structure ν_e will behave like a neutral particle. But, if two such particles approach one another, they will be either attracted or repulsed from each other because of van der Waals forces caused by their residual chromaticism and polarisation. The sign of this interaction depends on the twisting directions of the particles' currents. One can show [12] that the configuration of colour charges in the hexaplet ν_e matches (is attractive to) that of the triplet e if both particles have like-helicities (topological charges). On the contrary, the force between the particles of the same kind is attractive for the opposite helicities ($2e^+_{\circlearrowleft\circlearrowright}$ or $e^+_{\circlearrowleft}e^-_{\circlearrowright}$) and repulsive for like-helicities ($2e^+_{\circlearrowleft\circlearrowleft}$ or $e^+_{\circlearrowleft}e^-_{\circlearrowleft}$). So, the combined effective potential of the system $2e$ with unlike-helicities, will have an attractive inner and repulsive outer region, allowing an equilibrium configuration of the two particles. In the case of like-helicities, both inner and outer regions of the potential are repulsive and the particles e with like-helicities will never combine. This coheres with (and probably explains) the Pauli exclusion principle, suggesting that the helicity (topological charge) of a particle can straightforwardly be related to the quantum notion of spin. This conjecture is also supported by the fact that quantum spin is measured in units of angular momentum ($\hbar$), and so too — the topological charge in question, which is derived from the rotational motion of the tripoles Y around the ring-closed axis of the triplet e or hexaplet ν_e.

Relying upon the geometrical resemblance between the tripoles Y, triplets e, and hexaplets ν_e and following the pattern replicated on different complexity levels we can deduce how these structures will combine with each other. Obviously, the hexaplet ν_e, formed of twelve tripoles, is geometrically larger than a single tripole. Thus, these two structures can combine only when the former enfolds the latter. The combined structure, which we shall denote as $\mathsf{Y}_1 = \nu_e + \mathsf{Y}$, will have a mass derived from its 39 constituents: $m_{\mathsf{Y}_1} = n_{\nu_e} + m_{\mathsf{Y}} = 36 + 3 = 39\ [m_\circ]$. Its charge will be derived from the charge of its central tripole: $q_{\mathsf{Y}_1} = \pm 3\ [q_\circ]$. By their properties, the tripole, Y, and the "helical tripole", Y_1, are alike, except for the helicity property of the latter derived from the helicity of its constituent hexaplet.

When considering the combination of the hexaplet, ν_e, with the triplet, e, we can observe that the hexaplet must be stiffer than the triplet because of stronger bonds between the unlike-charged components of the former, while the repulsion between the like-charged components of the latter makes the bonds between them weaker. Then, the amplitude of the fluctuations of the triplet's radius will be larger than that of the hexaplet. Thus, in the combined structure, which we shall denote as $W = 6\mathsf{Y}\overline{\mathsf{Y}}3\mathsf{Y}$ (or $\nu_e e$), it is the triplet that would enfold the hexaplet. The charge of this structure will correspond to the charge of its charged component, e: $q_W = \pm 9\ [q_\circ]$; its mass can also be derived from the masses of its constituents if oscillations are dampened:

$$m_W = m_e + n_{\nu_e} = 9 + 36 = 45\ [m_\circ].$$

Like the simple Y-tripoles, the "helical" ones, Y_1, can form bound states with each other (doublets, strings, loops, etc.). Two hexaplets, if both enfold like-charged tripoles, will *always* have like-topological charges (helicities), which means that the force between them due to their topological charges will be repulsive (in addition to the usual repulsive force between like-charges). Thus, two like-charged helical tripoles Y_1 will never combine, unless there exists an intermediate hexaplet (ν_e) between them, with the topological charge opposite to that of the components of the pair. This would neutralise the repulsive force between these components and allow the formation of the following positively charged bound state ("helical" doublet):

$$u^+ = \mathsf{Y}_{1\circlearrowleft}\nu_{e\circlearrowright}\mathsf{Y}_{1\circlearrowleft} \quad \text{or} \quad \mathsf{Y}_1 \between \mathsf{Y}_1\ . \tag{10}$$

For brevity we have denoted the intermediate hexaplet with the symbol $\between$, implying that it creates a bond force between the otherwise repulsive components on its sides. By its properties, the helical doublet can be identified with the u-quark. Its net charge, $q_u = +6\ [q_\circ]$, is derived from the charges of its two charged components (Y_1-tripoles). Its mass is also derived from the number of particles that constitute these charged components: $m_u = 2{\times}39 = 78\ [m_\circ]$.

Table 1: Simple preon-based structures

Structure	Constituents of the structure	Number of colour charges in the structure	Charge ($q_\circ$ units)	Mass ($m_\circ$-units)
The primitive particle (preon Π)				
Π	1Π	1	$+1$	1
First-order structures (combinations of preons)				
ϱ	2Π	2	$+2$	2
g^0	$1\overline{\Pi}+1\Pi$	2	$-1+1=0$	~ 0
Υ	3Π	3	$+3$	3
Second-order structures (combinations of tripoles Υ)				
δ	2Υ	6	$+6$	6
γ	$1\overline{\Upsilon}+1\Upsilon$	6	$-3+3=0$	~ 0
e^-	$3\overline{\Upsilon}$	9	-9	9
Third-order structures				
$2e^-$	$3\overline{\Upsilon}+3\overline{\Upsilon}$	$9+9=18$	-18	18
e^-e^+	$3\overline{\Upsilon}+3\Upsilon$	$9+9=18$	$-9+9=0$	$\sim 16^\dagger$
ν_e	$6\overline{\Upsilon}\Upsilon$	$6\times(3+3)=36$	$6\times(-3+3)=0$	$7.9\times10^{-8\,\dagger}$
Υ_1	$\nu_e + \Upsilon$	$36+3=39$	$0-3=-3$	$36+3=39$
W^-	$\nu_e + e^-$	$36+9=45$	$0-9=-9$	$36+9=45$
u	$\Upsilon_1 \,\langle\!\rangle\, \Upsilon_1$	$39+36+39=114$	$+3+0+3=+6$	$39+39=78$
ν_μ	$\Upsilon_1 \,\vdots\, \overline{\Upsilon}_1$	$39+36+39=114$	$-3+0+3=0$	$1.4\times10^{-7\,\dagger}$
d	$u + W^-$	$114+45=159$	$+6-9=-3$	$78+45=123$
μ	$\nu_\mu + W^-$	$114+45=159$	$0-9=-9$	$\overline{48+39}^\ddagger$
and so on...				

†quantities estimated in [13]

‡system with two oscillating components (see further)

The positively charged u-quark can combine with the negatively charged structure $W^- = \overline{\nu}_e e^-$ (of 45-units mass), forming the d-quark:

$$d^- = u^+ + \overline{\nu}_e e^- \tag{11}$$

of a 123-units mass ($m_d = m_u + m_W = 78 + 45$). The charge of this structure will correspond to the charge of a single triplet: $q_d = q_u + q_e = +6 - 9 = -3\ [q_\circ]$ (see Fig. 6 that below).

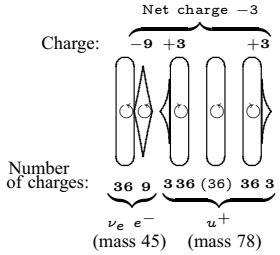

Fig. 6: Scheme of the d-quark. The symbol $\diamondsuit$ is used for the triplet (e), the symbols $\langle$ and $\rangle$ denote the tripoles (Υ-particles), and the symbols $[]$ denote the hexaplets (ν_e).

10 The second and third generations of the fundamental fermions

When two unlike-charged helical tripoles combine, their polarisation modes and helicity signs will *always* be opposite (simply because their central tripoles have opposite charges). This would cause an attractive force between these two particles, in addition to the usual attractive force corresponding to the opposite electric charges of Υ_1 and $\overline{\Upsilon}_1$. Since all the forces here are attractive, the components of this system will coalesce and then disintegrate into neutral doublets γ. However, this coalescence can be prevented by an additional hexaplet ν_e with oscillating polarisation, which would create a repulsive stabilising force (barrier) between the combining particles:

$$\nu_\mu = \Upsilon_{1\circlearrowleft}\nu_{e\circlearrowleft\circlearrowleft}\overline{\Upsilon}_{1\circlearrowleft}. \tag{12}$$

It is natural to identify this structure with the muon-neutrino — a neutral lepton belonging to the second family of the fundamental fermions. The intermediate hexaplet oscillates between the tripoles $\Upsilon_{1\circlearrowleft}$ and $\overline{\Upsilon}_{1\circlearrowleft}$, changing synchronously its polarisation state: $\nu_{e\circlearrowleft} \leftrightsquigarrow \nu_{e\circlearrowleft}$. For brevity, we shall use vertical dots separating the components of ν_μ to

denote this barrier-hexaplet:

$$\nu_\mu = \mathsf{Y}_1 \vdots \overline{\mathsf{Y}}_1 \,. \tag{13}$$

By analogy, we can derive the tau-neutrino structure:

$$\nu_\tau = \mathsf{Y}_1 \vdots \overline{\mathsf{Y}}_1 \vdots \mathsf{Y}_1 \vdots \overline{\mathsf{Y}}_1 \,, \tag{14}$$

as well as the structures of the muon (Fig. 7):

$$\mu^- = \nu_\mu \overline{\nu}_e e^- \tag{15}$$

and tau-lepton (Fig. 8):

$$\tau^- = \nu_\tau \overline{\nu}_\mu \mu^- . \tag{16}$$

Drawing also an analogy with molecular equilibrium configurations, where the rigidness of a system depends on the number of local minima of its combined effective potential [14], we can consider the second and third generation fermions as non-rigid structures with oscillating components (clusters) rather than stiff entities with dampened oscillations. In Fig. 7 and Fig. 8 we mark the supposedly clustered components of the μ- and τ-leptons with braces. Obtaining the ground-state energies (masses) of these complex structures is not a straightforward task because they may have a great variety of oscillatory modes contributing to the mass. However, in principle, these masses are computable, as can be shown by using the following empirical formula:

$$m_{\text{clust}} = \overline{m_1 + m_2 + \cdots + m_N} = m\widetilde{m}, \tag{17}$$

where N is the number of oscillating clusters, each with the mass m_i $(i = 1, \ldots, N)$; m is the sum of these masses:

$$m = m_1 + m_2 + \cdots + m_N,$$

and $\widetilde{m}$ is the reduced mass based on the components (3):

$$\widetilde{m}^{-1} = \widetilde{m}_1^{-1} + \widetilde{m}_2^{-1} + \cdots + \widetilde{m}_N^{-1}.$$

For simplicity, we assume that unit conversion coefficients in this formula are set to unity. Each substructure here contains a well-defined number of constituents (preons) corresponding to the configuration with the lowest energy. Therefore, the number of these constituents is fixed by the basic symmetry of the potential, implying that the input quantities in (17) are not free parameters. The fermion masses computed with the use of this formula are summarised in Table 2.

As an example, let us compute the muon's mass. The masses of the muon's substructures, according to Fig. 7, are: $m_1 = \widetilde{m}_1 = 48$, $m_2 = \widetilde{m}_2 = 39$ (in units of $m_\circ$). And the muon's mass will be: $m_\mu = \overline{48+39} = \dfrac{48+39}{1/48+1/39} = 1872[m_\circ]$. For the τ-lepton, the constituent masses are $m_1 = \widetilde{m}_1 = 201$, $m_2 = \widetilde{m}_2 = 156$ (Fig. 8), and its mass is $m_\tau = \overline{201+156} = 31356\,[m_\circ]$. For the proton, the positively charged fermion consisting of two up ($N_u = 2$), one down ($N_d = 1$) quarks and submerged into a cloud of gluons g^0, the masses of its components are $m_u = \widetilde{m}_u = 78$, $m_d = \widetilde{m}_d = 123$. The total number of primitive charges comprising the proton's structure is $N_p = 2m_u + m_d = 2{\times}78 + 123 = 279$, which would correspond to the number of gluons (N_g) interacting with each of these charges ($N_g = N_p = 279$). The masses of these gluons, according to (8), are $m_{g^0} = 1$, $\widetilde{m}_{g^0} = \infty$, and the resulting proton mass is

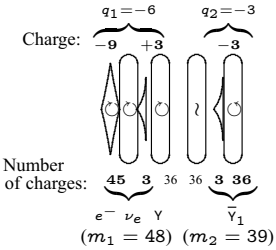

Fig. 7: Scheme of the muon.

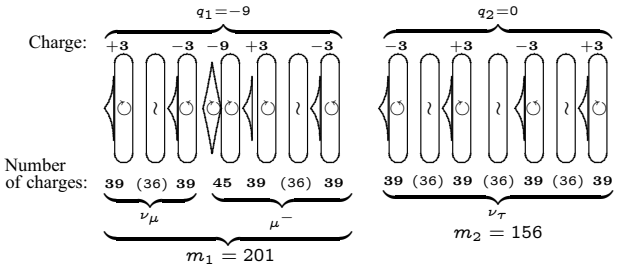

Fig. 8: Scheme of the tau-lepton.

$$m_p = \overline{N_u m_u + N_d m_d + N_g m_g} = 16523\,[m_\circ]\,, \tag{18}$$

which also reproduces the well-known but not yet explained proton-to-electron mass ratio, since $\frac{m_p}{m_e} = \frac{16523}{9} \approx 1836$.

With the value (18) one can convert m_e, m_μ, m_τ, and the masses of all other particles from units $m_\circ$ into proton mass units, m_p, thus enabling these masses to be compared with the experimental data. The computed fermion masses are listed in Table 2 where the symbols Y_1, Y_2 and Y_3 denote complex "helical" tripoles that replicate the properties of the simple tripole Y on higher levels of the hierarchy. These helical tripoles can be regarded as the combinations of "heavy neutrinos" with simple triplets. Like ν_e, the heavy neutrino consists of six pairs of helical triplets: $\nu_{\text{h}} = 6\mathsf{Y}_1\overline{\mathsf{Y}}_1$. They can further combine and form "ultra-heavy" neutrinos $\nu_{\text{uh}} = 3(\overline{\mathsf{Y}}_1\nu_{\text{h}}u)e^-$ and so on. The components Y_2 and Y_3 of the c and t quarks have the following structures: $\mathsf{Y}_2 = u\nu_e u\nu_e e^-$, consisting of 165 primitive particles, and $\mathsf{Y}_3 = \nu_{\text{uh}}\mathsf{Y}$, consisting of 1767 primitive particles.

Table 2: Computed masses of quarks and leptons. The values in the 4th column taken in units of $m_\circ$ are converted into proton mass units (5th column) m_p=16523, Eq.(18). The overlined ones are shorthands for Eq. (17). The masses of ν_e, ν_μ and ν_τ are estimated in [13].

Particle and its structure (components)		Number of charges in the non-cancelled mass components	Computed masses in units of $[m_p]$	Masses converted into m_p	Experimental masses [3] in units of $[m_p]$
First family					
ν_e	$6\mathsf{Y}\overline{\mathsf{Y}}$	≈ 0	7.864×10^{-8}	4.759×10^{-12}	$< 3\times10^{-9}$
e^-	$3\overline{\mathsf{Y}}$	9	9	0.0005447	0.0005446170232
u	$\mathsf{Y}_1 \between \mathsf{Y}_1$	78	78	0.004720	0.0021 to 0.0058
d	$u + \overline{\nu}_e e^-$	123	123	0.007443	0.0058 to 0.0115
Second family					
ν_μ	$\mathsf{Y}_1 \vdots \overline{\mathsf{Y}}_1$	≈ 0	1.4×10^{-7}	8.5×10^{-12}	$< 2\times10^{-4}$
μ^-	$\nu_\mu + \overline{\nu}_e e^-$	$\overline{48+39}$	1872	0.1133	0.1126095173
c	$\mathsf{Y}_2 \between \mathsf{Y}_2$	$\overline{165+165}$	27225	1.6477	1.57 to 1.95
s	$c + e^-$	$\overline{165+165+9}$	2751	0.1665	0.11 to 0.19
Third family					
ν_τ	$\mathsf{Y}_1 \vdots \overline{\mathsf{Y}}_1 \vdots \mathsf{Y}_1 \vdots \overline{\mathsf{Y}}_1$	≈ 0	1.5896×10^{-7}	9.6192×10^{-12}	$< 2\times10^{-2}$
τ^-	$\nu_\tau + \overline{\nu}_\mu \mu^-$	$\overline{156+201}$	31356	1.8977	1.8939 ± 0.0003
t	$\mathsf{Y}_3 \between \mathsf{Y}_3$	$\overline{1767+1767}$	3122289	188.94	189.7 ± 4.5
b	$t + \mu^-$	$\overline{1767+1767+48+39}$	76061.5	4.603	4.3 to 4.7

11 Conclusions

The results presented in Table 2 show that our model agree with experiment to an accuracy better then 0.5%. The discrepancies should be attributed to the simplifications we have assumed here (e. g., neglecting the binding and oscillatory energies, as well as the neutrino residual masses, which contribute to the masses of many structures in our model).

By matching the pattern of properties of the fundamental particles our results confirm that our conjecture about the dualism of space and the symmetry of the basic field corresponds, by a grand degree of confidence, to the actual situation. Thus, our model seems to unravel a new layer of physical reality, which bears the causal mechanisms underlying quantum phenomena. This sets a foundation from which one can explain many otherwise inexplicable observational facts that plague modern physics.

Acknowledgements

The author thanks Prof. V. V. Orlov for his valuable comments and Dr. L. V. Morrison for his linguistic support.

References

1. Kalman C. S. *Nucl. Phys. Proc. Suppl.*, 2005, v.142, 235–237.
2. Dugne J.-J. Higgs pain? Take a preon! arXiv: hep-ph/9709227. Peccei R. D. The mystery of flavor. arXiv: hep-ph/9712422. Weinberg S. *Phys. Rev. D*, 1976, v.13, 974.
3. Eidelman S., *et al.* (Particle Data Group), *Phys. Lett. B*, 2004, v. 592, 1–33 (online http://pdg.lbl.gov).
4. Pesteil P. *Apeiron*, 1991, v. 1, 15–29.
5. Golfand Yu. A. and Likhtman E. P. *JETP Lett.*, 1971, v. 13, 323. Randall L. and Sundrum R. *Phys. Rev. Lett.*, 1999, v. 83, 3370. Libanov M. and Nougaev E. *JHEP*, 2002, v. 204, 55. Spaans M. On the topological nature of fundamental interactions. arXiv: gr-qc/9901025.
6. Donoghue J. F. *Phys. Rev. D*, 1998, v. 57, 5499–5508.
7. D'Souza I. A. and Kalman C. S. Preons. World Scientific Publ., Singapore, 1992.
8. Kastrup H. A. in *Symmetries in physics (1600–1980)* (ed. by Doncel M. G.) World Sci. Publ., Singapore, 1988, 113–163.
9. Zelmanov A. L., Chronometric invariants (dissertation), 1944. Publ. CERN EXT-2004-117, 236 p.
10. Gödel K. in *Albert Einstein: philosopher, scientist*, (ed. by Schilpp P. A.) Harper Tordi Books, N.Y., 1959, v.II, 555–562.
11. Suisso E. F., de Melo J. P. B. C., Frederico T. *Phys. Rev. D*, 2002, v. 65, 094009.
12. Yershov V. N. *Few-Body Systems*, 2005, v. 37, 79–106.
13. Yershov V. N. Neutrino masses and the structure of the weak-gauge boson. arXiv: physics/0301034.
14. Burenin A. V. *Physics-Uspekhi*, 2002, v. 45(7), 753–776.

Dynamical Fractal 3-Space and the Generalised Schrödinger Equation: Equivalence Principle and Vorticity Effects

Reginald T. Cahill

School of Chemistry, Physics and Earth Sciences, Flinders University, Adelaide 5001, Australia

E-mail: Reg.Cahill@flinders.edu.au

The new dynamical "quantum foam" theory of 3-space is described at the classical level by a velocity field. This has been repeatedly detected and for which the dynamical equations are now established. These equations predict 3-space "gravitational wave" effects, and these have been observed, and the 1991 DeWitte data is analysed to reveal the fractal structure of these "gravitational waves". This velocity field describes the differential motion of 3-space, and the various equations of physics must be generalised to incorporate this 3-space dynamics. Here a new generalised Schrödinger equation is given and analysed. It is shown that from this equation the equivalence principle may be derived as a quantum effect, and that as well this generalised Schrödinger equation determines the effects of vorticity of the 3-space flow, or "frame-dragging", on matter, and which is being studied by the Gravity Probe B (GP-B) satellite gyroscope experiment.

1 Introduction

Extensive experimental evidence [1, 2, 3] has shown that a complex dynamical 3-space underlies reality. The evidence involves the repeated detection of the motion of the Earth relative to that 3-space using Michelson interferometers operating in gas mode [3], particularly the experiment by Miller [4] in 1925/26 at Mt.Wilson, and the coaxial cable RF travel time measurements by Torr and Kolen in Utah, and the DeWitte experiment in 1991 in Brussels [3]. All such 7 experiments are consistent with respect to speed and direction. It has been shown that effects caused by motion relative to this 3-space can mimic the formalism of spacetime, but that it is the 3-space that is "real", simply because it is directly observable [1].

The 3-space is in differential motion, that is one part has a velocity relative to other parts, and so involves a velocity field $\mathbf{v}(\mathbf{r}, t)$ description. To be specific this velocity field must be described relative to a frame of observers, but the formalism is such that the dynamical equations for this velocity field must transform covariantly under a change of observer. As shown herein the experimental data from the DeWitte experiment shows that $\mathbf{v}(\mathbf{r}, t)$ has a fractal structure. This arises because, in the absence of matter, the dynamical equations for $\mathbf{v}(\mathbf{r}, t)$ have no scale. This implies that the differential motion of 3-space manifests at all scales. This fractal differential motion of 3-space is missing from all the fundamental equations of physics, and so these equations require a generalisation. Here we report on the necessary generalisation of the Schrödinger equation, and which results in some remarkable results: (i) the equivalence principle emerges, as well as (ii) the effects of vorticity of this velocity field. These two effects are thus seen to be quantum-theoretic effects, i. e. consequences of the wave nature of matter. The equivalence principle, as originally formulated by Galileo and then Newton, asserts that the gravitational acceleration of an object is independent of its composition and speed. However we shall see that via the vorticity effect, the velocity of the object does affect the acceleration by causing rotations.

It has been shown [1, 5] that the phenomenon of gravity is a consequence of the time-dependence and inhomogeneities of $\mathbf{v}(\mathbf{r}, t)$. So the dynamical equations for $\mathbf{v}(\mathbf{r}, t)$ give rise to a new theory of gravity, when combined with the generalised Schrödinger equation, and the generalised Maxwell and Dirac equations. The equations for $\mathbf{v}(\mathbf{r}, t)$ involve the Newtonian gravitational constant G and a dimensionless constant that determines the strength of a new spatial self-interaction effect, which is missing from both Newtonian Gravity and General Relativity. Experimental data has revealed [1, 5] the remarkable discovery that this constant is the fine structure constant $\alpha \approx 1/137$. This dynamics then explains numerous gravitational anomalies, such as the bore hole g anomaly, the so-called "dark matter" anomaly in the rotation speeds of spiral galaxies, and that the effective mass of the necessary black holes at the centre of spherical matter systems, such as globular clusters and spherical galaxies, is $\alpha/2$ times the total mass of these systems. This prediction has been confirmed by astronomical observations [6].

The occurrence of α suggests that space is itself a quantum system undergoing on-going classicalisation. Just such a proposal has arisen in *Process Physics* [1] which is an information-theoretic modelling of reality. There quantum space and matter arise in terms of the Quantum Homotopic Field Theory (QHFT) which, in turn, may be related to the

standard model of matter. In the QHFT space at this quantum level is best described as a "quantum foam". So we interpret the observed fractal 3-space as a classical approximation to this "quantum foam".

While here we investigate the properties of the generalised Schrödinger equation, analogous generalisations of the Maxwell and Dirac equations, and in turn the corresponding generalisations to the quantum field theories for such systems, may also be made. In the case of the Maxwell equations we obtain the light bending effects, including in particular gravitational lensing, caused by the 3-space differential and time-dependent flow.

2 The physics of 3-space

Because of the dominance of the spacetime ontology, which has been the foundation of physics over the last century, the existence of a 3-space as an observable phenomenon has been overlooked, despite extensive experimental detection over that period, and earlier. This spacetime ontology is distinct from the role of spacetime as a mathematical formalism implicitly incorporating some real dynamical effects, though this distinction is rarely made. Consequently the existence of 3-space has been denied, and so there has never been a dynamical theory for 3-space. In recent years this situation has dramatically changed. We briefly summarise the key aspects to the dynamics of 3-space.

Relative to some observer 3-space is described by a velocity field $\mathbf{v}(\mathbf{r}, t)$. It is important to note that the coordinate $\mathbf{r}$ is not itself 3-space, rather it is merely a label for an element of 3-space that has velocity $\mathbf{v}$, relative to some observer. This will become more evident when we consider the necessary generalisation of the Schrödinger equation. Also it is important to appreciate that this "moving" 3-space is not itself embedded in a "space"; the 3-space is all there is, although as noted above its deeper structure is that of a "quantum foam".

In the case of zero vorticity $\nabla \times \mathbf{v} = 0$ the 3-space dynamics is given by, in the non-relativistic limit,

$$\nabla \cdot \left(\frac{\partial \mathbf{v}}{\partial t} + (\mathbf{v} \cdot \nabla)\mathbf{v} \right) + \frac{\alpha}{8} \left((\mathrm{tr} D)^2 - \mathrm{tr}(D^2) \right) = -4\pi G \rho \,, \tag{1}$$

where ρ is the matter density, and where

$$D_{ij} = \frac{1}{2} \left(\frac{\partial v_i}{\partial x_j} + \frac{\partial v_j}{\partial x_i} \right) . \tag{2}$$

The acceleration of an element of space is given by the Euler form

$$\mathbf{g}(\mathbf{r}, t) \equiv \lim_{\Delta t \to 0} \frac{\mathbf{v}\left(\mathbf{r} + \mathbf{v}(\mathbf{r}, t)\Delta t, t + \Delta t\right) - \mathbf{v}(\mathbf{r}, t)}{\Delta t} = \frac{\partial \mathbf{v}}{\partial t} + (\mathbf{v} \cdot \nabla)\mathbf{v} \,. \tag{3}$$

These forms are mandated by Galilean covariance under change of observer*. This non-relativistic modelling of the dynamics for the velocity field gives a direct account of the various phenomena noted above. A generalisation to include vorticity and relativistic effects of the motion of matter through this 3-space is given in [1]. From (1) and (2) we obtain that

$$\nabla \cdot \mathbf{g} = -4\pi G \rho - 4\pi G \rho_{DM} \,, \tag{4}$$

where

$$\rho_{DM}(\mathbf{r}) = \frac{\alpha}{32\pi G} \left((\mathrm{tr} D)^2 - \mathrm{tr}(D^2) \right) . \tag{5}$$

In this form we see that if $\alpha \to 0$, then the acceleration of the 3-space elements is given by Newton's Law of Gravitation, in differential form. But for a non-zero α we see that the 3-space acceleration has an additional effect, the ρ_{DM} term, which is an effective "matter density" that mimics the new self-interaction dynamics. This has been shown to be the origin of the so-called "dark matter" effect in spiral galaxies. It is important to note that (4) does not determine $\mathbf{g}$ directly; rather the velocity dynamics in (1) must be solved, and then with $\mathbf{g}$ subsequently determined from (3). Eqn. (4) merely indicates that the resultant non-Newtonian aspects to $\mathbf{g}$ could be mistaken as being the result of a new form of matter, whose density is given by ρ_{DM}. Of course the saga of "dark matter" shows that this actually happened, and that there has been a misguided and fruitless search for such "matter".

The numerous experimental confirmations of (1) imply that Newtonian gravity is not universal at all. Rather a key aspect to gravity was missed by Newton because it so happens that the 3-space self-interaction dynamics does not necessarily explicitly manifest outside of spherical matter systems, such as the Sun. To see this it is only necessary to see that the velocity field

$$\mathbf{v}(\mathbf{r}) = -\sqrt{\frac{2GM'}{r}}\, \hat{\mathbf{r}} \,, \tag{6}$$

is a solution to (1) external to a spherical mass M, where $M' = (1 + \frac{\alpha}{2})M + \ldots$ Then (6) gives, using (3), the resultant external "inverse square law" acceleration

$$\mathbf{g}(\mathbf{r}) = -\frac{GM'}{r^2}\, \hat{\mathbf{r}} \,. \tag{7}$$

Hence in this special case the 3-space dynamics predicts an inverse square law form for $\mathbf{g}$, as confirmed in the non-relativistic regime by Kepler's laws for planetary motion, with only a modified value for the effective mass M'. So for this reason we see how easy it was for Newton to have overlooked a velocity formalism for gravity, and so missed the self-interaction dynamics in (1). Inside a spherical matter

*However this does not exclude so-called relativistic effects, such as the length contraction of moving rods or the time dilations of moving clocks.

system Newtonian gravity and the new gravity theory differ, and it was this difference that explained the bore hole g anomaly data [5], namely that g does not decrease down a bore hole as rapidly as Newtonian gravity predicts. It was this anomaly that lead to the discovery that α was in fact the fine structure constant, up to experimental errors. As well the 3-space dynamics in (1) has "gravitational wave" solutions [7]. Then there are regions where the velocity differs slightly from the enveloping region. In the absence of matter these waves will be in general fractal because there is no dimensioned constant, and so no natural scale. These waves were seen by Miller, Torr and Kolen, and by DeWitte [1, 7] as shown in Fig. 2.

However an assumption made in previous analyses was that the acceleration of the 3-space itself, in (3), was also the acceleration of matter located in that 3-space. The key result herein is to derive this result by using the generalised Schrödinger equation. In doing so we discover the additional effect that vorticity in the velocity field causes quantum states to be rotated, as discussed in sect. 7.

3 Newtonian gravity and the Schrödinger equation

Let us consider what might be regarded as the conventional "Newtonian" approach to including gravity in the Schrödinger equation [8]. There gravity is described by the Newtonian potential energy field $\Phi(\mathbf{r},t)$, such that $\mathbf{g}=-\nabla\Phi$, and we have for a "free-falling" quantum system, with mass m,

$$i\hbar\,\frac{\partial\psi(\mathbf{r},t)}{\partial t}=-\frac{\hbar^2}{2m}\nabla^2\psi(\mathbf{r},t)+m\Phi(\mathbf{r},t)\,\psi(\mathbf{r},t)\equiv \equiv H(t)\psi\,, \tag{8}$$

where the hamiltonian is in general now time dependent, because the masses producing the gravitational acceleration may be moving. Then the classical-limit trajectory is obtained via the usual Ehrenfest method [9]: we first compute the time rate of change of the so-called position "expectation value"

$$\frac{d<\mathbf{r}>}{dt}\equiv\frac{d}{dt}(\psi,\mathbf{r}\psi)=\frac{i}{\hbar}(H\psi,\mathbf{r}\psi)-\frac{i}{\hbar}(\psi,\mathbf{r}H\psi)= =\frac{i}{\hbar}(\psi,[H,\mathbf{r}]\psi)\,, \tag{9}$$

which is valid for a normalised state ψ. The norm is time invariant when H is hermitian ($H^\dagger=H$) even if H itself is time dependent,

$$\frac{d}{dt}(\psi,\psi)=\frac{i}{\hbar}(H\psi,\psi)-\frac{i}{\hbar}(\psi,H\psi)= =\frac{i}{\hbar}(\psi,H^\dagger\psi)-\frac{i}{\hbar}(\psi,H\psi)=0\,. \tag{10}$$

Next we compute the matter "acceleration" from (9)

$$\frac{d^2<\mathbf{r}>}{dt^2}=\frac{i}{\hbar}\,\frac{d}{dt}(\psi,[H,\mathbf{r}]\psi)= =\Big(\frac{i}{\hbar}\Big)^2(\psi,\big[H,[H,\mathbf{r}]\big]\psi)+\frac{i}{\hbar}\left(\psi,\left[\frac{\partial H(t)}{\partial t},\mathbf{r}\right]\psi\right)= =-(\psi,\nabla\Phi\,\psi)=\big(\psi,\mathbf{g}(\mathbf{r},t)\psi\big)=<\mathbf{g}(\mathbf{r},t)>, \tag{11}$$

where for the commutator

$$\left[\frac{\partial H(t)}{\partial t},\mathbf{r}\right]=\left[m\,\frac{\partial\Phi(\mathbf{r},t)}{\partial t},\mathbf{r}\right]=0\,. \tag{12}$$

In the classical limit ψ has the form of a wavepacket where the spatial extent of ψ is much smaller than the spatial region over which $\mathbf{g}(\mathbf{r},t)$ varies appreciably. Then we have the approximation $<\mathbf{g}(\mathbf{r},t)>\approx\mathbf{g}(<\mathbf{r}>,t)$, and finally we arrive at the Newtonian 2nd-law equation of motion for the wavepacket,

$$\frac{d^2<\mathbf{r}>}{dt^2}\approx\mathbf{g}\,(<\mathbf{r}>,t)\,. \tag{13}$$

In this classical limit we obtain the equivalence principle, namely that the acceleration is independent of the mass m and of the velocity of that mass. But of course that followed by construction, as the equivalence principle is built into (8) by having m as the coefficient of Φ. In Newtonian gravity there is no explanation for the origin of Φ or $\mathbf{g}$. In the new theory gravity is explained in terms of a velocity field, which in turn has a deeper explanation within *Process Physics*.

4 Dynamical 3-space and the generalised Schrödinger equation

The key insight is that conventional physics has neglected the interaction of various systems with the dynamical 3-space. Here we generalise the Schrödinger equation to take account of this new physics. Now gravity is a dynamical effect arising from the time-dependence and spatial inhomogeneities of the 3-space velocity field $\mathbf{v}(\mathbf{r},t)$, and for a "free-falling" quantum system with mass m the Schrödinger equation now has the generalised form

$$i\hbar\left(\frac{\partial}{\partial t}+\mathbf{v}\cdot\nabla+\frac{1}{2}\,\nabla\cdot\mathbf{v}\right)\psi(\mathbf{r},t)=-\frac{\hbar^2}{2m}\,\nabla^2\psi(\mathbf{r},t)\,, \tag{14}$$

which we write as

$$i\hbar\,\frac{\partial\psi(\mathbf{r},t)}{\partial t}=H(t)\,\psi(\mathbf{r},t)\,, \tag{15}$$

where now

$$H(t)=-i\hbar\left(\mathbf{v}\cdot\nabla+\frac{1}{2}\,\nabla\cdot\mathbf{v}\right)-\frac{\hbar^2}{2m}\,\nabla^2\,. \tag{16}$$

This form for H specifies how the quantum system must couple to the velocity field, and it uniquely follows from two considerations: (i) the generalised Schrödinger equation must remain form invariant under a change of observer, i. e. with $t\to t$, and $\mathbf{r}\to\mathbf{r}+\mathbf{v}t$, where $\mathbf{v}$ is the relative velocity of the two observers. Then we compute that $\frac{\partial}{\partial t}+\mathbf{v}\cdot\nabla+\frac{1}{2}\nabla\cdot\mathbf{v}\to$

$\to \frac{\partial}{\partial t} + \mathbf{v}\cdot\nabla + \frac{1}{2}\nabla\cdot\mathbf{v}$, i. e. that it is an invariant operator, and (ii) requiring that $H(t)$ be hermitian, so that the wavefunction norm is an invariant of the time evolution. This implies that the $\frac{1}{2}\nabla\cdot\mathbf{v}$ term must be included, as $\mathbf{v}\cdot\nabla$ by itself is not hermitian for an inhomogeneous $\mathbf{v}(\mathbf{r},t)$. Then the consequences for the motion of wavepackets is uniquely determined; they are fixed by these two quantum-theoretic requirements.

Then again the classical-limit trajectory is obtained via the position "expectation value", first with

$$\begin{aligned}\mathbf{v}_{\mathrm{O}} &\equiv \frac{d<\mathbf{r}>}{dt} = \frac{d}{dt}(\psi, \mathbf{r}\psi) = \frac{i}{\hbar}(\psi, [H,\mathbf{r}]\psi) = \\ &= \left(\psi, \left(\mathbf{v}(\mathbf{r},t) - \frac{i\hbar}{m}\nabla\right)\psi\right) = <\mathbf{v}(\mathbf{r},t)> - \frac{i\hbar}{m}<\nabla>,\end{aligned} \tag{17}$$

on evaluating the commutator using $H(t)$ in (16), and which is again valid for a normalised state ψ.

Then for the "acceleration" we obtain from (17) that*

$$\begin{aligned}&\frac{d^2<\mathbf{r}>}{dt^2} = \frac{d}{dt}\left(\psi, \left(\mathbf{v} - \frac{i\hbar}{m}\nabla\right)\psi\right) = \\ &= \left(\psi, \left(\frac{\partial\mathbf{v}(\mathbf{r},t)}{\partial t} + \frac{i}{\hbar}\left[H, \left(\mathbf{v} - \frac{i\hbar}{m}\nabla\right)\right]\right)\psi\right) = \\ &= \left(\psi, \frac{\partial\mathbf{v}(\mathbf{r},t)}{\partial t}\psi\right) + \\ &+ \left(\psi, \left(\mathbf{v}\cdot\nabla + \frac{1}{2}\nabla\cdot\mathbf{v} - \frac{i\hbar}{2m}\nabla^2\right)\left(\mathbf{v} - \frac{i\hbar}{m}\nabla\right)\psi\right) - \\ &- \left(\psi, \left(\mathbf{v} - \frac{i\hbar}{m}\nabla\right)\left(\mathbf{v}\cdot\nabla + \frac{1}{2}\nabla\cdot\mathbf{v} - \frac{i\hbar}{2m}\nabla^2\right)\right)\psi\right) = \\ &= \left(\psi, \left(\frac{\partial\mathbf{v}(\mathbf{r},t)}{\partial t} + \big((\mathbf{v}\cdot\nabla)\mathbf{v}\big) - \frac{i\hbar}{m}(\nabla\times\mathbf{v})\times\nabla\right)\psi\right) + \\ &+ \left(\psi, \frac{i\hbar}{2m}\big(\nabla\times(\nabla\times\mathbf{v})\big)\psi\right) \approx \\ &\approx \frac{\partial\mathbf{v}}{\partial t} + (\mathbf{v}\cdot\nabla)\mathbf{v} + (\nabla\times\mathbf{v})\times\left(\frac{d<\mathbf{r}>}{dt} - \mathbf{v}\right) + \\ &+ \frac{i\hbar}{2m}\big(\nabla\times(\nabla\times\mathbf{v})\big) = \\ &= \frac{\partial\mathbf{v}}{\partial t} + (\mathbf{v}\cdot\nabla)\mathbf{v} + (\nabla\times\mathbf{v})\times\left(\frac{d<\mathbf{r}>}{dt} - \mathbf{v}\right) = \\ &= \frac{\partial\mathbf{v}}{\partial t} + (\mathbf{v}\cdot\nabla)\mathbf{v} + (\nabla\times\mathbf{v})\times\mathbf{v}_R\,,\end{aligned} \tag{18}$$

where in arriving at the 3rd last line we have invoked the small-wavepacket approximation, and used (17) to identify

$$\mathbf{v}_R \equiv -\frac{i\hbar}{m}<\nabla> = \mathbf{v}_{\mathrm{O}} - \mathbf{v}, \tag{19}$$

where $\mathbf{v}_{\mathrm{O}}$ is the velocity of the wavepacket or object "O" relative to the observer, so then $\mathbf{v}_R$ is the velocity of the wavepacket relative to the local 3-space. Then all velocity field terms are now evaluated at the location of the wavepacket. Note that the operator

$$-\frac{i\hbar}{m}(\nabla\times\mathbf{v})\times\nabla + \frac{i\hbar}{2m}\big(\nabla\times(\nabla\times\mathbf{v})\big) \tag{20}$$

is hermitian, but that separately neither of these two operators is hermitian. Then in general the scalar product in (18) is real. But then in arriving at the last line in (18) by means of the small-wavepacket approximation, we must then self-consistently use that $\nabla\times(\nabla\times\mathbf{v}) = 0$, otherwise the acceleration acquires a spurious imaginary part. This is consistent with (27) outside of any matter which contributes to the generation of the velocity field, for there $\rho = 0$. These observations point to a deep connection between quantum theory and the velocity field dynamics, as already argued in [1].

We see that the test "particle" acquires the acceleration of the velocity field, as in (3), and as well an additional vorticity induced acceleration which is the analogue of the Helmholtz acceleration in fluid mechanics. Hence we find that the equivalence principle arises from the unique generalised Schrödinger equation and with the additional vorticity effect. This vorticity effect depends on the absolute velocity $\mathbf{v}_R$ of the object relative to the local space, and so requires a change in the Galilean or Newtonian form of the equivalence principle.

The vorticity acceleration effect is the origin of the Lense-Thirring so-called "frame-dragging" effect† [10] discussed in sect. 7. While the generation of the vorticity is a relativistic effect, as in (27), the response of the test particle to that vorticity is a non-relativistic effect, and follows from the generalised Schrödinger equation, and which is not present in the standard Schrödinger equation with coupling to the Newtonian gravitational potential, as in (8). Hence the generalised Schrödinger equation with the new coupling to the velocity field is more fundamental. The Helmholtz term in (18) is being explored by the Gravity Probe B gyroscope precession experiment, however the vorticity caused by the motion of the Earth is extremely small, as discussed in sect. 7.

An important insight emerges from the form of (15) and (16): here the generalised Schrödinger equation involves two fields $\mathbf{v}(\mathbf{r},t)$ and $\psi(\mathbf{r},t)$, where the coordinate $\mathbf{r}$ is merely a label to relate the two fields, and is not itself the 3-space. In particular while $\mathbf{r}$ may have the form of a Euclidean 3-geometry, the space itself has time-dependence and inhomogeneities, and as well in the more general case will exhibit vorticity $\omega = \nabla\times\mathbf{v}$. Only in the unphysical case does the description of the 3-space become identified with the coordinate system $\mathbf{r}$, and that is when the velocity field $\mathbf{v}(\mathbf{r},t)$ becomes uniform and time independent. Then by a suitable choice of observer we may put $\mathbf{v}(\mathbf{r},t) = 0$, and the generalised Schrödinger equation reduces to the usual "free"

*Care is needed to indicate the range of the various ∇'s. Extra parentheses $(\dots)$ are used to limit the range when required.

†In the spacetime formalism it is mistakenly argued that it is "spacetime" that is "dragged".

Schrödinger equation. As we discuss later the experimental evidence is that $\mathbf{v}(\mathbf{r},t)$ is fractal and so cannot be removed by a change to a preferred observer. Hence the generalised Schrödinger equation in (15)–(16) is a major development for fundamental physics. Of course in general other non-3-space potential energy terms may be added to the RHS of (16). A prediction of this new quantum theory, which also extends to a generalised Dirac equation, is that the fractal structure to space implies that even at the scale of atoms etc there will be time-dependencies and inhomogeneities, and that these will affect transition rates of quantum systems. These effects are probably those known as the Shnoll effects [11].

5 Free-fall minimum proper-time trajectories

The acceleration in (18) also arises from the following argument, which is the analogue of the Fermat least-time formalism. Consider the elapsed time for a comoving clock travelling with the test particle. Then taking account of the Lamour time-dilation effect that time is given by

$$\tau[\mathbf{r}_0] = \int dt \left(1 - \frac{\mathbf{v}_R^2}{c^2}\right)^{1/2} \qquad (21)$$

with $\mathbf{v}_R$ given by (19) in terms of $\mathbf{v}_O$ and $\mathbf{v}$. Then this time effect relates to the speed of the clock relative to the local 3-space, and that c is the speed of light relative to that local 3-space. We are using a relativistic treatment in (21) to demonstrate the generality of the results*. Under a deformation of the trajectory

$$\mathbf{r}_0(t) \to \mathbf{r}_0(t) + \delta\mathbf{r}_0(t), \quad \mathbf{v}_0(t) \to \mathbf{v}_0(t) + \frac{d\delta\mathbf{r}_0(t)}{dt}, \quad (22)$$

and then

$$\begin{aligned} &\mathbf{v}\left(\mathbf{r}_0(t) + \delta\mathbf{r}_0(t), t\right) = \\ &= \mathbf{v}\left(\mathbf{r}_0(t), t\right) + \left(\delta\mathbf{r}_0(t)\cdot\nabla\right)\mathbf{v}\left(\mathbf{r}_0(t), t\right) + \dots \end{aligned} \qquad (23)$$

Evaluating the change in proper travel time to lowest order

$$\begin{aligned} &\delta\tau = \tau[\mathbf{r}_0 + \delta\mathbf{r}_0] - \tau[\mathbf{r}_0] = \\ &= -\int dt\, \frac{1}{c^2}\,\mathbf{v}_R\cdot\delta\mathbf{v}_R \left(1 - \frac{\mathbf{v}_R^2}{c^2}\right)^{-1/2} + \dots = \\ &= \int dt\, \frac{1}{c^2}\, \frac{\mathbf{v}_R\cdot(\delta\mathbf{r}_0\cdot\nabla)\mathbf{v} - \mathbf{v}_R\cdot\dfrac{d(\delta\mathbf{r}_0)}{dt}}{\sqrt{1 - \dfrac{\mathbf{v}_R^2}{c^2}}} = \\ &= \int dt\, \frac{1}{c^2} \left(\frac{\mathbf{v}_R\cdot(\delta\mathbf{r}_0\cdot\nabla)\mathbf{v}}{\sqrt{1 - \dfrac{\mathbf{v}_R^2}{c^2}}} + \delta\mathbf{r}_0\cdot\frac{d}{dt}\frac{\mathbf{v}_R}{\sqrt{1 - \dfrac{\mathbf{v}_R^2}{c^2}}} \right) = \\ &= \int dt\, \frac{1}{c^2}\delta\mathbf{r}_0\cdot \left(\frac{(\mathbf{v}_R\cdot\nabla)\mathbf{v} + \mathbf{v}_R\times(\nabla\times\mathbf{v})}{\sqrt{1 - \dfrac{\mathbf{v}_R^2}{c^2}}} + \frac{d}{dt}\frac{\mathbf{v}_R}{\sqrt{1 - \dfrac{\mathbf{v}_R^2}{c^2}}} \right). \end{aligned}$$

Hence a trajectory $\mathbf{r}_0(t)$ determined by $\delta\tau = 0$ to $O\left(\delta\mathbf{r}_0(t)^2\right)$ satisfies

$$\frac{d}{dt}\frac{\mathbf{v}_R}{\sqrt{1 - \dfrac{\mathbf{v}_R^2}{c^2}}} = -\frac{(\mathbf{v}_R\nabla)\mathbf{v} + \mathbf{v}_R\times(\nabla\times\mathbf{v})}{\sqrt{1 - \dfrac{\mathbf{v}_R^2}{c^2}}}\,. \qquad (24)$$

Substituting $\mathbf{v}_R(t) = \mathbf{v}_0(t) - \mathbf{v}\left(\mathbf{r}_0(t), t\right)$ and using

$$\frac{d\mathbf{v}\left(\mathbf{r}_0(t), t\right)}{dt} = \frac{\partial\mathbf{v}}{\partial t} + (\mathbf{v}_0\cdot\nabla)\mathbf{v}\,, \qquad (25)$$

we obtain

$$\begin{aligned} \frac{d\mathbf{v}_0}{dt} = \frac{\partial\mathbf{v}}{\partial t} + (\mathbf{v}\cdot\nabla)\mathbf{v} + (\nabla\times\mathbf{v})\times\mathbf{v}_R - \\ - \frac{\mathbf{v}_R}{1 - \dfrac{\mathbf{v}_R^2}{c^2}}\,\frac{1}{2}\,\frac{d}{dt}\left(\frac{\mathbf{v}_R^2}{c^2}\right). \end{aligned} \qquad (26)$$

Then in the low speed limit $v_R \ll c$ we may neglect the last term, and we obtain (18). Hence we see a close relationship between the geodesic equation, known first from General Relativity, and the 3-space generalisation of the Schrödinger equation, at least in the non-relativistic limit. So in the classical limit, i.e when the wavepacket approximation is valid, the wavepacket trajectory is specified by the least propertime geodesic.

The relativistic term in (26) is responsible for the precession of elliptical orbits and also for the event horizon effect. Hence the trajectory in (18) is a non-relativistic minimum travel-time trajectory, which is Fermat's Principle. The relativistic term in (26) will arise from a generalised Dirac equation which would then include the dynamics of 3-space.

6 Fractal 3-space and the DeWitte experimental data

In 1991 Roland DeWitte working within Belgacom, the Belgium telecommunications company, accidently made yet another detection of absolute motion, and one which was 1st-order in v/c. 5 MHz radio frequency (RF) signals were sent in both directions through two buried coaxial cables linking the two clusters of cesium atomic clocks.

Changes in propagation times were observed and eventually observations over 178 days were recorded. A sample of the data, plotted against sidereal time for just three days, is shown in Fig. 1. The DeWitte data was clear evidence of absolute motion with the Right Ascension for minimum/maximum propagation time agreeing almost exactly with

*A non-relativistic analysis may be alternatively pursued by first expanding (21) in powers of $1/c^2$.

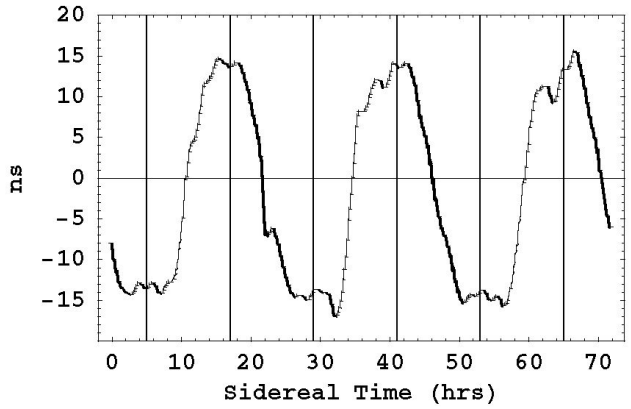

Fig. 1: Variations in twice the one-way travel time, in ns, for an RF signal to travel 1.5 km through a buried coaxial cable between Rue du Marais and Rue de la Paille, Brussels. An offset has been used such that the average is zero. The cable has a North-South orientation, and the data is $\pm$ difference of the travel times for NS and SN propagation. The sidereal time for maximum effect of $\sim$5hr (or $\sim$17hr) (indicated by vertical lines) agrees with the direction found by Miller[4]. Plot shows data over 3 sidereal days and is plotted against sidereal time. The main effect is caused by the rotation of the Earth. The superimposed fluctuations are evidence of turbulence i.e gravitational waves. Removing the Earth induced rotation effect we obtain the first experimental data of the fractal structure of space, and is shown in Fig. 2. DeWitte performed this experiment over 178 days, and demonstrated that the effect tracked sidereal time and not solar time[1].

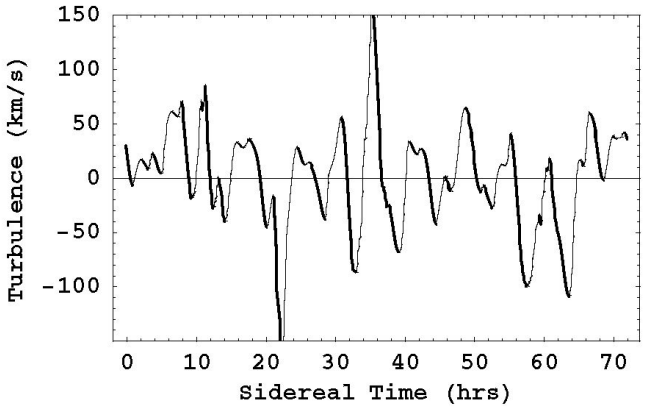

Fig. 2: Shows the velocity fluctuations, essentially "gravitational waves" observed by DeWitte in 1991 from the measurement of variations in the RF coaxial-cable travel times. This data is obtained from that in Fig. 1 after removal of the dominant effect caused by the rotation of the Earth. Ideally the velocity fluctuations are three-dimensional, but the DeWitte experiment had only one arm. This plot is suggestive of a fractal structure to the velocity field. This is confirmed by the power law analysis shown in Fig. 3.

Miller's direction* ($\alpha = 5.2^{\text{hr}}$, $\delta = -67^{\circ}$)†, and with speed 420 ± 30 km/s. This local absolute motion is different from the CMB motion, in the direction ($\alpha = 11.20^{\text{hr}}$, $\delta = -7.22^{\circ}$) with speed of 369 km/s, for that would have given the data a totally different sidereal time signature, namely the times for maximum/ minimum would have been shifted by 6hrs. The CMB velocity is motion relative to the distant early universe, whereas the velocity measured in the DeWitte and related experiments is the velocity relative to the local space. The declination of the velocity observed in this DeWitte experiment cannot be determined from the data as only three days of data are available. However assuming exactly the same declination as Miller the speed observed by DeWitte appears to be also in excellent agreement with the Miller speed. The dominant effect in Fig. 1 is caused by the rotation of the Earth, namely that the orientation of the coaxial cable with respect to the direction of the flow past the Earth changes as the Earth rotates. This effect may be approximately unfolded from the data, leaving the gravitational waves shown in Fig. 2. This is the first evidence that the velocity field describing 3-space has a complex structure, and is indeed fractal.

The fractal structure, i. e. that there is an intrinsic lack of scale, to these speed fluctuations is demonstrated by binning the absolute speeds $|v|$ and counting the number of speeds $p(|v|)$ within each bin. A least squares fit of the log–log plot to a straightline was then made. Plotting $\log[p(|v|)]$ vs $\log|v|$, as shown in Fig. 3 we see that the fit gives $p(v) \propto |v|^{-2.6}$. With the new experiment considerably more data will become available.

7 Observing 3-space vorticity

The vorticity effect in (18) can be studied experimentally in the Gravity Probe B (GP-B) gyroscope satellite experiment in which the precession of four on-board gyroscopes has been measured to unprecedented accuracy [12, 13]. In a generalisation of (1) [1] the vorticity $\nabla \times \mathbf{v}$ is generated by matter in motion through the 3-space, where here $\mathbf{v}_R$ is the absolute velocity of the matter relative to the local 3-space.

$$\nabla \times (\nabla \times \mathbf{v}) = \frac{8\pi G\rho}{c^2}\mathbf{v}_R\,. \tag{27}$$

We then obtain from (27) the vorticity (ignoring homogeneous vortex solutions)

$$\vec{\omega}(\mathbf{r},t) = \frac{2G}{c^2}\int d^3r'\,\frac{\rho(\mathbf{r}',t)}{|\mathbf{r}-\mathbf{r}'|^3}\,\mathbf{v}_R(\mathbf{r}',t)\times(\mathbf{r}-\mathbf{r}')\,. \tag{28}$$

*This velocity arises after removing the effects of the Earth's orbital speed about the Sun, 30 km/s, and the gravitational in-flow past the Earth towards the Sun, 42 km/s, as in (6).

†The opposite direction is not easily excluded due to errors within the data, and so should also be considered as possible. A new experiment will be capable of more accurately determining the speed and direction, as well as the fractal structure of 3-space. The author is constructung a more compact version of the Torr-Kolen - DeWitte coaxial cable RF travel-time experiment. New experimental techniques have been developed to increase atomic-clock based timing accuracy and stability, so that shorter cables can be used, which will permit 3-arm devices.

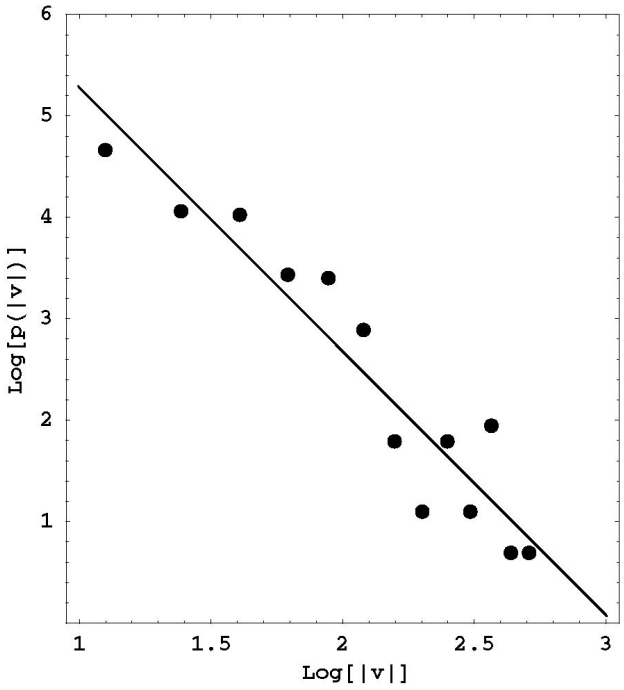

Fig. 3: Shows that the velocity fluctuations in Fig. 2 are scale free, as the probability distribution from binning the speeds has the form $p(v) \propto |v|^{-2.6}$. This plot shows $\log[p(v)]$ vs $\log|v|$. This shows that the velocity field has a fractal structure, and so requiring the generalisation of the Schrödinger equation, as discussed herein, and also the Maxwell and Dirac equations (to be discussed elsewhere).

For the smaller Earth-rotation induced vorticity effect $\mathbf{v}_R(\mathbf{r}) = \mathbf{w} \times \mathbf{r}$ in (28), where $\mathbf{w}$ is the angular velocity of the Earth, giving

$$\vec{\omega}(\mathbf{r})_{\rm rot} = 4\frac{G}{c^2}\frac{3(\mathbf{r}\cdot\mathbf{L})\,\mathbf{r} - r^2\mathbf{L}}{2r^5}, \qquad (29)$$

where $\mathbf{L}$ is the angular momentum of the Earth, and $\mathbf{r}$ is the distance from the centre.

In general the vorticity term in (18) leads to a apparent "torque", according to a distant observer, acting on the angular momentum $\mathbf{S}$ of the gyroscope,

$$\vec{\tau} = \int d^3r\,\rho(\mathbf{r})\;\mathbf{r} \times \left(\vec{\omega}(\mathbf{r}) \times \mathbf{v}_R(\mathbf{r})\right), \qquad (30)$$

where ρ is its density, and where now $\mathbf{v}_R$ is used here to describe the motion of the matter forming the gyroscope relative to the local 3-space. Then $d\mathbf{S} = \vec{\tau}dt$ is the change in $\mathbf{S}$ over the time interval dt. For a gyroscope $\mathbf{v}_R(\mathbf{r}) = \mathbf{s} \times \mathbf{r}$, where $\mathbf{s}$ is the angular velocity of the gyroscope. This gives

$$\vec{\tau} = \frac{1}{2}\,\vec{\omega} \times \mathbf{S} \qquad (31)$$

and so $\vec{\omega}/2$ is the instantaneous angular velocity of precession of the gyroscope. The component of the vorticity in (29) has been determined from the laser-ranged satellites LAGEOS (NASA) and LAGEOS 2 (NASA-ASI) [14], and the data implies the indicated coefficient on the RHS of (27) to $\pm 10\%$. For GP-B the direction of $\mathbf{S}$ has been chosen so that this precession is cumulative and, on averaging over an orbit, corresponds to some 7.7×10^{-6} arcsec per orbit, or 0.042 arcsec per year. GP-B has been superbly engineered so that measurements to a precision of 0.0005 arcsec are possible.

However for the Earth-translation induced precession if we use $v_R = 430\,$km/s (in the direction RA $= 5.2^{\rm hr}$, Dec $= -67^\circ$), (28) gives

$$\vec{\omega}(\mathbf{r})_{\rm trans} = \frac{2GM}{c^2}\frac{\mathbf{v}_R \times \mathbf{r}}{r^3}, \qquad (32)$$

and then the total vorticity is $\vec{\omega} = \vec{\omega}_{\rm rot} + \vec{\omega}_{\rm trans}$. The maximum magnitude of the speed of this precession component is $\omega_{\rm trans}/2 = gv_C/c^2 = 8\times10^{-6}$ arcsec/s, where here g is the usual gravitational acceleration at the altitude of the satellite. This precession has a different signature: it is not cumulative, and is detectable by its variation over each single orbit, as its orbital average is zero, to first approximation.

Essentially then these spin precessions are caused by the rotation of the "wavepackets" describing the matter forming the gyroscopes, and caused in turn by the vorticity of 3-space. The above analysis shows that the rotation is exactly the same as the rotation of the 3-space itself, just as the acceleration of "matter" was exactly the same as the acceleration of the 3-space. We this obtain a much clearer insight into the nature of motion, and which was not possible in the spacetime formalism.

8 Conclusions

We have seen herein that the new theory of 3-space has resulted in a number of fundamental developments, namely that a complex "quantum foam" dynamical 3-space exists and has a fractal "flow" structure, as revealed most clearly by the extraordinary DeWitte coaxial-cable experiment. This fractal structure requires that the fundamental equations of physics be generalised to take account of, for the first time, the physics of this 3-space and, in particular, here the inclusion of that dynamics within the dynamics of quantum systems. We saw that the generalisation of the Schrödinger equation is unique, and that from an Ehrenfest wavepacket analysis we obtained the equivalence principle, with the acceleration of "matter" being shown to be identical to the acceleration of the 3-space; which while not unexpected, is derived here for the first time. This result shows that the equivalence principle is really a quantum-theoretic effect. As well we obtained by that same analysis that any vorticity in the 3-space velocity field will result in a corresponding rotation of wavepackets, and just such an effect is being studied in the GP-B gyroscope experiment. So for the first time we see that the original Schrödinger equation actually lacked a key

dynamical ingredient. We saw that self-consistency within the small-wavepacket approximation imposed restrictions on the dynamical equations that determine the vorticity, giving yet another indication of the close connection between quantum theory and the phenomena of 3-space and gravity. As well because the 3-space is fractal the generalised Schrödinger equation now contains a genuine element of stochasticity.

This research is supported by an Australian Research Council Discovery Grant.

References

1. Cahill R. T. Process physics: from information theory to quantum space and matter. Nova Science Pub., N.Y., 2005.
2. Cahill R. T. Absolute motion and gravitational effects. *Apeiron*, 2004, v. 11, no.1, 53–111.
3. Cahill R. T. The Michelson and Morley 1887 experiment and the discovery of absolute motion. *Progress in Physics*, 2005, v. 3, 25–29; Cahill R. T. and Kitto K. *Apeiron*, 2003, v. 10, no. 2, 104–117.
4. Miller D. C. *Rev. Mod. Phys.*, 1933, v. 5, 203–242.
5. Cahill R. T. "Dark matter" as a quantum foam in-flow effect. *Trends in Dark Matter Research* (ed. by J. Val Blain), Nova Science Pub., N.Y., 2005; Cahill R. T. Gravitation, the "dark matter" effect, and the fine structure constant. *Apeiron*, 2005, v. 12, no.2, 155–177.
6. Cahill R. T. Black holes in elliptical and spiral galaxies and in globular clusters. *Progress in Physics*, 2005, v. 3, 51–56.
7. Cahill R. T. Quantum foam, gravity and gravitational waves. *Relativity, Gravitation, Cosmology*, Nova Science Pub., N.Y., 2004, 168–226.
8. Schrödinger E. *Ann. d. Physik*, 1926, v. 79, 361–376, 489–527, 734–756; *Die Naturwissenschaften*, 1926, v. 14, 664; *Phys. Rev.*, 1926, v. 28, 1049.
9. Ehrenfest P. *Z. Physik*, 1927, v. 45, 455.
10. Lense J. and Thirring H. *Phys. Z.*, 1918, v. 29, 156.
11. Shnoll S. E. *et al*. Experiments with radioactive decay of ^{239}Pu evidence sharp anisotropy of space. *Progress in Physics*, 2005, v. 1, 81–84, and references therein.
12. Cahill R. T. Novel gravity probe B frame-dragging effect. *Progress in Physics*, 2005, v. 3, 30–33.
13. Schiff L. I. *Phys. Rev. Lett.*, 1960, v. 4, 215.
14. Ciufolini I. and Pavlis E. *Nature*, 2004, v. 431, 958–960.

Zelmanov's Anthropic Principle and the Infinite Relativity Principle

Dmitri Rabounski
E-mail: rabounski@yahoo.com

Zelmanov's Anthropic Principle, although introduced in the 1940's, has been published only recently: "The Universe has the interior we observe because we observe the Universe in this way. It is impossible to divorce the Universe from the observer. If the observer is changed, then the observed world will present in some other way, so the Universe observed will also be changed. If no observers exist then the observable Universe as well does not exist." Zelmanov's mathematical apparatus of physical observable quantities employs the Principle to the General Theory of Relativity. Using this apparatus he developed the Infinite Relativity Principle: "In homogeneous isotropic cosmological models spatial infinity of the Universe and infinity of its evolution span depend on our choice of the observer's reference frame."

Abraham Zelmanov (1913–1987), a prominent cosmologist, introduced his Anthropic Principle in the 1940's, but it has been published only recently. It is probable that he reached his ideas not only from his pure mathematical studies on the General Theory of Relativity and relativistic cosmology — besides these he had an excellent knowledge of religious considerations on world-genesis and the origin of humanity. We can now only guess at the way in which he came to his idea of the Anthropic Principle. The fact is that for more than 60 years his Anthropic Principle remained known only a close circle of several of his pupils. His book containing his main fundamental studies on the General Theory of Relativity and relativistic cosmology was written in 1944 and had survived only in manuscript until it has been published in 2004 [1].

Zelmanov stated his Anthropic Principle in two versions. The first version sets forth the law of human evolution dependent upon fundamental physical constants:

> Humanity exists at the present day and we observe world constants completely because the constants bear their specific numerical values at this time. When the world constants bore other values humanity did not exist. When the constants change to other values humanity will disappear. That is, humanity can exist only with the specific scale of the numerical values of the cosmological constants. Humanity is only an episode in the life of the Universe. At the present time cosmological conditions are such that humanity develops.

In the second form he argues that any observer depends on the Universe he observes in the same way that the Universe depends on him:

> The Universe has the interior we observe, because we observe the Universe in this way. It is impossible to divorce the Universe from the observer. The observable Universe depends on the observer and the observer depends on the Universe. If the contemporary physical conditions in the Universe change then the observer is changed. And vice versa, if the observer is changed then he will observe the world in another way. So the Universe he observes will be also changed. If no observers is exist then the observable Universe as well does not exist.

It is probable that by proceeding from his Anthropic Principle, in 1941–1944 Zelmanov solved the well-known problem of physical observable quantities in the General Theory of Relativity [1, 2]. It should be noted, many researchers were working on the theory of observable quantities in the 1940's. For example, Landau and Lifshitz in their famous *The Classical Theory of Fields* [3] introduced observable time and the observable three-dimensional interval similar to those introduced by Zelmanov. But they limited themselves only to this particular case and did not arrive at general mathematical methods to define physical observable quantities in pseudo-Riemannian spaces. It was only Cattaneo, an Italian mathematician, who developed his own approach to the problem, not far removed from Zelmanov's solution. Cattaneo published his results on the theme in 1958 and later [4, 5].

In 1944 Zelmanov completed a complete mathematical apparatus [1, 2] to calculate physical observable quantities in four-dimensional pseudo-Riemannian space, that is the strict solution of that problem. He called the apparatus the *theory of chronometric invariants*. The essence of his theory is that if an observer accompanies his physical reference body, his observable quantities are projections of four-dimensional quantities on his time line and the spatial section — *chronometrically invariant quantities*, made by projecting operators $b^\alpha = \frac{dx^\alpha}{ds}$ and $h_{\alpha\beta} = -g_{\alpha\beta} + b_\alpha b_\beta$ which fully define his real reference space (here b^α is his velocity with respect to his real references). Thus, the chr.inv.-projections of a world-vector Q^α are $b_\alpha Q^\alpha = \frac{Q_0}{\sqrt{g_{00}}}$ and $h^i_\alpha Q^\alpha = Q^i$, while chr.inv.-projections of a world-tensor of the 2nd rank $Q^{\alpha\beta}$

are $b^{\alpha}b^{\beta}Q_{\alpha\beta}=\frac{Q_{00}}{g_{00}}$, $h^{i\alpha}b^{\beta}Q_{\alpha\beta}=\frac{Q^{i}_{0}}{\sqrt{g_{00}}}$, $h^{i}_{\alpha}h^{k}_{\beta}Q^{\alpha\beta}=Q^{ik}$. Physically observable properties of the space are derived from the fact that chr.inv.-differential operators $\frac{{}^{*}\partial}{\partial t}=\frac{1}{\sqrt{g_{00}}}\frac{\partial}{\partial t}$ and $\frac{{}^{*}\partial}{\partial x^{i}}=\frac{\partial}{\partial x^{i}}+\frac{1}{c^{2}}v_{i}\frac{{}^{*}\partial}{\partial t}$ are non-commutative $\frac{{}^{*}\partial^{2}}{\partial x^{i}\partial t}-\frac{{}^{*}\partial^{2}}{\partial t\,\partial x^{i}}=\frac{1}{c^{2}}F_{i}\frac{{}^{*}\partial}{\partial t}$ and $\frac{{}^{*}\partial^{2}}{\partial x^{i}\partial x^{k}}-\frac{{}^{*}\partial^{2}}{\partial x^{k}\partial x^{i}}=\frac{2}{c^{2}}A_{ik}\frac{{}^{*}\partial}{\partial t}$, and also from the fact that the chr.inv.-metric tensor h_{ik} may not be stationary. The observable characteristics are the chr.inv.-vector of gravitational inertial force F_{i}, the chr.inv.-tensor of angular velocities of the space rotation A_{ik}, and the chr.inv.-tensor of rates of the space deformations D_{ik}, namely

$$F_{i}=\frac{1}{\sqrt{g_{00}}}\left(\frac{\partial \mathrm{w}}{\partial x^{i}}-\frac{\partial v_{i}}{\partial t}\right),\quad \sqrt{g_{00}}=1-\frac{\mathrm{w}}{c^{2}}$$

$$A_{ik}=\frac{1}{2}\left(\frac{\partial v_{k}}{\partial x^{i}}-\frac{\partial v_{i}}{\partial x^{k}}\right)+\frac{1}{2c^{2}}\left(F_{i}v_{k}-F_{k}v_{i}\right),$$

$$D_{ik}=\frac{1}{2}\frac{{}^{*}\partial h_{ik}}{\partial t},\quad D^{ik}=-\frac{1}{2}\frac{{}^{*}\partial h^{ik}}{\partial t},\quad D^{k}_{k}=\frac{{}^{*}\partial \ln\sqrt{h}}{\partial t},$$

where w is gravitational potential, $v_{i}=-c\frac{g_{0i}}{\sqrt{g_{00}}}$ is the linear velocity of the space rotation, $h_{ik}=-g_{ik}+\frac{1}{c^{2}}v_{i}v_{k}$ is the chr.inv.-metric tensor, and also $h=\det\|h_{ik}\|$, $h\,g_{00}=-g$, $g=\det\|g_{\alpha\beta}\|$. Observable inhomogeneity of the space is set up by the chr.inv.-Christoffel symbols $\Delta^{i}_{jk}=h^{im}\Delta_{jk,m}$, which are built just like Christoffel's usual symbols $\Gamma^{\alpha}_{\mu\nu}=g^{\alpha\sigma}\Gamma_{\mu\nu,\sigma}$ using h_{ik} instead of $g_{\alpha\beta}$.

A four-dimensional generalization of the main chr.inv.-quantities F_{i}, A_{ik}, and D_{ik} (by Zelmanov, the 1960's [10]) is: $F_{\alpha}=-2c^{2}b^{\beta}a_{\beta\alpha}$, $A_{\alpha\beta}=ch^{\mu}_{\alpha}h^{\nu}_{\beta}a_{\mu\nu}$, $D_{\alpha\beta}=ch^{\mu}_{\alpha}h^{\nu}_{\beta}d_{\mu\nu}$, where $a_{\alpha\beta}=\frac{1}{2}\left(\nabla_{\alpha}b_{\beta}-\nabla_{\beta}b_{\alpha}\right)$, $d_{\alpha\beta}=\frac{1}{2}\left(\nabla_{\alpha}b_{\beta}+\nabla_{\beta}b_{\alpha}\right)$.

In this way, for any equations obtained using general covariant methods, we can calculate their physically observable projections on the time line and the spatial section of any particular reference body and formulate the projections in terms of their real physically observable properties, from which we obtain equations containing only quantities measurable in practice.

Zelmanov deduced chr.inv.-formulae for the space curvature [1]. He followed that procedure by which the Riemann-Christoffel tensor was built: proceeding from the non-commutativity of the second derivatives of an arbitrary vector ${}^{*}\nabla_{i}{}^{*}\nabla_{k}Q_{l}-{}^{*}\nabla_{k}{}^{*}\nabla_{i}Q_{l}=\frac{2A_{ik}}{c^{2}}\frac{{}^{*}\partial Q_{l}}{\partial t}+H^{\cdots j}_{lki\cdot}Q_{j}$, he obtained the chr.inv.-tensor $H^{\cdots j}_{lki\cdot}=\frac{{}^{*}\partial\Delta^{j}_{il}}{\partial x^{k}}-\frac{{}^{*}\partial\Delta^{j}_{kl}}{\partial x^{i}}+\Delta^{m}_{il}\Delta^{j}_{km}-\Delta^{m}_{kl}\Delta^{j}_{im}$, which is similar to Schouten's tensor from the theory of non-holonomic manifolds. The tensor $H^{\cdots j}_{lki}$ differs algebraically from the Riemann-Christoffel tensor because of the presence of the space rotation A_{ik} in the formula. Nevertheless its generalization gives the chr.inv.-tensor

$$C_{lkij}=\frac{1}{4}\left(H_{lkij}-H_{jkil}+H_{klji}-H_{iljk}\right),$$

which possesses all the algebraic properties of the Riemann-Christoffel tensor in this three-dimensional space and, at the same time, the property of chronometric invariance. Therefore Zelmanov called C_{iklj} the *chr.inv.-curvature tensor* as the tensor of the observable curvature of the observer's spatial section. Its contraction step-by-step

$$C_{kj}=C^{\cdots i}_{kij\cdot}=h^{im}C_{kimj},\qquad C=C^{j}_{j}=h^{lj}C_{lj}$$

gives the chr.inv.-scalar C, which is the *observable three-dimensional curvature* of this space.

Chr.inv.-projections of the Riemann-Christoffel tensor are [1]: $X^{ik}=-c^{2}\frac{R^{\cdot i\cdot k}_{0\cdot 0\cdot}}{g_{00}}$, $Y^{ijk}=-c\frac{R^{\cdot ijk}_{0\cdots}}{\sqrt{g_{00}}}$, $Z^{ijkl}=c^{2}R^{ijkl}$.

Solving Einstein's equations with this mathematical apparatus, Zelmanov obtained the total system of all cosmological models (senarios of the Universe's evolution) which could be possible as derived from the equations [1, 6]. In particular, he had arrived at the possibility that infinitude may be relative. Later, in the 1950's, he enunciated the *Infinite Relativity Principle*:

> In homogeneous isotropic cosmological models spatial infinity of the Universe depends on our choice of that reference frame from which we observe the Universe (the observer's reference frame). If the three-dimensional space of the Universe, being observed in one reference frame, is infinite, it may be finite in another reference frame. The same is just as well true for the time during which the Universe evolves.

In other words, using purely mathematical methods of the General Theory of Relativity, Zelmanov showed that any observer forms his world-picture from a comparison between his observation results and some standards he has in his laboratory — the standards of different objects and their physical properties. So the "world" we see as a result of our observations depends directly on that set of physical standards we have, so the "visible world" depends directly on our considerations about some objects and phenomena.

The mathematical apparatus of physical observable quantities and those results it gave in relativistic cosmology were the first results of Zelmanov's application of his Anthropic Principle to the General Theory of Relativity. To obtain the results with general covariant methods (standard in the General Theory of Relativity), where observation results do not depend on the observer's reference properties, would be impossible.

Now, according to the wishes of those who knew Zelmanov closely, I would like to say a few good words in memory of him.

Abraham Leonidovich Zelmanov was born in May 15, 1913 in Poltava Gubernya of the Russian Empire. His father

was a Judaic religious scientist, a specialist in comments on Torah and Kabbalah. In 1937 Zelmanov completed his education at the Mechanical Mathematical Department of Moscow University. After 1937 he was a research-student at the Sternberg Astronomical Institute in Moscow, where he presented his dissertation in 1944. In 1953 he was arrested for "cosmopolitism" within the framework of Stalin's campaign against Jews, however as soon as Stalin had died Zelmanov was set free after some months of in gaol. For several decades Zelmanov and his paralyzed parents lived in a room in a shared flat with neighbours. He took everyday care of his parents, so they lived into old age. Only in the 1970's did he obtain a personal municipal flat. He was married three times. Zelmanov worked on the academic staff of the Sternberg Astronomical Institute all life, until his death on the winter's day, the 2nd of February, 1987.

Abraham Zelmanov, 1940's

He was very thin in physique, like an Indian yogi, rather shorter than average, and a very delicate man. From his appearance it was possible to think that his life and thoughts were rather ordinary or uninteresting. However, in acquaintance with him and his scientific discussions in friendly company one formed another opinion about him. Those were discussions with a great scientist and humanist who reasoned in a very unorthodox way. Sometimes we thought that we were not speaking with a contemporary scientist of the 20th century, but some famous philosopher from Classical Greece or the Middle Ages. So the themes of those discussions are eternal — the interior of the Universe, what is the place of a human in the Universe, what are space and time.

Zelmanov liked to remark that he preferred to make mathematical "instruments" more than to use them in practice. Perhaps thereby his main goal in science was the mathematical apparatus of physical observable quantities in the General Theory of Relativity known as the *theory of chronometric invariants* [1, 2]. In developing the apparatus he also created other mathematical methods, namely — *kinemetric invariants* [9] and *monad formalism* [10]. Being very demanding of himself, Zelmanov published less than a dozen scientific articles during his life (see References), so every publication is a concentrate of his fundamental scientific ideas.

Most of his time was spent in scientific work, but he sometimes gave lectures on the General Theory of Relativity and relativistic cosmology as a science for the geometrical structure of the Universe. Stephen Hawking, a young scientist in the 1960's, attended Zelmanov's seminars on cosmology at the Sternberg Astronomical Institute in Moscow. Zelmanov presented him as a "promising young cosmologist". Hawking read a brief report at one of those seminars.

Because Zelmanov made scientific creation the main goal of his life writing articles was a waste of time to him. However he never regreted time spent on long discussions in friendly company, where he set forth his philosophic concepts on the geometrical structure of the Universe and the ways of human evolution. In those discussions he formulated his famous Anthropic Principle and the Infinite Relativity Principle.

Now everyone may read it. I hope that Zelmanov's classical works on the General Theory of Relativity and cosmology, in particular his Anthropic Principle and the Infinite Relativity Principle known to a very close circle of his pupils, will become more widely known and appreciated.

References

1. Zelmanov A. L. Chronometric invariants. Dissertation, 1944. First published: CERN, EXT-2004-117, 236 pages.
2. Zelmanov A. L. Chronometric invariants and co-moving coordinates in the general relativity theory. *Doklady Acad. Nauk USSR*, 1956, v. 107 (6), 815–818.
3. Landau L. D. and Lifshitz E. M. The classical theory of fields. GITTL, Moscow, 1939 (ref. with the 4th final exp. edition, Butterworth–Heinemann, 1980).
4. Cattaneo C. General Relativity: Relative standard mass, momentum, energy, and gravitational field in a general system of reference. *Il Nuovo Cimento*, 1958, v. 10 (2), 318–337.
5. Cattaneo C. Problèmes d'interprétation en Relativité Générale. *Colloques Internationaux du Centre National de la Recherche Scientifique*, No. 170 "Fluides et champ gravitationel en Relativité Générale", Éditions du Centre National de la Recherche Scientifique, Paris, 1969, 227–235.
6. Zelmanov A. L. To relativistic theory of anisotropic inhomogeneous Universe. *Proceedings of the 6th Soviet Conference on Cosmogony*, Nauka, Moscow, 1959, 144–174 (*in Russian*).
7. Zelmanov A. L. To statement of the problem of the infinity of space in the general relativity theory. *Doklady Acad. Nauk USSR*, 1959, v. 124 (5), 1030–1034.
8. Zelmanov A. L. To problem of the deformation of the co-moving space in Einstein's theory of gravitation. *Doklady Acad. Nauk USSR*, 1960, v. 135 (6), 1367–1370.
9. Zelmanov A. L. Kinemetric invariants and their relation to chronometric invariants in Einstein's theory of gravitation. *Doklady Acad. Nauk USSR*, 1973, v. 209 (4), 822–825.
10. Zelmanov A. L. Orthometric form of monad formalism and its relations to chronometric and kinemetric invariants. *Doklady Acad. Nauk USSR*, 1976, v. 227 (1), 78–81.
11. Zelmanov A. L. and Khabibov Z. R. Chronometrically invariant variations in Einstein's gravitation theory. *Doklady Acad. Nauk USSR*, 1982, v. 268 (6), 1378–1381.
12. Zelmanov A. L. and Agakov V. G. Elements of the General Theory of Relativity. Nauka, Moscow, 1989 (*in Russian*).

On Nonlinear Quantum Mechanics, Brownian Motion, Weyl Geometry and Fisher Information

Carlos Castro* and Jorge Mahecha†

*Center for Theoretical Studies of Physical Systems, Clark Atlanta University, Atlanta, Georgia, USA
†Institute of Physics, University of Antioquia, Medellín, Colombia

*E-mail: czarlosromanov@yahoo.com; castro@ctsps.cau.edu †E-mail: mahecha@fisica.udea.edu.co

A new nonlinear Schrödinger equation is obtained explicitly from the (fractal) Brownian motion of a massive particle with a complex-valued diffusion constant. Real-valued energy plane-wave solutions and solitons exist in the free particle case. One remarkable feature of this nonlinear Schrödinger equation based on a (fractal) Brownian motion model, over all the other nonlinear QM models, is that the quantum-mechanical energy functional coincides precisely with the field theory one. We finalize by showing why a *complex* momentum is essential to fully understand the physical implications of Weyl's geometry in QM, along with the interplay between Bohm's Quantum potential and Fisher Information which has been overlooked by several authors in the past.

1 Introduction

Over the years there has been a considerable debate as to whether linear QM can fully describe Quantum Chaos. Despite that the quantum counterparts of classical chaotic systems have been studied via the techniques of linear QM, it is our opinion that Quantum Chaos is truly a new paradigm in physics which is associated with non-unitary and nonlinear QM processes based on non-Hermitian operators (implementing time symmetry breaking). This Quantum Chaotic behavior should be linked more directly to the Nonlinear Schrödinger equation without any reference to the nonlinear behavior of the classical limit. For this reason, we will analyze in detail the fractal geometrical features underlying our Nonlinear Schrödinger equation obtained in [6].

Nonlinear QM has a practical importance in different fields, like condensed matter, quantum optics and atomic and molecular physics; even quantum gravity may involve nonlinear QM. Another important example is in the modern field of quantum computing. If quantum states exhibit small nonlinearities during their temporal evolution, then quantum computers can be used to solve NP-complete (non polynomial) and #P problems in polynomial time. Abrams and Lloyd [19] proposed logical gates based on non linear Schrödinger equations and suggested that a further step in quantum computing consists in finding physical systems whose evolution is amenable to be described by a NLSE.

On other hand, we consider that Nottale and Ord's formulation of quantum mechanics [1], [2] from first principles based on the combination of scale relativity and fractal spacetime is a very promising field of future research. In this work we extend Nottale and Ord's ideas to derive the nonlinear Schrödinger equation. This could shed some light on the physical systems which could be appropriately described by the nonlinear Schrödinger equation derived in what follows.

The contents of this work are the following: In section 2 we derive the nonlinear Schrödinger equation by extending Nottale-Ord's approach to the case of a fractal Brownian motion with a complex diffusion constant. We present a thorough analysis of such nonlinear Schrödinger equation and show why it cannot linearized by a naive complex scaling of the wavefunction $\psi \to \psi^{\lambda}$.

Afterwards we will describe the explicit interplay between Fisher Information, Weyl geometry and the Bohm's potential by introducing an action based on a *complex* momentum. The connection between Fisher Information and Bohm's potential has been studied by several authors [24], however the importance of introducing a *complex* momentum $P_k = p_k + iA_k$ (where A_k is the Weyl gauge field of dilatations) in order to fully understand the physical implications of Weyl's geometry in QM, along with the interplay between Bohm's quantum potential and Fisher Information, has been overlooked by several authors in the past [24], [25]. For this reason we shall review in section 3 the relationship between Bohm's Quantum Potential and the Weyl curvature scalar of the Statistical ensemble of particle-paths (an Abelian fluid) associated to a single particle that was initially developed by [22]. A Weyl geometric formulation of the Dirac equation and the nonlinear Klein-Gordon wave equation was provided by one of us [23]. In the final section 4, we summarize our conclusions and include some additional comments.

2 Nonlinear QM as a fractal Brownian motion with a complex diffusion constant

We will be following very closely Nottale's derivation of the ordinary Scrödinger equation [1]. Recently Nottale and

Celerier [1] following similar methods were able to derive the Dirac equation using bi-quaternions and after breaking the parity symmetry $dx^\mu \leftrightarrow -dx^\mu$, see references for details. Also see the Ord's paper [2] and the Adlers's book on quaternionic QM [16]. For simplicity the one-particle case is investigated, but the derivation can be extended to many-particle systems. In this approach particles do not follow smooth trajectories but fractal ones, that can be described by a continuous but non-differentiable fractal function $\vec{r}(t)$. The time variable is divided into infinitesimal intervals dt which can be taken as a given scale of the resolution.

Then, following the definitions given by Nelson in his stochastic QM approach (Lemos in [12] p. 615; see also [13, 14]), Nottale define mean backward an forward derivatives

$$\frac{d_\pm \vec{r}(t)}{dt} = \lim_{\Delta t \to \pm 0} \left\langle \frac{\vec{r}(t+\Delta t) - \vec{r}(t)}{\Delta t} \right\rangle , \qquad (1)$$

from which the forward and backward mean velocities are obtained,

$$\frac{d_\pm \vec{r}(t)}{dt} = \vec{b}_\pm \, . \qquad (2)$$

For his deduction of Schrödinger equation from this fractal space-time classical mechanics, Nottale starts by defining the complex-time derivative operator

$$\frac{\delta}{dt} = \frac{1}{2}\left(\frac{d_+}{dt} + \frac{d_-}{dt}\right) - i\,\frac{1}{2}\left(\frac{d_+}{dt} - \frac{d_-}{dt}\right) , \qquad (3)$$

which after some straightforward definitions and transformations takes the following form,

$$\frac{\delta}{dt} = \frac{\partial}{\partial t} + \vec{V}\cdot\vec{\nabla} - iD\nabla^2 , \qquad (4)$$

D is a real-valued diffusion constant to be related to the Planck constant.

The D comes from considering that the scale dependent part of the velocity is a Gaussian stochastic variable with zero mean, (see de la Peña at [12] p. 428)

$$\langle d\xi_{\pm i}\, d\xi_{\pm j}\rangle = \pm 2D\delta_{ij}dt \, . \qquad (5)$$

In other words, the fractal part of the velocity $\vec{\xi}$, proportional to the $\vec{\zeta}$, amount to a Wiener process when the fractal dimension is 2.

Afterwards, Nottale defines a set of complex quantities which are generalization of well known classical quantities (Lagrange action, velocity, momentum, etc), in order to be coherent with the introduction of the complex-time derivative operator. The complex time dependent wave function ψ is expressed in terms of a Lagrange action S by $\psi = e^{iS/(2mD)}$. S is a complex-valued action but D is real-valued. The velocity is related to the momentum, which can be expressed as the gradient of S, $\vec{p} = \vec{\nabla}S$. Then the following known relation is found,

$$\vec{V} = -2iD\vec{\nabla}\ln\psi \, . \qquad (6)$$

The Schrödinger equation is obtained from the Newton's equation (force = mass times acceleration) by using the expression of $\vec{V}$ in terms of the wave function ψ,

$$-\vec{\nabla}U = m\frac{\delta}{dt}\vec{V} = -2imD\frac{\delta}{dt}\vec{\nabla}\ln\psi \, . \qquad (7)$$

Replacing the complex-time derivation (4) in the Newton's equation gives us

$$-\vec{\nabla}U = -2im\left(D\frac{\partial}{\partial t}\vec{\nabla}\ln\psi\right) - 2D\vec{\nabla}\left(D\frac{\nabla^2\psi}{\psi}\right) . \qquad (8)$$

Simple identities involving the $\vec{\nabla}$ operator were used by Nottale. Integrating this equation with respect to the position variables finally yields

$$D^2\nabla^2\psi + iD\frac{\partial\psi}{\partial t} - \frac{U}{2m}\psi = 0 \, , \qquad (9)$$

up to an arbitrary phase factor which may set to zero. Now replacing D by $\hbar/(2m)$, we get the Schrödinger equation,

$$i\hbar\frac{\partial\psi}{\partial t} + \frac{\hbar^2}{2m}\nabla^2\psi = U\psi \, . \qquad (10)$$

The Hamiltonian operator is Hermitian, this equation is linear and clearly is homogeneous of degree one under the substitution $\psi \to \lambda\psi$.

Having reviewed Nottale's work [1] we can generalize it by relaxing the assumption that the diffusion constant is real; we will be working with a complex-valued diffusion constant; i. e. with a complex-valued $\hbar$. This is our new contribution. The reader may be immediately biased against such approach because the Hamiltonian ceases to be Hermitian and the energy becomes complex-valued. However this is not always the case. We will explicitly find plane wave solutions and soliton solutions to the nonlinear and non-Hermitian wave equations with real energies and momenta. For a detailed discussion on complex-valued spectral representations in the formulation of quantum chaos and time-symmetry breaking see [10]. Nottale's derivation of the Schrödinger equation in the previous section required a complex-valued action S stemming from the complex-valued velocities due to the breakdown of symmetry between the forwards and backwards velocities in the fractal zigzagging. If the action S was complex then it is not farfetched to have a complex diffusion constant and consequently a complex-valued $\hbar$ (with same units as the complex-valued action).

Complex energy is not alien in ordinary linear QM. They appear in optical potentials (complex) usually invoked to model the absorption in scattering processes [8] and decay of unstable particles. Complex potentials have also been used to describe decoherence. The accepted way to describe resonant states in atomic and molecular physics is based on the complex scaling approach, which in a natural way deals with complex energies [17]. Before, Nottale wrote,

$$\langle d\zeta_\pm\, d\zeta_\pm\rangle = \pm 2Ddt \, , \qquad (11)$$

with D and $2mD = \hbar$ real. Now we set

$$\langle d\zeta_{\pm}\, d\zeta_{\pm}\rangle = \pm(D + D^*)\, dt\,, \tag{12}$$

with D and $2mD = \hbar = \alpha + i\beta$ complex. The complex-time derivative operator becomes now

$$\frac{\delta}{dt} = \frac{\partial}{\partial t} + \vec{V}\cdot\vec{\nabla} - \frac{i}{2}\,(D + D^*)\,\nabla^2. \tag{13}$$

In the real case $D = D^*$. It reduces to the complex-time-derivative operator described previously by Nottale. Writing again the ψ in terms of the complex action S,

$$\psi = e^{iS/(2mD)} = e^{iS/\hbar}, \tag{14}$$

where S, D and $\hbar$ are complex-valued, the complex velocity is obtained from the complex momentum $\vec{p} = \vec{\nabla} S$ as

$$\vec{V} = -2iD\vec{\nabla}\ln\psi\,. \tag{15}$$

The NLSE (non-linear Schröedinger equation) is obtained after we use the generalized Newton's equation (force = mass times acceleration) in terms of the ψ variable,

$$-\vec{\nabla}U = m\,\frac{\delta}{dt}\,\vec{V} = -2imD\frac{\delta}{dt}\vec{\nabla}\ln\psi\,. \tag{16}$$

Replacing the complex-time derivation (13) in the generalized Newton's equation gives us

$$\begin{aligned}\vec{\nabla}U = 2im\Big[D\frac{\partial}{\partial t}\vec{\nabla}\ln\psi - 2iD^2(\vec{\nabla}\ln\psi\cdot\vec{\nabla})\times \\ \times(\vec{\nabla}\ln\psi) - \frac{i}{2}\,(D + D^*)\,D\,\nabla^2(\vec{\nabla}\ln\psi)\Big].\end{aligned} \tag{17}$$

Now, using the next three identities: (i) $\vec{\nabla}\nabla^2 = \nabla^2\vec{\nabla}$; (ii) $2\,(\vec{\nabla}\ln\psi\cdot\vec{\nabla})(\vec{\nabla}\ln\psi) = \vec{\nabla}(\vec{\nabla}\ln\psi)^2$; and (iii) $\nabla^2\ln\psi = \nabla^2\psi/\psi - (\vec{\nabla}\ln\psi)^2$ allows us to integrate such equation above yielding, after some straightforward algebra, the NLSE

$$i\hbar\frac{\partial\psi}{\partial t} = -\frac{\hbar^2}{2m}\,\frac{\alpha}{\hbar}\,\nabla^2\psi + U\psi - i\,\frac{\hbar^2}{2m}\,\frac{\beta}{\hbar}\big(\vec{\nabla}\ln\psi\big)^2\psi\,. \tag{18}$$

Note the crucial minus sign in front of the kinematic pressure term and that $\hbar = \alpha + i\beta = 2mD$ is complex. When $\beta = 0$ we recover the linear Schrödinger equation.

The nonlinear potential is now complex-valued in general. Defining

$$W = W(\psi) = -\frac{\hbar^2}{2m}\,\frac{\beta}{\hbar}\,\big(\vec{\nabla}\ln\psi\big)^2, \tag{19}$$

and U the ordinary potential, we rewrite the NLSE as

$$i\hbar\frac{\partial\psi}{\partial t} = \left(-\frac{\hbar^2}{2m}\,\frac{\alpha}{\hbar}\,\nabla^2 + U + iW\right)\psi\,. \tag{20}$$

This is the fundamental nonlinear wave equation of this work. It has the form of the ordinary Schrödinger equation with the complex potential $U + iW$ and the complex $\hbar$. The Hamiltonian is no longer Hermitian and the potential $V = U + iW(\psi)$ itself depends on ψ. Nevertheless one could have meaningful physical solutions with real valued energies and momenta, like the plane-wave and soliton solutions studied in the next section. Here are some important remarks.

• Notice that the NLSE above *cannot* be obtained by a *naive* scaling of the wavefunction

$$\begin{aligned}\psi = e^{iS/\hbar_0} \to \psi' = e^{iS/\hbar} = e^{(iS/\hbar_0)(\hbar_0/\hbar)} = \\ = \psi^{\lambda} = \psi^{\hbar_0/\hbar}, \qquad \hbar = \text{real}\end{aligned} \tag{21}$$

related to a scaling of the diffusion constant $\hbar_0 = 2mD_0 \to \hbar = 2mD$. Upon performing such scaling, the ordinary *linear* Schrödinger equation in the variable ψ will appear to be *nonlinear* in the new scaled wavefunction ψ'

$$\begin{aligned}i\hbar\frac{\partial\psi'}{\partial t} = -\frac{\hbar^2}{2m}\,\frac{\hbar_0}{\hbar}\,\nabla^2\psi' + U\psi' - \\ -\frac{\hbar^2}{2m}\Big(1-\frac{\hbar_0}{\hbar}\Big)\Big(\vec{\nabla}\ln\psi'\Big)^2\psi',\end{aligned} \tag{22}$$

but this apparent nonlinearity is only an *artifact* of the change of variables (the scaling of ψ).

Notice that the latter (apparent) nonlinear equation, despite having the same form as the NLSE, obtained from a complex-diffusion constant, differs *crucially* in the actual values of the coefficients multiplying each of the terms. The NLSE has the complex coefficients $\alpha/\hbar$ (in the kinetic terms), and $-i\beta/\hbar$ (in the nonlinear logarithmic terms) with $\hbar = \alpha + i\beta =$ complex. However, the nonlinear equation obtained from a naive scaling involves *real* and *different* numerical coefficients than those present in the NLSE. Therefore, the genuine NLSE *cannot* be obtained by a naive scaling (redefinition) of the ψ and the diffusion constant.

Notice also that even if one scaled ψ by a complex exponent $\psi \to \psi^{\lambda}$ with $\lambda = \hbar_0/\hbar$ and $\hbar =$ complex, the actual numerical values in the apparent nonlinear equation, in general, would have still been different than those present in the NLSE. However, there is an actual equivalence, if, and only if, the scaling exponent $\lambda = \hbar_0/\hbar$ obeyed the condition:

$$\alpha = \hbar_0 \;\Rightarrow 1 - \frac{\hbar_0}{\hbar} = 1 - \frac{\alpha}{\hbar} = 1 - \frac{\hbar - i\beta}{\hbar} = i\,\frac{\beta}{\hbar} \tag{23}$$

in this very special case, the NLSE would be obtained from a linear Schrödinger equation after scaling the wavefunction $\psi \to \psi^{\lambda}$ with a complex exponent $\lambda = \hbar_0/\hbar = \alpha/\hbar$. In this very special and restricted case, the NLSE could be *linearized* by a scaling of the wavefunction with complex exponent.

From this analysis one infers, immediately, that if one defines the norm of the complex $\hbar$: $\|\hbar\| = \sqrt{\alpha^2 + \beta^2} = \hbar_0$ to coincide precisely with the observed value $\hbar_0$ of Planck's constant, then $\alpha \neq \hbar_0$, $i\beta \neq \hbar - \hbar_0$ and, consequently, the

NLSE *cannot* be obtained from the ordinary (linear) Schrödinger equations after a naive scaling, with a complex exponent, $\psi \to \psi^{\lambda} = \psi^{\hbar_0/\hbar}$. Therefore, a complex diffusion constant $2mD = \hbar = \alpha + i\beta$, with the condition $2m\|D\| = \|\hbar\| = \sqrt{\alpha^2+\beta^2} = \hbar_0$ (observed value of Planck's constant) ensures that the NLSE is not a mere artifact of the scaling of the wavefunction $\psi \to \psi^{\lambda} = \psi^{\hbar_0/\hbar}$ in the ordinary linear Schrödinger equation.

It is important to emphasize that the diffusion constant is always chosen to be related to Planck constant as follows: $2m\|D\| = \|\hbar\| = \hbar_0$ which is just the transition length from a fractal to a scale-independence non-fractal regime discussed by Nottale in numerous occasions. In the relativistic scale it is the Compton wavelength of the particle (say an electron): $\lambda_c = \hbar_0/(mc)$. In the nonrelativistic case it is the de Broglie wavelength of the electron.

Therefore, the NLSE based on a fractal Brownian motion with a complex valued diffusion constant $2mD = \hbar = \alpha + i\beta$ represents truly a new physical phenomenon and a hallmark of nonlinearity in QM. For other generalizations of QM see experimental tests of quaternionic QM (in the book by Adler [16]). Equation (18) is the fundamental NLSE of this work.

• A Fractal Scale Calculus description of our NLSE was developed later on by Cresson [20] who obtained, on a rigorous mathematical footing, the same functional form of our NLSE equation above (although with different complex numerical coefficients) by using Nottale's fractal scale-calculus that obeyed a quantum bialgebra. A review of our NLSE was also given later on by [25]. Our nonlinear wave equation originated from a complex-valued diffusion constant that is related to a complex-valued extension of Planck's constant. Hence, a fractal spacetime is deeply ingrained with *nonlinear* wave equations as we have shown and it was later corroborated by Cresson [20].

• Complex-valued viscosity solutions to the Navier-Stokes equations were also analyzed by Nottale leading to the Fokker-Planck equation. Clifford-valued extensions of QM were studied in [21] C-spaces (Clifford-spaces whose enlarged coordinates are polyvectors, i. e. antisymmetric tensors) that involved a Clifford-valued number extension of Planck's constant; i. e. the Planck constant was a hypercomplex number. Modified dispersion relations were derived from the underlying QM in Clifford-spaces that lead to faster than light propagation in ordinary spacetime but without violating causality in the more fundamental Clifford spaces. Therefore, one should not exclude the possibility of having complex-extensions of the Planck constant leading to nonlinear wave equations associated with the Brownian motion of a particle in fractal spacetimes.

• Notice that the NLSE (34) obeys the homogeneity condition $\psi \to \lambda\psi$ for any constant λ. All the terms in the NLSE are scaled respectively by a factor λ. Moreover, our two parameters α, β are intrinsically connected to a complex Planck constant $\hbar = \alpha + i\beta$ such that $\|\hbar\| = \sqrt{\alpha^2+\beta^2} = \hbar_0$ (observed Planck's constant) rather that being *ah-hoc* constants to be determined experimentally. Thus, the nonlinear QM equation derived from the fractal Brownian motion with complex-valued diffusion coefficient is intrinsically tied up with a non-Hermitian Hamiltonian and with complex-valued energy spectra [10].

• Despite having a non-Hermitian Hamiltonian we still could have eigenfunctions with real valued energies and momenta. Non-Hermitian Hamiltonians (pseudo-Hermitian) have captured a lot of interest lately in the so-called PT symmetric *complex* extensions of QM and QFT [27]. Therefore these ideas cannot be ruled out and they are the subject of active investigation nowadays.

3 Complex momenta, Weyl geometry, Bohm's potential and Fisher information

Despite that the interplay between Fisher Information and Bohm's potential has been studied by several authors [24] the importance of introducing a *complex* momentum $P_k = p_k + iA_k$ in order to fully understand the physical implications of Weyl's geometry in QM has been overlooked by several authors [24], [25]. We shall begin by reviewing the relationship between the Bohm's Quantum Potential and the Weyl curvature scalar of the Statistical ensemble of particle-paths (a fluid) associated to a single particle and that was developed by [22]. A Weyl geometric formulation of the Dirac equation and the nonlinear Klein-Gordon wave equation was provided by one of us [23]. Afterwards we will describe the interplay between Fisher Information and the Bohm's potential by introducing an action based on a *complex* momentum $P_k = p_k + iA_k$.

In the description of [22] one deals with a geometric derivation of the nonrelativistic Schrödinger Equation by relating the Bohm's quantum potential Q to the Ricci-Weyl scalar curvature of an ensemble of particle-paths associated to *one* particle. A quantum mechanical description of many particles is far more complex. This ensemble of particle paths resemble an Abelian *fluid* that permeates spacetime and whose ensemble density ρ affects the Weyl curvature of spacetime, which in turn, determines the geodesics of spacetime in guiding the particle trajectories. See [22], [23] for details.

Again a relation between the *relativistic* version of Bohm's potential Q and the Weyl-Ricci curvature exists but without the ordinary nonrelativistic probabilistic connections. In relativistic QM one does not speak of probability density to find a particle in a given spacetime point but instead one refers to the particle number current $J^{\mu} = \rho dx^{\mu}/d\tau$. In [22], [23] one begins with an ordinary Lagrangian associated with a point particle and whose statistical ensemble average over all particle-paths is performed only over the random initial data (configurations). Once the initial data is specified the trajectories (or rays) are completely determined by the

Hamilton-Jacobi equations. The statistical average over the random initial Cauchy data is performed by means of the ensemble density ρ. It is then shown that the Schrödinger equation can be derived after using the Hamilton-Jacobi equation in conjunction with the continuity equation and where the "quantum force" arising from Bohm's quantum potential Q can be related to (or described by) the Weyl geometric properties of space. To achieve this one defines the Lagrangian

$$L(q,\dot{q},t) = L_C(q,\dot{q},t) + \gamma(\hbar^2/m)\,R(q,t)\,, \qquad (24)$$

where $\gamma = (1/6)(d-2)/(d-1)$ is a dimension-dependent numerical coefficient and R is the Weyl scalar curvature of the corresponding d-dimensional Weyl spacetime M where the particle lives.

Covariant derivatives are defined for contravariant vectors V^k: $V^k_{;\beta} = \partial_i V^k - \Gamma^k_{im} V^m$ where the Weyl connection coefficients are composed of the ordinary Christoffel connection plus terms involving the Weyl gauge field of dilatations A_i. The curvature tensor R^i_{mkn} obeys the same symmetry relations as the curvature tensor of Riemann geometry as well as the Bianchi identity. The Ricci symmetric tensor R_{ik} and the scalar curvature R are defined by the same formulas also, viz. $R_{ik} = R^n_{ink}$ and $R = g^{ik}R_{ik}$

$$R_{\text{Weyl}} = R_{\text{Riemann}} + \\ + (d-1)\left[(d-2)\,A_i\,A^i - \frac{2}{\sqrt{g}}\,\partial_i(\sqrt{g}A^i)\right], \qquad (25)$$

where R_{Riemann} is the ordinary Riemannian curvature defined in terms of the Christoffel symbols without the Weyl-gauge field contribution.

In the special case that the space is flat from the Riemannian point of view, after some algebra one can show that the Weyl scalar curvature contains only the Weyl gauge field of dilatations

$$R_{\text{Weyl}} = (d-1)(d-2)(A_k A^k) - 2(d-1)(\partial_k A^k)\,. \qquad (26)$$

Now the Weyl geometrical properties are to be derived from physical principles so the A_i cannot be arbitrary but must be related to the distribution of matter encoded by the ensemble density of particle-paths ρ and can be obtained by the same (averaged) least action principle giving the motion of the particle. The minimum is to be evaluated now with respect to the class of all Weyl geometries having arbitrarily Weyl-gauge fields but with fixed metric tensor.

A variational procedure [22] yields a minimum for

$$A_i(q,t) = -\frac{1}{d-2}\,\partial_k(\log\rho) \Rightarrow F_{ij} = \partial_i A_j - \partial_j A_i = 0\,, \qquad (27)$$

which means that the ensemble density ρ is Weyl-covariantly constant

$$\mathcal{D}_i\,\rho = 0 = \partial_i\,\rho + \omega(\rho)\,\rho\,A_i = 0 \;\Rightarrow \\ \Rightarrow\; A_i(q,t) = -\frac{1}{d-2}\,\partial_i(\log\rho)\,, \qquad (28)$$

where $\omega(\rho)$ is the Weyl weight of the density ρ. Since A_i is a *total* derivative the length of a vector transported from A to B along *different* paths changes by the *same amount*. Therefore, a vector after being transported along a *closed* path does *not* change its overall length. This is of fundamental importance to be able to solve in a satisfactory manner Einstein's objections to Weyl's geometry. If the lengths were to change in a path-dependent manner as one transports vectors from point A to point B, two atomic clocks which followed different paths from A to B will tick at *different* rates upon arrival at point B.

The continuity equation is

$$\frac{\partial\rho}{\partial t} + \frac{1}{\sqrt{g}}\,\partial_i(\sqrt{g}\,\rho\,v^i) = 0\,. \qquad (29)$$

In this spirit one goes next to a geometrical derivation of the Schrödinger equation. By inserting

$$A_k = -\frac{1}{d-2}\,\frac{\partial\log\rho}{\partial x^k} \qquad (30)$$

into

$$R_{\text{Weyl}} = (d-1)(d-2)(A_k A^k) - 2(d-1)\,\partial_k A^k \qquad (31)$$

one gets for the Weyl scalar curvature, in the special case that the space is flat from the Riemannian point of view, the following expression

$$R_{\text{Weyl}} = \frac{1}{2\gamma\sqrt{\rho}}(\partial_i\,\partial^i\sqrt{\rho})\,, \qquad (32)$$

which is precisely equal to the Bohm's Quantum potential up to numerical factors.

The Hamilton-Jacobi equation can be written as

$$\frac{\partial S}{\partial t} + H_C(q,S,t) - \gamma\left(\frac{\hbar^2}{2m}\right)R = 0\,, \qquad (33)$$

where the effective Hamiltonian is

$$H_C - \gamma\left(\frac{\hbar^2}{m}\right)R = \frac{1}{2m}\,g^{jk}p_j p_k + V - \gamma\,\frac{\hbar^2}{m}R = \\ = \frac{1}{2m}\,g^{jk}\frac{\partial S}{\partial x^j}\frac{\partial S}{\partial x^k} + V - \gamma\,\frac{\hbar^2}{m}R\,. \qquad (34)$$

When the above expression for the Weyl scalar curvature (Bohm's quantum potential given in terms of the ensemble density) is inserted into the Hamilton-Jacobi equation, in conjunction with the continuity equation, for a momentum given by $p_k = \partial_k S$, one has then a set of two nonlinear coupled partial differential equations. After some straightforward algebra, one can verify that these two coupled differential equations equations will lead to the Schrödinger equation after the substitution $\Psi = \sqrt{\rho}\,e^{iS/\hbar}$ is made.

For example, when $d=3$, $\gamma = 1/12$ and consequently, Bohm's quantum potential $Q = -(\hbar^2/12m)R$ (when R_{Riemann} is zero) becomes

$$R = \frac{1}{2\gamma\sqrt{\rho}}\partial_i\,g^{ik}\,\partial_k\sqrt{\rho} \sim \frac{1}{2\gamma}\,\frac{\Delta\sqrt{\rho}}{\sqrt{\rho}} \Rightarrow Q = -\frac{\hbar^2}{2m}\,\frac{\Delta\sqrt{\rho}}{\sqrt{\rho}} \qquad (35)$$

as is should be and from the two coupled differential equations, the Hamilton-Jacobi and the continuity equation, they both reduce to the standard Schrödinger equation in flat space

$$i\hbar\frac{\partial\Psi(\vec{x},t)}{\partial t}=-\frac{\hbar^2}{2m}\Delta\Psi(\vec{x}.t)+V\Psi(\vec{x},t) \qquad (36)$$

after, and only after, one defines $\Psi=\sqrt{\rho}\,e^{iS/\hbar}$.

If one had a *curved* spacetime with a nontrivial metric one would obtain the Schrödinger equation in a curved spacetime manifold by replacing the Laplace operator by the Laplace-Beltrami operator. This requires, of course, to write the continuity and Hamilton Jacobi equations in a explicit covariant manner by using the covariant form of the divergence and Laplace operator [22], [23]. In this way, the geometric properties of space are indeed affected by the presence of the particle and in turn the alteration of geometry acts on the particle through the quantum force $f_i=\gamma(\hbar^2/m)\partial_i R$ which depends on the Weyl gauge potential A_i and its derivatives. It is this peculiar feedback between the Weyl geometry of space and the motion of the particle which recapture the effects of Bohm's quantum potential.

The formulation above from [22] was also developed for a derivation of the Klein-Gordon (KG) equation. The Dirac equation and Nonlinear Relativistic QM equations were found by [23] via an average action principle. The *relativistic* version of the Bohm potential (for signature $-,+,+,+$) can be written

$$Q\sim\frac{1}{m^2}\frac{(\partial_\mu\partial^\mu\sqrt{\rho})}{\sqrt{\rho}} \qquad (37)$$

in terms of the D'Alambertian operator.

To finalize this section we will explain why the Bohm-potential/Weyl scalar curvature relationship in a flat spacetime

$$Q=-\frac{\hbar^2}{2m}\frac{1}{\sqrt{\rho}}g^{ik}\partial_i\partial_k\sqrt{\rho}=\frac{\hbar^2 g^{ik}}{8m}\left(\frac{2\partial_i\partial_k\rho}{\rho}-\frac{\partial_i\rho\partial_k\rho}{\rho^2}\right) \qquad (38)$$

encodes already the explicit connection between Fisher Information and the Weyl-Ricci scalar curvature R_{Weyl} (for Riemann flat spaces) after one realizes the importance of the *complex* momentum $P_k=p_k+iA_k$. This is typical of Electromagnetism after a minimal coupling of a charged particle (of charge e) to the $U(1)$ gauge field $\mathcal{A}_k$ is introduced as follows $\Pi_k=p_k+ie\mathcal{A}_k$. Weyl's initial goal was to unify Electromagnetism with Gravity. It was later realized that the gauge field of Weyl's dilatations A was *not* the same as the $U(1)$ gauge field of Electromagnetism $\mathcal{A}$.

Since we have reviewed the relationship between the Weyl scalar curvature and Bohm's Quantum potential, it is not surprising to find automatically a connection between Fisher information and Weyl Geometry after a *complex* momentum $P_k=p_k+iA_k$ is introduced. A complex momentum has already been discussed in previous sections within the context of fractal trajectories moving forwards and backwards in time by Nottale and Ord.

If ρ is defined over an d-dimensional manifold with metric g^{ik} one obtains a natural definition of the Fisher information associated with the ensemble density ρ

$$I=g^{ik}I_{ik}=\frac{g^{ik}}{2}\int\frac{1}{\rho}\frac{\partial\rho}{\partial y^i}\frac{\partial\rho}{\partial y^k}d^n y. \qquad (39)$$

In the Hamilton-Jacobi formulation of classical mechanics the equation of motion takes the form

$$\frac{\partial S}{\partial t}+\frac{1}{2m}g^{jk}\frac{\partial S}{\partial x^j}\frac{\partial S}{\partial x^k}+V=0\,. \qquad (40)$$

The momentum field p^j is given by $p^j=g^{jk}(\partial S/\partial x^k)$. The ensemble probability density of particle-paths $\rho(t,x^\mu)$ obeys the normalization condition $\int d^n x\rho=1$. The continuity equation is

$$\frac{\partial\rho}{\partial t}+\frac{1}{m}\frac{1}{\sqrt{g}}\frac{\partial}{\partial x^j}\left(\sqrt{g}\,\rho g^{jk}\frac{\partial S}{\partial x^k}\right)=0\,. \qquad (41)$$

These equations completely describe the motion and can be derived from the action

$$S=\int\rho\left(\frac{\partial S}{\partial t}+\frac{1}{2m}g^{jk}\frac{\partial S}{\partial x^j}\frac{\partial S}{\partial x^k}+V\right)dtd^n x \qquad (42)$$

using fixed endpoint variation in S and ρ.

The Quantization via the Weyl geometry procedure is obtained by defining the *complex* momentum in terms of the Weyl gauge field of dilatations A_k as $P_k=p_k+ieA_k$ and constructing the modified Hamiltonian in terms of the norm-squared of the *complex* momentum $P^kP_k^*$ as follows

$$H_{\text{Weyl}}=\frac{g^{jk}}{2m}\left[(p_j+ieA_j)(p_k-ieA_k)\right]+V. \qquad (43)$$

The *modified* action is now:

$$S_{\text{Weyl}}=\int dt\,d^n x\left[\frac{\partial S}{\partial t}+\frac{g^{jk}}{2m}(p_j+ieA_j)(p_k-ieA_k)+V\right]. \qquad (44)$$

The relationship between the Weyl gauge potential and the ensemble density ρ was

$$A_k\sim\frac{\partial\log(\rho)}{\partial x^k} \qquad (45)$$

the proportionality factors can be re-absorbed into the coupling constant e as follows $P_k=p_k+ieA_k=p_k+i\,\partial_k(\log\rho)$. Hence, when the spacetime metric is flat (diagonal) $g^{jk}=\delta^{jk}$, S_{Weyl} becomes

$$S_{\text{Weyl}}=\int dt\,d^n x\frac{\partial S}{\partial t}+\frac{g^{jk}}{2m}\left[\left(\frac{\partial S}{\partial x^j}+i\frac{\partial\log(\rho)}{\partial x^j}\right)\times\right.$$
$$\left.\times\left(\frac{\partial S}{\partial x^k}-i\frac{\partial\log(\rho)}{\partial x^k}\right)\right]+V=\int dt\,d^n x\left[\frac{\partial S}{\partial t}+V+\right. \qquad (46)$$
$$\left.+\frac{g^{jk}}{2m}\left(\frac{\partial S}{\partial x^j}\right)\left(\frac{\partial S}{\partial x^k}\right)\right]+\frac{1}{2m}\int dt\,d^n x\left[\frac{1}{\rho}\frac{\partial\rho}{\partial x^k}\right]^2.$$

The expectation value of S_{Weyl} is

$$<S_{\text{Weyl}}> \; = \; <S_C> + S_{\text{Fisher}} = \int dt\, d^n x\, \rho \left[\frac{\partial S}{\partial t} + \right.$$
$$\left. + \frac{g^{jk}}{2m} \left(\frac{\partial S}{\partial x^j} \right) \left(\frac{\partial S}{\partial x^k} \right) + V \right] + \frac{1}{2m} \int dt\, d^n x\, \rho \left[\frac{1}{\rho} \frac{\partial \rho}{\partial x^k} \right]^2 . \quad (47)$$

This is how we have reproduced the Fisher Information expression directly from the last term of $<S_{\text{Weyl}}>$:

$$S_{\text{Fisher}} \equiv \frac{1}{2m} \int dt\, d^n x\, \rho \left[\frac{1}{\rho} \frac{\partial \rho}{\partial x^k} \right]^2 . \quad (48)$$

An Euler variation of the expectation value of the action $<S_{\text{Weyl}}>$ with respect to the ρ yields:

$$\frac{\partial S}{\partial t} + \frac{\delta <S_{\text{Weyl}}>}{\delta \rho} - \partial_j \left(\frac{\delta <S_{\text{Weyl}}>}{\delta (\partial_j \rho)} \right) = 0 \; \Rightarrow \quad (49)$$

$$\frac{\partial S}{\partial t} + V + \frac{1}{2m} g^{jk} \left[\frac{\partial S}{\partial x^j} \frac{\partial S}{\partial x^k} + \right.$$
$$\left. + \left(\frac{1}{\rho^2} \frac{\partial \rho}{\partial x^j} \frac{\partial \rho}{\partial x^k} - \frac{2}{\rho} \frac{\partial^2 \rho}{\partial x^j \partial x^k} \right) \right] = 0 . \quad (50)$$

Notice that the last term of the Euler variation

$$\frac{1}{2m} g^{jk} \left[\left(\frac{1}{\rho^2} \frac{\partial \rho}{\partial x^j} \frac{\partial \rho}{\partial x^k} - \frac{2}{\rho} \frac{\partial^2 \rho}{\partial x^j \partial x^k} \right) \right] \quad (51)$$

is precisely the same as the Bohm's quantum potential , which in turn, is proportional to the Weyl scalar curvature. If the continuity equation is implemented at this point one can verify once again that the last equation is equivalent to the Schrödinger equation after the replacement $\Psi = \sqrt{\rho}\, e^{iS/\hbar}$ is made.

Notice that in the Euler variation variation of $<S_{\text{Weyl}}>$ w. r. t the ρ one must include those terms involving the derivatives of ρ as follows

$$-\partial_j \left(\frac{\delta \left[\rho (\partial_k \rho / \rho)^2 \right]}{\delta (\partial_j \rho)} \right) = -\frac{1}{\rho} \partial_j \left(\frac{\delta (\partial_k \rho)^2}{\delta (\partial_j \rho)} \right) = -\frac{2}{\rho} \partial_j \partial^j \rho . \quad (52)$$

This explains the origins of all the terms in the Euler variation that yield Bohm's quantum potential.

Hence, to conclude, we have shown how the *last* term of the Euler variation of the averaged action $<S_{\text{Weyl}}>$, that automatically incorporates the Fisher Information expression after a *complex* momentum $P_k = p_k + i\partial_k(\log \rho)$ is introduced via the Weyl gauge field of dilations $A_k \sim -\partial_k \log \rho$, generates once again Bohm's potential:

$$Q \sim \left(\frac{1}{\rho^2} \frac{\partial \rho}{\partial x^j} \frac{\partial \rho}{\partial x^k} - \frac{2}{\rho} \frac{\partial^2 \rho}{\partial x^j \partial x^k} \right) . \quad (53)$$

To conclude, the Quantization of a particle whose Statistical ensemble of particle-paths permeate a spacetime background endowed with a Weyl geometry allows to construct a *complex* momentum $P_k = \partial_k S + i\partial_k(\log \rho)$ that yields automatically the Fisher Information S_{Fisher} term. The latter Fisher Information term is crucial in generating Bohm's quantum potential Q after an Euler variation of the expectation value of the $<S_{\text{Weyl}}>$ with respect to the ρ is performed. Once the Bohm's quantum potential is obtained one recovers the Schrödinger equation after implementing the continuity equation and performing the replacement $\Psi = \sqrt{\rho}\, e^{iS/\hbar}$. This completes the relationship among Bohm's potential, the Weyl scalar curvature *and* Fisher Information *after* introducing a *complex* momentum.

4 Concluding remarks

Based on Nottale and Ord's formulation of QM from first principles; i. e. from the fractal Brownian motion of a massive particle we have derived explicitly a nonlinear Schrödinger equation. Despite the fact that the Hamiltonian is not Hermitian, real-valued energy solutions exist like the plane wave and soliton solutions found in the free particle case. The remarkable feature of the fractal approach versus *all* the Nonlinear QM equation considered so far is that the Quantum Mechanical energy functional coincides precisely with the field theory one.

It has been known for some time, see Puskarz [8], that the expression for the energy functional in nonlinear QM does *not* coincide with the QM energy functional, nor it is unique. The classic Gross-Pitaveskii NLSE (of the 1960's), based on a quartic interaction potential energy, relevant to Bose-Einstein condensation, contains the nonlinear cubic terms in the Schrödinger equation, after differentiation, $(\psi^* \psi)\psi$. This equation does not satisfy the Weinberg homogeneity condition [9] and also the energy functional differs from the E_{QM} by factors of two.

However, in the fractal-based NLSE there is no discrepancy between the quantum-mechanical energy functional and the field theory energy functional. Both are given by

$$H^{\text{NLSE}}_{\text{fractal}} = -\frac{\hbar^2}{2m} \frac{\alpha}{\hbar} \psi^* \nabla^2 \psi + U \psi^* \psi - \quad (54)$$
$$- i \frac{\hbar^2}{2m} \frac{\beta}{\hbar} \psi^* (\vec{\nabla} \ln \psi)^2 \psi .$$

This is why we push forward the NLSE derived from the fractal Brownian motion with a complex-valued diffusion coefficient. Such equation does admit plane-wave solutions with the dispersion relation $E = \vec{p}^{\,2}/(2m)$. It is not hard to see that after inserting the plane wave solution into the fractal-based NLSE we get (after setting $U = 0$),

$$E = \frac{\hbar^2}{2m} \frac{\alpha}{\hbar} \frac{\vec{p}^{\,2}}{\hbar^2} + i \frac{\beta}{\hbar} \frac{\vec{p}^{\,2}}{2m} = \frac{\vec{p}^{\,2}}{2m} \frac{\alpha + i\beta}{\hbar} = \frac{\vec{p}^{\,2}}{2m} , \quad (55)$$

since $\hbar = \alpha + i\beta$. Hence, the plane-wave *is* a solution to our fractal-based NLSE (when $U = 0$) with a real-valued energy and has the correct energy-momentum dispersion relation.

Soliton solutions, with real-valued energy (momentum) are of the form

$$\psi \sim \left[F(x-vt)+iG(x-vt)\right]e^{ipx/\hbar - iEt/\hbar}, \qquad (56)$$

with F, G two functions of the argument $x-vt$ obeying a coupled set of two nonlinear differential equations.

It is warranted to study solutions when one turns-on an external potential $U \neq 0$ and to generalize this construction to the Quaternionic Schrödinger equation [16] based on the Hydrodynamical Nonabelian-fluid Madelung's formulation of QM proposed by [26]. And, in particular, to explore further the consequences of the Non-Hermitian Hamiltonian (pseudo-Hermitian) associated with our NLSE (34) within the context of the so-called PT symmetric *complex* extensions of QM and QFT [27]. Arguments why a quantum theory of gravity should be nonlinear have been presented by [28] where a *different* non-linear Schrödinger equation, but with a similar logarithmic dependence, was found. This equation [28] is also similar to the one proposed by Doebner and Goldin [29] from considerations of unitary representations of the diffeomorphism group.

Acknowledgements

We acknowledge to the Center for Theoretical Studies of Physical Systems, Clark Atlanta University, Atlanta, Georgia, USA, and the Research Committee of the University of Antioquia (CODI), Medellín, Colombia for support.

References

1. Nottale L. *Chaos, Solitons and Fractals*, 1994, v. 4(3), 361; Celerier M. and Nottale L. Dirac equation in scale relativity. arXiv: hep-th/0112213.
2. Ord G. N. *Journal of Physics A: Math. Gen.*, 1983, v. 16, 1869.
3. Bialynicki-Birula I., Mycielsky J. *Annal of Physics*, 1976, v. 100, 62.
4. Pardy M. To the nonlinear QM. arXiv: quant-ph/0111105.
5. Bohm D. and Vigier J. *Phys. Rev.*, 1954, v. 96, 208.
6. Castro C., Mahecha J., and Rodriguez B. Nonlinear QM as a Fractal Brownian motion with complex diffusion constant. arXiv: quant-ph/0202026.
7. Madelung E. *Z. Physik*, 1926, v. 40, 322.
8. Staruszkiewicz A. *Acta Physica Polonica*, 1983, v. 14, 907; Puszkarz W. On the Staruszkiewicz modification of the Schrödinger equation. arXiv: quant-ph/9912006.
9. Weinberg S. *Ann. Phys.*, 1989, v. 194, 336.
10. Petrosky T., Prigogine I. *Chaos, Solitons and Fractals*, 1994, v. 4(3), 311.
11. Castro C. *Chaos, Solitons and Fractals*, 2001, v. 12, 101.
12. Gómez B., Moore S., Rodríguez A., and Rueda A. (eds). Stochatic processes applied to physics and other related fields. World Scientific, Singapore, 1983.
13. Lemos N. A. *Phys. Lett. A*, 1980, v. 78, 237; 1980, v. 78, 239.
14. Ghirardi G. C., Omero C., Rimini A., and Weber T. *Rivista del Nuovo Cimento*, 1978, v. 1, 1.
15. Kamesberger J., Zeilinger J. *Physica B*, 1988, v. 151, 193.
16. Adler S. L. Quaternionic quantum mechanics and quantum fields. Oxford University Press, Oxford, 1995.
17. Yaris R. and Winkler P. *J. Phys. B: Atom. Molec Phys.*, 1978, v. 11, 1475; 1978, v. 11, 1481; Moiseyev N. *Phys. Rep.*, 1998, v. 302, 211.
18. Mensky M. B. *Phys. Lett. A*, 1995, v. 196, 159.
19. Abrams D. S. and Lloyd S. *Phys. Rev. Lett.*, 1998, v. 81, 3992.
20. Cresson J. Scale Calculus and the Schrodinger Equation. arXiv: math.GM/0211071.
21. Castro C. *Foundations of Physics*, 2000, v. 8, 1301; *Chaos, Solitons and Fractals*, 2000, v. 11(11), 1663–1670; On the noncommutative Yang's spacetime algebra, holography, area quantization and C-space relativity. (*Submitted to European Journal of Physics C*); Castro C., Pavsic M. The Extended Relativity Theory in Clifford-spaces. *Progress in Physics*, 2005, v. 1, 31–64.
22. Santamato E. *Phys. Rev. D*, 1984, v. 29, 216; 1985, v. 32, 2615; *Jour. Math. Phys.*, 1984, v. 25, 2477.
23. Castro C. *Foundations of Physics*, 1992, v. 22, 569; *Foundations of Physics Letters*, 1991, v. 4, 81; *Jour. Math. Physics.*, 1990, v. 31(11), 2633.
24. Frieden B. Physics from Fisher Information. Cambridge University Press, Cambridge, 1998; Hall M., Reginatto M. *Jour. Phys. A*, 2002, v. 35, 3829; Frieden B., Plastino A., Plastino A. R., and Soffer B. A Schrödinger link between non-equilibrium theormodynamics and Fisher information. arXiv: cond-mat/0206107.
25. Carroll R. Fisher, Kahler, Weyl and the Quantum Potential. arXiv: quant-ph/0406203; Remarks on the Schrödinger Equation. arXiv: quant-ph/0401082.
26. Love P., Boghosian B. Quaternionic madelung transformation and Nonabelian fluid dynamics. arXiv: hep-th/0210242.
27. Bender C. Introduction to PT-Symmetric Quantum Theory. arXiv: quant-ph/0501052; Bender C., Cavero-Pelaez I., Milton K. A., Shajesh K. V. PT-Symmetric Quantum Electrodynamics. arXiv: hep-th/0501180.
28. Singh T., Gutti S., and Tibrewala R. Why Quantum Gravity should be Nonlinear. arXiv: gr-qc/0503116.
29. Doebner H. and Goldin G. *Phys. Lett. A*, 1992, v. 162, 397.

The Gravity of Photons and the Necessary Rectification of Einstein Equation

C. Y. Lo

Applied and Pure Research Institute, 17 Newcastle Drive, Nashua, NH 03060, USA

E-mail: c_y_lo@yahoo.com; C_Y_Lo@alum.mit.edu

It is pointed out that Special Relativity together with the principle of causality implies that the gravity of an electromagnetic wave is an accompanying gravitational wave propagating with the same speed. Since a gravitational wave carries energy-momentum, this accompanying wave would make the energy-stress tensor of the light to be different from the electromagnetic energy-stress tensor, and thus can produce a geodesic equation for the photons. Moreover, it is found that the appropriate Einstein equation must additionally have the photonic energy-stress tensor with the antigravity coupling in the source term. This would correct that, in disagreement with the calculations for the bending of light, existing solutions of gravity for an electromagnetic wave, is unbounded. This rectification is confirmed by calculating the gravity of electromagnetic plane-waves. The gravity of an electromagnetic wave is indeed an accompanying gravitational wave. Moreover, these calculations show the first time that Special Relativity and General Relativity are compatible because the physical meaning of coordinates has been clarified. The success of this rectification makes General Relativity standing out further among theories of gravity.

1 Introduction

The physical basis of Special Relativity is constancy of the light speed, which is also the velocity of an electromagnetic wave [1]. On the other hand, the physical basis of quantum mechanics is that light can be considered as consisting of the photons [2]. Currently, it seems, there is no theoretical connection between constancy of light speed and photons, except that both are proposed by Einstein. However, since constancy of the light speed and the notion of photon are two aspects of the same physical phenomenon, from the viewpoint of physics, a theoretical connection of these notions must exist. Moreover, such a connection would be a key to understand the relationship between these two theories.

To this end, General Relativity seems to hold a special position because of the bending of light. The fact that a photon follows the geodesic of a massless particle [3, 4] manifests that there is a connection between the light speed and the photon. This suggests that General Relativity may provide some insight on the existence of the photons. In other words, the existence of the photons, though an observed fact, may be theoretically necessary because the light speed is the maximum.

On the other hand, since electromagnetism is a source for gravity [5], an electromagnetic wave would generate gravity. Thus, it is natural to ask whether its gravity is related to the existence of the photon. In other words, would the existence of the photon be an integral part of the theory of General Relativity? It will be shown here that the answer is affirmative. In fact, this is also a consequence of Special Relativity provided that the theoretical framework of General Relativity is valid.

2 Special Relativity and the accompanying gravity of an electromagnetic wave

In a light ray, the massless light energy is propagating in vacuum with the maximum speed c. Thus, the gravity due to the light energy should be distinct from that generated by massive matter [6–7]. Since a field emitted from an energy density unit means a non-zero velocity relative to that unit, it is instructive to study the velocity addition. According to Special Relativity, the addition of velocities is as follows [1]:

$$u_x = \frac{\sqrt{1-v^2/c^2}}{1+u'_z v/c^2}\, u'_x\,, \quad u_y = \frac{\sqrt{1-v^2/c^2}}{1+u'_z v/c^2}\, u'_y\,, \quad \text{and} \quad u_z = \frac{u'_z + v}{1+u'_z v/c^2}\,, \tag{1}$$

where velocity $\vec{v}$ is in the z-direction, $(u'_x,\, u'_y,\, u'_z)$ is a velocity in a system moving with velocity v, c is the light speed, $u_x = dx/dt$, $u_y = dy/dt$, and $u_z = dz/dt$. When $v = c$, independent of $(u'_x,\, u'_y,\, u'_z)$ one has

$$u_x = 0\,, \quad u_y = 0\,, \quad \text{and} \quad u_z = c\,. \tag{2}$$

Thus, neither the direction nor the magnitude of the velocity $\vec{v}$ $(= \vec{c})$ have been changed.

This implies that nothing can be emitted from a light ray, and therefore no field can be generated outside the light ray. To be more specific, from a light ray, no gravitational field

can be generated outside the ray although, accompanying the light ray, a gravitational field g_{ab} ($\neq \eta_{ab}$ the flat metric) is allowed within the ray.

According to the principle of causality [7], this accompanying gravity g_{ab} should be a gravitational wave since an electromagnetic wave is the physical cause. This would put General Relativity into a severe test for theoretical consistency. However, this examination would also have the benefit of knowing that electrodynamics is completely compatible with General Relativity.

3 The accompanying gravitational wave and the photonic energy-stress tensor

Observations confirm that photons follow a geodesic. One may expect that the light energy-stress tensor $T(L)_{ab}$ would generate the photonic geodesic since the massive tensor $T(m)_{ab}$ generates the geodesic through $\nabla^c T(m)_{cb} = 0$ [5]. This means that $T(L)_{ab}$ is different from the electromagnetic energy-stress tensor $T(E)_{ab}$ since $\nabla^c T(E)_{cb}$ is the Lorentz force [7, 8].

Nevertheless, this can be resolved since a gravitational wave carries an additional energy-stress tensor $T(g)_{ab}$, i. e., one should have

$$T(L)_{ab} = T(E)_{ab} + T(g)_{ab} \tag{3}$$

since there is no other type of energy. Then, one may expect that Eq. (3) allows $\nabla^c T(L)_{cb} = 0$ to generate the necessary geodesic equation for photons.

If the light is emitted and absorbed in terms of photons, physically the photons contain all the energy of the light, i. e., the photonic energy-stress tensor,

$$T(P)_{ab} = T(L)_{ab}\,. \tag{4}$$

One might object on the ground that, in quantum theory, $T(E)_{ab}$ is considered as identical to the photonic energy-stress tensor $T(P)_{ab}$. However, one should note also that gravity is ignored in quantum electrodynamics.

4 The Einstein equation for an electromagnetic wave

Einstein [9] suggested the field equation for the gravity of an electromagnetic wave was

$$G_{ab} = -KT(E)_{ab}\,, \tag{5}$$

where G_{ab} is the Einstein tensor, and K is the coupling constant. However, to generate the photonic geodesic, the source term must include the photonic energy-stress $T(P)_{ab}$. The need of a modified equation is supported by the fact that all existing solutions, in disagreement with light bending calculation, are unbounded [7].

Moreover, if the gravity of an electromagnetic wave is a gravitational wave, validity of Eq. (5) is questionable. It has been known from the binary pulsar experiments, that when radiation is included, the anti-gravity coupling must be included in the Einstein equation [10],

$$G_{ab} = -K\big[T(m)_{ab} - t(g)_{ab}\big]\,, \tag{6}$$

where $T(m)_{ab}$ and $t(g)_{ab}$ are respectively the energy-stress tensors for massive matter and gravity. The need of $t(g)_{ab}$ was first conjectured by Hogarth [12]. The possibility of such an coupling was suggested by Pauli [13]. Moreover, if a space-time singularity is not a reality, the existence of an antigravity coupling is implicitly given by the singularity theorems which assume the coupling constants are of the same sign [14].

There are theories such as the Brans-Dicke's [15] and the Yilmaz's [16] that provide an extra source term in vacuum. However, it is not clear that they can provide the right formula for the gravity of an electromagnetic wave since their connection with the notion of photon was never mentioned. Besides, it is more appropriate to consider a fundamental problem from the basics.

The above analysis suggests that, to obtain an appropriate Einstein equation, one may start from considering the gravitational radiation with Einstein's radiation formula as follows:

(a) For the gravitational wave generated by massive matter, the gravitational energy-stress $t(g)_{ab}$ of Einstein's radiation formula is approximately [11].

$$t(g)_{ab} = \frac{G^{(2)}_{ab}}{K}\,, \quad \text{where} \quad G^{(2)}_{ab} = G_{ab} - G^{(1)}_{ab}\,, \tag{7}$$

where $G^{(1)}_{ab}$ consists of all first order terms of G_{ab}. Moreover, if the gravitational energy is the same as the gravitational wave energy, one has

$$t(g)_{ab} = T(g)_{ab}\,. \tag{8}$$

(b) Since g_{ab} is a wave propagating with the electromagnetic wave, one may have the linear terms, $G^{(1)}_{ab} = 0$ on a time average. This suggests $G_{ab} = KT(g)_{ab}$. Thus, it follows from Eqs. (3) and (4) that

$$G_{ab} = KT(g)_{ab} = -K\big[T(E)_{ab} - T(P)_{ab}\big] \tag{9}$$

would be the appropriate Einstein equation. Comparing with Eq. (5), there is an additional term $T(P)_{ab}$.

(c) Since the Lorentz force $\nabla^c T(E)_{cb}=0$ and $\nabla^c G_{cb}=0$, as expected, one has the necessary formula

$$\nabla^c T(P)_{cb} = 0 \tag{10}$$

generate the photonic geodesic equation. However, to verify Eq. (9), one must first show that Eq. (5) cannot be valid for at least one example and then find the photonic energy-stress tensor $T(P)_{ab}$ for Eq. (9).

Alternatively, Eq. (9) can be derived from the principle of causality [7, 8] since the electromagnetic plane-wave as a

spatial local idealization has been justified in electrodynamics. In general, without an idealization, to solve the gravity of an electromagnetic wave is very difficult [4].

5 The reduced Einstein equation for plane-waves

Due to the speed of light is the maximum, the influence of an electromagnetic wave to its accompanying gravity is spatially local. Thus, an electromagnetic plane-wave is also a valid modeling for the problem of gravity.

Now, let us consider the electromagnetic potential $A_k(t-z)$ which represents the photons moving in the z-direction. Then, Eq. (5) is reduced to a differential equation of $u\,(=t-z)$ [6] as follows:

$$\begin{aligned} &G'' - g'_{xx}g'_{yy} + (g'_{xy})^2 - G'\frac{g'}{2g} = 2GR_{tt} = \\ &= 2K\left(F_{xt}^2 g_{yy} + F_{yt}^2 g_{xx} - 2F_{xt}F_{yt}\,g_{xy}\right), \end{aligned} \tag{11}$$

where

$$G = g_{xx}g_{yy} - g_{xy}^2\,, \qquad g = \mid g_{ab} \mid$$

is the determinant of the metric, $F_{ab} = \partial_a A_b - \partial_b A_a$ is the electromagnetic field tensor, and R_{ab} is the Ricci tensor. The metric elements are connected as follows:

$$g = Gg_t^2, \quad \text{where} \quad g_t \equiv g_{tt} + g_{tz}. \tag{12}$$

Moreover, the massless of photons implies that

$$g_{tt} + 2g_{tz} + g_{zz} = 0, \quad \text{and} \quad g^{tt} - 2g^{tz} + g^{zz} = 0\,.$$

Note that Eq. (35.31) and Eq. (35.44) in reference [4] and Eq. (2.8) in reference [17] are special cases of Eq. (5). They believed that bounded wave solutions can be obtained [7].

It has been shown that A_t, g_{xt}, g_{yt}, and g_{zt} are allowed to be zero. Although there are four remaining metric elements (g_{xx}, g_{xy}, g_{yy}, and g_{tt}) to be determined, based on Einstein's notion of weak gravity and Eq. (5), it will be shown that there is no physical solution [6]. In other words, in contrast to Einstein's belief [9], the difficulty of his equation is not limited to mathematics.

6 Verification of the rectified Einstein equation

Now, consider an electromagnetic plane-waves of circular polarization, propagating to the z-direction

$$A_x = \frac{1}{\sqrt{2}}\,A_0\cos\omega u\,, \quad \text{and} \quad A_y = \frac{1}{\sqrt{2}}\,A_0\sin\omega u\,, \tag{13}$$

The rotational invariants with respect to the z-axis are constants. These invariants are: G_{tt}, R_{tt}, $T(E)_{tt}$, G, $(g_{xx}+g_{yy})$, g_{tz}, g_{tt}, g, and etc. It follows that [6, 7]

$$\begin{aligned} g_{xx} &= -1 - C + B_\alpha\cos(\omega_1 u + \alpha)\,, \\ g_{yy} &= -1 - C - B_\alpha\cos(\omega_1 u + \alpha)\,, \\ g_{xy} &= \pm\, B_\alpha\sin(\omega_1 u + \alpha)\,, \end{aligned} \tag{14}$$

where C and B_α are small constants, and $\omega_1 = 2\omega$. Thus, metric (14) is a circularly polarized wave with the same direction of polarization as the electromagnetic wave (13). On the other hand, one also has $G = (1+C)^2 - B_\alpha^2 \geqslant 0$,

$$G_{tt} = \frac{2\omega^2 B_\alpha^2}{G} \geqslant 0\,, \tag{15}$$

$$T(E)_{tt} = \frac{g_{yy}}{G}\,\omega^2 A_0^2\,(1 + C - B_\alpha\cos\alpha) > 0\,.$$

Thus, it is not possible to satisfy Einstein equation (5) because $T(E)_{tt}$ and G_{tt} have the same sign [6]. Thus, it is necessary to have a photonic energy-stress tensor.

Given that a geodesic equation must be produced, for a monochromatic wave, the form of a photonic energy tensor should be similar to that of massive matter. Observationally, there is very little interaction, if any, among photons of the same ray. Theoretically, since photons travel in the velocity of light, there should not be any interaction among them.

Therefore, the photonic energy tensor should be dust-like with the momentum of the photon P_a as follows:

$$T_{ab}(P) = \rho\,P_a\,P_b\,, \tag{16}$$

where ρ is a scalar and is a function of u. In the units $c = \hbar = 1$, $P_t = \omega$. It has been obtained [6] that

$$\rho(u) = -A_m\,g^{mn}A_n \geqslant 0\,. \tag{17}$$

Here, $\rho(u)$ is related to gravity through g^{mn}. Since light intensity is proportional to the square of the wave amplitude, ρ which is Lorentz gauge invariant, can be considered as the density function of photons. Then

$$\begin{aligned} T_{ab} &= -T(g)_{ab} = T(E)_{ab} - T(P)_{ab} = \\ &= T(E)_{ab} + A_m\,g^{mn}A_n\,P_a\,P_b\,. \end{aligned} \tag{18}$$

Thus, $T_{ab}(P)$ has been derived completely from the electromagnetic wave A_k and g_{ab}.

Physically, such a tensor should be unique. It remains to see whether all the severe physical requirements can be satisfied. In particular, validity of the light bending calculation requires compatibility with the notion of weak gravity [3]. Also, the photonic energy tensor of Misner et al. [4], is an approximation of the time average of $T_{ab}(P)$.

As expected, this tensor $T_{ab}(P)$ enables a gravity solution for wave (13). According to Eq. (8),

$$T_{tt} = -\frac{1}{G}\,\omega^2 A_0^2 B_\alpha\cos\alpha \leqslant 0\,, \tag{19}$$

since $B_\alpha = \frac{K}{2}\,A_0^2\cos\alpha$. the energy density of the photonic energy tensor is indeed larger than that of the electromagnetic wave. $T(g)_{tt}$ is of order K. Note that, pure electromagnetic waves can exist since $\cos\alpha = 0$ is also possible. To confirm the general validity of (16), consider a wave linearly polarized in the x-direction,

$$A_x = A_0 \cos\omega(t-z)\,. \tag{20}$$

Then, one has

$$T_{tt} = \frac{g_{yy}}{G}\,\omega^2 A_0^2 \cos 2\omega(t-z)\,, \tag{21}$$

since the gravitational component is not an independent wave, $T(g)_{tt}$ is allowed to be negative. Eq. (21) implies that its polarization has to be different.

It turns out that the solution is a linearly polarized gravitational wave and that the time-average of $T(g)_{tt}$ is positive of order K [7]. From the viewpoint of physics, for an x-directional polarization, gravitational components related to the y-direction, remains the same. In other words,

$$g_{xy} = 0, \quad \text{and} \quad g_{yy} = -1\,. \tag{22}$$

It follows that the general solution of wave (20) is:

$$\begin{aligned} &-g_{xx} = 1 + C_1 - \frac{K}{2}\,A_0^2 \cos 2\omega(t-z)\,,\\ &\text{and} \quad g_{tt} = -g_{zz} = \sqrt{\frac{g}{g_{xx}}}\,, \end{aligned} \tag{23}$$

where C_1 is a constant. Note that he frequency ratio is the same as that of a circular polarization, but there is no phase difference to control the amplitude of the gravitational wave.

For a polarization in the diagonal direction of the $x-y$ plane, the solution is:

$$g_{xx} = g_{yy} = -1 - \frac{C_1}{2} + \frac{K}{4}\,A_0^2 \cos 2\omega(t-z)\,, \tag{24}$$

$$g_{xy} = -\frac{C_1}{2} + \frac{K}{4}\,A_0^2 \cos 2\omega(t-z)\,, \tag{25}$$

$$g_{tt} = -g_{zz} = \sqrt{\frac{-g}{1-2g_{xy}}}\,. \tag{26}$$

Note that for a perpendicular polarization, the metric element g_{xy} changes sign. The time averages of their T_{tt} are also negative as required. If $g=-1$, relativistic causality requires $C_1 \geqslant KA_0^2/2$.

7 Compatibility between Special Relativity and General Relativity

We implicitly use the same coordinate system whether the calculation is done in terms of Special Relativity or General Relativity. However, according to Einstein's "covariance principle" [1], coordinates have no physical meaning whereas the coordinates in Special Relativity have very clear meaning [18]. Thus, all the above calculations could have no meaning. Recently, it has been proven that a physical coordinate system for General Relativity necessarily has a frame of reference(1) with the Euclidean-like structure [19–21]. Moreover, the time coordinate will be the same as in Special Relativity if the metric is asymptotically flat.

Many theorists, including Einstein, overlooked that the metric of a Riemannian space actually is compatible with the space coordinates with the Euclidean-like structure. Let us illustrate this with the Schwarzschild solution in quasi-Minkowskian coordinates [11],

$$\begin{aligned} -ds^2 = -\left(1-\frac{2M\kappa}{r}\right)c^2dt^2 + \left(1-\frac{2M\kappa}{r}\right)^{-1}dr^2 + \\ + r^2(d\theta^2 + \sin^2\theta d\varphi^2), \end{aligned} \tag{27}$$

where $(r,\,\theta,\,\varphi)$ transforms to $(x,\,y,\,z)$ by,

$$\begin{aligned} &x = r\sin\theta\,\cos\varphi\,, \quad y = r\sin\theta\,\sin\varphi\,,\\ &\text{and} \quad z = r\cos\theta\,. \end{aligned} \tag{28}$$

Coordinate transformation (28) tells that the space coordinates satisfy the Pythagorean theorem. The Euclidean-like structure represents this fact, but avoids confusion with the notion of a Euclidean subspace, determined by the metric. Metric (27) and the Euclidean-like structure (28) are complementary to each other in the Riemannian space. Then, a light speed ($ds^2=0$) is defined in terms of dx/dt, dy/dt, and dz/dt [1]. This is necessary though insufficient for a physical space [19–21].

Einstein's oversight made his theory inconsistent, and thus rejected by Whitehead [22] for being not a theory in physics. For instance, his theory of measurement is incorrect because it is modeled after(2) measurements for a Riemannian space embedded in a higher dimensional space [19–21]. In General Relativity, the local distance ($\sqrt{-ds^2}$, where $dt=0$) represents the space contraction, which is measured in a free fall local space [1, 3]. Thus, this is a dynamic measurement since the measuring instrument is in a free fall state.

Einstein's error is that he overlooked the free fall state, and thus has mistaken this dynamic local measurement as a static measurement. Moreover, having different states at different points, this makes such a measurement for an extended object not executable.

The Euclidean-like structure determines the distance between two points in a frame of reference, and the observed light bending supports this physical meaning. This is why the interpretation of Hubble's law as a consequence of receding velocity(3) is invalid [23]. Because the measurement theory of Einstein is invalid, the miles long arms of the laser interferometer in LIGO would not change their length under the influence of gravitational waves [24]. In other words, LIGO would inadvertently further confirm that Einstein's theory of measurement is invalid.

It has been solved that the coordinate system of General Relativity and that of Special Relativity are actually the same for this problem. We must show also that the plane waves

would satisfy the Maxwell equation in General Relativity, see [11; p. 125],

$$\frac{\partial}{\partial x^a}\sqrt{g}\,F^{ab} = -\sqrt{g}\,J^b, \tag{29}$$

$$\frac{\partial}{\partial x^a}F^{bc} + \frac{\partial}{\partial x^b}F^{ca} + \frac{\partial}{\partial x^c}F^{ab} = 0\,. \tag{30}$$

Since equation (30) is the same as in Special Relativity, it remains to show that (29) is satisfied for $J^a = 0$. To show this, we can use the facts that g^{ab} and F^{ab} are function of u, and that $g^{tt} + g^{zz} = 0$. It follows that

$$\begin{aligned}\frac{\partial}{\partial x^a}\sqrt{g}\,F^{ab} &= \frac{\partial\sqrt{g}}{\partial t}(F^{tb} - F^{zb}) = \\ &= \frac{\partial\sqrt{g}}{\partial t}\,g^{tt}\,(\partial_t A_c + \partial_z A_c)\,g^{cb} = 0\,.\end{aligned} \tag{31}$$

We thus complete the compatibility proof.

8 Conclusions and Discussions

A crucial argument for this case is that both Special Relativity and General Relativity use the same coordinate system. This is impossible, according to Einstein's theory of measurement. A major problem of Einstein's theory is that the physical meaning of coordinates is not only ambiguous, but also confusing[4] since the physical meaning of the coordinates depends on the metric. Moreover, Einstein's equivalence principle actually contradicts the so-called "covariance principle". P. Morrison of MIT [21, 25] remarked that the "covariance principle" is physically invalid because it disrupts the necessary physical continuity from Special Relativity to General Relativity.

Now, a photonic energy-stress tensor has been obtained as physics requires. The energy and momentum of a photon is proportional to its frequency although, as expected from a classical theory, their relationship with the Planck constant $\hbar$ is not yet clear; and the photonic energy-stress tensor is a source term in the Einstein equation. As predicted by Special Relativity, the gravity of an electromagnetic wave is an accompanying gravitational wave propagating with the same speed. Moreover, the gravity of light is proven to be compatible with the notion of weak gravity.

In the literature [4, 26–29], however, solutions of Eq. (5) are unbounded.[5] Thus, they are incompatible with the approximate validity of electrodynamics and violate physical principles including the equivalence principle and the principle of causality [7, 30]. (The existence of local Minkowski spaces is only a necessary condition[6] for Einstein's equivalence principle [31].) Naturally, one may question whether the gravity due to the light is negligible. Now, the claim that the bending of light experiment confirms General Relativity, is no longer inflated.

In addition, the calculation answers a long-standing question on the propagation of gravity in General Relativity. Since an electromagnetic wave has an accompanying gravitational wave, gravity should propagate in the same speed as electromagnetism. It is interesting to note that Rabounski [32] reached the same conclusion on the propagation of gravity with a completely different method, which is independent of the Einstein equation.

One might argue that since $E = mc^2$ and the gravitational effect of the wave energy density should be outside a light ray. However, this is a misinterpretation [33, 34]. One should not, as Tolman [35] did, ignore Special Relativity and the fact that the light energy density is propagating with the maximum velocity possible. There are intrinsically different characteristics in such an energy form according to Special Relativity. This calculation confirms a comment of Einstein [23] that $E = mc^2$ must be understood in the contact of energy conservation.

To illustrate this, consider the case of a linear polarization, for which Eq. (5) still has a solution [6]

$$-g_{xx} = 1 - \frac{K}{4}A_0^2\left[2\omega^2(t-z)^2 + \cos 2\omega(t-z)\right]. \tag{32}$$

However, solution (32) is invalid since $(t-z)^2$ grows very large as time goes by. This would "represent" the effects that the wave energy were equivalent to mass. This illustrates also that Einstein's notion of weak gravity may not be compatible with an inadequate source.

The theoretical consistency between Special Relativity and General Relativity is further established. This is a very strong confirming evidence for General Relativity beyond the requirements of the equivalence principle. Moreover, this rectification makes General Relativity standing out among all theories of gravity. Moreover, since light has a gravitational wave component, it would be questionable to quantize gravity independently as in the current approach.

Acknowledgments

The author gratefully acknowledges stimulating discussions with J. E. Hogarth, and P. Morrison. Special thanks are to D. Rabounski for valuable comments and useful suggestions. This work is supported in part by the Chan Foundation, Hong Kong.

Endnotes

[1] In a Riemannian geometry, a frame of reference may not exist since the coordinates can be arbitrary. However, for a physical space, a frame of reference with the Euclidean-like structure must exist because of physical requirements [19–21]. Note that the Euclidean-like structure is independent of the metric.

[2] In the initial development of Riemannian geometry, the metric was identified formally with the notion of distance in analogy as the case of the Euclidean space. Such geometry is often illustrated with the surface of a sphere, a subspace embedded in a flat space [4, 36]. Then, the distance is determined by the flat space and can be measured with a static method. For a general case, however, the issue of measurement was not addressed before Einstein's theory.

[3] Einstein's theory of measurements is not supported by observation, which requires [21, 37] that the light speed must be defined in terms of the Euclidean-like structure as in Einstein's own papers [1, 3].

[4] If the "covariance principle" was valid, it has been shown that the "event of horizon" for a black hole could be just any arbitrary constant [38].

[5] In fact, all existing solutions involving waves are unbounded because the term to accommodate gravitational wave energy-stress is missing. It is interesting that Einstein and Rosen are the first to discover the non-existence of wave solutions [39]. However, their arguments that led to their correct conclusion was incorrect. Robertson as a referee of Physical Review pointed out that the singularities mentioned are actually removable [39]. However, there are other reasons for a wave solution to be invalid. It has been found that a wave solution necessarily violates Einstein's equivalence principle and the principle of causality [10, 19].

[6] Many theorists do not understand Einstein's equivalence principle because they failed in understanding the Einstein-Minkowski condition that the local space of a particle under gravity must be locally Minkowskian [1, 3]. This condition is crucial to obtain the time dilation and space contractions [21].

References

1. Einstein A., Lorentz H. A., Minkowski H., and Weyl H. The Principle of Relativity. Dover, New York, 1923.
2. Einstein A. *Annalen der Physik*, 1905, Bd. 17, 132–148.
3. Einstein A. The Meaning of Relativity (1921). Princeton Univ. Press, 1954.
4. Misner C. W., Thorne K. S., and Wheeler J. A. Gravitation. Freeman, San Francisco, 1973.
5. Lo C. Y. *Phys. Essays*, 1997, v.10(4), 540–545.
6. Lo C. Y. *Proc. Sixth Marcel Grossmann Meeting On Gen. Relativity, Kyoto 1991*, ed. H. Sato, and T. Nakamura, World Sci., Singapore, 1992, 1496.
7. Lo C. Y. *Phys. Essays*, 1997, v.10(3),424–436.
8. Lo C. Y. *Phys. Essays*, 1999, v.12(2), 226–241.
9. Einstein A. Physics and Reality (1936) in Ideas and Opinions. Crown, New York, 1954, p. 311.
10. Lo C. Y. *Astrophys. J.*, 1995, v. 455, 421–428.
11. Weinberg S. Gravitation and Cosmology. John Wiley Inc., New York, 1972.
12. Hogarth J. E., Ph. D. Thesis, 1953, Dept. of Math. Royal Holloway College, University of London, p. 6.
13. Pauli W. Theory of Relativity. Pergamon Press, London, 1958, p. 163.
14. Hawking S. W. and Penrose R., *Proc. Roy. Soc. London A*, 1970, v. 314, 529–548.
15. Brans C. and Dicke R. H. *Phys. Rev.*, 1961, v. 124, 925.
16. Yilmaz H. *Hadronic J.*, 1979, v. 2, 997–1020.
17. Bondi H., Pirani F. A. E., and Robinson I. *Proc. R. Soc. London A*, 1959, v. 251, 519–533.
18. Einstein A. The Problem of Space, Ether, and the Field in Physics (1934) in Ideas and Opinions Crown, New York, 1954.
19. Lo C. Y. *Phys. Essays*, 2002, v. 15(3), 303–321.
20. Lo C. Y. *Chinese J. of Phys.*, 2003, v. 41(4), 1–11.
21. Lo C. Y. *Phys. Essays*, 2005, v. 18(4).
22. Whitehead A. N. The Principle of Relativity. Cambridge Univ. Press, Cambridge, 1962.
23. Lo C. Y. *Progress in Phys.*, 2006, v. 1, 10–13.
24. Lo C. Y. The Detection of Gravitational Wave with the Laser Interferometer and Einstein's Theoretical Errors on Measurements. (*In preparation*).
25. Lo C. Y. *Phys. Essays*, 2005, v. 18(1).
26. Peres A. *Phys. Rev.*, 1960, v. 118, 1105.
27. Penrose R. *Rev. Mod. Phys.*, 1965, v. 37(1), 215–220.
28. Bonnor W. B. *Commun. Math. Phys.*, 1969, v. 13, 173.
29. Kramer D., Stephani H., Herlt E., and MacCallum M. *Exact Solution of Einstein's Field Equations*, ed. E. Schmutzer, Cambridge Univ. Press, Cambridge, 1980.
30. Lo C. Y. *Phys. Essays*, 1994, v. 7(4), 453–458.
31. Lo C. Y. *Phys. Essays*, 1998, v. 11(2), 274–272.
32. Rabounski D. *Progress in Physics*, 2005, v. 1, 3–6.
33. Einstein A. $E = Mc^2$ (1946) Ideas and Opinions. Crown, New York, 1954, p. 337
34. Lo C. Y. *Astrophys. J.*, 1997, v. 477, 700–704.
35. Tolman R. C. Relativity, Thermodynamics, and Cosmology. Dover, New York, 1987, p. 273.
36. Dirac P. A. M. General Theory of Relativity. John Wiley, New York, 1975.
37. Lo C. Y. *Phys. Essays*, 2003, v. 16(1), 84–100.
38. Lo C. Y. *Chin. Phys.*, 2004, v. 13(2), 159.
39. Kennefick D. Einstein versus the Physical Review. *Physics Today*, September 2005.

On the Theory and Physics of the Aether

Ole D. Rughede

Copenhagen, DK-2200 N, Denmark

E-mail: ole.rughede@privat.dk

Physical Space is identified as the universal Aether Space. An Aether Equation is deduced, predicting the Temperature of the Cosmic Background Radiation T_{CMBR}, and indicating that G and c are universal dependent variables. The strong nuclear force is found to be a strong gravitational force at extreme energy densities of the neutron, indicating a Grand Unified Theory, when gravity is a process of enduring exchange of radiant energy between all astrophysical objects. The big bang hypothesis is refuted by interpretation of the Hubble redshift as evidence of gravitational work. Conditions for application of STR and GTR in the scientific cosmological research are deduced.

Gravity must be caused by an agent acting constantly according to certain laws; but whether this agent be material or immaterial, I have left to the consideration of my readers.

Newton. Letter to Bentley, 1693.

We assume to find in every point of space a flow in all directions of radiant energy from all astrophysical objects, meaning that space everywhere has a specific energy U [erg] and an energy density $u = U/V$ [erg/cm^3], which of course is a local variable depending on the position in space.

The radiant energy will we name the "Aether", and since it is present throughout the Universe, we will call space the "Aether-Space". Presuming the aether the medium sustaining all physical fields and forces, the aether-space is the universal physical space.

A set of equations can be found for this situation [1] from which may be derived the aether equation with the minimum energy U at the temperature T_{Aether}, which has been confirmed by the COBE observations of $T_{\text{CMBR}} = 2.735 \pm 0.06$ Kelvin [(1)]

$$\kappa UV = Ghc^2,$$

$$U = 3.973637 \times 10^{-13}\,\text{erg} \quad \text{at} \quad T_{\text{Aether}} = 2.692064\,\text{Kelvin},$$

$$K = Gc/\kappa L^2 = UL/hc = 2.000343 \times 10^3.$$

Defining $\kappa \equiv 1$ erg/(sec$\times$g^2) and $V = 1$ cm^3, it is seen that if U is a variable, then the Newtonian G and the velocity of light c are dependent variables if Planck's h is a universal constant.

At higher energy densities of the aether, such as in the galaxies, G and c would have other and higher values than $G = 6.672426 \times 10^{-8}$ cm^3/(g$\times$sec^2) and $c = 2.99792458 \times 10^{10}$ cm/sec of the aether equation and will need some coefficient ρ to G, while the maximum value of c is supposed from a possible coefficient function to be $c_{\max} = \sqrt{2}\,c$.

To have an idea of the extreme energy densities and their corresponding ρ-values, we will have a look at the Schwarzschild solution for the electron, from which to derive G: [(2)]

$$Gm_e/r_e c^2 = 1/\rho_e = Gm_e^2/e^2,$$

$$\rho_e G e^2 = c^4 r_e^2,$$

$$m_e = 9.109535 \times 10^{-28}\,\text{g},$$

$$e = 4.803242 \times 10^{-10}\,\text{esu},$$

$$r_e = 2.817937 \times 10^{-13}\,\text{cm},$$

$$\rho_e = 4.166705 \times 10^{42}.$$

Considering the composite neutron, the proton$^+$, and the neutron-meson$^-$ we find that the meson must be the mass difference between the neutron and the proton, and that the meson must be a special heavy neutron-electron, since the free neutron in relatively short time disintegrates into a proton, an electron, and some neutrino energy depending on the velocities and directions of the parting massive particles. We therefore have with α, the fine structure constant:

$$m_n = 1.674954 \times 10^{-24}\,\text{g},$$

$$m_p = 1.672648 \times 10^{-24}\,\text{g},$$

$$m_m = 2.305589 \times 10^{-27}\,\text{g},$$

$$m_p m_m/m_e^2 = \alpha K^2/2\pi = K^3 e^2/UL = \rho_e/\rho_{p,m} = 4.64723 \times 10^3,$$

$$\alpha = 7.297349 \times 10^{-3},$$

$$\rho_{p,m} = 8.965996 \times 10^{38}.$$

As an analogon to the Schwarzschild electron solution we find:

$$\rho_{p,m} G m_n/r_n c^2 = \rho_{p,m} G m_p m_m/e^2 = 1,$$

$r_n = 1.11492 \times 10^{-13}$ cm would then be the radius of the neutron, and if the proton is calculated with the same coefficient $\rho_{p,m}$,

$$\rho_{p,m} G m_p/r_p c^2 = 1,$$

$$r_p = 1.113386 \times 10^{-13}\,\text{cm}.$$

If the neutron-meson should in fact be a heavy electron, and $m_m/m_e \sim 2.53$, it would make sense if the mass-difference $m_m - m_e$ was the virtual gravitational mass of the neutron's intrinsic proton-electron pair, whence we find from a first calculation m_{vir}:

$$\rho_{p,m} G m_p m_e / r_n c^2 = 9.096998 \times 10^{-28} \text{ g},$$

$$\rho_{p,m} G m_p m_e / r_p c^2 = 9.109531 \times 10^{-28} \text{ g}.$$

We have hereby accounted for a neutron-meson of twice the electron's mass, while we need an explanation for the extra mass of $\frac{1}{2}$ electron-mass in the neutron-meson. We will abstain from further calculations here and for the moment consider it sufficient to have shown a double electron-mass in the meson, pointing to the self-gravitation also of the virtual mass as a probable solution to the deficiency of $\sim 4.83 \times 10^{-28}$ g meson-mass.

Regarding the self-gravitation of the neutron, it may be shown from a normalization of the neutron's gravitational potential P, that the potential with respect of the central proton, when the self-gravitation means an increment of the meson-mass from $\sim 2m_e$ to m_m, would result in a slightly greater value of ρ by a factor of $r_n/r_p = m_n/m_p = 1.001378$ [3] from $\rho_{p,m}$ to ρ_n, so that $\rho_n = 1.001378\, \rho_{p,m} = 8.978353 \times 10^{38}$. We then find from considering the gravitational potential of the neutron, as if produced by the central proton alone in the distance r_n, that it leads to the resulting potential

$$P = \rho_n G m_p / r_n = \rho_{p,m} G m_n / r_n = c^2,$$

$$\rho_n G m_p m_m / r_n = E_m .$$

$E_m = m_m c^2$ is the total energy of the heavily augmented neutron-electron to the full mass of the neutron-meson, $m_m = m_n - m_p$. That the virtual gravitational mass of the free neutron equals one electron-mass may be seen from the following equation, which interestingly shows the ratio between radii r_p and r_e. It appears then that all the relational conditions of the free neutron are completely deduced:

$$m_{\text{vir}} = \rho_{p,m} G m_p m_e / r_p c^2 = m_m r_p / r_e = e^2 / r_e c^2 = m_e ,$$

$$m_m = e^2 / r_p c^2 .$$

Having demonstrated that the Newtonian G must be a variable of very great values at extreme energy densities, such as in the composite neutron ($\rho_{p,m} G \sim 6 \times 10^{31}$), it seems reasonable to believe that the strong nuclear force is caused by such extreme values of the Newtonian gravitational factor.

We therefore assume that the neutron-meson would be able to bind two protons in the atomic nucleus by orbiting in such a way that it shifts constantly between the two protons, of which the one may be considered a neutron, when the other is a proton and vice versa in constant shifts of constitution in the neutron-proton pair of a nucleus.

The binding orbit may hence be thought of in a most simple theoretical illustration as the meson following an Oval of Cassini around the two heavy electrically positive charged particles, forcing them to the constant shifts of neutron-proton phase. And as will be known, the Lemniscate is the extreme curve of the Cassini Oval, with the parameters $a = b$, where the strong particle-binding would break in a proton and a free neutron that may possibly leave the nucleus.[4]

Of course, the real conditions of an "orbiting neutron-meson" cannot be made really lucid, since we know that the interaction is rather a question of probability of distribution of charges and masses, when we observe the weak magnetic moment of the electrically neutral neutron.

However, it seems that the strong nuclear force may be accounted for as a very strong gravitational force at extreme energy densities, to which it is remarked that in the galaxies, with their very intense radiation from stars and gasses, we may also expect special dynamics due to the variablility of the factor G, which would therefore account for the observed galactic differential velocities and probably would explain also the so-called "problem of missing mass in the Universe".

As in fact gravitational action according to the aether physics is an electromagnetic phenomenon of energy exchange in Planck quanta leaving an enduring train of impulses unto the gravitating masses, it seems that a unification of the four fundamental forces in nature may be expected from consideration of the physics of the aether.

From the aether equation we have found the constant K. Considering the composite neutron, $m_p + m_m = m_n$, we have the mass relation and the energy-charge relation:

$$(m_p m_m)/m_e^2 = K^3 (e^2/UL) = K^2 (e^2/hc),$$

$$E_e r_e = E_m r_p = E_p r_m = e^2 .$$

It further follows that $K\Phi/c = G m_x m_y / L^2$ for any pair of gravitating masses in mutual distance $L = 1$ cm, when the radiant flux Φ [erg/sec] is $\Phi_{x,y} = \kappa m_x m_y$.

We will therefore show that a radiant aether flux Φ is the common cause of the Coulomb force and the extremely strong force of gravity in the neutron, manifest as the strong nuclear force

$$e^2/r_n^2 = \rho_{p,m} [(K\Phi_{p,m})/c] \times [L^2/r_n^2] = \\ = \rho_{p,m} G m_p m_m / r_n^2 \text{ dynes},$$

$$e^2 c / r_n^2 = \rho_{p,m} K \Phi_{p,m} L^2 / r_n^2 = \rho_{p,m} G m_p m_m c / r_n^2 \text{ erg/sec},$$

$$e^2/m_p m_m = \rho_{p,m} K \kappa L^2 / c = \rho_{p,m} \kappa U V / hc^2 = \rho_{p,m} G ,$$

$$e^2/G = \rho_{p,m} m_p m_m = M_{\text{JS}}^2 .$$

For any pair of fundamental particles of unit charge $\pm$ esu there seems to exist a dimensionless factor of proportionality $\rho_{1,2}$, which, if made a coefficient of G, will balance the electrostatic Coulomb force and the Newtonian force of

gravity at any distance between the charged particles. For any charged pair of $mass_1$ and $mass_2$ the factor of proportionality will be ρ with the Johnstone-Stoney mass squared e^2/G as a constant: $\rho_{1,2} = M_{\text{JS}}^2/(m_1 m_2)$.

Demonstrating the validity of the foregoing derivations, it may be shown that, with the magnitude found for the coefficient $\rho_{p,m}$, the dimensions r_n, r_p, and r_m of the neutron masses m_n, m_p, and m_m are most easily given by the following simple relations:

$$\rho K \kappa m L^2/c^3 = \rho G m/c^2 = r\,;$$

as is with ρ_e and m_e the Schwarzschild radius of the electron r_e.

Generally, provided a local value of ρ can be found or estimated, the local gravitational potential P at any distance R from the center of a gravitating mass M will be:

$$P = \rho GM/R \text{ (cm/sec)}^2.$$

When, however, all ponderable matter is constituted as a sum of charged particles, and the force of gravity as shown is an electromagnetic phenomenon by energy exchange in the aether space between any pair of masses via a radiant flux Φ [erg/sec], which is proportional to the product of the two masses, we generally have with some local value of ρ the Newtonian force between M_1 and M_2:

$$F = \rho GM_1M_2/R^2 = \rho \kappa M_1 M_2 UV/hc^2R^2 = \\ = \rho K[\Phi/c] \times [L^2/R^2] \text{ dynes}.$$

The radiant flux $K\Phi$ may be thought of as aether energy at the velocity of light, which is bound in the line of distance R between the gravitating masses, representing the gravitational energy $K\Phi L^2/Rc$ and the equivalent virtual gravitational mass $K\Phi L^2/Rc^3$ that belongs to the binary system. It should therefore be added to the sum of gravitating masses for calculations of total potential and force including the self-gravitation of the aether energy in Φ.

In the composite neutron, however, only two elementary charges are acting, the proton's $+e$ esu and the meson-electron's $-e$ esu. The latter is an ordinary electron, when the neutron disintegrates, and we have no idea whatsoever of a variation in the elementary charge $e = 4.803242 \times 10^{-10}$ esu. We conclude from the neutron equation, as from Schwarzschild's electron solution:

$$e^2/r_n^2 = \rho_{p,m} G m_p m_m/r_n^2\,,$$

$$e^2/m_p m_m = \rho_{p,m} G\,,$$

that gravity is an electromagnetic phenomenon, and that it is the relation shown herein between charges and masses which governs the gravitational force between the neutron's proton and electron at the extreme energy density of the free neutron.

Presumably, it is the gravitational interaction between the free neutron and all other masses in the aether space, by enduring energy exchange with the radiant energy of the aether, that makes the neutron unstable by emitting more energy to the aether field than is absorbed in the same interval of time. This loss of energy is by radiation at the cost of the meson-mass, which diminishes, meaning a loss of mass and of the neutron's energy density, thereby a reduction of the coefficient ρ, of G. That means an increase in r_n, the radius of the free neutron, to a considerably greater dimension as a so-called "cold neutron" until the proton and the neutron-electron part with a random measure of the electron-meson's binding energy as a massless supply of neutrino-energy to the aether.

The aether energy represented in the radiant flux Φ is, according to the theory, present in the aether space of infinite energy as random radiation at all wavelengths and in all directions to and from the gravitating systems. Therefore the action of gravity is immediate, say if one of the gravitating masses is suddenly increased, while any change in the gravitating system will result in a signal which propagates in the aether space as a gravitational wave with the velocity of light. Such a signal may therefore be thought of as a modulation of the present radiant aether energy. The flux Φ is not a flow of energy from mass 1 to mass 2 and back again. It is a result of the energy exchange in all directions between the aether and the complete system and its single gravitating masses. According to the aether theory we have:

$$\alpha(Km_e)^2 = 2\pi m_p m_m \text{ g}^2,$$

$$\Updownarrow$$

$$[e^2/h\nu] \times [Gm_e^2/\lambda^2] = [L\Phi_{p,m}/U] \times [h/\lambda] \text{ erg}\,.$$

Aether energy which is absorbed by a mass is immediately re-emitted randomly to the aether, and in all directions. The action of gravity means work by impulses $h\nu/c = h/\lambda$ both at absorption and radiation of energy, while reflection means a double-pulse [2]. The gravitational work done by the aether causes an increasing loss of aether energy, shown in the Hubble-effect of increasing redshift with distance of all light from distant sources. The universal redshift thus is evidence of gravitational work, and not of any universal expansion interpreted as a Doppler-effect. The redshift is in complete accordance with the gravitational effect described by Einstein's theory of relativity, where we have to discriminate between two types of gravitational effects: (1) the local redshift of a single mass also deflecting passing rays of light; (2) the redshift of distance called the Hubble redshift.

The speculative big-bang hypothesis therefore seems absurd and way beyond rational science, since General Relativity has meaning only in application to a finite physical space of known and observable contents of masses and energy, while the Universe is for all reasons of an infinite mightiness beyond some apparent limit of observation, and

when the idea of the Newtonian gravitational factor G as an universal constant cannot be upheld. The multitude of individual "galactic worlds" of very different types and ages in some general ongoing process of creation and decay by age should, on the other hand, be an obvious goal for scientific cosmological research.

The loss of energy to gravitational work is replenished by the stars and all the energy producing astrophysical objects by irradiation of new energy into the aether space at the cost of their masses. It seems clear that there ought to exist a feedback effect working to keep the aether at a constant energy level, which, however, may be left to future research.

The replenishment of free radiant energy to the aether-space by irradiation of Planck quanta at the velocity of light is, as seen from the aether equation, regardless of any local coefficient ρ:

$$h\nu/c = \kappa UV/(Gc^2\lambda) = (U/Kc) \times L/\lambda\,;$$

$$Kh\nu = U \times L/\lambda\,.$$

By the foregoing presentation of the theory and physics of the aether we have shown that gravitation is an electromagnetic phenomenon, and that the force of gravity is the result of an enduring exchange of radiant energy between mass and aether, by which the energy of the fundamental particles fluctuates consistently with the QED-findings regarding the fundamental charge/mass proportion of the electron.

The theory of the aether thereby seems to confirm also Einstein's finding 1928 [3] that "The separation of the gravitational and the electromagnetic field appears artificial", — when, of course, the aether-space is the seat of all physical fields and forces.

In modern 5-dimensional Kaluza-Klein Theory the specific space energy of the aether, or some identical local aether-parameter, such as for instance T_{Aether} Kelvin, would apparently represent the 5th dimension.

Provided the speculative unphysical STR is defined with a local energy density u of the aether space, and with the condition that u shall be constant all over the actual physical space, ensuring a constant light-velocity c, the Special Theory of Relativity is a valid physical theory confirmed by observations.

Provided in any application of GTR the λ-term is defined with the parameters of a black body radiation of energy density u at the temperature $\mathrm{T}_{\text{Aether}}$ in the actual finite physical aether space, and provided the local coefficient ρ to the Einsteinian gravitational factor χ is estimated correct, the General Theory of Relativity may be applied to a first approximation.

STR and GTR thereby should be useful sub-theories in the Theory and Physics of the Aether which, as here described, appears as a natural continuation and extension of Drude's famous *Physik des Aethers* [4]. In thermodynamics it should be noted that gravitational energy exchange by radiation is a reversible process in open systems, therefore in no matter of the 2nd law.

Acknowledgements

I am indebted to Mr. Jeppe Kabell for the typesetting in LaTeX, and for his meticulous and patient help in corrections and proof-readings. For kind encouragements I thank with special gratitude the late professors Joseph Weber and Paul E. Kustanheimo, as also Emeritus Professor Bent Elbek, Professor Holger Bech Nielsen, Dr. Ole Remmer, and M. Sc. Frank Mundt.

Endnotes

(1) Since the aether is a perfect boson-gas, we have with $a = 8\pi V/c^3$ and $b = kT/h$, when $\zeta(x)$ is the Riemann ζ-function, $L = 1$ cm, $V = 1\,\text{cm}^3$, $m = 1$ g the following solutions:

$$pV/kT = a2b^3\zeta(4)\,, \qquad U = ah6b^4\zeta(4)\,;$$

$$p = u/3\,, \qquad pV = U/3\,;$$

$$R/N = R_G/N_A = k = 1.380662\times10^{-16} \text{ erg/Kelvin};$$

$$RT = ah2b^4\zeta(3) = kTN\,;$$

$$R_{\text{Aether}} = 5.464489\times10^{-14} \text{ erg/Kelvin}\,;$$

$$N_{\text{Aether}} = a2b^3\zeta(3) = 3.957876\times10^2;$$

$$S = 4U/3T = R\zeta(4)/\zeta(3) = 4Ghc^2/3kVT\,;$$

$$S_{\text{Aether}} = 1.968074\times10^{-13} \text{ erg/Kelvin}\,;$$

$$\kappa = \Phi/m^2 = \chi hc^4/8\pi UV = 4Ghc^2/3SVT\,;$$

$$\chi = \text{Einstein's gravitational factor}\,;$$

$$\Phi/L^2 = (Gm^2/L^2) \times (4hc^2/3SVT) = \kappa m^2/L^2.$$

(2) When for every mass m it holds that $E = mc^2$, and the de Broglie wavelength $\lambda_{\text{B}} = h/mv$, we have for $v = c$ that $E_m\lambda_{\text{B}=\text{C}} = hc$. When further the fine structure constant is $\alpha = 2\pi e^2/hc$, a precise theoretical value of the Newtonian G may be derived from iterations on the shown Schwarzschild solution for the electron and the very well known value of α.

This theoretical value of G, which of all physical magnitudes is the most difficult to measure experimentally, is the universal Newtonian constant $G = 6.672426\times10^{-8}$ $\text{cm}^3/(\text{g}\times\text{sec}^2)$ at the minimum specific energy of the aether at the defined universal mimimum temperature $T_{\text{Aether}} = 2.692064$ Kelvin $= T_{\text{CMBR}}$ according to the theory of the aether. At any higher aether temperature $T_{\text{Aether}} > T_{\text{CMBR}}$, thus at a proportionally greater local energy density u erg/cm^3, $u_{\text{Aether}} > u_{\text{CMBR}}$, the Newtonian constant becomes a variable: $\rho G > G_{\text{CMBR}}$ by a dimensionless coefficient of proportionality.

According to the aether equation we furthermore find $KE_m\lambda_{\text{C}} = UL$, confirming the derived magnitudes of U and G with utmost precision; thereby also the predicted temperature T_{Aether} comparable with the experimental value from measurements of T_{CMBR}.

The relation $K = UL/E_m\lambda_C = UL/hc$ may be of interest in particle physics as in wave mechanics, since according to Planck the fundamental particles may be regarded as oscillating electromagnetic energy in standing waves, with the oscillator parameters L [cm] and C [Farad], in which case we have for the elementary charged particles of energy E_m, and besides for the electron of energy $E_e = m_e c^2$ especially: $E_m = h\nu = mc^2 = hc/\lambda_{B=C} = mLC\omega^2$; $E_e = E_{m(e)} = = e^2/r_e$.

(3) One finds from the small factor $1.001378 = r_n/r_p = m_n/m_p$,

$$r_n m_p/r_p m_n = r_e m_e/r_p m_m = 1\,,$$

$$r_e m_e = e^2 m_e/m_e c^2 = e^2/c^2 = r_p m_m\,,$$

$$r_n m_p/r_e m_e = r_n/r'_p = r_n/(r_n - r_p)\,,$$

$$r_n - r_p = r'_p = e^2/m_p c^2\,,$$

$$r_e m_e m_n/m_m m_p r_n = 1\,,$$

$$[e^2/m_m m_p] \times m_n/r_n c^2 = 1\,,$$

$$e^2/(m_m m_p) = \rho_{p,m} G\,,$$

$$e^2/G = \rho_{p,m} m_m m_p = M_{JS}^2\,,$$

$$\rho_{p,m} G m_n/r_n = c^2,$$

that both $\rho_{p,m}G$ and the Johnstone-Stoney mass M_{JS}^2 can be derived with extreme precision alone from the found dimensions r_x and masses m_x, when at the same time showing correctly that the meson-mass m_m and the proton-mass m_p are both charged with e esu, whereas no electric charge occurs at the neutron m_n. It is such an overwhelming demonstration of the valid derivation of all the found dimensions, that no doubt seems possible.

The small extension $r'_p = 1.534 \times 10^{-16}$ cm of space the proton-radius up to the neutron-radius, which in fact would be the radius r'_p of the proton, if calculated strictly like the radius of the electron according to the Schwarzschild solution, is the thickness of an outer spherical shell surrounding the central proton of the free neutron, is why we may say that the volume of this spherical shell of extremely narrow depth r'_p is the location of the bound heavy neutron-meson.

Calculation of $r'_n = 1.532 \times 10^{-16}$ cm $= e^2/m_n c^2$ retains the ratio $1.001378 = r'_p/r'_n$ and the exceedingly small difference $r'_p - r'_n = 2.113 \times 10^{-19}$ cm < 0.002 pro mille of the neutron radius r_n. If of any relevance at all, it will have to await the results and precision of future research.

(4) From two protons in a torus of radii r_p and r_e may be generated the family of Cassini Ovals in planes parallel with the torus axis. The Lemniscate may be seen in a section cut in a plane parallel to the axis through a point on the inside of the torus, i. e. in the distance $(r_e - r_p)$ from the axis.

The mutual distance of the protons in the Lemniscate is $2\sqrt{(r_e)^2 - (r_e - r_p)^2} = 4.488 \times 10^{-13}$ cm, or $4.031 \times r_p$ cm apart (according to Pythagorean calculation).

In case of a change of radii, $r_e \to r_p$, or contrary $r_p \to r_e$, the torus will degenerate into a non-Riemannian surface with one singularity in the axis.

References

1. Yourgrau W., van der Merwe A., Raw G. Treatise on irreversible and statistical thermodynamics. The Macmillan Company, N.Y., 1966, Chap. 3–9, 10, Statistics of a photon gas. Blackbody radiation and the laws of Planck and Stefan. (The Dover edition 1982 is an unabridged and extensively corrected republication).
2. Einstein A. Zur Quantentheorie der Strahlung. *Physikalische Zeitschrift*, XVIII, Leipzig 1917, 121–128.
3. Einstein A. Neue Möglichkeit für eine einheitliche Feldtheorie von Gravitation und Elektrizität. *Sitzungber. K. Preuss. Akad. Wissenschaften*, Phys.-Math. Klasse, Berlin 1928, 224–227.
4. Drude P. Physik des Aethers auf Elektromagnetischer Grundlage. Stuttgart, Verlag von Ferdinand Enke, 1894.

Open Letter by the Editor-in-Chief

Declaration of Academic Freedom

(Scientific Human Rights)

Article 1: Preamble

The beginning of the 21st century reflects more than at any other time in the history of Mankind, the depth and significance of the role of science and technology in human affairs.

The powerfully pervasive nature of modern science and technology has given rise to a commonplace perception that further key discoveries can be made principally or solely by large government or corporation funded research groups with access to enormously expensive instrumentation and hordes of support personnel.

The common perception is however, mythical, and belies the true nature of how scientific discoveries are really made. Large and expensive technological projects, howsoever complex, are but the result of the application of the profound scientific insights of small groups of dedicated researchers or lone scientists, often working in isolation. A scientist working alone is now and in the future, just as in the past, able to make a discovery that can substantially influence the fate of humanity and change the face of the whole planet upon which we so insignificantly dwell.

Groundbreaking discoveries are generally made by individuals working in subordinate positions within government agencies, research and teaching institutions, or commercial enterprises. Consequently, the researcher is all too often constrained or suppressed by institution and corporation directors who, working to a different agenda, seek to control and apply scientific discovery and research for personal or organizational profit, or self-aggrandisement.

The historical record of scientific discovery is replete with instances of suppression and ridicule by establishment, yet in later years revealed and vindicated by the inexorable march of practical necessity and intellectual enlightenment. So too is the record blighted and besmirched by plagiarism and deliberate misrepresentation, perpetrated by the unscrupulous, motivated by envy and cupidity. And so it is today.

The aim of this Declaration is to uphold and further the fundamental doctrine that scientific research must be free of the latent and overt repressive influence of bureaucratic, political, religious and pecuniary directives, and that scientific creation is a human right no less than other such rights and forlorn hopes as propounded in international covenants and international law.

All supporting scientists shall abide by this Declaration, as an indication of solidarity with the concerned international scientific community, and to vouchsafe the rights of the citizenry of the world to unfettered scientific creation according to their individual skills and disposition, for the advancement of science and, to their utmost ability as decent citizens in an indecent world, the benefit of Mankind. Science and technology have been far too long the handmaidens of oppression.

Article 2: Who is a scientist

A scientist is any person who does science. Any person who collaborates with a scientist in developing and propounding ideas and data in research or application is also a scientist. The holding of a formal qualification is not a prerequisite for a person to be a scientist.

Article 3: Where is science produced

Scientific research can be carried out anywhere at all, for example, at a place of work, during a formal course of education, during a sponsored academic programme, in groups, or as an individual at home conducting independent inquiry.

Article 4: Freedom of choice of research theme

Many scientists working for higher research degrees or in other research programmes at academic institutions such as universities and colleges of advanced study, are prevented from working upon a research theme of their own choice by senior academic and/or administrative officials, not for lack of support facilities but instead because the academic hierarchy and/or other officials simply do not approve of the line of inquiry owing to its potential to upset mainstream dogma, favoured theories, or the funding of other projects that might be discredited by the proposed research. The authority of the orthodox majority is quite often evoked to scuttle a research project so that authority and budgets are not upset. This commonplace practice is a deliberate obstruction to free scientific thought, is unscientific in the extreme, and is criminal. It cannot be tolerated.

A scientist working for any academic institution, authority or agency, is to be completely free as to choice of a research theme, limited only by the material support and intellectual skills able to be offered by the educational institution, agency or authority. If a scientist carries out research as a member of a collaborative group, the research directors and team leaders shall be limited to advisory and consulting roles in relation to choice of a relevant research theme by a scientist in the group.

Article 5: Freedom of choice of research methods

It is frequently the case that pressure is brought to bear upon a scientist by administrative personnel or senior academics in relation to a research programme conducted within an academic environment, to force a scientist to adopt research methods other than those the scientist has chosen, for no reason other than personal preference, bias, institutional policy, editorial dictates, or collective authority. This practice, which is quite widespread, is a deliberate denial of freedom of thought and cannot be permitted.

A non-commercial or academic scientist has the right to develop a research theme in any reasonable way and by any reasonable means he considers to be most effective. The final decision on how the research will be conducted is to be made by the scientist alone.

If a non-commercial or academic scientist works as a member of a collaborative non-commercial or academic team of scientists the project leaders and research directors shall have only advisory and consulting rights and shall not otherwise influence, mitigate or constrain the research methods or research theme of a scientist within the group.

Article 6: Freedom of participation and collaboration in research

There is a significant element of institutional rivalry in the practice of modern science, concomitant with elements of personal envy and the preservation of reputation at all costs, irrespective of the scientific realities. This has often led to scientists being prevented from enlisting the assistance of competent colleagues located at rival institutions or others without any academic affiliation. This practice is too a deliberate obstruction to scientific progress.

If a non-commercial scientist requires the assistance of another person and that other person is so agreed, the scientist is at liberty to invite that person to lend any and all assistance, provided the assistance is within an associated research budget. If the assistance is independent of budget considerations the scientist is at liberty to engage the assisting person at his sole discretion, free of any interference whatsoever by any other person whomsoever.

Article 7: Freedom of disagreement in scientific discussion

Owing to furtive jealousy and vested interest, modern science abhors open discussion and wilfully banishes those scientists who question the orthodox views. Very often, scientists of outstanding ability, who point out deficiencies in current theory or interpretation of data, are labelled as crackpots, so that their views can be conveniently ignored. They are derided publicly and privately and are systematically barred from scientific conventions, seminars and colloquia so that their ideas cannot find an audience. Deliberate falsification of data and misrepresentation of theory are now frequent tools of the unscrupulous in the suppression of facts, both technical and historical. International committees of scientific miscreants have been formed and these committees host and direct international conventions at which only their acolytes are permitted to present papers, irrespective of the quality of the content. These committees extract large sums of money from the public purse to fund their sponsored projects, by resort to deception and lie. Any objection to their proposals on scientific grounds is silenced by any means at their disposal, so that money can continue to flow into their project accounts, and guarantee them well-paid jobs. Opposing scientists have been sacked at their behest; others have been prevented from securing academic appointments by a network of corrupt accomplices. In other situations some have been expelled from candidature in higher degree programmes such as the PhD, for expressing ideas that undermine a fashionable theory, however longstanding that orthodox theory might be. The fundamental fact that no scientific theory is definite and inviolable, and is therefore open to discussion and re-examination, they thoroughly ignore. So too do they ignore the fact that a phenomenon may have a number of plausible explanations, and maliciously discredit any explanation that does not accord with orthodox opinion, resorting without demur to the use of unscientific arguments to justify their biased opinions.

All scientists shall be free to discuss their research and the research of others without fear of public or private materially groundless ridicule, or be accused, disparaged, impugned or otherwise discredited by unsubstantiated allegations. No scientist shall be put in a position by which livelihood or reputation will be at risk owing to expression of a scientific opinion. Freedom of scientific expression shall be paramount. The use of authority in rebuttal of a scientific argument is not scientific and shall not be used to gag, suppress, intimidate, ostracise, or otherwise coerce or bar a scientist. Deliberate suppression of scientific facts or arguments either by act or omission, and the deliberate doctoring of data to support an argument or to discredit an opposing view is scientific fraud, amounting to a scientific crime. Principles of evidence shall guide all scientific discussion, be that evidence physical or theoretical or a combination thereof.

Article 8: Freedom to publish scientific results

A deplorable censorship of scientific papers has now become the standard practice of the editorial boards of major journals and electronic archives, and their bands of alleged expert referees. The referees are for the most part protected by anonymity so that an author cannot verify their alleged expertise. Papers are now routinely rejected if the author disagrees with or contradicts preferred theory and the mainstream orthodoxy. Many papers are now rejected automatically by virtue of the appearance in the author list of a

particular scientist who has not found favour with the editors, the referees, or other expert censors, without any regard whatsoever for the contents of the paper. There is a blacklisting of dissenting scientists and this list is communicated between participating editorial boards. This all amounts to gross bias and a culpable suppression of free thinking, and are to be condemned by the international scientific community.

All scientists shall have the right to present their scientific research results, in whole or in part, at relevant scientific conferences, and to publish the same in printed scientific journals, electronic archives, and any other media. No scientist shall have their papers or reports rejected when submitted for publication in scientific journals, electronic archives, or other media, simply because their work questions current majority opinion, conflicts with the views of an editorial board, undermines the bases of other current or planned research projects by other scientists, is in conflict with any political dogma or religious creed, or the personal opinion of another, and no scientist shall be blacklisted or otherwise censured and prevented from publication by any other person whomsoever. No scientist shall block, modify, or otherwise interfere with the publication of a scientist's work in the promise of any presents or other bribes whatsoever.

Article 9: Co-authoring of scientific papers

It is a poorly kept secret in scientific circles that many co-authors of research papers actually have little or nothing to do with the research reported therein. Many supervisors of graduate students, for instance, are not averse to putting their names to papers written by those persons who are but nominally working under their supervision. In many such cases, the person who actually writes the paper has an intellect superior to the nominal supervisor. In other situations, again for the purposes of notoriety, reputation, money, prestige, and the like, non-participating persons are included in a paper as co-author. The actual authors of such papers can only object at risk of being subsequently penalised in some way, or even being expelled from candidature for their higher research degree or from the research team, as the case may be. Many have actually been expelled under such circumstances. This appalling practice cannot be tolerated. Only those persons responsible for the research should be accredited authorship.

No scientist shall invite another person to be included and no scientist shall allow their name to be included as a co-author of a scientific paper if they did not significantly contribute to the research reported in the paper. No scientist shall allow himself or herself to be coerced by any representative of an academic institution, corporation, government agency, or any other person, to include their name as a co-author concerning research they did not significantly contribute to, and no scientist shall allow their name to be used as co-author in exchange for any presents or other bribes. No person shall induce or attempt to induce a scientist in howsoever a way to allow that scientist's name to be included as a co-author of a scientific paper concerning matters to which they did not significantly contribute.

Article 10: Independence of affiliation

Many scientists are now employed under short-term contracts. With the termination of the employment contract, so too is the academic affiliation. It is often the policy of editorial boards that persons without an academic or commercial affiliation will not be published. In the absence of affiliation many resources are not available to the scientist, and opportunities to present talks and papers at conferences are reduced. This is a vicious practice that must be stopped. Science does not recognise affiliation.

No scientist shall be prevented from presenting papers at conferences, colloquia or seminars, from publication in any media, from access to academic libraries or scientific publications, from attending scientific meetings, or from giving lectures, for want of an affiliation with an academic institution, scientific institute, government or commercial laboratory, or any other organisation.

Article 11: Open access to scientific information

Most specialised books on scientific matters and many scientific journals render little or no profit so that commercial publishers are unwilling to publish them without a contribution of money from academic institutions, government agencies, philanthropic foundations, and the like. Under such circumstances commercial publishers should allow free access to electronic versions of the publications, and strive to keep the cost of the printed materials to a minimum.

All scientists shall strive to ensure that their research papers are available to the international scientific community free of charge, or in the alternative, if it cannot be avoided, at minimum cost. All scientists should take active measures to make their technical books available at the lowest possible cost so that scientific information can be available to the wider international scientific community.

Article 12: Ethical responsibility of scientists

History testifies that scientific discoveries are used for ends both good and evil, for the benefit of some and the destruction of others. Since the progress of science and technology cannot stop, some means for the containment of malevolent application should be established. Only a democratically elected government, free of religious, racial and other bias, can safeguard civilisation. Only democratically elected government, tribunals and committees can safeguard the right of free scientific creation. Today, various undemocratic states and totalitarian regimes conduct active research into nuclear physics, chemistry, virology, genetic engineering, etc in order

to produce nuclear, chemical and biological weapons. No scientist should willingly collaborate with undemocratic states or totalitarian regimes. Any scientist coerced into work on the development of weapons for such states should find ways and means to slow the progress of research programmes and to reduce scientific output so that civilisation and democracy can ultimately prevail.

All scientists bear a moral responsibility for their scientific creations and discoveries. No scientist shall willingly engage in the design or construction of weapons of any sort whatsoever for undemocratic states or totalitarian regimes or allow his or her scientific skills and knowledge to be applied to the development of anything whatsoever injurious to Mankind. A scientist shall live by the dictum that all undemocratic government and the violation of human rights is crime.

November 22, 2005 *Dmitri Rabounski*

Editor-in-Chief,
Progress in Physics

The Journal on Advanced Studies in Theoretical and Experimental Physics, including Related Themes from Mathematics

PROGRESS IN PHYSICS

A quarterly issue scientific journal, registered with the Library of Congress (DC, USA). This journal is peer reviewed and included in the abstracting and indexing coverage of: Mathematical Reviews and MathSciNet (AMS, USA), DOAJ of Lund University (Sweden), Zentralblatt MATH (Germany), Referativnyi Zhurnal VINITI (Russia), etc.

Electronic version of this journal:
http://www.geocities.com/ptep_online

To order printed issues of this journal, contact the Editor in Chief.

Department of Mathematics, University of New Mexico, 200 College Road, Gallup, NM 87301, USA

This journal is powered by LaTeX

A variety of books can be downloaded free from the Digital Library of Science:
http://www.gallup.unm.edu/∼smarandache

ISSN: 1555-5534 (print)
ISSN: 1555-5615 (online)

Standard Address Number: 297-5092
Printed in the United States of America

APRIL 2006 **VOLUME 2**

CONTENTS

Information for Authors and Subscribers

Progress in Physics has been created for publications on advanced studies in theoretical and experimental physics, including related themes from mathematics. All submitted papers should be professional, in good English, containing a brief review of a problem and obtained results.

All submissions should be designed in LaTeX format using *Progress in Physics* template. This template can be downloaded from *Progress in Physics* home page http://www.geocities.com/ptep_online. Abstract and the necessary information about author(s) should be included into the papers. To submit a paper, mail the file(s) to Chief Editor.

All submitted papers should be as brief as possible. Beginning from 2006 we accept only papers, no longer than 8 journal pages. Short articles are preferable.

All that has been accepted for the online issue of *Progress in Physics* is printed in the paper version of the journal. To order printed issues, contact Chief Editor.

This journal is non-commercial, academic edition. It is printed from private donations.

Correct Linearization of Einstein's Equations

Dmitri Rabounski
E-mail: rabounski@yahoo.com

Routinely, Einstein's equations are be reduced to a wave form (linearly independent of the second derivatives of the space metric) in the absence of gravitation, the space rotation and Christoffel's symbols. As shown herein, the origin of the problem is the use of the general covariant theory of measurement. Herein the wave form of Einstein's equations is obtained in terms of Zelmanov's chronometric invariants (physically observable projections on the observer's time line and spatial section). The equations so obtained depend solely upon the second derivatives, even for gravitation, the space rotation and Christoffel's symbols. The correct linearization proves that the Einstein equations are completely compatible with weak waves of the metric.

1 Introduction

Gravitational waves are routinely considered as weak waves of the space metric, whereby, one takes a Galilean metric $g^{(0)}_{\alpha\beta}$, whose components are $g^{(0)}_{00}=1$, $g^{(0)}_{0i}=0$, $g^{(0)}_{ik}=-\delta_{ik}$, and says: because gravitating matter is connected to the field of the metric tensor $g_{\alpha\beta}$ by Einstein's equations*

$$R_{\alpha\beta}-\frac{1}{2}\,g_{\alpha\beta}R=-\kappa\,T_{\alpha\beta}+\lambda g_{\alpha\beta}\,,\quad \kappa=\text{const}>0\,,$$

gravitational waves are weak perturbations $\zeta_{\alpha\beta}$ of the Galilean metric. Thus the common metric, consisting of the initially undeformed and wave parts, is $g_{\alpha\beta}=g^{(0)}_{\alpha\beta}+\zeta_{\alpha\beta}$.

According to the theory of partial differential equations, a wave of a field is a Hadamard break [1] in the derivatives of the field function along the hypersurface of the field equations (the wave front). The first derivative of a function at a point determines a direction tangential to it, while the second derivative determines a normal direction. Thus, if a surface in a tensor field is the front of the field wave, the second derivatives of this tensor have breaks there. It is possible to prove in relation to this case in a Riemannian space with the metric $g_{\alpha\beta}$, that d'Alembert's operator $\Box=g^{\alpha\beta}\nabla_\alpha\nabla_\beta$ of this field equals zero†. For instance, the wave field of a tensor $Q_{\mu\nu}$ is characterized by the d'Alembert equations $\Box Q_{\mu\nu}=0$.

We can apply the d'Alembert operator to any tensor field and equate it to be zero. For this reason any claims that waves of the space metric cannot exist are wrong, even from the purely mathematical viewpoint, independently of those deductions that the authors of those claims adduced.

So, the front of weak wave perturbations $\zeta_{\alpha\beta}$ of a Galilean metric $g^{(0)}_{\alpha\beta}$ is determined by breaks in their second derivatives, while the wave field $\zeta_{\alpha\beta}$ itself is characterized by the d'Alembert equations

$$\Box\zeta_{\alpha\beta}=0\,.$$

If the left side of the Einstein equations for the common metric $g_{\alpha\beta}=g^{(0)}_{\alpha\beta}+\zeta_{\alpha\beta}$ reduced to $\Box\zeta_{\alpha\beta}$,‡ the equations could be reduced to the form

$$a\Box\zeta_{\alpha\beta}=-\kappa\,T_{\alpha\beta}+\lambda g_{\alpha\beta}\,,\qquad \text{where}\quad a=\text{const}\,,$$

which, in the absence of matter, become the wave equations $\Box\zeta_{\alpha\beta}=0$, meaning that the perturbations $\zeta_{\alpha\beta}$ are waves.

As one calculates the left side of the Einstein equations for the common metric, he obtains a large number of terms where only one is $\Box\zeta_{\alpha\beta}$ with a numerical coefficient. Thus one concludes: the Einstein equations are non-linear with respect to the second derivatives of $\zeta_{\alpha\beta}$.

In order to prove gravitational waves, theory should lead to cancellation of all the non-linear terms, as argued by Eddington [2], and Landau and Lifshitz [3]. This process is so-called the *linearization* of the Einstein equations.

2 Problems with the linearization

There is much literature about why the non-linear terms can be cancelled (see Lichnerowicz [4] or Zakharov [5] for details). All the reasons depend upon one initial factor: the theory of measurements we use.

We know two theories of measurements in General Relativity: Einstein's theory of measurements and Zelmanov's theory of physically observable quantities. The first one was built by Einstein in the 1910's. Following him§, we consider the space-time volume of nearby events in order to find a particular reference frame satisfying the properties of our real laboratory. We then express our general covariant equations in terms of the chosen reference frame. Some terms drop out, because of the properties of the chosen reference frame. Briefly, as one calculates the Ricci tensor $R_{\alpha\beta}=g^{\mu\nu}R_{\alpha\mu\nu\beta}$ by the contraction of the Riemann-Christoffel tensor

*We write the Einstein equations in the main form containing the λ-term, because our consideration is outside a discussion of the λ-term.

†Note that the d'Alembert operator consists of the second derivatives.

‡Actually, this problem is to reduce the Ricci tensor for the common metric $g_{\alpha\beta}=g^{(0)}_{\alpha\beta}+\zeta_{\alpha\beta}$ to $\Box\zeta_{\alpha\beta}$.

§Einstein gave his theory of measurements partially in many papers. You can see the complete theory in Synge's book [6], for instance.

$$R_{\alpha\mu\nu\beta} = -\Gamma^{\sigma}_{\mu\beta}\,\Gamma_{\alpha\nu,\sigma} + \Gamma^{\sigma}_{\mu\nu}\,\Gamma_{\alpha\beta,\sigma} + \\ + \frac{1}{2}\left(\frac{\partial^2 g_{\mu\nu}}{\partial x^{\alpha}\partial x^{\beta}} + \frac{\partial^2 g_{\alpha\beta}}{\partial x^{\nu}\partial x^{\mu}} - \frac{\partial^2 g_{\alpha\nu}}{\partial x^{\mu}\partial x^{\beta}} - \frac{\partial^2 g_{\mu\beta}}{\partial x^{\alpha}\partial x^{\nu}}\right)$$

for $g_{\alpha\beta} = g^{(0)}_{\alpha\beta} + \zeta_{\alpha\beta}$ (see §105 in [3]), he can reduce it to

$$R_{\alpha\beta} = \frac{1}{2}\,g^{(0)\mu\nu}\frac{\partial^2\zeta_{\alpha\beta}}{\partial x^{\mu}\partial x^{\nu}} = \frac{1}{2}\,\Box\,\zeta_{\alpha\beta}$$

and the left side of the Einstein equations to $\Box\,\zeta_{\alpha\beta}$, only if:

1. The reference frame is free of forces of gravity;
2. The reference frame is free of rotation;
3. Christoffel's symbols $\Gamma^{\alpha}_{\mu\nu}$, containing the inhomogeneity of space, are all zero.

Of course, we can find a reference frame where the gravitational potential, the space rotation, and the Christoffel symbols are zero at a given point*. However they cannot be reduced to zero in an area. Moreover, a gravitational wave detector consists of two bodies located far away from each other. In a Weber solid-body detector the distance is several metres, while in a laser interferometer the distance can take even millions of kilometres, as LISA in a solar orbit. It is wrong to interpret any of those as points. So, gravitational forces, the space rotation or the Christoffel symbols cannot be obviated in the equations. This is the main reason why:

> By the methods of Einstein's theory of measurements, the Einstein equations cannot be mathematically correctly linearized with respect to the second derivatives of the weak perturbations $\zeta_{\alpha\beta}$ of the space metric.

Some understand this incompatibility to mean that General Relativity does not permit weak waves of the metric.

This is absolutely wrong, even from the purely mathematical viewpoint: the d'Alembert operator $\Box = g^{\alpha\beta}\,\nabla_{\alpha}\nabla_{\beta}$ may be applied to any tensor field, the field of the weak perturbations $\zeta_{\alpha\beta}$ of the metric included, and equated to zero.

This obvious incompatibility can arise for one or both of the following reasons:

1. Einstein's equations in their current form are insufficient to describe our real world;
2. Einstein's theory of measurements is inadequate for the four-dimensional pseudo-Riemannian space.

Einstein's equations were born of his intuition, only the left side thereof is derived from the geometry. However main experimental tests of General Relativity, proceeding from the equations, verify the theory. So, the equations are adequate for describing our real world to within a first approximation.

At the same time, Einstein's theory of measurements has many deficiencies. There are no clear methods for recognition of physically observable components of a tensor field. It set up so that the three-dimensional components of a world-vector field compose its spatially observable part, while the time component is its scalar potential. However this problem becomes confused for a tensor of higher rank, because it has time, spatial, and mixed (space-time) components. There are also other drawbacks (see [8], for instance).

The required mathematical methods have been found by Zelmanov, who, in 1944, fused them into a complete theory of physically observable quantities [9, 10, 11].

3 The theory of physically observable quantities

According to Zelmanov, each observer has his own spatial section, set up by a coordinate net spanned over his real reference rest-body and extended far away with its gravitational field. The net is replete with a system of synchronized clocks†. Physically observed by him are projections of world-quantities onto his time line and spatial section, made by the projection operators $b^{\alpha} = \frac{dx^{\alpha}}{ds}$ and $h_{\alpha\beta} = -g_{\alpha\beta} + b_{\alpha}b_{\beta}$. Chr.inv.-projections of a world-vector Q^{α} are $b_{\alpha}Q^{\alpha} = \frac{Q_0}{\sqrt{g_{00}}}$ and $h^{i}_{\alpha}Q^{\alpha} = Q^{i}$, while those of a 2nd rank world-tensor $Q^{\alpha\beta}$ are $b^{\alpha}b^{\beta}Q_{\alpha\beta} = \frac{Q_{00}}{g_{00}}$, $h^{i\alpha}b^{\beta}Q_{\alpha\beta} = \frac{Q^{i}_{0}}{\sqrt{g_{00}}}$, $h^{i}_{\alpha}h^{k}_{\beta}Q^{\alpha\beta} = Q^{ik}$. Physically observable properties of the space are determined by the non-commutativity of the chr.inv.-operators $\frac{{}^{*}\partial}{\partial t} = \frac{1}{\sqrt{g_{00}}}\frac{\partial}{\partial t}$ and $\frac{{}^{*}\partial}{\partial x^{i}} = \frac{\partial}{\partial x^{i}} + \frac{1}{c^2}v_i\frac{{}^{*}\partial}{\partial t}$, and the fact that the chr.inv.-metric tensor $h_{ik} = -g_{ik} + \frac{1}{c^2}v_iv_k$ may not be stationary. They are the chr.inv.-quantities: the gravitational inertial force F_i, the space rotation tensor A_{ik}, and the space deformational rates D_{ik}

$$F_i = \frac{1}{\sqrt{g_{00}}}\left(\frac{\partial \mathrm{w}}{\partial x^{i}} - \frac{\partial v_i}{\partial t}\right), \qquad \sqrt{g_{00}} = 1 - \frac{\mathrm{w}}{c^2},$$

$$A_{ik} = \frac{1}{2}\left(\frac{\partial v_k}{\partial x^{i}} - \frac{\partial v_i}{\partial x^{k}}\right) + \frac{1}{2c^2}\left(F_iv_k - F_kv_i\right), \quad v_i = -\frac{cg_{0i}}{\sqrt{g_{00}}},$$

$$D_{ik} = \frac{1}{2}\frac{{}^{*}\partial h_{ik}}{\partial t}, \quad D^{ik} = -\frac{1}{2}\frac{{}^{*}\partial h^{ik}}{\partial t}, \quad D = D^{k}_{k} = \frac{{}^{*}\partial \ln\sqrt{h}}{\partial t},$$

where w is gravitational potential, v_i is the linear velocity of the space rotation, $h = \det\|h_{ik}\|$, and $\sqrt{-g} = \sqrt{h}\,\sqrt{g_{00}}$. The chr.inv.-Christoffel symbols $\Delta^{i}_{jk} = h^{im}\Delta_{jk,m}$ are built like the usual $\Gamma^{\alpha}_{\mu\nu} = g^{\alpha\sigma}\Gamma_{\mu\nu,\sigma}$, using h_{ik} instead of $g_{\alpha\beta}$.

By analogy with the Riemann-Christoffel curvature tensor, Zelmanov derived the chr.inv.-curvature tensor‡

$$C_{lkij} = \frac{1}{4}\left(H_{lkij} - H_{jkil} + H_{klji} - H_{iljk}\right),$$

from which the contraction $C_{kj} = C^{\cdots i}_{kij\cdot} = h^{im}C_{kimj}$ gives the chr.inv.-scalar observable curvature $C = C^{j}_{j} = h^{lj}C_{lj}$.

*See §7 *Special Reference Frames* in Petrov's book [7].

†Projections onto such a spatial section are independent of transformations of the time coordinate — they are *chronometric invariants*.

‡Here $H^{\cdots j}_{lki\cdot} = \frac{{}^{*}\partial\Delta^{j}_{il}}{\partial x^{k}} - \frac{{}^{*}\partial\Delta^{j}_{kl}}{\partial x^{i}} + \Delta^{m}_{il}\Delta^{j}_{km} - \Delta^{m}_{kl}\Delta^{j}_{im}$.

4 Correct linearization of Einstein's equations

We now show that Einstein's equations expressed with physically observable quantities may be linearized without problems; proof that waves of weak perturbations of the space metric are fully compatible with the Einstein equations.

Zelmanov already deduced [9] the Einstein equations in chr.inv.-components (the chr.inv.-Einstein equations) in the absence of matter: —

$$\frac{{}^*\partial D}{\partial t} + D_{jl}D^{jl} + A_{jl}A^{lj} + \left({}^*\nabla_j - \frac{1}{c^2}F_j\right)F^j = 0\,,$$

$${}^*\nabla_j\left(h^{ij}D - D^{ij} - A^{ij}\right) + \frac{2}{c^2}F_jA^{ij} = 0\,,$$

$$\frac{{}^*\partial D_{ik}}{\partial t} - \left(D_{ij}+A_{ij}\right)\left(D^j_k + A^{\cdot j}_{k\cdot}\right) + D\,D_{ik} + 3A_{ij}A^{\cdot j}_{k\cdot} + \\ + \frac{1}{2}\left({}^*\nabla_iF_k + {}^*\nabla_kF_i\right) - \frac{1}{c^2}F_iF_k - c^2C_{ik} = 0\,,$$

where Zelmanov's ${}^*\nabla_k$ denotes the chr.inv.-derivative*.

The components of the metric $g_{\alpha\beta} = g^{(0)}_{\alpha\beta} + \zeta_{\alpha\beta}$, consisting of a Galilean metric and its weak perturbations, are†

$$\begin{array}{lll} g_{00} = 1 + \zeta_{00}\,, & g_{0i} = \zeta_{0i}\,, & g_{ik} = -\delta_{ik} + \zeta_{ik}\,, \\ g^{00} = 1 - \zeta^{00}, & g^{0i} = -\zeta^{0i}, & g^{ik} = -\delta^{ik} - \zeta^{ik}, \\ h_{ik} = \delta_{ik} - \zeta_{ik}, & h^i_k = \delta^i_k\,, & h^{ik} = \delta^{ik} + \zeta^{ik}. \end{array}$$

Because $\zeta_{\alpha\beta}$ are weak, the products of their components or derivatives vanish. In such a case,

$$F_i = \frac{c}{1+\zeta_{00}}\left(\frac{\partial\zeta_{0i}}{\partial t} - \frac{c}{2}\frac{\partial\zeta_{00}}{\partial x^i}\right),$$

$$A_{ik} = \frac{c}{\sqrt{1+\zeta_{00}}}\left(\frac{\partial\zeta_{0i}}{\partial x^k} - \frac{\partial\zeta_{0k}}{\partial x^i}\right),$$

$$D_{ik} = -\frac{1}{2\sqrt{1+\zeta_{00}}}\frac{\partial\zeta_{ik}}{\partial t}\,, \quad D = h^{ik}D_{ik} = \delta^{ik}D_{ik}\,,$$

$$C_{imnk} = \frac{\partial^2\zeta_{mk}}{\partial x^i\partial x^n} + \frac{\partial^2\zeta_{in}}{\partial x^m\partial x^k} - \frac{\partial^2\zeta_{mn}}{\partial x^i\partial x^k} - \frac{\partial^2\zeta_{ik}}{\partial x^m\partial x^n}\,.$$

After some algebra, we obtain the chr.inv.-Einstein equations for the metric $g_{\alpha\beta} = g^{(0)}_{\alpha\beta} + \zeta_{\alpha\beta}$:

$$\frac{1}{c^2\left(1+\zeta_{00}\right)}\frac{\partial^2\zeta}{\partial t^2} + \frac{\delta^{km}}{\left(1+\zeta_{00}\right)}\left(\frac{\partial^2\zeta_{00}}{\partial x^k\partial x^m} - \frac{2}{c}\frac{\partial^2\zeta_{0m}}{\partial x^k\partial t}\right) = 0\,,$$

$$\frac{\delta^{ij}}{c^2\sqrt{1+\zeta_{00}}}\frac{\partial^2\zeta}{\partial x^j\partial t} - \frac{1}{c^2\sqrt{1+\zeta_{00}}}\frac{\partial^2\zeta^{ij}}{\partial x^j\partial t} + \\ + \frac{2\,\delta^{im}\delta^{jn}}{c\sqrt{1+\zeta_{00}}}\left(\frac{\partial^2\zeta_{0m}}{\partial x^j\partial x^n} - \frac{\partial^2\zeta_{0n}}{\partial x^j\partial x^m}\right) = 0\,,$$

$$\frac{1}{c^2\left(1+\zeta_{00}\right)}\frac{\partial^2\zeta_{ik}}{\partial t^2} - \frac{1}{c\left(1+\zeta_{00}\right)}\left(\frac{\partial^2\zeta_{0k}}{\partial x^i\partial t} - \frac{\partial^2\zeta_{0i}}{\partial x^k\partial t}\right) + \\ + 2\delta^{mn}\left(\frac{\partial^2\zeta_{mk}}{\partial x^i\partial x^n} + \frac{\partial^2\zeta_{in}}{\partial x^m\partial x^k} - \frac{\partial^2\zeta_{mn}}{\partial x^i\partial x^k} - \frac{\partial^2\zeta_{ik}}{\partial x^m\partial x^n}\right) = 0\,.$$

Note that the obtained equations are functions of only the second derivatives of the weak perturbations of the space metric. So, the Einstein equations have been linearized, even in the presence of gravitational inertial forces and the space rotation. This implies: —

> By the methods of Zelmanov's mathematical theory of chronometric invariants (physically observable quantities), **the Einstein equations are linearized in a mathematically correct way**, i. e. without the assumption of a specific reference frame where there are no gravitational forces or the space rotation.

This is the mathematical proof to the statement: —

> Waves of the weak perturbations of the space metric are fully compatible with the Einstein equations.

*So ${}^*\nabla_kQ^i = \frac{{}^*\partial Q^i}{\partial x^k} + \Delta^i_{mk}Q^m$ and ${}^*\nabla_kQ_i = \frac{{}^*\partial Q_i}{\partial x^k} - \Delta^m_{ik}Q_m$ are the chr.inv.-derivatives of a chr.inv.-vector Q^i.

†The contravariant tensor $g^{\alpha\beta}$, determined by the main property $g_{\alpha\sigma}g^{\sigma\beta} = \delta^\beta_\alpha$ of the fundamental metric tensor as $\left(g^{(0)}_{\alpha\sigma} + \zeta_{\alpha\sigma}\right)g^{\sigma\beta} = \delta^\beta_\alpha$, is $g^{\alpha\beta} = g^{(0)\alpha\beta} - \zeta^{\alpha\beta}$, while its determinant is $g = g^{(0)}\left(1+\zeta\right)$. This is easy to check, taking into account that, because the values of the weak corrections $\zeta_{\alpha\beta}$ are infinitesimal, their products vanish; while we may move indices in $\zeta_{\alpha\beta}$ by the Galilean metric tensor $g^{(0)}_{\alpha\beta}$.

References

1. Hadamard J. Leçons sur la propagation des ondes et les équations de l'hydrodynamique. Paris, Hermann, 1903.
2. Eddington A. S. The mathematical theory of relativity. Cambridge University Press, Cambridge, 1924.
3. Landau L. D. and Lifshitz E. M. The classical theory of fields. GITTL, Moscow, 1939 (ref. with the 4th final exp. edition, Butterworth–Heinemann, 1980).
4. Lichnerowicz A. Théories relativistes de la gravitation de l'électromagnétisme. Paris, Masson, 1955.
5. Zakharov V. D. Gravitational waves in Einstein's theory of gravitation. Moscow, Nauka, 1972.
6. Synge J. L. Relativity: the General Theory. North Holland, Amsterdam, 1960.
7. Petrov A. Z. Einstein spaces. Pergamon, London, 1969.
8. Lo C. Y. Space contraction, local light speeds and the question of gauge in General Relativity. *Chineese Journal of Physics* (Taipei), 2003, v. 41(4), 332–342.
9. Zelmanov A. L. Chronometric invariants. Dissertation, 1944. CERN, EXT-2004-117, 236 pages.
10. Zelmanov A. L. Chronometric invariants and co-moving coordinates in the general relativity theory. *Doklady Acad. Nauk USSR*, 1956, v. 107 (6), 815–818.
11. Rabounski D. Zelmanov's anthropic principle and the infinite relativity principle. *Progress in Physics*, 2006, v. 1, 35–37.

Einstein's Equivalence Principle and Invalidity of Thorne's Theory for LIGO

C. Y. Lo
Applied and Pure Research Institute, 17 Newcastle Drive, Nashua, NH 03060, USA
E-mail: c_y_lo@yahoo.com; C_Y_Lo@alum.mit.edu

The theoretical foundation of LIGO's design is based on the equation of motion derived by Thorne. His formula, motivated by Einstein's theory of measurement, shows that the gravitational wave-induced displacement of a mass with respect to an object is proportional to the distance from the object. On the other hand, based on the observed bending of light and Einstein's equivalence principle, it is concluded that such induced displacement has nothing to do with the distance from another object. It is shown that the derivation of Thorne's formula has invalid assumptions that make it inapplicable to LIGO. This is a good counter example for those who claimed that Einstein's equivalence principle is not important or even irrelevant.

1 Introduction

Since the behavior of binary pulsars has been interpreted successfully as due to gravitational radiation [1, 2], the existence of gravitational waves is generally accepted. Moreover, the Maxwell Newton Approximation,(1) which generates gravitational waves, has been established independent of the Einstein equation [3]. However, a direct observation of the gravitational waves has not been successful because a gravitational wave is very weak in nature [4].

To obtain the required sensitivity of detection for gravitational waves, two gigantic laser interferometer gravitational wave observatories (LIGO) have been built.(2) Currently they represent the hope of detecting the gravitational waves directly. The confidence on these new apparatus is based on the perceived high sensitivity [5] that is designed according to Thorne's equation, which is motivated on Einstein's theory of measurement [6, 7].

Thorne's [8] equation of motion is as follows [9]:

$$m\frac{d^2\delta x^j}{dt^2} = \frac{1}{2}\, m\frac{\partial^2 h^{\rm TT}_{jk}}{\partial t^2}\, x^k, \qquad (1)$$

where δx^k is the displacement of the test particle with mass m from a fixed object, x^k is the Euclidean-like distance (or the particle's Cartesian coordinate position) of the test particle from the fixed object (at the original the space coordinates), and $h^{\rm TT}_{jk}$ is the first order of the dimensionless "gravitational wave field" that induces the displacement. Then the integration of equation (1) gives,

$$\delta x^j = \frac{1}{2}\, h^{\rm TT}_{jk} x^k. \qquad (2)$$

The superscript TT on the gravitational field is to remind us that the field is "transverse and traceless".

On the other hand, according to Einstein's equivalence principle [10], the Euclidean-like structure [11, 12] that determines the distance between two points is independent of gravity, and this is supported the observed bending of light. Thus, the displacement from a fixed object induced by gravitational wave, according the geodesic equation, has nothing to do with the distance between them (see Section 2). In this paper, it will be shown the errors related to eqs. (1) and (2).

2 Problems in the theory of Thorne

Now let us first derive, according the theory of Thorne [8], the induced phase delay in the interferometer. Since the sources of the gravitational waves are very far away, the waves look very nearly planar as they pass through the observer's proper reference frame.(3) If we orient the x, y, z spatial axes, so the propagation in the z direction, then the transversality of the waves and traceless mean that the non-zero components of the wave field are $h^{\rm TT}_{xx} = -h^{\rm TT}_{yy}$, $h^{\rm TT}_{xy} = h^{\rm TT}_{yx}$, called respectively the $+$ and $\times$-polarization. For a $(+)$-polarization, if the arm length of the interferometer is L, we have

$$\begin{aligned} \delta x(t) &= \frac{1}{2}\, L h_+(t) \qquad \text{for mass on } x \text{ axis,} \\ \delta y(t) &= -\frac{1}{2}\, L h_+(t) \quad \text{for mass on } y \text{ axis.} \end{aligned} \qquad (3)$$

For a light wavelength λ, if B is the number of bounce back and forth in the arms, the total phase delay is

$$\triangle\phi_{\rm T} = 8\pi B\,\frac{\delta x}{\lambda} = 4\pi B\,\frac{L}{\lambda}\, h_+ \,. \qquad (4)$$

Thus, the sensitivity of the interferometer would be increased with longer arms. If Einstein's theory of measurement was valid, then eq. (3) would be an expected result. This explains that eq. (1) was accepted. To show the errors, some detailed analysis is needed.

In a Local frame of free fall, Manasse and Misner [12] claimed that the metric have approximately,

$$-ds^2=(1+R_{0l0m}x^l x^m)dt^2+\left(\frac{4}{3}R_{0ljm}x^l x^m\right)dx^j dt- \\ -\left(\delta_{ij}-\frac{1}{3}R_{iljm}x^l x^m\right)dx^i dx^j-\mathrm{O}(|x^j|^3)dx^\alpha dx^\beta \quad (5)$$

accurate to the second order in small $|x^j|$. The observer in the free fall is located at the origin of the local frame. Eq. (5) is the equation (13.73) in Misner et al. [9]. In the next step (35.12), they claimed to have the equation,

$$\frac{D^2 n^j}{d\tau^2}=-R^j_{0k0}\,n^k=-R_{j0k0}\,n^k, \\ \text{where}\quad n^j=x^j_{\text{B}}-x^j_{\text{A}}=x^j_{\text{B}} \quad (6)$$

since $x^j_{\text{A}}=0$. In eq. (5), $|x^j|$ is restricted to be small. However, a problem in this derivation is that R_{j0k0} may not be the same at points A and B. Nevertheless, one may argue that $\Gamma^\mu_{\alpha\beta}=0$ at A, and (6) is reduced to

$$\frac{d^2 x^j_{\text{B}}}{d\tau^2}=-R_{j0k0}\,x^k_{\text{B}}=\frac{1}{2}\frac{\partial h^{\text{TT}}_{jk}}{\partial\tau^2}\,x^k_{\text{B}}\,. \quad (7)$$

If it is applied to the case of LIGO, one must show at least a miles long x^j_{B} could be regarded as very small as (5) requires. From the geodesic equation, clearly it is impossible to justify (7) for any frame of reference.

More important, since LIGO is built on the Earth, its frame of reference is not at free fall when gravitational waves are considered. The radius of the Earth is 6.3×10^3 km, but the expected gravitational wave length is only about 15 km [9]. Thus, the Earth can no longer be considered as a test particle when only the gravity of the Sun is considered. In other words, (5) and (7) are inapplicable to LIGO.

Note that Misner et al. [9] have mistaken Pauli's version(4) as Einstein's equivalence principle [10], it is natural that they made related mistakes. For instance, Thorne [15] incorrectly criticized Einstein's equivalence principle as follows:

"In deducing his principle of equivalence, Einstein ignored tidal gravitation forces; he pretended they do not exist. Einstein justified ignoring tidal forces by imagining that you (and your reference frame) are very small."

However, Einstein has already explained these problems. For instance, the problem of tidal forces was answered in Einstein's letter of 12 July 1953 to Rehtz [16] as follows:

"The equivalence principle does not assert that every gravitational field (e. g., the one associated with the Earth) can be produced by acceleration of the coordinate system. It only asserts that the qualities of physical space, as they present themselves from an accelerated coordinate system, represent a special case of the gravitational field."

Clearly, his principle is for a space where physical requirements are sufficiently satisfied.

In fact, Misner et al. [9] do not understand Einstein's equivalence principle and related theorems in Riemannian space [14, 17]. A simple and clear evidence is in their eq. (40.14) [9; p. 1107], and they got a physically incorrect conclusion on the local time of the Earth in the solar system. Moreover, Ohanian and Ruffini [5; p. 198] also ignored the Einstein-Minkowski condition and had the same problems as shown in their eq. (50). However, Liu [18], Straumann [19], Wald [20], and Weinberg [4] did not make the same mistake. Note that Ohanian, Ruffini, and Wheeler have proclaimed that they are non-believers of Einstein's principles [5].

3 Remarks

In the theory of Thorne, there are major errors because his understanding of Einstein's equivalence principle is inadequate. His equation was motivated by Einstein's theory of measurement, and the superficial consistency with such a theory makes many theorists had confidence on his equation. Now, it is clear that such a support from an invalid theory is proven to be useless. Because Misner et al. [9] do not understand Einstein's equivalence principle, they cannot see that Einstein's theory of measurement is not self-consistent [21, 22].

In addition, since LIGO is built on the Earth, the frame is not at free fall. The radius of the Earth is 6.3×10^3 km, but the expected gravitational wave length is only about 15 km [9]. Thus, the Earth cannot be regarded as a test particle for gravitational waves. Moreover, Thorne was not aware that the Einstein equation has no wave solution [1, 2]. Although Misner, Thorne, and Wheeler [9] claimed plane wave solutions exist, their derivation has been found to be invalid [2, 23]. The second problem has been resolved by a modified Einstein equation, and it has the Maxwell-Newton Approximation as the first order equation [1].

In short, the current theory on the detection of gravitational waves for LIGO is incorrect. The root of these problems is due to that they do not understand Einstein's equivalence principle.(5) Consequently, they also failed to see the Euclidean-like structure is necessary(6) in a physical space [12]. This is a very good counter example for those who believed the Einstein's equivalence principle is not important or even irrelevant [2]. The sensitivity of LIGO will be addressed in a separate paper [24].

Acknowledgments

The author gratefully acknowledge stimulating discussions with Richard C. Y. Hui and David P. Chan. Special thanks are to L. Borissova and D. Rabounski for valuable comments and useful suggestions. This work is supported in part by the Chan Foundation, Hong Kong.

Endnotes

[1] The Maxwell-Newton Approximation, whose sources are massive matter, could be identified as a special case of the so-called linearized approximation that has been found to be incompatible with Einstein equation for a dynamic situation [1].

[2] M. Bartusiak [25] has written an interesting book on the great efforts to build LIGO.

[3] Einstein equation has no physically valid wave solution because there is no term in Einstein's equation to accommodate the energy-stress tensor of a gravitational wave that must move with the wave [23]. Thus, a wave solution must come from the modified equation of 1995.

[4] Pauli's [26] version of the principle of equivalence was commonly but mistakenly regarded as Einstein's principle, although Einstein strongly objected to this version as a misinterpretation [15]. In fact, Misner, Thorne, and Wheeler [9; p. 386] falsely claimed that Einstein's equivalence principle is as follows:

"In any and every local Lorentz frame, anywhere and anytime in the universe, all the (Nongravitational) laws of physics must take on their familiar special-relativistic form. Equivalently, there is no way, by experiments confined to infinitestimally small regions of spacetime, to distinguish one local Lorentz frame in one region of spacetime frame any other local Lorentz frame in the same or any other region."

However, this is only an alternative version of Pauli's because the Einstein-Minkowski condition,[7] which requires that the local space in a free fall must have a local Lorentz frame, is missing.

[5] There are other surprises. In spite of Einstein's clarification, many theorists, including the editors of Nature, Physical Review, and Science, still do not fully understand special relativity, in particular $E = mc^2$ [27–30].

[6] An existence of the Euclidean-like structure (that Einstein [6] called as "in the sense of Euclidean geometry") is necessary for a physical space [11, 12]. The Euclidean-like structure is operationally defined in terms of spatial measurements essentially the same as Einstein defined the frame of reference for special relativity [31]. Since the attached measuring instruments and the coordinates being measured are under the influence of the same gravity, a Euclidean-like structure emerges from such measurements as if gravity did not exist.

[7] For the Einstein-Minkowski condition, Einstein [10] addressed only the metrics without a crossing space-time element. This creates a false impression that the Einstein-Minkowski condition is trivial.

References

1. Lo C. Y. *Astrophys. J.*, 1995, v. 455, 421.
2. Lo C. Y. *Phys. Essays*, 2000, v. 13(4), 527.
3. Lo C. Y. *Phys. Essays*, 1999, v. 12(3), 508.
4. Weinberg S. Gravitation and cosmology. John Wiley Inc., New York, 1972.
5. Ohanian H. C. & Ruffini R. Gravitation and spacetime. Norton, New York, 1994.
6. Einstein A., Lorentz H. A., Minkowski H., & Weyl H. The principle of Relativity. Dover, New York, 1923.
7. Landau L. D. & Lifshitz E. M. The classical theory of fields. Pergamon Press, New York, 1975.
8. Thorne K. S. Gravitational radiation. In *300 Years of Gravitation*. Eds. S. W. Hawking & W. Israel, Camb. Univ. Press, New York, 1987.
9. Misner C. W., Thorne K. S., & Wheeler J. A. Gravitation. Freeman, San Francisco, 1973.
10. Einstein A. The meaning of Relativity (1921). Princeton Univ. Press, 1954.
11. Lo C. Y. *Phys. Essays*, 2002, v. 15(3), 303.
12. Lo C. Y. *Chinese J. of Phys.*, 2003, v. 41(4), 233.
13. Lo C. Y. *Phys. Essays*, 2003, v. 16(1), 84–100.
14. Manasse F. K. & Misner C. W., *J. Math. Phys.*, 1963, v. 4, 735–745.
15. Thorne K. S. Black holes & time warps. Norton, New York, 1994.
16. Norton J. What was Einstein's principle of equivalence? *Einstein's Studies*, v. 1: Einstein and the history of General Relativity, Eds. D. Howard and J. Stachel (Birkhäuser).
17. Synge J. L. Relativity: The General Theory. North-Holland, Amsterdam, 1971.
18. Liu Liao. General Relativity. High Education Press, Shanghai, China), 1987, p. 42.
19. Straumann N. General Relativity and relativistic astrophysics. Springer, New York, 1984.
20. Wald R. M. General Relativity. The Univ.of Chicago Press, Chicago, 1984.
21. Lo C. Y. *Phys. Essays*, 2005, v. 18(4).
22. Lo C. Y. *Progress in Physics*, 2006, v. 1, 10.
23. Lo C. Y. *Phys. Essays*, 1997, v. 10(3), 424.
24. Lo C. Y. The detection of gravitational wave with the laser interferometer and Einstein's theoretical errors on measurements. *In preparation*.
25. Bartusiak M. Einstein's unfinished symphony. Berkley Books, New York, 2000.
26. Pauli W. Theory of Relativity. Pergamon Press, London, 1958, p. 163.
27. Lo C. Y. *Astrophys. J.*, 1997, 477, 700–704.
28. Lo C. Y. *Phys. Essays*, 1997, v. 10 (4), 540–545.
29. Lo C. Y. Remarks on interpretations of the Eötvös experiment and misunderstandings of $E = mc^2$. *In preparation*.
30. Lo C. Y. *Progress in Physics*, 2006, v. 1, 46.
31. Einstein A. The problem of space, ether, and the field in physics. In *Ideas and Opinions*, Dover, 1982.

3-Space In-Flow Theory of Gravity: Boreholes, Blackholes and the Fine Structure Constant

Reginald T. Cahill

School of Chemistry, Physics and Earth Sciences, Flinders University, Adelaide 5001, Australia

E-mail: Reg.Cahill@flinders.edu.au

A theory of 3-space explains the phenomenon of gravity as arising from the time-dependence and inhomogeneity of the differential flow of this 3-space. The emergent theory of gravity has two gravitational constants: $G_{\rm N}$ — Newton's constant, and a dimensionless constant α. Various experiments and astronomical observations have shown that α is the fine structure constant $\approx 1/137$. Here we analyse the Greenland Ice Shelf and Nevada Test Site borehole g anomalies, and confirm with increased precision this value of α. This and other successful tests of this theory of gravity, including the supermassive black holes in globular clusters and galaxies, and the "dark-matter" effect in spiral galaxies, shows the validity of this theory of gravity. This success implies that the non-relativistic Newtonian gravity was fundamentally flawed from the beginning, and that this flaw was inherited by the relativistic General Relativity theory of gravity.

1 Introduction

In the Newtonian theory of gravity [1] the Newtonian gravitational constant $G_{\rm N}$ determining the strength of this phenomenon is difficult to measure because of the extreme weakness of gravity. Originally determined in laboratory experiments by Cavendish [2] in 1798 using a torsion balance, Airy [3] in 1865 presented a different method which compared the gravity gradients above and below the surface of the Earth. Then if the matter density within the neighbourhood of the measurements is sufficiently uniform, or at most is horizontally layered and known, then such measurements then permitted $G_{\rm N}$ to be determined, as discussed below, if Newtonian gravity was indeed correct. Then the mass of the Earth can be computed from the value of g at the Earth's surface. However two anomalies have emerged for these two methods: (i) the Airy method has given gravity gradients that are inconsistent with Newtonian gravity, and (ii) the laboratory measurements of $G_{\rm N}$ using various geometries for the test masses have not converged despite ever increasing experimental sophistication and precision. There are other anomalies involving gravity such as the so-called "dark-matter" effect in spiral galaxies, the systematic effects related to the supermassive blackholes in globular clusters and elliptical galaxies, the Pioneer 10/11 deceleration anomaly, the so-called galactic 'dark-matter' networks, and others, all suggest that the phenomenon of gravity has not been understood even in the non-relativistic regime, and that a significant dynamical process has been overlooked in the Newtonian theory of gravity, and which is also missing from General Relativity.

The discovery of this missing dynamical process arose from experimental evidence [4, 8, 9] that a complex dynamical 3-space underlies reality. The evidence involves the repeated detection of the motion of the Earth relative to that 3-space using Michelson interferometers operating in gas mode [8], particularly the experiment by Miller in 1925/26 at Mt. Wilson, and the coaxial cable RF travel time measurements by Torr and Kolen in Utah in 1985, and the DeWitte experiment in 1991 in Brussels [8]. In all 7 such experiments are consistent with respect to speed and direction. It has been shown that effects caused by motion relative to this 3-space can mimic the formalism of spacetime, but that it is the 3-space that is "real", simply because it is directly observable [4].

The 3-space is in differential motion, that is one part has a velocity relative to other parts, and so involves a velocity field $\mathbf{v}(\mathbf{r}, t)$ description. To be specific this velocity field must be described relative to a frame of observers, but the formalism is such that the dynamical equations for this velocity field must transform covariantly under a change of observer. It has been shown [4, 6] that the phenomenon of gravity is a consequence of the time-dependence and inhomogeneities of $\mathbf{v}(\mathbf{r}, t)$. So the dynamical equations for $\mathbf{v}(\mathbf{r}, t)$ give rise to a new theory of gravity when combined with the generalised Schrödinger equation, and the generalised Maxwell and Dirac equations [10]. The equations for $\mathbf{v}(\mathbf{r}, t)$ involve the gravitational constant* G and a dimensionless constant that determines the strength of a new 3-space self-interaction effect, which is missing from both Newtonian Gravity and General Relativity. Experimental data has revealed [4, 5, 6] the remarkable discovery that this constant is the fine structure constant $\alpha \approx e^2/\hbar c \approx 1/137$. This dynamics then explains numerous gravitational anomalies, such as the borehole g anomaly, the so-called "dark matter" anomaly in the rotation speeds of spiral galaxies, and that the effective

*This is different from the Newtonian effective gravitational constant $G_{\rm N}$ defined later.

mass of the necessary black holes at the centre of spherical matter systems, such as globular clusters and spherical galaxies, is $\alpha/2$ times the total mass of these systems. This prediction has been confirmed by astronomical observations [7].

Here we analyse the Greenland and Nevada Test Site borehole g anomalies, and confirm with increased precision this value of α.

The occurrence of α suggests that space is itself a quantum system undergoing on-going classicalisation. Just such a proposal has arisen in *Process Physics* [4] which is an information-theoretic modelling of reality. There quantum space and matter arise in terms of the Quantum Homotopic Field Theory (QHFT) which, in turn, may be related to the standard model of matter. In the QHFT space at this quantum level is best described as a "quantum foam". So we interpret the observed fractal* 3-space as a classical approximation to this "quantum foam" [10].

2 Dynamical 3-space

Relative to some observer 3-space is described by a velocity field $\mathbf{v}(\mathbf{r},t)$. It is important to note that the coordinate $\mathbf{r}$ is not itself 3-space, rather it is merely a label for an element of 3-space that has velocity $\mathbf{v}$, relative to some observer. Also it is important to appreciate that this "moving" 3-space is not itself embedded in a "space"; the 3-space is all there is, although as noted above its deeper structure is that of a "quantum foam".

In the case of zero vorticity $\nabla\times\mathbf{v}=\mathbf{0}$ the 3-space dynamics is given by [4, 6], in the non-relativistic limit,

$$\nabla\cdot\left(\frac{\partial\mathbf{v}}{\partial t}+(\mathbf{v}\cdot\nabla)\mathbf{v}\right)+\frac{\alpha}{8}\left((\mathrm{tr}D)^2-\mathrm{tr}(D^2)\right)=-4\pi G\rho\,, \quad (1)$$

where ρ is the matter density, and where

$$D_{ij}=\frac{1}{2}\left(\frac{\partial v_i}{\partial x_j}+\frac{\partial v_j}{\partial x_i}\right). \quad (2)$$

The acceleration of an element of space is given by the Euler form

$$\mathbf{g}(\mathbf{r},t)\equiv\lim_{\Delta t\to 0}\frac{\mathbf{v}\left(\mathbf{r}+\mathbf{v}(\mathbf{r},t)\Delta t,t+\Delta t\right)-\mathbf{v}(\mathbf{r},t)}{\Delta t}=\\ =\frac{\partial\mathbf{v}}{\partial t}+(\mathbf{v}\cdot\nabla)\mathbf{v}\,. \quad (3)$$

It was shown in [10] that matter has the same acceleration† as (3), which gave a derivation of the equivalence principle as a quantum effect in the Schrödinger equation when uniquely generalised to include the interaction of the quantum system with the 3-space. These forms are mandated by Galilean covariance under change of observer‡. This minimalist non-relativistic modelling of the dynamics for the velocity field

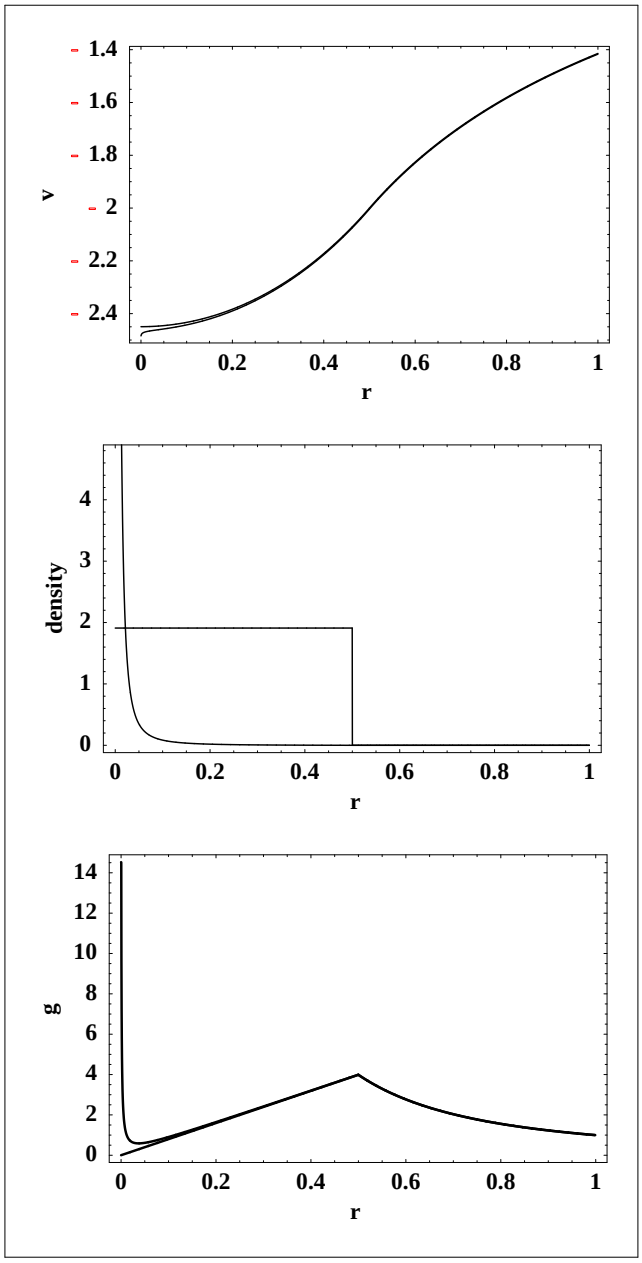

Fig. 1: Upper plot shows speeds from numerical iterative solution of (7) for a solid sphere with uniform density and radius $r=0.5$ for (i) upper curve the case $\alpha=0$ corresponding to Newtonian gravity, and (ii) lower curve with $\alpha=1/137$. These solutions only differ significantly near $r=0$. Middle plot shows matter density and "dark matter" density ρ_{DM}, from (5), with arbitrary scales. Lower plot shows the acceleration from (3) for (i) the Newtonian in-flow from the upper plot, and (ii) from the $\alpha=1/137$ case. The difference is only significant near $r=0$. The accelerations begin to differ just inside the surface of the sphere at $r=0.5$, according to (15). This difference is the origin of the borehole g anomaly, and permits the determination of the value of α from observational data. This generic singular-g behaviour, at $r=0$, is seen in the Earth, in globular clusters and in galaxies.

*The fractal property of 3-space was found [10] from the DeWitte data.

†Except for the acceleration component induced by vorticity.

‡However this does not exclude so-called relativistic effects, such as the length contraction of moving rods or the time dilations of moving clocks.

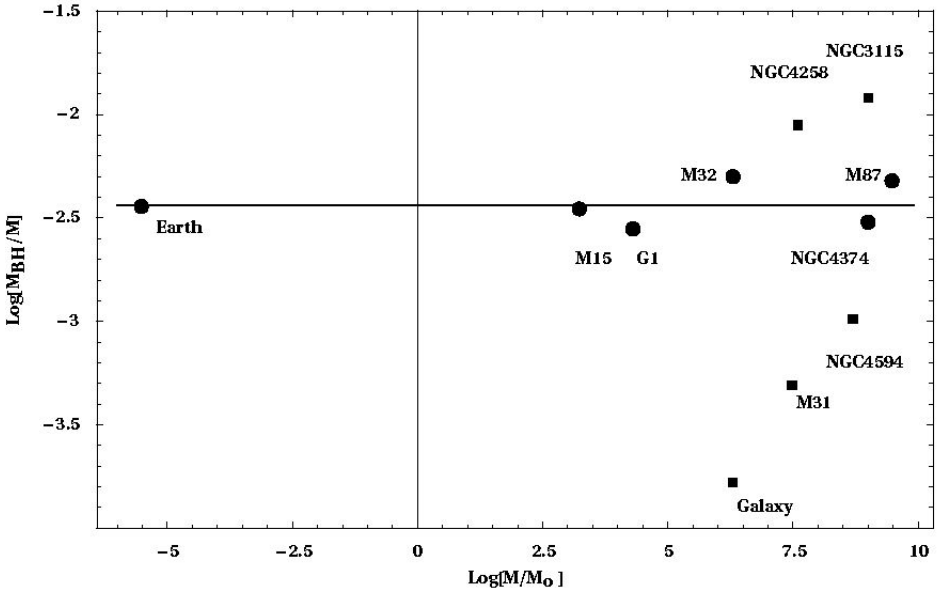

Fig. 2: The data shows $\mathrm{Log}_{10}[M_{BH}/M]$ for the "blackhole" or "dark matter" masses M_{BH} for a variety of spherical matter systems with masses M, shown by solid circles, plotted against $\mathrm{Log}_{10}[M/M_0]$, where M_0 is the solar mass, showing agreement with the "$\alpha/2$-line" ($\mathrm{Log}_{10}[\alpha/2] = -2.44$) predicted by (10), and ranging over 15 orders of magnitude. The "blackhole" effect is the same phenomenon as the "dark matter" effect. The data ranges from the Earth, as observed by the bore hole g anomaly, to globular cluster M15 and G1, and then to spherical "elliptical" galaxies M32 (E2), NGC 4374 (E1) and M87 (E0). Best fit to the data from these star systems gives $\alpha = 1/134$, while for the Earth data in Figs.3,4,5 give $\alpha = 1/137$. In these systems the "dark matter" or "black hole" spatial self-interaction effect is induced by the matter. For the spiral galaxies, shown by the filled boxes, where here M is the bulge mass, the blackhole masses do not correlate with the "$\alpha/2$-line". This is because these systems form by matter in-falling to a primordial blackhole, and so these systems are more contingent. For spiral galaxies this dynamical effect manifests most clearly via the non-Keplerian rotation-velocity curve, which decrease asymptotically very slowly. See [7] for references to the data.

gives a direct account of the various phenomena noted above. A generalisation to include relativistic effects of the motion of matter through this 3-space is given in [4]. From (1) and (3) we obtain that

$$\nabla \cdot \mathbf{g} = -4\pi G\rho - 4\pi G\rho_{DM}, \tag{4}$$

where

$$\rho_{DM}(\mathbf{r}) = \frac{\alpha}{32\pi G}\big((\mathrm{tr}D)^2 - \mathrm{tr}(D^2)\big). \tag{5}$$

In this form we see that if $\alpha \to 0$, then the acceleration of the 3-space elements is given by Newton's *Universal Law of Gravitation*, in differential form. But for a non-zero α we see that the 3-space acceleration has an additional effect, from the ρ_{DM} term, which is an effective "matter density" that mimics the new self-interaction dynamics. This has been shown to be the origin of the so-called "dark matter" effect in spiral galaxies. It is important to note that (4) does not determine $\mathbf{g}$ directly; rather the velocity dynamics in (1) must be solved, and then with $\mathbf{g}$ subsequently determined from (3). Eqn. (4) merely indicates that the resultant non-Newtonian $\mathbf{g}$ could be mistaken as the result of a new form of matter, whose density is given by ρ_{DM}. Of course the saga of "dark matter" shows that this actually happened, and that there has been a misguided and fruitless search for such "matter".

3 Airy method for determining α

We now show that the Airy method actually gives a technique for determining the value of α from Earth based borehole gravity measurements. For a time-independent velocity field (1) may be written in the integral form

$$|\mathbf{v}(\mathbf{r})|^2 = 2G\int d^3r' \frac{\rho(\mathbf{r}') + \rho_{DM}(\mathbf{r}')}{|\mathbf{r} - \mathbf{r}'|}. \tag{6}$$

When the matter density of the Earth is assumed to be spherically symmetric, and that the velocity field is now radial* (6) becomes

$$v(r)^2 = \frac{8\pi G}{r}\int_0^r s^2\left[\rho(s) + \rho_{DM}(s)\right]ds + \\ + 8\pi G\int_r^\infty s\left[\rho(s) + \rho_{DM}(s)\right]ds, \tag{7}$$

*This in-flow is additional to the observed velocity of the Earth through 3-space.

where, with $v' = dv(r)/dr$,

$$\rho_{DM}(r) = \frac{\alpha}{32\pi G}\left(\frac{v^2}{2r^2} + \frac{vv'}{r}\right). \tag{8}$$

Iterating (7) once we find to 1st order in α that

$$\rho_{DM}(r) = \frac{\alpha}{2r^2}\int_r^\infty s\,\rho(s)\,ds + \mathrm{O}(\alpha^2), \tag{9}$$

so that in spherical systems the "dark matter" effect is concentrated near the centre, and we find that the total "dark matter" is

$$\begin{aligned} M_{DM} &\equiv 4\pi\int_0^\infty r^2\rho_{DM}(r)\,dr = \\ &= \frac{4\pi\alpha}{2}\int_0^\infty r^2\rho(r)\,dr + \mathrm{O}(\alpha^2) = \frac{\alpha}{2}M + \mathrm{O}(\alpha^2), \end{aligned} \tag{10}$$

where M is the total amount of (actual) matter. Hence to $\mathrm{O}(\alpha)$ $M_{DM}/M = \alpha/2$ independently of the matter density profile. This turns out to be a very useful property as complete knowledge of the density profile is then not required in order to analyse observational data. As seen in Fig. 1 the singular behaviour of both v and g means that there is a *blackhole** singularity at $r = 0$. Interpreting M_{DM} in (10) as the mass of the blackholes observed in the globular clusters M15 and G1 and in the highly spherical "elliptical" galaxies M32, M87 and NGC 4374, we obtained [7] $\alpha \approx 1/134$, as shown in Fig. 2.

From (3), which is also the acceleration of matter [10], the gravity acceleration† is found to be, to 1st order in α, and using that $\rho(r) = 0$ for $r > R$, where R is the radius of the Earth,

$$g(r) = \begin{cases} \dfrac{\left(1+\frac{\alpha}{2}\right)GM}{r^2}, & r > R; \\ \dfrac{4\pi G}{r^2}\displaystyle\int_0^r s^2\rho(s)\,ds + & \\ + \dfrac{2\pi\alpha G}{r^2}\displaystyle\int_0^r\left(\int_s^R s'\rho(s')ds'\right)ds, & r < R. \end{cases} \tag{11}$$

This gives Newton's "inverse square law" for $r > R$, even when $\alpha \neq 0$, which explains why the 3-space self-interaction dynamics did not overtly manifest in the analysis of planetary orbits by Kepler and then Newton. However inside the Earth (11) shows that $g(r)$ differs from the Newtonian theory, corresponding to $\alpha = 0$, as Fig. 1, and it is this effect that allows the determination of the value of α from the Airy method.

Expanding (11) in r about the surface, $r = R$, we obtain, to 1st order in α and for an arbitrary density profile,

$$g(r) = \begin{cases} \dfrac{G_{\mathrm{N}}M}{R^2} - \dfrac{2G_{\mathrm{N}}M}{R^3}(r-R), & r > R; \\ \dfrac{G_{\mathrm{N}}M}{R^2} - \left(\dfrac{2G_{\mathrm{N}}M}{R^3} - 4\pi\left(1-\dfrac{\alpha}{2}\right)G_{\mathrm{N}}\rho\right)\times & \\ \times\,(r-R), & r < R. \end{cases} \tag{12}$$

where ρ is the matter density at the surface, M is the total matter mass of the Earth, and where we have defined

$$G_{\mathrm{N}} \equiv \left(1+\frac{\alpha}{2}\right)G. \tag{13}$$

The corresponding Newtonian gravity expression is obtained by taking the limit $\alpha \to 0$,

$$g_{\mathrm{N}}(r) = \begin{cases} \dfrac{G_{\mathrm{N}}M}{R^2} - \dfrac{2G_{\mathrm{N}}M}{R^3}(r-R), & r > R; \\ \dfrac{G_{\mathrm{N}}M}{R^2} - \left(\dfrac{2G_{\mathrm{N}}M}{R^3} - 4\pi G_{\mathrm{N}}\rho\right)(r-R), & r < R. \end{cases} \tag{14}$$

Assuming Newtonian gravity (14) then means that from the measurement of difference between the above-ground and below-ground gravity gradients, namely $4\pi G_{\mathrm{N}}\rho$, and also measurement of the matter density, permit the determination of G_{N}. This is the basis of the Airy method for determining G_{N} [3].

When analysing the borehole data it has been found [11, 12] that the observed difference of the density gradients was inconsistent with $4\pi G_{\mathrm{N}}\rho$ in (14), in that it was not given by the laboratory value of G_{N} and the matter density. This is known as the borehole g anomaly and which attracted much interest in the 1980's. The key point in understanding this anomaly is that even allowing for the dynamical rescaling of G, expressions (12) and (14) have a different dependence on $r - R$ beneath the surface. The borehole data papers [11, 12] report the discrepancy, i. e. the anomaly or the gravity residual as it is called, between the Newtonian prediction and the measured below-earth gravity gradient. Taking the difference between (12) and (14), assuming the same unknown value of G_{N} in both, we obtain an expression for the gravity residual

$$\Delta g(r) \equiv g_{\mathrm{N}}(r) - g(r) = \begin{cases} 0, & r > R; \\ 2\pi\alpha G_{\mathrm{N}}\rho(r-R), & r < R. \end{cases} \tag{15}$$

When $\alpha \neq 0$ we have a two-parameter theory of gravity, and from (11) we see that measurement of the difference between the above ground and below ground gravity gradients is $4\pi\left(1-\frac{\alpha}{2}\right)G_{\mathrm{N}}\rho$, and this is not sufficient to determine both G_{N} and α, given ρ, and so the Airy method is now understood not to be a complete measurement by itself, i. e. we need to combine it with other measurements. If we now use laboratory Cavendish experiments to determine G_{N}, then from the borehole gravity residuals we can determine the value of α, as already indicated in [5, 6]. As discussed in Sect. 7 these Cavendish experiments can only determine G_{N}

*These are called *blackholes* because there is an event horizon, but in all other aspects differ from the *blackholes* of General Relativity.

†We now use the convention that $g(r)$ is positive if it is radially inward.

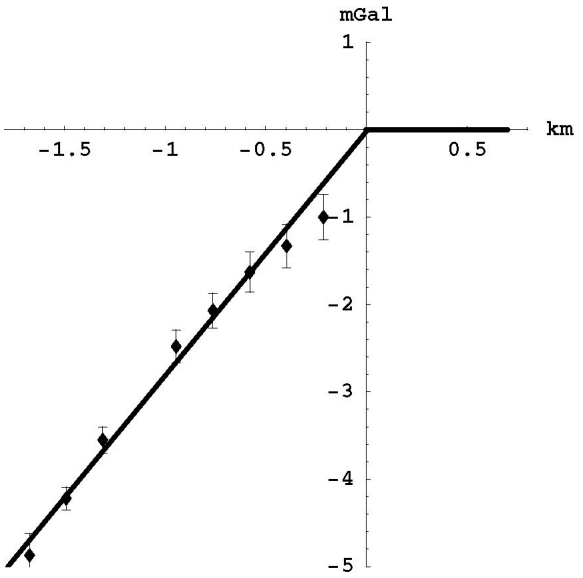

Fig. 3: The data shows the gravity residuals for the Greenland Ice Shelf [11] Airy measurements of the $g(r)$ profile, defined as $\Delta g(r) = g_{\text{Newton}} - g_{\text{observed}}$, and measured in mGal (1mGal $=$ $= 10^{-3}$ cm/s^2) and plotted against depth in km. The gravity residuals have been offset. The borehole effect is that Newtonian gravity and the new theory differ only beneath the surface, provided that the measured above surface gravity gradient is used in both theories. This then gives the horizontal line above the surface. Using (15) we obtain $\alpha^{-1} = 137.9 \pm 5$ from fitting the slope of the data, as shown. The non-linearity in the data arises from modelling corrections for the gravity effects of the irregular sub ice-shelf rock topography.

up to corrections of order $\alpha/4$, simply because the analysis of the data from these experiments assumed the validity of Newtonian gravity. So the analysis of the borehole residuals will give the value of α up to $O(\alpha^2)$ corrections, which is consistent with the $O(\alpha)$ analysis reported above.

4 Greenland Ice Shelf borehole data

Gravity residuals from a bore hole into the Greenland Ice Shelf were determined down to a depth of 1.5 km by Ander *et al.* [11] in 1989. The observations were made at the Dye 3 2033 m deep borehole, which reached the basement rock. This borehole is 60 km south of the Arctic Circle and 125 km inland from the Greenland east coast at an elevation of 2530 m. It was believed that the ice provided an opportunity to use the Airy method to determine G_{N}, but now it is understood that in fact the borehole residuals permit the determination of α, given a laboratory value for G_{N}. Various steps were taken to remove unwanted effects, such as imperfect knowledge of the ice density and, most dominantly, the terrain effects which arises from ignorance of the profile and density inhomogeneities of the underlying rock. The borehole gravity meter was calibrated by comparison with an absolute gravity meter. The ice density depends on pressure, temperature and air content, with the density rising to its average value of $\rho = 920$ kg/m^3 within some 200 m of the surface, due to compression of the trapped air bubbles. This surface gradient in the density has been modelled by the author, and is not large enough the affect the results. The leading source of uncertainty was from the gravitational effect of the bedrock topography, and this was corrected for using Newtonian gravity. The correction from this is actually the cause of the non-linearity of the data points in Fig. 3. A complete analysis would require that the effect of this rock terrain be also computed using the new theory of gravity, but this was not done. Using $G_{\text{N}} = 6.6742 \times 10^{-11}$ m^{3}s^{-2}kg^{-1}, which is the current CODATA value, see Sect. 7, we obtain from a least-squares fit of the linear term in (15) to the data points in Fig. 3 that $\alpha^{-1} = 137.9 \pm 5$, which equals the value of the fine structure constant $\alpha^{-1} = 137.036$ to within the errors, and for this reason we identify the constant α in (1) as being the fine structure constant. The first analysis [5, 6] of the Greenland Ice Shelf data incorrectly assumed that the ice density was 930 kg/m^3 which gave $\alpha^{-1} = 139 \pm 5$. However trapped air reduces the standard ice density to the ice shelf density of 920 kg/m^3, which brings the value of α immediately into better agreement with the value of $\alpha = e^2/\hbar c$ known from quantum theory.

5 Nevada Test Site borehole data

Thomas and Vogel [12] performed another borehole experiment at the Nevada Test Site in 1989 in which they measured the gravity gradient as a function of depth, the local average matter density, and the above ground gradient, also known as the free-air gradient. Their intention was to test the extracted G_{local} and compare with other values of G_{N}, but of course using the Newtonian theory. The Nevada boreholes, with typically 3 m diameter, were drilled as a part of the U.S. Government tests of its nuclear weapons. The density of the rock is measured with a $\gamma - \gamma$ logging tool, which is essentially a γ-ray attenuation measurement, while in some holes the rock density was measured with a coreing tool. The rock density was found to be 2000 kg/m^3, and is dry. This is the density used in the analysis herein. The topography for 1 to 2 km beneath the surface is dominated by a series of overlapping horizontal lava flows and alluvial layers. Gravity residuals from three of the bore holes are shown in Figs.4, 5 and 6. All gravity measurements were corrected for the Earth's tide, the terrain on the surface out to 168 km distance, and the evacuation of the holes. The gravity residuals arise after allowing for, using Newtonian theory, the local lateral mass anomalies but assumed that the matter beneath the holes occurs in homogeneous ellipsoidal layers. Here we now report a detailed analysis of the Nevada data. First we note that the gravity residuals from borehole U20AO, Fig. 6,

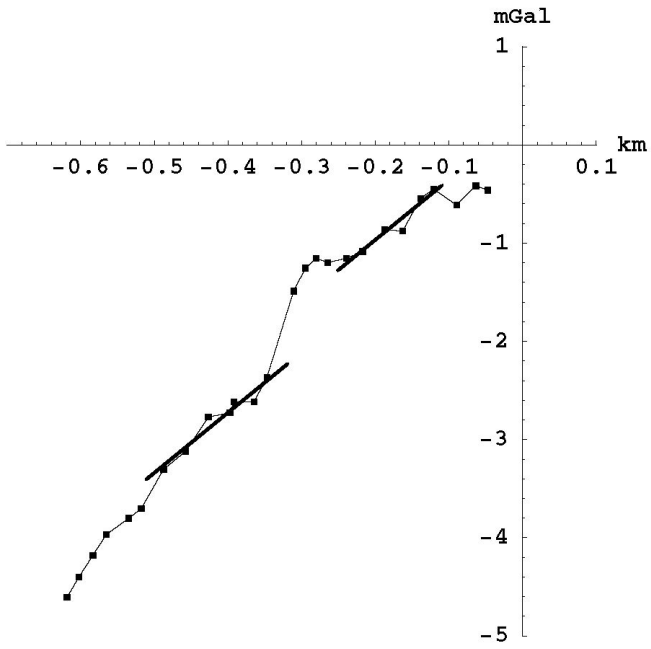

Fig. 4: The data shows the gravity residuals for the Nevada U20AK borehole Airy measurements of the $g(r)$ profile [12], defined as $\Delta g(r) = g_{\text{Newton}} - g_{\text{observed}}$, and measured in mGal, plotted against depth in km. This residual shows regions of linearity interspersed with regions of non-linearity, presumably arising from layers with a density different from the main density of 2000 kg/m^3. Density changes generate a change in the (arbitrary) residual offset. From a least-squares simultaneous fit of the linear form in (15) to the four linear regions in this data and that in Fig. 5 for the data from borehole U20AL, we obtain $\alpha^{-1} = 136.8 \pm 3$. The two fitted regions of data are shown by the two straight lines here and in Fig. 5.

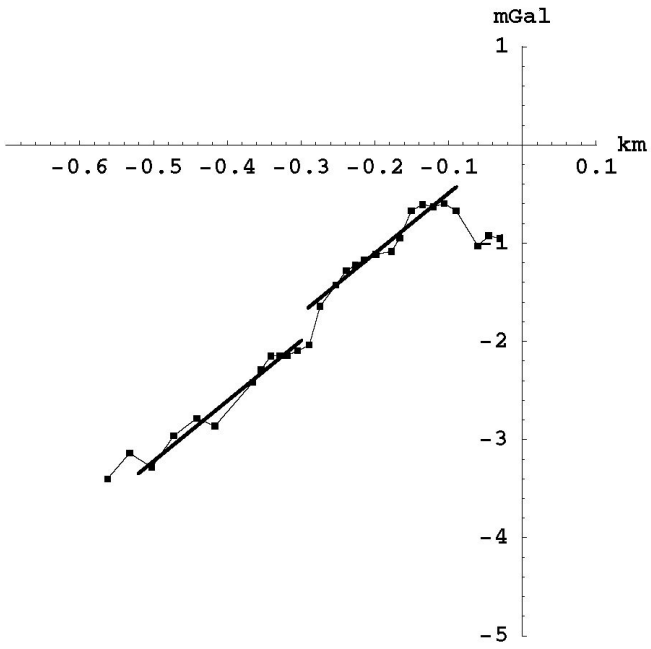

Fig. 5: The data shows the gravity residuals for the Nevada U20AL borehole Airy measurements of the $g(r)$ profile [12], defined as $\Delta g(r) = g_{\text{Newton}} - g_{\text{observed}}$, and measured in mGal, plotted against depth in km. This residual shows regions of linearity interspersed with regions of non-linearity, presumably arising from layers with a density different from the main density of 2000 kg/m^3. Density changes generate a change in the (arbitrary) residual offset. From a least-squares simultaneous fit of the linear form in (15) to the four linear regions in this data and that in Fig. 4 for the data from borehole U20AK in Fig. 4, we obtain $\alpha^{-1} = 136.8 \pm 3$. The two fitted regions of data are shown by the two straight lines here and in Fig. 4.

are not sufficiently linear to be useful. This presumably arises from density variations caused by the layering effect. For boreholes UA20AK, Fig. 4, and UA20AL, Fig. 5, we see segments where the gravity residuals are linear with depth, where the density is the average value of 2000 kg/m^3, but interspersed by layers where the residuals show non-linear changes with depth. It is assumed here that these non-linear regions are caused by variable density layers. So in analysing this data we have only used the linear regions, and a simultaneous least-squares fit to (15), with again $G_{\text{N}} = 6.6742 \times 10^{-11}$ m^3 s^{-2}kg^{-1} as for the Greenland data analysis, of these four linear regions gives $\alpha^{-1} = 136.8 \pm 3$, which again is in extraordinary agreement with the value of 137.04 from quantum theory.

6 Ocean measurements

The ideal Airy experiment would be one using the ocean, as all relevant physical aspects are accessible. Such an experiment was carried out by Zumberge *et al.* in 1991 [13] using submersibles. Corrections for sea floor topography, seismic profiles and sea surface undulations were carried out. However a true Airy experiment appears not to have been performed. That would have required the measurement of the above and below sea-surface gravity gradients. Rather only the below sea-surface gradients were measured, and compared with a predicted gravity gradient using the density of the water and a laboratory value of G_{N} from only one such experiment and, as shown in Fig. 7, these have a large uncertainty. Hence this experiment does not permit an analysis of the data of the form applied to the Greenland and Nevada observations. The value of G_{N} from this ocean experiment is shown in Fig. 7 as experiment #12.

7 G experiments

The new theory of gravity, given in (1) for the case of zero vorticity and in the non-relativistic limit, is a two-parameter theory; G and α. Hence in experiments to determine G (or G_{N}) we expect to see systematic discrepancies if the

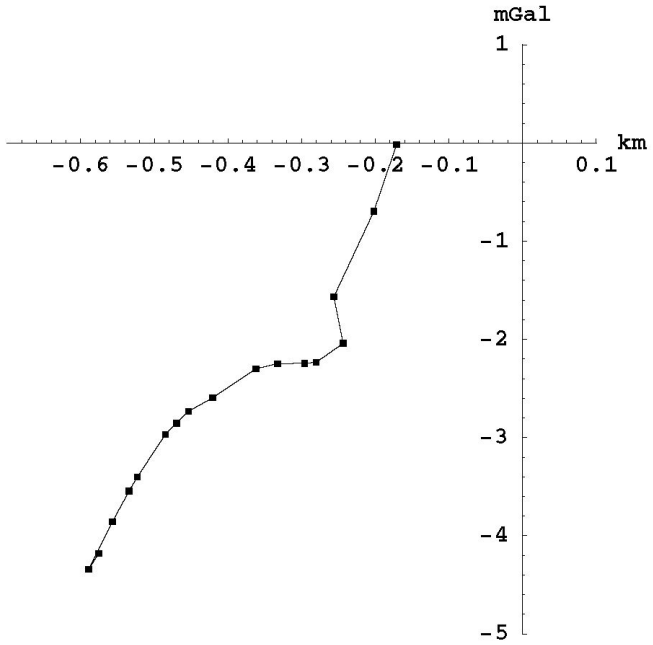

Fig. 6: The data shows the gravity residuals from the third Nevada U20AO borehole Airy measurements of the $g(r)$ profile [12]. This data is not of sufficient linearity, presumably due to non-uniformity of density, to permit a fit to the linear form in (15), but is included here for completeness. There is an arbitrary offset in the residual.

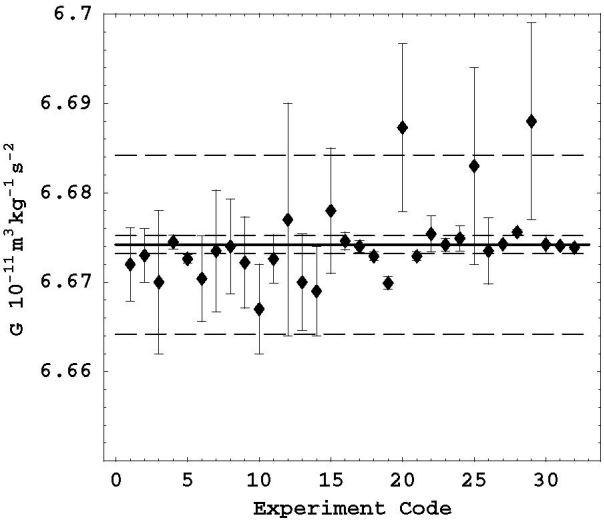

Fig. 7: Results of precision measurements of $G_{\rm N}$ published in the last sixty years in which the Newtonian theory was used to analyse the data. These results show the presence of a systematic effect, not in the Newtonian theory, of fractional size up to $\Delta G_{\rm N}/G_{\rm N} \approx \alpha/4$, which corresponded with the 1998 error bars on $G_{\rm N}$ (outer dashed lines), with the full line being the current CODATA value of $G_{\rm N} = 6.6742(10)\times10^{-11}$ m^{2}s^{-2}kg^{-1}. In 2005 CODATA [20] reduced the error bars by a factor of 10 (inner dashed lines) on the basis of some recent experiments, and so neglecting the presence of the systematic effect.

Newtonian theory is used to analyse the data. This is clearly the case as shown in Fig. 7 which shows the results of such analyses over the last 60 years. The fundamental problem is that non-Newtonian effects of size $\Delta G_{\rm N}/G_{\rm N} \approx \alpha/4$ are clearly evident, and effects of this size are expected from (1). To correctly analyse data from these experiments the full theory in (1) must be used, and this would involve (i) computing the velocity field for each configuration of the test masses, and then (ii) computing the forces by using (3) to compute the acceleration field. These computations are far from simple, especially when the complicated matter geometries of recent experiments need to be used. Essentially the flow of space results in a non-Newtonian effective "dark matter" density in (5). This results in deviations from Newtonian gravity which are of order $\alpha/4$. The prediction is that when laboratory Cavendish-type experiments are correctly analysed the data will permit the determination of both $G_{\rm N}$ and α, and the large uncertainties in the determination of $G_{\rm N}$ will no longer occur. Until then the value of $G_{\rm N}$ will continue to be the least accurately known of all the fundamental constants. Despite this emerging insight CODATA* in 2005 [20] reduced the apparent uncertainties in $G_{\rm N}$ by a factor of 10, and so ignoring the manifest presence of a systematic effect. The occurrence of the fine structure constant α, in giving the magnitude of the spatial self-interaction effect in (1), is a fundamental development in our understanding of 3-space and the phenomenon of gravity. Indeed the implication is that α arises here as a manifestation of quantum processes inherent in 3-space.

*CODATA is the Task Group on Fundamental Constants of the Committee on Data for Science and Technology, established in 1969.

8 Some history

Here we have simply applied the new two-parameter theory of 3-space, and hence of gravity, to the existing data from borehole experiments. However the history of these experiments shows that, of course, the nature of the gravitational anomaly had not been understood, and so the implications for fundamental physics that are now evident could not have been made. The first indications that some non-Newtonian effect was being observed arose from Yellin [14] and Hinze *et al.* [15]. It was Stacey *et al.* in 1981 [17, 16, 18] who undertook systematic studies at the Mt. Isa mine in Queensland, Australia. In the end a mine site is very unsuited for such a gravitational anomaly experiment as by their very nature mines have non-uniform poorly-known density and usually, as well, irregular surface topography. In the end it was acknowledged that the Mt. Isa mine data was unreliable. Nevertheless those reports motivated the Greenland, Nevada and Ocean experiments, as well as above-ground tower expe-

riments [19], all with the assumption that the non-Newtonian effects were being caused by a modification to Newton's *inverse square law* by an additional short-range force — which also involved the notion of a possible "5th-force" [21]. However these interpretations were not supported by the data, and eventually the whole phenomenon of these gravitational borehole anomalies was forgotten.

9 Conclusions

We have extended the results from an earlier analysis [5, 6] of the Greenland Ice Shelf borehole g anomaly data by correcting the density of ice from the assumed value to the actual value. This brought the extracted value of α from approximately 1/139 to approximately 1/137, and so into even closer agreement with the quantum theory value. As well the analysis was extended to the Nevada borehole anomaly data, again giving $\alpha \approx 1/137$. This is significant as the rock density is more than twice the ice density. As well we have included the previous results [7] from analysis of the blackhole masses in globular clusters and elliptical "spherical" galaxies, which gave $\alpha \approx 1/134$, but with larger uncertainty. So the conclusion that α is actually the fine structure constant from quantum theory is now extremely strong. These results, together with the successful explanation for the so-called spiral galaxy "dark-matter" effect afforded by the new theory of gravity, implies that the Newtonian theory of gravity [1] is fundamentally flawed, even at the non-relativistic level, and that the disagreement with experiment and observation can be of fractional order α, or in the case of spiral galaxies and blackholes, extremely large. This failure implies that General Relativity, which reduces to the Newtonian theory in the non-relativistic limit, must also be considered as flawed and disproven.

References

1. Newton I. Philosophiae Naturalis Principia Mathematica. 1687.
2. Cavendish H. Philosophical Transactions. 1798.
3. Airy G. B. *Philos. Trans. R. Soc. London*, 1856, v. 146, 297; v. 146, 343.
4. Cahill R. T. Process Physics: from information theory to quantum space and matter. Nova Science Pub., NY, 2005.
5. Cahill R. T. Gravitation, the "dark matter" effect, and the fine structure constant. *Apeiron*, 2005, v. 12(2), 155–177.
6. Cahill R. T. "Dark matter" as a quantum foam in-flow effect. In *Trends in Dark Matter Research*, ed. by J. Val Blain, Nova Science Pub., NY., 2005, 96–140.
7. Cahill R. T. Black holes in elliptical and spiral galaxies and in globular clusters. *Progress in Physics*, 2005, v. 3, 51–56.
8. Cahill R. T. The Michelson and Morley 1887 experiment and the discovery of absolute motion. *Progress in Physics*, 2005, v. 3, 25–29; Cahill R. T. and Kitto K. *Apeiron*, 2003, v. 10(2), 104–117.
9. Cahill R. T. Absolute motion and gravitational effects. *Apeiron*, 2004, v. 11(1), 53–111.
10. Cahill R. T. Dynamical fractal 3-space and the generalised Schrödinger equation: Equivalence principle and vorticity effects. *Progress in Physics*, 2006, v. 1, 27–34.
11. Ander M. E. *et al.* Test of Newton's inverse-square law in the Greenland Ice Cap. *Phys. Rev. Lett.*, 1989, v. 62, 985–988.
12. Thomas J. and Vogel P. Testing the inverse-square law of gravity in boreholes at the Nevada Test Site. *Phys. Rev. Lett.*, 1990, v. 65, 1173–1176.
13. Zumberge M. A. *et al.* Submarine measurement of the Newtonian gravitational constant. *Phys. Rev. Lett.*, 1991, v. 67, 3051–3054.
14. Yellin M. J. ESSA Operational data report C & GSDR-2. U.S. Dept. Commerce, Washington, 1968.
15. Hinze W. J., Bradley J. W., and Brown A. R. *J. Geophys. Res.*, 1978, v. 83, 5864.
16. Stacey F. C. *et al.* Constraints on the planetary scale of the Newtonian gravitational constant from the gravity profile within a mine. *Phys. Rev. D*, 1981, v. 23, 1683–1692.
17. Stacey F. D. and Tuck G. J. Geophysical evidence for non-Newtonian gravity. *Nature*, 1981, v. 292, 16–22.
18. Holding S. C., Stacey F. D., and Tuck G. J. Gravity in mines — an investigation of Newton's law. *Phys. Rev. D*, 1986, v. 33, 3487–3494.
19. Thomas J. *et al.* Testing the inverse-square law of gravity on a 465-m tower. *Phys. Rev. Lett.*, 1989, v. 63, 1902–1905.
20. Mohr P. J. and Taylor B. N. CODATA recommended values of the fundamental physical constants: 2002. *Rev. Mod. Phys.*, 2005, v. 77(1), 1–107.
21. Fischbach E. and Talmadge C. Ten years of the fifth force. arXiv: hep-ph/9606249, and references therein.

The Solar Photosphere: Evidence for Condensed Matter

Pierre-Marie Robitaille
130 Means Hall, 1654 Upham Drive, The Ohio State University, Columbus, Ohio 43210, USA
E-mail: robitaille.1@osu.edu

The stellar equations of state treat the Sun much like an ideal gas, wherein the photosphere is viewed as a sparse gaseous plasma. The temperatures inferred in the solar interior give some credence to these models, especially since it is counterintuitive that an object with internal temperatures in excess of 1 MK could be existing in the liquid state. Nonetheless, extreme temperatures, by themselves, are insufficient evidence for the states of matter. The presence of magnetic fields and gravity also impact the expected phase. In the end, it is the physical expression of a state that is required in establishing the proper phase of an object. The photosphere does not lend itself easily to treatment as a gaseous plasma. The physical evidence can be more simply reconciled with a solar body and a photosphere in the condensed state. A discussion of each physical feature follows: (1) the thermal spectrum, (2) limb darkening, (3) solar collapse, (4) the solar density, (5) seismic activity, (6) mass displacement, (7) the chromosphere and critical opalescence, (8) shape, (9) surface activity, (10) photospheric/coronal flows, (11) photospheric imaging, (12) the solar dynamo, and (13) the presence of Sun spots. The explanation of these findings by the gaseous models often requires an improbable combination of events, such as found in the stellar opacity problem. In sharp contrast, each can be explained with simplicity by the condensed state. This work is an invitation to reconsider the phase of the Sun.

Introduction

The stellar phase has important consequences, not only for modeling the Sun, but indeed, for the proper treatment of nearly every aspect of astrophysics. Recently, the accepted temperature of the photosphere has been questioned [1]. This hinges on the proper understanding of both blackbody radiation [2] and the liquid state [3]. In modern theory, stars can be essentially infinitely compressed without ever becoming liquid. Outside the Earth's oceans, the liquid state appears all but non-existent in the universe. By invoking the gaseous equations of state [i. e. 4] without the possibility of condensation to the liquid and solid state, the accepted models continue to ignore laboratory findings relative to the existence of these transformations. These issues are not simple. However, sufficient evidence exists to bring into question the gaseous models of the Sun.

The physical evidence

1. The thermal spectrum:

It is hard to imagine that, after more than 100 years, our understanding of blackbody radiation could be questioned. If this is the case, it is because of shortcomings in the work of Gustav Kirchhoff [5, 6] which have previously been overlooked [7]. The arguments hinged on whether or not blackbody radiation is in fact universal as initially advanced by Kirchhoff [5, 6], echoed by Planck [2] and theoretically confirmed by Einstein [8]. In order to dissect the problem, Kirchhoff and Planck are treated together, along with the experimental proof [7]. Einstein's work [8] can then be examined from a conceptual viewpoint [9] without bringing into question any of Einstein's mathematics. Thus, arguments against the universality of blackbody radiation have already been made both on an experimental basis [7] and on a theoretical one [9]. In reality, the entire foundation for the liquid model of the Sun rests on the soundness of these arguments [7, 9]. The belief is that claims of universality are not only overstated, they are incorrect [9]. As such, it is improper to assign any astrophysical temperature based on the existence of a thermal spectrum in the absence of a known isothermal (not adiabatic) and perfectly absorbing enclosure [1, 7, 9].

The Sun possesses a thermal signature as reported early on by Langley [10, 11]. The fact that this spectrum is continuous in nature leads to difficulties for the gaseous models [1]. This is because gases are known to emit radiation only in discrete bands [12]. Consequently, in order to produce the thermal spectrum of the Sun, theoretical astrophysics must currently invoke the summation of numerous spectroscopic processes. Furthermore, this must occur in a slightly shifted manner within each internal layer of the Sun. Many distinct physical processes (bound-bound, bound-free, and free-free) are used to arrive at a single spectrum [i. e. 4]. This constitutes the stellar opacity problem: the summation of many distinct spectroscopic processes to yield a single spectroscopic signature.

In reality, each spectroscopic signature, including the

thermal spectrum, must arise from a single spectroscopic process [1]. Just as an NMR spectrum arises from an NMR process, so must a thermal spectrum arise from a thermal process. Whatever process takes place with graphite on Earth must be taking place on the surface of the Sun. That the gaseous models require many spectroscopic processes along with gradually and systematically changing stellar opacities [i. e. 4] is perhaps their greatest obstacle. Gases simply cannot generate thermal spectra in the absence of a rigid body (condensed matter) enclosure. They are restricted to emission in bands.

In contrast, condensed matter can easily generate continuous spectra [13, 14, 15] as a manifestation of its inherent lattice structure. Thus, relative to the existence of a continuous solar spectrum, a condensed matter model of the Sun has distinct advantages.

2. Limb darkening:

The Sun is also characterized by limb darkening. The solar spectrum becomes less bright when viewing the Sun from the center to the limb. Since a change in the thermal spectrum is involved, the gaseous models must once again invoke the stellar opacity problem. Limb darkening is explained by inferring the sampling of varying optical depths. The Sun must be able to slowly and gradually change its thermal spectrum from one temperature to another based on depth using a perfect combination of bound-bound, bound-free and free-free processes at every location inside the Sun. Gaseous theory therefore places a tremendous constraint on nature relative to limb darkening. As stated above, it is not reasonable to expect that a single spectrum is actually resultant from the infinite sum of many distinct and unrelated spectroscopic processes. If a thermal spectrum is produced by the Sun, it must invoke the same mechanism present in the piece of graphite on Earth. That the gaseous models rely on varying optical depths in order to explain limb darkening might appear elegant, but lacks both clarity and support in experimental physics.

In sharp contrast, angle dependence in thermal emission is extremely well documented for condensed matter [14, 15]. Changes in optical depth are not required. Rather, a subtle change in the angle of observation is sufficient. This is precisely what is observed when we monitor the Sun. For instance, even the oceans of the Earth are known to have angle dependent emission intensities at microwave frequencies [16]. Thus, in the condensed matter scenario, limb darkening is an expression of angle of observation without having to make any arguments based on optical depth.

3. Solar collapse:

One of the key requirements of the gaseous models is the need to prevent solar collapse as a result of gravitational forces. Currently, it is advocated that solar collapse is prevented by electron gas pressure in the solar interior and, for larger stars, by radiation pressure. However, the existence of gas pressure relies on the presence of a rigid surface [i. e. 4]. The atmosphere of the Earth does not collapse due to the relatively rigid oceanic and continental surfaces. Within the gaseous models of the stars however, there is no mechanism to introduce the rigid surface required to maintain gas pressure. Theoretical arguments are made [i. e. 4] without experimental foundation. The same holds for internal radiation pressure. There is no experimental basis on Earth for radiation pressure internal to a single object [13, 14, 15]. It is well-established that for the gaseous models of the Sun, complete solar collapse would take place in a matter of seconds should electron gas pressure and internal radiation pressure cease [i. e. 4]. In sharp contrast, relative incompressibility is a characteristic of the liquid state. A liquid Sun is by definition essentially incompressible, and experimental evidence for such behavior in liquids is abundant. Stellar collapse is excluded by the very nature of the phase invoked.

4. Solar density:

The Sun has an average density of 1.4 g/cm^3. The gaseous models distribute this density with radial dependence with the core of the Sun typically approaching a density of 150 g/cm^3 and the photosphere 10^{-7} g/cm^3. If the Sun were truly a gaseous plasma, it would have been much more convenient if the average density did not so well approximate the density of the condensed state (> 1 g/cm^3). The gaseous models would be in a much stronger position if the average solar density, for instance, was 10^{-4} g/cm^3. Such a density would clearly not lend itself to the condensed state. In contrast, the known density of the Sun is ideal for a condensed model whose primary constituents are hydrogen and helium. Moreover, for the condensed models [1], the radial dependence of density is not critical to the solution and a uniform distribution of mass may be totally acceptable.

The density of the Sun very closely approaches that of all the Jovian planets. Nonetheless, a great disparity in mass exists between the Sun and these planets. As such, it is probably best not to enter into schemes which involve great changes in internal solar densities. The liquid model maintains simplicity in this area and such a conclusion is viewed as important.

5. Seismology:

The Sun is a laboratory of seismology [17]. Yet, on Earth, seismology is a science of the condensed state. It is interesting to highlight how the gaseous models of the Sun fail to properly fit seismological data. In the work by Bahcall et. al. [18] for instance, experimental and theoretical siesmological findings are compared as a function of Solar radius. Precise fits are obtained for most of the solar sphere. In fact, it is surprising how the interior of the Sun can be so accurately fitted, given that all the data is being acquired

from the solar surface. At the same time, this work is unable to fit the data in the exterior 5% of the Sun [18]. Yet, this is precisely the point from which all the data is being collected. The reason that this region cannot be fitted is that the gaseous models are claiming that the photosphere has a density on the order of 10^{-7} g/cm^3. This is lower than practical vacuums on Earth. Thus, the gaseous models are trying to conduct seismology in a vacuum by insisting on a photospheric density unable to sustain seismic activity. For the condensed models of the Sun, this complication is eliminated.

6. Mass displacement:

On July 9, 1996, the SOHO satellite obtained Doppler images of the solar surface in association with the eruption of a flare [19, 20]. These images reveal the clear propagation of transverse waves on the solar surface. The authors of the scientific paper refer to the mass displacement exactly like the action resulting from a pebble thrown in a pond. This is extremely difficult to explain for the gaseous models, yet trivial for the condensed model. The Doppler images show the presence of transverse waves. This is something unique to the condensed state. Gases propagate energy longitudinally. It can be theoretically argued perhaps that gases can sustain transverse waves. These however would be on the order of a few atomic radii at best. In sharp contrast, the waves seen on the Sun extend over thousands of kilometers. Once again, the condensed state provides a greatly superior alternative to the study of transverse waves on the solar surface.

7. The chromosphere and critical opalescence:

Critical opalescence occurs when a material is placed at the critical point, that combination of temperature, pressure, magnetic field and gravity wherein the gas/liquid interface disappears. At the critical point, a transparent liquid becomes cloudy due to light scattering, hence the term critical opalescence. The gas is regaining order, as it becomes ready to enter the condensed phase. It would appear that the Sun, through the chromosphere, is revealing to us behavior at the solar critical point. Under this scenario, the chromosphere is best viewed as the transition phase between the condensed photosphere and the gaseous corona.

In order to shed light on this problem, consider that in the lower region of the corona, the gaseous material exists at a temperature just beyond the critical temperature. The temperature is sufficiently elevated, that it is impossible for condensation to occur, given the gravity present. However, as one moves towards the Sun, the critical temperature increases as a result of increased gravity. Consequently, a point will eventually be reached where the temperature of the region of interest is in fact below the critical temperature. Condensation can begin to occur. As the surface of the Sun is increasingly approached, the critical temperature increases further. This is a manifestation of increased gravity and magnetic forces. By the time the photosphere is reached, the region of interest is now well below the critical temperature and the liquid state becomes stable. The surface at this point is visualized.

Therefore, in the liquid model, the chromosphere represents that region where matter projected into the corona is now in the process of re-condensing in order to enter the liquid state of the photosphere. Such an elegant explanation of the chromosphere is lacking for the gaseous models. Indeed, for these models, the understanding of the chromosphere requires much more than elementary chemical principles.

8. Shape:

The Sun is not a perfect sphere. It is oblate. Solar oblateness [21] is a direct manifestation of solar rotation and can best be understood by examining the rotation of liquid masses [22]. The oblateness of the solar disk has recently come under re-evaluation. While exact measurements have differed in the extent of solar oblateness, it appears that the most reliable studies currently place solar oblateness at 8.77×10^{-6} [21]. In order to understand solar oblateness, astrophysics is currently invoking a relative constant solar density as a function of radial position [21]. This is in keeping with our understanding of liquid body rotations [22], but is in direct opposition to the densities calculated using the gaseous equations of state [i. e. 4]. Interestingly, a relatively constant density is precisely what is invoked in the condensed matter model of the Sun [1]. The question becomes even more important when one considers stars like Achanar whose oblateness approaches 1.5 [23]. Such an observation would be difficult to rationalize were the Sun truly gaseous.

9. Surface activity:

The Sun has extensive surface activity and appears to be boiling. Indeed, several undergraduate texts actually refer to the Sun as a boiling gas. In addition to the boiling action, the Sun is characterized by numerous solar eruptions. Both of these phenomena (boiling and solar eruptions) are extremely difficult to rationalized for the gaseous models. Gases do not boil. They are the result of such action. It is an established fact that liquids boil giving rise to gases. There is no evidence on Earth that superheating a gas can give rise to a region of different density capable of erupting from the gaseous mass. These are extremely complex issues for the gaseous models since actions resembling both boiling and superheating must be generated without having recourse to the liquid state.

In contrast, the presence of superheated liquids within the solar interior could easily explain the production of solar eruptions. The existence of boiling action is well documented for the liquid. Nothing further need be added. Phenomena easily explained in the liquid model, become exceedingly difficult for the gaseous equations of state.

10. Photospheric/coronal flow:

It has been well established that the Sun displays pronounced flows at the surface. Matter can be seen rising from, and descending into, the solar interior. However, matter is also traversing the solar surface in a manner perpendicular to established flows in the corona. The photosphere is characterized not simply by a change in opacity as the gaseous models theorize, but by drastically altered directions of material flow relative to the corona. In the liquid model, the interface delineated by flow directions can be explained based on the existence of a phase transition between the photosphere and the corona. In fact, the orthogonality of mass displacement at the solar surface relative to the corona is reminiscent of the orthogonality observed on Earth between the currents in the oceans and the upward and downwards drafts sometimes observed in the overlying air. It is not trivial for the gaseous models to account for the orthogonality of flow between the photosphere and the corona. By contrast, this is a natural extension of current knowledge relative to liquid/gaseous interfaces for the liquid model.

11. Photospheric imaging:

The solar surface has recently been imaged in high resolution using the Swedish Solar Telescope [24, 25]. These images reveal a clear solar surface in 3D with valleys, canyons, and walls. Relative to these findings, the authors insist that a true surface is not being seen. Such statements are prompted by belief in the gaseous models of the Sun. The gaseous models cannot provide an adequate means for generating a real surface. Solar opacity arguments are advanced to caution the reader against interpretation that a real surface is being imaged. Nonetheless, a real surface is required by the liquid model. It appears that a real surface is being seen. Only our theoretical arguments seem to support our disbelief that a surface is present.

12. Dynamo action:

The Sun is characterized by strong magnetic fields. These magnetic fields can undergo complex winding and protrusions. On Earth however, strong magnetic fields are always produced from condensed matter. The study of dynamos relies on the use of molten sodium [26], not gaseous sodium. It is much more realistic to generate powerful magnetic fields in condensed matter than in sparse gaseous plasmas. Consequently, the liquid model and its condensed phase lends itself much more readily to the requirements that the Sun possesses strong magnetic fields.

13. Sun spots:

The presence of Sun spots have long been noted on the solar sphere. Sun spots are often associated with strong magnetic activity. The gaseous models explain the existence of Sun spots with difficulty. The problem lies in the requirement that different types of order (disorder) can coexist in stellar gases, based on the presence of a magnetic field. While there is ample room here for theoretical arguments justifying the existence of Sun spots in a gaseous model, the situation is less complex in the liquid model. Thus, if one considers that the bulk of the solar photosphere exists with hydrogen and helium adhering to a certain lattice structure, all that is required is a concentration of magnetic fields within a region to produce a change in the lattice. The surface of the Sun is changed from a hypothetical "Type I lattice" to a "Type II lattice". The requirement that a strong magnetic field alters the structure of condensed matter in an ordered lattice from one form to another, is much less than would be required to alter the structure of a gaseous plasma (something which has no inherent lattice).

Conclusion

The evidence in favor of a condensed matter model of the Sun is overwhelming. For every avenue explored, the condensed model holds clear advantages in simplicity of understanding. In fact, it remains surprising that the gaseous models have been able to survive for so long. This is partially due to the elegance with which the theoretical framework is established. Moreover, the gaseous equations of state have such profound implications for astrophysics.

Consequently, it is recognized that the acceptance of any condensed matter model will require such dramatic changes in astrophysics that such adoption cannot be swift. In the meantime, it is important to set out the physical evidence for a liquid model both in manuscript [1] and abstract form [27–30]. Eventually, astrophysics may well be forced to abandon the gaseous models and their equations of state. It is likely that this will occur when the field more fully appreciates the lack of universality in blackbody radiation [7, 9, 31]. At this time, gases will no longer be hypothesized as suitable candidates for the emission of thermal radiation. The need for condensed matter will be self-evident.

References

1. Robitaille P. M. L. A high temperature liquid plasma model of the Sun. 2004, arXiv: astro-ph/0410075.
2. Planck M. Ueber das Gesetz der Energieverteilung in Normalspectrum. *Annalen der Physik*, 1901, Bd. 4, 553.
3. March N. H., Tosi M. P. Introduction to liquid state physics. World Scientific, New Jersey, 2002.
4. Kippenhahn R., Weigert A. Stellar structure and evolution. 3rd ed., Springer-Verlag, Berlin, 1994.
5. Kirchhoff G. Ueber den Zusammenhang von Emission und Absorption von Licht und Warme. *Monatsberichte der Akademie der Wissenschaften zu Berlin*, Sessions of Dec. 1859, 1860, 783.

6. Kirchhoff G. Ueber das Verhaltnis zwischen dem Emissionsvermogen und dem Absorptionsvermogen der Korper fur Warme und Litcht. *Annalen der Physik*, 1860, Bd. 109, 275.
7. Robitaille P. M. L. On the validity of Kirchhoff's law of thermal emission. *IEEE Trans. Plasma Science*, 2003, v. 31(6).
8. Einstein A. *Phys. Zs.*, 1917, Bd. 18, 121; English Translation: On the quantum theory of radiation, by D. der Haar, the old quantum theory. Pergamon Press, New York, 1967, 167.
9. Robitaille P. M. L. An analysis of universality in blackbody radiation. 2005, arXiv: physics/0507007.
10. Langley S. P. Experimental determination of wave-lengths in the invisible spectrum. *Mem. Natl. Acad. Sci.*, 1883, v. 2, 147.
11. Langley S. P. On hitherto unrecognized wave-lengths. *Phil. Mag.*, 1886, v. 22, 149.
12. Penner S. S. Quantitative molecular spectroscopy and gas emissivities. Addison-Wesley Publishing Company, Inc., Reading MA, 1959.
13. Knudsen J. G., Hottel H. C., Sarofim A. F., Wankat P. C., Knaebel K. S. Heat transmission. *Perry's Chemical Engineers' Handbook*, 7th ed., R. H. Perry, D. W. Green and J. O. Maloney, Eds. The McGraw-Hill Book Company, New York, 1997, v. 5, 23.
14. Siegel R., Howell J. Thermal radiation heat transfer. 4th ed., Taylor and Francis, New York, 2002,
15. Touloukian Y. S., Ho C. Y. Thermophysical properties of matter. Plenum, New York, 1970, v. 1–8.
16. Ulaby F. T., Moore R. K., Fung A. K. Microwave remote sensing active and passive: radar remote sensing and surface scattering and emission theory. Addison-Wesley Publishing Company, London, 1982, v. 2, 880.
17. Gough D. O. Seismology of the Sun and the distant stars. D. Reidel Publishing Company, Dordrecht, 1986.
18. Bahcall J. N., Pinsonneault M. H., Basu S. Solar models: current epoch and time dependences, neutrinos, and helioseismological properties. *Astrophysical J.*, 2001, v. 555, 990.
19. Kosovichev A. G., Zharkova V. V. X-ray flare sparks quake inside the Sun. *Nature*, 1998, v. 393, 28.
20. Fleck B., Brekke P., Haugan S., Duarte L. S., Domingo V., Gurman J. B., Poland A. I. Four years of SOHO discoveries — some highlighs. *ESA Bulletin*, 2000, v. 102, 68.
21. Godier S., Rozelot J. P. The Solar oblateness and its relationship with the structure of the tacholine and the Sun's subsurface. *Astron. Astrophys.*, 2000, v. 355, 365–374.
22. Littleton R. A. The stability of rotating liquid masses. Cambridge University Press, Cambridge, 1953.
23. Domiciana de Souza A., Kervella P., Jankov S., Abe L., Vakili F., di Folco E., Paresce F. The spinning-top be star achernar from VLTI-VINCI. *Astron. Astrophys.*, 2003, v. 407, L47–L50.
24. Roberts A. M. Solar faculae stand exposed. *Sky and Telescope*, 2003, v. 106(4), 26.
25. Scharmer G. B., Gudiksen B. V., Kiselman D., Lfdahl M. G., Rouppe van der Voort L. H. M. Dark cores in sunspot pernumbral filaments. *Nature*, 2002, v. 420, 151.
26. Nornberg M. D., Spence E. J., Kendrick R. D., Forest C. B. Measurement of the magnetic field induced by a turbulent flow liquid metal. 2005, arXiv: physics/0510265.
27. Robitaille P. M. L. Evidence for a liquid plasma model of the Sun. APS April 2004, http://www.aps.org/meet/APR04/baps/abs/S280002.html.
28. Robitaille P. M. L. The Sun as a hot liquid plasma: additional evidence. APS Ohio Spring 2004, http://www.aps.org/meet/OSS04/baps/abs/S50002.html.
29. Robitaille P. M. L. The photosphere as condensed matter. APS Ohio Fall 2004, http://meeting.aps.org/meet/OSF04/baps/abs/S60005.html.
30. Robitaille P. M. L. The Sun as a hot liquid plasma: more evidence. APS NE Fall 2004, http://www.aps.org/meet/NEF04/baps/abs/S10004.html.
31. Robitaille P. M. L. Blackbody radiation: Kirchhoff's error propagates beyond Einstein. APS NE Spring 2005, http://meetings.aps.org/Meeting/NES05/Event/31261.

An Analysis of Universality in Blackbody Radiation

Pierre-Marie Robitaille
130 Means Hall, 1654 Upham Drive, The Ohio State University, Columbus, Ohio 43210, USA
E-mail: robitaille.1@osu.edu

Through the formulation of his law of thermal emission, Kirchhoff conferred upon blackbody radiation the quality of universality [G. Kirchhoff, *Annalen der Physik*, 1860, v. 109, 275]. Consequently, modern physics holds that such radiation is independent of the nature and shape of the emitting object. Recently, Kirchhoff's experimental work and theoretical conclusions have been reconsidered [P. M. L. Robitaille. *IEEE Transactions on Plasma Science*, 2003, v. 31(6), 1263]. In this work, Einstein's derivation of the Planckian relation is reexamined. It is demonstrated that claims of universality in blackbody radiation are invalid.

From the onset, blackbody radiation was unique in possessing the virtue of universality [1, 2]. The nature of the emitting object was irrelevant to emission. Planck [3], as a student of Kirchhoff, adopted and promoted this concept [4, 5]. Nonetheless, he warned that objects sustaining convection currents should not be treated as blackbodies [5].

As previously discussed in detail [6], when Kirchhoff formulated his law of thermal emission [1, 2], he utilized two extremes: the perfect absorber and the perfect reflector. He had initially observed that all materials in his laboratory displayed distinct emission spectra. Generally, these were not blackbody in appearance and were not simply related to temperature changes. Graphite, however, was an anomaly, both for the smoothness of its spectrum and for its ability to simply disclose its temperature. Eventually, graphite's behavior became the basis of the laws of Stefan [7], Wien [8] and Planck [3].

For completeness, the experimental basis for universality is recalled [1, 2, 5, 6]. Kirchhoff first set forth to manufacture a box from graphite plates. This enclosure was a near perfect absorber of light ($\varepsilon = 1$, $\kappa = 1$). The box had a small hole through which radiation escaped. Kirchhoff placed various objects in this device. The box would act as a transformer of light [6]. From the graphitic light emitted, Kirchhoff was able to gather the temperature of the enclosed object once thermal equilibrium had been achieved. A powerful device had been constructed to ascertain the temperature of any object. However, this scenario was strictly dependent on the use of graphite.

Kirchhoff then sought to extend his findings [1, 2, 5]. He constructed a second box from metal, but this time the enclosure had perfectly reflecting walls ($\varepsilon = 0$, $\kappa = 0$). Under this second scenario, Kirchhoff was never able to reproduce the results he had obtained with the graphite box. No matter how long he waited, the emitted spectrum was always dominated by the object enclosed in the metallic box. The second condition was unable to produce the desired spectrum.

As a result, Kirchhoff resorted to inserting a small piece of graphite into the perfectly reflecting enclosure [5]. Once the graphite particle was added, the spectrum changed to that of the classic blackbody. Kirchhoff believed he had achieved universality. Both he, and later, Planck, viewed the piece of graphite as a "catalyst" which acted only to increase the speed at which equilibrium was achieved [5]. If only time was being compressed, it would be mathematically appropriate to remove the graphite particle and to assume that the perfect reflector was indeed a valid condition for the generation of blackbody radiation.

However, given the nature of graphite, it is clear that the graphite particle was in fact acting as a perfect absorber. Universality was based on the validity of the experiment with the perfect reflector. Yet, in retrospect, and given a modern day understanding of catalysis and of the speed of light, the position that the graphite particle acted as a catalyst is untenable. In fact, by adding a perfect absorber to his perfectly reflecting box, it was as if Kirchhoff lined the entire box with graphite. He had unknowingly returned to the first case. Consequently, universality remains without any experimental basis.

Nonetheless, physics has long since dismissed the importance of Kirchhoff's work [9]. The basis for universality no longer rests on the experimental proof [i. e. 9], but rather on Einstein's theoretical formulation of the Planckian relation [10, 11]. It has been held [i. e. 9] that with Einstein's derivation, universality was established beyond doubt based strictly on a theoretical platform. Consequently, there appears to no longer be any use for the experimental proof formulated by Kirchhoff [1, 2, 5]. Physics has argued [9] that Einstein's derivation of the Planckian equations had moved the community beyond the limited confines of Kirchhoff's enclosure. Einstein's derivation, at least on the surface, appeared totally independent of the nature of the emitting compound. Blackbody radiation was finally free of the constraints of enclosure.

In his derivation of the Planckian relation, Einstein has

recourse to his well-known coefficients [10, 11]. Thermal equilibrium and the quantized nature of light ($E = \hbar\nu$) are also used. All that is required appears to be (1) transitions within two states, (2) absorption, (3) spontaneous emission, and (4) stimulated emission. However, Einstein also requires that gaseous atoms act as perfect absorbers and emitters or radiation. In practice, of course, isolated atoms can never act in this manner. In all laboratories, isolated groups of atoms act to absorb and emit radiation in narrow bands and this only if they possess a dipole moment. This is well-established in the study of gaseous emissions [12]. As such, Einstein's requirement for a perfectly absorbing atom, knows no physical analogue on earth. In fact, the only perfectly absorbing materials known, exist in the condensed state. Nonetheless, for the sake of theoretical discussion, Einstein's perfectly absorbing atoms could be permitted.

In his derivation, Einstein also invokes the requirement of thermal equilibrium with a Wien radiation field [8], which of course, required enclosure [1, 2]. However, such a field is uniquely the product of the solid state. To be even more specific, a Wien's radiation field is currently produced with blackbodies typically made either from graphite itself or from objects lined with soot. In fact, it is interesting that graphite (or soot) maintain a prominent role in the creation of blackbodies currently used at the National Bureau of Standards [13–17].

Consequently, through his inclusion of a Wien's radiation field [8], Einstein has recourse to a physical phenomenon which is known to be created exclusively by a solid. Furthermore, a Wien's field, directly involves Kirchhoff's enclosure. As a result, claims of universality can no longer be supported on the basis of Einstein's derivation of the Planckian relation. A solid is required. Therefore, blackbody radiation remains exclusively a property of the solid state. The application of the laws of Planck [3], Stefan [7] and Wien [8] to non-solids is without both experimental and theoretical justification.

References

1. Kirchhoff G. Ueber den Zusammenhang von Emission und Absorption von Licht und Warme. *Monatsberichte der Akademie der Wissenschaften zu Berlin*, sessions of Dec. 1859, 1860, 783.
2. Kirchhoff G. Ueber das Verhaltnis zwischen dem Emissionsvermogen und dem Absorptionsvermogen der Korper fur Warme und Litcht. *Annalen der Physik*, 1860, v. 109, 275.
3. Planck M. Ueber das Gesetz der Energieverteilung in Normalspectrum. *Annalen der Physik*, 1901, v. 4, 553.
4. Planck M. The new science. Meridian Books, Inc., New York, 1959, 18.
5. Planck M. The theory of heat radiation. P. Blakiston's Son & Co., Philadelphia, PA, 1914.
6. Robitaille P. M. L. On the validity of Kirchhoff's law of thermal emission. *IEEE Trans. Plasma Sci.*, 2003, v. 31(6), 1263.
7. Stefan J. Ueber die Beziehung zwischen der Warmestrahlung und der Temperatur. *Wein. Akad. Sitzber.*, 1879, v. 79, 391.
8. Wien W. Ueber die Energieverteilung im Emissionspektrum eines schwarzen Korpers. *Annalen der Physik*, 1896, v. 58, 662.
9. Schirrmacher A. Experimenting theory: the proofs of Kirchhoff's radiation law before and after Planck. http://www.mzwtg.mwn.de/arbeitspapiere/Schirrmacher_2001_1.pdf.
10. Einstein A. Strahlungs-Emission und Absorption nach der Quantentheorie. *Verhandlunger der Deutschen Physikalischen Gesellschaft*, 1916, v. 18, 318.
11. Einstein A. *Phys. Zs.*, 1917, v. 18, 121; English Translation: On the quantum theory of radiation, by D. der Haar, the old quantum theory. Pergamon Press, New York, 1967, 167.
12. Penner S. S. Quantitative molecular spectroscopy and gas emissivities. Addison-Wesley Publishing Company, Inc., Reading, MA, 1959.
13. Fowler J. B. A Third generation water bath based blackbody source. *J. Res. Natl. Inst. Stand. Technol.*, 1995, v. 100, 591.
14. Fowler J. B. An oil-based 293 K to 473 K blackbody source. *J. Res. Natl. Inst. Stand. Technol.*, 1996, v. 101, 629.
15. Murphy A. V., Tsai B. K., Saunders R. D. Comparative calibration of heat flux sensors in two blackbody facilities. *J. Res. Natl. Inst. Stand. Technol.*, 1999, v. 104, 487.
16. Murphy A. V., Tsai B. K., Saunders R. D. Transfer calibration validation tests on a heat flux sensor in the 51 mm high-temperature blackbody. *J. Res. Natl. Inst. Stand. Technol.*, 2001, v. 106, 823.
17. Navarro M., Bruce S. S., Johnson B. C., Murphy A. V., Saunders R. D. Vacuum processing technique for development of primary standard blackbodies. *J. Res. Natl. Inst. Stand. Technol.*, 1999, v. 104, 253.

Exotic Material as Interactions Between Scalar Fields

Glen A. Robertson
Gravi Atomic Research, 265 Ita Ann Ln., Madison, Al 35757, USA
E-mail: gravi_atomic@hotmail.com

Many theoretical papers refer to the need to create exotic materials with average negative energies for the formation of space propulsion anomalies such as "wormholes" and "warp drives". However, little hope is given for the existence of such material to resolve its creation for such use. From the standpoint that non-minimally coupled scalar fields to gravity appear to be the current direction mathematically. It is proposed that exotic material is really scalar field interactions. Within this paper the Ginzburg-Landau (GL) scalar fields associated with superconductor junctions is investigated as a source for negative vacuum energy fluctuations, which could be used to study the interactions among energy fluctuations, cosmological scalar (i. e., Higgs) fields, and gravity.

1 Introduction

Theoretically, exotic material can be used to establish wormholes by gravitationally pushing the walls apart [1] and for the formation of a warp bubble [2] by providing the negative energy necessary to warp spacetime. Exotic material in combination with gravitation might also produce a net acceleration force for highly advanced propellant-less space propulsion engine cycles.

Negative energy is encountered in models of elementary particles. For example, Jackson [3] invokes Poincare stress, to suppress the TeV/c^2 contribution of electromagnetic field energy to the MeV/c^2 mass of an electron. Also, the Reissner-Nordstrom metric [4], devised 50 years before the development of scalar fields, predicts effects which are negligible more than a few *femtometers* $[10^{-15}\,\mathrm{m}]$ from a charged particle.

Exotic material has the requirement of a "negative average energy density", which violates several energy conditions and breaks Lorentz symmetries. Pospelov and Romalis [5] tell us that the breaking of Lorentz symmetry enables the CPT symmetry, which combines charge conjugation (C), parity (P), and time-reversal (T) symmetries, to be violated. In conventional field theories, the Lorentz and CPT symmetries are automatically preserved. But in quantum gravity, certain restrictive conditions such as locality may no longer hold, and symmetries may be broken. They also suggest that quintessence, a very low-energy 5 keV/cm^3 scalar field ψ with wavelength comparable to the size of the observable universe, is a candidate for dark energy. For in addition to its effect on the expansion of the universe, quintessence might also manifest itself through its possible interactions with matter and radiation [6, 7]. This scalar interaction could lead to a modification of a mass as a function of coordinates and violates the equivalence principle: The mass feels an extra force in the direction of $\nabla\phi$ (ϕ is the phase of the scalar field ψ).

The question is then "Where do we look for exotic material on the scale of laboratory apparatus?" From the standpoint that non-minimally coupled scalar fields to gravity appear to be the current direction mathematically [8]. It is proposed that exotic material is really scalar field interactions.

Within this paper the Ginzburg-Landau (GL) scalar fields associated with superconductor junctions is investigated as a source for negative vacuum energy fluctuations, which could be used to study the interactions among energy fluctuations, cosmological scalar (i. e., Higgs) fields, and gravity. Such an analogy is not much a stretch as it is not hard to show that the Higgs model is simply a relativistic generalization of the GL theory of superconductivity, and the classical field in the Higgs model is analog of cooper-pair Bose condensate [9]. Here, the mechanisms for scalar field interactions or the production of exotic material from the superconductor are discussed and an analogy to energy radiated in gravitational waves is presented.

2 Background

Theoretical work [1] has shown that vacuum fluctuations near a black hole's horizon are exotic due to curvature distortion of space-time. Vacuum fluctuations come about from the notion that when one tries to remove all electric and magnetic fields from some region of space to create a perfect vacuum, there always remain an excess of random, unpredictable electromagnetic oscillations, which under normal conditions averages to zero. However, curvature distortion of space-time as would occur near black holes causes vacuum energy fluctuations to become negative and therefore are "exotic". In earlier wormhole theories [10, 11], exotic material was

generally thought to only occur in quantum systems [1]. It seems that the situation has changed drastically; for it has now been shown that even classical systems, such as those built from scalar fields non-minimally coupled to gravity; violate all energy conditions [8]. Gradually, these energy conditions are losing their status, which theoretically could lead even to a workable "warp drive" [12]. Further, recent mathematical models have shown that the amount of energy needed for producing wormholes (and possibly warp drives) is much less than originally thought [13], which may open the door to laboratory scale experiments.

Given that the answer to exotic material for practical propulsion applications is somewhere in between vacuum fluctuation in curved space-time and scalar fields non-minimally coupled to gravity, Ginzburg-Landau (GL) scalar fields associated with superconductor junctions could present themselves as a medium for studying the interactions among energy fluctuations, cosmological scalar fields, and gravity. As in superconductors, the GL scalar field is known [14] to extend small distances beyond the boundaries of a superconducting material. That is, in describing the operation of a Josephson junction array, two or more superconductors can be entangled over gaps of several micrometers, which is large compared to atomic distances.

The introduction of scalar fields into cosmology has been problematic. For example, the Higgs scalar field [15] of particle physics must have properties much different from the scalar field hypothesized to cause the universe to increase its expansion rate 5G years ago. However, the study of particle physics in conjunction with inflationary cosmology presents a new understanding of present day physics through the notion of symmetry breaking [9]. This suggests that the GL scalar field could possibly bridge the gap between the subatomic energy and distance scale of particle physics and the galactic scale of scalar fields in cosmology?

3 Landau-Ginzburg field in the superconductor

The Landau-Ginzburg (GL) field ψ is described as a scalar function

$$\psi = \sqrt{n}\, e^{j\theta}, \tag{1}$$

where $\sqrt{n}$ infers the degree of electron interactions in the superconductor and θ is the phase factor of these interactions.

Electrons in a room temperature superconductor material or normal conductor with no applied external fields are either confined to an atom or move about the composite molecules with random phases; $\sum \phi \approx 0$ (disorder state). However, they are generally thought to be confined to the vicinity of background ions and are positionally fixed. When the superconductor material is cooled to its critical temperature at which time a phase transition occurs, the electrons suddenly agree on a common phase; $\sum \phi > 0$ (ordered state). Again they are generally thought to be confined to the vicinity of background ions and are localized as opposed to gathering in some region creating a large space charge potential.

In a type I superconductor and as the bulk superconductor material cools down (or warms up), various size domains (depending on the cool-down, or warm up, profile) of superconductive material can form surrounded by normal conductive material. When two or more domains are in close proximity, a superconductor-normal conductor-superconductor Josephson junction is formed. In a typical bulk type I superconductor, composed of small randomly arranged crystals or grains, proximity effects would cause the electrons of a single grain to go superconductive (or normal) as a group.

In the type II YBCO superconductor this is also true with the exception that weakly coupled Josephson junctions [16] can also form between individual molecules across the copper oxide planes and across grain boundaries typically composed of an oxide layer. These are referred to as superconductor-insulator-superconductor junctions. The insulation planes degrade the time for proximity effects to cause the electrons of a single grain to go superconductive (or normal) as a group. Therefore in the type II superconductor, a superconductor domain can be as small as one molecule of superconductor material or composed of a multitude of molecules (i. e., grains).

In both the type I & II superconductor at temperatures below ~ 44 K, coherence encompasses all domains, in effect producing one single domain of phase ϕ.

When multiple domains exist, gradients between domains of differing phase ϕ are accompanied by currents that tunnel between the domains as the spaces between the domains form Josephson junctions [14]. The possible current patterns are restricted by the requirement that the GL scalar function ψ must be single-valued and infers a current flow of density $\vec{J}$ given by

$$\vec{\nabla} \arg \psi = \vec{\nabla}\phi = \frac{m}{2\hbar e|\psi|^2}\, \vec{J}; \tag{2}$$

neglecting contributions from external magnetic fields.

3.1 The Landau-Ginzburg free energy potential

The Landau-Ginzburg free energy potential $V(\psi)$ refers to the energy density in the superconductor, and anywhere the scalar field is non-zero. It can even extend into a region μm outside the superconductor. The potential contribution to the free energy (neglecting contributions from external magnetic fields) is given by the energy density function:

$$V(\psi) = \alpha\,|\psi|^2 + \frac{1}{2}\,\beta\,|\psi|^4, \tag{3}$$

where equation (3) can be viewed as a series expansion in powers of $|\psi|^2$.

Two cases arise as depending whether α is positive or negative. If α is positive, the minimum free energy occurs at $|\psi|^2 = 0$, corresponding to the normal state. On the other

hand, if $\alpha < 0$, the minimum occurs when

$$|\psi|^2 = |\psi_\infty|^2 = \frac{1}{2}\sqrt{n_1 n_2} \approx \frac{n_{3D}}{2} \quad (4)$$

for identical domain materials (which is assumed hereon) where the notation ψ_∞ is conventionally used because ψ approaches this value infinitely deep in the interior of the superconductor [17], where it is screened from any surface fields or currents. If the two domains are similar in crystalline structure, the two domains can be viewed as a single bulk superconductor and the Landau-Ginzburg free energy potential case for $\alpha < 0$ applies. For $\alpha < 0$

$$V(\psi_\infty) = \frac{-\alpha^2}{2\beta} = \frac{1}{2}\alpha|\psi_\infty|^2, \quad (5)$$

which gives

$$\alpha = \frac{2}{|\psi_\infty|^2}V(\psi_\infty); \qquad \beta = \frac{2}{|\psi_\infty|^4}V(\psi_\infty). \quad (6)$$

4 High power flow during phase transition

Given a uniform superconductor, the average energy E_J in the junction between domains is defined by

$$E_J \leqslant \Delta|\psi|^2\overline{V}_g \approx \frac{1}{2}\Delta n_{3D}\overline{V}_g. \quad (7)$$

For the Type II YBCO superconductor $n_{3D} \approx 1.69\times10^{28}$ m^3 and $\Delta = 0.014$ eV [17, 18]. Given that grain size diameters in a typical sinter YBCO superconductor are on the order of 1 micron, then for an average domain volume $\overline{V}_g \approx 10^{-18}$ m^3, the energy in the junction $E_J \approx 10^2$ GeV. If the junction energy dissipates on the superconductor relaxation time τ_{sc}, the powers flow $E_J/\tau_{sc} \approx 10^{24}$ eV/s for the YBCO relaxation time $\tau_{sc} \approx 10^{16}$ s.

Such high energy changes during a normal state transition seems a bit extreme, especially considering that not much (if any) is mentioned of this phenomena in the literature. The main reason is that most of the energy should not be seen external to the superconductor since the initial energy transfer from the state change is an internal process. However radiation is known to accompany processes involving charged particles, such as β decay.

Jackson [3] tells us that the radiation accompanying β decay is a Bremsstrahlung spectrum: It sometimes bears the name "inner bremsstrahlung" to distinguish it from bremsstrahlung emitted by the same beta particle in passing through matter. It appears that the spectrum extends to infinity, thereby violating conservation of energy. Qualitative agreement with conservation of energy can obtain by appealing to the uncertainty principle. That is, the acceleration time τ must be of the order of $\tau = \hbar/E$, thereby satisfying the conservation of energy requirement at least qualitatively.

In the superconductor, the uncertainty principle (at least qualitatively) allows for the violation of energy conservation through rapid state change processes, which can produce vortices in the superconductor when proper phase alignment exists among domains [19]. In such a case, high energy radiation, such as Bremsstrahlung accompanying the rapid magnetic field formation cannot be ruled out as theories of superconductivity are not sufficiently understood. This is especially true with the type II superconductor, which exhibits flux pinning throughout the body of the superconductor and allows for flux motion during phase transition.

Further, energy levels of $E_J \approx 10^2$ GeV in the domain junctions could produce tunneling electrons with critical temperature for a phase transition in the Glashow-Weinberg-Salam theory of weak and electromagnetic interactions [20]. Such high energy phase transitions could then lead to effects similar to cosmology inflation, an anti-gravity force thought responsible for the acceleration of the universe [21].

5 Mechanisms for exotic material in the superconductor

In order to produce exotic material or negative vacuum energy fluctuations from superconductors in terms of curvature distortion of spacetime, asymmetric energy fluctuations must be produced. Since the Landau-Ginzburg free energy density is fixed by the number superconductor electrons, the average time rate of change or phase transition time of the superconductor electrons must be asymmetric. That is the power flow eV/s in the phase transition to the superconductor state must be higher than the power in the phase transition to the normal state or vise versa. This process of creating a time varying GL scalar field might then result in a gradient in the surrounding global vacuum scalar field (Higgs, quintessence, or etc.) in the direction of $\nabla\phi$; being measurable as a gravitation disturbance.

Asymmetric phase transitions would require electrons with group velocities that are higher than their normal relaxation times, which are already relativity short. The combination of two phenomena associated with superconductors could achieve this requirement. They are:

(1) The dissipation of the Landau-Ginzburg free energy potential during a rapid superconductor quench referred to as spontaneous symmetry breaking phase transition [22], which implies state changes on very short time scales;

(2) The Hartman effect [23], which implies that the effective group velocity of the electrons across a superconductor junction can become arbitrarily large.

Both spontaneous symmetry breaking and the Hartman effect illustrates Hawking's [24] point about the elusive definition of time in a quantum mechanical process. That is, uncertainty in the theory allow time intervals to be chosen to illustrate how measurable effects might be produced outside the superconductor without contradicting experiments with

conventional solid state physics detectors. One such time interval of notice is that which occurs during a spontaneous symmetry breaking phase transitions.

5.1 Spontaneous symmetry breaking phase transition

Phase transitions between the high and low temperature phases of a superconductor involve spontaneous symmetry breaking between order (superconductor electron pair) and disorder (electron) states when the transition occurs over shorter time periods than depicted by the normal relaxation times. Kibble [25] explains that symmetry-breaking phase transitions are ubiquitous in condensed matter systems and in quantum field theories. There is also good reason to believe that they feature in the very early history of the Universe. At which time many such transitions topological defects of one kind or another are formed. Because of their inherent stability, they can have important effects on the subsequent behavior of the system. Experimental evidence validates this by the presence of a magnetic field [26, 27, 19, 28] during spontaneous symmetry breaking phase transition experiments.

In general, each superconductor domain must be taken to follow normal phase transition symmetry, which follows that the energy within these domains is conserved as anomalous energy effects have not been observed during rapid superconductor quenching of low temperature superconductive systems, which have been around for decades. However, it is conceivable that, a small fraction of the energy could be expended in disturbing nearby vacuum fields, without being noticed by crystal-switching apparatus. Since experimentally, the formation of vortices does occur during spontaneous symmetry breaking phase transitions of coupled domains in the Type II superconductor, Lorentz symmetry is violated. This allows for energy conservation violation, whereby, the assumption can be made that the energy fluctuations in the junction between superconductor domains interacts with the vacuum field on a time scale that approaches that of the Planck scale.

Evidence of this comes from Pospelov and Romalis [5], who point out that Lorentz violation could possibly be due to unknown dynamics at the Planck scale. Further, when dealing with interactions described by massless vector particles (gluons) within a relativistic local quantum field theory, Binder [42] indicates that Planck units are assigned to the background fluctuation level and provide for a common base. The gluon field plays the same role for quarks as Jackson's Poincare stress plays for electrons. Therefore, the choice for the energy fluctuation time during a spontaneous symmetry breaking phase transition of electron pairs is taken to be the Planck time T_{pl} .

However, the Planck time is too fast to be observed, which implies that human units must be artificially imposed when measuring superconductor electron fluctuations (or any other Planck time phenomena). To explain this, it is noted that just before electron phase transition and superconductor pair bonding, each electron had an energy deficit ≈ 1 eV. From the uncertainty principle, the electron can maintain this deficit before pairing for a time t according to

$$t = \frac{\hbar}{E}\,, \tag{8}$$

which for the paired electron $E \approx 2$ eV giving $t \approx 3.3 \times 10^{-16}$ sec. Then by noting

$$E_p\, T_{pl} = E\, t = \hbar \tag{9}$$

a limitation on the electron power flow exist at $E = E_p$ (the Planck energy) and $t = T_{pl}$. This limitation gives the human artificial units for Planck time events according to

$$t = \frac{E_p}{E}\, T_{pl}\,. \tag{10}$$

For example, during an electron pair transition where $t \approx 3.3 \times 10^{-16}$ s, a power flow $E/T_{pl} = E_p/t \approx 10^{43}$ eV/s per superconductor electron pair is produced, which is much less than the limit defined by $E_p/T_{pl} \approx 10^{71}$ eV/s.

That is, even though the event could have occurred on the Planck time T_{pl}, it took a time t to observe/measure the energy released. According to the uncertainty principle, the observed/measured value of the energy is then

$$E = \left(\frac{T_{pl}}{t}\right) E_p\,. \tag{11}$$

Equation (11) then tells us that energy events that occur on the Planck time are reduced by the ratio of the Planck time to the observed/measured time.

The question is then, "Can this uncertainly in the energy be captured in such a way as to be useable on the human scale?" Evidence for a yes answer arises in superluminal electron velocities in nature, which have been associated with cosmological events, lasers and electrostatic acceleration [29, 30, 31]. In these events however, the total energy in the system is interpreted from the average group velocity, whereby energy is conserved.

5.2 The Hartman effect

In the superconductor another superluminal electron phenomena exists, the Hartman effect [23, 32, 33], which is associated with the junction tunnelling process. The Hartman effect indicates that for sufficiently large barrier widths, the effective group velocity of the electrons across a superconductor junction can become arbitrarily large, inferring a violation of energy conservation.

Muga [34] tells us that defining "tunnelling times" has produced controversial discussion. Some of the definitions proposed lead to tunnelling conditions with very short times,

which can even become negative in some cases. This may seem to contradict simple concepts of causality. The classical causality principle states that the particle cannot exit a region before entering it. Thus the traversal time must be positive. However, when trying to extend this principle to the quantum case, one encounters the difficulty that the traversal time concept does not have a straightforward and unique translation in quantum theory. In fact for some of the definitions proposed, in particular for the so called "extrapolated phase time" [35], the naпve extension of the classical causality principle does not apply for an arbitrary potential, even though it does work in the absence of bound states.

Generally, the Hartman effect occurs when the time of passage of the transmitted wave packet in a tunnelling collision of a quantum particle with an opaque square barrier or junction becomes essentially independent of the barrier width [23, 36] and the velocity may exceed arbitrarily large numbers. This "fast tunnelling" has been frequently interpreted as, or related to, a "superluminal effect", see e. g. [37, 38, 39, 40, 41].

The Hartman effect illustrates Hawking's (1988) discussion about ambiguities in defining time in relation to quantum mechanics and cannot be ruled out during spontaneous symmetry breaking phase transition. Therefore, large power flows across the junctions between the domains or junctions are allowed.

6 Energy radiated in gravitational waves

Arbitrarily large electron group velocities (the Hartman effect) induced by spontaneous symmetry breaking phase transitions could conceivably result in a space-like (gravitational) disturbance in nearby vacuum scalar fields with possible momentum and energy transfer about these disturbances for space propulsion applications. Although, a theory that connects the GL scalar field to gravity has yet to be presented, here the general formulation for calculating gravitational radiation from quadrupolar motion [43] is used to illustrate the possible energy radiated in a gravitational wave from the instantaneous power flow through a type II superconductor.

The power radiated L_{rad} in gravitational waves is roughly approximated from the ratio of the square of the internal power flow $\Delta E/\Delta t$ by

$$L_{rad} = \left(\frac{G}{c^5}\right)\left(\frac{\Delta E}{\Delta t}\right)^2 . \qquad (12)$$

The time parameter Δt in equation (11) is ill-defined, since General Relativity cannot incorporate the uncertainties of quantum mechanics. For as previously pointed out, even times as short as the Planck time can be used without violating experimental observations.

Here, the time parameter is determined by noting that at the instant of the release of the GL free energy there is a freeze out time:

$$\hat{t} = \sqrt{T_{pl}\,\tau_{sc}} \qquad (13)$$

between the transition from the adiabatic (Planck time fluctuations T_{pl}) and impulse (relaxation time τ_{sc}) regimes [26]. This implies an inherent limitation on the power flow though the superconductor, which from equation (10) implies that

$$\frac{\Delta E}{\Delta t} = \frac{E}{T_{pl}} \rightarrow \frac{E_p}{\eta\hat{t}} \qquad (14)$$

where $\Delta t = \eta\hat{t}$ and where η combines geometric (i. e., size, shape, number of domains, & etc.), I-V junction characteristics [44, 45], and any other influence on the propagation of the electrons through the superconductor.

Given that the observed/measured propagation speed of the GL free energy (i. e., electron motion) through the superconductor is limited to the speed of light c, then

$$\eta \rightarrow \frac{T_h}{c\hat{t}} \qquad (15)$$

Combining equation (12) with equations (14 & 15) the instantaneous power radiated in gravitational waves is given by

$$L_{rad} \rightarrow \left(\frac{G}{c^5}\right)\left(\frac{E_p}{\eta\,\hat{t}}\right)^2 \approx \left(\frac{G}{c^5}\right)\left(\frac{E_p\,c}{T_h}\right)^2 \qquad (16)$$

and the radiated energy in gravitational waves:

$$E_{rad} \rightarrow L_{rad}\,\hat{t} \qquad (17)$$

from the freeze-out motion within the superconductor and noting that the gravitational waves is not effected by the superconductor properties (i. e., η).

Assuming a superconductor of thickness $T_h \approx 0.0254$ m, gives the maximum instantaneous power radiated in gravitational waves $L_{rad} \approx 10^{42}$ eV/s and radiated gravitational waves energy $E_{rad} \approx 10^{13}$ eV or $\approx 10^{-4}$ J; measurable on the laboratory scale.

7 Conclusions

The Ginzburg-Landau scalar field associated with the type II superconductor was discussed as a source of exotic material to produce gravitational forces for highly advanced propulsion related systems. Arbitrarily large electron group velocities (the Hartman effect) induced by spontaneous symmetry breaking phase transitions were discussed as the mechanisms for setting up a time-varying GL scalar field, which could conceivably result in gravitational disturbances in nearby vacuum scalar fields applicable to space propulsion. The short time scale behavior discussed provides a possible signature for an experimentalist to verify that new physics is occurring. Such experiments could provide insight into the laws of scalar fields, which need to be formulated for space propulsion engine cycles.

Nomenclature

$V(\psi)$ = energy density (eV/m^3)
n = electron probability density (electrons/m^3)
ϕ = phase of the scalar field
J = current through a superconductor junction (A/m^2)
n_{3D} = 3-D electron density (m^3)
2Δ = BCS gap energy (eV)
$\overline{V_g}$ = average domains volume (m^3)
T_{pl} = Planck Time = $\sqrt{\hbar G/c^5} \approx 5\times10^{-44}$ (s)
$\hbar$ = Plank's Constant $\approx 1.06\times10^{-34}$ (J s)
G = gravitation constant = 6.673×10^{-11} (N m^2/kg^2)
c = speed of light = 2.9979×10^{8} (m/s)
E_p = Planck Power $\hbar/T_{pl} \approx 10^{28}$ (eV)
T_h = superconductor thickness (m)

Acknowledgments

The author expresses thanks to Dr. Raymond Lewis who suggested that energy fluctuations in the superconductor could occur on the Planck time and for his expertise in particle physics.

References

1. Thorne K. S. Black holes and time warps. W. W. Norton & Company, NY, 1994.
2. Alcubierre M. The warp drive: hyper-fast travel within general relativity. *Classical and Quantum Gravity*, 1994, v. 11, L73–L77; arXiv: gr-qc/0009013.
3. Jackson J. D. Classical Electrodynamics. (Section 15.7), John Wiley & Sons Inc., 1962.
4. D'Inverno R. Introducing Einstein's relativity. Clarendon Press, 1992.
5. Pospelov M. and Romalis M. Lorentz invariance on trial. *Physics Today*, July, 2004.
6. Will C. M. Theory and experiment in gravitational physics, Cambridge Univ. Press, New York, 1993.
7. Caroll S. M. Quintessence and the rest of the world. *Phys. Rev. Lett.*, 1998, v. 81; arXiv: astro-ph/9806099.
8. Barceló C. and Visser M. Scalar fields, energy conditions and traversable wormholes. *Class. Quantum Grav.*, 2000, v. 17, 3843–3864.
9. Linde A. Particle physics and inflationary cosmology. *Contemporary Concepts in Physics*, Volume 5, Harwood Academic Publishers, 1990.
10. Morris M. S., Thorne K. S., and Yurtsever U. Wormholes, time machines, and the weak energy condition. *Phys. Rev. Lett.*, 1988, v. 61, 1446.
11. Morris M. S. and Thorne K. S. Wormholes in spacetime and their use for interstellar travel: a tool for teaching General Relativity. *Am. J. Phys.*, 1988, v. 56, 395.
12. Lobo F. S. N. and Visser M. Fundamental limitations on "warp drive" spacetimes. arXiv: gr-qc/0406083.
13. Visser M., Kar S., and Dadhich N. Traversable wormholes with arbitrarily small energy condition violations. *Phys. Rev. Lett.*, 2003, v. 90.
14. Josephson B. D. Supercurrents through barriers. *Adv. Phys.*, 1965, v. 14, 419.
15. Csa'ki Csaba, Grojean C., Pilo L., and Terning J. Towards a realistic model of Higgsless electroweak symmetry breaking. *Phys. Rev. Lett.*, 2004, v. 92.
16. Clem J. R. Two-dimensional vortices in a stack of thin superconducting films: A model for high-temperature superconducting multilayers. *Phys. Rev. B*, 1991, v. 43, 101.
17. Tinkham M. Introduction to superconductivity. McGraw-Hill, 1996.
18. Poole C. P., Farach H. A., Creswick R. J. Superconductivity. Academic Press, 1995.
19. Carmi R., Polturak E., Koren G., and Auerbach A. Spontaneous macroscopic magnetization at the superconducting transition temperature of $YBa_2Cu_3O_{7-\delta}$. *Nature*, 2000, v. 404, 853.
20. Glashow S. L. Partial symmetries of weak interactions. *Nucl. Phys.*, 1961, v. 22, 579.
21. Guth A. H. Inflationary Universe: A possible solution to the horizon and flatness problem. *Phys. Rev. D*, 1981, v. 23, 347.
22. Kibble T. W. B. Topology of cosmic domains and strings. *J. Phys. A*, 1976, v. 8, 1387.
23. Hartman T. E. Tunneling of a wave packet. *J. Appl. Phys.*, 1962, v. 33, 3427.
24. Hawking S. A brief history of time. Bantam Press, 1988 (ISBN: 0-553-05340-X).
25. Kibble T. W. B. Symmetry breaking and deffects. arXiv: cond-mat/0211110.
26. Zurek W. H. Cosmological experiments in condensed matter systems. *Physics Reports*, 1996, v. 276, 177–221.
27. Polturak E. and Koren G. Observation of spontaneous flux generation in a multi-josephson-junction loop. *Phys. Rev. Lett.*, 2000, v. 84(21).
28. Kibble T. W. B. and Rajantie A. Estimation of vortex density after superconducting film quench. arXiv: cond-mat/0306633.
29. Esser R. and Edgar R. Differential flow speeds of ions of the same element: Effects on Solar wind ionization fractions. *ApL*, 2001, v. 563, 1055–1062.
30. Andreev A. A. and Limpouch J. Ion acceleration in short-pulse laser-target interactions. *J. Plasma Physics*, 1999, v. 62, part 2, 179–193.
31. Kerlick G. S., Dymoke-Bradshaw A. K. L., and Dangor A. E. Observations of ion acceleration by relativistic electron beam. *J. Phys. D: Appl. Phys.*, 1983, v. 16, 613–629.
32. Olkhovsky V. S. and Recami E. Recent developments in time analysis of tunneling processes. *Phys. Reports*, 1992, v. 214, 340.
33. Winful H. G. Delay time and the hartman effect in quantum tunneling. *Phys. Rev. Lett.*, 2003, v. 91(26), 260401.
34. Muga J. G., Egusquiza I. L., Damborenea J. A., and Delgado F. Bounds and enhancements for the Hartman effect. arXiv: quant-ph/0206181.

35. Hauge E. H. and Stovneng J. A. Tunneling times: A critical-review. *Rev. Mod. Phys.*, 1989, v. 61, 17.

36. Fletcher J. R. Time delay in tunnelling through a potential barrier. *J. Phys. C: Solid State Phys.*, 1985, v.18.

37. Enders A. and Nimtz G. Evanescent-mode propagation and quantum tunneling. *Phys. Rev. E*, 1993, v. 48, 632.

38. Mugnai D., Ranfagni A., Ruggeri R., Agresti A., and Recami E. Superluminal processes and signal velocity in tunneling simulation. *Phys. Lett. A*, 1995, v. 209, 227.

39. Jakiel J. On superluminal motions in photon and particle tunnellings. arXiv: quant-ph/9810053.

40. Chiao R. Y. Tunneling times and superluminality: A tutorial. arXiv: quant-ph/9811019.

41. Nimtz G. Superluminal signal velocity. *Ann. Phys.* (Leipzig), 1998, v. 7, 618.

42. Binder B. Iterative coupling and balancing currents. e-Book, 2003, ISBN: 3-00-010972-2; With iterative and bosonized coupling towards fundamental particle properties. (2002, online http://www.quanics.com).

43. Misner W., Thorne K. S., and Wheeler J. A. Gravitation. (Chapter 36), W. H. Freeman and Company, 1973.

44. Watanabe M. Quantum effects in small-capacitance single Josephson junctions. *Phys. Rev. B*, 2003, v. 67; arXiv: cond-mat/0301467.

45. Watanabe M. Small-capacitance Josephson junctions: One-dimensional arrays and single junctions. arXiv: cond-mat/ 0301340.

Exact Theory of a Gravitational Wave Detector. New Experiments Proposed

Dmitri Rabounski and Larissa Borissova
E-mail: rabounski@yahoo.com; lborissova@yahoo.com

We deduce exact solutions to the deviation equation in the cases of both free and spring-connected particles. The solutions show that gravitational waves may displace particles in a two-particle system only if they are in motion with respect to each other or the local space (there is no effect if they are at rest). We therefore propose a new experimental statement for the detection of gravitational waves: use a suspended solid-body detector self-vibrating so that there are relative oscillations of its butt-ends. Or, in another way: use a free-mass detector fitted with suspended, vibrating mirrors. Such systems may have a relative displacement of the butt-ends and a time shift in the butt-ends, produced by a falling gravitational wave.

The authors dedicate this paper to the memory of Joseph Weber, who pioneered the detection of gravitational waves.

1 Introduction

As Borissova recently showed [1] by the Synge equation for deviating geodesic lines and the Synge-Weber equation for deviating non-geodesics, Weber's experimental statement on gravitational waves [2] is inadequate. His conclusions were not based upon an exact solution to the equations, but on an approximate analysis of what could be expected. Weber expected that a plane weak wave of the space metric (gravitational wave) may displace two particles at rest with respect to one another. The Weber equations and their solutions formulated in terms of the physically observable quantities show instead that gravitational waves cannot displace resting particles; some effect may be produced only if the particles are in motion.

Here we deduce exact solutions to both the Synge equation and the Synge-Weber equation (the exact theory to free-mass and solid-body detectors). The exact solutions show that we may alter the construction of both solid-body and free-mass detectors so that they may register oscillations produced by gravitational waves. Weber most probably detected them as claimed in 1968 [3, 4, 5], as his room-temperature solid-body pigs may have their own relative oscillations of the butt-ends, whereas the oscillations are inadvertently suppressed as noise in the detectors developed by his all followers, who have had no positive result in over 35-years.

2 Main equations of the theory

We consider two cases of a simple system consisting of two particles, either free or connected by a spring. A falling gravitational wave as a wave of the space metric deforming the space should produce some effect in such a system. Therefore we call such a system a gravitational wave detector.

We will determine the effect produced by a gravitational wave in both kinds of the two-particle systems.

If the particles are connected by a non-gravitational force Φ^α, they move along neighbouring non-geodesic world-lines, according to the non-geodesic equations of motion*

$$\frac{dU^\alpha}{ds} + \Gamma^\alpha_{\mu\nu} U^\mu U^\nu = \frac{\Phi^\alpha}{m_0 c^2}\,, \tag{1}$$

while relative oscillations of the world-lines (particles) are described by the so-called Synge-Weber equation† [2]

$$\frac{\mathrm{D}^2\eta^\alpha}{ds^2} + R^\alpha_{\cdot\beta\gamma\delta}\, U^\beta U^\delta \eta^\gamma = \frac{1}{m_0 c^2}\frac{\mathrm{D}\Phi^\alpha}{dv}dv\,. \tag{2}$$

If two neighbouring particles are free ($\Phi^\alpha = 0$), they move along neighbouring geodesic lines, according to the geodesic equations of motion

$$\frac{dU^\alpha}{ds} + \Gamma^\alpha_{\mu\nu} U^\mu U^\nu = 0\,, \tag{3}$$

while relative oscillations of the geodesics (particles) are given by the so-called Synge equations [6]

$$\frac{\mathrm{D}^2\eta^\alpha}{ds^2} + R^\alpha_{\cdot\beta\gamma\delta}\, U^\beta U^\delta \eta^\gamma = 0\,. \tag{4}$$

A solution to the deviation equations (4) or (2) gives the deviation $\eta^\alpha = (\eta^0, \eta^1, \eta^2, \eta^3)$ between the particles in the acting gravitational field. Because the field is unspecified in the equations (it is hidden in the formula for the metric ds), the equations allow the deviation to be described in both regular and wave fields of gravitation. Thus to determine

*Here $U^\alpha = \frac{dx^\alpha}{ds}$ is the four-dimensional velocity vector of the particle, tangential to its world-line. It is a unit world-vector: $U_\alpha U^\alpha = 1$. The space-time interval ds along the world-line is used as a parameter for differentiation, m_0 is the rest-mass of the particle, $\Gamma^\alpha_{\mu\nu}$ are Christoffel's symbols of the 2nd kind.

†Here $\frac{\mathrm{D}}{ds}$ is the absolute (covariant) differentiation operator; $R^\alpha_{\cdot\beta\gamma\delta}$ is the Riemann-Christoffel curvature tensor; $\eta^\alpha = \frac{\partial x^\alpha}{\partial v}dv$ is the relative deviation vector of the particles; v is a parameter having the same numerical value along a neighbouring world-line, while dv is the difference between its values in the world-lines.

how a gravitational wave causes two test-particles to deviate from one another, we should use the metric ds for this wave field and obtain exact solutions to the deviation equation.

Currently, two main kinds of gravitational wave detectors are presumed:

1. Weber's solid-body detector — a freely suspended bulky cylindrical pig, approximated by two masses connected by a spring (i. e. non-gravitational force). Oscillations of the butt-ends of the pig in the field of a falling gravitational wave are formulated by the Synge-Weber equation of deviating non-geodesics;
2. A free-mass detector, consisting of two freely suspended mirrors, distantly separated. Each mirror is fitted with a laser range-finder for producing measurements of the distance between them. Oscillations of the mirrors under a falling gravitational wave formulated by the Synge equation of deviating geodesics.

Both detectors have a common theory — the Synge-Weber equation, in comparison to the Synge equation, has just the non-zero right side with a force Φ^α connecting the particles. We may solve them using the same method. Before doing that however, we analyse Weber's approach to the main equations and his simplifications.

3 Weber's approach and criticism thereof

Weber proceeded from the proposition that a falling gravitational wave should deform a solid-body pig, represented by a system of two particles connected by a spring. He proposed the relative displacement of the particles η^α consisting of a "basic" displacement r^α (covariantly constant) and an infinitely small relative displacement ζ^α in the butt-ends of the cylinder caused by a falling gravitational wave

$$\eta^\alpha = r^\alpha + \zeta^\alpha, \qquad \zeta^\alpha \ll r^\alpha, \qquad \frac{\mathrm{D}\, r^\alpha}{ds} = 0\,. \tag{5}$$

Thus the non-geodesic deviation equation is

$$\frac{\mathrm{D}^2\zeta^\alpha}{ds^2} + R^\alpha_{\cdot\beta\gamma\delta}\, U^\beta U^\delta \left(r^\gamma + \zeta^\gamma\right) = \frac{\Phi^\alpha}{m_0 c^2}\,, \tag{6}$$

which he transformed to*

$$\frac{\mathrm{D}^2\zeta^\alpha}{ds^2} + \frac{d^\alpha_\sigma}{m_0 c^2}\frac{\mathrm{D}\zeta^\sigma}{ds} + \frac{k^\alpha_\sigma}{m_0 c^2}\zeta^\sigma = -R^\alpha_{\cdot\beta\gamma\delta}\left(r^\gamma + \zeta^\gamma\right). \tag{7}$$

This equation is like the equation of forced oscillations, where the curvature tensor is a forcing factor. Weber then finally transformed the equation to

$$\frac{d^2\zeta^\alpha}{dt^2} + \frac{d^\alpha_\sigma}{m_0}\frac{d\zeta^\sigma}{dt} + \frac{k^\alpha_\sigma}{m_0}\zeta^\sigma = -c^2 R^\alpha_{\cdot 0\sigma 0}\, r^\sigma, \tag{8}$$

which can only be obtained under his assumptions:

1. The length r of the pig to be covariantly constant $r = \sqrt{g_{\mu\nu} r^\mu r^\nu}$, which is a "background" for the infinitesimal displacement of the butt-ends $\zeta^\alpha \ll r^\alpha$ caused by a falling gravitational wave. Note that r isn't the length η of the pig in the "equilibrium state". Weber postulated r^α to be covariantly constant, so r is the "unchanged length". In such a case Weber has actually two detectors at the same time: (1) a pig having the covariantly constant length r, which remains unchanged in the field of a falling gravitational wave, (2) a pig having the length ζ, which, being made from the same material and connected to the first pig, changes its length under the same gravitational wave. In actual experiments a solid-body pig has a monolithic body which reacts as a whole to external influences. In other words, by introducing the splitting term $\eta^\alpha = r^\alpha + \zeta^\alpha$ into the equation of the deviating non-geodesics (2), Weber postulated that a falling gravitational wave is an external entity that forces the particles into resonant oscillations;
2. Because the cylindrical pig is freely suspended, it is in free fall;
3. Christoffel's symbols are all zero, so covariant derivatives became regular derivatives. (Of course, we can choose a specific reference frame where $\Gamma^\alpha_{\mu\nu} = 0$ at each given point. Such a reference frame is known as locally geodesic. However, since the curvature tensor is different from zero, $\Gamma^\alpha_{\mu\nu}$ cannot be reduced to zero in a finite area [7]. Therefore, if we connect one particle to a locally geodesic reference frame, in the neighbouring particle $\Gamma^\alpha_{\mu\nu} \neq 0$);
4. The butt-ends of the pig are at rest with respect to the observer ($U^i = 0$) all the time before a gravitational wave passes. This was assumed because the pig was regularly cooled down to a temperature close to 0 K in order to suppress internal molecular motions. With $U^i = 0$, there can only be resonant oscillations of the butt-ends. Parametric oscillations cannot appear there. Therefore Weber and all his followers have expected registration of a signal if a falling gravitational wave produces resonant oscillations in the detector.

Because the same assumptions were applied to the geodesic deviation equation, all that has been said is applicable to a free-mass detector.

Weber didn't solve his final equation (8). He limited himself by using $R^\alpha_{\cdot 0\sigma 0}\, r^\sigma$ as a forcing factor in his calculations of expected oscillations in solid-body detectors. Exact solution of Weber's final equation with all his assumptions was obtained by Borissova in the 1970's [8]. The assumptions actually mean that the solution of the Weber equation (8), with his requirement for r^α and its length $r = \sqrt{g_{\mu\nu} r^\mu r^\nu}$, must be covariantly constant: $\frac{\mathrm{D}\, r^\alpha}{ds} = 0$. Borissova showed that in the case of a gravitational wave linearly polarized

*Weber takes Φ^α as the sum of the returning (elastic) force $k^\alpha_\sigma \zeta^\sigma$ and the force $d^\alpha_\sigma \frac{\mathrm{D}\zeta^\sigma}{ds}$ setting up the damping factor (tensors k^α_σ and d^α_σ describe the peculiarities of the spring).

in the x^2 direction, and propagating along x^1, the equation $\frac{\mathrm{D}r^\alpha}{ds}=0$ gives $r^2=r^2_{(0)}\left[1-A\sin\frac{\omega}{c}\left(ct+x^1\right)\right]$ (the detector oriented along x^2). From this result, she obtained the Weber equation (8) in the form*

$$\frac{d^2\zeta^2}{dt^2}+2\lambda\frac{d\zeta^2}{dt}+\Omega_0^2\zeta^2=-A\omega^2r^2_{(0)}\sin\frac{\omega}{c}\left(ct+x^1\right), \quad (9)$$

i. e. an equation of forced oscillations, where the forcing factor is the relative displacement of the particles caused by the gravitational wave. She then obtained the exact solution: the relative displacement $\eta^2=\eta_y$ of the butt-ends is

$$\eta^2=r^2_{(0)}\left[1-A\sin\frac{\omega}{c}\left(ct+x^1\right)\right]+Me^{-\lambda t}\sin(\Omega t+\alpha)-\\ -\frac{A\omega^2r^2_{(0)}}{\left(\Omega_0^2-\omega^2\right)^2}\cos\left(\omega t+\delta+\frac{\omega}{c}x^1\right), \quad (10)$$

where $\Omega=\sqrt{\Omega_0^2-\omega^2}$, $\delta=\arctan\frac{2\lambda\omega}{\omega^2-\Omega_0^2}$, while M and α are constants. In this solution the relative oscillations consist of the "basic" harmonic oscillations and relaxing oscillations (first two terms), and the resonant oscillations (third term). As soon as the source's frequency ω coincides with the basic frequency of the detector $\Omega_0=\omega$, resonance occurs: in such a case even weak oscillations may be registered.

Thus, by his equation (6), Weber actually postulated that gravitational waves force rest-particles to undergo relative resonant oscillations. It was amazing that the exact solution showed that! Moreover, his assumptions led to a specific construction of the detectors, where parametric oscillations are obviated. As we show further by the exact solution of the deviation equations, gravitational waves may produce oscillations in only moving particles, in both solid-body and free-mass detectors.

4 Correct solution: a resting detector (Weber's case)

Our solution of the deviation equations depends on a specific formula for the space metric whereby we calculate the Riemann-Christoffel tensor. Because the sources of gravitational waves (double stars, pulsars, etc.) are far away from us, we expect received gravitational waves to be weak and plane. Therefore we consider the well-known metric of weak plane gravitational waves

$$ds^2=c^2dt^2-(dx^1)^2-(1+a)(dx^2)^2+\\ +\ 2b\,dx^2dx^3-(1-a)(dx^3)^2, \quad (11)$$

where a and b are functions of $ct+x^1$ (if propagation is along x^1), while a and b are infinitesimal so that squares and products of their derivatives vanish. The wave field described by this metric has a purely deformational origin, because it is derived from the non-stationarity of the spatial components g_{ik} of the fundamental metric tensor $g_{\alpha\beta}$. This metric is preferred because it satisfies Einstein's equations in vacuum $R_{\alpha\beta}=0$ ($R_{\alpha\beta}$ is Ricci's tensor).

Because we seek solutions applicable to real experiments, we solve the deviation equations in the terms of physically observable quantities†.

The non-geodesic equations of motion (1) have two physically observable projections [11]

$$\frac{dm}{d\tau}-\frac{m}{c^2}F_i\mathrm{v}^i+\frac{m}{c^2}D_{ik}\mathrm{v}^i\mathrm{v}^k=\frac{\sigma}{c},\\ \frac{d}{d\tau}(m\mathrm{v}^i)-mF^i+2m\left(D^i_k+A^i_{k\cdot}\right)+m\Delta^i_{kn}\mathrm{v}^k\mathrm{v}^n=f^i, \quad (12)$$

where m is the relativistic mass of the particle; $\mathrm{v}^i=\frac{dx^i}{d\tau}$ is its three-dimensional observable velocity, the square of which is $\mathrm{v}^2=h_{ik}\mathrm{v}^i\mathrm{v}^k$; $h_{ik}=-g_{ik}+\frac{g_{0i}g_{0k}}{g_{00}}$ is the observable metric tensor; $d\tau=\sqrt{g_{00}}\,dt+\frac{g_{0i}}{c\sqrt{g_{00}}}dx^i$ is the observable time interval, which is different to the coordinate time interval $dt=\frac{1}{c}dx^0$; $F_i=\frac{1}{\sqrt{g_{00}}}\left(\frac{\partial\mathrm{w}}{\partial x^i}-\frac{\partial v_i}{\partial t}\right)$ is the observable gravitational inertial force, where w is the gravitational potential, while $\sqrt{g_{00}}=1-\frac{\mathrm{w}}{c^2}$; $v_i=-\frac{cg_{0i}}{\sqrt{g_{00}}}$ is the linear velocity of the space rotation; $A_{ik}=\frac{1}{2}\left(\frac{\partial v_k}{\partial x^i}-\frac{\partial v_i}{\partial x^k}\right)+\frac{1}{2c^2}(F_iv_k-F_kv_i)$ is the tensor of observable angular velocities of the space rotation; $D_{ik}=\frac{1}{2\sqrt{g_{00}}}\frac{\partial h_{ik}}{\partial t}$ the tensor of observable rates of the space deformations; $\Delta^i_{kn}=h^{im}\Delta_{kn,m}$ are the spatially observable Christoffel symbols, built like Christoffel's usual symbols $\Gamma^\alpha_{\mu\nu}=g^{\alpha\sigma}\Gamma_{\mu\nu,\sigma}$ using h_{ik} instead of $g_{\alpha\beta}$; $\sigma=\frac{\Phi_0}{\sqrt{g_{00}}}$ is the observable projection of the non-gravitational force Φ^α onto the observer's time line, while $f^i=\Phi^i$ is its observable projection onto his spatial section.

If a particle rests with respect to an observer ($\mathrm{v}^i=0$), its observable equations of motion (12) take the form

$$\frac{dm_0}{d\tau}=\frac{\sigma}{c}=0, \qquad m_0F^i=-f^i. \quad (13)$$

Clearly, if a two-particle system is in free fall ($F^i=0$) and also rests with respect to an observer (as happens with a solid-body detector in Weber's experimental statement), a non-gravitational force connecting the particles has no effect on their motion: two resting particles connected by a spring have the same behaviour as free ones.

Therefore, to find what effect is produced by a gravitational wave on a resting solid-body detector or a free-mass detector, we should solve the same Synge equations of the deviating geodesics.

If, as Weber assumed, the observer's reference frame is "synchronous" ($F^i=0$, $A_{ik}=0$, $dt=d\tau$), the metric of weak

*Here $2\lambda=\frac{b}{m_0}$ and $\Omega^2_{(0)}=\frac{k}{m_0}$ are derived from the formula for the non-gravitational force $\Phi^2=-k\zeta^2-b\dot\zeta^2$, acting along x^2 in this case. The elastic coefficient of the "spring" is k, the friction coefficient is b.

†Physically observable (chronometrically invariant) are the projections of a four-dimensional quantity onto the time line and the spatial section of an observer [9]. See a brief account of that in [10], for instance.

plane gravitational waves (11) has just $D_{ik}=\frac{1}{2\sqrt{g_{00}}}\frac{\partial h_{ik}}{\partial t}\neq 0$. Let the wave propagate along x^1. Then $D_{22}=-D_{33}=\frac{1}{2}\dot{a}$ and $D_{23}=\frac{1}{2}\dot{b}$, where the dot means differentiation by t. The rest of the components of D_{ik} are zero. In such a case the time observable projection of the Synge equation (4) vanishes, while its spatial observable projection is

$$\frac{d^2\eta^i}{dt^2}+2D^i_k\frac{d\eta^k}{dt}=0\,, \tag{14}$$

which is, in component notation,

$$\begin{aligned}
&\frac{d^2\eta^1}{dt^2}=0\,,\\
&\frac{d^2\eta^2}{dt^2}+\frac{da}{dt}\frac{d\eta^2}{dt}+\frac{db}{dt}\frac{d\eta^3}{dt}=0\,,\\
&\frac{d^2\eta^3}{dt^2}-\frac{da}{dt}\frac{d\eta^3}{dt}+\frac{db}{dt}\frac{d\eta^2}{dt}=0\,.
\end{aligned} \tag{15}$$

The first of these (the deviating acceleration along the wave propagation direction x^1) shows that transverse waves don't produce an effect in the direction of propagation.

We look for exact solutions to the remaining two equations of (15) in the case where a gravitational wave is linearly polarized in the x^2 direction ($b=0$). First integrals of the equations are $\frac{d\eta^2}{dt}=C_1e^{-a}$ and $\frac{d\eta^3}{dt}=C_2e^{+a}$. Expanding e^{-a} and e^{+a} into series (high order terms vanish there), we obtain

$$\frac{d\eta^2}{dt}=C_1(1-a)\,,\qquad \frac{d\eta^3}{dt}=C_2(1+a)\,. \tag{16}$$

Let the gravitational wave be simple harmonic $\omega=\text{const}$ with a constant amplitude $A=\text{const}$: $a=A\sin\frac{\omega}{c}(ct+x^1)$. We then obtain exact solutions to the equations — the nonzero relative displacements produced in the two-particle system by the gravitational wave falling along x^1:

$$\begin{aligned}
\eta^2&=\dot{\eta}^2_{(0)}\Big[t+\frac{A}{\omega}\cos\frac{\omega}{c}(ct+x^1)\Big]+\eta^2_{(0)}-\frac{A}{\omega}\dot{\eta}^2_{(0)}\,,\\
\eta^3&=\dot{\eta}^3_{(0)}\Big[t-\frac{A}{\omega}\cos\frac{\omega}{c}(ct+x^1)\Big]+\eta^3_{(0)}-\frac{A}{\omega}\dot{\eta}^3_{(0)}\,.
\end{aligned} \tag{17}$$

These are the exact solutions of the Synge equation in a particular case, realised today in all solid-body and free-mass detectors. Looking at the solutions, we conclude:

> Transverse gravitational waves of a deformational sort may produce an effect in a two-particle system, resting as a whole with respect to the observer, only if the particles initially oscillate with respect to each other. If the particles are at rest in the initial moment of time, a falling gravitational wave cannot produce relative displacement of the particles.

Therefore the correct theory of a gravitational wave detector we have built states:

> Solid-body and free-mass detectors of current construction cannot register gravitational waves in principle; in cooling a solid-body detector and initially placing two distant mirrors at rest in a free-mass detector, inherent free oscillations are suppressed, thereby preventing registration of gravitational waves by the detectors.

In order to make the detectors sensitive to gravitational waves, we propose the following changes to their current construction:

For a free-mass detector: Introduce relative oscillations of the mirrors along their mutual line of sight. Such a modified system may have a reaction to a falling gravitational wave as an add-on to the relative velocity of the mirrors on the background of their basic relative oscillations.

For a solid-body detector: Don't cool the cylindrical pig, or better, apply relative oscillations of the butt-ends. Then the pig may have a reaction to a falling gravitational wave: an add-on to the noise of the self-deforming oscillations regularly detected as a piezoelectric effect*.

By the foregoing modifications to the exact theory of a gravitational wave detector, a solid-body detector, and especially a free-mass detector, may register gravitational waves.

Our theoretical result shows that to detect gravitational waves, the best method would be a detector consisting of two moving "particles". From the purely theoretical perspective, this is a general case of the deviation equations, where both particles move with respect to the observer at the initial moment of time. We obtain therefore, exact solutions for the general case and, as a result, consider detectors built on moving "particles" — a suspended, self-vibrating solid-body pig or suspended, vibrating mirrors in a free-mass detector.

5 Correct solution: a moving detector (general case)

If Weber had solved the deviation equation in conjunction with the equations of motion, he would have come to the same conclusion as us: gravitational waves of the deformational sort may produce an effect in a two-particle system only if the particles are in motion. Therefore we are going to solve the deviation equation in conjunction with the equations of motion in the general case where both particles move initially

*Because of this, it is most probable that Weber really detected gravitational waves in his experiments of 1968–1970 [3, 4, 5] where he used room-temperature detectors "... spaced about 2 km. A number of coincident events have been observed, with extremely small probability that they are statistical. It is clear that on rare occasions these instruments respond to a common external excitation which may be gravitational radiation" [3]. "Coincidences have been observed on gravitational-radiation detectors over a base line of about 1000 km at Argonne National Laboratory and at the University of Maryland. The probability that all of these coincidences were accidental is incredibly small" [4]. "Other experiments involve observations to rule out the possibility that the detectors are being excited electromagnetically. These results are evidence supporting an earlier claim that gravitational radiation is being observed" [5].

We both highly appreciate the work of Joseph Weber (1919–2000). Surely, if he was still alive he would be enthusiastic about our current results, and with us, immediately undertake new experiments for the detection of gravitational waves.

with respect to the observer ($U^i \neq 0$). (We mean that both particles move at the same velocity.)

We do this with the Synge-Weber equation of the deviating non-geodesics, because the Synge equation of the deviating geodesics is actually the same when the right side is zero.

We write the Synge-Weber equation (2) in the expanded form (with similar terms reduced)

$$\frac{d^2\eta^\alpha}{ds^2}+2\Gamma^\alpha_{\mu\nu}\frac{d\eta^\mu}{ds}U^\nu+\frac{\partial\Gamma^\alpha_{\beta\delta}}{\partial x^\gamma}U^\beta U^\delta\eta^\gamma=\frac{1}{m_0c^2}\frac{\partial\Phi^\alpha}{\partial x^\gamma}\eta^\gamma, \quad (18)$$

where ds may be expressed through the observable time interval $d\tau=\sqrt{g_{00}}\,dt+\frac{g_{0i}}{c\sqrt{g_{00}}}dx^i$ as $ds=cd\tau\sqrt{1-\mathrm{v}^2/c^2}$.

According to Zelmanov [9], any vector Q^α has two observable projections $\frac{Q_0}{\sqrt{g_{00}}}$ and Q^i, where the time projection may be calculated as $\frac{Q_0}{\sqrt{g_{00}}}=\sqrt{g_{00}}\,Q^0-\frac{1}{c}v_iQ^i$. We denote $\sigma=\frac{\Phi_0}{\sqrt{g_{00}}}$ and $f^i=\Phi^i$ for the connecting force Φ^α, while $\varphi=\frac{\eta_0}{\sqrt{g_{00}}}$ and η^i for the deviation η^α.

We consider the Synge-Weber equation (18) in a non-relativistic case, because the velocity of the particles is obviously small. In such a case, in the metric of weak plane gravitational waves (11), we have*

$$\begin{aligned}&d\tau=dt\,, \qquad \eta^0=\eta_0=\varphi\,, \quad \Phi^0=\Phi_0=\sigma\,,\\ &\Gamma^0_{kn}=\frac{1}{c}D_{kn}\,, \quad \Gamma^i_{0k}=\frac{1}{c}D^i_k\,, \quad \Gamma^i_{kn}=\Delta^i_{kn}\,,\end{aligned} \quad (19)$$

while all other Christoffel symbols are zero. We obtain the time and spatial observable projections of the Synge-Weber equation (18), which are

$$\begin{aligned}&\frac{d^2\varphi}{dt^2}+\frac{2}{c}D_{kn}\frac{d\eta^k}{dt}\mathrm{v}^n+\left(\varphi\frac{\partial D_{kn}}{\partial t}+c\frac{\partial D_{kn}}{\partial x^m}\eta^m\right)\frac{\mathrm{v}^k\mathrm{v}^n}{c^2}=\\ &\qquad=\frac{1}{m_0}\left(\frac{\varphi}{c}\frac{\partial\sigma}{\partial t}+\frac{\partial\sigma}{\partial x^m}\eta^m\right),\\ &\frac{d^2\eta^i}{dt^2}+\frac{2}{c}D^i_k\left(\frac{d\varphi}{dt}\mathrm{v}^k+c\frac{d\eta^k}{dt}\right)+2\Delta^i_{kn}\frac{d\eta^k}{dt}\mathrm{v}^n+\\ &+2\left(\frac{\varphi}{c}\frac{\partial D^i_k}{\partial t}+\frac{\partial D^i_k}{\partial x^m}\eta^m\right)\mathrm{v}^k+\left(\frac{\varphi}{c}\frac{\partial\Delta^i_{kn}}{\partial t}+\frac{\partial\Delta^i_{kn}}{\partial x^m}\eta^m\right)\mathrm{v}^k\mathrm{v}^n=\\ &\qquad=\frac{1}{m_0}\left(\frac{\varphi}{c}\frac{\partial f^i}{\partial t}+\frac{\partial f^i}{\partial x^m}\eta^m\right).\end{aligned} \quad (20)$$

We solve the deviation equations (20) in the field of a weak plane gravitational wave falling along x^1 and linearly polarized in the x^2 direction ($b=0$). In such a field we have

$$\begin{aligned}&D_{22}=-D_{33}=\frac{1}{2}\dot a\,, \qquad \frac{d}{dx^1}=\frac{1}{c}\frac{d}{dt}\,,\\ &\Delta^1_{22}=-\Delta^1_{33}=-\frac{1}{2c}\dot a\,, \quad \Delta^2_{12}=-\Delta^3_{13}=\frac{1}{2c}\dot a\,,\end{aligned} \quad (21)$$

so that the deviation equations (20) in component form are

$$\begin{aligned}&\frac{d^2\varphi}{dt^2}+\frac{\dot a}{c}\left(\frac{d\eta^2}{dt}\mathrm{v}^2-\frac{d\eta^3}{dt}\mathrm{v}^3\right)+\\ &+\frac{\ddot a}{2c^2}\left(\varphi+\eta^1\right)\left((\mathrm{v}^2)^2-(\mathrm{v}^3)^2\right)=\frac{1}{m_0}\left(\frac{1}{c}\frac{\partial\sigma}{\partial t}+\frac{\partial\sigma}{\partial x^m}\eta^m\right),\\ &\frac{d^2\eta^1}{dt^2}-\frac{\dot a}{c}\left(\frac{d\eta^2}{dt}\mathrm{v}^2-\frac{d\eta^3}{dt}\mathrm{v}^3\right)-\\ &-\frac{\ddot a}{2c^2}\left(\varphi+\eta^1\right)\left((\mathrm{v}^2)^2-(\mathrm{v}^3)^2\right)=\frac{1}{m_0}\left(\frac{1}{c}\frac{\partial f^1}{\partial t}+\frac{\partial f^1}{\partial x^m}\eta^m\right),\\ &\frac{d^2\eta^2}{dt^2}+\frac{\dot a}{c}\left(\frac{d\varphi}{dt}+\frac{d\eta^1}{dt}\right)\mathrm{v}^2+\dot a\frac{d\eta^2}{dt}\left(1+\frac{\mathrm{v}^1}{c}\right)+\\ &+\frac{\ddot a}{c}\left(\varphi+\eta^1\right)\left(1+\frac{\mathrm{v}^1}{c}\right)\mathrm{v}^2=\frac{1}{m_0}\left(\frac{1}{c}\frac{\partial f^2}{\partial t}+\frac{\partial f^2}{\partial x^m}\eta^m\right),\\ &\frac{d^2\eta^3}{dt^2}-\frac{\dot a}{c}\left(\frac{d\varphi}{dt}+\frac{d\eta^1}{dt}\right)\mathrm{v}^3-\dot a\frac{d\eta^3}{dt}\left(1+\frac{\mathrm{v}^1}{c}\right)-\\ &-\frac{\ddot a}{c}\left(\varphi+\eta^1\right)\left(1+\frac{\mathrm{v}^1}{c}\right)\mathrm{v}^3=\frac{1}{m_0}\left(\frac{1}{c}\frac{\partial f^3}{\partial t}+\frac{\partial f^3}{\partial x^m}\eta^m\right).\end{aligned} \quad (22)$$

This is a system of 2nd order differential equations with respect to φ, η^1, η^2, η^3, where the variable coefficients of the functions are the quantities $\dot a$, $\ddot a$, v^1, v^2, v^3.

We may find a from the given metric of the gravitational wave field, while v^i are the solutions to the non-geodesic equations of motion (12). By the given non-relativistic case in a field of weak plane linearly polarized gravitational wave, the equations of motion take the form

$$\begin{aligned}&\frac{\dot a}{2c}\left((\mathrm{v}^2)^2-(\mathrm{v}^3)^2\right)=\frac{\sigma}{m_0}\,,\\ &\frac{d\mathrm{v}^1}{dt}-\frac{\dot a}{2c}\left((\mathrm{v}^2)^2-(\mathrm{v}^3)^2\right)=\frac{f^1}{m_0}\,,\\ &\frac{d\mathrm{v}^2}{dt}+\dot a\,\mathrm{v}^2\left(1+\frac{\mathrm{v}^1}{c}\right)=\frac{f^2}{m_0}\,,\\ &\frac{d\mathrm{v}^3}{dt}-\dot a\,\mathrm{v}^3\left(1+\frac{\mathrm{v}^1}{c}\right)=\frac{f^3}{m_0}\,.\end{aligned} \quad (23)$$

5.1 Solution for a free-mass detector

We first find the solution for a simple case, where two particles don't interact with each other ($\Phi^\alpha=0$) — the right side is zero in the equations. This is a case of a free-mass detector. We find the quantities v^i from the equations of motion (23), which, since $\Phi^\alpha=0$, become geodesic

$$\begin{aligned}&(\mathrm{v}^2)^2-(\mathrm{v}^3)^2=0\,, \qquad \frac{d\mathrm{v}^1}{dt}=0\,,\\ &\frac{d\mathrm{v}^2}{dt}+\dot a\,\mathrm{v}^2=0\,, \qquad \frac{d\mathrm{v}^3}{dt}+\dot a\,\mathrm{v}^3=0\,.\end{aligned} \quad (24)$$

From this we see that a transverse gravitational wave doesn't produce an effect in the longitudinal direction: $\mathrm{v}^1=\mathrm{v}^1_{(0)}=\mathrm{const}$. Therefore, henceforth, $\mathrm{v}^1_{(0)}=0$.

*By the metric of weak plane gravitational waves (11), there is no difference between upper and lower indices.

The remaining equations of (24) may be integrated without problems. We obtain: $\mathrm{v}^2 = \mathrm{v}^2_{(0)} e^{-a}$, $\mathrm{v}^3 = \mathrm{v}^3_{(0)} e^{+a}$. Assuming the wave simple harmonic, $\omega = \text{const}$, with a constant amplitude, $A = \text{const}$, i. e. $a = A \sin \frac{\omega}{c}(ct + x^1)$, and expanding the exponent into series, we obtain

$$\begin{aligned} \mathrm{v}^2 &= \mathrm{v}^2_{(0)} \left[1 - A \sin \frac{\omega}{c}(ct + x^1)\right], \\ \mathrm{v}^3 &= \mathrm{v}^3_{(0)} \left[1 + A \sin \frac{\omega}{c}(ct + x^1)\right], \end{aligned} \tag{25}$$

i. e. a gravitational wave has an effect only in directions orthogonal to its propagation. Clearly, a gravitational wave doesn't affect particles at rest with respect to the local space where the wave propagates.

Substituting the solutions (25) into the equations of the deviating non-geodesics (22) and setting the right side to zero as for geodesics, we obtain

$$\begin{aligned} &\frac{d^2\varphi}{dt^2} + \frac{\dot a}{c}\left(\frac{d\eta^2}{dt}\mathrm{v}^2_{(0)} - \frac{d\eta^3}{dt}\mathrm{v}^3_{(0)}\right) = 0, \\ &\frac{d^2\eta^1}{dt^2} - \frac{\dot a}{c}\left(\frac{d\eta^2}{dt}\mathrm{v}^2_{(0)} - \frac{d\eta^3}{dt}\mathrm{v}^3_{(0)}\right) = 0, \\ &\frac{d^2\eta^2}{dt^2} + \dot a\frac{d\eta^2}{dt} + \frac{\dot a}{c}\left(\frac{d\varphi}{dt} + \frac{d\eta^1}{dt}\right)\mathrm{v}^2_{(0)} + \frac{\ddot a}{c}\left(\varphi + \eta^1\right)\mathrm{v}^2_{(0)} = 0, \\ &\frac{d^2\eta^3}{dt^2} - \dot a\frac{d\eta^3}{dt} - \frac{\dot a}{c}\left(\frac{d\varphi}{dt} + \frac{d\eta^1}{dt}\right)\mathrm{v}^2_{(0)} - \frac{\ddot a}{c}\left(\varphi + \eta^1\right)\mathrm{v}^2_{(0)} = 0. \end{aligned} \tag{26}$$

Summing the first two equations and integrating the sum, we obtain $\varphi + \eta^1 = B_1 t + B_2$, where $B_{1,2}$ are integration constants. Substituting these into the other two, we obtain

$$\begin{aligned} &\frac{d^2\eta^2}{dt^2} + \dot a\frac{d\eta^2}{dt} + \frac{\dot a}{c}B_1\mathrm{v}^2_{(0)} + \frac{\ddot a}{c}\left(B_1 t + B_2\right)\mathrm{v}^2_{(0)} = 0, \\ &\frac{d^2\eta^3}{dt^2} - \dot a\frac{d\eta^2}{dt} - \frac{\dot a}{c}B_1\mathrm{v}^3_{(0)} - \frac{\ddot a}{c}\left(B_1 t + B_2\right)\mathrm{v}^3_{(0)} = 0. \end{aligned} \tag{27}$$

The equations differ solely in the sign of a, and can therefore be solved in the same way. We introduce a new variable $y = \frac{d\eta^2}{dt}$. Then we have a linear uniform equation of the 1st order with respect to y

$$\dot y + \dot a y = -\frac{\dot a}{c}B_1\mathrm{v}^2_{(0)} - \frac{\ddot a}{c}\left(B_1 t + B_2\right)\mathrm{v}^2_{(0)}, \tag{28}$$

which has the solution

$$y = e^{-F}\left(y_0 + \int_0^t g(t)\, e^F dt\right), \quad F(t) = \int_0^t f(t)\, dt, \tag{29}$$

where $F(t) = \dot a$, $g(t) = -\frac{\dot a}{c}B_1\mathrm{v}^2_{(0)} - (B_1 t + B_2)\mathrm{v}^2_{(0)}$. Expanding the exponent into series in the solution, and then integrating, we obtain

$$\begin{aligned} y = \dot\eta^2 = \dot\eta^2_{(0)} &\left[1 - A \sin \frac{\omega}{c}(ct + x^1)\right] - \\ &- \frac{A\omega}{c}\mathrm{v}^2_{(0)}\left(B_1 t + B_2\right)\cos\frac{\omega}{c}(ct + x^1) + \frac{A\omega}{c}B_2\mathrm{v}^2_{(0)}. \end{aligned} \tag{30}$$

Integrating this equation, and applying the same method for η^3, we arrive at the final solutions: the relative displacements η^2 and η^3 in a free-mass detector are

$$\begin{aligned} \eta^2 = \eta^2_{(0)} &+ \left(\dot\eta^2_{(0)} + \frac{A\omega B_2\mathrm{v}^2_{(0)}}{c}\right)t + \frac{A}{\omega}\left(\dot\eta^2_{(0)} - \frac{\mathrm{v}^2_{(0)}}{c}B_1\right)\times \\ &\times\left[\cos\frac{\omega}{c}(ct + x^1) - 1\right] - \frac{A\mathrm{v}^2_{(0)}}{c}\left(B_1 t + B_2\right)\sin\frac{\omega}{c}(ct + x^1), \end{aligned} \tag{31}$$

$$\begin{aligned} \eta^3 = \eta^3_{(0)} &+ \left(\dot\eta^3_{(0)} - \frac{A\omega B_2\mathrm{v}^3_{(0)}}{c}\right)t - \frac{A}{\omega}\left(\dot\eta^3_{(0)} - \frac{\mathrm{v}^3_{(0)}}{c}B_1\right)\times \\ &\times\left[\cos\frac{\omega}{c}(ct + x^1) - 1\right] + \frac{A\mathrm{v}^3_{(0)}}{c}\left(B_1 t + B_2\right)\sin\frac{\omega}{c}(ct + x^1). \end{aligned} \tag{32}$$

With $\dot\eta^2$ and $\dot\eta^3$, we integrate the first two equations of (26). We obtain thereby the relative displacement η^1 in a free-mass detector and the time shift φ at its ends, thus

$$\eta^1 = \dot\eta^1_{(0)} t - \frac{A}{\omega c}\left(\mathrm{v}^2_{(0)}\dot\eta^2_{(0)} - \mathrm{v}^3_{(0)}\dot\eta^3_{(0)}\right)\left[1 - \cos\frac{\omega}{c}(ct + x^1)\right] + \eta^1_{(0)}, \tag{33}$$

$$\varphi = \dot\varphi_{(0)} t + \frac{A}{\omega c}\left(\mathrm{v}^2_{(0)}\dot\eta^2_{(0)} - \mathrm{v}^3_{(0)}\dot\eta^3_{(0)}\right)\left[1 - \cos\frac{\omega}{c}(ct + x^1)\right] + \eta^1_{(0)}. \tag{34}$$

Finally, we substitute φ and η^1 into $\varphi + \eta^1 = B_1 t + B_2$ to fix the integration constants $B_1 = \dot\varphi_{(0)} + \dot\eta^1_{(0)}$ and $B_2 = \varphi_{(0)} + \eta^1_{(0)}$.

Thus we have obtained the solutions to the Synge equation of deviating geodesics. We see that relative displacements of two free particles in the directions x^2 and x^3, transverse to that of gravitational wave propagation consist of:

1. Displacements, increasing linearly with time;
2. Harmonic oscillations at the frequency ω of a falling gravitational wave;
3. Oscillations, the amplitude of which increases linearly with time (last term in the solutions).

The first two of the displacements are permitted in the transverse direction x^2 or x^3, only if the particles initially move in this direction with respect to the local space ($\mathrm{v}^2 \neq 0$ or $\mathrm{v}^3 \neq 0$) or with respect to each other ($\dot\eta^2 \neq 0$ or $\dot\eta^3 \neq 0$). For instance, if they are at rest with respect to x^2, an x^1-directed gravitational wave doesn't displace them in this direction.

The third of the displacements is permitted only if the particles initially move with respect to each other in the longitudinal direction ($\dot\eta^1 \neq 0$).

We see from the solution for η^1 that gravitational waves may displace the particles even in the same direction of the wave propagation, if the particles initially move in this direction with respect to each other.

The solution φ is the time shift in the clocks located at both particles, caused by a falling gravitational wave*. From (34), this effect is permitted if the particles move both with

*We assume $\varphi_{(0)} = 0$: time count starts from zero. We assume as well $\dot\varphi_{(0)} = 0$: time flows uniformly in the absence of a wave gravitational field.

respect to the local space and each other in at least one of the transverse directions x^2 and x^3.

In view of these results, we propose a new experimental statement for the detection of gravitational waves, based on a free-mass detector.

New experiment for a free-mass detector: A free-mass detector, where two mirrors are suspended and vibrating so that they have free oscillations with respect to each other or along parallel (vertical or horizontal) lines. With the mirrors oscillating along parallel lines, such a system moves with respect to the local space ($\mathrm{v}^i_{(0)} \neq 0$), while with the mirrors oscillating with respect to each other the system has non-stationary relative displacements of the butt-ends ($\eta^i_{(0)} \neq 0$, $\dot{\eta}^i_{(0)} \neq 0$). According to the exact theory of a free-mass detector given above, a falling gravitational wave produces a relative displacement of the mirrors, that may be registered with a laser range-finder (or similar system). Moreover, as the theory predicts, a time shift is produced in the mirrors, that may be registered by synchronized clocks located with each of the mirrors: their asynchronization implies a gravitational wave detection.

5.2 Solution for a solid-body detector

We assume an elastic force connecting two particles in a solid-body detector to be $\Phi^\alpha = -k^\alpha_\sigma x^\sigma$, where k^α_σ is the elastic coefficient. We assume the force Φ^α to be independent of time, i. e. $k^0_\sigma = 0$. In such a case the equations of motion of the particles (23) take the form

$$\begin{aligned}
&(\mathrm{v}^2)^2 - (\mathrm{v}^3)^2 = 0\,,\\
&\frac{d\mathrm{v}^1}{dt} - \frac{\dot{a}}{2c}\Big((\mathrm{v}^2)^2 - (\mathrm{v}^3)^2\Big) = -\frac{k^1_\sigma}{m_0}\,x^\sigma,\\
&\frac{d\mathrm{v}^2}{dt} + \dot{a}\,\mathrm{v}^2\left(1 + \frac{\mathrm{v}^1}{c}\right) = -\frac{k^2_\sigma}{m_0}\,x^\sigma,\\
&\frac{d\mathrm{v}^3}{dt} - \dot{a}\,\mathrm{v}^3\left(1 + \frac{\mathrm{v}^1}{c}\right) = -\frac{k^3_\sigma}{m_0}\,x^\sigma.
\end{aligned} \tag{35}$$

Thus a transverse gravitational wave doesn't produce an effect in the longitudinal direction x^1: $\mathrm{v}^1 = \mathrm{v}^1_{(0)} = \mathrm{const}$. Therefore, henceforth, $\mathrm{v}^1 = 0$ and $k^1_\sigma = 0$. In such a case the equations of motion take the form

$$\frac{d\mathrm{v}^2}{dt} + \dot{a}\,\mathrm{v}^2 = -\frac{k^2_\sigma}{m_0}\,x^\sigma, \qquad \frac{d\mathrm{v}^3}{dt} - \dot{a}\,\mathrm{v}^3 = -\frac{k^3_\sigma}{m_0}\,x^\sigma. \tag{36}$$

The equations differ solely by the sign of $\dot{a}$. Therefore we solve only the first of them. The second equation may be solved following the same method.

Let $k^2_\sigma = k^3_\sigma = k = \mathrm{const}$, i. e. the solid-body pig is elastic in only two directions transverse to the direction x^1 of the gravitational wave propagation. With that, the equation of motion in the x^2 direction is

$$\frac{d^2x^2}{dt^2} + \frac{k}{m_0}\,x^2 = -A\,\omega\cos\frac{\omega}{c}\,(ct + x^1)\,\frac{dx^2}{dt}\,. \tag{37}$$

Denoting $x^2 \equiv x$, $\frac{k}{m_0} = \Omega^2$, $A\omega = -\mu$, we reduce this equation to the form

$$\ddot{x} + \Omega^2 x = \mu\cos\frac{\omega}{c}\,(ct + x^1)\,\dot{x}\,, \tag{38}$$

where μ is the so-called "small parameter". This is a "quasi-harmonic" equation: with $\mu = 0$, such an equation is a harmonic oscillation equation; while if $\mu \neq 0$ the right side plays the rôle of an forcing factor — we obtain a forced oscillation equation.

We solve this equation using the small parameter method of Poincaré, known also as the perturbation method: we consider the right side as a perturbation of a harmonic oscillation described by the left side. The Poincaré method is related to exact solution methods, because a solution produced with the method is a power series expanded by the small parameter μ (see Lefschetz, Chapter XII, §2 [12]).

Before we solve (38) we introduce a new variable $t' = \Omega t$ in order to make it dimensionless as in [12], and $\mu' = \frac{\mu}{\Omega}$

$$\ddot{x} + x = \mu'\cos\frac{\omega}{\Omega c}\,(ct' + \Omega x^1)\,\dot{x}\,, \tag{39}$$

where we differentiate by t'. A general solution of this equation, representable as the equivalent system

$$\dot{x} = y\,, \qquad \dot{y} = -x + \mu'\cos\frac{\omega}{\Omega c}\,(ct' + \Omega x^1)\,y \tag{40}$$

with the initial data $x_{(0)}$ and $y_{(0)}$ at $t' = 0$, is determined by the series pair (Lefschetz)

$$\left.\begin{aligned}
x &= P_0\,(x_{(0)}, y_{(0)}, t') + \mu' P_1\,(x_{(0)}, y_{(0)}, t') + \dots\\
y &= \dot{P}_0\,(x_{(0)}, y_{(0)}, t') + \mu' \dot{P}_1\,(x_{(0)}, y_{(0)}, t') + \dots
\end{aligned}\right\}. \tag{41}$$

We substitute these into (40) and, equating coefficients in the same orders of μ', obtain the recurrent system

$$\left.\begin{aligned}
&\ddot{P}_0 + P_0 = 0\\
&\ddot{P}_1 + P_1 = \dot{P}_0\cos\frac{\omega}{\Omega c}\,(ct' + \Omega x^1)\\
&\dots\dots\dots\dots\dots\dots\dots\dots\dots\dots
\end{aligned}\right\} \tag{42}$$

with the initial data $P_0(0) = \xi$, $\dot{P}_0(0) = \vartheta$, $P_1(0) = \dot{P}_1(0) = 0$ ($n > 0$) at $t' = 0$. Because the amplitude A (we have it in the variable $\mu' = -\frac{\omega}{\Omega}A$) is small, this problem takes only the first two equations into account. The first of them is a harmonic oscillation equation, with the solution

$$P_0 = \xi\cos t' + \vartheta\sin t', \tag{43}$$

while the second equation, with this solution, is

$$\ddot{P}_1 + P_1 = (-\xi\sin t' + \vartheta\cos t')\cos\frac{\omega}{\Omega c}\,(ct' + \Omega x^1)\,. \tag{44}$$

This is a linear uniform equation. We solve it following Kamke (Part III, Chapter II, §2.5 in [13]). The solution is*

*Here we go back to the initial variables.

$$P_1 = \frac{\vartheta\Omega^2}{2}\left\{\frac{\cos\left[(\Omega-\omega)t-\frac{\omega}{c}x^1\right]}{\Omega^2-(\Omega-\omega)^2}+\frac{\cos\left[(\Omega+\omega)t+\frac{\omega}{c}x^1\right]}{\Omega^2-(\Omega+\omega)^2}\right\} - \\ -\frac{i\xi\Omega^2}{2}\left\{\frac{\sin\left[(\Omega-\omega)t-\frac{\omega}{c}x^1\right]}{\Omega^2-(\Omega-\omega)^2}+\frac{\sin\left[(\Omega+\omega)t+\frac{\omega}{c}x^1\right]}{\Omega^2-(\Omega+\omega)^2}\right\}, \quad (45)$$

where the brackets contain the real and imaginary parts of the formula $e^{i(\Omega-\omega)t-\frac{\omega}{c}x^1}+e^{i(\Omega+\omega)t+\frac{\omega}{c}x^1}$. Going back to $x^2=x$, we obtain the final solution in the reals

$$x^2 = \xi\cos\Omega t+\vartheta\sin\Omega t - \\ -\frac{A\omega\Omega\vartheta}{2}\left\{\frac{\cos\left[(\Omega-\omega)t-\frac{\omega}{c}x^1\right]}{\Omega^2-(\Omega-\omega)^2}+\frac{\cos\left[(\Omega+\omega)t+\frac{\omega}{c}x^1\right]}{\Omega^2-(\Omega+\omega)^2}\right\}, \quad (46)$$

while the solution for x^3 will differ solely in the sign of the amplitude A.

With this result we solve the equations of the deviating non-geodesics (22). Because a solid-body detector has a freedom for motion less than a free-mass detector, we assume $\mathrm{v}^1=0$, $\mathrm{v}^2=\mathrm{v}^3$, $\Phi^1=0$, $\Phi^2=-\frac{k}{m_0}\eta^2$, $\Phi^3=-\frac{k}{m_0}\eta^3$. Note that $\mathrm{v}^2=\mathrm{v}^3$ means that the initial conditions ξ and ϑ are the same in both the directions x^2 and x^3. Therefore we obtain

$$\frac{d^2\varphi}{dt^2}=0\,, \qquad \frac{d^2\eta^1}{dt^2}=0\,, \quad (47)$$

i. e. a gravitational wave doesn't change both the vertical size of the pig and the time shift φ at its butt-ends: we may put $\varphi=0$ and $\eta^1=0$. With all these, the deviation equation along x^2 takes the form*

$$\frac{d^2\eta^2}{dt^2}+\frac{k}{m_0}\eta^2=-A\omega\cos\frac{\omega}{c}(ct+x^1)\frac{d\eta^2}{dt}\,, \quad (48)$$

having the same form as equation (37). So the solution η^2 is like (46), but with the difference that the initial constants ξ and ϑ depend on $\eta^2_{(0)}$, $\eta^3_{(0)}$ and $\dot\eta^2_{(0)}$, $\dot\eta^3_{(0)}$. It is

$$\eta^2 = \xi\cos\Omega t+\vartheta\sin\Omega t - \\ -\frac{A\omega\Omega\vartheta}{2}\left\{\frac{\cos\left[(\Omega-\omega)t-\frac{\omega}{c}x^1\right]}{\Omega^2-(\Omega-\omega)^2}+\frac{\cos\left[(\Omega+\omega)t+\frac{\omega}{c}x^1\right]}{\Omega^2-(\Omega+\omega)^2}\right\}. \quad (49)$$

Thus two spring-connected particles in the field of a gravitational wave may experience the following effects:

1. Free relative oscillations at a frequency Ω;
2. Forced relative oscillations, caused by the gravitational wave of frequency ω; they occur in the directions transverse to the wave propagation;
3. Resonant oscillations, which occur as soon as the gravitational wave's frequency becomes double the frequency of the particle's free oscillation ($\omega=2\Omega$); in such a case even weak oscillations caused by the gravitational wave may be detected;

*We write and solve only the equation for η^2, because it differs to that for η^3 solely by the sign of the amplitude A. See (22).

The second and third effects are permitted only if the particles have an initial relative oscillation. If there is no initial oscillation, gravitational waves cannot produce an effect in such a system. Owing to this result, we propose a new experimental statement for the detection of gravitational waves by a solid-body detector.

New experiment for a solid-body detector: Use a solid-body cylindrical pig, horizontally suspended and self-vibrating so that there are relative oscillations of its butt-ends ($\eta^2_{(0)}\neq0$, $\dot\eta^2_{(0)}\neq0$). Such an oscillation may be induced by alternating electromagnetic current or something like this. Or, alternatively, use a similarly suspended, vibrating pig so that it has an oscillation in the horizontal plane. Such a system has a non-zero velocity with respect to the observer's local space ($\mathrm{v}^2_{(0)}\neq0$, $\mathrm{v}^3_{(0)}\neq0$). Both systems, according to the exact theory of a solid-body detector, may have a reaction to gravitational waves (up to resonance) that may be measured as a piezo-effect in the pig.

References

1. Borissova L. Gravitational waves and gravitational inertial waves in the General Theory of Relativity: a theory and experiments. *Progress in Physics*, 2005, v. 2, 30–62.
2. Weber J. General Relativity and gravitational waves. R. Marshak, New York, 1961.
3. Weber J. Gravitational-wave-detector events. *Phys. Rev. Lett.*, 1968, v. 20, 1307–1308.
4. Weber J. Evidence for discovery of gravitational radiation. *Phys. Rev. Lett.*, 1969, v. 22, 1320–1324.
5. Weber J. Gravitational radiation experiments. *Phys. Rev. Lett.*, 1970, v. 24, 276–279.
6. Synge J. L. Relativity: the General Theory. North Holland, Amsterdam, 1960.
7. Petrov A. Z. Einstein spaces. Pergamon, London, 1969.
8. Borissova L. B. Quadrupole mass-detector in a field of weak plane gravitational waves. *Izvestia VUZov*, *Physica*, 1978, v. 10, 109–114.
9. Zelmanov A. L. Chronometric invariants and co-moving coordinates in the general relativity theory. *Doklady Acad. Nauk USSR*, 1956, v. 107 (6), 815–818.
10. Rabounski D. Zelmanov's anthropic principle and the infinite relativity principle. *Progress in Physics*, 2006, v. 1, 35–37.
11. Borissova L. and Rabounski D. Fields, vacuum, and the mirror Universe. Editorial URSS, Moscow, 2001 (2nd rev. ed.: CERN, EXT-2003-025).
12. Lefschetz S. Differential equations: geometric theory. Interscience Publishers, New York, 1957.
13. Kamke E. Differentialgleichungen: Lösungsmethoden und Lösungen. Chelsea Publishing Co., New York, 1959.

Changes in the Fine Structure of Stochastic Distributions as a Consequence of Space-Time Fluctuations

Simon E. Shnoll

Department of Physics, Moscow State University, Moscow 119992, Russia
Institute of Theoretical and Experimental Biophysics, Russian Academy of Sciences, Pushchino, Moscow Region, 142290, Russia

E-mail: shnoll@iteb.ru

This is a survey of the fine structure stochastic distributions in measurements obtained by me over 50 years. It is shown: (1) The forms of the histograms obtained at each geographic point (at each given moment of time) are similar with high probability, even if we register phenomena of completely different nature — from biochemical reactions to the noise in a gravitational antenna, or α-decay. (2) The forms of the histograms change with time. The iterations of the same form have the periods of the stellar day (1.436 min), the solar day (1.440 min), the calendar year (365 solar days), and the sidereal year (365 solar days plus 6 hours and 9 min). (3) At the same instants of the local time, at different geographic points, the forms of the histograms are the same, with high probability. (4) The forms of the histograms depend on the locations of the Moon and the Sun with respect to the horizon. (5) All the facts are proof of the dependance of the form of the histograms on the location of the measured objects with respect to stars, the Sun, and the Moon. (6) At the instants of New Moon and the maxima of solar eclipses there are specific forms of the histograms. (7) It is probable that the observed correlations are not connected to flow power changes (the changes of the gravity force) — we did not find the appropriate periods in changes in histogram form. (8) A sharp anisotropy of space was discovered, registered by α-decay detectors armed with collimators. Observations at 54° North (the collimator was pointed at the Pole Star) showed no day-long periods, as was also the case for observations at 82° North, near the Pole. Histograms obtained by observations with an Easterly-directed collimator were determined every 718 minutes (half stellar day) and with observations using a Westerly-directed collimator. (9) Collimators rotating counter-clockwise, in parallel with the celestial equator, gave the probability of changes in histograms as the number of the collimator rotations. (10) Collimators rotating clockwise once a day, show no day-long periods, and similarly, collimators pointed at the Pole Star, and measurements taken near the North Pole. All the above lead us to the conclusion (proposition) that the fine structure of the histograms should be a result of the interference of gravitational waves derived from orbital motions of space masses (the planets and stars).

Introduction

Earlier we showed that the fine structure of the spectrum of amplitude variations in the results of measurements of processes of different nature (in other words, the fine structure of the dispersion of results or the pattern of the corresponding histograms) is subject to "*macroscopic fluctuations*", changing regularly with time. These changes indicate that the "dispersion of results" that remains after all artifacts are excluded inevitably accompanies any measurements and reflects very basic features of our world. In our research, we have come to the conclusion that this dispersion of results is the effect of space-time fluctuations, which, in their turn, are caused by the movement of the measured object in an anisotropic gravitational field. Among other things, this conclusion means that the examination of the detailed pattern of distributions obtained from the results of measurement of the dynamics of processes of different nature uncovers laws which cannot be revealed using traditional methods for the analysis of time series.

These assertions are based on the results of long-term experimental investigations conducted for many decades. The major part of these results, begun in 1958, is published in Russian. The goal of this paper is to give a brief review of those results and provide corresponding references.

The most general conclusion of our research is that there is evidence that the fine structure of stochastic distributions is not accidental. In other words, noncasual is the pattern of histograms plotted from a rather small number of the results of measurement of the dynamics of processes of different nature, from biochemical reactions and noise in gravitational antennae, to α-decay [1–24].

1 The "effect of near zone"

The first element of evidence of the histogram pattern changing regularly in time is the "effect of near zone". This effect means that similar histograms are significantly more likely to appear in the nearby (neighbouring) intervals of the time series of the results of measurements. The similarity of the pattern of histograms plotted from independent intervals of a time series implies the presence of an external (towards the process studied) factor, which determines the pattern of the histogram. The independence of the "near zone" effect of the nature of the process indicates that this factor has a quite general nature.

2 Measurements of processes of different nature

The second element of evidence comes from the similarity of the pattern of histograms plotted from the results of simultaneous independent measurements of processes of different nature at the same geographical point. In view of the fundamental difference in the nature of those processes and methods of their measurement, such a similarity also means that the factor, determining the histogram pattern, has a quite general nature. The similarity of histograms when under study are the processes, in which the ranges of transduced energy differ by dozens of orders (40 orders if the matter concerns the noise in a gravitational antenna, and the phenomenon of α-decay), implies that this factor has no relation to energy.

3 Regular changes in the histogram patterns

The third element of evidence for noncasuality of the histogram patterns is their regular changing with time. The regularities are revealed in the existence of the following periods in the change of the probability of similar histograms to appear.

3.1. Near-daily periods; these are well-resolvable "sidereal" (1436 min) and "solar" (1440 min) daily periods. These periods imply dependence of the histogram pattern on the rotation of the Earth around its axis. The pattern is determined by two independent factors: the position relative to the starry sky and that relative to the Sun.

3.2. Approximately 27-day periods. These periods can be considered as an indication of the dependence of the histogram pattern on the position relative to the nearby celestial bodies: the Sun, the Moon and, probably, the planets.

3.3. Yearly periods; these are well-resolvable "calendar" (365 solar days) and "sidereal" (365 solar days plus 6 h and 9 min) yearly periods.

All these periods imply the dependence of the obtained histogram pattern on two factors of rotation — (1) rotation of the Earth around its axis, and (2) movement of the Earth along its circumsolar orbit.

4 The observed local-time synchronism

The dependence of the histogram pattern on the Earth rotation around its axis is clearly revealed in the phenomenon of *synchronization at the local time*, when similar histograms are very likely to appear at different geographical points (from Arctic to Antarctic, in the Western and Eastern hemispheres) at the same *local* time. It is astonishing that the local-time synchronism with the precision of 1 min is observed independently of the regional latitude at the most extreme distances — as extreme as possible on the Earth (about 15,000 km).

5 The synchronism observed at different latitudes

The dependence of the histogram pattern on the Earth rotation around its axis is also revealed in the disappearance of the near-daily periods close to the North Pole. Such measurements were conducted at the latitude of 82° North in 2000. The analysis of histograms from the 15-min and 60-min segments showed no near-daily periods, but these periods remain in the sets of histograms plotted from the 1-min segments. Also remaining was the local-time synchronism in the appearance of similar histograms.

Following these results, it would be very interesting to conduct measurements as close as possible to the North Pole. That was unfeasible, and so we performed measurements with collimators, which channel α-particles emitted in a certain direction from a sample of ^{239}Pu. The results of those experiments made us change our views fundamentally.

6 The collimator directed at the Pole Star

Measurements were taken with the collimator directed at the Pole Star. In the analysis of histograms plotted from the results of counting α-particles that were travelling North (in the direction of the Pole Star), the near-daily periods were not observed, nor was the near-zone effect. The measurements were made in Pushchino (54° latitude North), but the effect is as would be expected at 90° North, i. e. at the North Pole. This means that the histogram pattern depends on the spatial direction of the process measured. Such a dependence, in its turn, implies a sharp anisotropy of space. Additionally, it becomes clear that the matter does not concern any "effect" or "influence" on the object under examination. The case in point is changes, fluctuations of the space-time emerging from the rotation of the Earth around its axis and the movement of the planet along its circumsolar orbit [9, 13, 14, 15, 19, 20, 21].

7 The East and West-directed collimators

This effect was confirmed in experiments with two collimators, directed East and West correspondingly. In those experiments, two important effects were discovered.

7.1. The histograms registered in the experiments with the East-directed collimator ("east histograms") are similar to those "west histograms" that are delayed by 718 min, i. e. by half of the sidereal day.

7.2. No similar histograms were observed in the simultaneous measurements with the "east" and "west" collimators. Without collimators, it is highly probable for similar histograms to appear at the same place and time. This space-time synchronism disappears when α-particles streaming in the opposing directions are counted.

These results are in agreement with the concept that the histogram pattern depends on the vector of the α-particle emission relative to a certain point at the coelosphere [20].

8 The experiments with the rotating collimators

These investigations were naturally followed by experiments with rotating collimators [22, 24].

8.1. With the collimator rotating counter-clockwise (i. e., together with the Earth), the coelosphere was scanned with a period equal to the number of the collimator rotations per day plus one rotation made by the Earth itself. We examined the dependence of the probability of similar histograms to appear on the number of collimator rotations per day. Just as expected, the probability turned out to jump with periods equal to 1440 min divided by the number of collimator rotations per day plus 1. We evaluated data at 1, 2, 3, 4, 5, 6, 7, 11 and 23 collimator rotations per day and found periods equal to 12, 8, 6 etc. hours. The analysis of highly resolved data (with a resolution of 1 min) revealed that each of these periods had two extrema: "sidereal" and "solar". These results indicate that the histogram pattern is indeed determined by how the direction of the α-particle emission relates to the "picture of the heaven" [24].

8.2. When the collimator made 1 clockwise rotation per day, the rotation of the Earth was compensated for (α-particles always undergo emission in the direction of the same region of the coelosphere) and, correspondingly, the daily periods dissappeared. This result was completely analogous to the results of measurements near the North Pole and measurements with the immobile collimator directed towards the Pole Star [20].

8.3. With the collimator placed in the ecliptic plane, directed at the Sun and making 1 clockwise rotation per day, α-particles are constantly emitted in the direction of the Sun. As was expected, the near-daily periods, both solar and sidereal, disappeared under such conditions.

9 The 718-min period

The pattern of histograms is determined by a complex set of cosmo-physical factors. It follows from the existence of the near-27-day periods, that amongst these factors may be the relative positions and states of the Sun, the Moon and the Earth. We repeatedly observed similar histograms during the risings and settings of the Sun and the Moon. A very large volume of work has been carried out. Yet we have not found a histogram pattern which would be characteristic for those instants. A review and analysis of the corresponding results will be given in a special paper. Here, I shall note one quite paradoxical result: on the days of equinox one can see a clear period in the appearance of similar histograms, which is equal to 718 min (i. e. half of the sidereal day). There is no such period on the days of solstice. This phenomenon indicates that the histogram pattern depends on the ecliptic position of the Sun. If that is indeed so, we can expect that on the equator the period of 718 min will be observed year-round.

10 The observations during eclipses

All the results presented above were obtained by the evaluation of tens of thousands of histogram pairs in every experiment, so these results have a stochastic character. A completely different approach is used in the search for characteristic histogram patterns in the periods of the New Moon and solar eclipses. In these cases, we go right to the analysis of the histogram patterns at a certain predetermined moment. Doing so, we have discovered an amazing phenomenon. At the moment of the New Moon, a certain characteristic histogram appears practically simultaneously at different longitudes and latitudes — all over the Earth. This characteristic histogram corresponds to a time segment of 0.5–1.0 min [21]. When the solar eclipse reaches maximum (as a rule, this moment does not coincide with the time of the New Moon), a specific histogram also appears; however, it has a different pattern. Such specific patterns emerge not only in the moments of the New Moon or solar eclipses. But the probability of their appearance at these very moments at different places and on different dates (months, years) being accidental is extremely low. These specific patterns do not relate to tidal effects. Nor do they depend on position on the Earth's surface, where the Moon's shadow falls during the eclipse or the New Moon.

11 The possible nature of "macroscopic fluctuations"

I have presented above a brief review of the main phenomena that are united by the notion of "macroscopic fluctuations". A number of works suggested different hypotheses on the nature of those phenomena [3, 9, 10, 13–15, 19, 27–31], concerning some general categories such as discreteness and continuity, symmetry, the nature of numbers, stochasticity. In this section of the paper I draw attention to the question of how some of the discovered phenomena can be considered in relation to these general categories.

11.1. The non-energetic nature of the phenomena. Fluctuations of space-time [14, 19].

It is clear that we deal with non-energetic phenomena. As mentioned above, the ranges of energies in biochemical reactions, noise in gravitational antennae, and α-decay, differ by many orders. At the same time, the corresponding histogram patterns are similar with a high probability at the same local time at different geographical points. The only thing common to such different processes is the space-time in which they occur. Therefore, the characteristics of space-time change every successive moment.

It is important to note that the "macroscopic fluctuations" do not result from the effect of any factors on the object under examination. They just reflect the state of the space-time.

The changes in space-time can follow the alterations of the gravitational field. These alterations are determined by the movement of the examined object in a heterogeneous gravitational field. The heterogeneity results from the existence of "mass thicknesses", i. e. heavenly bodies. The movement includes the daily rotation of the Earth, its translocation along its circumsolar orbit and, probably, the drift of the solar system in the galaxy. All these forms of movement seem to be reflected in the corresponding periods of variation of histogram patterns. How the fluctuations of space-time transform into the pattern of histograms is unclear.

11.2. Fractality [14, 19].

We suppose that the histogram pattern varies due to the change of the cosmo-physical conditions in the process of the Earth movement around its axis and along its circumsolar orbit. Then we might expect that the shorter are the intervals for which histograms are plotted, the more similar would be the histogram patterns. This corresponds to the concept of "lifetime" of a certain idea of form. This concept is an obvious consequence of the "effect of near zone", when the probability of histogram patterns to be similar is higher for the histograms from the neighbouring intervals.

However, we failed to find such a short interval for which the histogram pattern "would not have time to change". The maximum probability for histograms to be similar only in the first, the nearest interval, does not change upon variation of this interval from several hours to milliseconds. This phenomenon corresponds to the notion of "fractality"; however, the physical meaning of this fractality needs to be clarified.

Following the dependence of the histogram pattern on direction obtained in the experiments with collimators, we deal with a spatial heterogeneity on the scale of the order of 10^{-13} cm: the dependence of the histogram pattern should be determined before the emission of α-particles from the nucleus. Therefore, to "stop the instant", stop the histogram changing, we should have worked with correspondingly small time intervals. Perhaps this will be possible someday soon.

11.3. The mirror symmetry, chirality of histograms [7].

Quite often (up to 30% of cases), the patterns of the successive histograms are reflection symmetric. There are right and left forms, and they may be very complex. This phenomenon possibly means that chirality is an inherent feature of space-time.

11.4. "Stochasticity along abscissa and regularity along ordinate".

Our main result — evidence of non-stochasticity of the fine structure of sampling distributions, i. e. the fine structure of the spectrum of amplitude fluctuations in processes of any nature, i. e. the fine structure of the corresponding histograms — implies the existence of a particular class of macroscopic stochastic processes.

Among such processes is radioactive decay. This is an "*a priori* stochastic" (i. e. stochastic according to the accepted criteria) process. However, the pattern of histograms (i. e. the fine structure of the amplitudes of fluctuations of the decay rate) changes regularly with time.

The point is that in the majority of cases, stochasticity is treated as an irregular succession of events — succession in time, just one after another. This is "stochasticity along the axis of abscisses".

For macroscopic processes, the distributions of the amplitudes of fluctuations of measured quantities are considered to correspond to smooth distributions of Gauss-Poisson type. The available fitting criteria are integral, they are based on averaging, smoothing of those fluctuations. Such fitting criteria cannot "sense" the fine structure of distributions. According to these criteria, the processes we study, such as radioactive decay, correspond well to traditional views.

However, known for more then a hundred years is a noticeable exception — atomic spectra. While the transitions of electrons from one level to another are "*a priori* stochastic", the energies of the levels are sharply discrete. The "stochastic along the abscissa" process of transition is "regular along the ordinate".

The result of our work is the discovery of analogous macroscopic processes. In the process of fluctuating, the measured quantities take values, some of which are observed more often than the others; there are "forbidden" and "allowed" values of the measured quantities. This is what we see in the fine structure of histograms, with all its "peaks and troughs". The "macroscopic quantization" differs from the quantization in the microworld. Here only the "idea of histogram form" remains invariant, whereas the concrete values, corresponding to extrema, can change. This is the main difference between the spectra of amplitude fluctuations of macroscopic processes and the atomic spectra.

11.5. The fine structure of histograms. The presence of "peaks and troughs" in histogram patterns is a consequence of two causes: arithmetic (algorithmic) and physical [7, 14, 19].

11.5.1. The arithmetic or algorithmic cause of discreteness [7, 14, 19] lies in a very unequal number of factors (divisors) corresponding to the natural sequence. If the measured value is a result of operations based on the algorithms of division, multiplication, exponentiation, then discreteness will be

unavoidable. Correspondingly, the histogram patterns will be determined by these algorithms. This can be seen, for example, in the computer simulation of the process of radioactive decay (Poisson statistics). The pattern of some histograms obtained in such a simulation is indistinguishable from the pattern of histograms plotted for the radioactive decay data. However, the sequence of "computer" histogram patterns, in contrast to that of "physical" ones, does not depend on time and can be reproduced over and over again by launching the simulation program with the same parameters. This sequence is determined by the nature of numbers and the algorithms used. In our work we experienced an unusual incident, when the sequence of histogram patterns created by a random number generator was similar, with high probability, to the sequence obtained from the radioactive decay data. If studied systematically, this case might give a clue to the nature of those "physical algorithms" that determine the time changes of the patterns of physical histograms [19].

11.5.2. The physical cause of discreteness is the interference of wave fluxes [19].

The fine structure of histograms, the presence of narrow extrema, cannot have a probabilistic nature. According to Poisson statistics, with which radioactive decay roughly accords, the width of such extrema should be of order $N^{1/2}$.

Therefore, if neighbouring extrema in the histogram pattern have similar values of N, they should overlap, but they do not. Such narrow extrema can arise only as a result of interference. Hence, the fine structure of histograms plotted from the results of measurements of any nature would be a result of an interference of some waves. As follows from all the material presented above, the issue concerns processes caused by the movement of the Earth (and objects on its surface) relative to the "mass thicknesses". So it would be logical to define the waves whose interference is reflected in the histogram patterns as "gravitational".

The results of experiments with collimators, producing narrow beams of α-particles, lead us to conclude for a sharp anisotropy of our world. The corresponding wave fluxes should be very narrow.

Collimators are not necessary to reveal this anisotropy. We observe highly resolved daily and yearly periods in the changing of the probability of a certain histogram pattern to appear repeatedly (the resolution is 1 min). The histogram patterns specific for the New Moon and solar eclipses can appear at different geographical points synchronously, with an accuracy of 0.5 min. The local-time synchronism at different geographical points (almost 15,000 km apart) is also determined by a sharp extremum on the curve of distribution over intervals with a resolution of 1 min. In the experiments with the rotation of collimators, the "sidereal" and "solar" periods are also observed with one-minute resolution.

Taken together, all these facts can mean that we deal with narrowly directed wave fluxes, "beams". The narrowness of these putative fluxes or beams is smaller than the aperture of collimators. Collimators with the diameter of 0.9 mm and length of 10 mm isolate in the coelosphere a window of about 5°, corresponding to approximately 20 min of the Earth's daily rotation rate. This fact, noted by Kharakoz, could be explained if we admit that the "beams" are more narrow than the aperture of our collimators.

Even with the fact that the matter concerns the changes of the histogram pattern and the movement of the Earth relative to the sphere of fixed stars, the Moon and the Sun, it is not necessary to consider anisotropy as being only due to the heterogeneous distribution of masses (presence of celestial bodies) in space. It is possible that this anisotropy is caused by a preferential direction, which, for example, is due to the drift of the solar system towards the constellation of Hercules. The existence of such a direction is an old problem of physics. In this connection, of great value for us are the results of the interference experiments of Dayton Miller [43], the experiments and conception of Alais [42], de Witte's measurements [47] and Cahill's conception [44, 46]. It is necessary to mention that several years ago, Lyapidevsky [29] and Dmitrievsky [30] considered the preferential direction in space as the cause of the effects we observed.

In this case, we can say that for many years, we have studied phenomena indicating the existence of gravitational waves. Then the problem of detection of gravitational waves can be approached differently: instead of using bulky and expensive devices, such as Weber's antennae, one could register the changes of the fine structure of histograms plotted from the results of measurements of certain chosen processes.

The fine structure of the histogram pattern we registered while solar eclipses manifests a resonance in an interference picture, built by a bulky space masses. Most probable this is a gravitational wave pattern. The histogram patterns specific for solar eclipses recall to Crother's analysis of Kepler's laws in General Relativity, wherein he showed that space-time is locally anisotropic for a rotating spherical body [49]. In this situation, we suppose that of principal importance are works by Borissova [50] and Rabounski [51] on the theory and methods of detection of gravitational waves and the concept of "global scaling" advanced by Hartmut Muller [52].

Acknowledgements

I thank my colleagues I. A. Rubinshtein, V. A. Shlekhtarev, V. A. Kolombet, N. V. Udaltsova, E. V. Pozharsky, T. A. Zenchenko, K. I. Zenchenko, A. A. Konradov, L. M. Ovchinnikova, T. S. Malova, T. Ya. Britsina and N. P. Ivanova for many years of collaboration. I appreciate valuable comments and psychological support from D. P. Kharakoz, V. I. Bruskov, F. I. Ataullakhanov, V. N. Morozov, I. I. Berulis, B. M. Vladimirsky, V. K. Lyapidevsky, I. M. Dmitrievsky, B. U. Rodionov, S. N. Shapovalov, O. A. Troshichev, E. S. Gorshkov, A. V. Makarevich, V. A. Sadovnichy, Yu. S. Vladimirov,

V. A. Namiot, N. G. Esipova, G. V. Lisichkin, Yu. A. Baurov, D. S. Chernavsky, B. V. Komberg, V. L. Ginzburg, E. L. Feinberg, G. T. Zatsepin. Invaluable advice, psychological and financial support of M. N. Kondrashova and V. P. Tikhonov are in the foundations of the results obtained. I am grateful to G. M. Frank, G. R. Ivanitsky, E. E. Fesenko, V. A. Tverdislov for many years of patience and support. Special thanks to my respected teacher Sergey E. Severin and my older friend Lev A. Blumenfeld for years of joyful conversations. I thank D. Rabounski and L. Borissova for remarks to this paper and discussion. I am also grateful to S. J. Crothers for his help in the preparing of this paper.

References

1. Perevertun T. V., Udaltzova N. V., Kolombet V. A., Ivanova N. P., Britsina T. Ya., and Shnoll S. E. Macroscopic fluctuations in aqueous solutions of proteins and other substances as a possible consequence of cosmo-geophysical factors. *Biophysics*, 1981, v. 26(4), 613–624.
2. Shnoll S. E., Namiot V. A., Zhvirblis V. E., Morozov V. N., Temnov A. V., and Morozova T. Ya. Possible common nature of macroscopic fluctuations of the rates of biochemical and chemical reactions, electrophoretic mobility of the cells and fluctuations in measurements of radioactivity, optical activity and flicker noise. *Biophysics*, 1983, v. 28(1), 164–168.
3. Shnoll S. E. Discrete amplitude spectra (histograms) of macroscopic fluctuations in processes of various nature. *Itogi Nauki i Techniki. Molecular Biology Series*, ed. V. P. Skulachev, 1985, v. 5, Moscow, VINITI, 130–200.
4. Udaltzova N. V., Kolombet V. A., and Shnoll S. E. A possible cosmophysical origin of macroscopic fluctuations in various processes. Puschino, ONTI NtsBI, 1987.
5. Udaltzova N. V., Kolombet V. A., and Shnoll S. E. The possible gravitational nature of factor influensing discrete macroscopic fluctuations. *Proc. First Intern. Congress on Geo-Cosmic Relations*, Wageningen, Netherlands, 1989, 174–180.
6. Shnoll S. E. Correlation of the shape of macroscopic fluctuations amplitude spectra with position of the Moon relative to the horizon. *Biophysics*, 1989, v. 34(5), 911–912.
7. Shnoll S. E., Udaltsova N. V., Kolombet V. A., Namiot V. A., and Bodrova N. B. Patterns in the discrete distributions of the results of measurements (cosmophysical aspects). *Biophysics*, 1992, v. 37(3), 378–398.
8. Shnoll S. E. The form of the spectra of states realized in the course of macroscopic fluctuations depends on the rotation of the Earth about its axis. *Biophysics*, 1995, v. 40(4), 857–866.
9. Shnoll S. E., Kolombet V. A., Pozharski E. V., Zenchenko T. A., Zvereva I. M., and Konradov A. A., Realization of discrete states during fluctuations in macroscopic processes. *Physics-Uspekhi*, 1998, v. 162(10), 1129–1140.
10. Shnoll S. E., Kolombet V. A., Zenchenko T. A., Pozharski E. V., Zvereva I. M., and Konradov A. A. Cosmophysical origin of "macroscopic fluctations". *Biophysics*, 1998, v. 43(5), 909–915.
11. Zvereva I. M., Zenchenko T. A., Pozharski E. V., Kolombet V. A., Konradov A. A., and Shnoll S. E. Radioactive decay of radium family isotopes as an illustration of synchronous changes in the fine structure of measurement result distributions. *Biophysics*, 1998, v. 43(4), 693–695.
12. Shnoll S. E., Pozharski E. V., Zenchenko T. A., Kolombet V. A., Zvereva I. M., and Konradov A. A. Fine structure of distributions in measurements of different processes as affected by geophysical and cosmophysical factors. *Phys. & Chem. Earth A: Solid Earth & Geod.*, 1999, v. 24(8), 711–714.
13. Shnoll S. E., Zenchenko T. A., Zenchenko K. I., Pozharski E. V., Kolombet V. A., and Konradov A.A.: Regular variation of the fine structure of statistical distributions as a consequence of cosmophysical agents. *Physics-Uspekhi*, 2000, v. 43(2), 205–209.
14. Shnoll S. E. Discrete distribution patterns: arithmetic and cosmophysical origins of their macroscopic fluctuations. *Biophysics*, 2001, v. 46(5), 733–741.
15. Shnoll S. E., Zenchenko K. I., Zenchenko T. A., Fedorov M. V., and Konradov A. A. The non-random character of fine structure of various measurement results distributions as a possible consequence of cosmophysical and arithmetical causes. *Gravitation & Cosmology*, 2002, v. 8, Supppl., 231.
16. Fedorov M. V., Belousov L. V., Voeikov V. L., Zenchenko T. A., Zenchenko K. I., Pozharski E. V., Konradov A. A., Shnoll S. E. Synchronous changes in dark current fluctuations in two separate photomultipliers in relation to Earth rotation *Astrophysics and Space Science*, 2003, v. 283, 3–10.
17. Shnoll S. E., Rubinstein I. A., Zenchenko K. I., Zenchenko T. A., Konradov A. A., Shapovalov S. N., Makarevich A. V., Gorshkov E. S., and Troshichev O. A. Dependence of "macroscopic fluctuations" on geographic coordinates (by data of Arctic and Antarctic expeditions). *Biophysics*, 2003, v. 48(5), 1123–1131.
18. Shnoll S. E., Zenchenko K. I., Berulis I. I., Udaltsova N. V., Zhirkov S. S., and Rubinstein I. A. The dependence of "macroscopic fluctuations" on cosmophysical factors. Spatial anisotropy. *Biophysics*, 2004, v. 49(1), 129–139.
19. Shnoll S. E. Periodical changes in the fine structure of statistic distributions in stochastic processes as a result of arithmetic and cosmophysical reasons. *Time, Chaos, and Math. Problems*, No. 3, University Publ. House, Moscow, 2004, 121–154.
20. Shnoll S. E., Zenchenko K. I., Berulis I. I., Udaltsova N. V., and Rubinstein I. A. Fine structure of histograms of α-activity measurements depends on direction of alpha particles flow and the Earth rotation: experiments with collimators. arXiv: physics/0412007.
21. Shnoll S. E., Zenchenko K. I., Shapovalov S. N., Gorshkov S. N., Makarevich A. V., and Troshichev O. A. The specific form of histograms presenting the distribution of data of α-decay measurements appears simultaneously in the moment of New Moon in different points from Arctic to Antarctic. arXiv: physics/0412152.
22. Shnoll S. E., Rubinshtein I. A., Zenchenko K. I, Shlekhtarev V. A., Kaminsky A. V., Konradov A. A., Udaltsova N. V. Experiments with rotating collimators cutting out pencil of

α-particles at radioactive decay of Pu-239 evidence sharp anisotropy of space. arXiv: physics/0501004.

23. Shnoll S. E., Zenchenko K. I., and Udaltsova N. V. Cosmophysical effects in structure of the daily and yearly periods of change in the shape of the histograms constructed by results of measurements of α-activity Pu-239. arXiv: physics/0504092.
24. Shnoll S. E., Rubinshtein I. A., Zenchenko K. I, Shlekhtarev V. A., Kaminsky A. V., Konradov A. A., Udaltsova N. V. Experiments with rotating collimators cutting out pencil of α-particles at radioactive decay of Pu-239 evidence sharp anisotropy of space. *Progress in Physics*, 2005, v. 1, 81–84.
25. Goleminov N. G. Possible nuclear activity of dark matter. *Gravitation & Cosmology*, 2002, v. 8, Supplement, 219.
26. Rodionov B. U. On the way to new physics. *Gravitation & Cosmology*, 2002, v. 8, Supplement, 214–215.
27. Namiot V. A. On the theory of the effect of "macroscopic fluctuations". *Biophysics*, 2001, v. 46(5), 856–858.
28. Blumenfeld L. A. and Zenchenko T. A. Quantum transitions between states and cosmophysical fluctuations. *Biophysics*, 2001, v. 46(5), 859–861.
29. Lyapidevskii V. K. Diurnal variations in the flux of α-particles as possible evidence for changes in the vector of velocity of movement of an experimental set-up relative to a relic system. *Biophysics*, 2001, v. 46(5), 850–851.
30. Dmitrievski I. M. A possible explanation of the phenomenon of cosmophysical fluctuations. *Biophysics*, 2001, v. 46(5), 852–855.
31. Kirillov A. A. and Zenchenko K. I. On the probability of of disturbance of the poisson statistics in processes of radioactive decay type. *Biophysics*, 2001, v. 46(5), 841–849.
32. Baurov Yu. A., Konradov A. A., Kuznetsov E. A., Kushniruk V. F., Ryabov Y. B., Senkevich A. P., Sobolev Yu. G., and Zadorozsny S. Experimental investigations of changes in beta-decay rate of ^{60}Co and ^{137}Cs. *Mod. Phys. Lett. A*, 2001, v. 16(32), 2089.
33. Baurov Yu. A. and Shutov V. L. On influence of the vector magnetic potentials of the Earth and the Sun in the в-decay rate. *Applied Physics*, 1995, No. 1, 40.
34. Baurov Yu. A., Klimenko E. Yu., and Novikov S. I. Observations of magnetic anisotropy of the space in experiments. *Doklady Akad. Sci. USSR*, 1990, v. 315(5), 1116.
35. Baurov Yu. A. Space magnetic anisotropy and a new interaction in nature. *Phys. Lett. A*, 1993, v. 181, 283.
36. Baurov Yu. A., Timofeev I. B., Chernikov V. A., and Chalkin S. I. Experimental research for space anisotropy in the radiations by impulse plasmatron. *Appl. Physics*, 2002, No. 4, 48–57.
37. Zenchenko T. A., Konradov A. A., and Zenchenko K. I. Correlation between dynamics of the "nearest zone effect" amplitude and parameters of the interplanetary magnetic field. *Geophysical Processes and Biosphere*, 2005, v. 4, No. 1/2, 125–132.
38. Zenchenko T. A., Konradov A. A., and Zenchenko K. I. Macroscopic fluctuations: on the fact that the "nearest zone effect" appears periodically. *Biophysics*, 2003, v. 48(6), 1132–1136.
39. Qian-shen Wang, Xin-she Yang, Chuan-zhen Wu, Hong-gang Guo, Hong-chen Liu, and Chang-chai Hua. Precise measurement of gravity variations during a total solar eclipse. *Phys. Rev. D*, 2000, v. 62, 041101.
40. Vezzoli G. Private communications.
41. Lucatelli F. Private communications.
42. Allais M. L'anisotropie de l'espace. Paris, Éditions Clement Juglar, 1997.
43. Miller D. C. The ether-drift experiment and the determination of the absolute motion of the Earth. *Review of Modern Physics*, 1933, v. 5, 204–241.
44. Cahill R. T. Gravitation, the "dark matter" effect and the fine structure constant. arxiv: physics/0401047.
45. Cahill R. T. Novel Gravity Probe B gravitational wave detection. arXiv: physics/0408097.
46. Cahill R. T. Absolute motion and gravitational effects. *Apeiron*, 2004, v. 11(1), 53–111.
47. The DeWitte Experiment: 1991, R. DeWitte.
48. DeMeo J. Critical review of the Shankland et al. analysis of Dayton Miller's aether-drift experiments. *Meetings of the Natural Philosophy Alliance*, Berkeley (California) and Storrs (Connecticut), May and June, 2000.
49. Crothers S. J. On the generalisation of Kepler's 3rd law for the vacuum field of the point-mass. *Progress in Physics*, 2005, v. 2, 70–75.
50. Borissova L. Gravitational waves and gravitational inertial waves in the General Theory of Relativity. A theory and experiments. *Progress in Physics*, 2005, v. 2, 59–91.
51. Rabounski D. A theory of gravity like electrodynamics. *Progress in Physics*, 2005, v. 2, 15–29.
52. Muller H. Global Scaling. Die Basis ganzheitlicher Naturwissenschaft. *Raum & Zeit*, Special 1, 2004.

On the Coupling Constants, Geometric Probability and Complex Domains*

Carlos Castro
Center for Theoretical Studies of Physical Systems, Clark Atlanta University, Atlanta, Georgia, USA
E-mail: czarlosromanov@yahoo.com; castro@ctsps.cau.edu

By recurring to Geometric Probability methods it is shown that the coupling constants, $\alpha_{EM}, \alpha_W, \alpha_C$, associated with the electromagnetic, weak and strong (color) force are given by the *ratios* of measures of the sphere S^2 and the Shilov boundaries $Q_3 = S^2 \times RP^1$, *squashed* S^5, respectively, with respect to the Wyler measure $\Omega_{Wyler}[Q_4]$ of the Shilov boundary $Q_4 = S^3 \times RP^1$ of the poly-disc D_4 (8 real dimensions). The latter measure $\Omega_{Wyler}[Q_4]$ is linked to the geometric coupling strength α_G associated to the gravitational force. In the conclusion we discuss briefly other approaches to the determination of the physical constants, in particular, a program based on the Mersenne primes p-adic hierarchy. The most important conclusion of this work is the role played by higher dimensions in the determination of the coupling constants from pure geometry and topology alone and which does *not* require to invoke the anthropic principle.

1 Geometric probability

Geometric Probability [1] is the study of the probabilities involved in geometric problems — the distributions of length, area, volume, etc. for geometric objects under stated conditions. One of the most famous problem is the Buffon's Needle Problem of finding the probability that a needle of length l will land on a line, given a floor with equally spaced parallel lines a distance d apart. The problem was posed by the French naturalist Buffon in 1733. For $l < d$ the probability is

$$P = \frac{1}{2\pi}\int_0^{2\pi} d\theta \frac{l|\cos\theta|}{d} = \frac{4l}{2\pi d}\int_0^{\frac{\pi}{2}} \cos\theta = \frac{2l}{\pi d} = \frac{2ld}{\pi d^2}. \quad (1.1)$$

Hence, the Geometric Probability is essentially the *ratio* of the areas of a rectangle of length $2d$, and width l and the area of a circle of radius d. For $l > d$, the solution is slightly more complicated [1]. The Buffon needle problem provides with a numerical experiment that determines the value of π empirically. Geometric Probability is a vast field with profound connections to Stochastic Geometry.

Feynman long ago speculated that the fine structure constant may be related to π. This is the case as Wyler found long ago [2]. We will take the fine structure constant based on Feynman's physical interpretation of the electron's charge as the probability amplitude that an electron emits/absorbs a photon. The clue to evaluate this probability within the context of Geometric Probability theory is provided by the electron self-energy diagram. Using Feynman's rules, the self-energy $\Sigma(p)$ as a function of the electron's incoming/outgoing energy-momentum p_μ is given by the integral involving the photon and electron propagator along the internal lines

$$-i\Sigma(p) = (-ie)^2 \int \frac{d^4k}{(2\pi)^4}\gamma^\mu \frac{i}{\gamma^\rho(p_\rho - k_\rho) - m}\frac{-ig_{\mu\nu}}{k^2}\gamma^\nu. \quad (1.2)$$

The integral is taken with respect to the values of the photon's energy-momentum k^μ. By inspection one can see that the electron self-energy is proportional to the fine structure constant $\alpha_{EM} \sim e^2$, the square of the probability amplitude (in natural units of $\hbar = c = 1$) and physically represents the electron's emission of a virtual photon (off-shell, $k^2 \neq 0$) of energy-momentum k_ρ at a given moment, followed by an absorption of this virtual photon at a later moment.

Based on this physical picture of the electron self-energy graph, we will evaluate the Geometric Probability that an electron emits a photon at $t = -\infty$ (infinite past) and reabsorbs it at a much later time $t = +\infty$ (infinite future). The off-shell (virtual) photon associated with the electron self-energy diagram *asymptotically* behaves on-shell at the very moment of emission ($t = -\infty$) and absorption ($t = +\infty$). However, the photon can remain off-shell in the intermediate region between the moments of emission and absorption by the electron. The fact that Geometric Probability is a classical theory does not mean that one cannot derive the fine structure constant (which involves the Planck constant) because the electron self-energy diagram is itself a quantum (one-loop) Feynman process; i. e. one can recur to Geometric Probability to assign proper geometrical measures to Feynman diagrams, not unlike the Twistor-diagrammatic version of the Feynman rules of QFT.

The topology of the boundaries (at conformal infinity) of the past and future light-cones are spheres S^2 (the celestial sphere). This explains why the (Shilov) boundaries are essential mathematical features to understand the geometric derivation of all the coupling constants. In order to describe the physics at infinity we will recur to Penrose's ideas [12] of conformal compactifications of Minkowski spacetime by attaching the light-cones at conformal infinity. Not unlike the one-point compactification of the complex plane by adding the points at infinity leading to the Gauss-Riemann sphere.

*This paper is based on a talk given at the Second Intern. p-adic Conference in Mathematics and Physics (Belgrade, Serbia, September, 2005).

The conformal group leaves the light-cone fixed and it does not alter the causal properties of spacetime despite the rescalings of the metric. The topology of the conformal compactification of real Minkowski spacetime $\bar{M}_4 = S^3 \times S^1/Z_2 = = S^3 \times RP^1$ is precisely the same as the topology of the Shilov boundary Q_4 of the 4 complex-dimensional poly-disc D_4. The action of the discrete group Z_2 amounts to an antipodal identification of the future null infinity $\mathcal{I}^+$ with the past null infinity $\mathcal{I}^-$; and the antipodal identification of the past timelike infinity i^- with the future timelike infinity, i^+, where the electron emits, and absorbs the photon, respectively.

Shilov boundaries of homogeneous (symmetric spaces) complex domains, G/K [9]–[11] are not the same as the ordinary topological boundaries (except in some special cases). The reason being that the action of the isotropy group K of the origin is not necesarily *transitive* on the ordinary topological boundary. Shilov boundaries are the minimal subspaces of the ordinary topological boundaries which implement the Maldacena-'T Hooft-Susskind holographic principle [15] in the sense that the holomorphic data in the interior (bulk) of the domain is fully determined by the holomorphic data on the Shilov boundary. The latter has the property that the maximum modulus of any holomorphic function defined on a domain is attained at the Shilov boundary.

For example, the poly-disc D_4 of 4 complex dimensions is an 8 real-dim Hyperboloid of constant negative scalar curvature that can be identified with the conformal relativistic *curved* phase space associated with the electron (a particle) moving in a $4D$ Anti de Sitter space AdS_4. The poly-disc is a Hermitian symmetric homogeneous coset space associated with the $4D$ conformal group $SO(4, 2)$ since $D_4 = SO(4, 2) /SO(4) \times SO(2)$. Its Shilov boundary $Shilov\ (D_4) = Q_4$ has precisely the *same* topology as the $4D$ conformally compactified real Minkowski spacetime $Q_4 = \bar{M}_4 = S^3 \times S^1/Z_2 = = S^3 \times RP^1$. For more details about Shilov boundaries, the conformal group, future tubes and holography we refer to the article by Gibbons [14] and [9], [18].

The role of the conformal group in gravity in these expressions (besides the holographic bulk/boundary *AdS*/*CFT* duality correspondence [15]) stems from the MacDowell Mansouri-Chamseddine-West formulation of gravity based on the conformal group $SO(3, 2)$ which has the same number of 10 generators as the $4D$ Poincaré group. The $4D$ vielbein e^a_μ which gauges the spacetime translations is identified with the $SO(3, 2)$ generator $A^{[a5]}_\mu$, up to a crucial scale factor R, given by the size of the Anti de Sitter space (de Sitter space) throat. It is known that the Poincaré group is the Wigner-Inonu group contraction of the de Sitter Group $SO(4,1)$ after taking the throat size $R = \infty$. The spin-connection ω^{ab}_μ that gauges the Lorentz transformations is identified with the $SO(3, 2)$ generator $A^{[ab]}_\mu$. In this fashion, the e^a_μ, ω^{ab}_μ are encoded into the $A^{[mn]}_\mu$ $SO(3, 2)$ gauge fields, where m, n run over the group indices 1, 2, 3, 4, 5. A word of caution, gravity is a gauge theory of the full diffeomorphisms group which is infinite-dimensional and which includes the translations. Therefore, strictly speaking gravity is not a gauge theory of the Poincaré group. The Ogiovetsky theorem shows that the diffeomorphisms algebra in $4D$ can be generated by an infinity of *nested* commutators involving the $GL(4, R)$ and the $4D$ Conformal Group $SO(4, 2)$ generators.

In [19] we have shown why the MacDowell-Mansouri-Chamseddine-West formulation of gravity, with a cosmological constant and a topological Gauss-Bonnet invariant term, can be obtained from an action inspired from a BF-Chern-Simons-Higgs theory based on the conformal $SO(3, 2)$ group. The AdS_4 space is a natural vacuum of the theory. The vacuum energy density was *derived* to be precisely the geometric-mean between the UV Planck scale and the IR throat size of de Sitter (Anti de Sitter) space. Setting the throat size to coincide with the future horizon scale (of an accelerated de Sitter Universe) given by the Hubble scale (today) R_H, the geometric mean relationship yields the observed value of the vacuum energy density $\rho \sim (L_P R_H)^{-2} = = (L_P)^{-4}(L_P^2/R_H^2) \sim 10^{-120} M^4_{Planck}$. Nottale [24] gave a different argument to explain the small value of ρ based on Scale Relativistic arguments. It was also shown in [19] why the Euclideanized AdS_{2n} spaces are $SO(2n-1, 2)$ instantons solutions of a non-linear sigma model obeying a double self duality condition.

A typical objection to the possibility of being able to derive the values of the coupling constants, from pure thought alone, is that there are an infinite number of possible analytical expressions that accurately reproduce the values of the couplings within the experimental error bounds. However, this is not our case because once the gauge groups $U(1)$, $SU(2)$, $SU(3)$ are known there are *unique* expressions stemming from Geometric Probability which furnish the values of the couplings. Another objection is that it is a meaningless task to try to derive these couplings because these are not constants per se but vary with respect to the energy scale. The running of the coupling constants is an *artifact* of the perturbative Renormalization Group program. We will see that the values of the couplings derived from Geometric Probability are precisely those values that correspond to the natural physical scales associated with the EM, Weak and Strong forces.

Another objection is that physical measurements of irrational numbers are impossible because there are always experimental limitations which rule out the possibility of actually measuring the *infinite* number of digits of an irrational number. This experimental constraint does not exclude the possibility of deriving exact expressions based on π as we shall see. We should not worry also about obtaining numerical values within the error bars in the table of the coupling constants since these numbers are based on the values of *other* physical constants; i. e. they are based on the particular *consensus* chosen for all of the other physical constants.

In our conventions, $\alpha_{EM} = e^2/4\pi = 1/137.036\ldots$ in the natural units of $\hbar = c = 1$, and the quantities $\alpha_{weak}, \alpha_{color}$ are the Geometric Probabilities $\tilde{g}_w^2, \tilde{g}_c^2$, after *absorbing* the factors of 4π of the conventional $\alpha_W = (g_w^2/4\pi)$, $\alpha_C = (g_c^2/4\pi)$ definitions used in the Renormalization Group (RG) program.

2 The fine structure constant

In order to define the Geometric Probability associated with this process of the electron's emission of a photon at i^- ($t = -\infty$), followed by an absorption at i^+ ($t = +\infty$), we must take into account the important fact that the photon is on-shell $k^2 = 0$ *asymptotically* (at $t = \pm\infty$), but it can move off-shell $k^2 \neq 0$ in the intermediate region which is represented by the *interior* of the $4D$ conformally compactified real Minkowski spacetime which agrees with the Shilov boundary of D_4 (the four-complex-dimensional poly-disc) $Q_4 = \bar{M}_4 = S^3 \times S^1/Z_2 = S^3 \times RP^1$. The Q_4 has four-real-dimensions which is half the real-dimensions of D_4 (2×4=8).

The measure associated with the celestial spheres S^2 (associated with the future/past light-cones) at timelike infinity i^+, i^-, respectively, is $V(S^2) = 4\pi r^2 = 4\pi$ ($r = 1$). Thus, the *net* measure corresponding to the two celestial spheres S^2 at timelike infinity $i^{\pm}$ requires an overall factor of 2 giving $2V(S^2) = 8\pi$ ($r = 1$). The factor of $8\pi = 2{\times}4\pi$ can also be interpreted in terms of the two-helicity degrees of freedom, corresponding to a spin 1 massless photon, assigned to the area of the celestial sphere. The Geometric Probability is defined by the ratio of the (dimensionless volumes) measures associated with the celestial spheres S^2 at i^+, i^- timelike infinity, where the photon moves on-shell, relative to the Wyler measure $\Omega_{Wyler}[Q_4]$ associated with the full *interior* region of the conformally compactified $4D$ Minkwoski space $Q_4 = \bar{M}_4 = S^3 \times S^1/Z_2 = S^3 \times RP^1$, where the massive electron is confined to move, as it propagates from i^- to i^+, (and *off-shell* photons can also live in):

$$\alpha_{EM} = \frac{2V(S^2)}{\Omega_{Wyler}[Q_4]} = \frac{8\pi}{\Omega_{Wyler}[Q_4]} = \frac{1}{137.03608\ldots} \quad (2.1a)$$

after inserting the Wyler measure

$$\Omega_{Wyler}[Q_4] = \frac{V(S^4)V(Q_5)}{[V(D_5)]^{\frac{1}{4}}} = \frac{8\pi^2}{3}\frac{8\pi^3}{3}\left(\frac{\pi^5}{2^4{\times}5!}\right)^{-\frac{1}{4}}. \quad (2.1b)$$

The Wyler measure $\Omega_{Wyler}[Q_4]$ [2] is *not* the standard measure (dimensionless volume) $V(Q_4) = 2\pi^3$ calculated by Hua [10] but requires some elaborate procedure.

It was realized by Smith [5] that the presence of the Wyler measure in the expression for α_{EM} given by eq.-(2.1) was consistent with Wheeler ideas that the observed values of the coupling constants of the Electromagnetic, Weak and Strong Force can be obtained if the geometric force strengths (measures related to volumes of complex homogenous domains associated with the $U(1)$, $SU(2)$, $SU(3)$ groups, respectively) are all *divided* by the geometric force strength of gravity α_G (related to the $SO(3,2)$ MMCW Gauge Theory of Gravity) and which is not the same as the $4D$ Newton's gravitational constant $G_N \sim m_{Planck}^{-2}$. Hence, upon dividing these geometric force strengths by the geometric force strength of gravity α_G one is dividing by the Wyler measure factor because (see below) $\alpha_G \equiv \Omega_{Wyler}[Q_4]$.

Furthermore, the expression for $\Omega_{Wyler}[Q_4]$ is also consistent with the Kaluza-Klein compactification procedure of obtaining Maxwell's EM in $4D$ from *pure* gravity in $5D$ since Wyler's expression involves a $5D$ domain D_5 from the very start; i. e. in order to evaluate the Wyler measure $\Omega_{Wyler}\ [Q_4]$ one requires to embed D_4 into D_5 because the Shilov boundary space $Q_4 = S^3 \times RP^1$ is *not* adequate enough to implement the action of the $SO(5)$ group, the compact version of the Anti de Sitter Group $SO(3,2)$ that is required in the MacDowell-Mansouri-Chamseddine-West (MMCW) $SO(3,2)$ gauge formulation of gravity. However, the Shilov boundary of D_5 given by $Q_5 = S^4 \times RP^1$ is adequate enough to implement the action of $SO(5)$ via isometries (rotations) on the internal symmetry space $S^4 = SO(5)/SO(4)$. This justifies the embedding procedure of $D_4 \to D_5$

The 5 complex-dimensional poly-disc $D_5 = SO(5,2)/SO(5) \times SO(2)$ is the 10 real-dim Hyperboloid $\mathcal{H}^{10}$ corresponding to the relativistic curved phase space of a particle moving in $5D$ Anti de Sitter Space AdS_5. The Shilov boundary Q_5 of D_5 has 5 real dimensions (half of the 10-real-dim of D_5). One cannot fail to notice that the hyperboloid $\mathcal{H}^{10}$ can be embedded in the 11-dim pseudo-Euclidean $R^{9,2}$ space, with two-time like directions. This is where 11-dim lurks into our construction.

Having displayed Wyler's expression of the fine structure constant α_{EM} in terms of the ratio of dimensionless measures, we shall present a Fiber Bundle (a sphere bundle fibration over a complex homogeneous domain) derivation of the Wyler expression based on the bundle $S^4 \to E \to D_5$, and explain below why the propagation (via the determinant of the Feynman propagator) of the electron through the *interior* of the domain D_5 is what accounts for the "obscure" factor $V(D_5)^{1/4}$ in Wyler's formula for α_{EM}.

We begin by explaining why Wyler's measure $\Omega_{Wyler}[Q_4]$ in eq.-(2.1) corresponds to the measure of a S^4 bundle fibered over the base curved-space $D_5 = SO(5,2)/SO(5) \times SO(2)$ and *weighted* by a factor of $V(D_5)^{-1/4}$. This $S^4 \to E \to D_5$ bundle is linked to the MMCW $SO(3,2)$ Gauge Theory formulation of gravity and explains the essential role of the gravitational interaction of the electron in Wyler's formula [5] corroborating Wheeler's ideas that one must normalize the geometric force strengths with respect to gravity in order to obtain the coupling constants. The subgroup $H = SO(5)$ of the isotropy group (at the origin) $K = SO(5) \times SO(2)$ acts naturally on the Fibers $F = S^4 = SO(5)/SO(4)$, the internal symmetric space, via isometries (rotations). Locally, and only locally, the Fiber bundle E is the product $D_5 \times S^4$.

The restriction of the Fiber bundle E to the Shilov boundary Q_5 is written as $E|_{Q_5}$ and *locally* is the product of $Q_5 \times S^4$, but this is *not* true globally unless the fiber bundle admits a global section (the bundle is trivial). So, the volume $V(E|_{Q_5})$ does not necessary always factorize as $V(Q_5) \times V(S^4)$. Setting aside this subtlety, we shall pursue a more physical route, suggested by Wyler in unpublished work [3]*, to explain the origin of the "obscure normalization" factor $V(D_5)^{1/4}$ in Wyler's measure $\Omega_{Wyler}[Q_4] = (V(S^4) \times V(Q_5)/V(D_5)^{1/4})$, which suggests that the volumes may not factorize.

The relevant physical feature of this measure factor $V(D_5)^{1/4}$ is that it encodes the *spinorial* degrees of freedom of the electron, like the factor of 8π encodes the two-helicity states of the massless photon. The Feynman propagator of a massive scalar particle (inverse of the Klein-Gordon operator) $(D_\mu D^\mu - m^2)^{-1}$ corresponds to the *kernel* in the Feynman path integral that in turn is associated with the Bergman kernel $K_n(z, z')$ of the complex homogenous domain D_n, proportional to the Bergman constant $k_n \equiv 1/V(D_n)$, i. e.

$$(D_\mu D^\mu - m^2)^{-1}(x^\mu) = \frac{1}{(2\pi\mu)^D} \int d^D p \frac{e^{-ip_\mu x^\mu}}{p^2 - m^2 + i\epsilon} \leftrightarrow$$
$$\leftrightarrow K_n(\mathbf{z}, \bar{\mathbf{z}}') = \frac{1}{V(D_n)}(1 - \mathbf{z}\bar{\mathbf{z}}')^{-2n}, \tag{2.2}$$

where we have introduced a momentum scale μ to match units in the Feynman propagator expression, and the Bergman Kernel $K_n(\mathbf{z}, \bar{\mathbf{z}}')$ of D_n whose dimensionless entries are $\mathbf{z} = (z_1, z_2, \ldots, z_n)$, $\mathbf{z}' = (z'_1, z'_2, \ldots, z'_n)$ is given as

$$K_n(\mathbf{z}, \bar{\mathbf{z}}') = \frac{1}{V(D_n)}(1 - \mathbf{z}\bar{\mathbf{z}}')^{-2n} \tag{2.3a}$$

$V(D_n)$ is the dimensionless Euclidean volume found by Hua $V(D_n) = (\pi^n / 2^{n-1} n!)$ and satisfies the reproducing and normalization properties

$$f(z) = \int_{D_n} f(\xi)\, K_n(z, \xi) d^n\xi d^n\bar{\xi}\,, \quad \int_{D_n} K_n(z, \bar{z}) d^n z d^n \bar{z} = 1. \tag{2.3b}$$

The *key* result that can be inferred from the Feynman propagator (kernel) $\leftrightarrow$ Bergman kernel K_n correspondence, when $\mu = 1$, is the $(2\pi)^{-D} \leftrightarrow (V(D_n))^{-1}$ correspondence; i. e. the fundamental hyper-cell in momentum space $(2\pi)^D$ (when $\mu = 1$) corresponds to the dimensionless volume $V(D_n)$ of the domain, where $D = 2n$ real dimensions. The regularized vacuum-to-vacuum amplitude of a free *real* scalar field is given in terms of the zeta function $\zeta(s) = \sum_i \lambda_i^{-s}$ associated with the eigenvalues of the Klein-Gordon operator by

$$Z = <0|0> = \sqrt{\det(D_\mu D^\mu - m^2)^{-1}} \sim \exp\left[\frac{1}{2}\frac{d\zeta}{ds}(s=0)\right]. \tag{2.4}$$

In case of a *complex* scalar field we have to *double* the number of degrees of freedom, the amplitude then factorizes into a product and becomes $Z = \det(D_\mu D^\mu - m^2)^{-1}$.

Since the Dirac operator $\mathcal{D} = \gamma^\mu D_\mu + m$ is the "square-root" of the Klein-Gordon operator $\mathcal{D}^\dagger \mathcal{D} = D_\mu D^\mu - m^2 + \mathcal{R}$ ($\mathcal{R}$ is the scalar curvature of spacetime that is zero in Minkowski space) we have the numerical correspondence

$$\sqrt{\det(\mathcal{D})^{-1}} = \sqrt{\det\left(D_\mu D^\mu - m^2\right)^{-1/2}} =$$
$$= \sqrt{\sqrt{\det\left(D_\mu D^\mu - m^2\right)^{-1}}} \leftrightarrow k_n^{1/4} = \left(\frac{1}{V(D_n)}\right)^{1/4}, \tag{2.5}$$

because $\det \mathcal{D}^\dagger = \det \mathcal{D}$, and

$$\det \mathcal{D} = e^{\mathrm{tr}\ln \mathcal{D}} = e^{\mathrm{tr}\ln(D_\mu D^\mu - m^2)^{1/2}} =$$
$$= e^{\frac{1}{2}\mathrm{tr}\ln(D_\mu D^\mu - m^2)} = \sqrt{\det(D_\mu D^\mu - m^2)}\,. \tag{2.6}$$

The vacuum-to-vacuum amplitude of a *complex* Dirac field Ψ (a fermion, the electron) is $Z = \det(\gamma^\mu D_\mu + m) = \det \mathcal{D} \sim \exp[-(d\zeta/ds)(s=0)]$. Notice the $\det(\mathcal{D})$ behavior of the fermion versus the $\det(D_\mu D^\mu - m^2)^{-1}$ behavior of a complex scalar field due to the Grassmanian nature of the Gaussian path integral of the fermions. The vacuum-to-vacuum amplitude of a Majorana (real) spinor (half of the number of degrees of freedom of a complex Dirac spinor) is $Z = \sqrt{\det(\gamma^\mu D_\mu + m)}$. Because the complex Dirac spinor encodes both the dynamics of the electron and its anti-particle, the positron (the negative energy solutions), the vacuum-to-vacuum amplitude corresponding to the electron (positive energy solutions, propagating forward in time) must be then $Z = \sqrt{\det(\gamma^\mu D_\mu + m)}$.

Therefore, to sum up, the origin of the "obscure" factor $V(D_5)^{1/4}$ in Wyler's formula is the *normalization* condition of $V(S^4) \times V(Q_5)$ by a factor of $V(D_5)^{1/4}$ stemming from the correspondence $V(D_5)^{1/4} \leftrightarrow Z = \sqrt{\det(\gamma^\mu D_\mu + m)}$ and which originates from the vacuum-to-vacuum amplitude of the fermion (electron) as it propagates forward in time in the domain D_5. These last relations emerge from the correspondence between the Feynman fermion (electron) propagator in Minkowski spacetime and the Bergman Kernel of the complex homogenous domain after performing the Wyler map between an unbounded domain (the interior of the future lightcone of spacetime) to a bounded one. In general, the Bergman Kernel gives rise to a Kahler potential $F(z, \bar{z}) = \log K(z, \bar{z})$ in terms of which the Bergman metric on D_n is given by

$$g_{i\bar{j}} = \frac{\partial^2 F}{\partial z^i \partial \bar{z}^i}. \tag{2.7}$$

We must emphasize that this Geometric probability explanation *is very different* from the interpretations provided in [2, 5, 6, 7] and properly accounts for all the numerical factors. Concluding, the Geometric Probability that an electron emits a photon at $t = -\infty$ and absorbs it at $t = +\infty$, is given by the *ratio* of the dimensionless measures (volumes):

$$\alpha_{EM} = \frac{2V(S^2)}{\Omega_{Wyler}[Q_4]} = 8\pi \frac{1}{V(S^4)} \frac{1}{V(Q_5)} [V(D_5)]^{\frac{1}{4}} =$$
$$= \frac{9}{8\pi^4}\left(\frac{\pi^5}{2^4 \times 5!}\right)^{1/4} = \frac{1}{137.03608\ldots} \tag{2.8}$$

*I thank Frank (Tony) Smith for this information and many discussions.

in very good agreement with the experimental value. This is easily verified after one inserts the values of the Euclideanized *regularized* volumes found by Hua [10]

$$V(D_5)=\frac{\pi^5}{2^4\times 5!},\ V(Q_5)=\frac{8\pi^3}{3},\ V(S^4)=\frac{8\pi^2}{3}. \quad (2.19)$$

In general

$$V(D_n)=\frac{\pi^n}{2^{n-1}n!},\qquad V(S^{n-1})=\frac{2\pi^{n/2}}{\Gamma(n/2)}, \quad (2.10)$$

$$V(Q_n)=V(S^{n-1}\times RP^1)=V(S^{n-1})\times V(RP^1)= \\ =\frac{2\pi^{n/2}}{\Gamma(n/2)}\times\pi=\frac{2\pi^{(n+2)/2}}{\Gamma(n/2)}. \quad (2.11)$$

Objections were raised to Wyler's original expression by Robertson [4]. One of them was that the hyperboloids (discs) are *not* compact and whose volumes diverge because the Lobachevsky metric diverges on the boundaries of the poly-discs. Gilmore explained [4] why one requires to use the Euclideanized regularized volumes because Wyler had shown that it is possible to map an unbounded physical domain (the interior of the future light cone) onto the interior of a homogenous bounded domain without losing the causal structure and on which there exist also a complex structure. A study of Shilov boundaries, holography and the future tube can be found in [14].

Furthermore, in order to resolve the scaling problems of Wyler's expression raised by Robertson, Gilmore showed why it is essential to use *dimensionless* volumes by setting the throat sizes of the Anti de Sitter hyperboloids to $r=1$, because this is the only choice for r where all elements in the bounded domains are also coset representatives, and therefore, amount to honest group operations. Hence the scaling objections against Wyler raised by Robertson were satisfactory solved by Gilmore [4]. Thus, all the volumes in this section and forth, are based on setting the scaling factor $r=1$.

The question as to *why* the value of α_{EM} obtained in Wyler's formula is precisely the value of α_{EM} observed at the *scale* of the Bohr radius a_B, has not been solved, to our knowledge. The Bohr radius is associated with the ground (most stable) state of the Hydrogen atom [5]. The spectrum generating group of the Hydrogen atom is well known to be the conformal group $SO(4,2)$ due to the fact that there are two conserved vectors, the angular momentum and the Runge-Lentz vector. After quantization, one has two commuting $SU(2)$ copies $SO(4)=SU(2)\times SU(2)$. Thus, it makes physical sense why the Bohr-scale should appear in this construction. Bars [16] has studied the many physical applications and relationships of many seemingly distinct models of particles, strings, branes and twistors, based on the (super) conformal groups in diverse dimensions. In particular, the relevance of two-time physics in the formulation of M, F, S theory has been advanced by Bars for some time. The Bohr radius corresponds to an energy of $137.036\times 2\times 13.6\,\mathrm{eV}\sim 3.72\times 10^3\,\mathrm{eV}$. It is well known that the Rydberg scale, the Bohr radius, the Compton wavelength of electron, and the classical electron radius are all related to each other by a successive scaling in products of α_{EM}.

To finalize this section and based on the MMCW $SO(3,2)$ Gauge Theory formulation of gravity, with a Gauss-Bonnet topological term plus a cosmological constant, the (dimensionless) Wyler measure was *defined* as the geometric coupling strength of gravity [5]:

$$\Omega_{Wyler}[Q_4]=\frac{V(S^4)V(Q_5)}{[V(D_5)]^{\frac{1}{4}}}\equiv\alpha_G\,. \quad (2.12)$$

The relationship between α_G and the Newtonian gravitational G constant is based on the value of the coupling $(1/16\pi G)$ appearing in the Einstein-Hilbert Lagrangian $(R/16\pi G)$, and goes as follows:

$$(16\pi G)(m^2_{Planck})=\alpha_{EM}\alpha_G=8\pi\Rightarrow \\ \Rightarrow G=\frac{1}{16\pi}\frac{8\pi}{m^2_{Planck}}=\frac{1}{2m^2_{Planck}}\Rightarrow \\ \Rightarrow Gm^2_{proton}=\frac{1}{2}\left(\frac{m_{proton}}{m_{Planck}}\right)^2\sim 5.9\times 10^{-39} \quad (2.13)$$

and in natural units $\hbar=c=1$ yields the physical force strength of gravity at the Planck Energy scale 1.22×10^{19} GeV. The Planck mass is obtained by equating the Schwarzschild radius $2Gm_{Planck}$ to the Compton wavelength $1/m_{Planck}$ associated with the mass; where $m_{Planck}\sqrt{2}=1.22\times 10^{19}$ GeV and the proton mass is 0.938 GeV. Some authors define the Planck mass by absorbing the factor of $\sqrt{2}$ inside the definition of $m_{Planck}=1.22\times 10^{19}$ GeV.

3 The weak and strong couplings

We turn now to the derivation of the other coupling constants. The Fiber Bundle picture of the previous section is essential in our construction. The Weak and the Strong geometric coupling constant strength, defined as the probability for a particle to emit and later absorb a $SU(2)$, $SU(3)$ gauge boson, can both be obtained by using the main formula derived from Geometric Probability (as ratios of dimensionless measures/volumes) after one identifies the suitable homogeneous domains and their Shilov boundaries to work with.

Since massless gauge bosons live on the lightcone, a null boundary in Minkowski spacetime, upon performing the Wyler map, the gauge bosons are confined to live on the Shilov boundary. Because the $SU(2)$ bosons $W^{\pm}$, Z^0 and the eight $SU(3)$ gluons have *internal* degrees of freedom (they carry weak and color charges) one must also include the measure associated with the their respective internal spaces; namely, the measures relevant to Geometric Probability calculations are the measures corresponding to the appropriate sphere bundles fibrations defined over the complex bounded homogenous domains $S^m\to E\to\mathcal{D}_n$.

Furthermore, the Geometric Probability interpretation for $\alpha_{weak}, \alpha_{strong}$ agrees with Wheeler's ideas [5] that one must normalize these geometric force strengths with respect to the geometric force strength of gravity $\alpha_G = \Omega_{Wyler}[Q_4]$ found in the last section. Hence, after these explanations, we will show below why the weak and strong couplings are given, respectively, by the *ratio* of the measures (dimensionless volumes):

$$\alpha_{weak} = \frac{\Omega[Q_3]}{\Omega_{Wyler}[Q_4]} = \frac{\Omega[Q_3]}{\alpha_G} = \frac{\Omega[Q_3]}{(8\pi/\alpha_{EM})}, \quad (3.1)$$

$$\alpha_{color} = \frac{\Omega[squashed\, S^5]}{\Omega_{Wyler}[Q_4]} = \frac{\Omega[sq.S^5]}{\alpha_G} = \frac{\Omega[sq.S^5]}{(8\pi/\alpha_{EM})}. \quad (3.2)$$

As always, one must insert the values of the regularized (Euclideanized) dimensionless volumes provided by Hua [10] (set the scale $r = 1$). We must also clarify and emphasize that we define the quantities $\alpha_{weak}, \alpha_{color}$ as the probabilities $\tilde{g}_W^2$, $\tilde{g}_C^2$, by absorbing the factors of 4π in the conventional $\alpha_W = (g_W^2/4\pi)$, $\alpha_C = (g_C^2/4\pi)$ definitions (based on the Renormalization Group (RG) program) into our definitions of probability $\tilde{g}_W^2$, $\tilde{g}_C^2$.

Let us evaluate the α_{weak}. The internal symmetry space is $CP^1 = SU(2)/U(1)$ (a sphere $S^2 \sim CP^1$) where the isospin group $SU(2)$ acts via isometries on CP^1. The Shilov boundary of D_2 is $Q_2 = S^1 \times RP^1$ but is not adequate enough to accommodate the action of the isospin group $SU(2)$. One requires to have the Shilov boundary of D_3 given by $Q_3 = S^2 \times S^1/Z_2 = S^2 \times RP^1$ that can accommodate the action of the $SU(2)$ group on S^2. A Fiber Bundle over $D_3 = SO(3,2)/SO(3) \times SO(2)$ whose $H = SO(3) \sim SU(2)$ subgroup of the isotropy group (at the origin) $K = SO(3) \times SO(2)$ acts on S^2 by simple rotations. Thus, the relevant measure is related to the fiber bundle E restricted to Q_3 and is written as $V(E|_{Q_3})$.

One must notice that due to the fact that the $SU(2)$ group is a double-cover of $SO(3)$, as one goes from the $SO(3)$ action on S^2 to the $SU(2)$ action on S^2 , one must take into account an extra factor of 2 giving then

$$V(CP^1) = V\big(SU(2)/U(1)\big) = \\ = 2V\big(SO(3)/U(1)\big) = 2V(S^2) = 8\pi\,. \quad (3.3)$$

In order to obtain the weak coupling constant due to the exchange of $W^{\pm}Z^0$ bosons in the four-point tree-level processes involving four leptons, like the electron, muon, tau, and their corresponding neutrinos (leptons are fundamental particles that are lighter than mesons and baryons) which are confined to move in the interior of the domain D_3, and can emit (absorb) $SU(2)$ gauge bosons, $W^{\pm}Z^0$, in the respective s, t, u channels, one must take into account a factor of the square root of the determinant of the fermionic propagator, $\sqrt{\det \mathcal{D}^{-1}} = \sqrt{\det\,(\gamma^\mu D_\mu + m)^{-1}}$, for each *pair* of leptons, as we did in the previous section when an electron emitted and absorbed a photon. Since there are *two* pairs of leptons in these four-point tree-level processes involving *four* leptons, one requires *two* factors of $\sqrt{\det\,(\gamma^\mu D_\mu + m)^{-1}}$, giving a net factor of $\det\,(\gamma^\mu D_\mu + m)^{-1}$ and which corresponds now to a net normalization factor of $k_n^{1/2} = (1/V(D_3))^{1/2}$, after implementing the Feynman kernel $\leftrightarrow$ Bergman kenel correspondence. Therefore, after taking into account the result of eq.-(3.3), the measure of the $S^2 \to E \to D_3$ bundle, restricted to the Shilov boundary Q_3, and weighted by the net normalization factor $(1/V(D_3))^{1/2}$, is

$$\Omega(Q^3) = 2V(S^2)\frac{V(Q_3)}{V(D_3)^{1/2}}\,. \quad (3.4)$$

Therefore, the Geometric probability expression is given by the ratio of measures (dimensionless volumes):

$$\alpha_{weak} = \frac{\Omega[Q^3]}{\Omega_{Wyler}[Q_4]} = \frac{\Omega[Q^3]}{\alpha_G} = \frac{2V(S^2)V(Q_3)}{V(D_3)^{1/2}}\frac{\alpha_{EM}}{8\pi} = \\ = (8\pi)(4\pi^2)\left(\frac{\pi^3}{24}\right)^{-\frac{1}{2}}\frac{\alpha_{EM}}{8\pi} = 0.2536\ldots \quad (3.5)$$

that corresponds to the weak coupling constant ($g^2/4\pi$ based on the RG convention) at an energy of the order of

$$E = M = 146\ \text{GeV} \sim \sqrt{M_{W_+}^2 + M_{W_-}^2 + M_Z^2} \quad (3.6)$$

after the expressions inserted (setting the scale $r = 1$)

$$V(S^2) = 4\pi\,,\ \ V(Q_3) = 4\pi^2,\ \ V(D_3) = \frac{\pi^3}{24} \quad (3.7)$$

into the formula (3-5). The relationship to the Fermi coupling goes as follows (with the energy scale $E = M = 146$ GeV):

$$G_F \equiv \frac{\alpha_W}{M^2} \Rightarrow G_F\, m_{proton}^2 = \left(\frac{\alpha_W}{M^2}\right) m_{proton}^2 = \\ = 0.2536 \times \left(\frac{m_{proton}}{146\ \text{GeV}}\right)^2 \sim 1.04 \times 10^{-5} \quad (3.8)$$

in very good agreement with experimental observations. Once more, it is unknown why the value of α_{weak} obtained from Geometric Probability corresponds to the energy scale related to the W_+, W_-, Z_0 boson mass, after spontaneous symmetry breaking.

Finally, we shall derive the value of α_{color} from eq.-(3.2) after one defines what is the suitable fiber bundle. The calculation is based on the book by L. K. Hua [10, p. 40, 93]. The symmetric space with the $SU(3)$ color force as a local group is $SU(4)/SU(3) \times U(1)$ which corresponds to a bounded symmmetric domain of type $I(1,3)$ and has a Shilov boundary that Hua calls the "characteristic manifold" $CI(1,3)$. The volume $V\big(CI(m,n)\big)$ is:

$$V(CI) = \frac{(2\pi)^{mn - m(m-1)/2}}{(n-m)!\,(n-m+1)!\ldots(n-1)!} \quad (3.9)$$

so that for $m = 1$ and $n = 3$ the relevant volume is then $V(CI) = (2\pi)^3/2! = 4\pi^3$. We must remark at this point that $CI(1,3)$ is *not* the standard round S^5 but is the *squashed*

five-dimensional $\tilde{S}^5$.*

The domain of which $CI(1,3)$ is the Shilov boundary is denoted by Hua as $RI(1,3)$ and whose volume is

$$V(RI) = \frac{1!\,2!\ldots(m-1)!\,1!\,2!\ldots(n-1)!\,\pi^{mn}}{1!\,2!\ldots(m+n-1)!} \quad (3.10)$$

so that for $m=1$ and $n=3$ it gives $V(RI)=1!\,2!\,\pi^3/1!\,2!\,3!=$ $=\pi^3/6$ and it also agrees with the volume of the standard six-ball.

The internal symmetry space (fibers) is as follows $CP^2=$ $=SU(3)/U(2)$ whose isometry group is the color $SU(3)$ group. The base space is the $6D$ domain $B_6=SU(4)/U(3)=$ $=SU(4)/SU(3)\times U(1)$ whose subgroup $SU(3)$ of the isotropy group (at the origin) $K=SU(3)\times U(1)$ acts on the internal symmetry space CP^2 via isometries. In this special case, the Shilov and ordinary topological boundary of B_6 both coincide with the *squashed* S^5 [5].

Since Gilmore, in response to Robertson's objections to Wyler's formula [2], has shown that one must set the scale $r=1$ of the hyperboloids $\mathcal{H}^n$ (and S^n) and use *dimensionles* volumes, if we were to equate the volumes $V(CP^2)=$ $=V(S^4, r=1)$ [5], this would be tantamount of choosing another scale [25] R (the unit of geodesic distance in CP^2) that is *different* from the unit of geodesic distance in S^4 when the radius $r=1$, as required by Gilmore. Hence, a bundle map $E\to E'$ from the bundle $CP^2\to E\to B_6$ to the bundle $S^4\to E'\to B_6$, would be required that would allow us to replace the $V(CP^2)$ for $V(S^4, r=1)$. Unless one decides to *calibrate* the unit of geodesic distance in CP^2 by choosing $V(CP^2)=V(S^4)$.

Using again the same results described after eq.-(2.2), since a quark can emit and absorb later on a $SU(3)$ gluon (in a one-loop process), and is confined to move in the interior of the domain B_6, there is *one* factor only of the square root of the determinant of the Dirac propagator $\sqrt{\det \mathcal{D}^{-1}}=$ $=\sqrt{\sqrt{\det\,(D_\mu D^\mu - m^2)^{-1}}}$ and which is associated with a normalization factor of $k_n^{1/4}=(1/V(B_6))^{1/4}$. Therefore, the measure of the bundle $S^4\to E'\to B_6$ restricted to the *squashed* S^5 (Shilov boundary of B^6), and weighted by the normalization factor $(1/V(B_6))^{1/4}$, is then

$$\Omega[\textit{squashed}\,S^5] = \frac{V(S^4)\,V(\textit{squashed}\,S^5)}{V(B_6)^{1/4}} \quad (3.11)$$

and the ratio of measures

$$\alpha_S = \frac{\Omega[sq.S^5]}{\Omega_{Wyler}[Q_4]} = \frac{\Omega[sq.S^5]}{\alpha_G} = \frac{V(S^4)V(sq.S^5)}{V(B_6)^{1/4}}\,\frac{\alpha_{EM}}{8\pi} = \left(\frac{8\pi^2}{3}\right)(4\pi^3)\left(\frac{\pi^3}{6}\right)^{-1/4}\frac{\alpha_{EM}}{8\pi} = 0.6286\ldots \quad (3.12)$$

matches, remarkably, the strong coupling value $\alpha=g^2/4\pi$ at an energy E related precisely to the pion masses [5]

$$E = 241\ \text{MeV} \sim \sqrt{m_{\pi^+}^2 + m_{\pi^-}^2 + m_{\pi^0}^2}. \quad (3.13)$$

The one-loop Renormalization Group flow of the coupling is given by [28]:

$$\alpha_s(E^2)=\alpha_s(E_0^2)\left[1+\frac{\left(11-\frac{2}{3}N_f(E^2)\right)}{4\pi}\alpha_s(E_0^2)\ln\left(\frac{E^2}{E_0^2}\right)\right]^{-1} \quad (3.14)$$

where $N_f(E^2)$ is the number of quark flavors whose mass $M^2<E^2$. For the specific numerical details of the evaluation (in energy-intervals given by the diverse quark masses) of the Renormalization Group flow equation (3-14) that yields $\alpha_s(E=241\ \text{MeV})\sim 0.6286$ we refer to [5]. Once more, it is unknown why the value of α_{color} obtained from Geometric Probability corresponds to the energy scale $E=241$ MeV related to the masses of the pions. The pions are the known lightest quark-antiquark pairs that feel the strong interaction.

Rigorously speaking, one should include higher-loop corrections to eq.-(3.14) as Weinberg showed [28] to determine the values of the strong coupling at energy scales $E=241$ MeV. This issue and the subtleties behind the calibration of scales (volumes) by imposing the condition $V(CP^2)=V(S^4)$ need to be investigated. For example, one could calibrate lengths in terms of the units of geodesic distance in CP^2 (based on Gilmore's choice of $r=1$) giving $V(CP^2)=$ $=V(S^5; r=1)/V(S^1; r=1)=\pi^2/2!$ [25], and it leads now to the value of $\alpha_S=0.1178625$ which is very close to the value of α_S at the energy scale of the Z-boson mass (91.2 GeV) and given by $\alpha_S=0.118$ [28].

4 Mersenne primes p-adic hierarchy. Other approaches

To conclude, we briefly mention other approaches to the determination of the physical parameters. A hierarchy of coupling constants, including the cosmological constant, based on Seifert-spheres fibrations was undertaken by [26]. The ratios of particle masses, like the proton to electron mass ratio $m_p/m_e\sim 6\pi^5$ has also been calculated using the volumes of homogeneous bounded domains [5, 6]. A charge-mass-spin relationship was investigated in [27]. It is not known whether this procedure should work for Grand Unified Theories (GUT) based on the groups like $SU(5)$, $SO(10)$, E_6, E_7, E_8, meaning whether or not one could obtain, for example, the $SU(5)$ coupling constant consistent with the Grand Unification Models based on the $SU(5)$ group and with the Renormalization Group program at the GUT scale.

Beck [8] has obtained all of the Standard Model parameters by studying the numerical minima (and zeros) of certain potentials associated with the Kaneko coupled two-dim lattices (two-dim non-linear sigma-like models which resemble Feynman's chess-board lattice models) based on Stochastic Quantization methods. The results by Smith [5] (also based on Feynman's chess board models and hyper-diamond lattices) are analytical rather than being numerical [8] and it is not clear if there is any relationship between

*Frank (Tony) Smith, private communication.

these latter two approaches. Noyes has proposed an iterated numerical hierarchy based on Mersenne primes $M_p = 2^p - 1$ for *certain* values of $p = primes$ [20], and obtained a quite large number of satisfactory values for the physical parameters. An interesting coincidence is related to the iterated Mersenne prime sequence

$$\begin{aligned} &M_2 = 2^2 - 1 = 3\,, \qquad M_3 = 2^3 - 1 = 7\,,\\ &M_7 = 2^7 - 1 = 127\,, \quad 3 + 7 + 127 = 137\,,\\ &M_{127} = 2^{127} - 1 \sim 1.69{\times}10^{38} \sim \left(\frac{M_{Planck}}{m_{proton}}\right)^2. \end{aligned} \tag{4.1}$$

Pitkanen has also developed methods to calculate physical masses recurring to a p-adic hierarchy of scales based on Mersenne primes [21].

An important connection between anomaly cancellation in string theory and perfect even numbers was found in [23]. These are numbers which can be written in terms of sums of its divisors, including unity, like $6 = 1 + 2 + 3$, and are of the form $P(p) = \frac{1}{2}\,2^p(2^p - 1)$ if, and only if, $2^p - 1$ is a Mersenne prime. Not all values of $p = prime$ yields primes. The number $2^{11} - 1$ is not a Mersenne prime, for example. The number of generators of the anomaly free groups $SO(32)$, $E_8 \times E_8$ of the 10-dim superstring is 496 which is an even perfect number. Another important group related to the unique tadpole-free bosonic string theory is the $SO(2^{13}) = SO(8192)$ group related to the bosonic string compactified on the $E_8 \times SO(16)$ lattice. The number of generators of $SO(8192)$ is an even perfect number since $2^{13} - 1$ is a Mersenne prime. For an introduction to p-adic numbers in Physics and String theory see [22].

A lot more work needs to be done to be able to answer the question: is all this just a mere numerical coincidence or is it design? However, the results of the previous sections indicate that it is very *unlikely* that these results were just a mere numerical coincidence (senseless numerology) and that indeed the values of the physical constants could be actually calculated from pure thought, rather than invoking the anthropic principle; i. e. namely, based on the interplay of harmonic analysis, geometry, topology, higher dimensions and, ultimately, number theory. The fact that the coupling constants involved the ratio of measures (volumes) may cast some light on the role of the world-sheet areas of strings, and world volumes of p-branes, as they propagate in target spacetime backgrounds of diverse dimensions.

References

1. Klein D. A. and Rota G. C. Introduction to geometric probability. New York, Cambridge University Press, 1997.
2. Wyler A. *C. R. Acad. Sci. Paris*, 1969, v. A269, 743; 1971, v. A272, 186.
3. Wyler's unpublished papers: http://www.valdostamuseum.org/hamsmith/WylerIAS.pdf.
4. Gilmore R. *Phys. Rev. Lett.*, 1972, v. 28, 462; Robertson B. *Phys. Rev. Lett.*, 1972, v. 27, 1845.
5. Smith F. D., Jr. *Int. J. Theor. Phys.*, 1985, v. 24, 155; 1985, v. 25, 355; arXiv: hep-ph/9708379; CERN CDS EXT-2003-087.
6. Gonzalez-Martin G. Physical geometry. Univ. of S. Bolivar Publ., Caracas, 2000; arXiv: physics/0009052; 0009051.
7. Smilga W. arXiv: hep-th/0304137.
8. Beck C. Spatio-temporal vacuum fluctuations of quantized fields. World Scientific, Singapore, 2002.
9. Coquereaux R., Jadcyk A. *Rev. Math. Phys.*, 1990, v. 2, 1.
10. Hua L. K. Harmonic analysis of functions of several complex variables in the classical domains. Birkhauser, Boston-Basel-Berlin, 2000.
11. Faraut J., Kaneyuki S., Koranyi A., Qi-keng Lu, Roos G. *Progress in Math.*, v. 185, Birkhauser, Boston-Basel-Berlin.
12. Penrose R., Rindler W. Spinors and space-time. Cambridge Univ. Press, 1986.
13. Hugget S. A., Todd K. P. An introduction to twistor theory. Cambridge Univ. Press, 1985.
14. Gibbons G. arXiv: hep-th/9911027.
15. Maldacena J. arXiv: hep-th/9711200.
16. Bars I. arXiv: hep-th/0502065.
17. Bergman S. The kernel function and conformal mapping. *Math. Surveys*, 1970, v. 5, AMS, Providence.
18. Odzijewicz A. *Int. Jour. of Theor. Phys.*, 1986, v. 107, 561.
19. Castro C. *Mod. Phys. Letts.*, 2002, v. A17, 2095; *Class. Quan. Grav.*, 2003, v. 20, 3577.
20. Noyes P. Bit-strings physics: a discrete and finite approach to natural philosophy. *Knots in Physics*, v. 27, Singapore, World Scientific, 2001.
21. Pitkanen M. *Chaos, Solitons, Fractals*, 2002, v. 13(6), 1205.
22. Vladimorov V., Volovich I., Zelenov I. p-adic numbers in mathematical physics. Singapore, World Scientific, 1994; Brekke L., Freund P. *Physics Reports*, 1993, v. 1, 231.
23. Frampton P., Kephart T. *Phys. Rev. D*, 1999, v. 60, 08790.
24. Nottale L. Fractal spacetime and microphysics, towards the theory of scale relativity. World Scientific, Singapore 1992; *Chaos, Solitons and Fractals*, 2003, v. 16, 539.
25. Boya L., Sudarshan E.C.G., Tilma T. arXiv: math-ph/0210033.
26. Efremov V., Mitskievich N. arXiv: gr-qc/0309133.
27. Castro C. *Foundations of Physics*, 2004, v. 34, 107.
28. Weinberg S. The quantum theory of fields. Vol. 2. Cambridge Univ. Press, 1996; Greiner W. and Schafer A. Quantum Chromodynamics. Springer, Berlin-Heidelberg-New York 1994.

A Brief History of Black Holes

Stephen J. Crothers
Sydney, Australia
E-mail: thenarmis@yahoo.com

Neither the layman nor the specialist, in general, have any knowledge of the historical circumstances underlying the genesis of the idea of the Black Hole. Essentially, almost all and sundry simply take for granted the unsubstantiated allegations of some ostentatious minority of the relativists. Unfortunately, that minority has been rather careless with the truth and is quite averse to having its claims corrected, notwithstanding the documentary evidence on the historical record. Furthermore, not a few of that vainglorious and disingenuous coterie, particularly amongst those of some notoriety, attempt to dismiss the testimony of the literature with contempt, and even deliberate falsehoods, claiming that history is of no importance. The historical record clearly demonstrates that the Black Hole has been conjured up by combination of confusion, superstition and ineptitude, and is sustained by widespread suppression of facts, both physical and theoretical. The following essay provides a brief but accurate account of events, verifiable by reference to the original papers, by which the scandalous manipulation of both scientific and public opinion is revealed.

It has frequently been alleged by theoretical physicists (e. g. [1, 2]) that Newton's theory of gravitation either predicts or adumbrates the black hole. This claim stems from a suggestion originally made by John Michell in 1784 that if a body is sufficiently massive, "all light emitted from such a body would be made to return to it by its own power of gravity". The great French scientist, P. S. de Laplace, made a similar conjecture in the eighteenth century and undertook a mathematical analysis of the matter.

However, contrary to popular and frequent expert opinion, the Michell-Laplace dark body, as it is actually called, is not a black hole at all. The reason why is quite simple.

For a gravitating body we identify an escape velocity. This is a velocity that must be achieved by an object to enable it to leave the surface of the host body and travel out to infinity, where it comes to rest. Therefore, it will not fall back towards the host. It is said to have escaped the host. At velocities lower than the escape velocity, the object will leave the surface of the host, travel out to a finite distance where it momentarily comes to rest, then fall back to the host. Consequently, a suitably located observer will see the travelling object twice, once on its journey outward and once on its return trajectory. If the initial velocity is greater than or equal to the escape velocity, an observer located outside the host, anywhere on the trajectory of the travelling object, will see the object just once, as it passes by on its outward unidirectional journey. It escapes the host. Now, if the escape velocity is the speed of light, this means that light can leave the host and travel out to infinity and come to rest there. It escapes the host. Therefore, all observers located anywhere on the trajectory will see the light once, as it passes by on its outward journey. However, if the escape velocity is greater than the speed of light, then light will travel out to a finite distance, momentarily come to rest, and fall back to the host, in which case a suitably located observer will see the light twice, once as it passes by going out and once upon its return. Furthermore, an observer located at a sufficiently large and finite distance from the host will not see the light, because it does not reach him. To such an observer the host is dark: a Michell-Laplace dark body. But this does not mean that the light cannot leave the surface of the host. It can, as testified by the closer observer. Now, in the case of the black hole, it is claimed by the relativists that no object and no light can even leave the event horizon (the "surface") of the black hole. Therefore, an observer, no matter how close to the event horizon, will see nothing. Contrast this with the escape velocity for the Michell-Laplace dark body where, if the escape velocity is the speed of light, all observers located on the trajectory will see the light as it passes out to infinity where it comes to rest, or when the escape velocity is greater than the speed of light, so that a suitably close observer will see the light twice, once when it goes out and once when it returns. This is completely opposite to the claims for the black hole. Thus, there is no such thing as an escape velocity for a black hole, and so the Michell-Laplace dark body is not a black hole. Those who claim the Michell-Laplace dark body a black hole have not properly understood the meaning of escape velocity and have consequently been misleading as to the nature of the alleged event horizon of a black hole. It should also be noted that nowhere in the argument for the Michell-Laplace dark body is there gravitational collapse to a point-mass, as is required for the black hole.

The next stage in the genesis of the black hole came with Einstein's General Theory of Relativity. Einstein himself

never derived the black hole from his theory and never admitted the theoretical possibility of such an object, always maintaining instead that the proposed physical basis for its existence was incorrect. However, he was never able to demonstrate this mathematically because he did not understand the basic geometry of his gravitational field. Other theoreticians obtained the black hole from Einstein's equations by way of arguments that Einstein always objected to. But Einstein was over-ruled by his less cautious colleagues, who also failed to understand the geometry of Einstein's gravitational field.

The solution to Einstein's field equations, from which the black hole has been extracted, is called the "Schwarzschild" solution, after the German astronomer Karl Schwarzschild, who, it is claimed by the experts, first obtained the solution and first predicted black holes, event horizons, and Schwarzschild radii, amongst other things. These credits are so commonplace that it comes as a surprise to learn that the famous "Schwarzschild" solution is not the one actually obtained by Karl Schwarzschild, even though all the supposed experts and all the textbooks say so. Furthermore, Schwarzschild did not breathe a word about black holes, because his true solution does not allow them.

Shortly after Einstein published the penultimate version of his theory of gravitation in November 1915, Karl Schwarzschild [3] obtained an exact solution for what is called the static vacuum field of the point-mass. At that time Schwarzschild was at the Russian Front, where he was serving in the German army, and suffering from a rare skin disease contracted there. On the 13th January 1916, he communicated his solution to Einstein, who was astonished by it. Einstein arranged for the rapid publication of Schwarzschild's paper. Schwarzschild communicated a second paper to Einstein on the 24th February 1916 in which he obtained an exact solution for a sphere of homogeneous and incompressible fluid. Unfortunately, Schwarzschild succumbed to the skin disease, and died about May 1916, at the age of 42.

Working independently, Johannes Droste [4] obtained an exact solution for the vacuum field of the point-mass. He communicated his solution to the great Dutch scientist H. A. Lorentz, who presented the solution to the Dutch Royal Academy in Amsterdam at a meeting on the 27th May 1916. Droste's paper was not published until 1917. By then Droste had learnt of Schwarzschild's solution and therefore included in his paper a footnote in acknowledgement. Droste anticipated the mathematical procedure that would later lead to the black hole, and correctly pointed out that such a procedure is not permissible, because it would lead to a non-static solution to a static problem. Contra-hype!

Next came the famous "Schwarzschild" solution, actually obtained by the great German mathematician David Hilbert [5], in December 1916, a full year after Schwarzschild obtained his solution. It bears a little resemblance to Schwarzschild's solution. Hilbert's solution has the same form as Droste's solution, but differs in the range of values allowed for the incorrectly assumed radius variable describing how far an object is located from the gravitating mass. It is this incorrect range on the incorrectly assumed radius variable by Hilbert that enabled the black hole to be obtained. The variable on the Hilbert metric, called a radius by the relativists, is in fact not a radius at all, being instead a real-valued parameter by which the true radii in the spacetime manifold of the gravitational field are rightly calculated. None of the relativists have understood this, including Einstein himself. Consequently, the relativists have never solved the problem of the gravitational field. It is amazing that such a simple error could produce such a gigantic mistake in its wake, but that is precisely what the black hole is — a mistake for enormous proportions. Of course, the black hole violates the static nature of the problem, as pointed out by Droste, but the black hole theoreticians have ignored this important detail.

The celebrated German mathematician, Hermann Weyl [6], obtained an exact solution for the static vacuum field of the point-mass in 1917, by a very elegant method. He derived the same solution that Droste had obtained.

Immediately after Hilbert's solution was published there was discussion amongst the physicists as to the possibility of gravitational collapse into the nether world of the nascent black hole. During the Easter of 1922, the matter was considered at length at a meeting at the Collège de France, with Einstein in attendance.

In 1923 Marcel Brillouin [7] obtained an exact solution by a valid transformation of Schwarzschild's original solution. He demonstrated quite rigorously, in relation to his particular solution, that the mathematical process, which later spawned the black hole, actually violates the geometry associated with the equation describing the static gravitational field for the point-mass. He also demonstrated rigorously that the procedure leads to a non-static solution to a static problem, just as Droste had pointed out in 1916, contradicting the very statement of the initial problem to be solved — what is the gravitational field associated with a spherically symmetric gravitating body, where the field is unchanging in time (static) and the spacetime outside the body is free of matter (i. e. vacuum), other than for the presence of a test particle of negligible mass?

In mathematical terms, those solutions obtained by Schwarzschild, Droste and Weyl, and Brillouin, are mutually consistent, in that they can be obtained from one another by an admissible transformation of coordinates. However, Hilbert's solution is inconsistent with their solutions because it cannot be obtained from them or be converted to one of them by an admissible transformation of coordinates. This fact alone is enough to raise considerable suspicions about the validity of Hilbert's solution. Nonetheless, the relativists have not recognised this problem either, and have carelessly adopted Hilbert's solution, which they invariably call "Schwarzschild's" solution, which of course, it is cer-

tainly not.

In the years following, a number of investigators argued, in one way or another, that the "Schwarzschild" solution, as Hilbert's solution became known and Schwarzschild's real solution neglected and forgotten, leads to the bizarre object now called the black hole. A significant subsequent development in the idea came in 1949, when a detailed but erroneous mathematical study of the question by the Irish mathematical physicist J. L. Synge [8], was read before the Royal Irish Academy on the 25th April 1949, and published on the 20th March 1950. The study by Synge was quite exhaustive but being based upon false premises its conclusions are generally false too. Nonetheless, this paper was hailed as a significant breakthrough in the understanding of the structure of the spacetime of the gravitational field.

It was in 1960 that the mathematical description of the black hole finally congealed, in the work of M. D. Kruskal [9] in the USA, and independently of G. Szekeres [10] in Australia. They allegedly found a way of mathematically extending the "Schwarzschild" solution into the region of the nascent black hole. The mathematical expression, which is supposed to permit this, is called the Kruskal-Szekeres extension. This formulation has become the cornerstone of modern relativists and is the fundamental argument upon which they rely for the theoretical justification of the black hole, which was actually christened during the 1960's by the American theoretical physicist, J. A. Wheeler, who coined the term.

Since about 1970 there has been an explosion in the number of people publishing technical research papers, textbooks and popular science books and articles on various aspects of General Relativity. A large proportion of this includes elements of the theory of black holes. Quite a few are dedicated exclusively to the black hole. Not only is there now a simple black hole with a singularity, but also naked singularities, black holes without hair, supermassive black holes at the centres of galaxies, black hole quasars, black hole binary systems, colliding black holes, black hole x-ray sources, charged black holes, rotating black holes, charged and rotating black holes, primordial black holes, mini black holes, evaporating black holes, wormholes, and other variants, and even white holes! Black holes are now "seen" everywhere by the astronomers, even though no one has ever found an event horizon anywhere. Consequently, public opinion has been persuaded that the black hole is a fact of Nature and that anyone who questions the contention must be a crackpot. It has become a rather lucrative business, this black hole. Quite a few have made fame and fortune peddling the shady story.

Yet it must not be forgotten that all the arguments for the black hole are theoretical, based solely upon the erroneous Hilbert solution and the meaningless Kruskal-Szekeres extension on it. One is therefore lead to wonder what it is that astronomers actually "see" when they claim that they have found yet another black hole here or there.

Besides the purely mathematical errors that mitigate the black hole, there are also considerable physical arguments against it, in addition to the fact that no event horizon has ever been detected.

What does a material point mean? What meaning can there possibly be in the notion of a material object without any spatial extension? The term material point (or point-mass) is an oxymoron. Yet the black hole singularity is supposed to have mass and no extension. Moreover, there is not a single shred of experimental evidence to even remotely suggest that Nature makes material points. Even the electron has spatial extent, according to experiment, and to quantum theory. A "point" is an abstraction, not a physical object. In other words, a point is a purely mathematical object. Points and physical objects are mutually exclusive by definition. No one has ever observed a point, and no one ever will because it is unobservable, not being physical. Therefore, Nature does not make material points. Consequently, the theoretical singularity of the black hole cannot be a point-mass.

It takes an infinite amount of observer time for an object, or light, to reach the event horizon, irrespective of how far that observer is located from the horizon. Similarly, light leaving the surface of a body undergoing gravitational collapse, at the instant that it passes its event horizon, takes an infinite amount of observer time to reach an observer, however far that observer is from the event horizon. Therefore, the black hole is undetectable to the observer since he must wait an infinite amount of time to confirm the existence of an event horizon. Such an object has no physical meaning for the observer. Furthermore, according to the very same theoreticians, the Universe started with a Big Bang, and that theory gives an alleged age of 14 billion years for the Universe. This is hardly enough time for the black hole to form from the perspective of an external observer. Consequently, if black holes exist they must have been created at the instant of the Bang. They must be primordial black holes. But that is inconsistent with the Bang itself, because matter at that "time", according to the Big Bang theoreticians, could not form lumps. Even so, they cannot be detected by an external observer owing to the infinite time needed for confirmation of the event horizon. This now raises serious suspicions as to the validity of the Big Bang, which is just another outlandish theory, essentially based upon Friedmann's expanding Universe solution, not an established physical reality as the astronomers would have us believe, despite the now commonplace alleged observations they adduce to support it.

At first sight it appears that the idea of a binary system consisting of two black holes, or a hole and a star, and the claim that black holes can collide, are physical issues. However, this is not quite right, notwithstanding that the theoreticians take them as well-defined physical problems. Here are the reasons why these ideas are faulty. First, the

black hole is allegedly predicted by General Relativity. What the theoreticians routinely fail to state clearly is that the black hole comes from a solution to Einstein's field equations when treating of the problem of the motion of a test particle of negligible mass in the vicinity of a single gravitating body. The gravitational field of the test particle is considered too small to affect the overall field and is therefore neglected. Therefore, Hilbert's solution is a solution for one gravitating body interacting with a test particle. It is not a solution for the interaction of two or more comparable masses. Indeed, there is no known solution to Einstein's field equations for more than one gravitating body. In fact, it is not even known if Einstein's field equations actually admit of solutions for multi-body configurations. Therefore, there can be no meaningful theoretical discussion of black hole binaries or colliding black holes, unless it can be shown that Einstein's field equations contain, hidden within them, solutions for such configurations of matter. Without at least an existence theorem for multi-body configurations, all talk of black hole binaries and black hole collisions is twaddle (see also [11]). The theoreticians have never provided an existence theorem.

It has been recently proved that the black hole and the expanding Universe are not predicted by General Relativity at all [12, 13], in any circumstances. Since the Michell-Laplace dark body is not a black hole either, there is no theoretical basis for it whatsoever.

References

1. Hawking S., Ellis G. F. R. The large-scale structure of space-time. Cambridge University Press, Cambridge, 1973.
2. Misner C. W., Thorne K. S., Wheeler J. A. Gravitation. W. H. Freeman and Company, New York, 1973.
3. Schwarzschild K. On the gravitational field of a mass point according to Einstein's theory. *Sitzungsber. Preuss. Akad. Wiss.*, *Phys. Math Kl.*, 1916, 189; http://www.geocities.com/theometria/schwarzschild.pdf.
4. Droste J. The field of a single centre in Einstein's theory of gravitation, and the motion of a particle in that field. *Ned. Acad. Wet.*, *S. A.*, 1917, v. 19, 197; http://www.geocities.com/theometria/Droste.pdf.
5. Hilbert D. *Nachr. Ges. Wiss. Gottingen*, *Math. Phys. Kl.*, v. 53, 1917; http://www.geocities.com/theometria/hilbert.pdf.
6. Weyl H. *Ann. Phys.* (Leipzig), 1917, v. 54, 117.
7. Brillouin M. The singular points of Einstein's universe. *Journ. Phys. Radium*, 1923, v. 23, 43; http://www.geocities.com/theometria/brillouin.pdf.
8. Synge J. L. The gravitational field of a particle. *Proc. Roy. Irish Acad.*, 1950, v. 53, 83.
9. Kruskal M. D. Maximal extension of Schwarzschild metric. *Phys. Rev.*, 1960, v. 119, 1743.
10. Szekeres G. On the singularities of a Riemannian manifold. *Math. Debreca.*, 1960, v. 7, 285.
11. McVittie G. C. Laplace's alleged "black hole". *The Observatory*, 1978, v. 98, 272; http://www.geocities.com/theometria/McVittie.pdf.
12. Crothers S. J. On the general solution to Einstein's vacuum field and its implications for relativistic degeneracy. *Progress in Physics*, 2005, v. 1, 68–73.
13. Crothers S. J. On the general solution to Einstein's vacuum field for the point-mass when $\lambda \neq 0$ and its implications for relativistic cosmology. *Progress in Physics*, 2005, v. 3, 7–18.

The Neutrosophic Logic View to Schrödinger's Cat Paradox

Florentin Smarandache* and Vic Christianto†

*Department of Mathematics, University of New Mexico, Gallup, NM 87301, USA
E-mail: smarand@unm.edu

†Sciprint.org — a Free Scientific Electronic Preprint Server, http://www.sciprint.org
E-mail: admin@sciprint.org

This article discusses Neutrosophic Logic interpretation of the Schrödinger's cat paradox. We argue that this paradox involves some degree of indeterminacy (unknown) which Neutrosophic Logic could take into consideration, whereas other methods including Fuzzy Logic could not. For a balanced discussion, other interpretations have also been discussed.

1 Schrödinger equation

As already known, Schrödinger equation is the most used equation to describe non-relativistic quantum systems. Its relativistic version was developed by Klein-Gordon and Dirac, but Schrödinger equation has wide applicability in particular because it resembles classical wave dynamics. For introduction to non-relativistic quantum mechanics, see [1].

Schrödinger equation begins with definition of total energy $E = \vec{p}^2/2m$. Then, by using a substitution

$$E = i\hbar \frac{\partial}{\partial t}\,, \qquad P = \frac{\hbar}{i}\nabla, \tag{1}$$

one gets [2]

$$\left[i\hbar \frac{\partial}{\partial t} + \hbar \frac{\bar{\nabla}^2}{2m} - U(x) \right] \psi = 0 \tag{2}$$

or

$$\frac{i\partial}{\partial t}\,\psi = H\psi\,. \tag{3}$$

While this equation seems quite clear to represent quantum dynamics, the physical meaning of the wavefunction itself is not so clear. Soon thereafter Born came up with hypothesis that the square of the wavefunction has the meaning of chance to find the electron in the region defined by dx (Copenhagen School). While so far his idea was quickly adopted as "standard interpretation", his original "guiding field" interpretation has been dropped after criticism by Heisenberg over its physical meaning [3]. Nonetheless, a definition of "Copenhagen interpretation" is that it gives the wavefunction a role in the actions of something else, namely of certain macroscopic objects, called "measurement apparatus", therefore it could be related to phenomenological formalism [3].

Nonetheless, we should also note here that there are other approaches different from Born hypothesis, including:

- The square of the wavefunction represents a measure of the density of matter in region defined by dx (Determinism school [3, 4, 5]). Schrödinger apparently preferred this argument, albeit his attempt to demonstrate this idea has proven to be unfruitful;
- The square of wavefunction of Schrödinger equation as the vorticity distribution (including topological vorticity defects) in the fluid [6];
- The wavefunction in Schrödinger equation represents tendency to make structures;
- The wavemechanics can also be described in terms of topological Aharonov effect, which then it could be related to the notion of topological quantization [7, 8]. Aharonov himself apparently argues in favour of "realistic" meaning of Schrödinger wave equation, whose interpretation perhaps could also be related to Kron's work [9].

So forth we will discuss solution of this paradox.

2 Solution to Schrödinger's cat paradox

2.1 Standard interpretation

It is known that Quantum Mechanics could be regarded more as a "mathematical theory" rather than a physical theory [1, p. 2]. It is wave mechanics allowing a corpuscular duality. Already here one could find problematic difficulties: i. e. while the quantity of wavefunction itself could be computed, the physical meaning of wavefunction itself remains *indefinable* [1]. Furthermore, this notion of wavefunction corresponds to another fundamental indefinable in Euclidean geometry: the point [1, p. 2]. It is always a baffling question for decades, whether the electron could be regarded as wave, a point, or we should introduce a *non-zero* finite entity [4]. Attempts have been made to describe wave equation in such non-zero entity but the question of the physical meaning of wavefunction itself remains mystery.

The standard Copenhagen interpretation advertised by Bohr and colleagues (see DeBroglie, Einstein, Schrödinger who advocated "realistic" interpretation) asserts that it is practically *impossible* to know what really happens in quantum scale. The quantum measurement itself only represents reading in *measurement apparatus*, and therefore it is difficult to separate the object to be measured and the measurement

apparatus itself. Bohr's phenomenological viewpoint perhaps could be regarded as pragmatic approach, starting with the request not to attribute a deep meaning to the wave function but immediately go over to statistical likelihood [10]. Consequently, how the process of "wave collapse" could happen remains mystery.

Heisenberg himself once emphasized this viewpoint when asked directly the question: Is there a fundamental level of reality? He replied as follows:

> "This is just the point: I do not know what the words fundamental reality mean. They are taken from our daily life situation where they have a good meaning, but when we use such terms we are usually extrapolating from our daily lives into an area very remote from it, where we cannot expect the words to have a meaning. This is perhaps one of the fundamental difficulties of philosophy: that our thinking hangs in the language. Anyway, we are forced to use the words so far as we can; we try to extend their use to the utmost, and then we get into situations in which they have no meaning" [11].

A modern version of this interpretation suggests that at the time of measurement, the wave collapses instantaneously into certain localized object corresponding to the action of measurement. In other words, the measurement processes define how the wave should define itself. At this point, the wave ceases to become coherent, and the process is known as "decoherence". Decoherence may be thought of as a way of making real for an observer in the large scale world only one possible history of the universe which has a likelihood that it will occur. Each possible history must in addition obey the laws of logic of this large-scale world. The existence of the phenomenon of decoherence is now supported by laboratory experiments [12]. It is worthnoting here, that there are also other versions of decoherence hypothesis, for instance by Tegmark [13] and Vitiello [14].

In the meantime, the "standard" Copenhagen interpretation emphasizes the role of observer where the "decoherence viewpoint" may not. The problem becomes more adverse because the axioms of standard statistical theory themselves are not fixed forever [15, 16]. And here is perhaps the source of numerous debates concerning the interpretation and philosophical questions implied by Quantum Mechanics. From this viewpoint, Neutrosophic Logic offers a new viewpoint to problems where indeterminacy exists. We will discuss this subsequently. For a sense of balance, we also discuss a number of alternative interpretations. Nonetheless this article will not discuss all existing interpretations of the quantum wavefunction in the literature.

2.2 Schrödinger's cat paradox

To make the viewpoint on this paradox a bit clearer, let us reformulate the paradox in its original form.

According to Uncertainty Principle, any measurement of a system must disturb the system under investigation, with a resulting lack of precision in the measurement. Soon after reading Einstein-Podolsky-Rosen's paper discussing incompleteness of Quantum Mechanics, Schrödinger in 1935 came up with a series of papers in which he used the "cat paradox" to give an illustration of the problem of viewing these particles in a "thought experiment" [15, 17]:

> "One can even set up quite ridiculous cases. A cat is penned up in a steel chamber, along with the following diabolical device (which must be secured against direct interference by the cat): in a Geiger counter there is a bit of radioactive substance, *so* small, that *perhaps* in the course of one hour one of the atoms decays, but also, with equal probability, perhaps none; if it happens, the counter tube discharges and through a relay releases a hammer which shatters a small flask of hydrocyanic acid. If one has left this entire system to itself for an hour, one would say that the cat still lives *if* meanwhile no atom has decayed. The first atomic decay would have poisoned it. The wave-function of the entire system would express this by having in it the living and the dead cat (pardon the expression) mixed or smeared into equal parts."

In principle, Schrödinger's thought experiment asks whether the cat is dead or alive after an hour. The most logical solution would be to wait an hour, open the box, and see if the cat is still alive. However once you open the box to determine the state of the cat you have viewed and hence disturbed the system and introduced a level of uncertainty into the results. The answer, in quantum mechanical terms, is that before you open the box the cat is in a state of being half-dead and half-alive.

Of course, at this point one could ask whether it is possible to find out the state of the cat without having to disturb its wavefunction via action of "observation".

If the meaning of word "observation" here is defined by *to open the box and see the cat*, and then it seems that we could argue whether it is possible to propose another equally possible experiment where we introduce a pair of twin cats, instead of only one. A cat is put in the box while another cat is located in a separate distance, let say 1 meter from the box. If the state of the cat inside the box altered because of poison reaction, it is likely that we could also observe its effect to its twin, perhaps something like "sixth sense" test (perhaps via monitoring frequency of the twin cat's brain).

This plausible experiment could be viewed as an alternative "thought experiment" of well-known Bell-Aspect-type experiment. One could also consider an entangled pair of photons instead of twin cats to conduct this "modified" cat paradox. Of course, for this case then one would get a bit complicated problem because now he/she should consider two probable state: the decaying atom and the photon pair.

We could also say that using this alternative configuration, we know exact information about the Cat outside, while indeterminate information about the Cat inside. However, because both Cats are entangled (twin) we are sure of all the properties of the Cat inside "knows" the state of the Cat outside the box, via a kind of "spooky action at distance" reason (in Einstein's own word)*.

Therefore, for experimental purpose, perhaps it would be useful to simplify the problem by using "modified" Aspect-type experiment [16]. Here it is proposed to consider a decaying atom of Cesium which emits two correlated photons, whose polarization is then measured by Alice (A) on the left and by Bob (B) on the right (see Fig. 1). To include the probable state as in the original cat paradox, we will use a switch instead of Alice A. If a photon comes to this switch, then it will turn on a coffee-maker machine, therefore the observer will get a cup of coffee†. Another switch and coffee-maker set also replace Bob position (see Fig. 2). Then we encapsulate the whole system of decaying atom, switch, and coffee-maker at A, while keeping the system at B side open. Now we can be sure, that by the time the decaying atom of Cesium emits photon to B side and triggers the switch at this side which then turns on the coffee-maker, it is "likely" that we could also observe the same cup of coffee at A side, even if we do not open the box.

We use term "likely" here because now we encounter a "quasi-deterministic" state where there is also small chance that the photon is shifted different from -0.0116, which is indeed what the Aspect, Dalibard and Roger experiment demonstrated in 1982 using a system of two correlated photons [16]. At this "shifted" phase, it could be that the switch will not turn on the coffee-maker at all, so when an observer opens the box at A side he will not get a cup of coffee.

If this hypothetical experiment could be verified in real world, then it would result in some wonderful implications, like prediction of ensembles of multi-particles system, — or a colony of cats.

Another version of this cat paradox is known as GHZ paradox: "The Greenberger-Horne-Zeilinger paradox exhibits some of the most surprising aspects of multiparticle entanglement" [18]. But we limit our discussion here on the original cat paradox.

2.3 Hidden-variable hypothesis

It would be incomplete to discuss quantum paradoxes, in particular Schrödinger's cat paradox, without mentioning hidden-variable hypothesis. There are various versions of this argument, but it could be summarised as an assertion that there is "something else" which should be included in the Quantum Mechanical equations in order to explain thoroughly all quantum phenomena. Sometimes this assertion can be formulated in question form [19]: Can Quantum Mechanics be considered complete? Interestingly, however, the meaning of "complete" itself remains quite abstract (fuzzy).

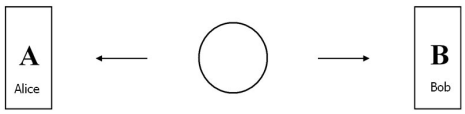

Figure 1: Aspect-type experiment

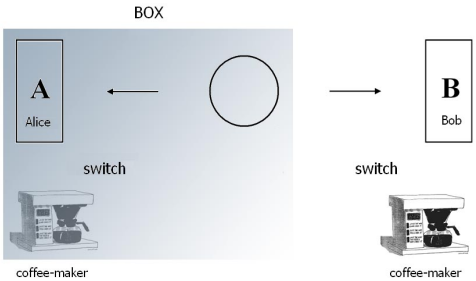

Figure 2: Aspect-type experiment in box

An interpretation of this cat paradox suggests that the problem arises because we mix up the macroscopic systems (observer's wavefunction and apparatus' wavefunction) from microscopic system to be observed. In order to clarify this, it is proposed that "... the measurement apparatus should be described by a classical model in our approach, and the physical system eventually by a quantum model" [20].

2.4 Hydrodynamic viewpoint and diffusion interpretation

In attempt to clarify the meaning of wave collapse and decoherence phenomenon, one could consider the process from (dissipative) hydrodynamic viewpoint [21]. Historically, the hydrodynamic/diffusion viewpoint of Quantum Mechanics has been considered by some physicists since the early years of wave mechanics. Already in 1933, Fuerth showed that Schrödinger equation could be written as a diffusion equation with an imaginary diffusion coefficient [1]

$$D_{qm} = \frac{i\hbar}{2m}\,. \tag{4}$$

But the notion of imaginary diffusion is quite difficult to comprehend. Alternatively, one could consider a classical Markov process of diffusion type to consider wave mechanics equation. Consider a continuity equation

$$\frac{\partial \rho}{\partial t} = -\nabla\,(\rho v)\,, \tag{5}$$

where $v = v_0 = D\nabla \ln \rho$ (see [1]), which is a Fokker-Planck equation. Then the expectation value for the energy of particle can be written as [1]

*The authors are grateful to Dmitri Rabounski for his valuable comments discussing a case of entangled twin Cats.

†The "coffee-maker" analogue came to mind after a quote: "A mathematician is a device for turning coffee into theorems" — Alfréd Rényi, a Hungarian mathematician, 1921–1970. (As quoted by Christopher J. Mark.)

$$<E> = \int \left(\frac{mv^2}{2} + \frac{D^2 m}{2} D \ln \rho^2 + eV \right) \rho d^3 x \,. \quad (6)$$

Alternatively, it could be shown that there is exact mapping between Schrödinger equation and viscous dissipative Navier-Stokes equations [6], where the square of the wavefunction of Schrödinger equation as the vorticity distribution (including topological vorticity defects) in the fluid [6]. This Navier-Stokes interpretation differs appreciably from more standard Euler-Madelung fluid interpretation of Schrödinger equation [1], because in Euler method the fluid is described only in its inviscid limit.

2.5 How neutrosophy could offer solution to Schrödinger's paradox

In this regard, Neutrosophic Logic as recently discussed by one of these authors [22, 23, 24] could offer an interesting application in the context of Schrödinger's cat paradox. It could explain how the "mixed" state could be. It could be shown, that Neutrosophic probability is useful to those events, which involve some degree of indeterminacy (unknown) and more criteria of evaluation — as quantum physics. This kind of probability is necessary because it provides a better representation than classical probability to uncertain events [25]. This new viewpoint for quantum phenomena is required because it is known that Quantum Mechanics is governed by uncertainty, but the meaning of "uncertainty" itself remains uncertain [16].

For example the Schrödinger's Cat Theory says that the quantum state of a photon can basically be in more than one place in the same time which, translated to the neutrosophic set, means that an element (quantum state) belongs and does not belong to a set (a place) in the same time; or an element (quantum state) belongs to two different sets (two different places) in the same time. It is a problem of "alternative worlds theory well represented by the neutrosophic set theory.

In Schrödinger's equation on the behavior of electromagnetic waves and "matter waves" in quantum theory, the wave function ψ, which describes the superposition of possible states, may be simulated by a neutrosophic function, i. e. a function whose values are not unique for each argument from the domain of definition (the vertical line test fails, intersecting the graph in more points).

Now let's return to our cat paradox [25]. Let's consider a Neutrosophic set of a collection of possible locations (positions) of particle x. And let A and B be two neutrosophic sets. One can say, by language abuse, that any particle x neutrosophically belongs to any set, due to the percentages of truth/indeterminacy/falsity involved, which varies between $^-0$ and 1^+. For example: x (0.5, 0.2, 0.3) belongs to A (which means, with a probability of 50% particle x is in a position of A, with a probability of 30% x is not in A, and the rest is undecidable); or y (0, 0, 1) belongs to A (which normally means y is not for sure in A); or z (0, 1, 0) belongs to A (which means one does know absolutely nothing about z's affiliation with A). More general, x {(0.2–0.3), (0.40–0.45) ∪ [0.50–0.51], (0.2, 0.24, 0.28)} belongs to the set A, which mean:

- Owning a likelihood in between 20–30% particle x is in a position of A (one cannot find an exact approximate because of various sources used);
- Owning a probability of 20% or 24% or 28% x is not in A;
- The indeterminacy related to the appurtenance of x to A is in between 40–45% or between 50–51% (limits included);
- The subsets representing the appurtenance, indeterminacy, and falsity may overlap, and $n\_\sup = 30\% + 51\% + 28\% > 100\%$ in this case.

To summarize our proposition [25], given the Schrödinger's cat paradox is defined as a state where the cat can be dead, or can be alive, or it is undecided (i. e. we don't know if it is dead or alive), then herein the Neutrosophic Logic, based on three components, truth component, falsehood component, indeterminacy component (T, I, F), works very well. In Schrödinger's cat problem the Neutrosophic Logic offers the possibility of considering the cat neither dead nor alive, but undecided, while the fuzzy logic does not do this. Normally indeterminacy (I) is split into uncertainty (U) and paradox (conflicting) (P).

We could expect that someday this proposition based on Neusotrophic Logic could be transformed into a useful guide for experimental verification of quantum paradox [15, 10].

Above results will be expanded into details in our book *Multi-Valued Logic, Neutrosophy, and Schrödinger Equation* that is in print.

References

1. Rosu H. C. arXiv: gr-qc/9411035.
2. Englman R., Yahalom H. arXiv: physics/0406149.
3. Durr D., et al. arXiv: quant-ph/0308039.
4. Hofer W. A. arXiv: physics/9611009; quant-ph/9801044.
5. Hooft G. arXiv: quant-ph/0212095.
6. Kiehn R. M. An interpretation of wavefunction as a measure of vorticity. http://www22.pair.com/csdc/pdf/cologne.pdf.
7. Post E. J. The electromagnetic origin of quantization and the ensuing changes of Copenhagen interpretation. *Annales de la Fondation Louis de Broglie*, 2002, no. 2, 217–240;
8. Aharonov Y., et al. arXiv: quant-ph/0311155.
9. Kron G. Electric circuit model of Schrödinger equation. *Phys. Rev.*, 1945, v. 67, 39–43.
10. Lesovik G., Lebedev A., Blatter G. Appearance of Schrödinger Cat states in measurement process. arXiv: quant-ph/0307044.

11. Buckley P., Peat F. D. A question of physics: conversations in physics and biology. Routledge and Kegan Paul, London and Henley, 1979.
12. Zurek W. *Physics Today*, 1999, v. 44, 36; *Los Alamos Science*, 2002, No. 27; arXiv: quant-ph/0306072; *Rev. Mod. Phys.*, 2003, v. 75, 715; *Complexity, Entropy and the Physics of Information*, Santa Fe Institute Studies, Addison-Wesley, 1990; Haroche S. *Physics Today*, 1998, v. 36.
13. Tegmark M. arXiv: quant-ph/9907009.
14. Vitiello G. arXiv: hep-th/9503135.
15. Schrödinger E. Die gegenwartige Situation in der Quantenmechanik. *Naturwissenschaften*, 1935, Bd. 23; English transl. in: *Quantum Mechanics and Measurement*, ed. J. A. Wheeler and W. Zurek, Princeton UP, 1983.
16. Meglicki Z. Two and three photons: Bell's inequality. http://beige.ucs.indiana.edu/M743/node70.html.
17. Edwards P. M. 75 years of Schrödinger wave equation in 2001. http://ublib.buffalo.edu/libraries/units/sel/exhibits/schrodinger/e_schro.html.
18. Exploring quantum physics. http://xqp.physik.uni-muenchen.de/explore/prog.html.
19. Vaidman L. E. arXiv: hep-th/9310176.
20. Aerts D. *Int. J. Theor. Phys.*, 1998, v. 37, 291–304.
21. Na K., Wyatt R. E. Decoherence demystified: the hydrodynamic viewpoint. arXiv: quant-ph/0201108.
22. Smarandache F. Neutrosophy / neutrosophic probability, set, and logic. American Research Press, Rehoboth, 1998; A unifying field in logics: neutrosophic logic. Neutrosophy, neutrosophic set, neutrosophic probability. 3rd ed., American Research Press, 2003.
23. Smarandache F. A unifying field in logics: neutrosophic logic. *Multiple Valued Logic / An International Journal*, 2002, v. 8(3), 385–438.
24. Smarandache F. Definitions derived from neutrosophics. *Multiple Valued Logic / An International Journal*, 2002, v. 8 (5–6), 591–604.
25. Smarandache F. An introduction to the neutrosophic probability applied in quantum physics. *Bull. Pure and Appl. Sciences*, Ser. D (Physics), 2003, v. 22D, No. 1, 13–25.

Schrödinger Equation and the Quantization of Celestial Systems

Florentin Smarandache* and Vic Christianto†

*Department of Mathematics, University of New Mexico, Gallup, NM 87301, USA
E-mail: smarand@unm.edu

†Sciprint.org — a Free Scientific Electronic Preprint Server, http://www.sciprint.org
E-mail: admin@sciprint.org

In the present article, we argue that it is possible to generalize Schrödinger equation to describe quantization of celestial systems. While this hypothesis has been described by some authors, including Nottale, here we argue that such a macroquantization was formed by topological superfluid vortice. We also provide derivation of Schrödinger equation from Gross-Pitaevskii-Ginzburg equation, which supports this superfluid dynamics interpretation.

1 Introduction

In the present article, we argue that it is possible to generalize Schrödinger equation to describe quantization of celestial systems, based on logarithmic nature of Schrödinger equation, and also its exact mapping to Navier-Stokes equations [1].

While this notion of macro-quantization is not widely accepted yet, as we will see the logarithmic nature of Schrödinger equation could be viewed as a support of its applicability to larger systems. After all, the use of Schrödinger equation has proved itself to help in finding new objects known as extrasolar planets [2, 3]. And we could be sure that new extrasolar planets are to be found in the near future. As an alternative, we will also discuss an outline for how to derive Schrödinger equation from simplification of Ginzburg-Landau equation. It is known that Ginzburg-Landau equation exhibits fractal character, which implies that quantization could happen at *any scale*, supporting topological interpretation of quantized vortices [4].

First, let us rewrite Schrödinger equation in its common form [5]

$$\left[i \frac{\partial}{\partial t} + \frac{\bar{\nabla}^2}{2m} - U(x) \right] \psi = 0 \qquad (1)$$

or

$$i \frac{\partial \psi}{\partial t} = H \psi \,. \qquad (2)$$

Now, it is worth noting here that Englman and Yahalom [5] argues that this equation exhibits logarithmic character

$$\ln \psi(x,t) = \ln \left(|\psi(x,t)| \right) + i \arg\big(\psi(x,t)\big) \,. \qquad (3)$$

Schrödinger already knew this expression in 1926, which then he used it to propose his equation called "eigentliche Wellengleichung" [5]. Therefore equation (1) can be rewritten as follows

$$2m \frac{\partial \big(\ln|\psi|\big)}{\partial t} + 2\bar{\nabla} \ln|\psi| \, \bar{\nabla} \arg\big[\psi\big] + \bar{\nabla}\bar{\nabla} \arg\big[\psi\big] = 0 \,. \qquad (4)$$

Interestingly, Nottale's scale-relativistic method [2, 3] was also based on generalization of Schrödinger equation to describe quantization of celestial systems. It is known that Nottale-Schumacher's method [6] could predict new exoplanets in good agreement with observed data. Nottale's scale-relativistic method is essentially based on the use of first-order scale-differentiation method defined as follows [2]

$$\frac{\partial V}{\partial (\ln \delta t)} = \beta(V) = a + b\,V + \dots \,. \qquad (5)$$

Now it seems clear that the natural-logarithmic derivation, which is essential in Nottale's scale-relativity approach, also has been described properly in Schrödinger's original equation [5]. In other words, its logarithmic form ensures applicability of Schrödinger equation to describe macro-quantization of celestial systems. [7, 8]

2 Quantization of celestial systems and topological quantized vortices

In order to emphasize this assertion of the possibility to describe quantization of celestial systems, let us quote Fischer's description [4] of relativistic momentum from superfluid dynamics. Fischer [4] argues that the circulation is in the relativistic dense superfluid, defined as the integral of the momentum

$$\gamma_s = \oint p_\mu \, dx^\mu = 2\pi N_v \hbar \,, \qquad (6)$$

and is quantized into multiples of Planck's quantum of action. This equation is the covariant Bohr-Sommerfeld quantization of γ_s. And then Fischer [4] concludes that the Maxwell equations of ordinary electromagnetism can be written in the form of conservation equations of relativistic perfect fluid hydrodynamics [9]. Furthermore, the topological character of equation (6) corresponds to the notion of topological electronic liquid, where compressible electronic liquid represents superfluidity [25]. For the plausible linkage between superfluid dynamics and cosmological phenomena, see [16–24].

It is worth noting here, because vortices could be defined as elementary objects in the form of stable topological excitations [4], then equation (6) could be interpreted as Bohr-Sommerfeld-type quantization from *topological quantized vortices*. Fischer [4] also remarks that equation (6) is quite interesting for the study of superfluid rotation in the context of gravitation. Interestingly, application of Bohr-Sommerfeld quantization for celestial systems is known in literature [7, 8], which here in the context of Fischer's arguments it has special meaning, i. e. it suggests that *quantization of celestial systems actually corresponds to superfluid-quantized vortices at large-scale* [4]. In our opinion, this result supports known experiments suggesting neat correspondence between condensed matter physics and various cosmology phenomena [16–24].

To make the conclusion that quantization of celestial systems actually corresponds to superfluid-quantized vortices at large-scale a bit conceivable, let us consider the problem of quantization of celestial orbits in solar system.

In order to obtain planetary orbit prediction from this hypothesis we could begin with the Bohr-Sommerfeld's conjecture of quantization of angular momentum. This conjecture may originate from the fact that according to BCS theory, superconductivity can exhibit macroquantum phenomena [26, 27]. In principle, this hypothesis starts with observation that in quantum fluid systems like superfluidity [28]; it is known that such vortexes are subject to quantization condition of integer multiples of 2π, or $\oint v_s\, dl = 2\pi n\hbar/m$. As we know, for the wavefunction to be well defined and unique, the momenta must satisfy Bohr-Sommerfeld's quantization condition [28]

$$\oint_{\Gamma} p\, dx = 2\pi n\hbar \tag{6a}$$

for any closed classical orbit Γ. For the free particle of unit mass on the unit sphere the left-hand side is [28]

$$\int_0^T v^2 d\tau = \omega^2 T = 2\pi\omega\,, \tag{7}$$

where $T = 2\pi/\omega$ is the period of the orbit. Hence the quantization rule amounts to quantization of the rotation frequency (the angular momentum): $\omega = n\hbar$. Then we can write the force balance relation of Newton's equation of motion [28]

$$\frac{GMm}{r^2} = \frac{mv^2}{r}\,. \tag{8}$$

Using Bohr-Sommerfeld's hypothesis of quantization of angular momentum, a new constant g was introduced [28]

$$mvr = \frac{ng}{2\pi}\,. \tag{9}$$

Just like in the elementary Bohr theory (before Schrödinger), this pair of equations yields a known simple solution for the orbit radius for any quantum number of the form [28]

$$r = \frac{n^2 g^2}{4\pi^2 GMm^2}\,, \tag{10}$$

which can be rewritten in the known form of gravitational Bohr-type radius [2, 7, 8]

$$r = \frac{n^2 GM}{v_0^2}\,, \tag{11}$$

where r, n, G, M, v_0 represents orbit radii, quantum number ($n = 1, 2, 3, \dots$), Newton gravitation constant, and mass of the nucleus of orbit, and specific velocity, respectively. In this equation (11), we denote [28]

$$v_0 = \frac{2\pi}{g}\, GMm\,. \tag{12}$$

The value of m is an adjustable parameter (similar to g) [7, 8]. In accordance with Nottale, we assert that the specific velocity v_0 is 144 km/sec for planetary systems. By noting that m is meant to be mass of celestial body in question, then we could find g parameter (see also [28] and references cited therein).

Using this equation (11), we could predict quantization of celestial orbits in the solar system, where for Jovian planets we use least-square method and use M in terms of reduced mass $\mu = \frac{(M_1 + M_2)}{M_1 M_2}$. From this viewpoint the result is shown in Table 1 below [28].

For comparison purpose, we also include some recent observation by Brown-Trujillo team from Caltech [29–32]. It is known that Brown et al. have reported not less than four new planetoids in the outer side of Pluto orbit, including 2003EL61 (at 52 AU), 2005FY9 (at 52 AU), 2003VB12 (at 76 AU, dubbed as Sedna). And recently Brown-Trujillo team reported a new planetoid finding, called 2003UB31 (97 AU). This is not to include their previous finding, Quaoar (42 AU), which has orbit distance more or less near Pluto (39.5 AU), therefore this object is excluded from our discussion. It is interesting to remark here that all of those new "planetoids" are within 8% bound from our prediction of celestial quantization based on the above Bohr-Sommerfeld quantization hypothesis (Table 1). While this prediction is not so precise compared to the observed data, one could argue that the 8% bound limit also corresponds to the remaining planets, including inner planets. Therefore this 8% uncertainty could be attributed to macroquantum uncertainty and other local factors.

While our previous prediction only limits new planet finding until $n = 9$ of Jovian planets (outer solar system), it seems that there are sufficient reasons to suppose that more planetoids in the Oort Cloud will be found in the near future. Therefore it is recommended to extend further the same quantization method to larger n values. For prediction purpose, we include in Table 1 new expected orbits based

Object	No.	Titius	Nottale	CSV	Observ.	Δ, %
	1		0.4	0.43		
	2		1.7	1.71		
Mercury	3	4	3.9	3.85	3.87	0.52
Venus	4	7	6.8	6.84	7.32	6.50
Earth	5	10	10.7	10.70	10.00	−6.95
Mars	6	16	15.4	15.4	15.24	−1.05
Hungarias	7		21.0	20.96	20.99	0.14
Asteroid	8		27.4	27.38	27.0	1.40
Camilla	9		34.7	34.6	31.5	−10.00
Jupiter	2	52		45.52	52.03	12.51
Saturn	3	100		102.4	95.39	−7.38
Uranus	4	196		182.1	191.9	5.11
Neptune	5			284.5	301	5.48
Pluto	6	388		409.7	395	−3.72
2003EL61	7			557.7	520	−7.24
Sedna	8	722		728.4	760	4.16
2003UB31	9			921.8	970	4.96
Unobserv.	10			1138.1		
Unobserv.	11			1377.1		

Table 1: Comparison of prediction and observed orbit distance of planets in Solar system (in 0.1AU unit) [28].

on the same quantization procedure we outlined before. For Jovian planets corresponding to quantum number $n = 10$ and $n = 11$, our method suggests that it is likely to find new orbits around 113.81 AU and 137.71 AU, respectively. It is recommended therefore, to find new planetoids around these predicted orbits.

As an interesting alternative method supporting this proposition of quantization from superfluid-quantized vortices (6), it is worth noting here that Kiehn has argued in favor of re-interpreting the square of the wavefunction of Schrödinger equation as the vorticity distribution (including topological vorticity defects) in the fluid [1]. From this viewpoint, Kiehn suggests that there is *exact mapping* from Schrödinger equation to Navier-Stokes equation, using the notion of quantum vorticity [1]. Interestingly, de Andrade and Sivaram [33] also suggest that there exists formal analogy between Schrödinger equation and the Navier-Stokes viscous dissipation equation:

$$\frac{\partial V}{\partial t} = \nu \nabla^2 V \,, \qquad (13)$$

where ν is the kinematic viscosity. Their argument was based on propagation torsion model for quantized vortices [23]. While Kiehn's argument was intended for ordinary fluid, nonetheless the neat linkage between Navier-Stokes equation and superfluid turbulence is known in literature [34, 24].

At this point, it seems worth noting that some criticism arises concerning the use of quantization method for describing the motion of celestial systems. These criticism proponents usually argue that quantization method (wave mechanics) is oversimplifying the problem, and therefore cannot explain other phenomena, for instance planetary migration etc. While we recognize that there are phenomena which do not correspond to quantum mechanical process, at least we can argue further as follows:

1. Using quantization method like Nottale-Schumacher did, one can expect to predict new exoplanets (extrasolar planets) with remarkable result [2, 3];
2. The "conventional" theories explaining planetary migration normally use fluid theory involving *diffusion* process;
3. Alternatively, it has been shown by Gibson et al. [35] that these migration phenomena could be described via Navier-Stokes approach;
4. As we have shown above, Kiehn's argument was based on *exact-mapping* between Schrödinger equation and Navier-Stokes equations [1];
5. Based on Kiehn's vorticity interpretation one these authors published prediction of some new planets in 2004 [28]; which seems to be in good agreement with Brown-Trujillo's finding (March 2004, July 2005) of planetoids in the Kuiper belt;
6. To conclude: while our method as described herein may be interpreted as an oversimplification of the real planetary migration process which took place sometime in the past, at least it could provide us with useful tool for prediction;
7. Now we also provide new prediction of other planetoids which are likely to be observed in the near future (around 113.8 AU and 137.7 AU). It is recommended to use this prediction as guide to finding new objects (in the inner Oort Cloud);
8. There are of course other theories which have been developed to explain planetoids and exoplanets [36]. Therefore quantization method could be seen as merely a "plausible" theory between others.

All in all, what we would like to emphasize here is that the quantization method does not have to be the *true* description of reality with regards to celestial phenomena. As always this method could explain some phenomena, while perhaps lacks explanation for other phenomena. But at least it can be used to predict something quantitatively, i. e. measurable (exoplanets, and new planetoids in the outer solar system etc.).

In the meantime, it seems also interesting here to consider a plausible generalization of Schrödinger equation in particular in the context of viscous dissipation method [1]. First, we could write Schrödinger equation for a charged particle

interacting with an external electromagnetic field [1] in the form of Ulrych's unified wave equation [14]

$$\left[(-i\hbar\nabla - qA)_\mu(-i\hbar\nabla - qA)^\mu\psi\right] = \\ = \left[-i2m\frac{\partial}{\partial t} + 2mU(x)\right]\psi\,. \quad (14)$$

In the presence of electromagnetic potential, one could include another term into the LHS of equation (14)

$$\left[(-i\hbar\nabla - qA)_\mu(-i\hbar\nabla - qA)^\mu + eA_0\right]\psi = \\ = 2m\left[-i\frac{\partial}{\partial t} + U(x)\right]\psi\,. \quad (15)$$

This equation has the physical meaning of Schrödinger equation for a charged particle interacting with an external electromagnetic field, which takes into consideration Aharonov effect [37]. Topological phase shift becomes its immediate implication, as already considered by Kiehn [1].

As described above, one could also derived equation (11) from scale-relativistic Schrödinger equation [2, 3]. It should be noted here, however, that Nottale's method [2, 3] differs appreciably from the viscous dissipative Navier-Stokes approach of Kiehn [1], because Nottale only considers his equation in the Euler-Newton limit [3]. Nonetheless, it shall be noted here that in his recent papers (2004 and up), Nottale has managed to show that his scale relativistic approach has linkage with Navier-Stokes equations.

3 Schrödinger equation derived from Ginzburg-Landau equation

Alternatively, in the context of the aforementioned superfluid dynamics interpretation [4], one could also derive Schrödinger equation from simplification of Ginzburg-Landau equation. This method will be discussed subsequently. It is known that Ginzburg-Landau equation can be used to explain various aspects of superfluid dynamics [16, 17]. For alternative approach to describe superfluid dynamics from Schrödinger-type equation, see [38, 39].

According to Gross, Pitaevskii, Ginzburg, wavefunction of N bosons of a reduced mass m^* can be described as [40]

$$-\left(\frac{\hbar^2}{2m^*}\right)\nabla^2\psi + \kappa\left|\psi\right|^2\psi = i\hbar\frac{\partial\psi}{\partial t}\,. \quad (16)$$

For some conditions, it is possible to replace the potential energy term in equation (16) with Hulthen potential. This substitution yields

$$-\left(\frac{\hbar^2}{2m^*}\right)\nabla^2\psi + V_{\text{Hulthen}}\psi = i\hbar\frac{\partial\psi}{\partial t}\,, \quad (17)$$

where

$$V_{\text{Hulthen}} = -Ze^2\frac{\delta\, e^{-\delta r}}{1 - e^{-\delta r}}\,. \quad (18)$$

This equation (18) has a pair of exact solutions. It could be shown that for small values of δ, the Hulthen potential (18) approximates the effective Coulomb potential, in particular for large radius

$$V^{\text{eff}}_{\text{Coulomb}} = -\frac{e^2}{r} + \frac{\ell(\ell+1)\,\hbar^2}{2mr^2}\,. \quad (19)$$

By inserting (19), equation (17) could be rewritten as

$$-\left(\frac{\hbar^2}{2m^*}\right)\nabla^2\psi + \left[-\frac{e^2}{r} + \frac{\ell(\ell+1)\hbar^2}{2mr^2}\right]\psi = i\hbar\frac{\partial\psi}{\partial t}\,. \quad (20)$$

For large radii, second term in the square bracket of LHS of equation (20) reduces to zero [41],

$$\frac{\ell(\ell+1)\,\hbar^2}{2mr^2} \to 0\,, \quad (21)$$

so we can write equation (20) as

$$\left[-\left(\frac{\hbar^2}{2m^*}\right)\nabla^2 + U(x)\right]\psi = i\hbar\frac{\partial\psi}{\partial t}\,, \quad (22)$$

where Coulomb potential can be written as

$$U(x) = -\frac{e^2}{r}\,. \quad (22a)$$

This equation (22) is nothing but Schrödinger equation (1), except for the mass term now we get mass of Cooper pairs. In other words, we conclude that it is possible to re-derive Schrödinger equation from simplification of (Gross-Pitaevskii) Ginzburg-Landau equation for superfluid dynamics [40], in the limit of small screening parameter, δ. Calculation shows that introducing this Hulthen effect (18) into equation (17) will yield essentially similar result to (1), in particular for small screening parameter. Therefore, we conclude that for most celestial quantization problems the result of TDGL-Hulthen (20) is *essentially* the same with the result derived from equation (1). Now, to derive gravitational Bohr-type radius equation (11) from Schrödinger equation, one could use Nottale's scale-relativistic method [2, 3].

4 Concluding remarks

What we would emphasize here is that this derivation of Schrödinger equation from (Gross-Pitaevskii) Ginzburg-Landau equation is in good agreement with our previous conjecture that equation (6) implies macroquantization corresponding to superfluid-quantized vortices. This conclusion is the main result of this paper. Furthermore, because Ginzburg-Landau equation represents superfluid dynamics at low-temperature [40], the fact that we can derive quantization of celestial systems from this equation seems to support the idea of Bose-Einstein condensate cosmology [42, 43]. Nonetheless, this hypothesis of Bose-Einstein condensate cosmology deserves discussion in another paper.

Above results are part of our book *Multi-Valued Logic, Neutrosophy, and Schrödinger Equation* that is in print.

Acknowledgments

The authors would like to thank to Profs. C. Castro, A. Rubcic, R. M. Kiehn, M. Pitkänen, E. Scholz, A. Kaivarainen and E. Bakhoum for valuable discussions.

References

1. Kiehn R. M. An interpretation of wavefunction as a measure of vorticity. http://www22.pair.com/csdc/pdf/cologne.pdf.
2. Nottale L., et al., *Astron. Astrophys.*, 1997, v. 322, 1018.
3. Nottale L. *Astron. Astrophys.*, 1997, v. 327, 867-889.
4. Fischer U. W. arXiv: cond-mat/9907457 (1999).
5. Englman R. and Yahalom H. arXiv: physics/0406149 (2004).
6. Nottale L., Schumacher G., Levefre E. T. *Astron. Astrophys.*, 2000, v. 361, 379–387.
7. Rubcic A. and Rubcic J. The quantization of solar-like gravitational systems. *Fizika B*, 1998, v. 7(1), 1–13.
8. Agnese A. G. and Festa R. Discretization of the cosmic scale inspired from the Old Quantum Mechanics. *Proc. Workshop on Modern Modified Theories of Grav. and Cosmology*, 1997; arXiv: astro-ph/9807186.
9. Fischer U. W. arXiv: cond-mat/9907457.
10. Aharonov Y., et al. arXiv: quant-ph/0311155.
11. Hofer W. A. arXiv: physics/9611009; quant-ph/9801044.
12. Hooft G. arXiv: quant-ph/0212095.
13. Blasone M., et al. arXiv: quant-ph/0301031.
14. Rosu H. C. arXiv: gr-qr-qc/9411035.
15. Oudet X. The quantum state and the doublets. *Annales de la Fondation Louis de Broglie*, 2000, v. 25(1).
16. Zurek W. Cosmological experiments in superfluids and superconductors. *Proc. Euroconference Formation and Interaction of Topological Defects*, ed. A. Davis and R. Brandenberger, Plenum, 1995; arXiv: cond-mat/9502119.
17. Volovik G. Superfluid analogies of cosmological phenomena. arXiv: gr-qc/0005091.
18. Volovik G. Links between gravity and dynamics of quantum liquids. *Int. Conf. Cosmology. Relativ. Astrophysics. Cosmoparticle Physics* (COSMION-99); arXiv: gr-qc/0004049.
19. Volovik G. arXiv: gr-qc/0104046.
20. Nozieres P. and Pines D. The theory of quantum liquids: Superfluid Bose Liquid. Addison-Wesley, 1990, 116–124.
21. Winterberg F. *Z. Naturforsch.*, 2002, v. 57a, 202–204; presented at *9th Canadian Conf. on General Relativity and Relativ. Astrophysics*, Edmonton, May 24–26, 2001.
22. Winterberg F. Maxwell's aether, the Planck aether hypothesis, and Sommerfeld's fine structure constant. http://www.znaturforsch.com/56a/56a0681.pdf.
23. Kaivarainen A. arXiv: physics/020702.
24. Kaivarainen A. Hierarchic models of turbulence, superfluidity and superconductivity. arXiv: physics/0003108.
25. Wiegmann P. arXiv: cond-mat/9808004.
26. Schrieffer J. R. Macroscopic quantum phenomena from pairing in superconductors. Lecture, December 11th, 1972.
27. Coles P. arXiv: astro-ph/0209576.
28. Christianto V. *Apeiron*, 2004, v. 11(3).
29. NASA News Release (Jul 2005), http://www.nasa.gov/vision/universe/solarsystem/newplanet-072905.html.
30. *BBC News* (Oct 2004), http://news.bbc.co.uk/1/hi/sci/tech/4730061.stm.
31. Brown M., et al. *ApJ. Letters*, Aug. 2004; arXiv: astro-ph/0404456; *ApJ.*, forthcoming issue (2005); astro-ph/0504280.
32. Brown M. (July 2005), http://www.gps.caltech.edu/∼mbrown/planetlila/.
33. de Andrade L. G. and Sivaram C. arXiv: hep-th/9811067.
34. Godfrey S. P., et al. A new interpretation of oscillating flow experiments in superfluid Helium II, *J. Low Temp. Physics*, Nos. 112, Oct 2001.
35. Gibson C. and Schild R. arXiv: astro-ph/0306467.
36. Griv E. and Gedalin M. The formation of the Solar System by Gravitational Instability. arXiv: astro-ph/0403376.
37. Anandan J. S. *Quantum Coherence and Reality, Proc. Conf. Fundamental Aspects of Quantum Theory*, Columbia SC., ed. by J. S. Anandan and J. L. Safko, World Scientific, 1994; arXiv: gr-qc/9504002.
38. Varma C. M. arXiv: cond-mat/0109049.
39. Lipavsky P., et al. arXiv: cond-mat/0111214.
40. Infeld E., et al. arXiv: cond-mat/0104073.
41. Pitkänen M. http://www.physics.helsinki.fi/∼matpitka/articles/nottale.pdf.
42. Trucks M. arXiv: gr-qc/9811043.
43. Castro C., et al. arXiv: hep-th/0004152.

Non-Euclidean Geometry and Gravitation

Nikias Stavroulakis
Solomou 35, 15233 Chalandri, Greece
E-mail: nikias.stavroulakis@yahoo.fr

A great deal of misunderstandings and mathematical errors are involved in the currently accepted theory of the gravitational field generated by an isotropic spherical mass. The purpose of the present paper is to provide a short account of the rigorous mathematical theory and exhibit a new formulation of the problem. The solution of the corresponding equations of gravitation points out several new and unusual features of the stationary gravitational field which are related to the non-Euclidean structure of the space. Moreover it precludes the black hole from being a mathematical and physical notion.

1 Introduction

If the structure of the spacetime is actually non-Euclidean as is postulated by general relativity, then several non-Euclidean features will manifest themselves in the neighbourhoods of the sources of the gravitational field. So, a spherical distribution of matter will appear as a non-Euclidean ball and the concentric with it spheres will possess the structure of non-Euclidean spheres. Specifically, if this distribution of matter is isotropic, such a sphere will be characterised completely by its radius, say ρ, and its curvature radius which is a function of ρ, say $g(\rho)$, defining the area $4\pi(g(\rho))^2$ of the sphere as well as the length of circumference $2\pi g(\rho)$ of the corresponding great circles. It is then expected that the function $g(\rho)$ will play a significant part in the conception of the metric tensor related to the gravitational field of the spherical mass. Of course, in formulating the problem, we must distinguish clearly the radius ρ, which is introduced as a given length, from the curvature radius $g(\rho)$, the determination of which depends on the equations of gravitation. However the classical approach to the problem suppresses this distinction and assumes that the radius af the sphere is the unknown function $g(\rho)$. This glaring mistake underlies the pseudo-theorem of Birkhoff as well as the classical solutions, which have distorted the theory of the gravitational field.

Another glaring mistake of the classical approach to the problem is related to the topological space which underlies the definition of the metric tensor. The spatial aspect of the problem suggests to identify the centre of the spherical mass with the origin of the vector space $\mathbb{R}^3$ which is moreover considered with the product topology of three real lines. Regarding the time t , several assumptions suggest to consider it (or rather ct) as a variable describing the real line $\mathbb{R}$. It follows that the topological space pertaining to the considered situation is the space $\mathbb{R}\times\mathbb{R}^3$ equipped with the product topology of four real lines. This simple and clear algebraic and topological situation has been altered from the beginnings of general relativity by the introduction of the so-called polar coordinates of $\mathbb{R}^3$ which destroy the topological structure of $\mathbb{R}^3$ and replace it by the manifold with boundary $[0,+\infty[\times S^2$. The use of polar coordinates is allowed in the theory of integration, because the open set $]0,+\infty[\times]0,2\pi[\times]0,\pi[$, described by the point (r,ϕ,θ), is transformed diffeomorphically onto the open set

$$\mathbb{R}^3-\left\{(x_1,x_2,x_3)\in\mathbb{R}^3;\ \ x_1\geqslant 0,\ \ x_2=0\right\}$$

and moreover the half-plane

$$\left\{(x_1,x_2,x_3)\in\mathbb{R}^3;\ \ x_1\geqslant 0,\ \ x_2=0\right\}$$

is of zero measure in $\mathbb{R}^3$. But in general relativity this half-plane cannot be omitted. Then by choosing two systems of geographic coordinates covering all of S^2, we define a C^∞ mapping of $[0,+\infty[\times S^2$ onto $\mathbb{R}^3$ transgressing the fundamental principle according to which only diffeomorphisms are allowed. In fact, this mapping is not even one-to-one: All of $\{0\}\times S^2$ is transformed into the origin of $\mathbb{R}^3$. This situation gives rise to inconsistent assertions. So, although the origin of $\mathbb{R}^3$ disappears in polar coordinates, the meaningless term "the origin $r=0$" is commonly used. Of course, the value $r=0$ does not define a point but the boundary $\{0\}\times S^2$ which is an abstract two-dimensional sphere without physical meaning. In accordance with the idea that the value $r=0$ defines the origin, the relativists introduce transformations of the form $r=h(\overline{r})$, $\overline{r}\geqslant 0$, in order to "change the origin". This extravagant idea goes back to Droste, who claims that by setting $r=\overline{r}+2\mu$, $\mu=\frac{km}{c^2}$, we define a "new radial coordinate $\overline{r}$" such that the sphere $r=2\mu$ reduces to the "new origin $\overline{r}=0$". Rosen [2] claims also that the transformation $r=\overline{r}+2\mu$ allows to consider a mass point placed at the origin $\overline{r}=0$! The same extravagant ideas are introduced in the definition of the so-called harmonic coordinates by Lanczos (1922) who begins by the introduction of the transformation $r=\overline{r}+\mu$ in order to define the "new radial coordinate $\overline{r}$".

The introduction of the manifold with boundary $[0,+\infty[\times S^2$ instead of $\mathbb{R}^3$, hence also the introduction of $\mathbb{R}\times[0,+\infty[\times S^2$ instead of $\mathbb{R}\times\mathbb{R}^3$, gives also rise to misunderstandings and mistakes regarding the space metrics and the spacetime metrics as well.

Given a C^∞ Riemannian metric on $\mathbb{R}^3$, its transform in polar coordinates is a C^∞ quadratic form on $[0,+\infty[\times S^2$,

positive definite on $]0,+\infty[\times S^2$ and null on $\{0\}\times S^2$. (This is, in particular, true for the so-called metric of $\mathbb{R}^3$ in polar coordinates, namely $ds^2=dr^2+r^2d\omega^2$ with $d\omega^2=$ $=\sin^2\theta d\phi^2+d\theta^2$ in the domain of validity of (ϕ,θ).) But the converse is not true. A C^∞ form on $[0,+\infty[\times S^2$ satisfying the above conditions is associated in general with a form on $\mathbb{R}^3$ presenting discontinuities at the origin of $\mathbb{R}^3$. So the C^∞ form $2dr^2+r^2d\omega^2$, conceived on $[0,+\infty[\times S^2$, results from a uniquely defined form on $\mathbb{R}^3$, namely

$$dx^2+\frac{(xdx)^2}{\|x\|^2},$$

(here $dx^2=dx_1^2+dx_2^2+dx_3^2$, $xdx=x_1dx_1+x_2dx_2+x_3dx_3$) which is discontinuous at $x=(0,0,0)$.

Now, given a C^∞ spacetime metric on $\mathbb{R}\times\mathbb{R}^3$, its transform in polar coordinates is a C^∞ form degenerating on the boundary $\mathbb{R}\times\{0\}\times S^2$. But the converse is not true. A C^∞ spacetime form on $\mathbb{R}\times[0,+\infty[\times S^2$ degenerating on the boundary $\mathbb{R}\times\{0\}\times S^2$ results in general from a spacetime form on $\mathbb{R}\times\mathbb{R}^3$ presenting discontinuities. For instance, the so-called Bondi metric

$$ds^2=e^{2A}dt^2+2e^{A+B}dtdr-r^2d\omega^2$$

where $A=A(t,r)$, $B=B(t,r)$, conceals singularities, because it results from a uniquely defined form on $\mathbb{R}\times\mathbb{R}^3$, namely

$$ds^2=e^{2A}dt^2+2e^{A+B}\frac{(xdx)}{\|x\|}dt-dx^2+\frac{(xdx)^2}{\|x\|}$$

which is discontinuous at $x=(0,0,0)$. It follows that the current practice of formulating problems with respect to $\mathbb{R}\times[0,+\infty[\times S^2$, instead of $\mathbb{R}\times\mathbb{R}^3$, gives rise to misleading conclusions. The problems must be always conceived with respect to $\mathbb{R}\times\mathbb{R}^3$.

2 SΘ(4)-invariant and Θ(4)-invariant tensor fields on $\mathbb{R}\times\mathbb{R}^3$.

The metric tensor is conceived naturally as a tensor field invariant by the action of the rotation group $SO(3)$. However, although $SO(3)$ acts naturally on $\mathbb{R}^3$, it does not the same on $\mathbb{R}\times\mathbb{R}^3$, and this is why we are led to introduce the group SΘ(4) consisting of the matrices

$$\begin{pmatrix}1 & O_H\\ O_V & A\end{pmatrix}$$

with $O_H=(0,0,0)$, $O_V=\begin{pmatrix}0\\0\\0\end{pmatrix}$ and $A\in SO(3)$. We introduce also the group Θ(4) consisting of the matrices of the same form for which $A\in O(3)$. Obviously SΘ(4) is a subgroup of Θ(4).

With these notations, the metric tensor related to the isotropic distribution of matter is conceived as a SΘ(4)-invariant tensor field on $\mathbb{R}\times\mathbb{R}^3$. SΘ(4)-invariant tensor fields appear in several problems of relativity, so that it is convenient to study them in detail. Their rigorous theory appears in a previous paper [7] together with the theory of the *pure SΘ(4)-invariant tensor fields* which are not used in the present paper.

It is easily seen that a function $h(x_0,x_1,x_2,x_3)$ is SΘ(4)-invariant (or Θ(4)-invariant) if and only if it is of the form $f(x_0,\|x\|)$. Of course we confine ourselves to the case where $f(x_0,\|x\|)$ is C^∞ with respect to the coordinates x_0, x_1, x_2, x_3 on $\mathbb{R}\times\mathbb{R}^3$.

Proposition 2.1 *$f(x_0,\|x\|)$ is C^∞ on $\mathbb{R}\times\mathbb{R}^3$ if and only if the function $f(x_0,u)$ with $(x_0,u)\in\mathbb{R}\times[0,+\infty[$ is C^∞ on $\mathbb{R}\times[0,+\infty[$ and such that its derivatives of odd order with respect to u at $u=0$ vanish.*

The functions satisfying these conditions constitute an algebra which will be denoted by Γ_0. As a corollary, we see that $f(x_0,\|x\|)$ belongs to Γ_0 if and only if the function $h(x_0,u)$ defined by setting

$$h(x_0,u)=h(x_0,-u)=f(x_0,u),\quad u\geqslant 0$$

is C^∞ on $\mathbb{R}\times\mathbb{R}$. It follows in particular that, if the function $f(x_0,\|x\|)$ belongs to Γ_0 and is strictly positive, then the functions $\frac{1}{f(x_0,\|x\|)}$ and $\sqrt{f(x_0,\|x\|)}$ belong also to Γ_0. Now, if $T(x_0,x)$, $x=(x_1,x_2,x_3)$, is an SΘ(4)-invariant (or Θ(4)-invariant) tensor field on $\mathbb{R}\times\mathbb{R}^3$, then, for every function $f\in\Gamma_0$, the tensor field $f(x_0,\|x\|)\,T(x_0,x)$ is also SΘ(4)-invariant (or Θ(4)-invariant). Consequently the set of SΘ(4)-invariant (or Θ(4)-invariant) tensor fields constitutes a Γ_0-module. In particular, we are interesting in the sub-module consisting of the covariant tensor fields of degree 2. The proof of the following proposition is given in the paper [7].

Proposition 2.2 *Let $T(x_0,x)$ be an SΘ(4)-invariant C^∞ covariant symmetric tensor field of degree 2 on $\mathbb{R}\times\mathbb{R}^3$. Then there exist four functions $q_{00}\in\Gamma_0$, $q_{01}\in\Gamma_0$, $q_{11}\in\Gamma_0$, $q_{22}\in\Gamma_0$ such that*

$$\begin{aligned}T(x_0,x)&=q_{00}(x_0,\|x\|)(dx_0\otimes dx_0)+\\&+q_{01}(x_0,\|x\|)\big(dx_0\otimes F(x)+F(x)\otimes dx_0\big)+\\&+q_{11}(x_0,\|x\|)E(x)+q_{22}(x_0,\|x\|)\big(F(x)\otimes F(x)\big),\end{aligned}$$

where $E(x)=\sum_1^3(dx_i\otimes dx_i)$ and $F(x)=\sum_1^3x_idx_i$. Moreover $T(x_0,x)$ is Θ(4)-invariant.

So, the components $g_{\alpha\beta}$ of $T(x_0,x)$ are defined by means of the four functions q_{00}, q_{01}, q_{11}, q_{22} as follows

$$\begin{aligned}&g_{00}=q_{00},&&g_{0i}=g_{i0}=x_iq_{01},\\&g_{ii}=q_{11}+x_i^2q_{22},&&g_{ij}=x_ix_jq_{22},\end{aligned}$$

where $i,j=1,2,3$; $i\neq j$. Suppose now that the tensor field $T(x_0,x)$ is a metric tensor, namely a symmetric tensor field of signature $(+1,-1,-1,-1)$. Then we write it usually as a quadratic form

$$ds^2=q_{00}dx_0^2+2q_{01}(xdx)dx_0+q_{11}dx^2+q_{22}(xdx)^2.$$

Since $x_0 = t$ is the time coordinate, we have $q_{00} = q_{00}(x_0, \|x\|) > 0$ for all $(x_0, x) \in \mathbb{R}\times\mathbb{R}^3$, so the function $f = f(x_0, \|x\|) = \sqrt{q_{00}(x_0, \|x\|)}$ is strictly positive and C^∞ on $\mathbb{R}\times\mathbb{R}^3$. Consequently the function $f_1 = \frac{q_{01}}{f}$ is also C^∞ on $\mathbb{R}\times\mathbb{R}^3$, namely a function belonging to Γ_0, and we can write the metric into the form

$$ds^2 = \big(f dt + f_1 (x dx)\big)^2 + q_{11} dx^2 + \big(q_{22} - f_1^2\big)(x dx)^2$$

which makes explicit the corresponding spatial (positive definite) metric $-q_{11}dx^2 - \big(q_{22} - f_1^2\big)(x dx)^2$ with $-q_{11} > 0$ and $-q_{11} - \big(q_{22} - f_1^2\big)\|x\|^2 > 0$ on $\mathbb{R}\times\mathbb{R}^3$. So we can introduce the strictly positive C^∞ functions

$$\ell_1 = \ell_1(t, \|x\|) = \sqrt{-q_{11}(t, \|x\|)}$$

and

$$\ell = \ell(t, \|x\|) = \sqrt{\ell_1^2 - \|x\|^2\big(q_{22} - f_1^2\big)}$$

which possess a clear geometrical meaning:

> ℓ_1 serves to define the curvature radius $g(t,\rho) = g(t, \|x\|) = \|x\|\,\ell_1(t, \|x\|) = \rho\,\ell_1(t,\rho)$, $(\rho = \|x\|)$, of the non-Euclidean spheres centered at the origin of $\mathbb{R}^3$, whereas ℓ defines the element of length on the spatial radial geodesics.

Consequently it is very convenient to put the metric into a form exhibiting explicitly ℓ_1 and ℓ. This is obtained by remarking that the C^∞ function $q_{22} - f_1^2$ can be written as

$$\frac{\ell_1^2 - \ell^2}{\rho^2}\,.$$

Of course the last expression is C^∞ everywhere on account of the condition $\ell_1(t,0) = \ell(t,0)$ and the fact that $\ell_1 \in \Gamma_0$, $\ell \in \Gamma_0$. It follows that

$$ds^2 = \big(f dt + f_1 (x dx)\big)^2 - \ell_1^2 dx^2 - \frac{\ell^2 - \ell_1^2}{\rho^2}(x dx)^2 \quad (2.1)$$

or

$$ds^2 = f^2 dt^2 + 2 f f_1 (x dx)\, dt - \ell_1^2 dx^2 + \left(\frac{\ell_1^2 - \ell^2}{\rho^2} + f_1^2\right)(x dx)^2 \quad (2.2)$$

with the components

$$g_{00} = f^2, \qquad g_{0i} = g_{i0} = x_i f f_1\,,$$

$$g_{ii} = -\ell_1^2 + x_i^2\left(\frac{\ell_1^2 - \ell^2}{\rho^2} + f_1^2\right),$$

$$g_{ij} = x_i x_j\left(\frac{\ell_1^2 - \ell^2}{\rho^2} + f_1^2\right), \qquad i,j = 1,2,3;\ \ i \neq j\,.$$

There are two significant functions which do not appear in (2. 1) and are not C^∞ on $\mathbb{R}\times\mathbb{R}^3$:

1. First the already considered curvature radius $g(t,\rho) = \rho\,\ell_1(t,\rho)$ of the non-Euclidean spheres centered at the origin;
2. Secondly the function $h(t,\rho) = \rho f_1(t,\rho)$ which appears in the equations defining the radial motions of photons outside the matter, namely the equations

   $$(f dt + f_1 \rho\, d\rho)^2 = \ell^2 d\rho^2 \quad \text{or} \quad f dt + \rho f_1 d\rho = \pm \ell\, d\rho$$

   which imply necessarily $|h| \leqslant \ell$ in order that both the ingoing and outgoing motions be possible [4]. In any case the condition $|h| \leqslant \ell$ must also be valid inside the matter in order that the nature of the variable t as time coordinate be preserved. Moreover h vanishes for $\rho = 0$.

Of course g and h are C^∞ with respect to $(t,\rho) \in \mathbb{R}\times[0, +\infty[$, but since $\rho = \|x\|$ is not differentiable at the origin, they are not differentiable on the subspace $\mathbb{R}\times\{(0,0,0)\}$ of $\mathbb{R}\times\mathbb{R}^3$. However, on account of their geometrical and physical significance, we introduce them in the computations remembering that, for any global solution on $\mathbb{R}\times\mathbb{R}^3$, the functions $\ell_1 = \frac{g}{\rho}$ and $f_1 = \frac{h}{\rho}$ appearing in (2.1) must be elements of the algebra Γ_0.

3 The Ricci tensor and the equations of gravitation

In order to obtain the equations of gravitation related to (2.1), we have first to introduce the Christoffel symbols and then compute the components of the Ricci tensor. At first sight the computations seem to be extremely complicated, but the $\Theta(4)$-invariance of the metric allows to obtain a great deal of simplification in accordance with the following proposition, the proof of which is given in the paper [8].

Proposition 3.1 **(a)** *The Christoffel symbols of the first kind as well as those of the second kind related to (2.2) are the components of a $\Theta(4)$-invariant tensor field*; **(b)** *The curvature tensor, the Ricci tensor, and the scalar curvature related to (2.2) are $\Theta(4)$-invariant*; **(c)** *If an energy-momentum tensor satisfies the equations of gravitation related to (2.2), it is $\Theta(4)$-invariant.*

Corollary 3.1. *The Christoffel symbols of the second kind related to (2.2) depend on ten C^∞ functions $B_\alpha = B_\alpha(t,\rho)$, $(\alpha = 0,1,2,\ldots,9)$, as follows*:

$$\Gamma^0_{00} = B_0\,, \qquad \Gamma^0_{0i} = \Gamma^0_{i0} = B_1 x_i\,, \qquad \Gamma^i_{00} = B_2 x_i\,,$$
$$\Gamma^0_{ii} = B_3 + B_4 x_i^2, \qquad \Gamma^0_{ij} = \Gamma^0_{ji} = B_4 x_i x_j\,,$$
$$\Gamma^i_{i0} = \Gamma^i_{0i} = B_5 + B_6 x_i^2, \qquad \Gamma^i_{j0} = \Gamma^i_{0j} = B_6 x_i x_j\,,$$
$$\Gamma^i_{ii} = B_7 x_i^3 + (B_8 + 2B_9) x_i\,,$$
$$\Gamma^i_{jj} = B_7 x_i x_i^2 + B_8 x_i\,, \quad \Gamma^j_{ij} = \Gamma^j_{ji} = B_7 x_i x_j^2 + B_9 x_i\,,$$
$$\Gamma^i_{jk} = B_7 x_i x_j x_k\,, \qquad i,j,k = 1,2,3;\ \ j \neq k \neq i\,.$$

Regarding the Ricci tensor $R_{\alpha\beta}$, since it is symmetric and $\Theta(4)$-invariant, its components are defined, according to proposition 2.2, by four functions $Q_{00} = Q_{00}(t,\rho)$, $Q_{01} = Q_{01}(t,\rho)$, $Q_{11} = Q_{11}(t,\rho)$, $Q_{22} = Q_{22}(t,\rho)$ as follows:

$$R_{00} = Q_{00}\,, \quad R_{0i} = R_{i0} = Q_{01} x_i\,, \quad R_{ii} = Q_{11} + x_i^2 Q_{22}\,,$$
$$R_{ij} = x_i x_j Q_{22}\,, \qquad i,j = 1,2,3;\ \ i \neq j\,.$$

In the same way, an energy-momentum tensor $W_{\alpha\beta}$ satisfying the equations of gravitation related to (2.2) is defined by four functions of (t,ρ), say E_{00}, E_{01}, E_{11}, E_{22}:

$$W_{00}=E_{00}\,,\quad W_{0i}=x_iE_{01}\,,\quad W_{ii}=E_{11}+x_i^2E_{22}\,,$$
$$W_{ij}=x_ix_jE_{22}\,,\qquad i,j=1,2,3;\ \ i\neq j\,.$$

Moreover, since the scalar curvature $R=Q$ is $\Theta(4)$-invariant, it is a function of (t,ρ): $R=Q=Q(t,\rho)$.

It follows that the equations of gravitation (with cosmological constant -3λ)

$$R_{\alpha\beta}-\left(\frac{Q}{2}+3\lambda\right)g_{\alpha\beta}+\frac{8\pi k}{c^4}W_{\alpha\beta}=0$$

can be written from the outset as a system of four equations depending uniquely on (t,ρ):

$$Q_{00}-\left(\frac{Q}{2}+3\lambda\right)f^2+\frac{8\pi k}{c^4}E_{00}=0\,,$$
$$Q_{01}-\left(\frac{Q}{2}+3\lambda\right)ff_1+\frac{8\pi k}{c^4}E_{01}=0\,,$$
$$Q_{11}+\left(\frac{Q}{2}+3\lambda\right)\ell_1^2+\frac{8\pi k}{c^4}E_{11}=0\,,$$
$$Q_{22}-\left(\frac{Q}{2}+3\lambda\right)\left(\frac{\ell_1^2-\ell^2}{\rho^2}+f_1^2\right)+\frac{8\pi k}{c^4}E_{22}=0\,.$$

Note that it is often convenient to replace the last equation by the equation

$$Q_{11}+\rho^2Q_{22}-\left(\frac{Q}{2}+3\lambda\right)\left(\rho^2f_1^2-\ell^2\right)+\frac{8\pi k}{c^4}\left(E_{11}+\rho^2E_{22}\right)=0.$$

In order to apply these equations to special situations, it is necessary to give the explicit expressions of Q_{00}, Q_{01}, Q_{11}, Q_{22} by means of the functions B_α, $(\alpha=0,1,2,...,9)$, appearing in the Christoffel symbols. We recall the results of computation

$$Q_{00}=\frac{\partial}{\partial t}\left(3B_5+\rho^2B_6\right)-\rho\frac{\partial B_2}{\partial\rho}-$$
$$-B_2\left(3+4\rho^2B_9-\rho^2B_1+\rho^2B_8+\rho^2B_7\right)-$$
$$-3B_0B_5+3B_5^2+\rho^2B_6\left(-B_0+2B_5+\rho^2B_6\right),$$

$$Q_{01}=\frac{\partial}{\partial t}\left(\rho^2B_7+B_8+4B_9\right)-\frac{1}{\rho}\frac{\partial B_5}{\partial\rho}-\rho\frac{\partial B_6}{\partial\rho}+$$
$$+B_2\left(B_3+\rho^2B_4\right)-2B_6\left(2+\rho^2B_9\right)-B_1\left(3B_5+\rho^2B_6\right),$$

$$Q_{11}=-\frac{\partial B_3}{\partial t}-\rho\frac{\partial B_8}{\partial\rho}-\left(B_0+B_5+\rho^2B_6\right)B_3+$$
$$+\left(1-\rho^2B_8\right)\left(B_1+\rho^2B_7+B_8+2B_9\right)-3B_8\,,$$

$$Q_{22}=-\frac{\partial B_4}{\partial t}+\frac{1}{\rho}\frac{\partial}{\partial\rho}\left(B_1+B_8+2B_9\right)+B_1^2+B_8^2-$$
$$-2B_9^2-2B_1B_9+2B_3B_6+\left(-B_0-B_5+\rho^2B_6\right)B_4+$$
$$+\left(-3+\rho^2\left(-B_1+B_8-2B_9\right)\right)B_7.$$

4 Stationary vacuum solutions

The radial motion of the isotropic spherical distribution of matter generates a non-stationary (dynamical) gravitational field extending beyond the boundary in the exterior space. This field is defined by non-stationary $\Theta(4)$-invariant vacuum solutions of the equations of gravitation and exhibits essential and unusual features related to the propagation of gravitation. Several problems related to it are not yet clarified. But, in any case, in order to establish and understand the dynamical solutions, a previous knowledge of the stationary solutions is necessary. This is why, in the sequel we confine ourselves to the simple problems related to the stationary vacuum solutions. So we suppose that we have a stationary metric

$$ds^2=\left(fdt+f_1\left(xdx\right)\right)^2-\ell_1^2dx^2-\frac{\ell^2-\ell_1^2}{\rho^2}\left(xdx\right)^2,\ (4.1)$$

where $f=f(\rho)$, $f_1=f_1(\rho)$, $\ell_1=\ell_1(\rho)$, $\ell=\ell(\rho)$.

Of course, we have also to take into account the significant functions

$$h=h(\rho)=\rho f_1(\rho)\,,\qquad g=g(\rho)=\rho\ell_1(\rho)\,,$$

which are not differentiable at the origin $(0,0,0)$. Every half-line issuing from the origin, $x_1=\alpha_1\rho$, $x_2=\alpha_2\rho$, $x_3=\alpha_3\rho$ (where $0\leqslant\rho<+\infty$ and $\alpha_1^2+\alpha_2^2+\alpha_3^2=1$) is a geodesic of the spatial metric $\ell_1^2dx^2+\frac{\ell^2-\ell_1^2}{\rho^2}\left(xdx\right)^2$ so that the geodesic distance δ of the origin from the point $x=(x_1,x_2,x_3)$ is defined by the integral

$$\delta=\int_0^\rho\ell(u)du,\qquad\rho=\|x\|.$$

As already noticed, the function $\ell(\rho)$, where $0\leqslant\rho<+\infty$, is strictly positive, but it cannot be arbitrarily given. Suppose, for instance, that

$$\ell(\rho)=\frac{\epsilon}{\rho^2},\qquad\epsilon=\text{const}>0$$

on $[1,+\infty[$. Then the geodesic distance $\delta=\int_0^1\ell(u)du+$ $+\int_1^\rho\frac{\epsilon}{u^2}du=\int_0^1\ell(u)du+\epsilon-\frac{\epsilon}{\rho}$ tends to the finite value $\int_0^1\ell(u)du+\epsilon$ as $\rho\to\infty$, which cannot be physically accepted. Consequently the positive function $\ell(\rho)$ is allowable only if the integral $\int_0^\rho\ell(u)du$ tends to $+\infty$ as $\rho\to+\infty$.

This being said, it is easy to see that the functions $B_\alpha=B_\alpha(\rho)$, $(\alpha=0,1,\ldots,9)$, occurring in the Christoffel symbols resulting from the stationary metric (4.1) are defined by the following formulae:

$$B_0=-\frac{hf'}{\ell^2}\,,\quad B_1=\frac{f'}{\rho f}-\frac{h^2f'}{\rho f\ell^2}\,,$$
$$B_2=\frac{ff'}{\rho\,\ell^2}\,,\qquad B_3=\frac{hgg'}{\rho^2f\ell^2}\,,$$
$$B_4=\frac{hf'}{\rho^2f^2}-\frac{h^3f'}{\rho^2f^2\ell^2}+\frac{h'}{\rho^2f}-\frac{h\ell'}{\rho^2f\ell}-\frac{hgg'}{\rho^4f\ell^2}\,,$$

$$B_5 = 0\,, \qquad B_6 = \frac{hf'}{\rho^2\ell^2}\,,$$
$$B_7 = \frac{h^2 f'}{\rho^3 f\ell^2} + \frac{\ell'}{\rho^3\ell} + \frac{gg'}{\rho^5\ell^2} - \frac{2g'}{\rho^3 g} + \frac{1}{\rho^4}\,,$$
$$B_8 = \frac{1}{\rho^2} - \frac{gg'}{\rho^3\ell^2}\,, \qquad B_9 = -\frac{1}{\rho^2} + \frac{g'}{\rho g}\,.$$

Then inserting these expressions in the formulae brought out at the end of the previous section, we find the functions

$$Q_{00} = f\left(-\frac{f''}{\ell^2} + \frac{f'\ell'}{\ell^3} - \frac{2f'g'}{\ell^2 g}\right), \qquad g = \rho\ell_1\,,$$
$$Q_{01} = \frac{h}{\rho f}\,Q_{00}\,, \qquad h = \rho f_1\,,$$
$$Q_{11} = \frac{1}{\rho^2}\left(-1 + \frac{g'^2}{\ell^2} + \frac{gg''}{\ell^2} - \frac{\ell' gg'}{\ell^3} + \frac{f'gg'}{f\ell^2}\right),$$
$$Q_{11} + \rho^2 Q_{22} = \frac{f''}{f} + \frac{2g''}{g} - \frac{f'\ell'}{f\ell} - \frac{2\ell' g'}{\ell g} + \frac{h^2}{f^2}\,Q_{00}\,,$$

which are everywhere valid, namely outside as well as inside the matter, Specifically, by using them, we can establish the gravitational equations outside the matter with electromagnetic field and cosmological constant. However, in the present short account, our purpose is to put forward the most significant elementary facts, and this is why we confine ourselves to the pure gravitational field outside the matter without cosmological constant. Then $Q = R = 0$, $\lambda = 0$, so that $Q_{00} = 0$, $Q_{01} = 0$, $Q_{11} = 0$, $Q_{11} + \rho^2 Q_{22} = 0$. Since $Q_{00} = 0$ implies $Q_{01} = 0$, we have finally the following three equations

$$-f'' + \frac{f'\ell'}{\ell} - \frac{2f'g'}{g} = 0\,, \tag{4.2}$$
$$-1 + \frac{g'^2}{\ell^2} + \frac{gg''}{\ell^2} - \frac{\ell' gg'}{\ell^3} + \frac{f'gg'}{f\ell^2} = 0\,, \tag{4.3}$$
$$f'' + \frac{2fg''}{g} - \frac{f'\ell'}{\ell} - \frac{2f\ell' g'}{\ell g} = 0\,, \tag{4.4}$$

By adding (4.2) to (4.4) we obtain

$$\frac{f'g'}{f} = g'' - \frac{\ell' g'}{\ell} \tag{4.5}$$

and inserting this expression of $\frac{f'g'}{f}$ into (4.3), we find the equation

$$-1 + \frac{g'^2}{\ell^2} + \frac{2gg''}{\ell^2} - \frac{2\ell' gg'}{\ell^3} = 0$$

which implies $\frac{d}{d\rho}\left(-g + \frac{gg'^2}{\ell^2}\right) = 0$ so that

$$-g + \frac{gg'^2}{\ell^2} = -2A = \text{const}. \tag{4.6}$$

On the other hand (4.5) can be written as $(f\ell)'g' = (f\ell)\,g''$ whence $\frac{d}{d\rho}\left(\frac{g'}{f\ell}\right) = 0$ and

$$f\ell = cg', \qquad (\text{where } c = \text{const})\,. \tag{4.7}$$

The equations (4.6) and (4.7) define the general stationary solution outside the matter. The function h does not appear in them, but it is not empty of physical meaning as is usually believed. It occurs in the problem as a function satisfying the condition $|h| \leqslant \ell$. The different allowable choices of h correspond to different significations of the time coordinate.

Proposition 4.1. *If $A = 0$, the solution defined by (4.6) and (4.7) is a pseudo-Euclidean metric (or, better, a family of pseudo-Euclidean metrics).*

Proof. On account of $A = 0$, (4.6) implies $g' = \ell$ and next (4.7) gives $f = c$. Referring to (4.1) and setting $\int_0^\rho v f(v)dv = \alpha(\rho)$, we have

$$d\alpha(\rho) = \rho f_1(\rho)d\rho = f_1(\rho)x dx$$

and

$$f(\rho)dt + f_1(\rho)x dx = d\big(ct + \alpha(\rho)\big)\,,$$

which suggests the transformation $\tau = t + \frac{\alpha(\rho)}{c}$. On the other hand, since $\ell = g' = (\rho\ell_1)' = \rho\ell_1' + \ell_1$, we have

$$\ell_1^2 dx^2 + \frac{\ell^2 - \ell_1^2}{\rho^2}\,(x dx)^2 = \ell_1^2 dx^2 + 2\ell_1\ell_1'\frac{(x dx)^2}{\|x\|} + \ell_1'^2\,(x dx)^2 =$$
$$= \left(\ell_1 dx_1 + x_1\ell_1'\frac{x dx}{\rho}\right)^2 + \left(\ell_1 dx_2 + x_2\ell_1'\frac{x dx}{\rho}\right)^2 +$$
$$+ \left(\ell_1 dx_3 + x_3\ell_1'\frac{x dx}{\rho}\right)^2 = \big(d(\ell_1 x_1)\big)^2 + \big(d(\ell_1 x_2)\big)^2 + \big(d(\ell_1 x_3)\big)^2$$

so that by setting $y_1 = \ell_1 x_1$, $y_2 = \ell_1 x_2$, $y_3 = \ell_1 x_3$, we obtain the metric in the standard pseudo-Euclidean form $ds^2 = c^2 d\tau^2 - (dy_1^2 + dy_2^2 + dy_3^2)$. In the sequel we give up this trivial case and assume $A \neq 0$.

5 Punctual sources of the gravitational field do not exist

(4.6) is a first order differential equation with respect to the unknown function $g = g(\rho)$, so that its general solution depends on an arbitrary constant. But (4.6) contains already the constant A and moreover the function $\ell = \ell(\rho)$ which is not given. Consequently the general solution of (4.6) contains two constants. Moreover, it seems that it depends on the function $\ell(\rho)$, namely that to every allowable function $\ell(\rho)$ there corresponds a solution of (4.6) depending on two constants. However, we can prove that the function $\ell(\rho)$ is not actually involved in the general solution of (4.6).

Since the geodesic distance $\delta = \int_0^\rho \ell(u)du = \beta(\rho)$ is a strictly increasing function of ρ tending to $+\infty$ as $\rho \to +\infty$, the inverse function $\rho = \gamma(\delta)$ is also a strictly increasing function of δ tending to $+\infty$ as $\delta \to +\infty$. Consequently $g(\rho)$ can be considered as a function of δ:

$$G(\delta) = g\big(\gamma(\delta)\big).$$

It follows that the determination of $G(\delta)$ as a function of the geodesic distance δ, which possesses an intrinsic meaning with respect to the stationary metric, allows its definition with respect to any other radial coordinate depending diffeomorphically on δ.

Now, since $\delta = \beta\big(\gamma(\delta)\big)$, we have $1 = \frac{d\beta}{d\rho}\frac{d\rho}{d\delta} = \ell(\rho)\gamma'(\delta)$ and $G' = G'(\delta) = g'(\rho)\gamma'(\delta) = \frac{g'(\rho)}{\ell(\rho)}$, so that the equation (4.6) takes the form $-G + GG'^2 = -2A$ or

$$GG'^2 = G - 2A \tag{5.1}$$

which does not contain the function ℓ.

Regarding (4.7), it is obviously replaced by the equation

$$F = cG'$$

with $F = F(\delta) = f\big(\gamma(\delta)\big)$. The functions F and G are related to a stationary metric which results from the stationary metric (4.1) by the introduction of the new space coordinates:

$$y_i = \frac{\delta}{\rho}x_i = \frac{\beta(\rho)}{\rho}x_i\,, \tag{5.2}$$

where $i = 1, 2, 3$; $\|y\| = \delta$; $\|x\| = \rho$. This transformation is C^∞ everywhere, even at the origin, because the function $B(\rho) = \frac{\beta(\rho)}{\rho}$ (where $B(0) = \ell(0)$) belongs to the algebra Γ_0. In fact, since $\beta'(\rho) = \ell(\rho)$, we have $\beta(\rho) = \rho\int_0^1 \beta'(\rho u)du = \rho\int_0^1 \ell(\rho u)du$ and

$$B(\rho) = \int_0^1 \ell(\rho u)du\,,$$

consequently $B^{(2m+1)}(\rho) = \int_0^1 \ell^{(2m+1)}(\rho u)\,u^{2m+1}du$ and since $\ell \in \Gamma_0$ implies $\ell^{(2m+1)}(0) = 0$, we obtain

$$B^{(2m+1)}(0) = 0\,, \qquad (m = 0, 1, 2, 3, \dots)$$

and, from proposition 2.1, it follows that $B \in \Gamma_0$.

The inverse of (5.2) is defined by the equations

$$x_i = \Delta(\delta)\,y_i\,, \qquad i = 1, 2, 3\,, \tag{5.3}$$

where $\Delta(\delta) = \frac{\rho}{\beta(\rho)} = \frac{\gamma(\delta)}{\delta}$. Since $\gamma(\delta) = \delta\int_0^1 \gamma'(\delta u)du = \delta\int_0^1 \frac{du}{\ell(\gamma(\delta u))}$, it can be shown by induction that the function $\Delta(\delta) = \frac{\gamma(\delta)}{\delta} = \int_0^1 \frac{du}{\ell(\gamma(\delta u))}$ is an element of the algebra Γ_0, so that (5.3) is universally valid. A simple computation gives

$$x\,dx = \sum_1^3 x_i\,dx_i = \frac{\gamma\gamma'}{\delta}\,(y\,dy)\,,$$

$$dx^2 = \sum_1^3 dx_i^2 = \left(\frac{\gamma'^2}{\delta^2} - \frac{\gamma^2}{\delta^4}\right)(y\,dy)^2 + \frac{\gamma^2}{\delta^2}dy^2$$

so that, by setting $F(\delta) = f\big(\gamma(\delta)\big)$, $F_1(\delta) = f_1\big(\gamma(\delta)\big)\frac{\gamma(\delta)\gamma'(\delta)}{\delta}$, $L_1(\delta) = \ell_1\big(\gamma(\delta)\big)\frac{\gamma(\delta)}{\delta}$, $L(\delta) = \ell\big(\gamma(\delta)\big)\gamma'(\delta) = 1$, we obtain the transformed metric

$$ds^2 = \big(F\,dt + F_1(y\,dy)\big)^2 - \left(L_1^2\,dy^2 + \frac{1 - L_1^2}{\delta^2}(y\,dy)^2\right) \tag{5.4}$$

which is related to the geodesic distance $\delta = \|y\|$ and the functions F and G. Instead of $h(\rho)$, we have now the function $H = H(\delta) = \delta F_1(\delta)$, and moreover the invariant curvature radius of the spheres $\delta = \text{const.}$ is given by the function

$$G = G(\delta) = \delta L_1(\delta)\,.$$

Before solving the equation (5.1), we can anticipate that the values of the solution $G(\delta)$ do not cover the whole half-line $[0, +\infty[$ or, possibly, the whole open half-line $]0, +\infty[$, because by taking a sequence of positive values $\delta_n \to 0$, we have $G(\delta_n) \to 0$ and then the equation (5.1) implies $A = 0$ contrary to our assumption $A \neq 0$. (This conclusion follows also from (4.6), because $g(0) = 0$ implies $A = 0$.) So, we are led to anticipate that the values of the solution $G(\delta)$ cover a half-line $[\alpha, +\infty[$ with $\alpha > 0$. This important property, which implies that the source of the field cannot be reduced to a point, will be verified by the explicit expression of the solution.

Now, since $G(\delta) \geqslant \alpha > 0$ and $G - 2A \geqslant 0$ according to (5.1), the function $G(\delta)$ is obtained by the equation

$$\frac{dG}{d\delta} = \sqrt{1 - \frac{2A}{G}}$$

and since $\sqrt{1 - \frac{2A}{G}} > 0$, $G(\delta)$ is a strictly increasing function of δ. Moreover $G(\delta)$ can not remain bounded because $\frac{dG}{d\delta} \to 1$ as $G \to +\infty$.

Technically, we have first to obtain the inverse function $\delta = P(G)$ by integrating the equation

$$\frac{d\delta}{dG} = \frac{1}{\sqrt{1 - \frac{2A}{G}}}$$

which implies also that $\delta = P(G)$ is a strictly increasing and not bounded function of G. Now, we introduce an auxiliary fixed positive length ξ which will not appear in the final result, but it is needed in order to carry out correctly the computations. In fact, since G, A, $G - 2A$ represent also lengths, the ratios $\frac{G}{\xi}$, $\frac{G-2A}{\xi}$ are dimensionless, so that we can introduce the logarithm

$$\ln\left(\sqrt{\frac{G}{\xi}} + \sqrt{\frac{G - 2A}{\xi}}\right)$$

and since $\frac{d}{dG}\left(\sqrt{G\,(G-2A)} + 2A\ln\left(\sqrt{\frac{G}{\xi}} + \sqrt{\frac{G-2A}{\xi}}\right)\right) = \frac{1}{\sqrt{1 - \frac{2A}{G}}}$ the preceding equation gives $\delta = P(G)$,

$$\delta = B + \sqrt{G(G-2A)} + 2A\ln\left(\sqrt{\frac{G}{\xi}} + \sqrt{\frac{G-2A}{\xi}}\right) \tag{5.5}$$

where $B = \text{const.}$ It follows that

$$\frac{\delta}{G(\delta)} = \frac{P(G)}{G} = \frac{B}{G} + \sqrt{1 - \frac{2A}{G}} + \frac{2A}{G}\ln\left(\sqrt{\frac{G}{\xi}} + \sqrt{\frac{G-2A}{\xi}}\right)$$

and since we have $\frac{2A}{G}\ln\left(\sqrt{\frac{G}{\xi}} + \sqrt{\frac{G-2A}{\xi}}\right) = \frac{2A}{G}\ln\sqrt{\frac{G}{\xi}} + \frac{2A}{G}\ln\left(1 + \sqrt{1 - \frac{2A}{G}}\right) \to 0$ as $G \to +\infty$ we have

$$\frac{\delta}{G(\delta)} = 1 + \epsilon(\delta), \qquad \frac{G(\delta)}{\delta} = \frac{1}{1+\epsilon(\delta)}$$

with $\epsilon(\delta) \to 0$ as $\delta \to +\infty$. This property allows to determine the constant A by using the so-called Newtonian approximation of the metric (5.4) for the great values of the distance δ. Classically this approximation is referred to the static metric, namely to the case where $F_1 = 0$. We have already seen that $|\delta F_1(\delta)| \leqslant 1$, but this condition does not imply that $\delta F_1(\delta)$ possesses a limit as $\delta \to +\infty$. So we accept the condition $F_1(\delta) = 0$ for the derivation of the Newtonian approximation, without forgetting that we have to do with a specific choice of F_1 used for convenience in the case of a special problem.

This being said, the Newtonian approximation is obtained by setting $\epsilon(\delta) = 0$ and $F_1 = 0$. Then since $F = cG' = c\sqrt{1 - \frac{2A}{G}} = c\sqrt{1 - \frac{2A}{\delta} - \frac{2A\epsilon(\delta)}{\delta}}$, $1 - L_1^2 = 1 - \left(\frac{1}{1+\epsilon(\delta)}\right)^2$, and $\frac{\|y\|}{\delta} = 1$, we get the form

$$ds^2 = c^2\left(1 - \frac{2A}{\delta}\right)dt^2 - dy^2$$

which, by means of a known argument, leads to identify $\frac{c^2 A}{\delta}$ with $\frac{km}{\delta}$, whence $A = \frac{km}{c^2} = \mu$.

Since $G - 2A \geqslant 0$, we have $G(\delta) \geqslant 2\mu$, so that, as anticipated, $G(\delta)$ possesses the strictly positive greatest lower bound 2μ, which, as we see, is independent of the second constant B appearing in the solution (5.5). It follows that the strictly increasing function $G(\delta)$ appears as an implicit function defined by the equation

$$\delta = B + \sqrt{G(G-2\mu)} + 2\mu \ln\left(\sqrt{\frac{G}{\xi}} + \sqrt{\frac{G-2\mu}{\xi}}\right).$$

The greatest lower bound 2μ is obtained for $\delta = B + 2\mu \ln\sqrt{\frac{2\mu}{\xi}}$ and this is why it is convenient to introduce, instead of B, the constant $\delta_0 = B + 2\mu \ln\sqrt{\frac{2\mu}{\xi}}$, which allows to write $\delta = \delta_0 + \sqrt{G(G-2\mu)} + 2\mu \ln\left(\sqrt{\frac{G}{2\mu}} + \sqrt{\frac{G}{2\mu} - 1}\right)$ or

$$\delta = \delta_0 + \int_{2\mu}^{G} \frac{du}{\sqrt{1 - \frac{2\mu}{u}}}, \qquad G = G(\delta) \geqslant 2\mu$$

which does not contain the auxiliary length ξ. The solution is completed by the determination of the function

$$F = cG' = c\sqrt{1 - \frac{2\mu}{G(\delta)}}.$$

As far as $H(\delta) = \delta F_1(\delta)$ is concerned, we repeat that it is introduced simply as a C^∞ function vanishing for $\delta = 0$ and satisfying the condition $|H(\delta)| \leqslant 1$.

What about the new constant δ_0 ? From the mathematical point of view, negative values of δ_0 are not excluded. So, we distinguish the following cases (see Figure):

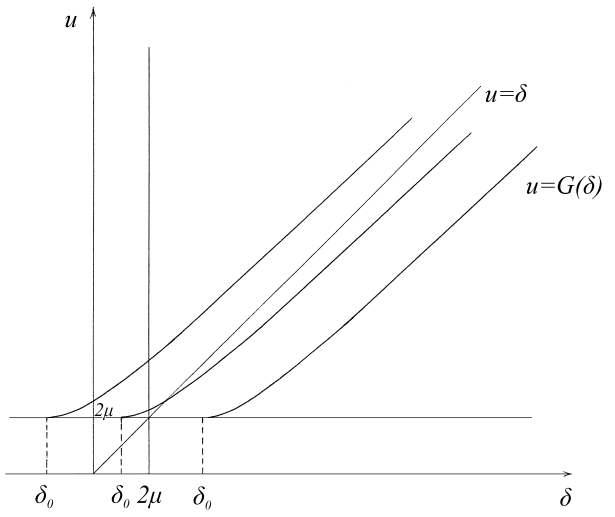

(a) $\delta_0 < 0$. Then the values of $G(\delta)$ for $\delta_0 \leqslant \delta < 0$ are meaningless physically, because $G(\delta)$ is conceived on $[0, +\infty[$. But the value $\delta = 0$ is also excluded because

$$\int_{2\mu}^{G(0)} \frac{du}{\sqrt{1 - \frac{2\mu}{u}}} = -\delta_0 > 0$$

implies $G(0) > 2\mu$ contrary to the geometrical condition $G(0) = 0$. Consequently there exists a constant $\delta_1 > 0$ (the radius of the considered distribution of matter) such that only the restriction of $G(\delta)$ to $[\delta_1, +\infty[$ is taken into account.

(b) $\delta_0 = 0$. Then

$$\int_{2\mu}^{G(0)} \frac{du}{\sqrt{1 - \frac{2\mu}{u}}} = 0$$

so that $G(0) = 2\mu$ contrary to the geometrical condition $G(0) = 0$. Consequently the solution is valid, as previously, on a half-line $[\delta_1, +\infty[$ with $\delta_1 > 0$.

(c) $\delta_0 > 0$. Then $G(\delta_0) = 2\mu$, $F(\delta_0) = 0$, so that the metric degenerates for $\delta = \delta_0$. A degenerate metric does not possess physical meaning. Consequently, there exists a constant $\delta_1 > \delta_0$ (the radius of the sphere bounding the matter) such that the solution is physically valid only on the half-line $[\delta_1, +\infty[$.

Whatever the case may be, the vacuum solution is not defined for $\delta < \delta_1$. In other words, the ball $\|y\| \leqslant \delta_1$ is occupied by matter, so that the source of the field cannot be reduced to a point. The constant δ_0 is related to a boundary condition, namely the value of the curvature radius of the sphere bounding the matter. In fact, if δ_1 is the radius of this sphere, and the value $G(\delta_1)$ is known, then the value δ_0 is easily obtained:

$$\delta_0 = \delta_1 - \sqrt{G(\delta_1)\,(G(\delta_1) - 2\mu)} - 2\mu \ln\left(\sqrt{\frac{G(\delta_1)}{2\mu}} + \sqrt{\frac{G(\delta_1)}{2\mu} - 1}\right).$$

However, it is difficult, even impossible, to obtain $G(\delta_1)$ by direct measurements. So the value δ_0 is to be found indirectly by taking into account the phenomena induced by δ_0. This problem will be treated in another paper.

The most impressive characteristic of the solution is perhaps the non-Euclidean structure of the space and specifically the strong non-Euclidean properties in the neighbourhood of the origin. If the theory is applicable to the elementary particles, then strong deviations from the Euclidean geometry are to be expected in the world of microphysics. Together with the new geometrical ideas, the solution brings about an improvement of the law of gravitation in accordance with Poincaré's prediction: "Il est difficile de ne pas supposer que la loi véritable contient des termes complémentaires qui deviendraient sensibles aux petites distances" [1]. In fact, the Newton potential

$$-\frac{km}{\delta}$$

is an approximation of the more accurate expression

$$-\frac{km}{G(\delta)}$$

which depends on the curvature radius $G(\delta)$. There is a significant discrepancy between the two formulae. Although, as shown earlier, the ratio $\frac{G(\delta)}{\delta}$ converges to 1, the difference

$$\delta - G(\delta) = P(G) - G = \delta_0 + \\ + 2\mu \ln\left(\sqrt{\frac{G}{2\mu}} + \sqrt{\frac{G}{2\mu} - 1}\right) - \frac{2\mu}{1 + \sqrt{1 - \frac{2\mu}{G}}}$$

tends to $+\infty$ as $\delta \to +\infty$. Moreover $G(\delta)$ depends not only on the radius δ, but also on the constant δ_0. Of course, the distinction between Newton's theory and Einstein's theory does not reduce to the distinction between δ and $G(\delta)$. Einstein's theory provides a new entity, namely a spacetime metric.

A last question regards the "boundary conditions at infinity". Classically it is required that the metric admit as limit form the standard pseudo-Euclidean metric as $\delta \to +\infty$. Since, as already remarked, $\delta F_1(\delta)$ does not possess a limit as $\delta \to +\infty$, this requirement presupposes that $F_1 = 0$, namely that we are dealing with a static metric. Then the metric can be written as

$$ds^2 = c^2\left(1 - \frac{2\mu}{G(\delta)}\right)dt^2 - \\ - \left(\left(\frac{G(\delta)}{\delta}\right)^2 dy^2 + \frac{1}{\delta^2}\left(1 - \left(\frac{G(\delta)}{\delta}\right)^2\right)(ydy)^2\right)$$

and since $G(\delta) \to +\infty$, $\frac{G(\delta)}{\delta} \to 1$, $\frac{\|y\|}{\delta} = 1$, we find, in fact, "at infinity" the standard pseudo-Euclidean form

$$ds^2 = c^2 dt^2 - dy^2.$$

Note that, if we introduce the so-called polar coordinates, this conclusion fails. In fact, then we have the form

$$ds^2 = c^2\left(1 - \frac{2\mu}{G(\delta)}\right)dt^2 - \left(d\delta^2 + \left(G(\delta)\right)^2\left(\sin^2\theta d\phi^2 + d\theta^2\right)\right)$$

which does not possess a limit form as $\delta \to +\infty$.

6 Black holes do not exist

The pseudo-theory of black holes appeared as a consequence of misunderstandings and mathematical errors brought out in detail in the papers [3, 5, 6]. We emphasize that the so-called "horizon" does not represent an observable value of the curvature radius $G(\delta)$. According to the established rigorous solution, 2μ is the greatest lower bound of the vacuum solution $G(\delta)$ and is defined for a certain value δ_0 of the new constant. If $\delta_0 \leqslant 0$ there exists no real sphere with the curvature radius 2μ, and the physically valid part of the solution is defined for $\delta \geqslant \delta_1$, where δ_1 is a strictly positive value such that $G(\delta_1) > 2\mu$. On the other hand, if $\delta_0 > 0$, the degeneracy of the metric for $\delta = \delta_0$ implies that the corresponding sphere lies inside the matter, so that the vacuum solution is valid for $\delta \geqslant \delta_1$ where $\delta_1 > \delta_0$ and $G(\delta_1) > 2\mu$. Whatever the case may be, the notion of black hole is inconceivable.

References

1. Poincaré H. La science et l'hypothèse. Champs, Flammarion, Paris, 1968.
2. Rosen N. General Relativity with a background metric. *Found. of Phys.*, 1980, 10, Nos. 9/10, 673–784.
3. Stavroulakis N. Mathématiques et trous noirs. *Gazette des mathématicients*, No. 31, Juillet 1986, 119–132.
4. Stavroulakis N. Sur la fonction de propagation des ébranlements gravitationnels. *Annales Fond. Louis de Broglie*, 1995, v. 20, No. 1, 1–31.
5. Stavroulakis N. On the principles of general relativity and the $\Theta(4)$-invariant metrics. *Proceedings of the 3rd Panhellenic Congress of Geometry*, Athens, 1997, 169–182.
6. Stavroulakis N. Vérité scientifique et trous noirs (première partie). Les abus du formalisme. *Annales Fond. Louis de Broglie*, 1999, v. 24, No. 1, 67–l09.
7. Stavroulakis N. Vérité scientifique et trous noirs (deuxième partie) Symétries relatives au groupe des rotations. *Annales Fond. Louis de Broglie*, 2000, v. 25, No. 2, 223–266.
8. Stavroulakis N. Vérité scientifique et trous noirs (troisième partie). Equations de gravitation relatives à une métrique $\Theta(4)$-invariante. *Annales Fond. Louis de Broglie*, 2001, v. 26, No. 4, 605–631.
9. Stavroulakis N. On a paper by J. Smoller and B. Temple. *Annales Fond. Louis de Broglie*, 2002, v. 27, No. 3, 511–521.
10. Stavroulakis N. A statical smooth extension of Schwarzschild's metric. *Lettere al Nuovo Cimento*, Serie 2, 26/10/1974, v. 11, No. 8, 427–430.

Gravitational Perturbations as a Possible Cause for Instability in the Measurements of Positron Annihilation

Boris P. Vikin*

The Faculty of Physics, Voronezh State University, Voronezh, Russia

The annihilation of positrons is measured in a wide range of studies in the field of physical chemistry [1, 2]. One of the problems in these studies is the instability of the results of measurements [3–5]. As shown in our research, instability may result from the change of nonregistering gravitational effects related to alteration of the tidal forces upon the change of moon phases and the seasonal changes of the distance between the Earth and the Sun.

1 Materials and methods

A sample of ^{22}Na (5 mCu) was used as a source of positrons. The yield of positronium (I_2) and the parameters of its annihilation at the passage through organic liquids were measured by two techniques: either angular (parapositronium) or temporal (orthopositronium) correlations of annihilation quanta were registered. The yield of positronium was measured with a setup of "fast-slow coincidences". The setup was assembled according to a typical scheme, had the time resolution of 0.5 ns and was connected to a multichannel amplitude recorder [1, 2].

2 Results

In the experiments, I_2-parameter and spectra of triplet positronium were measured in the toluol samples purified from oxygen by the method of vacuum freezing-out and the samples under oxygen (0.6 atm). The measurements were conducted daily over a period of 3 months (November, 1981 — February, 1982).

Fig. 1 shows that in the oxygen-depleted samples, regular fluctuations in the positronium yield are observed, which correlate with the changes of the moon phase. The yield is maximal in the times close to the new moon and minimal in the times close to the full moon.

In the presence of oxygen, Fig. 2, no reliable effects were revealed. It can be explained by a specific influence of oxygen on the processes of formation and annihilation of positronium [1, 2]. However, these experiments indicate stability of the setup itself.

In addition to periodical fluctuations, one can see a trend in the series of measurements: the mean level of I_2 grows from November to February. This trend may be due to the seasonal change of the distance between the Earth and the Sun.

In more large scale the seasonal changes of positronium yield apparent from Fig. 3, which presents average results

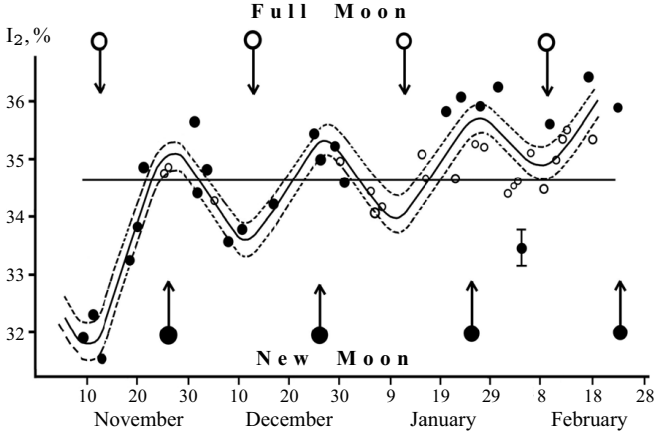

Fig. 1: Yield of positronium correlate with the changes of the Moon phases.

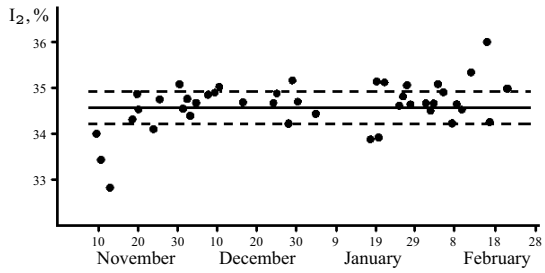

Fig. 2: Yield of positronium in the presence of oxygen.

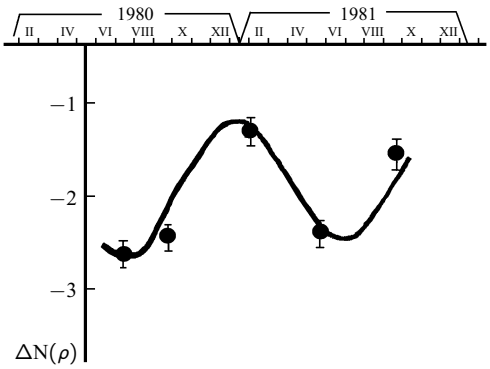

Fig. 3: Seasonal changes of positronium yield in 1980–1981.

*Submitted via Simon E. Shnoll. All correspondence addressed to the author should be directed to Simon E. Shnoll (e-mail: shnoll@iteb.ru).

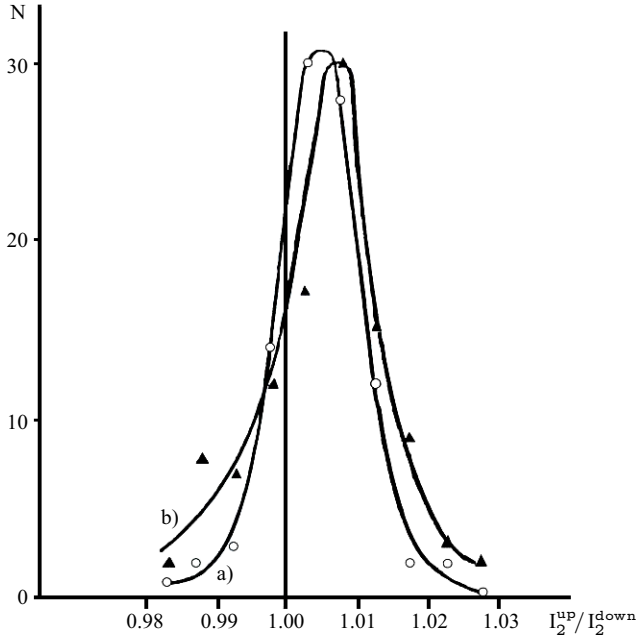

Fig. 4: Distribution of measuring results of positronium yield at the case of the experimental setup relocating up (triangles) and down (circles), with the height difference 1.5 m.

of large number of experiments provided in 1980–1981. It's possible to see that minimal yield is observable for summer solstice (June — July) and maximal yield for winter solstice (December — February).

The reliability of the conclusion that the yield of positronium depends on the tidal changes in gravity force was checked in the experiments of 1984–1985, in which the setup used for measuring I_2 was relocating up-and-down, with the height difference of 1.5 m. The measurements (1500 in total) were alternated (up/down) every 20 min. Finally, an I_2^{up}/I_2^{down} ratio was calculated. Fig. 4 shows a smoothed distribution of the results obtained. The mean of this ratio is 1.00447 for all the measurements. The root-mean-square error equals to ± 0.00064. Thus, lifting the setup 1.5 m higher results in a reliable increase in the positronium yield (the difference amounts to 7σ).

References

1. Goldansky V. I. Physical chemistry of the positron and the positronium. *Atomic Energy Review*, IAEA, Vienna, 1968, v.6, 3–148. (Referred with the 2nd, Russian edition, Nauka Publ., Moscow, 1968.)
2. Goldansky V. I. and Firsov V. G. Chemistry of new atoms. *Progress in Chemistry* (Russian) 1971, v. 40(8), 1353–1393.
3. Vikin B. P., Martsinkovsky E. V. and Litvinov V. I. A method for calculation of the parameters of annihilation. In *Radiophysics and Microelectronics*, Voronezh University Press, Voronezh, 1970, p. 60.
4. Vikin B. P., Zalukaev L. P., Perfil'ev L. P., et al. The study of toluol association by the method of positron annihilation. *Theor. Exp. Chem.* (Kiev), 1977, v. 14(2).
5. Campbell J. L. and Schutte A. A problem of stability in the energy spectroscopy of annihilation photons. *Appl. Physics*, 1980, v. 21(1), 19.

Photon Physics of Revised Electromagnetics

Bo Lehnert

Alfvén Laboratory, Royal Institute of Technology, S-10044, Stockholm, Sweden

E-mail: Bo.Lehnert@ee.kth.se

Conventional theory, as based on Maxwell's equations and associated quantum electrodynamical concepts in the vacuum, includes the condition of zero electric field divergence. In applications to models of the individual photon and to dense light beams such a theory exhibits several discrepancies from experimental evidence. These include the absence of angular momentum (spin), and the lack of spatially limited geometry in the directions transverse to that of the propagation. The present revised theory includes on the other hand a nonzero electric field divergence, and this changes the field equations substantially. It results in an extended quantum electrodynamical approach, leading to nonzero spin and spatially limited geometry for photon models and light beams. The photon models thereby behave as an entirety, having both particle and wave properties and possessing wave-packet solutions which are reconcilable with the photoelectric effect, and with the dot-shaped marks and interference patterns on a screen by individual photons in a two-slit experiment.

1 Introduction

Conventional electromagnetic theory based on Maxwell's equations and quantum mechanics has been very successful in its applications to numerous problems in physics, and has sometimes manifested itself in an exceptionally good agreement with experiments. Nevertheless there exist areas within which these joint theories do not provide fully adequate descriptions of physical reality. As stated by Feynman [1], there are difficulties associated with the *ideas* of Maxwell's theory which are not solved by and not directly associated with quantum mechanics. Thus the classical theory of electromagnetism is in its conventional form an unsatisfactory theory of its own.

Maxwell's equations have served as a guiding line and basis for conventional quantum electrodynamics (QED) in which there is a vacuum state with a vanishing electric field divergence [2]. The quantized equations become equivalent to the classical field equations in which all field quantities are replaced by their expectations values [3]. According to Schiff [2] and Heitler [3], the Poynting vector further forms the basis for the quantized field momentum. Consequently, QED will also become subject to the shortcomings of a conventional field theory.

When applying such a theory to photon physics, it will lead to irrelevant results in a number of important cases. This occurs with the experimentally confirmed existence of angular momentum of individual photons and of light beams with a spatially limited cross-section, with the behaviour of individual photons as needle radiation in the photoelectric effect and in two-slit experiments, and with the particle-wave duality of the photon.

As a consequence of the revealed limitations, modified theories leading beyond Maxwell's equations have been elaborated by several authors. Among these there is an approach described in this paper [4–9]. It is based on a vacuum state that can give rise to local space charges and currents in addition to the displacement current. This changes the field equations in a substantial way, thus resulting in an extended quantum electrodynamical ("EQED") approach.

In the applications to photon physics the nonzero electric field divergence may appear as small, but it still comes out to have an essential effect on the end result. In other applications of the present theory, such as on an electron model [6, 7] not being treated here, the electric field divergence terms appear as large contributions already in the basic field equations.

2 Basis of present theory

The vacuum is not merely an empty space. There is a nonzero level of its ground state, the zero-point-energy, which derives from the quantum states of the harmonic oscillator [2]. An experimentally verified example of the related electromagnetic vacuum fluctuations is the Casimir effect [10]. Electron-positron pair formation due to an energetic photon also indicates that local positive and negative electric charges can be created out of an electrically neutral vacuum state. The basic physical concept of the present theory is therefore the appearance of a local charge density in such a state. In its turn, this becomes associated with a nonzero electric field divergence. The inclusion of the latter can as well be taken as a starting point of a corresponding field theory.

2.1 Lorentz invariant field equations

In presence of electric space charges and related current densities, a general form of the Proca-type equation

$$\Box A_\mu \equiv \left(\frac{1}{c^2} \frac{\partial^2}{\partial t^2} - \nabla^2 \right) A_\mu = \mu_0 J_\mu \,, \quad \mu = 1, 2, 3, 4 \quad (1)$$

can be taken as a four-dimensional starting point of the pre-

sent field equations, given in SI units. Here $A_\mu = (\mathbf{A}, i\phi/c)$, where $\mathbf{A}$ and ϕ are the magnetic vector potential and the electrostatic potential in three-space, and

$$J_\mu = (\mathbf{j},\, \mathrm{i}c\bar{\rho}) \tag{2}$$

is the four-current density. The right-hand member of equation (1) and the form (2) are now given a new interpretation, where $\bar{\rho}$ is the nonzero electric charge density in the vacuum, and $\mathbf{j}$ stands for an associated three-space current density. Maxwell's equations are recovered when the current density (2) disappears, and equation (1) reduces to the d'Alembert equation. The present charge and current densities should not become less conceivable than the conventional concepts of a nonzero curl of the magnetic field and an associated displacement current. All these concepts can be regarded as intrinsic properties of the electromagnetic field.

Physical experience further supports that also the present revised and extended field equations should remain Lorentz invariant. This implies that the current (2) has to transform as a four-vector, and its square then becomes invariant to a transform from one inertial frame K to another such frame K′. Thus

$$j^2 - c^2\bar{\rho}^2 = j'^2 - c^2\bar{\rho}'^2 = \text{const}\,. \tag{3}$$

In addition, the current density $\mathbf{j}$ should exist only when there is also a charge density $\bar{\rho}$, and this implies that the constant in equation (3) vanishes. Since $\mathbf{j}$ and $\bar{\rho}$ must behave as space and time parts of J_μ, the disappearance of this constant merely becomes analogous to the choice of origin for the space and time coordinates. Consequently the final form of he current density (2) becomes

$$\mathbf{j} = \bar{\rho}\,(\mathbf{C},\, \mathrm{i}c) \qquad \mathbf{C}^2 = c^2. \tag{4}$$

It is obvious that $\bar{\rho}$ as well as the velocity vector $\mathbf{C}$ vary from one inertial frame to another and do not become Lorentz invariant, whereas this is the case of J_μ.

It can be shown [6, 7] that there is a connection between the current density (4) and the electron theory by Dirac. A different form of the current density in equation (1) has further been introduced by de Broglie and Vigier [11] and applied by Evans and Vigier [12]. It explicitly includes a small nonzero photon rest mass.

The three-dimensional representation of the extended equations *in the vacuum* now becomes

$$\text{curl}\ \mathbf{B}/\mu_0 = \varepsilon_0(\text{div}\ \mathbf{E})\,\mathbf{C} + \varepsilon_0\partial\mathbf{E}/\partial t \tag{5}$$

$$\text{curl}\ \mathbf{E} = -\partial\mathbf{B}/\partial t \tag{6}$$

$$\text{div}\ \mathbf{E} = \bar{\rho}/\varepsilon_0 \tag{7}$$

for the electric and magnetic fields $\mathbf{E}$ and $\mathbf{B}$. Here the first term of the right-hand member of equation (5) and equation (7) are the new parts introduced. Thus, there is a change from a homogeneous to an inhomogeneous system of equations, a new degree of freedom is introduced by the nonzero electric field divergence, and the latter produces an asymmetry in the appearance of the electric and magnetic fields.

The presence in equations (5) and (7) of the dielectric constant ε_0 and the magnetic permeability μ_0 of the conventional vacuum may require further explanation. In the present approach the vacuum is considered not to include electrically polarized or magnetized atoms or molecules. In this respect equation (7) is the same as in the theory of plasmas which contain freely moving charged particles in a background of empty vacuum space.

A nonzero magnetic field divergence is not adopted in this theory, because this is so far a possible but not experimentally supported supposition which is here left as an open question.

Using vector identities, the basic equations (5)–(7) yield the local momentum equation

$$\text{div}^2\mathbf{S} = \bar{\rho}\,(\mathbf{E} + \mathbf{C}\times\mathbf{B}) + \frac{\partial}{\partial t}\,\mathbf{g} \tag{8}$$

and the local energy equation

$$-\text{div}\ \mathbf{S} = \bar{\rho}\,\mathbf{E}\cdot\mathbf{C} + \frac{\partial}{\partial t}\,w_f\,. \tag{9}$$

Here $\frac{1}{c^2}\,\mathbf{S}$ is the electromagnetic stress tensor,

$$\mathbf{g} = \varepsilon_0\,\mathbf{E}\times\mathbf{B} = \frac{1}{c^2}\,\mathbf{S} \tag{10}$$

can be interpreted as an electromagnetic momentum density with $\mathbf{S}$ denoting the Poynting vector, and

$$w_f = \frac{1}{2}\,\varepsilon_0\left(\mathbf{E}^2 + c^2\mathbf{B}^2\right) \tag{11}$$

representing the electromagnetic field energy density. The angular momentum density becomes

$$\mathbf{s} = \mathbf{r}\times\mathbf{S}/c^2 \tag{12}$$

where $\mathbf{r}$ is the radius vector from the origin.

Combination of equations (5) and (6) results in an extended wave equation for the electric field

$$\left(\frac{\partial^2}{\partial t^2} - c^2\,\nabla^2\right)\mathbf{E} + \left(c^2\,\nabla + \mathbf{C}\,\frac{\partial}{\partial t}\right)(\text{div}\ \mathbf{E}) = 0\,. \tag{13}$$

A divergence operation on equation (5) results in

$$\left(\frac{\partial}{\partial t} + \mathbf{C}\cdot\nabla\right)(\text{div}\ \mathbf{E}) = 0\,, \tag{14}$$

provided that $\text{div}\ \mathbf{C} = 0$.

2.2 Quantization of the revised theory

In the conventional QED formalism Maxwell's equations with a vanishing electric field divergence have been used as a basis, also including the Poynting vector in the representation

of the quantized field momentum [2, 3]. The quantized equations then become equivalent to the classical ones in which the field quantities are replaced by their expectation values.

A similar situation also has to apply to the present revised equations. The resulting solutions are expected not to be too far from the truth, by representing the most probable trajectories. A rigorous extended quantum electrodynamical (EQED) formulation would imply that the field equations are quantized already from the outset. However, to simplify the analysis, we will instead solve the extended equations as they stand, and impose relevant quantum conditions afterward. For the considered photon models these conditions are given by the energy $h\nu$ related to the frequency ν, and by the angular momentum $h/2\pi$ of the individual photon with the property of a boson particle.

3 Axisymmetric model of the individual photon

When elaborating a model of the individual photon as a propagating boson, a wave or wave-packet with preserved and limited geometrical shape and undamped motion in a defined direction of space has to be taken as a starting point. This leads to cylindrical geometry and waves. A cylindrical frame (r, φ, z) becomes appropriate, with its z-axis in the direction of propagation. We further introduce a velocity vector of helical geometry

$$\mathbf{C} = c\,(0, \cos\alpha, \sin\alpha) \tag{15}$$

where the angle α is constant and $0 < \cos\alpha \ll 1$ for reasons to be clarified later. As will be shown, the component C_z is related to the wave propagation in the axial direction, and the component C_φ to the angular momentum and an associated small nonzero rest mass. Here we choose the positive values of $\sin\alpha$ and $\cos\alpha$, but have in general both signs representing the two directions of propagation and the two spin directions.

The wave equation (13) now leads to

$$\left(D_1 - \frac{1}{r^2} + \frac{1}{r^2}\frac{\partial^2}{\partial\varphi^2}\right) E_r - \frac{2}{r^2}\frac{\partial}{\partial\varphi} E_\varphi = \frac{\partial}{\partial r}(\mathrm{div}\ \mathbf{E}) \tag{16}$$

$$\left(D_1 - \frac{1}{r^2} + \frac{1}{r^2}\frac{\partial^2}{\partial\varphi^2}\right) E_\varphi - \frac{2}{r^2}\frac{\partial}{\partial\varphi} E_r = \\ = \left[\frac{1}{r}\frac{\partial}{\partial\varphi} + \frac{1}{c}(\cos\alpha)\frac{\partial}{\partial t}\right](\mathrm{div}\ \mathbf{E}) \tag{17}$$

$$\left(D_1 + \frac{1}{r^2}\frac{\partial^2}{\partial\varphi^2}\right) E_z = \left[\frac{\partial}{\partial z} + \frac{1}{c}(\sin\alpha)\frac{\partial}{\partial t}\right](\mathrm{div}\ \mathbf{E}) \tag{18}$$

where

$$D_1 = \frac{\partial^2}{\partial r^2} + \frac{1}{r}\frac{\partial}{\partial r} + \frac{\partial^2}{\partial z^2} - \frac{1}{c^2}\frac{\partial^2}{\partial t^2}\,. \tag{19}$$

Equation (14) further becomes

$$\left(\frac{\partial}{\partial t} + c\cos\alpha\,\frac{1}{r}\frac{\partial}{\partial\varphi} + c\sin\alpha\,\frac{\partial}{\partial z}\right)(\mathrm{div}\ \mathbf{E}) = 0\,. \tag{20}$$

In this section restriction is made to purely axisymmetric normal modes for which $\partial/\partial\varphi = 0$, and where every quantity Q has the form $Q = \hat{Q}\,(r)\exp\left[\mathrm{i}\,(-\omega t + kz)\right]$ with a given angular frequency ω and wave number k.

3.1 Shortcomings of a conventional model

Turning first to a model based on Maxwell's equations, the system (16)–(18) with a vanishing electric field divergence results in the electric field components

$$\begin{aligned} \hat{E}_r &= k_{1r}\,r + k_{2r}/r \\ \hat{E}_\varphi &= k_{1\varphi}\,r + k_{2\varphi}/r \\ \hat{E}_z &= k_{1z}\ln r + k_{2z} \end{aligned} \tag{21}$$

and similar expressions for the magnetic field. The solutions for E_r and E_φ were first deduced by Thomson [13] who called attention to their divergent character, thus becoming unsuitable for a limited model.

However, an even more serious shortcoming arises from the requirement that the divergences of the fields have to vanish. Thus the second order equations (16)–(18) and their solutions (21) have to be checked with respect to the first order equations of an *identically* vanishing field divergence. This implies that

$$2k_{r_1} + \mathrm{i}k\,(k_{1z}\ln r + k_{2z}) \equiv 0 \tag{22}$$

for all k and r. Consequently E_z and k_{1r} have to vanish, only E_φ and k_{2r} remain nonzero, and similar results apply to the magnetic field. This implies that the wave becomes purely transverse, that the Poynting vector (10) has a component in the direction of propagation only, and that there is no spin in the axial direction.

3.2 Axisymmetric models in revised theory

For an axisymmetric normal mode, equation (20) of the revised theory yields the dispersion relation

$$\omega/k = c\sin\alpha = v\,, \qquad k^2 - \omega^2/c^2 = k^2\cos^2\alpha \tag{23}$$

where v stands for the phase velocity which becomes equal to the group velocity $\partial\omega/\partial k$. The parameter $\cos\alpha$ must be small here, such as not to get in conflict with experiments of the Michelson-Morley type. For $\cos\alpha \leqslant 10^{-4}$ the difference between v and c would thus become less than a change in the eight decimal of c. Equations (16), (17) and (23) further combine to

$$-k^2\cos^2\alpha\,E_r = \mathrm{i}k\,\frac{\partial E_z}{\partial r} \tag{24}$$

$$\left(\frac{\partial^2}{\partial r^2} + \frac{1}{r}\frac{\partial}{\partial r} - \frac{1}{r^2} - k^2\cos^2\alpha\right) E_\varphi = \\ = -(\mathrm{tg}\ \alpha)\left(\frac{\partial^2}{\partial r^2} + \frac{1}{r}\frac{\partial}{\partial r} - k^2\cos^2\alpha\right) E_z\,. \tag{25}$$

A *generating function*

$$G_0 \cdot G = E_z + (\cot\alpha)E_\varphi\,, \quad G = R(\rho)\,\mathrm{e}^{\mathrm{i}(-\omega t + kz)} \tag{26}$$

can now be found which has the amplitude G_0, a normalized dimensionless part G, the normalized coordinate $\rho = r/r_0$, and the characteristic radius r_0 of the configuration represented by the radial function R. The function (26) generates the solutions

$$E_r = -\mathrm{i}G_0\left(\theta\cos^2\alpha\right)^{-1}\frac{\partial}{\partial\rho}\Big[\left(1-\rho^2 D\right)G\Big] \tag{27}$$

$$E_\varphi = G_0\,(\mathrm{tg}\,\alpha)\,\rho^2 DG \tag{28}$$

$$E_z = G_0\left(1-\rho^2 D\right)G \tag{29}$$

where

$$D = D_\rho - \theta^2\cos^2\alpha\,, \qquad D_\rho = \frac{\partial^2}{\partial\rho^2} + \frac{1}{\rho}\frac{\partial}{\partial\rho} \tag{30}$$

and $\theta = kr_0$. The solutions (27)–(29) are reconfirmed by insertion into equations (16)–(18). The magnetic field components are derived from the induction law (6). The helical-like structure of the obtained solution, with its axial field components, is similar but not identical to that deduced by Evans and Vigier [12].

From the normal modes a wave packet solution is now formed which has finite extensions, and a narrow line width as required by experimental observation. We are free to rewrite the amplitude factor (26) as $G_0 = g_0\cos^2\alpha$. The wave packet has the amplitude

$$A_k = \left(\frac{k}{k_0^2}\right)\mathrm{e}^{-z_0^2(k-k_0)^2} \tag{31}$$

in the interval $\mathrm{d}k$ being centered around the main wave number k_0. Here $2z_0$ represents the axial length of the packet. With $z = \bar{z} - vt$ and the notation

$$\bar{E}_0 = E_0(\bar{z}) = \left(\frac{g_0}{k_0 r_0}\right)\left(\frac{\sqrt{\pi}}{k_0 z_0}\right)\exp\left[-\left(\frac{\bar{z}}{2z_0}\right)^2 + \mathrm{i}\,k_0\bar{z}\right] \tag{32}$$

the spectral averages of the field components are

$$\bar{E}_r = -\mathrm{i}E_0\left[R_5 + (\theta_0')^2 R_1\right] \tag{33}$$

$$\bar{E}_\varphi = E_0\theta_0(\sin\alpha)(\cos\alpha)\left[R_3 - (\theta_0')^2 R_1\right] \tag{34}$$

$$\bar{E}_z = E_0\theta_0(\cos^2\alpha)\left[R_4 + (\theta_0')^2 R_1\right] \tag{35}$$

where $\theta_0 = k_0 r_0$, $\theta_0' = \theta_0\cos\alpha$ and

$$R_1 = \rho^2 R, \quad R_3 = \rho^2 D_\rho R, \quad R_4 = \left(1-\rho^2 D_\rho\right)R, \tag{36}$$

$$R_5 = \frac{d}{d\rho}\Big[\left(1-\rho^2 D_\rho\right)R\Big], \quad R_7 = \left(\frac{d}{d\rho} + \frac{1}{\rho}\right)\left(\rho^2 R\right). \tag{37}$$

The packet components $\left(\bar{E}_\varphi, \bar{E}_z, \bar{B}_r\right)$ are in phase with the generating function (26). The components $\left(\bar{E}_r, \bar{B}_\varphi, \bar{B}_z\right)$ are ninety degrees out of phase with it. We now choose the real part of the function (26), i. e. $G = R(\rho)\cos k\bar{z}$, which is symmetric with respect to the axial center $\bar{z} = 0$ of the moving wave packet. Then the real part of the form (32) is adopted, from which $\left(\bar{E}_\varphi, \bar{E}_z, \bar{B}_r\right)$ become symmetric and $\left(\bar{E}_r, \bar{B}_\varphi, \bar{B}_z\right)$ antisymmetric. Under these conditions the integrated electric charge and magnetic moment vanish.

The electromagnetic field energy density (11) defines an equivalent total mass

$$m = \frac{1}{c^2}\int w_f\,dV \cong \frac{2\pi\varepsilon_0}{c^2}\int_{-\infty}^{+\infty} r\,E_r^2\,dr d\bar{z} \tag{38}$$

to lowest order. Integration and quantization yields

$$m = a_0 W_m \cong \frac{h\nu_0}{c^2}\,, \qquad W_m = \int \rho\,R_5^2\,d\rho\,, \tag{39}$$

where

$$a_0 = \varepsilon_0\,\pi^{5/2}\sqrt{2}\,z_0\left(g_0/ck_0^2 z_0\right)^2 \equiv 2a_0^* g_0^2 \tag{40}$$

and $\nu_0 = c/\lambda_0$. Here the slightly reduced phase and group velocity (23) can be associated with a very small nonzero photon rest mass $m_0 = m\cos\alpha$.

Turning finally to the momentum balance, all integrated volume forces in equation (8) vanish on account of the symmetry properties, and expression (12) gives

$$s = \int s_z\,dV = -2\pi\varepsilon_0\int_{-\infty}^{+\infty}\int r^2\bar{E}_r\bar{B}_z\,dr d\bar{z}\,. \tag{41}$$

It reduces to the quantum condition

$$s = a_0 r_0 c(\cos\alpha)W_s = \frac{h}{2\pi}\,, \quad W_s = -\int \rho^2 R_5 R_7\,d\rho\,. \tag{42}$$

So far the radial function R has not been specified. We first consider the case where it is finite at the axis $\rho = 0$ and tends to zero at large ρ, as in the form

$$R(\rho) = \rho^\gamma \mathrm{e}^{-\rho} \tag{43}$$

where $\gamma > 0$. In principle, the factor in front of the exponential would have to be replaced by a power series of ρ, but since we will proceed to the limit of large γ, only one dominating term becomes sufficient. The exponential factor in (43) is further included to secure the convergence of any moment with R. The function (43) has a sharply defined maximum at the radius $\hat{r} = \gamma r_0$. Combination of relations (39) and (42) finally results in an effective photon diameter

$$2\hat{r} = \frac{\lambda_0}{\pi\cos\alpha} \tag{44}$$

being independent of γ and the exponential factor in equation (43).

We next consider the alternative of a radial function R which *diverges* at the axis, i. e.

$$R(\rho) = \rho^{-\gamma}\mathrm{e}^{-\rho}. \tag{45}$$

Here $\hat{r} = r_0$ can be taken as an effective radius. To obtain *finite* integrated values of the total mass m and spin s, small lower limits ρ_m and ρ_s are now introduced in the integrals of W_m and W_s. We further introduce

$$r_0 = c_r \cdot \varepsilon\,, \qquad g_0 = c_g \cdot \varepsilon^{\beta} \tag{46}$$

such as to make the characteristic radius r_0 and the factor g_0 shrink to small but nonzero values as the lower limits ρ_m and ρ_s approach zero. In equations (46), ε is an independent smallness parameter, $0 < \varepsilon \ll 1$, and c_r, c_g and β stand for positive constants. Equations (40), (39) and (44) combine to

$$m = a_0^* \gamma^5 c_g^2 \left(\varepsilon^{2\beta}/\rho_m^{2\gamma}\right) \cong h/\lambda_0 c\,, \tag{47}$$

$$s = a_0^* \gamma^5 c_g^2 c_r c(\cos\alpha) \left(\varepsilon^{2\beta+1}/\rho_m^{2\gamma-1}\right) = h/2\pi\,. \tag{48}$$

To obtain finite m and s it is then necessary that

$$\rho_m = \varepsilon^{\beta/\gamma}, \qquad \rho_s = \varepsilon^{(2\beta+1)(2\gamma-1)}. \tag{49}$$

We are here free to choose $\beta = \gamma \gg 1$ by which $\rho_s \cong \rho_m = \varepsilon$. This leads to a similar set of geometrical configurations which have a shape being independent of ρ_m, ρ_s and ε in the range of small ε. From equations (47) and (48) the effective photon diameter finally becomes

$$2\hat{r} = \frac{\varepsilon\lambda_0}{\pi\cos\alpha} \tag{50}$$

which is independent of γ, β and the exponential factor.

3.3 Summary on the photon model

- Conventional theory results in a model of the individual photon which has no spin, and is not reconcilable with a limited geometrical shape.
- The present axisymmetric wave packet model is radially polarized, does not consist of purely transverse elementary waves as in conventional theory, has a nonzero spin and an associated very small rest mass, and a helical-like field structure.
- The spatial dimensions of the present model are limited. The solutions are reconcilable with the concepts of needle radiation proposed by Einstein. This provides an explanation of the photoelectric effect in which a photon knocks out an electron from an atom, and of the dot-shaped marks on a screen in two-slit experiments on individual photons as reported by Tsuchiya et al. [14]. As an example with $\cos\alpha = 10^{-4}$ and $\lambda_0 = 3\times10^{-7}$m, equation (44) yields a diameter $2\hat{r} = 10^{-3}$m, and equation (50) results in $2\hat{r} \leqslant 10^{-7}$m when $\varepsilon \leqslant \cos\alpha$ for needle-like radiation.
- The present individual photon model is relevant in respect to particle-wave dualism. A subdivision into a particle and an associated pilot wave is not necessary, because the rest mass merely constitutes an integrating part of the total field energy. The wave packet behaves as an entirety, having particle and wave properties at the same time. There is a particle like behaviour such as by needle radiation and a nonzero rest mass, and a wave-like behaviour in terms of interference between cylindrical waves. The rest mass may make possible "photon oscillations" between different modes [8], such as those of the results (44) and (50).

4 Screw-shaped light

In a review by Battersby [15] new results have been reported on twisted light in which the energy travels along a cork-screw-shaped path. These discoveries are expected to become important in communication and microbiology.

In this section, equations (16)–(18) will be applied to screw-shaped waves with the factor

$$\exp\Big[\mathrm{i}(-\omega t + \bar{m}\varphi + kz)\Big] = \exp(\mathrm{i}\theta_m) \tag{51}$$

and $\bar{m}$ as a positive or negative integer. Since the analysis is similar to that of Section 3.2, we shall leave out its details.

4.1 Shortcomings of the conventional analysis

With Maxwell's equations the system (16)–(18) reduces to

$$\left[D_\rho - \frac{\left(1+\bar{m}^2\right)}{\rho^2}\right](E_r, \mathrm{i}E_\varphi) - \frac{2\bar{m}^2}{\rho^2}(\mathrm{i}E_\varphi, E_r) = 0\,, \tag{52}$$

$$\left[D_\rho - \frac{\bar{m}^2}{\rho^2}\right] E_z = 0\,. \tag{53}$$

For nonzero values of $\bar{m}$, equations (52) combine to

$$\hat{E}_r = c_{1r}\rho^{1\pm\bar{m}} + c_{2r}\rho^{-(1\pm\bar{m})} = \pm\mathrm{i}\hat{E}_\varphi \tag{54}$$

when $1 \pm \bar{m} \neq 0$ and

$$\hat{E}_r = c_{1r0} + c_{2r0}\ln\rho = \pm\mathrm{i}\hat{E}_\varphi \tag{55}$$

when $1 \pm \bar{m} = 0$. Further equation (53) gives

$$\hat{E}_z = c_{1z}\rho^{\bar{m}} + c_{2z}\rho^{-\bar{m}}. \tag{56}$$

As in Section 3.1 these results become divergent.

An even more serious shortcoming is again due to an identically vanishing electric and magnetic field divergence. This makes the axial components E_z and B_z disappear, thus resulting in a vanishing spin.

4.2 Twisted modes in revised theory

For nonzero values of $\bar{m}$, the second term in equation (20) introduces complications. This problem is approached by limiting the analysis to sufficient small $\cos\alpha$, and the dispersion relation to be approximated by relations (23). From

equation (18) can be seen that E_z is of the order of $\cos^2\alpha$ as compared to E_r and E_φ when $\bar{m} \neq 0$. Equation (16) then takes the approximate form

$$E_r \cong -\left(\frac{r}{\bar{m}}\right)\left[1-k^2\left(\cos^2\alpha\right)\left(\frac{r}{\bar{m}}\right)^2\right]\left(\frac{\partial}{\partial r}+\frac{1}{r}\right)\left(\mathrm{i}E_\varphi\right). \quad (57)$$

When inserting this relation into equation (17), the latter is identically satisfied up to the order $\cos^2\alpha$. The component $\mathrm{i}E_\varphi$ can be used as a generating function

$$\mathrm{i}E_\varphi = G_0\, G \qquad G = R(\rho)\,\mathrm{e}^{\mathrm{i}\theta_m}. \quad (58)$$

The analysis proceeds in forming a wave packet of narrow line width, as given in detail elsewhere [9]. The radial forms (43) and (45) lead to effective diameters for which a factor $|\bar{m}|^{3/2}$ has to be added in the denominators of expressions (44) and (50). These diameters also apply to radially polarized dense light beams, because the mass and angular momentum are both proportional to the same number of photons.

5 Boundary conditions and spin of light beams

A light beam of low photon density can merely be regarded as a stream of non-interacting photons. At high photon densities a unidirectional beam of limited cross-section becomes more complex. The observed angular momentum of such a linearly or elliptically polarized beam has been proposed to be due to transverse spatial derivatives at its boundary [3, 16]. The angular momentum which would have existed for the individual photons in the beam core have been imagined to be substituted by the momentum generated in the boundary region. However, the detailed explanation is so far not clear.

In this section a dense light beam is considered where the individual photons in the beam core overlap each other, such as to form a plane classical electromagnetic (EM) wave as conceived in earlier considerations [7, 8]. Outside the beam there is a vacuum region. The main purpose is to analyze the boundary conditions and the angular momentum of this system.

5.1 Definitions of beam conditions

A beam is considered having an arbitrary cross-section of large size as compared to its characteristic wave lengths. The analysis of a general case with elliptically polarized modes of various wave lengths can be subdivided into a study on each of the included elementary and linearly polarized modes of a specific wave length. A further simplification is provided by the narrow boundary region where the boundary conditions can be applied separately to every small local segment. The analysis is then limited to one linearly polarized core wave. In its turn, this wave can be subdivided into two waves of the same frequency, but having electric field vectors which are perpendicular and parallel to the local segment.

The following analysis starts with an investigation in terms of Maxwell's equations. It then proceeds by the revised theory, first on a flat-shaped configuration with main electric field vectors being either perpendicular or parallel to the boundary. Finally a simplified study is undertaken on a beam of circular cross-section.

5.2 Shortcomings of the conventional analysis

We consider a beam which propagates in the z-direction of a frame (x, y, z) and where every field quantity Q has the form $\hat{Q}(x, y)\exp\left[\mathrm{i}\left(-\omega t + kz\right)\right]$. The conventional limit of the field equation (13) then reduces to

$$\left[k_0^2 - \left(\frac{\partial^2}{\partial x^2}+\frac{\partial^2}{\partial y^2}\right)\right](\mathbf{E}, \mathbf{B}) = 0 \quad (59)$$

where $k_0^2 = k^2 - \left(\frac{\omega}{c}\right)^2$ can have any value. A separable form $X(x)\cdot Y(y)$ of each component then leads to

$$k_0^2 = k_{0x}^2 + k_{0y}^2\,, \quad X''/X = k_{0x}^2\,, \quad Y''/Y = k_{0y}^2\,, \quad (60)$$

where k_{0x}^2 and k_{0y}^2 can have any sign and value. The solution for the electric field becomes

$$\begin{aligned}\bar{E}_\nu = &\left[a_{\nu_1}\exp(k_{0x}x) + a_{\nu_2}\exp(-k_{0x}x)\right]\cdot \\ &\cdot\left[b_{\nu_1}\exp(k_{0y}y) + b_{\nu_2}\exp(-k_{0y}y)\right]\end{aligned} \quad (61)$$

with $\nu = x, y, z$ and an analogous form for the magnetic field. The divergences have to vanish identically. With the solution (61), this leads to a purely transverse wave with zero spin as shown by equation (12). Further one should either have $E_x = E_y = 0$ and $B_x = B_y = 0$, or $k_{0x} = k_{0y} = k_0 = 0$ and $\omega^2 = k^2c^2$. There are no transverse derivatives in an exact solution.

The alternative has also be taken into account where k_0 is zero already from the beginning. Then

$$\bar{E}_\nu = \left(c_{\nu_1}x + c_{\nu_2}\right)\left(d_{\nu_1}y + d_{\nu_2}\right). \quad (62)$$

With these solutions inserted into the condition of vanishing field divergence

$$\bar{E}_x = c_0\,x + c_1\,y + c_2\,,\ \ \bar{E}_y = c_3\,x - c_0\,y + c_4\,,\ \ \bar{E}_z = 0\,. \quad (63)$$

All the obtained solutions thus have a vanishing spin, and are not reconcilable with a beam of spatially limited cross-section.

5.3 Revised equations of flat-shaped geometry

We now proceed to a revised analysis of flat-shaped beam geometry. With z still in the direction of propagation and x along the normal of the boundaries of a slab-like beam, all field quantities become independent of y. The velocity vector is given by a form similar to (15), having a small

component C_y along the boundary and a large component C_z in the direction of propagation.

Now equation (14) yields the same dispersion relation as (23), and the three component equations reduce to

$$E_x = -\frac{\mathrm{i}}{k\cos^2\alpha}\frac{\partial E_z}{\partial x}\,, \tag{64}$$

$$\left(k^2\cos^2\alpha - \frac{\partial^2}{\partial x^2}\right)\left(E_y + \frac{\sin\alpha}{\cos\alpha}E_z\right) = 0\,. \tag{65}$$

Consequently E_z can be considered as a generating function of E_x and E_y. One solution of equation (65) is found where E_y has the same spatial profile as E_z and

$$E_y = -\frac{\sin\alpha}{\cos\alpha}\,E_z\,. \tag{66}$$

5.4 Two special cases of flat-shaped geometry

A flat-shaped (slab-like) beam is now considered which has a core region $-a < x < a$ and two narrow boundary regions, $-(a+b) < x < -a$ and $a < x < a+b$, with thickness $d = b - a$. With the frame chosen in Section 5.3, we first consider the case where E_x is the main electric component. Within the core a homogeneous linearly polarized EM wave is assumed to exist, having the constant components E_{0x} and B_{0y}. In the boundary region an axial field component E_z is chosen which increases linearly with x, from zero at $x = a$, and in such a way that E_x of equation (64) becomes matched to E_{0x} at $x = a$. In the same region the field E_z further passes a maximum, and then drops to zero at the vacuum interface $x = a + b$. The resulting field E_x is reversed in the boundary layer, having a maximum strength of the order of E_{0x}. With $E_{0x} = \mathrm{O}(1)$ in respect to the smallness parameter $\cos\alpha$, equations (64) and (66) show that $E_z = \mathrm{O}(\cos^2\alpha)$ and $E_y = \mathrm{O}(\cos\alpha)$. Here B_y is of zero order and matches B_{0y} at the edge of the core. The components of the Poynting vector are $S_x = 0$ and

$$S_y \cong c\,(\cos\alpha)\,\varepsilon_0\,E_x^2\,, \qquad S_z \cong c\,(\sin\alpha)\,\varepsilon_0\,E_x^2\,. \tag{67}$$

Thus there is a primary flow of momentum S_z in the direction of propagation, and a secondary flow S_y along the boundary, but no flow across it. The field energy density finally becomes $w_f \cong \varepsilon_0 E_x^2$.

Turning to the second case where E_y is the main electric component and is parallel to the boundary, there is an EM core wave with the components E_{0y} and B_{0x}. In a small range of x near $x = a$ the axial field E_z is assumed to be constant, and $E_x = 0$. Relation (66) then makes it possible to match E_y to E_{0y} at $x = a$. Moreover, the field E_z is chosen to decrease towards zero when approaching the outer boundary $x = a + b$. According to equation (64) the field E_x increases from zero at $x = a$ to a maximum, and then drops towards zero when approaching the outer boundary at $x = a + b$. Combination of equations (64) and (66) yields

$$|E_x/E_y| = \lambda/2\pi L_{cy}\cos\alpha \tag{68}$$

where $\lambda = 2\pi/k$ and L_{cy} stands for the characteristic length of the derivative of E_y. As an example with $\lambda/L_{cy} = 10^{-4}$ and $\cos\alpha = 10^{-4}$, equation (68) gives a ratio of about 0.16. The Poynting vector components become $S_x = 0$ and

$$S_y = c\,(\cos\alpha)\,\varepsilon_0\,E_y^2\left[1 + \sin^2\alpha\,(E_x/E_y)^2\right]/\sin^2\alpha\,, \tag{69}$$

$$S_z = c\,\varepsilon_0\,E_y^2\left[1 + \sin^2\alpha\,(E_x/E_y)^2\right]/\sin^2\alpha\,. \tag{70}$$

The energy density is $w_f \cong \varepsilon_0 E_y^2$ as long as $E_x^2 \ll E_y^2$.

5.5 Simplified analysis on the spin of a beam

A simplified analysis is performed on a beam of circular cross-section. The frame is redefined for a linearly polarized EM core wave $\mathbf{E}_0 = (E_0, 0, 0)$ and $\mathbf{B}_0 = (0, B_0, 0)$. With the angle θ between the y-direction and the radial direction, the electric components are

$$E_{0\perp} = E_0\sin\theta\,, \qquad E_{0\parallel} = E_0\cos\theta \tag{71}$$

in the perpendicular and parallel directions of the boundary. The solutions of Section 5.4 are now matched to these core components at the inner surface of the boundary layer. The energy density is $w_f = \varepsilon_0\,\mathbf{E}^2$ where $\mathbf{E}^2 = \mathbf{E}_0^2$ at the edge of the beam core.

With the numerical example of Section 5.4 as a reference where $E_x^2 \ll E_y^2$, the Poynting vector components in the transverse direction now add up to

$$S_t = c(\cos\alpha)\,\varepsilon_0\,\mathbf{E}^2\,. \tag{72}$$

The energy density of the beam core can be written as

$$\varepsilon E_0^2 = n_p hc/\lambda \tag{73}$$

where n_p is the number of equivalent photons per unit volume. With the spin $h/2\pi$ of each photon, the core contains a total angular momentum per unit length

$$s_c = r_0^2 n_p h/2 = \varepsilon_0 E_0^2 \lambda r_0^2/2c \tag{74}$$

with r_0 standing for the core radius. From equations (12) and (72) the angular momentum generated per axial length in the boundary layer becomes on the other hand

$$s_b = 2\pi(\cos\alpha)\,\varepsilon\,E_0^2\,f_E\,r_0^2\,d/c \tag{75}$$

where d is the thickness of the boundary layer and $f_E < 1$ is a profile factor of $\mathbf{E}^2$ across the layer. Thus

$$\frac{s_b}{s_c} = \frac{4\pi\,(\cos\alpha)f_E\,d}{\lambda}\,. \tag{76}$$

Here $s_b = s_c$ when the equivalent angular momentum of the core is compensated by that generated in the boundary layer. As an example, for $\lambda = 3\times10^{-7}$m, $f_E = 0.2$ and $d = 10^{-3}$m this becomes possible when $\cos\alpha = 10^{-4}$.

5.6 Summary of the analysis on a dense light beam

- Conventional theory leads to a vanishing spin, and is not reconcilable with a beam of limited extensions in its transverse directions. A limited cross-section can only appear in an approximate solution when the characteristic lengths of the transverse derivatives are much larger than the included wavelengths.
- The present revised theory leads to a Poynting vector with a primary component in the direction of propagation, and a secondary component in the transverse directions which generates a spin.
- The angular momentum represented by the spin of the photons in the beam core is substituted by a real spin generated in the boundary layer.
- Even large transverse spatial derivatives and a corresponding limited beam cross-section can exist according to the revised theory.

6 Conclusions

Conventional theory which is based on Maxwell's equations and the associated quantum electrodynamical concepts in the vacuum state includes the condition of zero electric field divergence. When being applied to the physics of the individual photon and of dense light beams, such a theory exhibits a number of discrepancies from experimental evidence. These shortcomings include the absence of spin and of spatially limited geometry in the directions which are transverse to that of the propagation.

The present revised theory on the vacuum state is based on a nonzero electric field divergence which introduces an additional degree of freedom into the field equations, thereby changing the latter and their solutions substantially as compared to the conventional ones. The resulting extended quantum electrodynamics (EQED) makes it possible for both individual photons and for dense light beams to possess a nonzero spin, and to have a spatially limited geometry in the transverse directions. Moreover the individual photon models behave as an entirety in having both particle and wave properties. There are wave-packet solutions with the character of needle radiation which become reconcilable with the photoelectric effect, and with the dot-shaped marks and interference patterns due to individual photons in two-slit experiments.

References

1. Feynman R. P. Lectures in physics: mainly electromagnetism and matter. Addison-Wesley, Reading, Massachusetts, 1964, p. 28.
2. Schiff L. I. Quantum Mechanics. McGraw-Hill Book Comp. Inc., New York, 1949, Ch. XIV, Ch. IV.
3. Heitler W. The quantum theory of radiation. Third edition, Clarendon Press, Oxford, 1954, Appendix and Ch. II, p. 58.
4. Lehnert B. An extended formulation of Maxwell's equations. *Spec. Sci. Technol.*, 1986, v. 9, 177–184.
5. Lehnert B. Basic concepts of an extended electromagnetic theory. *Spec. Sci. Technol.*, 1994, v. 17, 259–273.
6. Lehnert B., Roy S. Extended electromagnetic theory. World Scientific Publishers, Singapore, 1998.
7. Lehnert B. Optical effects of an extended electromagnetic theory. In: *Advances in Chemical Physics*, v. 119. Edited by M. W. Evans, I. Prigogine, and S. A. Rice, John Wiley and Sons, Inc., New York, 2001, 1–77.
8. Lehnert B. Photon wave and particle concepts of an extended electromagnetic theory. *Physics Scripta*, 2002, v. 66, 105–113.
9. Lehnert B. Screw-shaped light in extended electromagnetics. *Physics Scripta*, 2005, v. 72, 359–365.
10. Casimir H. B. G. On the attraction between two perfectly conducting plates. *Proc. K. Ned. Akad. Wet.*, 1948, v. 51, 793–795.
11. de Broglie L., Vigier J. P. Photon mass and new experimental result on longitudinal displacements of laser beams near total reflection. *Phys. Rev. Lett.*, 1872, v. 28, 1001–1004.
12. Evans M., Vigier J. P. The enigmatic photon. Kluwer Academic Publishers, Dordrecht, v. 1, 1994, v. 2, 1995.
13. Thomson Sir J. J. The nature of light. *Nature*, 1936, v. 137, 232–233.
14. Tsuchiya Y., Inuzuka E., Kurono T., Hosoda M. Photon-counting imaging and its applications. *Advances in Electronics and Electron Physics*, 1985, v. 64A, 21–31.
15. Battersby S. Twisting the light away. *New Scientist*, 2004, 12 June, 37–40.
16. Ditchburn R. W. Light. Academic Press, London, New York, San Francisco, 1976, Third Edition, Sec. 17.24.

On Area Coordinates and Quantum Mechanics in Yang's Noncommutative Spacetime with a Lower and Upper Scale

Carlos Castro

Center for Theoretical Studies of Physical Systems, Clark Atlanta University, Atlanta, Georgia, USA

E-mail: czarlosromanov@yahoo.com; castro@ctsps.cau.edu

We explore Yang's Noncommutative space-time algebra (involving *two* length scales) within the context of QM defined in Noncommutative spacetimes and the holographic area-coordinates algebra in Clifford spaces. Casimir invariant wave equations corresponding to Noncommutative coordinates and momenta in d-dimensions can be recast in terms of *ordinary* QM wave equations in $d+2$-dimensions. It is conjectured that QM over Noncommutative spacetimes (Noncommutative QM) may be described by ordinary QM in *higher* dimensions. Novel Moyal-Yang-Fedosov-Kontsevich star products deformations of the Noncommutative Poisson Brackets are employed to construct star product deformations of scalar field theories. Finally, generalizations of the Dirac-Konstant and Klein-Gordon-like equations relevant to the physics of D-branes and Matrix Models are presented.

1 Introduction

Yang's noncommutative space time algebra [1] is a generalization of the Snyder algebra [2] (where now both coordinates and momenta are not commuting) that has received more attention recently, see for example [3] and references therein. In particular, Noncommutative p-brane actions, for even $p+1 = 2n$-dimensional world-volumes, were written explicitly [15] in terms of the *novel* Moyal-Yang (Fedosov-Kontsevich) star product deformations [11, 12] of the Noncommutative Nambu Poisson Brackets (NCNPB) that are associated with the *noncommuting* world-volume coordinates q^A, p^A for $A = = 1, 2, 3, \ldots n$. The latter noncommuting coordinates obey the noncommutative Yang algebra with an ultraviolet L_P (Planck) scale and infrared (R) scale cutoff. It was shown why the novel p-brane actions in the "classical" limit $\hbar_{\text{eff}} = = \hbar L_P/R \to 0$ still acquire nontrivial noncommutative *corrections* that differ from ordinary p-brane actions. Super p-branes actions in the light-cone gauge are also amenable to Moyal-Yang star product deformations as well due to the fact that p-branes moving in flat spacetime backgrounds, in the light-cone gauge, can be recast as gauge theories of volume-preserving diffeomorphisms. The most general construction of noncommutative super p-branes actions based on non (anti) commuting superspaces and quantum group methods remains an open problem.

The purpose of this work is to explore further the consequences of Yang's Noncommutative spacetime algebra within the context of QM in Noncommutative spacetimes and the holographic area-coordinates algebra in Clifford spaces [14]. In section 2 we study the interplay among Yang's Noncommutative spacetime algebra and the former area-coordinates algebra in Clifford spaces. In section 3 we show how Casimir invariant wave equations corresponding to Noncommutative coordinates and momenta in D-dimensions, can be recast in terms of ordinary QM wave equations in $D+2$-dimensions. In particular, we shall present explicit solutions of the D'Alambertian operator in the *bulk* of AdS spaces and explain its correspondence with the Casimir invariant wave equations associated with the Yang's Noncommutative spacetime algebra at the projective *boundary* of the conformally compactified AdS spacetime. We conjecture that QM over Noncommutative spacetimes (Noncommutative QM) may be described by ordinary QM in *higher* dimensions.

In section 4 we recur to the *novel* Moyal-Yang (Fedosov-Kontsevich) star products [11, 12] deformations of the Noncommutative Poisson Brackets to construct Moyal-Yang star product deformations of scalar field theories. The role of star products in the construction of p-branes actions from the large N limit of $SU(N)$ Yang-Mills can be found in [6] and in the Self-Dual Gravity/$SU(\infty)$ Self Dual Yang-Mills relation in [7, 8, 9, 10]. Finally, in the conclusion 5, we present the generalizations of the Dirac-Konstant equations (and their "square" Klein-Gordon type equations) that are relevant to the incorporation of fermions and the physics of D-branes and Matrix Models.

2 Noncommutative Yang's spacetime algebra in terms of area-coordinates in Clifford spaces

The main result of this section is that there is a *subalgebra* of the C-space operator-valued coordinates [13] which is *isomorphic* to the Noncommutative Yang's spacetime algebra [1, 3]. This, in conjunction to the discrete spectrum of angular momentum, leads to the discrete area quantization in multiples of Planck areas. Namely, the $4D$ Yang's Noncommutative space-time algebra [3] (written in terms of $8D$ phase-space coordinates) is isomorphic to the 15-dimensional *subalgebra* of the C-space operator-valued coordinates associated with the *holographic areas* of C-space. This connection

between Yang's algebra and the $6D$ Clifford algebra is possible because the $8D$ phase-space coordinates x^μ, p^μ (associated to a $4D$ spacetime) have a one-to-one correspondence to the $\hat{X}^{\mu 5}$; $\hat{X}^{\mu 6}$ holographic area-coordinates of the C-space (corresponding to the $6D$ Clifford algebra). Furhermore, Tanaka [3] has shown that the Yang's algebra [1] (with 15 generators) is related to the $4D$ conformal algebra (15 generators) which in turn is isomorphic to a subalgebra of the $4D$ Clifford algebra because it is known that the 15 generators of the $4D$ conformal algebra $SO(4,2)$ can be explicitly realized in terms of the $4D$ Clifford algebra as shown in [13].

The correspondence between the holographic area coordinates $X^{AB} \leftrightarrow \lambda^2 \Sigma^{AB}$ and the angular momentum variables when $A, B = 1, 2, 3, \ldots 6$ yields an isomorphism between the holographic area coordinates algebra in Clifford spaces [14] and the noncommutative Yang's spacetime algebra in $D = 4$. The scale λ is the ultraviolet lower Planck scale. We begin by writing the exchange algebra between the position and momentum coordinates encapsulated by the commutator

$$\begin{aligned} &\left[\hat{X}^{\mu 6}, \hat{X}^{56}\right] = -i\lambda^2 \eta^{66} \hat{X}^{\mu 5} \;\leftrightarrow \\ &\left[\frac{\lambda^2 R}{\hbar}\,\hat{p}^\mu,\ \lambda^2 \Sigma^{56}\right] = -i\lambda^2 \eta^{66} \lambda \hat{x}^\mu \end{aligned} \tag{2.1}$$

from which we can deduce that

$$\left[\hat{p}^\mu,\ \Sigma^{56}\right] = -i\eta^{66} \frac{\hbar}{\lambda R}\,\hat{x}^\mu, \tag{2.2}$$

hence, after using the definition $\mathcal{N} = (\lambda/R)\Sigma^{56}$, where R is the infrared upper scale, one has the exchange algebra commutator of p^μ and $\mathcal{N}$ of the Yang's spacetime algebra given by

$$[\hat{p}^\mu, \mathcal{N}] = -i\eta^{66} \frac{\hbar}{R^2}\,\hat{x}^\mu. \tag{2.3}$$

From the commutator

$$\begin{aligned} &\left[\hat{X}^{\mu 5}, \hat{X}^{56}\right] = -\left[\hat{X}^{\mu 5}, \hat{X}^{65}\right] = i\eta^{55} \lambda^2 \hat{X}^{\mu 6} \;\leftrightarrow \\ &\left[\lambda \hat{x}^\mu, \lambda^2 \Sigma^{56}\right] = i\eta^{55} \lambda^2 \lambda^2 \frac{R}{\hbar}\,\hat{p}^\mu \end{aligned} \tag{2.4}$$

we can deduce that

$$\left[\hat{x}^\mu, \Sigma^{56}\right] = i\eta^{55} \frac{\lambda R}{\hbar}\,\hat{p}^\mu \tag{2.5}$$

and after using the definition $\mathcal{N} = (\lambda/R)\Sigma^{56}$ one has the exchange algebra commutator of x^μ and $\mathcal{N}$ of the Yang's spacetime algebra

$$[\hat{x}^\mu, \mathcal{N}] = i\eta^{55} \frac{\lambda^2}{\hbar}\,\hat{p}^\mu. \tag{2.6}$$

The other relevant holographic area-coordinates commutators in C-space are

$$\left[\hat{X}^{\mu 5}, \hat{X}^{\nu 5}\right] = -i\eta^{55} \lambda^2 \hat{X}^{\mu\nu} \leftrightarrow [\hat{x}^\mu, \hat{x}^\nu] = -i\eta^{55} \lambda^2 \Sigma^{\mu\nu} \tag{2.7}$$

that yield the noncommuting coordinates algebra after having used the representation of the C-space operator holographic area-coordinates

$$i\hat{X}^{\mu\nu} \leftrightarrow i\lambda^2 \frac{1}{\hbar}\,\mathcal{M}^{\mu\nu} = i\lambda^2 \Sigma^{\mu\nu}, \quad i\hat{X}^{56} \leftrightarrow i\lambda^2 \Sigma^{56}, \tag{2.8}$$

where we appropriately introduced the Planck scale λ as one should to match units. From the correspondence

$$\hat{p}^\mu = \frac{\hbar}{R}\,\Sigma^{\mu 6} \leftrightarrow \frac{\hbar}{R}\frac{1}{\lambda^2}\,\hat{X}^{\mu 6} \tag{2.9}$$

one can obtain nonvanishing momentum commutator

$$\left[\hat{X}^{\mu 6}, \hat{X}^{\nu 6}\right] = -i\eta^{66} \lambda^2 \hat{X}^{\mu\nu} \leftrightarrow [\hat{p}^\mu, \hat{p}^\nu] = -i\eta^{66} \frac{\hbar^2}{R^2} \Sigma^{\mu\nu}. \tag{2.10}$$

The signatures for AdS_5 space are $\eta^{55} = +1$; $\eta^{66} = -1$ and for the *Euclideanized* AdS_5 space are $\eta^{55} = +1$ and $\eta^{66} = +1$. Yang's space-time algebra corresponds to the latter case. Finally, the *modified* Heisenberg algebra can be read from the following C-space commutators

$$\begin{aligned} &\left[\hat{X}^{\mu 5}, \hat{X}^{\nu 6}\right] = i\eta^{\mu\nu} \lambda^2 \hat{X}^{56} \;\leftrightarrow \\ &[\hat{x}^\mu, \hat{p}^\mu] = i\hbar \eta^{\mu\nu} \frac{\lambda}{R}\,\Sigma^{56} = i\hbar \eta^{\mu\nu} \mathcal{N}. \end{aligned} \tag{2.11}$$

Eqs-(2.1–2.11) are the defining relations of Yang's Noncommutative $4D$ spacetime algebra [1] involving the $8D$ phase-space variables. These commutators obey the Jacobi identities. There are other commutation relations like $[\mathcal{M}^{\mu\nu}, x^\rho], \ldots$ that we did not write down. These are just the well known rotations (boosts) of the coordinates and momenta.

When $\lambda \to 0$ and $R \to \infty$ one recovers the ordinary *commutative* spacetime algebra. The Snyder algebra [2] is recovered by setting $R \to \infty$ while leaving λ intact. To recover the ordinary Weyl-Heisenberg algebra is more subtle. Tanaka [3] has shown the the *spectrum* of the operator $\mathcal{N} = (\lambda/R)\Sigma^{56}$ is discrete given by $n(\lambda/R)$. This is not suprising since the angular momentum generator $\mathcal{M}^{56}$ associated with the *Euclideanized* AdS_5 space is a rotation in the now compact $x^5 - x^6$ directions. This is not the case in AdS_5 space since $\eta^{66} = -1$ and this timelike direction is no longer compact. Rotations involving timelike directions are equivalent to noncompact boosts with a continuous spectrum.

In order to recover the standard Weyl-Heisenberg algebra from Yang's Noncommutative spacetime algebra, and the standard uncertainty relations $\Delta x \Delta p \geqslant \hbar$ with the ordinary $\hbar$ term, rather than the $n\hbar$ term, one needs to take the limit $n \to \infty$ limit in such a way that the net combination of $n\frac{\lambda}{R} \to 1$. This can be attained when one takes the *double* scaling limit of the quantities as follows

$$\begin{aligned} &\lambda \to 0, \quad R \to \infty, \quad \lambda R \to L^2, \\ &\lim_{n\to\infty} n\frac{\lambda}{R} = n\frac{\lambda^2}{\lambda R} = \frac{n\lambda^2}{L^2} \to 1. \end{aligned} \tag{2.12}$$

From eq-(2.12) one learns then that

$$n\lambda^2 = \lambda R = L^2. \tag{2.13}$$

The spectrum n corresponds to the quantization of the angular momentum operator in the $x^5 - x^6$ direction (after

embedding the $5D$ hyperboloid of throat size R onto $6D$). Tanaka [3] has shown why there is a *discrete spectra* for the *spatial* coordinates and *spatial* momenta in Yang's spacetime algebra that yields a *minimum* length λ (ultraviolet cutoff in energy) and a minimum momentum $p=\hbar/R$ (maximal length R, infrared cutoff). The energy and temporal coordinates had a continous spectrum.

The physical interpretation of the double-scaling limit of eq-(2.12) is that the the area $L^2=\lambda R$ becomes now *quantized* in units of the Planck area λ^2 as $L^2=n\lambda^2$. Thus the quantization of the area (via the double scaling limit) $L^2=\lambda R=n\lambda^2$ is a result of the *discrete* angular momentum spectrum in the x^5-x^6 directions of the Yang's Noncommutative spacetime algebra when it is realized by (angular momentum) differential operators acting on the *Euclideanized* AdS_5 space (two branches of a $5D$ hyperboloid embedded in $6D$). A general interplay between quantum of areas and quantum of angular momentum, for arbitrary values of spin, in terms of the square root of the Casimir $\mathbf{A}\sim\lambda^2\sqrt{j(j+1)}$, has been obtained a while ago in Loop Quantum Gravity by using spin-networks techniques and highly technical area-operator regularization procedures [4].

The advantage of this work is that we have arrived at similar (not identical) area-quantization conclusions in terms of minimal Planck areas and a discrete angular momentum spectrum n via the double scaling limit based on Clifford algebraic methods (C-space holographic area-coordinates). This is not surprising since the norm-squared of the holographic Area operator has a correspondence with the quadratic Casimir $\Sigma_{AB}\Sigma^{AB}$ of the conformal algebra $SO(4,2)$ ($SO(5,1)$ in the Euclideanized AdS_5 case). This quadratic Casimir must not be confused with the $SU(2)$ Casimir J^2 with eigenvalues $j(j+1)$. Hence, the correspondence given by eqs-(2.3–2.8) gives $\mathbf{A}^2\leftrightarrow\lambda^4\Sigma_{AB}\Sigma^{AB}$.

In [5] we have shown why AdS_4 gravity with a topological term; i. e. an Einstein-Hilbert action with a cosmological constant plus Gauss-Bonnet terms can be obtained from the vacuum state of a **BF**-Chern-Simons-Higgs theory *without* introducing by *hand* the zero torsion condition imposed in the McDowell-Mansouri-Chamsedine-West construction. One of the most salient features of [5] was that a *geometric mean* relationship was found among the cosmological constant Λ_c, the Planck area λ^2 and the AdS_4 throat size squared R^2 given by $(\Lambda_c)^{-1}=(\lambda)^2(R^2)$. Upon setting the throat size to be of the order of the Hubble scale R_H and $\lambda=L_P$ (Planck scale), one recovers the observed value of the cosmological constant $L_P^{-2}R_H^{-2}=L_P^{-4}(L_P/R_H)^2\sim 10^{-120}M_P^4$. A similar geometric mean relation is also obeyed by the condition $\lambda R=$ $=L^2(=n\lambda^2)$ in the double scaling limit of Yang's algebra which suggests to identify the cosmological constant as $\Lambda_c=$ $=L^{-4}$. This geometric mean condition remains to be investigated further. In particular, we presented the preliminary steps how to construct a Noncommutative Gravity via the Vasiliev-Moyal star products deformations of the $SO(4,2)$ algebra used in the study of higher conformal massless spin theories in AdS spaces by taking the inverse-throat size $1/R$ as a deformation parameter of the $SO(4,2)$ algebra. A Moyal deformation of ordinary Gravity via $SU(\infty)$ gauge theories was advanced in [7].

3 Noncommutative QM in Yang's spacetime from ordinary QM in higher dimensions

In order to write wave equations in non-commuting spacetimes we start with a Hamiltonian written in *dimensionless* variables involving the terms of the relativistic oscillator (let us say oscillations of the center of mass) and the rigid rotor/top terms (rotations about the center of mass)

$$H=\left(\frac{p_\mu}{\hbar/R}\right)^2+\left(\frac{x_\mu}{L_P}\right)^2+\left(\Sigma^{\mu\nu}\right)^2 \qquad (3.1)$$

with the fundamental difference that the coordinates x^μ and momenta p^μ obey the non-commutative Yang's space time algebra. For this reason one *cannot* naively replace p^μ any longer by the differential operator $-i\hbar\partial/\partial x^\mu$ nor write the $\Sigma^{\mu\nu}$ generators as $\frac{1}{\hbar}(x^\mu\partial_{x_\nu}-x^\nu\partial_{x_\mu})$. The correct coordinate realization of Yang's noncommutative spacetime algebra requires, for example, embedding the 4-dim space into 6-dim and expressing the coordinates and momenta operators as follows

$$\begin{aligned}
&\frac{p_\mu}{(\hbar/R)}\ \leftrightarrow\ \Sigma^{\mu 6}=i\,\frac{1}{\hbar}\left(X^\mu\partial_{X_6}-X^6\partial_{X_\mu}\right),\\
&\frac{x_\mu}{L_P}\ \leftrightarrow\ \Sigma^{\mu 5}=i\,\frac{1}{\hbar}\left(X^\mu\partial_{X_5}-X^5\partial_{X_\mu}\right),\\
&\Sigma^{\mu\nu}\ \leftrightarrow\ i\,\frac{1}{\hbar}\left(X^\mu\partial_{X_\nu}-X^\nu\partial_{X_\mu}\right),\\
&\mathcal{N}=\Sigma^{56}\ \leftrightarrow\ i\,\frac{1}{\hbar}\left(X^5\partial_{X_6}-X^6\partial_{X_5}\right).
\end{aligned} \qquad (3.2)$$

This allows to express H in terms of the standard angular momentum operators in 6-dim. The $X^A=X^\mu,X^5,X^6$ coordinates ($\mu=1,2,3,4$) and $P^A=P^\mu,P^5,P^6$ momentum variables obey the standard commutation relations of ordinary QM in 6-dim, namely $-\left[X^A,X^B\right]=0$, $\left[P^A,P^B\right]=0$, $\left[X^A,P^B\right]=i\hbar\eta^{AB}$, so that the momentum admits the standard realization as $P^A=-i\hbar\partial/\partial X_A$.

Therefore, concluding, the Hamiltonian H in eq-(3.1) associated with the non-commuting coordinates x^μ and momenta p^μ in $d-1$-dimensions can be written in terms of the standard angular momentum operators in $(d-1)+2=d+1$-dim as $H=\mathcal{C}_2-\mathcal{N}^2$, where $\mathcal{C}_2$ agrees precisely with the quadratic Casimir operator of the $SO(d-1,2)$ algebra in the spin $s=0$ case,

$$\mathcal{C}_2=\Sigma_{AB}\Sigma^{AB}=(X_A\partial_B-X_B\partial_A)(X^A\partial^B-X^B\partial^A). \qquad (3.4)$$

One remarkable feature is that $\mathcal{C}_2$ also agrees with the d'Alambertian operator for the Anti de Sitter Space AdS_d of *unit radius* (throat size) $(D_\mu D^\mu)_{AdS_d}$ as shown by [18].

The proof requires to show that the d'Alambertian operator for the $d+1$-dim embedding space (expressed in terms of the X^A coordinates) is related to the d'Alambertian operator in AdS_d space of *unit* radius expressed in terms of the $z^1, z^2, \ldots, z^d$ *bulk intrinsic* coordinates as

$$(D_\mu D^\mu)_{R^{d+1}} = -\frac{\partial^2}{\partial\rho^2} - \frac{d}{\rho}\frac{\partial}{\partial\rho} + \frac{1}{\rho^2}(D_\mu D^\mu)_{AdS} \Rightarrow$$
$$C_2 = \rho^2 (D_\mu D^\mu)_{R^{d+1}} + \left[(d-1) + \rho\frac{\partial}{\partial\rho}\right]\rho\frac{\partial}{\partial\rho} = (D_\mu D^\mu)_{AdS_d}. \quad (3.5)$$

This result is just the hyperbolic-space generalization of the standard decomposition of the Laplace operator in spherical coordinates in terms of the radial derivatives plus a term containing the square of the orbital angular momentum operator L^2/r^2. In the case of nontrivial spin, the Casimir $C_2 = \Sigma_{AB}\Sigma^{AB} + S_{AB}S^{AB}$ has additional terms stemming from the spin operator.

The quantity $\Phi(z^1, z^2, \ldots, z^d)|_{\text{boundary}}$ restricted to the $d-1$-dim projective boundary of the conformally compactified AdS_d space (of unit throat size, whose topology is $S^{d-2}\times S^1$) is the sought-after solution to the Casimir invariant wave equation associated with the non-commutative x^μ coordinates and momenta p^μ of the Yang's algebra ($\mu = 1, 2, \ldots, d-1$). Pertaining to the boundary of the conformally compactified AdS_d space, there are two radii R_1, R_2 associated with S^{d-2} and S^1, respectively, and which must not be confused with the two scales R, L_P appearing in eq. (3.1). One can choose the units such that the present value of the Hubble scale (taking the Hubble scale as the infrared cutoff) is $R=1$. In these units the Planck scale L_P will be of the order of $L_P \sim 10^{-60}$. In essence, there has been a trade-off of two scales L_P, R with the two radii R_1, R_2.

Once can parametrize the coordinates of $AdS_d = AdS_{p+2}$ by writing there, according to [17], $X_0 = R\cosh(\rho)\cos(\tau)$, $X_{p+1} = R\cosh(\rho)\sin(\tau)$, $X_i = R\sinh(\rho)\Omega_i$.

The metric of $AdS_d = AdS_{p+2}$ space in these coordinates is $ds^2 = R^2\left[-(\cosh^2\rho)d\tau^2 + d\rho^2 + (\sinh^2\rho)d\Omega^2\right]$, where $0\leqslant\rho$ and $0\leqslant\tau<2\pi$ are the global coordinates. The topology of this hyperboloid is $S^1\times R^{p+1}$. To study the causal structure of AdS it is convenient to unwrap the circle S^1 (closed-timelike coordinate τ) to obtain the universal covering of the hyperboloid without closed-timelike curves and take $-\infty\leqslant\tau\leqslant+\infty$. Upon introducing the new coordinate $0\leqslant\theta<\frac{\pi}{2}$ related to ρ by $\tan(\theta) = \sinh(\rho)$, the metric is

$$ds^2 = \frac{R^2}{\cos^2\theta}\left[-d\tau^2 + d\theta^2 + (\sinh^2\rho)\,d\Omega^2\right]. \quad (3.6)$$

It is a conformally-rescaled version of the metric of the Einstein static universe. Namely, $AdS_d = AdS_{p+2}$ can be conformally mapped into one-half of the Einstein static universe, since the coordinate θ takes values $0\leqslant\theta<\frac{\pi}{2}$ rather than $0\leqslant\theta<\pi$. The boundary of the conformally compactified AdS_{p+2} space has the topology of $S^p\times S^1$ (identical to the conformal compactification of the $p+1$-dim Minkowski space). Therefore, the equator at $\theta=\frac{\pi}{2}$ is a *boundary* of the space with the topology of S^p. Ω_p is the solid angle coordinates corresponding to S^p and τ is the coordinate which parametrizes S^1. For a detailed discussion of AdS spaces and the AdS/CFT duality see [17].

The d'Alambertian in AdS_d space (of radius R, later we shall set $R=1$) is

$$D_\mu D^\mu = \frac{1}{\sqrt{g}}\partial_\mu(\sqrt{g}g^{\mu\nu}\partial_\nu) =$$
$$= \frac{\cos^2\theta}{R^2}\left[-\partial_\tau^2 + \frac{1}{(R\tan\theta)^p}\partial_\theta\left((R\tan\theta)^p\partial_\theta\right)\right] + \frac{\mathcal{L}^2}{R^2\tan^2\theta} \quad (3.7)$$

where $\mathcal{L}^2$ is the Laplacian operator in the p-dim sphere S^p whose eigenvalues are $l(l+p-1)$.

The scalar field can be decomposed as follows $\Phi = e^{\omega R\tau}Y_l(\Omega_p)G(\theta)$; the wave equation $(D_\mu D^\mu - m^2)\Phi = 0$ leads to the equation $\left[\cos^2\theta\left(\omega^2 + \partial_\theta^2 + \frac{p}{\tan\theta\cos^2\theta}\partial_\theta\right) + \right.$ $\left. + \frac{l(l+p-1)}{\tan^2\theta} - m^2R^2\right]G(\theta) = 0$, whose solution is

$$G(\theta) = (\sin\theta)^l(\cos\theta)^{\lambda_+}\,{}_2F_1(a,b,c;\sin\theta). \quad (3.8)$$

The hypergeometric function is defined as

$${}_2F_1(a,b,c,z) = \sum\frac{(a)_k(b)_k}{(c)_k k!}z^n, \quad (3.9)$$

where $|z|<1$, $(\lambda)_0 = 1$, $(\lambda)_k = \frac{\Gamma(\lambda+k)}{\Gamma(\lambda)} = \lambda(\lambda+1)(\lambda+2)\ldots(\lambda+k-1)$, $k=1,2,\ldots$, while $a = \frac{1}{2}(l+\lambda_+-\omega R)$, $b = \frac{1}{2}(l+\lambda_+ + \omega R)$, $c = l + \frac{1}{2}(p+1) > 0$, $\lambda_+ = \frac{1}{2}(p+1) \pm \frac{1}{2}\sqrt{(p+1)^2 + 4(mR)^2}$.

The analytical continuation of the hypergeometric function for $|z|\geqslant 1$ is

$${}_2F_1(a,b,c,z) =$$
$$= \frac{\Gamma(c)}{\Gamma(b)\Gamma(c-b)}\int_0^1 t^{b-1}(1-t)^{c-b-1}(1-tz)^{-a}dt \quad (3.10)$$

with $Real(c) > 0$ and $Real(b) > 0$. The boundary value when $\theta = \frac{\pi}{2}$ gives

$$\lim_{z\to 1^-} F(a,b,c;z) = \frac{\Gamma(c)\Gamma(c-a-b)}{\Gamma(c-a)\Gamma(c-b)}. \quad (3.11)$$

Let us study the behaviour of the solution $G(\theta)$ in the massless case: $m=0$, $\lambda_- = 0$, $\lambda_+ = p+1$.

Solutions with $\lambda_+ = p+1$ yield a trivial value of $G(\theta)=0$ at the boundary $\theta=\frac{\pi}{2}$ since $\cos\left(\frac{\pi}{2}\right)^{p+1} = 0$. Solutions with $\lambda_- = 0$ lead to $\cos(\theta)^{\lambda_-} = \cos(\theta)^0 = 1$ *prior* to taking the limit $\theta = \frac{\pi}{2}$. The expression $\cos\left(\frac{\pi}{2}\right)^{\lambda_-} = 0^0$ is ill defined. Upon using l'Hospital rule it yields 0. Thus, the limit $\theta=\frac{\pi}{2}$ must be taken afterwards the limit $\lambda_- = 0$:

$$\lim_{\theta\to\frac{\pi}{2}}\left[\cos(\theta)^{\lambda_-}\right] = \lim_{\theta\to\frac{\pi}{2}}\left[\cos(\theta)^0\right] = \lim_{\theta\to\frac{\pi}{2}}[1] = 1. \quad (3.12)$$

In this fashion the value of $G(\theta)$ is well defined and nonzero at the boundary when $\lambda_- = 0$ and leads to the value of the wavefunction at the boundary of the conformally compactified AdS_d (for $d = p+2$ with radius R)

$$\Phi_{\rm bound} = e^{i\omega\tau} Y_l(\Omega_p) \frac{\Gamma\left(l+\frac{p+1}{2}\right)\Gamma\left(\frac{p+1}{2}\right)}{\Gamma\left(\omega R+\frac{l+p+1}{2}\right)\Gamma\left(-\omega R+\frac{l+p+1}{2}\right)}\,. \quad (3.13a)$$

upon setting the radius of AdS_d space to *unity* it gives

$$\Phi_{\rm bound} = e^{i\omega\tau} Y_l(\Omega_p) \frac{\Gamma\left(l+\frac{p+1}{2}\right)\Gamma\left(\frac{p+1}{2}\right)}{\Gamma\left(\omega+\frac{l+p+1}{2}\right)\Gamma\left(-\omega+\frac{l+p+1}{2}\right)}\,. \quad (3.13b)$$

Hence, $\Phi_{\rm bound}$ in eq-(3.13b) is the solution to the Casimir invariant wave equation in the *massless* $m = 0$ case

$$C_2\Phi = \left[\left(\frac{p_\mu}{\hbar/R}\right)^2 + \left(\frac{x_\mu}{L_P}\right)^2 + \left(\Sigma^{\mu\nu}\right)^2 + \mathcal{N}^2\right]\Phi = 0 \quad (3.14)$$

and (when $R = 1$)

$$\left[\left(\frac{p_\mu}{\hbar/R}\right)^2 + \left(\frac{x_\mu}{L_P}\right)^2 + \left(\Sigma^{\mu\nu}\right)^2\right]\Phi = \left[C_2 - \mathcal{N}^2\right]\Phi = -\omega^2\Phi \quad (3.15)$$

since $\mathcal{N} = \Sigma^{56}$ is the rotation generator along the S^1 component of AdS space. It acts as $\partial/\partial\tau$ only on the $e^{i\omega R\tau}$ piece of Φ. Concluding: $\Phi(z^1, z^2, \ldots, z^d)|_{\rm boundary}$, restricted to the $d-1$-dim projective boundary of the conformally compactified AdS_d space (of *unit* radius and topology $S^{d-2}\times S^1$) given by eq-(3.12), is the sought-after solution to the wave equations (3.13, 3.14) associated with the non-commutative x^μ coordinates and momenta p^μ of the Yang's algebra and where the indices μ range over the dimensions of the *boundary* $\mu = 1, 2, \ldots, d-1$. This suggests that QM over Yang's Noncommutative Spacetimes could be well defined in terms of ordinary QM in *higher* dimensions! This idea deserves further investigations. For example, it was argued by [16] that the *quantized* Nonabelian gauge theory in d dimensions can be obtained as the infrared limit of the corresponding *classical* gauge theory in $d+1$-dim.

4 Star products and noncommutative QM

The ordinary Moyal star-product of two functions in phase space $f(x,p)$, $g(x,p)$ is

$$(f*g)(x,p) = \sum_s \frac{\hbar^s}{s!}\sum_{t=0}^{s}(-1)^t C(s,t)\times \times \left(\partial_x^{s-t}\partial_p^t f(x,p)\right)\left(\partial_x^t\partial_p^{s-t} g(x,p)\right) \quad (4.1)$$

where $C(s,t)$ is the binomial coefficient $s!/t!(s-t)!$. In the $\hbar\to 0$ limit the star product $f*g$ reduces to the ordinary pointwise product fg of functions. The Moyal product of two functions of the $2n$-dim phase space coordinates (q_i, p_i) with $i = 1, 2\ldots n$ is

$$(f*g)(x,p) = \sum_i^n\sum_s \frac{\hbar^s}{s!}\sum_{t=0}^{s}(-1)^t C(s,t)\times \times \left(\partial_{x_i}^{s-t}\partial_{p_i}^t f(x,p)\right)\left(\partial_{x_i}^t\partial_{p_i}^{s-t} g(x,p)\right). \quad (4.2)$$

The noncommutative, associative Moyal bracket is

$$\{f,g\}_{\rm MB} = \frac{1}{i\hbar}\left(f*g - g*f\right). \quad (4.3)$$

The task now is to construct *novel* Moyal-Yang star products based on the noncommutative spacetime Yang's algebra. A novel star product deformations of (super) p-brane actions based on the noncommutative spacetime Yang's algebra where the deformation parameter is $\hbar_{\rm eff} = \hbar L_P/R$, for nonzero values of $\hbar$, was obtained in [15] The modified (noncommutative) Poisson bracket is now given by

$$\begin{aligned}&\{\mathcal{F}(q^m,p^m),\mathcal{G}(q^m,p^m)\}_\Omega = \\ &= (\partial_{q^m}\mathcal{F})\{q^m,q^n\}(\partial_{q^n}\mathcal{G}) + (\partial_{p^m}\mathcal{F})\{p^m,p^n\}(\partial_{p^n}\mathcal{G}) + \\ &+ (\partial_{q^m}\mathcal{F})\{q^m,p^n\}(\partial_{p^n}\mathcal{G}) + (\partial_{p^m}\mathcal{F})\{p^m,q^n\}(\partial_{q^n}\mathcal{G}),\end{aligned} \quad (4.4)$$

where the entries $\{q^m,q^n\}\neq 0$, $\{p^m,p^n\}\neq 0$, and also $\{p^m,q^n\} = -\{q^n,p^m\}$ can be read from the commutators described in section 2 by simply defining the deformation parameter $\hbar_{\rm eff}\equiv\hbar(L_P/R)$. One can generalize Yang's original 4-dim algebra to noncommutative $2n$-dim world-volumes and/or spacetimes by working with the $2n+2$-dim angular-momentum algebra $SO(d,2) = SO(p+1,2) = SO(2n,2)$.

The Noncommutative Poisson brackets $\Omega(q^m,q^n) = \{q^m,q^n\}_{\rm NCPB}$, $\Omega(p^m,p^n) = \{p^m,p^n\}_{\rm NCPB}$, $\Omega(q^m,p^n) = -\Omega(p^n,q^m) = \{q^m,p^n\}_{\rm NCPB}$

$$\Omega(q^m,q^n) = \lim_{\hbar_{\rm eff}\to 0}\frac{1}{i\hbar_{\rm eff}}\left[q^m,q^n\right] = -\frac{L^2}{\hbar}\,\Sigma^{mn}, \quad (4.5a)$$

$$\Omega(p^m,p^n) = \lim_{\hbar_{\rm eff}\to 0}\frac{1}{i\hbar_{\rm eff}}\left[p^m,p^n\right] = -\frac{\hbar}{L^2}\,\Sigma^{mn}, \quad (4.5b)$$

$$\Omega(q^m,p^n) = \lim_{\hbar_{\rm eff}\to 0}\frac{1}{i\hbar_{\rm eff}}\left[q^m,p^n\right] = -\eta^{mn}, \quad (4.5c)$$

defined by above expressions, where Σ^{mn} is the "classical" $\hbar_{\rm eff} = (\hbar L_P/R)\to 0$ limit ($R\to\infty$, $L_P\to 0$, $RL_P = L^2$, $\hbar\neq 0$) of the quantity $\Sigma^{mn} = \frac{1}{\hbar}(X^mP^n - X^nP^m)$, after embedding the $d-1$-dimensional spacetime (boundary of AdS_d) into an ordinary $(d-1)+2$-dimensional one. In the $R\to\infty$, ... limit, the AdS_d space (the hyperboloid) degenerates into a *flat* Minkowski spacetime and the coordinates q^m, p^n, in that infrared limit, *coincide* with the coordinates X^m, P^n. Concluding, in the "classical" limit ($R\to\infty,\ldots$, flat limit) one has

$$\Sigma^{mn}\equiv\frac{1}{\hbar}\left(X^mP^n - X^nP^m\right)\to\frac{1}{\hbar}\left(q^mp^n - q^np^m\right) \quad (4.5d)$$

and then one recovers in that limit the ordinary definition of the angular momentum in terms of commuting coordinates q's and commuting momenta p's.

Denoting the coordinates (q^m, p^m) by Z^m and when the Poisson structure Ω^{mn} is given in terms of *constant* numerical coefficients, the Moyal star product is defined in terms of the deformation parameter $\hbar_{\text{eff}} = \hbar L_P/R$ as

$$(\mathcal{F} * \mathcal{G})(z) \equiv \\ \equiv \exp\left[(i\hbar_{\text{eff}})\Omega^{mn}\partial_m^{(z_1)}\partial_n^{(z_2)}\right]\mathcal{F}(z_1)\mathcal{G}(z_2)|_{z_1=z_2=z} \tag{4.6}$$

where the derivatives $\partial_m^{(z_1)}$ act only on the $\mathcal{F}(z_1)$ term and $\partial_n^{(z_2)}$ act only on the $\mathcal{G}(z_2)$ term. In our case the generalized Poisson structure Ω^{mn} is given in terms of *variable* coefficients, it is a function of the coordinates, then $\partial\Omega^{mn} \neq 0$, since the Yang's algebra is basically an angular momentum algebra, therefore the suitable Moyal-Yang star product given by Kontsevich [11] will contain the appropriate *corrections* $\partial\Omega^{mn}$ to the ordinary Moyal star product.

Denoting by $\partial_m = \partial/\partial z^m = (\partial/\partial q^m; \partial/\partial p^m)$ the Moyal-Yang-Kontsevich star product, let us say, of the Hamiltonian $H(q,p)$ with the density distribution in phase space $\rho(q,p)$ (not necessarily positive definite), $H(q,p) * \rho(q,p)$ is

$$H\rho + i\hbar_{\text{eff}}\Omega^{mn}(\partial_m H\partial_n\rho) + \\ + \frac{(i\hbar_{\text{eff}})^2}{2}\Omega^{m_1n_1}\Omega^{m_2n_2}(\partial^2_{m_1m_2}H)(\partial^2_{n_1n_2}\rho) + \\ + \frac{(i\hbar_{\text{eff}})^2}{3}\left[\Omega^{m_1n_1}(\partial_{n_1}\Omega^{m_2n_2}) \times \right. \\ \left. \times(\partial_{m_1}\partial_{n_2}H\partial_{n_2}\rho - \partial_{m_2}H\partial_{m_1}\partial_{n_2}\rho)\right] + \mathrm{O}(\hbar^3_{\text{eff}}), \tag{4.7}$$

where the explicit components of Ω^{mn} are given by eqs-(4.5a–4.5d). The Kontsevich star product is associative up to second order [11] $(f * g) * h = f * (g * h) + \mathrm{O}(\hbar^3_{\text{eff}})$.

The most general expression of the Kontsevich star product in Poisson manifold is quite elaborate and shall not be given here. Star products in *curved* phase spaces have been constructed by Fedosov [12]. Despite these technical subtlelties it did not affect the final expressions for the "classical" Noncommutative p-brane actions as shown in [15] when one takes the $\hbar_{\text{eff}} \to 0$ "classical" limit. In that limit there are still *nontrivial noncommutative corrections* to the ordinary p-brane actions.

In the Weyl-Wigner-Gronewold-Moyal quantization scheme in phase spaces one writes

$$H(x,p) * \rho(x,p) = \rho(x,p) * H(x,p) = E\rho(x,p), \tag{4.8}$$

where the Wigner density function in phase space associated with the Hilbert space state $|\Psi>$ is

$$\rho(x,p,\hbar) = \frac{1}{2\pi}\int dy\ \Psi^*\Big(x - \frac{\hbar y}{2}\Big)\Psi\Big(x + \frac{\hbar y}{2}\Big)e^{\frac{ipy}{\hbar}} \tag{4.9}$$

plus their higher dimensional generalizations. It remains to be studied if this Weyl-Wigner-Gronewold-Moyal quantization scheme is appropriate to study QM over Noncommutative Yang's spacetimes when we use the above Moyal-Yang-Kontsevich star products. A recent study of the Yang's Noncommutative algebra and *discrete* Hilbert (Buniy-Hsu-Zee) spaces was undertaken by Tanaka [3].

Let us write down the Moyal-Yang-Konstevich star deformations of the field theory Lagrangian corresponding to the scalar field $\Phi = \Phi(X^{AB})$ which depends on the holographic-area coordinates X^{AB} [13]. The reason one should *not* try to construct the star product of $\Phi(x^m) * \Phi(x^n)$ based on the Moyal-Yang-Kontsevich product, is because the latter star product given by eq-(4.7) will introduce explicit *momentum* terms in the r.h.s of $\Phi(x^m) * \Phi(x^m)$, stemming from the expression $\Sigma^{mn} = x^m p^n - x^n p^m$ of eq-(4.5d), and thus it invalidates writing $\phi = \phi(x)$ in the first place. If the Σ^{mn} were *numerical constants*, like Θ^{mn}, then one could write the $\Phi(x^m) * \Phi(x^m)$ in a straightforward fashion as it is done in the literature.

The reason behind choosing $\Phi = \Phi(X^{AB})$ is more clear after one invokes the area-coordinates and angular momentum correspondence discussed in detail in section 2. It allows to properly define the star products. A typical Lagrangian is

$$\mathcal{L} = -\Phi * \partial^2_{X^{AB}}\Phi\big(X^{AB}\big) + \frac{m^2}{2}\Phi\big(X^{AB}\big) * \Phi\big(X^{AB}\big) + \\ + \frac{g^n}{n}\Phi\big(X^{AB}\big) * \Phi\big(X^{AB}\big) * \cdots *_n \Phi\big(X^{AB}\big) \tag{4.10}$$

and leads to the equations of motion

$$-\big(\partial/\partial X^{AB}\big)\big(\partial/\partial X^{AB}\big)\Phi\big(X^{AB}\big) + m^2\Phi\big(X^{AB}\big) + \\ + g^n\,\Phi\big(X^{AB}\big) * \Phi\big(X^{AB}\big) * \cdots *_{n-1}\Phi\big(X^{AB}\big) = 0 \tag{4.11}$$

when the multi-symplectic Ω^{ABCD} form is coordinate-independent, the star product is

$$(\Phi * \Phi)(Z^{AB}) \equiv \exp\Big[\big(i\lambda\Omega^{ABCD}\partial_{X^{AB}}\partial_{Y^{AB}}\big)\Big] \times \\ \times \Phi(X^{AB})\Phi\big(Y^{AB}\big)\big|_{X=Y=Z} = \\ = \exp\Big[\big(\Sigma^{ABCD}\partial_{X^{AB}}\partial_{Y^{AB}}\big)\Big]\Phi\big(X^{AB}\big)\Phi\big(Y^{AB}\big)\big|_{X=Y=Z} \tag{4.12}$$

where Σ^{ABCD} is derived from the structure constants of the holographic area-coordinate algebra in C-spaces [14] as: $\big[X^{AB}, X^{CD}\big] = \Sigma^{ABCD} \equiv iL_P^2\big(\eta^{AD}X^{BC} - \eta^{AC}X^{BD} + \\ + \eta^{BC}X^{AD} - \eta^{BD}X^{AC}\big)$. There are nontrivial derivative terms acting on Σ^{ABCD} in the definition of the star product $(\Phi * \Phi)(Z^{MN})$ as we have seen in the definition of the Kontsevich star product $H(x,p) * \rho(x,p)$ in eq-(4.7). The expansion parameter in the star product is the Planck scale squared $\lambda = L_P^2$. The star product has the same functional form as (4-7) with the only difference that now we are taking derivatives w.r.t the area-coordinates X^{AB} instead of derivatives w.r.t the variables x, p, hence to order $\mathrm{O}(L_P^4)$, the star product is

$$\Phi * \Phi = \Phi^2 + \Sigma^{ABCD}(\partial_{AB}\Phi\,\partial_{CD}\Phi) + \\ + \frac{1}{2}\Sigma^{A_1B_1C_1D_1}\Sigma^{A_2B_2C_2D_2}(\partial^2_{A_1B_1A_2B_2}\Phi)(\partial^2_{C_1D_1C_2D_2}\Phi) + \\ + \frac{1}{3}\big[\Sigma^{A_1B_1C_1D_1}(\partial_{C_1D_1}\Sigma^{A_2B_2C_2D_2}) \times \\ \times(\partial_{A_1B_1}\partial_{A_2B_2}\Phi\,\partial_{C_2D_2}\Phi - B_1 \leftrightarrow B_2)\big]. \tag{4.13}$$

Notice that the powers of iL_P^2 are encoded in the definition of Σ^{ABCD}. The star product is noncommutative but is also nonassociative at the order $O(L_P^6)$ and beyond. The Jacobi identities would be anomalous at that order and beyond. The derivatives acting on Σ^{ABCD} are

$$\begin{aligned}&(\partial_{C_1D_1}\Sigma^{A_2B_2C_2D_2}) = \\ &= iL_P^2\left(\eta^{A_2D_2}\,\delta^{B_2C_2}_{C_1D_1} - \eta^{A_2C_2}\,\delta^{B_2D_2}_{C_1D_1}\right) + \\ &+ iL_P^2\left(\eta^{B_2C_2}\,\delta^{A_2D_2}_{C_1D_1} - \eta^{B_2D_2}\,\delta^{A_2C_2}_{C_1D_1}\right).\end{aligned} \tag{4.14}$$

where $\delta^{AB}_{CD} = \delta^A_C\delta^B_D - \delta^A_D\delta^B_C$ and the higher derivatives like $\partial^2_{A_1B_1C_1D_1}\Sigma^{A_2B_2C_2D_2}$ will be zero.

5 On the generalized Dirac-Konstant equation in Clifford spaces

To conclude this work we will discuss the wave equations relevant to fermions. The "square" of the Dirac-Konstant equation $(\gamma^{[\mu\nu]}\Sigma_{\mu\nu})\,\Psi = \lambda\Psi$ yields

$$\begin{aligned}&(\gamma^{[\mu\nu]}\gamma^{[\rho\tau]}\Sigma_{\mu\nu}\Sigma_{\rho\tau})\,\Psi = \lambda^2\Psi \;\Rightarrow \\ &\Big[\gamma^{[\mu\nu\rho\tau]} + (\eta^{\mu\rho}\gamma^{[\nu\tau]} - \eta^{\mu\tau}\gamma^{[\nu\rho]} + \dots) + \\ &+ (\eta^{\mu\rho}\eta^{\nu\tau}\mathbf{1} - \eta^{\mu\tau}\eta^{\nu\rho}\mathbf{1})\Big]\,\Sigma_{\mu\nu}\Sigma_{\rho\tau}\Psi = \lambda^2\Psi\end{aligned} \tag{5.2}$$

where we omitted numerical factors. The generalized Dirac equation in Clifford spaces is given by [13]

$$\begin{aligned}-i\left(\frac{\partial}{\partial\sigma} + \gamma^\mu\frac{\partial}{\partial x^\mu} + \gamma^{[\mu\nu]}\frac{\partial}{\partial x^{\mu\nu}} + \dots\right. \\ \left. + \gamma^{[\mu_1\mu_2\dots\mu_d]}\frac{\partial}{\partial x^{\mu_1\mu_2\dots\mu_d}}\right)\Psi = \lambda\Psi\,,\end{aligned} \tag{5.3}$$

where $\sigma, x^\mu, x^{\mu\nu}, \dots$ are the generalized coordinates associated with the Clifford *polyvector* in C-space

$$X = \sigma\mathbf{1} + \gamma^\mu x_\mu + \gamma^{\mu_1\mu_2}x_{\mu_1\mu_2} + \dots\gamma^{\mu_1\mu_2\dots\mu_d}x_{\mu_1\mu_2\dots\mu_d} \tag{5.4}$$

after the length scale expansion parameter is set to unity. The generalized Dirac-Konstant equations in Clifford-spaces are obtained after introducing the generalized angular momentum operators [14]

$$\begin{aligned}&\Sigma^{[[\mu_1\mu_2\dots\mu_n][\nu_1\nu_2\dots\nu_n]]} = X^{[[\mu_1\mu_2\dots\mu_n]}P^{[\nu_1\nu_2\dots\nu_n]]} = \\ &= X^{[\mu_1\mu_2\dots\mu_n]}\frac{i\partial}{\partial X_{[\nu_1\nu_2\dots\nu_n]}} - X^{[\nu_1\nu_2\dots\nu_n]}\frac{i\partial}{\partial X_{[\mu_1\mu_2\dots\mu_n]}}\end{aligned} \tag{5.5}$$

by writing

$$\sum_n\gamma^{[[\mu_1\mu_2\dots\mu_n]}\gamma^{[\nu_1\nu_2\dots\nu_n]]}\Sigma_{[[\mu_1\mu_2\dots\mu_n][\nu_1\nu_2\dots\nu_n]]}\Psi = \lambda\Psi \tag{5.6}$$

and where we sum over all polyvector-valued indices (antisymmetric tensors of arbitrary rank). Upon squaring eq-(5.4), one obtains the Clifford space extensions of the $D0$-brane field equations found in [3] which are of the form

$$\begin{aligned}&\left[X^{AB}\frac{\partial}{\partial X_{CD}} - X^{CD}\frac{\partial}{\partial X_{AB}}\right]\times \\ &\times\left[X_{AB}\frac{\partial}{\partial X^{CD}} - X_{CD}\frac{\partial}{\partial X^{AB}}\right]\Psi = 0\,,\end{aligned} \tag{5.6}$$

where $A, B = 1, 2, \dots, 6$. It is warranted to study all these equations in future work and their relation to the physics of D-branes and Matrix Models [3]. Yang's Noncommutative algebra should be extended to superspaces, meaning non-anti-commuting Grassmanian coordinates and noncommuting bosonic coordinates.

Acknowledgments

We are indebted to C. Handy and M. Bowers for encouragement and support.

References

1. Yang C. N. *Phys. Rev.*, 1947, v. 72, 874; *Proc. of the Intern. Conference on Elementary Particles*, 1965, Kyoto, 322–323.
2. Snyder S. *Phys. Rev.*, 1947, v. 71, 38; *ibid.*, 1947, v. 71, 78.
3. Tanaka S. *Nuovo Cimento*, 1999, v. 114B, 49; arXiv: hep-th/0511023; hep-th/0406166; hep-th/0002001; hep-th/0303105.
4. Ashtekar A., Rovelli C., and Smolin L. *Phys. Rev. Lett.*, 1992, v. 69, 237.
5. Castro C. *Mod. Phys. Lett.*, 2002, v. A17, No. 32, 2095.
6. Castro C. arXiv: hep-th/9908115; Ansoldi S., Castro C., and Spallucci E. *Phys. Lett.*, 2001, v. B504, 174; *Class. Quan. Gravity*, 2001, v. 18, L17–L23; *Class. Quan. Gravity*, 2001, v. 18, 2865; Ansoldi S., Castro C., Guendelman E., and Spallucci E. *Class. Quant. Gravity*, 2002, v. 19, L135.
7. Castro C. *General Relativity and Gravitation*, 2004, v. 36, No. 12, 2605.
8. Castro C. *Jour. Math. Phys.*, 1993, v. 34, 681; *Phys. Lett.*, 1992, v. B288, 291.
9. Park Q. H. *Int. Jour. Mod. Phys.*, 1992, v. A7, 1415; Garcia-Compean H., Plebanski J., and Przanowski M. arXiv: hep-th/9702046.
10. Hoppe J. Quantum theory of a relativistic surface. Ph.D Thesis, MIT, 1982.
11. Kontsevich M. arXiv: q-alg/9709040.
12. Fedosov B. *J. Diff. Geom.*, 1994, v. 40, No. 2, 213.
13. Castro C. and Pavšič M. *Progress in Physics*, 2005, v. 1, 31–64.
14. Castro C. *Foundations of Physics*, 2005, v. 35, No. 6, 971.
15. Castro C. *Phys. Lett.*, 2005, v. B626, 209; *Foundations of Physics*, 2000, v. 8, 1301.
16. Biro T., Mueller B., and Matinyan S. arXiv: hep-th/0301131.
17. Aharony O., Gubser S., Maldacena J., Ooguri H., and Oz Y. *Phys. Rep.*, 2000, v. 323, 183.
18. de Witt B. and Herger I. arXiv: hep-th/9908005.

The Journal on Advanced Studies in Theoretical and Experimental Physics, including Related Themes from Mathematics

PROGRESS IN PHYSICS

A quarterly issue scientific journal, registered with the Library of Congress (DC, USA). This journal is peer reviewed and included in the abstracting and indexing coverage of: Mathematical Reviews and MathSciNet (AMS, USA), DOAJ of Lund University (Sweden), Zentralblatt MATH (Germany), Referativnyi Zhurnal VINITI (Russia), etc.

Electronic version of this journal:
http://www.geocities.com/ptep_online

To order printed issues of this journal, contact the Editor in Chief.

Department of Mathematics, University of New Mexico, 200 College Road, Gallup, NM 87301, USA

ISSN: 1555-5534 (print)
ISSN: 1555-5615 (online)

Standard Address Number: 297-5092
Printed in the United States of America

JULY 2006 **VOLUME 3**

CONTENTS

Information for Authors and Subscribers

Progress in Physics has been created for publications on advanced studies in theoretical and experimental physics, including related themes from mathematics. All submitted papers should be professional, in good English, containing a brief review of a problem and obtained results.

All submissions should be composed in LaTeX format using the *Progress in Physics* template. This template can be downloaded from the *Progress in Physics* home page http://www.geocities.com/ptep_online. An abstract and the necessary information about authors should be included in the papers. To submit a paper, mail the files to the Editor in Chief.

All submitted papers should be as brief as possible. Beginning from 2006 we accept only papers no longer than 8 journal pages. Short articles are preferable.

Before preparing your paper please contact Editor in Chief for the current terms and conditions.

All material accepted for the online issue of *Progress in Physics* is printed in the paper version of the journal. To order printed issues, contact the Editor in Chief.

This journal is a non-commercial, academic edition. It is printed from private donations.

Open Letter by the Editor-in-Chief: Declaration of Academic Freedom (Scientific Human Rights)
*The Dutch Translation**

Declaratie van Academische Vrijheid

(Wetenschappelijke Mensenrechten)

Artikel 1: Preambule

Meer dan welke tijd dan ook in de geschiedenis van de mensheid weerspiegelt het begin van de 21e eeuw de diepgaande betekenis van de rol van wetenschap en technologie in menselijke aangelegenheden.

Het krachtige doordringende karakter van de moderne wetenschap en technologie heeft de algemene opvatting doen ontstaan dat verdere hoofdontdekkingen in principe alleen gemaakt kunnen worden door grote onderzoeksgroepen die gesubsidieerd worden door de overheid of het bedrijfsleven en die de beschikking hebben over uitzonderlijk dure instrumentatie en geassisteerd worden door hordes ondersteunend personeel.

Deze algemene opvatting is echter van mythische aard en is in tegenspraak met hoe wetenschappelijke ontdekkingen werkelijk gedaan worden. Grote en kostbare technologische projecten, hoe complex ook, zijn slechts het resultaat van het toepassen van diepe wetenschappelijke inzichten van kleine groepen toegewijde onderzoekers of alleen werkende wetenschappers die vaak in een isolement werken. Een wetenschapper die alleen werkt is nu en in de toekomst, net als in het verleden, in staat om een ontdekking te doen die een substantiële invloed heeft op het lot van de mensheid en die het aangezicht van de hele planeet waar we zo onbetekenend op verblijven verandert.

Fundamentele ontdekkingen worden over het algemeen gedaan door individuen op ondergeschikte posities binnen overheidsinstellingen, onderzoeks- en opleidingsinstituten of commerciële ondernemingen. Onderzoekers worden maar al te vaak beperkt en onderdrukt door instituten en bedrijfsdirecteuren die met een andere agenda werken en vanuit persoonlijke belangen of in het belang van het instituut of het bedrijf of door grootheidswaanzin wetenschappelijke ontdekkingen en onderzoek proberen te controleren en/of toe te passen.

De annalen van de wetenschap zijn bezaaid met wetenschappelijke ontdekkingen die onderdrukt en bespot werden door de gevestigde orde, maar die in latere jaren bekendheid kregen en in het gelijk gesteld werden door de onverbiddelijke opmars van praktische noodzakelijkheid en intellectuele verlichting. Daarnaast zijn de wetenschappelijke annalen bevlekt en besmeurd door plagiaat en opzettelijk valse voorstellingen, daden begaan door mensen zonder scrupules, mensen die gemotiveerd werden door jaloezie en hebzucht. En zo is het nog steeds.

Het doel van deze declaratie is het ondersteunen en bevorderen van het grondbeginsel dat stelt dat wetenschappelijk onderzoek vrij moet zijn van verborgen en openlijk onderdrukkende invloeden van bureaucratische, politieke, religieuze en commerciële aard en dat wetenschappelijke creatie niet minder een mensenrecht is dan andere soortgelijke rechten en wanhopige ondernemingen zoals die voorgesteld zijn in internationale verdragen en het internationale recht.

Wetenschappers die deze declaratie ondersteunen behoren zich eraan houden als teken van solidariteit en betrokkenheid met de internationale wetenschapsgemeenschap en als waarborg voor de rechten van alle wereldburgers om naar vermogen individuele vaardigheden en aanleg te gebruiken voor ongeremde wetenschappelijke creatie, dit ter bevordering van de wetenschap en, naar hun uiterste vermogen als betamelijke burgers in een onbetamelijke wereld, voor de vooruitgang van de mensheid. Wetenschap en technologie zijn veel te lang dienaren van onderdrukking geweest.

Artikel 2: Wie is een wetenschapper

Een wetenschapper is ieder persoon die aan wetenschap doet. Ieder persoon die met een wetenschapper samenwerkt in het ontwikkelen, produceren en voorstellen van ideeën en data tijdens onderzoek of toepassing is ook een wetenschapper.

Artikel 3: Waar wordt er wetenschap geproduceerd

Wetenschappelijk onderzoek kan overal worden uitgevoerd, bijvoorbeeld op een werkplek, tijdens een formele educatiecursus, tijdens een gesponsord academisch programma, in groepen, of als individu die thuis onafhankelijk onderzoek doet.

Artikel 4: Vrijheid van keuze van onderzoeksthema

Veel wetenschappers die werken voor een hogere onderzoeksgraad of in andere onderzoeksprogramma's op academische instituten zoals universiteiten of hogescholen worden verhinderd om te werken aan een onderzoeksonderwerp naar eigen keuze door begeleidende academici en/of administra-

*Original text published in English: *Progress in Physics*, 2006, v. 1, 57–60. Online — http://www.geocities.com/ptep_online/.

Originele Engelse versie door Dmitri Rabounski, hoofdredacteur van het tijdschrift *Progress in Physics*. E-mail: rabounski@yahoo.com.

Vertaald door Eit Gaastra. E-mail: eitgaastra@freeler.nl.

tieve ambtenaren, niet vanwege het ontbreken van ondersteunende faciliteiten maar omdat de academische hiërarchie en/of andere ambtenaren doodeenvoudig de onderzoeksrichting niet goedkeuren als het voorgestelde onderzoek de potentie heeft om voor onrust te zorgen ten aanzien van heersende dogma's en favoriete theorieën, of als het voorgestelde onderzoek de subsidies van andere projecten in gevaar kan brengen. Het gezag van de orthodoxe meerderheid meent zeer vaak een onderzoeksproject te moeten torpederen zodat gezag en budgetten onaangetast blijven. Deze alledaagse praktijken zijn weloverwogen belemmeringen om vrije wetenschappelijke gedachten tegen te houden, ze zijn extreem onwetenschappelijk en crimineel. Ze mogen niet getolereerd worden.

Een wetenschapper die werkt voor een academisch instituut, autoriteit of instelling behoort volkomen vrij te zijn ten aanzien van de keuze van het onderzoeksonderwerp en mag enkel beperkt worden door de materiële ondersteuning en intellectuele vaardigheden die geboden worden door het opleidingsinstituut, de instelling of de autoriteit. Als de wetenschapper een onderzoek uitvoert als lid van een samenwerkende groep behoren de onderzoeksdirecteuren en teamleiders zich te beperken tot een adviserende en consulterende rol met betrekking tot de keuze van een relevant onderzoeksthema door een wetenschapper in de groep.

Artikel 5: Vrijheid van keuze van onderzoeksmethoden

Het gebeurt vaak dat er op een wetenschapper druk wordt uitgeoefend door administratief personeel of begeleidende academici met betrekking tot een onderzoeksprogramma dat in een academische omgeving wordt uitgevoerd. Deze druk wordt uitgeoefend om een wetenschapper er toe te dwingen om andere onderzoeksmethoden te gebruiken dan de wetenschapper heeft gekozen, dit vanwege geen andere reden dan persoonlijke voorkeur, vooroordeel, institutioneel beleid, redactionele voorschriften of verenigde autoriteit. Deze praktijk, die zeer wijdverbreid is, is een weloverwogen ontkenning van de vrijheid van gedachten en kan niet toegestaan worden.

Een non-commerciële of academische wetenschapper heeft het recht om een onderzoeksthema te ontwikkelen op elke redelijke manier en met alle redelijke middelen die hij als het meest effectief beschouwt. De uiteindelijke beslissing ten aanzien van hoe het onderzoek uitgevoerd zal worden behoort te worden gemaakt door de wetenschapper zelf.

Als een non-commerciële of academische wetenschapper werkt als lid van een samenwerkend non-commercieel of academisch team van wetenschappers behoren de projectleiders en onderzoeksdirecteuren enkel adviserende en consulterende rechten te hebben en behoren zij niet op een andere manier de onderzoeksmethoden of het onderzoeksthema van de wetenschapper in de groep te beïnvloeden, matigen of beperken.

Artikel 6: Vrijheid van samenwerking en deelname in een onderzoek

Er is een aanzienlijke hoeveelheid institutionele rivaliteit in de alledaagse praktijk van de moderne wetenschap die samengaat met gevallen van persoonlijke jaloezie en het ten koste van alles zorgen voor het behoud van reputaties, ongeacht het wetenschappelijke wezen. Dit heeft er vaak toe geleid dat wetenschappers belet werden de hulp in te roepen van competente collega's van rivaliserende instituten of anderen zonder enige binding met een academisch instituut. Ook deze praktijken zijn weloverwogen belemmeringen van wetenschappelijke vooruitgang.

Als een non-commerciële wetenschapper assistentie van een ander persoon nodig heeft en deze andere persoon stemt daarin toe dan heeft de wetenschapper de vrijheid om die persoon uit te nodigen om enige of alle mogelijke assistentie te verlenen mits de assistentie binnen het aan het onderzoek verbonden budget valt. Als de assistentie onafhankelijk is van budgetoverwegingen heeft de wetenschapper de vrijheid om de assisterende persoon naar eigen goeddunken in dienst te nemen, vrij van enige bemoeienis door welk ander persoon dan ook.

Artikel 7: Vrijheid van meningsverschil in wetenschappelijke discussies

Door heimelijke jaloezie en oude gevestigde belangen verafschuwt de moderne wetenschap openlijke discussie en verbant zij moedwillig wetenschappers die twijfelen aan de orthodoxe standpunten. Zeer vaak worden uitzonderlijk bekwame wetenschappers die op de tekortkomingen in de gangbare theorieën of interpretatie van data wijzen gelabeld als zonderlingen, zodat hun denkbeelden probleemloos genegeerd kunnen worden. Ze worden publiekelijk en privé bespot en het wordt hen systematisch belet om conferenties, seminaries en colloquia te bezoeken, zodat hun ideeën geen publiek kunnen vinden. Opzettelijke vervalsing van data en het verkeerd voorstellen van theorieën zijn nu veel gebruikte werktuigen van onscrupuleuzen in het onderdrukken van feiten, zowel technisch als historisch. Er hebben zich internationale commissies van wetenschappelijke onverlaten gevormd en deze commissies treden als gastheer op tijdens door henzelf in het leven geroepen internationale conferenties waar alleen hun volgelingen toegestaan wordt om lezingen te presenteren, ongeacht de kwaliteit van de inhoud. Deze commissies halen enorme sommen geld uit de publieke portemonnee om hun gesponsorde projecten te subsidiëren door hun toevlucht te nemen tot misleiding en leugens. Iedere op wetenschappelijke gronden berustende tegenwerping ten aanzien van hun voorstellen wordt op hun instigatie volledig doodgezwegen, zodat geld naar hun projecten kan blijven stromen en hun goedbetaalde banen gegarandeerd blijven. Opponerende wetenschappers zijn in

hun opdracht ontslagen; anderen is het belet om zekerheidbiedende academische aanstellingen te krijgen door een netwerk van corrupte medeplichtigen. In andere situaties zijn sommigen verdreven van een kandidatuur voor programma's voor een hogere graad, zoals promotie naar een doctortitel, omdat ze ideeën hebben geuit die de gangbare theorie zouden kunnen ondermijnen, hoe oud die orthodoxe theorie ook was. Het fundamentele feit dat geen wetenschappelijke theorie definitief noch onschendbaar is en daarom open staat voor discussie en her-evaluatie wordt door hen grondig genegeerd. Ook negeren ze het feit dat een fenomeen meerdere aannemelijke verklaringen kan hebben en brengen ze iedere verklaring die niet in overeenstemming is met de orthodoxe opinie kwaadaardig in diskrediet. Zonder aarzelen nemen ze hun toevlucht tot het gebruik van onwetenschappelijke argumenten om hun vooringenomen mening te rechtvaardigen.

Alle wetenschappers behoren vrij te zijn om over hun onderzoek en het onderzoek van anderen te discussiëren zonder angst om publiekelijk of privé zonder wezenlijke argumenten belachelijk gemaakt te worden of te worden beschuldigd, gekleineerd, betwist of anderszins in diskrediet gebracht te worden door ongefundeerde aantijgingen. Geen wetenschapper mag in een positie gebracht worden waar levensonderhoud of reputatie in gevaar zijn als gevolg van het uiten van een wetenschappelijke mening. Vrijheid van wetenschappelijke expressie behoort een uiterst hoog goed te zijn. Het gebruik van macht in het weerleggen van een wetenschappelijk argument is niet wetenschappelijk en behoort niet gebruikt te worden om te muilkorven, onderdrukken, intimideren, verbannen of anderszins een wetenschapper te dwingen of uit te sluiten. Opzettelijke onderdrukking van wetenschappelijke feiten of argumenten, zowel actief door daad als passief door weglaten, en opzettelijke vervalsing van data om een argument te ondersteunen of om een opponerende opvatting in diskrediet te brengen is wetenschappelijke fraude en dient beschouwd te worden als een wetenschappelijke misdaad. Grondbeginselen ten aanzien van bewijsmateriaal behoren iedere wetenschappelijke discussie te begeleiden, of het bewijsmateriaal nu experimenteel, theoretisch of een combinatie van die twee is.

Artikel 8: Vrijheid van publicatie van wetenschappelijke resultaten

Een betreurenswaardige censuur is nu de standaardpraktijk geworden bij redacties van de belangrijke wetenschapstijdschriften en elektronische archieven en hun bendes zogenaamde deskundige referees. De referees worden voor het grootste deel beschermd door anonimiteit zodat de auteur niet hun zogenaamde deskundigheid kan verifiëren. Stukken worden momenteel routinematig geweigerd als de auteur de dominante theorie en gangbare orthodoxie verwerpt of weerlegt. Veel stukken worden nu automatisch geweigerd omdat bij de referenties een wetenschapper staat die in ongenade is gevallen bij de redacteuren, referees of andere deskundige censoren, zonder dat men zich ook maar enigszins over de inhoud van het stuk bekommert. Er bestaat een zwarte lijst van wetenschappers die een afwijkende mening hebben en deze lijst gaat over en weer tussen participerende redacties. Dit alles draagt bij aan grove vooringenomenheid en een misdadige onderdrukking van vrije gedachten en dient veroordeeld te worden door de internationale wetenschapsgemeenschap.

Alle wetenschappers behoren het recht te hebben om hun wetenschappelijke onderzoeksresultaten geheel of gedeeltelijk te presenteren op relevante wetenschapconferenties en hetzelfde te publiceren in gedrukte wetenschapstijdschriften, elektronische archieven en welke andere media dan ook. Van geen enkele wetenschapper behoren stukken of verslagen die ter publicatie aangeboden worden aan wetenschapstijdschriften, elektronische archieven of andere media geweigerd te worden alleen maar omdat het werk de gangbare meerderheidsmening ter discussie stelt, in conflict is met de opvattingen van de redactie, de bases ondermijnt van andere in gang gezette of geplande onderzoeksprojecten van andere wetenschappers, of botst met een politiek dogma, religieus geloof of persoonlijke mening van een ander, en geen enkele wetenschapper behoort op een zwarte lijst te staan of anderszins gecensureerd te worden noch verhinderd te worden om tot publicatie te komen door welk ander persoon dan ook. Geen wetenschapper behoort door de belofte van een geschenk of andere vergoeding ter omkoping de publicatie van het werk van een andere wetenschapper te blokkeren, modificeren of anderszins met de publicatie van het werk te interfereren.

Artikel 9: Het co-auteurschap van wetenschappelijke artikelen

Het is een slecht verborgen gehouden geheim binnen wetenschappelijke kringen dat veel co-auteurs van onderzoeksartikelen eigenlijk weinig of niks van doen hebben met het onderzoek waarover gerapporteerd wordt. Veel supervisors van afstuderende studenten bijvoorbeeld zijn er niet afkerig van om hun namen op artikelen te zetten van personen die slechts nominaal onder hun supervisie werken. In veel van die gevallen heeft degene die het artikel schrijft een superieur begrip ten aanzien van de materie vergeleken met de supervisor. In andere situaties, ook nu weer met als doel algemene bekendheid, reputatie, geld, prestige en dergelijke, worden niet-participerende personen aan het artikel toegevoegd als co-auteur. De werkelijke auteurs van dergelijke artikelen kunnen hiertegen enkel protesteren in het besef dat ze het risico lopen om later hiervoor gestraft te worden of, naar gelang de omstandigheden, zelfs uitgesloten te worden van de kandidatuur voor een hogere onderzoeksgraad of van de onderzoeksgroep. Velen zijn feitelijk ver-

bannen onder dergelijke omstandigheden. Deze ontstellende praktijken kunnen niet getolereerd worden. Alleen de personen verantwoordelijk voor het onderzoek behoren als auteur geaccrediteerd te worden.

Geen wetenschapper behoort een ander persoon uit te nodigen om toegevoegd te worden en geen wetenschapper behoort het toe te staan dat zijn of haar naam toegevoegd wordt als co-auteur van een wetenschappelijk artikel als hij of zij niet significant heeft bijgedragen aan het onderzoek waarover gerapporteerd wordt in het artikel. Geen wetenschapper behoort het toe te staan dat hij of zij door een vertegenwoordiger van een academisch instituut, corporatie, overheidsinstelling of enig ander persoon als co-auteur toegevoegd wordt aan een artikel dat een onderzoek betreft waar hij of zij niet significant aan heeft bijgedragen, en geen wetenschapper behoort het toe te staan dat zijn of haar naam gebruikt wordt als co-auteur met als tegenprestatie welk geschenk of andere vergoeding ter omkoping dan ook. Geen persoon behoort een wetenschapper op wat voor manier dan ook ertoe te bewegen of proberen ertoe te bewegen om het toe te staan dat de naam van de wetenschapper toegevoegd wordt als co-auteur van een wetenschappelijk artikel dat een inhoud heeft waar hij of zij niet significant aan heeft bijgedragen.

Artikel 10: Onafhankelijkheid van affiliatie

Veel wetenschappers zijn nu in dienst met een korte termijn contract. Met de beëindiging van het dienstverband komt er ook een einde aan de academische affiliatie. Redacties voeren vaak het beleid dat personen zonder een academische of commerciële affiliatie niet gepubliceerd worden. Zonder affiliatie kan een wetenschapper van veel middelen niet gebruik maken en de mogelijkheden om lezingen te geven en artikelen te presenteren op conferenties worden er door beperkt. Dit is een verdorven praktijk die gestopt moet worden. Wetenschap herkent geen affiliatie.

Geen wetenschapper behoort belet te worden om artikelen te presenteren op conferenties, colloquia te geven op seminaries, te publiceren in welke media dan ook, toegang te krijgen tot academische bibliotheken of wetenschappelijke publicaties, wetenschappelijke bijeenkomsten bij te wonen of lezingen te geven, vanwege het niet geaffilieerd zijn met een academisch instituut, wetenschappelijk instituut, overheids- of bedrijfslaboratorium, of welke andere organisatie dan ook.

Artikel 11: Vrije toegang tot wetenschappelijke informatie

De meeste gespecialiseerde boeken over wetenschappelijke aangelegenheden en veel wetenschappelijke tijdschriften leveren weinig tot geen winst op zodat commerciële uitgevers niet bereid zijn ze te publiceren zonder een geldbijdrage van academische instituten, overheidsinstellingen, filantropische stichtingen en dergelijke. Onder zulke omstandigheden zouden commerciële uitgevers vrije toegang tot elektronische versies van de publicaties toe moeten staan en ernaar moeten streven de kosten van het gedrukte materiaal tot een minimum te beperken.

Alle wetenschappers behoren ernaar te streven dat hun onderzoeksartikelen gratis beschikbaar zijn voor de internationale wetenschapsgemeenschap of, als dat niet mogelijk is, beschikbaar zijn voor zo weinig mogelijk kosten. Alle wetenschappers zouden actief maatregelen moeten nemen om hun technische boeken verkrijgbaar te maken voor zo weinig mogelijk kosten, zodat de wetenschappelijke informatie beschikbaar kan zijn voor een bredere internationale wetenschapsgemeenschap.

Artikel 12: Ethische verantwoordelijkheid van wetenschappers

De geschiedenis toont ons dat wetenschappelijke ontdekkingen gebruikt worden voor zowel goed als kwaad en dat ze sommigen ten goede komen en anderen vernietigen. Omdat de vooruitgang van wetenschap en technologie niet kan stoppen zullen er bepaalde middelen moeten komen om kwaadaardige toepassingen te voorkomen. Enkel een democratisch gekozen regering die vrij is van religieuze, raciale en andere vooroordelen kan de beschaafde wereld waarborgen. Enkel democratisch gekozen regeringen, tribunalen en commissies kunnen het recht van vrije wetenschappelijke creatie waarborgen. Momenteel zijn er verscheidene ondemocratische staten en totalitaire regimes die actief onderzoek uitvoeren op het gebied van nucleaire fysica, chemie, virologie, genetische manipulatie, etc. om nucleaire, chemische en biologische wapens te produceren. Geen wetenschapper behoort vrijwillig samen te werken met ondemocratische staten of totalitaire regimes. Iedere wetenschapper die gedwongen wordt om te werken aan het ontwikkelen van wapens voor zulke staten behoort wegen en middelen te vinden om de vooruitgang van de onderzoeksprogramma's te vertragen en de wetenschappelijke output te beperken, zodat beschaving en democratie ten slotte kunnen zegevieren.

Alle wetenschappers dragen een morele verantwoordelijkheid voor hun wetenschappelijke creaties en ontdekkingen. Geen wetenschapper behoort zich vrijwillig bezig te houden met het ontwerpen of vervaardigen van wapens van welke soort dan ook voor ondemocratische staten of totalitaire regimes, of toestaan dat zijn of haar wetenschappelijke vaardigheden of kennis gebruikt wordt voor de ontwikkeling van wat dan ook dat de mensheid kan beschadigen. Een wetenschapper behoort te leven met het dictum dat iedere ondemocratische regering en iedere schending van de mensenrechten misdadig is.

28 maart 2006

On Isotropic Coordinates and Einstein's Gravitational Field

Stephen J. Crothers

Queensland, Australia

E-mail: thenarmis@yahoo.com

It is proved herein that the metric in the so-called "isotropic coordinates" for Einstein's gravitational field is a particular case of an infinite class of equivalent metrics. Furthermore, the usual interpretation of the coordinates is erroneous, because in the usual form given in the literature, the alleged coordinate length $\sqrt{dx^2+dy^2+dz^2}$ is not a coordinate length. This arises from the fact that the geometrical relations between the components of the metric tensor are invariant and therefore bear the same relations in the isotropic system as those of the metric in standard Schwarzschild coordinates.

1 Introduction

Petrov [1] developed an algebraic classification of Einstein's field equations. Einstein's field equations can be written as,

$$R_{\alpha\beta} - \frac{1}{2} R g_{\alpha\beta} = \kappa T_{\alpha\beta} - \lambda g_{\alpha\beta} ,$$

where κ is a constant, and λ the so-called cosmological constant. If $T_{\alpha\beta} \propto g_{\alpha\beta}$, the associated space is called an Einstein space. Thus, Einstein spaces include those described by partially degenerate metrics of this form. Consequently, such metrics become non-Einstein only when

$$g = \det \|g_{\alpha\beta}\| = 0 .$$

A simple source is a spherically symmetric mass (a mass island), without charge or angular momentum. A simple source giving rise to a static gravitational field in vacuum, where space is isotropic and homogeneous, constitutes a Schwarzschild space. The associated field equations external to the simple source are

$$R_{\alpha\beta} - \frac{1}{2} R g_{\alpha\beta} = 0 ,$$

or, more simply,

$$R_{\alpha\beta} = 0 .$$

Thus, a Schwarzschild space is an Einstein space. There are four types of Einstein spaces. The Schwarzschild space is a type 1 Einstein space. It gives rise to a spherically symmetric gravitational field.

The simple source interacts with a "test" particle, which has no charge, no angular momentum, and effectively no mass, or so little mass that its own gravitational field can be neglected entirely. A similar concept is utilised in electrodynamics in the notion of a "test" charge.

The only solutions known for Einstein's field equations involve a single gravitating source interacting with a test particle. There are no known solutions for two or more interacting comparable masses. In fact, it is not even known if Einstein's field equations admit of solutions for multi-body configurations, as no existence theorem has even been adduced. It follows that there is no theoretical sense to concepts such as black hole binaries, or colliding or merging black holes, notwithstanding the all too common practice of assuming them well-posed theoretical problems allegedly substantiated by observations.

The metric for Einstein's gravitational field in the usual isotropic coordinates is, in relativistic units ($c = G = 1$),

$$ds^2 = \frac{\left(1-\frac{m}{2r}\right)^2}{\left(1+\frac{m}{2r}\right)^2} dt^2 - \left(1+\frac{m}{2r}\right)^4 \left[dr^2 + r^2\left(d\theta^2 + \sin^2\theta\, d\varphi^2\right)\right] = \tag{1a}$$

$$= \frac{\left(1-\frac{m}{2r}\right)^2}{\left(1+\frac{m}{2r}\right)^2} dt^2 - \left(1+\frac{m}{2r}\right)^4 \left(dx^2+dy^2+dz^2\right) , \tag{1b}$$

having set $r = \sqrt{x^2+y^2+z^2}$. This metric describes a Schwarzschild space.

By virtue of the factor $(dx^2+dy^2+dz^2)$ it is usual that $0 \leqslant r < \infty$ is taken. However, this standard range on r is due entirely to assumption, based upon the misconception that because $0 \leqslant r < \infty$ is defined on the usual Minkowski metric, this must also hold for (1a) and (1b). Nothing could be further from the truth, as I shall now prove.

2 Proof

Consider the standard Minkowski metric,

$$\begin{aligned} ds^2 &= dt^2 - dx^2 - dy^2 - dz^2 \equiv \\ &\equiv dt^2 - dr^2 - r^2(d\theta^2 + \sin^2\theta d\varphi^2) , \\ &0 \leqslant r < \infty . \end{aligned} \tag{2}$$

The spatial components of this metric describe a sphere of radius $r \geqslant 0$, centred at $r = 0$. The quantity r is an Efcleeth-

ean* distance since Minkowski space is pseudo-Efcleethean.

Now (2) is easily generalised [2] to

$$ds^2 = dt^2 - dr^2 - (r - r_0)^2(d\theta^2 + \sin^2\theta\, d\varphi^2) = \tag{3a}$$

$$= dt^2 - \frac{(r - r_0)^2}{|r - r_0|^2}\, dr^2 - |r - r_0|^2(d\theta^2 + \sin^2\theta\, d\varphi^2)\,, \tag{3b}$$

$$= dt^2 - d|r - r_0|^2 - |r - r_0|^2(d\theta^2 + \sin^2\theta\, d\varphi^2)\,, \tag{3c}$$

$$0 \leqslant |r - r_0| < \infty\,.$$

The spatial components of equations (3) describe a sphere of radius $R_c(r) = |r - r_0|$, centred at a point located anywhere on the 2-sphere r_0. Only if $r_0 = 0$ does (3) describe a sphere centred at the origin of the coordinate system. With respect to the underlying coordinate system of (3), $R_c(r)$ is the radial distance between the 2-spheres $r = r_0$ and $r \neq r_0$.

The usual practice is to supposedly generalise (2) as

$$ds^2 = A(r)dt^2 - B(r)\big(dr^2 + r^2 d\theta^2 + r^2\sin^2\theta\, d\varphi^2\big) \tag{4}$$

to finally obtain (1a) in the standard way, with the assumption that $0 \leqslant r < \infty$ on (2) must hold also on (4), and hence on equations (1). However, this assumption has never been proved by the theoreticians. The assumption is demonstrably false. Furthermore, this procedure does not produce a generalised solution in terms of the parameter r, but instead a particular solution.

Since (3) is a generalisation of (2), I use it to generalise (4) to

$$ds^2 = e^{\nu}dt^2 - e^{\mu}\big(dh^2 + h^2 d\theta^2 + h^2\sin^2\theta\, d\varphi^2\big) \tag{5}$$

$$h = h(r) = h(|r - r_0|),\quad \nu = \nu(h(r)),\quad \mu = \mu(h(r))\,.$$

Note that (5) can be written in the mixed form

$$ds^2 = e^{\nu}dt^2 - e^{\mu}\left[\left(\frac{dh}{dr}\right)^2 dr^2 + h^2 d\theta^2 + h^2\sin^2\theta d\varphi^2\right], \tag{6}$$

from which the particular form (4) usually used is recovered if $h(|r - r_0|) = r$. However, no particular form for $h(|r - r_0|)$ should be pre-empted. Doing so, in the routine fashion of the majority of the relativists, produces only a particular solution in terms of the Minkowski r, with all the erroneous assumptions associated therewith.

Now (5) must satisfy the energy-momentum tensor equations for the simple, static, vacuum field:

$$0 = e^{-\mu}\left(\frac{\mu'^2}{4} + \frac{\mu'\nu'}{2} + \frac{\mu' + \nu'}{h}\right)$$

$$0 = e^{-\mu}\left(\frac{\mu''}{2} + \frac{\nu''}{2} + \frac{\nu'^2}{r} + \frac{\mu' + \nu'}{2h}\right)$$

$$0 = e^{-\mu}\left(\mu'' + \frac{\mu'^2}{4} + \frac{2\mu'}{h}\right),$$

where the prime indicates d/dh. This gives, in the usual way,

$$ds^2 = \frac{\left(1 - \frac{m}{2h}\right)^2}{\left(1 + \frac{m}{2h}\right)^2}\, dt^2 - \\ - \left(1 + \frac{m}{2h}\right)^4\left[dh^2 + h^2\left(d\theta^2 + \sin^2\theta\, d\varphi^2\right)\right], \tag{7}$$

from which the admissible form for $h(|r - r_0|)$ and the value of the constant r_0 must be rigorously ascertained from the intrinsic geometrical properties of the metric itself.

Now the intrinsic geometry of the metric (2) is the same on all the metrics given herein in terms of the spherical coordinates of Minkowski space, namely, the radius of curvature R_c in the space described by the metric is always the square root of the coefficient of the angular terms of the metric and the proper radius R_p is always the integral of the square root of the component containing the differential element of the radius of curvature. Thus, on (2),

$$R_c(r) \equiv r,\quad R_p(r) \equiv \int_0^r dr = r \equiv R_c(r)\,,$$

and on (3),

$$R_c(r) \equiv |r - r_0|\,,$$

$$R_p(r) \equiv \int_0^{|r - r_0|} dr = |r - r_0| \equiv R_c(r)\,,$$

whereby it is clear that $R_c(r)$ and $R_p(r)$ are identical, owing to the fact that the spatial coordinates of (2) and (3) are Efcleethean.

Now consider the general metric of the form

$$ds^2 = A(r)dt^2 - B(r)dr^2 - C(r)(d\theta^2 + \sin^2\theta\, d\varphi^2) \tag{8}$$

$$A, B, C > 0.$$

In this case,

$$R_c(r) = \sqrt{C(r)},\quad R_p(r) = \int\sqrt{B(r)}\, dr\,.$$

I remark that although (8) is mathematically valid, it is misleading. In the cases of (2) and (3), the respective metrics are given in terms of the radius of curvature and its differential element. This is not the case in (8) where the first and second components are in terms of the parameter r of the radius of curvature, not the radius of curvature itself. I therefore write (8) in terms of only the radius of curvature on (8), thus

$$ds^2 = A^*\big(\sqrt{C(r)}\big)dt^2 - B^*\big(\sqrt{C(r)}\big)d\sqrt{C(r)}^{\,2} - \\ - C(r)(d\theta^2 + \sin^2\theta\, d\varphi^2)\,, \tag{9a}$$

$$A^*, B^*, C > 0\,.$$

*Due to Efcleethees, incorrectly Euclid, so the geometry is rightly Efcleethean.

Note that (9a) can be written as,

$$ds^2 = A^*\left(\sqrt{C(r)}\right)dt^2 - B^*\left(\sqrt{C(r)}\right)\left(\frac{d\sqrt{C(r)}}{dr}\right)^2 dr^2 - \\ - C(r)\left(d\theta^2 + \sin^2\theta\, d\varphi^2\right), \tag{9b}$$

$$A^*, B^*, C > 0,$$

and by setting

$$B^*\left(\sqrt{C(r)}\right)\left(\frac{d\sqrt{C(r)}}{dr}\right)^2 = B(r),$$

equation (8) is recovered, proving that (8) and equations (9) are mathematically equivalent, and amplifying the fact that (8) is a mixed-term metric. Note also that if $C(r)$ is set equal to r^2, the alleged general form used by most relativists is obtained. However, the form of $C(r)$ should not be pre-empted, for by doing so only a particular parametric solution is obtained, and with the form chosen by most relativists, the properties of r in Minkowski space are assumed (incorrectly) to carry over into the metric for the gravitational field.

It is also clear from (8) and equations (9) that $|r - r_0|$ is the Efcleethean distance between the centre of mass of the field source and a test particle, in Minkowski space, and which is mapped into $R_c(r)$ and $R_p(r)$ of the gravitational field by means of functions determined by the structure of the gravitational metric itself, namely the functions given by

$$R_c(r) = \sqrt{C(r)},$$

$$R_p(r) = \int \sqrt{B^*\left(\sqrt{C(r)}\right)}\, d\sqrt{C(r)} = \int \sqrt{B(r)}\, dr.$$

In the case of the usual metric the fact that $|r - r_0|$ is the Efcleethean distance between the field source and a test particle in Minkowski space is suppressed by the choice of the particular function $\sqrt{C(r)} = r^2$, so that it is not immediately apparent that when r goes down to $\alpha = 2m$ on that metric, the parametric distance between field source and test particle has gone down to zero. Generally, as the parametric distance goes down to zero, the proper radius in the gravitational field goes down to zero, irrespective of the location of the field source in parameter space. Thus, the field source is always located at $R_p = 0$ as far as the metric for the gravitational field is concerned.

It has been proved elsewhere [3, 4] that in the case of the simple "point-mass" (a fictitious object), metrics of the form (8) or (9) are characterised by the following scalar invariants,

$$R_p(r_0) \equiv 0, \quad R_c(r_0) \equiv 2m, \quad g_{00}(r_0) \equiv 0, \tag{10}$$

so that the actual value of r_0 is completely irrelevant.

Now (7) can be written as

$$ds^2 = \frac{\left(1 - \frac{m}{2h}\right)^2}{\left(1 + \frac{m}{2h}\right)^2} dt^2 - \\ - \left(1 + \frac{m}{2h}\right)^4 dh^2 - h^2\left(1 + \frac{m}{2h}\right)^4 \left(d\theta^2 + \sin^2\theta\, d\varphi^2\right), \tag{11}$$

$$h = h(r) = h(|r - r_0|).$$

Since the geometrical relations between the components of the metric tensor are invariant it follows that on (11),

$$R_c(r) = h(r)\left(1 + \frac{m}{2h(r)}\right)^2, \tag{12a}$$

$$R_p(r) = \int \left(1 + \frac{m}{2h(r)}\right)^2 dh(r) = \\ = h(r) + m\ln h(r) - \frac{m^2}{2}\frac{1}{h(r)} + K,$$

where $K = \text{constant}$,

$$R_p(r) = h(r) + m\ln\frac{h(r)}{K_1} - \frac{m^2}{2}\frac{1}{h(r)} + K_2 \tag{12b}$$

where K_1 and K_2 are constants.

It is required that $R_p(r_0) \equiv 0$, so

$$0 = h(r_0) + m\ln\frac{h(r_0)}{K_1} - \frac{m^2}{2}\frac{1}{h(r_0)} + K_2,$$

which is satisfied only if

$$h(r_0) = K_1 = K_2 = \frac{m}{2}. \tag{13}$$

Therefore,

$$R_p(r) = h(r) + m\ln\left(\frac{2h(r)}{m}\right) - \frac{m^2}{2}\frac{1}{h(r)} + \frac{m}{2}. \tag{14}$$

According to (12a), and using (13),

$$R_c(r_0) = \frac{m}{2}\left(1 + \frac{m}{2\frac{m}{2}}\right)^2 = 2m,$$

satisfying (10) as required.

Now from (11),

$$g_{00}(r) = \frac{\left(1 - \frac{m}{2h(r)}\right)^2}{\left(1 + \frac{m}{2h(r)}\right)^2},$$

and using (13),

$$g_{00}(r_0) = \frac{\left(1 - \frac{2m}{2m}\right)^2}{\left(1 + \frac{2m}{2m}\right)^2} = 0,$$

satisfying (10) as required.

It remains now to ascertain the general admissible form of $h(r) = h(|r - r_0|)$.

By (6),

$$\frac{dh}{dr} \neq 0 \quad \forall \quad r \neq r_0.$$

It is also required that (11) become Minkowski in the infinitely far field, so

$$\lim_{|r-r_0|\to\infty} \frac{h^2(r)\left(1+\frac{m}{2h(r)}\right)^4}{|r-r_0|^2} \to 1\,,$$

must be satisfied.

When there is no matter present ($m=0$), $h(r)$ must reduce the metric to Minkowski space.

Finally, $h(r)$ must be able to be arbitrarily reduced to r by a suitable choice of arbitrary constants so that the usual metric (1a) in isotropic coordinates can be recovered at will.

The only form for $h(r)$ that satisfies all the requirements is

$$h(r)=\left[|r-r_0|^n+\left(\frac{m}{2}\right)^n\right]^{\frac{1}{n}}, \qquad n\in\Re^+,\quad r_0\in\Re,\quad r\neq r_0\,, \tag{15}$$

where n and r_0 are entirely arbitrary constants. The condition $r\neq r_0$ is necessary since the "point-mass" is not a physical object.

Setting $n=1$, $r_0=\frac{m}{2}$, and $r>r_0$ in (15) gives the usual metric (1a) in isotropic coordinates. Note that in this case $r_0=\frac{m}{2}$ is the location of the fictitious "point-mass" in parameter space (i. e. in Minkowski space) and thus as the distance between the test particle and the source, located at $r_0=\frac{m}{2}$, goes to zero in parameter space, the proper radius in the gravitational field goes to zero, the radius of curvature goes to $2m$, and g_{00} goes to zero. Thus, the usual claim that the term $dr^2+r^2(d\theta^2+\sin^2\theta\,d\varphi^2)$ (or $dx^2+dy^2+dz^2$) describes a coordinate length is false. Note that in choosing this case, the resulting metric suppresses the true nature of the relationship between the r-parameter and the gravitational field because, as clearly seen by (15), $r_0=\frac{m}{2}$ drops out. Note also that (15) generalises the mapping so that distances on the real line are mapped into the gravitational field.

Consequently, there is no black hole predicted by the usual metrics (1) in isotropic coordinates. The black hole concept has no validity in General Relativity (and none in Newton's theory either since the Michell-Laplace dark body is not a black hole [5, 6]).

The singularity at $R_p(r_0)\equiv 0$ is insurmountable because

$$\lim_{|r-r_0|\to 0} \frac{2\pi R_c(r)}{R_p(r)} \to \infty\,,$$

according to the admissible forms of $R_p(r)$, $R_c(r)$, and $h(r)$.

Note also that only in the infinitely far field are $R_c(r)$ and $R_p(r)$ identical; where the field becomes Efcleethean (i. e. Minkowski),

$$\lim_{|r-r_0|\to\infty} \frac{2\pi R_c(r)}{R_p(r)} \to 2\pi\,.$$

It has been proved elsewhere [3, 2] that there are no curvature singularities in Einstein's gravitational field. In particular the Riemann tensor scalar curvature invariant (the Kretschmann scalar) $f=R_{\alpha\beta\sigma\rho}R^{\alpha\beta\sigma\rho}$ is finite everywhere, and and in the case of the fictitious point-mass takes the invariant value

$$f(r_0)\equiv\frac{12}{(2m)^4}\,,$$

completely independent of the value of r_0.

Since the intrinsic geometry of the metric is invariant, (11) with (15) must also satisfy this invariant condition. A tedious calculation gives the Kretschmann scalar for (11) at

$$f(r)=\frac{48m^2}{h^6\left(1+\frac{m}{2h}\right)^{12}}\,,$$

which by (15) is

$$f(r)=\frac{48m^2}{\left[|r-r_0|^n+\left(\frac{m}{2}\right)^n\right]^{\frac{6}{n}}\left(1+\frac{m}{2\left[|r-r_0|^n+\left(\frac{m}{2}\right)^n\right]^{\frac{1}{n}}}\right)^{12}}\,.$$

Then

$$f(r_0)\equiv\frac{12}{(2m)^4}\,,$$

completely independent of the value of r_0, as required by the very structure of the metric.

The structure of the metric is also responsible for the Ricci flatness of Einstein's static, vacuum gravitational field (satisfying $R_{\alpha\beta}=0$). Consequently, all the metrics herein are Ricci flat (i. e. $R=0$). Indeed, all the given metrics can be transformed into

$$ds^2=\left(1-\frac{2m}{R_c}\right)dt^2-\left(1-\frac{2m}{R_c}\right)^{-1}dR_c^2-\\ -R_c^2(d\theta^2+\sin^2\theta\,d\varphi^2)\,, \tag{16}$$

$$R_c=R_c(r)=\sqrt{C(r)}\,,\quad 2m<R_c(r)<\infty\,,$$

which is Ricci flat for any analytic function $R_c(r)$, which is easily verified by using the variables

$$x^0=t\,,\quad x^1=R_c(r)\,,\quad x^2=\theta\,,\quad x^3=\varphi\,,$$

in the calculation of the Ricci curvature from (16), using,

$$R=g^{\mu\nu}\left\{\frac{\partial^2}{\partial x^\mu\partial x^\nu}\left(\ln\sqrt{|g|}\right)-\right.\\ \left.-\frac{1}{\sqrt{|g|}}\frac{\partial}{\partial x^\rho}\left(\sqrt{|g|}\,\Gamma^\rho_{\mu\nu}\right)+\Gamma^\rho_{\mu\sigma}\Gamma^\sigma_{\rho\nu}\right\}.$$

Setting

$$\frac{\chi}{2\pi}=R_c(r)=h(r)\left(1+\frac{m}{2h(r)}\right)^2,$$

transforms the metric (7) into,

$$ds^2 = \left(1 - \frac{2\pi\alpha}{\chi}\right) dt^2 - \left(1 - \frac{2\pi\alpha}{\chi}\right)^{-1} \frac{d\chi^2}{4\pi^2} - \\ - \frac{\chi^2}{4\pi^2}(d\theta^2 + \sin^2\theta d\varphi^2)\,, \qquad (17)$$

$$2\pi\alpha < \chi < \infty\,, \quad \alpha = 2m\,,$$

which is the metric for Einstein's gravitational field in terms of the only theoretically measurable distance in the field – the circumference χ of a great circle [2]. This is a truly coordinate independent expression. There is no need of the r-parameter at all.

Furthermore, equation (17) is clear as to what quantities are radii in the gravitational field, *viz.*

$$R_c(\chi) = \frac{\chi}{2\pi}\,,$$

$$R_p(\chi) = \int_{2\pi\alpha}^{\chi} \sqrt{\frac{\frac{\chi}{2\pi}}{\left(\frac{\chi}{2\pi} - \alpha\right)}}\, \frac{d\chi}{2\pi} = \\ = \sqrt{\frac{\chi}{2\pi}\left(\frac{\chi}{2\pi} - \alpha\right)} + \alpha \ln \left| \frac{\sqrt{\frac{\chi}{2\pi}} + \sqrt{\frac{\chi}{2\pi} - \alpha}}{\sqrt{\alpha}} \right|.$$

3 Epilogue

The foregoing is based, as has all my work to date, upon the usual manifold with boundary, $[0\,, +\infty[\times S^2$. By using the very premises of most relativists, including their $[0, +\infty[\times S^2$, I have demonstrated herein that black holes (see also [4, 7]), and elsewhere as a logical consequence [8], that big bangs are not consistent with General Relativity. Indeed, cosmological solutions for isotropic, homogeneous, type 1 Einstein spaces do not exist. Consequently, there is currently no valid relativistic cosmology at all. The Standard Cosmological Model, the Big Bang, is false.

Stavroulakis [9] has argued that $[0, +\infty[\times S^2$ is inadmissible because it destroys the topological structure of $\mathbb{R}^3$. He has maintained that the correct topological space for Einstein's gravitational field should be $\mathbb{R} \times \mathbb{R}^3$. He has also shown that black holes are not predicted by General Relativity in $\mathbb{R} \times \mathbb{R}^3$.

However, the issue of whether or not $[0, +\infty[\times S^2$ is admissible is not relevant to the arguments herein, given the objectives of the analysis.

Although χ is measurable in principle, it is apparently beyond measurement in practice. This severely limits the utility of Einstein's theory.

The historical analysis of Einstein's gravitational field proceeded in ignorance of the fact that only the circumference χ of a great circle is significant. It has also failed to realise that there are two different immeasurable radii defined in Einstein's gravitational field, as an inescapable consequence of the intrinsic geometry on the metric, and that these radii are identical only in the infinitely far field where space becomes Efcleethean (i. e. Minkowski). Rejection summarily of the oddity of two distinct immeasurable radii is tantamount to complete rejection of General Relativity; an issue I have not been concerned with.

Minkowski's metric in terms of χ is,

$$ds^2 = dt^2 - \frac{d\chi^2}{4\pi^2} - \frac{\chi^2}{4\pi^2}(d\theta^2 + \sin^2\theta\, d\varphi^2)\,,$$

$$0 \leqslant \chi < \infty\,.$$

It is generalised to

$$ds^2 = A\left(\frac{\chi}{2\pi}\right) dt^2 - B\left(\frac{\chi}{2\pi}\right)^{-1} \frac{d\chi^2}{4\pi^2} - \\ - \frac{\chi^2}{4\pi^2}(d\theta^2 + \sin^2\theta\, d\varphi^2)\,, \qquad (18)$$

$$\chi_0 < \chi < \infty\,, \qquad A, B > 0\,,$$

which leads, in the usual way, to the line-element of (17), from which χ_0 and the radii associated with the gravitational field are determined via the intrinsic and invariant geometry of the metric.

Setting $R_c(r) = \sqrt{C(r)}$ in (16) gives,

$$ds^2 = \left(1 - \frac{\alpha}{\sqrt{C(r)}}\right) dt^2 - \left(1 - \frac{\alpha}{\sqrt{C(r)}}\right)^{-1} d\sqrt{C(r)}^{\,2} - \\ - C(r)(d\theta^2 + \sin^2\theta d\varphi^2)\,, \qquad (19)$$

where [2]

$$C(r) = \left(\left|r - r_0\right|^n + \alpha^n\right)^{\frac{2}{n}}, \qquad (20)$$

$$n \in \Re^+, \quad r_0 \in \Re\,, \quad \alpha = 2m\,, \quad r \neq r_0\,,$$

and where n and r_0 are entirely arbitrary constants. Note that if $n = 1$, $r_0 = \alpha$, $r > r_0$, the usual line-element is obtained, but the usual claim that r can go down to zero is clearly false, since when $r = \alpha$, the parametric distance between field source and test particle is zero, which is reflected in the fact that the proper radius on (19) is then zero, $R_c = \alpha = 2m$, and $g_{00} = 0$, as required. The functions (20) are called Schwarzschild forms [4, 7], and they produce an infinite number of equivalent Schwarzschild metrics.

The term $\sqrt{dx^2 + dy^2 + dz^2}$ of the standard metric in "isotropic coordinates" is not a coordinate length as commonly claimed. This erroneous idea stems from the fact that the usual choice of $C(r) = r^2$ in the metric (19) suppresses the true nature of the mapping of parametric distances into the true radii of the gravitational field. This arises from the additional fact that the location of the field source at $r_0 = \alpha$

in parameter space drops out of the functional form $C(r)$ as given by (20), in this particular case. The subsequent usual transformation to the usual metric (1a) carries with it the erroneous assumptions about r, inherited from the misconceptions about r in (19) with the reduction of $C(r)$ to r^2, which, in the usual conception, violates (20), and hence the entire structure of the metric for the gravitational field. Obtaining (1a) from first principles using the expression (5) with $h(r) = r^2$ and the components of the energy-momentum tensor, already presupposes the form of $h(r)$ and generates the suppression of the true nature of r in similar fashion.

The black hole, as proved herein and elsewhere [4, 7], and the Big Bang, are due to a serious neglect of the intrinsic geometry of the gravitational metric, a failure heretofore to understand the structure of type 1 Einstein spaces, with the introduction instead, of extraneous and erroneous hypotheses by which the intrinsic geometry is violated.

Since Nature does not make point-masses, the point-mass referred to Einstein's gravitational field must be regarded as merely the mathematical artifice of a centre-of-mass of the source of the field. The fact that the gravitational metric for the point-mass disintegrates at the point-mass is a theoretical indication that the point-mass is not physical, so that the metric is undefined when $r = r_0$ in parameter space, which is at $R_p(r_0) \equiv 0$ on the metric for the gravitational field. The usual concept of gravitational collapse itself collapses.

To fully describe the gravitational field there must therefore be two metrics, one for the interior of an extended gravitating body and one for the exterior of that field source, with a transition between the two at the surface of the body. This has been achieved in the idealised case of a sphere of incompressible and homogeneous fluid in vacuum [10, 11]. No singularities then arise, and gravitational collapse to a "point-mass" is impossible.

Acknowledgements

I thank Dr. Dmitri Rabounski for his comments concerning elaboration upon certain points I addressed too succinctly in an earlier draft, or otherwise took for granted that the reader would already know.

References

1. Petrov A. Z. Einstein spaces. Pergamon Press, London, 1969.
2. Crothers S. J. On the geometry of the general solution for the vacuum field of the point-mass. *Progress in Physics*, v. 2, 3–14, 2005.
3. Abrams L. S. Black holes: the legacy of Hilbert's error. *Can. J. Phys.*, 1989, v. 67, 919 (see also in arXiv: gr-qc/0102055).
4. Crothers S. J. On the general solution to Einstein's vacuum field and it implications for relativistic degeneracy. *Progress in Physics*, v. 1, 68–73, 2005.
5. Crothers S. J. A short history of black holes. *Progress in Physics*, v. 2, 54–57, 2006.
6. McVittie G. C. Laplace's alleged "black hole". *The Observatory*, 1978, v. 98, 272; http://www.geocities.com/theometria/McVittie.pdf.
7. Crothers S. J. On the ramifications of the Schwarzschild space-time metric. *Progress in Physics*, v. 1, 74–80, 2005.
8. Crothers S. J. On the general solution to Einstein's vacuum field for the point-mass when $\lambda \neq 0$ and its consequences for relativistic cosmology. *Progress in Physics*, v. 2, 7–18, 2005.
9. Stavroulakis N. Non-Euclidean geometry and gravitation. *Progress in Physics*, v. 2, 68–75, 2006.
10. Schwarzschild K. On the gravitational field of a sphere of incompressible fluid according to Einstein's theory. *Sitzungsber. Preuss. Akad. Wiss., Phys. Math. Kl.,* 1916, v. 424 (see also in arXiv: physics/9912033).
11. Crothers S. J. On the vacuum field of a sphere of incompressible fluid. *Progress in Physics*, v. 2, 43–47, 2005.

S-Denying of the Signature Conditions Expands General Relativity's Space

Dmitri Rabounski, Florentin Smarandache, Larissa Borissova

Department of Mathematics, University of New Mexico, Gallup, NM 87301, USA

E-mail: rabounski@yahoo.com; fsmarandache@yahoo.com; lborissova@yahoo.com

We apply the S-denying procedure to signature conditions in a four-dimensional pseudo-Riemannian space — i. e. we change one (or even all) of the conditions to be partially true and partially false. We obtain five kinds of expanded space-time for General Relativity. Kind I permits the space-time to be in collapse. Kind II permits the space-time to change its own signature. Kind III has peculiarities, linked to the third signature condition. Kind IV permits regions where the metric fully degenerates: there may be non-quantum teleportation, and a home for virtual photons. Kind V is common for kinds I, II, III, and IV.

1 Einstein's basic space-time

Euclidean geometry is set up by Euclid's axioms: (1) given two points there is an interval that joins them; (2) an interval can be prolonged indefinitely; (3) a circle can be constructed when its centre, and a point on it, are given; (4) all right angles are equal; (5) if a straight line falling on two straight lines makes the interior angles on one side less than two right angles, the two straight lines, if produced indefinitely, meet on that side. Non-Euclidean geometries are derived from making assumptions which deny some of the Euclidean axioms. Three main kinds of non-Euclidean geometry are conceivable — Lobachevsky-Bolyai-Gauss geometry, Riemann geometry, and Smarandache geometry.

In Lobachevsky-Bolyai-Gauss (hyperbolic) geometry the fifth axiom is denied in the sense that there are infinitely many lines passing through a given point and parallel to a given line. In Riemann (elliptic) geometry*, the axiom is satisfied formally, because there is no line passing through a given point and parallel to a given line. But if we state the axiom in a broader form, such as "through a point not on a given line there is only one line parallel to the given line", the axiom is also denied in Riemann geometry. Besides that, the second axiom is also denied in Riemann geometry, because herein the straight lines are closed: an infinitely long straight line is possible but then all other straight lines are of the same infinite length.

In Smarandache geometry one (or even all) of the axioms is false in at least two different ways, or is false and also true [1, 2]. This axiom is said to be Smarandachely denied (S-denied). Such geometries have mixed properties of Euclidean, Lobachevsky-Bolyai-Gauss, and Riemann geometry. Manifolds that support such geometries were introduced by Iseri [3].

Riemannian geometry is the generalization of Riemann geometry, so that in a space of Riemannian geometry:

(1) The differentiable field of a 2nd rank non-degenerate symmetric tensor $g_{\alpha\beta}$ is given so that the distance ds between any two infinitesimally close points is given by the quadratic form

$$ds^2 = \sum_{0\leqslant\alpha,\beta\leqslant n} g_{\alpha\beta}(x)\, dx^\alpha dx^\beta = g_{\alpha\beta}\, dx^\alpha dx^\beta,$$

known as the Riemann metric†. The tensor $g_{\alpha\beta}$ is called the fundamental metric tensor, and its components define the geometrical structure of the space;

(2) The space curvature may take different numerical values at different points in the space.

Actually, a Riemann geometry space is the space of the Riemannian geometry family, where the curvature is constant and has positive numerical value.

In the particular case where $g_{\alpha\beta}$ takes the diagonal form

$$g_{\alpha\beta} = \begin{pmatrix} 1 & 0 & \dots & 0 \\ 0 & 1 & \dots & 0 \\ \vdots & \vdots & \ddots & \vdots \\ 0 & 0 & \dots & 1 \end{pmatrix},$$

the Riemannian space becomes Euclidean.

Pseudo-Riemannian spaces consist of specific kinds of Riemannian spaces, where $g_{\alpha\beta}$ (and the Riemannian metric ds^2) has sign-alternating form so that its diagonal components bear numerical values of opposite sign.

Einstein's basic space-time of General Relativity is a four-dimensional pseudo-Riemannian space having the sign-alternating signature $(+---)$ or $(-+++)$, which reserves one dimension for time $x^0 = ct$ whilst the remaining three are reserved for three-dimensional space, so that the space metric is‡

$$ds^2 = g_{\alpha\beta}\, dx^\alpha dx^\beta = g_{00}\, c^2 dt^2 + 2g_{0i}\, c\, dt\, dx^i + g_{ik}\, dx^i dx^k.$$

**Elleipein* — "to fall short"; *hyperballein* — "to throw beyond" (Greek).

†Here is a space of n dimensions.

‡Landau and Lifshitz in *The Classical Theory of Fields* [4] use the signature $(-+++)$, where the three-dimensional part of the four-dimensional impulse vector is real. We, following Eddington [5], use the signature $(+---)$, because in this case the three-dimensional *observable impulse*, being the projection of the four-dimensional impulse vector on an observer's spatial section, is real. Here $\alpha, \beta = 0, 1, 2, 3$, while $i, k = 1, 2, 3$.

In general the four-dimensional pseudo-Riemannian space is curved, inhomogeneous, gravitating, rotating, and deforming (any or all of the properties may be anisotropic). In the particular case where the fundamental metric tensor $g_{\alpha\beta}$ takes the strictly diagonal form

$$g_{\alpha\beta} = \begin{pmatrix} 1 & 0 & 0 & 0 \\ 0 & -1 & 0 & 0 \\ 0 & 0 & -1 & 0 \\ 0 & 0 & 0 & -1 \end{pmatrix},$$

the space becomes four-dimensional pseudo-Euclidean

$$ds^2 = g_{\alpha\beta}\, dx^\alpha dx^\beta = c^2 dt^2 - dx^2 - dy^2 - dz^2,$$

which is known as Minkowski's space (he had introduced it first). It is the basic space-time of Special Relativity.

2 S-denying the signature conditions

In a four-dimensional pseudo-Riemannian space of signature $(+---)$ or $(-+++)$, the basic space-time of General Relativity, there are *four signature conditions* which define this space as pseudo-Riemannian.

Question: What happens if we S-deny one (or even all) of the four signature conditions in the basic space-time of General Relativity? What happens if we postulate that one (or all) of the signature conditions is to be denied in two ways, or, alternatively, to be true and false?

Answer: If we S-deny one or all of the four signature conditions in the basic space-time, we obtain a new expanded basic space-time for General Relativity. There are five main kinds of such expanded spaces, due to four possible signature conditions there.

Here we are going to consider each of the five kinds of expanded spaces.

Starting from a purely mathematical viewpoint, the signature conditions are derived from sign-alternation in the diagonal terms g_{00}, g_{11}, g_{22}, g_{33} in the matrix $g_{\alpha\beta}$. From a physical perspective, see §84 in [4], the signature conditions are derived from the requirement that the three-dimensional observable interval

$$d\sigma^2 = h_{ik}\, dx^i dx^k = \left(-g_{ik} + \frac{g_{0i} g_{0k}}{g_{00}} \right) dx^i dx^k$$

must be positive. Hence the three-dimensional observable metric tensor $h_{ik} = -g_{ik} + \frac{g_{0i} g_{0k}}{g_{00}}$, being a 3×3 matrix defined in an observer's reference frame accompanying its references, must satisfy three obvious conditions

$$\det \| h_{11} \| = h_{11} > 0\,,$$

$$\det \begin{Vmatrix} h_{11} & h_{12} \\ h_{21} & h_{22} \end{Vmatrix} = h_{11}\, h_{22} - h_{12}^2 > 0\,,$$

$$h = \det \| h_{ik} \| = \det \begin{Vmatrix} h_{11} & h_{12} & h_{13} \\ h_{21} & h_{22} & h_{23} \\ h_{31} & h_{32} & h_{33} \end{Vmatrix} > 0\,.$$

From here we obtain the signature conditions in the fundamental metric tensor's matrix $g_{\alpha\beta}$. In a space of signature $(+---)$, the signature conditions are

$$\det \| g_{00} \| = g_{00} > 0\,, \qquad \text{(I)}$$

$$\det \begin{Vmatrix} g_{00} & g_{01} \\ g_{10} & g_{11} \end{Vmatrix} = g_{00}\, g_{11} - g_{01}^2 < 0\,, \qquad \text{(II)}$$

$$\det \begin{Vmatrix} g_{00} & g_{01} & g_{02} \\ g_{10} & g_{11} & g_{12} \\ g_{20} & g_{21} & g_{22} \end{Vmatrix} > 0\,, \qquad \text{(III)}$$

$$g = \det \| g_{\alpha\beta} \| = \det \begin{Vmatrix} g_{00} & g_{01} & g_{02} & g_{03} \\ g_{10} & g_{11} & g_{12} & g_{13} \\ g_{20} & g_{21} & g_{22} & g_{23} \\ g_{30} & g_{31} & g_{32} & g_{33} \end{Vmatrix} < 0\,. \qquad \text{(IV)}$$

An expanded space-time of kind I: In such a space-time the first signature condition $g_{00} > 0$ is S-denied, while the other signature conditions remain unchanged. Given the expanded space-time of kind I, the first signature condition is S-denied in the following form

$$\det \| g_{00} \| = g_{00} \geqslant 0\,,$$

which includes two particular cases, $g_{00} > 0$ and $g_{00} = 0$, so $g_{00} > 0$ is partially true and partially false.

Gravitational potential is $\mathrm{w} = c^2(1 - \sqrt{g_{00}})$ [6, 7], so the S-denied first signature condition $g_{00} \geqslant 0$ means that in such a space-time $\mathrm{w} \leqslant c^2$, i. e. two different states occur

$$\mathrm{w} < c^2\,, \qquad \mathrm{w} = c^2.$$

The first one corresponds to the regular space-time, where $g_{00} > 0$. The second corresponds to a special space-time state, where the first signature condition is simply denied $g_{00} = 0$. This is the well-known condition of gravitational collapse.

Landau and Lifshitz wrote, "nonfulfilling of the condition $g_{00} > 0$ would only mean that the corresponding system of reference cannot be accomplished with real bodies" [4].

Conclusion on the kind I: An expanded space-time of kind I ($g_{00} \geqslant 0$) is the generalization of the basic space-time of General Relativity ($g_{00} > 0$), including regions where this space-time is in a state of collapse, ($g_{00} = 0$).

An expanded space-time of kind II: In such a space-time the second signature condition $g_{00}\, g_{11} - g_{01}^2 < 0$ is S-denied, the other signature conditions remain unchanged. Thus, given the expanded space-time of kind II, the second signature condition is S-denied in the following form

$$\det \begin{Vmatrix} g_{00} & g_{01} \\ g_{10} & g_{11} \end{Vmatrix} = g_{00}\, g_{11} - g_{01}^2 \leqslant 0\,,$$

which includes two different cases

$$g_{00}\,g_{11} - g_{01}^2 < 0\,, \qquad g_{00}\,g_{11} - g_{01}^2 = 0\,,$$

whence the second signature condition $g_{00}\,g_{11} - g_{01}^2 < 0$ is partially true and partially false.

The component g_{00} is defined by the gravitational potential $\mathrm{w} = c^2(1 - \sqrt{g_{00}})$. The component g_{0i} is defined by the space rotation linear velocity (see [6, 7] for details)

$$v_i = -c\frac{g_{0i}}{\sqrt{g_{00}}}\,, \quad v^i = -c\,g^{0i}\sqrt{g_{00}}\,, \quad v_i = h_{ik}\,v^k.$$

Then we obtain the S-denied second signature condition $g_{00}\,g_{11} - g_{01}^2 \leqslant 0$ (meaning the first signature condition is not denied $g_{00} > 0$) as follows

$$g_{11} - \frac{1}{c^2}\,v_1^2 \leqslant 0\,,$$

having two particular cases

$$g_{11} - \frac{1}{c^2}\,v_1^2 < 0\,, \qquad g_{11} - \frac{1}{c^2}\,v_1^2 = 0\,.$$

To better see the physical sense, take a case where g_{11} is close to -1.* Then, denoting $v^1 = v$, we obtain

$$v^2 > -c^2, \qquad v^2 = -c^2.$$

The first condition $v^2 > -c^2$ is true in the regular basic space-time. Because the velocities v and c take positive numerical values, this condition uses the well-known fact that positive numbers are greater than negative ones.

The second condition $v^2 = -c^2$ has no place in the basic space-time; it is true as a particular case of the common condition $v^2 \geqslant -c^2$ in the expanded spaces of kind II. This condition means that as soon as the linear velocity of the space rotation reaches light velocity, the space signature changes from $(+---)$ to $(-+++)$. That is, given an expanded space-time of kind II, the transit from a non-isotropic sub-light region into an isotropic light-like region implies change of signs in the space signature.

Conclusion on the kind II: An expanded space-time of kind II ($v^2 \geqslant -c^2$) is the generalization of the basic space-time of General Relativity ($v^2 > -c^2$) which permits the peculiarity that the space-time changes signs in its own signature as soon as we, reaching the light velocity of the space rotation, encounter a light-like isotropic region.

An expanded space-time of kind III: In this space-time the third signature condition is S-denied, the other signature conditions remain unchanged. So, given the expanded space-time of kind III, the third signature condition is

$$\det \begin{Vmatrix} g_{00} & g_{01} & g_{02} \\ g_{10} & g_{11} & g_{12} \\ g_{20} & g_{21} & g_{22} \end{Vmatrix} \geqslant 0\,,$$

*Because we use the signature $(+---)$.

which, taking the other form of the third signature condition into account, can be transformed into the formula

$$\det \begin{Vmatrix} h_{11} & h_{12} \\ h_{21} & h_{22} \end{Vmatrix} = h_{11}\,h_{22} - h_{12}^2 \geqslant 0\,,$$

that includes two different cases

$$h_{11}\,h_{22} - h_{12}^2 > 0\,, \qquad h_{11}\,h_{22} - h_{12}^2 = 0\,,$$

so that the third initial signature condition $h_{11}\,h_{22} - h_{12}^2 > 0$ is partially true and partially false. This condition is not clear. Future research is required.

An expanded space-time of kind IV: In this space-time the fourth signature condition $g = \det\|g_{\alpha\beta}\| < 0$ is S-denied, the other signature conditions remain unchanged. So, given the expanded space-time of kind IV, the fourth signature condition is

$$g = \det\|g_{\alpha\beta}\| = \det \begin{Vmatrix} g_{00} & g_{01} & g_{02} & g_{03} \\ g_{10} & g_{11} & g_{12} & g_{13} \\ g_{20} & g_{21} & g_{22} & g_{23} \\ g_{30} & g_{31} & g_{32} & g_{33} \end{Vmatrix} \leqslant 0\,,$$

that includes two different cases

$$g = \det\|g_{\alpha\beta}\| < 0\,, \qquad g = \det\|g_{\alpha\beta}\| = 0\,,$$

so that the fourth signature condition $g < 0$ is partially true and partially false: $g < 0$ is true in the basic space-time, $g = 0$ could be true in only he expanded spaces of kind IV.

Because the determinants of the fundamental metric tensor $g_{\alpha\beta}$ and the observable metric tensor h_{ik} are connected as follows $\sqrt{-g} = \sqrt{h}\,\sqrt{g_{00}}$ [6, 7], degeneration of the fundamental metric tensor ($g = 0$) implies that the observable metric tensor is also degenerate ($h = 0$). In such fully degenerate areas the space-time interval ds^2, the observable spatial interval $d\sigma^2 = h_{ik}\,dx^i dx^k$ and the observable time interval $d\tau$ become zero†

$$ds^2 = c^2 d\tau^2 - d\sigma^2 = 0\,, \qquad c^2 d\tau^2 = d\sigma^2 = 0\,.$$

Taking formulae for $d\tau$ and $d\sigma$ into account, and also the fact that in the accompanying reference frame we have $h_{00} = h_{0i} = 0$, we write $d\tau^2 = 0$ and $d\sigma^2 = 0$ as

$$d\tau = \left[1 - \frac{1}{c^2}\left(\mathrm{w} + v_i u^i\right)\right] dt = 0\,, \qquad dt \neq 0\,,$$

$$d\sigma^2 = h_{ik}\,dx^i dx^k = 0\,,$$

where the three-dimensional coordinate velocity $u^i = dx^i/dt$ is different to the observable velocity $\mathrm{v}^i = dx^i/d\tau$.

†Note, $ds^2 = 0$ is true not only at $c^2 d\tau^2 = d\sigma^2 = 0$, but also when $c^2 d\tau^2 = d\sigma^2 \neq 0$ (in the isotropic region, where light propagates). The properly observed time interval is determined as $d\tau = \sqrt{g_{00}}\,dt + \frac{g_{0i}}{c\sqrt{g_{00}}}dx^i$, where the coordinate time interval is $dt \neq 0$ [4, 5, 6, 7].

With $h_{ik} = -g_{ik} + \frac{1}{c^2} v_i v_k$, we obtain aforementioned physical conditions of degeneration in the final form

$$\mathrm{w} + v_i u^i = c^2, \qquad g_{ik} u^i u^k = c^2 \Big(1 - \frac{\mathrm{w}}{c^2}\Big)^2 .$$

As recently shown [8, 9], the degenerate conditions permit non-quantum teleportation and also virtual photons in General Relativity. Therefore we expect that, employing an expanded space of kind IV, one may join General Relativity and Quantum Electrodynamics.

Conclusion on the kind IV: An expanded space-time of kind IV ($g \leqslant 0$) is the generalization of the basic space-time of General Relativity ($g < 0$) including regions where this space-time is in a fully degenerate state ($g = 0$). From the viewpoint of a regular observer, in a fully degenerate area time intervals between any events are zero, and spatial intervals are zero. Thus, such a region is observable as a point.

An expanded space-time of kind V: In this space-time all four signature conditions are S-denied, therefore given the expanded space-time of kind V the signature conditions are

$$\det \| g_{00} \| = g_{00} \geqslant 0 ,$$

$$\det \begin{Vmatrix} g_{00} & g_{01} \\ g_{10} & g_{11} \end{Vmatrix} = g_{00}\, g_{11} - g_{01}^2 \leqslant 0 ,$$

$$\det \begin{Vmatrix} g_{00} & g_{01} & g_{02} \\ g_{10} & g_{11} & g_{12} \\ g_{20} & g_{21} & g_{22} \end{Vmatrix} \geqslant 0 ,$$

$$g = \det \| g_{\alpha\beta} \| = \det \begin{Vmatrix} g_{00} & g_{01} & g_{02} & g_{03} \\ g_{10} & g_{11} & g_{12} & g_{13} \\ g_{20} & g_{21} & g_{22} & g_{23} \\ g_{30} & g_{31} & g_{32} & g_{33} \end{Vmatrix} \leqslant 0 ,$$

so all four signature conditions are partially true and partially false. It is obvious that an expanded space of kind V contains expanded spaces of kind I, II, III, and IV as particular cases, it being a common space for all of them.

Negative S-denying expanded spaces: We could also S-deny the signatures with the possibility that say $g_{00} > 0$ for kind I, but this means that the gravitational potential would be imaginary, or, even take into account the "negative" cases for kind II, III, etc. But most of them are senseless from the geometrical viewpoint. Hence we have only included five main kinds in our discussion.

3 Classification of the expanded spaces for General Relativity

In closing this paper we repeat, in brief, the main results.

There are currently three main kinds of non-Euclidean geometry conceivable — Lobachevsky-Bolyai-Gauss geometry, Riemann geometry, and Smarandache geometries. A four-dimensional pseudo-Riemannian space, a space of the Riemannian geometry family, is the basic space-time of General Relativity. We employed S-denying of the signature conditions in the basic four-dimensional pseudo-Riemannian space, when a signature condition is partially true and partially false. S-denying each of the signature conditions (or even all the conditions at once) gave an expanded space for General Relativity, which, being an instance of the family of Smarandache spaces, include the pseudo-Riemannian space as a particular case. There are four signature conditions. So, we obtained five kinds of the expanded spaces for General Relativity:

Kind I Permits the space-time to be in collapse;

Kind II Permits the space-time to change its own signature as reaching the light speed of the space rotation in a light-like isotropic region;

Kind III Has some specific peculiarities (not clear yet), linked to the third signature condition;

Kind IV Permits full degeneration of the metric, when all degenerate regions become points. Such fully degenerate regions provide trajectories for non-quantum teleportation, and are also a home space for virtual photons.

Kind V Provides an expanded space, which has common properties of all spaces of kinds I, II, III, and IV, and includes the spaces as particular cases.

The foregoing results are represented in detail in the book [10], which is currently in print.

4 Extending this classification: mixed kinds of the expanded spaces

We can S-deny one axiom only, or two axioms, or three axioms, or even four axioms simultaneously. Hence we may have: $C_4^1 + C_4^2 + C_4^3 + C_4^4 = 2^4 - 1 = 15$ kinds of expanded spaces for General Relativity, where C_n^i denotes combinations of n elements taken in groups of i elements, $0 \leqslant i \leqslant n$. And considering the fact that each axiom can be S-denied in three different ways, we obtain $15 \times 3 = 45$ kinds of expanded spaces for General Relativity. Which expanded space would be most interesting?

We collect all such "mixed" spaces into a table. Specific properties of the mixed spaces follow below.

1.1.1: $g_{00} \geqslant 0$, $h_{11} > 0$, $h_{11} h_{22} - h_{12}^2 > 0$, $h > 0$. At $g_{00} = 0$, we have the usual space-time permitting collapse.

1.1.2: $g_{00} > 0$, $h_{11} \geqslant 0$, $h_{11} h_{22} - h_{12}^2 > 0$, $h > 0$. At $h_{11} = 0$ we have $h_{12}^2 < 0$ that is permitted for imaginary values of h_{12}: we obtain a complex Riemannian space.

1.1.3: $g_{00} > 0$, $h_{11} > 0$, $h_{11} h_{22} - h_{12}^2 \geqslant 0$, $h > 0$. At $h_{11} h_{22} - h_{12}^2 = 0$, the spatially observable metric $d\sigma^2$ permits purely spatial isotropic lines.

1.1.4: $g_{00} > 0$, $h_{11} > 0$, $h_{11} h_{22} - h_{12}^2 > 0$, $h \geqslant 0$. At $h = 0$, we have the spatially observed metric $d\sigma^2$ completely degenerate. An example — zero-space [9], obtained as a completely degenerate Riemannian space. Because $h = -\frac{g}{g_{00}}$, the

Positive S-denying spaces, $N \geqslant 0$		Negative S-denying spaces, $N \leqslant 0$		S-denying spaces, where $N > 0 \cup N < 0$	
Kind	Signature conditions	Kind	Signature conditions	Kind	Signature conditions
One of the signature conditions is S-denied					
1.1.1	$I \geqslant 0,\ II > 0,\ III > 0,\ IV > 0$	1.2.1	$I \leqslant 0,\ II > 0,\ III > 0,\ IV > 0$	1.3.1	$I \gtrless 0,\ II > 0,\ III > 0,\ IV > 0$
1.1.2	$I > 0,\ II \geqslant 0,\ III > 0,\ IV > 0$	1.2.2	$I > 0,\ II \leqslant 0,\ III > 0,\ IV > 0$	1.3.2	$I > 0,\ II \gtrless 0,\ III > 0,\ IV > 0$
1.1.3	$I > 0,\ II > 0,\ III \geqslant 0,\ IV > 0$	1.2.3	$I > 0,\ II > 0,\ III \leqslant 0,\ IV > 0$	1.3.3	$I > 0,\ II > 0,\ III \gtrless 0,\ IV > 0$
1.1.4	$I > 0,\ II > 0,\ III > 0,\ IV \geqslant 0$	1.2.4	$I > 0,\ II > 0,\ III > 0,\ IV \leqslant 0$	1.3.4	$I > 0,\ II > 0,\ III > 0,\ IV \gtrless 0$
Two of the signature conditions are S-denied					
2.1.1	$I \geqslant 0,\ II \geqslant 0,\ III > 0,\ IV > 0$	2.2.1	$I \leqslant 0,\ II \leqslant 0,\ III > 0,\ IV > 0$	2.3.1	$I \gtrless 0,\ II \gtrless 0,\ III > 0,\ IV > 0$
2.1.2	$I \geqslant 0,\ II > 0,\ III \geqslant 0,\ IV > 0$	2.2.2	$I \leqslant 0,\ II > 0,\ III \leqslant 0,\ IV > 0$	2.3.2	$I \gtrless 0,\ II > 0,\ III \gtrless 0,\ IV > 0$
2.1.3	$I \geqslant 0,\ II > 0,\ III > 0,\ IV \geqslant 0$	2.2.3	$I \leqslant 0,\ II > 0,\ III > 0,\ IV \leqslant 0$	2.3.3	$I \gtrless 0,\ II > 0,\ III > 0,\ IV \gtrless 0$
2.1.4	$I > 0,\ II \geqslant 0,\ III > 0,\ IV \geqslant 0$	2.2.4	$I > 0,\ II \leqslant 0,\ III > 0,\ IV \leqslant 0$	2.3.4	$I > 0,\ II \gtrless 0,\ III > 0,\ IV \gtrless 0$
2.1.5	$I > 0,\ II \geqslant 0,\ III \geqslant 0,\ IV > 0$	2.2.5	$I > 0,\ II \leqslant 0,\ III \leqslant 0,\ IV > 0$	2.3.5	$I > 0,\ II \gtrless 0,\ III \gtrless 0,\ IV > 0$
2.1.6	$I > 0,\ II > 0,\ III \geqslant 0,\ IV \geqslant 0$	2.2.6	$I > 0,\ II > 0,\ III \leqslant 0,\ IV \leqslant 0$	2.3.6	$I > 0,\ II > 0,\ III \gtrless 0,\ IV \gtrless 0$
Three of the signature conditions are S-denied					
3.1.1	$I > 0,\ II \geqslant 0,\ III \geqslant 0,\ IV \geqslant 0$	3.2.1	$I > 0,\ II \leqslant 0,\ III \leqslant 0,\ IV \leqslant 0$	3.3.1	$I > 0,\ II \gtrless 0,\ III \gtrless 0,\ IV \gtrless 0$
3.1.2	$I \geqslant 0,\ II > 0,\ III \geqslant 0,\ IV \geqslant 0$	3.2.2	$I \leqslant 0,\ II > 0,\ III \leqslant 0,\ IV \leqslant 0$	3.3.2	$I \gtrless 0,\ II > 0,\ III \gtrless 0,\ IV \gtrless 0$
3.1.3	$I \geqslant 0,\ II \geqslant 0,\ III > 0,\ IV \geqslant 0$	3.2.3	$I \leqslant 0,\ II \leqslant 0,\ III > 0,\ IV \leqslant 0$	3.3.3	$I \gtrless 0,\ II \gtrless 0,\ III > 0,\ IV \gtrless 0$
3.1.4	$I \geqslant 0,\ II \geqslant 0,\ III \geqslant 0,\ IV > 0$	3.2.4	$I \leqslant 0,\ II \leqslant 0,\ III \leqslant 0,\ IV > 0$	3.3.4	$I \gtrless 0,\ II \gtrless 0,\ III \gtrless 0,\ IV > 0$
All the signature conditions are S-denied					
4.1.1	$I \geqslant 0,\ II \geqslant 0,\ III \geqslant 0,\ IV \geqslant 0$	4.2.1	$I \leqslant 0,\ II \leqslant 0,\ III \leqslant 0,\ IV \leqslant 0$	4.3.1	$I \gtrless 0,\ II \gtrless 0,\ III \gtrless 0,\ IV \gtrless 0$

Table 1: The expanded spaces for General Relativity (all 45 mixed kinds of S-denying). The signature conditions are denoted by Roman numerals

metric ds^2 is also degenerate.

1.2.1: $g_{00} \leqslant 0,\ h_{11} > 0,\ h_{11}h_{22} - h_{12}^2 > 0,\ h > 0$. At $g_{00} = 0$, we have kind 1.1.1. At $g_{00} < 0$ physically observable time becomes imaginary $d\tau = \frac{g_{0i}\,dx^i}{c\sqrt{g_{00}}}$.

1.2.2: $g_{00} > 0,\ h_{11} \leqslant 0,\ h_{11}h_{22} - h_{12}^2 > 0,\ h > 0$. At $h_{11} = 0$, we have kind 1.1.2. At $h_{11} < 0$, distances along the axis x^1 (i. e. the values $\sqrt{h_{11}}dx^1$) becomes imaginary, contradicting the initial conditions in General Relativity.

1.2.3: $g_{00} > 0,\ h_{11} > 0,\ h_{11}h_{22} - h_{12}^2 \leqslant 0,\ h > 0$. This is a common space built on a particular case of kind 1.1.3 where $h_{11}h_{22} - h_{12}^2 = 0$ and a subspace where $h_{11}h_{22} - h_{12}^2 < 0$. In the latter subspace the spatially observable metric $d\sigma^2$ becomes sign-alternating so that the space-time metric has the signature $(+-+-)$ (this case is outside the initial statement of General Relativity).

1.2.4: $g_{00} > 0,\ h_{11} > 0,\ h_{11}h_{22} - h_{12}^2 > 0,\ h \leqslant 0$. This space is built on a particular case of kind 1.1.2 where $h = 0$ and a subspace where $h < 0$. At $h < 0$ we have the spatial metric $d\sigma^2$ sign-alternating so that the space-time metric has the signature $(+--+)$ (this case is outside the initial statement of General Relativity).

1.3.1: $g_{00} \gtrless 0,\ h_{11} > 0,\ h_{11}h_{22} - h_{12}^2 > 0,\ h > 0$. Here we have the usual space-time area ($g_{00} > 0$) with the signature $(+---)$, and a sign-definite space-time ($g_{00} < 0$) where the signature is $(----)$. There are no intersections of the areas in the common space-time; they exist severally.

1.3.2: $g_{00} > 0,\ h_{11} \gtrless 0,\ h_{11}h_{22} - h_{12}^2 > 0,\ h > 0$. Here we have a common space built on two separated areas where $(+---)$ (usual space-time) and a subspace where $(++--)$. The areas have no intersections.

1.3.3: $g_{00} > 0,\ h_{11} > 0,\ h_{11}h_{22} - h_{12}^2 \gtrless 0,\ h > 0$. This is a common space built on the usual space-time and a particular space-time of kind 1.2.3, where the signature is $(+-+-)$. The areas have no intersections.

1.3.4: $g_{00} > 0,\ h_{11} > 0,\ h_{11}h_{22} - h_{12}^2 > 0,\ h \gtrless 0$. This is a common space built on the usual space-time and a particular space-time of kind 1.2.4, where the signature is $(+--+)$. The areas have no intersections.

2.1.1: $g_{00} \geqslant 0,\ h_{11} \gtrless 0,\ h_{11}h_{22} - h_{12}^2 > 0,\ h > 0$. This is a complex Riemannian space with a complex metric $d\sigma^2$, permitting collapse.

2.1.2: $g_{00} \gtrless 0,\ h_{11} > 0,\ h_{11}h_{22} - h_{12}^2 \gtrless 0,\ h > 0$. This space permits collapse, and purely spatial isotropic directions.

2.1.3: $g_{00} \gtrless 0,\ h_{11} > 0,\ h_{11}h_{22} - h_{12}^2 > 0,\ h \gtrless 0$. This space permits complete degeneracy and collapse. At $g_{00} = 0$ and $h = 0$, we have a collapsed zero-space.

2.1.4: $g_{00} > 0,\ h_{11} \gtrless 0,\ h_{11}h_{22} - h_{12}^2 > 0,\ h \gtrless 0$. Here we have a complex Riemannian space permitting complete degeneracy.

2.1.5: $g_{00} > 0,\ h_{11} \geqslant 0,\ h_{11}h_{22} - h_{12}^2 \geqslant 0,\ h > 0$. At

$h_{11}=0$, we have $h_{12}^2=0$: a partial degeneration of the spatially observable metric $d\sigma^2$.

2.1.6: $g_{00}>0,\ h_{11}>0,\ h_{11}h_{22}-h_{12}^2\geqslant 0,\ h\geqslant 0$. This space permits the spatially observable metric $d\sigma^2$ to completely degenerate: $h=0$.

2.2.1: $g_{00}\leqslant 0,\ h_{11}\leqslant 0,\ h_{11}h_{22}-h_{12}^2>0,\ h>0$. At $g_{00}=0$ and $h_{11}=0$, we have a particular space-time of kind 2.1.1. At $g_{00}<0,\ h_{11}<0$ we have a space with the signature $(----)$ where time is like a spatial coordinate (this case is outside the initial statement of General Relativity).

2.2.2: $g_{00}\leqslant 0,\ h_{11}>0,\ h_{11}h_{22}-h_{12}^2\leqslant 0,\ h>0$. At $g_{00}=0$ and $h_{11}h_{22}-h_{12}^2=0$, we have a particular space-time of kind 2.1.2. At $g_{00}<0$ and $h_{11}h_{22}-h_{12}^2<0$, we have a space with the signature $(-+-+)$ (it is outside the initial statement of General Relativity).

2.2.3: $g_{00}\leqslant 0,\ h_{11}>0,\ h_{11}h_{22}-h_{12}^2>0,\ h\leqslant 0$. At $g_{00}=0$ and $h=0$, we have a particular space-time of kind 2.1.3. At $g_{00}<0$ and $h_{11}h_{22}-h_{12}^2<0$, we have a space-time with the signature $(---+)$ (it is outside the initial statement of General Relativity).

2.2.4: $g_{00}>0,\ h_{11}\leqslant 0,\ h_{11}h_{22}-h_{12}^2\leqslant 0,\ h>0$. At $h_{11}=0$ and $h_{11}h_{22}-h_{12}^2=0$, we have a particular space-time of kind 2.1.5. At $h_{11}<0$ and $h_{11}h_{22}-h_{12}^2<0$, we have a space-time with the signature $(++-+)$ (outside the initial statement of General Relativity).

2.2.5: $g_{00}>0,\ h_{11}\leqslant 0,\ h_{11}h_{22}-h_{12}^2\geqslant 0,\ h\leqslant 0$. At $h_{11}=0$ and $h=0$, we have a particular space-time of kind 2.1.4. At $h_{11}<0$ and $h<0$, a space-time with the signature $(+--+)$ (outside the initial statement of General Relativity).

2.2.6: $g_{00}>0,\ h_{11}>0,\ h_{11}h_{22}-h_{12}^2\leqslant 0,\ h\leqslant 0$. At $h_{11}h_{22}-h_{12}^2=0$ and $h=0$, we have a particular space-time of kind 2.1.6. At $h_{11}h_{22}-h_{12}^2<0$ and $h<0$, we have a space-time with the signature $(+-++)$ (outside the initial statement of General Relativity).

2.3.1: $g_{00}\gtrless 0,\ h_{11}\gtrless 0,\ h_{11}h_{22}-h_{12}^2>0,\ h>0$. This is a space built on two areas. At $g_{00}>0$ and $h_{11}>0$, we have the usual space-time. At $g_{00}<0$ and $h_{11}<0$, we have a particular space-time of kind 2.2.1. The areas have no intersections: the common space is actually built on non-intersecting areas.

2.3.2: $g_{00}\gtrless 0,\ h_{11}>0,\ h_{11}h_{22}-h_{12}^2\gtrless 0,\ h>0$. This space is built on two areas. At $g_{00}>0$ and $h_{11}h_{22}-h_{12}^2>0$, we have the usual space-time. At $g_{00}<0$ and $h_{11}h_{22}-h_{12}^2<0$, we have a particular space-time of kind 2.2.2. The areas, building a common space, have no intersections.

2.3.3: $g_{00}\gtrless 0,\ h_{11}>0,\ h_{11}h_{22}-h_{12}^2>0,\ h\gtrless 0$. This space is built on two areas. At $g_{00}>0$ and $h_{11}>0$, we have the usual space-time. At $g_{00}<0$ and $h_{11}<0$, a particular space-time of kind 2.2.3. The areas, building a common space, have no intersections.

2.3.4: $g_{00}>0,\ h_{11}\gtrless 0,\ h_{11}h_{22}-h_{12}^2>0,\ h\gtrless 0$. This space is built on two areas. At $h_{11}>0$ and $h>0$, we have the usual space-time. At $h_{11}<0$ and $h<0$, a particular space-time of kind 2.2.4. The areas, building a common space, have no intersections.

2.3.5: $g_{00}>0,\ h_{11}\gtrless 0,\ h_{11}h_{22}-h_{12}^2\gtrless 0,\ h>0$. This space is built on two areas. At $h_{11}>0$ and $h_{11}h_{22}-h_{12}^2>0$, we have the usual space-time. At $h_{11}<0$ and $h_{11}h_{22}-h_{12}^2<0$, a particular space-time of kind 2.2.5. The areas, building a common space, have no intersections.

2.3.6: $g_{00}>0,\ h_{11}>0,\ h_{11}h_{22}-h_{12}^2\gtrless 0,\ h\gtrless 0$. This space is built on two areas. At $h_{11}h_{22}-h_{12}^2>0$ and $h>0$, we have the usual space-time. At $h_{11}h_{22}-h_{12}^2<0$ and $h<0$, a particular space-time of kind 2.2.6. The areas, building a common space, have no intersections.

3.1.1: $g_{00}>0,\ h_{11}\geqslant 0,\ h_{11}h_{22}-h_{12}^2\geqslant 0,\ h\geqslant 0$. This space permits complete degeneracy. At $h_{11}>0,\ h_{11}h_{22}-h_{12}^2>0,\ h>0$, we have the usual space-time. At $h_{11}=0,\ h_{11}h_{22}-h_{12}^2=0,\ h=0$, we have a particular case of a zero-space.

3.1.2: $g_{00}\geqslant 0,\ h_{11}>0,\ h_{11}h_{22}-h_{12}^2\geqslant 0,\ h\geqslant 0$. At $g_{00}>0,\ h_{11}h_{22}-h_{12}^2>0,\ h>0$, we have the usual space-time. At $g_{00}=0,\ h_{11}h_{22}-h_{12}^2=0,\ h=0$, we have a particular case of a collapsed zero-space.

3.1.3: $g_{00}\geqslant 0,\ h_{11}\geqslant 0,\ h_{11}h_{22}-h_{12}^2>0,\ h\geqslant 0$. At $g_{00}>0,\ h_{11}>0,\ h>0$, we have the usual space-time. At $g_{00}=0,\ h_{11}=0,\ h=0$, we have a collapsed zero-space, derived from a complex Riemannian space.

3.1.4: $g_{00}\geqslant 0,\ h_{11}\geqslant 0,\ h_{11}h_{22}-h_{12}^2\geqslant 0,\ h>0$. At $g_{00}>0,\ h_{11}>0,\ h_{11}h_{22}-h_{12}^2>0$, we have the usual space-time. At $g_{00}=0,\ h_{11}=0,\ h_{11}h_{22}-h_{12}^2=0$, we have the usual space-time in a collapsed state, while there are permitted purely spatial isotropic directions $\sqrt{h_{11}}dx^1$.

3.2.1: $g_{00}>0,\ h_{11}\leqslant 0,\ h_{11}h_{22}-h_{12}^2\leqslant 0,\ h\leqslant 0$. At $h_{11}=0,\ h_{11}h_{22}-h_{12}^2=0$ and $h=0$, we have a particular space-time of kind 3.1.1. At $h_{11}<0,\ h_{11}h_{22}-h_{12}^2<0$ and $h<0$, we have a space-time with the signature $(++++)$ (outside the initial statement of General Relativity).

3.2.2: $g_{00}\leqslant 0,\ h_{11}>0,\ h_{11}h_{22}-h_{12}^2\leqslant 0,\ h\leqslant 0$. At $g_{00}=0,\ h_{11}h_{22}-h_{12}^2=0$ and $h=0$, we have a particular space-time of kind 3.1.2. At $h_{11}<0,\ h_{11}h_{22}-h_{12}^2<0$ and $h<0$, we have a space-time with the signature $(--++)$ (outside the initial statement of General Relativity).

3.2.3: $g_{00}\leqslant 0,\ h_{11}\leqslant 0,\ h_{11}h_{22}-h_{12}^2>0,\ h\leqslant 0$. At $g_{00}=0,\ h_{11}=0$ and $h=0$, we have a particular space-time of kind 3.1.3. At $h_{11}<0,\ h_{11}h_{22}-h_{12}^2<0$ and $h<0$, we have a space-time with the signature $(-+-+)$ (outside the initial statement of General Relativity).

3.2.4: $g_{00}\leqslant 0,\ h_{11}\leqslant 0,\ h_{11}h_{22}-h_{12}^2\leqslant 0,\ h>0$. At $g_{00}=0,\ h_{11}=0$ and $h_{11}h_{22}-h_{12}^2=0$, we have a particular space-time of kind 3.1.4. At $g_{00}<0,\ h_{11}<0$ and $h_{11}h_{22}-h_{12}^2<0$, we have a space-time with the signature $(-++-)$ (outside the initial statement of General Relativity).

3.3.1: $g_{00}>0,\ h_{11}\gtrless 0,\ h_{11}h_{22}-h_{12}^2\gtrless 0,\ h\gtrless 0$. This is a space built on two areas. At $h_{11}>0,\ h_{11}h_{22}-h_{12}^2>0$ and $h_{11}>0$, we have the usual space-time. At $h_{11}<0,\ h_{11}h_{22}-h_{12}^2<0$ and $h_{11}<0$, we have a particular space-time of kind 3.2.1. The areas have no intersections: the

common space is actually built on non-intersecting areas.

3.3.2: $g_{00} \gtrless 0,\ h_{11} > 0,\ h_{11}h_{22} - h_{12}^2 \gtrless 0,\ h \gtrless 0$. This space is built on two areas. At $g_{00} > 0$, $h_{11}h_{22} - h_{12}^2 > 0$ and $h > 0$, we have the usual space-time. At $g_{00} < 0$, $h_{11}h_{22} - h_{12}^2 < 0$ and $h < 0$, we have a particular space-time of kind 3.2.2. The areas, building a common space, have no intersections.

3.3.3: $g_{00} \gtrless 0,\ h_{11} \gtrless 0,\ h_{11}h_{22} - h_{12}^2 > 0,\ h \gtrless 0$. This space is built on two areas. At $g_{00} > 0$, $h_{11} > 0$ and $h > 0$, we have the usual space-time. At $g_{00} < 0$, $h_{11} < 0$ and $h < 0$, we have a particular space-time of kind 3.2.3. The areas, building a common space, have no intersections.

3.3.4: $g_{00} \gtrless 0,\ h_{11} \gtrless 0,\ h_{11}h_{22} - h_{12}^2 \gtrless 0,\ h > 0$. This space is built on two areas. At $g_{00} > 0$, $h_{11} > 0$ and $h_{11}h_{22} - h_{12}^2 > 0$, we have the usual space-time. At $g_{00} < 0$, $h_{11} < 0$ and $h_{11}h_{22} - h_{12}^2 < 0$, a particular space-time of kind 3.2.4. The areas, building a common space, have no intersections.

4.4.1: $g_{00} \geqslant 0,\ h_{11} \geqslant 0,\ h_{11}h_{22} - h_{12}^2 \geqslant 0,\ h \geqslant 0$. At $g_{00} > 0$, $h_{11} > 0$, $h_{11}h_{22} - h_{12}^2 \geqslant 0$ and $h \geqslant 0$, we have the usual space-time. At $g_{00} = 0$, $h_{11} = 0$, $h_{11}h_{22} - h_{12}^2 = 0$ and $h = 0$, we have a particular case of collapsed zero-space.

4.4.2: $g_{00} \leqslant 0,\ h_{11} \leqslant 0,\ h_{11}h_{22} - h_{12}^2 \leqslant 0,\ h \leqslant 0$. At $g_{00} = 0$, $h_{11} = 0$, $h_{11}h_{22} - h_{12}^2 = 0$ and $h = 0$, we have a particular case of space-time of kind 4.4.1. At $g_{00} < 0$, $h_{11} < 0$, $h_{11}h_{22} - h_{12}^2 < 0$ and $h < 0$, we have a space-time with the signature $(----)$ (outside the initial statement of General Relativity). The areas have no intersections.

4.4.3: $g_{00} \gtrless 0,\ h_{11} \gtrless 0,\ h_{11}h_{22} - h_{12}^2 \gtrless 0,\ h \gtrless 0$. At $g_{00} > 0$, $h_{11} > 0$, $h_{11}h_{22} - h_{12}^2 > 0$ and $h > 0$, we have the usual space-time. At $g_{00} < 0$, $h_{11} < 0$, $h_{11}h_{22} - h_{12}^2 < 0$ and $h < 0$, we have a space-time with the signature $(----)$ (outside the initial statement of General Relativity). The areas have no intersections.

References

1. Smarandache F. Paradoxist mathematics. *Collected papers*, v. II, Kishinev University Press, Kishinev, 1997, 5–29.
2. Kuciuk L. and Antholy M. An introduction to Smarandache geometries. *New Zealand Math. Coll.*, Massey Univ., 2001, http://atlas-conferences.com/c/a/h/f/09.htm; Also *Intern. Congress of Mathematicians ICM-2002*, Beijing, China, 2002, http://www.icm2002.org.cn/B/Schedule_Section04.htm.
3. Iseri H. Smarandache manifolds. American Research Press, Rehoboth, 2002.
4. Landau L. D. and Lifshitz E. M. The classical theory of fields. GITTL, Moscow, 1939 (referred with the 4th final expanded edition, Butterworth–Heinemann, 1980).
5. Eddington A. S. The mathematical theory of relativity. Cambridge University Press, Cambridge, 1924 (referred with the 3rd expanded edition, GTTI, Moscow, 1934).
6. Zelmanov A. L. Chronometric invariants. Dissertation, 1944. Published: CERN, EXT-2004-117.
7. Zelmanov A. L. Chronometric invariants and co-moving coordinates in the general relativity theory. *Doklady Acad. Nauk USSR*, 1956, v. 107 (6), 815–818.
8. Borissova L. B. and Rabounski D. D. Fields, vacuum, and the mirror Universe. Editorial URSS, Moscow, 2001, 272 pages (the 2nd revised ed.: CERN, EXT-2003-025).
9. Borissova L. and Rabounski D. On the possibility of instant displacements in the space-time of General Relativity. *Progress in Physics*, 2005, v. 1, 17–19; Also in: *Physical Interpretation of Relativity Theory* (PIRT-2005), Proc. of the Intern. Meeting., Moscow, 2005, 234–239; Also in: *Today's Takes on Einstein's Relativity*, Proc. of the Confer., Tucson (Arizona), 2005, 29–35.
10. Rabounki D., Smarandache F., Borissova L. Neutrosophic Methods in General Relativity. Hexis, Phoenix (Arizona), 2005.

Nonlocal Effects of Chemical Substances on the Brain Produced through Quantum Entanglement

Huping Hu and Maoxin Wu

Biophysics Consulting Group, 25 Lubber Street, Stony Brook, NY 11790, USA

E-mail: hupinghu@quantumbrain.org

Photons are intrinsically quantum objects and natural long-distance carriers of information. Since brain functions involve information and many experiments have shown that quantum entanglement is physically real, we have contemplated from the perspective of our recent hypothesis on the possibility of entangling the quantum entities inside the brain with those in an external chemical substance and carried out experiments toward that end. Here we report that applying magnetic pulses to the brain when an anesthetic or pain medication was placed in between caused the brain to feel the effect of the said substance for several hours after the treatment as if the test subject had actually inhaled the same. The said effect is consistently reproducible. We further found that drinking water exposed to magnetic pulses, laser light or microwave when a chemical substance was placed in between also causes consistently reproducible brain effects in various degrees. Further, through additional experiments we have verified that the said brain effect is the consequence of quantum entanglement between quantum entities inside the brain and those of the chemical substance under study, induced by the photons of the magnetic pulses or applied lights. We suggest that the said quantum entities inside the brain are nuclear and/or electron spins and discuss the profound implications of these results.

1 Introduction

Quantum entanglement is ubiquitous in the microscopic world and manifests itself macroscopically under some circumstances [1, 3, 4]. Further, quantum spins of electrons and photons have now been successfully entangled in various ways for the purposes of quantum computation, memory and communication [5, 6]. In the field of neuroscience, we have recently suggested that nuclear and/or electronic spins inside the brain may play important roles in certain aspects of brain functions such as perception [2]. Arguably, we could test our hypothesis by first attempting to entangle these spins with those of a chemical substance such as a general anaesthetic and then observing the resulting brain effects such an attempt may produce, if any. Indeed, instead of armchair debate on how the suggested experiments might not work, we just went ahead and carried out the experiments over a period of more than a year. Here, we report our results. We point out from the outset that although it is commonly believed that quantum entanglement alone cannot be used to transmit classical information, the function of the brain may not be totally based on classical information [2].

2 Methods, test subjects and materials

Figure 1A (see end sheet) illustrates a typical setup for the first set of experiments. It includes a magnetic coil with an estimated 20 W output placed at one inch above the right side of a test subject's forehead, a small flat glass-container inserted between the magnetic coil and the forehead, and an audio system with adjustable power output and frequency spectrum controls connected to the magnetic coil. When music is played on the audio system, the said magnetic coil produces magnetic pulses with frequencies in the range of 5 Hz to 10 kHz. Experiments were conducted with said container being filled with different general anaesthetics, medications, or nothing/water as control, and the test subject being exposed to the magnetic pulses for 10 min and not being told the content in the container or details of the experiments.

The indicators used to measure the brain effect of the treatment were the first-person experiences of any unusual sensations such as numbness, drowsiness and/or euphoria which the subject felt after the treatment and the relative degrees of these unusual sensations on a scale of 10 with 0 = nothing, 1 = weak, 2 = light moderate, 3 = moderate, 4 = light strong, 5 = strong, 6 = heavily strong, 7 = very strong, 8 = intensely strong, 9 = extremely strong and 10 = intolerable. The durations of the unusual sensations and other symptoms after the treatment, such as nausea or headache, were also recorded.

Figure 1B illustrates a typical setup for the second set of experiments. It includes the magnetic coil connected to the audio system, a large flat glass-container filled with 200 ml fresh tap water and the small flat glass-container inserted between the magnetic coil and larger glass-container. Figure 1C illustrates a typical setup for the second set of experiments when a red laser with a 50 mW output and wavelengths of

635 nm–675 nm was used. All Experiments were conducted in the dark with the small flat glass-container being filled with different general anaesthetics, medications, or nothing/water as control, the large glass-container being filled with 200 ml of fresh tap water and exposed to the magnetic pulses or laser light for 30 min and the test subject consuming the treated tap water but not being told the content in the small container or details of the experiments. The indicators used for measuring the brain effects were the same as those used in the first set of experiments. Experiments were also carried out respectively with a 1200 W microwave oven and a flashlight powered by two size-D batteries. When the microwave oven was used, a glass tube containing 20 ml of fresh tap water was submerged into a larger glass tube containing 50 ml of general anaesthetic and exposed to microwave radiation for 5 sec. The said procedure was repeated numerous times, to collect a total of 200 ml of treated tap water for consumption. When the flashlight was used, the magnetic coil shown in Figure 1B was replaced with the flashlight.

To verify that the brain effects experienced by the test subjects were the consequences of quantum entanglement between quantum entities inside the brain and those in the chemical substances under study, the following additional experiments were carried out. Figure 1D shows a typical setup of the entanglement verification experiments. The setup is the reverse of the setup shown in Figure 1C. In addition, the small flat glass-container with a chemical substance or nothing/water as control was positioned with an angle to the incoming laser light to prevent reflected laser light from re-entering the large glass-container.

In the first set of entanglement verification experiments, the laser light from the red laser first passed through the large glass-container with 200 ml of fresh tap water and then through the small flat glass-container filled with a chemical substance or nothing/water as control located about 300 cm away. After 30 min of exposure to the laser light, a test subject consumed the exposed tap water without being told the content in the small container or details of the experiments and reported the brain effects felt for the next several hours.

In the second set of entanglement verification experiments, 400 ml of fresh tap water in a glass-container was first exposed to the radiation of the magnetic coil for 30 min or that of the 1500W microwave oven for 2 min. Then the test subject immediately consumed one-half of the water so exposed. After 30 min from the time of consumption the other half was exposed to magnetic pulses or laser light for 30 minutes using the setup shown in Figure 1B and Figure 1D respectively. The test subject reported, without being told the content in the small container or details of the experiments, the brain effects felt for the whole period from the time of consumption to several hours after the exposure had stopped. In the third set of entanglement verification experiments, one-half of 400 ml Poland Spring water with a shelve time of at least three months was immediately consumed by the test subject. After 30 min from the time of consumption the other half was exposed to the magnetic pulses or laser light for 30 min using the setup shown in Figure 1B and Figure 1D respectively. Test subject reported, without being told the content in the small container or details of the experiments, the brain effects felt for the whole period from the time of consumption to several hours after the exposure had stopped.

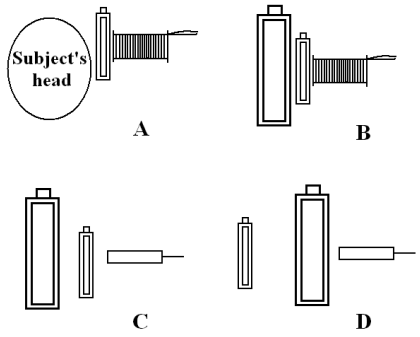

Fig. 1: Schematic view of typical experimental setups used in our study

In the fourth set of entanglement verification experiments, the test subject would take one-half of the 400 ml fresh tap water exposed to microwave for 2 min or magnetic pulses for 30 min to his/her workplace located more than 50 miles away (in one case to Beijing located more than 6,500 miles away) and consumed the same at the workplace at a specified time. After 30 min from the time of consumption, the other half was exposed to magnetic pulses or laser light for 30 min at the original location using the setup shown in Figure 1B and Figure 1D respectively. The test subject reported the brain effects felt without being told the content in the small container or details of the experiments for the whole period from the time of consumption to several hours after the exposure had stopped.

With respect to the test subjects, Subject A and C are respectively the first author and co-author of this paper and Subject B and C are respectively the father and mother of the first author. All four test subjects voluntarily consented to the proposed experiments. To ensure safety, all initial experiments were conducted on Subject A by himself. Further, all general anaesthetics used in the study were properly obtained for research purposes and all medications were either leftover items originally prescribed to Subject C's late mother or items available over the counter. To achieve proper control, repeating experiments on Subject A were carried out by either Subject B or C in blind settings, that is, he was not told whether or what general anaesthetic or medication were applied before the end of the experiments. Further, all experiments on Subject B, C and D were also carried out in blind settings, that is, these test subjects were not told about the details of the experiments on them or whether or what general anaesthetic or medication were applied.

	1st Set: Magn. Coil		2nd Set: Magn. Coil		Red laser		Flashlight		Microwave	
	Test ♯	Effect	Test ♯	Effect	Test ♯	Effect	Test ♯	Effect	Test ♯	Effect
Anaesthetics										
Subject A	13	yes	16	yes	22	yes	8	yes	3	yes
Subject B	2	yes	2	yes	3	yes	0	n/a	1	yes
Subject C	2	yes	6	yes	6	yes	0	n/a	1	yes
Subject D	2	yes	1	yes	5	yes	0	n/a	0	n/a
Medications										
Subject A	17	yes	14	yes	16	yes	1	yes	3	yes
Subject B	1	yes	1	yes	3	yes	0	n/a	2	yes
Subject C	3	yes	1	yes	4	yes	0	n/a	1	yes
Subject D	0	n/a	0	n/a	3	yes	0	n/a	1	yes
Control										
Subject A	12	no	5	no	11	no				
Subject B	3	no	0	n/a	1	no				
Subject C	1	no	2	no	4	no				
Subject D	0	n/a	0	n/a	1	no				

Table 1: Summary of results obtained from the first two sets of experiments

3 Results

Table 1 summarizes the results obtained from the first two sets of experiments described above and Table 2 details the summary into each general anaesthetic studied plus morphine in the case of medications. In the control studies for the first set of experiments, all test subjects did not feel anything unusual from the exposure to magnetic pulses except vague or weak local sensation near the site of exposure. In contrast, all general anaesthetics studied produced clear and completely reproducible brain effects in various degrees and durations as if the test subjects had actually inhaled the same. These brain effects were first localized near the site of treatment and then spread over the whole brain and faded away within several hours. But residual brain effects (hangover) lingered on for more than 12 hours in most cases. Among the general anaesthetics studied, chloroform and deuterated chloroform (chloroform D) produced the most pronounced and potent brain effects in strength and duration followed by isoflorance and diethyl ether. Tribromoethanol dissolved in water (1:50 by weight) and ethanol also produced noticeable effects but they are not summarized in the table.

As also shown in Table 1, while the test subjects did not feel anything unusual from consuming the tap water treated in the control experiments with magnetic pulses or laser light, all the general anaesthetics studied produced clear and completely reproducible brain effects in various degrees and durations respectively similar to the observations in the first set of experiments. These effects were over the whole brain, intensified within the first half hour after the test subjects consumed the treated water and then faded away within the next few hours. But residual brain effects lingered on for more than 12 hours as in the first set of experiments. Among the general anaesthetics studied, again chloroform and deuterated chloroform produced the most pronounced and potent effect in strength and duration followed by isoflorance and diethyl ether as illustrated in Figure 2. Tribromoethanol dissolved in water (1:50 by weight) and ethanol also produced noticeable effects but they are not summarized in the table.

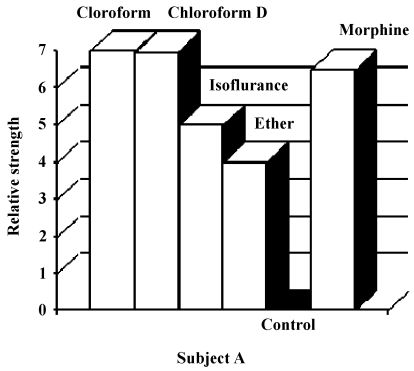

Fig. 2: Illustration of relative strengths of brain effects of several anesthetics and morphine

In addition, available results with flashlight and microwave as photon sources are also summarized in Table 1 respectively. In both cases general anaesthetics studied produced clear and reproducible brain effects. But the brain effects produced with microwave exposure were much stronger than those by flashlight.

Table 1 also summarizes results obtained with several medications including morphine, fentanyl, oxycodone, nicotine and caffeine in first and second sets of experiments. We

found that they all produced clear and completely reproducible brain effects such as euphoria or hastened alertness in various degrees and durations respectively. For example, in the case of morphine in the first set of experiments the brain effect was first localized near the site of treatment and then spread over the whole brain and faded away within several hours. In the case of morphine in the second set of experiments the brain effect was over the whole brain, first intensified within the first half hour after the test subjects consumed the treated water and then faded away within the next a few hours as illustrated in Figure 3.

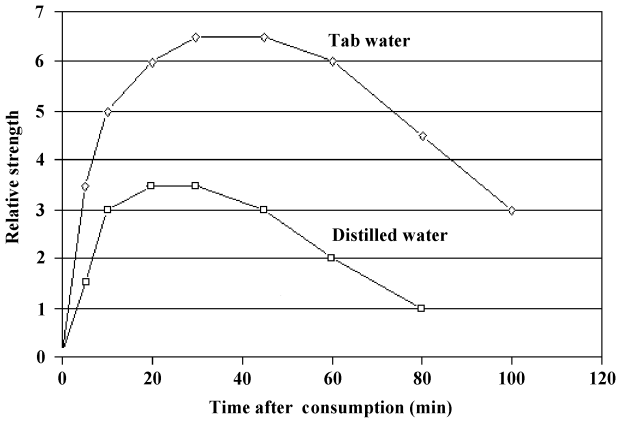

Fig. 3: Illustration of dynamics of brain effects produced by two types of water exposed to morphine

Comparative experiments were also done on Subject A and C with chloroform and diethyl ether by asking them to inhale the vapours of chloroform and diethyl respectively for 5 sec and compare the brain effect felt with those in the two sets of experiments described above. The brain effects induced in these comparative experiments were qualitatively similar to those produced in various experiments described above when chloroform and diethyl ether were respectively used for the exposure to photons of various sources.

Furthermore, through additional experiments we also made the following preliminary observations. First, the brain effects in the first set of experiments could not be induced by a permanent magnet in the place of the magnetic coil. Nor could these effects be produced by a third magnetic coil placed directly above the head of the test subject and connected to a second magnetic coil through an amplifier with the second magnetic coil receiving magnetic pulses from a first magnetic coil after the said magnetic pulses first passed through the anaesthetic sample. That is, the brain effects could not be transmitted through an electric wire. Second, in the second set of experiments the water exposed to magnetic pulses, laser light, microwave and flashlight when a chemical substance was present tasted about the same as that before the exposure. Third, heating tap water exposed to magnetic pulses or laser light in the presence of a chemical substance diminished the brain effect of the said substance. Fourth, when distilled water was used instead of fresh tap water the observed brain effects were markedly reduced as illustrated in Figure 6 in the case of morphine.

Table 3 summarizes the results obtained with the entanglement verification experiments carried out so far with chloroform, deuterated chloroform, diethyl ether and morphine. With all four sets of experiments, clear and consistently reproducible brain effects were experienced by the test subjects above and beyond what were noticeable in the control portions of the experiments under blind settings. More specifically, in the first set of entanglement verification experiments, the brain effects experienced by the test subjects were the same as those in which the setup shown in Figure 1C was used. In the second, third and fourth sets of these experiments, all test subjects did not feel anything unusual in the first half hour after consuming the first half of the water either exposed to microwave/magnetic pulses or just sit on the shelf for more than 3 months. But within minutes after the second half of the same water was exposed to the laser light or magnetic pulses in the presence of general anaesthetics, the test subjects would experience clear and completely reproducible brain effect of various intensities as if they have actually inhaled the general anaesthetic used in the exposure of the second half of the water. The said brain effects were over the whole brain, first intensified within minutes after the exposure began and persisted for the duration of the said exposure and for the next several hours after the exposure had stopped. Further, all other conditions being the same, magnetic coil produced more intense brain effects than the red laser. Furthermore, all other conditions being the same, the water exposed to microwave or magnetic pulses before consumption produced more intense brain effects than water just sitting on the shelve for more than 3 months before consumption.

4 Discussion

With respect to the second, third and fourth sets of entanglement verification experiments, the only possible explanation for the brain effects experienced by the test subjects are that they were the consequences of quantum entanglement because the water consumed by the test subjects was never directly exposed to the magnetic pulses or the laser lights in the presence of the chemical substances. There are other indications that quantum entanglement was the cause of the brain effects experienced by the test subjects. First, the brain effect inducing means could not be transmitted through an electrical wire as already reported above. Second, the said inducing means did not depend on the wavelengths of the photons generated. Thus, mere interactions among the photons, a chemical substance and water will induce brain effects after a test subject consumes the water so interacted.

While designing and conducting the herein described experiments, the first author became aware of the claims

	1st Set: Magn. Coil		2nd Set: Magn. Coil		Red laser		Flashlight		Microwave	
	Test ♯	Effect	Test ♯	Effect	Test ♯	Effect	Test ♯	Effect	Test ♯	Effect
Chloroform										
Subject A	2	yes	2	yes	5	yes	2	yes	3	yes
Subject B	0	n/a	0	n/a	1	yes	0	n/a	1	yes
Subject C	1	yes	2	yes	3	yes	0	n/a	1	yes
Subject D	1	yes	0	n/a	2	yes	0	n/a	0	n/a
Chloroform D										
Subject A	3	yes	2	yes	2	yes	1	yes		
Subject B	1	yes	0	n/a	1	yes	0	n/a		
Subject C	0	n/a	0	n/a	1	yes	0	n/a		
Subject D	0	n/a	0	n/s	0	n/a	0	n/a		
Isoflurance										
Subject A	3	yes	6	yes	5	yes	4	yes		
Subject B	0	n/a	1	yes	0	n/a	0	0		
Subject C	0	n/a	1	yes	1	n/a	0	0		
Subject D	1	yes	1	yes	1	n/a	0	0		
Diethyl Ether										
Subject A	5	yes	6	yes	10	yes	1	yes		
Subject B	1	yes	1	yes	1	yes	0	n/a		
Subject C	1	yes	3	yes	1	yes	0	n/a		
Subject D	0	n/a	0	n/a	2	yes	0	n/a		
Morphine										
Subject A	5	yes	7	yes	5	yes				
Subject B	0	n/a	1	yes	2	yes				
Subject C	0	n/a	1	yes	2	yes				
Subject D	0	n/a	0	n/a	2	yes				
Other Medications										
Subject A	7	yes	4	yes						
Subject B	1	yes	0	n/a						
Subject C	3	yes	0	n/a						
Subject D	0	n/a	0	n/a						

Table 2: Breakdown of the summary in Table 1 into each general anesthetic studied plus morphine in the case of medications

	First Set		Second Set		Third Set		Fourth Set	
	Test ♯	Effect	Test ♯	Effect	Test ♯	Effect	Test ♯	Effect
Subject A	8	yes	8	yes	3	yes	3	yes
Subject B	2	yes	3	yes	2	yes	1	yes
Subject C	3	yes	2	yes	1	yes	1	yes
Control								
Subject A	2	no	8	no	3	no	3	no
Subject B	0	n/a	3	no	2	no	1	no
Subject C	1	no	2	no	1	no	1	no

Table 3: Summary of the results obtained with the entanglement verification experiments carried out so far with chloroform, deuterated chloroform, diethyl ether and morphine

related to the so called "water memory" [7]. However, since these claims were said to be non-reproducible, we do not wish to discuss them further here except to say that we currently do not subscribe to any of the existing views on the subject and readers are encouraged to read our recent online paper on quantum entanglement [8].

We would like to point out that although the indicators used to measure the brain effects were qualitative and subjective, they reflect the first-person experiences of the qualities, intensities and durations of these effects by the test subjects since their brains were directly used as experimental probes. Further, these effects are completely reproducible under blind experimental settings so that possible placebo effects were excluded. However, as with many other important new results, replications by others are the key to independently confirm our results reported here. Our experiments may appear simple and even "primitive" but the results and implications are profound.

We first chose general anaesthetics in our experiments because they are among the most powerful brain-influencing substances. Our expectation was that, if nuclear and/or electronic spins inside the brain are involved in brain functions such as perception as recently hypothesized by us, the brain may be able to sense the effect of an external anaesthetic sample through quantum entanglement between these spins inside the brain and those of the said anaesthetic sample induced by the photons of the magnetic pulses by first interacting with the nuclear and/or electronic spins inside the said anaesthetic sample, thus carrying quantum information about the anaesthetic molecules, and then interacting with the nuclear and/or electronic spins inside the brain.

We suggest here that the said quantum entities inside the brains are likely nuclear and/or electronic spins for the reasons discussed below. Neural membranes and proteins contain vast numbers of nuclear spins such as 1H, 13C, 31P and 15N. These nuclear spins and unpaired electronic spins are the natural targets of interaction with the photons of the magnetic pulses or other sources. These spins form complex intra- and inter-molecular networks through various intramolecular J- and dipolar couplings and both short- and long-range intermolecular dipolar couplings. Further, nuclear spins have relatively long relaxation times after excitations [9]. Thus, when a nematic liquid crystal is irradiated with multi-frequency pulse magnetic fields, its 1H spins can form long-lived intra-molecular quantum coherence with entanglement for information storage [10]. Long-lived (0.05 ms) entanglement of two macroscopic electron spin ensembles at room temperature has also been achieved [3]. Furthermore, spin is a fundamental quantum process with intrinsic connection to the structure of space-time [11] and was shown to be responsible for the quantum effects in both Hestenes and Bohmian quantum mechanics [12, 13]. Thus, we have recently suggested that these spins could be involved in brain functions at a more fundamental level [2].

5 Conclusions

In light of the results from the entanglement verification experiments, we conclude that the brain effects experienced by the test subjects were the consequences of quantum entanglement between quantum entities inside the brains and those of the chemical substances under study induced by the entangling photons of the magnetic pulses or applied lights. More specifically, the results obtained in the first set of experiments can be interpreted as the consequence of quantum entanglement between the quantum entities in the brain and those in the chemical substances induced by the photons of the magnetic pulses. Similarly, the results obtained from the second sets of experiments can be explained as quantum entanglement between the quantum entities in the chemical substance and those in the water induced by the photons of the magnetic pulses, laser light, microwave or flashlight and the subsequent physical transport of the water entangled with the said chemical substance to the brain after consumption by the test subject which, in turn, produced the observed brain effects through the entanglement of the quantum entities inside the brain with those in the consumed water.

Several important conclusions and implications can be drawn from our findings. First, biologically and chemically meaningful information can be communicated via quantum entanglement from one place to another by photons and possibly other quantum objects such as electrons, atoms and even molecules. Second, both classical and quantum information can be transmitted between locations of arbitrary distances through quantum entanglement alone. Third, instantaneous signalling is physically real which implies that Einstein's theory of relativity is in real (not just superficial) conflict with quantum theory. Fourth, brain processes such as perception and other biological processes likely involve quantum information and nuclear and/or electronic spins may play important roles in these processes. Further, our findings provide important new insights into the essence and implications of the mysterious quantum entanglement and clues for solving the long-standing measurement problem in quantum theory including the roles of the observer and/or consciousness. Very importantly, our findings also provide a unified scientific framework for explaining many paranormal and/or anomalous effects such as telepathy, telekinesis and homeopathy, if they do indeed exist, thus transforming these paranormal and anomalous effects into the domains of conventional sciences.

Finally, with respect to applications, our findings enable various quantum entanglement technologies be developed. Some of these technologies can be used to deliver the therapeutic effects of many drugs to various biological systems such as human bodies without physically administrating the same to the said systems. This will dramatically reduce waste and increase productivity because the same drugs can be

repeatedly used to deliver their therapeutic effects to the mass on site or from remote locations of arbitrary distances. Further, many substances of nutritional and recreational values can be repeatedly administrated to desired biological systems such as human bodies through the said technologies either on site or from remote locations. Other such technologies can be used for instantaneous communications between remote locations of arbitrary distances in various ways. Potentially, these technologies can also be used to entangle two or more human minds for legitimate and beneficial purposes.

Acknowledgements

We wish to thank Yongchang Hu and Cuifang Sun for their participation in the experiments and Robert N. Boyd for our visit to his place of research.

References

1. Julsgaard B., Sherson J., Cirac J. I., Fiurasek J., Polzik E. S. Experimental demonstration of quantum memory for light. *Nature*, 2004, v. 432, 482–485.
2. Hu H. P., Wu M. X. Spin-mediated consciousness theory. *Med. Hypotheses*, 2004, v. 63, 633–646; arXiv: quant-ph/0208068.
3. Julsgaard B., Kozhekin A., Polzik E. S. Experimentally long-lived entanglement of two macroscopic objects. *Nature*, 2001, v. 413, 400–403.
4. Ghosh S., Rosenbaum T. F., Aeppli G., Coppersmith S. N. Entangled quantum state of magnetic dipoles. *Nature*, 2003, v. 425, 48–51.
5. Matsukevich D. N., Kuzmich A. Quantum state transfer between matter and light. *Science*, 2004, v. 306, 663–666.
6. Chanelière T. et al. Storage and retrieval of single photons transmitted between remote quantum memory. *Nature*, 2005, v. 438, 833–836.
7. Davenas E. et al. Human basophil degranulation triggered by very dilute antiserum against IgE. *Nature*, 1988, v. 333, 816–818.
8. Hu H. P., Wu M. X. Thinking outside the box: the essence and implications of quantum entanglement. *NeuroQuantology*, 2006, v. 4, 5–16; Cogprints: ID4581.
9. Gershenfeld N., Chuang I. L. Bulk spin resonance quantum computation. *Science*, 1997, v. 275, 350–356.
10. Khitrin A. K., Ermakov V. L., Fung B. M. Information storage using a cluster of dipolar-coupled spins. *Chem. Phys. Lett.*, 2002, v. 360, 160–166.
11. Dirac P. A. M. The quantum theory of the electron. *Proc. R. Soc.*, 1928, v. A117, 610–624.
12. Hestenes D. Quantum mechanics from self-interaction. *Found. Phys.*, 1983, v. 15, 63–78.
13. Salesi G., Recami E. Hydrodynamics of spinning particles. *Phys. Rev.*, 2004, v. A57, 98–105.

The Extended Relativity Theory in Clifford Spaces: Reply to a Review by W. A. Rodrigues, Jr.

Carlos Castro* and Matej Pavšič†

*Center for Theor. Studies of Physical Systems, Clark Atlanta University, Atlanta, USA
E-mail: czarlosromanov@yahoo.com; castro@ctsps.cau.edu

†Jožef Stefan Institute, Jamova 39, 1000 Ljubljana, Slovenia
E-mail: Matej.Pavsic@ijs.si

In a review, W. A. Rodrigues, Jr., wrote that we confused vector and affine spaces, and that we misunderstood the concept of curvature. We reply to those comments, and point out, that in our paper there was an explicit expression for the curvature of a connection. Therefore we were quite aware — contrary to what asserted the reviewer — that the curvature of a manifold has nothing to do with a choice of a frame field which, of course, even in a flat manifold can be position dependent.

In 2005 we published a paper entitled *The Extended Relativity Theory in Clifford Spaces* [1] which was reviewed by W.A. Rodrigues, Jr. [2]. A good review, even if critical, is always welcome, provided that the criticism is correct and relevant. Unfortunately the reviewer produced some statements which need a reply. He wrote:

> "Two kinds of Clifford spaces are introduced in their paper, flat and curved. According to their presentation, which is far from rigorous by any mathematical standard, we learn that flat Clifford space is a vector space, indeed the vector space of a Clifford algebra of real vector space $\mathbb{R}^D$ equipped with a metric of signature $P+Q=D$. As such the authors state that the coordinates of Clifford space are noncommutative Clifford-valued quantities. It is quite obvious for a mathematician that the authors confuse a vector space with an affine space. This is clear when we learn their definition of a curved Clifford space, which is a 16-dimensional manifold where the tangent vectors are position dependent and at any point are generators of a Clifford algebra $C_{P,Q}$. The authors, as is the case of many physicists, seem not to be aware that the curvature of a manifold has to do with the curvature of a connection that we may define on such a manifold, and has nothing to do with the fact that we may choose even in flat manifold a section of the frame bundle consisting of vectors that depend on the coordinates of the manifold points in a given chart of the maximal atlas of the manifold."

When introducing flat C-space we just said that the Clifford-valued polyvector denotes the position of a point in a manifold, called Clifford space, or C-space. It is a common practice to consider coordinates, e. g., four coordinates x^μ, $\mu=0,1,2,3$, of a point $\mathcal{P}$ of a flat spacetime as components of a radius vector from a chosen point $\mathcal{P}_0$ ("the origin") to $\mathcal{P}$. If we did not provide at this point a several pages course on vector and affine spaces, this by no means implies that we were not aware of a distinction of the two kinds of spaces. That position in flat spacetime is described by radius vector is so common that we do not need to provide any further explanation in this respect. Our paper is about *physics* and not mathematics. We just *use* the well established mathematics. Of course a spacetime manifold (including a flat one) is not the same space as a vector space, but, choosing an "origin" in spacetime, to every point there corresponds a vector, so that there is a one-to-one correspondence between the two spaces. This informal description is true, regardless of the fact that there exist corresponding rigorous, formal, mathematical descriptions (to be found in many textbooks on physics and mathematics).

The correspondence between points and vectors does no longer hold in a curved space, at least not according to the standard wisdom practiced in the textbooks on differential geometry. However, there exists an alternative approach adopted by Hestenes and Sobcyk in their book [3], according to which even the points of a curved space are described by vectors. Moreover, there is yet another possibility, described in refs. [4, 5], which employs vector fields $a^\mu(x)\gamma_\mu$ in a curved space $\mathcal{M}$, where γ_μ, $\mu=0,1,2,\ldots,n-1$, are the coordinate basis vector fields. At every point $\mathcal{P}$ the vectors $\gamma_\mu|_\mathcal{P}$ span a tangent space $T_\mathcal{P}\mathcal{M}$ which is a vector space.

A particular case can be such that in a given coordinate system* we have $a^\mu(x)=x^\mu$. Then at every point $\mathcal{P}\in\mathcal{M}$, the object $x(\mathcal{P})=x^\mu(\mathcal{P})\gamma_\mu(\mathcal{P})$ is a tangent vector. So we have one-to-one correspondence between the points $\mathcal{P}$ of $\mathcal{M}$ and the tangent vectors $x(\mathcal{P})=x^\mu(\mathcal{P})\gamma_\mu(\mathcal{P})$, shortly $x^\mu\gamma_\mu$. The set of objects $x(\mathcal{P})$ for all point $\mathcal{P}$ in a region $R\subset\mathcal{M}$ we call the coordinate vector field [4]. So although the manifold is curved, every point in it can be described by a tangent

*"Coordinate system" or simply "coordinates" is an abbreviation for "the coordinates of the manifold points in a given chart of the maximal atlas of the manifold".

vector at that point, the components of the tangent vector being equal to the coordinates of that point.* Those tangent vectors $x^\mu(\mathcal{P})\gamma_\mu(\mathcal{P})$ are now "house numbers" assigned to a point $\mathcal{P}$. We warn the reader not to confuse the tangent vector $x(\mathcal{P})$ at a point $\mathcal{P}$ with the vector pointing from $\mathcal{P}_0$ (a coordinate origin) to a point $\mathcal{P}$, a concept which is ill defined in a curved manifold.

Analogous holds for Clifford space C. It is a manifold whose points $\mathcal{E}$ can be physically interpreted as extended "events". One possible way to describe those points is by means of a *polyvector field* $A(X) = A^M(X)\gamma_M(X) = X^M\gamma_M$, where $\gamma_M|_\mathcal{E}$, $M = 1, 2, \ldots, 2^n$, are tangent polyvectors that at every point $\mathcal{E} \in C$ span a Clifford algebra. At a given point $\mathcal{E} \in C$ it may hold [6, 5]

$$\gamma_M = \gamma_{\mu_1} \wedge \gamma_{\mu_2} \wedge \ldots \wedge \gamma_{\mu_r}\,, \qquad r = 0, 1, 2, \ldots, n \quad (1)$$

i. e., γ_M are defined as wedge product of vectors γ_μ, $\mu = 0, 1, 2, \ldots, n-1$. The latter property cannot hold in a general curved Clifford space [6, 5]. In refs. [7, 1] we considered a particular subclass of curved C-spaces, for which it does hold.

If we choose a particular point $\mathcal{E}_0 \in C$, to which we assign coordinates $X^M(\mathcal{E}_0) = 0$, then we have a correspondence between points $\mathcal{E} \in C$ and Clifford numbers $X^M(\mathcal{E})\,\gamma_M(\mathcal{E})$. In this sense one has to understand the sentence of ref. [1]:

> "An element of C-space is a Clifford number, called also polyvector or Clifford aggregate which we now write in the form $X = s\gamma + x^\mu\gamma_\mu + x^{\mu\nu}\gamma_\mu\wedge\gamma_\nu + \ldots$"

Therefore, a more correct formulation would be, e. g.,

> "An element of C-space is an extended event $\mathcal{E}$, to which one can assign a Clifford number, called polyvector, $X^M(\mathcal{E})\gamma_M(\mathcal{E}) \equiv X^M\gamma_M$."

together with an explanation in the sense as given above. So a rigorous formulation is, not that an element of C-space *is* a Clifford number, but that to a point of C-space there *corresponds* a Clifford number, and that this holds for all points within a domain $\Omega \subset C$ corresponding to a given chart of the maximal atlas of C.

On the one hand we have a 2^n-dimensional manifold $C \equiv \{\mathcal{E}\}$ of points (extended events) $\mathcal{E}$, and on the other hand the 2^n-dimensional space $\{X(\mathcal{E})\}$ of Clifford numbers $X(\mathcal{E}) = X^M(\mathcal{E})\,\gamma\,(\mathcal{E})$ for $\mathcal{E} \in \Omega \subset C$. The latter space $\{X(\mathcal{E})\}$, of course, is not a Clifford algebra. It is a subspace of 2×2^n-dimensional tangent bundle TC of the manifold C. At every point $\mathcal{E} \in C$ there is a also another subspace of TC, namely the 2^n-dimensional tangent space $T_\mathcal{E}C$, which is a Clifford algebra $\mathcal{C}_n$. Since there is a one-to-one correspondence between the spaces $\{X(\mathcal{E})\}$ and $\{\mathcal{E}\}$, the space $\{X(\mathcal{E})\}$ can be used for description of the space $\{\mathcal{E}\}$.

It is true that physicists are often sloppy with mathematical formulations and usage of language, but it is also true that mathematicians often read *physics papers* superficially and see misconceptions, "errors", erroneous mathematical statements, etc., instead of trying to figure out the true content behind an informal (and therefore necessarily imprecise) description, whose emphasis is on physics and not mathematics.

A culmination is when the reviewer writes

> "The authors, as is the case of many physicists, seem not to be aware that curvature... has nothing to do with the fact that we may choose even in flat manifold a section of the frame bundle consisting of vectors that depend on coordinates of the manifold points..."

That curvature has nothing to do with coordinate transformations† is clear to everybody who has ever studied the basis of general relativity. Everyone who has a good faith that the author(s) of a paper have a minimal level of competence would interpret a text such as [1]

> "In flat C-space the basis polyvectors γ_M are constant. In a curved C-space this is no longer true. Each γ_M is a function of C-space coordinates X^M..."

according to

> "In flat C-space one can always find coordinates‡ in which γ_M are constant. In a curved C-space this is no longer true. Each γ_M depends on position in C-space." Or equivalently, "Each γ_M is a function of the C-space coordinates".

However, even our formulation as it stands in ref. [1] makes sense within the context in which we first consider flat space in which we *choose* a constant frame field, i. e., constant basis polyvectors. We denote the latter polyvectors as γ_M. If we then deform§ the flat space into a curved one, then the *same* (poly)vector fields γ_M in general can no longer be independent of position. In this sense the formulation as it stands in our paper is quite correct.

We then define a *connection* on our manifold C, and the corresponding *curvature* (see eqs. (77), (78) of ref. [1]). That

*If we change coordinate system, then $a^\mu(x)\gamma_\mu = x^\mu\gamma_\mu = a'^\mu(x')\gamma'_\mu(x')$, with $a'^\mu = a^\nu(x)(\partial x'^\mu/\partial x^\nu) = x^\nu(\partial x'^\mu/\partial x^\nu)$. In another coordinate system S' one can then take another vector field, such that $b^\mu(x') = x'^\mu$. Let us stress that $b^\mu(x') = x'^\mu$ is a different field from $a'^\mu(x')$, therefore the reader should not think that we say $x'^\mu = x^\nu(\partial x'^\mu/\partial x^\nu)$ which is, of course, wrong. What we say is $a'^\mu(x') = (\partial x'^\mu/\partial x^\nu)a^\nu(x)$, where, in particular, $a^\nu(x) = x^\nu$.

†For instance, in flat spacetime one can introduce a curvilinear coordinate system of coordinates, like the use of polar coordinates in the plane and spherical coordinates in $\mathbb{R}^3$. However, the introduction of a curvilinear coordinate system does not convert the original flat space into a curved one. And vice versa, one can introduce a non-Euclidean metric (non-flat metric) on a two-dim flat surface, for example, like the hyperbolic Lobachevsky metric of constant negative scalar curvature.

‡We renounce to use here the lengthy formulation provided by the reviewer. Usage of the term "coordinates" is sufficient, and it actually means "coordinates of the manifold point in a given chart of the maximal atlas of the manifold".

§This is easy to imagine, if we consider a flat surface embedded in a higher dimensional space, and then deform the surface. In general, we may deform the surface so that is is curved not only extrinsically, but also intrinsically.

the reviewer reproaches us of being ignorant of the fact that the curvature of a manifold has to do with the curvature of a connection is therefore completely out of place, to say at least.

Finally, let us mention that in the review of another paper [8] the same reviewer ascribed to one of us (M.P) an incorrect mathematical statement. But I was quite aware of the well known fact that Clifford algebras associated with vector spaces of different signatures (p, q), with $p + q = n$, are not all isomorphic (in the sense as stated, e. g., in the book by Porteous [9]). What I discussed in that paper was something different. This should be clear from my description, therefore I did not explicitly warn the reader about the difference (although I was aware of the danger that at superficial reading some people might believe me of committing an error). However, in subsequent ref. [1] we did warn the reader about the possibility of such a confusion.

References

1. Castro C. and Pavšič M. The extended relativity theory in Clifford spaces. *Progress in Physics*, 2005, v. 1, 31.
2. Rodrigues W. A., Jr. *Mathematical Reviews*, MR2150508 (2006c:83068).
3. Hestenes D. and Sobcyk G. Clifford algebra to geometric calculus. D. Reidel, Dordrecht, 1984.
4. Pavšič M. The landscape of theoretical physics: a global view; From point particles to the brane world and beyond, in search of a unifying principle. Kluwer Academic Publishers, Amsterdam, 2001.
5. Pavšič M. Spin gauge theory of gravity in Clifford space: A realization of Kaluza-Klein theory in 4-dimensional space-time. arXiv: gr-qc/0507053, to appear in *Int. J. Mod. Phys. A*.
6. Pavšič M. Kaluza-Klein theory without extra dimensions: Curved Clifford space. *Phys. Lett. B*, 2005, v. 614, 85. arXiv: hep-th/0412255.
7. Castro C. and Pavšič M. Higher derivative gravity and torsion from the geometry of C-spaces. *Phys. Lett. B*, 2002, v. 539, 133. arXiv: hep-th/0110079.
8. Pavšič M. Clifford algebra based polydimensional relativity and relativistic dynamics. *Found. Phys.*, 2001, v. 31, 1185. arXiv: hep-th/0011216.
9. Porteous I. R. Topological geometry. Second edition, Cambridge Univ. Press, Cambridge, 1982.

On the Regge-Wheeler Tortoise and the Kruskal-Szekeres Coordinates

Stephen J. Crothers

Queensland, Australia

E-mail: thenarmis@yahoo.com

The Regge-Wheeler tortoise "coordinate" and the the Kruskal-Szekeres "extension" are built upon a latent set of invalid assumptions. Consequently, they have led to fallacious conclusions about Einstein's gravitational field. The persistent unjustified claims made for the aforesaid alleged coordinates are not sustained by mathematical rigour. They must therefore be discarded.

1 Introduction

The Regge-Wheeler tortoise coordinate was not conjured up from thin air. On the contrary, is was obtained *a posteriori* from the Droste/Weyl/(Hilbert) [1, 2, 3] (the DW/H) metric for the static vacuum field; or, more accurately, from Hilbert's corruption of the spacetime metric obtained by Johannes Droste.

The first presentation and misguided use of the Regge-Wheeler coordinate was made by A. S. Eddington [4] in 1924. Finkelstein [5], years later, in 1958, presented much the same; since then virtually canonised in the so-called "Eddington-Finkelstein" coordinates. Kruskal [6], and Szekeres [7], in 1960, compounded the errors with additional errors, all built upon the very same fallacious assumptions, by adding even more fallacious assumptions. The result has been a rather incompetent use of mathematics to produce nonsense on an extraordinary scale.

Orthodox relativists are now so imbued with the misconceptions that they are, for the most part, no longer capable of rational thought on the subject. Although the erroneous assumptions of the orthodox have been previously demonstrated to be false [8–18] they have consistently and conveniently ignored the proofs.

I amplify the erroneous assumptions of the orthodox relativists in terms of the Regge-Wheeler tortoise, and consequently in the Kruskal-Szekeres phantasmagoria.

2 The orthodox confusion and delusion

Consider the DW/H line-element

$$ds^2 = \left(1 - \frac{\alpha}{r}\right) dt^2 - \left(1 - \frac{\alpha}{r}\right)^{-1} dr^2 - \\ - r^2 \left(d\theta^2 + \sin^2\theta \, d\varphi^2\right), \qquad (1)$$

where $\alpha = 2m$. Droste showed that $\alpha < r < \infty$ is the correct domain of definition on (1), as did Weyl some time later. Hilbert however, claimed $0 < r < \infty$. Modern orthodox relativists claim two intervals, $0 < r < \alpha$, $\alpha < r < \infty$, and call the latter the "exterior" Schwarzschild solution and the former a "black hole", notwithstanding that (1) with $0 < r < \infty$ was never proposed by K. Schwarzschild [19]. Astonishingly, the vast majority of orthodox relativists, it seems, have never even heard of Schwarzschild's true solution.

I have proved elsewhere [11, 12, 13] that the orthodox, when considering (1), have made three invalid assumptions, to wit

(a) r is a proper radius;

(b) r can go down to zero;

(c) A singularity must occur where the Riemann tensor scalar curvature invariant (the Kretschmann scalar), $f = R_{\alpha\beta\rho\sigma} R^{\alpha\beta\rho\sigma}$, is unbounded.

None of these assumptions have ever been proved true with the required mathematical rigour by any orthodox relativist. Notwithstanding, they blindly proceed on the assumption that they are all true. The fact remains however, that they are all demonstrably false.

Consider assumption (a). By what rigorous argument have the orthodox identified r as a radial quantity on (1)? Moreover, by what rigorous mathematical means have they ever indicated what they mean by a radial quantity on (1)? Even a cursory reading of the literature testifies to the fact that the orthodox relativists have never offered any mathematical rigour to justify assumption (a). Mathematical rigour actually proves that this assumption is false.

Consider assumption (b). By what rigorous means has it ever been proved that r can go down to zero on (1)? The sad fact is that the orthodox have never offered a rigorous argument. All they have ever done is inspect (1) and claim that there are singularities at $r = \alpha$ and at $r = 0$, and thereafter concocted means to make one of them ($r = 0$) a "physical" singularity, and the other a "coordinate" singularity, and vaguely refer to the latter as a "pathology" of coordinates, whatever that means. The allegation of singularities at $r = \alpha$ and at $r = 0$ also involves the unproven assumption (a). Evidently the orthodox consider that assumptions (a) and (b) are self-evident, and so they don't even think about them. However, assumptions (a) and (b) are not self-evident and if they are to be justifiably used, they must first be proved. No

orthodox relativist has ever bothered to attempt the necessary proofs. Indeed, none it would seem have ever seen the need for proofs, owing to their "self-evident" assumptions.

Assumption (c) is an even more curious one. Indeed, it is actually a bit of legerdemain. Having just assumed (a) and (b), the orthodox needed some means to identify their "physical" singularity. They went looking for it at a suitable unbounded curvature scalar, found it in the Kretschmann scalar, after a series of misguided transformations of "coordinates" leading to the Kruskal-Szekeres "extension", and thereafter have claimed singularity of the Kretschmann type in the static vacuum field.

Furthermore, using these unproved assumptions, the orthodox relativists have claimed a process of "gravitational collapse" to a "point-mass". And with this they have developed what they have called grandiosely and misguidedly, "singularity theorems", by which it is alleged that "physical" singularities and "trapped surfaces" are a necessary consequence of gravitational collapse, and even cosmologically, called Friedmann singularities.

The orthodox relativists must first prove their assumptions by rigorous mathematics. Unless they do this, their analyses are unsubstantiated and cannot be admitted.

Since the orthodox assumptions have in fact already been rigorously proved entirely false, the theory that the orthodox have built upon them is also false.

3 The Regge-Wheeler tortoise; the Kruskal-Szekeres phantasmagoria

Since the Regge-Wheeler tortoise does not come from thin air, from where does it come?

First consider the general static line-element

$$ds^2 = A\left(\sqrt{C(r)}\right)dt^2 - B\left(\sqrt{C(r)}\right)d\sqrt{C(r)}^2 - \\ - C(r)\left(d\theta^2 + \sin^2\theta\, d\varphi^2\right), \quad (2)$$

$$A, B, C > 0\,.$$

It has the solution

$$ds^2 = \left(1-\frac{\alpha}{\sqrt{C(r)}}\right)dt^2 - \left(1-\frac{\alpha}{\sqrt{C(r)}}\right)^{-1} d\sqrt{C(r)}^2 - \\ - C(r)\left(d\theta^2 + \sin^2\theta\, d\varphi^2\right), \quad (3)$$

and setting $R_c(r) = \sqrt{C(r)}$ for convenience, this becomes

$$ds^2 = \left(1-\frac{\alpha}{R_c(r)}\right)dt^2 - \left(1-\frac{\alpha}{R_c(r)}\right)^{-1} dR_c^2(r) - \\ - R_c^2(r)\left(d\theta^2 + \sin^2\theta d\varphi^2\right), \quad (4)$$

for some analytic function $R_c(r)$. Clearly, if $R_c(r)$ is set equal to r, then (1) is obtained.

Reduce (4) to two dimensions, thus

$$ds^2 = \left(1-\frac{\alpha}{R_c(r)}\right)dt^2 - \left(1-\frac{\alpha}{R_c(r)}\right)^{-1} dR_c^2(r)\,. \quad (5)$$

The null geodesics are given by

$$ds^2 = 0 = \left(1-\frac{\alpha}{R_c(r)}\right)dt^2 - \left(1-\frac{\alpha}{R_c(r)}\right)^{-1} dR_c^2(r)\,.$$

Consequently

$$\left(\frac{dt}{dR_c(r)}\right)^2 = \left(\frac{R_c(r)}{R_c(r)-\alpha}\right)^2,$$

and therefore,

$$t = \pm\left[R_c(r) + \alpha\ln\left|\frac{R_c(r)}{\alpha} - 1\right|\right] + \text{const.}$$

Now

$$R^*(r) = R_c(r) + \alpha\ln\left|\frac{R_c(r)}{\alpha} - 1\right| \quad (6)$$

is the so-called Regge-Wheeler tortoise coordinate. If $R_c(r) = r$, then

$$r^* = r + \alpha\ln\left|\frac{r}{\alpha} - 1\right|, \quad (7)$$

which is the standard expression used by the orthodox. They never use the general expression (6) because they only ever consider the particular case $R_c(r) = r$, owing to the fact that they do not know that their equations relate to a particular case. Furthermore, with their unproven and invalid assumptions (a) and (b), many orthodox relativists claim

$$0 = 0 + \alpha\ln\left|\frac{0}{\alpha} - 1\right| \quad (8)$$

so that $r_0^* = r_0 = 0$. But as explained above, assuming $r_0 = 0$ in (1) has no rigorous basis, so (8) is rather misguided.

Let us now consider (2). I identify therein the radius of curvature $R_c(r)$ as the square root of the coefficient of the angular terms, and the proper radius $R_p(r)$ as the integral of the square root of the component of the metric tensor containing the squared differential element of the radius of curvature. Thus, on (2),

$$R_c(r) = \sqrt{C(r)}\,, \\ R_p(r) = \int\sqrt{B(\sqrt{C(r)})}\; d\sqrt{C(r)} + \text{const.} \quad (9)$$

In relation to (4) it follows that,

$$R_c(r) \quad \text{is the radius of curvature,} \\ R_p(r) = \int\sqrt{\frac{R_c(r)}{(R_c(r)-\alpha)}}\; dR_c(r) + K\,, \quad (10)$$

where K is a constant to be rigorously determined by a boundary condition. Note that according to (10) there is no *a priori* reason for $R_p(r)$ and $R_c(r)$ to be identical in Einstein's gravitational field.

Now consider the usual Minkowski metric,

$$ds^2 = dt^2 - dr^2 - r^2\left(d\theta^2 + \sin^2\theta d\varphi^2\right), \qquad (11)$$

$$0 \leqslant r < \infty,$$

where

$$R_c(r) = r, \qquad R_p(r) = \int_0^r dr = r \equiv R_c(r). \qquad (12)$$

In this case $R_p(r)$ is identical to $R_c(r)$. The identity is due to the fact that the spatial components of Minkowski space are Efcleethean*. But (4), and hence (10), are non-Efcleethean, and so there is no reason for $R_p(r)$ and $R_c(r)$ to be identical therein.

The geometry of a spherically symmetric line-element is an intrinsic and invariant property, by which radii are rigorously determined. The radius of curvature is always the square root of the coefficient of the angular terms and the proper radius is always the integral of the square root of the component containing the square of the differential element of the radius of curvature. Note that in general $R_c(r)$ and $R_p(r)$ are analytic functions of r, so that r is merely a parameter, and not a radial quantity in (2) and (4). So $R_c(r)$ and $R_p(r)$ map the parameter r into radii (i. e. distances) in the gravitational field. Note further that r is actually defined in Minkowski space. Thus, a distance in Minkowski space is mapped into corresponding distances in Einstein's gravitational field by the mappings $R_c(r)$ and $R_p(r)$.

It has been proved [11, 12] that the admissible form for $R_c(r)$ is,

$$R_c(r) = \left(\left|r - r_0\right|^n + \alpha^n\right)^{\frac{1}{n}}, \qquad (13)$$

$$n \in \Re^+, \quad r_0 \in \Re, \quad \alpha = 2m, \quad r \neq r_0,$$

where n and r_0 are entirely arbitrary constants, and that

$$R_p(r) = \sqrt{R_c(r)\left(R_c(r) - \alpha\right)} + \alpha \ln\left|\frac{\sqrt{R_c(r)} + \sqrt{R_c(r) - \alpha}}{\sqrt{\alpha}}\right|.$$

If $n=1$, $r_0=\alpha$, $r>r_0$ are chosen, then by (13), $R_c(r)=r$ and equation (1) is recovered; but by (13), $\alpha < r < \infty$ is then the range on the r-parameter. Note that in this case

$$R_c(\alpha) = \alpha, \qquad R_p(\alpha) = 0,$$

and that in general,

$$R_c(r_0) = \alpha, \qquad R_p(r_0) = 0,$$

$$\alpha < R_c(r) < \infty,$$

since the value of r_0 is immaterial. I remark in passing that if $n=3$, $r_0=0$, $r>0$ are chosen, Schwarzschild's original solution results.

Returning now to the Regge-Wheeler tortoise, it is evident that

$$-\infty < R^*(r) < \infty,$$

and that $R^*(r)=0$ when $R(r) \approx 1.278465\,\alpha$. Now according to (13), $\alpha < R_c(r) < \infty$, so the Regge-Wheeler tortoise can be written generally as,

$$R^*(r) = R_c(r) + \alpha \ln\left(\frac{R_c(r)}{\alpha} - 1\right), \qquad (14)$$

which is, in the particular case invariably used by the orthodox relativists,

$$r^* = r + \alpha \ln\left(\frac{r}{\alpha} - 1\right),$$

and so, by (13) and (14), the orthodox claim that

$$0 = 0 + \alpha \ln\left|\frac{0}{\alpha} - 1\right|,$$

is nonsense. It is due to the invalid assumptions (a) and (b) which the orthodox relativists have erroneously taken for granted. Of course, the tortoise, r^*, cannot be interpreted as a radius of curvature, since in doing so would violate the intrinsic geometry of the metric. This is clearly evident from (13), which specifies the permissible form of a radius of curvature on a metric of the form (4).

So what is the motivation to the Regge-Wheeler tortoise and the subsequent Kruskal-Szekeres extension? Very simply this, to rid (1) of the singularity at $r=\alpha$ and make $r=0$ a "physical" singularity, satisfying the *ad hoc* assumption (c), under the mistaken belief that† $r=\alpha$ is not a physical singularity (but it is a true singularity, however, not a Kretschmann curvature-type). This misguided notion is compounded by a failure to realise that there are two radii in Einstein's gravitational field and that they are never identical, except in the infinitely far field where spacetime becomes Minkowski, and that what they treat as a proper radius in the gravitational field is in fact the radius of curvature in their particular metric, which cannot go down to zero. Only the proper radius can approach zero, although it cannot take the value of zero, i. e. $r \neq r_0$ in (13), since $R_p(r_0) \equiv 0$ marks the location of the centre of mass of the source of the field, which is not a physical object.

*Owing to the geometry due to Efcleethees, for those ignorant of Greek; usually and incorrectly Euclid.

†Indeed, that $\left(R_c(r_0) \equiv \alpha\right) \equiv \left(R_p(r_0) \equiv 0\right)$.

The mechanical procedure to the Kruskal-Szekeres extension is well-known, so I will not reproduce it here, suffice to say that it proposes the following null coordinates u and v,

$$u = t - R^*(r)\,,$$
$$v = t + R^*(r)\,,$$

which is always given by the orthodox relativists in the particular case

$$u = t - r^*\,,$$
$$v = t + r^*\,.$$

Along the way to the Kruskal-Szekeres extension, the sole purpose of which is to misguidedly drive the radius of curvature r in (1) down to zero, owing to their invalid assumptions (a), (b) and (c), the orthodox obtain

$$ds^2 = -\frac{\alpha e^{-\frac{r}{\alpha}}}{r}\, e^{\frac{(v-u)}{2\alpha}}\, du\, dv\,,$$

which in general terms is

$$ds^2 = -\frac{\alpha e^{-\frac{R_c(r)}{\alpha}}}{R_c(r)}\, e^{\frac{(v-u)}{2\alpha}}\, du\, dv\,,$$

and erroneously claim that the metric components of (1) have been factored into a piece, $\frac{e^{-r/\alpha}}{r}$, which is non-singular as $r \to \alpha$, times a piece with u and v dependence [20]. The claim is of course completely spurious, since it is based upon the false assumptions (a), (b), and (c). The orthodox relativists have not, contrary to their claims, developed a coordinate patch to cover a part of an otherwise incompletely covered manifold. What they have actually done, quite unwittingly, is invent a completely separate manifold, which they glue onto the manifold of the true Schwarzschild field, and confound this new and separate manifold as a part of the original manifold, and by means of the Kruskal-Szekeres extension, leap between manifolds in the mistaken belief that they are moving between coordinate patches on one manifold. The whole procedure is ludicrous; and patently false. Loinger [21] has also noted that the alleged "interior" of the Hilbert solution is a different manifold.

The fact that the Hilbert solution is not diffeomorphic to Schwarzschild's solution was proved by Abrams [9], who showed that the Droste/Weyl metric is diffeomorphic to Schwarzschild's original solution. This is manifest in (13), and can be easily demonstrated alternatively by a simple transformation, as follows. In the Hilbert metric, denote the radius of curvature by r^*, and equate this to Schwarzschild's radius of curvature thus,

$$r^* = \left(r^3 + \alpha^3\right)^{\frac{1}{3}}\,. \qquad (15)$$

Since $0 < r < \infty$ in Schwarzschild's original solution, it follows from this that

$$\alpha < r^* < \infty\,,$$

which is precisely what Droste obtained; later confirmed by Weyl. There is no "interior" associated with the DW/H metric, and no "trapped surface". The transformation (15) simply shifts the location of the centre of mass of the source in parameter space from $r_0 = 0$ to $r_0 = \alpha$, as given explicitly in (13).

4 Recapitulation and general comments

The standard school of relativists has never attempted to rigorously prove its assumptions about the variable r appearing in the line-element (1). It has never provided any rigorous argument as to what constitutes a radial quantity in Einstein's gravitational field. It has invented a curvature condition, in the behaviour of the Kretschmann scalar, as an *ad hoc* basis for singularity in Einstein's gravitational field.

The Regge-Wheeler tortoise has been thoroughly misinterpreted by the standard school of relativists. The Kruskal-Szekeres extension is a misguided procedure, and does not lead to a coordinate patch, but in fact, to a completely separate manifold having nothing to do with a Schwazschild space. The motivation to the Eddington-Finkelstein coordinates and the Kruskal-Szekeres extension is due to the erroneous assumptions that the variable r in (1) is a proper radius and can therefore go down to zero.

The standard school has failed to see that there are two radii in Einstein's gravitational field, which are determined by the intrinsic geometry of the metric. Thus, it has failed to understand the geometrical structure of type 1 Einstein spaces. Consequently, the orthodox relativists have incorrectly treated the variable r in (1) as a proper radius, failing to see that it is in fact the radius of curvature in (1), and that the proper radius must in fact be calculated by the geometrical relations intrinsic to the metric. They have failed to realise that the quantity r is in general nothing more than a parameter, defined in Minkowski space, which is mapped into the radii of the gravitational field, thereby making Minkowski space a parameter space from which Efcleethean distance is mapped into the corresponding true radii of Einstein's pseudo-Riemannian gravitational field.

The so-called "singularity theorems" are not theorems at all, as they are based upon false concepts. The "point-mass" is actually nothing more than the location of the centre of mass of the source of the gravitational field, and has no physical significance. Moreover, the alleged theorems are based upon the invalid construction of "trapped surfaces", essentially derived from the false assumptions (a), (b) and (c). The Friedmann singularities simply do not exist at all, either physically or mathematically, as it has been rigorously proved that cosmological solutions for isotropic type 1 Einstein spaces do not even exist [14], so that the Standard Cosmological model is completely invalid.

My own experience has been that most orthodox relativists just ignore the facts, resort to aggressive abuse when

confronted with them, and merrily continue with their demonstrably false assumptions. But here is a revelation: abuse and ignorance are not scientific methods. Evidently, scientific method is no longer required in science.

I have in the past, invited certain very substantial (and some not so substantial) elements of the orthodox relativists, literally under a torrent of vicious abuse, both gutter and eloquent, depending upon the person, (to which I have on occasion responded in kind after enduring far too much), to prove their assumptions (a), (b), and (c). Not one of them took up the invitation. I have also invited them to prove me wrong by simply providing a rigorous demonstration that the radius of curvature is not always the square root of the coefficient of the angular terms of the metric, and that the proper radius is not always the integral of the square root of the component containing the square of the differential element of the radius of curvature. Not one of them has taken up that invitation either. To refute my analysis is very simple in principle — rigorously prove the foregoing.

Alas, the orthodox are evidently unwilling to do so, being content instead to foist their errors upon all and sundry in the guise of profundity, to salve their need of vainglory, and ignore or abuse those who ask legitimate questions as to their analyses. And quite a few persons who have pointed out serious errors in the standard theory, have been refused any and all opportunity to publish papers on these matters in those journals and electronic archives which constitute the stamping grounds of the orthodox.

I give the foregoing in illustration of how modern science is now being deliberately censored and falsified. This cannot be allowed to continue, and those responsible must be exposed and penalised. It is my view that what the modern orthodox relativists have done amounts to scientific fraud. The current situation is so appalling that to remain silent would itself be criminal.

References

1. Droste J. The field of a single centre in Einstein's theory of gravitation, and the motion of a particle in that field. *Ned. Acad. Wet., S.A.*, v. 19, 1917, 197 (www.geocities.com/theometria/Droste.pdf).
2. Weyl H. Zur Gravitationstheorie. *Ann. Phys.*, (*Leipzig*), 1917, v. 54, 117.
3. Hilbert D. *Nachr. Ges. Wiss. Gottingen, Math. Phys. Kl.*, v. 53, 1917 (see also in arXiv: physics/0310104).
4. Eddington A. S. A comparison of Whitehead's and Einstein's formulas. *Nature*, 1924, v. 113, 192.
5. Finkelstein D. Past-future asymmetry of the gravitational field of a point particle. *Phys. Rev.*, 1958, v. 110, 965.
6. Kruskal M. D. Maximal extension of Schwarzschild metric. *Phys. Rev.*, 1960, v. 119, 1743.
7. Szekeres G. On the singularities of a Riemannian manifold. *Math. Debreca.*, 1960, v. 7, 285.
8. Brillouin M. The singular points of Einstein's Universe. *Journ. Phys. Radium*, 1923, v. 23, 43 (see also in arXiv: physics/0002009).
9. Abrams L. S. Black holes: the legacy of Hilbert's error. *Can. J. Phys.*, 1989, v. 67, 919 (see also in arXiv: gr-qc/0102055).
10. Abrams L. S. The total space-time of a point charge and its consequences for black holes. *Int. J. Theor. Phys.*, v. 35, 1996, 2661 (see also in arXiv: gr-qc/0102054).
11. Crothers S. J. On the general solution to Einstein's vacuum field and it implications for relativistic degeneracy. *Progress in Physics*, 2005, v. 1, 68–73.
12. Crothers S. J. On the ramifications of the Schwarzschild spacetime metric. *Progress in Physics*, 2005, v. 1, 74–80.
13. Crothers S. J. On the geometry of the general solution for the vacuum field of the point-mass. *Progress in Physics*, 2005, v. 2, 3–14.
14. Crothers S. J. On the general solution to Einstein's vacuum field for the point-mass when $\lambda \neq 0$ and its consequences for relativistic cosmology. *Progress in Physics*, 2005, v. 3, 7–14.
15. Stavroulakis N. A statical smooth extension of Schwarzschild's metric. *Lettere al Nuovo Cimento*, 1974, v. 11, 8 (see also in www.geocities.com/theometria/Stavroulakis-3.pdf).
16. Stavroulakis N. On the principles of General Relativity and the $S\Theta(4)$-invariant metrics. *Proc. 3rd Panhellenic Congr. Geometry*, Athens, 1997, 169 (see also in www.geocities.com/theometria/Stavroulakis-2.pdf).
17. Stavroulakis N. On a paper by J. Smoller and B. Temple. *Annales de la Fondation Louis de Broglie*, 2002, v. 27, 3 (see also in www.geocities.com/theometria/Stavroulakis-1.pdf).
18. Stavroulakis N. Non-Euclidean geometry and gravitation *Progress in Physics*, 2006, v. 2, 68–75.
19. Schwarzschild K. On the gravitational field of a mass point according to Einstein's theory. *Sitzungsber. Preuss. Akad. Wiss., Phys. Math. Kl.*, 1916, 189 (www.geocities.com/theometria/schwarzschild.pdf).
20. Wal R. M. General Relativity. The University of Chicago Press, Chicago, 1984.
21. Loinger A. On black holes and gravitational waves. *La Goliardica Pavese*, Pavia, 2002, 22–25; arXiv: gr-qc/0006033.

Complexity Science for Simpletons

Craig Alan Feinstein

2712 Willow Glen Drive, Baltimore, Maryland 21209, USA

E-mail: cafeinst@msn.com

In this article, we shall describe some of the most interesting topics in the subject of Complexity Science for a general audience. Anyone with a solid foundation in high school mathematics (with some calculus) and an elementary understanding of computer programming will be able to follow this article. First, we shall explain the significance of the P versus NP problem and solve it. Next, we shall describe two other famous mathematics problems, the Collatz $3n+1$ Conjecture and the Riemann Hypothesis, and show how both Chaitin's incompleteness theorem and Wolfram's notion of "computational irreducibility" are important for understanding why no one has, as of yet, solved these two problems.

1 Challenge

Imagine that you have a collection of one billion lottery tickets scattered throughout your basement in no particular order. An official from the lottery announces the number of the winning lottery ticket. For a possible prize of one billion dollars, is it a good idea to search your basement until you find the winning ticket or until you come to the conclusion that you do not possess the winning ticket? Most people would think not — even if the winning lottery ticket were in your basement, performing such a search could take $10^9/(60 \times 60 \times 24 \times 365.25)$ years, over thirty work-years, assuming that it takes you at least one second to examine each lottery ticket. Now imagine that you have a collection of only one thousand lottery tickets in your basement. Is it a good idea to search your basement until you find the winning ticket or until you come to the conclusion that you do not possess the winning ticket? Most people would think so, since doing such would take at most a few hours.

From these scenarios, let us postulate a general rule that the maximum time that it may take for one person to search N unsorted objects for one specific object is directly proportional to N. This is clearly the case for physical objects, but what about abstract objects? For instance, let us suppose that a dating service is trying to help n single women and n single men to get married. Each woman gives the dating service a list of characteristics that she would like to see in her potential husband, for instance, handsome, caring, athletic, domesticated, etc. And each man gives the dating service a list of characteristics that he would like to see in his potential wife, for instance, beautiful, obedient, good cook, thrifty, etc. The dating service is faced with the task of arranging dates for each of its clients so as to satisfy everyone's preferences.

Now there are $n!$ (which is shorthand for $n \times (n-1) \times (n-2) \times \cdots \times 2 \times 1$) possible ways for the dating service to arrange dates for each of its clients, but only a fraction of such arrangements would satisfy all of its clients. If $n = 100$, it would take too long for the dating service's computer to evaluate all 100! possible arrangements until it finds an arrangement that would satisfy all of its clients. (100! is too large a number of possibilities for any modern computer to handle.) Is there an efficient way for the dating service's computer to find dates with compatible potential spouses for each of the dating service's clients so that everyone is happy, assuming that it is possible to do such? Yes, and here is how:

Matchmaker algorithm — Initialize the set $M = \emptyset$. Search for a list of compatible relationships between men and women that alternates between a compatible relationship $\{x_1, x_2\}$ not contained in set M, followed by a compatible relationship $\{x_2, x_3\}$ contained in set M, followed by a compatible relationship $\{x_3, x_4\}$ not contained in set M, followed by a compatible relationship $\{x_4, x_5\}$ contained in set M, and so on, ending with a compatible relationship $\{x_{m-1}, x_m\}$ not contained in set M, where both x_1 and x_m are not members of any compatible relationships contained in set M. Once such a list is found, for each compatible relationship $\{x_i, x_{i+1}\}$ in the list, add $\{x_i, x_{i+1}\}$ to M if $\{x_i, x_{i+1}\}$ is not contained in M or remove $\{x_i, x_{i+1}\}$ from M if $\{x_i, x_{i+1}\}$ is contained in M. (Note that this procedure must increase the size of set M by one.) Repeat this procedure until no such list exists.

Such an algorithm is guaranteed to **efficiently** find an arrangement M that will satisfy all of the dating service's clients whenever such an arrangement exists [30]. So we see that with regard to abstract objects, it is not necessarily the case that the maximum time that it may take for one to search N unsorted objects for a specific object is directly proportional to N; in the dating service example, there are $n!$ possible arrangements between men and women, yet it is not necessary for a computer to examine all $n!$ arrangements in order to find a satisfactory arrangement. One might think that the problem of finding a satisfactory dating arrangement is easy for a modern computer to solve because the list of pairs of men and women who are compatible is relatively small (of size at most n^2, which is much smaller than the number of possible arrangements $n!$) and because it is

easy to verify whether any particular arrangement will make everyone happy. But this reasoning is invalid, as we shall demonstrate.

2 The SUBSET-SUM problem

Consider the following problem: You are given a set $A = \{a_1, \ldots, a_n\}$ of n integers and another integer b which we shall call the *target integer*. You want to know if there exists a subset of A for which the sum of its elements is equal to b. (We shall consider the sum of the elements of the empty set to be zero.) This problem is called the *SUBSET-SUM problem* [10]. Now, there are 2^n subsets of A, so one could naïvely solve this problem by exhaustively comparing the sum of the elements of each subset of A to b until one finds a subset-sum equal to b, but such a procedure would be infeasible for even the fastest computers in the world to implement when $n = 100$. Is there an algorithm which can considerably reduce the amount of work for solving the SUBSET-SUM problem? Yes, there is an algorithm discovered by Horowitz and Sahni in 1974 [21], which we shall call the *Meet-in-the-Middle algorithm*, that takes on the order of $2^{n/2}$ steps to solve the SUBSET-SUM problem instead of the 2^n steps of the naïve exhaustive comparison algorithm:

Meet-in-the-Middle algorithm — First, partition the set A into two subsets, $A^+ = \{a_1, \ldots, a_{\lceil \frac{n}{2} \rceil}\}$ and $A^- = \{a_{\lceil \frac{n}{2} \rceil + 1}, \ldots, a_n\}$. Let us define S^+ and S^- as the sets of subset-sums of A^+ and A^-, respectively. Sort sets S^+ and $b - S^-$ in ascending order. Compare the first elements in both of the lists. If they match, then stop and output that there is a solution. If not, then compare the greater element with the next element in the other list. Continue this process until there is a match, in which case there is a solution, or until one of the lists runs out of elements, in which case there is no solution.

This algorithm takes on the order of $2^{n/2}$ steps, since it takes on the order of $2^{n/2}$ steps to sort sets S^+ and $b - S^-$ (assuming that the computer can sort in linear-time) and on the order of $2^{n/2}$ steps to compare elements from the sorted lists S^+ and $b - S^-$. Are there any faster algorithms for solving SUBSET-SUM? $2^{n/2}$ is still a very large number when $n = 100$, even though this strategy is a vast improvement over the naïve strategy. It turns out that no algorithm with a better worst-case running-time has ever been found since the Horowitz and Sahni paper [40]. And the reason for this is because it is impossible for such an algorithm to exist. Here is an explanation why:

Explanation: To understand why there is no algorithm with a faster worst-case running-time than the Meet-in-the-Middle algorithm, let us travel back in time seventy-five years, long before the internet. If one were to ask someone back then what a computer is, one would have gotten the answer, "a person who computes (usually a woman)" instead of the present day definition, "a machine that computes" [18]. Let us imagine that we knew two computers back then named Mabel and Mildred (two popular names for women in the 1930's [34]). Mabel is very efficient at sorting lists of integers into ascending order; for instance she can sort a set of ten integers in 15 seconds, whereas it takes Mildred 20 seconds to perform the same task. However, Mildred is very efficient at comparing two integers a and b to determine whether $a < b$ or $a = b$ or $a > b$; she can compare ten pairs of integers in 15 seconds, whereas it takes Mabel 20 seconds to perform the same task.

Let's say we were to give both Mabel and Mildred the task of determining whether there exists a subset of some four element set, $A = \{a_1, a_2, a_3, a_4\}$, for which the sum of its elements adds up to b. Since Mildred is good at comparing but not so good at sorting, Mildred chooses to solve this problem by comparing b to all of the sixteen subset-sums of A. Since Mabel is good at sorting but not so good at comparing, Mabel decides to solve this problem by using the Meet-in-the-Middle algorithm. In fact, of all algorithms that Mabel could have chosen to solve this problem, the Meet-in-the-Middle algorithm is the most efficient for her to use on sets A with only four integers. And of all algorithms that Mildred could have chosen to solve this problem, comparing b to all of the sixteen subset-sums of A is the most efficient algorithm for her to use on sets A with only four integers.

Now we are going to use the principle of mathematical induction to prove that the best algorithm for Mabel to use for solving the SUBSET-SUM problem for large n is the Meet-in-the-Middle algorithm: We already know that this is true when $n = 4$. Let us assume that this is true for n, i. e., that of all possible algorithms for Mabel to use for solving the SUBSET-SUM problem on sets with n integers, the Meet-in-the-Middle algorithm has the best worst-case running-time. Then we shall prove that this is also true for $n + 1$:

Let S be the set of all subset-sums of the set $A = \{a_1, a_2, \ldots, a_n\}$. Notice that the SUBSET-SUM problem on the set $A \cup \{a'\}$ of $n+1$ integers and target b is equivalent to the problem of determining whether (1) $b \in S$ or (2) $b' \in S$ (where $b' = b - a'$). (The symbol $\in$ means "is a member of".) Also notice that these two subproblems, (1) and (2), are independent from one another in the sense that the values of b and b' are unrelated to each other and are also unrelated to set S; therefore, in order to determine whether $b \in S$ or $b' \in S$, it is necessary to solve both subproblems (assuming that the first subproblem solved has no solution). So it is clear that if Mabel could solve both subproblems in the fastest time possible and also whenever possible make use of information obtained from solving subproblem (1) to save time solving subproblem (2) and whenever possible make use of information obtained from solving subproblem (2) to save time solving subproblem (1), then Mabel would be able to solve the problem of determining whether (1) $b \in S$ or (2) $b' \in S$ in the fastest time possible [15].

We shall now explain why the Meet-in-the-Middle algorithm has this characteristic for sets of size $n+1$: It is clear that by the induction hypothesis, the Meet-in-the-Middle algorithm solves each subproblem in the fastest time possible, since it works by applying the Meet-in-the-Middle algorithm to each subproblem, without loss of generality sorting and comparing elements in lists S^+ and $b-S^-$ and also sorting and comparing elements in lists S^+ and $b'-S^-$ as the algorithm sorts and compares elements in lists S^+ and $b-[S^- \cup (S^-+a')]$. There are two situations in which it is possible for the Meet-in-the-Middle algorithm to make use of information obtained from solving subproblem (1) to save time solving subproblem (2) or to make use of information obtained from solving subproblem (2) to save time solving subproblem (1). And the Meet-in-the-Middle algorithm takes advantage of both of these opportunities:

- Whenever the Meet-in-the-Middle algorithm compares two elements from lists S^+ and $b-S^-$ and the element in list S^+ turns out to be less than the element in list $b-S^-$, the algorithm makes use of information obtained from solving subproblem (1) (the fact that the element in list S^+ is less than the element in list $b-S^-$) to save time, when n is odd, solving subproblem (2) (the algorithm does not consider the element in list S^+ again).
- Whenever the Meet-in-the-Middle algorithm compares two elements from lists S^+ and $b'-S^-$ and the element in list S^+ turns out to be less than the element in list $b'-S^-$, the algorithm makes use of information obtained from solving subproblem (2) (the fact that the element in list S^+ is less than the element in list $b'-S^-$) to save time, when n is odd, solving subproblem (1) (the algorithm does not consider the element in list S^+ again).

Therefore, we can conclude that the Meet-in-the-Middle algorithm whenever possible makes use of information obtained from solving subproblem (1) to save time solving subproblem (2) and whenever possible makes use of information obtained from solving subproblem (2) to save time solving subproblem (1). So we have completed our induction step to prove true for $n+1$, assuming true for n.

Therefore, the best algorithm for Mabel to use for solving the SUBSET-SUM problem for large n is the Meet-in-the-Middle algorithm. But is the Meet-in-the-Middle algorithm the best algorithm for Mildred to use for solving the SUBSET-SUM problem for large n? Since the Meet-in-the-Middle algorithm is not the fastest algorithm for Mildred to use for small n, is it not possible that the Meet-in-the-Middle algorithm is also not the fastest algorithm for Mildred to use for large n? It turns out that for large n, there is no algorithm for Mildred to use for solving the SUBSET-SUM problem with a faster worst-case running-time than the Meet-in-the-Middle algorithm. Why?

Notice that the Meet-in-the-Middle algorithm takes on the order of $2^{n/2}$ steps regardless of whether Mabel or Mildred applies it. And notice that the algorithm of naïvely comparing the target b to all of the 2^n subset-sums of set A takes on the order of 2^n steps regardless of whether Mabel or Mildred applies it. So for large n, regardless of who the computer is, the Meet-in-the-Middle algorithm is faster than the naïve exhaustive comparison algorithm — from this example, we can understand the general principle that the asymptotic running-time of an algorithm does not differ by more than a polynomial factor when run on different types of computers [40, 41]. Therefore, since no algorithm is faster than the Meet-in-the-Middle algorithm for solving SUBSET-SUM for large n when applied by Mabel, we can conclude that no algorithm is faster than the Meet-in-the-Middle algorithm for solving SUBSET-SUM for large n when applied by Mildred. And furthermore, using this same reasoning, we can conclude that no algorithm is faster than the Meet-in-the-Middle algorithm for solving SUBSET-SUM for large n when run on a modern computing machine. □

So it doesn't matter whether the computer is Mabel, Mildred, or any modern computing machine; the fastest algorithm which solves the SUBSET-SUM problem for large n is the Meet-in-the-Middle algorithm. Because once a solution to the SUBSET-SUM problem is found, it is easy to verify (in polynomial-time) that it is indeed a solution, we say that the SUBSET-SUM problem is in class NP [5]. And because there is no algorithm which solves SUBSET-SUM that runs in polynomial-time (since the Meet-in-the-Middle algorithm runs in exponential-time and is the fastest algorithm for solving SUBSET-SUM, as we have shown above), we say that the SUBSET-SUM problem is not in class P [5]. Then since the SUBSET-SUM problem is in class NP but not in class P, we can conclude that $P \neq NP$, thus solving the P versus NP problem [15]. The solution to the P versus NP problem demonstrates that it is possible to hide abstract objects (in this case, a subset of set A) without an abundance of resources — it is, in general, more difficult to find a subset of a set of only one hundred integers for which the sum of its elements equals a target integer than to find the winning lottery-ticket in a pile of one billion unsorted lottery tickets, even though the lottery-ticket problem requires much more resources (one billion lottery tickets) than the SUBSET-SUM problem requires (a list of one hundred integers).

3 Does $P \neq NP$ really matter?

Even though $P \neq NP$, might there still be algorithms which efficiently solve problems that are in NP but not P in the average-case scenario? (Since the $P \neq NP$ result deals only with the worst-case scenario, there is nothing to forbid this from happening.) The answer is yes; for many problems which are in NP but not P, there exist algorithms which efficiently solve them in the average-case scenario [28, 39],

so the statement that $P \neq NP$ is not as ominous as it sounds. In fact, there is a very clever algorithm which solves almost all instances of the SUBSET-SUM problem in polynomial-time [11, 26, 28]. (The algorithm works by converting the SUBSET-SUM problem into the problem of finding the shortest non-zero vector of a lattice, given its basis.) But even though for many problems which are in NP but not P, there exist algorithms which efficiently solve them in the average-case scenario, in the opinion of most complexity-theorists, it is probably false that for all problems which are in NP but not P, there exist algorithms which efficiently solve them in the average-case scenario [3].

Even though $P \neq NP$, might it still be possible that there exist polynomial-time *randomized* algorithms which correctly solve problems in NP but not in P with a high probability regardless of the problem instance? (The word "randomized" in this context means that the algorithm bases some of its decisions upon random variables. The advantage of these types of algorithms is that whenever they fail to output a solution, there is still a good chance that they will succeed if they are run again.) The answer is probably no, as there is a widely believed conjecture that $P = BPP$, where BPP is the class of decision problems for which there are polynomial-time randomized algorithms that correctly solve them at least two-thirds of the time regardless of the problem instance [22].

4 Are quantum computers the answer?

A *quantum computer* is any computing device which makes direct use of distinctively quantum mechanical phenomena, such as superposition and entanglement, to perform operations on data. As of today, the field of practical quantum computing is still in its infancy; however, much is known about the theoretical properties of a quantum computer. For instance, quantum computers have been shown to efficiently solve certain types of problems, like factoring integers [35], which are believed to be difficult to solve on a *classical computer*, e. g., a human-computer like Mabel or Mildred or a machine-computer like an IBM PC or an Apple Macintosh.

Is it possible that one day quantum computers will be built and will solve problems like the SUBSET-SUM problem efficiently in polynomial-time? The answer is that it is generally suspected by complexity theorists to be impossible for a quantum computer to solve the SUBSET-SUM problem (and all other problems which share a characteristic with the SUBSET-SUM problem in that they belong to a subclass of NP problems known as *NP-complete* problems [5]) in polynomial-time. A curious fact is that if one were to solve the SUBSET-SUM problem on a quantum computer by brute force, the algorithm would have a running-time on the order of $2^{n/2}$ steps, which (by coincidence?) is the same asymptotic running-time of the fastest algorithm which solves SUBSET-SUM on a classical computer, the Meet-in-the-Middle algorithm [1, 4, 19].

In any case, no one has ever built a practical quantum computer and some scientists are even of the opinion that building such a computer is impossible; the acclaimed complexity theorist, Leonid Levin, wrote: "QC of the sort that factors long numbers seems firmly rooted in science fiction. It is a pity that popular accounts do not distinguish it from much more believable ideas, like Quantum Cryptography, Quantum Communications, and the sort of Quantum Computing that deals primarily with locality restrictions, such as fast search of long arrays. It is worth noting that the reasons why QC must fail are by no means clear; they merit thorough investigation. The answer may bring much greater benefits to the understanding of basic physical concepts than any factoring device could ever promise. The present attitude is analogous to, say, Maxwell selling the Daemon of his famous thought experiment as a path to cheaper electricity from heat. If he did, much of insights of today's thermodynamics might be lost or delayed" [25].

5 Unprovable conjectures

In the early twentieth century, the famous mathematician, David Hilbert, proposed the idea that all mathematical facts can be derived from only a handful of self-evident axioms. In the 1930's, Kurt Gödel proved that such a scenario is impossible by showing that for any proposed finite axiom system for arithmetic, there must always exist true statements that are unprovable within the system, if one is to assume that the axiom system has no inconsistencies. Alan Turing extended this result to show that it is impossible to design a computer program which can determine whether any other computer program will eventually halt. In the latter half of the 20th century, Gregory Chaitin defined a real number between zero and one, which he calls Ω, to be the probability that a computer program halts. And Chaitin proved that:

Theorem 1: For any mathematics problem, the bits of Ω, when Ω is expressed in binary, completely determine whether that problem is solvable or not.

Theorem 2: The bits of Ω are random and only a finite number of them are even possible to know.

From these two theorems, it follows that the very structure of mathematics itself is random and mostly unknowable! [8]

Even though Hilbert's dream to be able derive every mathematical fact from only a handful of self-evident axioms was destroyed by Gödel in the 1930's, this idea has still had an enormous impact on current mathematics research [43]. In fact, even though mathematicians as of today accept the incompleteness theorems proven by Gödel, Turing, and Chaitin as true, in general these same mathematicians also believe that these incompleteness theorems ultimately have no impact on traditional mathematics research, and they have thus adopted Hilbert's paradigm of deriving mathematical

facts from only a handful of self-evident axioms as a practical way of researching mathematics. Gregory Chaitin has been warning these mathematicians for decades now that these incompleteness theorems are actually very relevant to advanced mathematics research, but the overwhelming majority of mathematicians have not taken his warnings seriously [7]. We shall directly confirm Chaitin's assertion that incompleteness is indeed very relevant to advanced mathematics research by giving very strong evidence that two famous mathematics problems, determining whether the Collatz $3n+1$ Conjecture is true and determining whether the Riemann Hypothesis is true, are impossible to solve:

The Collatz $3n+1$ Conjecture — Here's a fun experiment that you, the reader, can try: Pick any positive integer, n. If n is even, then compute $n/2$ or if n is odd, then compute $(3n+1)/2$. Then let n equal the result of this computation and perform the whole procedure again until $n=1$. For instance, if you had chosen $n=11$, you would have obtained the sequence $(3\times11+1)/2=17$, $(3\times17+1)/2=26$, $26/2=13, 20, 10, 5, 8, 4, 2, 1$.

The Collatz $3n+1$ Conjecture states that such an algorithm will always eventually reach $n=1$ and halt [23]. Computers have verified this conjecture to be true for all positive integers less than $224\times2^{50}\approx2.52\times10^{17}$ [33]. Why does this happen? One can give an informal argument as to why this may happen [12] as follows: Let us assume that at each step, the probability that n is even is one-half and the probability that n is odd is one-half. Then at each iteration, n will decrease by a multiplicative factor of about $\left(\frac{3}{2}\right)^{1/2}\left(\frac{1}{2}\right)^{1/2}=$ $=\left(\frac{3}{4}\right)^{1/2}$ on average, which is less than one; therefore, n will eventually converge to one with probability one. But such an argument is **not** a rigorous mathematical proof, since the probability assumptions that the argument is based upon are not well-defined and even if they were well-defined, it would still be possible (although extremely unlikely, with probability zero) that the algorithm will never halt for some input.

Is there a rigorous mathematical proof of the Collatz $3n+1$ Conjecture? As of today, no one has found a rigorous proof that the conjecture is true and no one has found a rigorous proof that the conjecture is false. In fact, Paul Erdös, who was one of the greatest mathematicians of the twentieth century, commented about the Collatz $3n+1$ Conjecture: "Mathematics is not yet ready for such problems" [23]. We can informally demonstrate that there is no way to deductively prove that the conjecture is true, as follows:

Explanation: First, notice that in order to be certain that the algorithm will halt for a given input n, it is necessary to know whether the value of n at the beginning of each iteration of the algorithm is even or odd. (For a rigorous proof of this, see *The Collatz Conjecture is Unprovable* [16].) For instance, if the algorithm starts with input $n=11$, then in order to know that the algorithm halts at one, it is necessary to know that 11 is odd, $(3\times11+1)/2=17$ is odd, $(3\times17+1)/2=26$ is even, $26/2=13$ is odd, 20 is even, 10 is even, 5 is odd, 8 is even, 4 is even, and 2 is even. We can express this information (odd, odd, even, odd, even, even, odd, even, even, even) as a vector of zeroes and ones, $(1,1,0,1,0,0,1,0,0,0)$. Let us call this vector the *parity vector* of n. (If n never converges to one, then its parity vector must be infinite-dimensional.) If one does not know the parity vector of the input, then it is impossible to know what the algorithm does at each iteration and therefore impossible to be certain that the algorithm will converge to one. So any proof that the algorithm applied to n halts must specify the parity vector of n. Next, let us give a definition of a *random vector*:

Definition — We shall say that a vector $\mathbf{x}\in\{0,1\}^m$ is *random* if $\mathbf{x}$ cannot be specified in less than m bits in a computer text-file [6].

Example 1 — The vector of one million concatenations of the vector $(0,1)$ is **not** random, since we can specify it in less than two million bits in a computer text-file. (We just did.)

Example 2 — The vector of outcomes of one million coin-tosses has a good chance of fitting our definition of "random", since much of the time the most compact way of specifying such a vector is to simply make a list of the results of each coin-toss, in which one million bits are necessary.

Now let us suppose that it were possible to prove the Collatz $3n+1$ Conjecture and let B be the number of bits in a hypothetical computer text-file containing such a proof. And let $(x_0,x_1,x_2,\ldots,x_B)$ be a random vector, as defined above. (It is not difficult to prove that at least half of all vectors with $B+1$ zeroes and ones are random [6].) There is a mathematical theorem [23] which says that there must exist a number n with the first $B+1$ bits of its parity vector equal to $(x_0,x_1,x_2,\ldots,x_B)$; therefore, any proof of the Collatz $3n+1$ Conjecture must specify vector $(x_0,x_1,x_2,\ldots,x_B)$ (as we discussed above), since such a proof must show that the Collatz algorithm halts when given input n. But since vector $(x_0,x_1,x_2,\ldots,x_B)$ is random, $B+1$ bits are required to specify vector $(x_0,x_1,x_2,\ldots,x_B)$, contradicting our assumption that B is the number of bits in a computer text-file containing a proof of the Collatz $3n+1$ Conjecture; therefore, a formal proof of the Collatz $3n+1$ Conjecture cannot exist [16]. □

The Riemann Hypothesis — There is also another famous unresolved conjecture, the Riemann Hypothesis, which has a characteristic similar to that of the Collatz $3n+1$ Conjecture, in that it too can never be proven true. In the opinion of many mathematicians, the Riemann Hypothesis is the most important unsolved problem in mathematics [13]. The reason why it is so important is because a resolution of the Riemann Hypothesis would shed much light on the distribution of prime numbers: It is well known that the number of prime numbers less than n is approximately $\int_2^n\frac{dx}{\log x}$. If the Riemann Hypothesis is true, then for large n, the error in this approxi-

mation must be bounded by $cn^{1/2}\log n$ for some constant $c>0$ [38], which is also a bound for a *random walk*, i. e., the sum of n independent random variables, X_k, for $k=1,2,\ldots,n$ in which the probability that $X_k=-c$ is one-half and the probability that $X_k=c$ is one-half.

The Riemann-Zeta function $\zeta(s)$ is a complex function which is defined to be $\zeta(s)=\frac{s}{s-1}-s\int_1^\infty\frac{x-\lfloor x\rfloor}{x^{s+1}}dx$ when the real part of the complex number s is positive. The Riemann Hypothesis states that if $\rho=\sigma+ti$ is a complex root of ζ and $0<\sigma<1$, then $\sigma=1/2$. It is well known that there are infinitely many roots of ζ that have $0<\sigma<1$. And just like the Collatz $3n+1$ Conjecture, the Riemann Hypothesis has been verified by high-speed computers — for all $|t|<T$ where $T\approx 2.0\times 10^{20}$ [29]. But it is still unknown whether there exists a $|t|\geqslant T$ such that $\zeta(\sigma+ti)=0$, where $\sigma\neq 1/2$. And just like the Collatz $3n+1$ Conjecture, one can give a heuristic probabilistic argument that the Riemann Hypothesis is true [17], as follows:

It is well known that the Riemann Hypothesis follows from the assertion that for large n, $M(n)=\Sigma_{k=1}^{n}\mu(k)$ is bounded by $cn^{1/2}\log n$ for some constant $c>0$, where μ is the Möbius Inversion function defined on $\mathbb{N}$ in which $\mu(k)=-1$ if k is the product of an odd number of distinct primes, $\mu(k)=1$ if k is the product of an even number of distinct primes, and $\mu(k)=0$ otherwise. If we were to assume that $M(n)$ is distributed as a random walk, which is certainly plausible since there is no apparent reason why it should not be distributed as a random walk, then by probability theory, $M(n)$ is bounded for large n by $cn^{1/2}\log n$ for some constant $c>0$, with probability one; therefore, it is very likely that the Riemann Hypothesis is true. We shall now explain why the Riemann Hypothesis is unprovable, just like the Collatz $3n+1$ Conjecture:

Explanation: The Riemann Hypothesis is equivalent to the assertion that for each $T>0$, the number of real roots t of $\zeta(1/2+ti)$, where $0<t<T$, is equal to the number of roots of $\zeta(s)$ in $\{s=\sigma+ti\colon 0<\sigma<1,\ 0<t<T\}$. It is well known that there exists a continuous **real** function $Z(t)$ (called the Riemann-Siegel function) such that $|Z(t)|=|\zeta(1/2+ti)|$, so the real roots t of $\zeta(1/2+ti)$ are the same as the real roots t of $Z(t)$. (The formula for $Z(t)$ is $\zeta(1/2+ti)e^{i\vartheta(t)}$, where $\vartheta(t)=\arg\left[\Gamma(\frac{1}{4}+\frac{1}{2}it)\right]-\frac{1}{2}t\ln\pi$.) Then because the formula for the real roots t of $\zeta(1/2+ti)$ cannot be reduced to a formula that is simpler than the equation, $\zeta(1/2+ti)=0$, the only way to determine the number of real roots t of $\zeta(1/2+ti)$ in which $0<t<T$ is to count the changes in sign of the real function $Z(t)$, where $0<t<T$ [31].

So in order to prove that the number of real roots t of $\zeta(1/2+ti)$, where $0<t<T$, is equal to the number of roots of $\zeta(s)$ in $\{s=\sigma+ti:\ 0<\sigma<1,\ 0<t<T\}$, which can be computed via a theorem known as the *Argument Principle* **without** counting the changes in sign of $Z(t)$, where $0<t<T$ [27, 31, 32], it is necessary to count the changes in sign of $Z(t)$, where $0<t<T$. (Otherwise, it would be possible to determine the number of real roots t of $\zeta(1/2+ti)$, where $0<t<T$, without counting the changes in sign of $Z(t)$ by computing the number of roots of $\zeta(s)$ in $\{s=\sigma+ti\colon 0<\sigma<1,\ 0<t<T\}$ via the Argument Principle.) As T becomes arbitrarily large, the time that it takes to count the changes in sign of $Z(t)$, where $0<t<T$, approaches infinity for the following reasons: (1) There are infinitely many changes in sign of $Z(t)$. (2) The time that it takes to evaluate the sign of $Z(t)$ approaches infinity as $t\to\infty$ [31]. Hence, an infinite amount of time is required to prove that for each $T>0$, the number of real roots t of $\zeta(1/2+ti)$, where $0<t<T$, is equal to the number of roots of $\zeta(s)$ in $\{s=\sigma+ti:\ 0<\sigma<1,\ 0<t<T\}$ (which is equivalent to proving the Riemann Hypothesis), so the Riemann Hypothesis is unprovable. □

Chaitin's incompleteness theorem implies that mathematics is filled with facts which are both true and unprovable, since it states that the bits of Ω completely determine whether any given mathematics problem is solvable and only a finite number of bits of Ω are even knowable [8]. And we have shown that there is a very good chance that both the Collatz $3n+1$ Conjecture and the Riemann Hypothesis are examples of such facts. Of course, we can never formally prove that either one of these conjectures is both true and unprovable, for obvious reasons. The best we can do is prove that they are unprovable and provide computational evidence and heuristic probabilistic reasoning to explain why these two conjectures are most likely true, as we have done. And of course, it is conceivable that one could find a counter-example to the Collatz $3n+1$ Conjecture by finding a number n for which the Collatz algorithm gets stuck in a nontrivial cycle or a counter-example to the Riemann Hypothesis by finding a complex root, $\rho=\sigma+ti$, of ζ for which $0<\sigma<1$ and $\sigma\neq 1/2$. But so far, no one has presented any such counter-examples.

The theorems that the Collatz $3n+1$ Conjecture and the Riemann Hypothesis are unprovable illustrate a point which Chaitin has been making for years, that mathematics is not so much different from empirical sciences like physics [8, 14]. For instance, scientists universally accept the law of gravity to be true based on experimental evidence, but such a law is by no means absolutely certain — even though the law of gravity has been observed to hold in the past, it is not inconceivable that the law of gravity may cease to hold in the future. So too, in mathematics there are conjectures like the Collatz $3n+1$ Conjecture and the Riemann Hypothesis which are strongly supported by experimental evidence but can never be proven true with absolute certainty.

6 Computational irreducibility

Up until the last decade of the twentieth century, the most famous unsolved problem in all of mathematics was to prove

the following conjecture:

Fermat's Last Theorem (FLT) — When $n > 2$, the equation $x^n + y^n = z^n$ has no nontrivial integer solutions.

After reading the explanations in the previous section, a skeptic asked the author what the difference is between the previous argument that the Collatz $3n+1$ Conjecture is unprovable and the following argument that Fermat's Last Theorem is unprovable (which cannot possibly be valid, since Fermat's Last Theorem was proven by Wiles and Taylor in the last decade of the twentieth century [37]):

Invalid Proof that FLT is unprovable: Suppose that we have a computer program which computes $x^n + y^n - z^n$ for each $x, y, z \in \mathbb{Z}$ and $n > 2$ until it finds a nontrivial (x, y, z, n) such that $x^n + y^n - z^n = 0$ and then halts. Obviously, Fermat's Last Theorem is equivalent to the assertion that such a computer program can never halt. In order to be certain that such a computer program will never halt, it is necessary to compute $x^n + y^n - z^n$ for each $x, y, z \in \mathbb{Z}$ and $n > 2$ to determine that $x^n + y^n - z^n \neq 0$ for each nontrivial (x, y, z, n). Since this would take an infinite amount of time, Fermat's Last Theorem is unprovable. □

This proof is invalid, because the assertion that "it is necessary to compute $x^n + y^n - z^n$ for each $x, y, z \in \mathbb{Z}$ and $n > 2$ to determine that $x^n + y^n - z^n \neq 0$ for each nontrivial (x, y, z, n)" is false. In order to determine that an equation is false, it is not necessary to compute both sides of the equation — for instance, it is possible to know that the equation $6x + 9y = 74$ has no integer solutions without evaluating $6x + 9y$ for every $x, y \in \mathbb{Z}$, since one can see that if there were any integer solutions, the left-hand-side of the equation would be divisible by three but the right-hand-side would not be divisible by three.

Question — So why can't we apply this same reasoning to show that the proof that the Collatz $3n + 1$ Conjecture is unprovable is invalid? Just as it is not necessary to compute $x^n + y^n - z^n$ in order to determine that $x^n + y^n - z^n \neq 0$, is it not possible that one can determine that the Collatz algorithm will converge to one without knowing what the algorithm does at each iteration?

Answer — Because what the Collatz algorithm does at each iteration **is** what determines whether or not the Collatz sequence converges to one [16], it is necessary to know what the Collatz algorithm does at each iteration in order to determine that the Collatz sequence converges to one. Because the exact values of $x^n + y^n - z^n$ are **not** relevant to knowing that $x^n + y^n - z^n \neq 0$ for each nontrivial (x, y, z, n), it is not necessary to compute each $x^n + y^n - z^n$ in order to determine that $x^n + y^n - z^n \neq 0$ for each nontrivial (x, y, z, n).

Exercise — You are given a deck of n cards labeled $1, 2, 3, \ldots, n$. You shuffle the deck. Then you perform the following "reverse-card-shuffling" procedure: Look at the top card labeled k. If $k = 1$, then stop. Otherwise, reverse the order of the first k cards in the deck. Then look at the top card again and repeat the same procedure. For example, if $n = 7$ and the deck were in order 5732416 (where 5 is the top card), then you would obtain $4237516 \to 7324516 \to 6154237 \to \to 3245167 \to 4235167 \to 5324167 \to 1423567$. Now, we present two problems:

- Prove that such a procedure will always halt for any n and any shuffling of the n cards.
- Find a closed formula for the maximum number of iterations that it may take for such a procedure to halt given the number of cards in the deck, or prove that no such formula exists. (The maximum number of iterations for $n = 1, 2, 3, \ldots, 16$ are $0, 1, 2, 4, 7, 10, 16, 22, 30, 38, 51, 65, 80, 101, 113, 139$ [36].)

It is easy to use the principle of mathematical induction to solve the first problem. As for the second problem, it turns out that there is no closed formula; in other words, in order to find the maximum number of iterations that it may take for such a procedure to halt given the number of cards n in the deck, it is necessary to perform the reverse-card-shuffling procedure on every possible permutation of $1, 2, 3, \ldots, n$. This property of the Reverse-Card-Shuffling Problem in which there is no way to determine the outcome of the reverse-card-shuffling procedure without actually performing the procedure itself is called *computational irreducibility* [42]. Notice that the notion of computational irreducibility also applies to the Collatz $3n+1$ Conjecture and the Riemann Hypothesis in that an infinite number of irreducible computations are necessary to prove these two conjectures.

Stephen Wolfram, who coined the phrase "computational irreducibility", argues in his famous book, *A New Kind of Science* [42], that our universe is computationally irreducible, i.e., the universe is so complex that there is no general method for determining the outcome of a natural event without either observing the event itself or simulating the event on a computer. The dream of science is to be able to make accurate predictions about our natural world; in a computationally irreducible universe, such a dream is only possible for very simple phenomena or for events which can be accurately simulated on a computer.

7 Open problems in mathematics

In the present year of 2006, the most famous unsolved number theory problem is to prove the following:

Goldbach's Conjecture — Every even number greater than two is the sum of two prime numbers.

Just like the Collatz $3n + 1$ Conjecture and the Riemann Hypothesis, there are heuristic probabilistic arguments which support Goldbach's Conjecture, and Goldbach's Conjecture has been verified by computers for a large number of even numbers [20]. The closest anyone has come to proving Goldbach's Conjecture is a proof of the following:

Chen's Theorem — Every sufficiently large even integer is either the sum of two prime numbers or the sum of a prime number and the product of two prime numbers [9].

Although the author cannot prove it, he believes the following:

Conjecture 1 — Goldbach's Conjecture is unprovable.

Another famous conjecture which is usually mentioned along with Goldbach's Conjecture in mathematics literature is the following:

The Twin Primes Conjecture — There are infinitely many prime numbers p for which $p + 2$ is also prime [20].

Just as with Goldbach's Conjecture, the author cannot prove it, but he believes the following:

Conjecture 2 — The Twin Primes Conjecture is undecidable, i. e., it is impossible to know whether the Twin Primes Conjecture is true or false.

8 Conclusion

The $P \neq NP$ problem, the Collatz $3n+1$ Conjecture, and the Riemann Hypothesis demonstrate to us that as finite human beings, we are all severely limited in our ability to solve abstract problems and to understand our universe. The author hopes that this observation will help us all to better appreciate the fact that there are still so many things which G-d allows us to understand.

Acknowledgements

I thank G-d, my parents, my wife, and my children for their support.

References

1. Aaronson S. NP-complete problems and physical reality. *SIGACT News*, *Complexity Theory Column*, March 2005.
2. Belaga E. Reflecting on the $3x + 1$ mystery: Outline of a scenario. Univ. Strasbourg preprint, 10 pages, 1998.
3. Ben-David S., Chor B., Goldreich O., and Luby M. *Journal of Computer and System Sciences*, 1992, v. 44, No. 2, 193–219.
4. Bennett C., Bernstein E., Brassard G., and Vazirani U. *SIAM J. Comput.*, 1997, v. 26(5), 1510–1523.
5. Bovet P. B. and Crescenzi P. Introduction to the theory of complexity. Prentice Hall, 1994.
6. Chaitin G. J. Algorithmic information theory. Rev. 3rd ed., Cambridge University Press, 1990.
7. Chaitin G. J. arXiv: math/0306042.
8. Chaitin G. J. Meta Math! Pantheon, October 2005.
9. Chen J. R. *Kexue Tongbao*, 1966, v. 17, 385–386.
10. Cormen T. H., Leiserson C. E., and Rivest R. L., Introduction to algorithms. McGraw-Hill, 1990.
11. Coster M. J., Joux A., LaMacchia B. A., Odlyzko A. M., Schnorr C. P., and Stern J. *Computational Complexity*, 1992, No. 2, 111–128.
12. Crandall R. E. *Math. Comp.*, 1978, v. 32, 1281–1292.
13. Derbyshire J. Prime obsession. Joseph Henry Press, 2003.
14. Dombrowski K. *Progress in Physics*, 2005, v. 1, 65–67.
15. Feinstein C. A. arXiv: cs/0310060.
16. Feinstein C. A. arXiv: math/0312309.
17. Good I. J. and Churchhouse R. F. *Math. Comp.*, 1968, v. 22, 857–861.
18. Grier D. A. When computers were human. Princeton University Press, 2005.
19. Grover L. K. *Proc. 28th Annual ACM Symp. on the Theory of Computing*, May 1996, 212–219.
20. Guy R. K. Unsolved problems in number theory. 3rd ed., New York, Springer-Verlag, 2004.
21. Horowitz E. and Sahni S. *Journal of the ACM*, 1974, v. 2l, No. 2, 277–292.
22. Impagliazzo R. and Wigderson A. *Proc. of the Twenty-Ninth Annual ACM Symp. on Theory of Computing*, 1997, 220–229.
23. Lagarias J. C. *Amer. Math. Monthly*, 1985, v. 92, 3–23. Repr. in: *Conf. on Organic Math.*, Canad. Math. Soc. Conf. Proc., v. 20, 1997, 305–331; http://www.cecm.sfu.ca/organics/papers.
24. Lagarias J. C. arXiv: math/0309224.
25. Levin L. A. *Probl. Inform. Transmis.*, 2003, v. 39(1), 92–103.
26. Menezes A., van Oorschot P., and Vanstone S. Handbook of applied cryptography. CRC Press, 1996.
27. Odlyzko A. M. *Math. of Computation 1943-1993*, W. Gautschi (ed.), AMS, Proc. Symp. Appl. Math., v. 48, 1994, 451–463.
28. Odlyzko A. M. *Cryptol. and Comput. Num. Theory*, C. Pomerance (ed.), AMS, Proc. Symp. Appl. Math., 1990, v. 42, 75–88.
29. Odlyzko A.M. *Supercomputing'89, Conf. Proc.*, L.P. Kartashev and S.I. Kartashev (eds.), Int. Supercomp. Inst., 1989, 348–352.
30. Papadimitriou C. H. and Steiglitz K. Combinatorial optimization: Algorithms and complexity. Prentice-Hall, Englewood Cliffs, NJ, 1982.
31. Pugh G. R. Master's thesis, Univ. of British Columbia, 1998.
32. Rao M. and Stetkaer H. Complex analysis. World Sci., 1991.
33. Roosendaal E. http://personal.computrain.nl/eric/wondrous/.
34. Shackleford M. W. *Actuarial Note 139*, Social Security Admin., May 1998; http://www.ssa.gov/OACT/babynames/.
35. Shor P. *Proc. 35th Ann. Symp. on Found. of Computer Sci., Santa Fe, NM, USA, 1994*, IEEE Comp. Soc. Press, 124–134.
36. Sloane N.J.A. *Online Enc. of Integer Seq.*, No. A000375, 2005.
37. Weisstein E. W. Fermat's last theorem. *Concise Enc. of Math.*, 2nd ed., CRC Press, Boca Raton (FL), 2003, 1024–1027.
38. Weisstein E. W. Riemann Hypothesis. *Ibid.*, 2550–2551.
39. Wilf H. S. *Inform. Proc. Lett.*, 1984, v. 18, 119–122.
40. Woeginger G. J. *Lecture Notes in Computer Sci.*, Springer-Verlag Heidelberg, 2003, v. 2570, 185–207.
41. Wolfram S. *Phys. Rev. Lett.*, 1985, v. 54, 735–738.
42. Wolfram S. A new kind of science. Wolfram Media, Champaign, IL, 2002.
43. Zach R. arXiv: math/0508572.

Steady Particle States of Revised Electromagnetics

Bo Lehnert

Alfvén Laboratory, Royal Institute of Technology, S-10044, Stockholm, Sweden

E-mail: Bo.Lehnert@ee.kth.se

A revised Lorentz invariant electromagnetic theory leading beyond Maxwell's equations, and to a form of extended quantum electrodynamics, has been elaborated on the basis of a nonzero electric charge density and a nonzero electric field divergence in the vacuum state. Among the applications of this theory, there are steady electromagnetic states having no counterpart in conventional theory and resulting in models of electrically charged and neutral leptons, such as the electron and the neutrino. The analysis of the electron model debouches into a point-charge-like geometry with a very small characteristic radius but having finite self-energy. This provides an alternative to the conventional renormalization procedure. In contrast to conventional theory, an integrated radial force balance can further be established in which the electron is prevented from "exploding" under the action of its net self-charge. Through a combination of variational analysis and an investigation of the radial force balance, a value of the electronic charge has been deduced which deviates by only one percent from that obtained in experiments. This deviation requires further investigation. A model of the neutrino finally reproduces some of the basic features, such as a small but nonzero rest mass, an angular momentum but no magnetic moment, and long mean free paths in solid matter.

1 Introduction

Maxwell's equations in a vacuum state with a vanishing electric field divergence have served as a basis for quantum electrodynamics (QED) in its conventional form [1]. This theory has been very successful in many applications, but as stated by Feynman [2], there still exist areas within which it does not provide fully adequate descriptions of physical reality. When applying conventional theory to attempted models of the electron, there thus appear a number of incomprehensible and unwieldy problems. These include the existence of a steady particle state, the unexplained point-charge-like geometry, the question of infinite self-energy and the associated physical concept of renormalization with extra added counter terms [3], the lack of radial force balance of the electron under the action of its self-charge [4], and its unexplained quantized charge. Also the models of an electrically neutral state of the neutrino include a number of questions, such as those of a nonzero but small rest mass, a nonzero angular momentum and a vanishing magnetic moment, and excessively long mean free paths for interaction with solid matter.

The limitations of conventional theory have caused a number of authors to elaborate modified electromagnetic approaches aiming beyond Maxwell's equations. Among these there is a theory [5–12] to be described in this paper. It is based on a vacuum state that can give rise to local space charges and an associated nonzero electric field divergence, leading to a current in addition to the displacement current. The field equations are then changed in a substantial manner, to result in a form of extended quantum electrodynamics ("EQED").

In applications of the present theory to photon physics, the nonzero electric field divergence appears as a small quantity, but it still comes out to have an essential effect on the end results [11, 12]. For the steady particle states to be treated here, the field equations contain electric field divergence terms which appear as large contributions already at the outset.

2 Basic field equations

The basic physical concept of the present theory is the appearance of a local electric charge density in the vacuum state in which there are quantum mechanical electromagnetic fluctuations. This charge density is associated with a nonzero electric field divergence. When imposing the condition of Lorentz invariance on the system, there arises a local "space-charge current density" in addition to the displacement current. The detailed deductions are described in earlier reports by the author [5–12]. The revised field equations *in the vacuum* are given by

$$\operatorname{curl}\mathbf{B}/\mu_0 = \varepsilon_0(\operatorname{div}\mathbf{E})\,\mathbf{C} + \varepsilon_0\partial\mathbf{E}/\partial t\,, \tag{1}$$

$$\operatorname{curl}\mathbf{E} = -\partial\mathbf{B}/\partial t\,, \tag{2}$$

$$\mathbf{B} = \operatorname{curl}\mathbf{A}\,, \qquad \operatorname{div}\mathbf{B} = 0\,, \tag{3}$$

$$\mathbf{E} = -\nabla\phi - \partial\mathbf{A}/\partial t\,, \qquad \operatorname{div}\mathbf{E} = \bar{\rho}/\varepsilon_0 \tag{4}$$

for the electric and magnetic fields $\mathbf{E}$ and $\mathbf{B}$, the electric

charge density $\bar{\rho}$, the magnetic vector potential $\mathbf{A}$, the electrostatic potential ϕ, and the velocity vector $\mathbf{C}$, where $\mathbf{C}^2 = c^2$. In analogy with the direction to be specified for the current density in conventional theory, the unit vector $\mathbf{C}/c$ depends on the geometry of the particular configuration to be studied.

Using well-known vector identities, equations (1) and (2) can be recast into the local momentum equation

$$\operatorname{div} {}^2\mathbf{S} = \bar{\rho}\,(\mathbf{E} + \mathbf{C} \times \mathbf{B}) + \varepsilon_0 \frac{\partial}{\partial t}\,\mathbf{g} \tag{5}$$

and the local energy equation

$$-\operatorname{div} \mathbf{S} = \bar{\rho}\,\mathbf{E} \cdot \mathbf{C} + \frac{1}{2}\,\varepsilon_0 \frac{\partial}{\partial t}\,w_f\,. \tag{6}$$

Here ${}^2\mathbf{S}$ is the electromagnetic stress tensor,

$$\mathbf{g} = \varepsilon_0\,\mathbf{E} \times \mathbf{B} = \frac{1}{c^2}\,\mathbf{S} \tag{7}$$

can be interpreted as an electromagnetic momentum density with $\mathbf{S}$ denoting the Poynting vector, and

$$w_f = \frac{1}{2}\left(\varepsilon_0\,\mathbf{E}^2 + \mathbf{B}^2/\mu_0\right) \tag{8}$$

representing the electromagnetic field energy density. An electromagnetic source energy density

$$w_s = \frac{1}{2}\,\bar{\rho}\,(\phi + \mathbf{C} \cdot \mathbf{A}) \tag{9}$$

can also be deduced and related to the density (8) as shown earlier [12].

As distinguished from Maxwell's equations, the present theory includes steady electromagnetic states in which all explicit time derivatives vanish in equations (1)–(6). The volume integrals of w_f and w_s then become equal for certain configurations which are limited in space.

3 Steady axisymmetric states

Among the steady axisymmetric states the analysis is here restricted to particle-shaped ones where the configuration is bounded both in the axial and radial directions. There are also string-shaped states being uniform in the axial directions, as described elsewhere [7, 12].

3.1 General features of particle-shaped states

In particle-shaped geometry a frame (r, θ, φ) of spherical coordinates is introduced, where all relevant quantities are independent of the angle φ. The analysis is further limited to a current density $\mathbf{j} = (0, 0, C\bar{\rho})$ and a vector potential $\mathbf{A} = (0, 0, A)$. Here $C = \pm\, c$ represents the two possible spin directions. The basic equations (1)–(4) then take the form

$$\frac{(r_0\,\rho)^2\,\bar{\rho}}{\varepsilon_0} = D\phi = \left[D + (\sin\theta)^{-2}\right](CA)\,, \tag{10}$$

where the dimensionless radial variable $\rho = r/r_0$ has been introduced with r_0 as a characteristic radial dimension, and where the operator $D = D_\rho + D_\theta$ is defined by

$$D_\rho = -\frac{\partial}{\partial\rho}\left(\rho^2 \frac{\partial}{\partial\rho}\right), \qquad D_\theta = -\frac{\partial^2}{\partial\theta^2} - \frac{\cos\theta}{\sin\theta}\frac{\partial}{\partial\theta}\,. \tag{11}$$

The general solution of equations (10) is obtained in terms of a *generating function*

$$F(r, \theta) = CA - \phi = G_0 \cdot G(\rho, \theta)\,, \tag{12}$$

where G_0 stands for a characteristic amplitude and G for a normalized dimensionless part. The solutions become

$$CA = -(\sin^2\theta)\,DF\,, \tag{13}$$

$$\phi = -\left[1 + (\sin^2\theta)\,D\right]F\,, \tag{14}$$

$$\bar{\rho} = -\left(\frac{\varepsilon_0}{r_0^2\,\rho^2}\right) D\left[1 + (\sin^2\theta)\,D\right]F\,. \tag{15}$$

The extra degree of freedom introduced by the nonzero electric field divergence and the inhomogeneity of equations (10) are underlying this general result.

Using expressions (13)–(15), (9), and the functions

$$f(\rho, \theta) = -(\sin\theta)\,D\left[1 + (\sin^2\theta)\,D\right]G\,, \tag{16}$$

$$g(\rho, \theta) = -\left[1 + 2(\sin^2\theta)\,D\right]G \tag{17}$$

integrated field quantities can be obtained which represent a net electric charge q_0, magnetic moment M_0, mass m_0, and angular momentum s_0. The magnetic moment is obtained from the local contributions of the current density, and the mass and angular momentum from those of w_s/c^2 and the energy relation by Einstein. The current density behaves as a common convection current. The mass flow originates from the velocity vector, having the same direction for positive and negative charge elements. Thus the integrated quantities become

$$q_0 = 2\pi\varepsilon_0\,r_0\,G_0\,J_q\,, \qquad I_q = f\,, \tag{18}$$

$$M_0 = \pi\varepsilon_0\,C\,r_0^2\,G_0\,J_M\,, \qquad I_M = \rho\,(\sin\theta) f\,, \tag{19}$$

$$m_0 = \pi(\varepsilon_0/c^2)\,r_0\,G_0^2\,J_m\,, \qquad I_m = fg\,, \tag{20}$$

$$s_0 = \pi(\varepsilon_0 C/c^2)\,r_0^2\,G_0^2\,J_s\,, \qquad I_s = \rho\,(\sin\theta) fg \tag{21}$$

with the normalized integrals

$$J_k = \int_{\rho_k}^{\infty}\!\!\int_0^{\pi} I_k\,d\rho\,d\theta\,, \qquad k = q, M, m, s\,. \tag{22}$$

Here ρ_k are small radii of circles centered around the origin $\rho = 0$ when G is divergent there, and $\rho_k = 0$ when G is convergent at $\rho = 0$.

At this point a further step is taken by restricting the analysis to a separable generating function

$$G(\rho, \theta) = R(\rho) \cdot T(\theta)\,. \tag{23}$$

The integrands of the normalized forms then become

$$I_q = \tau_0 R + \tau_1 (D_\rho R) + \tau_2 D_\rho (D_\rho R) , \quad (24)$$

$$I_M = \rho (\sin\theta) I_q , \quad (25)$$

$$I_m = \tau_0\tau_3 R^2 + (\tau_0\tau_4 + \tau_1\tau_3) R (D_\rho R) + \tau_1\tau_4 (D_\rho R)^2 + + \tau_2\tau_3 R D_\rho (D_\rho R) + \tau_2\tau_4 (D_\rho R) [D_\rho (D_\rho R)] , \quad (26)$$

$$I_s = \rho (\sin\theta) I_m , \quad (27)$$

where

$$\tau_0 = -(\sin\theta)(D_\theta T) - (\sin\theta) D_\theta \left[(\sin^2\theta)(D_\theta T)\right] , \quad (28)$$

$$\tau_1 = -(\sin\theta) T - (\sin\theta) D_\theta \left[(\sin^2\theta) T\right] - \sin^3\theta (D_\theta T) , \quad (29)$$

$$\tau_2 = -(\sin^3\theta) T , \quad (30)$$

$$\tau_3 = -T - 2(\sin^2\theta)(D_\theta T) , \quad (31)$$

$$\tau_4 = -2(\sin^2\theta) T . \quad (32)$$

The restriction (23) of separability becomes useful here for configurations having sources $\bar{\rho}$ and $\mathbf{j}$ that are mainly localized to a region near the origin, such as for a particle of limited extent. The analysis further concerns a radial function R which can become convergent or divergent at the origin, and a finite polar function T with finite derivatives which can be symmetric or antisymmetric in respect to the "equatorial plane" (midplane) defined by $\theta = \pi/2$. Repeated partial integration of expressions (22) for J_q and J_M leads to the following results as described in detail elsewhere [7, 8, 12]:

- The integrated charge q_0 and magnetic moment M_0 vanish in all cases where R is convergent at the origin and T has top-bottom symmetry as well as antisymmetry in respect to the equatorial plane. These cases lead to models of electrically neutral particles, such as the neutrino;
- The charge q_0 and magnetic moment M_0 are both nonzero provided that R is divergent at the origin and T has top-bottom symmetry. This case leads to models of charged particles, such as the electron. As will be seen from the analysis to follow, the *divergence* of R can still becomes reconcilable with *finite* values of q_0, M_0, m_0, and s_0 provided that the characteristic radius r_0 is made to shrink to the very small values of a point-charge-like state, as also being supported by experimental observations.

3.2 Quantum conditions of steady states

In this analysis a simplified road is chosen by imposing relevant quantum conditions afterwards on the obtained general solutions of the field equations. This is expected to be a rather good approximation to a rigorous approach where the extended field equations are quantized from the outset. The quantized equations namely become equivalent to the original ones in which the field quantities are replaced by their expectation values according to Heitler [13].

The angular momentum (spin) condition to be imposed on a model of the electron in the capacity of a fermion particle, as well as of the neutrino, is combined with equation (21) to result in

$$s_0 = \pi \left(\varepsilon_0 C / c^2\right) r_0^2 G_0^2 J_s = \pm h/4\pi . \quad (33)$$

In particular, for a charged particle such as the electron, muon, tauon or their antiparticles, equations (18) and (33) combine to

$$q^* \equiv |q_0/e| = \sqrt{f_0 J_q^2 / 2 J_s} , \qquad f_0 = 2\varepsilon_0 c h / e^2 . \quad (34)$$

Here q^* is a dimensionless charge which is normalized with respect to the experimentally determined elementary charge "e", and $f_0 \cong 137.036$ is the inverted value of the fine-structure constant.

According to Dirac, Schwinger, and Feynman [14] the quantum condition of the magnetic moment of a charged particle such as the electron becomes

$$M_0 m_0 / q_0 s_0 = 1 + \delta_M , \qquad \delta_M = 1/2\pi f_0 , \quad (35)$$

which shows excellent agreement with experiments. Here the unity term of the right hand member is due to Dirac who obtained the correct Landé factor, and δ_M is a small quantum mechanical correction due to Schwinger and Feynman. Conditions (33) and (35) can also be made plausible by elementary physical arguments based on the present picture of a particle-shaped state of "self-confined" radiation [7, 12].

In a charged particle-shaped state the electric current distribution generates a total magnetic flux Γ_{tot}. Here we consider the electron to be a system having both quantized angular momentum s_0 and a quantized charge q_0. The magnetic flux should then be quantized as well, and be given by the specific values of the two quantized concepts s_0 and q_0. This leads to the relation

$$\Gamma_{tot} = |s_0/q_0| . \quad (36)$$

4 A model of the electron

The analysis in this section will show that finite and nonzero integrated field quantities can be obtained in terms of the shrinking characteristic radius of a point-charge-like state. This does not imply that r_0 has to become strictly equal to zero, which would end up into the unphysical situation of a structureless point.

4.1 The integrated field quantities

The generating function to be considered has the parts

$$R = \rho^{-\gamma} e^{-\rho}, \qquad \gamma > 0 , \quad (37)$$

$$T = 1 + \sum_{\nu=1}^{n} \left\{ a_{2\nu-1} \sin[(2\nu-1)\theta] + a_{2\nu} \cos(2\nu\theta) \right\} . \quad (38)$$

The radial part (37) appears at first glance to be somewhat special. Generally one could have introduced a negative power series of ρ. However, for a limited number of terms, that with the largest negative power will in any case dominate at the origin. Due to the analysis which follows the same series has further to contain one term only, with a locked special value of γ. Moreover, the exponential factor in the form (37) secures the convergence of any moment with R, but will not appear in the end result.

The radial form (37) is now inserted into the integrands (24)–(27). Then the integrals (22) take a form $J_k = J_{k\rho} J_{k\theta}$. Here $J_{k\rho}$ is a part resulting from the integration with respect to ρ, and which is dominated by terms of the strongest negative power. The part $J_{k\theta}$ further results from the integration with respect to θ. In the integrals $J_{k\rho}$ divergences appear when the lower limits ρ_k approach zero. To outbalance this, we introduce a shrinking characteristic radius

$$r_0 = c_0\,\varepsilon\,, \qquad c_0 > 0\,, \qquad 0 < \varepsilon \ll 1\,, \tag{39}$$

where ε is a dimensionless smallness parameter. The integrated field quantities (18)–(21) then become

$$q_0 \;=\; 2\pi\varepsilon_0 c_0 G_0\,[J_{q\theta}/(\gamma-1)]\,(\varepsilon/\rho_q^{\gamma-1})\,, \tag{40}$$

$$M_0 m_0 \;=\; \pi^2(\varepsilon_0^2 C/c^2)c_0^3 G_0^3\cdot \\ \cdot\,[J_{M\theta}J_{m\theta}/(\gamma-2)(2\gamma-1)]\,(\varepsilon^3/\rho_M^{\gamma-2}\rho_m^{2\gamma-1})\,, \tag{41}$$

$$s_0 \;=\; \pi(\varepsilon_0 C/c^2)c_0^2 G_0^2\,[J_{s\theta}/2(\gamma-1)]\,(\varepsilon/\rho_s^{\gamma-1})^2. \tag{42}$$

The reason for introducing the compound quantity $M_0 m_0$ in expression (41) is that this quantity appears as a single entity in all finally obtained relations of the present analysis. The configuration with its integrated quantities is now required to scale in such a way that the geometry is preserved by becoming independent of ρ_k and ε. Such a uniform scaling implies that

$$\rho_q = \rho_M = \rho_m = \rho_s = \varepsilon \tag{43}$$

and that the parameter γ has to approach the value 2 from above, as specified by

$$\gamma(\gamma-1) = 2+\tilde{\delta}\,, \quad 0 \leqslant \tilde{\delta} \ll 1\,, \quad \gamma \approx 2+\tilde{\delta}/3\,. \tag{44}$$

As a result of this

$$J_{k\theta} = \int_0^{\pi} I_{k\theta}\,d\theta\,, \tag{45}$$

where

$$I_{q\theta} \;=\; -2\tau_1 + 4\tau_2\,, \tag{46}$$

$$I_{M\theta}/\tilde{\delta} \;=\; (\sin\theta)(-\tau_1+4\tau_2)\,, \tag{47}$$

$$I_{m\theta} \;=\; \tau_0\tau_3 - 2(\tau_0\tau_4+\tau_1\tau_3) + \\ +\,4(\tau_1\tau_4+\tau_2\tau_3) - 8\tau_2\tau_4\,, \tag{48}$$

$$I_{s\theta} \;=\; (\sin\theta)\,I_{m\theta}\,. \tag{49}$$

Then

$$q_0 \;=\; 2\pi\varepsilon_0 c_0 G_0 A_q\,, \tag{50}$$

$$M_0 m_0 \;=\; \pi^2(\varepsilon_0^2 C/c^2)c_0^3 G_0^3 A_M A_m\,, \tag{51}$$

$$s_0 \;=\; (1/2)\pi(\varepsilon_0 C/c^2)c_0^2 G_0^2 A_s \tag{52}$$

with $A_q \equiv J_{q\theta}$, $A_M \equiv J_{M\theta}/\tilde{\delta}$, $A_m \equiv J_{m\theta}$, and $A_s \equiv J_{s\theta}$.

The uniform scaling due to relations (39) and (43) in the range of small ε requires the characteristic radius r_0 to be very small, but does not specify its absolute value. One possibility of estimating this radius is by a crude modification of the field equations by an effect of General Relativity originating from the circulatory spin motion [7, 12]. This yields an upper limit of r_0 of about 10^{-19} meters for which this modification can be neglected.

As expressed by equations (39) and (43), the present results also have an impact on the question of Lorentz invariance of the electron radius. In the limit $\varepsilon \to 0$ the deductions will thus in a formal way satisfy such an invariance, in terms of a vanishing radius. At the same time the range of small ε becomes applicable to the physically relevant case of a very small but nonzero radius of a configuration having an internal structure.

4.2 The magnetic flux

According to equation (13) the magnetic flux function becomes

$$\Gamma = 2\pi r\,(\sin\theta)A = -2\pi r_0\,(G_0/c)\,\rho(\sin^3\theta)\,DG\,. \tag{53}$$

Making use of equations (37) and (39), it takes the form

$$\Gamma = 2\pi(c_0 G_0/C)\sin^3\theta\,\big\{\big[\gamma(\gamma-1)+2(\gamma-1)\rho+\rho^2\big]\,T - \\ -\;D_\theta\,T\big\}\,\big(\varepsilon/\rho^{\gamma-1}\big)\,e^{-\rho}\,. \tag{54}$$

To obtain a nonzero and finite magnetic flux function at the spherical surface $\rho = \varepsilon$ when γ approaches the value 2 from above, one has then to choose a corresponding dimensionless lower radius limit $\rho_\Gamma = \varepsilon$, in analogy with the condition (43).

In the further analysis a normalized flux function

$$\Psi \equiv \Gamma_{(\rho=\varepsilon,\theta)}/2\pi(c_0 G_0/C) = \sin^3\theta\,(D_\theta T - 2T) \tag{55}$$

is introduced at $\rho = \varepsilon$. A detailed study [8, 9, 12] of this function shows that there is a main magnetic flux

$$\Psi_0 = \Psi(\pi/2) \equiv A_\Gamma\,, \tag{56}$$

which intersects the equatorial plane, and that the total flux of equation (36) also includes that of two separate magnetic "islands" situated above and below the equatorial plane. As a consequence, the derivative $d\Psi/d\theta$ has two zero points at θ_1 and $\theta_2 > \theta_1$ in the range $0 \leqslant \theta \leqslant \pi/2$. These define the particular fluxes Ψ_1 in the range $0 < \theta \leqslant \theta_1$ and Ψ_2 in the

range $\theta_2 < \theta < \pi/2$. The total normalized magnetic flux thus becomes

$$\Psi_{tot} = f_{\Gamma f}\,\Psi_0\,, \quad f_{\Gamma f} = \left[2(\Psi_1 + \Psi_2) - \Psi_0\right]/\Psi_0\,, \quad (57)$$

where $f_{\Gamma f} > 1$ is the *obtained* flux factor including the additional contributions from the magnetic islands.

4.3 Quantum conditions

For the angular momentum and its associated charge relation (34) the quantum condition becomes

$$q^* = \sqrt{f_0 A_q^2/A_s} \quad (58)$$

according to equations (50) and (52). The magnetic moment condition (35) further reduces to

$$A_M A_m/A_q A_s = 1 + \delta_M\,. \quad (59)$$

Combination of equations (36), (50), (52), and (56) finally yields

$$8\pi f_{\Gamma q} A_\Gamma A_q = A_s\,, \quad (60)$$

where $f_{\Gamma q}$ is the flux factor being *required* by the quantum condition. For a self-consistent solution the two flux factors of equations (57) and (60) have to become equal to a common factor $f_\Gamma = f_{\Gamma f} = f_{\Gamma q}$.

4.4 Variational analysis of the integrated charge

Since the elementary electronic charge appears to represent the smallest quantum of free charge, the question may be raised whether there is a more profound reason for such a charge to exist, possibly in terms of variational analysis. In a first attempt efforts have therefore been made to search for an extremum of the normalized charge (58), under the two subsidiary quantum conditions (59) and (60) and including Lagrange multipliers. The available variables are then the amplitudes (a_1, a_2, a_3, ...) of the polar function (38). However, such a conventional procedure is found to be upset by difficulties. It namely applies when there are well-defined and localized points of extremum, but not when such single points are replaced by a flat plateau in parameter space.

The plateau behaviour is in fact what occurs here, and an alternative analysis is then applied in terms of an increasing number of amplitudes that are "swept" (scanned) across their entire range of variation [9, 12]. One illustration of this is presented in Fig. 1 for the first four amplitudes, and with a flux factor $f_\Gamma = 1.82$. The figure shows the behaviour of the normalized charge q^* when scanning the ranges of the remaining amplitudes a_3 and a_4. There is a steep barrier in the upper part of Fig. 1, from which q^* drops down to a flat plateau being quite close to the level $q^* = 1$ which represents the experimental value:

- A detailed analysis of the four-amplitude case clearly demonstrates the asymptotic flat plateau behaviour at large amplitudes a_3 and a_4. The self-consistent minimum values of q^* obtained along the perimeter of the plateau have been found to vary from $q^* = 0.969$ for $f_\Gamma = 1.81$ to $q^* = 1.03$ for $f_\Gamma = 1.69$. Consequently, the plateau is found to be slightly "warped", being partly below and partly above the level $q^* = 1$;
- For an increasing number of amplitudes beyond four there is a similar plateau behaviour, with only a slight increase in the level. This is not in conflict with the principle of the variational analysis. Any function q^* can thus have minima in the hyperspace of amplitudes at points where some of these amplitudes vanishes;
- The preserved plateau behaviour at an increasing number of amplitudes can be understood from the fact that the ratio A_q^2/A_s in equation (58) becomes a slow function of the higher "multipole" terms of the expansion (38);
- With these plateau solutions the normalized charge q^* is still left with some additional degrees of freedom. These are eliminated by the analysis of the force balance in the following subsection. There it will be shown that the lowest value of q^* obtained from the variational analysis solely does not become reconcilable with the radial force balance.

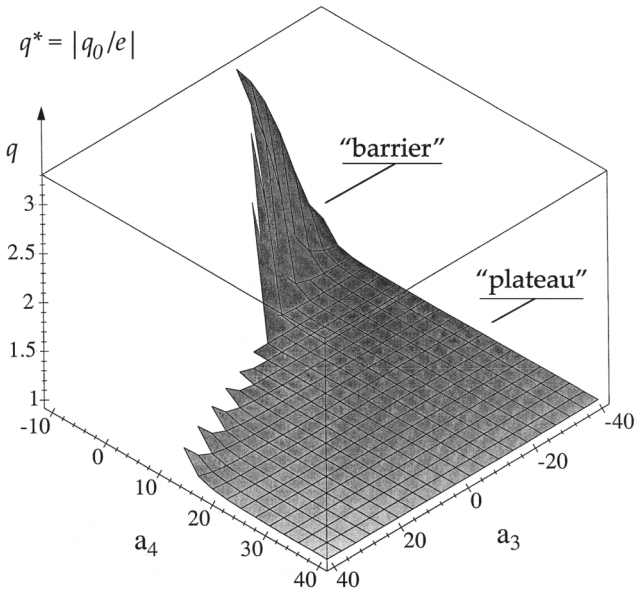

Fig. 1: The normalized electron charge $q^* \equiv |q_0/e|$ as a function of the two amplitudes a_3 and a_4 in the four amplitude case.

4.5 The radial force balance

The fundamental description of a charged particle in conventional theory is deficient also in respect to its radial force balance. Thus, an equilibrium cannot be maintained by the classical electrostatic force $\bar{\rho}\,\mathbf{E}$ in equation (5) only, but

is then assumed to require forces of a nonelectromagnetic character to be present as described by Jackson [4]. In other words, the electron would otherwise "explode" under the action of its self-charge.

Turning to the present revised theory, however, there is an additional magnetic term $\bar{\rho}\,\mathbf{C}\times\mathbf{B}$ in equation (5) which under certain conditions provides the radial force balance of an equilibrium. With the already obtained results based on equations (10)–(15), the integrated radial force of the right-hand member in equation (5) becomes

$$F_r = -2\pi\varepsilon_0 G_0^2 \iint \left[DG + D\left(s^2 DG\right)\right] \cdot \cdot \left[\frac{\partial G}{\partial \rho} - \frac{1}{\rho}\, s^2 DG\right] \rho^2 s\, d\rho\, d\theta\,, \qquad (61)$$

where $s \equiv \sin\theta$. For the point-charge-like model of Sections 4.1–4.4 this force is represented by the form

$$F_r = I_+ - I_-\,, \qquad (62)$$

where I_+ and I_- are the positive and negative contributions to F_r. The results are as follows [10]:

- The ratio I_+/I_- in the plateau region of the four-amplitude case decreases from 1.27 at $q^* = 0.98$ to 0.37 at $q^* = 1.01$, thereby passing a sharply defined equilibrium point $I_+/I_- = 1$ at $q^* \cong 0.988$. The remaining degrees of freedom of this case have then been used up;
- With more than four amplitudes slightly higher values of q^* have been obtained in a corresponding plateau region. Even when there exists a force balance at higher values of q^* than that of the four-amplitude solution, the latter still corresponds to the lowest q^* for an integrated radial force balance;
- The obtained small deviation of $q^* \cong 0.988$ from the experimental value $q^* = 1$ is a remaining problem. One possible explanation could be provided by a small quantum mechanical correction of the magnetic flux condition (60), in analogy with the correction δ_M of the magnetic moment condition (59). Another possibility to be further examined is simply due to some uncertainty in the numerical calculations of a rather complex system of relations, being subject to iterations in several consecutive steps;
- The present analysis of the integrated (total) forces, performed instead of a treatment of their local parts, is in full analogy with the earlier deductions of the integrated charge, magnetic moment, mass, and angular momentum.

With the obtained radial force balance, we finally return to the radial constant c_0 of equation (39). As shown earlier [7], the mass and magnetic moment become $m_0 = K_m/c_0$ and $M_0 = K_M c_0$ where K_m and K_M include the normalized integrals A_m, A_M, and A_s. Introducing the relation $h\nu = m_0 c^2$ by Planck and Einstein and the related Compton wavelength $\lambda_C = c/\nu = h/m_0 c$ combination with $m_0 = K_m/c_0$ then yields $6\pi c_0/\lambda_C = A_m/A_s$. In the radial force balance $A_m/A_s = 1.07$. Choosing the three-fold circumference based on the radius c_0 to be equal to the Compton wavelength then results in masses of the electron, muon, and tauon which deviate by only seven percent from the experimental values. This three-fold circumference requires further investigation.

5 A model of the neutrino

The electrically neutral steady states described in Section 3.1 will now be used as a basis for models of the neutrino. Since the analysis is restricted to a steady particle-shaped configuration, it includes the concept of a nonzero rest mass. This is supported by the observed neutrino oscillations. The present neutrino models are described in detail elsewhere [7, 12, 15], and will only be outlined in this section.

5.1 A convergent generating function

A separable generating function is now adopted, having a convergent radial part R and a polar part T of top-bottom symmetry, as given by

$$R = \rho^\gamma e^{-\rho}\,, \qquad T = \sin^\alpha\theta\,, \qquad (63)$$

where $\gamma \gg \alpha \gg 1$. At increasing values of ρ the part R first reaches a maximum at $\rho = \hat{\rho} = \hat{r}/r_0 = \gamma$, after which it drops steeply to zero at large ρ. Therefore $\hat{r} = \gamma r_0$ can be taken as an effective radius of the configuration. Inserting the forms (63) into equations (24)–(32) and the integrated expressions (20)–(22) for the total mass and angular momentum, we obtain the ratio

$$J_m/J_s = 15/38\,\gamma\,. \qquad (64)$$

Combination of equations (20), (21), (64), and the quantum condition (33) then yields the mass-radius relation

$$m_0\hat{r} = m_0\gamma r_0 = 15h/152\pi c \cong 7{\times}10^{-44}\ [\mathrm{kg}{\times}\mathrm{m}]\,. \qquad (65)$$

For a case with top-bottom antisymmetry of T there is little difference as compared to the result obtained here.

5.2 A divergent generating function

We now turn to a generating function having a divergent radial part of the same form (37) as that for the electron model, and with a polar part of top-bottom antisymmetry. When $\rho = r/r_0$ increases from $\rho = 0$, the radial part decreases from a high level, down to $R = 1/e$ at $\rho = 1$, and further to very small values. Thus $\hat{r} = r_0$ can here be taken as an effective radius of the configuration.

The analysis of the radial integrals is analogous to that of the electron model. To obtain nonzero and finite values of mass m_0 and angular momentum s_0, a shrinking effective radius $\hat{r}$ and a shrinking amplitude factor G_0 are introduced through the relations

$$\hat{r} = r_0 = c_r \cdot \varepsilon\,, \qquad G_0 = c_G \cdot \varepsilon^{\beta}, \tag{66}$$

where c_r, c_G, and β are positive constants and $0 < \varepsilon \ll 1$. Expressions (20) and (21) then take the forms

$$m_0 = \pi(\varepsilon_0/c^2) c_r c_G^2 (2\gamma-1)^{-1} J_{m\theta}\left[\varepsilon^{1+2\beta}/\rho_m^{2\gamma-1}\right], \tag{67}$$

$$s_0 = \pi(\varepsilon_0 C/c^2) c_r^2 c_G^2 [2\,(\gamma-1)]^{-1} J_{s\theta}\left[\varepsilon^{2(1+\beta)}/\rho_s^{2(\gamma-1)}\right], \tag{68}$$

where the lower limits ρ_m and ρ_s of the integrals (22) have been introduced. For nonzero and finite values of m_0 and s_0 it is then required that

$$\rho_m = \varepsilon^{(1+2\beta)/(2\gamma-1)}\,, \qquad \rho_s = \varepsilon^{(1+\beta)/(\gamma-1)}\,. \tag{69}$$

With the quantum condition (33) relations (66)–(69) further combine to

$$m_0 \hat{r} = \frac{h}{2\pi c}\,\frac{\gamma-1}{2\gamma-1}\,(J_{m\theta}/J_{s\theta})\,\varepsilon\,. \tag{70}$$

The ratio $J_{m\theta}/J_{s\theta}$ is here expected to become a slow function of the profile shapes of $T(\theta)$ and $I_{m\theta}$, as obtained for a number of test functions for $I_{m\theta}$. An additional specific example with $\gamma = 3$ and $\beta = 3/2$ yields $\rho_m = \varepsilon^{4/5}$ and $\rho_s = \varepsilon^{5/4}$ making ρ_m and ρ_s almost linear functions of ε. In a first crude approximation relation (70) can therefore be written as

$$m_0 \hat{r} \cong 2{\times}10^{-43}\,\varepsilon\ [\mathrm{kg{\times}m}]\,. \tag{71}$$

5.3 Neutrino penetration into solid matter

The mass m_0 has to be reconcilable with observed data. The upper bounds of the neutrino mass are about 4.7 eV for the electron-neutrino, 170 keV for the muon-neutrino, and 18 MeV for the tauon-neutrino. Neutrinos can travel as easily through the Earth as a bullet through a bank of fog. They pass through solid matter consisting of nucleons, each having a radius $r_N \cong 6{\times}10^{-15}$ meters. Concerning the present neutrino models, there are the following options:

- With the result (65) the ratio $\hat{r}/r_N$ becomes about 10^6, 40, and 0.4 for the electron-neutrino, muon-neutrino, and the tauon-neutrino. The interaction with the electron-neutrino is then expected to take place between the short-range nucleon field as a whole and a very small part of the neutrino field. The latter field could then "heal" itself in terms of a restoring tunneling effect. Then the electron-neutrino would represent the "fog" and the nucleon the "bullet". The mean free paths of the muon- and tauon-neutrinos would on the other hand become short for this option;
- With the result (71) the corresponding values of $\hat{r}/r_N$ become about $4{\times}10^6\,\varepsilon$, $100\,\varepsilon$, and ε, respectively. Here sufficiently small values of ε would make the neutrino play the role of the "bullet" and the nucleon that of the "fog".

6 Conclusions

The present steady electromagnetic equilibria, and their applications to leptons, have no counterparts in conventional theory. The electron model, and that of the muon, tauon and corresponding antiparticles, embrace new aspects and explanations of a number of so far unsolved problems:

- To possess a nonzero electric net charge, the characteristic radius of the particle-shaped states has to shrink to that of a point-charge-like geometry. This agrees with experimental observation;
- Despite the success of the conventional renormalization procedure, physically more satisfactory ways are needed in respect to the infinite self-energy problem of a point-charge, and to the extra added counter terms by which a finite result is obtained from the difference of two "infinities". Such a situation is avoided through the present theory where the "infinity" (divergence) of the generating function is outbalanced by the "zero" of a shrinking characteristic radius;
- In the present approach the Lorentz invariance of the electron radius is formally satisfied at the limit $r_0 \to 0$. At the same time the theory includes a parameter range of small but nonzero radii being reconcilable with an internal structure;
- In contrast to conventional theory, an integrated radial force balance can be provided by the present space-charge current density which prevents the electron from "exploding" under the action of its electric self-charge. Possibly a corresponding situation may arise for the bound quarks in the interior of baryons. Here the strong force provides an equilibrium for their mutual interactions, but this does not fully explain how the individual quarks are kept in equilibrium in respect to their self-charges;
- The variational analysis results in a parameter range of the normalized charge q^* which is close to the experimental value $q^* = 1$. Within this range the remaining degrees of freedom in the analysis become exhausted when imposing the additional condition of an integrated radial force balance. This results in $q^* \cong 0.99$ which deviates by only one percent from the experimental value. The reason for the deviation is not clear at the present stage, but it should on the other hand be small enough to be regarded as an experimental support of the theory. It can also be taken as an indirect confirmation of a correctly applied value

of the Landé factor, because a change of the latter by a factor of two would result in entirely different results. Provided that the value $q^* = 1$ can be obtained after relevant correction, the elementary charge would no longer remain as an independent constant of nature, but is then derived from the velocity of light, Planck's constant, and the permittivity of the vacuum.

The steady states having a vanishing net charge also form possible models for a least some of the basic properties of the neutrino:

- A small but nonzero rest mass is in conformity with the analysis;
- The steady state includes an angular momentum, but no magnetic moment;
- Long mean free paths are predicted in solid matter, but their detailed comparison with observed data is so far an open question.

References

1. Schiff L. I. Quantum Mechanics. McGraw-Hill Book Comp. Inc., New York, 1949, Ch XIV.
2. Feynman R. P. Lectures in physics: mainly electromagnetism and matter. Addison-Wesley, Reading, Massachusetts, 1964, p. 28–1.
3. Ryder L. H. Quantum field theory. Second edition. Cambridge Univ. Press, 1996, Ch. 9.3.
4. Jackson J. D. Classical Electrodynamics. John Wiley and Sons, Inc., New York–London–Sydney, 1962, Ch. 17.4.
5. Lehnert B. An extended formulation of Maxwell's equations. *Spec. Sci. Technol.*, 1986, v. 9, 177–184.
6. Lehnert B. Basic concepts of an extended electromagnetic theory. *Spec. Sci. Technol.*, 1994, v. 17, 259–273.
7. Lehnert B., Roy S. Extended electromagnetic theory. World Scientific Publishers, Singapore, 1998.
8. Lehnert B. Optical effects of an extended electromagnetic theory. In: *Advances in Chemical Physics*, v. 119. Edited by M. W.Evans, I. Prigogine, and S. A. Rice, John Wiley and Sons, Inc., New York, 2001, 1–77.
9. Lehnert B., Scheffel J. On the minimum elementary charge of an extended electromagnetic theory. *Physica Scripta*, 2002, v. 65, 200–207.
10. Lehnert B. The electron as a steady-state confinement system. *Physica Scripta*, 2004, v. T113, 41–44.
11. Lehnert B. Photon physics of revised electromagnetics. *Progress in Physics*, 2006, v. 2, 78–85.
12. Lehnert B. Revised electromagnetics with fundamental applications. Report TRITA-ALF-2004-02, Fusion Plasma Physics, Alfvén Laboratory, Royal Institute of Technology, Stockholm, 2004, 1–126.
13. Heitler W. The quantum theory of radiation. Third edition. Clarendon Press, Oxford, 1954, Appendix, p. 409
14. Feynman R. P. QED: The strange theory of light and matter, Penguin, London, 1990.
15. Lehnert B. Neutral particle states of an extended electromagnetic theory. In: *Dirac equation, neutrinos and beyond*, Edited by V. V. Dvoeglazov. *Ukrainian Journal: Electromagnetic Phenomena*, 2003, T. 3, v. 9, 49–55.

Positive, Neutral and Negative Mass-Charges in General Relativity

Larissa Borissova and Florentin Smarandache
Department of Mathematics, University of New Mexico, Gallup, NM 87301, USA
E-mail: lborissova@yahoo.com; fsmarandache@yahoo.com

As shown, any four-dimensional proper vector has two observable projections onto time line, attributed to our world and the mirror world (for a mass-bearing particle, the projections posses are attributed to positive and negative mass-charges). As predicted, there should be a class of neutrally mass-charged particles that inhabit neither our world nor the mirror world. Inside the space-time area (membrane) the space rotates at the light speed, and all particles move at as well the light speed. So, the predicted particles of the neutrally mass-charged class should seem as light-like vortices.

1 Problem statement

As known, neutrosophy is a new branch of philosophy which extends the current dialectics by the inclusion of neutralities. According to neutrosophy [1, 2, 3], any two opposite entities <A> and <Anti-A> exist together with a whole class of neutralities <Neut-A>.

Neutrosophy was created by Florentin Smarandache and then applied to mathematics, statistics, logic, linguistic, and other branches of science. As for geometry, the neutrosophic method expanded the Euclidean set of axioms by denying one or more of them in at least two distinct ways, or, alternatively, by accepting one or more axioms true and false in the same space. As a result, it was developed a class of Smarandache geometries [4], that includes Euclidean, Riemann, and Lobachevski-Gauss-Bolyai geometries as partial cases.

In nuclear physics the neutrosophic method theoretically predicted "unmatter", built on particles and anti-particles, that was recently observed in CERN and Brookhaven experiments (see [5, 6] and References there). In General Relativity, the method permits the introduction of entangled states of particles, teleportation of particles, and also virtual particles [7], altogether known before in solely quantum physics. Aside for these, the method permits to expand the basic space-time of General Relativity (the four-dimensional pseudo-Riemannian space) by a family of spaces where one or more space signature conditions is permitted to be both true and false [8].

In this research we consider another problem: mass-charges of particles. Rest-mass is a primordial property of particles. Its numerical value remains unchanged. On the contrary, relativistic mass has "charges" dependent from relative velocity of particles. Relativistic mass displays itself in only particles having interaction. Therefore theory considers relativistic mass as mass-charge.

Experimental physics knows two kinds of regular particles. Regular mass-bearing particles possessing non-zero rest-masses and relativistic masses (masses-in-motion). Massless light-like particles (photons) possess zero rest-masses, while their relativistic masses are non-zeroes. Particles of other classes (as virtual photons, for instance) can be considered as changed states of mass-bearing or massless particles.

Therefore, following neutrosophy, we do claim:

Aside for observed positively mass-charged (i. e. mass-bearing) particles and neutrally mass-charged (light-like) particles, there should be a third class of "negatively" mass-charged particles unknown in today's experimental physics.

We aim to establish such a class of particles by the methods of General Relativity.

2 Two entangled states of a mass-charge

As known, each particle located in General Relativity's space-time is characterized by its own four-dimensional impulse vector. For instance, for a mass-bearing particle the proper impulse vector P^α is

$$P^\alpha = m_0 \frac{dx^\alpha}{ds}\,, \quad P_\alpha P^\alpha = 1\,, \quad \alpha = 0,1,2,3\,, \qquad (1)$$

where m_0 is the rest-mass of this particle. Any vector or tensor quantity can be projected onto an observer's time line and spatial section. Namely the projections are physically observable quantities for the observer [9]. As recently shown [10, 11], the four-dimensional impulse vector (1) has two projections onto the time line*

$$\frac{P_0}{\sqrt{g_{00}}} = \pm m\,, \qquad \text{where } \; m = \frac{m_0}{\sqrt{1-\mathrm{v}^2/c^2}}\,, \qquad (2)$$

and solely the projection onto the spatial section

$$P^i = \frac{m}{c}\,\mathrm{v}^i = \frac{1}{c}\,p^i, \quad \text{where } \; \mathrm{v}^i = \frac{dx^i}{d\tau}\,, \;\; i = 1,2,3\,, \quad (3)$$

where p_i is the three-dimensional observable impulse. Therefore, we conclude:

*Where $d\tau = \sqrt{g_{00}}dt + \frac{g_{0i}}{c\sqrt{g_{00}}}dx^i$ is the properly observed time interval [9, 12].

> Any mass-bearing particle, having two time projections, exists in two observable states, entangled to each other: the positively mass-charged state is observed in our world, while the negatively mass-charged state is observed in the mirror world.

The mirror world is almost the same that ours with the following differences:

1. The particles bear negative mass-charges and energies;
2. "Left" and "right" have meanings opposite to ours;
3. Time flows oppositely to that in our world.

From the viewpoint of an observer located in the mirror world, our world will seem the same that his world for us.

Because both states are attributed to the same particle, and entangled, both our world and the mirror world are two entangled states of the same world-object.

To understand why the states remain entangled and cannot be joined into one, we consider the third difference between them — the time flow.

Terms "direct" and "opposite" time flows have a solid mathematical ground in General Relativity. They are connected to the sign of the derivative of the coordinate time interval by the proper time interval . The derivative arrives from the purely geometrical law that the square of a unit four-dimensional vector remains unchanged in a four-dimensional space. For instance, the four-dimensional velocity vector

$$U^\alpha U_\alpha = g_{\alpha\beta}\, U^\alpha U^\beta = 1\,, \qquad U^\alpha = \frac{dx^\alpha}{ds}\,. \tag{4}$$

Proceeding from by-component notation of this formula, and using $\mathrm{w} = c^2(1-\sqrt{g_{00}})$ and $v_i = -c\frac{g_{0i}}{\sqrt{g_{00}}}$, we arrive to a square equation

$$\left(\frac{dt}{d\tau}\right)^2 - \frac{2v_i\mathrm{v}^i}{c^2\left(1-\frac{\mathrm{w}}{c^2}\right)}\frac{dt}{d\tau} + \\ + \frac{1}{\left(1-\frac{\mathrm{w}}{c^2}\right)^2}\left(\frac{1}{c^4}\,v_iv_k\mathrm{v}^i\mathrm{v}^k - 1\right) = 0\,, \tag{5}$$

which solves with two roots

$$\left(\frac{dt}{d\tau}\right)_{1,2} = \frac{1}{1-\frac{\mathrm{w}}{c^2}}\left(\frac{1}{c^2}\,v_i\mathrm{v}^i \pm 1\right). \tag{6}$$

Observer's proper time lows anyhow directly $d\tau > 0$, because this is a relative effect connected to the his viewpoint at clocks. Coordinate time t flows independently from his views. Accordingly, the direct flow of time is characterized by the time function $dt/d\tau > 0$, while the opposite flow of time is $dt/d\tau < 0$.

If $dt/d\tau = 0$ happens, the time flow stops. This is a boundary state between two entangled states of a mass-charged particle, one of which is located in our world (the positively directed time flow $dt/d\tau > 0$), while another — in the mirror world (where the time flow is negatively directed $dt/d\tau < 0$).

From purely geometric standpoints, the state $dt/d\tau = 0$ describes a space-time area, which, having special properties, is the boundary space-time membrane between our world and the mirror world (or the mirror membrane, in other word). Substituting $dt/d\tau = 0$ into the main formula of the space-time interval $ds^2 = g_{\alpha\beta}\, dx^\alpha dx^\beta$

$$ds^2 = c^2dt^2 + 2g_{0i}cdtdx^i + g_{ik}\, dx^i dx^k, \tag{7}$$

we obtain the metric of the space within the area

$$ds^2 = g_{ik}\, dx^i dx^k. \tag{8}$$

So, the mirror membrane between our world and the mirror world has a purely spatial metric which is also stationary.

As Kotton showed [13], any three-dimensional Riemannian space permits a holonomic orthogonal reference frame, in respect to which the three-dimensional metric can be reduced to the sum of Pythagorean squares. Because our initially four-dimensional metric ds^2 is sign-alternating with the signature $(+---)$, the three-dimensional metric of the mirror membrane between our world and the mirror world is negatively defined and has the form

$$ds^2 = -H_1^2(dx^1)^2 - H_2^2(dx^2)^2 - H_3^2(dx^3)^2, \tag{9}$$

where $H_i\,(x^1, x^2, x^3)$ are Lamé coefficients (see for Lamé coefficients and the tetrad formalism in [14]). Determination of this metric is connected to the proper time of observer, because we mean therein.

Substituting $dt = 0$ into the time function (6), we obtain the physical conditions inside the area (mirror membrane)

$$v_i\, dx^i = \pm c^2 d\tau\,. \tag{10}$$

Owning the definition of the observer's proper time

$$d\tau = \sqrt{g_{00}}\, dt + \frac{g_{0i}\, dx^i}{\sqrt{g_{00}}} = \left(1-\frac{\mathrm{w}}{c^2}\right)dt - \frac{1}{c^2}\, v_i dx^i, \tag{11}$$

and using $dx^i = v^i d\tau$ therein, we obtain: the observer's proper state $d\tau > 0$ can be satisfied commonly with the state $dt = 0$ inside the membrane only if there is*

$$v_i\mathrm{v}^i = -c^2 \tag{12}$$

thus we conclude:

> The space inside the mirror membrane between our world and the mirror world seems as the rotating at the light speed, while all particles located there move at as well the light speed. So, particles that inhabit the space inside the membrane seem as light-like vortices.

*Here is a vector product of two vectors v_i and v^i, dependent on the cosine between them (which can be both positive and negative). Therefore the modules may not be necessarily imaginary quantities.

Class of mass-charge	Particles	Energies	Class of motion	Area
Positive mass-charges, $m > 0$	mass-bearing particles	$E > 0$	move at sub-light speeds	our world
Neutral mass-charges, $m = 0$	massless (light-like) particles	$E > 0$	move at the light speed	our world
	light-like vortices	$E = 0$	move at the light speed within the area, rotating at the light speed	the membrane
	massless (light-like) particles	$E < 0$	move at the light speed	the mirror world
Negative mass-charges, $m < 0$	mass-bearing particles	$E < 0$	move at sub-light speeds	the mirror world

This membrane area is the "barrier", which prohibits the annihilation between positively mass-charged particles and negatively mass-charged particles — the barrier between our world and the mirror world. In order to find its mirror twin, a particle should be put in an area rotating at the light speed, and accelerated to the light speed as well. Then the particle penetrates into the space inside the membrane, where annihilates with its mirror twin.

As a matter of fact, no mass-bearing particle moved at the light speed: this is the priority of massless (light-like) particles only. Therefore:

> Particles that inhabit the space inside the membrane seem as light-like vortices.

Their relativistic masses are zeroes $m = 0$ as those of massless light-like particles moving at the light speed. However, in contrast to light-like particles whose energies are non-zeroes, the particles inside the membrane possess zero energies $E = 0$ because the space metric inside the membrane (8) has no time term.

The connexion between our world and the mirror world can be reached by matter only filled in the light-like vortical state.

3 Two entangled states of a light-like matter

As known, each massless (light-like) particle located in General Relativity's space-time is characterized by its own four-dimensional wave vector

$$K^\alpha = \frac{\omega}{c}\frac{dx^\alpha}{d\sigma}\,, \qquad K_\alpha K^\alpha = 0\,, \tag{13}$$

where ω is the proper frequency of this particle linked to its energy $E = \hbar\omega$, and $d\sigma = \left(-g_{ik} + \frac{g_{0i}g_{0k}}{g_{00}}\right)dx^i dx^k$ is the measured spatial interval. (Because massless particles move along isotropic trajectories, the trajectories of light, one has $ds^2 = 0$, however the measured spatial interval and the proper interval time are not zeroes.)

As recently shown [10, 11], the four-dimensional wave vector has as well two projections onto the time line

$$\frac{K_0}{\sqrt{g_{00}}} = \pm\omega\,, \tag{14}$$

and solely the projection onto the spatial section

$$K^i = \frac{\omega}{c}c^i = \frac{1}{c}p^i, \quad \text{where } c^i = \frac{dx^i}{d\tau}\,, \tag{15}$$

while c^i is the three-dimensional observable vector of the light velocity (its square is the world-invariant c^2, while the vector's components c^i can possess different values). Therefore, we conclude:

> Any massless (light-like) particle, having two time projections, exists in two observable states, entangled to each other: the positively energy-charged state is observed in our world, while the negatively energy-charged state is observed in the mirror world.

Because along massless particles' trajectories $ds^2 = 0$, the mirror membrane between the positively energy-charged massless states and their entangled mirror twins is characterized by the metric

$$ds^2 = g_{ik}\,dx^i dx^k = 0\,, \tag{16}$$

or, expressed with Lamé coefficients $H_i\,(x^1, x^2, x^3)$,

$$ds^2 = -H_1^2(dx^1)^2 - H_2^2(dx^2)^2 - H_3^2(dx^3)^2 = 0\,. \tag{17}$$

As seen, this is a particular case, just considered, the membrane between the positively mass-charged and negatively mass-charge states.

4 Neutrosophic picture of General Relativity's world

As a result we arrive to the whole picture of the world provided by the purely mathematical methods of General Relativity, as shown in Table.

It should be noted that matter inside the membrane is not the same as the so-called zero-particles that inhabit fully degenerated space-time areas (see [15] and [8]), despite the fact they posses zero relativistic masses and energies too. Fully degenerate areas are characterized by the state $w + v_i u^i = c^2$ as well as particles that inhabit them*. At first, inside the membrane the space is regular, non-degenerate. Second. Even in the absence of gravitational fields, the zero-space state becomes $v_i u^i = c^2$ that cannot be trivially reduced to $v_i u^i = -c^2$ as inside the membrane.

*Here $u^i = dx^i/dt$ is so-called the coordinate velocity.

Particles inside the membrane between our world and the mirror world are filled into a special state of light-like vortices, unknown before.

This is one more illustration to that, between the opposite states of positively mass-charge and negatively mass-charge, there are many neutral states characterized by "neutral" mass-charge. Probably, further studying light-like vortices, we'd find more classes of neutrally mass-charged states (even, probably, an infinite number of classes).

References

1. Smarandache F. Neutrosophy/neutrosophic probability, set, and logic. American Research Press, Rehoboth, 1998.
2. Smarandache F. A unifying field in logic: neutrosophic logic. Neutrosophy, neutrosophic set, neutrosophic probability. 3rd ed., American Research Press, Rehoboth, 2003.
3. Smarandache F. and Liu F. Neutrosophic dialogues. Xiquan Publishing House, Phoenix, 2004.
4. Iseri H. Smarandache manifolds. American Research Press, Rehoboth, 2002.
5. Smarandache F. A new form of matter — unmatter, composed of particles and anti-particles. *Progress in Physics*, 2005, v. 1, 9–11.
6. Smarandache F. and Rabounski D. Unmatter entities inside nuclei, predicred by the Brightsen Nucleon Cluster Model. *Progress in Physics*, 2006, v. 1, 14–18.
7. Rabounki D., Borissova L., Smarandache F. Entangled particles and quantum causality threshold in the General Theory of Relativity. *Progress in Physics*, 2005, v. 2, 101–107.
8. Rabounki D., Smarandache F., Borissova L. Neutrosophic methods in General Relativity. Hexis, Phoenix (Arizona), 2005.
9. Zelmanov A. L. Chronometric invariants and co-moving coordinates in the general relativity theory. *Doklady Acad. Nauk USSR*, 1956, v. 107(6), 815–818.
10. Borissova L. and Rabounski D. Fields, vacuum, and the mirror Universe. Editorial URSS, Moscow, 2001, 272 pages (2nd rev. ed.: CERN, EXT-2003-025).
11. Rabounski D. D. and Borissova L. B. Particles here and beyond the Mirror. Editorial URSS, Moscow, 2001, 84 pages.
12. Landau L. D. and Lifshitz E. M. The classical theory of fields. GITTL, Moscow, 1939 (ref. with the 4th final exp. edition, Butterworth-Heinemann, 1980).
13. Kotton E. Sur les variétés a trois dimensions. *Ann. Fac. Sci. Toulouse* (2), v. 1, Thése, Paris, 1899.
14. Petrov A. Z. Einstein spaces. Pergamon, Oxford, 1969.
15. Borissova L. and Rabounski D. On the possibility of instant displacements in the space-time of General Relativity. *Progress in Physics*, 2005, v. 1, 17–19; Also in: *Physical Interpretation of Relativity Theory* (PIRT-2005), Proc. of the Intern. Meeting., Moscow, 2005, 234–239; Also in: *Today's Take on Einstein's Relativity*, Proc. of the Confer., Tucson (Arizona), 2005, 29–35.

Much Ado about Nil: Reflection from Moving Mirrors and the Interferometry Experiments

Christo I. Christov

Dept. of Mathematics, University of Louisiana at Lafayette, Lafayette, LA 70504, USA

E-mail: christov@louisiana.edu

The emitter and receiver Doppler effects are re-examined from the point of view of boundary condition on a moving boundary. Formulas are derived for the frequencies of the waves excited on receiver's and emitter's surfaces by the waves traveling thorough the medium. It is shown that if the emitting source and the reflection mirror are moving with the same speed in the same direction relative to a medium at rest, there is no observable Doppler effect. Hence, the nil effect of Michelson and Morley experiment (MME) is the only possible outcome and cannot be construed as an indication about the existence or nonexistence of an absolute continuum. The theory of a new experiment that can give conclusive information is outlined and the possible experimental set-up is sketched.

5 Introduction

Since the groundlaying work of Fizeau, interferometry has been one of the most often used methods to investigate the properties of light. The idea of interferometry was also applied to detecting the presence of an absolute medium in the Michelson and Morley experiment (MME) [1]. The expected effect was of second order $O(v^2/c^2)$ with respect to the ratio between the Earth speed v and speed of light c and it is generally accepted now that Michelson-Morley experiment yielded a nil result, in the sense that the fringes that were observed corresponded to a much smaller (assumed to be negligible) speed than actual Earth's speed. Around the end of Nineteen Century, the nil result of MME prompted Fitz-Gerald and Lorentz to surmise that the lengths are contracted in the direction of motion by the Lorentz factor $\sqrt{1 - v^2/c^2}$ that cancels exactly the expected effect. Since then the Lorentz contraction has been many times verified and can be considered now as an established fact. The Lorentz contraction does not need MME anymore in order to survive as the main vehicle of the modern physics of processes at high speeds.

On another note, the nil effect of MME was eventually interpreted as an indication that there exists no absolute (resting) medium where the light propagates. The problem with this conclusion is that nobody *actually* proposed a theory for MME in which a continuous medium was considered with the correct boundary conditions. Rather, the emission theory of light was used whose predictions contradicted the experimental evidence. In the present paper we show that if a medium at rest is assumed and if this medium is not entrained by the moving bodies, the exact effect from MME is nil, i. e., the expected second-order effect was an artifact from the fact that the emission theory of light (essentially corpuscular in its nature) was applied to model the propagation of light in a continuous medium.

The best way to judge about the existence of the absolute medium is to stage first-order experiments (one way experiments). Along these lines are organized many experimental works, most notably [2, 3] where the sought effect was the anisotropy of speed of light. In our opinion, it is not quite clear how one can discriminate between an anisotropic speed of light on one hand and a first-order Doppler effect, on the other. Yet, we believe that the solution of the conundrum about the existence or nonexistence of an absolute continuum will be solved by a first-order experiment. To this end we also propose an interference experiment that should be able to measure the first-order effect. The most important thing is that first-order effect has actually been observed (see [2, 3], among others). This being said, one should be aware that the "second-order" re-interpretations of the slightly nontrivial results of [4] are also a valid avenue of research in the quest for detecting the absolute medium (or as the modern euphemism goes "the preferred frame"). In this connection, an important contribution seems to be [5]. Another source of higher-order effects can also be the local dependence of speed of light on the strength of the gravitational field. This kind of dependence is very important in any experiment conducted on Earth and in order to figure out the more subtle effects, one should use a theory in which the fundamental tensor of space affects the propagation of light. In the framework of the present approach it will result into a wave equation for the light which has non-constant coefficients, the latter depending on the curvature tensor. It goes beyond the scope of the present short note to delve into this more complicated case.

The aim of the present paper is to be understood in a very limited fashion: we show that the main effect of MME must be zero when it is considered in a purely Euclidean space without gravitational effects on the propagation of light. We

pose correctly the problem of propagation and reflection of waves in a resting medium when both the source and the mirror are moving with respect to the medium. We show that the strict result from the interference is nil which invalidates most of the conclusions drawn from the perceived nil effect of MME.

6 Conditions on moving boundaries

Here we follow [6] (see also [7] for application to MME) where emitter's Doppler effect was explained with boundary conditions (b. c.) on a moving boundary. Consider the $(1+1)\,D$ linear wave equation

$$\phi_{tt} = c^2 \phi_{xx}\,, \tag{1}$$

whose solution is the harmonic wave.

$$\phi\,(x,t) = e^{i\hat{k}x \pm i\hat{\omega}t}, \quad \text{where} \quad \hat{k} = \frac{\hat{\omega}}{c}\,, \tag{2}$$

where c is the characteristic speed and "$\pm$" signs refer to the left- and right-going waves, respectively.

Consider now a boundary (a point in 1D) moving with velocity u, at which a wave with temporal frequency ω is created. This means that the wave propagating inside the medium satisfies the following boundary condition

$$\begin{aligned}\phi\,(ut,t) = e^{i(\omega_1 t - k_1 x)} = e^{i\omega_1 (t - x/c)} = \\ = e^{i\omega_1 t(1-u/c)} = e^{i\omega t},\end{aligned} \tag{3}$$

where it is tacitly assumed that the right going wave is of interest. The above b. c. gives that

$$\omega_1 \left(1 - \frac{u}{c}\right) = \omega, \quad \rightarrow \quad \omega_1 = \frac{\omega}{1 - u/c}\,. \tag{4}$$

The last formula is the well known emitter's Doppler effect which shows how the frequency of the propagating wave is related to the frequency of the moving emitter

If the receiver is at rest, it will measure a frequency ω_1. The situation is completely different if the receiver is also moving, say with velocity v in the positive x-direction (to the right). Then due to the b. c. $\phi\,(vt,t) = e^{i\omega_1 t - i\frac{\omega_1}{c} vt} = e^{i\omega_2 t}$, the traveling wave of frequency ω_1 and wave number $k_1 = \frac{\omega_1}{c}$ will generate an oscillation of frequency ω_2 at the moving boundary point $x = vt$:

$$\omega_2 = \omega_1 \left(1 - \frac{v}{c}\right) = \omega\, \frac{1 - v/c}{1 - u/c}\,, \tag{5}$$

i. e., the measuring instruments in the moving frame of the receiver will detect a standing wave of frequency ω_2. We observe here that if the receiver is moving exactly with the speed of the emitter, then the frequency measured in receiver's frame will be exactly equal to emitter's frequency. In other words, a receiver that is moving with the same speed as the emitter does not observe a Doppler effect and cannot discover the motion.

This conclusion appears in an implicit form in the standard texts, e. g. [8, 9, p.164], where it is claimed that a Doppler effect is observed only for relative motion of the emitter and the receiver. Unfortunately, this correct observation did not lead to posing the question about the relevance of MME despite of the conspicuous lack of *relative motion* between the emitter and the receiver (mirror) in MME. The explanation in [8] was that "[F]or electromagnetic waves there evidently exists *no preferred frame*". We believe that the rigorous statement is that absolute rest (the "preferred frame") *cannot be detected* from measurements of Doppler effect between a source and a receiver which are moving together with identical speed through the absolute continuum.

After a consensus has been reached between the present work and the literature that the luminiferous continuum cannot be detected from an experiment in which a single source and a receiver are moving together as a non-deformable system, then the interesting question which remains is whether the absolute continuum can be detected when the emitter and the mirror are in relative motion, i. e. when they move with different speeds relative to the resting frame. To this end, consider now the situation when the receiver is a mirror which sends back a left going wave $e^{i\omega_3 t + ik_3 x}$ generated by the oscillations with frequency ω_2 at the point $x = vt$ namely, $e^{i\omega_3 t + ik_3 vt} = e^{i\omega_2 t}$. Then

$$\omega_3\,(1 + v/c) = \omega_2, \;\; \Rightarrow \;\; \omega_3 = \omega\, \frac{1 - v/c}{(1 + v/c)(1 - u/c)}\,. \tag{6}$$

Now, the wave of frequency ω_3 is traveling through the continuum to the left. The frequency, ω_4, of the wave excited on the *moving* surface of the emitter by this traveling wave has to satisfy the moving b. c. $e^{i\hat{\omega}_4} = e^{i(\hat{\omega}_3 t + \omega_3 \frac{u}{c} t)}$. Then

$$\omega_4 = \omega_3 \left(1 + \frac{u}{c}\right), \;\; \Rightarrow \quad \omega_4 = \omega\, \frac{(1 - v/c)(1 + u/c)}{(1 + v/c)(1 - u/c)}\,. \tag{7}$$

The above result is illustrated in Fig. 1.

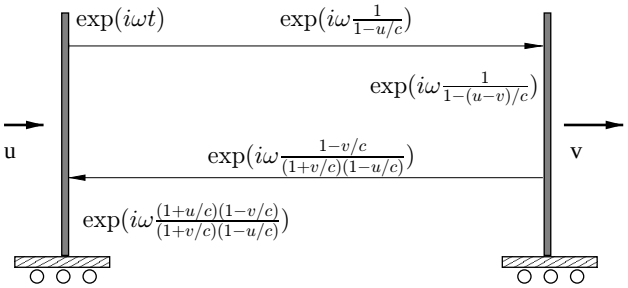

Fig. 1: Moving emitter and receiver

The case of waves propagating transversely to the emitter and receiver gives a trivial result in 1D, in the sense that the frequency and wave number of the propagating wave are not affected by the motion of the source or the receiver. The most general treatment for point source in 3D is given by

the eikonal equation [6, p.225] for the inhomogeneous wave equation that is obtained in a frame moving with prescribed speed in certain direction.

An interesting limiting case is presented when $u, v \ll c$. Then the product uv/c^2 can be neglected in comparison with $(u-v)/c$ (provided that $u-v \simeq \mathrm{O}(u)$) and the above formula reduces to

$$\omega_4 = \frac{1+(u-v)/c}{1-(u-v)/c},$$

which is the formula from [8, 9] for zero angle between the relative speed and the line of the emitter and observer. The discrepancies of order (uv/c^2) can be the cause of the so-called Pioneer anomaly [10]. It will be interesting to reexamine the raw data from Pioneer 10 eliminating the formula for relativistic Doppler effect and using in its place Eq. 7. Then what appears as an anomaly, can actually give the information about the absolute velocities of Earth and of the space ship. It is not necessary, of course, to go as far as Pioneer 10 and 11 went. The experiment can be done with an interferometer whose arms are the distances between two different satellites moving with different orbital speeds in the vicinity of Earth.

7 Michelson-Morley experiment (MME)

It was argued that because of the motion of the experimental equipment (the interferometer), the time taken by light to travel in the direction of motion will be different from the time needed to return, and these times together will differ from the time to travel in lateral direction. The argument that led to the prediction that the effect is of second order (see, [11, p.149], [1]) was typically corpuscular in its nature. The emission theory of light assumed that the "particles" of light were supposed to move in a resting continuum with velocity c. However when these particles were emitted by a moving surface in the direction of motion, they acquired speed $c+v$, whereas the particles emitted against the motion would move with speed $c-v$. The emission theory claimed that the total time for a ray to complete the full path in longitudinal direction is

$$t_1 = \frac{l}{c+v} + \frac{l}{c-v} = \frac{2l}{c(1-v^2/c^2)}, \qquad (8)$$

where l is the length of the longitudinal and transverse arms of the interferometer. The arguments about the nature of reflections in the transverse arm of the interferometer are similarly based on the emission theory. In the transverse direction the length of the path traveled by one light corpuscle is calculated using the Pythagorean theorem and the total time needed for the light particle to complete the return trip to the lateral mirror is given by (see [1])

$$t_2 = \frac{2l}{c}\sqrt{1+\frac{v^2}{c^2}}. \qquad (9)$$

Then the difference in the times needed to traverse the longitudinal and the transverse arms is

$$t_1 - t_2 \approx \frac{2l}{c}\left[1+2\frac{v^2}{c^2}-1-\frac{v^2}{c^2}+\mathrm{O}\left(\frac{v^4}{c^4}\right)\right] \approx l\,\frac{v^2}{c^2}. \qquad (10)$$

Under the standard analogies of corpuscular approach, at this point the arguments usually go back to the wave theory of light assuming that the change in travel time of light particles somehow materializes as change of the emitted or received frequency.

Although the scientific community gradually elevated MME to the status of one of the *experimenta crucis* for the theory of relativity, the above argument was never critically revisited after the postulate of the constancy of speed of light was accepted. The only work known to the present author is [12] where the emission theory and wave theory of Doppler effect are compared and shown to coincide within the first order in v/c but no conclusions about the actual applicability of the above corpuscular-based formula are made.

The problem with applying a corpuscular approach to a wave phenomenon in a medium is that a propagation speed $c+v$ is impossible since all propagation speeds are limited by the characteristic speed of the medium. Yet, the above derivations were repeated in [11, 13] and now feature prominently in many of the most authoritative modern textbooks, such as [9, 14]. So we are faced with a very peculiar situation: The formula used to explain the results of one of the most important for relativity theory experiments contradict the second postulate of the same theory.

The fallacy of the argumentation is as follows:

(i) The existence of a continuous medium in which the light propagates is stipulated (luminiferous continuum);

(ii) An irrelevant to continuum description theoretical formula is derived using the corpuscular concept of light (emission theory of light);

(iii) An experiment is designed for which it is believed that it can allow the measurement of the variable involved in the irrelevant theoretical formula;

(iv) Measurements obtained from the experiment do not show the expected effect;

(v) Conclusion is drawn that the contradiction is due to the fact that the original assumption of the presence of a continuum at rest is wrong;

(vi) The concept of existing of a material luminiferous continuum (i) is abandoned altogether.

This kind of fallacy is called *ignoratio elenchi* ("pure and simple irrelevance") and consists in using an argument that is supposed to prove one proposition but succeeds only in proving a different one. Clearly, there can be at least two causes for the nil result of the experiment. Before assuming that (i) is wrong, one has to examine (ii) from the point of view of the wave theory of light under the condition of

constancy of speed of light. The only way to pass judgment on the presence or absence of an absolute continuum is to derive a formula for the interference effect that is based on the assumption that the space between the different parts of the equipment is filled with a continuous medium in which the propagation speed of linear waves is a given constant. In doing so, the reflection from the mirror has to be treated as an excitation of a wave on moving material surface. Then the frequency of the excited wave (which then travels back as the reflected wave) is subject to the motion of the mirror itself. In this short note we make an attempt to correctly pose the problem (using the adequate mathematical approach to solving the wave equation with b. c. on moving boundaries) and to show the consequences of this for the interpretation of interferometry experiments involving moving mirrors that are moving translatory with respect to the supposed absolute continuum. Only after the proper theoretical formula based on the idea that the continuum is at rest and that the equipment is moving relative to it, is derived and only after the predictions of this *relevant* formula are found to contradict the experimental evidence, one rule out the existence of an absolute continuum at rest in which the light waves are propagating as shear waves in a material medium.

It has been shown above that if the source of light and the mirror are moving together with the same velocity relative to the resting medium, then the Doppler effect is strictly equal to zero. This means that no Doppler effect can be detected from an experiment in which the emitter and the mirror are moving together through a quiescent continuum. This means that a nil effect from the celebrated experiment of Michelson and Morley should be interpreted as an evidence about the existence of a material continuum at rest and that this absolute continuum is not entrained by the moving bodies. The flawed arguments of the emission theory of light introduced an error of $\mathrm{O}(v^2/c^2)$ in the formulas which was, in fact, the perceived effect in MME. At the same time, the correct solution (see the previous section) shows that the effect must be strictly nil provided that an absolute continuum fills the space between the different parts of the interferometer and that this continuum is not entrained.

8 A possible experimental set-up

If MME is irrelevant to detecting the absolute medium, then the question arises of is it possible at all to detect the latter by means of an interferometry experiment whose parts are moving together with the Earth. The answer (as already suggested in [7]) is in the positive if one can use two *independent* sources of light of virtually identical frequencies and avoid reflections. This means that one has to aim the beams against each other as shown in Fig. 2.

Assume now that two waves of identical frequencies are excited at two *different* points that are moving together in the same direction with the same velocity relative to the resting medium. The interference between the right-going wave from the left source and the left-going wave from the right source is given by

$$\begin{aligned} e^{i\omega(t-x/c)/(1-u/c)} + e^{i\omega(t+x/c)/(1+u/c)} = \\ = \left[\cos(\omega_1 t - k_1 x) + \cos(\omega_2 t + k_2 x)\right] + \\ + i\left[\sin(\omega_1 t - k_1 x) + \sin(\omega_2 t + k_2 x)\right] = \\ = 2\cos(\tilde{\omega} t + \hat{k} x)\exp\left[i(\hat{\omega} t + \tilde{k} x)\right], \end{aligned} \tag{11}$$

where

$$\tilde{\omega} = \frac{\omega_1+\omega_2}{2} = \omega\left(1-\frac{u^2}{c^2}\right), \quad \hat{\omega} = \frac{\omega_2-\omega_1}{2} = -\frac{u}{c}\tilde{\omega},$$

are the carrier and beat frequencies, and $\tilde{k} = \tilde{\omega}/c$, $\hat{k} = \hat{\omega}/c$. The wave excited at certain point, say $x = 0$, is

$$2\cos(\tilde{\omega} t)\exp(i\hat{\omega} t). \tag{12}$$

In Fig. 2 we show a possible experimental set-up which makes use of two independent sources of coherent light. Note that using two lasers, does not make our experiment similar to the set-up used in [15] because the latter involves mirrors and as it has been shown above, using mirrors dispels any possible effect.

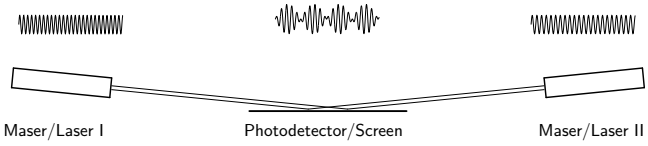

Fig. 2: Experimental set-up involving two lasers/masers

One of the ways to find the beat frequency is to use a photodetector in a point of the region of interference of the two waves. Note that the carrier frequency of the visible light is very high and cannot be detected in principle. The problem is that and even the beat frequency, Eq. 12, can be too high for the resolution of the available photodetectors. Apart from the fact that mirrors were used in [16], the high beat frequency could be another reason why it was not detected in those experiments. In fact they were after the beat frequency connected with the second-order effects and found practically no beat which is exactly what is to be expected in the light of the theory above presented. This is additional confirmation of the theory proposed here because we claim that no effect (neither first- nor second-order not higher-order) can exist if reflections are involved.

The other way to conduct the experiment is to measure the beat wave number $\hat{k}$ by taking a snapshot of the wave at certain moment of time. Then the spatial distribution of the wave amplitude is

$$2\cos(\hat{k}x)\,\exp(i\tilde{k}x), \tag{13}$$

which will produce an interference pattern in the resting continuum that can be observed on a screen (as shown

alternatively in Fig. 2). Note that in this case the screen is "parallel" or "tangent" to the vibrating part of the absolute continuum, and what is observed, are the dark and light strips corresponding the the different values of the amplitude of the beat wave. Clearly, the effect will be best observed if the two lasers beams have identical polarization.

The requirements for the frequency stabilization of the sources of light stem from the magnitudes of the beat frequency. It is accepted nowadays that the speed of the so-called Local Standard of Rest (LSR) to which solar system belongs, is of order of $v \approx 300$ km/s relative to the center of the local cluster of galaxies [17]. The speed of LSR is an upper estimate of the speed with respect to the absolute medium. This maximum can be reached only if the center of cluster of galaxies is at rest relative to the medium. Thus, the upper limit for the dimensionless parameter $\varepsilon = v/c$ is 10^{-3}, which places very stringent requirements on the resolution in case that a photodetector is involved. For red-light lasers, the beat frequency is of order of 600 GHz which is well beyond the sensitivity of the available photodetectors. This means that one should opt for terahertz masers when the beat frequency ω_b will be smaller than 1–3 GHz.

In the alternative implementation of the experimental set-up a detecting screen is used to get the spatial distribution of the interference pattern. In such a case, one can use standard visible-light lasers. For instance, the red light has wavelength approximately in the range of $600\,\mathrm{m}^{-9}$, then the beat wave length is expected to be $\varepsilon^{-1} \approx 1000$ times longer. This means 0.6 mm which is technically feasible to observe on a screen. Conversely, using terahertz masers in this case could make the wave length of the beat wave of order of 20–50 cm.

Now, in order to have reliable results from the proposed interferometry experiment, one needs frequency stabilization a couple of orders of magnitude better than the sought effect. To be on the safe side, we mention that the lowest value for ε is 10^{-4} which corresponds to the orbital speed of Earth. Then the best stabilization of the frequency needed is 10^{-7}. This is well within the stabilization limits for the currently available low-power lasers. For example, Coherent, Inc. offers the series 899-21 that are Actively Stabilized, Scanning Single-Frequency Ring Lasers with stabilization 10^{-9}.

9 Conclusion

The theory of Michelson-Morley interference experiment is revisited from the point of view of the wave theory of light. The fallacy of using the accepted formula based on the emission theory of light is shown and new formulas are derived based on the correct posing of the boundary conditions at moving boundaries for a hyperbolic equation. It is shown that when the source of light and the reflector are moving with the same speed through a non-entrained absolute continuum, the reflected wave as received back at the emitter's place shows no Doppler shift, and hence no fringes can be expected. The situation is different if the emitter and the reflector are in relative motion with respect to each other. The meaning of the results of the present work is that the only correct conclusion from a nil effect from interferometry experiment involving reflection is not that absolute medium does not exist, but that an absolute continuum exist which is not entrained by the motion of the measuring instrument (the system of emitters and mirrors). Naturally, the nil effect of Michelson-Morley experiment should not be used as the sole verification of the absolute medium and to this end a new experimental set-up is proposed.

References

1. Michelson A. A., Morley E. W. On the relat. motion of the earth and the luminiferous ether. *Am. J. Sci.*, 1887, v.34, 333–345.
2. Torr D. G., Kolen P. An experiment to measure relative variations in the one-way velocity of light. *Prec. Measur. Fund. Const. II*, Natl. Bur. Stand. (US), Sp. Publ. 617, 1984, 675–679.
3. Krisher T.P., Maleki L., Lutes G.F., Primas L.E., Logan R.T., Anderson J. D. Test of isotropy of the one-way speed of light using hydrogen-maser standards. *Phys. Rev. D*, 1990, v. 42, 731–734.
4. Miller D. C. The ether-drift experiment and the determination of the absolute motion of earth. *Reviews of Modern Physics*, 1933, v. 5, 203–242.
5. Cahill R. T. The Michelson and Morley 1887 experiment and the discovery of absolute motion. *Progress in Physics*, 2005, v. 3, 25–29.
6. Whitham G. B. Linear and nonlinear waves. Wiley, NY, 1974.
7. Christov C. I. Discrete out of continuous: Dynamics of phase patterns in continua. *Continuum Models and Discrete Systems — Proc. of CMDS8*, World Sci., Singapore, 1996, 370–394.
8. Elmore W. C., Heald M. A. Physics of waves. Dover, NY, 1969.
9. Dichtburn R. W. Light, volume 1. Acad. Press, London, 1976.
10. Anderson J. D., Laing P. A., Lau E. L., Liu A. S., Nieto M. M., Turyshev S. G. Study of the anomalous acceleration of Pioneer 10 and 11. *Phys. Rev. D*, 2002, v. 65, 082004.
11. Michelson A. A. Studies in optics. Univ. Chicago Press, 1927.
12. Tolman R. C. The second postulate of relativity. *Physical Review*, 1910, v. 31, 26–40.
13. Lorentz H. A. The theory of electrons and its applications to the phenomena of light and radiant heat. Dover, NY, 1952.
14. Hecht E., Zajaz A. Optics. Adison-Wesley, Reading, 1974.
15. Jaseda T. S., Javan A., Townes C. H. Frequency stability of He-Ne masers and measurements of length. *Phys. Rev. Lett.*, 1963, v. 10, 165–167.
16. Jaseda T. S., Javan A., Murray J, Townes C. H. Test of special relativity or of the isotropy of space by use of infrared masers. *Phys. Rev. A*, 1964, v. 113, 1221–1225.
17. Smoot G. F., Gorenstein M. V., Miller R. A. Detection of anisotropy in the Cosmic Blackbody Radiation. *Phys. Rev. Lett.*, 1977, v. 39, 898–901.

The Roland De Witte 1991 Experiment (to the Memory of Roland De Witte)

Reginald T. Cahill

School of Chemistry, Physics and Earth Sciences, Flinders University, Adelaide 5001, Australia

E-mail: Reg.Cahill@flinders.edu.au

In 1991 Roland De Witte carried out an experiment in Brussels in which variations in the one-way speed of RF waves through a coaxial cable were recorded over 178 days. The data from this experiment shows that De Witte had detected absolute motion of the earth through space, as had six earlier experiments, beginning with the Michelson-Morley experiment of 1887. His results are in excellent agreement with the extensive data from the Miller 1925/26 detection of absolute motion using a gas-mode Michelson interferometer atop Mt. Wilson, California. The De Witte data reveals turbulence in the flow which amounted to the detection of gravitational waves. Similar effects were also seen by Miller, and by Torr and Kolen in their coaxial cable experiment. Here we bring together what is known about the De Witte experiment.

Preface of the Editor-in-Chief

Today, on the 15th anniversary of De Witte's experiment, I would like to comment on an erroneous discussion of the "supposed disparity" between the De Witte results and Einstein's Principle of Relativity, and the whole General Theory of Relativity, due to the measured anisotropy of the velocity of light. The same should be said about the Torr-Kolen experiment (1981, Utah State Univ., USA) and the current experiment by Cahill (Flinders Univ., Australia).

The discussion was initiated by people having a poor knowledge of General Relativity, having learnt it from "general purpose" books, and bereft of native abilities to learn even the basics of tensor calculus and Riemannian geometry — mainly so-called "anti-relativists" and mere anti-semites, to whom Einstein's genius and discoveries give no rest.

Roland De Witte was excellent experimentalist, not a master in theory. He was misled about the "disparity" by the anti-relativists, that resulted his deep depression and death.

It is well known that in a four-dimensional pseudo-Riemannian space (the basic space-time of General Relativity), the velocity of light c is said to be general covariantly invariant; its value is independent of the reference frame we use. However a real observer is located in his three-dimensional spatial section $x^0 = \text{const}$ (inhomogeneous, curved, and deforming), pierced by time lines $x^i = \text{const}$ (also inhomogeneous and curved). The space can bear a gravitational potential $\mathrm{w} = c^2(1-\sqrt{g_{00}})$, and be non-holonomic — the time lines are non-othogonal to the spatial section, that is displayed as the space three-dimensional rotation at the linear velocity $v_i = -c\frac{g_{0i}}{\sqrt{g_{00}}}$. These factors lead to the fact that the physically observable time interval is $d\tau = \sqrt{g_{00}}\,dt - \frac{1}{c^2}\,v_i dx^i$, which is different to the coordinate time interval dt. Anyone can find all this in *The Classical Theory of Fields* by Landau and Lifshitz [1], the bible of General Relativity, and other literature.

The complete theory of physically observable quantities was developed in the 1940's by Abraham Zelmanov, by which the observable quantities are determined by the projections of four-dimensional quantities onto an observer's real time line and spatial section. (See [2,3,4,5] and References therein.) From this we see that the physically observable velocity of light is a three-dimensional vector $c^i = \frac{dx^i}{d\tau}$ dependent on the gravitational potential and the space non-holonomity (rotation) through the physically observable time interval $d\tau$. In particular, c^i can be distributed anisotropically in the spatial section, if it completely rotates. At the same time the complete general covariantly invariant c remains unchanged.

Therefore the anisotropy of the observed value of the velocity of light does not contradict Einstein's Principle of Relativity. On the contrary, such an experimental result can be viewed as a new verification of Einstein's theory.

Moreover, as already shown by Zelmanov [2] in the 1940's, General Relativity's space permits absolute reference frames connected to the anisotropy of the fields of the spatial non-holonomity or deformation, i. e. connected to globally polarized fields which are likely a global background giro. Therefore, absolute reference frames connected to the spatial anisotropy of the velocity of light or the Cosmic Microwave Background can also be viewed as additional verifications of General Relativity.

Roland De Witte didn't published his experimental results. All we possess subsequent to his death is his public letter of 1998 and letters to his colleagues wherein he described his experimental set up in detail. I therefore asked Prof. Cahill to prepare a brief description of the De Witte experiment so that any interested person may thereby have a means of referring to De Witte's results as published. Reginald T. Cahill is an expert in such experimental techniques and currently prepares a new experiment, similar to that by De Witte (but with a precision in measurement a thousand times greater using current technologies). Therefore his description of the De Witte experiment is accurate.

Dmitri Rabounski

[1] Landau L. D., Lifshitz E. M. The classical theory of fields. 4th ed., Butterworth–Heinemann, 1980.

[2] Zelmanov A. L. Chronometric invariants. Dissertation thesis, 1944. 2nd ed., American Research Press, Rehoboth (NM), 2006.

[3] Zelmanov A. L. Chronometric invariants and co-moving coordinates in the general relativity theory. *Doklady Acad. Nauk USSR*, 1956, v. 107(6).

[4] Zelmanov A. L., Agakov V. G. Elements of General Relativity. Moscow, Nauka, 1988.

[5] Rabounski D. Zelmanov's anthropic principle and the infinite relativity principle. *Progress in Physics*, 2006, v. 1.

1 Introduction


R. De Witte

Ever since the 1887 Michelson-Morley experiment [1] to detect absolute motion, that is motion relative to space, by means of the anisotropy of the speed of light, physicists in the main have believed that such absolute motion was unobservable, and even meaningless. This was so after Einstein proposed as one of his postulates for his Special Theory of Relativity that the speed of light is invariant quantity. However the Michelson-Morley experiment did observe small fringe shifts of the form indicative of an anisotropy of the light speed*. The whole issue has been one of great confusion over the last 100 years or so. This confusion arose from deep misunderstandings of the theoretical structure of Special Relativity, but also because ongoing detections of the anisotropy of the speed of light were treated with contempt, rather than being rationally discussed. The intrinsic problem all along has been that the observed anisotropy of the speed of light also affects the very apparatus being used to measure the anisotropy. In particular the Lorentz-Fitzgerald length contraction effect must be included in the analysis of the interferometer when the calibration constant for the device is calculated. The calibration constant determines what value of the speed of light anisotropy is to be determined from an observed fringe shift as the apparatus is rotated. Only in 2002 was it discovered that the calibration constant is very much smaller than had been assumed [2, 3], and that the observed fringe shifts corresponded to a speed in excess of 0.1% of the speed of light. That discovery showed that the presence of a gas in the light path is essential if the interferometer is to act as a detector of absolute motion, and that a vacuum operated interferometer is totally incapable of detecting absolute motion. That physics has suppressed this effect for over 100 years is a major indictment of physics. There have been in all seven detections of such anisotropy, with five being Michelson interferometer experiments [1, 4, 5, 6, 7], and two being one-way RF coaxial cable propagation time experiments, see [9, 10] for extensive discussion and analysis of the experimental data. The most thorough interferometer experiment was by Miller in 1925/26. He accumulated sufficient data that in conjunction with the new calibration understanding, the velocity of motion of the solar system could be determined† as ($\alpha = 5.2^{\text{hr}}$, $\delta = -67^\circ$), with a speed of 420 ± 30 km/s. This local (in the galactic sense) absolute motion is different from the Cosmic Microwave Background (CMB) anisotropy determined motion, in the direction ($\alpha = 11.20^{\text{hr}}$, $\delta = -7.22^\circ$) with speed 369 km/s; this is motion relative to the source of the CMB, namely relative to the distant universe.

*The older terminology was that of detecting motion relative to an *ether* that was embedded in a geometrical space. However the more modern understanding does away with both the ether and a geometrical space, and uses a structured dynamical *3-space*, as in [9, 10].

†There is a possibility that the direction is opposite to this direction.

The first one-way coaxial cable speed-of-propagation experiment was performed at the Utah State University in 1981 by Torr and Kolen [8]. This involved two rubidium vapor clocks placed approximately 500 m apart with a 5 MHz sinewave RF signal propagating between the clocks via a buried nitrogen filled coaxial cable maintained at a constant pressure of ~ 2 psi. Unfortunately the cable was orientated in an East-West direction which is not a favourable orientation for observing absolute motion in the Miller direction. There is no reference to Miller's result in the Torr and Kolen paper, otherwise they would presumably not have used this orientation. Nevertheless there is a small projection of the absolute motion velocity onto the East-West cable and Torr and Kolen did observe an effect in that, while the round speed time remained constant within $0.0001\%\, c$, variations in the one-way travel time were observed. The maximum effect occurred, typically, at the times predicted using the Miller velocity [9, 10]. So the results of this experiment are also in remarkable agreement with the Miller direction, and the speed of 420 km/s. As well Torr and Kolen reported fluctuations in both the magnitude, from 1–3 ns, and the time of maximum variations in travel time.

However during 1991 Roland De Witte performed the most extensive RF travel time experiment, accumulating data over 178 days. His data is in complete agreement with the 1925/26 Miller experiment. These two experiments will eventually be recognised as two of the most significant experiments in physics, for independently and using different experimental techniques they detected the same velocity of absolute motion. But also they detected turbulence in the flow of space past the earth; non other than gravitational waves. Both Miller and De Witte have been repeatably attacked for their discoveries. Of course the experiments indicated the anisotropy of the speed of light, but that is not in conflict with the confirmed correctness of various relativistic effects. While Miller was able to publish his results [4], and indeed the original data sheets were recently discovered at Case Western Reserve University, Cleveland, Ohio, De Witte was never permitted to publish his data in a physics journal. The only source of his data was from a e-mail posted in 1998, and a web page that he had established. This paper is offered as a resource so that De Witte's extraordinary discoveries may be given the attention and study that they demand, and that others may be motivated to repeat the experiment, for that is the hallmark of science‡.

2 The De Witte experiment

In a 1991 research project within Belgacom, the Belgium telcommunications company, another (serendipitous) detection of absolute motion was performed. The study was undertaken by Roland De Witte. This organisation had two sets of atomic

‡The author has been developing and testing new techniques for doing one-way RF travel time experiments.

clocks in two buildings in Brussels separated by 1.5 km and the research project was an investigation of the task of synchronising these two clusters of atomic clocks. To that end 5 MHz radio frequency (RF) signals were sent in both directions through two buried coaxial cables linking the two clusters. The atomic clocks were caesium beam atomic clocks, and there were three in each cluster: A1, A2 and A3 in one cluster, and B1, B2, and B3 at the other cluster. In that way the stability of the clocks could be established and monitored. One cluster was in a building on Rue du Marais and the second cluster was due south in a building on Rue de la Paille. Digital phase comparators were used to measure changes in times between clocks within the same cluster and also in the propagation times of the RF signals. Time differences between clocks within the same cluster showed a linear phase drift caused by the clocks not having exactly the same frequency, together with short term and long term noise. However the long term drift was very linear and reproducible, and that drift could be allowed for in analysing time differences in the propagation times between the clusters.

The atomic clocks (OSA 312) and the digital phase comparators (OS5560) were manufactured by Oscilloquartz, Neuchâtel, Switzerland. The phase comparators produce a change of 1 V for a phase variation of 200 ns between the two input signals. At both locations the comparison between local clocks, A1–A2 and A1–A3, and between B1–B2, B1–B3, yielded linear phase variations in agreement with the fact that the clocks have not exactly the same frequencies due to the limited reproducible accuracy together with a short term and long term phase noise (A. O. Mc Coubrey, *Proc. of the IEEE*, Vol. 55, No. 6, June, 1967, 805–814). Even if the long term frequency instability were 2×10^{-13} this is able to produce a phase shift of 17 ns a day, but this instability was not often observed and the ouputs of the phase comparators have shown that the local instability was typically only a few nanoseconds a day (5 ns) between two local clocks.

But between distant clocks A1 toward B1 and B1 toward A1, in addition to the same linear phase variations (but with identical positive and negative slopes, because if one is fast, the other is slow), there is also an additional clear sinusoidal-like phase undulation ($\approx$ 24 h period) of the order of 28 ns peak to peak.

The possible instability of the coaxial lines cannot be responsible for the phase effects observed because these signals are in phase opposition and also because the lines are identical (same place, length, temperature, etc. . .) causing the cancellation of any such instabilities. As well the experiment was performed over 178 days, making it possible to measure with accuracy ($\pm$ 25 s) the period of the phase signal to be the sidereal day (23 h 56 min), thus permitting to conclude that absolute motion had been detected, even with apparent turbulence.

According to the manufacturer of the clocks, the typical humidity sensitivity is $df/f = 10^{-14}$ % humidity, so the effect observed between two distant clocks (24 ns in 12 h) needs, for example, a differential step of variation of humidity of 55%, two times a day, over 178 days. So the humidity variations cannot be responsible for the persistent periodic phase shift observed. As for pressure effects, the manufacturer confirmed that no measurable frequency change during pressure variations around 760 mm Hg had been observed. When temperature effects are considered, the typical sensitivity around room temperature is $df/f = 0.25\times10^{-13}$ °C and implies, for example, a differential step of room temperature variation of 24°C, two times a day, over 178 days to produce the observed time variations. Moreover the room temperature was maintained at nearly a constant around 20°C by the thermostats of the buildings. So the possible temperature variations of the clocks could not be responsible for the periodic phase shift observed between distant clocks. As well the heat capacity of the housings of the clocks would even further smooth out possible temperature variations. Finally, the typical magnetic sensitivity of $df/f = 1.4\times10^{-13}$ Gauss needs, for example, differential steps of field induction of 4 Gauss variation, two times a day, over 178 days. But the terrestrial magnetic induction in Belgium is only in the order of 0.2 Gauss and thus its variations are much less (except during a possible magnetic storm). As for possible parasitic variable DC currents in the vicinity of the clocks, a 4 Gauss change needs a variation of 2000 amperes in a conductor at 1 m, and thus can be excluded as a possible effect. So temperature, pressure, humidity and magnetic induction effects on the frequencies of the clocks were thus completely negligible in the experiment.

Changes in propagation times were observed over 178 days from June 3 1991 7 h 19 m GMT to 27 Nov 19 h 47 m GMT and recorded. A sample of the data, plotted against sidereal time for just three days, is shown in Fig. 1. De Witte recognised that the data was evidence of absolute motion but he was unaware of the Miller experiment and did not realise that the Right Ascension for minimum/maximum propagation time agreed almost exactly with Miller's direction ($\alpha = 5.2^{\mathrm{hr}}$, $\delta = -67°$). In fact De Witte expected that the direction of absolute motion should have been in the CMB direction, but that would have given the data a totally different sidereal time signature, namely the times for maximum/minimum would have been shifted by 6 hrs. The declination of the velocity observed in this De Witte experiment cannot be determined from the data as only three days of data are available. However assuming exactly the same declination as Miller the speed observed by De Witte appears to be also in excellent agreement with the Miller speed, which in turn is in agreement with that from the Michelson-Morley and other experiments.

Being 1st-order in v/c the Belgacom experiment is easily analysed to sufficient accuracy by ignoring relativistic effects, which are 2nd-order in v/c. Let the projection of the

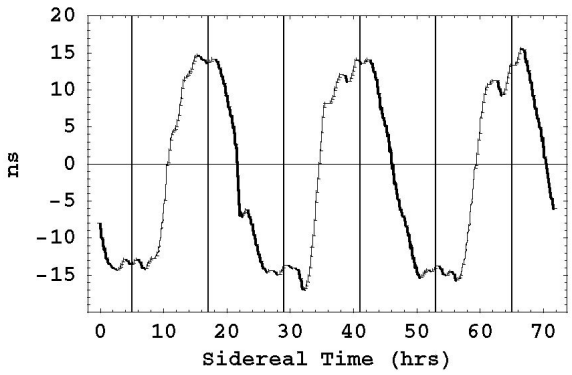

Fig. 1: Variations in twice the one-way travel time, in ns, for an RF signal to travel 1.5 km through a buried coaxial cable between Rue du Marais and Rue de la Paille, Brussels, by subtracting the Paille Street phase shift data from the Marais Street phase shift data. An offset has been used such that the average is zero. The cable has a North-South orientation, and the data is $\pm$ difference of the travel times for NS and SN propagation. The sidereal time for maximum effect of $\sim$5 hr (or $\sim$17 hr) (indicated by vertical lines) agrees with the direction found by Miller [4]. Plot shows data over 3 sidereal days and is plotted against sidereal time. The main effect is caused by the rotation of the earth. The superimposed fluctuations are evidence of turbulence i.e gravitational waves. Removing the earth induced rotation effect we obtain the first experimental data of the turbulent structure of space, and is shown in Fig. 2. De Witte performed this experiment over 178 days, and demonstrated that the effect tracked sidereal time and not solar time, as shown in Fig. 3.

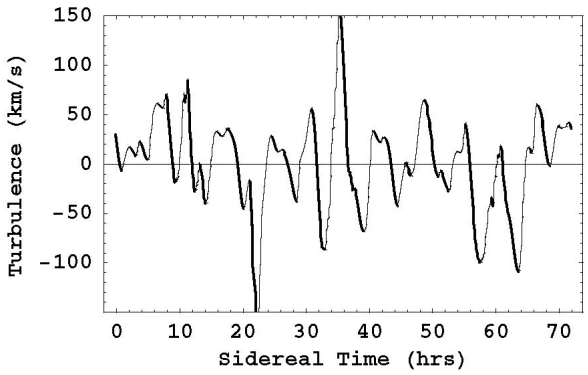

Fig. 2: Shows the speed fluctuations, essentially "gravitational waves" observed by De Witte in 1991 from the measurement of variations in the RF coaxial-cable travel times. This data is obtained from that in Fig. 1 after removal of the dominant effect caused by the rotation of the earth. Ideally the velocity fluctuations are three-dimensional, but the De Witte experiment had only one arm. This plot is suggestive of a fractal structure to the velocity field. This is confirmed by the power law analysis shown in Fig. 4. From [11].

absolute velocity vector $\mathbf{v}$ onto the direction of the coaxial cable be v_P. Then the phase comparators reveal the *difference* between the propagation times in NS and SN directions. Consider a simple analysis to establish the magnitude of the observed speed.

$$\Delta t = \frac{L}{\frac{c}{n} - v_P} - \frac{L}{\frac{c}{n} + v_P} = \\ = 2\,\frac{L}{c/n}\,n\,\frac{v_P}{c} + \mathrm{O}\left(\frac{v_P^2}{c^2}\right) \approx 2t_0\,n\,\frac{v_P}{c}\,.$$

Here $L = 1.5$ km is the length of the coaxial cable, $n = 1.5$ is the assumed refractive index of the insulator within the coaxial cable, so that the speed of the RF signals is approximately $c/n = 200,000$ km/s, and so $t_0 = nL/c = 7.5\times10^{-6}$ sec is the one-way RF travel time when $v_P = 0$. Then, for example, a value of $v_P = 400$ km/s would give $\Delta t = 30$ ns. De Witte reported a speed of 500 km/s. Because Brussels has a latitude of 51° N then for the Miller direction the projection effect is such that v_P almost varies from zero to a maximum value of $|\mathbf{v}|$. The De Witte data in Fig. 1 shows Δt plotted with a false zero, but shows a variation of some 28 ns. So the De Witte data is in excellent agreement with the Miller's data.

The actual days of the data in Fig. 1 are not revealed by De Witte so a detailed analysis of the data is not possible. If all of De Witte's 178 days of data were available then a detailed analysis would be possible.

De Witte does however reveal the sidereal time of the cross-over time, that is a "zero" time in Fig. 1, for all 178 days of data. This is plotted in Fig. 3 and demonstrates that the time variations are correlated with sidereal time and not local solar time. A least squares best fit of a linear relation to that data gives that the cross-over time is retarded, on average, by 3.92 minutes per solar day. This is to be compared with the fact that a sidereal day is 3.93 minutes shorter than a solar day. So the effect is certainly galactic and not associated with any daily thermal effects, which in any case would be very small as the cable is buried. Miller had also compared his data against sidereal time and established the same property, namely that, up to small diurnal effects identifiable with the earth's orbital motion, the dominant features in the data tracked sidereal time and not solar time, [4].

The De Witte data is also capable of resolving the question of the absolute direction of motion found by Miller. Is the direction ($\alpha = 5.2^{\mathrm{hr}}$, $\delta = -67°$) or the opposite direction? Being a 2nd-order Michelson interferometer experiment Miller had to rely on the earth's orbital effects in order to resolve this ambiguity, but his analysis of course did not take account of the gravitational in-flow effect [9, 10]. The De Witte experiment could easily resolve this ambiguity by simply noting the sign of Δt. Unfortunately it is unclear as to how the sign in Fig. 1 is actually defined, and De Witte does not report a direction expecting, as he did, that the direction should have been the same as the CMB direction.

The dominant effect in Fig. 1 is caused by the rotation of the earth, namely that the orientation of the coaxial cable with respect to the direction of the flow past the earth changes as the earth rotates. This effect may be approximately unfolded from the data, see [9, 10], leaving the gravitational waves shown in Fig. 2. This is the first evidence that the velocity

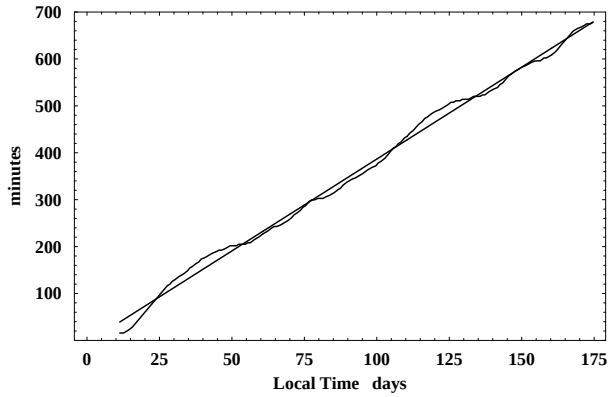

Fig. 3: Plot of the negative of the drift of the cross-over time between minimum and maximum travel-time variation each day (at $\sim 10^{\mathrm{h}} \pm 1^{\mathrm{h}}$ ST) versus local solar time for some 178 days, from June 3 1991 7 h 19 m GMT to 27 Nov 19 h 47 m GMT. The straight line plot is the least squares fit to the experimental data, giving an average slope of 3.92 minutes/day. The time difference between a sidereal day and a solar day is 3.93 minutes/day. This demonstrates that the effect is related to sidereal time and not local solar time.

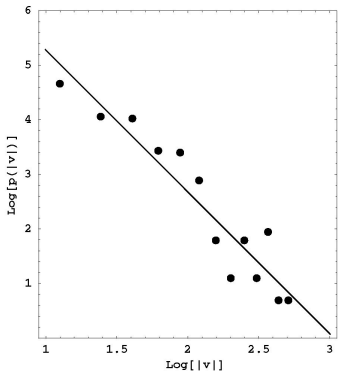

Fig. 4: Shows that the speed fluctuations in Fig. 2 are scale free, as the probability distribution from binning the speeds has the form $p(v) \propto |v|^{-2.6}$. This plot shows $\log[p(v)]$ vs $|v|$. From [11].

field describing the flow of space has a complex structure, and is indeed fractal. The fractal structure, i.e. that there is an intrinsic lack of scale to these speed fluctuations, is demonstrated by binning the absolute speeds $|v|$ and counting the number of speeds $p(|v|)$ within each bin. Plotting $\log[p(|v|)]$ vs $|v|$, as shown in Fig. 4 we see that $p(v) \propto |v|^{-2.6}$. The Miller data also shows evidence of turbulence of the same magnitude. So far the data from three experiments, namely Miller, Torr and Kolen, and De Witte, show turbulence in the flow of space past the earth. This is what can be called gravitational waves [9, 10].

3 Biography of De Witte

These short notes were extracted from De Witte's webpage.

Roland De Witte was born September 29, 1953 in the small village of Halanzy in the south of Belgium. He became the apprentice to an electrician and learned electrical wiring of houses. At the age of fourteen he decided to take private correspondence courses in electronics from the EURELEC company, and obtained a diploma at the age of sixteen. He decided to stop work as an apprentice and go to school. Without a state diploma it was impossible for him to be admitted into an ordinary school with teenagers of his age. After working for a scrap company where he used dynamite, he was finally admitted into a secondary school with the assistance of the director, but with the condition that he pass some tests from the board of the state examiners, called the Central Jury, for the first three years. After having sat the exams he became a legitimate schoolboy. But when he was in the last but one year in secondary school he decided to prepare for the entrance exam in physics at the University of Liège, and became a university student in physics one year before his friends. During secondary school years he was interested in all the scientific activities and became a schoolboy president of the Scientific Youths of the school in Virton. Simple physics experiments were performed: Millikan, photoelectric effect, spectroscopy, etc... and a small electronics laboratory was started. He also took part in different scientific short talks contests, and became a prizewinner for a talk about "special relativity", and received a prize from the Belgian Shell Company which had organised the contest. De Witte even visited the house where Einstein lived for a few months in Belgium when he left Germany. The house is the "Villa Savoyarde" at "Coq-Sur-Mer" Belgium, and is just 200 m from the North Sea. During secondary school De Witte had hobbies such as astronomy and pirate radio transmission on 27 Mhz with a hand-made transmitter, with his best long distance communication being with Denmark.

De Witte says that he is not able to study by "heart", and during secondary school, even with his bad memory which caused problems in history and english, he nevertheless always achieved the maximum of points in physics, chemistry and mathematics and was the top of his class. At University he obtained the diploma from the two year degree in physics but was not able to continue due to the "impossibility to study by heart several thousands of pages of erroneous calculations" like the others did to obtain the graduate diploma. Thus even though considered to be intelligent by several teachers, he decided to leave the University and became the manager of a retail electronic components shop. He did this job for ten years while also performing his physics experiments and studying theoretical physics. He was interested in microwaves and became an IEEE member and reader of the publications of the Microwave Theory & Techniques and Instrumentation & Measurement Societies. During that period he built an electron spin resonance spectrometer for the pleasure of studying the electron and free radicals. By chance he was invited by Dr. Yves Lion of the Physics Institute of the University of Liège to help them for a few weeks in their researches on the photoionisation mechanism of the tryptophan amino-acid with the powerful EPR spectrometer. He was also interested in TV satellite reception and Meteosat images. He built several microwave microstrip circuits such as an 18 dB

low noise amplifier using GaAs-Fets for 11.34 GHz. He also developed some apparatus using microprocessors for a digital storage system for Meteosat's images.

In 1990 he became a civil servant in the Metrology Department of the Transmission Laboratories of Belgacom (Belgium Telephone Company). His job was to test the synchronization of rubidium frequency standards on a distant master ceasium beam clock. It is there that he took the time to compare the phase of distant ceasium clocks and discovered the periodic phase shift signal with a sidereal day period. De Witte retired from the Department, reporting that he had been dismissed, and worked on theoretical physics and philosophy of science, while performing various cheap experiments to test his electron theory and also develop a new working process for a beamless ceasium clock.

De Witte acknowledged assistance from J. Tamborijn, the Engineer Cerfontaine, and particularly Engineer and Executive Director B. Daspremont, all from the Metrology, Fiber Optics and Transmission Laboratory of Belgacom in Brussels, for the use of the six caesium atomic clocks, the comparators, the recorder and the underground lines, and also Paul Pàquet, Director of the Royal Observatory of Belgium, for explanations and documentation provided about the realisation of UTC in Belgium.

4 De Witte's letter

Roland De Witte was not able to have his experimental results published in a physics journal. His only known publications are that of an e-mail posted to the newsgroup sci.physics.research. The e-mail is reproduced here:

> * Subject: Ether-wind detected!
> * From: "DE WITTE Roland" <roland.dewitte@ping.be>
> * Date: 07 Dec 1998 00:00:00 GMT
> * Approved: baez@math.ucr.edu
> * Newsgroups: sci.physics.research
> * Organization: EUnet Belgium, Leuven, Belgium
>
> I have performed an interesting experiment with cesium beam frequency standards.
>
> A 5 Mhz signal from one clock (A) is sent to another clock (B) 1.5 km apart in Brussels by the use of an underground coaxial cable of the Belgium Telephone Company. There, the 5Mhz signal from clock A is compared to the one of clock B, by the use of a digital phase comparator (like those used in PLL).
>
> Incredibly, the output of the phase comparator shows a clear and important sinus-like undulation which permits to conclude of the existence of a periodic variation (24 h period) of the speed of light in the coaxial cable around 500 km/s.
>
> In performing the experiment during 178 days, with six caesium beam clocks, the period of the phase signal has been accurately measured and is 23 h 56 m $\pm$25 s. and thus is the sidereal day.
>
> This result, like the one of D. G. Torr and P. Kolen (Natl. Bur. Stand. (U.S.), Spec. Publ. 617, 1984) is well understood with a new space-time theory based on a new electron theory.
>
> It is also the case for the nearly negative result of the experiment of Krisher et al., with a fiber optics instead of a coaxial cable (Physical Review D, Vol. 42, Number 2, 1990, pp. 731–734).
>
> All the details of the experiment is on my web-site under construction: www.ping.be/electron/belgacom.htm together with already a few arguments against Einstein's special theory of relativity.
>
> DE WITTE Roland
> www.ping.be/electron
>
> [Moderator's note: needless to say, there are many potential causes of daily variations that need to be studied in interpreting an experiment of this sort. — jb]

5 Conclusions

The De Witte experiment was truly remarkable considering that initially it was serendipitous. DeWiite's data like that of Miller is extremely valuable and needs to be made available for detailed analysis. Regrettably Roland De Witte has died, and the bulk of the data was apparently lost when he left Belgacom.

References

1. Michelson A. A. and Morley E. W. *Philos. Mag.*, 1887, S. 5, v. 24, No. 151, 449–463.
2. Cahill R. T. and Kitto K. Michelson-Morley experiments revisited. *Apeiron*, 2003, v. 10(2), 104–117.
3. Cahill R. T. The Michelson and Morley 1887 experiment and the discovery of absolute motion. *Progress in Physics*, 2005, v. 3, 25–29.
4. Miller D. C. *Rev. Mod. Phys.*, 1933, v. 5, 203–242.
5. Illingworth K. K. *Phys. Rev.*, 1927, v. 3, 692–696.
6. Joos G. *Ann. d. Physik* 1930, Bd. 7, 385.
7. Jaseja T. S. *et al. Phys. Rev. A*, 1964, v. 133, 1221.
8. Torr D. G. and Kolen P. *Precision Measurements and Fundamental Constants*, Taylor B. N. and Phillips W. D. eds. Natl. Bur. Stand. (U.S.), Spec. Pub., 1984, v. 617, 675.
9. Cahill R. T. Process Physics: From information theory to quantum space and matter. Nova Science Pub., NY, 2005.
10. Cahill R. T. Absolute motion and gravitational effects. *Apeiron*, 2004, v. 11, 53–111.
11. Cahill R. T. Dynamical fractal 3-Space and the generalised Schrödinger equation: Equivalence principle and vorticity effects. *Progress in Physics*, 2006, v. 1, 27–34.

Effect of Alpha-Particle Energies on CR-39 Line-Shape Parameters using Positron Annihilation Technique

M. A. Abdel-Rahman*, M. Abdel-Rahman*, M. Abo-Elsoud†, M. F. Eissa†, Y. A. Lotfy*, and E. A. Badawi*

*Physics Department, Faculty of Science, Minia University, Egypt
†Physics Department, Faculty of Science, Beni-suef University, Egypt
E-mail: maboelsoud24@yahoo.com <M. Abo-Elsoud>; emadbadawi@yahoo.com <E. A. Badawi>

Polyally diglycol carbonate "CR-39" is widely used as etched track type particle detector. Doppler broadening positron annihilation (DBPAT) provides direct information about core and valance electrons in (CR-39) due to radiation effects. It provides a non-destructive and non-interfering probe having a detecting efficiency. This paper reports the effect of irradiation α-particle intensity emitted from ^{241}Am (5.486 MeV) source on the line shape S- and W-parameters for CR-39 samples. Modification of the CR-39 samples due to irradiation were studied using X-ray diffraction (XRD) and scanning electron microscopy (SEM) techniques.

1 Introduction

Polyallyl diglycol carbonate ($C_{12}H_{18}O_7, \rho = 1310\,kg/m^3$) is a thermoset polymer [1]. Polyallyl diglycol carbonate, CR-39, has been used in heavy ion research such as composition of cosmic rays, heavy ion nuclear reactions, radiation dose due to heavy ions, exploration of extra heavy elements etc. Its availability in excellent quality from different manufactures is also an advantage for further applications [1].

Swift heavy ions (SHI) produce permanent damage in polymeric materials as latent tracks along their path due to dissociation of valence bonds, cross linking and formation of free radicals [2, 3].

Positron Annihilation Technique (PAT) has been employed for the investigating Polymorphism in several organic materials [4] and it has emerged as a unique and potent probe for characterizing the properties of polymers [5]. In PAT, the positron is used as a nuclear probe which is repelled by the ion cores and preferentially localized in the atomic size free-volume holes [6] of the polymeric material. The motion of the electron-positron pair causes a Doppler shift on the energy of the annihilation radiation. As a consequence, the line-shape gives the distribution of the longitudinal momentum component of the annihilating pair. Positron Annihilation Doppler Broadening Spectroscopy (PADBS) is a well established tool to characterize defects [7]. The 0.511 MeV peak is Doppler broadened by the longitudinal momentum of the annihilating pairs. Since the positrons are thermalized, the Doppler broadening measurements provide information about the momentum distributions of electrons at the annihilation site.

Essentially all prior Doppler broadening measurements [8, 9] have been performed using either slow positron beams or wide-energy-spectrum positron beams from radioactive sources. Two parameters S (for shape), and W (for wings) [10] are usually used to characterize the annihilation peak. The S-parameter is more sensitive to the annihilation with low momentum valence and unbound electrons. The S-parameter defined by Mackenzie et al. [11] as the ratio of the integration over the central part of the annihilation line to the total integration. Diffraction peaks are analyzed through common fitting procedures, which result in parameters like the center of gravity and the width of the distribution. The W-parameter is more sensitive to the annihilation with high momentum core electrons and is defined as the ratio of counts in the wing regions of the peak to the total counts in the peak.

Fig. 1 shows Doppler broadening line-shape from which the S- and W-parameters are calculated using the following equations:

$$S = \frac{\int_{xc-g1}^{xc+g1} y(x)dx}{area},$$

$$W = \frac{\int_{xc-g3}^{xc-g2} y(x)dx + \int_{xc-g2}^{xc-g3} y(x)dx}{area},$$

where $area = \int_{g\,\min}^{g\,\max} y(x)dx$, and xc is the center of the peak.

In this regard, the main goal of the positron annihilation technique experiments is to point out the CR-39 line-shape parameters resulting from the effect of α-particle energies.

2 Experimental technique

Track detectors "CR-39" were normally irradiated in air by different α-particle energies with different fluxes from 1476.42 particles/cm^2 at 1.13 MeV to 48130.25 particles/cm^2 at 4.95 MeV from 0.1 μCi ^{241}Am source. Collimators of different thickness were used to change the α-particle energy.

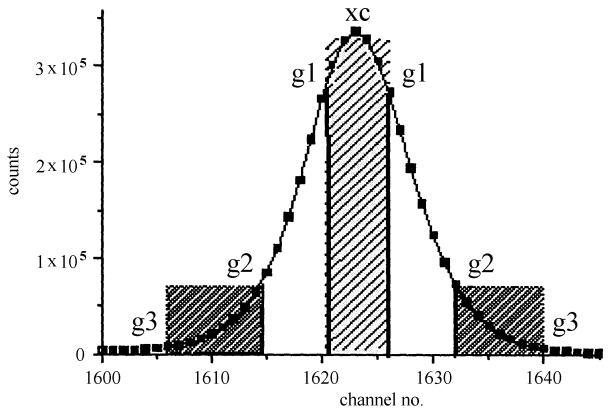

Fig. 1: Definition of the S- and W-parameters [12] (note, that the limits $g1$, $g2$, $g3$ are arbitrary to a certain degree, but have to be the same for all annihilation lines analyzed).

After irradiations, the samples were etched in 6.25 M NaOH solution at 70°C for 6 hr.

The simplest way to guide the positrons into the samples is to use a sandwich configuration as shown in Fig. 2. ^{22}Na is the radioactive isotope used in our experiment.

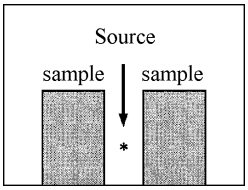

Fig. 2: Sandwich configuration of the positron source respect to a pair of specimen.

The positron source of 1mCi free carrier ^{22}NaCl was evaporated from an aqueous solution of sodium chloride and deposited on a thin Kapton foil of 7.5 μm in thickness. The ^{22}Na decays by positron emission and electron capture (E. C.) to the first excited state (at 1.274 MeV) of ^{22}Na. This excited state de-excites to the ground state by the emission of a 1.274 MeV gamma ray with half life $T_{1/2}$ of 3×10^{-12} sec. The positron emission is almost simultaneous with the emission of the 1.274 MeV gamma ray while the positron annihilation is accompanied by two 0.511 MeV gamma rays. The measurements of the time interval between the emission of 1.274 MeV and 0.511 MeV gamma rays can yield the lifetime τ of positrons. The source has to be very thin so that only small fractions of the positron annihilate in the source.

The system which has been used to determine the Doppler broadening S-and W-parameters consists of an Ortec HPGe detector with an energy resolution of 1.95 keV for 1.33 MeV line of ^{60}Co, an Ortec 5 kV bais supply 659, Ortec amplifier 575 and trump 8 k MCA. Fig. 3 shows a schematic diagram of the experimental setup. Doppler broadening is caused by the distribution of the velocity of the annihilating electrons in the directions of gamma ray emission. The signal coming from the detector enters the input of the preamplifier and the output from the preamplifier is fed to the amplifier. The

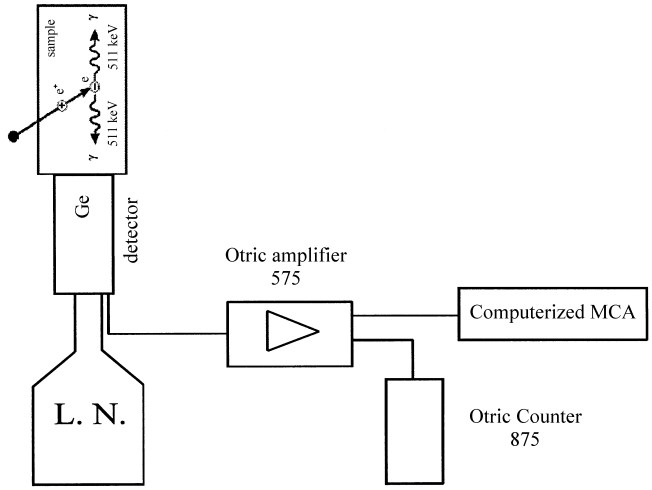

Fig. 3: Block diagram of HPGe-detector and electronics for Doppler broadening line-shape measurements.

input signal is a negative signal. The output signal from the amplifier is fed to a computerized MCA. All sample spectra are acquired for 30 min.

3 Results and discussion

3.1 Positron annihilation measurements

Fig. 4 shows the Doppler broadening line shape parameters measured for unirradiated and irradiated CR-39 samples at α-particle energies of 2.86 and 4.86 MeV. The measured line-shape profiles reveal similar line-shape counts for samples (unirradiated and irradiated with α-particle energy, i. e. 4.86 MeV). A minimum line-shape counts are obtained at 2.86 MeV. The other observation is that the Full Width at Half Maximum (FWHM) for 2.86 MeV irradiated sample is more broadening than others. From such behavior it is clear that either something happened during irradiation with 2.86 MeV and it recovers again at higher energies or some kind of transition occurs at 2.86 MeV of α-particle energy.

The Doppler broadening line-shape S- and W-parameters are calculated using SP ver. 1.0 program [13] which designed to automatically analyze of the positron annihilation line in a fully automated fashion.

The S- and W-parameters calculated using the previous program were correlated as a function of α-particle energy with different fluxes deposit into CR-39 detector, the results are illustrated in Fig. 5. The S-parameters has values around 46% while values of about 15% are obtained for W-parameters. An abrupt change definitely observed at irradiation energy 2.86 MeV of α-particles for both S- and W-parameters. At this energy a drastically decrease in the S-parameter comparable with a drastically increase in the W-parameter. Values of about 35% and 28% were observed for the S- and W-parameters respectively at 2.86 MeV of α-particle energy.

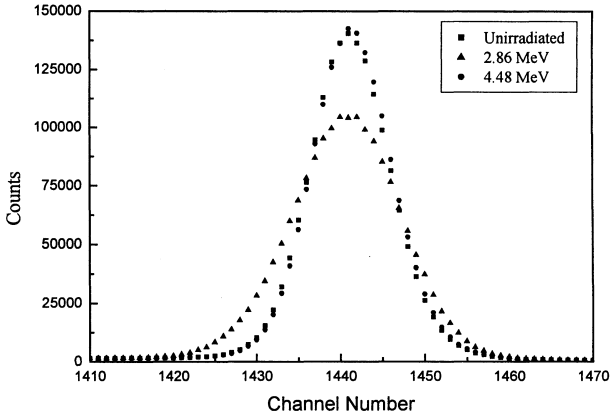

Fig. 4: The line shape spectra of the unirradiated sample and irradiated with α-particle energies of 2.86 and 4.84 MeV.

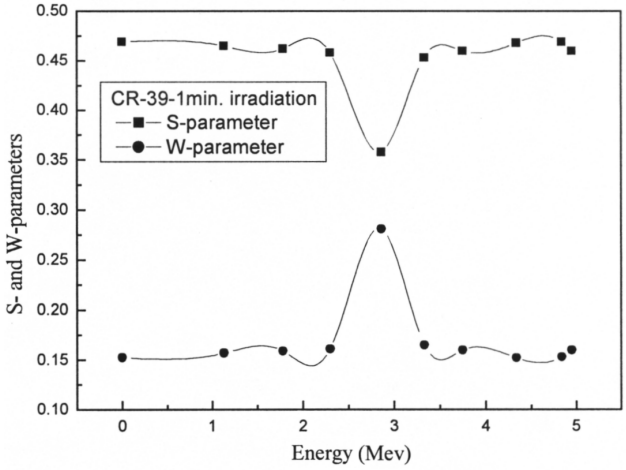

Fig. 5: The behavior of the S- and W-parameters as a function of α-particle energies.

A high concentration of defects, or an increase in the mean size of defects, leads to a larger contribution of annihilation photons from low momentum electrons because positrons are trapped at defects [14]. This is reflected in Doppler broadening measurements by an increase in S-parameter and a decrease in W-parameter. The behavior of S- and W-parameters reveal an abrupt change at the position of the transition. The behavior of the line-shape S- and W-parameters can be related to the different phases. Like many others molecular materials, the use of PAT also proven a very valuable in the study of phase transition in polymers. The same results have been obtained by Schiltz et al. [15]. Walker's et al. [4] measurements have indicated the conversion of one polymorphism to another. Srivastana et al. [16] have investigated polymorphic transitions in DL-norlevcine and hexamethyl benzene.

The transitions in the crystalline phase are related to the lattice transformation from monoclinic to hexagonal and setting in of torsional oscillations in the polymer chain.

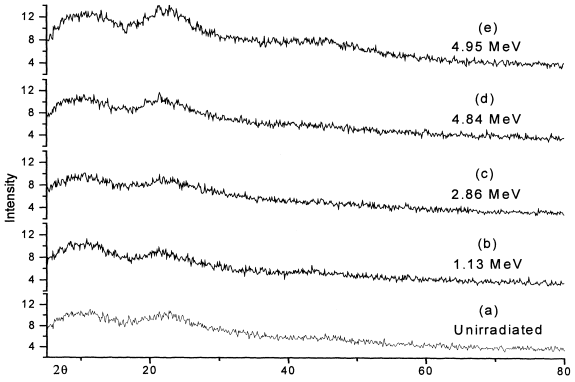

Fig. 6: X-ray diffraction pattern of "CR-39" Polyallyl diglycol carbonate.

3.2 X-ray diffraction pattern (XRD) and Scanning Electron Microscopy (SEM)

The X-ray diffraction analysis was used to obtain information about the transformation as a result of change in α-irradiation intensity. The XRD intensity measurements as a function of diffraction angle (2θ) for unirradiated sample and samples irradiated at different α-particle energies are shown in Fig. 6.

From the X-ray charts it is observed that, an increase in the intensity is obtained at higher α-irradiation intensity 4.84 and 4.95 MeV. At these energies, the XRD chart reveals a new peak that start to appear at 2.86 MeV α-particle energy. The one prominent X-ray peak is located at $2\theta = 21.5^{\circ}$ and it grows up with increasing α-particle energy. The appearance of this peak might be related to phase transition.

A number of papers on the study of polymer show that the amorphous state is altered by structural relaxation and crystallization processes. Positron annihilation behavior in the amorphous state has been described both in terms of topological short range ordering (TSRO) and chemical short-range ordering (CSRO) at the basis of the structural relaxation mechanisms [11, 15, 17–19]. During crystallization the positron behavior is determined by the phase diagram of the amorphous and crystallized system. On our X-ray diffraction patterns might be the first sign of the crystallization onset appears at 2.86 MeV. This sign is increased at higher α-particle energies as shown in the Fig. 6.

The SEM images taken for unirradiated and irradiated CR-39 samples at 4.84 MeV with magnification of 500 are shown in Fig. 7a and b. Tracks are obtained as a result of exposure of α-particle energy. A different magnified (15000) image for one track is shown at Fig. 7c. Cumbrera et al. [19] showed that rings of the structure (metastable structure) were already present in the scanning electron micrographs.

4 Conclusion

Doppler broadening positron annihilation (DBPAT) provides direct information about core and valance electrons in CR-

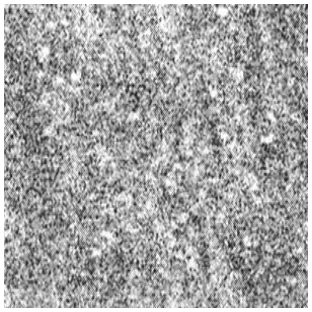

(a) Unirradiated ($M = 500$)

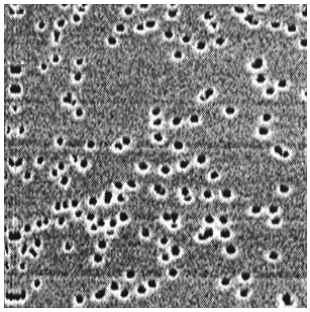

(b) 4.84 MeV ($M = 500$)

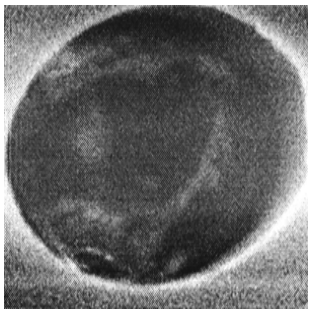

(c) 4.84 MeV ($M = 15\,000$)

Fig. 7: SEM for unirradiated sample and irradiated sample at 4.84 MeV α-particle energies for different magnifications

39 due to radiation effects. The behavior of the S- and W-parameters supports the idea that positrons are trapped by defects and inhomogeneities inherently present in the as-received CR-39 polycarbonate. The annihilation characteristics of positrons are very sensitive to phase transitions. The phase transition in the CR-39 polycarbonate remain complex. XRD pattern and SEM technique of polymers studied in the present work clearly show crystalline and amorphous regions in the samples.

References

1. Rajta I., Baradács E., Bettiol A. A., Csige I., Tökési K., Budai L. and Kiss Á Z. *Nucl. Instr. and Meth. in Phys. Res. B*, 2005, v. 231, 384–388.
2. Myler U., Xu X. L., Coleman M. R. and Simpson P. J. Ion implant-induced change in polimide films monitored by variable energy positron annihilation spectroscopy. *J. Polym. Sci. B. Polym. Phys.*, 1998, v. 36, 2413–2421.
3. Kumar R., Rajguru S., Das D. and Prasad R. *Radiation Measurements*, 2003, v. 36, issues 1–6, 151–154.
4. Walker W. W. and Kline D. C. *J. Chem. Phys.*, 1974, v. 60, 4990.
5. Jean Y. C. In: A. Dupasquier and A. P. Mills Jr., eds., *Positron Spectroscopy of Solids*, IOS Publ., Amsterdam, 1995, 563–569.
6. Schrador D. M., Jean Y. C. (Eds). Positron and positronium chemistry, studies in physical and theoretical. Elsevier, Amsterdam, 1988, v. 57.
7. Dupasquier A., Mills A. P. (Eds.) Positron Spectroscopy of Solids. 1995.
8. Escobar Galindo R., Van Veen A., Alba Garcia A., Schut H., De Hosson J. Th. In: *Proc. of the Twelfth Conf. on Positron Annihilation*, 2000, 499.
9. Hori F., Oshima R. In: *Proc. of the Twelfth Conf. on Positron Annihilation*, 2000, 204.
10. Urban-Klaehen J. M., Quarles C. A. *J. Appl. Phys.*, 1989, v. 86, 355.
11. Mackenzie I. K., Eady J. A. and Gingerich R. R. *Phys. Lett. 33A*, 1970, 279.
12. Priesmeyer H. G., Bokuchava G. *Applied Radiation and Isotopes*, 2005, v. 63, 751–755.
13. http://www.ifj.edu.pl/∼mdryzek.
14. Osipowicz A., Harting M., Hempel M., Britton D. T., Bauer-Kugelmann W., Triftshauser W. *Appl. Surf. Sci.*, 1999, v. 149, 198.
15. Schiltz A., Liolios A., Dalas M. In: *Proc. of the 7th Int. Conf. on Positron Annihilation*, New Delhi, 1985.
16. Srivastana P. K., Singh K. P. and Jain P. C. *Solid state comun.*, 1986, v. 58, 147.
17. Tsumbu M., Segers D., Dorikend M. and Dorikens-Vanpraet L. *Rev. Phys. Appl.*, 1985, v. 20, 831–836.
18. Mbungu T., Segers D. In: *Proc. of the 6th Int. Conf. on Positron Annihilation*, Texas, Arlington, 1982.
19. Cumbrera F. L., Millan M., Conde A., *J. Mater. Sci.*, 1982, v. 17, 861.

Planck Particles and Quantum Gravity

Stephen J. Crothers* and Jeremy Dunning-Davies†

*Queensland, Australia; †Department of Physics, University of Hull, England
E-mail: thenarmis@yahoo.com; j.dunning-davies@hull.ac.uk

The alleged existence of so-called Planck particles is examined. The various methods for deriving the properties of these "particles" are examined and it is shown that their existence as genuine physical particles is based on a number of conceptual flaws which serve to render the concept invalid.

1 Introduction

The idea of the so-called Planck particle seems to have been around for quite some time now but has appeared in a number of totally different contexts. It seems to have been used initially as a means of making equations and expressions dimensionless by making use of suitable combinations of the universal constants c, the speed of light, G, Newton's universal constant of gravitation, and finally Planck's constant. As far as the third and final constant is concerned, it has appeared variously as the original h and in the reduced form $\hbar$. The combinations considered were those which ended up with the dimensions of mass or length or time and so, the idea of a "Planck particle" emerged.

Hence, initially the notion seems to have occurred via expressions deduced from dimensional considerations; no mention of an actual "particle" would have been included at this point presumably. Later, however, other arguments were introduced which lead to the same expressions. These included examining the equivalence of the Compton wavelength and Schwarzschild radius of a particle or drawing on results from Special Relativity and Quantum Mechanics. Finally, because the expressions incorporate the Planck constant, which is normally associated with quantum phenomena, and both the speed of light and the universal constant of gravitation, which are often associated with relativistic and gravitational phenomena, these "particles" seem to have been elevated to a position of importance and even physical reality which is difficult to justify.

Here the various methods of determining the expressions for the various physical quantities, such as mass and length, of these so-called Planck "particles" will be examined, before some conclusions about the actual "particles" themselves — including their physical existence — will be discussed.

2 The "Planck" quantities

(a) Dimensional analysis

Using the fundamental ideas of dimensional analysis allows the derivation of the Planck mass, Planck length, and all the other Planck quantities to be accomplished very easily. Taking c, G and h as the three basic quantities, the expression for the Planck mass is found easily by putting

$$\left(LT^{-1}\right)^{\alpha}\left(ML^2T^{-1}\right)^{\beta}\left(M^{-1}L^3T^{-2}\right)^{\gamma}=M\,,$$

where $\left(LT^{-1}\right)$, $\left(ML^2T^{-1}\right)$, $\left(M^{-1}L^3T^{-2}\right)$ are the dimensions of c, G and h respectively. Equating coefficients immediately gives

$$\text{Planck mass}\equiv\sqrt{\frac{ch}{G}}\,.$$

Similar manipulations give

$$\text{Planck length}\equiv\sqrt{\frac{hG}{c^3}}\quad\text{and}\quad\text{Planck time}\equiv\sqrt{\frac{hG}{c^5}}\,.$$

It is easy to see how expressions such as these could prove useful in making equations dimensionless and so more suitable for numerical work. However, the derivation of these expressions is seen to have been accomplished by a purely mathematical exercise; absolutely no physical argument has been involved!

(b) Compton wavelength and Schwarzschild radius

Another derivation involves the consideration of a body whose Compton wavelength equals its Schwarzschild or gravitational radius [1]. Immediately, this equivalence leads to

$$\frac{h}{mc}=\frac{2Gm}{c^2}\,,$$

from which it follows that

$$m=\sqrt{\frac{hc}{2G}}\,.$$

Corresponding expressions for the Planck length and Planck time follow easily and it is seen that the ratio of Planck mass to Planck length equals $c^2/2G$, which would make such a body, if it truly existed, a Michell-Laplace dark body or a Schwarzschild black hole.

However, the expressions derived by this route are seen to involve an extra figure two. This apparent little problem is overcome by using $\hbar$ instead of h in the dimensional analysis approach and by putting the Compton wavelength equal to π multiplied by the Schwarzschild or gravitational radius in the approach. Since the equivalence is purely arbitrary, introducing an extra arbitrary factor of π is not really a problem.

(c) The quantum/relativity approach

This approach makes use of the Heisenberg uncertainty principle [2]. The starting point is provided by the introduction of a Planck time, t_p, for which quantum fluctuations are felt to exist on the scale of the Planck length which is defined to be equal to $\ell_p = ct_p$. If a Planck density is denoted by ρ_p, a Planck mass may then be $m_p \cong \rho_p \ell_p^3$. Then, using Heisenberg's uncertainty principle in the form

$$\Delta E\, \Delta t \cong m_p c^2 t_p \cong \rho_p \left(ct_p\right)^3 c^2 t_p \cong \frac{c^5 t_p^4}{G t_p^2} \cong \hbar\,,$$

leads to

$$t_p \cong \sqrt{\frac{\hbar G}{c^5}} \cong 5.4{\times}10^{-44}\ \text{sec}\,.$$

Here the reduced Planck constant, $\hbar$, has been used as is more usual. The expressions for both the Planck mass and Planck length follow easily and their numerical values are

$$m_p \cong 2.2{\times}10^{-8}\ \text{kg} \quad \text{and} \quad \ell_p \cong 1.6{\times}10^{-35}\ \text{m}$$

respectively, where the value of the reduced Planck constant has been used.

These are the three basic properties associated with these so-called Planck "particles". It is quite common to note also that the corresponding Planck energy and Planck temperature are then given by

$$E_p = m_p c^2 \cong \sqrt{\frac{\hbar c^5}{G}} \cong 1.2{\times}10^{19}\ \text{GeV}$$

and

$$T_p = \frac{E_p}{k} \cong \sqrt{\frac{\hbar c^5}{G k^2}} \cong 1.4{\times}10^{32}\ \text{K}\,.$$

3 Planck particles as black holes

The arbitrary equality of the Compton wavelength to the alleged "Schwarzschild radius" has resulted in the claim that the so-called Planck particles are black holes. This conclusion is inadmissible for a number of reasons.

The expression

$$R = \frac{2Gm}{c^2}, \tag{1}$$

describes the Michell-Laplace dark body, a theoretical astronomical object having an escape velocity equal to that of light. This expression can be generalised to

$$R \leqslant \frac{2Gm}{c^2}, \tag{2}$$

to include escape velocities greater than that of light.

The radius R described by (1) and (2) is Euclidean, and therefore measurable in principle. The Compton wavelength is also measurable in principle because it too is Euclidean. However, (1) is routinely claimed to be the "Schwarzschild radius", the radius of the event horizon of the alleged black hole. (1) is also claimed to show that the escape velocity associated with a black hole is the velocity of light. Actually this is false. An alleged black hole has no escape velocity since it is claimed also that neither material object nor light may leave the event horizon. On the other hand, an escape velocity does not mean that a material object having an initial velocity less than the escape velocity cannot leave the surface of a gravitating body. A material object possessing an initial velocity less than the escape velocity may leave the surface of the host object, travel radially outward to a finite distance where it comes to rest momentarily before falling radially backwards to the host. If the escape velocity is the velocity of light, then light itself may leave the surface and travel radially outward to infinity and, therefore, escape. Hence, equation (1) does not specify an escape velocity for the alleged black hole. In truth, black holes have no escape velocity associated with them [3, 4].

Furthermore, in the case of the Michell-Laplace dark body, equation (1) specifies a Euclidean radius, whereas, in the case of the alleged black hole, the Schwarzschild radius is non-Euclidean. Moreover, in principle, R is a measurable length in the Euclidean space of Newton's theory, but in General Relativity R is not measurable in principle. Hence equating the Euclidean Compton wavelength to R given by (1) is conceptually flawed. In addition, in Einstein's gravitational field there are two radii — the proper radius and the radius of curvature. These are the same only in the infinitely far field where space-time is asymptotically Minkowski, (that is, pseudo-Euclidean) where the radii coalesce to become identical because, in Euclidean space, the radius of curvature and the proper radius are identical. Therefore, when the Compton wavelength is equated to (1) in the context of the black hole, which non-Euclidean Einstein radius does R specify?

It has been shown [5, 6] that when (1) is interpreted in terms of Einstein's gravitational field, the Schwarzschild radius R is actually the invariant radius of curvature of the fictitious point-mass, which corresponds to an associated invariant proper radius of zero. In ignorance of the fact that Einstein's gravitational field yields two different radii, physicists erroneously interpret R in equation (1) as a proper radius in Einstein's gravitational field and, therefore, allow it to go to zero, which is false! In their conception of R as

a proper radius they also treat R as a measurable quantity in Einstein's gravitational field, as it is in Euclidean space, which is also false!

Hence, even if the equality of the Compton wavelength to the gravitational radius of curvature of a point-mass could be admitted, the alleged Planck particles would necessarily be point-masses, which are not only fictitious but also contradict the very meaning of the Compton wavelength and, indeed, the foundations of Quantum Mechanics. However, there can be no meaning to the equality of a measurable Euclidean length to an immeasurable non-Euclidean length to begin with. Not only that, there can be no meaning to the equality of a Euclidean length which is both the proper radius and the radius of curvature in Euclidean space and a non-Euclidean radius of curvature, which is not the same as the corresponding non-Euclidean proper radius. Consequently, claims that Planck particles are black holes are false, even if black holes actually exist. It might well be noted at this juncture that General Relativity, contrary to widespread claims, doesn't even predict the existence of black holes [5, 6].

Planck particles are presumed to be able to interact with one another. However, the black hole is allegedly derived from a solution to Einstein's gravitational field for a "point-mass". Therefore, the black hole is the result of a solution involving a *single* gravitating body interacting with a "test particle". It is *not* the result of a solution involving the gravitational coupling of two comparable masses. Since there are no known solutions to Einstein's field equations for multi-body configurations and since it is not even known if Einstein's field equations admit multi-body configurations [3], all conceptions of black hole interactions are meaningless. Consequently, Schwarzschild radius Planck particle interactions are also meaningless.

The claim that Planck particles were prolific during the early Universe but are now extremely rare is also erroneous. This follows since it has been proved that cosmological solutions to Einstein's field equations for isotropic type 1 Einstein spaces, from which the expanding Universe and the Big Bang have allegedly been derived, do not even exist.[7].

4 Comments and conclusions

Above, three ways of deducing expressions for the so-called Planck quantities have been outlined. In many ways, the first method indicates a good idea of the physical standing for the so-called Planck "particles". This first method is purely a mathematical manipulation of three man-made constants. At the end of the day, all numbers originate in a man-made model and so these three numbers, although assigned a seemingly exalted status as universal constants, are still members of that group of man-made objects. As mentioned already, the first method contains no physics and makes absolutely no pretensions to contain any. The second and third derivations, on the other hand, do seem to contain some physics as a basis for what follows. However, closer examination casts real doubt on this initial feeling. What physical basis is there in asserting the equivalence of the Compton wavelength and the Schwarzschild or gravitational radius of a particle? If one believes modern ideas, this merely asserts that the said particle is a "Schwarzschild black hole", and does so from the outset. The second of these two is simply a mathematical manipulation of symbols using Heisenberg's uncertainty principle as a starting point. The manipulations, as such, are reasonable enough, but is it valid to then make physical assertions about "particles" whose very existence depends only on these mathematical manipulations?

The alleged link between Quantum mechanics and General Relativity via the interpretation of the Compton wavelength as a Schwarzschild radius is clearly seen to be false. All that remains is an interpretation of Planck particles via equation (1) as it relates to the Michell-Laplace dark body radius. In this case, one may say only that the escape velocity associated with a Planck particle is the velocity of light in the flat three-dimensional Euclidean space of Newton. Of course, the Planck particles are thereby robbed of their more mysterious relativistic qualities and their primordial profusion. Black hole creation in the collision of a high energy photon with a particle and concomitant digestion of the photon is fallacious. Likewise there is no possibility of micro black holes being formed by fermion collision in particle accelerators.

There can be little doubt that Planck "particles" originated purely out of mathematical manipulations and there seems no reason to suppose that they exist or ever have existed as genuine physical particles. It is for that reason that it is worrying to see these objects being assigned an actual physical role in models of the early universe. Most books on this subject seem to regard Planck "particles" as genuine particles — mini black holes — which existed in large numbers during the very early stages of the formation of the universe but are now thought to be extremely rare, if not actually extinct. The grounds for this belief seem very shaky and it is claimed, for example, that the decay of a single Planck "particle" could lead to the production of 5×10^{18} baryons [1]. It is also claimed that theory as presently available doesn't allow examination back beyond a time of approximately 10^{-43} seconds, the Planck "time" because, beyond that time, a theory of quantum gravity would be necessary. Hence, this time is effectively regarded as an actual barrier between the quantum and non-quantum world. Why? The relevance of this question lies in the fact that it is a purely arbitrary figure. The fact that it and the other Planck quantities depend on the reduced Planck constant, which is regarded as being a quantity associated with quantum mechanics, and the speed of light and the universal constant of gravitation, which are associated with relativistic and gravitational phenomena, is something which comes out of human choice not something which occurs naturally. It is

interesting that quantities which have the dimensions of mass, length and time may be constructed from these three constants which appear so frequently in so many areas of theoretical science but that is all it is — interesting! It is not, at least as far as current scientific knowledge is concerned, any more significant than that. Playing around with numbers and combinations of numbers can be very fascinating but, if attempts are made to assign physical reality to the outcomes of such mathematical diversions, scientific chaos could, and probably will, ensue!

References

1. Hoyle F., Burbidge G., Narlikar J. A different approach to cosmology. Cambridge University Press, 2000.
2. Coles P., Lucchin F. Cosmology. John Wiley & Sons.
3. McVittie G. C. Laplace's alleged "black hole". *The Observatory*, v. 98, 1978, 272; http://www.geocities.com/theometria/McVittie.pdf.
4. Crothers S. J. A brief history of black holes. *Progress in Physics*, 2006, v. 2, 54–57.
5. Abrams L. S. Black holes: the legacy of Hilbert's error. *Can. J. Phys.*, 1989, v. 67, 919; arXiv: gr-qc/0102055.
6. Crothers S. J. On the general solution to Einstein's vacuum field and it implications for relativistic degeneracy. *Progress in Physics*, 2005, v. 1, 68–73.
7. Crothers S. J. On the general solution to Einstein's vacuum field for the point-mass when $\lambda \neq 0$ and its consequences for relativistic cosmology. *Progress in Physics*, 2005, v. 3, 7–14.

The Quantum Space Phase Transitions for Particles and Force Fields

Ding-Yu Chung* and Volodymir Krasnoholovets†

*P.O. Box 180661, Utica, Michigan 48318, USA
†Institute for Basic Research, 90 East Winds Court, Palm Harbor, FL 34683, USA
E-mail: chung@wayne.edu; v_kras@yahoo.com

We introduce a phenomenological formalism in which the space structure is treated in terms of attachment space and detachment space. Attachment space attaches to an object, while detachment space detaches from the object. The combination of these spaces results in three quantum space phases: binary partition space, miscible space and binary lattice space. Binary lattice space consists of repetitive units of alternative attachment space and detachment space. In miscible space, attachment space is miscible to detachment space, and there is no separation between attachment space and detachment spaces. In binary partition space, detachment space and attachment space are in two separate continuous regions. The transition from wavefunction to the collapse of wavefuction under interference becomes the quantum space phase transition from binary lattice space to miscible space. At extremely conditions, the gauge boson force field undergoes a quantum space phase transition to a "hedge boson force field", consisting of a "vacuum" core surrounded by a hedge boson shell, like a bubble with boundary.

1 The origin of the space structure

The conventional explanation of the hidden extra space dimensions is the compactization of the extra space dimensions. For example, six space dimensions become hidden by the compactization, so space-time appears to be four dimensional. Papers [1, 2] propose the other explanation of the reduction of >4D space-time into 4D space-time by slicing >4D space-time into infinitely many 4D slices surrounding the 4D core particle. Such slicing of >4D space-time is like slicing 3-space D object into 2-space D object in the way stated by Michel Bounias as follows: "You cannot put a pot into a sheet without changing the shape of the 2-D sheet into a 3-D dimensional packet. Only a 2-D slice of the pot could be a part of sheet".

This paper proposes that the space structure for such reduction of >4D space-time can also be derived from the cosmic digital code [3, 4], which one can consider as "the law of all laws". The cosmic digital code consists of mutually exclusive attachment space and detachment space. Attachment space attaches to an object, while detachment space detaches from the object. The cosmic digital code is analogous to two-value digital code for computer with two mutually exclusive values: 1 and 0, representing *on* and *off*. In terms of the cosmic digital code, attachment space and detachment space are represented as 1 and 0, respectively. The object with >4D space-time attaches to >4D attachment space, which can be represented by

$(i\ 1_{3+k})_m$ as $>$ 4D attachment space with m repetitive units of time (i) and $3+k$ space dimension.

The slicing of >4D attachment space is through 4D detachment space, represented by

$(i\ 0_3)_n$ as detachment space with n repetitive units of time (i) and three space dimension.

The slicing of >4D attachment space by 4D detachment space is the space-time dimension number reduction equation as follows

$$\underbrace{(i\ 1_{3+k})_m}_{\text{4D attachment space}} \xrightarrow{slicing} \underbrace{(i\ 1_3)_m}_{\text{4D core attachment space}} + \underbrace{\sum_{k=1}^{k}((i\ 0_3)\ (i\ 1_3))_{n,k}}_{k\text{ types 4D slices}} \quad (1)$$

The two products of the slicing are the 4D-core attachment space and 4D slices represented by n repetitive units of alternative 4D attachment space and 4D detachment space. They are k types of 4D slices, representing the total number of space dimensions greater than three-dimensional space. For example, the slicing of 10D attachment space produces 4D core attachment space and six types of 4D slices. The value of n approaches to infinity for infinitely many 4D slices.

The core attachment space surrounded by infinitely many 4D slices corresponds to the core particle surrounded by infinitely many small 4D particles. Gauge force fields are made of such small 4D particles surrounding the core particle. The space with repetitive units (of alternative attachment space and detachment space) is binary lattice space.

The combination of attachment space (1) and detachment space (0) results in three quantum space phases: miscible space, binary partition space, or binary lattice space for four-dimensional space-time.

$$\begin{array}{l}(1_4)_n \text{ attachment space} + (0_4)_n \text{ detachment space}\\ \overset{combination}{\longrightarrow} \text{ three quantum space phases:}\\ (1_4\ 0_4)_n \text{ binary lattice space, miscible space, or}\\ (1_4)_n\,(0_4)_n \text{ binary partition space.}\end{array} \tag{2}$$

Binary lattice space consists of repetitive units of alternative attachment space and detachment space. In miscible space, attachment space is miscible to detachment space, and there is no separation of attachment space and detachment space. In binary partition space, detachment space and attachment space are in two separate continuous regions.

2 The quantum space phase transition for particles

Binary lattice space, $(1_40_4)_n$, consists of repetitive units of alternative attachment space and detachment space. Thus, binary lattice space consists of multiple quantized units of attachment space separated from one another by detachment space. Binary lattice space is the space for wavefunction, which thus appears as not an abstract entity but a real one filled with a substance, that is in line with works [5, 6]. In wavefunction

$$|\psi\rangle \;=\; \sum_{i=1}^{n} c_i|\,\phi_i\rangle \tag{3}$$

each individual basis element $|\phi_i\rangle$ attaches to attachment space, and separates from the adjacent basis element by detachment space. Detachment space detaches from object. Binary lattice space with n units of four-dimensional, $(1_40_4)_n$, contains n units of basis elements.

Detachment space contains no object that carries information. Without information, detachment space is outside of the realm of causality. Without causality, distance (space) and time do not matter to detachment space, resulting in non-localizable and non-countable space-time. The requirement for the system (binary lattice space) containing non-localizable and non-countable detachment space is the absence of net information by any change in the space-time of detachment space. All changes have to be coordinated to result in zero net information. This coordinated non-localized binary lattice space corresponds to nilpotent space. All changes in energy, momentum, mass, time, space have to result in zero as defined by the generalized nilpotent Dirac equation [7, 8]

$$\begin{aligned}\big(\mp\mathbf{k}\,\partial/\partial t \pm \mathbf{i}\nabla + \mathbf{j}m\big)\big(\pm i\mathbf{k}E \pm \mathbf{ip} + \mathbf{j}m\big)\times\\ \times\exp\big(i(-Et + \mathbf{pr})\big) = 0\,,\end{aligned} \tag{4}$$

where E, $\mathbf{p}$, m, t and $\mathbf{r}$ are respectively energy, momentum, mass, time, space and the symbols ±1, $\pm i$, $\pm\boldsymbol{i}$, $\pm\boldsymbol{j}$, $\pm\boldsymbol{k}$, $\pm\mathbf{i}$, $\pm\mathbf{j}$, $\pm\mathbf{k}$ are used to represent the respective units required by the scalar, pseudoscalar, quaternion and multivariate vector groups. The changes involve the sequential iterative path from nothing (nilpotent) through conjugation, complexification, and dimensionalization. The non-local property of binary lattice space for wavefunction provides the violation of Bell inequalities [9] in quantum mechanics in terms of faster-than-light influence and indefinite property before measurement. The non-locality in Bell inequalities does not result in net new information.

In binary lattice space, for every attachment space, there is its corresponding adjacent detachment space. Thus, a basis element attached to attachment space can never be at rest with complete localization even at the absolute zero degree. The adjacent detachment space forces the basis element to delocalize.

In binary lattice space, for every detachment space, there is its corresponding adjacent attachment space. Thus, no part of the object can be irreversibly separated from binary lattice space, and no part of a different object can be incorporated in binary lattice space. Binary lattice space represents coherence as wavefunction. Binary lattice space is for coherent system.

Any destruction of the coherence by the addition of a different object to the object causes the collapse of binary lattice space into miscible space. The collapse is a quantum space phase transition from binary lattice space to miscible space.

$$\begin{array}{l}\underbrace{\big((0_4)\ (1_4)\big)_n}\\ \text{binary lattice space}\\ \overset{quantum\ space\ phase\ transition}{\longrightarrow} \text{ miscible space.}\end{array} \tag{5}$$

In miscible space, attachment space is miscible to detachment space, and there is no separation of attachment space and detachment space. In miscible space, attachment space contributes zero speed, while detachment space contributes the speed of light. A massless particle is on detachment space continuously, and detaches from its own space continuously. For a moving massive particle, the massive part with rest mass m_0 belongs to attachment space and the other part of the particle mass, which appears due to the motion, induces an additional energy, namely the kinetic energy K, that changes properties of attachment space and leads to the propagation speed v lesser than the speed of light c.

To maintain the speed of light constant for a moving particle, the time (t) in a moving particle has to be dilated, and the length (L) has to be contracted relative to the rest frame

$$\begin{aligned}t &= \frac{t_0}{\sqrt{1 - v^2/c^2}} = t_0\gamma\,,\\ L &= L_0/\gamma\,,\\ E &= K + m_0c^2 = \gamma m_0c^2,\end{aligned} \tag{6}$$

where $\gamma = 1/\sqrt{1-v^2/c^2}$ is the Lorentz factor for time dilation and length contraction, E is the total energy and K is the kinetic energy.

The information in such miscible space is contributed by the combination of both attachment space and detachment space, so detachment space with information can no longer be non-localize. Any value in miscible space is definite. All observations in terms of measurements bring about the collapse of wavefunction, resulting in miscible space that leads to eigenvalue as definite quantized value. Such collapse corresponds to the appearance of eigenvalue E by a measurement operator H on a wavefunction ψ, i. e.

$$H\psi = E\psi\,. \tag{7}$$

Another way for the quantum space phase transition from binary lattice space to miscible space is gravity. Penrose [10] pointed out that the gravity of a small object is not strong enough to pull different states into one location. On the other hand, the gravity of large object pulls different quantum states into one location to become binary partition space. Therefore, a small object without outside interference is always in binary lattice space, while a large object is never in binary latticespace.

3 The quantum space phase transitions for force fields

At zero temperature or extremely high pressure, binary lattice space for a gauge force field undergoes a quantum space phase transition to become binary partition space. In binary partition space, detachment space and attachment space are in two separate continuous regions as follows

$$\underbrace{(1_4)_m + \sum_{k=1}^{k}\big((0_4)\ (1_4)\big)_{n,k}}_{\text{particle gauge boson field in binary lattice space}} \longrightarrow \underbrace{(1_4)_m}_{\text{hedge particle}} + \underbrace{\sum_{k=1}^{k}(0_4)_{n,k}\ (1_4)_{n,k}}_{\substack{\text{hedge boson field in binary}\\ \text{partition space}}} \tag{8}$$

The force field in binary lattice space is a gauge boson force field, the force field in binary partition space is denoted as a *hedge boson force field*. The detachment space in hedge boson field is a "vacuum" core, while hedge bosons attached to attachment space form the hedge boson shell. Gauge boson force field has no boundary, while the attachment space in the binary partition space acts as the boundary for hedge boson force field. Hedge boson field is like a bubble with core vacuum surrounded by membrane where hedge bosons locate.

Hedge boson force is incompatible to gauge boson force field. The incompatibility of hedge boson force field and gauge boson force field manifests in the Meissner effect, where superconductor repels external magnetism. The energy (stiffness) of hedge boson force field can be determined by the penetration of boson force field into hedge boson force field as expressed by the London equation for the Meissner effect

$$\nabla^2 H = -\lambda^{-2} H\,, \tag{9}$$

where H is an external boson field and λ is the depth of the penetration of magnetism into hedge boson shell. Eq. (9) indicates that the external boson field decays exponentially as it penetrate into hedge boson force field.

The Meissner effect is the base for superconductivity. It is also the base for gravastar, an alternative to black hole [11–13]. Gravastar is a spherical void as Bose-Einstein condensate surrounded by an extremely durable form of matter. This paper proposes gravastar based on hedge boson field.

Before the gravitational collapse of large or supermassive star, the fusion process in the core of the star to create the outward pressure counters the inward gravitational pull of the star's great mass. When the core contains heavy elements, mostly iron, the fusion stops. Instantly, the gravitational collapse starts. The great pressure of the gravity collapses atoms into neutrons. Further pressure collapses neutrons to quark matter and heavy quark matter.

Eventually, the high gravitational pressure transforms the gauge gluon force field into the hedge gluon force field, consisting of a vacuum core surrounded by a hedge gluon shell, like a bubble. The exclusion of gravity by the hedge gluon force field as in the Meissner effect prevents the gravitational collapse into singularity. To keep the hedge gluon force field from collapsing, the vacuum core in the hedge gluon force field acquires a non-zero vacuum energy whose density (ρ) is equal to negative pressure (P). The space for the vacuum core becomes de Sitter space. The vacuum energy of the vacuum core comes from the gravitons in the exterior region surrounding the hedge gluon force field as in the Chapline's dark energy star. The external region surrounding the hedge gluon force field becomes the vacuum exterior region. Thus, the core of gravastar can be divided into three regions: the vacuum core, the hedge gluon shell, and the vacuum exterior region

$$\begin{aligned} &\text{vacuum core region:} && \rho = -P\\ &\text{hedge gluon shell region:} && \rho = +P\\ &\text{vacuum exterior region:} && \rho = P = 0 \end{aligned} \tag{10}$$

Quarks without the strong force field are transformed into the decayed products as electron-positron and neutrino-antineutrino denoted as the "lepton composite"

$$\text{quarks} \xrightarrow{quark\ decay} \underbrace{e^- + e^+ + \bar{\nu} + \nu}_{\text{the lepton composite}} \tag{11}$$

The result is that the core of the collapsed star consists of the lepton composite surrounded by the hedge gluon field. This lepton composite-hedge gluon force field core constitutes the core for gravastar. The star consisting of the lepton composite-hedge gluon field core (LHC) and the matter shell is "gravastar". The matter shell consists of different layers of matters: heavy quark matter layer, quark matter layer, neutron layer, and heavy element layer one after the other:

$$\begin{array}{l}\text{LHC (lepton composite}\\ \qquad\text{— hedge gluon force field core):}\\ \quad\text{lepton composite region:}\quad \rho = +P\\ \quad\text{vacuum core region:}\quad \rho = -P\\ \quad\text{hedge gluon shell region:}\quad \rho = +P\\ \quad\text{vacuum exterior region:}\quad \rho = P = 0\\ \text{MATTER SHELL}\\ \quad\text{(heavy quark layer}\\ \quad\text{quark layer}\\ \quad\text{neutron layer}\\ \quad\text{heavy element layer):}\quad \rho = +P\end{array} \qquad (12)$$

4 Summary

Thus our formal phenomenological approach allows us to conclude that the quantum space phase transition is the quantum phase transition for space. The approach that is developed derives the space structure from attachment space and detachment space. Attachment space attaches to an object, while detachment space detaches from the object. The combination of attachment space and detachment space results in three quantum space phases: binary partition space, miscible space, or binary lattice space. Binary lattice space consists of repetitive units of alternative attachment space and detachment space. In miscible space, attachment space is miscible to detachment space, and there is no separation of attachment space and detachment space. In binary partition space, detachment space and attachment space are in two separate continuous regions. For a particle, the transition from wavefunction to the collapse of wavefuction under interference is the quantum space phase transition from binary lattice space to miscible space.

At zero temperature or extremely high pressure, gauge boson force field undergoes a quantum space phase transition to "hedge boson force field", consisting of a vacuum core surrounded by a hedge boson shell, like a bubble with boundary. In terms of the quantum space phase, gauge boson force field is in binary lattice space, while hedge boson force field is in binary partition space. The hedge boson force fields include superconductivity and gravastar.

References

1. Bounias M. and Krasnoholovets V. Scanning the structure of ill-known spaces: Part 1. Founding principles about mathematical constitution of space. *Kybernetes: The International Journal of Systems and Cybernetics*, 2003, v. 32 (7/8), 945–975. arXiv: physics/0211096.
2. Bounias M. and Krasnoholovets V. Scanning the structure of ill-known spaces: Part 2. Principles of construction of physical space. *Ibid.*, 2003, v. 32 (7/8), 976–1004. arXiv: physics/0211096.
3. Chung D. The cosmic digital code and quantum mechanics. arXiv: quan-ph/0204033.
4. Chung D. and Krasnoholovets V. The cosmic organism theory. arXiv: physics/0512026.
5. Krasnoholovets V. Submicroscopic deterministic quantum mechanics. *Int. J. Computing Anticipatory Systems*, 2002, v. 11, 164–179. arXiv: quant-ph/0109012.
6. Krasnoholovets V. On the origin of conceptual difficulties of quantum mechanics. In: *Developments in Quantum Physics*, Eds.: F. Columbus and V. Krasnoholovets, 2004, Nova Science Publishers Inc., New York, 85–109. arXiv: physics/0412152.
7. Rowlands P. Some interpretations of the Dirac algebra. *Speculat. Sci. Tech.*, 1996, v. 19, 243–51.
8. Rowlands P. and Cullerne J. P. The Dirac algebra and its physical interpretation, 1994. arXiv: quant-ph/0010094.
9. Bell J. S. On the Einstein-Podolsky-Rosen paradox. *Physics*, 1964, v. 1, 195–199.
10. Penrose R. Wavefunction collapse as a real gravitational effect. In: *Mathematical Physics*, eds: by A. Fokas, A. Grigoryan, T. W. B. Kibble and B. Zegarlinski, 2000, Imperial College, London, 266–282.
11. Mazur P. O. and Mottola E. Gravitational condensate stars: an alternative to black holes. Preprint LA-UR-01-5067, 2001. arXiv: gr-qc/0109035.
12. Mazur P. O. and Mottol E. Gravitational condensate stars. *Proc. Nat. Acad. Sci.*, 2004, v. 111, 9545–9550. arXiv: gr-qc/0407075.
13. Chapline G. Dark energy stars. arXiv: astro-ph/0503200.

Spectral Emission of Moving Atom Exhibits always a Redshift

J. X. Zheng-Johansson

Institute of Fundamental Physics Research, 611 93 Nyköping, Sweden
E-mail: jxzj@iofpr.org

A renewed analysis of the H. E. Ives and G. R. Stilwell's experiment on moving hydrogen canal rays (*J. Opt. Soc. Am.*, 1938, v. 28, 215) concludes that the spectral emission of a moving atom exhibits always a redshift which informs not the direction of the atom's motion. The conclusion is also evident from a simple energy relation: atomic spectral radiation is emitted as an orbiting electron consumes a portion of its internal energy on transiting to a lower-energy state which however has in a moving atom an additional energy gain; this results in a redshift in the emission frequency. Based on auxiliary experimental information and a scheme for de Broglie particle formation, we give a vigorous elucidation of the mechanism for deceleration radiation of atomic electron; the corresponding prediction of the redshift is in complete agreement with the Ives and Stilwell's experimental formula.

1 Introduction

Charged de Broglie particles such as the electron and the proton can be decelerated by emitting electromagnetic radiation. This occurs in all different kinds of processes, including atomic spectral emission produced in laboratory [1, 2] or from celestial processes[3], and charged particle synchrotron radiation [4, 5]. The electromagnetic radiation emission from sources of this type is in common converted from a portion of the *internal energy* or the *mass* of a de Broglie particle involved, which often involves a final state in motion, hence moving source. The associated source-motion effect has except for admitting a relativistic effect connected to high source velocity thus far been taken as no different from the ordinary Doppler effect that consists in a red- or blue-shift depending on the source is moving away or toward the observer. The ordinary Doppler effects are directly observable with moving sources of a "conventional type", like an external-field-driven oscillating electron, an automobile horn, and others, that are externally driven into oscillation which does not add directly to the mass of the source. In this paper we first (Sec. 2) examine the property, prominently an invariable redshift, of moving atom radiation as informed by the hydrogen canal ray experiment [1] of Ives and Stilwell performed at the Bell Labs in 1938 for a thorougher investigation of the associated anomalous Doppler effect then known. Combining with auxiliary experimental information and a scheme for de Broglie particle formation[6], we then elucidate (Secs. 3–5) the mechanism for spectral emission of moving atom, or in essence the underlying (relative) deceleration radiation of moving de Broglie electron, and predict Ives and Stilwell's experimental formula for redshift.

2 Indication by Ives-Stilwell's experiment on fast moving hydrogen atoms

In their experiment on fast moving hydrogen canal ray spectral emission[1], Ives and Stilwell let positively charged hydrogen ions H_i^+ of mass M_{H_i} and charge q_i ($i=2,3$) be accelerated into a canal ray of high velocity, v, across accurately controlled electric potential $\mathscr{V}$ correlated with v through the work-energy relation $q\mathscr{V}=\frac{1}{2}M_{\mathrm{H}_i}v^2$; or

$$v/c = A\sqrt{\mathscr{V}} \tag{1}$$

with c the speed of light, and $A=\sqrt{\frac{2q_i}{c^2 M_{\mathrm{H}_i}}}$. For $\mathscr{V}\sim 6700$–20755 volts, $v\sim 10^6$ m/s as from (1). By neutralization and dissociation the ions are at exit converted to excited atoms that are unstable and will transit to ground state by emitting Balmer spectral lines. The wavelength, λ_r, of the emitted Hβ line is then measured using diffraction grating (Fig. 1a) as a function of $\mathscr{V}$. For a finite v, the spectral line produces a first-diffraction peak at $P(v)$, at distance $y(v)=PO$ from the center O; for a hydrogen at rest, $v=0$, the line has a wavelength $\lambda_{r_0}=4861$ angst. and produces a first peak at P_0, $y_0=P_0O$. These have the geometric relations: $\lambda_r=\frac{\lambda_{r_0}}{y_0}y$, and

$$\Delta\lambda_r=\lambda_r-\lambda'_{r_0}=(\lambda_{r_0}/y_0)(y-y_0) \tag{2}$$

$\Delta\lambda_r$ being the mean displacement of the Doppler lines at a given v. The measured spectrogram, Fig. 1b, informs $y-y_0=B'\sqrt{\mathscr{V}}$ with B' a constant; this combining with (2) is:

$$\Delta\lambda_r/\lambda_{r_0}=(\lambda_r-\lambda'_{r_0})/\lambda_{r_0}=B\sqrt{\mathscr{V}} \tag{3}$$

where $B=B'\lambda_{r_0}/y_0$.

If *assuming*

$$\frac{\Delta\lambda_r}{\lambda_{r_0}}=+\frac{v}{c}, \tag{4}$$

then this and (3) give $\frac{v}{c}=B\sqrt{\mathscr{V}}$. But $\frac{v}{c}$ and $\sqrt{\mathscr{V}}$ must satisfy (1); thus $B\equiv A$; that is (3) writes:

$$\Delta\lambda_r/\lambda_{r_0}=A\sqrt{\mathscr{V}}. \tag{3'}$$

In [1], the two variables $\frac{\Delta\lambda_r}{\lambda_{r_0}}$ and $\sqrt{\mathscr{V}}$ are separately

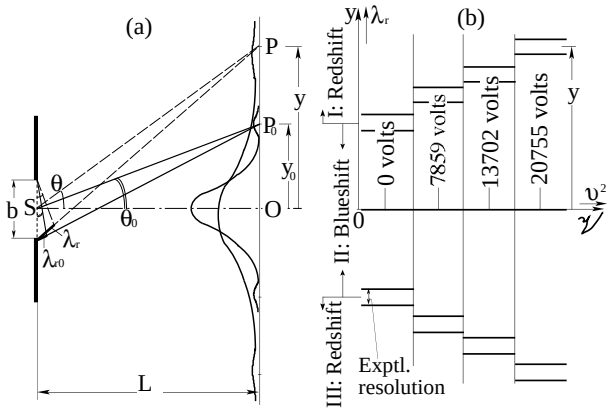

Fig. 1: (a) Schematic single-slit diffraction grating. (b) Experimental spectrogram, peak coordinates $y\,(\propto \lambda_r)$ at several voltages $\mathscr{V}\,(\propto v^2)$, 7859, ..., 20755 volts, after original Fig. of Ref. [1]. Spectral lines at finite $\mathscr{V}$ values all fall in the redshift regions I and III beyond the $\mathscr{V}=0$ ($v^2=0$)-lines illustrated in this plot.

measured and thus given an experimental relation, shown in Fig. 10, of [1, p. 222], which agrees completely with (3′); accordingly (4) is directly confirmed. Furthermore there is a shift of center of gravity of λ'_{r_0} from λ_{r_0}: $\Delta'\lambda_r=\lambda_{r_0}-\lambda'_{r_0}=$ $=\frac{1}{2}(\frac{v}{c})^2$; or $\lambda'_{r_0}=\lambda_{r_0}\left(1-\frac{1}{2}(\frac{v}{c})^2\right)\simeq\lambda_{r_0}\sqrt{1-(v/c)^2}$. With this and (4) in the first equation of (3) or similarly of (2), one gets:

$$\lambda_r=\sqrt{1-(v/c)^2}\,\lambda_{r_0}+(v/c)\lambda_{r_0}; \qquad (5)$$

(5) gives $\lambda_r-\lambda_{r_0}>\frac{v}{c}-\frac{1}{2}(\frac{v}{c})^2\geqslant 0$; or, λ_r is always elongated for $|v|>0$. Furthermore, (4)–(5) are obtained in [1] for both the cases where source and observer move toward and away from each other: The source velocity v is in the fixed $+x$-direction; waves emitted parallel with v (Fig. 2) strike on the diffraction grating D (observer 1) directly (Fig. 2b), and waves antiparallel with v (Fig. 2c) strike on mirror M (observer 2) first and are then reflected to D. That is, (5) is regardless of the direction of the vector c. Therefore from Ives and Stilwell's experiment we conclude:

> The wavelength of spectral line emitted from an atom in motion is always *longer*, or *red-shifted*, than from one at rest, irrespective if the atom is moving away or toward the observer; the faster the atom moves, the longer wavelength its spectral line is shifted to.

This apparently contrasts with the conventional Doppler effect where wavelengths will be $\lambda_r=\lambda_{r_0}(1-v/c)$ and $\lambda_r=$ $=\lambda_{r_0}(1+v/c)$ and show a blue or red shift according to if the source is moving toward or away from the observer.

3 Emission frequency of a moving atom

If a H atom is at rest in the vacuum, its electron, of charge $-e$ in circular motion at velocity u_{n+1} about the atomic nucleus in an excited $n+1$th orbit, has from quantum-mechanical solution (and also solution based on the unification scheme [6]) an eigen energy $\varepsilon_{u.n+1}=-\hbar^2/\left[2m_{e_0}(n+1)^2a_{B_0}^2\right]$, where $n=1,2,\ldots$ and $m_{e_0}=\gamma_0 M_e$, $\gamma_0=1/\left[1-(u_{n+1}/c)^2\right]^{-1/2}$ with u_n being high ($\sim 10^6$ m/s), M_e the electron rest mass, and a_{B_0} Bohr's radius (should already contain $1/\gamma_0$, see below). If now the electron transits to an unoccupied nth orbit, the atom lowers its energy to $\varepsilon_{u.n}$ and emits an electromagnetic wave of frequency

$$\nu_{r_0}=\frac{\varepsilon_{u.n+1}(0)-\varepsilon_{u.n}(0)}{h}=\frac{\hbar^2(2n+1)}{h2m_e(n+1)^2n^2a_B^2}; \qquad (6)$$

accordingly $\lambda_{r_0}=c/\nu_{r_0}$ and $k_{r_0}=2\pi/\lambda_{r_0}=2\pi\nu_{r_0}/c$.

If now the atom is moving at a velocity v in $+x$-direction, $(v/c)^2\gg 0$, then in the motion direction, its orbital radius is Lorentz contracted to $a_B=a_{B_0}/\gamma$, and its mass augmented according to Einstein to $m_e=\gamma m_{e_0}=\gamma\gamma_0 M_e$ (see also the classical-mechanics solutions [6]), where $\gamma=1/\sqrt{1-(v/c)^2}$. With a_B and m_e for a_{B_0} and m_{e_0} in (6), we have $\nu_r=$ $=\frac{\varepsilon_{u.n+1}(v)-\varepsilon_{u.n}(v)}{h}=\gamma\nu_{r_0}$; including in this an additional term $\delta\nu_r$ which we will justify below to result because of an energy gain of the moving source, the spectral frequency for the $n+1\to n$ transition for the moving atom then writes

$$\nu_r=\gamma\left(\nu_{r_0}+\delta\nu_r\right). \qquad (7)$$

4 Atomic spectral emission scheme

We now inspect how an electron transits, from an initial $n+1$th to final nth orbit in an atom moving in general, here at velocity v in $+x$-direction. To the initial-state electron, with a velocity u_{n+1} if $v=0$, the finite v of the traveling atom will at each point on the orbit project a component $v\cos\theta$ onto $u_{n+1}(\theta)$, with θ in $(0,2\pi)$; the average is $\bar{u}_{n+1}=$ $=\int_{\theta=0}^{2\pi}[u_{n+1}+v\cos\theta]d\theta=u_{n+1}$. That is, $\bar{u}_{n+1}$ and any its derivative dynamic quantities of the stationary-state orbiting electron are not affected by v except through the second order factor $\gamma(v)$. The situation however differs during the $n+1\to n$ transition which distinct features may be induced as follows:

(i) The transition ought realistically be a mechanical process in which, in each sampling, the electron comes off orbit $n+1$ at a single definite location, e. g. A in Fig. 2a. That where A is located on the orbit in any sampling, is a statistic event.

(ii) The spectral radiation is a single monochromatic electromagnetic wave emitted in forward direction of the orbiting electron at the point (A) it comes off orbit $n+1$, as based on observations for decelerating electron radiation in a storage ring in synchrotron experiments [4], which is no different from an orbiting atomic electron except for its macroscopic orbital size.

(iii) It follows from (i)–(ii) combined with momentum conservation condition that the transition electron coming off at A, will migrate across shortest-distance AB, perpendicular

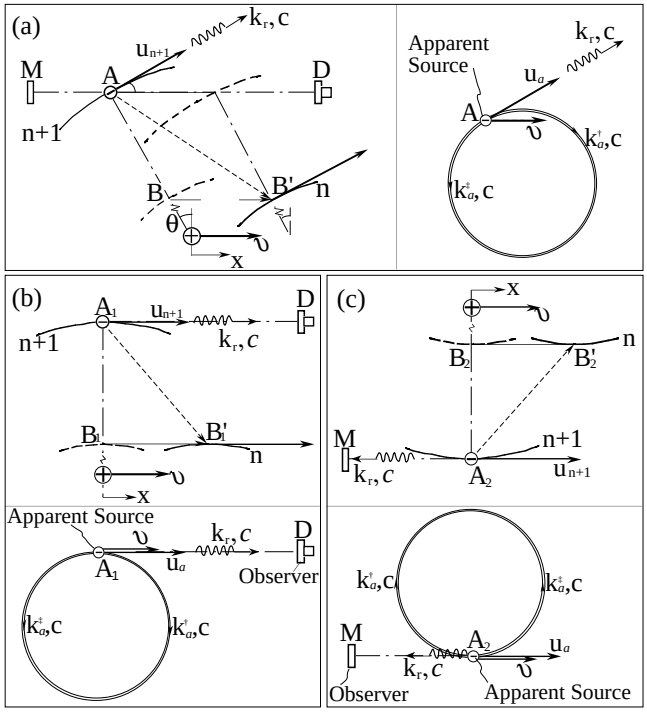

Fig. 2: An atomic electron comes off orbit $n+1$ statistically e. g. at A in (a), emitting in brief time δt a single electromagnetic wave of energy $h\nu_r$ in forward (u_{n+1}) direction, and then migrates (transits) along AB, $\perp u_{n+1}$, to orbit n for an atom of $v = 0$, and across AB' in time $t_{AB'}$ for finite v in $+x$-direction; $\mathrm{BB}' = vt_{AB'}$. In (a): $\angle c, v = \theta$; (b): $c\|v$; (c): $-c\|v$. The insets in (a)-(c) illustrate the radiation from an apparent source.

to u_{n+1}, to orbit n, at B if the atom is at rest, or at B' if the atom is moving at velocity v in x-direction, given after vector addition.

(iv) A stationary-state orbiting electron on orbit n^* ($= n+1$ or n), $\psi_{k_{dn^*}}$, is [6] a (*single*) beat or de Broglie phase wave convoluted from the opposite-traveling component total waves $\{\varphi^j_{kn}\}$ generated by an oscillatory massless (vaculeon) charge $-e$, of wavevectors $k^\dagger_{n^*}$ and $k^\ddagger_{n^*}$, which being Doppler shifted for the source moving at velocity u^j_{n+1}. An $n+1 \to n$ transition emits the difference between the two *single* waves, $\psi_{k_{dn+1}}$ and $\psi_{k_{dn}}$ — the emitted radiation is naturally also a *single* wave. And,

(v) The component total waves making up the electron beat wave at A is generated by the source in a brief time δt when at A, a wave frequency $\sim \mathcal{V} = 511\,\mathrm{keV}/h \simeq 10^{20}\,\mathrm{s}^{-1}$; so the the time for detaching the entire radiation wave trains from the source is estimated $\delta t \sim 1/\mathcal{V} = 8\times10^{-21}$ s. In contrast, the orbiting period of the electron is $\tau_{d.n+1} = 1/\nu_{d.n+1} = (n_1)^2 1.5\times10^{-16}$ s. So in time $\delta t \ll \tau_{d.n+1}$, the electron is essentially not moved along orbit $n+1$ as well as path AB or AB'; hence u_{n^*} ($\simeq u_{n+1}$) (thus c) and v are at fixed angle θ. Specifically if the electron comes off at A_1 and A_2 as in Fig. 2b and c, respectively, we have the approaching and receding source and observer

$$c \,\|\, v \qquad \text{and} \qquad -c \,\|\, v\,. \tag{8}$$

The wave and dynamic variables for the nonstationary transition process would not be a simple difference between solutions of the stationary states. However, we can try to represent the process effectively using an apparent source such that:

(v.1) the total wave detached from the apparent source gives the same observed radiation as due to the actual source; and

(v.2) the apparent source in transition has the same motion as the (actual source of the) transition electron, that is, translating at the velocity v (cf. item iv) in $+x$-direction here.

5 A theoretical formula for the redshift

In fulfilling (v.1), the apparent source ought to be an oscillatory charge (q) executing in stationary state circular motion at velocity u_a on orbit $n+1$ (insets in Fig. 2). Let first the orbit $n+1$ be at rest, $v = 0$, and so must be the apparent source as by (v.2). The apparent source generates two identical monochromatic electromagnetic waves traveling oppositely along orbit $n+1$, of wavevectors $k^\dagger_{a0} = k^\ddagger_{a0} = k_{a0}$, which superpose into a single electromagnetic wave $\psi_{k_{a0}}$. On transition, the source emits the entire $\psi_{k_{a0}}$ in the direction parallel with $u_a(\theta)$, by simply detaching it; thus $k_{a0} \equiv k_{r_0} = 2\pi/\lambda_{r_0}$.

Let now orbit $n+1$ be in motion at velocity v in $+x$-direction, and so must be the apparent source. Let the source comes off orbit $n+1$ at point A_1 (Fig. 2b). In a brief time δt before this, the apparent source was essentially at A_1 and generating two waves $\varphi^\dagger_{k^\dagger_a}$ parallel and antiparallel with u_a, thus v; their wavelengths were owing to the source motion of v Doppler shifted, to $\lambda^\dagger_a = \lambda_{r_0}(1-\frac{v}{c})$, $\lambda^\ddagger_a = \lambda_{r_0}(1+\frac{v}{c})$, and wavevectors $k^\dagger_a = \frac{2\pi}{\lambda^\dagger_a}$, $k^\ddagger_a = \frac{2\pi}{\lambda^\ddagger_a}$ with the Doppler shifts

$$k^\dagger_a - k_{r_0} = \frac{(v/c)k_{r_0}}{1-v/c}\ (a); \quad k_{r_0} - k^\ddagger_a = \frac{(v/c)k_{r_0}}{1+v/c}\ (b). \tag{9}$$

The two waves superpose to $\psi_{k_a} = \varphi^\dagger_{k^\dagger_a} + \varphi^\ddagger_{k^\ddagger_a}$, being according to [6] now a single beat, or de Broglie phase wave of the moving apparent source. On transition the source detaches the entire single beat wave ψ_{k_a}, which is no longer "regulated" by the source and will relax into a pure electromagnetic wave ψ_{k_r}, but in conserving momentum, retains in the single direction parallel with u_a thus v. Similarly, if the source exits at A_2 (Fig. 2c), a single electromagnetic wave will be emitted parallel with $u_a(A_2)$, or, $-v\cdot\psi_{k_a}$ has a de Broglie wavevector given[6] by the geometric mean of (9a) and (b):

$$k_{a.d} = \sqrt{(k^\dagger_a - k_{r_0})(k_{r_0} - k^\ddagger_a)} = \frac{\left(\frac{v}{c}\right)k_{r_0}}{\sqrt{1-(v/c)^2}}$$

$$\text{or} \qquad k_{a.d} = \gamma\left(\frac{v}{c}\right)k_{r_0}\,. \tag{10}$$

We below aim to express the $k_{a.d}$-effected radiation variables k_r, ν_r and λ_r, which being directly observable. Momentum conservation requires $|\hbar k_{a.d}| = |\hbar \delta k_r|$; $k_{a.d}$ is associated with an energy *gain* of the apparent source, $\varepsilon_{a.v} = \frac{(\hbar k_{a.d})^2}{2m_e}$, owing to its motion, and thus an energy *deficit* in the emitted radiation wave ψ_{k_r},

$$\begin{aligned} &\delta\varepsilon_r (= \hbar \delta k_r c) = -\varepsilon_{a.v}\,, \\ &\text{for either} \quad c \parallel v \quad \text{or} \quad -c \parallel v\,, \end{aligned} \tag{11}$$

and accordingly momentum and frequency deficits in the emission

$$\delta k_r = -k_{a.d} = -(v/c) k_{r_0}\,, \tag{12}$$

$$\delta \nu_r = \delta k_r c = -(v/c) k_{r_0} c = -(v/c)\nu_{r_0}\,. \tag{13}$$

With (13) in (7), we have

$$\nu_r = \gamma \left(1 - \frac{v}{c}\right) \nu_{r_0} \simeq \gamma \nu_{r_0} - \left(\frac{v}{c}\right) \nu_{r_0} \tag{14}$$

where γ in front of $\delta\nu_r$ is higher order thus dropped. With (14) we can further compute for the emitted wave:

$$k_r = \frac{2\pi\nu_r}{c} = \gamma \left(1 - \frac{v}{c}\right) k_{r_0} \simeq \gamma k_{r_0} - \left(\frac{v}{c}\right) k_{r_0}\,, \tag{15}$$

$$\lambda_r = \frac{c}{\nu_r} = \frac{c}{\nu_{r_0}(1/\gamma - v/c)} \simeq \frac{\lambda_{r_0}}{\gamma} + \left(\frac{v}{c}\right) \lambda_{r_0}\,. \tag{16}$$

The theoretical prediction (16) for λ_r above is seen to agree exactly with Ives and Stilwell's experimental formula, (5). Notice especially that the prediction gives $\delta\nu_r < 0$ and $\delta\lambda_r > 0$ for both $c \parallel v$ and $-c \parallel v$ as follows from (11); that is, they represent always a redshift in the emission spectral line, regardless if the wave is emitted parallel or antiparallel with v.

6 Discussion

From the forgoing analysis of the direct experimental spectral data of Ives and Stilwell on hydrogen canal rays, and with the elucidation of the underlying mechanism, we conclude without ambiguity that, the spectral emission of a moving hydrogen atom exhibits always a redshift compared to that from an atom at rest; the faster the atom moves, the redder-shift it shows. This is not an ordinary Doppler effect associated with a conventional moving source, but rather is an energy deficiency resulting from the de Broglie electron kinetic energy gain in transition to a moving frame, a common feature elucidated in [7] to be exhibited by the deceleration radiation of all de Broglie particles. This redshift does not inform the direction of motion of the source (the atom).

It is on the other hand possible for an atomic spectral emission to exhibit blue shift for other reasons, for example, when the observer is moving toward the source as based on Galilean transformation. The author thanks P.-I. Johansson for his support of the research and the Studsvik Library for helping acquiring needed literature.

References

1. Ives H. E. and Stilwell G. R. An experimental study of the rate of a moving atomic clock. *J. Opt. Soc. Am.*, 1938, v. 28, 215–226.
2. Kuhn H. G. Atomic spectra. Longmans, London, 1962.
3. Freedman W. L. The Hubble constant and the expansion age of the Universe. *Phys. Rept.*, 2000, v. 333, 13–31; arXiv: astro-ph/9909076; Riess A. G., The case for an accelerating Universe from supernovae. *Pub. of Astronom. Soc. Pacific*, 2000, v. 112, 1284–1299.
4. Crasemann B. Synchrotron radiation in atomic physics. *Can. J. Phys.*, 1998, v. 76, 251–272.
5. Winick H. and Doniach S., editors. Synchrotron radiation research. Plenum Press, New York, 1980.
6. Zheng-Johansson J. X. and Johansson P-I., Fwd. Lundin R., Unification of Classical, Quantum and Relativistic Mechanics and of the four forces. Nova Sci. Pub., NY, 2006; Inference of Schrödinger equation from classical-mechanics solution. *Quantum Theory and Symmetries IV*, ed Dobrev V. K., Heron Press, Sofia, 2006; (with Lundin R.) Cause of gravity. Prediction of gravity between charges in a dielectric medium. *ibid.*; also arxiv: phyiscs/0411134; arxiv physics/0411245; *Bull. Am. Phys. Soc.*, 2006, Topics in Quantum Foundations, B40; *ibid.*, 2004, in: Charm Quark States, D10; *ibid.*, 2004, C1.026; Origin of mass. Mass and mass-energy equation from classical-mechanics solution. arxiv: physics/0501037; *Bull. Am. Phys. Soc.*, 2005, New Ideas in Particle Theory, Y9; Electromagnetic radiation of a decelerating moving de Broglie particle: always a redshift, *ibid.*, 2005, Intermediate Energy Accelerators, Radiation Sources, and New Acceleration Methods, T13; Unification of Classical and Quantum Mechanics, & the theory of relative motion. *Bull. Am. Phys. Soc.*, 2003, General Physics, G35.01; *ibid.*, 2004, General Theory, Y38.
7. Zheng-Johansson J. X. and Johansson P-I., Fwd. Lundin R. Inference of basic laws of Classical, Quantum and Relativistic Mechanics from first-principles classical-mechanics solutions. Nova Sci. Pub., NY, 2006.

Dark Matter and Dark Energy: Breaking the Continuum Hypothesis?

Emilio Casuso Romate and John Beckman
Instituto de Astrofísica de Canarias, E-38200 La Laguna, Tenerife, Spain
E-mail: eca@iac.es

In the present paper an attempt is made to develop a fractional integral and differential, deterministic and projective method based on the assumption of the essential discontinuity observed in real systems (note that more than 99% of the volume occupied by an atom in real space has no matter). The differential treatment assumes continuous behaviour (in the form of averaging over the recent past of the system) to predict the future time evolution, such that the real history of the system is "forgotten". So it is easy to understand how problems such as unpredictability (chaos) arise for many dynamical systems, as well as the great difficulty to connecting Quantum Mechanics (a probabilistic differential theory) with General Relativity (a deterministic differential theory). I focus here on showing how the present theory can throw light on crucial astrophysical problems like dark matter and dark energy.

1 Introduction

In 1999 I published [1] the preliminaries of a new theory: the General Interactivity. It was a sketched presentation of the mathematical basis of the theory, i. e. the fractional integral treatment of time evolution. In the present paper we extend the ideas of General Interactivity to the fractional derivatives, and so we can explain the outer flatness of rotation curves, last measures of SN Ia at high redshifts, the fluctuations in the CMB radiation and the classical cosmology theory.

In 1933 Zwicky [2] found that the Coma cluster of galaxies ought to contain more matter than is inferred from optical observations: many of the thousands of galaxies in the cluster move at speeds faster than the escape velocity expected from the amount of visible matter and from the Newton theory of gravitation. In the 1970's, many authors discovered that the speed of stars and clouds of hydrogen atoms rotating in a galactic disk is nearly constant all the way out to the edge of the galaxy [3, 4]. Using Newton's law of gravitation, this implied that the amount of matter at increasing radius is not falling away, against the observed star-light suggests. Over past two decades, the measured deflection of light from a distant star by a massive object like a galaxy (gravitational lens) points to a mass-to-light ratio for the lensing galaxies of about 150, and yet if galaxies contained only observed stars the expected value would be between 5 and 10 [5]. From the observed cosmic microwave background (CMB, the relic radiation of the Big Bang that fills the Universe) fluctuations, we need that 23% of the Universe is dark matter, and 73% is dark energy [6, 7, 8, 9, 10]. Recent observations of SN Ia brightness show that the expansion of the Universe has been speeding up. This unexpected acceleration is also ascribed to an amount of dark energy that is very similar than 73% of the Universe [11].

In Section 2 we show a review of the theory, in Section 3 we apply the theory to account for the observed dark matter and dark energy, and in Section 4 we develop the conclusions.

2 The model

I start from two hypothesis: (1) the irreversibility in time of natural systems and (2) the interactivity among all the systems in the Universe. These hypotheses imply an intricate, unsettled and discontinuous (and hence non-differentiable) space-time. The differential treatment projects a variable $X(t)$, whose value is known at a time t, to a successive time, $t+\Delta t$, through the assumption of a knowledge of their time derivative, $X'(t)$, as follows: $X(t+\Delta t) = X(t) + + X'(t)\Delta t$. In many cases, to a good approximation, there is proportionality between $X(t)$ and $X'(t)$ so that $X'(t) \propto X(t+\Delta t)$. Here I extend this projection, but with two crucial modifications: (a) I project a complete distribution of real values (a set of measured values ordered in time) instead of individual values at one time, and (b) I generalize the derivative to the Liouville fractional derivative (to take into account the possibility of the discontinuous space-time of the system under study). This then gives the fundamental equation of the new dynamics:

$$\frac{d^{\beta}_{FRAC}}{dt}\, X(t_{past}) \propto X(t_{future})\,. \qquad (1)$$

$X(t_{past})$ being a table of values of the variable X until the present time, $X(t_{future})$ the same number of values of X but from the present time to the future (a projection), and β a value between 0 and 1 that includes the key information about the history of the system.

But for more physical sense, one must take the inverse of equation (1), i. e.

$$X(t_{past}) \propto \frac{1}{\Gamma(\beta)} \int_{t_{past}}^{T} \frac{X(t_{future})}{(t_{past} - t_{future})^{1-\beta}} dt_{future} \qquad (2)$$

which is the fractional integration (or the Riemann-Liouville integral) of $X(t_{future})$, T being a time-period characteristic of each system. The first hypothesis, irreversibility, suggests the necessity of projecting the values of $X(t)$, weighted by a function of time that must be similar to the function characteristic of critical points, such as observed in the well known irreversible phase transitions in Thermodynamics; for example, the form $(T_E - T_{EC})^{-0.64}$ for the time correlation length of an infinite set of spins with a temperature T_E near the critical temperature T_{EC} [12]. Compare this with the term $(t_{past} - t_{future})^{\beta-1}$ in equation (2). I call this weighting "generalized inertia"; it is characteristic of each system in the sense of incorporating into the β exponent the history of all the interactions suffered by the system, including those interactions avoided by the differential approximation (high order terms in Taylor expansions) due to its small values.

To use the fundamental equation (1) with maximum efficiency, I invert equation (2) because this is an Abel integral transform, and there is a technique developed by Simmoneau et al. [13] to optimize the inversion of Abel transforms. This technique consists in making a spectral expansion using a special kind of polynomials whose coefficients are obtained by means of numerical integration, thus avoiding the basic problem of amplification of the errors, a problem inherent in numerical differentiation; in the technique of Simmoneau et al., measurement errors are incorporated into the coefficients of the spectral expansion and then propagate with time without being amplified.

In the present context one can see the time as a critical variable, each "present" being an origin of time coordinates, with two time dimensions: the past and the future. We should note that in Quantum Mechanics two independent wave functions are needed (the real part and the imaginary part of the total wave function) to describe the state of a system at each moment in time.

One can view General Interactivity as a third approximation to reality: the first was the conception of continuous and flat space-time by Newton, the second was that of continuous and curved space-time by Einstein. Here I see a discontinuous space-time whose degree of intricacy measures the essential cause of changing. As in Newtonian Dynamics, where the forces are the causes of changing, and in General Relativity, where modifications of the metric of space-time are the cause of changes in the motion of all massive systems, in General Interactivity the exponent β gives us a measure of the intricacy of the space-time "seen" by each system through a given variable X. But how can we see Gravity from the new point of view of General Interactivity? From (differential) Potential Theory we know that the modulus of the gravity force per unit mass is the following function of mass distribution, $\rho(x)$, in space:

$$F_G(x) = G \int \frac{\rho(x')}{|x' - x|^2} d^3x' \qquad (3)$$

and, comparing with the three-dimensional fractional integration of $\rho(x)$ we have:

$$R_\beta\big[\rho(x)\big] = \pi^{\beta-\frac{\pi}{2}} \frac{\Gamma\left(\frac{3-\beta}{2}\right)}{\Gamma\left(\frac{\beta}{2}\right)} \int \frac{\rho(x')}{|x - x'|^{3-\beta}} d^3x'; \qquad (4)$$

$F_G(x)$ can be identified with the 1-integral of $\rho(x)$ in three-dimensional space ($\beta = 1$) except for a constant. So in the present context the gravity force can be interpreted as a one-dimensional projection of the three-dimensional continuous distribution of matter. It is not, then, a complete integral (this would be $\beta = 3$) and so the sum (integral) for obtaining the gravity is more intricate than the mass distribution (continuous by definition), i. e. the real discontinuity of mass distributions is transferred to the fractional integral instead of working with a discontinuous $\rho(x)$. Gravity, like the electrostatic force, whose expression is very similar to $F_G(x)$, is seen as an inertial reaction of space-time, which would tend to its initial (less intricate,i. e. simpler) state, towards a structure in which the masses were all held together without relative motions; both forces are seen as reactions against the action of progressive intricacy in the general expansion of the Universe following the Big Bang.

We take the total mass-energy of the Universe as the observable magnitude $X(t)$ to evolve in time using Eq. (2). The constancy of this variable gives $1 = \frac{1}{\beta^2}(T^2 - t_{past}^2)^\beta$ (where I take squared variables for simplicity in the use of Simmoneau et al.'s inversion technique). The greater past-time variable, t_{past}, less β indicating that the space-time is more intricate with time; this is the reason for integrating more fractionally (less β). So the parameter β can also be considered as a measure of the entropy of the Universe.

Another key to understand General Interactivity comes from the classical Gaussian and Planckian distribution functions, to which real systems in equilibrium tend. The equilibrium distribution function for systems of particles, for collisional and for collisionless systems (in the non-degenerate limit [14]) is Gaussian; classical Brownian motion is an example [15]; the equilibrium distribution function for systems of waves is a Planckian, and a key example is blackbody radiation. If both distribution functions evolve in time, then, using the inversion of equation (2), we have the same final result: the Planckian distribution. This tells us that whatever the initial distribution at the beginning of the Big Bang (perhaps both the Planckian characteristic of interacting waves and the Gaussian characteristic of interacting particles coexisted), their time evolution leads to a Planckian distribution, thereby connecting with the actual observed spectrum of the Cosmic Microwave Background, which appears to be almost perfectly Planckian.

But, why is the Planckian more stable than the Gaussian with the passing of time? The answer I propose is that successive critical transitions (at each time), due to the complexity caused by interactions at large distances, tend to amplify the Gaussian distribution to all range of energies, making it

flatter. This breaks the thermal homogeneity because of the very different time evolution of many regions, due to the delay in the transmission of information from any one zone to others that are far away (note that the speed of the light is a constant). This amplification goes preferentially to high energies because there is no limit, in contrast with lower energies, for which the limit is the vacuum energy.

In this context, then, the Universe is seen as an expansion of objects that emitting information (electromagnetic waves) in all directions, and one can differentiate between two basic kinds of interactions: (a) at small distances (the distance travelled by light during a time that is characteristic of each system) forming coupled systems showing macroscopic (ensemble) characteristics, such as temperature or density, well differentiated from those of their surroundings; and (b) at large distances, interfering one system from another in a complex manner due to the permanent change in the relative distances due to the constancy of the speed of light, the huge number of interactions and the internal variation of the sources themselves. Note that this distinction between small and large distances can be extended relative to each physical system. For instance, a cloud of water vapour (as in the Earth's atmosphere) constitutes a system of water molecules interacting over short distances, while the interaction between one cloud and another is considered to take place over a large distance. Inside a galaxy, the stars in a cluster are considered to interact over short distances, while the interactions between that cluster and the remaining stars and gas clouds in the galaxy are considered as interactions over large distances.

In General Relativity there are no point objects; instead, all the objects in Nature are considered as systems of other objects, even subatomic particles appearing to be composed of others yet smaller.

I now focus on one of the most puzzling interpretations of Quantum Mechanics: the wave-particle duality. In Quantum Mechanics the objects under study show a double behaviour depending on what type of experiment one makes. An electron behaves as a particle in collisions with other electrons, but the same electron passing through two gaps (enough small and enough near each other) behaves as a wave in that the outcoming electrons form an interference pattern. In General Interactivity each "particle" is considered as a system, and we know that the equilibrium distribution of random particles is Gaussian, and that after the time evolution given by Eq. (2) the distribution transforms into a Planckian (the interaction with the other systems "drives" the random set of particles) which is the distribution to which a set of interacting waves in a cavity naturally tend. Furthermore, the Planckian can be decomposed into a set of Gaussians, so that the double nature of matter/energy is ensured. The fact that a Planckian can be the result of the addition of Gaussians of different centres and amplitudes is interpreted as the Planckian representing an ensemble of random motions in turn represented by Gaussians, which find a series of walls to which resulting in certain reflexion and certain absorption. As already demonstrated [15], both processes, reflexion and absorption by a barrier, are equivalent to the addition and the subtraction, respectively, of two Gaussians: the main Gaussian and that which emerge as a consequence of the barrier (by displacing its centre to the other side of the barrier). A Gaussian, then, converts into a set of several other Gaussians at progressively smaller amplitudes as a consequence of the existence of barriers, and the envelope is a Planckian. There is a partial reflection at each barrier in the direction of higher energies, while the reflection is total to the lower energies and the absorption of unreflected part must be added to the left of the barrier. This argument can be applied to explain the Planckian distribution observed in the Cosmic Microwave Background Radiation: the energy barriers can be thought of as the consequence of the existence of wrinkles in space-time, caused by the finiteness of the Universe (closed box) and the uncoupled expansion of the content with respect to the box, or by breaking of the expansion because of the collision of the outer parts with another medium, or by the succession of several bangs at the beginning, instead of only one bang.

3 Dark Matter and Dark Energy

Another example of application of this theory is the generalization of one of the most important theorems in Field Theory, Gauss's theorem, leading to a possible solution (as a kind of Modified Newtonian Dynamics theory) of the well known problem of the "lost mass" of the Universe and its associated problem of "dark matter" [16]. Assuming the well known observation of the infinitesimal volume occupied by matter relative to holes in Nature (the nucleus of an atom occupy less than 1% of the atom's volume, and gas clouds in the interstellar medium have densities of 1 atom per cubic centimeter or less), one must consider the possibility of relaxing the continuum hypothesis. The Gauss's theorem can be expressed, simplified and for the gravitational field, as

$$\int_S g_N dS = -4\pi GM\,, \tag{5}$$

where g_N is the intensity of the gravity field over a closed surface, S, which contains the mass, M, which is the origin of the field, on the assumption of continuity, and G is the universal gravity constant. So, integrating Eq. (5) on the assumption of $g_N \simeq$ constant over S, we get $g_N = -4\pi GM/S$, with $S = \int_S dS$. If we take as the starting point the differential form of Gauss theorem, and then we take in Eq. (5) the fractional, instead of the full, integral and also assume $g \simeq$ const, we have

$$g(r) = \frac{-4\pi GM}{\frac{\pi^{\beta-1}\Gamma\left(\frac{2-\beta}{2}\right)}{\Gamma\left(\frac{\beta}{2}\right)} \int_S \frac{dX}{|S-X|^{2-\beta}}}\,. \tag{6}$$

Because β is less than 2, g is greater than g_N, and this result could explain the observational fact of g_N being very

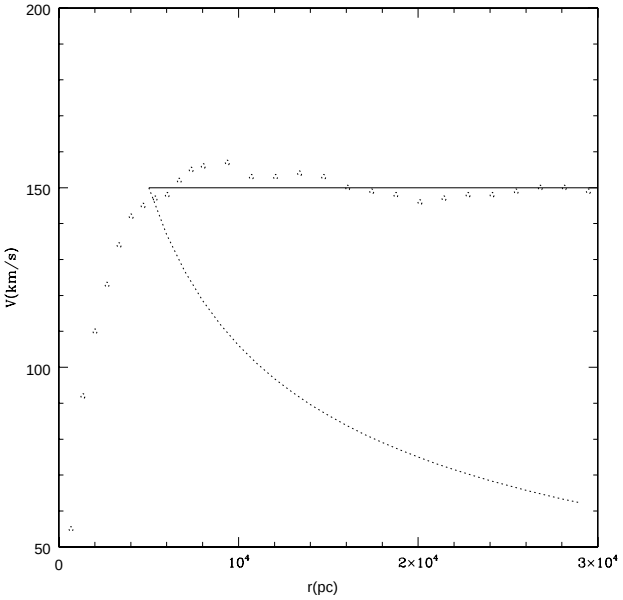

Fig. 1: Rotation curve (kms^{-1}) for NGC3198. Crosses are observational data points taken from van Albada et al. [17]. Full line is the prediction of the present theory, and dashed line is the prediction by the Newton law of gravitation.

small in explaining, for instance, many galactic rotation curves far from the central regions. For, assuming spherical simetry one has:

$$g(r) = g_N \frac{4\pi r^2}{\frac{\pi^{\beta-1}\Gamma\left(\frac{2-\beta}{2}\right)}{\Gamma\left(\frac{\beta}{2}\right)} \int_0^{2\pi} \frac{2\pi r^2 \sin\theta d\theta}{r^{2-\beta}}} \,. \tag{7}$$

And taking $\beta = 1$ one has $g(r) = g_N r$, which introduced in the classical centrifugal equilibrium identity $\frac{V^2}{r} = g$ leads to the amazingly $V = (GM)^{1/2} \simeq$ constant as is observed for flat rotation curves that needs dark matter (see Fig. 1).

More complicated treatment can be made: in the integral treatment one can consider the basic constituents of matter (the atoms) and the infinitesimal size of the volume occupied by the atomic mass (the nucleus) with respect to the size of the atom, and then one finds the necessity of take into account that ubiquitous nature of the big holes existing inside the matter (the atoms and molecules inside the very low density galactic gas clouds amplify the hole effect respect to the whole cloud and then amplify the influence in the macroscopic gravitational (massive) behaviour). So one can consider the hypothesis of continuity as a first approximation, and one can re-examine the Gauss' theorem

$$\int_S g dS = -4\pi G \int_V \rho dV \,, \tag{8}$$

where g is the gravitational field over the surface S, S is any closed surface containing the massive object which is the source of the field, G is the gravitational constant, ρ is the density, and V is the volume contained within the surface S. And one can generalize Eq. (5) in the sense of take both integrals as fractional integrals (α and β respectively) which leads to normal integrals for some especial case. If one assumes, for simplicity, spherical symmetry for the gas mass distribution in the galaxy, one has:

$$\rho = \rho_0 \, e^{\frac{-(r-r_0)}{r'}} \tag{9}$$

and assuming $g \simeq$ constant over the now non-necessary continue surface (the fractional integration takes this into account) one has:

$$g = -\frac{16\pi^2 G\rho_0 C_2(\beta)}{f(\alpha) r^2 C_1(\alpha)} \, r^{2-\alpha} \int r^2 r^{\beta-3} e^{-\frac{r-r_0}{r'}} dr \,, \tag{10}$$

where $f(\alpha)$ is some function of α,

$$C_2(\beta) = \pi^{\beta-3/2} \frac{\Gamma\left(\frac{3-\beta}{2}\right)}{\Gamma\left(\frac{\beta}{2}\right)} \,, \tag{11}$$

$$C_1(\alpha) = \pi^{\alpha-1} \frac{\Gamma\left(\frac{2-\alpha}{2}\right)}{\Gamma\left(\frac{\alpha}{2}\right)} \,, \tag{12}$$

while

$$g_N = -\frac{4\pi G\rho_0}{r^2} \int r^2 e^{-\frac{r-r_0}{r'}} dr \,. \tag{13}$$

So, in the especial case when $\beta = 3$ and $\alpha = 2$ we have $g = g_N$. Then, expanding $r^{\beta-3} \simeq 1 + (\beta-3)\log r + \ldots$ as $\beta \to 3$ and $r^{2-\alpha} \simeq 1 - (\alpha-2)\log r + \ldots$ as $\alpha \to 2$, and including the expansions into Eq. (13) one has

$$\begin{aligned} g \simeq & \frac{8\pi C_2(\beta)}{f(\alpha) C_1(\alpha)} \big(1 - (\alpha-2)\log r\big) \times \\ & \times \left(g_N - \frac{4\pi G\rho_0}{r^2} \int (\beta-3)(\log r) r^2 e^{-\frac{r-r_0}{r'}} dr \right). \end{aligned} \tag{14}$$

And integrating by parts and taking very large values for r, we have

$$g \simeq g_N \frac{8\pi C_2(\beta)}{f(\alpha) C_1(\alpha)} \big(1 + (\alpha-2)(3-\beta)\log^2 r\big) \,. \tag{15}$$

And for typical values of observed flat rotation curves ($5\mathrm{kpc} \leqslant r \leqslant 20\mathrm{kpc}$) we have that $g \propto g_N r$ represents a good approximation. So, for certain values of α and β (α less than 2 and β greater than 3) one has that outer rotation curves can be flat as observed.

But the most puzzling problem up-to-date in cosmology is the necessity of adding "ad hoc" a dark energy or negative pressure (the so called by Einstein cosmological constant) to the main equation of General Relativity to account for the last measures on supernovae Ia and the fluctuations in the cosmic microwave background radiation which implies a flat accelerating expanding universe. The field equation of General Relativity was formulated by Einstein as the

generalization of the classic Poisson equation which relates the second derivative of the potential ϕ associated to the gravitational field with the assumed continuous mass distribution represented by the volume density ρ:

$$\Delta^2\phi + 4\pi G\rho = 0\,. \tag{16}$$

For comparison, the similar equation in General Relativity, which relates the mass and energy distribution with the differential changes in the geometry of the continuum space-time, is (see e. g. Einstein [18]):

$$\left(R_{\mu\nu} - \frac{1}{2}\,g_{\mu\nu}R\right) + \kappa\,T_{\mu\nu} = 0\,. \tag{17}$$

But for the last equation be coherent with the last independent measures of SN Ia and fluctuations of CMB radiation, we need to add a term $g_{\mu\nu}\Lambda$ to the left side of equation which represents near 73% of all the other terms. This problem is avoided naturally if we consider a discontinuous space-time, and then we re-formulate the equations by using the fractional derivative instead the full derivative. In that case, the second derivative is less than the full derivative, and then the cosmological constant is not needed at all to equilibrate the equations. In fact the μ-fractional derivative of the function r^λ is given by [19]:

$$D^\mu r^\lambda = \frac{\Gamma(\lambda+1)}{\Gamma(\lambda-\mu+1)}r^{\lambda-\mu} \tag{18}$$

for λ greater than -1, μ greater than 0. But as $\lambda\to-1$, $r^\lambda\to\propto\phi$ being ϕ the gravitational potential. And as one can see, taken a fixed value of λ, as μ increase, the μ-derivative decrease. Or to be more precise, if we assume that the constant to be added to the left side of Eq. (17) represents the 73% of all the matter and energy in the Universe, one has:

$$\lim_{\lambda\to-1}\frac{\Gamma(\lambda-\mu+1)R^{-\lambda-2}}{\Gamma(\lambda-2+1)R^{-\lambda-\mu}} \simeq 1.73\,, \tag{19}$$

where R is a characteristic scale-length of the Universe. And the relation (19) works for values of μ greater but very near 2, being 2 the value corresponding to the usual second derivative. So we conclude that taking a value, for the derivatives in the field equations, slightly greater than the usual 2, we are able of include the cosmological constant inside the new fractional derivative of the classical field equations.

4 Conclusions

The new theory of the General Interactivity can be applied to many fields of natural science and constitutes a new step forward in the approximation to the real behaviour of Nature. It assumes the necessity of explicitly taking into account the real history of a system and projecting to the future. However, it also takes into account the non-uniformity of the distribution of holes in the Nature and is therefore a theory of discontinuity. The new theory can account for naturally the needed amounts of dark matter and dark energy as a light modification of classical field equations.

Acknowledgements

This work was supported by project AYA2004-08251-CO2-01 of the Spanish Ministry of Education and Science, and P3/86 of the Instituto de Astrofísica de Canarias.

References

1. Casuso E. *I.J.M.P.A.*, 1999, v. 14, No. 20, 3239.
2. Zwicky F. *Hel. Phys. Acta*, 1933, v. 6, 110.
3. Sancisi R., van Albada T. S. In: *Dark Matter in the Universe*, (eds. Knapp G., Kormendy J.), I.A.U. Symp. No. 117, 67 Reidel, Dordrecht, 1987.
4. Battaner E., Florido E. *Fund. of Cosmic Phys.*, 2000, v. 21, 1.
5. Mc Kay T. A. et al. *ApJ*, 2002, v. 571, L85.
6. Riess A. G. et al. *AJ*, 1998, v. 116, 1009.
7. Perlmutter S. et al. *ApJ*, 1999, v. 517, 565.
8. de Bernardis P. et al. *Nature*, 2000, v. 404, 955.
9. Hanany S. et al. *ApJ*, 2000, v. 545, L5.
10. Halverson N. W. et al. *ApJ*, 2002, v. 568, 38.
11. Kirshner R. P. *Science*, 2003, v. 300, 1914.
12. Wilson K. G., Kogut J. *Physics Reports*, 1974, v. 12, No. 2, 75.
13. Simmoneau E., Varela A. M., Munoz-Tunon C. *J.Q.S.R.T.*, 1993, v. 49, 149.
14. Nakamura J. *ApJ*, 2000, v. 531, 739.
15. Chandrasekhar S. *Rev. Mod. Phys.*, 1943, v. 15(1), 20.
16. Binney J., Tremaine S. In: *Galactic Dynamics*, Princeton Univ. Press, 1987.
17. van Albada T. S., Bahcall J. N., Begeman K., Sancisi R. *ApJ*, 1985, v. 295, 305.
18. Einstein A. In: *El Significado de la Relatividad*, ed. Planeta-Agostini, Spain, 1985.
19. Oldham K. B., Spanier J. In: *The Fractional Calculus: Integrations and Differentiations of Arbitrary Order*, New York, Academic Press, 1974.

Phenomenological Model for Creep Behaviour in Cu-8.5 at.% Al Alloy

M. Abo-Elsoud

Mater. Sci. Lab., Physics Department, Faculty of Science, Beni-Suef University, Egypt

E-mail: maboelsoud24@yahoo.com

Creep experiments were conducted on Cu-8.5 at.% Al alloy in the intermediate temperature range from 673 to 873 K, corresponding to 0.46–0.72 T_m where T_m is the absolute melting temperature. The present analysis reveals the presence of two distinct deformation regions (climb and viscous glide) in the plot of $\log \dot{\varepsilon}$ vs. $\log \sigma$. The implications of these results on the transition from power-law to exponential creep regime are examined. The results indicated that the rate controlling mechanism for creep is the obstacle-controlled dislocation glide. A phenomenological model is proposed which assumes that cell boundaries with sub-grains act as sources and obstacles to gliding dislocations.

1 Introduction

The importance of accurate experimental data on the creep properties of polycrystalline metals and alloys is well known.

Creep resistance is an important attribute of high temperature alloys and mechanisms that control! creep in alloys must be well understood for design of alloys that resist creep. These mechanisms can be classified into different types depending on the values of the activation energy for creep and temperatures. Several of these mechanism were reviewed by Raj and Langdon [1].

The creep resistance of Cu was shown to increase as the Al content is increased although the creep increment was small above 8.5 at.% Al. The creep response of Cu-Al binary solid solutions has been described in one of two ways: (i) those alloys in which dislocation climb is the rate-controlling step during deformation and (ii) where dislocation glide becomes rate controlling due to solute drag on moving dislocations [2]. More detailed knowledge of dislocation processes in cell walls and for sub-boundaries in creep that could lead to a greater understanding of the creep mechanisms has been emphasized [3]. From out point of view, the two models which represent an important step in this direction are as follows: (a) the model of soft (i.e. sub-grain interior) and hard (i. e. sub-boundaries) regions introduced by Nix-Ilschner [4], and developed with considerable detail by Rodriguez et al. [5]; (b) the bowing-out model of sub-boundaries due to Argon and Takeuchi [6]. From an experimental point of view, Aldrete [7] measured local stresses in the sub-grain structure formed during steady state creep in Cu-16 at.% Al solid solution alloy. Their results show that the internal stress σ_i [3] mainly originates in cell wall regions.

The objective of this paper is to study the phenomenological model for creep behaviour in Cu-8.5 at.% Al alloy, and examine the mechanism controlling the creep regime at intermediate temperature region.

2 Experimental procedure

The Cu-8.5 at.% Al alloy was prepared from melting high purity copper and aluminum (99.99%) by aspiration through a quartz crucible of induction melted alloy under a helium atmosphere [8]. The cooling rate of the alloy is between $4{\times}10^2$ and $10^3\,\mathrm{K s^{-1}}$. The ingot was swaged in wire form of diameter 1 mm and ≈ 50 mm gauge length. The wire specimens were pre-annealed at 873 K for 1h to check what happens to the distribution of Al, and to remove the effects of machining with producing a stable uniform grain size [9], in a quartz ampoule after evacuating to at least $5.3{\times}10^4$ Pa. After this treatment the samples were considered to be precipitated [10]. Fairly reproducible and equiaxed grains were obtained from the heat treatment, and the average linear intercept grain size obtained from a statistical sample size of grains was $\cong 10\mu$m.

Creep tests were conducted at the intermediate temperature range from 673 to 873 K, corresponding to $0.46-0.72\,T_m$, with an accuracy of ± 1 K under constant stress condition in a home-made creep machine with a Andrade-Chalmers lever arm. All tests were conducted under a flowing argon atmosphere maintained at a slightly positive pressure.

Some temperature change tests were conducted in order to determine the activation energy for creep Q_c.

3 Results and discussion

All creep curves showed a normal primary stage and a reasonably well-established steady-state region. The duration of the tertiary stage was short and abrupt, although the contribution of the tertiary strain to the total strain was often quite large. Typical creep curves are shown in Fig. 1 for a temperature 773 K and different stress levels.

Usually creep tests are carried out on annealed samples; then we can assume that, during the first minutes of the test,

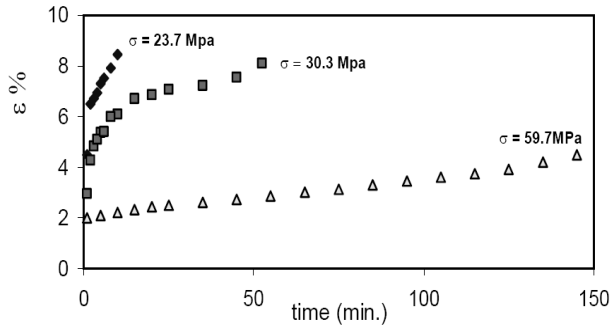

Fig. 1: Representative creep curves at different stress levels and at $T = 823\,\mathrm{K}$.

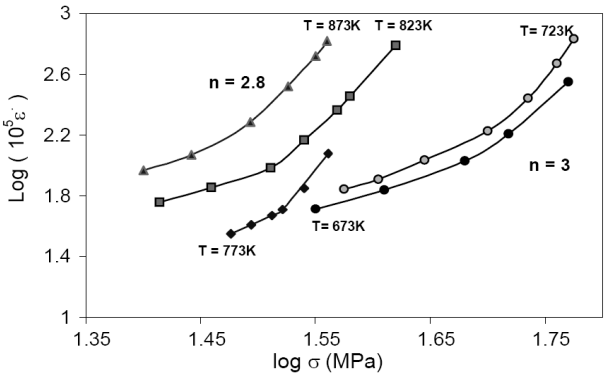

Fig. 2: Stress dependence of minimal creep rate at different temperatures. The creep rates show a change in slopes from $n = 3$ to $n = 2.8$ at the transition stresses.

the annihilation events are negligible as compared with the creation of dislocations. Therefore, considering that all the dislocations are mobile, the change ρ_m in is due to the creation of new dislocations. Also, according to Montemayor-Aldrete et al. [7] the creation rate $\dot{\rho}_m^+$ of dislocations is given as

$$\dot{\rho}_m^+ = \frac{\alpha\sigma\,\dot{\varepsilon}}{\bar{u}}\,, \qquad (1)$$

where $\bar{u}$ is the mean value for the self-energy of dislocations per unit length, α is the average geometrical factor relating the tensile deformation to the shear deformation for samples, and $\dot{\varepsilon}$ is the deformation rate.

Since the strain in the secondary region was often quite small, especially at the lower temperatures, it was necessary to assume that the minimum creep rate was representative of secondary behaviour. Fig. 2 shows the variation of the minimum creep rate $\dot{\varepsilon}$ with applied stress plotted logarithmically. As indicated, the stress exponent, n, $(n = \partial \ln \dot{\varepsilon}/\partial \ln \sigma_a)_{T,t}$ decreases from $\cong 3.2 \pm 0.2$ at the lowest temperature of 673 K to $\cong 2.8 \pm 0.2$ at temperature above $\cong 773\,\mathrm{K}$. These values of stress exponent are typical for a rate controlling process due to a transition from viscous glide mechanism to climb of dislocation along the shear planes [2]. However, Fig. 2 assumes implicitly that the power-law relationship is valid and this may not be true to for all of the datum

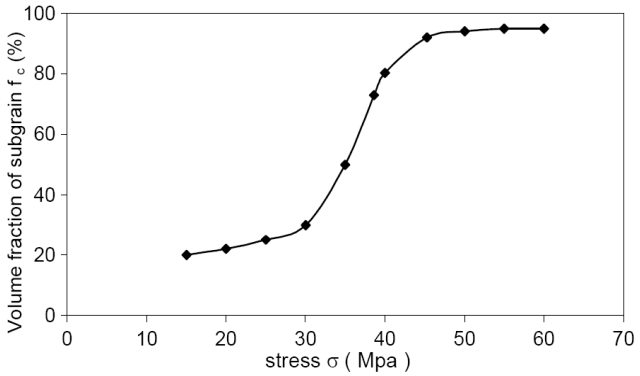

Fig. 3: The dependence of the volume fraction fc of subgrains near grain boundaries on applied stress at $T = 773\,\mathrm{K}$.

points. This observation suggested that there is a connection between creep behaviour and the internal microstructure of the primary sub-grains. It is found that the primary sub-grains become elongated in the transition region between power-law and exponential creep, and they often contain fewer secondary sub-boundaries, larger numbers of coarse-walled cells and a higher dislocation density in comparison to their equiaxed neighbors [1]. Similar microstructures consisting of cells and equiaxed and elongated sub-grains have also been observed in Al [9], Cu [11], Fe [12].

From a phenomenological point of view, the qualitative features of the our model consider that in the early primary transient stage of deformation the only difference between viscous glide and power-law creep is due to the dependence of the glide velocity on the effective stress σ_e. Here $\sigma_e = \sigma - \sigma_i$, with σ the applied stress and σ_i the internal stress. At the higher stress level in the power law creep regime, the apparent creep mechanism is determined by the relative volume fraction of climb-and viscous-glide-controlled regions as presented in Fig. 3. If the above arguments are reasonable, then it is suggested that the creep rate in a grain of a polycrystalline aggregate can be represented by summation of the viscous glide and climb rates as follows [13]:

$$\dot{\varepsilon}_{app} = (1 - f_c)\,\dot{\varepsilon}_g + f_c\,\dot{\varepsilon}_c\,, \qquad (2)$$

where $\dot{\varepsilon}_{app}$ is the apparent creep rate, and $\dot{\varepsilon}_g$ and $\dot{\varepsilon}_c$ are the rates of the viscous glide and climb processes respectively. The volume fraction of sub-grains near the boundary is f_c. The volume fraction of the region controlled by the viscous glide process is $1 - f_c$. If grain boundaries migrate only, the value of f_c becomes zero.

Fig. 4 shows a schematic representation of the deformation behaviour in the vicinity of grain boundaries and development of sub-grains in $n \approx 3$ stress region. It shows a large equiaxed primary sub-grain which is formed during power-law creep and subdivided by cells; for simplicity, secondary sub-boundaries are not shown (see Fig. 4a). Under steady-state conditions, a dislocation generated at a cell boundary under the action of a shear stress, τ, can glide across to the

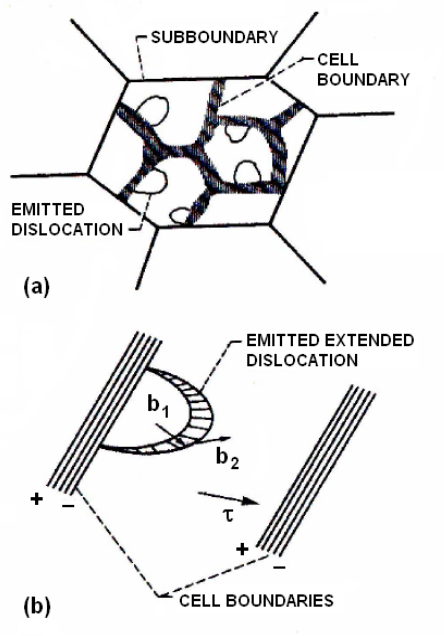

Fig. 4: A phenomenological model for creep showing (a) cells and dislocations within a sub-grain and (b) emission of extended dislocations from a cell wall; b_1 and b_2 are the Burgers vectors of the partial dislocations.

opposite boundary fairly easily (Fig. 4b), where its motion is obstructed or it is annihilated. This process is similar to mechanisms suggested for cyclic deformation [14] but unlike the earlier two phase creep models [2], the present mechanism is consistent with recent experimental observations [15] since it assumes that the cell rather than the sub-grain boundaries govern steady-state behaviour. This difference is important because, in order to accommodate strain inhomogeneity in the material, a cell boundary is more likely than a sub-boundary to breakup due to its smaller misorientation angle (about 0.1°), and thus it is more likely to release new dislocations into the sub-grain interior. In this way, the cell boundaries act as the major sources and sinks for dislocations during creep. The transition from power-law to exponential creep can be envisaged [4, 7] to occur when these microstructural changes are sufficiently large that they influence the nature and magnitudes of the internal stresses acting within the primary sub-grains, thereby resulting in an increase in their aspect ratio. The internal stresses within elongated sub-grains are expected to be higher than that within equiaxed sub-grain, and this difference can lead to sub-boundary migration if the sub-boundaries are mobile. This is consistent with experimental observations on many materials [16].

Fig. 5 shows a comparison of the experimental activation energies Q_c for the alloy with those predicted by the Nix-Ilschner model [4] for obstacle-controlled glide Q_g vs. normalized stress σ/G. It suggest that obstacle controlled dislocation glide is the dominant mechanism in Cu-8.5 at.% Al alloy

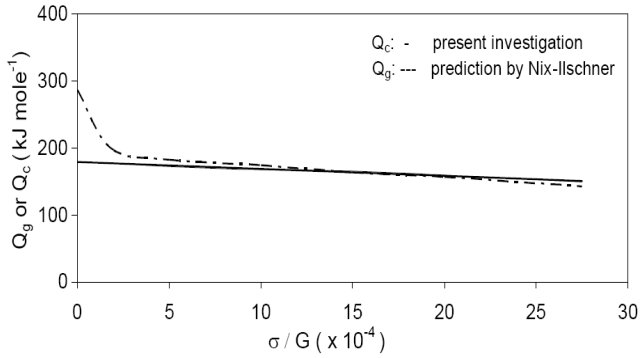

Fig. 5: A comparing between the experimental activation energies, Q_c, for Al-8.5 at.% Cu alloy, and the prediction by the Nix-Ilschner model [4] for obstacle-controlled glide, Q_g at $T = 773$ K.

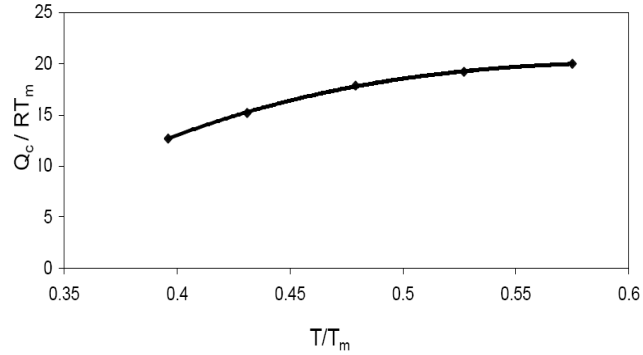

Fig. 6: The normalized activation energies, Q_c, dependence of the T/T_m for the increasing strain rates.

at intermediate temperature region when $\sigma/G \geqslant 5\times10^{-5}$, corresponding to the exponential creep regime [17].

Although the Nix-Ilschner model [4] is in excellent agreement with the experimental data, it is conceptually limited because since it assumes that the deformation processes occurring within the sub-grain interior (i. e. the soft regions) are coupled with recovery mechanisms taking place at the sub-boundaries (i. e. the hard regions). While this assumption predicts that the power-law and the exponential creep mechanisms will act independently, it dose not satisfy the strain compatibility conditions which must maintained between the hard and soft regions to ensure that the slowest deforming phase determines the overall creep rate in both deformation regimes. Support this phenomenological model is also found in Cottrell-Stokes type experiments [18].

Additionally, Fig. 6 reveals that the normalized activation energies, Q_g/RT_m, extrapolate smoothly to the values obtained at lower homologous temperatures where obstacle-controlled glide was established as the dominant deformation process.

4 Conclusion

1. A detailed analysis of creep data on Cu-8.5 at.% Al alloy, obtained at intermediate temperatures between

$0.46-0.72\,T_m$, showed that the obstacle-controlled glide is the rate-controlling mechanism in the transition from power-law to exponential creep regime.

2. A phenomenological model for creep is proposed which is based on the premise that cell boundaries in the sub-grain interior act as sources and obstacles for dislocations.
3. The soft and hard regions model for the internal stress σ_i for a power-law creep curve can only be explained by considering the contribution to σ_i arising from the cell wall dislocations, as well as from dislocations that do not belong to the cell walls.

References

1. Raj S. V. and Langdon T. G. *Acta Metall.*, 1991, v. 39, 1817.
2. Guyot P., Canova G., *Philos. Mag.*, 1999, v. A79, 2815.
3. Cadek J. *Mater. Sci. Eng.*, 1987, v. 94, 79.
4. Nix W. D. and Ilschner B. Strength of Metals and Alloys (ICSMA5), ed. by Haasen P., Gerold V. and Kostorz G., v. 3, p. 1503, Pergamon Press, Oxford, 1980.
5. Poddriguez P. P., Ibarra A., Iza-Mendia A., San Juan J. and No M. L. *Mater. Sci. and Eng.*, 2004, v. A378, 263–268.
6. Argon A. S. and Takeuchi S. *Acta Metall.*, 1981, v. 29, 1877.
7. Montemayor-Aldrete J. *Mater. Sci. and Eng.*, 1993, v. A160, 71–79.
8. Kang S. S., Dobois J. M. *Philos. Mag.*, 1992, v. A66, No. 1, 151.
9. Soliman M. S. J. *Mater. Sci.*, 1993, v. 28, 4483.
10. Murray J. L. *Int. Met. Rev.*, 1985, v. 30, 211.
11. Hasegawa T., Karashima S. *Metall. Trans.*, 1971, v. 2, 1449.
12. Ichihashi K., Oikawa H. *Trans. Japan Inst. Metals*, 1976, v. 17, 408.
13. Dong-Heon Lee, dong Hyuk Shin and Soo Woo Nam. *Mater. Sci. and Eng.*, 1992, v. A156, 43–52.
14. Mughrabi H. Strength of Metals and Alloys (ICSMA5), ed. by Haasen P., Gerold V. and Kostorz G., v. 3, p. 1615, Pergamon Press, Oxford, 1980.
15. Yuwei Xun, Farghalli, Mohamed A., *Acta Metr.*, 2004, v. 52, 4401–4412.
16. Caillard D. and Martin J. L. *Rev. Phys. Appl.*, 1987, v. 22, 169.
17. Raj S. V. and Langdon T. G. *Acta Metall.*, 1989, v. 37, 843.
18. Giacometti E., Balue N., Bonneville J. In: Dubois J. M., Thiel P. A., Tsai A. P., Urban K. (Eds.), *Quasicrystals, Proceedings of the Materials Research Society Symposium*, v. 553, p. 295, *Materials Research Society*, 1999.

Positron Annihilation Line Shape Parameters for CR-39 Irradiated by Different Alpha-Particle Doses

M. Abdel-Rahman*, M. Abo-Elsoud†, M. F. Eissa†, N. A. Kamel*, Y. A. Lotfy*, and E. A. Badawi*

*Physics Department, Faculty of Science, Minia University, Egypt
†Physics Department, Faculty of Science, Beni-suef University, Egypt
E-mail: maboelsoud24@yahoo.com <M. Abo-Elsoud>; emadbadawi@yahoo.com <E. A. Badawi>

Doppler broadening positron annihilation technique (DBPAT) provides direct information about the change of core and valance electrons in Polyallyl diglycol carbonate (CR-39). CR-39 is widely used as etched track type particle detector. This work aims to study the variation of line-shape parameters (S- and W-parameters) with different α-particle doses of ^{241}Am (5.486 MeV) on CR-39 samples at different energies. The relation between both line-shape parameters was also reported. The behavior of the line-shape S- and W-parameters can be related to the different phases.

1 Introduction

Positron Annihilation Technique (PAT) has been used to probe a variety of material properties as well as carry out research in solid state physics. Recently this technique has become established as a useful tool in material science and is successfully applied for investigation of defect structures present in metal alloys. PAT has been employed for the investigating Polymorphism in several organic materials [1] and it has emerged as a unique and potent probe for characterizing the properties of polymers [2].

Positron Annihilation Doppler Broadening Spectroscopy (PADBS) is a well established tool to characterize defects [3]. The 511 keV peak is Doppler broadened by the longitudinal momentum of the annihilating pairs. Since the positrons are thermalized, the Doppler broadening measurements provide information about the momentum distributions of electrons at the annihilation site.

Two parameters S (for shape), and W (for wings) [4] are usually used to characterize the annihilation peak. The S-parameter is more sensitive to the annihilation with low momentum valence and unbound electrons. The S-parameter defined by Mackenzie et al. [5] as the ratio of the integration over the central part of the annihilation line to the total integration. The W-parameter is more sensitive to the annihilation with high momentum core electrons and is defined as the ratio of counts in the wing regions of the peak to the total counts in the peak.

CR-39 is a polymer of Polyallyl diglycol carbonate (PADC) has been used in heavy ion research such as composition of cosmic rays, heavy ion nuclear reactions, radiation dose due to heavy ions and exploration of extra heavy elements. Some applications include studies of exhalation rates of radon from soil and building materials [6, 7] and neutron radiology [8]. When a charged particle passes through a polyallyl diglycol carbonate, $C_{12}H_{18}O_7$ (CR-39) a damage zone are created, this zone is called latent track. The latent track of the particle after chemical etching is called "etch pit" [9]. The etch pit may be seen under an optical microscope. Positron trapping in vacancies (the size of the etch pit in the CR-39 sample) results in an increase (decrease) in S (W) since annihilation with low momentum valence electrons is increased at vacancies.

2 Experimental technique

Various holder collimators with different heights are used to normally irradiate the INTERCAST CR-39 in air by α-particles [10]. Track detectors "CR-39" were normally irradiated in air by different α-particle energies from 0.1 μCi ^{241}Am source.

The heights of the holders are 12.47, 17.55, 21.58, 24.93, 28.7, 31.55 and 34.6 mm they would reduce the energy of 5.486 MeV α-particles from ^{241}Am to 4.34, 3.75, 3.3, 2.86, 2.3, 1.78 and 1.13 MeV, respectively. The irradiations were verified at 0.5, 2, 3, 4.5 min. After exposures, the detectors were etched chemically in 6.25 M NaOH solution at 70°C for 6 h. The simplest way to guide the positrons into the samples is to use a sandwich configuration. ^{22}Na is the radioactive isotope used in our experiment.

The positron source of 1 mCi free carrier ^{22}NaCl was evaporated from an aqueous solution of sodium chloride and deposited on a thin Kapton foil of 7.5 μm in thickness. The ^{22}Na decays by positron emission and electron capture (E. C.) to the first excited state (at 1.274 MeV) of ^{22}Na. This excited state de-excites to the ground state by the emission of a 1.274 MeV gamma ray with half life $T_{1/2}$ of 3×10^{-12} sec. The positron emission is almost simultaneous with the emission of the 1.274 MeV gamma ray while the positron annihilation is accompanied by two 0.511 MeV gamma rays. The measurements of the time interval between the emission of 1.274 MeV and 0.511 MeV gamma rays can

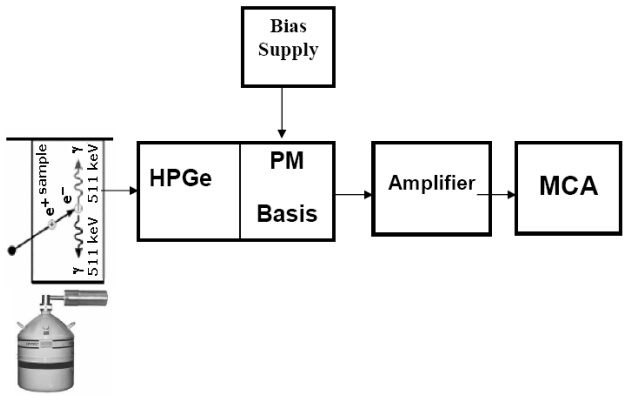

Fig. 1: Block diagram of HPGe-detector and electronics for Doppler broadening line shape measurements.

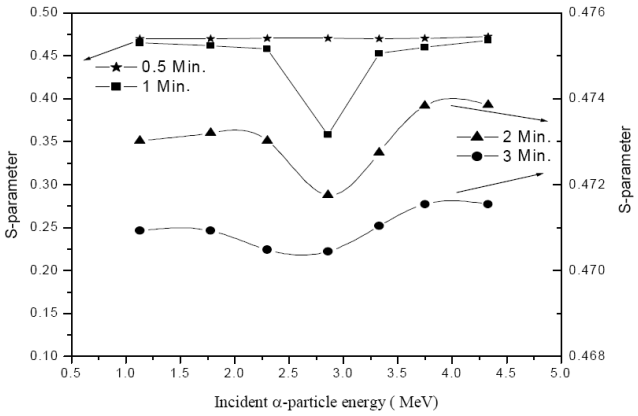

Fig. 2: The variation of S-parameter as a function of irradiation energy for 0.5, 1, 2 and 3 min. irradiation time.

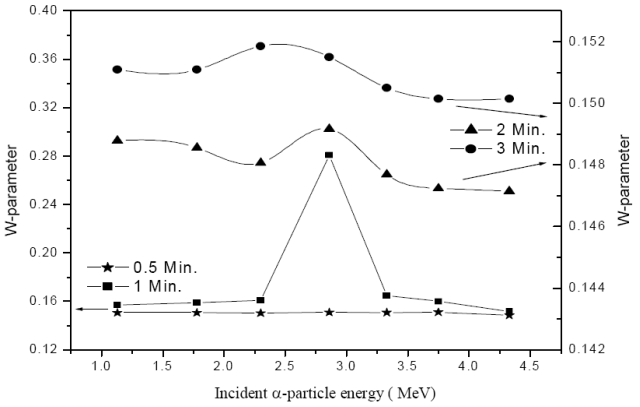

Fig. 3: The variation of W-parameter as a function of irradiation energy for 0.5, 1, 2 and 3 min irradiation time.

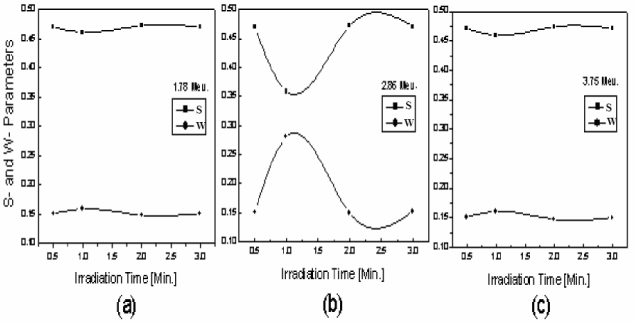

Fig. 4: The variation of S and W parameters as a function of irradiation time for CR-39 samples.

yield the lifetime τ of positrons. The source has to be very thin so that only small fractions of the positron annihilate in the source.

The system which has been used in the present work to determine the Doppler broadening S- and W-parameters consists of an Ortec HPGe detector with an energy resolution of 1.95 keV for 1.33 MeV line of ^{60}Co, an Ortec 5 kV bais supply 659, Ortec amplifier 575 and trump 8 k MCA. Figure 1, shows a schematic diagram of the experimental setup. Doppler broadening is caused by the distribution of the velocity of the annihilating electrons in the directions of gamma ray emission. The signal coming from the detector enters the input of the preamplifier and the output from the preamplifier is fed to the amplifier. The input signal is a negative signal. The output signal from the amplifier is fed to a computerized MCA. All samples spectrum are collected for 30 min.

3 Results and discussion

The Doppler broadening line-shape parameters were measured for irradiated CR-39 samples of different α-particle energies at different doses (0.5, 1, 2 and 3 min). The data of S-and W-parameters at 1 min were calculated by Abdel-Rahman et. al. [11]. The Doppler broadening line-shape S- and W-parameters are calculated using SP ver. 1.0 program [12] which designed to automatically analyze of the positron annihilation line in a fully automated fashion but the manual control is also available. The most important is to determine the channel with the maximum which is associated with the energy 511 keV. The maximum is necessary because it is a base for definition of the regions for calculations of S- and W-parameters.

The results of S- and W-parameters as a function of α-particle energy at different irradiation doses into CR-39 polymer are shown in Figures 2 and 3. From these figures one notice a linear behavior of S- and W-parameters obtained at minimum irradiation time of 0.5 min. The effect of such small irradiation time is very weak to make any variation in line-shape parameters. The values of S- and W-parameters are 47% and 15% respectively at 0.5 min. At longer time (1 min) the S-parameter has values around 46% while values of about 15% are obtained for W-parameter. An abrupt change at 1 min definitely observed at irradiation energy of 2.86 MeV of α-particles for both S- and W-parameters. At this energy a drastically decrease in the S-parameter with deviation of about $\Delta S = 11\%$ comparable with a drastically increase in the W-parameter with deviation of about $\Delta W = 13\%$ [11].

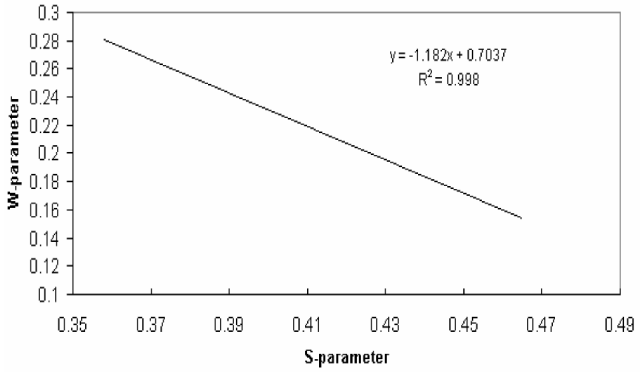

Fig. 5: The correlation between the W-parameter and S-parameter at irradiation time of 1 min.

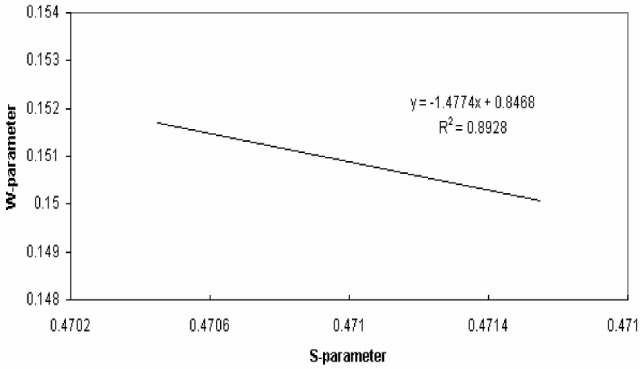

Fig. 6: The correlation between the W-parameter and S-parameter at irradiation time of 3 min.

The S-parameter decreases while W-parameter increases with increasing of irradiation time. Values of about 35% and 25% for S-parameter are obtained at 2 and 3 min respectively for lower energies. The deviation of both S- and W-parameters at 2.86 MeV become very small at longer time as measured at 2 and 3 min. The deviations of $\triangle$S and $\triangle$W reach values less than 0.1% at 3 min (notice different scale on Figures 2 and 3). The behavior of S- and W-parameters reveal an abrupt change at the position of the transition (1 min at 2.86 MeV). The behavior of the line-shape S- and W-parameters can be related to the different phases. Like many others molecular materials, the use of PAT also proven a very valuable in the study of phase transition in polymers.

To recognize more clear the effect of both irradiation time and energy, we take 3 values of energies from presented figures and draw them as a function of irradiation time. Figure 4 (a, b, and c) represent the S- and W-parameters as a function irradiation time for samples irradiated at energies of 1.78, 2.86 and 3.75 MeV respectively. It is much more clear from these figures a slightly change of S- and W-parameters are obtained only at 1 min at irradiation energies of 1.78 and 3.75 MeV. Much more pronounced change in both S- and W-parameters are obtained at the same irradiation time at energy of 2.86 MeV.

The values of W-parameter as a function of S-parameter at 1 and 3 min are plotted in Figs. 5 and 6. It is obvious from these Figures that W-parameter increases as S-parameter decreases for all irradiation times. In addition there are a good correlation with $r^2 = 0.998$ and 0.8928 between S-parameter and W-parameter for 1 and 3 min respectively.

4 Conclusion

The variation of line-shape parameters (S- and W-parameters) at different α-particle doses of ^{241}Am on CR-39 samples for different energies have been studied. The behavior of line-shape parameters at different α-particle doses reveals a pronounced decrease and increase in both S- and W-parameters respectively. A linear behavior of S- and W-parameters are obtained at minimum irradiation time of 0.5 min. An abrupt change of both line-shape parameters, obtained at 2.86 MeV and irradiation dose of 1 min. The W-parameter increases as S-parameter decreases for all irradiation times.

Acknowledgment

We thank Prof. Dr. M. A. Abdel-Rahman for his encouragements and support facilities during preparation of this work.

References

1. Walker W. W., Kline D. C. *J. Chem. Phys.*, 1974, v. 60, 4990.
2. Jean Y. C. In: A. Dupasquier and A. P. Mills Jr. (Eds), *Positron Spectroscopy of Solids*, IOS Publ., Amsterdam, 1995, 563–569.
3. Dupasquier A., Mills A. P. (Eds.) *Positron Spectroscopy of Solids*, IOS Publ., Amsterdam, 1995
4. Urban-Klaehen J. M., Quarles C. A. *J. Appl. Phys.*, 1999, v. 86, 355.
5. Mackenzie I. K., Eady J. A. and Gingerich R. R. *Phys. Lett.*, 1970, v. 33A, 279.
6. Sroor A., El-Bahia S. M., Ahmed F., Abdel-Haleem A. S. Natural radioactivity and radon exhalation rate of soil in southern Egypt. *Applied Radiation and Isotopes*, 2001, v. 55, 873–879.
7. Sharma N. and Virk H. S. Exhalation rate study of radon/thoron in some building materials. *Radiation Measurements*, 2001, v. 34, 467–469.
8. Majeed A. and Durrani S. A., High-energy neutron spectrum measurements using electrochemically etched CR-39 detectors with radiators and degraders. *Nucl. Track Radiat. Meas.*, 1991, v. 19, No. 1–4, pp. 489–494.
9. Durrani S. A., Bull R. K. Solid-state nuclear track, principles, methods and applications formation. Pergamon, Oxford, 1987.
10. Enge W. Introduction to plastic nuclear track detectors. *Nuclear Track*, 1980, No. 4, 283–308.
11. Abdel-Rahman M. A., Abdel-Rahman M., Abo-Elsoud M., Eissa M. F., Lotfy Y. A. and Badawi E. A. *Progress in Physics*, 2006, v. 3, 66–69.
12. http://www.ifj.edu.pl/∼mdryzek.

The Journal on Advanced Studies in Theoretical and Experimental Physics, including Related Themes from Mathematics

PROGRESS IN PHYSICS

A quarterly issue scientific journal, registered with the Library of Congress (DC, USA). This journal is peer reviewed and included in the abstracting and indexing coverage of: Mathematical Reviews and MathSciNet (AMS, USA), DOAJ of Lund University (Sweden), Zentralblatt MATH (Germany), Referativnyi Zhurnal VINITI (Russia), etc.

Electronic version of this journal:
http://www.ptep-online.com
http://www.geocities.com/ptep_online

To order printed issues of this journal, contact the Editor in Chief.

Department of Mathematics, University of New Mexico, 200 College Road, Gallup, NM 87301, USA

This journal is powered by LaTeX

A variety of books can be downloaded free from the Digital Library of Science:
http://www.gallup.unm.edu/∼smarandache

ISSN: 1555-5534 (print)
ISSN: 1555-5615 (online)

Standard Address Number: 297-5092
Printed in the United States of America

OCTOBER 2006 **VOLUME 4**

CONTENTS

Information for Authors and Subscribers

Progress in Physics has been created for publications on advanced studies in theoretical and experimental physics, including related themes from mathematics. All submitted papers should be professional, in good English, containing a brief review of a problem and obtained results.

All submissions should be designed in LaTeX format using *Progress in Physics* template. This template can be downloaded from *Progress in Physics* home page http://www.ptep-online.com. Abstract and the necessary information about author(s) should be included into the papers. To submit a paper, mail the file(s) to Chief Editor.

All submitted papers should be as brief as possible. Commencing 1st January 2006 we accept brief papers, no larger than 8 typeset journal pages. Short articles are preferable. Papers larger than 8 pages can be considered in exceptional cases (such as discoveries, etc.) to the section *Special Reports* intended for such publications in the journal.

All that has been accepted for the online issue of *Progress in Physics* is printed in the paper version of the journal. To order printed issues, contact Chief Editor.

This journal is non-commercial, academic edition. It is printed from private donations.

New Effect of General Relativity: Thomson Dispersion of Light in Stars as a Machine Producing Stellar Energy

Dmitri Rabounski
E-mail: rabounski@yahoo.com

Given a non-holonomic space, time lines are non-orthogonal to the spatial section therein, which manifests as the three-dimensional space rotation. It is shown herein that a global non-holonomity of the background space is an experimentally verifiable fact revealing itself by two fundamental fields: a field of linear drift at 348 km/sec, and a field of rotation at 2,188 km/sec. Any local rotation or oscillation perturbs the background non-holonomity. In such a case the equations of motion show additional energy flow and force, produced by the non-holonomic background, in order to compensate the perturbation in it. Given the radiant transportation of energy in stars, an additional factor is expected in relation to Thomson dispersion of light in free electrons, and provides the same energy radiated in the wide range of physical conditions from dwarfs to super-giants. It works like a machine where the production of stellar energy is regulated by radiation from the surface. This result, from General Relativity, accounts for stellar energy by processes different to thermonuclear reactions, and coincides with data of observational astrophysics. The theory leads to practical applications of new energy sources working much more effectively and safely than nuclear energy.

1 Introduction. The mathematical basis

We aim to study the effects produced on a particle, if the space is non-holonomic. We then apply the result to the particles of the gaseous constitution of stars.

To do this we shall study the equations of motion. To obtain a result applicable to real experiment, we express the equations in terms of physically observable quantities. Mathematical methods for calculating observable quantities in General Relativity were invented by A. Zelmanov, in the 1940's [1, 2, 3]. We now present a brief account thereof.

A regular observer perceives four-dimensional space as the three-dimensional spatial section $x^0 = \text{const}$, pierced at each point by time lines $x^i = \text{const}$.* Therefore, physical quantities perceived by an observer are actually *projections* of four-dimensional quantities onto his own time line and spatial section. The spatial section is determined by a three-dimensional coordinate net spanning a real reference body. Time lines are determined by clocks at those points where the clocks are located. If time lines are everywhere orthogonal to the spatial section, the space is known as *holonomic*. If not, there is a field of the space non-holonomity — the non-orthogonality of time lines to the spatial section, manifest as a three-dimensional rotation of the reference body's space. Such a space is said to be *non-holonomic*.

By mathematical means, four-dimensional quantities can be projected onto an observer's time line and spatial section by the projecting operators: $b^\alpha = \frac{dx^\alpha}{ds}$, the observer's four-dimensional velocity vector tangential to his world-line, and $h_{\alpha\beta} = -g_{\alpha\beta} + b_\alpha b_\beta$. For a real observer at rest with respect to his reference body ($b^i = 0$), the projections of a vector Q^α are $b^\alpha Q_\alpha = \frac{Q_0}{\sqrt{g_{00}}}$ and $h^i_\alpha Q^\alpha = Q^i$, while for a tensor of the 2nd rank $Q^{\alpha\beta}$ we have the projections $b^\alpha b^\beta Q_{\alpha\beta} = \frac{Q_{00}}{g_{00}}$, $h^{i\alpha} b^\beta Q_{\alpha\beta} = \frac{Q^i_0}{\sqrt{g_{00}}}$, $h^i_\alpha h^k_\beta Q^{\alpha\beta} = Q^{ik}$. Such projections are invariant with respect to the transformation of time in the spatial section: they are *chronometrically invariant quantities*.

In the observer's spatial section the chr.inv.-tensor

$$h_{ik} = -g_{ik} + b_i b_k = -g_{ik} + \frac{g_{0i}\, g_{0k}}{g_{00}}\,, \qquad (1)$$

possesses all the properties of the fundamental metric tensor $g_{\alpha\beta}$. Furthermore, the spatial projection of it is $h^\alpha_i h^\beta_k g_{\alpha\beta} = -h_{ik}$. Therefore h_{ik} is the *observable metric tensor*.

The chr.inv.-differential operators

$$\frac{{}^*\partial}{\partial t} = \frac{1}{\sqrt{g_{00}}}\frac{\partial}{\partial t}\,, \qquad \frac{{}^*\partial}{\partial x^i} = \frac{\partial}{\partial x^i} - \frac{g_{0i}}{g_{00}}\frac{\partial}{\partial x^0}\,, \qquad (2)$$

are different to the usual differential operators, and are non-commutative: $\frac{{}^*\partial^2}{\partial x^i \partial t} - \frac{{}^*\partial^2}{\partial t\, \partial x^i} = \frac{1}{c^2} F_i \frac{{}^*\partial}{\partial t}$ and $\frac{{}^*\partial^2}{\partial x^i \partial x^k} - \frac{{}^*\partial^2}{\partial x^k \partial x^i} = \frac{2}{c^2} A_{ik} \frac{{}^*\partial}{\partial t}$. The non-commutativity determines the chr.inv.-vector for the gravitational inertial force F_i and the chr.inv.-tensor of angular velocities of the space rotation A_{ik}

$$F_i = \frac{1}{\sqrt{g_{00}}}\left(\frac{\partial \mathrm{w}}{\partial x^i} - \frac{\partial v_i}{\partial t}\right), \quad \sqrt{g_{00}} = 1 - \frac{\mathrm{w}}{c^2}\,, \qquad (3)$$

$$A_{ik} = \frac{1}{2}\left(\frac{\partial v_k}{\partial x^i} - \frac{\partial v_i}{\partial x^k}\right) + \frac{1}{2c^2}\left(F_i v_k - F_k v_i\right), \qquad (4)$$

where w is the gravitational potential, and $v_i = -c\,\frac{g_{0i}}{\sqrt{g_{00}}}$ is the linear velocity of the space rotation†. Other observable

*Greek suffixes are the space-time indices $0, 1, 2, 3$, Latin ones are the spatial indices $1, 2, 3$. So the space-time interval is $ds^2 = g_{\alpha\beta}\, dx^\alpha dx^\beta$.

†Its contravariant component is $v^i = -c\, g^{0i} \sqrt{g_{00}}$, so $v^2 = h_{ik} v^i v^k$.

properties of the reference space are presented with the chr. inv.-tensor of the rates of the space deformations

$$D_{ik} = \frac{1}{2\sqrt{g_{00}}}\frac{\partial h_{ik}}{\partial t} = \frac{1}{2}\frac{^*\partial h_{ik}}{\partial t} \quad (5)$$

and the chr.inv.-Christoffel symbols

$$\Delta^i_{jk} = h^{im}\Delta_{jk,m} = \frac{1}{2}h^{im}\left(\frac{^*\partial h_{jm}}{\partial x^k} + \frac{^*\partial h_{km}}{\partial x^j} - \frac{^*\partial h_{jk}}{\partial x^m}\right) \quad (6)$$

built just like Christoffel's usual symbols $\Gamma^\alpha_{\mu\nu} = g^{\alpha\sigma}\Gamma_{\mu\nu,\sigma}$ using h_{ik} instead of $g_{\alpha\beta}$.

Within infinitesimal vicinities of any point in a Riemannian space the fundamental metric tensor can be represented as the scalar product $g_{\alpha\beta} = \vec{e}_{(\alpha)}\vec{e}_{(\beta)}$ of the basis vectors, tangential to curves and non-orthogonal to each coordinate line of the space. Hence $g_{\alpha\beta} = e_{(\alpha)}e_{(\beta)}\cos(x^\alpha; x^\beta)$. Therefore the linear velocity of the space rotation

$$v_i = -c\frac{g_{0i}}{\sqrt{g_{00}}} = -ce_{(i)}\cos(x^0; x^i) \quad (7)$$

shows how much the time line inclines to the spatial section, and is the actual value of the space non-holonomity.

The observable time interval $d\tau$ and spatial displacements are the projections of the world-displacement dx^α:

$$d\tau = \frac{1}{c}b_\alpha dx^\alpha = \sqrt{g_{00}}\,dt - \frac{1}{c^2}v_k dx^k, \quad (8)$$

while the observable spatial displacements coincide with the coordinate ones $h^i_\alpha dx^\alpha = dx^i$. The observable spatial interval is $d\sigma^2 = h_{ik}dx^i dx^k$, while $ds^2 = c^2d\tau^2 - d\sigma^2$.

Using these techniques, we can calculate the physically observable projections of any world-quantity, then express them through the observable properties of the space.

2 A global non-holonomity of the background space — an experimentally verifiable fact

Can such a case exist, where, given a non-holonomic space, the linear velocity of its rotation is $v_i \neq 0$, while the angular velocity is $A_{ik} = 0$? Yes, it is possible. If v_i has the same numerical value $v_i = \bar{v}_i = \text{const}$ at each point of a space, we have $A_{ik} = 0$ everywhere therein. In such a case, by formula (7), there is a stationary homogeneous *background field of the space non-holonomity*: all time lines, piercing the spatial section, have the same inclination $\cos(x^0; x^i) = -\frac{\bar{v}_i}{ce_{(i)}}$ to the spatial section at each its points.

Is such a background truly present in our real space? If yes, what is the "primordial" value $\bar{v}_i = \text{const}$? These questions can be answered using research of the 1960's, carried out by Roberto di Bartini [4, 5].

In his research di Bartini used topological methods. He considered "a predicative unbounded and hence unique specimen A. [...] A coincidence group of points, drawing elements of the set of images of the object A, is a finite symmetric system, which can be considered as a topological spread mapped into the spherical space R^n" [5].

Given the spread R^n, di Bartini studied "sequences of stochastic transitions between different dimension spreads as stochastic vector quantities, i. e. as fields. Then, given a distribution function for frequencies of the stochastic transitions dependent on n, we can find the most probable number of the dimension of the ensemble" [5]. He found extrema of the distribution function at $n = \pm 6$, "hence the most probable and most improbable extremal distributions of primary images of the object A are presented in the 6-dimensional closed configuration: the existence of the total specimen A we are considering is 6-dimensional. [...] a spherical layer of R^n, homogeneously and everywhere densely filled by doublets of the elementary formations A, is equivalent to a vortical torus, concentric with the spherical layer. The mirror image of the layer is another concentric homogeneous double layer, which, in turn, is equivalent to a vortical torus coaxial with the first one. Such formations were studied by Lewis and Larmore for the $(3+1)$-dimensional case" [5].

For the $(3+1)$-dimensional image, di Bartini calculated the ratio between the torus diameter D and the radius of the circulation r which satisfies the condition of stationary vortical motion (the current lines coincide with the trajectory of the vortex core). He obtained $E = \frac{D}{r} = 274.074\,996$, i. e.

$$\frac{R}{r} = 137.037\,498. \quad (9)$$

Applying this bizarre result to General Relativity, we see that if our real space satisfies the most probable topological shape, we should observe two fundamental drift-fields:

1. A field of the constant rotating velocity 2,187.671 km/sec — a field of the background space non-holonomity.

This comes with the fact that the frequency distribution Φ_n of the stochastic transitions between different dimensions "is isomorphic to the function of the surface's value $S_{(n+1)}$ of a unit radius hypersphere located in an $(n+1)$-dimensional space (this value is equal to the volume of an n-dimensional hypertorus). This isomorphism is adequate for the ergodic concept, according to which the spatial and time spreads are equivalent aspects of a manifold" [5].

In such a case the radius of the circulation r (the spatial spread's function) is expressed through a velocity v just like the torus' radius R (the time spread's function) is expressed through the velocity of light $c = 2.997\,930 \times 10^{10}$ cm/sec. Thus, we obtain the analytical value of the velocity $\bar{v}_i$:

$$\bar{v} = \frac{2c}{E} = \frac{cr}{R} = 2.187\,671 \times 10^8 \text{ cm/sec}, \quad (10)$$

Because the vortical motion is stationary, the linear velocity $\bar{v}_i$ of the circulation r is constant everywhere within it. In other words, $\bar{v}_i = 2{,}187.671$ km/sec is the linear velocity of the space rotation characterizing a stationary homogeneous

field of the background space non-holonomity: there in the space all time lines have the same inclination to the spatial section at each of its points

$$\cos(x^0; x^i) = -\frac{\bar{v}}{c} = -\frac{1}{137.037498} = -0.0072972728. \quad (11)$$

The background non-holonomity should produce an effect in v_i-dependent phenomena. Hence the non-holonomic background should be an experimentally verifiable fact.

In such an experiment we should take into account the fact that all v_i-dependent physical factors should initially contain the background space rotation $\bar{v}_i = 2{,}187.671\,\text{km/sec}$. Therefore, the background cannot itself be isolated; it can be shown only by the changes of the quantities expected to be affected by local perturbations of the background.

2. A field of constant linear velocity 348.1787 km/sec — a field of the background drift-velocity.

This comes from the fact that the background becomes polarized while "the shift of the field vector at $\frac{\pi}{2}$ in its parallel transfer along closed arcs of radii R and r in the affine coherence space R^n" [5]. Hence, we find that the unpolarized component of the field $\bar{v}_i = 2{,}187.671\,\text{km/sec}$ is a field of a constant dipole-fit velocity

$$\bar{\mathrm{v}} = \frac{\bar{v}}{2\pi} = 3.481787 \times 10^7\,\text{cm/sec}\,. \quad (12)$$

In other words, it should be a global-drift field of the constant dipole-fit linear velocity $\bar{\mathrm{v}} = 348.1787\,\text{km/sec}$, represented in the circulation r (three-dimensional spread).

Our analytically obtained value 348.1787 km/sec is in close agreement with the linear drift-velocity $365 \pm 18\,\text{km/sec}$ extracted from the recently discovered anisotropy of the Cosmic Microwave Background.

The Cosmic Microwave Background Radiation was discovered in 1965 by Penzias and Wilson at Bell Telephone Lab. In 1977, Smoot, Gorenstein, and Muller working with a twin antenna Dicke radiometer at Lawrence Berkeley Lab, discovered an anisotropy in the Background as the dipole-fit linear velocity $390 \pm 60\,\text{km/sec}$ [9]. Launched by NASA, in 1989, the Cosmic Background Explorer (COBE) satellite produced observations from which the dipole-fit velocity was extracted more precisely at $365 \pm 18\,\text{km/sec}$. The Wilkinson Microwave Anisotropy Probe (WMAP) satellite by NASA, launched in 2001, verified the COBE data [10].

As already shown by Zelmanov, in the 1940's [1], General Relativity permits absolute reference frames connected to the anisotropy of the fields of the space non-holonomity or deformation — the globally polarized fields similar to a global gyro. Therefore the drift-fields analytically obtained above provide a theoretical basis for an absolute reference frame in General Relativity, connected to the anisotropy of the Cosmic Microwave Background.

In the next Section we study the effects we expect on a test-particle due to the background space non-holonomity.

3 A test-particle in a non-holonomic space. Effects produced by the background space non-holonomity

Free particles move along the shortest (geodesic) lines. The equations of free motion are derived from the fact that any tangential vector remains parallel to itself when transferred along a geodesic, so the general covariant derivative of the vector is zero along the line. A particle's four-dimensional impulse vector is $P^\alpha = m_0 \frac{dx^\alpha}{ds}$, so the general covariant equations of free motion are

$$\frac{dP^\alpha}{ds} + \Gamma^\alpha_{\mu\nu} P^\mu \frac{dx^\nu}{ds} = 0\,; \quad (13)$$

their observable chr.inv.-projections, by Zelmanov [1], are

$$\begin{aligned} &\frac{dE}{d\tau} - mF_i \mathrm{v}^i + mD_{ik}\mathrm{v}^i\mathrm{v}^k = 0\,, \\ &\frac{dp^i}{d\tau} - mF^i + 2m\left(D^i_k + A^{\cdot i}_{k\cdot}\right)\mathrm{v}^k + m\Delta^i_{nk}\mathrm{v}^n\mathrm{v}^k = 0\,, \end{aligned} \quad (14)$$

where $\mathrm{v}^i = \frac{dx^i}{d\tau}$ and $p^i = m\mathrm{v}^i$ are the observable velocity and impulse of the particle, m and $E = mc^2$ are its relativistic mass and energy. Each term in the equations is an observable chr.inv.-quantity*. The scalar equation is the chr.inv.-energy law. The vector equations are the three-dimensional chr.inv.-equations of motion, setting up the 2nd Newtonian law.

In non-free motion, a particle deviates from a geodesic line, so the right sides of the equations of motion become non-zero, expressing a deviating force.

We will now fit the chr.inv.-equations of motion according to the most probable topological configuration of the space, as propounded by di Bartini. In such a case we can represent dx^i as $dx^i = v^i\,dt$ while the time interval is $dx^0 = cdt$. Such a representation coincides with the ergodic concept, where the spatial and time spreads are equivalent elements of a manifold; so the transformation $dx^i = v^i\,dt$ should be understood to be "ergodic".

Applying the "ergodic transformation", after some algebra we find that in such a space the metric ds^2 takes the form†

$$ds^2 = g_{00}\,c^2 dt^2 \left\{ \left(1 + \frac{v^2}{c^2\sqrt{g_{00}}}\right)^2 - \frac{v^2}{c^2 g_{00}} \right\}, \quad (15)$$

while the physically observable time interval is

$$d\tau = \left(\sqrt{g_{00}} - \frac{v^2}{c^2}\right) dt = \left\{1 - \frac{1}{c^2}\left(\mathrm{w} + v^2\right)\right\} dt\,, \quad (16)$$

where $v^2 = v_i\,v^i = h_{ik}\,v^i v^k$. Looking at the resultant metric from the geometric viewpoint, we note an obvious feature:

> In such a metric space the flow of time is equivalent to a *turn of the spatial section*.

*Given a chr.inv.-quantity, we can raise/lower its indices by the chr.inv.-metric tensor h_{ik}: $h_{ik} = -g_{ik} + \frac{1}{c^2} v_i v_k$, $h^{ik} = -g^{ik}$, and $h^i_k = \delta^i_k$.

†Because $v_i = -c\,\frac{g_{0i}}{\sqrt{g_{00}}}$, $v^i = -c\,g^{0i}\sqrt{g_{00}}$, $h_{ik} = -g_{ik} + \frac{1}{c^2} v_i v_k$.

In the (3+1)-dimensional vortical torus, the ratio between its diameter D and the radius of the circulation r is the fundamental constant $E=\frac{D}{r}=274.074\,996$ [4, 5]. Hence the circulation velocity $\bar{v}=\frac{2c}{E}=2{,}187.671\ \text{km/sec}$ (the linear velocity of the background space rotation) is covariantly constant. On the other hand, locally in the spatial section, the components of the vector $v_i=-c\frac{g_{0i}}{\sqrt{g_{00}}}$ can be different from 2,187.671 km/sec due to the locally non-holonomic perturbations in the background*. In other words, the field v_i is built on two factors: (1) the background remaining constant and uniform $\bar{v}_i=2{,}187.671$ km/sec at any point or direction in the space, and (2) a local perturbation $\tilde{v}_i$ in the background produced by rotating bodies located nearby.

As a result, within an area in which the non-holonomic background $\bar{v}_i$ is perturbed by a local rotation $\tilde{v}_i$,

$$dx^i=v^i\,dt=\left(\bar{v}^i+\tilde{v}^i\right)dt\,. \tag{17}$$

That is, with the same displacement dx^i the turn dt can be different depending on how much the non-holonomic background is perturbed by a local rotation.

The non-holonomic background remaining constant does not produce an effect in the differentiated quantities. An effect is expected to be due only from the expansion of the differential operator $\frac{\partial}{\partial t}$ where we represent dt, according to the metric (15), as a turn of the spatial section. As such, dt should be expressed through the ergodic transformation $dx^i=v^i\,dt=\left(\bar{v}^i+\tilde{v}^i\right)dt$. Expanding $\frac{\partial}{\partial t}$ in such a way, after algebra, we obtain the corrected formulae for the main physically observable chr.inv.-characteristics of the space that take the background space non-holonomity into account†

$$F_i=\frac{1}{\sqrt{g_{00}}}\left\{\frac{\partial \mathrm{w}}{\partial x^i}-\left(1+\delta^m_n\frac{\tilde{v}^n}{\bar{v}^m}\right)\frac{\partial\tilde{v}_i}{\partial\bar{t}}\right\}, \tag{18}$$

$$A_{ik}=\frac{1}{2}\left(\frac{\partial\tilde{v}_k}{\partial x^i}-\frac{\partial\tilde{v}_i}{\partial x^k}\right)+\frac{1}{2c^2}\left(F_i\tilde{v}_k-F_k\tilde{v}_i\right), \tag{19}$$

$$D_{ik}=\frac{1}{2\sqrt{g_{00}}}\left(1+\delta^m_n\frac{\tilde{v}^n}{\bar{v}^m}\right)\frac{\partial h_{ik}}{\partial\bar{t}}\,, \tag{20}$$

$$\begin{aligned}\Delta^i_{jk}&=\frac{1}{2}\,h^{im}\left(\frac{\partial h_{jm}}{\partial x^k}+\frac{\partial h_{km}}{\partial x^j}-\frac{\partial h_{jk}}{\partial x^m}\right)+\\&+\frac{1}{c^2}\,h^{im}\left(1+\delta^m_n\frac{\tilde{v}^n}{\bar{v}^m}\right)\left(v_k D_{jm}+v_j D_{km}+v_m D_{jk}\right),\end{aligned} \tag{21}$$

where the differential operator $\frac{\partial}{\partial\bar{t}}$ is determined in the unperturbed background $\bar{v}_i$, while the additional multiplier sets up a correction for a local perturbation $\tilde{v}_i$ in it.

If there is no non-holonomic background, but only locally non-holonomic fields due to rotating small bodies, the above formulae revert to their original shape through $\bar{v}^i=0$ in the transformation $dx^i=v^i\,dt=\left(\bar{v}^i+\tilde{v}^i\right)dt$. The above transformation is impossible in a holonomic space since therein the spatial coordinates aren't functions of the time coordinate; $x^i\neq f\left(x^0\right)$. So the foregoing is true only if the space is non-holonomic, and the spatial and time spreads are equivalent elements of the manifold.

From the formulae obtained, we conclude that:

> The main physically observable chr.inv.-properties of the reference space, such as the gravitational inertial force F_i, the angular velocity of the space rotation A_{ik}, the rate of the space deformation D_{ik}, and the space non-uniformity (set up by the chr.inv.-Christoffel symbols Δ^i_{jk}) are dependent on the ratio between the value of the local non-holonomity $\tilde{v}_i$ (due to nearby rotating bodies) and the background space non-holonomity $\bar{v}_i=2{,}187.671$ km/sec.

What effect does this have on the motion of a particle? Let's recall the chr.inv.-equations of motion (14). While a particle is moved along dx^i by an external force (or several forces), the acceleration gained by the particle is determined by the fact that its spatial impulse vector p^i, being transferred along dx^i, undergoes a space-time turn dt expressed by the ergodic transformation (17).

The entire motion of a particle is expressed by the term with $\frac{d}{d\tau}$ in the scalar and chr.inv.-vector equations of motion (14). The remaining terms in the scalar equation express the work spent on the motion by external forces, while the remaining terms in the vector equation account for the forces themselves. Therefore, for the entire motion of a particle, we have no need of expanding $\frac{\partial}{\partial t}$ by the ergodic transformation, for each force acting thereon. We simply need to apply the expansion to the chr.inv.-derivative with respect to the observable time $\frac{d}{d\tau}$ in the equations of motion (14).

By definition (8), $d\tau=\sqrt{g_{00}}\,dt-\frac{1}{c^2}\,v_k dx^k$, so we have $dt=\frac{1}{\sqrt{g_{00}}}\left(1+\frac{1}{c^2}\,v_k\mathrm{v}^k\right)d\tau$. The differential is $d=\frac{\partial}{\partial x^\alpha}\,dx^\alpha$, so $d=\frac{1}{\sqrt{g_{00}}}\left(1+\frac{1}{c^2}\,v_k\mathrm{v}^k\right)\frac{\partial}{\partial t}\,d\tau+\frac{\partial}{\partial x^k}\,dx^k$ and, finally

$$\frac{d}{d\tau}=\frac{1}{\sqrt{g_{00}}}\left(1+\frac{1}{c^2}\,v_k\mathrm{v}^k\right)\frac{\partial}{\partial t}+\mathrm{v}^k\frac{\partial}{\partial x^k}\,. \tag{22}$$

Expanding this formula with the ergodic transformation $dx^i=v^i\,dt=\left(\bar{v}^i+\tilde{v}^i\right)dt$, we obtain it in the form

$$\begin{aligned}\frac{d}{d\tau}&=\left(1+\delta^m_n\frac{\tilde{v}^n}{\bar{v}^m}\right)\frac{d}{d\bar{\tau}}+\delta^m_n\frac{\tilde{v}^n}{\bar{v}^m}\,\mathrm{v}^k\frac{\partial}{\partial x^k}+\\&+\frac{1}{c^2\sqrt{g_{00}}}\left(1+\delta^m_n\frac{\tilde{v}^n}{\bar{v}^m}\right)\tilde{v}_k\mathrm{v}^k\frac{\partial}{\partial\bar{t}}\end{aligned} \tag{23}$$

where the non-holonomic background $\bar{v}_i=2{,}187.671$ km/sec is taken into account. Here $\frac{\partial}{\partial\bar{\tau}}$ and $\frac{\partial}{\partial\bar{t}}$ are also determined in the unperturbed background $\bar{v}_i$.

*Note that Minkowski space of Special Relativity is free of gravitational fields ($g_{00}=1$) and rotations ($g_{0i}=0$). So all the effects we are considering are attributed only to General Relativity's space.

†Here $\delta^m_n=\left(\begin{smallmatrix}1&0&0\\0&1&0\\0&0&1\end{smallmatrix}\right)$ is the unit three-dimensional tensor, the spatial part of the four-dimensional Kronecker unit tensor δ^α_β used for replacing the indices. So δ^m_n replaces the indices in three-dimensional tensors.

In particular, if a moving particle is slow with respect to light and the differentiated quantity is distributed uniformly in the spatial section, we have $\frac{1}{c^2}\tilde{v}_k \mathrm{v}^k = 0$ and $\frac{\partial}{\partial x^k} = 0$ in the above formula, so we obtain

$$\frac{d}{d\tau} \simeq \frac{1}{\sqrt{g_{00}}}\frac{\partial}{\partial t} = \frac{1}{\sqrt{g_{00}}}\left(\bar{v}^k + \tilde{v}^k\right)\frac{\partial}{\partial x^k} = \\ = \left(1 + \delta^m_n \frac{\tilde{v}^n}{\bar{v}^m}\right)\frac{d}{d\bar{\tau}}\,. \tag{24}$$

In such a case, by the chr.inv.-equations of motion (14), the total force moving the particle $\Phi^i = \frac{dp^i}{d\tau}$ and the total energy flow $W = \frac{dE}{d\tau}$ expended on the motion are

$$W = \frac{dE}{d\tau} = \left(1 + \delta^m_n \frac{\tilde{v}^n}{\bar{v}^m}\right) W_{(0)} = W_{(0)} + \delta^m_n \frac{\tilde{v}^n}{\bar{v}^m} W_{(0)} \tag{25}$$

$$\Phi^i = \frac{dp^i}{d\tau} = \left(1 + \delta^m_n \frac{\tilde{v}^n}{\bar{v}^m}\right)\Phi^i_{(0)} = \Phi^i_{(0)} + \delta^m_n \frac{\tilde{v}^n}{\bar{v}^m}\Phi^i_{(0)} \tag{26}$$

where $\Phi^i_{(0)}$ and $W_{(0)}$ are the acting force and energy flow in the unperturbed non-holonomic background (before a local rotation $\tilde{v}^i$ was started). The additional force $\delta^m_n \frac{\tilde{v}^n}{\bar{v}^m}\Phi^i_{(0)}$ and energy flow $\delta^m_n \frac{\tilde{v}^n}{\bar{v}^m} W_{(0)}$ are produced by the stationary homogeneous field of the background space non-holonomity $\bar{v}_i$ in order to compensate for a perturbation in it caused by a local rotation $\tilde{v}_i$. As a result we conclude that:

> The presence of a background space non-holonomity manifests in a particle as an addition to its acceleration, gained from an external force (or forces) moving it. This additional force appears only if the non-holonomic background is perturbed by a local rotation in the area where the particle moves. (Being unperturbed, the non-holonomic background does not produce any forces.) The force appears independently of the origin of the forces moving the particle, and is proportional to the ratio between the linear velocity of the local rotation $\tilde{v}_i$ and that of the background space rotation $\bar{v}_i = 2{,}187.671\ \mathrm{km/sec}$.

Such an additional force should appear on any particle accelerated near a rotating body. On the other hand, because the space background rotates rapidly, at 2,187.671 km/sec, such a force is expected only near rapid rotations, comparable with 2,187.671 km/sec.

For instance, consider a high speed gyro as used in aviation navigation technology: 250 g rotor of 1.65″ diameter, rotating at 24,000 rpm. With current technology, the latter is almost the ultimate speed for such a mechanically rotating system. In such a case the non-holonomic background near the gyro is perturbed as $\tilde{v} = 5.3\times10^3$ cm/sec, i. e. 53 m/sec*. So near the gyro, by our formula (26), we expect to have an additional factor of 2.4×10^{-5} of any force accelerating a particle near the gyro. In other words, the expected effect is very small near such mechanically rotating systems.

The terrestrial globe rotates at 465 m/sec at its equator, so the non-holonomic space background is perturbed there by Earth's rotation by the factor 2.2×10^{-4}. Hence, given a specific experiment performed at the equator, an additional force produced by the non-holonomic background in order to compensate the perturbation in it should be 2.2×10^{-4} of the force acting in the experiment. This effect decreases with latitude owing to concomitant reduction of the linear velocity of the Earth's rotation, and completely vanishes at the poles.

However, the additional force can be much larger if the non-holonomic background is perturbed by particles rotated or oscillated by electromagnetic fields. In such a case a local rotation velocity can even reach that of the background, i. e. 2,187.671 km/sec, in which case the main force accelerating the particle is doubled. In the next Section we consider a particular example of such a doubled force, expected in relation to Thomson dispersion of light in free electrons within stars.

In forthcoming research we show how such an additional force can be detected in experiment, and applied to the development on a device whose motion is based on principles, completely different from those employed in aviation and space technology today. Such a device should revolutionize aviation and space travel.

It is interesting to note that a similar conclusion on the time flow as a turn and additional forces produced by it were drawn by the famous astronomer and experimental physicist, N. A. Kozyrev, within the framework of his "nonsymmetrical mechanics" [8]. Kozyrev proceeded from his research on the insufficiency of Classical Mechanics and thermodynamics in order to explain some effects in rotating bodies and also the specific physical conditions in stars. He didn't construct an exact theory, limiting himself to phenomenological conclusions and general speculations. On the other hand, his phenomenologically deduced formula for a force additional to Classical Mechanics is almost the same as our purely theoretical result $\delta^m_n \frac{\tilde{v}^n}{\bar{v}^m}\Phi^i_{(0)}$ obtained by means of General Relativity in the non-holonomic four-dimensional space of General Relativity, in the low velocity approximation. Therefore this coincidence can be viewed as an auxiliary verification of our theory.

We see that there is no need to change the basic physics as Kozyrev did. Naturally, all the results we have obtained are derived from the background non-holonomity of the four-dimensional space of General Relativity. Classical Mechanics uses a three-dimensional flat Euclidean space that does not contain the time spread and, hence, the non-holonomic property. Classical Mechanics is therefore insufficient for explaining the effects of the background space non-holonomity predicted herein by means of General Relativity. So the additional force and energy flow are new effects predicted within the framework of Einstein's theory.

*Mechanical gyros used in aviation and submarine navigation systems have rotations at speeds in the range 6,000 – 30,000 rpm. The upper speed is limited by problems derived from friction in such a mechanical system.

4 Thomson dispersion of light in stars as a machine producing stellar energy due to the background space non-holonomity

Here we apply the foregoing results to the particles of the gaseous constitution of stars.

The physical conditions in stars result from the comparison of well-known correlations of observational astrophysics and two main equations of equilibrium in stars (mechanical and thermal equilibrium). Such a comparison is made in the extensive research started in the 1940's by Kozyrev. The final version was printed in 2005 [6].

In brief, a star is a gaseous ball in a stable state, because mechanical and thermal equilibrium therein are expressed by two equations: (1) the mechanical equilibrium equation — gravity pushing each cm^3 of the gas to the centre of a star is balanced by the gaseous pressure from within; (2) the thermal equilibrium equation — the energy flow produced within one cm^3 of the gas equals the energy loss by radiation. The comparison of the equilibrium equations with the mass–luminosity relation and the period — average density of Cepheids, a well verified correlation of observational astrophysics, resulted in the stellar energy diagram wherein the isoergs show the productivity of stellar energy sources per second [6]. The diagram is reproduced below. The energy output of thermonuclear reactions gives a surface, whose intersection with the diagram is the dashed arc. Because stars have a completely different distribution in the diagram, it is concluded that thermonuclear synthesis can be the source of stellar energy in only a minority of stars, located along the dashed arc. Naturally, stars in the diagram are distributed along a straight line that runs from the right upper region to the left lower region, with a ball-like concentration at the centre of the diagram. The equation of the main direction is

$$\frac{B}{n_e} = \text{const} = 1.4\times10^{-11}\,\text{erg}\,, \qquad (27)$$

and is the relation between the radiant energy density B and the concentration of free electrons in stars. In other words, this is the energy produced per free electron in stars, and it is constant throughout the widest range of the physical conditions in stars: from dwarfs to super-giants. This is the actual physical condition under which the mechanism that generates stellar energy works, even in the low-temperature stars such as red super-giants like the infrared satellite of ε Aurigae, wherein the temperature is about 200,000° and the pressure about one atmosphere. In other words, the relation characterizes the source of stellar energy. According to the stellar energy relation (27), constant in any kind of star, Kozyrev concluded that "the energy productivity in stars is determined by the energy drainage (radiation) only. [...] In contrast to reaction, such a mechanism should be called a machine. [...] In other words, stars are *machines* which generate radiant energy. The heat drainage is the power regulation mechanism in the machines" [6].

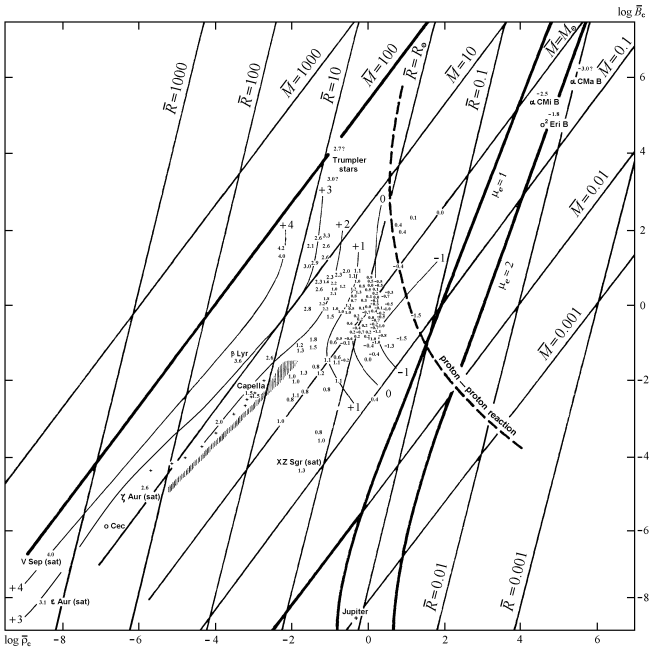

Fig. 1: Diagram of stellar energy: the productivity of stellar energy sources. The abscissa is the logarithm of the density of matter, the ordinate is the logarithm of the radiant energy density (both are taken at the centre of stars in multiples of the corresponding values at the centre of the Sun). Reproduced from [6].

I note that the stellar energy relation (27) — the result of comparing the two main equilibrium equations and observational data — is pure phenomenology, independent of our theoretical views on the origin of stellar energy.

Let's consider the stellar energy relation (27) by means of our theory developed in Section 3 herein. By this relation we have $\frac{B}{n_e} = \text{const} = 1.4\times10^{-11}$erg: the energy produced per electron is constant in any kind of star, under any temperature or pressure therein. So the mechanism producing stellar energy works by a process related to electrons in stars. There is just one process of such a kind — Thomson dispersion of light in free electrons in the radiant transportation of energy from the centre to the surface.

We therefore consider the Thomson process. When a light wave having the average density of energy q encounters a free electron, the flow of the wave energy $\sigma c q$ is stopped in the electron's "square" $\sigma = 6.65\times10^{-25}\,\text{cm}^2$ (the square of Thomson dispersion). As a result the electron gains an acceleration σq, directed orthogonally to the wave front. In other words, the electron is propelled by a force produced by the wave energy flow stopped in its square, and in the direction of the wave propagation.

We will determine the force by means of electrodynamics in the terms of physically observable chr.inv.-quantities*. The

*The basics of electrodynamics such as the theory of an electromagnetic field and a charged particle moving in it, expressed in terms of chronometric invariants, was developed in the 1990's [11, Chapter 3].

chr. inv.-energy density q and chr.inv.-impulse density J^i are the chr.inv.-projections $q=\frac{T_{00}}{g_{00}}$ and $J^i=\frac{cT_0^i}{\sqrt{g_{00}}}$ of the energy-momentum tensor $T^{\alpha\beta}$ of an electromagnetic field

$$q=\frac{1}{8\pi}\left(E_iE^i+H_{ik}H^{ik}\right),\qquad J^i=\frac{c}{4\pi}E_kH^{ik},\quad(28)$$

where $E^i=\frac{F_{0\cdot}^{\ i}}{\sqrt{g_{00}}}$ and $H^{ik}=F^{ik}$ are the chr.inv.-projections of the electromagnetic field tensor $F_{\alpha\beta}$ — the physically observable electric and magnetic strengths of the field [11]. We consider radiation within stars to be isotropic. In an isotropic electromagnetic field $E_iE^i=H_{ik}H^{ik}$ [11], so

$$q=\frac{1}{4\pi}E_iE^i,\qquad J^2=h_{ik}\,J^iJ^k=q^2c^2,.\qquad(29)$$

Hence, the wave impulse flow along the x^1 direction the wave travels is

$$J^1=\frac{qc}{\sqrt{h_{11}}},\qquad(30)$$

while the flow of the wave energy stopped in an electron's surface σ, i. e. the force pushing the electron in the x^1 direction, orthogonal to the wave front, is

$$\Phi^1=\frac{\sigma q}{\sqrt{h_{11}}}=\frac{\sigma q}{\sqrt{1+\frac{1}{c^2}v_1v_1}}.\qquad(31)$$

On the other hand, according to our theory, developed in Section 3, the total force Φ^1 acting on an electron and the energy flow W expended on it via the Thomson process should be

$$W=\frac{dE}{d\tau}=W_{(0)}+\delta_n^m\frac{\tilde v^n}{\bar v^m}W_{(0)},\qquad(32)$$

$$\Phi^1=\frac{dp^1}{d\tau}=\Phi^1_{(0)}+\delta_n^m\frac{\tilde v^n}{\bar v^m}\Phi^1_{(0)},\qquad(33)$$

depending on a local perturbation $\tilde v^i$ in the background space non-holonomity $\bar v_i=2{,}187.671\ \text{km/sec}$.

What is the real value of the local perturbation $\tilde v^i$ in Thomson dispersion of light in stars? We calculate the value of $\tilde v^i$, proceeding from the self-evident geometrical truth that the origin of a non-holonomity of a space is any motion along a closed path in it, such as rotations or oscillations.

When a light wave falls upon an electron, the electron oscillates in the plane of the wave because of the oscillations of the electric field strength E^i in the plane. The spatial equation of motion of such an electron is the equation of forced oscillations. For oscillations in the x^2 direction, in a homogeneous non-deformed space, the equation of motion is

$$\ddot x^2+\omega_0^2x^2=\frac{e}{m_e}E_0^2\cos\omega t,\qquad(34)$$

where ω is the frequency of the wave and ω_0 is the proper frequency of the electron. This equation has the solution

$$x^2=\frac{eE_0^2\cos\omega t}{m_e(\omega_0^2-\omega^2)}\simeq\frac{eE_0^2\cos\omega t}{m_e\omega^2}\qquad(35)$$

so the components of the linear velocity $\tilde v^i$ of the local space rotation, approximated by the oscillation, are

$$\tilde v^2=\frac{eE_0^2}{m_e\omega},\qquad\tilde v^1=0,\qquad\tilde v^3=0.\qquad(36)$$

The electric field strength E in a light wave, according to (29), is $E=\sqrt{4\pi q}=\sqrt{4\pi B}$ where B is the radiant energy density. Therefore the value of $\tilde v^2$ is

$$\tilde v=\frac{e\sqrt{4\pi}}{m_e}\frac{\sqrt{B}}{\omega}=\frac{e\sqrt{4\pi\alpha}}{m_e}\frac{T^2}{\omega},\qquad(37)$$

where $\alpha=7.59\times10^{-15}\ \text{erg/cm}^3\times\text{degree}^4$ is Stefan's constant, T is temperature. Therefore the total energy flow $W=W_{(0)}+\frac{\tilde v^2}{\bar v^2}W_{(0)}=W_{(0)}+\frac{\tilde v}{\bar v}W_{(0)}$ and force $\Phi^1=\Phi^1_{(0)}+\frac{\tilde v^2}{\bar v^2}\Phi^1_{(0)}$ acting on an electron orthogonally to the wave plane in the Thomson process should be

$$W=W_{(0)}+\frac{e\sqrt{4\pi}}{m_e\bar v}\frac{\sqrt{B}}{\omega}W_{(0)},\qquad(38)$$

$$\Phi^1=\Phi^1_{(0)}+\frac{e\sqrt{4\pi}}{m_e\bar v}\frac{\sqrt{B}}{\omega}\Phi^1_{(0)},\qquad(39)$$

where $\bar v=2{,}187.671\,\text{km/sec}$. So the additional energy flow $\Delta W=\frac{\tilde v}{\bar v}W_{(0)}$ and force $\Delta\Phi^1=\frac{\tilde v}{\bar v}\Phi^1_{(0)}$ are twice the initial acting factors W and Φ if the multiplier

$$\frac{\tilde v}{\bar v}=\frac{e\sqrt{4\pi}}{m_e\bar v}\frac{\sqrt{B}}{\omega}\qquad(40)$$

becomes close to unity ($\tilde v$ becomes close to $\bar v$). In such a case the background non-holonomic field produces the same energy and forces as those acting in the system, so the energy flow and forces acting in the process are doubled.

Given the frequency $\nu=\frac{\omega}{2\pi}\approx5\times10^{14}\,\text{Hz}$, close to the spectral class of the Sun*, we deduce by formula (37) that there in the Sun $\tilde v$ reaches the linear velocity of the background space rotation $\bar v\simeq2.2\times10^8\ \text{cm/sec}$, if the radiant energy density is $B=1.4\times10^{11}\ \text{erg/cm}^3$, which is close to the average value of B in the Sun. From phenomenological data [6], in the central region of the Sun $B\simeq10^{13}\ \text{erg/cm}^3$ so $\tilde v\simeq2\times10^9\,\text{cm/sec}$ there, i. e. ten times larger than the average in the Sun. In the surface layer where $T\simeq6\times10^3$, we obtain the much smaller value $\tilde v\simeq2\times10^3\,\text{cm/sec}$.

This calculation verifies the phenomenological conclusion [6] that the sources of energy aren't located exclusively in the central region of a star (as would be the case for thermonuclear reactions), but are distributed throughout the whole volume of a star, with some concentration at the centre. With the above mechanism generating energy by the background space non-holonomity field, the sources of stellar energy should be working in even the surface layer of the

*A light wave doesn't change its proper frequency in the Thomson process, so the frequency remains the same while light travels from the inner region of a star to the surface where it determines the spectral class (visible colour) of the star.

Sun, but with much less power.

Because the productivity of such an energy generator is determined by the multiplier $\frac{\tilde{v}}{\bar{v}} = \frac{e\sqrt{4\pi}}{m_e \bar{v}} \frac{\sqrt{B}}{\omega}$ (40), in the additional energy flow $\Delta W = \frac{\tilde{v}}{\bar{v}} W_{(0)}$ and the force $\Delta \Phi^1 = \frac{\tilde{v}}{\bar{v}} \Phi^1_{(0)}$. So the energy output ε of the mechanism is determined mainly by the radiant energy density B in stars, i.e. the drainage of energy by radiation*. Therefore, given the above mechanism of energy production by the background space non-holonomity, stars are *machines* producing radiation, the power of which (the energy output) is regulated by their luminosity.

By the stellar energy relation (27) determined from observations, the radiant energy density per electron is constant $\frac{B}{n_e} = 1.4 \times 10^{-11}$erg in any kind of star. Even such different stars as white dwarfs, having the highest temperatures and pressures (the right upper region in the stellar energy diagram), and low-temperature and pressure infrared super-giants (the left lower region therein) satisfy the stellar energy relation. We therefore conclude that:

> Stellar energy is generated in Thomson dispersion of light while light travels from the inner region of a star to the surface. When a light wave is dispersed by a free electron, the electron oscillates in the electric field of the wave. The oscillation causes a local perturbation of the non-holonomic background space of the Universe, so the background non-holonomic field produces an additional energy flow and force in the Thomson process in order to compensate for the local perturbation in itself. Given the physical conditions in stars, the additional energy and forces are the same as those radiated throughout the wide range of physical conditions in stars — from dwarfs to super-giants. Such energy sources work in the whole volume of a star, even in the surface layer, but with some concentration at the centre. Moreover, the power of the mechanism is regulated by the energy drainage (the radiation from the surface). This is a self-regulating machine, actuated by the background space non-holonomity, and is independent of thermonuclear reactions.

This theoretical result, from General Relativity, verifies the conclusion drawn by Kozyrev from his analysis of well-known phenomenological correlations of observational astrophysics [6]. But having no exact theory of stellar energy sources, Kozyrev had no possibility of calculating similar effects under the physical conditions different than those in stars whose temperatures and pressures are hardly reproducible in a laboratory.

With the theory of the phenomenon established, we can simulate similar effects in a laboratory for low temperature and pressure conditions (with less energy output). We can as well discover, in a laboratory, similar additional energy flow and force in processes much more simply realizable than Thomson dispersion of light. So the theoretical results of Sections 3 and 4 can be used as a basis for forthcoming developments of new energy sources.

As is well known, current employment of nuclear energy produces ecological problems because of radioactive waste. Besides that, events of recent years testify that such energy sources are dangerous if atomic power stations are destroyed by natural or human-made causes: the nuclear fuel, even without atomic explosion, produces many heavy particles and other deadly radiations.

We therefore conclude that new energy sources similar to stellar energy sources described herein, being governed by the energy output, and producing no hard radiation, can work in a laboratory conditions much more effectively and safely than nuclear energy, and replace atomic power stations in the near future.

*The frequency ω determining the spectral class of a star undergoes a much smaller change, within 1 order, along the whole range of stars.

References

1. Zelmanov A. L. Chronometric invariants. Dissertation thesis, 1944. American Research Press, Rehoboth (NM), 2006.
2. Zelmanov A. L. Chronometric invariants and co-moving coordinates in the general relativity theory. *Doklady Acad. Nauk USSR*, 1956, v. 107(6), 815–818.
3. Rabounski D. Zelmanov's anthropic principle and the infinite relativity principle. *Progress in Physics*, 2005, v. 1, 35–37.
4. Oros di Bartini R. Some relations between physical constants. *Doklady Acad. Nauk USSR*, 1965, v. 163, No. 4, 861–864.
5. Oros di Bartini R. Relations between physical constants. *Progress in Physics*, 2005, v. 3, 34–40.
6. Kozyrev N. A. Sources of stellar energy and the theory of the internal constitution of stars. *Prog. in Phys.*, 2005, v. 3, 61–99.
7. Kozyrev N. A. Physical peculiarities of the components of double stars. *Colloque "On the Evolution of Double Stars"*, *Comptes rendus*, Communications du Observatoire Royal de Belgique, ser. B, no. 17, Bruxelles, 1967, 197–202.
8. Kozyrev N. A. On the possibility of experimental investigation of the properties of time. *Time in Science and Philosophy*, Academia, Prague, 1971, 111–132.
9. Smoot G. F., Gorenstein M. V., and Muller R. A. Detection of anisotropy in the Cosmic Blackbody Radiation. *Phys. Rev. Lett.*, 1977, v. 39, 898–901.
10. Bennett C. L. et al. First-year Wilkinson Microwave Anisotropy Probe (WMAP) observations: preliminary maps and basic results. *Astrophys. Journal Suppl. Series*, 2003, v. 148, 1–27.
11. Borissova L. and Rabounski D. Fields, vacuum, and the mirror Universe. Editorial URSS, Moscow, 2001. (2nd revised ed.: CERN, EXT-2003-025).

Frequency Resolved Detection over a Large Frequency Range of the Fluctuations in an Array of Quantum Dots

Aziz N. Mina* and Adel H. Phillips†

*Faculty of Science, Cairo University, Beni-Suef Branch, Egypt
†Faculty of Engineering, Ain Shams University, Cairo, Egypt
E-mail: adel_phillips@yahoo.com

Quantum noise effects in an array of quantum dots coupled to superconducting leads are studied. The effect of broadband fluctuations on the inelastic rate in such tunable system has been taken into account. The quantum shot noise spectrum is expressed in terms of the time dependent fluctuations of the current around its average value. Numerical calculation has been performed over a wide range of frequencies of the induced photons. Our results show an asymmetry between absorption and emission processes. This research is very important for optoelectronic nanodevices.

1 Introduction

Semiconductor nanostructures based on two dimensional electron gas (2 DEG) could form the basis of future nanodevices for sensing, information processing and quantum computation. Coherent electron transport through mesoscopic system in the presence of a time-varying potential has been a subject of increasing interest in the past recent years [1]. Applying the microwave field with frequency, ω, to an electron with energy, E, the electron wavefunction possesses sideband components with energies $E + n\hbar\omega$ ($n = 0, \pm 1, \pm 2, \dots$). The coherence of sideband components characterizes transport properties of electrons such as photon-assisted tunneling (PAT) [2–6]. Shot noise measurements provide a powerful tool to study electron transport in mesoscopic systems [7]. Shot noise can be enhanced in devices with superconducting leads by virtue of the Andreev-reflection process taking place at the interface between a semiconductor and superconductor [8–10]. A remarkable feature of the current noise in the presence of timedependent potentials is its dependence on the phase of the transmission amplitudes [11]. Moreover, for high driving frequencies, the driving can be treated within a self-consistent perturbation theory [12]. In the present paper, a shot noise spectrum of a mesoscopic device is derived and analyzed over a wide range of frequencies of the induced microwave field.

2 Model of calculations

The present studied mesoscopic device is formed of an array of semiconductor quantum dots coupled weakly to two superconducting leads via tunnel barriers. Electrical shot noise is the time-dependent fluctuation of the current around its average value, due to the discreteness of the charge carriers. The nonsymmetrized shot noise spectrum is given by [13]:

$$P(\omega) = 2 \int_{-\infty}^{\infty} dt\, e^{i\omega t} \left\langle \Delta\hat{I}(t)\, \Delta\hat{I}(0) \right\rangle , \qquad (1)$$

where $\Delta\hat{I}(t)$ is the time-dependent fluctuations of the current around its average value [14]. The average current operator is given by [15]:

$$\left\langle \hat{I}(t) \right\rangle = \frac{e}{h} \sum_{\alpha,\beta} \int_0^{\infty} d\varepsilon \int_0^{\infty} d\varepsilon' I_{\alpha,\beta}(\varepsilon, \varepsilon') \times \times \hat{a}_{\alpha}^{+}(\varepsilon)\, \hat{a}_{\beta}(\varepsilon')\, e^{i(\varepsilon-\varepsilon')t/\hbar}, \qquad (2)$$

where $\hat{a}_{\alpha}^{+}(\varepsilon)$ and $\hat{a}_{\alpha}(\varepsilon)$ are the creation and annihilation operators of the scattering states $\psi_{\alpha}(\varepsilon)$ respectively. $I_{\alpha\beta}(\varepsilon, \varepsilon')$ is the matrix element of the current operator between states $\psi_{\alpha}(\varepsilon)$ and $\psi_{\beta}(\varepsilon')$. The indices α and β (Eq. 2) denote mode number (m) as well as whether it concerns electron $\alpha = (m, e)$ or hole $\alpha = (m, h)$ propagation, due to Andreev reflection processes at semiconductor-superconductor interface [16]. The scattering states $\psi_{\alpha}(\varepsilon)$ and $\psi_{\beta}(\varepsilon')$ are determined by solving the Bogoliubov-deGennes equation (BdG) [17, 18] and are given by:

$$\Psi_{\alpha j}(x, \varepsilon) = \left[A_j \exp(ik_j x) \begin{pmatrix} 1 \\ 0 \end{pmatrix} + B_j \exp(-ik_j x) \begin{pmatrix} 0 \\ 1 \end{pmatrix} \right] \times \times \sum_{n=0}^{\infty} J_n \left(\frac{eV_0}{\hbar\omega} \right) \exp\left[-i\,(\varepsilon + n\hbar\omega)\, t/\hbar \right] \qquad (3)$$

where ω is the frequency of the induced microwave field, J_n is the n-th order Bessel function of first kind and V_0 is the amplitude of the ac-voltage. Eq. (3) represents the eigenfunction inside the quantum dot in the j-th region and the corresponding eigenfunction inside the superconducting leads is given by:

$$\Psi_{\alpha}(x, \varepsilon) = \left[C \exp(ik'x) \begin{pmatrix} u \\ v \end{pmatrix} + D \exp(-ik'x) \begin{pmatrix} v \\ u \end{pmatrix} \right] \times \times \sum_{n=-\infty}^{\infty} J_n \left(\frac{eV_0}{\hbar\omega} \right) \exp\left[-i\,(\varepsilon + n\hbar\omega)\, t/\hbar \right] . \qquad (4)$$

The wave vectors k_j and k' are the wave vectors inside j-th quantum dot and inside the superconducting leads and

they are given by:

$$k_j = \frac{\left(2m^*(V_{\text{eff}} \pm \varepsilon + n\hbar\omega)\right)^{0.5}}{\hbar} \tag{5}$$

and

$$k' = \frac{\left(2m^*(E_F - V_b \pm \sqrt{(\varepsilon + n\hbar\omega)^2 - \Delta^2}\right)^{0.5}}{\hbar} \tag{6}$$

where V_{eff} is expressed as:

$$V_{\text{eff}} = V_b + \frac{U_c N^2}{2} + E_F + e\eta V_g \tag{7}$$

in which V_b is the Schottky barrier height, U_c is the charging energy of the quantum dot, E_F is the Fermi-energy, Δ is the energy gap of superconductor, V_g is the gate voltage and η is the lever arm. The eigenfunctions u and v (Eq. 4) of the corresponding electron/hole due to Andreev reflection process at the semiconductor-superconductor interface are given by:

$$u = \sqrt{\frac{1}{2}\left(1 + \frac{\left((\varepsilon + n\hbar\omega)^2 - \Delta^2\right)^{0.5}}{\varepsilon + n\hbar\omega}\right)} \tag{8}$$

and

$$v = \sqrt{\frac{1}{2}\left(1 - \frac{\left((\varepsilon + n\hbar\omega)^2 - \Delta^2\right)^{2}}{\varepsilon + n\hbar\omega}\right)}. \tag{9}$$

Now, in order to evaluate the shot noise spectrum, this can be achieved by substituting the current operator Eq. 2 into Eq. 1 and determining the expectation value [19] and after simple algebraic steps, we get a formula for the shot noise spectrum $P(\omega)$ [20] as:

$$P(\omega) = \frac{2eP_0}{h} \sum_{\alpha,\beta} \int_0^\infty d\varepsilon \, |\Gamma(\varepsilon)| \, f_{\alpha FD}(\varepsilon) \times \times \left[1 - f_{\beta FD}(\varepsilon + n\hbar\omega)\right], \tag{10}$$

where P_0 is the Poissonian shot noise spectrum and $f_{\beta FD}(\varepsilon + n\nabla\omega)$ are the Fermi distribution functions.

The tunneling rate, $\gamma(\varepsilon)$ through the barrier must be modified due to the influence of the induced microwave field as [21]:

$$\tilde{\gamma}(\varepsilon) = \sum_{n=-\infty}^{\infty} J_n^2\left(\frac{eV_0}{\hbar\omega}\right)\gamma(\varepsilon + n\hbar\omega). \tag{11}$$

The tunneling rate, $\gamma(\varepsilon)$ is related to the tunneling probability, $\Gamma(\varepsilon)$ [21] as:

$$\gamma(\varepsilon) = \frac{2\pi}{\hbar} \int_{E_F}^{E_F + 2\Delta\hbar\omega} d\varepsilon \, \Gamma(\varepsilon)\rho(\varepsilon) f_{FD}(\varepsilon) \times \times \left(1 - f_{FD}(\varepsilon - \Delta F)\right) \tag{12}$$

in which ΔF is the difference in final and initial free energy after and before the influence of microwave field. The tunneling probability, $\Gamma(\varepsilon)$, Eq. 10 has been determined by the authors [22, 23] using the transfer matrix method and it is expressed as:

$$\Gamma(\varepsilon + n\hbar\omega) = \frac{1}{\left(1 + C_1^2 C_2^2\right)} \tag{13}$$

where C_1 and C_2 are expressed as:

$$C_1 = \frac{V_{\text{eff}} \sinh(kb)}{2\sqrt{L_1}} \tag{14}$$

and

$$C_2 = 2\cosh(kb)\cos(k'a) - C_3. \tag{15}$$

We have used the following notations:

$$\begin{aligned} L_1 &= (\varepsilon + n\hbar\omega)\left(V_{\text{eff}} - \varepsilon - n\hbar\omega\right), \\ C_3 &= \left(\frac{L_2}{\sqrt{L_1}}\right)\sin(k'a)\exp(2kb), \\ L_2 &= 2(\varepsilon + n\hbar\omega) - V_{\text{eff}}. \end{aligned} \tag{16}$$

The parameters a and b represent the quantum dot size and the width of the barrier.

Now substituting Eq. 13 into Eq. 10 an expression for the frequency dependent shot noise spectrum and it depends on the geometrical dimension of the device under study.

3 Results and discussion

The shot noise spectrum, $P(\omega)$, Eq. 10 has been computed over a wide range of frequencies of the induced microwave field and at different temperatures. We considered a double quantum dots which they are a fully controllable two-level system. These quantum dots are AlGaAs-GaAs heterostructure and the leads are Nb superconductor. The calculations were performed for the cases: absorption of quanta from the environment (Fig. 1) and emission case (Fig. 2). The Schottky barrier height, V_b, was calculated by using a Monte-Carlo technique [24] and found to be equal to 0.47 eV. This value is in good agreement with those found by the authors [25]. As shown in Fig. 1 and Fig. 2, the normalized shot noise spectrum exhibits resonances at certain frequencies for both absorption and emission processes. The present results show that the Coulomb oscillations are modified by frequency of the induced microwave field over a wide range. Also, the Andreev reflection processes at the semiconductor-superconductor interface plays very important role for the appearance of these resonances. Our results show that the interplay between electronic transport and excitation by microwave is a particular interest. As high frequency perturbations are expected to yield a new nonequilibrium situation resulted from additional phase variations in energy states [26, 27, 28].

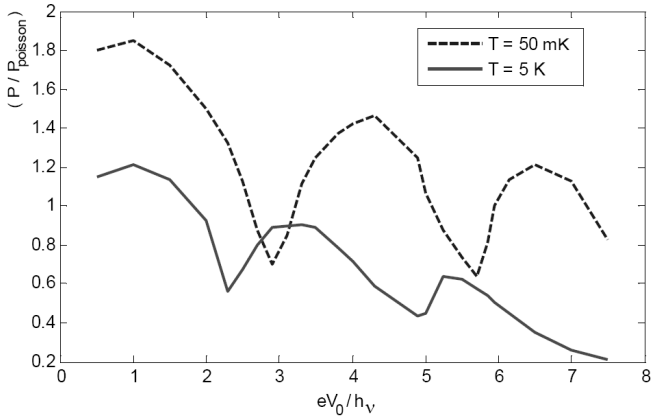

Fig. 1: The dependence of the normalized shot noise spectrum ($P/P_{poisson}$) on the normalized strength of the driving field (absorption case).

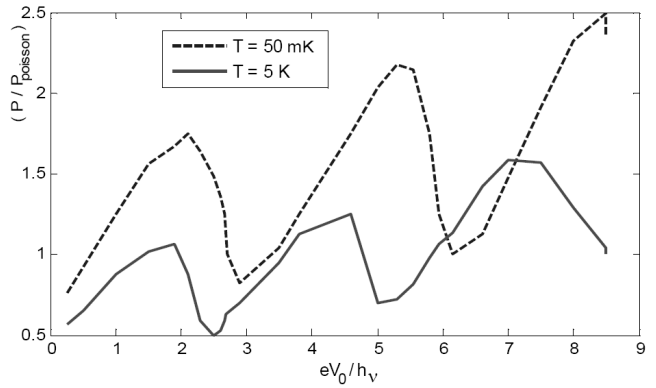

Fig. 2: The dependence of the normalized shot noise spectrum ($P/P_{poisson}$) on the normalized strength of the driving field (emission case).

4 Conclusions

In present paper, an expression for the shot noise spectrum has been deduced. The present studied mesoscopic device is modeled as double quantum dots coupled weakly to superconducting leads. The tunneling through the device is induced by microwave field of wide range of frequencies. The effect of both Andreev reflection processes and the Coulomb blockade had been taken into consideration. The resonances show the interplay between the forementioned effects and the photon induced microwave field. Our results show a concordant with those in the literature.

References

1. Toyoda E., Takayanagi H. and Nakano H. *J. Phys. Soc. Jpn*, 2000, v. 69, 1801.
2. Dayem A. H. and Martin R. J. *Phys. Rev. Lett.*, 1962, v. 8, 246.
3. Tien P. K. and Gordon J. P. *Phys. Rev.*, 1963, v. 129, 647.
4. Kouwenhoven L. P., Jauhar S., Orenstein J., McEuen P. L., Nagamune Y., Motohisa J., and Sakaki H. *Phys. Rev. Lett.*, 1994, v. 73, 3443.
5. Wiel V., Fujisawa W. G., Osterkamp T. H., and Kouwenhoven L. P. *Physica B*, 1999, v. 272, 31.
6. Keay B. J., Zeuner S., and Allen S. J. *Phys. Rev. Lett.*, 1995, v. 75, 4102.
7. Blanter Ya. M. and Buttiker M. *Phys. Rep.*, 2000, v. 336, 1.
8. Nagaev K. E. and Buttiker M. *Phys. Rev.*, 2001, v. B63, 081301(R).
9. Hoffmann C., Lefloch F., and Sanquer M. *Eur. Phys. J.*, 2002, v. B29, 629.
10. Phillips A. H. *Second Spring School on Current Activities of Materials Science*, Assiut University, Assiut, Egypt, 2000.
11. Camalet S., Lehmann J., Kohler S., and Hanggi P. *Phys. Rev. Lett.*, 2003, v. 90, 210602.
12. Brandes J. *Phys. Rev.*, 1997, v. B56, 1213.
13. DeJong M. J. M. and Beenakker C. W. Shot noise in mesoscopic systems. arXiv: cond-mat/9611140.
14. Aguado R. and Kouwenhoven L. P. *Phys. Rev. Lett.*, 2000, v. 84, 1986.
15. DeJong M. J. M. and Beenakker C. W. J. In: *Proceedings of Advanced Study Institute on Mesoscopic Electron Transport*, edited by Sohn L. L., Kouwenhoven L. P. and Schon G., Kluwer, Dordrecht, 1997.
16. Andreev A. F. *Sov. Phys. JETP*, 1964, v. 19, 1228.
17. Furusaki A., Takayanagi H., and Tsukada M. T. *Phys. Rev.*, 1992, v. B45, 10563.
18. Aly A. H., Phillips A. H., and Kamel R. *Egypt. J. Phys.*, 1999, v. 30, 32.
19. Beenakker C. W. J. and Buttiker M. *Phys. Rev.*, 1992, v. B46, R1889.
20. Blanter Ya. M. and Sukhorukov E. V. *Phys. Rev. Lett.*, 2000, v. 84, 1280.
21. Platero G. and Aguado R. Photon-assisted transport in semiconductor nanostructures. arXiv: cond-mat/0311001.
22. Mina A. N. *Egypt. J. Phys.*, 2001, v. 32, 253.
23. Atallah A. S. and Phillips A. H. *Proceedings of The International Conference on Materials Science and Technology*, Faculty of Science, Cairo University, Beni-Suef, Egypt, April 2–4, 2001.
24. Aly A. H. and Phillips A. H. *Phys. Stat. Sol. (B)*, 2002, v. 232, 238.
25. Becker Th., Muck M., and Heiden Ch. *Physica B*, 1995, v. 204, 14286.
26. Fujisawa T. and Hirayama Y. *Appl. Phys. Lett.*, 2000, v. 77, 543.
27. Camalet S., Kohler S., and Hanggi P. arXiv: cond-mat/0402182.
28. Phillips A. H., Mina A. N., Sobhy M. S., and Fouad E. A. Accepted for publ. in *J. Comput. & Theor. Nanoscience*, 2006.

Completing Einstein's Proof of $E=mc^2$

C. Y. Lo

Applied and Pure Research Institute, 17 Newcastle Drive, Nashua, NH 03060, USA

E-mail: c_y_lo@yahoo.com; C_Y_Lo@alum.mit.edu

It is shown that Einstein's proof for $E = mc^2$ is actually incomplete and therefore is not yet valid. A crucial step is his implicit assumption of treating the light as a bundle of massless particles. However, the energy-stress tensor of massless particles is incompatible with an electromagnetic energy-stress tensor. Thus, it is necessary to show that the total energy of a light ray includes also non-electromagnetic energy. It turns out, the existence of intrinsic difference between the photonic and the electromagnetic energy tensors is independent of the coupling of gravity. Nevertheless, their difference is the energy-stress tensor of the gravitational wave component that is accompanying the electromagnetic wave component. Concurrently, it is concluded that Einstein's formula $E = mc^2$ necessarily implies that the photons include non-electromagnetic energy and that the Einstein equation of 1915 must be rectified.

1 Introduction

In physics, the most famous formula is probably $E = mc^2$ [1]. However, it is also this formula that many(1) do not understand properly [2, 3]. Einstein has made clear that this formula must be understood in terms of energy conservation [4]. In other words, there is energy related to a mass, but there may not be an equivalent mass for any type of energy [2]. As shown by the Riessner-Nordstrom metric [5, 6], the gravity generated by mass and that by the electromagnetic energy are different because an electromagnetic energy stress tensor is traceless. Thus, the relationship between mass and energy would be far more complicated than as commonly believed.

In Einstein's 1905 derivation,(2) he believed [7] that the corresponding was between mass and any type of energy although he dealt with only the light, which may include more than just electromagnetic energy. Moreover, although his desired generality has not been attained, his belief was very strong. On this, Stachel [7] wrote,

> "Einstein returned to the relation between inertial mass and energy in 1906 and in 1907 giving more general arguments for their complete equivalence, but he did not achieve the complete generality to which he inspired. In his 1909 Salzburg talk, Einstein strongly emphasized that inertial mass is a property of all form of energy, and therefore electromagnetic radiation must have mass. This conclusion strengthened Einstein's belief in the hypothesis that light quanta manifest particle-like properties."

Apparently, the publications of the papers of Reissner [6] and Nordstrom [5] have changed the view of Einstein as shown in his 1946 article [4].

Perhaps, a root of misunderstanding $E = mc^2$ is related to the fact that the derivation of this formula [8] has not been fully understood. In Einstein's derivation, a crucial step is his implicit assumption of treating light as a bundle of massless particles. However, because gravity has been ignored in Einstein's derivation, it was not clear that an electromagnetic energy-stress tensor is compatible with the energy-stress tensor of massless particles.

Such an issue is valid since the divergence of an electromagnetic energy-stress tensor $\nabla_c T(E)^{cb}$ (where ∇_c is a covariant derivative) generates only the Lorentz force, whereas the divergence of a massive energy-stress tensor $\nabla_c T(m)^{cb}$ would generate the geodesic equation [9].

Thus, the energy-stress of photons $T(L)_{ab}$ would be

$$T(L)_{ab} = T(E)_{ab} + T(N)_{ab} \qquad (1)$$

or

$$T(N)_{ab} = T(L)_{ab} - T(E)_{ab}$$

where $T(E)_{ab}$ and $T(N)_{ab}$ are respectively the electromagnetic energy-stress tensor and a non-electromagnetic energy-stress tensor. Besides, being intrinsically traceless, $T(E)_{cb}$ would not be compatible with Einstein's formula $\triangle E = \triangle mc^2$. Based on the fact that the electromagnetic energy is dominating experimentally, it is natural to assume as shown later that $T(N)_{ab}$ is in fact the gravitational energy-stress tensor $T(g)_{ab}$.

2 A field equation for the accompanying gravitational wave

Physics requires also that the energy-stress tensor for photons $T(L)_{ab}$ is: (1) traceless, (2) $T(L)_{ab} \approx T(E)_{ab}$ and $\left[T(L)_{tt} - T(E)_{tt}\right] > 0$ on the average, and (3) related to a gravitational wave, i. e. satisfying

$$R_{ab} - \frac{1}{2} g_{ab} R = KT(g)_{ab} = -K\left[T(E)_{ab} - T(L)_{ab}\right], \qquad (2)$$

where R_{ab} is the Ricci tensor, and $R = g^{mn} R_{mn}$. Eq. (2) dif-

fers from Einstein equation with an additional term $T(L)_{ab}$ having a coupling of different sign. However, Eq. (2) is similar to the modified Einstein equation,

$$G_{ab} = R_{ab} - \frac{1}{2}\, g_{ab}R = -K\big[T(m)_{ab} - T(g)_{ab}\big]\,, \qquad (3)$$

which is necessitated by the Hulse-Taylor experiment [10, 11]. $T(g)_{ab}$ is non-zero since a gravitational wave carries energy. From Eq. (2), we have $\nabla_c T(L)^{cb} = 0$ since there $\nabla_c T(E)^{cb} = 0$ and $\nabla_c G^{cb} \equiv 0$.

Related to Eq. (2), a crucial question is whether the Einstein equation with only the electromagnetic wave energy-stress tensor as the source is valid. It has been found that such an equation cannot produce a physically valid solution [12]. Historically, it is due to that the Einstein equation does have a physical plane-wave solution that the need of a photonic energy-stress tensor is recognized (see also Sect. 3). One may object that the general form of gravitational energy-stress tensor is not yet known although its approximation for the weak gravity with the massive source is known to be equivalent to Einstein's pseudo-tensor for the gravitational energy-stress [10]. However, for this case, the related gravitational energy-stress tensor is defined by formula (1).

Now the remaining question is whether (2) would produce a gravitational wave. However, we should address first whether an electromagnetic wave has an accompanying gravitational wave. The answer is affirmative because the electromagnetic energy is propagating with the allowed maximum speed in Special Relativity.(3) Thus, the gravity due to the light energy should be distinct from that generated by massive matter [13] .

Since a field emitted from an energy density unit means a non-zero velocity relative to that unit, it is instructive to study the velocity addition. According to Special Relativity, the addition of velocities is as follows:

$$u_x = \frac{\sqrt{1-v^2/c^2}}{1+u'_z v/c^2}\, u'_x\,, \quad u_y = \frac{\sqrt{1-v^2/c^2}}{1+u'_z v/c^2}\, u'_y\,, \quad \text{and} \quad u_z = \frac{u'_z + v}{1+u'_z v/c^2}\,, \qquad (4)$$

where velocity $\vec{v}$ is in the z-direction, $(u'_x,\ u'_y,\ u'_z)$ is a velocity w. r. t. a system moving with velocity v, c is the light speed, $u_x = dx/dt$, $u_y = dy/dt$, and $u_z = dz/dt$. When $v = c$, independent of $(u'_x,\ u'_y,\ u'_z)$ one has

$$u_x = 0\,, \quad u_y = 0\,, \quad \text{and} \quad u_z = c\,. \qquad (5)$$

Thus, neither the direction nor the magnitude of the velocity $\vec{v}$ $(= \vec{c})$ have been changed.

This implies that nothing can be emitted from a light ray, and therefore no field can be generated outside the light ray. To be more specific, from a light ray, no gravitational field can be generated outside the ray although, accompanying the light ray, a gravitational field $g_{ab} (\neq \eta_{ab}$ the flat metric) is allowed within the ray.

According to the principle of causality [13], this accompanying gravity g_{ab} should be a gravitational wave since an electromagnetic wave is the physical cause. This would put General Relativity into a severe test for theoretical consistency. But, this examination would also have the benefit of knowing whether Einstein's implicit assumption in his proof for $E = mc^2$ is valid.

Let us consider the energy-stress tensor $T(L)_{ab}$ for photons. If a geodesic equation must be produced, for a monochromatic wave with frequency ω, the form of a photonic energy tensor should be similar to that of massive matter. Observationally, there is very little interaction, if any, among photons of the same ray. Theoretically, since photons travel in the velocity of light, there should not be any interaction (other than collision) among them. Therefore, the photons can be treated as a bundle of massless particles just as Einstein [8] did.

Thus, the photonic energy tensor of a wave of frequency ω should be dust-like and traceless as follows:

$$T^{ab}(L) = \rho\, P^a P^b, \qquad (6)$$

where ρ is a scalar and is a function of $u\,(= ct - z)$. In the units $c = h = 1$, $P^t = \omega$. The geodesic equation, $P^c \nabla_c P^b = 0$, is implied by $\nabla_c T(L)^{cb} = 0$ and also $\nabla_c(\rho P^c) = 0$. Since $\nabla_c(\rho P^c) = \big[\rho g^{bc} g'_{bc} + \rho'\big](P^t - P^z) = 0$, formula (6) does produces a geodesic equation if Eq. (2) is satisfied.

3 The reduced Einstein equation for an electromagnetic plane wave

Let us consider a ray of uniform electromagnetic waves (i. e. a laser beam) propagating in the z-direction. Within the ray, one can assume that the wave amplitude is independent of x and y. Thus, the electromagnetic potentials are plane-waves, and in the unit that light speed $c = 1$,

$$A_k(x, y, z, t) = A_k(t - z)\,, \text{ where } k = x, y, z, t. \qquad (7)$$

Due to the principle of causality, the metric g_{ab} is functions of $u\,(= t - z)$, i. e.,

$$g_{ab}(x, y, z, t) = g_{ab}(u)\,, \text{ where } a, b = x, y, z, t. \qquad (8)$$

Since, for this case, the coordinates for Special Relativity are also valid for General Relativity [14–16], such a consideration is valid. Let P^k be the momentum of a photon. If a photon is massless, one obtains the conditions,

$$P^z = P^t, \quad P^x = P^y = 0\,, \quad \text{and} \quad P^m g_{mk} = P_k = 0\,, \qquad (9)$$

for $k = x, y$, and $v\,(= t + z)$. Eq. (9a) is equivalent to

$$g_{xt} + g_{xz} = 0\,, \qquad g_{yt} + g_{yz} = 0\,, \qquad \text{and} \quad g_{tt} + 2\,g_{tz} + g_{zz} = 0\,, \qquad (10)$$

or

$$g^{xt} - g^{xz} = 0\,, \qquad g^{yt} - g^{yz} = 0\,, \\ \text{and} \;\; g^{tt} - 2g^{zt} + g^{zz} = 0\,. \tag{11}$$

The transverse of an electromagnetic wave implies

$$P^m A_m = 0\,, \\ \text{or equivalently} \;\; A_z + A_t = 0\,. \tag{12}$$

Eqs. (7) to (9) imply that not only the geodesic equation, the Lorentz gauge, but also Maxwell's equation are satisfied. Moreover, the Lorentz gauge becomes equivalent to a covariant expression.

For an electromagnetic wave being the source, Einstein [17] believed the field equation is $G_{ab} = -KT(E)_{ab}$, where $T(E)_{ab} = -g^{mn}F_{ma}F_{nb} + \frac{1}{4}g_{ab}F^{mn}F_{mn}$, while $F_{ab} = \partial_a A_b - \partial_b A_a$ is the field tensor. Since the trace of the energy-stress tensor is zero, $R = 0$. It follows that

$$R_{tt} = -R_{tz} = R_{zz}\,, \tag{13}$$

because $F^{mn}F_{mn} = 0$ due to Eq. (9). The other components are zero [12]. Then,

$$R_{tt} \equiv -\frac{\partial \Gamma^m_{tt}}{\partial x^m} + \frac{\Gamma^m_{mt}}{\partial t} - \Gamma^m_{mn}\Gamma^n_{tt} + \Gamma^m_{nt}\Gamma^n_{mt} = \\ = -KT(E)_{tt} = Kg^{mn}F_{mt}F_{nt}\,. \tag{14}$$

After some lengthy algebra [12], Eq. (14) is simplified to a differential equation of u as follows:

$$G'' - g'_{xx}g'_{yy} + (g'_{xy})^2 - G'(g'/2g) = 2GR_{tt} = \\ = 2K\left(F^2_{xt}g_{yy} + F^2_{yt}g_{xx} - 2F_{xt}F_{yt}g_{xy}\right), \tag{15}$$

where

$$G \equiv g_{xx}g_{yy} - g^2_{xy}, \;\; \text{and} \;\; g = |g_{ab}|\,,$$

the determinant of the metric. The metric elements are connected by the following relation:

$$-g = Gg_t^2, \;\; \text{where} \;\; g_t = g_{tt} + g_{tz}\,. \tag{16}$$

Note that Eqs. (35.31) and (35.44) in reference [18] and Eq. (2.8) in reference [19] are special cases of Eq. (15). But, their solutions are unbounded [17]. However, compatibility with Einstein's notion of weak gravity is required by the light bending calculation and is implied by the equivalence principle [20].

Equations (9)–(16) allow A_t, g_{xt}, g_{yt}, and g_{zt} to be set to zero. In any case, these assigned values have little effect in subsequent calculations. For the remaining metric elements (g_{xx}, g_{xy}, g_{yy}, and g_{tt}), however, Eq. (15) is sufficient to show that there is no physical solution. In other words, in contrast to Einstein's belief [17], the difficulty of this equation is not limited to mathematics.

4 Verification of the rectified Einstein equation

Now, consider an electromagnetic plane-wave of circular polarization, propagating to the z-direction

$$A_x = \frac{1}{\sqrt{2}}A_0\cos\omega u\,, \;\; \text{and} \;\; A_y = \frac{1}{\sqrt{2}}A_0\sin\omega u\,, \tag{17}$$

where A_0 is a constant. The rotational invariants with respect to the z-axis are constants. These invariants are: G_{tt}, R_{tt}, $T(E)_{tt}$, G, $(g_{xx} + g_{yy})$, g_{tz}, g_{tt}, g, and etc. It follows that [12–13]

$$g_{xx} = -1 - C + B_\alpha\cos(\omega_1 u + \alpha)\,, \\ g_{yy} = -1 - C - B_\alpha\cos(\omega_1 u + \alpha)\,, \\ g_{xy} = \pm B_\alpha\sin(\omega_1 u + \alpha)\,, \tag{18}$$

where C and B_α are small constants, and $\omega_1 = 2\omega$. Thus, metric (18) is a circularly polarized wave with the same direction of polarization as the electromagnetic wave (17). On the other hand, one also has

$$G_{tt} = 2\omega^2 B^2_\alpha/G \geqslant 0\,, \quad \text{and} \\ T(E)_{tt} = \frac{1}{2G}\,\omega^2 A_0^2(1 + C - B_\alpha\cos\alpha) > 0\,, \tag{19}$$

where $G = (1+C)^2 - B^2_\alpha > 0$. Thus, it is not possible to satisfy Einstein's equation because $T(E)_{tt}$ and G_{tt} have the same sign. Therefore, it is necessary to have a photonic energy-stress tensor.

If the photons are massless particles, the photonic energy-stress tensor (6) has a density function [12],

$$\rho\,(u) = -A_m\,g^{mn}A_n \geqslant 0 \tag{20}$$

which is a scalar function of $u\,(= t - z)$. Since light intensity is proportional to the square of the wave amplitude, which is Lorentz gauge invariant, $\rho\,(u)$ can be considered as the density function of photons. Then

$$T_{ab} = -T(g)_{ab} = T(E)_{ab} - T(L)_{ab} = \\ = T(E)_{ab} + A_m g^{mn}A_n P_a P_b\,. \tag{21}$$

Note that since $\rho\,(u)$ is a positive non-zero scalar consisting of A_k and/or fields such that, on the average, $T(L)_{ab}$ is approximately $T(E)_{ab}$ and Eq. (2) would have physical solutions, $\rho = -A_m g^{mn}A_n$ is the only choice.

As expected, tensor $T(L)_{ab}$ enables a valid solution for wave (17). According to Eq. (2) and formula (21),

$$T_{tt} = -\frac{1}{G}\,\omega^2 A_0^2 B_\alpha\cos\alpha < 0\,, \tag{22}$$

since $B_\alpha = (K/2)\,A_0^2\cos\alpha$. Thus, $T(g)_{tt} = -T_{tt}$ is of order K. It will be shown that $\cos\alpha = 1$.

To confirm the general validity of (2) further, consider a wave linearly polarized in the x-direction,

$$A_x = A_0 \cos\omega(t-z)\,. \tag{23}$$

Then,

$$\begin{aligned} T(E)_{tt} &= -\frac{g_{yy}}{2G}\,\omega^2 A_0^2\left[1-\cos 2\omega(t-z)\right] \text{ and} \\ T_{tt} &= \frac{g_{yy}}{2G}\,\omega^2 A_0^2 \cos 2\omega(t-z)\,. \end{aligned} \tag{24}$$

Note that independent of the coupling K, T_{tt} is non-zero. Since the gravitational component is not an independent wave, $T(g)_{tt}(=-T_{tt})$ is allowed to be negative or positive [13]. Eq.(19) implies $(g_{xx}+g_{yy})'$ to be of first order [13], and thus its polarization has to be different.

It turns out that the solution is a linearly polarized gravitational wave and that, as expected, the time-average of $T(g)_{tt}$ is positive of order K [13]. From the viewpoint of physics, for an x-directional polarization, gravitational components related to the y-direction, remains the same. In other words,

$$g_{xy}=0 \;\text{ and }\; g_{yy}=-1\,. \tag{25}$$

It follows [10, 11] that $G=-g_{xx}$ and the general solution for wave (18) is:

$$\begin{aligned} -g_{xx} &= 1+C_1-(K/2)A_0^2\cos\left[2\omega(t-z)\right], \\ \text{and }\; g_{tt} &= -g_{zz}=\sqrt{g/g_{xx}}\,, \end{aligned} \tag{26}$$

where C_1 is a constant and g is the determinant of the metric. The frequency ratio is the same as that of a circular polarization. However, there is no phase difference as α in (18). According to the principle of causality, α has a value, and to be consistent with (26) $\alpha=0$.

However, if $T(L)_{ab}$ were absent, one would have,

$$\begin{aligned} -g_{xx} = 1+C_1-(K/4)\,A_0^2\,\big(&2\omega^2(t-z)^2+ \\ &+\cos\left[2\omega(t-z)\right]\big)+C_2(t-z)\,, \end{aligned} \tag{27}$$

where C_1 and C_2 are constants. But solution (27) is invalid in physics since $(t-z)^2$ grows very large as time goes by. This would "represent" the effects if Special Relativity were invalid, and the wave energy were equivalent to mass. This illustrates that Einstein's notion of weak gravity, which is the theoretical basis for his calculation on the bending of light, may not be compatible with the Einstein equation with an inadequate source term.

5 Conclusions and discussions

A photonic energy-stress tensor has been obtained to satisfy the demanding physical requirements. The energy and momentum of a photon are proportional to its frequency although, as a classical theory, their relation-ship with the Planck constant h is not yet clear. Just as expected from Special Relativity, indeed, the gravity of an electromagnetic wave is an accompanying gravitational wave propagating with the same speed.(4) Concurrently, for this case, the need of modifying the Einstein equation is accomplished. Then, clearly the gravity due to the light is negligible in calculating the light bending [8].

In this derivation, it is crucial that the spatial coordinates are proven the same in Special and General Relativity [14–16] because the space coordinates must have the Euclidean-like structure.(5) For this case, even the time coordinate is the same, and the plane wave satisfied the Maxwell equation in terms of both Special and General Relativity [16], Thus, Special Relativity and General Relativity are consistent with each other. Einstein's proof is clearly incomplete since the energy-stress tensor of photons is different from that of electromagnetism.

A particle such as the photon has no inertial mass since it is subjected to only absorption and emission, but not acceleration and deceleration. Based on Special Relativity, it has been shown that the electromagnetic energy is distinct from the energy of a rest mass.(6) Interestingly, *it is precisely because of this non-equivalence of mass and energy that photonic energy-stress tensor* (6) *is valid, and the formula* $E=mc^2$ *can be proven.*

One might argue that experiment shows the notion of massless photons is valid, and thus believed the equivalence of mass and electromagnetic energy. However, while the addition of two massless particles may end up with a rest mass, the energy-stress tensor of electromagnetism cannot represent a rest mass since such a tensor is traceless. Thus, the formula(7) $\triangle E=\triangle mc^2$ necessarily implies that $T(L)_{ab}$ must include non-electromagnetic energy. Note that $\left[T(L)_{tt}-T(E)_{tt}\right]$ being non-zero, is independent of the gravitational coupling constant K. This makes it clear that the photonic energy tensor is intrinsically different from the electromagnetic energy tensor.

Although the formula $E=mc^2$ has been verified in numerous situations [1, 18], its direct physical meaning related to gravity was not understood;(8) and thus this formula is often misinterpreted, in conflict with General Relativity [2, 9], as any type of energy being equivalent to a mass [3]. A related natural question is how to measure the gravitational component of a light ray. However, in view of the difficulties encountered in measuring pure gravitational waves, the quantitative measurement of such a gravitational component is probably very difficult with our present level of technology although its qualitative existence is proven by the formula $E=mc^2$.

Both quantum theory and relativity are based on the phenomena of light. The gravity of photons finally shows that there is a link between them. It is gravity that makes the notion of photons compatible with electromagnetic waves.

Clearly, gravity is no longer just a macroscopic phenomena, but also a microscopic phenomena of crucial importance to the formula $E = mc^2$. In Einstein's proof, it has not been shown whether his implicit assumption is compatible with electromagnetism. This crucial problem is resolved with the gravity of an electromagnetic wave. Einstein probably would smile heartily since his formula confirms the link that relates gravity to quantum theory.

Acknowledgments

The author gratefully acknowledges stimulating discussions with David P. Chan, S.-J. Chang, A. J. Coleman, G. R. Goldstein, Benson P. Ho, J. E. Hogarth, Richard C. Y. Hui, J.-J. Pi, H.-M. Wang, Eric J. Weinberg, Chuen Wong, and H. Yilmaz. This work is supported in part by Innotec Design Inc., U.S.A.

Endnotes

(1) They include, but not limited to, Fock [21], Hawking [22], Misner, Thorne, & Wheeler [18], Tolman [23], and Will [3].

(2) In 1907 Plank [24] criticized the Einstein argument, and presented his own argument to show that the transfer of heat is associated with a similarly related transfer of inertial mass [7].

(3) In this paper, the convention of the metric signature for Special Relativity is $(1, -1, -1, -1)$.

(4) Some arguments, which were presented differently in the literature [13], are included in this paper for the convenience of the readers. For instance, now the value of α in (18) is obtained.

(5) Einstein called this structure as "in the sense of Euclidean geometry" [8], but failed to understand its physical meaning in terms of measurements [15, 25]. Weinberg [26] has showed, however, that in a curved space the coordinates can be straight.

(6) However, there are theorists such as Tolman [23], who incorrectly saw no difference in terms of gravity between mass and the energy in a light ray.

(7) Einstein's formula $\triangle E = \triangle mc^2$ is proven for radiating energy. Thus, it is applicable to the atomic bomb.

(8) Bodanis [1] gives a good account of how the formula $E = mc^2$ is applied. However, like many others, he also misinterpreted the formula as general equivalence between any type of energy and mass.

References

1. Bodanis D. $E = mc^2$: A biography of the world's most famous equation. The Berkley Publishing Group, New York, 2001.
2. Lo C. Y. *Astrophys. J.*, 1997, v. 477, 700–704.
3. Will C. M. Theory and experiment in gravitational physics. Cambridge Univ. press, Cambridge, 1981.
4. Einstein A. $E = Mc^2$ (from science illustrated 1946) ideas and opinions. Crown, New York, 1954, p. 337.
5. Reissner H. *Annalen der Physik*, 1916, Bd. 50, 106–120.
6. Nordstrom G. On the energy of gravitational field in Einstein's theory. *Proc. Kon. Ned. Akad. Wet.*, 1918, v. 20, 1238.
7. Stachel J., Editor. Einstein's miraculous year. Princeton Press, 1998, p.118.
8. Einstein A., Lorentz H. A., Minkowski H., and Weyl H. The Principle of Relativity. Dover, New York, 1923.
9. Lo C. Y. *Phys. Essays*, 1997, v. 10(4), 540–545.
10. Lo C. Y. *Astrophys. J.*, 1995, v. 455, 421–428.
11. Lo C. Y. *Phys. Essays*, 2000, v. 13(4), 527–539.
12. Lo C. Y. *Phys. Essays*, 1999, v. 12(2), 226–241.
13. Lo C. Y. *Phys. Essays*, 1997, v. 10(3), 424–436.
14. Lo C. Y. *Phys. Essays*, 2002, v. 15(3), 303–321.
15. Lo C. Y. *Chinese J. of Phys.*, 2003, v. 41(4), 1–11.
16. Lo C. Y. *Progress in Physics*, 2006, v. 1, 46.
17. Einstein A. Physics and reality (1936) in ideas and opinions. Crown, New York, 1954, p. 311.
18. Misner C. W., Thorne K. S., and Wheeler J. A. Gravitation. Freeman, San Francisco, 1973.
19. Bondi H., Pirani F. A. E., and Robinson I. *Proc. R. Soc. London A*, 1959, v. 251, 519–533.
20. Lo C. Y. *Phys. Essays*, 1999, v. 11(3), 508–526.
21. Fock V. A. The theory of space time and gravitation. Pergamon Press, 1964.
22. Hawking S. A brief history of time. Bantam Books, New York, 1988.
23. Tolman R. C. Relativity, thermodynamics, and cosmology. Dover, New York, 1987.
24. Planck M. *Annalen der Physik*, 1907, Bd. 22, 180–190.
25. Lo C. Y. *Phys. Essays*, 2005, v. 18(4).
26. Weinberg S. Gravitation and cosmology. John Wiley Inc., New York, 1972, p. 6.

A Source of Energy for Any Kind of Star

Dmitri Rabounski
E-mail: rabounski@yahoo.com

We discuss a recently predicted mechanism whereby energy is produced by the background space non-holonomic field (the global space rotation) in Thomson dispersion of light in free electrons. We compare the mechanism to the relations of observational astrophysics — the mass-luminosity relation and the stellar energy relation. We show that by such a mechanism generating energy in a star, the luminosity of a star L is proportional to its volume, with a progression associated with increasing radius. The obtained relation $L \sim R^{3.4}$ explains why there are no stars of a size close to that of the bulky planets. This also explains the extremely high thermal flow from within Jupiter, which most probably has the same energy sources as those within a star, but with a power much less than that required to radiate like a star. The theory, being applied to a laboratory condition, suggests new energy sources, working much more effectively and safely than nuclear energy.

1 The mechanism that generates energy in stars

By way of introduction, a brief account of my theory of the mechanism producing energy in stars [1] built within the framework of General Relativity, is presented. Then, in the next section, we analyse consequences of the theory in comparison with the correlations of observational astrophysics.

Given a non-holonomic space*, time lines piercing the spatial section (our proper three-dimensional space) are not orthogonal to the spatial section therein, which manifests as the three-dimensional space rotation. If all time lines have the same inclination to the spatial section at each of its points, there is a field of the background space non-holonomity. Such a non-holonomic background field, if perturbed by a local rotation, can produce a force and energy flow in order to compensate for the perturbation in itself. Such a force and energy flow were deduced on the basis of the equations of motion in a non-holonomic space: they manifest as additions to the total force $\Phi^i_{(0)}$ driving a particle and the total power $W_{(0)}$ spent on the motion

$$W = \frac{dE}{d\tau} = W_{(0)} + \delta^m_n \frac{\tilde{v}^n}{\bar{v}^m} W_{(0)} \,, \qquad (1)$$

$$\Phi^i = \frac{dp^i}{d\tau} = \Phi^i_{(0)} + \delta^m_n \frac{\tilde{v}^n}{\bar{v}^m} \Phi^i_{(0)} \,, \qquad (2)$$

where $\bar{v}^i$ is the constant linear velocity of the background space rotation, while $\tilde{v}^i$ is the linear velocity of a local rotation perturbing the background. As obtained within the framework of General Relativity [1], the value of $\bar{v}^i$ is the fundamental constant $\bar{v} = 2.187\,671 \times 10^8$ cm/sec connected to the value $\bar{\nu} = \frac{\bar{v}}{2\pi} = 3.481787 \times 10^7$ cm/sec of a dipole-fit velocity $\bar{\nu}^i$ characterizing the anisotropy of the rotating background (which is similar to a global gyro). The analytical value $\bar{\nu}$ is in close agreement with the dipole-fit velocity 365 ± 18 km/sec extracted from the recently discovered anisotropy of the Cosmic Microwave Background Radiation.

Such an additional factor should appear in Thomson dispersion of light in free electrons in stars. When a light wave of average energy density B encounters a free electron, the flow of the wave energy $c\sigma B$ is stopped in the electron's square $\sigma = 6.65 \times 10^{-25}$ cm^2 (the Thomson square of dispersion). As a result the electron gains an acceleration σB, directed orthogonally to the wave front. With this process the electron oscillates in the plane of the wave at the frequency ω of the wave's electric strength E^i oscillating in the plane. Let the wave travel in the x^1-direction, so $E^2 = E$, $E^1 = E^3 = 0$. The oscillation equation gives the linear velocity $\tilde{v}^i$ of the local space rotation, caused by the oscillating electron,

$$\tilde{v}^2 = \frac{eE}{m_e \omega} \,, \qquad \tilde{v}^1 = 0 \,, \qquad \tilde{v}^3 = 0 \,. \qquad (3)$$

Because the density of energy in an isotropic electromagnetic field is $B = \frac{1}{4\pi} E_i E^i$, the additional force and the power produced in the Thomson process by the global non-holonomic background should be

$$\Delta W = \frac{\tilde{v}^2}{\bar{v}^2} W_{(0)} = \frac{e\sqrt{4\pi}}{m_e \bar{v}} \frac{\sqrt{B}}{\omega} W_{(0)} \,, \qquad (4)$$

$$\Delta \Phi^1 = \frac{\tilde{v}^2}{\bar{v}^2} \Phi^1_{(0)} = \frac{e\sqrt{4\pi}}{m_e \bar{v}} \frac{\sqrt{B}}{\omega} \Phi^1_{(0)} \,, \qquad (5)$$

so the output of energy ε produced by the non-holonomic background in the process (within one cm^3 per second) is

$$\varepsilon = \frac{\tilde{v}}{\bar{v}} c n_e \sigma B = \frac{c\sigma e\sqrt{4\pi}}{m_e \bar{v}} \frac{n_e B^{3/2}}{\omega} \,. \qquad (6)$$

In other words, our equation (6) is the *formula for stellar energy*. The factor $\frac{c\sigma e\sqrt{4\pi}}{m_e \bar{v}}$ is constant, while the second fac-

*A four-dimensional pseudo-Riemannian space, which is the basic space-time of General Relativity.

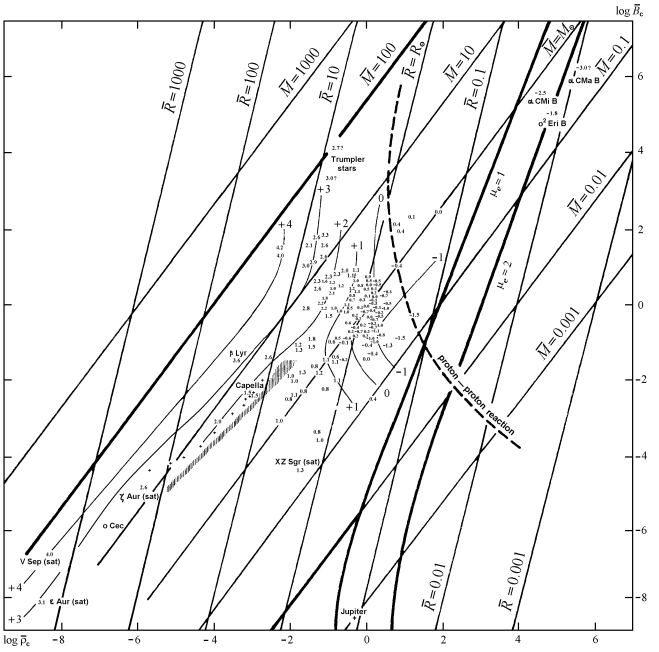

Fig. 1: Diagram of stellar energy: the productivity of stellar energy sources. The abscissa is the logarithm of the density of matter, the ordinate is the logarithm of the radiant energy density (both are taken at the centre of stars in multiples of the corresponding values at the centre of the Sun). Reproduced from [2]. Stars in the diagram are distributed along a straight line that runs from the right upper region to the left lower region, with a ball-like concentration at the centre of the diagram. The equation of the main direction is $\frac{B}{n_e} = 1.4\times10^{-11}$ erg (n_e is the concentration of free electrons).

tor depends mainly on the radiant energy density B in a star*.

Given the frequency $\nu = \frac{\omega}{2\pi} \approx 5\times10^{14}$ Hz (by the spectral class of the Sun), $\tilde{v}$ reaches the background space rotation $\bar{v} \simeq 2.2\times10^{8}$ cm/sec (so the additional energy flow fully compensates for the radiation) at $B = 1.4\times10^{11}$ erg/cm^3, which is close to the average value of B in the Sun. The theoretical result coincides with the phenomenological data [2] by which energy is generated throughout the whole volume of a star with some concentration at the centre (in contrast to thermonuclear reactions working exclusively in the central region).

Besides the main direction $\frac{B}{n_e} = \text{const}$, along which stars are distributed in the stellar energy diagram, Fig. 1 testifies that the power of a mechanism that generates energy in stars is regulated by the density of radiant energy, i. e. by the energy loss by radiation. So the real mechanism producing stellar energy works similar to a self-regulated machine and is independent of the inner resources reserved in stars.

Our formula for stellar energy (6) satisfies this condition, because the energy output is regulated by the radiant energy density B. So a mechanism that works by formula (6) at an oscillation velocity $\tilde{v}$ close to $\bar{v} \simeq 2.2\times10^{8}$ cm/sec behaves as an universal self-regulating generator of energy: the output of energy ε the non-holonomic background produces in order to compensate for a perturbation $\tilde{v}$ in itself is regulated by the density of radiant energy B in the system, while the perturbation in the background $\tilde{v} = \frac{e\sqrt{4\pi}}{m_e\bar{v}}\frac{\sqrt{B}}{\omega}$ is caused by the oscillation of free electrons, also regulated by the radiant energy density B. If the average oscillation velocity of electrons $\tilde{v}$ in a star becomes larger than that of the background $\bar{v} \simeq 2.2\times10^{8}$ cm/sec, temperature increases, and so the star expands until a new state of thermal equilibrium is reached, with a larger luminosity that compensates for the increased generation of energy within. If the average oscillation velocity of electrons becomes less than $\bar{v} \simeq 2.2\times10^{8}$ cm/sec, the star contracts until a new thermal equilibrium with lower luminosity is attained.

*And, to a much smaller extent, on ω, which has changes within 1 order of magnitude along the whole range of the spectral classes of stars.

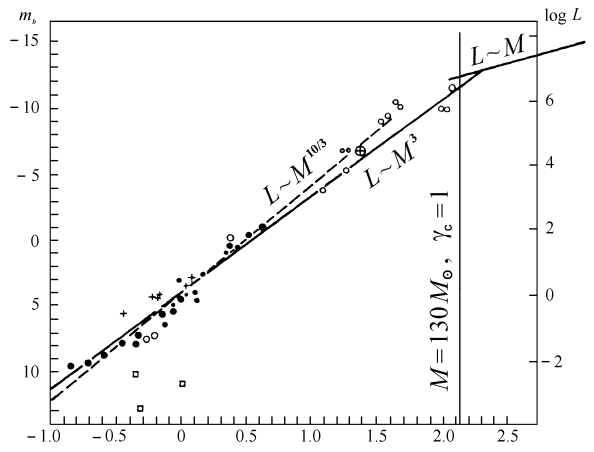

Fig. 2: The mass-luminosity relation. Here points are visual binaries, circles are spectral-binaries and eclipse variable stars, crosses are stars in Giades, squares are white dwarfs, the crossed circle is the satellite of ε Aurigae. Reproduced from [2].

If there were no other active factors slowly discharging the inner resources of a star (e. g. nuclear transformations of a different kind, etc), such a mechanism could generate stellar energy eternally, keeping stars in a stable radiating state.

2 Comparing the theory of stellar energy to observational data. The "volume-luminosity" correlation

We now analyse the implications of our formula (6) for stellar energy in comparison to the phenomenological data of observational astrophysics: the stellar energy relation (Fig. 1) and the mass-luminosity relation (Fig. 2).

We consider characteristics of a star in multiples of the corresponding values of the parameters for the Sun. We therefore operate with dimensionless characteristics: mass $\bar{M} = \frac{M}{M_\odot}$, radius $\bar{R} = \frac{R}{R_\odot}$, luminosity $\bar{L} = \frac{L}{L_\odot}$, productivity of energy $\bar{\varepsilon} = \frac{\varepsilon}{\varepsilon_\odot}$, etc. Using this notation, our formula (6) for stellar energy takes the form

$$\bar{\varepsilon} = \frac{\bar{n}_e\bar{B}^{3/2}}{\bar{\omega}} \simeq \bar{n}_e\bar{B}^{3/2}, \qquad (7)$$

or, considering the hydrogen constitution of most stars, so that $n_e = \frac{\rho}{m_p}$ (i. e. $\bar{n}_e = \bar{\rho}$),

$$\bar{\varepsilon} = \frac{\bar{\rho}\bar{B}^{3/2}}{\bar{\omega}} \simeq \bar{\rho}\bar{B}^{3/2}. \quad (8)$$

By the stellar energy relation $\frac{B}{n_e} = \text{const}$ from the stellar energy diagram (see Fig. 1), we have $\bar{B} = \bar{n}_e = \bar{\rho}$ throughout the whole range of stars. We can therefore write the stellar energy formula (8) in the final form

$$\bar{\varepsilon} = \bar{\rho}\bar{B}^{3/2} = \bar{B}^{5/2}. \quad (9)$$

By the data of observational astrophysics, stars obey the principles of an ideal gas, except for the white dwarfs wherein the gas is in a state on the boundary of degeneration. We therefore obtain by the equation for an ideal gas $p = \frac{\Re T\rho}{\mu}$ (where $\Re$ is Clapeyron's constant, μ is the molecular weight), $\bar{p} = \frac{\bar{T}\bar{\rho}}{\bar{\mu}}$, or, with a similar molecular composition throughout the whole range of stars, $\bar{p} = \bar{T}\bar{\rho}$. The gaseous pressure p is determined by the state of mechanical equilibrium in a star, according to which the pressure from within is equal to the pressure of a column of the star's contents, so we obtain $\bar{p} = \frac{\bar{M}}{\bar{R}^2}\bar{\rho}\bar{R} = \frac{\bar{M}}{\bar{R}^2}\frac{\bar{M}}{\bar{R}^3}\bar{R} = \frac{\bar{M}^2}{\bar{R}^4}$. Therefore the density of radiant energy in a star is $\bar{B} = \bar{T}^4 = \frac{\bar{M}^4}{\bar{R}^4}$. So the stellar energy formula takes the final form,

$$\bar{\varepsilon} = \bar{B}^{5/2} = \frac{\bar{M}^{10}}{\bar{R}^{10}}. \quad (10)$$

We analyze this result, taking the mass-luminosity relation into account. According to well verified data of observational astrophysics, stars satisfy the mass-luminosity relation $\bar{L} = \bar{M}^{10/3} \simeq \bar{M}^{3.3}$ (see Fig. 2). The relation $\bar{L} = \bar{M}^3$ can be deduced from theory. Here is how. Thermal equilibrium in a star is characterized by the equation [2]

$$\varepsilon = -\frac{c}{\kappa\rho}\frac{dB}{dr}, \quad (11)$$

which means that the flow of energy generated in a star is balanced by the flow of radiant energy therein (κ is the coefficient of absorption). In other words, this formula is the *condition of energy drainage* in a star — the condition of radiation. From this formula we have, for stars of approximately the same chemical composition,

$$\bar{\varepsilon} = \frac{\bar{B}}{\bar{\rho}\bar{R}} = \frac{\bar{M}^3}{\bar{R}^2}, \quad (12)$$

and hence, because the luminosity of a star is $\bar{L} = \bar{\varepsilon}\bar{R}^2$, we obtain the mass-luminosity relation $\bar{L} = \bar{M}^3$.

As a matter of fact, ε determined by the energy drainage condition in a star should coincide with ε determined by the mechanism producing stellar energy — an *energy production condition*. In our theory of stellar energy, such an energy production condition is represented by the stellar energy formula $\bar{\varepsilon} = \bar{n}_e\bar{B}^{3/2} = \bar{\rho}\bar{B}^{3/2} = \bar{B}^{5/2}$.

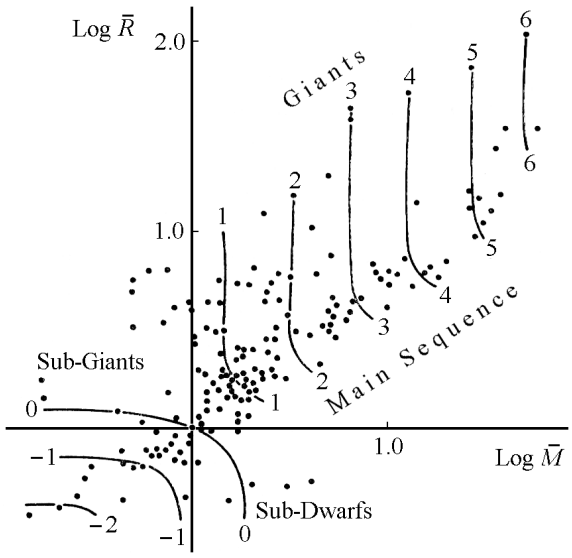

Fig. 3: Diagram of "mass–radius" devised by N. A. Kozyrev, the famous astronomer and experimental physicist, in the late 1970's. The arcs are isoergs of stellar matter. (Courtesy of V. V. Nassonov, Kozyrev's assistant, who had frequent meetings with the author in 1984–1985.)

We therefore substitute the observed mass-luminosity relation $\bar{L} = \bar{M}^{10/3}$ and the theoretical relation $\bar{L} = \bar{M}^3$ into our formula for stellar energy reduced to the absolute mass and radius of a star $\bar{\varepsilon} = \bar{B}^{5/2} = \frac{\bar{M}^{10}}{\bar{R}^{10}}$ (10). Because $\bar{L} = \bar{\varepsilon}\bar{R}^2$, our formula for stellar energy, in common with the observed mass-luminosity relation $\bar{L} = \bar{M}^{10/3}$, gives

$$\bar{L} = \bar{R}^4, \quad (13)$$

while with the theoretical relation $\bar{L} = \bar{M}^3$ our formula gives a slightly smaller exponent,

$$\bar{L} = \bar{R}^{3.4}. \quad (14)$$

In other words, for both the observed and theoretical mass-luminosity relation, our formula for stellar energy says that,

> On the basis of stellar energy being generated by the background space non-holonomity field, in Thomson dispersion of light in free electrons, the luminosity L of a star is proportional to its volume $V = \frac{4}{3}\pi R^3$, with a small progression with an increase of radius. We will refer to the newly discovered correlation as the *volume-luminosity relation*.

The predicted volume-luminosity relation $\bar{L} = \bar{R}^4$–$\bar{R}^{3.4}$ is derived from the condition of energy production by the non-holonomic space background in Thomson dispersion of light in stars (our theory of stellar energy). If such a correlation (the condition of energy production) is true, the correlation, in common with the energy drainage condition (the mass-luminosity relation $\bar{L} = \bar{M}^3$–$\bar{M}^{10/3}$), should produce another correlation; mass-radius $\bar{M} = \bar{R}^{1.1}$–$\bar{R}^{1.2}$. Fig. 3

shows a diagram devised by Kozyrev in the 1970's on the basis of observational data, along with many other diagrams within the framework of his extensive phenomenological research into stellar energy and the internal constitution of stars. As seen from the diagram, stars are distributed along the average direction $\bar{M} \sim \bar{R}$, which perfectly verifies the expected correlation $\bar{M} = \bar{R}^{1.1}$–$\bar{R}^{1.2}$ predicted on the basis of our formula for stellar energy. Hence the relation $\bar{M} \sim \bar{R}$ verifies as well the whole theory of the stellar energy mechanism we have built here and in [1].

The deduced volume-luminosity relation clearly depends upon the chemical composition of stars. Naturally, because the gravitational pressure in a star $\bar{p} = \frac{\bar{M}}{\bar{R}^2}\,\bar{\rho}\,\bar{R} = \frac{\bar{M}^2}{\bar{R}^4}$ is balanced by the gaseous pressure calculated by the equation for an ideal gas $\bar{p} = \frac{\bar{T}\bar{\rho}}{\bar{\mu}}$, we have $\bar{B} = \bar{T}^4 = \bar{\mu}^4 \frac{\bar{M}^4}{\bar{R}^4}$. On the other hand, Kozyrev has found, from the stellar energy diagram (Fig. 1), that "The main direction wonderfully traces an angle of exactly 45°. Hence, all stars are concentrated along the line, determined by the equation $B \sim \rho\mu^4$" [2]. We therefore substitute $\bar{n}_e = \bar{\rho} = \frac{\bar{B}}{\bar{\mu}^4}$ and $\bar{B} = \bar{\mu}^4 \frac{\bar{M}^4}{\bar{R}^4}$ into our initial formula for stellar energy $\bar{\varepsilon} = \bar{n}_e \bar{B}^{3/2}$ (7). As a result we obtain the formula for stellar energy in the form, where the molecular weight of the stellar contents is taken into account,

$$\bar{\varepsilon} = \bar{\mu}^6 \frac{\bar{M}^{10}}{\bar{R}^{10}}\,, \tag{15}$$

from which, because $\bar{L} = \bar{\varepsilon}\bar{R}^2$, we obtain, with the observed mass-luminosity relation $\bar{L} = \bar{M}^{10/3}$,

$$\bar{L} = \frac{1}{\bar{\mu}^3}\,\bar{R}^4, \tag{16}$$

while with the theoretical relation $\bar{L} = \bar{M}^3$ our updated formula (8) gives

$$\bar{L} = \frac{1}{\bar{\mu}^{2.6}}\,\bar{R}^{3.4}. \tag{17}$$

As is clearly seen, our deduced relation — the proportionality of the luminosity of a star to its volume $L \sim V \sim R^3$ — is inversely proportional to $\sim$3 orders of the molecular weight of the gas consisting a star. The greater the molecular weight of the gaseous contents of a star, the smaller its luminosity for the same volume. For instance, for a star consisting, instead of Hydrogen, of Helium or other heavy elements, the luminosity of such a star should be many times less than a completely hydrogen star of the same size.

3 The same stellar energy formula applied to brown dwarfs and the bulky planets

So the mass-luminosity relation $\bar{L} = \bar{M}^3$ is derived from the energy drainage condition $\bar{\varepsilon} = \frac{\bar{B}}{\bar{\rho}\bar{R}} = \frac{\bar{M}^3}{\bar{R}^2}$. The necessary coincidence with the energy production condition, the stellar energy formula $\bar{\varepsilon} = \bar{n}_e \bar{B}^{3/2} = \bar{\rho}\,\bar{B}^{3/2} = \bar{B}^{5/2}$, gives a new relation between the observable characteristics of stars — the volume-luminosity relation: $\bar{L} = \bar{R}^{3.4}$ for the theoretical relation $\bar{L} = \bar{M}^3$, or $\bar{L} = \bar{R}^4$ for the observed $\bar{L} = \bar{M}^{10/3}$.

Table 1: Brown dwarfs

	$\bar{L} = \bar{M}^{10/3}$	$\bar{L} = \bar{M}^3$	$\bar{L} = \bar{R}^4$	$\bar{L} = \bar{R}^{3.4}$
$\bar{L} = 10^{-4}$	$\bar{M} = 0.06$	$\bar{M} = 0.05$	$\bar{R} = 0.1$	$\bar{R} = 0.07$
$\bar{L} = 10^{-5}$	$\bar{M} = 0.03$	$\bar{M} = 0.02$	$\bar{R} = 0.06$	$\bar{R} = 0.03$

In this section we shall look at how our stellar energy formula can be applied to space objects of extremely small luminosity — recently discovered brown dwarfs, and also the bulky planets (Jupiter, Saturn, Uranus, and Neptune) whose radiated energy exceeds that received from the Sun (so they have their own internal sources of energy).

Brown dwarfs

These have masses $\bar{M} \leqslant 0.08$, luminosity $\bar{L} = 10^{-4}$–10^{-5}, and temperature at the surface $T \approx 700\,\mathrm{K}$, which determines their observed brown colour.

Proceeding from the luminosity $\bar{L}$ of brown dwarfs, we calculate: (1) their masses $\bar{M}$ by the mass-luminosity relation (the energy drainage condition), and also (2) their radii $\bar{R}$ by the volume-luminosity relation (the energy production condition) that characterizes the generation of stellar energy by the background space non-holonomity in Thomson dispersion of light. The results are given in Table 1.

By the observed mass-luminosity relation $\bar{L} = \bar{M}^{10/3}$, we obtained the masses in the range $\bar{M} = 0.03$–0.06 that satisfies the masses $\bar{M} \leqslant 0.08$ required for stars of such class. Brown dwarfs therefore satisfy the condition of energy drainage.

The radii of brown dwarfs $\bar{R} = 0.06$–0.1 we calculated by the condition of energy production — the volume-luminosity relation $\bar{L} = \bar{R}^4$ — are within the range of the bulky planets (from $\bar{R} = 0.034$ for Uranus to $\bar{R} = 0.10$ for Jupiter). Hence, from our calculations we conclude that:

> Brown dwarfs are stars of a size similar to Jupiter or Saturn. Their energy source is the same as that in stars of other kinds — the background space non-holonomity that generates energy in Thomson dispersion of light in free electrons. However, in contrast to the bulky planets, the radii of brown dwarfs satisfy the volume-luminosity relation, so the physical conditions therein are such that the stellar energy mechanism produces enough energy to compensate for the radiation from the surface.

The bulky planets

By direct measurements made by NASA's space missions (Pioneer, Voyager, Galileo, Cassini), the bulky planets have $\sim$75–90% hydrogen content (see http://www.nasa.gov for the details). So, because of the huge pressure in the central region, enough to ionize hydrogen, we propose the same energy source as that in any star. We can therefore calculate a table similar to that herein for brown dwarfs.

Table 2: The bulky planets

	$\bar{R}$	$\bar{M}$	T_{eff}	T_{ac}	B_{eff}	B_{ac}	$\bar{L}_{\text{p}}$	$\bar{L}=\bar{M}^x$	$\bar{L}=\bar{R}^y$	$\bar{L}=\bar{R}^4$
JUPITER:	0.10	9.5×10^{-4}	125 K	105 K	1.3×10^{4}	0.69×10^{4}	1.0×10^{-9}	$x=3.0$	$y=9.0$	$R=4{,}000$ km
SATURN:	0.086	2.9×10^{-4}	95 K	74 K	4.6×10^{3}	1.7×10^{3}	3.4×10^{-10}	$x=2.7$	$y=8.9$	$R=3{,}000$ km
URANUS:	0.034	4.4×10^{-5}	57 K	55 K	6.0×10^{2}	5.2×10^{2}	1.5×10^{-12}	$x=2.7$	$y=7.8$	$R=770$ km
NEPTUNE:	0.036	5.2×10^{-5}	59 K	38 K	6.9×10^{2}	1.2×10^{2}	1.2×10^{-11}	$x=2.5$	$y=7.4$	$R=1{,}300$ km

In Table 2 we use the effective temperature T_{eff} and the temperature T_{ac} acquired from the Sun, determined from the direct measurements made by the NASA satellites. The proper luminosity of each planet $L_{\text{p}}=4\pi R^2 B_{\text{p}}$ is calculated through the density of the proper radiant energy $B_{\text{p}}=B_{\text{eff}}-B_{\text{ac}}=$ $=\sigma\left(T_{\text{eff}}^4-T_{\text{ac}}^4\right)$, where $\sigma=5.67\times10^{-5}\ \text{erg/cm}^2\times\text{sec}\times\text{deg}$.

As seen from Table 2, the bulky planets have the luminosity $\bar{L}=\bar{M}^{2.5}$–$\bar{M}^{3.0}$. Many stars have a greater deviation from the average mass-luminosity relation $\bar{L}=\bar{M}^{10/3}$ (see Fig. 2), than the planets. We therefore conclude that,

> The bulky planets satisfy the mass-luminosity relation, which is the condition of energy drainage, so they radiate energy similar to stars.

Another result is provided by the volume-luminosity relation $\bar{L}\sim\bar{R}^y$, which characterizes the condition of energy production. The bulky planets have $\bar{L}=\bar{R}^{7.4}$–$\bar{R}^{9.0}$, while the coincidence of the energy drainage with the energy production in stars requires $\bar{L}=\bar{R}^{3.4}$–$\bar{R}^{4.0}$. The last column in Table 2 gives the values of the radii which should result if the energy loss is completely balanced by the energy produced within. So the bulky planets would be like stars. As seen, in such a case the bulky planets would be a bit smaller than the Earth: Jupiter and Saturn would have a size similar to Mars, Neptune would be similar to the Moon, while Uranus would be half the Moon. The obtained result implies that:

> The real radii of the bulky planets are so large that the energy produced within the planets is substantially less than that radiated from the surface: the planets are cooling down, in contrast to stars whose temperature is stable on the average.

So there is no crucial difference between stars and the bulky planets built on the gaseous contents. Looking at the evolution of the bulky planets, we see that as soon as the gravitational pressure compresses the planets down to radii satisfying the volume-luminosity relation $\bar{L}=\bar{R}^{3.4}$–$\bar{R}^{4.0}$, the energy output within the planets becomes balanced by the radiation from the surface, so the planets become stars. In such a case the density of the planets would become enormous.

Such high densities are conceivable, along the whole range of known stars, only within white dwarfs, which are mostly satellites of the most bulky stars. Compare Sirius' satellite ($\bar{R}=0.025$) and Procyon's satellite ($\bar{R}=0.013$), typical white dwarfs, which have a density $\rho\approx10^4$. We there therefore conclude that:

Table 3: The bulky planets, if becoming stars

	Radius, $\bar{R}$	Radius, km	Average density
JUPITER:	0.0057	4,000 km	7.1×10^{3} g/cm^3
SATURN:	0.0043	3,000 km	5.0×10^{3} g/cm^3
URANUS:	0.0011	770 km	4.6×10^{4} g/cm^3
NEPTUNE:	0.0019	1,300 km	1.1×10^{4} g/cm^3

> White dwarfs were formerly bulky planets like Jupiter and the great jovian planets, which, containing mostly hydrogen, were compressed by gravitational pressure to such a state that the energy produced within is the same as that radiated from the surface.
>
> So Jupiter and the jovian planets are stars in an early stage of their evolution. As soon as the gravitational pressure compresses each of them to the appropriate radius, they become white dwarfs — star-satellites of the Sun, so that the solar system becomes a multiple-star system.

4 A perspective for the new energy source

Accordingly, our theory that stellar energy is generated by the background space in Thomson dispersion of light in free electrons is readily verified. All that we need to reproduce the mechanism is ionized hydrogen: even if the temperature is much lower than in stars, we should obtain some energy output if the theory is correct. The ionization energy of a hydrogen atom is 13.6 eV; suitable equipment is accessible in even a junior college laboratory. Moreover, proceeding from the above theory, we can predict additional forces and energy output produced by the non-holonomic space background in phenomena other than Thomson dispersion of light. So the stellar energy theory herein, applied to laboratory conditions, predicts new energy sources working much more effectively and safely than nuclear energy.

References

1. Rabounski D. *Progress in Physics*, 2006, v. 4, 3–10.
2. Kozyrev N. A. *Progress in Physics*, 2005, v. 3, 61–99.

The Thermodynamics Associated with Santilli's Hadronic Mechanics

Jeremy Dunning-Davies

Department of Physics, University of Hull, England
Institute for Basic Research, P. O. Box 1577, Palm Harbor, Florida 346822, USA
E-mail: j.dunning-davies@hull.ac.uk

The new mathematics, referred to as iso-mathematics and geno-mathematics, introduced by Santilli to help explain a number of outstanding problems in quantum chemistry as well as in other areas of science such as astrophysics, has been applied successfully in a number of physical situations. This new formalism has, for the first time, provided an irreversible description of thermodynamics via an irreversible differential calculus together with the related mathematics. However, the associated thermodynamics has not been considered so far. That defect is remedied here.

1 Introduction

For many years now, science has harboured the belief that the theories of relativity and quantum mechanics offered the means to solve all outstanding theoretical problems. One person who has felt for many years that these theories are not complete is Ruggero Santilli. He has devoted his life to searching for extensions to these undoubtedly extremely successful theories. He was driven to this by the realisation that, despite a multitude of successes, a number of basic issues remained unresolved by orthodox quantum chemistry. Although a mountain of publications preceded it, the culmination of this work was presented in a monograph, *Foundations of Hadronic Chemistry* [1], which was produced in an attempt to provide possible explanations for a number of problems which had persisted for many years in the general area of quantum chemistry. In this book, he suggests a generalisation, or covering, of quantum chemistry, under the name "hadronic chemistry", which appears to resolve many of the outstanding problems. The suggested solution originates with the assumption that valence forces are nonlinear (in the wavefunction), non-local, and of non-potential type due to the deep overlapping of the wavepackets of valence electrons in singlet coupling. In turn, this "valence force" may not be represented quantitatively via conventional quantum chemistry since the latter is linear, local and potential. The covering of quantum chemistry for the invariant representation of the indicated new valence forces is based on a new mathematics called "iso-mathematics", which is itself based on real-valued (hermitian), nowhere singular yet arbitrary integro-differential units. Being, by fundamental assumption, incapable of representation via a Hamiltonian, these new valence forces are represented with the generalised integro-differential units. In turn, the representation of the new valence forces with a unit ensures the invariance of the theory, since the unit is known to be the basic invariant. The provision of simple means, utilising non-unitary transforms, for the construction of hadronic chemistry ensures that it differs from conventional theories.

In addition, an invariant formulation of irreversibility was presented also. The starting point for this was the historical legacy of Lagrange and Hamilton of representing irreversibility with the external terms in their celebrated equations — terms which are frequently ignored in modern expositions of the subject. For reasons of consistency, Santilli reformulates identically the original analytic equations in a form admitting a Lie-admissible structure in the sense of the American mathematician A. A. Albert. The formulation is extended from the classical to all branches. In this way, irreversibility emerges as originating from the most elementary levels of nature. Therefore, a possible resolution of the problem of reducing a macroscopic irreversible classical system to a finite collection of elementary particles, all in reversible conditions, is offered. This suggested formulation of irreversibility is based on an additional new form of mathematics known as "geno-mathematics". This is characterised by two real-valued, non-singular, non-symmetric, generalised units, interconnected by hermitian conjugates, one of which is assumed to characterise motion forward in time and the other, motion backward in time. The differences between the basic units for the two directions of time guarantee irreversibility for all possible reversible Hamiltonians. Since all potential interactions are reversible, these non-symmetric, generalised units represent the interactions responsible for irreversibility — namely, Lagrange's and Hamilton's external terms. This second set of methods is intended for an invariant representation of open irreversible processes, such as chemical reactions, and is part of the so-called genotopic branch of hadronic mechanics and chemistry.

However, the above generalisations were found not to resolve problems relating to anti-matter. To resolve these problems, it was found necessary to introduce yet more new mathematics. These further forms of mathematics are anti-isomorphic to the proposed iso- and geno-mathematics, have their own channel of quantisation, and the operator images are indeed antiparticles, defined as charge conjugates of con-

ventional particles on a Hilbert space. As far as the applicability of well-known thermodynamics' results is concerned, it is only the thermodynamics of anti-matter via Santilli's isodualities which has been considered [2]. It remains to consider the position of the powerful thermodynamic results in iso-mathematics and geno-mathematics.

2 Iso-thermodynamics

The basic rules for iso-mathematics are laid out clearly in Santilli's book [1] but what must be noted at the outset is the importance of realising that in such typical thermodynamic expressions as TdS, multiplication of T by dS is indicated. Hence,

$$TdS = T \times dS \to \hat{T} \hat{\times} \hat{d}\hat{S} \to T \times \hat{I} \times \hat{K} \times \hat{d}\hat{S} \to T \times \hat{d}\hat{S} ,$$

where

$$I \to \hat{I} = \frac{1}{\hat{K}} > 0 .$$

Then

$$T \times dS \to T \times \hat{d}\hat{S} = T \times \hat{I} \times d\left(S \times \hat{I}\right) = \hat{I} \times TdS .$$

Hence, it follows immediately that,

$$dQ = dU + pdV \to \hat{d}\hat{Q} = \hat{d}\hat{U} + \hat{p} \times \hat{d}\hat{V} \to \hat{I} \times dQ = \\ = \hat{I} \times (dU + pdV) \Rightarrow dQ = dU + pdV$$

and

$$dQ = TdS \to \hat{d}\hat{Q} = \hat{T} \hat{\times} \hat{d}\hat{S} \to \hat{I} \times dQ = \hat{I} \times TdS \Rightarrow \\ \Rightarrow dQ = TdS .$$

This means that, within the iso-mathematical framework, the equations representing the first and second laws of thermodynamics hold in their familiar forms. A moment's consideration indicates that other familiar thermodynamic relations will also retain the familiar forms; for example, the Euler relation

$$TS = U + pV - \mu N ,$$

the Gibbs-Duhem relation

$$SdT - Vdp + Nd\mu = 0 ,$$

and the expressions for the well-known thermodynamic potentials

$$\text{enthalpy: } H = U + pV,$$
$$\text{Helmholtz Free Energy: } F = U - TS,$$
$$\text{Gibbs Free Energy: } G = U + pV - TS.$$

3 Geno-thermodynamics

As far as the extension to include geno-mathematics is concerned, the basic rules of manipulation are again laid out in Santilli's book [1]. Application of these leads, for the combined first and second laws of thermodynamics, to

$$TdS = dU + pdV \to T^{>} > d^{>}S^{>} = d^{>}U^{>} + p^{>} > d^{>}V^{>}$$

which becomes

$$(TI^{>})\, I^{>-1}\left[I^{>-1} d\,(SI^{>})\right] = TdS = I^{>-1} d\,(UI^{>}) + \\ + (pI^{>})\, I^{>-1}\left[I^{>-1} d\,(VI^{>})\right] = dU + pdV .$$

However, here the genounit has been assumed constant. If the genounit depends on local variables

$$dS \to d^{>}S^{>} = I^{>-1} d\,(SI^{>}) = dS + SI^{>-1} dI^{>} ,$$

and similarly for dQ and dW. Hence, in these circumstances the equation representing the second law takes the form

$$T^{>} > d^{>}S^{>} = d^{>}U^{>} + p^{>} > d^{>}V^{>} \to \\ \to TdS + TSI^{>-1} dI^{>} = \\ = dU + UI^{>-1} dI^{>} + pdV + pVI^{>-1} dI^{>} \Rightarrow \\ \Rightarrow TdS = dU + pdV ,$$

since $TS = U + pV$.

Hence, even if the genounit does depend on local variables, the form of the equation representing a combination of the first and second laws of thermodynamics retains its familiar form. It may be noted that this is true of all the fundamental equations of thermodynamics when the extension into geno-mathematics is considered, just as was the case for iso-mathematics.

4 Conclusions

The end result of this discussion is simply to conclude that the familiar results of thermodynamics remain valid in their familiar forms in both iso-mathematics and geno-mathematics. These results all follow easily but are, nevertheless, important in that it confirms that the various results of thermodynamics may be used with confidence in conjunction with both iso-mathematics and geno-mathematics. It is worth remembering, however, that Santilli's new formalism achieves an irreversible description of thermodynamics through an irreversible differential calculus together with the related mathematics. Although it is shown here that the familiar thermodynamic results remain applicable in their familiar forms, it should be noted that the overall new formalism may be used to describe departures from the conventional laws which appear in several areas of science. This overall subject is relatively new and so the full extent of this claim is simply not known at present. Hence, it is important to embrace this new material with a truly open mind.

Further, it might be noted that, while a large number of Santilli's applications refer to what are essentially small systems and thermodynamics is a macroscopic theory, exactly how thermodynamics will apply in these cases is not yet completely clear. However, if a lead is taken from the work

of Hill [3], it is readily seen that the familiar equations as modified for application to these small systems remain valid in both iso-mathematics and geno-mathematics.

Finally, it is worth realising that, for all its background as a collection of "facts of experience", thermodynamics in its well-known form continues to be applicable in all situations which arise for consideration. It is certainly a topic which can lay claim to be at the very heart of physics.

References

1. Santilli R. M. Foundations of Hadronic Chemistry. Kluwer Academic Publishers, Dordrecht, 2001; *Il Nuovo Cimento B* (in press) and http://www.i-b-f.org/Hadronic-Mechanics.htm
2. Dunning-Davies J. *Found. Phys. Lett.*, 1999, v. 12, 593–599.
3. Hill T. L. Thermodynamics of small systems. Benjamin, New York, 1963.

A Note on Geometric and Information Fusion Interpretation of Bell's Theorem and Quantum Measurement*

Florentin Smarandache† and Vic Christianto‡

†*Department of Mathematics, University of New Mexico, Gallup, NM 87301, USA*
E-mail: smarand@unm.edu

‡*Sciprint.org — a Free Scientific Electronic Preprint Server, http://www.sciprint.org*
E-mail: admin@sciprint.org

In this paper we present four possible extensions of Bell's Theorem: Bayesian and Fuzzy Bayesian intrepretation, Information Fusion interpretation, Geometric interpretation, and the viewpoint of photon fluid as medium for quantum interaction.

1 Introduction

It is generally accepted that Bell's theorem [1] is quite exact to describe the linear hidden-variable interpretation of quantum measurement, and hence "quantum reality". Therefore null result of this proposition implies that no hidden-variable theory could provide good explanation of "quantum reality".

Nonetheless, after further thought we can find that Bell's theorem is nothing more than another kind of abstraction of quantum observation based on a set of assumptions and propositions [7]. Therefore, one should be careful before making further generalization on the null result from experiments which are "supposed" to verify Bell's theorem. For example, the most blatant assumption of Bell's theorem is that it takes into consideration only the classical statistical problem of chance of outcome A or outcome B, as result of adoption of Von Neumann's definition of "quantum logic". Another critic will be discussed here, i. e. that Bell's theorem is only a reformulation of statistical definition of correlation; therefore it is merely tautological [5].

Therefore in the present paper we will discuss a few plausible extension of Bell's theorem:

(a) Bayesian and Fuzzy Bayesian interpretation.

(b) Information Fusion interpretation. In particular, we propose a modified version of Bell's theorem, which takes into consideration this multivalued outcome, in particular using the information fusion Dezert-Smarandache Theory (DSmT) [2, 3, 4]. We suppose that in quantum reality the outcome of $P(A \cup B)$ and also $P(A \cap B)$ shall also be taken into consideration. This is where DSmT and Unification of Fusion Theories (UFT) could be found useful [2, 17].

(c) Geometric interpretation, using a known theorem connecting geometry and imaginary plane. In turn, this leads us to 8-dimensional extended-Minkowski metric.

(d) As an alternative to this geometric interpretation, we submit the viewpoint of photon fluid as medium for quantum interaction. This proposition leads us to Gross-Piteavskii equation which is commonly used to describe bose condensation phenomena. In turn we provide a route where Maxwell equations and Schrödinger equation could be deduced from Gross-Pitaevskii equation by using known algebra involving bi-quaternion number. In our opinion, this new proposition provides us a physical mechanism of quantum interaction, beyond conventional "quantum algebra" which hides causal explanation.

By discussing these various approaches, we use an expanded logic beyond "yes" or "no" type logic [3]. In other words, there could be new possibilities to describe quantum interaction: "both can be wrong", or "both can be right", as described in Table 1 below.

In Belnap's four-valued logic there are, besides Truth (T) and Falsehood (F), also Uncertainty (U) and Contradiction (C) but they are inter-related [30]. Belnap's logic is a particular case of Neutrosophic Logic (which considers three components: Truth, Falsehood, and Indeterminacy (I)) when indeterminacy is split into Uncertainty and Contradiction. In our article we have: Yes (Y), No (N), and Indeterminacy (I, which means: neither Yes nor No), but Indeterminacy is split into "both can be wrong" and "both can be right".

It could be expected that a combined interpretation represents multiple-facets of quantum reality. And hopefully it could bring better understanding on the physical mechanism beneath quantum measurement, beyond simple algebraic notions. Further experiments are of course recommended in order to verify or refute this proposition.

2 Bell's theorem. Bayesian and fuzzy Bayesian interpretation

Despite widespread belief of its ability to describe hidden-variables of quantum reality [1], it shall be noted that Bell's theorem starts with a set of assumptions inherent in its formulation. It is assumed that each pair of particles possesses a particular value of λ, and we define quantity $p(\lambda)$ so that probability of a pair being produced between λ and $\lambda + d\lambda$

*Note: The notion "hronir wave" introduced here was inspired from Borges' Tlon, Uqbar, Orbis Tertius.

Alternative	Bell's theorem	Implications	Special relativity
QM is nonlocal	Invalid	Causality breaks down; Observer determines the outcome	Is not always applicable
QM is local with hidden variable	Valid	Causality preserved; The moon is there even without observer	No interaction can exceed the speed of light
Both can be right	Valid, but there is a way to explain QM without violating Special Relativity	QM, special relativity and Maxwell electromagnetic theory can be unified. New worldview shall be used	Can be expanded using 8-dimensional Minkowski metric with imaginary plane
Both can be wrong	Invalid, and so Special Relativity is. We need a new theory	New nonlocal QM theory is required, involving quantum potential	Is not always applicable

Table 1: Going beyond classical logic view of QM

is $p(\lambda)\,d\lambda$. It is also assumed that this is normalized so that:

$$\int p(\lambda)\,d\lambda = 1\,. \tag{1}$$

Further analysis shows that the integral that measures the correlation between two spin components that are at an angle of $(\delta - \phi)$ with each other, is therefore equal to $C''(\delta - \phi)$. We can therefore write:

$$|C''(\phi) - C''(\delta)| - C''(\delta - \phi) \leqslant 1 \tag{2}$$

which is known as Bell's theorem, and it was supposed to represent any local hidden-variable theorem. But it shall be noted that actually this theorem cannot be tested completely because it assumes that all particle pairs have been detected. In other words, we find that a hidden assumption behind Bell's theorem is that it uses classical probability assertion [12], which may or may be not applicable to describe Quantum Measurement.

It is wothnoting here that the standard interpretation of Bell's theorem includes the use of Bayesian posterior probability [13]:

$$P(\alpha\,|\,x) = \frac{p(\alpha)\,p(x\,|\,\alpha)}{\sum_\beta p(\beta)\,p(x\,|\,\beta)}\,. \tag{3}$$

As we know Bayesian method is based on classical two-valued logic. In the meantime, it is known that the restriction of classical propositional calculus to a two-valued logic has created some interesting paradoxes. For example, the Barber of Seville has a rule that all and only those men who do not shave themselves are shaved by the barber. It turns out that the only way for this paradox to work is if the statement is both *true and false simultaneously* [14]. This brings us to *fuzzy Bayesian approach* [14] as an extension of (3):

$$P(s_i|\underline{M}) = \frac{p(\underline{M}\,|\,s_i)\,p(s_i)}{p(\underline{M})}\,, \tag{4}$$

where [14, p. 339]:

$$p(\underline{M}\,|\,s_i) = \sum_{k=1}^{r} p(x_k\,|\,s_i)\,\mu_{\underline{M}}(x_k)\,. \tag{5}$$

Nonetheless, it should also be noted here that there is shortcoming of this Bayesian approach. As Kracklauer points out, Bell's theorem is nothing but a reformulation of statistical definition of correlation [5]:

$$\mathrm{Corr}\,(A, B) = \frac{\langle|AB|\rangle - \langle A\rangle\langle B\rangle}{\sqrt{\langle A^2\rangle\langle B^2\rangle}}\,. \tag{6}$$

When $\langle A\rangle$ or $\langle B\rangle$ equals to zero and $\langle A^2\rangle\langle B^2\rangle = 1$ then equation (6) reduces to Bell's theorem. Therefore as such it could be considered as merely tautological [5].

3 Information fusion interpretation of Bell's theorem. DSmT modification

In the context of physical theory of information [8], Barrett has noted that "there ought to be a set theoretic language which applies directly to all quantum interactions". This is because the idea of a bit is itself straight out of *classical set theory*, the definitive and unambiguous assignment of an element of the set $\{0, 1\}$, and so the assignment of an information content of the photon itself is fraught with the same difficulties [8]. Similarly, the problem becomes more adverse because the fundamental basis of conventional statistal theories is the same classical set $\{0, 1\}$.

Not only that, there is also criticism over the use of Bayesian approach, i. e.: [13]

(a) In real world, neither class probabilities nor class densities are precisely known;

(b) This implies that one should adopt a parametric model for the class probabilities and class densities, and then use empirical data.

(c) Therefore, in the context where multiple sensors can be used, information fusion approach could be a better alternative to Bayes approach.

In other words, we should find an extension to standard proposition in statistical theory [8, p. 388]:

$$P(AB|C) = P(A|BC)P(B|C) \quad (7)$$
$$= P(B|AC)P(A|C) \quad (8)$$
$$P(A|B) + P(\bar{A}|B) = 1\,. \quad (9)$$

Such an extension is already known in the area of information fusion [2], known as Dempster-Shafer theory:

$$m(A) + m(B) + m(A \cup B) = 1\,. \quad (10)$$

Interestingly, Chapline [13] noted that neither Bayesian theory nor Dempster-Shafer could offer insight on how to minimize overall energy usage in the network. In the meantime, Dezert-Smarandache (DSmT) [2] introduced further improvement of Dempster-Shafer theory by taking into consideration chance to observe intersection between A and B:

$$m(A) + m(B) + m(A \cup B) + m(A \cap B) = 1\,. \quad (11)$$

Therefore, introducing this extension from equation (11) into equation (2), one finds a modified version of Bell's theorem in the form:

$$|C''(\phi) - C''(\delta)| - \\ - C''(\delta - \phi) + C''(\delta \cup \phi) + C''(\delta \cap \phi) \leqslant 1\,, \quad (12)$$

which could be called as modified Bell's theorem according to Dezert-Smarandache (DSmT) theory [2]. Its direct implications suggest that it could be useful to include more sensors in order to capture various possibilities beyond simple $\{0, 1\}$ result, which is typical in Bell's theorem.

Further generalization of DSmT theory (11) is known as Unification of Fusion Theories [15, 16, 17]:

$$m(A) + m(B) + m(A \cup B) + m(A \cap B) + \\ + m(\bar{A}) + m(\bar{B}) + m(\bar{A} \cup \bar{B}) + m(\bar{A} \cap \bar{B}) = 1\,, \quad (13)$$

where $\bar{A}$ is the complement of A and $\bar{B}$ is the complement of B (if we consider the set theory).

(But if we consider the logical theory then $\bar{A}$ is the negation of A and $\bar{B}$ is the negation of B. The set theory and logical theory in this example are equivalent, hence doesn't matter which one we use from them.) In equation (13) above we have a complement/negation for A. We might define the $\bar{A}$ as the entangle of particle A. Hence we could expect to further extend Bell's inequality considering UFT; nonetheless we leave this further generalization for the reader.

Of course, new experimental design is recommended in order to verify and to find various implications of this new proposition.

4 An alternative geometric interpretation of Bell-type measurement. Gross-Pitaevskii equation and the "hronir wave"

Apart from the aforementioned Bayesian interpretation of Bell's theorem, we can consider the problem from purely geometric viewpoint. As we know, there is linkage between geometry and algebra with imaginary plane [18]:

$$x + iy = \rho e^{i\phi}. \quad (14)$$

Therefore one could expect to come up with geometrical explanation of quantum interaction, provided we could generalize the metric using imaginary plane:

$$X + iX' = \rho e^{i\phi}. \quad (15)$$

Interestingly, Amoroso and Rauscher [19] have proposed exactly the same idea, i. e. generalizing Minkowski metric to become 8-dimensional metric which can be represented as:

$$Z^{\mu} = X^{\mu}_{re} + iX^{\mu}_{im} = \rho e^{i\phi}. \quad (16)$$

A characteristic result of this 8-dimensional metric is that "space separation" vanishes, and quantum-type interaction could happen in no time.

Another viewpoint could be introduced in this regard, i. e. that the wave nature of photon arises from "photon fluid" medium, which serves to enable photon-photon interaction. It has been argued that this photon-fluid medium could be described using Gross-Pitaevskii equation [20]. In turns, we could expect to "derive" Schrödinger wave equation from the Gross-Pitaevskii equation.

It will be shown, that we could derive Schrödinger wave equation from Gross-Pitaevskii equation. Interestingly, a new term similar to equation (14) arises here, which then we propose to call it "hronir wave". Therefore one could expect that this "hronir wave" plays the role of "invisible light" as postulated by Maxwell long-time ago.

Consider the well-known Gross-Pitaevskii equation in the context of superfluidity or superconductivity [21]:

$$i\hbar\,\frac{\partial \Psi}{\partial t} = -\frac{\hbar^2}{2m}\Delta\Psi + \left(V(x) - \gamma\,|\Psi|^{p-1}\right)\Psi, \quad (17)$$

where $p < 2N/(N-2)$ if $N \geqslant 3$. In physical problems, the equation for $p = 3$ is known as Gross-Pitaevskii equation. This equation (17) has standing wave solution quite similar to Schrödinger equation, in the form:

$$\Psi(x,t) = e^{-iEt/\hbar} \cdot u(x)\,. \quad (18)$$

Substituting equation (18) into equation (17) yields:

$$-\frac{\hbar^2}{2m}\,\Delta u + \big(V(x) - E\big)\,u = |u|^{p-1}\,u\,, \quad (19)$$

which is nothing but time-independent linear form of Schrödinger equation, except for term $|u|^{p-1}$ [21]. In case the right-hand side of this equation is negligible, equation (19) reduces to standard Schrödinger equation. Using Maclaurin series expansion, we get for (18):

$$\Psi(x,t) = \left(1 - \frac{iEt}{\hbar} + \frac{\left(\frac{iEt}{\hbar}\right)^2}{2!} + \frac{\left(-\frac{iEt}{\hbar}\right)^3}{3!} + \dots\right) \cdot u(x)\,. \quad (20)$$

Therefore we can say that standing wave solution of Gross-Pitaevskii equation (18) is similar to standing wave

solution of Schrödinger equation (u), except for nonlinear term which comes from Maclaurin series expansion (20). By neglecting third and other higher order terms of equation (20), one gets an approximation:

$$\Psi(x,t) = \left[1 - iEt/\hbar\right] \cdot u(x)\,. \tag{21}$$

Note that this equation (21) is very near to hyperbolic form $z = x + iy$ [18]. Therefore one could conclude that standing wave solution of Gross-Pitaevskii equation is merely an extension from ordinary solution of Schrödinger equation into Cauchy (imaginary) plane. In other words, there shall be "hronir wave" part of Schrödinger equation in order to describe Gross-Pitaevskii equation. We will use this result in the subsequent section, but first we consider how to derive bi-quaternion from Schrödinger equation.

It is known that solutions of Riccati equation are logarithmic derivatives of solutions of Schrödinger equation, and *vice versa* [22]:

$$u'' + vu = 0\,. \tag{22}$$

Bi-quaternion of differentiable function of $x = (x_1, x_2, x_3)$ is defined as [22]:

$$Dq = -\mathrm{div}\,(q) + \mathrm{grad}\,(q_0) + \mathrm{rot}\,(q)\,. \tag{23}$$

By using alternative representation of Schrödinger equation [22]:

$$\left[-\Delta + u\right] f = 0\,, \tag{24}$$

where f is twice differentiable, and introducing quaternion equation:

$$Dq + q^2 = -u\,. \tag{25}$$

Then we could find q, where q is purely vectorial differentiable bi-quaternion valued function [22].

We note that solutions of (24) are related to (25) as follows [22]:

- For any nonvanishing solution f of (24), its logarithmic derivative:
$$q = \frac{Df}{f}\,, \tag{26}$$
is a solution of equation (25), and *vice versa* [22].

Furthermore, we also note that for an arbitrary scalar twice differentiable function f, the following equality is permitted [22]:

$$\left[-\Delta + u\right] f = \left[D + M^h\right]\left[D - M^h\right] f\,, \tag{27}$$

provided h is solution of equation (25).

Therefore we can summarize that given a particular solution of Schrödinger equation (24), the general solution reduces to the first order equation [22, p. 9]:

$$\left[D + M^h\right] F = 0\,, \tag{28}$$

where

$$h = \frac{D\sqrt{\varepsilon}}{\varepsilon}\,. \tag{29}$$

Interestingly, equation (28) is equivalent to **Maxwell equations**. [22] Now we can generalize our result from the preceding section, in the form of the following conjecture:

Conjecture 1 *Given a particular solution of Schrödinger equation (24), then the approximate solution of Gross-Pitaevskii equation (17) reduces to the first order equation:*

$$\left[1 - iEt/\hbar\right]\left[D + M^h\right] F = 0\,. \tag{30}$$

Therefore we can conclude here that there is neat linkage between Schrödinger equation, Maxwell equation, Riccati equation via biquaternion expression [22, 23, 24]. And approximate solution of Gross-Pitaevskii equation is similar to solution of Schrödinger equation, except that it exhibits a new term called here "*the hronir wave*" (30).

Our proposition is that considering equation (30) has imaginary plane wave, therefore it could be expected to provided "physical mechanism" of quantum interaction, in the same sense of equation (14). Further experiments are of course recommended in order to verify or refute this

5 Some astrophysical implications of Gross-Pitaevskii description

Interestingly, Moffat [25, p. 9] has also used Gross-Pitaevskii in his "phion condensate fluid" to describe CMB spectrum. Therefore we could expect that this equation will also yield interesting results in cosmological scale.

Furthermore, it is well-known that Gross-Pitaevskii equation could exhibit *topologically* non-trivial vortex solutions [26, 27], which can be expressed as quantized vortices:

$$\oint p \bullet dr = N_v\, 2\pi\hbar\,. \tag{31}$$

Therefore an implication of Gross-Pitaevskii equation [25] is that topologically quantized vortex could exhibit in astrophysical scale. In this context we submit the viewpoint that this proposition indeed has been observed in the form of Tifft's quantization [28, 29]. The following description supports this assertion of topological quantized vortices in astrophysical scale.

We start with standard definition of Hubble law [28]:

$$z = \frac{\delta\lambda}{\lambda} = \frac{Hr}{c} \tag{32}$$

or

$$r = \frac{c}{H}\, z\,. \tag{33}$$

Now we suppose that the major parts of redshift data could be explained via Doppler shift effect, therefore [28]:

$$z = \frac{\delta\lambda}{\lambda} = \frac{v}{c}\,. \tag{34}$$

In order to interpret Tifft's observation of quantized redshift corresponding to quantized velocity 36.6 km/sec and

72.2 km/sec, then we could write from equation (34):

$$\frac{\delta v}{c} = \delta z = \delta\left(\frac{\delta\lambda}{\lambda}\right). \tag{35}$$

Or from equation (33) we get:

$$\delta r = \frac{c}{H}\,\delta z\,. \tag{36}$$

In other words, we submit the viewpoint that Tifft's observation of quantized redshift implies a quantized distance between galaxies [28], which could be expressed in the form:

$$r_n = r_0 + n\,(\delta r)\,. \tag{35a}$$

It is proposed here that this equation of quantized distance (5) is resulted from topological quantized vortices (31), and agrees with Gross-Pitaevskii (quantum phion condensate) description of CMB spectrum [25]. Nonetheless, further observation is recommended in order to verify the above proposition.

Concluding remarks

In the present paper we review a few extension of Bell's theorem which could take into consideration chance to observe outcome beyond classical statistical theory, in particular using the information fusion theory. A new geometrical interpretation of quantum interaction has been considered, using Gross-Pitaevskii equation. Interestingly, Moffat [25] also considered this equation in the context of cosmology.

It is recommended to conduct further experiments in order to verify and also to explore various implications of this new proposition, including perhaps for the quantum computation theory [8, 13].

Acknowledgment

The writers would like to thank to Profs. C. Castro, J. Dezert, P. Vallin, T. Love, D. Rabounski, and A. Kaivarainen for valuable discussions. The new term "*hronir wave*" introduced here was inspired from Borges' *Tlon, Uqbar, Orbis Tertius*. Hronir wave is defined here as "almost symmetrical mirror" of Schrödinger-type wave.

References

1. Shimony A. http://plato.stanford.edu/entries/bell-theorem/ ; http://plato.stanford.edu/entries/kochen-specker/.
2. Smarandache F. and Dezert J. Advances and applications of of DSmT for information fusion. American Research Press, Rehoboth, 2004.
3. Smarandache F. *Bulletin of Pure and Applied Sciences*, Ser. Physics, 2003, v. 22D, No. 1, 13–25.
4. Smarandache F. and Christianto V. Multivalued logic, neutrosophy and Schrödinger equation. Hexis, Phoenix, 2005.
5. Kracklauer A. La theorie de Bell, est-elle la plus grande meprise de l'histoire de la physique? *Annales de la Fondation Louis de Broglie*, v. 25, 2000, 193.
6. Aharonov Y. *et al.* arXiv: quant-ph/0311155.
7. Rosu H. C. arXiv: gr-qc/9411035.
8. Zurek W. (ed.), Complexity, entropy and the physics of information. Santa Fe Inst. Studies, Addison-Wesley, 1990.
9. Schrieffer J. R. Macroscopic quantum phenomena from pairing in superconductors. Lecture, December 11, 1972.
10. Anandan J. S. In: *Quantum Coherence and Reality*. Columbia SC, World Sci., 1994; arXiv: gr-qc/9504002.
11. Goldstein S. Quantum theory without observers — part one. *Physics Today*, March 1998, 42–46.
12. Pitowski I. arXiv: quant-ph/0510095.
13. Chapline G. arXiv: adap-org/9906002; quant-ph/9912019; Granik A. and Chapline G. arXiv: quant-ph/0302013; http://www.whatsnextnetwork.com/technology/index.php/2006/03/.
14. Ross T. J. fuzzy logic with engineering applications. McGraw-Hill, 1995, 196–197, 334–341.
15. Smarandache F. Unification of Fusion Theories (UFT). *Intern. J. of Applied Math. & Statistics*, 2004, v. 2, 1–14.
16. Smarandache F. An in-depth look at information fusion rules and unification of fusion theories. Invited speech at NASA Langley Research Center, Hampton, VA, USA, Nov 5, 2004.
17. Smarandache F. Unification of the fusion theory (UFT). Invited speech at NATO Advance Study Institute, Albena, Bulgaria, May 16–27, 2005.
18. Gogberashvili M. arXiv: hep-th/0212251.
19. Rauscher E. A. and Amoroso R. *Intern. J. of Comp. Anticipatory Systems*, 2006.
20. Chiao R. *et al.*. arXiv: physics/0309065.
21. Dinu T. L. arXiv: math.AP/0511184.
22. Kravchenko V. arXiv: math.AP/0408172.
23. Lipavsky P. *et al*. arXiv: cond-mat/0111214.
24. De Haas E. P. *Proc. of the Intern. Conf. PIRT-2005*, Moscow, MGTU Publ., 2005.
25. Moffat J. arXiv: astro-ph/0602607.
26. Smarandache F. and Christianto V. *Progress in Physics*, 2006, v. 2, 63–67.
27. Fischer U. arXiv: cond-mat/9907457; cond-mat/ 0004339.
28. Russell Humphreys D. Our galaxy is the centre of the universe, "quantized" red shifts show. *TJ Archive*, 2002, v. 16(2), 95–104; http://answersingenesis.org/tj/v16/i2/galaxy.asp.
29. Setterfield B. http://www.journaloftheoretics.com.
30. Belnap N. A useful four-valued logic, modern uses of multiple-valued logic. (D. Reidel, editor), 8–37, 1977.

Developing de Broglie Wave

J. X. Zheng-Johansson* and Per-Ivar Johansson†

*Institute of Fundamental Physics Research, 611 93 Nyköping, Sweden
E-mail: jxzj@iofpr.org

†Uppsala University, Studsvik, 611 82 Nyköping, Sweden
E-mail: Per-Ivar.Johansson@studsvik.uu.se

The electromagnetic component waves, comprising together with their generating oscillatory massless charge a material particle, will be Doppler shifted when the charge hence particle is in motion, with a velocity v, as a mere mechanical consequence of the source motion. We illustrate here that two such component waves generated in opposite directions and propagating at speed c between walls in a one-dimensional box, superpose into a traveling beat wave of wavelength $\Lambda_d = \frac{v}{c}\Lambda$ and phase velocity $c^2/v + v$ which resembles directly L. de Broglie's hypothetic phase wave. This phase wave in terms of transmitting the particle mass at the speed v and angular frequency $\Omega_d = 2\pi v/\Lambda_d$, with Λ_d and Ω_d obeying the de Broglie relations, represents a de Broglie wave. The standing-wave function of the de Broglie (phase) wave and its variables for particle dynamics in small geometries are equivalent to the eigen-state solutions to Schrödinger equation of an identical system.

1 Introduction

As it stood at the turn of the 20th century, M. Planck's quantum theory suggested that energy (ε) is associated with a certain periodic process of frequency (ν), $\varepsilon = h\nu$; and A. Einstein's mass-energy relation suggested the total energy of a particle (ε) is connected to its mass (m), $\varepsilon = mc^2$. Planck and Einstein together implied that mass was associated with a periodic process $mc^2 = h\nu$, and accordingly a larger ν with a moving mass. Incited by such a connection but also a clash with this from Einstein's relativity theory which suggested a moving mass is associated with a slowing-down clock and thus a smaller ν, L. de Broglie put forward in 1923 [1] a hypothesis that a matter particle (moving at velocity v) consists of an internal periodic process describable as a packet of phase waves of frequencies dispersed about ν, having a phase velocity $W = \frac{\nu}{k} = c^2/v$, with c the speed of light, and a group velocity of the phase-wave packet equal to v. Despite the hypothetic phase wave appeared supernatural and is today not held a standard physics notion, the de Broglie wave has proven in modern physics to depict accurately the matter particles, and the de Broglie relations proven their fundamental relations.

So inevitably the puzzles with the de Broglie wave persist, involving the hypothetic phase waves or not, and are unanswered prior to our recent unification work [2]: What is waving with a de Broglie wave and more generally Schrödinger's wave function? If de Broglie's phase wave is indeed a reality, what is then transmitted at a speed (W) being $\frac{c}{v}$ times the speed of light c? How is the de Broglie (phase) wave related to the particle's charge, which if accelerated generates according to Maxwell's theory electromagnetic (EM) waves of speed c, and how is it in turn related to the EM waves, which are commonplace emitted or absorbed by a particle which changes its internal state? In [2] we showed that a physical model able to yield all of the essential properties of a de Broglie particle, in terms of solutions in a unified framework of the three basic mechanics, is provided by a single harmonic oscillating, massless charge $+e$ or $-e$ (termed a *vaculeon*) and the resulting electromagnetic waves. The solutions for a basic material particle generally in motion, with the charge quantity (accompanied with a spin) and energy of the charge as the sole inputs, predict accurately the inertial mass, total wave function, total energy equal to the mass times c^2, total momentum, kinetic energy and linear momentum of the particle, and that the particle is a de Broglie wave, it obeys Newton's laws of motion, de Broglie relations, Schrödinger equation in small geometries, Newton's law of gravitation, and Galilean-Lorentz-Einstein transformation at high velocities. In this paper we give a self-contained illustration of the process by which the electromagnetic component waves of such a particle in motion superpose into a de Broglie (phase) wave.

2 Particle; component waves; dynamic variables

A free massless vaculeon charge (q) endowed with a kinetic energy $\mathcal{E}_q$ at its creation, being not dissipatable except in a pair annihilation, will tend to move about in the vacuum, and yet at larger displacement restored, fully if $\mathcal{E}_q$ below a threshold, toward equilibrium by the potential field of the surrounding dielectric vacuum being here polarized under the charge's own field [2]. As a result the charge oscillates in the vacuum, at a frequency Ω_q; once in addition unidirectionally driven, it will also be traveling at a velocity v here in a one-dimensional box of length L along X-axis firstly in $+X$-direction. Let axis X' be attached to the moving charge, $X' = X - vT$; let v be low so that $(v/c)^2 \to 0$,

with c the velocity of light; accordingly $T' = T$. The charge will according to Maxwell's theory generate electromagnetic waves to both $+X$ and $-X$-directions, being by the standard solution a plane wave, given in dimensionless displacements (of the medium or fields in it):

$$\varphi^{\dagger}(X', T) = C_1 \sin\left[K^{\dagger} X' - \Omega^{\dagger} T + \alpha_0\right], \quad \text{(a)}$$

$$\varphi^{\ddagger}(X', T) = -C_1 \sin\left[K^{\ddagger} X' + \Omega^{\ddagger} T - \alpha_0\right], \quad \text{(b)} \qquad (1)$$

where $\begin{bmatrix} K^{\dagger} \\ K^{\ddagger} \end{bmatrix} = \lim_{(v/c)^2 \to 0} \begin{bmatrix} k^{\dagger} \\ k^{\ddagger} \end{bmatrix} = K \pm K_d$, $\begin{bmatrix} k^{\dagger} \\ k^{\ddagger} \end{bmatrix} = \frac{K}{1 \mp v/c}$ being wavevectors Doppler-shifted due to the source motion from their zero-v value, K; $\Lambda = 2\pi/K$, and $\Omega = cK$; $\Omega = \Omega_q$ for the classical electromagnetic radiation. On defining $k_d = \sqrt{(k^{\dagger} - K)(K - k^{\ddagger})} = \left(\frac{v}{c}\right) k$, with $k = \gamma K$, $\gamma = \frac{1}{\sqrt{1-(v/c)^2}}$, we have at classic-velocity limit:

$$K_d = \lim_{(v/c)^2 \to 0} k_d = \left(\frac{v}{c}\right) K; \qquad (2)$$

$\begin{bmatrix} \Omega^{\dagger} \\ \Omega^{\ddagger} \end{bmatrix} = \begin{bmatrix} K^{\dagger} c \\ K^{\ddagger} c \end{bmatrix} = \Omega \pm K_d c$, and α_0 is the initial phase. Assuming $\mathcal{E}_q$ is large and radiated in $J\,(\gg 1)$ wave periods if without re-fuel, the wavetrain of φ^j of a length $L_\varphi = JL$ will wind about the box L in $J \gg 1$ loops.

The electromagnetic wave φ^j of an angular frequency $\omega^j = k^j c$, $j = \dagger$ or $\ddagger$, has according to M. Planck a wave energy $\varepsilon^j = \hbar\omega^j$, with $2\pi\hbar$ the Planck constant. The waves are here the components of a particle; the geometric mean of their wave energies, $\sqrt{\varepsilon^{\dagger}\varepsilon^{\ddagger}} = \hbar\sqrt{\omega^{\dagger}\omega^{\ddagger}} = \gamma\hbar\Omega$ gives thereby the total energy of the particle. $\varepsilon_v = \gamma\hbar\Omega - \hbar\Omega = \frac{1}{2}\hbar\Omega_d\left[1 + \frac{3}{4}\left(\frac{v}{c}\right)^2 + \ldots\right]$ gives further the particle's kinetic energy and in a similar fashion its linear momentum p_v (see [2]), and

$$\mathcal{E}_v = \lim_{(v/c)^2 \to 0} \varepsilon_v = \tfrac{1}{2}\hbar\left(\tfrac{v}{c}\right)^2 \Omega, \qquad (3)$$

$$P_v = \lim_{(v/c)^2 \to 0} p_v = \sqrt{2m_0 \mathcal{E}_v} = \hbar\left(\tfrac{v}{c}\right) K. \qquad (4)$$

The above continues to indeed imply as L. de Broglie noted that a moving mass has a larger $\gamma\Omega/2\pi$ $(= \nu)$, and thus a clash with the time-dilation of Einstein'smoving clock. This conflict however vanishes when the underlying physics becomes clear-cut [2, 2006c].

3 Propagating total wave of particle

A tagged wave front of say $\varphi^{\dagger}(X', T)$ generated by the vaculeon charge, of $v > 0$, to its right at location X' at time T, will after a round-trip of distance $2L$ in time $\delta T = 2L/c$ return from left and propagate again to the right to X' at time $T^* = T + \delta T$. Here it gains a total extra phase $\alpha' = K2L + 2\pi$ due to $2L$ (with $\frac{(K^{\dagger} + K^{\ddagger})}{2} = K$) and the twice reflections at the massive walls, and becomes

$$\varphi_r^{\dagger}(X', T^*) = C_1 \sin\left[K^{\dagger} X' - \Omega^{\dagger} T + \alpha_0 + \alpha'\right]. \quad \text{(1a)}'$$

$\varphi_r^{\dagger}$ meets $\varphi^{\dagger}(X', T^*)$ just generated to the right, an identical wave except for an α', and superposes with it to a maximum if assuming $K2L = N2\pi$, $N = 0, 1, \ldots$, returning the same $\varphi^{\dagger}$ (assuming normalized). Meanwhile, $\varphi_r^{\dagger}(X', T^*)$ meets $\varphi^{\ddagger}(X_1', T^*)$ just generated to the left (Fig. 1a) and superposes with it as $\widetilde{\psi} = \varphi_r^{\dagger} + \varphi^{\ddagger}$. Using the trigonometric identity (TI), denoting $\widetilde{\psi}(X', T) = \widetilde{\psi}(X', T^*)$, this is $\widetilde{\psi}(X', T) = 2C_1 \cos(KX' - K_d cT) \sin(K_d X' - \Omega T + \alpha_0)$. With $X' = X - vT$, we have on the X-axis:

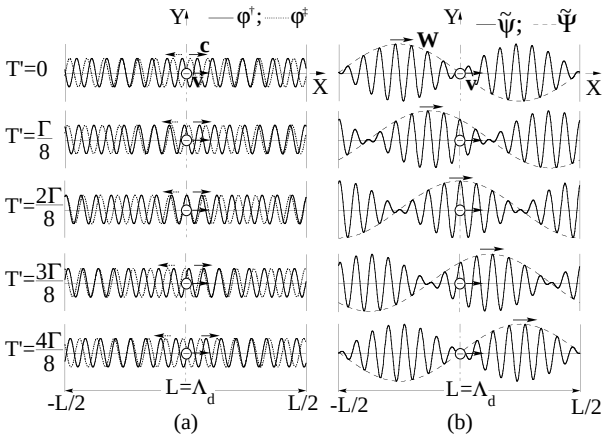

Fig. 1: (a) The time development of electromagnetic waves with wave speed c and wavelength Λ, $\varphi^{\dagger}$ generated to the right of (1a)$'$ and $\varphi^{\ddagger}$ to the left of (1b) by a charge $(\ominus)$ traveling at velocity v in $+X$ direction in a one-dimensional box of side L. (b) $\varphi^{\dagger}$ and $\varphi^{\ddagger}$ superpose to a beat, or de Broglie phase wave $\widetilde{\psi}$ of (5) traveling at phase velocity $W \simeq \frac{c^2}{v}$, of wavelength Λ_d. For the plot: $\Lambda = 0.067\Lambda_d$, and $\alpha_0 = -\frac{\pi}{2}$; $T' = T - \frac{\Gamma}{4}$; $v = (\frac{\Lambda}{\Lambda_d})c \ll c$.

$$\widetilde{\psi}(X, T) = \widetilde{\Phi}(X, T)\, \widetilde{\Psi}(X, T), \qquad (5)$$

$$\widetilde{\Phi}(X, T) = 2C_1 \cos(KX - 2K_d cT), \qquad (6)$$

$$\widetilde{\Psi}(X, T) = \sin\left[K_d X - (\Omega + \Omega_d) T + \alpha_0\right], \qquad (7)$$

where $Kv = K_d c$, and

$$\Omega_d = K_d v = \left(\frac{v}{c}\right)^2 \Omega. \qquad (8)$$

$\widetilde{\psi}$ expressed by (5) is a *traveling beat wave*, as plotted versus X in Fig. 1b for consecutive time points during $\Gamma/2$, or Fig. 2a during $\Gamma_d/2$. $\widetilde{\psi}$ is due to all the component waves of the particle while its charge is moving in one direction, and thus represents the (propagating) total wave of the particle, to be identified as a *de Broglie phase wave* below.

$\widetilde{\psi}$ has one product component $\widetilde{\Phi}$ oscillating rapidly on the X-axis with the wavelength $\Lambda = 2\pi/K$, and propagating at the speed of light c at which the total wave energy is transported. The other, $\widetilde{\Psi}$, envelops about $\widetilde{\Phi}$, modulating it into a slow varying beat $\widetilde{\psi}$ which has a wavevector, wavelength and angular frequency given by:

$$K_{\mathrm{b}} = K_d, \quad \Lambda_{\mathrm{b}} = \frac{2\pi}{K_{\mathrm{b}}} = \frac{2\pi}{K_d} = \Lambda_d, \quad \Omega_{\mathrm{b}} = \Omega + \Omega_d; \qquad (9)$$

$$\text{where} \quad \Lambda_d = \left(\frac{c}{v}\right)\Lambda. \qquad (10)$$

As follows (9), the beat $\widetilde{\psi}$ travels at the *phase velocity*

$$W = \frac{\Omega_{\rm b}}{K_{\rm b}} = \frac{\Omega}{K_d} + v = \left(\frac{c}{v}\right) c + v\,. \qquad (11)$$

4 De Broglie wave

Transmitted along with its beat wave, of a wavelength Λ_d, with $K_d = 2\pi/\Lambda_d$, is the mass of the particle at the velocity v. The beat wave conjoined with its transportation of the particle's mass represents thereby a periodic process of the particle, of a wavelength and wavevector equal to Λ_d and K_d of the beat wave. K_d and v define for the particle dynamics an angular frequency, $K_d v = \Omega_d$, as expressed by (8). Combining (10) and (4), and (8) and (3) respectively yield just the *de Broglie relations*:

$$P_v = \hbar K_d\,; \qquad (12) \qquad \mathcal{E}_v = \frac{1}{2}\,\hbar\Omega_d\,. \qquad (13)$$

Accordingly K_d, Λ_d, and Ω_d represent the de Broglie wave-vector, wavelength and angular frequency. The beat wave $\widetilde{\psi}$ of a phase velocity W resembles thereby the *de Broglie phase wave* and it in the context of transmitting the particle mass represents the *de Broglie wave* of the particle.

5 Virtual source. Reflected total particle wave

At an earlier time $T_1 = T - \Delta T$, at a distance L advancing its present location X, with $\Delta T = L/v$, the actual charge was traveling to the left, let axis $X''(= X + vT)$ be fixed to it. This past-time charge, said being virtual, generated at location X'' at time T_1 similarly one component wave $\varphi^{\dagger\,\rm vir}(X'', T_1^*)$ to the right, which after traversing $2L$ returned from left to X'' at time $T_1^* = T_1 + \delta T$ as $\varphi^{\dagger\,\rm vir}_r(X'', T_1^*) = $ $= C_1 \sin(K^{\dagger}_{-v} X'' - \Omega^{\dagger}_{-v} T_1^* + \alpha_0 + \alpha')$, where $K^{\dagger}_{-v} = K - K_d$, $K^{\ddagger}_{-v} = K + K_d$, and $\Omega^{j}_{-v} = K^{j}_{-v} c$ are the Doppler shifted wavevectors and angular frequencies; $\alpha' = (2N+1)\pi$ as earlier. Here at X'' and T_1^*, $\varphi^{\dagger\,\rm vir}_r$ meets the wave the virtual charge just generated to the left, $\varphi^{\ddagger\,\rm vir}(X'', T_1^*) = -C_1 \times$ $\times \sin(K^{\ddagger}_{-v} X'' + \Omega^{\dagger}_{-v} T_1^* - \alpha_0)$, and superpose with it to $\widetilde{\psi}^{\rm vir}(X, T_1^*) = \varphi^{\dagger\,\rm vir}_r + \varphi^{\ddagger\,\rm vir} = 2C_1 \cos(KX'' + K_d c T_1) \times$ $\times \sin\big[-K_d X'' - 2\Omega T_1 - \alpha_0\big]$.

With $J \gg 1$ and being nondamping, $\widetilde{\psi}^{\rm vir}$ will be looping continuously, up to the present time T. Its present form $\widetilde{\psi}^{\rm vir}(X'', T)$ is then as if just produced by the virtual charge at time T but at a location of a distance L advancing the actual charge; it accordingly has a phase advance $\beta = $ $= \frac{(K^{\dagger} - K^{\dagger}_{-v})}{2} L = K_d L$ relative to $\widetilde{\psi}$ (the phase advance in time yields no never feature). Including this β, using TI and with some algebra, $\widetilde{\psi}^{\rm vir}(X'', T)$ writes on axis X as

$$\widetilde{\psi}^{\rm vir}(X, T) = \widetilde{\Phi}^{\rm vir}(X, T)\, \widetilde{\Psi}^{\rm vir}(X, T)\,, \qquad (14)$$

$$\widetilde{\Phi}^{\rm vir}(X, T) = 2C_1 \cos\big[(KX + 2K_d c T\big]\,, \qquad (15)$$

$$\widetilde{\Psi}^{\rm vir}(X, T) = -\sin\big[K_d X + (\Omega + \Omega_d) T + \alpha_0 + \beta\big]\,. \qquad (16)$$

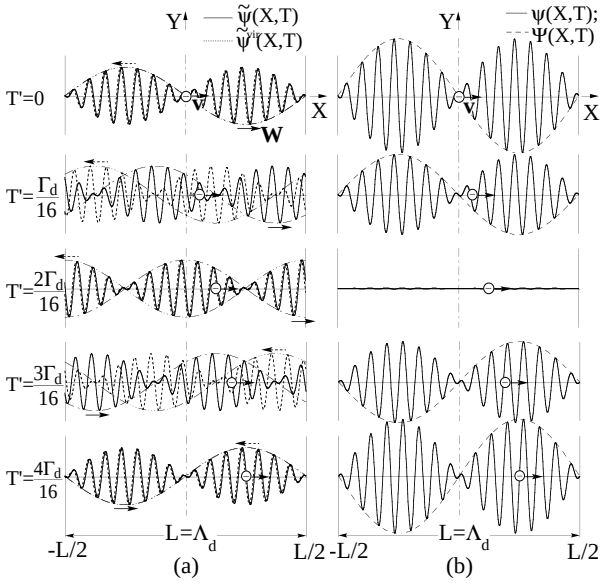

Fig. 2: (a) The beat waves $\widetilde{\psi}$ traveling at a phase velocity W to the right as in Fig. 1b and $\widetilde{\psi}^{\rm vir}$ at $-W$ to the left, of a wavelength Λ_d, due to the right- and left- traveling actual and virtual sources respectively. (b) $\widetilde{\psi}$ and $\widetilde{\psi}^{\rm vir}$ superpose to a standing beat or de Broglie phase wave ψ of wavelength Λ_d, angular frequency $\sim \Omega$. Along with the ψ process, the particle's center of mass ($\ominus$) is transported at the velocity v, of a period $\frac{2\pi}{\Omega_d} = \Lambda_d/v$.

$\widetilde{\psi}^{\rm vir}$ of the virtual or reflected charge is seen to be similarly a traveling beat or de Broglie phase wave to the left of a phase velocity $-W$ and wave parameters $K_{\rm b}$, $\Lambda_{\rm b}$ and $\Omega_{\rm b}$ as of (9).

6 Standing total wave and de Broglie wave

Now if $K_d L (= \beta) = n\pi$, i. e.

$$K_{dn} = \frac{n\pi}{L}\,, \quad n = 1, 2, \ldots\,, \qquad (17)$$

and accordingly $\Lambda_{dn} = \frac{2L}{n}$, then $\widetilde{\psi}^{\rm vir}$ and $\widetilde{\psi}$ superposed onto themselves from different loops are each a maximum. Also at (X, T), $\widetilde{\psi}^{\rm vir}$ and $\widetilde{\psi}$ meet and superpose, as $\psi = \widetilde{\psi} + \widetilde{\psi}^{\rm vir} = $ $= \widetilde{\Phi}\widetilde{\Psi} + \widetilde{\Phi}^{\rm vir}\widetilde{\Psi}^{\rm vir}$. On the scale of Λ_d, or K_d, the time variations in $\widetilde{\Phi}$ and $\widetilde{\Phi}^{\rm vir}$ are higher-order ones; thus for $K \gg K_d$, we have to a good approximation $\widetilde{\Phi}(X, T) \simeq \widetilde{\Phi}^{\rm vir}(X, T) \simeq$ $\simeq 2C_1 \cos(KX) = F(X)$ and $\psi(X, T) = F(X)\big[\widetilde{\Psi} + \widetilde{\Psi}^{\rm vir}\big] = $ $= C_4 \cos(KX) \sin\big[(\Omega + \Omega_d) T\big] \cos(K_d X + \alpha_0)$; $C_4 = 4C_1$. As a mechanical requirement at the massive walls,

$$\psi(0, T) = \psi(L, T) = 0\,. \qquad (18)$$

Condition (18) requires $\alpha_0 = -\frac{\pi}{2}$; ψ is thus now

$$\psi(X, T) = \Phi(X, T)\, \Psi_X(X)\,; \qquad (19)$$

$$\Psi_X(X) = \sin(K_d X)\,, \qquad (20)$$

$$\Phi(X, T) = C_4 \cos(KX) \sin\big[(\Omega + \Omega_d) T\big]\,. \qquad (21)$$

ψ of (18) is a standing beat or standing de Broglie phase wave; it includes all of the component waves due to both the actual and virtual charges and hence represents the (standing) total wave of the particle.

7 Eigen-state wave function and variables

Equation (13) showed the particle's kinetic energy is transmitted at the angular frequency $\frac{1}{2}\Omega_d$, half the value Ω_d for transporting the particle mass, and is a source motion effect of order $(\frac{v}{c})^2$. This is distinct from, actually exclusive of, the source motion effect, of order v, responsible for the earlier beat wave formation. We here include the order $(\frac{v}{c})^2$ effect only simply as a multiplication factor to ψ, and thus have $\psi' = \psi(X,T)\, e^{-i\frac{1}{2}\hbar\Omega_d T}$ which describes the particle's kinetic energy transmission. Furthermore, in typical applications $K \gg K_d$, $\Omega \gg \Omega_d$; thus on the scale of $(K_d,\ \Omega_d)$, we can to a good approximation ignore the rapid oscillation in Φ of (21), and have

$$\Phi(X,T) \simeq C_4 \equiv \text{constant} \qquad (21)'$$

and $\psi(X,T)=C\Psi_X(X)$. The time-dependent wave function, in energy terms, is thus $\Psi(X,T)=\psi'(X,T)=\psi e^{-i\frac{\Omega_d}{2}T}=$ $= C\Psi_X(X)e^{-i\frac{\Omega_d}{2}T}$, or

$$\Psi(X,T) = C\sin(K_d X)\, e^{-i\frac{1}{2}\Omega_d T}\,, \qquad (22)$$

where $C=\frac{1}{\int_0^L \psi^2 dX}=\frac{\sqrt{2/L}}{C_4}$ is a normalization constant. With (17) for K_{dn} in (12)–(13), for a fixed L we have the permitted dynamic variables

$$P_{vn} = \frac{n\hbar\pi}{L}\,, \qquad (23) \qquad \mathcal{E}_{vn} = \frac{n^2\hbar^2\pi^2}{2ML^2}\,, \qquad (24)$$

where $n = 1, 2, \ldots$ These dynamic variables are seen to be quantized, pronouncingly for L not much greater than Λ_d, as the direct result of the standing wave solutions. As shown for the three lowest energy levels in Fig. 3a, the permitted $\Psi(X)$, $\equiv \Psi(X,T_0)$ with T_0 a fixed time point, describing the envelopes (dotted lines) of $\psi(X) \equiv \psi(X,T_0)$ which rapid oscillations have no physical consequence to the particle dynamics, are in complete agreement with the corresponding solution of Schrödinger equation for an identical system, $\Psi_S(X)$, indicated by the same dotted lines.

The total wave of a particle, hence its total energy, mass, size, all extend in (real) space throughout the wave path. A portion of the particle, hence the probability of finding the particle, at a given position X in real space is proportional to the wave energy stored in the infinitesimal volume at X, $\mathcal{E}(X) = B\big(\psi(X)\big)^2$, with B a conversion constant [2], $\psi(X)$ as shown in Fig. 3b.

With (23) in $\Delta P_v = P_{v.n+1} - P_{v.n}$ we have $\Delta P_v\, 2L = h$, which reproduces Heisenberg's uncertainty relation. It follows from the solution that the uncertainty in finding a particle in real space results from the particle is an extensive

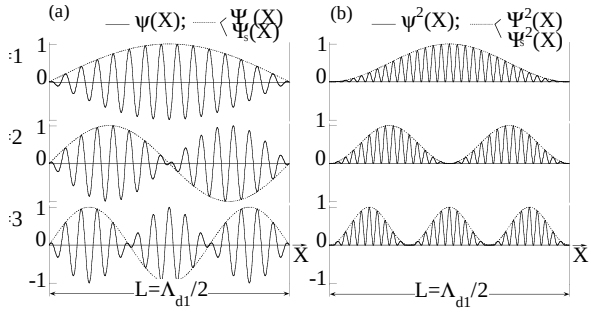

Fig. 3: (a) The total wave of particle $\psi(X)$ of (19) with rapid oscillation, and the de Broglie wave $\Psi(X)$ as the envelop, for three lowest energy levels $n = 1, 2, 3$; Ψ coincides with Schrödinger eigen-state functions Ψ_S. (b) The corresponding probabilities.

wave over L, and in momentum space from the standing wave solution where waves interfering destructively are cancelled and inaccessible to an external observer.

8 Concluding remarks

We have seen that the total wave superposed from the electromagnetic component waves generated by a traveling oscillatory vaculeon charge, which together make up our particle, has actually the requisite properties of a de Broglie wave. It exhibits in spatial coordinate the periodicity of the de Broglie wave, by the wavelength Λ_d, facilitated by a beat or de Broglie phase wave traveling at a phase velocity $\sim c^2/v$, with the beat in the total wave resulting naturally from the source-motion resultant Doppler differentiation of the electromagnetic component waves. Λ_d conjoined with the particle's center-of-mass motion leads to a periodicity of the de Broglie wave on time axis, the angular frequency Ω_d. The Λ_d and Ω_d obey the de Broglie relations. The particle's standing wave solutions in confined space agree completely with solutions for Schrödinger equation for an identical system.

References

1. De Broglie L., *Comptes rendus*, 1923, v. 177, 507–510; PhD Thesis, Univ. of Paris, 1924; *Phil. Mag.* 1924, v. 47, 446.
2. Zheng-Johansson J. X. and Johansson P.-I., Unification of classical, quantum and relativistic mechanics and of the four forces (Foreword by R. Lundin). Nova Science, N.Y., 2006a, 2nd printing (later 2006); *Quantum Theory and Symmetries IV*, ed. by V. K. Dobrev, Heron Press, Sofia, 2006b (one of two papers with R. Lundin); arxiv: phyiscs/0411134(v4); phyiscs/0411245; physics/0501037(v3); Inference of basic laws of classical, quantum and relativistic mechanics from first-principles classical-mechanics solutions (updated title), Nova Science, N.Y., 2006c.

The Classical Theory of Fields Revision Project (CTFRP):

Collected Papers Treating of Corrections to the Book "The Classical Theory of Fields" by L. Landau and E. Lifshitz

CALL FOR PAPERS

The "Course in Theoretical Physics" by L. Landau and E. Lifshitz has for decades served as a set of outstanding textbooks for students and reference for researchers. Many continue to learn their basic physics from this lucid and extensive exposition of physical theory and relevant mathematical methods.

The second volume of this series of texts, "The Classical Theory of Fields", is a mainstay source for physicists learning or conducting research in General Relativity*. However, it has been realised over the years that "The Classical Theory of Fields" contains a number of serious theoretical errors. The errors are in general not peculiar to this book alone, but are fundamental misconceptions that appear routinely in all textbooks on General Relativity, without exception.

Save for the errors alluded to above, "The Classical Theory of Fields" remains an authoritative and skilful exposition of Einstein's theory of gravitation. To enhance its already great standing in the scientific literature, the Editorial Board of Progress in Physics proposes a series of papers dealing with corrections of the now obsolete, although rather standard, erroneous arguments contained in "The Classical Theory of Fields". Any person interested in contributing to this project is invited to submit, for the consideration of the Editorial Board, a paper correcting one or more errors in the book. All papers will undergo review just as any research paper, and be published in Progress in Physics if accepted.

It is envisaged that accepted papers will also be collected together as a supplementary pamphlet to "The Classical Theory of Fields", which will be made available free as a download from the Progress in Physics website. Each author's contribution will bear the author's name, just like any research paper. All authors must agree to free dissemination in this fashion as a condition of contribution.

Should the pamphlet, at any future time, be considered by the Publisher's of the "Course in Theoretical Physics", or any other publisher besides Progress in Physics, as a published supplement packaged with the "Course in Theoretical Physics", all authors will be notified and can thereafter negotiate, if they wish, issues of royalties with the publisher directly. Progress in Physics will still reserve the right to provide the supplementary pamphlet free, from its website, irrespective of any other publication of the supplementary pamphlet by the publishers of the "Course in Theoretical Physics" or any other publisher. No author shall hold Progress in Physics, its Editorial Board or its Servants and Agents liable for any royalties under any circumstances, and all contributors will be required to sign a contract with Progress in Physics to that effect, so that there will be no dispute as to terms and conditions. The Editorial Board of Progress in Physics shall reserve all rights as to inclusion or rejection of contributions.

Those interested in making a contribution should express that interest in an email to the Editors of Progress in Physics who manage this project.

Dmitri Rabounski, Editor-in-Chief
Stephen J. Crothers, Associate Editor
(*the CTFRP organisers*)

*The first edition of "The Classical Theory of Fields" was completed in 1939, and originally published in Russian. Four revised editions of the book were later published in English in 1951, 1962, 1971, and 1975. (After Landau was severely injured in a car crash in 1962, Lifshitz alone expanded upon subsequent editions.) As a result the volume of the fourth edition doubled the volume of the first edition. Lifshitz, until his death in 1985, introduced numerous corrections, which are also included in the reprints. "The Classical Theory of Fields" was translated from the Russian, in all its editions, by Prof. Morton Hamermesh (University of Minnesota). Reprints of "The Classical Theory of Fields" are produced by Butterworth-Heinemann (Elsevier) almost annually.

Plausible Explanation of Quantization of Intrinsic Redshift from Hall Effect and Weyl Quantization

Florentin Smarandache* and Vic Christianto†

*Department of Mathematics, University of New Mexico, Gallup, NM 87301, USA
E-mail: smarand@unm.edu

†Sciprint.org — a Free Scientific Electronic Preprint Server, http://www.sciprint.org
E-mail: admin@sciprint.org

Using phion condensate model as described by Moffat [1], we consider a plausible explanation of (Tifft) intrinsic redshift quantization as described by Bell [6] as result of Hall effect in rotating frame. We also discuss another alternative to explain redshift quantization from the viewpoint of Weyl quantization, which could yield Bohr-Sommerfeld quantization.

1 Introduction

In a recent paper by Moffat [1] it is shown that quantum phion condensate model with Gross-Pitaevskii equation yields an approximate fit to data corresponding to CMB spectrum, and it also yields a modified Newtonian acceleration law which is in good agreement with galaxy rotation curve data. It seems therefore interesting to extend further this hypothesis to explain quantization of redshift, as shown by Tifft *et al.* [2, 6, 7]. We also argue in other paper that this redshift quantization could be explained as signature of topological quantized vortices, which also agrees with Gross-Pitaevskiian description [3, 5].

Nonetheless, there is remaining question in this quantized vortices interpretation, i. e. how to provide explanation of "intrinsic redshift" argument by Bell [6]. In the present paper, we argue that it sounds reasonable to interpret the intrinsic redshift data from the viewpoint of rotating Hall effect, i. e. rotational motion of clusters of galaxies exhibit quantum Hall effect which can be observed in the form of "intrinsic redshift". While this hypothesis is very new, it could be expected that we can draw some prediction, including possibility to observe small "blue-shift" effect generated by antivortex part of the Hall effect [5a].

Another possibility is to explain redshift quantization from the viewpoint of Weyl-Moyal quantization theory [25]. It is shown that Schrödinger equation can be derived from Weyl approach [8], therefore quantization in this sense comes from "graph"-type quantization. In large scale phenomena like galaxy redshift quantization one could then ask whether there is possibility of "super-graph" quantization.

Further observation is of course recommended in order to verify or refute the propositions outlined herein.

2 Interpreting quantized redshift from Hall effect. Cosmic String

In a recent paper, Moffat [1, p. 9] has used Gross-Pitaevskii in conjunction with his *phion condensate fluid* model to describe CMB spectrum data. Therefore we could expect that this equation will also yield interesting results in galaxies scale. See also [1b, 1c, 13] for other implications of low-energy phion fluid model.

Interestingly, it could be shown, that we could derive (approximately) Schrödinger wave equation from Gross-Pitaevskii equation. We consider the well-known Gross-Pitaevskii equation in the context of superfluidity or superconductivity [14]:

$$i\hbar\frac{\partial\Psi}{\partial t} = -\frac{\hbar^2}{2m}\Delta\Psi + \big(V(x) - \gamma\,|\Psi|^{p-1}\big)\Psi, \qquad (1)$$

where $p < 2N/(N-2)$ if $N \geqslant 3$. In physical problems, the equation for $p = 3$ is known as Gross-Pitaevskii equation. This equation (1) has standing wave solution quite similar to solution of Schrödinger equation, in the form:

$$\Psi(x,t) = e^{-iEt/\hbar}\cdot u(x) \qquad (2)$$

Substituting equation (2) into equation (1) yields:

$$-\frac{\hbar^2}{2m}\Delta u + \big(V(x) - E\big)\,u = |u|^{p-1}\,u\,, \qquad (3)$$

which is nothing but a time-independent linear form of Schrödinger equation, except for term $|u|^{p-1}$ [14]. If the right-hand side of this equation is negligible, equation (3) reduces to standard Schrödinger equation.

Now it is worth noting here that from Nottale *et al.* we can derive a gravitational equivalent of Bohr radius from generalized Schrödinger equation [4]. Therefore we could also expect a slight deviation of this gravitational Bohr radius in we consider Gross-Pitaevskii equation instead of generalized Schrödinger equation.

According to Moffat, the phion condensate model implies a modification of Newtonian acceleration law to become [1, p. 11]:

$$a(r) = -\frac{G_\infty M}{r^2} + K\,\frac{\exp\left(-\mu_\phi r\right)}{r^2}\left(1+\mu_\phi r\right), \qquad (4)$$

where

$$G_\infty = G\left[1+\sqrt{\frac{M_0}{M}}\right]. \tag{5}$$

Therefore we can conclude that the use of phion condensate model implies a modification of Newton gravitational constant, G, to become (5). Plugging in this new equation (5) into a Nottale's gravitational Bohr radius equation [4] yields:

$$r_n \approx n^2\,\frac{GM}{v_0^2}\left[1+\sqrt{\frac{M_0}{M}}\right] \approx \chi\cdot n^2\,\frac{GM}{v_0^2}\,, \tag{6}$$

where n is integer (1,2,3 ...) and:

$$\chi = \left[1+\sqrt{\frac{M_0}{M}}\right]. \tag{7}$$

Therefore we conclude that — provided the higher order Yukawa term of equation (4) could be neglected — one has a *modified* gravitational Bohr-radius in the form of (6). It can be shown (elsewhere) that using similar argument one could expect to explain a puzzling phenomenon of *receding Moon* at a constant rate of $\pm 1.5''$ per year. And from this observed fact one could get an estimate of this χ factor. It is more interesting to note here, that a number of *coral reef* data also seems to support the same idea of modification factor in equation (5), but discussion of this subject deserves another paper.

A somewhat similar idea has been put forward by Masreliez [18] using the metric:

$$ds^2 = e^{\alpha\beta}\left[dx^2+dy^2+dz^2-(icdt)^2\right]. \tag{8}$$

Another alternative of this metric has been proposed by Socoloff and Starobinski [19] using multi-connected hypersurface metric:

$$ds^2 = dx^2 + e^{-2x}\left(dy^2+dz^2\right) \tag{9}$$

with boundaries: $e^{-x}=\Lambda$.

Therefore one can conclude that the use of phion condensate model has led us to a form of expanding metric, which has been discussed by a few authors.

Furthermore, it is well-known that Gross-Pitaevskii equation could exhibit *topologically* non-trivial vortex solutions [4, 5], which also corresponds to quantized vortices:

$$\oint p\cdot dr = N_v\,2\pi\hbar\,. \tag{10}$$

Therefore an implication of Gross-Pitaevskii equation [1] is that topologically quantized vortex could exhibit in astrophysical scale. In this context we submit the viewpoint that this proposition indeed has been observed in the form of Tifft's redshift quantization [2, 6]:

$$\delta r = \frac{c}{H}\,\delta z\,. \tag{11}$$

In other words, we submit the viewpoint that Tifft's observation of quantized redshift implies a quantized distance between galaxies [2, 5], which could be expressed in the form:

$$r_n = r_0 + n(\delta r)\,, \tag{12}$$

where n is integer (1,2,3,...) similar to quantum number. Because it can be shown using standard definition of Hubble law that redshift quantization implies quantized distance between galaxies in the same cluster, then one could say that this equation of quantized distance (11) is a result of *topological* quantized vortices (9) in astrophysical scale [5]; and it agrees with Gross-Pitaevskii (quantum phion condensate) description of CMB spectrum [1]. It is perhaps more interesting if we note here, that from (11) then we also get an equivalent expression of (12):

$$\frac{c}{H}\,z_n = \frac{c}{H}\,z_0 + n\left(\frac{c}{H}\,\delta z\right) \tag{13}$$

or

$$z_n = z_0 + n(\delta z) \tag{14}$$

or

$$z_n = z_0\left[1+n\left(\frac{\delta z}{z_0}\right)\right]. \tag{15}$$

Nonetheless, there is a problem here, i. e. how to explain intrinsic redshift related to Tifft quantization as observed in Fundamental Plane clusters and also from various quasars data [6, 6a]:

$$z_{iQ} = z_f\left[N-0.1M_N\right] \tag{16}$$

where $z_f = 0.62$ is assumed to be a fundamental redshift constant, and $N(=1,2,3\ldots)$, and M is function of N [6a]. Meanwhile, it is interesting to note here similarity between equation (15) and (16). Here, the number M seems to play a rôle similar to second quantum number in quantum physics [7].

Now we will put forward an argument that intrinsic redshift quantization (16) could come from rotating quantum Hall effect [5a].

It is argued by Fischer [5a] that "Hall quantization is of necessity derivable from a *topological quantum number* related to this (quantum) coherence". He used total particle momentum [5a]:

$$p = mv + m\Omega\times r + qA\,. \tag{17}$$

The uniqueness condition of the collective phase represented in (9) then leads, if we take a path in the bulk of electron liquid, for which the integral of mv can be neglected, to the quantization of the sum of a *Sagnac flux*, and the magnetic flux [5a]:

$$\Phi = q\oint A\cdot dr + m\oint \Omega\times r\cdot dr = \\ = \iint B\cdot dS = N_v\,2\pi\hbar\,. \tag{18}$$

This flux quantization rule corresponds to the fact that a *vortex* is fundamentally characterised by the winding number N alone [5a]. In this regard the vortex could take the form of cosmic string [22]. Now it is clear from (15) that quantized vortices could be formed by different source of flux.

After a few more reasonable assumptions one could obtain a generalised Faraday law, which in rotating frame will give in a non-dissipative Hall state the quantization of Hall conductivity [5a].

Therefore one could observe that it is quite natural to interpret the quantized distance between galaxies (11) as an implication of quantum Hall effect in rotating frame (15). While this proposition requires further observation, one could think of it in particular using known analogy between condensed matter physics and cosmology phenomena [10, 22]. If this proposition corresponds to the facts, then one could think that redshift quantization is an imprint of generalized quantization in various scales from microphysics to macrophysics, just as Tifft once put it [2]:

> "The redshift has imprinted on it a pattern that appears to have its origin in microscopic quantum physics, yet it carries this imprint across cosmological boundaries".

In the present paper, Tifft's remark represents natural implication of topological quantization, which could be formed at any scale [5]. We will explore further this proposition in the subsequent section, using Weyl quantization.

Furthermore, while this hypothesis is new, it could be expected that we can draw some new prediction, for instance, like possibility to observe small "blue-shift" effect generated by the Hall effect from antivortex-galaxies [23]. Of course, in order to observe such a "blue-shift" one shall first exclude other anomalous effects of redshift phenomena [6]. (For instance: one could argue that perhaps Pioneer spacecraft anomaly's blue-shifting of Doppler frequency may originate from the same effect as described herein.)

One could expect that further observation in particular in the area of low-energy neutrino will shed some light on this issue [20]. In this regard, one could view that the Sun is merely a remnant of a neutron star in the past, therefore it could be expected that it also emits neutrino similar to neutron star [21].

3 An alternative interpretation of astrophysical quantization from Weyl quantization. Graph and quantization

An alternative way to interpret the above proposition concerning topological quantum number and topological quantization [5a], is by using Weyl quantization.

In this regards, Castro [8, p. 5] has shown recently that one could derive Schrödinger equation from Weyl geometry using continuity equation:

$$\frac{\partial \rho}{\partial t} + \frac{1}{\sqrt{g}}\,\partial_i\left(\sqrt{g}\rho v^i\right) \qquad (19)$$

and Weyl metric:

$$R_{\text{Weyl}} = (d-1)(d-2)\left(A_k A^k\right) - 2(d-1)\,\partial_k A^k\,. \qquad (20)$$

Therefore one could expect to explain astrophysical quantization using Weyl method in lieu of using generalised Schrödinger equation as Nottale did [4]. To our knowledge this possibility has never been explored before elsewhere.

For instance, it can be shown that one can obtain Bohr-Sommerfeld type quantization rule from Weyl approach [24, p. 12], which for kinetic plus potential energy will take the form:

$$2\pi N\hbar = \sum_{j=0}^{\infty} \hbar^j S_j(E)\,, \qquad (21)$$

which can be solved by expressing $E = \sum \hbar^k E_k$ as power series in $\hbar$ [24]. Now equation (10) could be rewritten as follows:

$$\oint p \cdot dr = N_v\, 2\pi\hbar = \sum_{j=0}^{\infty} \hbar^j S_j(E)\,. \qquad (22)$$

Or if we consider quantum Hall effect, then equation (18) can be used instead of equation (10), which yields:

$$\begin{aligned}\Phi = q\oint A\cdot dr + m\oint \Omega\times r\cdot dr \;=\\ = \iint B\cdot dS = \sum_{j=0}^{\infty}\hbar^j S_j(E)\,.\end{aligned} \qquad (23)$$

The above method is known as "graph kinematic" [25] or Weyl-Moyal's quantization [26]. We could also expect to find Hall effect quantization from this deformation quantization method.

Consider a harmonic oscillator, which equation can be expressed in the form of deformation quantization instead of Schrödinger equation [26]:

$$\left(\left(x + \frac{i\hbar}{2}\partial_p\right)^2 + \left(p - \frac{i\hbar}{2}\partial_x\right)^2 - 2E\right) f(x,p) = 0\,. \qquad (24)$$

This equation could be separated to become two simple PDEs. For imaginary part one gets [26]:

$$\left(x\,\partial_p - p\,\partial_x\right) f = 0\,. \qquad (25)$$

Now, considering Hall effect, one can introduce our definition of total particle momentum (17), therefore equation (25) may be written:

$$\left(x\,\partial_p - (mv + m\Omega\times r + qA)\,\partial_x\right) f = 0\,. \qquad (26)$$

Our proposition here is that in the context of deformation quantization it is possible to find quantization solution of harmonic oscillator without Schrödinger equation. And

because it corresponds to graph kinematic [25], generalized Bohr-Sommerfeld quantization rule for quantized vortices (22) in astrophysical scale could be viewed as signature of "*super-graph*"*quantization*.

This proposition, however, deserves further theoretical considerations. Further experiments are also recommended in order to verify and explore further this proposition.

Concluding remarks

In a recent paper, Moffat [1] has used Gross-Pitaevskii in his "phion condensate fluid" to describe CMB spectrum data. We extend this proposition to explain Tifft redshift quantization from the viewpoint of topological quantized vortices. In effect we consider that the intrinsic redshift quantization could be interpreted as result of Hall effect in rotating frame.

Another alternative to explain redshift quantization is to consider quantized vortices from the viewpoint of Weyl quantization (which could yield Bohr-Sommerfeld quantization).

It is recommended to conduct further observation in order to verify and also to explore various implications of our propositions as described herein.

Acknowledgment

The writers would like to thank to Profs. C. Castro, T. Love, E. Scholz, D. Rabounski, and A. Kaivarainen for valuable discussions.

References

1. Moffat J. arXiv: astro-ph/0602607; [1a] Consoli M. arXiv: hep-ph/0109215; [1b] Consoli M. *et al.* arXiv: physics/0306094.
2. Russell Humphreys D. Our galaxy is the centre of the universe, "quantized" red shifts show. *TJ Archive*, 2002, v. 16(2), 95–104; http://answersingenesis.org/tj/v16/i2/galaxy.asp.
3. Smarandache F. and Christianto V. A note on geometric and information fusion interpretation of Bell theorem and quantum measurement. *Progress in Physics*, 2006, v. 4, 27–31.
4. Smarandache F. and Christianto V. Schrödinger equation and the quantization of celestial systems. *Progress in Physics*, 2006, v. 2, 63–67.
5. Fischer U. arXiv: cond-mat/9907457; [5a] arXiv: cond-mat/0004339.
6. Bell M. B. arXiv: astro-ph/0111123; [6a] arXiv: astro-ph/0305112; [6b] arXiv: astro-ph/0305060.
7. Setterfield B. http://www.journaloftheoretics.com; http://www.setterfield.org.
8. Castro C. and Mahecha J. On nonlinear Quantum Mechanics, Brownian motion, Weyl geometry, and Fisher information. *Progress in Physics*, 2006, v. 1, 38–45.
9. Schrieffer J. R. Macroscopic quantum phenomena from pairing in superconductors. Lecture, December 11, 1972.
10. Zurek W. H. Cosmological experiments in superfluids and superconductors. In: *Proc. Euroconference in Formation and Interaction of Topological Defects*, Plenum Press, 1995; arXiv: cond-mat/9502119.
11. Anandan J. S. In: *Quantum Coherence and Reality, Proc. Conf. Fundamental Aspects of Quantum Theory*, Columbia SC., edited by J. S. Anandan and J. L. Safko, World Scientific, 1994; arXiv: gr-qc/9504002.
12. Rauscher E. A. and Amoroso R. The physical implications of multidimensional geometries and measurement. *Intern. J. of Comp. Anticipatory Systems*, 2006.
13. Chiao R. *et al.* arXiv: physics/0309065.
14. Dinu T. L. arXiv: math.AP/0511184.
15. Kravchenko V. arXiv: math.AP/0408172.
16. Lipavsky P. *et al.* arxiv: cond-mat/0111214.
17. De Haas E. P. *Proc. of the Intern. Conf. PIRT-2005*, Moscow, MGTU Publ., 2005.
18. Masreliez J. *Apeiron*, 2005, v. 12.
19. Marc L.-R. and Luminet J.-P. arXiv: hep-th/9605010.
20. Lanou R. arXiv: hep-ex/9808033.
21. Yakovlev D. *et al.* arXiv: astro-ph/0012122.
22. Volovik G. arXiv: cond-mat/0507454.
23. Balents L. *et al.* arXiv: cond-mat/9903294.
24. Gracia-Saz A. *Ann. Inst. Fourier*, Grenoble, 2005, v. 55(5), 1001–1008.
25. Asribekov V. L. arXiv: physics/0110026.
26. Zachos C. arXiv: hep-th/0110114.

Geometrical Dynamics in a Transitioning Superconducting Sphere

James R. Claycomb* and Rambis K. Chu†

*Department of Mathematics and Physics, Houston Baptist University, Houston, TX 77074-3298, USA
E-mail: jclaycomb@hbu.edu

†Bio-Nano Computational Laboratory RCMI-NCRR and Physics Department,
Texas Southern University, Houston, TX 77004, USA
E-mail: chu_rk@tsu.edu

Recent theoretical works have concentrated on calculating the Casimir effect in curved spacetime. In this paper we outline the forward problem of metrical variation due to the Casimir effect for spherical geometries. We consider a scalar quantum field inside a hollow superconducting sphere. Metric equations are developed describing the evolution of the scalar curvature after the sphere transitions to the normal state.

1 Introduction

The classical Casimir effect [1, 2] may be viewed as vacuum reduction by mode truncation where the presence of conducting boundaries, or capacitor plates, excludes vacuum modes with wavelengths longer than the separation between the conductors. The exclusion of longer wavelengths results in a lower vacuum pressure between the plates than in external regions. The resulting pressure difference, or Casimir force, may act to push the conductors together, effectively collapsing the reduced vacuum phase. This tiny force has been measured experimentally [3, 4] in agreement with the predictions of quantum electrodynamics. Boyer gives the first detailed treatment of the vacuum modes inside a conducting sphere [5] with more a recent account by Milton [6]. The Casimir effect for spherical conducting shells in external electromagnetic fields has been investigated [7, 8]. Applications of the Casimir effect to the bag model have been studied for massive scalar [9] and Dirac [10] fields confined to the interior of the shell. An example of the Casimir effect in curved spacetime has been considered for spherical geometries [11] in de Sitter space [12] and in the background of static domain wall [13]. In this paper we investigate the metrical variations resulting from vacuum pressure differences established by a spherical superconducting boundary. We first consider the static case when the sphere is superconducting and then the dynamical case as the sphere passes to the normal state.

2 The static case

Our idealized massless, thin sphere of radius R_0 has zero conductivity in the normal state. In the superconducting state, the vacuum inside the hollow is reduced so that there exists a pressure difference Δp inside and outside the sphere. In general, all quantum fields will contribute to the vacuum energy. When the sphere of volume V transitions to the superconducting state, a latent heat of vacuum phase transition ΔpV is exchanged. The distribution of vacuum pressure, energy density and space-time geometry are described by the semi-classical Einstein field equations taking $c=1$,

$$R_{\mu\nu} - \frac{1}{2} R\, g_{\mu\nu} = 8\pi G \left\langle T_{\mu\nu} \right\rangle , \tag{1}$$

where $R_{\mu\nu}$ and R are the Ricci tensor and scalar curvature, respectively. $\langle T_{\mu\nu} \rangle$ is the vacuum expectation of the stress energy tensor. Regulation procedures for calculating the renormalized stress energy tensor are given in [14] for various geometries. The most general line element with spherical symmetry is

$$ds^2 = B(r,t)\, dt^2 - A(r,t)\, dr^2 - C(r,t)\, dr dt - \\ - r^2 d\theta^2 - r^2 \sin^2\theta\, d\phi^2 , \tag{2}$$

where A, B, and C are arbitrary functions of time and the radial coordinate. (2) can be written under normal coordinate transformation [15],

$$ds^2 = \tilde{B}(r,t)\, dt^2 - \tilde{A}(r,t)\, dr^2 - r^2 d\theta^2 - r^2 \sin^2\theta\, d\phi^2 . \tag{3}$$

The metric tensor then becomes, dropping tildes,

$$g_{\mu\nu} = \mathrm{Diag}\left(B(r,t) , -A(r,t) , -r^2 , -r^2 \sin^2\theta \right) . \tag{4}$$

For a diagonal stress energy tensor, the solutions to equation (3) relating A and B are

$$-\frac{1}{r^2} + \frac{1}{r^2 A} - \frac{A'}{rA^2} = 8\pi G \frac{1}{B} \left\langle T_{00} \right\rangle , \tag{5}$$

$$\frac{1}{r^2} - \frac{1}{r^2 A} - \frac{B'}{rAB} = 8\pi G \frac{1}{A} \left\langle T_{11} \right\rangle , \tag{6}$$

$$\frac{A'}{2rA^2} - \frac{B'}{2rAB} + \frac{A'B'}{4A^2 B} - \frac{B'^2}{4AB^2} - \\ - \frac{B''}{2AB} = 8\pi G \frac{1}{r^2} \left\langle T_{22} \right\rangle , \tag{7}$$

with a fourth equation identical to (7). The prime denotes ∂_r.

Note that all time derivatives cancel from the field equations when the metric is in standard form and the stress energy tensor is diagonal. When the sphere is in the superconducting state, the scalar curvature $R = g^{\mu\nu} R_{\mu\nu}$ is given by

$$R = \frac{2}{r^2} - \frac{2}{r^2 A} + \frac{2A'}{rA^2} - \frac{2B'}{rAB} + \\ + \frac{A'B'}{2A^2 B} + \frac{B'^2}{2AB^2} - \frac{B''}{AB}\,. \tag{8}$$

In calculating the Casimir force, one properly calculates differences in vacuum pressure established by the conducting boundaries [2]. In the present case, it is only meaningful to consider changes in scalar curvature due to variations in vacuum pressure.

3 The dynamical case

If the sphere passes from the superconducting to the normal state, the pressure should equalize as the vacuum relaxes. The diagonal form of the stress energy tensor results in the cancellation of all time derivatives in the field equations. External electromagnetic fields will contribute off-diagonal terms, however we wish to consider how the pressure equalizes in absence of external fields. The key is that the required time dependence is provided by the zero point field fluctuations. As the simplest example, we consider the massless scalar quantum field with stress energy tensor [14]

$$T_{\mu\nu} = \phi_{,\mu}\,\phi_{,\nu} - \frac{1}{2}\, g_{\mu\nu}\, g^{\alpha\beta}\, \phi_{,\alpha}\,\phi_{,\beta}\,. \tag{9}$$

The non-zero components of $T_{\mu\nu}$ are

$$T_{00} = \frac{1}{2}\,\dot{\phi}^2 + \frac{B}{2A}\,\phi'^2, \tag{10}$$

$$T_{11} = \frac{1}{2}\,\phi'^2 + \frac{A}{2B}\,\dot{\phi}^2, \tag{11}$$

$$T_{22} = r^2 \left(\frac{1}{2B}\,\dot{\phi}^2 + \frac{1}{2A}\,\phi'^2 \right), \tag{12}$$

$$T_{33} = r^2 \sin^2\theta \left(\frac{1}{2B}\,\dot{\phi}^2 + \frac{1}{2A}\,\phi'^2 \right), \tag{13}$$

$$T_{01} = \dot{\phi}\,\phi', \tag{14}$$

where $T_{01} = T_{10}$. The semi-classical field equations become

$$-\frac{1}{r^2} + \frac{1}{r^2 A} - \frac{A'}{rA^2} = 8\pi G\,\frac{1}{B}\,\langle T_{00}\rangle\,, \tag{15}$$

$$\frac{1}{r^2} - \frac{1}{r^2 A} - \frac{B'}{rAB} = 8\pi G\,\frac{1}{A}\,\langle T_{11}\rangle\,, \tag{16}$$

$$-\frac{\dot{A}^2}{4A^2 B} - \frac{\dot{A}\dot{B}}{4AB^2} + \frac{\ddot{A}}{2AB} + \frac{A'}{2r^2 A} - \frac{B'}{2rAB} + \\ + \frac{A'B'}{4A^2 B} + \frac{B'^2}{4AB^2} - \frac{B''}{2AB} = 8\pi G\,\frac{1}{r^2}\,\langle T_{22}\rangle\,, \tag{17}$$

$$-\frac{\dot{A}}{rA} = 8\pi G\,\langle T_{01}\rangle\,. \tag{18}$$

Equations (15) and (16) are identical to (5) and (6). Two additional equations are identical to (17) and (18). Expressions for A and B may be obtained from equation (18) and (15) or (16), respectively. The scalar curvature is given by

$$R = \frac{2}{r^2} - \frac{2}{r^2 A} - \frac{\dot{A}^2}{2A^2 B} - \frac{\dot{A}\dot{B}}{AB} + \\ + \frac{\ddot{A}}{AB} + \frac{2A'}{rA^2} - \frac{2B'}{rAB} + \frac{A'B'}{2A^2 B} + \frac{B'^2}{2AB^2} - \frac{B''}{AB}\,. \tag{19}$$

Combining equation (19) with (15–17) and (10–12) reveals

$$R = 16\pi G \left\langle \frac{\dot{\phi}^2}{2B} - \frac{\phi'^2}{2A} \right\rangle. \tag{20}$$

When evaluating changes in scalar curvature, the expression for R in absence of the sphere should be subtracted from that obtained for a given quantum field.

4 Conclusion

When a hollow sphere transitions between the normal and superconducting state a latent heat of vacuum phase transition is exchanged. In the dynamical case, zero-point field fluctuations result in off-diagonal components of the stress energy tensor that give rise to time dependent field equations. The analysis presented here may be extended to include massive fields with coupling or spin (0, $\frac{1}{2}$ and 1) as well as other superconducting geometries.

Acknowledgments

This work was supported, in part, by RCMI through NCRR-NIH (Grant No. G12-RR-03045), Texas Southern University Research Seed Grant 2004/2005, and the State of Texas through the Texas Center for Superconductivity at University of Houston.

References

1. Casimir H. B. G. On the attraction between two perfectly conducting plates. *Proc. K. Ned. Akad. Wet.*, 1948, v. 51, 793.
2. Milonni P. W. The quantum vacuum: An introduction to Quantum Electrodynamics. Academic Press, London, 1994.
3. Lamoreaux S. K. Demonstration of the Casimir force in the 0.6 to 6 μm range. *Phys. Rev. Lett.*, 1997, v. 78, 5–8.
4. Mohideen U., Roy A. Precision measurement of the Casimir force from 0.1 to 0.9 μm. *Phys. Rev. Lett.*, 1998, v. 81, 4549–4552.
5. Boyer T. H. Quantum electromagnetic zero-point energy of a conducting spherical shell and the Casimir model for a charged particle. *Phys. Rev.*, 1968, v. 25, 1764–1776.

6. Milton K. A. Vector Casimir effect for a D-dimensional sphere. *Phys. Rev. D*, 1997, v. 55, 4940–4946.
7. Milton K. A., DeRaad L. L., Schwinger J. *Ann. Phys.*, 1978, v. 115, 338.
8. Nesterenko V. V., Pirozhenko I. G. Simple method for calculating the Casimir energy for a sphere. *Phys. Rev. D*, 1998, v. 57, 1284–1290.
9. Bordag M., Elizalde E., Kirsten K., Leseduarte S. Casimir energies for massive scalar fields in a spherical geometry. *Phys. Rev. D*, 1997, v. 56, 4896–4904.
10. Elizalde E., Bordag M., Kirsten K. Casimir energy for a massive fermionic quantum field with a spherical boundary. *J. Phys. A*, 1998, v. 31, 1743–1759.
11. Bayin S., Ozcan M. Casimir energy in a curved background with a spherical boundary: An exactly solvable case. *Phys. Rev. D*, 1993, v. 48, 2806–2812.
12. Setare M. R., Saharian A. A. Casimir effect for a spherical shell in de Sitter space. *Class. Quantum Grav.*, 2001, v. 18, 2331–2338.
13. Setare M. R., Saharian A. A. Casimir effect in background of static domain wall. *Int. J. Mod. Phys. A*, 2001, v. 16, 1463–1470.
14. Birrell N. D., Davies P. C. W. Quantum fields in curved space. Cambridge University Press, Cambridge, 1994.
15. Weinberg S. Gravitation and Cosmology Wiley, New York, 1972.

Black Holes and Quantum Theory: The Fine Structure Constant Connection

Reginald T. Cahill

School of Chemistry, Physics and Earth Sciences, Flinders University, Adelaide 5001, Australia

E-mail: Reg.Cahill@flinders.edu.au

The new dynamical theory of space is further confirmed by showing that the effective "black hole" masses M_{BH} in 19 spherical star systems, from globular clusters to galaxies, with masses M, satisfy the prediction that $M_{BH} = \frac{\alpha}{2}M$, where α is the fine structure constant. As well the necessary and unique generalisations of the Schrödinger and Dirac equations permit the first derivation of gravity from a deeper theory, showing that gravity is a quantum effect of quantum matter interacting with the dynamical space. As well the necessary generalisation of Maxwell's equations displays the observed light bending effects. Finally it is shown from the generalised Dirac equation where the spacetime mathematical formalism, and the accompanying geodesic prescription for matter trajectories, comes from. The new theory of space is non-local and we see many parallels between this and quantum theory, in addition to the fine structure constant manifesting in both, so supporting the argument that space is a quantum foam system, as implied by the deeper information-theoretic theory known as Process Physics. The spatial dynamics also provides an explanation for the "dark matter" effect and as well the non-locality of the dynamics provides a mechanism for generating the uniformity of the universe, so explaining the cosmological horizon problem.

1 Introduction

Physics has had two distinct approaches to space. Newton asserted that space existed, but was non-dynamical and unobservable. Einstein, in contrast, asserted that space was merely an illusion, a perspective effect in that it is four-dimensional spacetime which is real and dynamical, and that the foliation into space and a geometrical model of time was observer dependent; there was no observer independent space. Hence also according to Einstein space was necessarily unobservable. However both approaches have been challenged by the recent discovery that space had been detected again and again over more than 100 years [1–11], and that the dynamics of space is now established*. The key discovery [2] in 2002 was that the speed of light is anisotropic — that it is c only with respect to space itself, and that the solar system has a large speed of some 400 km/s relative to that space, which causes the observed anisotropy. This discovery changes all of physics†. The problem had been that from the very beginning the various gas-mode Michelson interferometer experiments to detect this anisotropy had been incorrectly calibrated‡, and that the small fringe shifts actually seen corresponded to this high speed. As well it has been incorrectly assumed that the success of the Special Relativity formalism requires that the speed of light be isotropic, that an actual 3-space be unobservable. Now that space is known to exist it must presumably also have a dynamics, and this dynamics has been discovered and tested by explaining various phenomena such as (i) gravity, (ii) the "dark matter" effect, (iii) the bore hole g anomalies, (iv) novel black holes, (v) light bending and gravitational lensing in general, and so on. Because space has been overlooked in physics as a dynamical aspect of reality all of the fundamental equations of physics, such as Maxwell's equations, the Schrödinger equation, the Dirac equation and so on, all lacked the notion that the phenomena described by these equations were excitations, of various kinds, of the dynamical space itself. The generalisation of the Schrödinger equation [12] then gave the first derivation and explanation for gravity: it is a quantum effect in which the wave functions are refracted by the inhomogeneities and time variations of the structured space. However the most striking discovery is that the internal dynamics of space is determined by the fine structure constant [13–16]. In this paper we report further observational evidence for this discovery by using a more extensive collection of "black hole" masses in spherical galaxies and globular clusters§. As well we give a more insightful explanation for the dynamics of space. We also show how this quantum-theoretic explanation for gravity leads to a derivation of the spacetime construct where, we emphasise, this is purely a mathematical construct and not an aspect of reality. This is important as it explains why the spacetime dynamics appeared to be successful, at

*At least in the limit of zero vorticity.

†Special Relativity does not require that the speed of light be isotropic, as is usually incorrectly assumed.

‡Special relativity effects and the presence of gas in the light paths both play critical roles in determining the calibration. In vacuum mode the interferometer is completely insensitive to absolute motion effects, i. e. to the anisotropy of light.

§The generic term "black hole" is used here to refer to the presence of a compact closed event horizon enclosing a spatial in-flow singularity.

least in those cases where the "dark matter" effect was not apparent. However in general the metric tensor of this induced spacetime does not satisfy the General Relativity (GR) equations.

2 Dynamics of space

At a deeper level an information-theoretic approach to modelling reality (Process Physics [1]) leads to an emergent structured "space" which is 3-dimensional and dynamic, but where the 3-dimensionality is only approximate, in that if we ignore non-trivial topological aspects of space, then it may be embedded in a 3-dimensional geometrical manifold. Here the space is a real existent discrete but fractal network of relationships or connectivities, but the embedding space is purely a mathematical way of characterising the 3-dimensionality of the network. This is illustrated in Fig. 1. This is not an ether model; that notion involved a duality in that both the ether and the space in which it was embedded were both real. Now the key point is that how we embed the network in the embedding space is very arbitrary: we could equally well rotate the embedding or use an embedding that has the network translating. These general requirements then dictate the minimal dynamics for the actual network, at a phenomenological level. To see this we assume at a coarse grained level that the dynamical patterns within the network may be described by a velocity field $\mathbf{v}(\mathbf{r},t)$, where $\mathbf{r}$ is the location of a small region in the network according to some arbitrary embedding. For simplicity we assume here that the global topology of the network is not significant for the local dynamics, and so we embed in an E^3, although a generalisation to an embedding in S^3 is straightforward. The minimal dynamics then follows from the above by writing down the lowest order zero-rank tensors, with dimension $1/t^2$, that are invariant under translation and rotation, giving*

$$\nabla\cdot\left(\frac{\partial\mathbf{v}}{\partial t}+(\mathbf{v}\cdot\nabla)\,\mathbf{v}\right)+ +\frac{\alpha}{8}\,(\mathrm{tr}\,D)^2+\frac{\beta}{8}\,\mathrm{tr}\,(D^2)=-4\pi G\rho\,, \tag{1}$$

where ρ is the effective matter density, and where

$$D_{ij}=\frac{1}{2}\left(\frac{\partial v_i}{\partial x_j}+\frac{\partial v_j}{\partial x_i}\right). \tag{2}$$

In Process Physics quantum matter are topological defects in the network, but here it is sufficient to give a simple description in terms of an effective density, but which can also model the "dark energy" effect and electromagnetic energy effects, which will be discussed elsewhere. We see

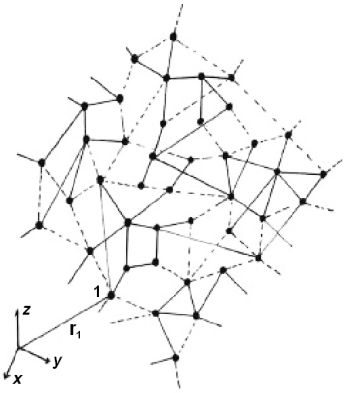

Fig. 1: This is an iconic graphical representation of how a dynamical network has its inherent approximate 3-dimensionality displayed by an embedding in a mathematical space such as an E^3 or an S^3. This space is not real; it is purely a mathematical artifact. Nevertheless this embeddability helps determine the minimal dynamics for the network, as in (1). At a deeper level the network is a quantum foam system [1]. The dynamical space is not an ether model, as the embedding space does not exist.

that there are only four possible terms, and so we need at most three possible constants to describe the dynamics of space: G, α and β. G will turn out to be Newton's gravitational constant, and describes the rate of non-conservative flow of space into matter. To determine the values of α and β we must, at this stage, turn to experimental data.

However most experimental data involving the dynamics of space is observed by detecting the so-called gravitational acceleration of matter, although increasingly light bending is giving new information. Now the acceleration $\mathbf{a}$ of the dynamical patterns in space is given by the Euler or convective expression

$$\mathbf{a}(\mathbf{r},t)\equiv\lim_{\Delta t\to 0}\frac{\mathbf{v}(\mathbf{r}+\mathbf{v}(\mathbf{r},t)\,\Delta t,t+\Delta t)-\mathbf{v}(\mathbf{r},t)}{\Delta t}= =\frac{\partial\mathbf{v}}{\partial t}+(\mathbf{v}\cdot\nabla)\mathbf{v} \tag{3}$$

and this appears in one of the terms in (1). As shown in [12] and discussed later herein the acceleration $\mathbf{g}$ of quantum matter is identical to this acceleration, apart from vorticity and relativistic effects, and so the gravitational acceleration of matter is also given by (3).

Outside of a spherically symmetric distribution of matter, of total mass M, we find that one solution of (1) is the velocity in-flow field given by†

$$\mathbf{v}(\mathbf{r})=-\hat{\mathbf{r}}\sqrt{\frac{2GM(1+\frac{\alpha}{2}+\dots)}{r}} \tag{4}$$

but only when $\beta=-\alpha$, for only then is the acceleration of matter, from (3), induced by this in-flow of the form

$$\mathbf{g}(\mathbf{r})=-\hat{\mathbf{r}}\,\frac{GM(1+\frac{\alpha}{2}+\dots)}{r^2} \tag{5}$$

which is Newton's Inverse Square Law of 1687, but with an effective mass that is different from the actual mass M.

*Note that then, on dimensional grounds, the spatial dynamics cannot involve the speed of light c, except on the RHS where relativistic effects come into play if the speed of matter relative to the local space becomes large, see [1]. This has significant implications for the nature and speed of so-called "gravitational" waves.

†To see that the flow is inward requires the modelling of the matter by essentially point-like particles.

So Newton's law requires $\beta = -\alpha$ in (1) although at present a deeper explanation has not been found. But we also see modifications coming from the α-dependent terms.

A major recent discovery [13–16] has been that experimental data from the bore hole g anomaly has revealed that α is the fine structure constant, to within experimental errors: $\alpha = e^2/\hbar c \approx 1/137.04$. This anomaly is that g does not decrease as rapidly as predicted by Newtonian gravity or GR as we descend down a bore hole. The dynamics in (1) and (3) gives the anomaly to be

$$\Delta g = 2\pi\alpha G\rho d \tag{6}$$

where d is the depth and ρ is the density, being that of glacial ice in the case of the Greenland Ice Shelf experiments, or that of rock in the Nevada test site experiment. Clearly (6) permits the value of α to be determined from the data, giving $\alpha = 1/(137.9 \pm 5)$ from the Greenland Ice Shelf data and, independently, $\alpha = 1/(136.8 \pm 3)$ from the Nevada test site data [16].

In general because (1) is a scalar equation it is only applicable for vorticity-free flows $\nabla \times \mathbf{v} = \mathbf{0}$, for then we can write $\mathbf{v} = \nabla u$, and then (1) can always be solved to determine the time evolution of $u(\mathbf{r}, t)$ given an initial form at some time t_0.*

The α-dependent term in (1) (with now $\beta = -\alpha$) and the matter acceleration effect, now also given by (3), permits (1) to be written in the form

$$\nabla \cdot \mathbf{g} = -4\pi G\rho - 4\pi G\rho_{DM}, \tag{7}$$

where

$$\rho_{DM}(\mathbf{r}, t) \equiv \frac{\alpha}{32\pi G}\left((\mathrm{tr}\, D)^2 - \mathrm{tr}\,(D^2)\right), \tag{8}$$

where ρ_{DM} is an effective matter density that would be required to mimic the α-dependent spatial self-interaction dynamics. Then (7) is the differential form for Newton's law of gravity but with an additional non-matter effective matter density. It has been shown [13–16] that this effect explains the so-called "dark matter" effect in spiral galaxies. As shown elsewhere it also explains, when used with the generalised Maxwell's equations, the gravitational lensing of light by this "dark matter" effect.

An intriguing aspect to the spatial dynamics is that it is non-local. Historically this was first noticed by Newton who called it action-at-a-distance. To see this we can write (1) as an integro-differential equation

$$\frac{\partial \mathbf{v}}{\partial t} = -\nabla\left(\frac{\mathbf{v}^2}{2}\right) + \\ + G\int d^3 r' \, \frac{\rho_{DM}(\mathbf{r}', t) + \rho(\mathbf{r}', t)}{|\mathbf{r} - \mathbf{r}'|^3}(\mathbf{r} - \mathbf{r}'). \tag{9}$$

This shows a high degree of non-locality and non-linearity, and in particular that the behaviour of both ρ_{DM} and ρ manifest at a distance irrespective of the dynamics of the intervening space. This non-local behaviour is analogous to that in quantum systems. The non-local dynamics associated with the α dynamics has been tested in various situations, as discussed herein, and so its validity is well established. This implies that the minimal spatial dynamics in (1) involves non-local connectivities.

We term the dynamics of space in (1) as a "flowing space". This term can cause confusion because in normal language a "flow" implies movement of something relative to a background space; but here there is no existent background space, only the non-existent mathematical embedding space. So here the "flow" refers to internal relative motion, that one parcel of space has a motion relative to a nearby parcel of space. Hence the absolute velocities in (1) have no observable meaning; that despite appearances it is only the relative velocities that have any dynamical significance. Of course it is this requirement that determined the form of (1), and as implemented via the embedding space technique.

However there is an additional role for the embedding space, namely as a coordinate system used by a set of cooperating observers. But again while this is useful for their discourse it is not real; it is not part of reality.

3 Black holes

Eqn. (1) has "black hole" solutions. The generic term "black hole" is used because they have a compact closed event horizon where the in-flow speed relative to the horizon equals the speed of light, but in other respects they differ from the putative black holes of General Relativity† — in particular their gravitational acceleration is not inverse square law. The evidence is that it is these new "black holes" from (1) that have been detected. There are two categories: (i) an in-flow singularity induced by the flow into a matter system, such as, herein, a spherical galaxy or globular cluster. These black holes are termed minimal black holes, as their effective mass is minimal, (ii) primordial naked black holes which then attract matter. These result in spiral galaxies, and the effective mass of the black hole is larger than required merely by the matter induced in-flow. These are therefore termed non-minimal black holes. These explain the rapid formation of structure in the early universe, as the gravitational acceleration is approximately $1/r$ rather than $1/r^2$. This is the feature that also explains the so-called "dark matter" effect in spiral galaxies. Here we consider only the minimal black holes.

Consider the case where we have a spherically symmetric matter distribution at rest, on average with respect to distant space, and that the in-flow is time-independent and radially symmetric. Then (1) is best analysed via (9), which can now

*Eqn.(1) also has Hubble expanding space solutions.

†It is probably the case that GR has no such solutions — they do not obey the boundary conditions at the singularity, see Crothers [17].

Galaxy	Type	$M_{BH}(+,-)$	M	Ref
M87	E0	$3.4\,(1.0,1.0)\times10^{9}$	$6.2\pm1.7\times10^{11}$	1
NGC4649	E1	$2.0\,(0.4,0.6)\times10^{9}$	$8.4\pm2.2\times10^{11}$	2
M84	E1	$1.0\,(2.0,0.6)\times10^{9}$	$5.0\pm1.4\times10^{11}$	3
M32	E2	$2.5\,(0.5,0.5)\times10^{6}$	$9.6\pm2.6\times10^{8}$	4
NGC4697	E4	$1.7\,(0.2,0.1)\times10^{8}$	$2.0\pm0.5\times10^{11}$	2
IC1459	E3	$1.5\,(1.0,1.0)\times10^{9}$	$6.6\pm1.8\times10^{11}$	5
NGC3608	E2	$1.9\,(1.0,0.6)\times10^{8}$	$9.9\pm2.7\times10^{10}$	2
NGC4291	E2	$3.1\,(0.8,2.3)\times10^{8}$	$9.5\pm2.5\times10^{10}$	2
NGC3377	E5	$1.0\,(0.9,0.1)\times10^{8}$	$7.8\pm2.1\times10^{10}$	2
NGC4473	E5	$1.1\,(0.4,0.8)\times10^{8}$	$6.9\pm1.9\times10^{10}$	2
Cygnus A	E	$2.9\,(0.7,0.7)\times10^{9}$	$1.6\pm1.1\times10^{12}$	6
NGC4261	E2	$5.2\,(1.0,1.1)\times10^{8}$	$4.5\pm1.2\times10^{11}$	7
NGC4564	E3	$5.6\,(0.3,0.8)\times10^{7}$	$5.4\pm1.5\times10^{10}$	2
NGC4742	E4	$1.4\,(0.4,0.5)\times10^{7}$	$1.1\pm0.3\times10^{10}$	8
NGC3379	E1	$1.0\,(0.6,0.5)\times10^{8}$	$8.5\pm2.3\times10^{10}$	9
NGC5845	E3	$2.4\,(0.4,1.4)\times10^{8}$	$1.9\pm0.5\times10^{10}$	2
NGC6251	E2	$6.1\,(2.0,2.1)\times10^{8}$	$6.7\pm1.8\times10^{11}$	10
Globular cluster		$M_{BH}(+,-)$	M	Ref
M15		$1.7\,(2.7,1.7)\times10^{3}$	4.9×10^{5}	10
G1		$1.8\,(1.4,0.8)\times10^{4}$	$1.35\pm0.5\times10^{7}$	11

Table 1. Black Hole masses and host masses for various spherical galaxies and globular clusters. References: (1) Macchetto *et al.* 1997; (2) Gebhardt *et al.* 2003; (3) average of Bower *et al.* 1998; Maciejewski & Binney 2001; (4) Verolme *et al.* 2002; (5) average of Verdoes Klein *et al.* 2000 and Cappellari *et al.* 2002; (6) Tadhunter *et al.* 2003; (7) Ferrarese *et al.* 1996; (8) Tremaine *et al.* 2002; (9) Gebhardt *et al.* 2000; (10) Ferrarese & Ford 1999; (11) Gerssen *et al.* 2002; (12) Gebhardt *et al.* 2002. Least squares best fit of this data to $\mathrm{Log}[M_{BH}] = \mathrm{Log}[\frac{\alpha}{2}] + x\mathrm{Log}[M]$ gives $\alpha = 1/137.4$ and $x = 0.974$. Data and best fit are shown in Fig. 2. Table adapted from Table 1 of [18].

be written in the form

$$|\mathbf{v}(\mathbf{r})|^2 = 2G \int d^3r' \, \frac{\rho_{DM}(\mathbf{r}') + \rho(\mathbf{r}')}{|\mathbf{r} - \mathbf{r}'|} \qquad (10)$$

in which the angle integrations may be done to yield

$$v(r)^2 = \frac{8\pi G}{r} \int_0^r s^2 \left[\rho_{DM}(s) + \rho(s)\right] ds + \\ + 8\pi G \int_r^\infty s \left[\rho_{DM}(s) + \rho(s)\right] ds \,, \qquad (11)$$

where with $v' = dv(r)/dr$,*

$$\rho_{DM}(r) = \frac{\alpha}{8\pi G} \left(\frac{v^2}{2r^2} + \frac{vv'}{r} \right). \qquad (12)$$

To obtain the induced in-flow singularity to $\mathrm{O}(\alpha)$ we substitute the non-α term in (11) into (12) giving the effective matter density that mimics the spatial self-interaction of the in-flow,

$$\rho_{DM}(r) = \frac{\alpha}{2r^2} \int_r^\infty s\,\rho(s)\, ds + \mathrm{O}(\alpha^2) \,. \qquad (13)$$

We see that the effective "dark matter" effect is concentrated near the centre, and we find that the total effective "dark matter" mass is

$$M_{DM} \equiv 4\pi \int_0^\infty r^2 \rho_{DM}(r)\, dr = \\ = \frac{4\pi\alpha}{2} \int_0^\infty r^2 \rho(r)\, dr + \mathrm{O}(\alpha^2) = \frac{\alpha}{2} M + \mathrm{O}(\alpha^2) \,. \qquad (14)$$

This result applies to any spherically symmetric matter distribution, and is the origin of the α terms in (4) and (5). It is thus responsible for the bore hole anomaly expression in (6). This means that the bore hole anomaly is indicative of an in-flow singularity at the centre of the Earth. This contributes some 0.4% of the effective mass of the Earth, as defined by Newtonian gravity. However in star systems this minimal black hole effect is more apparent, and we label M_{DM} as M_{BH}. Table 1 shows the effective "black hole" masses attributed to various spherically symmetric star systems based upon observations and analysis of the motion of gases and stars in these systems. The prediction of the dynamics of space is that these masses should obey (14). The data from Table 1 is plotted in Fig. 2, and we see the high precision to which (14) is indeed satisfied, and over some 6 orders of magnitude, giving from this data that $\alpha \approx 1/137.4$.

The application of the spatial dynamics to spiral galaxies is discussed in [13–16] where it is shown that a complete non-matter explanation of the spiral galaxy rotation speed anomaly is given: there is no such stuff as "dark matter" — it is an α determined spatial self-interaction effect. Essentially even in the non-relativistic regime the Newtonian theory of gravity, with its "universal" Inverse Square Law, is deeply flawed.

4 Spacetime

The curved spacetime explanation for gravity is widely known. Here an explanation for its putative success is given, for there is a natural definition of a spacetime that arises from (1), but that it is purely a mathematical construction with no ontological status — it is a mere mathematical artifact.

First consider the generalised Schrödinger [12]

$$i\hbar \frac{\partial \psi(\mathbf{r},t)}{\partial t} = H(t)\,\psi(\mathbf{r},t), \qquad (15)$$

where the free-fall hamiltonian is

$$H(t) = -i\hbar \left(\mathbf{v}\cdot\nabla + \frac{1}{2}\nabla\cdot\mathbf{v} \right) - \frac{\hbar^2}{2m}\nabla^2 \qquad (16)$$

As discussed in [12] this is uniquely defined by the requirement that the wave function be attached to the dynam-

*Previous papers had a typo error in this expression. Thanks to Andree Blotz for noting that.

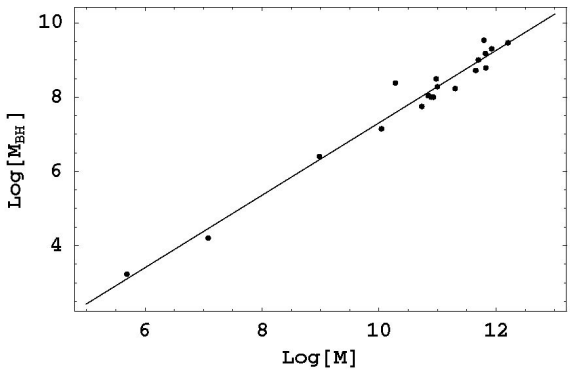

Fig. 2: Log-Log plot of black hole masses M_{BH} and host galaxy or globular cluster masses M (in solar units) from Table 1. Straight line is least squares best fit to $\mathrm{Log}[M_{BH}] = \mathrm{Log}[\frac{\alpha}{2}] + x\mathrm{Log}[M]$, giving $\alpha = 1/137.4$ and $x = 0.974$. The borehole g-anomaly gives $\alpha = 1/(137.9 \pm 5)$ from the Greenland Ice Shelf data and $\alpha = 1/(136.8 \pm 3)$ from the Nevada test site data [16].

ical space, and not to the embedding space, which is a mere mathematical artifact. We can compute the acceleration of a localised wave packet according to

$$\mathbf{g} \equiv \frac{d^2}{dt^2}\left(\psi(t), \mathbf{r}\,\psi(t)\right) = \\ = \frac{\partial \mathbf{v}}{\partial t} + (\mathbf{v}\cdot\nabla)\mathbf{v} + (\nabla\times\mathbf{v})\times\mathbf{v}_R \tag{17}$$

where $\mathbf{v}_R = \mathbf{v}_0 - \mathbf{v}$ is the velocity of the wave packet relative to the local space, as $\mathbf{v}_0$ is the velocity relative to the embedding space. Apart from the vorticity term which causes rotation of the wave packet* we see, as promised, that this matter acceleration is equal to that of the space itself, as in (3). This is the first derivation of the phenomenon of gravity from a deeper theory: gravity is a quantum effect — namely the refraction of quantum waves by the internal differential motion of the substructure patterns to space itself. Note that the equivalence principle has now been explained, as this "gravitational" acceleration is independent of the mass m of the quantum system.

An analogous generalisation of the Dirac equation is also necessary giving the coupling of the spinor to the actual dynamical space, and again not to the embedding space as has been the case up until now,

$$i\hbar\frac{\partial\psi}{\partial t} = -i\hbar\left(c\vec{\alpha}\cdot\nabla + \mathbf{v}\cdot\nabla + \frac{1}{2}\nabla\cdot\mathbf{v}\right)\psi + \beta mc^2\psi \tag{18}$$

where $\vec{\alpha}$ and β are the usual Dirac matrices. Repeating the analysis in (17) for the space-induced acceleration we obtain†

$$\mathbf{g} = \frac{\partial\mathbf{v}}{\partial t} + (\mathbf{v}\cdot\nabla)\mathbf{v} + (\nabla\times\mathbf{v})\times\mathbf{v}_R - \frac{\mathbf{v}_R}{1-\frac{\mathbf{v}_R^2}{c^2}}\frac{1}{2}\frac{d}{dt}\left(\frac{\mathbf{v}_R^2}{c^2}\right) \tag{19}$$

*This is the Lense-Thirring effect, and such vorticity is being detected by the Gravity Probe B satellite gyroscope experiment [33].

†Some details are incomplete in this analysis.

which generalises (17) by having a term which limits the speed of the wave packet relative to space to be $< c$. This equation specifies the trajectory of a spinor wave packet in the dynamical space.

We shall now show how this leads to both the spacetime mathematical construct and that the geodesic for matter worldlines in that spacetime is equivalent to trajectories from (19). First we note that (19) may be obtained by extremising the time-dilated elapsed time

$$\tau\left[\mathbf{r}_0\right] = \int dt\left(1 - \frac{\mathbf{v}_R^2}{c^2}\right)^{1/2} \tag{20}$$

with respect to the particle trajectory $\mathbf{r}_0(t)$ [1]. This happens because of the Fermat least-time effect for waves: only along the minimal time trajectory do the quantum waves remain in phase under small variations of the path. This again emphasises that gravity is a quantum effect. We now introduce a spacetime mathematical construct according to the metric

$$ds^2 = dt^2 - \frac{\left(d\mathbf{r} - \mathbf{v}(\mathbf{r},t)\,dt\right)^2}{c^2} = g_{\mu\nu}dx^\mu dx^\nu. \tag{21}$$

Then according to this metric the elapsed time in (20) is

$$\tau = \int dt\sqrt{g_{\mu\nu}\frac{dx^\mu}{dt}\frac{dx^\nu}{dt}}, \tag{22}$$

and the minimisation of (22) leads to the geodesics of the spacetime, which are thus equivalent to the trajectories from (20), namely (19). Hence by coupling the Dirac spinor dynamics to the space dynamics we derive the geodesic formalism of General Relativity as a quantum effect, but without reference to the Hilbert-Einstein equations for the induced metric. Indeed in general the metric of this induced spacetime will not satisfy these equations as the dynamical space involves the α-dependent dynamics, and α is missing from GR. So why did GR appear to succeed in a number of key tests where the Schwarzschild metric was used? The answer is provided by identifying the induced spacetime metric corresponding to the in-flow in (4) outside of a spherical matter system, such as the Earth. Then (21) becomes

$$ds^2 = dt^2 - \frac{1}{c^2}\left(dr + \sqrt{\frac{2GM(1+\frac{\alpha}{2}+\dots)}{r}}\,dt\right)^2 - \\ - \frac{1}{c^2}\,r^2\left(d\theta^2 + \sin^2\theta\,d\phi^2\right). \tag{23}$$

Making the change of variables‡ $t \to t'$ and $\mathbf{r} \to \mathbf{r}' = \mathbf{r}$ with

$$t' = t - \frac{2}{c}\sqrt{\frac{2GM(1+\frac{\alpha}{2}+\dots)\,r}{c^2}} + \\ + \frac{4GM(1+\frac{\alpha}{2}+\dots)}{c^3}\tanh^{-1}\sqrt{\frac{2GM(1+\frac{\alpha}{2}+\dots)}{c^2 r}} \tag{24}$$

‡No unique choice of variables is required. This choice simply leads to a well-known form for the metric.

this becomes (and now dropping the prime notation)

$$ds^2 = \left(1 - \frac{2GM(1+\frac{\alpha}{2}+\dots)}{c^2 r}\right) dt^2 - \\ -\frac{1}{c^2} r^2 \left(d\theta^2 + \sin^2\theta\, d\phi^2\right) - \frac{dr^2}{c^2\left(1 - \frac{2GM(1+\frac{\alpha}{2}+\dots)}{c^2 r}\right)} \quad (25)$$

which is one form of the the Schwarzschild metric but with the α-dynamics induced effective mass shift. Of course this is only valid outside of the spherical matter distribution, as that is the proviso also on (4). As well the above particular change of coordinates also introduces spurious singularities at the event horizon*, but other choices do not do this. Hence in the case of the Schwarzschild metric the dynamics missing from both the Newtonian theory of gravity and General Relativity is merely hidden in a mass redefinition, and so didn't affect the various standard tests of GR, or even of Newtonian gravity. Note that as well we see that the Schwarzschild metric is none other than Newtonian gravity in disguise, except for the mass shift. While we have now explained why the GR formalism appeared to work, it is also clear that this formalism hides the manifest dynamics of the dynamical space, and which has also been directly detected in gas-mode interferometer and coaxial-cable experiments.

One of the putative key tests of the GR formalism was the gravitational bending of light. This also immediately follows from the new space dynamics once we also generalise the Maxwell equations so that the electric and magnetic fields are excitations of the dynamical space. The dynamics of the electric and magnetic fields must then have the form, in 'empty' space,

$$\nabla \times \mathbf{E} = -\mu \left(\frac{\partial \mathbf{H}}{\partial t} + \mathbf{v}\cdot\nabla\mathbf{H}\right)$$
$$\nabla \times \mathbf{H} = \epsilon \left(\frac{\partial \mathbf{E}}{\partial t} + \mathbf{v}\cdot\nabla\mathbf{E}\right) \quad (26)$$
$$\nabla\cdot\mathbf{H} = \mathbf{0}, \qquad \nabla\cdot\mathbf{E} = \mathbf{0}$$

which was first suggested by Hertz in 1890 [34]. As discussed elsewhere the speed of EM radiation is now $c = 1/\sqrt{\mu\,\epsilon}$ with respect to the space, and in general not with respect to the observer if the observer is moving through space, as experiment has indicated again and again. In particular the in-flow in (4) causes a refraction effect of light passing close to the Sun, with the angle of deflection given by

$$\delta = 2\,\frac{v^2}{c^2} = \frac{4GM(1+\frac{\alpha}{2}+\dots)}{c^2 d} \quad (27)$$

where v is the in-flow speed at the surface of the Sun, and d is the impact parameter, essentially the radius of the Sun. Hence the observed deflection of 8.4×10^{-6} radians is actually a measure of the in-flow speed at the Sun's surface, and that gives $v = 615$ km/s. At the Earth distance the Sun induced spatial in-flow speed is 42 km/s, and this has been extracted from the 1925/26 gas-mode interferometer Miller data [1, 3]. These radial in-flows are to be vectorially summed to the galactic flow of some 400 km/s, but since that flow is much more uniform it does not affect the light bending by the Sun in-flow component†. Hence the deflection of light by the Sun is a way of directly measuring the in-flow speed at the Sun's surface, and has nothing to do with "real" curved spacetime. These generalised Maxwell equations also predict gravitational lensing produced by the large in-flows associated with new "black holes" in galaxies. So again this effect permits the direct observation of the these black hole effects with their non-inverse square law accelerations.

5 Conclusions

We have shown how minimal assumptions about the internal dynamics of space, namely how embeddability in a mathematical space such as an E^3 or an S^3, expressing its inherent 3-dimensionality, leads to various predictions ranging from the anisotropy of the speed of light, as expressed in the required generalisation of Maxwell' s equations, and which has been repeatedly observed since the Michelson-Morley experiment [5] of 1887, to the derivation of the phenomenon of gravity that follows after we generalise the Schrödinger and Dirac equations. This shows that the gravitational acceleration of matter is a quantum effect: it follows from the refraction of quantum waves in the inhomogeneities and time-dependencies of the flowing dynamical space. In particular the analysis shows that the acceleration of quantum matter is identical to the convective acceleration of the structured space itself. This is a non-trivial result. As well in the case of the Dirac equation we derive the spacetime formalism as well as the geodesic description of matter trajectories, but in doing so reveal that the spacetime is merely a mathematical construct. We note that the relativistic features of the Dirac equation are consistent with the absolute motion of the wave function in the dynamical 3-space. This emphasis yet again that Special Relativity does not require the isotropy of the speed of light, as is often incorrectly assumed.

Here we have further extended the observational evidence that it is the fine structure constant that determines the strength of the spatial self-interaction in this new physics by including data from black hole masses in 19 spherical star systems. Elsewhere we have already shown that the new space dynamics explains also the spiral galaxy rotation velocity anomaly; that it is not caused by a new form of matter, that the notion of "dark matter" is just a failure of

*The event horizon of (25) is at a different radius from the actual event horizon of the black hole solutions that arise from (1).

†The vector superposition effect for spatial flows is only approximate, and is discussed in more detail in [35]. The solar system has a galactic velocity of some 420±30 km/s in the direction RA=5.2 hr, Dec=−67°.

Newtonian gravity and GR. We have also shown that the space dynamics is non-local, a feature that Newton called action-at-a-distance. This is now extended to include the effects of the spatial self-interaction. The numerous confirmations of that dynamics, summarised herein, demonstrate the validity of this non-local physics. Of course since Newton we have become more familiar with non-local effects in the quantum theory. The new space dynamics shows that non-local effects are more general than just subtle effects in the quantum theory, for in the space dynamics this non-local dynamics is responsible for the supermassive black holes in galaxies. This non-local dynamics is responsible for two other effects: (i) that the dynamics of space within an event horizon, say enclosing a black hole in-flow singularity affects the space outside of the horizon, even though EM radiation and matter cannot propagate out through the event horizon, as there the in-flow speed exceeds the speed of light. So in this new physics we have the escape of information from within the event horizon, and (ii) that the universe overall is more highly connected than previously thought. This may explain why the universe is more uniform than expected on the basis of interactions limited by the speed of light, i. e. we probably have a solution to the cosmological horizon problem.

Elsewhere [1] we have argued that the dynamical space has the form of a quantum foam and so non-local quantum effects are to be expected. So it might be argued that the successful prediction of the masses of these black hole masses, and their dependence on the fine structure constant, is indicative of a grand unification of space and the quantum theory. This unification is not coming from the quantisation of gravity, but rather from a deeper modelling of reality as an information-theoretic system with emergent quantum-space and quantum matter.

This work is supported by an Australian Research Council Discovery Grant.

References

1. Cahill R. T. Process Physics: From information theory to quantum space and matter. Nova Science, N.Y., 2005.
2. Cahill R. T. and Kitto K. Michelson-Morley experiments revisited. *Apeiron*, 2003, v. 10(2), 104–117.
3. Cahill R. T. Absolute motion and gravitational effects. *Apeiron*, 2004, v. 11(1), 53–111.
4. Cahill R. T. The Michelson and Morley 1887 experiment and the discovery of absolute motion. *Progress in Physics*, 2005, v. 3, 25–29.
5. Michelson A. A. and Morley E. W. *Philos. Mag.*, S. 5, 1887, v. 24, No. 151, 449–463.
6. Miller D. C. *Rev. Mod. Phys.*, 1933, v. 5, 203–242.
7. Illingworth K. K. *Phys. Rev.*, 1927, v. 3, 692–696.
8. Joos G. *Ann. der Physik*, 1930, Bd 7, 385.
9. Jaseja T. S. *et al. Phys. Rev.*, v. A133, 1964, 1221.
10. Torr D. G. and Kolen P. *Precision Measurements and Fundamental Constants*, ed. by Taylor B. N. and Phillips W. D. Nat. Bur. Stand. (U.S.), Spec. Pub., 1984, v. 617, 675.
11. Cahill R. T. The Roland DeWitte 1991 experiment. *Progress in Physics*, 2006, v. 3, 60–65.
12. Cahill R. T. Dynamical fractal 3-space and the generalised Schrödinger equation: Equivalence Principle and vorticity effects. *Progress in Physics*, 2006, v. 1, 27–34.
13. Cahill R. T. Gravity, "dark matter" and the fine structure constant. *Apeiron*, 2005, v. 12(2), 144–177.
14. Cahill R. T. "Dark matter" as a quantum foam in-flow effect. In: *Trends in Dark Matter Research*, ed. J. Val Blain, Nova Science, N.Y., 2005, 96–140.
15. Cahill R. T. Black holes in elliptical and spiral galaxies and in globular clusters. *Progress in Physics*, 2005, v. 3, 51–56.
16. Cahill R. T. 3-Space in-flow theory of gravity: Boreholes, blackholes and the fine structure constant. *Progress in Physics*, 2006, v. 2, 9–16.
17. Crothers S. J. A brief history of black holes. *Progress in Physics*, 2006, v. 2, 54–57.
18. Marconi A. and Hunt L. K. *ApJ*, 2003, v. 589, L21–L24, part 2.
19. Macchetto F. *et al. ApJ*, 1997, v. 489, 579.
20. Gebhardt K. *et al. ApJ*, 2003, v. 583, 92.
21. Bower G. A. *et al. ApJ*, 2001, v. 550, 75.
22. Maciejewski F. and Binney J. *MNRAS*, 2001, v. 323, 831.
23. Verolme E. K. *et al. MNRAS*, 2002, v. 335, 517.
24. Verdoes Klein G. A. *et al. AJ*, 2000, v. 120, 1221.
25. Cappellari M. *et al. ApJ*, 2002, v. 578, 787.
26. Tadhunter C. *et al. MNRAS*, 2003, v. 342, 861.
27. Ferrarese L. *et al. ApJ*, 1996, v. 470, 444.
28. Tremaine S. *et al. ApJ*, 2002, v. 574, 740.
29. Gebhardt K. *et al. ApJ*, 2000, v. 539, L13.
30. Ferrarese L. and Ford H. C. *ApJ*, 1999, v. 515, 583.
31. Gerssen J. *et al. Astron. J.*, 2002, v. 124, 3270–3288; Addendum 2003, v. 125, 376.
32. Gebhardt K. *et al. ApJ.*, 2002, v. 578, L41.
33. Cahill R. T. Novel Gravity Probe B frame-dragging effect. *Progress in Physics*, 2005, v. 3, 30–33.
34. Hertz H. On the fundamental equations of electro-magnetics for bodies in motion. *Wiedemann's Ann.*, 1890, v. 41, 369; Electric waves. Collection of scientific papers. Dover Publ., N.Y., 1962.
35. Cahill R. T. The dynamical velocity superposition effect in the quantum-foam in-flow theory of gravity. arXiv: physics/0407133.

Preferred Spatial Directions in the Universe: a General Relativity Approach

Larissa Borissova
E-mail: lborissova@yahoo.com

Herein is constructed, using General Relativity, the space metric along the Earth's trajectory in the Galaxy, where the Earth traces outs a complicated spiral in its orbital motion around the Sun and its concomitant motion with the solar system around the centre of the Galaxy. It is deduced herein that this space is inhomogeneous and anisotropic. The observable properties of the space, characterizing its gravitation, rotation, deformation, and curvature, are obtained. The theory predicts that the observable velocity of light is anisotropic, due to the anisotropy and inhomogeneity of space caused by the presence of gravitation and the space rotation, despite the world-invariance of the velocity of light remaining unchanged. It is calculated that two pairs of synchronised clocks should record a different speed of light for light beams travelling towards the Sun and orthogonal to this direction, of about $4\times10^{-4}\,c$ (i. e. 120 km/sec, 0.04% of the measured velocity of light c). This effect should have oscillations with a 12-hour period (due to the daily rotation of the Earth) and 6 month period (due to the motion of the Earth around the Sun). The best equipment for detecting the effect is that being used by R. T. Cahill (Flinders University, Australia) in his current experiments measuring the velocity of light in an RF coaxial-cable equipped with a pair of high precision synchronized Rb atomic clocks.

The geniality of geometry, its applicability to our real world, can be verified by observation or experiment, not logical deduction.

N. A. Kozyrev

1 Introduction

We construct herein, by General Relativity, a mathematical model for a space body moving around another body (the centre of attraction), both moving in an observer's reference space. The Earth rotates around the Sun, and orbits in common with it around the centre of the Galaxy; the Sun rotates around the centre of the Galaxy and orbits in common with the Galaxy around the centre of the Local Group of galaxies; etc. As a result there are preferred directions determined by orbital motions, so the real Universe is *anisotropic* (inequivalence of directions). Because there are billions of centres of gravitational attraction, the Universe is also *inhomogeneous* (inequivalence of points). Hence, for the real Universe, we cannot ignore the anisotropy of space and gravitation.

On the other hand, most cosmologists use the concept of a homogeneous isotropic Universe wherein all points and directions are equivalent. Such a model can be built only by an observer who, observing matter in the Universe from afar, doesn't see such details as stars and galaxies. Such conceptions lead to a vicious circle — most cosmologists are sure that our Universe is a homogeneous isotropic ball expanding from an initial point-like state (singularity); they ignore the anisotropy of space and gravitation in such models.

Relativistic models of a homogeneous isotropic universe (which include the Friedmann solutions) are only a few partial solutions to Einstein's equations. Besides, as shown during the last decade, many popular cosmological metrics (including the Friedmann solutions) are inadmissible, because the difference between the radial coordinate and the proper radius isn't taken into account there (see [1, 2] and References therein).

And so forth, we shall show that the homogeneous isotropic metric spaces contain no rotation and gravitation, and that they can only undergo deformation: no stars, galaxies or other space bodies exist in such a universe*. Why do the scientists use such solutions? The answer is clearly evident: such solutions are simple, and thereby easier to study.

We shall consider another problem statement, the case of an inhomogeneous anisotropic universe as first set up in 1944 by A. Zelmanov [4, 5]. Such a consideration is applicable to any local part of the Universe. We show in this paper that along such a preferred direction, caused by the orbital motion of a space body, an *anisotropy of the observable velocity of light* can be deduced, despite the world-invariance of the velocity of light remaining unchanged†. Using this result as a basis, we will show in a subsequent paper (now in preparation) that not only is the anisotropy of the velocity of light expected along a satellite's trajectory, but even its motion is permitted only in a non-empty space filled by a distribution of matter and a λ-field (both derived from the right side of Einstein's equations). This conclusion leads to

*This situation is similar to the standard solution of the gravitational wave problem, which considers them as space deformation waves in a space free of rotation and gravitation [3].

†The observable velocity of light is different to the world-invariant velocity of light if considered by means of the mathematical apparatus of physically observed quantities in General Relativity — so-called chronometric invariants [4, 5].

the possibility of a new source of energy working in a rotating (non-holonomic) space, and has a direct link to the conclusion that stars produce energy due to the background space non-holonomity (as recently derived by means of General Relativity in [6, 7]).

2 Observed characteristics of space in the Earth's motion in the Galaxy

How do the Earth and the planets move in space? The Earth rotates around its own axis at 465 m/sec at the equator, with an approximately 24-hour period, and moves at 30 km/sec around the Sun with a 365.25-day period (astronomical year). The Sun, in common with the planets, moves at 250 km/sec around the centre of the Galaxy with an ~ 200 million year period. And so the Earth's orbit traces a cylinder, the axis of which is the galactic trajectory of the Sun. As a result, the local space of the Earth draws a very stretched spiral, spanned over the "galactic" cylinder of the Earth's orbit. Each planet traces a similar spiral in the Galaxy.

We aim to build a metric for the space along the Earth's transit in the Galaxy. We do this in two steps. First, the metric along the Earth's transit in the gravitational field of the Sun. Second, using the Lorentz transformation to change to the reference frame moving (with respect to the first frame) along the axis coinciding with the direction in which the Earth moves in the Galaxy.

We use a reference frame which rotates and moves forwards in a weak gravitational field. We therefore use cylindrical coordinates. Then the metric along the Earth's transit in the gravitational field of the Sun has the form*

$$ds^2 = \left(1 - \frac{2GM}{c^2 r} - \frac{\omega^2 r^2}{c^2}\right) c^2 dt^2 - \frac{2\omega r^2}{c}\, c dt\, d\varphi - \\ - \left(1 + \frac{2GM}{c^2 r}\right) dr^2 - r^2 d\varphi^2 - dz^2, \tag{1}$$

where ω is the angular velocity of the Earth's rotation around the Sun: $\omega = \frac{v_{orb}}{r} = 2\times 10^{-7}\,\mathrm{sec}^{-1}$.

We now change to a reference frame that rotates in a weak gravitational field and moves uniformly with a velocity v (associated with the motion of the Sun in the Galaxy) along the z-axis. We apply the Lorentz transformations

$$\tilde{z} = \frac{z + \mathrm{v}t}{\sqrt{1 - \frac{\mathrm{v}^2}{c^2}}}, \qquad \tilde{t} = \frac{t + \frac{\mathrm{v}z}{c^2}}{\sqrt{1 - \frac{\mathrm{v}}{c^2}}}, \tag{2}$$

where $\tilde{z}$ and $\tilde{t}$ are corresponding coordinates in the new reference frame. We differentiate $\tilde{z}$ and $\tilde{t}$, then substitute the resulting $d\tilde{z}^2$, $d\tilde{t}^2$ and $d\tilde{t}$ into (2). For $\mathrm{v} = 250$ km/sec we have $\mathrm{v}^2/c^2 = 7\times 10^{-7}$, hence $\frac{1}{\sqrt{1-\mathrm{v}^2/c^2}} \approx 1 + \mathrm{v}^2/2c^2$. We ignore terms in powers higher than $\frac{1}{c^2}$. As a result we obtain the metric along the Earth's trajectory in the Galaxy (dropping the tilde from the formulae)

$$ds^2 = \left(1 - \frac{2GM}{c^2 r} - \frac{\omega^2 r^2}{c^2}\right) c^2 dt^2 - \frac{2\omega r^2}{c}\, c dt\, d\varphi - \\ - \left(1 + \frac{2GM}{c^2 r}\right) dr^2 - r^2 d\varphi^2 - \frac{2\omega \mathrm{v} r^2}{c^2}\, d\varphi\, dz - dz^2. \tag{3}$$

This metric differs from (1), because of a spatial term $2\omega r^2 \mathrm{v}/c^2$ depending upon the linear velocity v.

In order to obtain really observable effects expected in the metric (3), we use the mathematical method of physical observed quantities [4, 5], which considers a fixed spatial section connected to a real reference frame of an observer. For such an observer the fundamental metrical tensor† has the three-dimensional invariant form

$$h_{ik} = -g_{ik} + \frac{1}{c^2}\, v_i v_k\,, \qquad i,k = 1,2,3, \tag{4}$$

dependent upon the linear velocity of the space rotation $v_i = -\frac{c g_{0i}}{\sqrt{g_{00}}}$. In (3) the metric tensor has the components

$$h_{11} = 1 + \frac{2GM}{c^2 r}\,, \quad h_{22} = r^2\left(1 + \frac{\omega^2 r^2}{c^2}\right), \\ h_{23} = \frac{\omega r^2 \mathrm{v}}{c^2}\,, \qquad h_{33} = 1\,, \tag{5}$$

while its contravariant components are

$$h^{11} = 1 - \frac{2GM}{c^2 r}\,, \quad h^{22} = \frac{1 - \frac{\omega^2 r^2}{c^2}}{r^2}\,, \\ h^{23} = -\frac{\omega \mathrm{v}}{c^2}\,, \qquad h^{33} = 1\,. \tag{6}$$

According to the theory [4, 5], any reference space has principal observable (chronometrically invariant) characteristics: the chr.inv.-vector of gravitational inertial force

$$F_i = \frac{1}{1 - \frac{\mathrm{w}}{c^2}} \left(\frac{\partial \mathrm{w}}{\partial x^i} - \frac{\partial v_i}{\partial t}\right); \tag{7}$$

the chr.inv.-tensor of the angular velocity of the space rotation

$$A_{ik} = \frac{1}{2}\left(\frac{\partial v_k}{\partial x^i} - \frac{\partial v_i}{\partial x^k}\right) + \frac{1}{2c^2}\left(F_i v_k - F_k v_i\right); \tag{8}$$

and the chr.inv.-tensor of the rates of the space deformation

$$D_{ik} = \frac{1}{2}\frac{{}^*\partial h_{ik}}{\partial t}\,, \tag{9}$$

*See any textbook on relativity. Note that the gravitational field is included in the components of the fundamental metric tensor $g_{\alpha\beta}$ as $\frac{GM}{c^2 r}$. The mass of the Sun is $M_\odot = 2\times 10^{33}$ g, the mass of the Earth is $M_\oplus = 6\times 10^{27}$ g; the distance between the Sun and the Earth is 15×10^{11} cm, the Earth's radius is 6.37×10^8 cm. We obtain $\frac{GM_\odot}{c^2 r} = 10^{-8}$, $\frac{GM_\oplus}{c^2 r} = 10^{-10}$. So, in this consideration we mean the daily rotation of the Earth and its gravitational field neglected (quasi-Newtonian approximation).

†The spatial indices 1, 2, 3 are denoted by Roman letters, while the space-time indices 0, 1, 2, 3 are denoted by Greek letters.

where $\mathrm{w} = c^2\left(1-\sqrt{g_{00}}\right)$, while $\frac{{}^*\partial}{\partial t} = \frac{1}{\sqrt{g_{00}}}\frac{\partial}{\partial t}$ is the so-called chronometrically invariant time derivative.

Calculating these for the metric space (3), we obtain

$$F^1 = \left(\omega^2 r - \frac{GM}{r^2}\right)\left(1+\frac{\omega^2 r^2}{c^2}\right); \qquad (10)$$

$$A^{12} = \frac{\omega}{r}\left(1-\frac{2GM}{c^2 r}+\frac{\omega^2 r^2}{2c^2}\right), \quad A^{31} = \frac{\omega^2 \mathrm{v} r}{c^2}. \qquad (11)$$

All components of D_{ik} equal zero. Hence the reference body gravitates, rotates, and moves forward at a constant velocity. Appropriate characteristics of the metrics (1) and (3) coincide, aside for A^{31}: $A^{31}=0$ in (3).

The observable time interval $d\tau$ contains v_i [4, 5]:

$$d\tau = \left(1-\frac{\mathrm{w}}{c^2}\right)dt - \frac{1}{c^2}\,v_i\,dx^i. \qquad (12)$$

Within an area wherein $A_{ik}=0$ (holonomic space) the time coordinate $x^0=ct$ can be transformed so that all $v_i=0$. In other words, the time interval between two events at different points does not depend on the path of integration: time is *integrable*, so a global synchronization of clocks is possible. In such a space the spatial section $x^0=\mathrm{const}$ is everywhere orthogonal to time lines $x^i=\mathrm{const}$. If $A_{ik}\neq 0$ (non-holonomic space), it is impossible for all v_i to be zero: the spatial section is not orthogonal to the time lines, and the time interval between two events at different points depends on the path of integration (time is *non-integrable*).

Zelmanov also introduced the chr.inv.-pseudovector of the angular velocity of the space rotation [4]

$$\Omega_i = \frac{1}{2}\,\varepsilon_{ijk}\,A^{jk}, \qquad (13)$$

where $\varepsilon_{ijk} = \frac{e_{ijk}}{\sqrt{h}}$ is the three-dimensional discriminant tensor, e_{ijk} is the completely antisymmetric three-dimensional tensor, $h=\det\|h_{ik}\|$. Hence, $\Omega_1=A^{23}$, $\Omega_2=A^{31}$, $\Omega_3=A^{12}$.

In our statement we have two bodies, both rotating and gravitating. The first body is at rest with respect to the observer, whilst the second body moves with a linear velocity. As seen from (11), for the rest body only $\Omega_3\neq 0$. For the moving body we also obtain $\Omega_2\neq 0$ and $\Omega_3\neq 0$.* In other words, any linear motion of an observer with respect to his reference body provides an additional degree of freedom to rotations of his reference space.

Besides the aforementioned observable "physical" characteristics F_i, A_{ik}, and D_{ik}, every reference space also has an observable geometric characteristic [4]: the chr.inv.-tensor of the three-dimensional space curvature

$$C_{lkij} = H_{lkij} - \frac{1}{c^2}\big(2A_{ki}D_{jl} + A_{ij}D_{kl} + \\ + A_{jk}D_{il} + A_{kl}D_{ij} + A_{li}D_{kj}\big), \qquad (14)$$

which possesses all the properties of the Riemann-Christoffel curvature tensor $R_{\alpha\beta\gamma\delta}$ in the spatial section. Here $H_{lkij} = h_{jm}H^{\cdots m}_{lki\cdot}$, where $H^{\cdots m}_{lki\cdot}$ is the chr.inv-tensor similar to Schouten's tensor [8]:

$$H^{\cdots j}_{lki\cdot} = \frac{{}^*\partial\Delta^j_{il}}{\partial x^k} - \frac{{}^*\partial\Delta^j_{kl}}{\partial x^i} + \Delta^m_{il}\Delta^j_{km} - \Delta^m_{kl}\Delta^j_{im}. \qquad (15)$$

If all A_{ik} or D_{ik} are zero in a space, $C_{iklj}=H_{iklj}$. Zelmanov also introduced $H_{ik}=h^{mn}H_{imkn}$, $H=h^{ik}H_{ik}$, $C_{ik}=h^{mn}C_{imkn}$ and $C=h^{ik}C_{ik}$.

The chr.inv.-Christoffel symbols of the first and second kinds, by Zelmanov, are

$$\Delta^k_{ij} = h^{km}\Delta_{ij,m} = \frac{1}{2}\left(\frac{{}^*\partial h_{im}}{\partial x^j} + \frac{{}^*\partial h_{jm}}{\partial x^i} - \frac{{}^*\partial h_{ij}}{\partial x^m}\right), \qquad (16)$$

where $\frac{{}^*\partial}{\partial x^i} = \frac{\partial}{\partial x^i} - \frac{1}{c^2}\frac{{}^*\partial}{\partial t}$ is the so-called chr.inv.-spatial derivative.

Calculating the components of Δ^k_{ij} for the metric (3), we obtain

$$\Delta^1_{22} = -r\left(1-\frac{2GM}{c^2 r}+\frac{2\omega^2 r^2}{c^2}\right),$$
$$\Delta^1_{11} = \frac{GM}{c^2 r^2}, \qquad \Delta^1_{23} = -\frac{\omega \mathrm{v} r}{c^2}, \qquad (17)$$
$$\Delta^2_{12} = \frac{1}{r}\left(1+\frac{\omega^2 r^2}{c^2}\right), \quad \Delta^2_{13} = \frac{\omega \mathrm{v}}{c^2 r},$$

while non-zero components of C_{iklj}, C_{ik} and C are

$$C_{1212} = -\frac{GM}{c^2 r} + \frac{3\omega^2 r^2}{c^2},$$
$$C_{11} = -\frac{GM}{c^2 r^3} + \frac{3\omega^2}{c^2}, \quad C_{22} = -\frac{GM}{c^2 r} + \frac{3\omega^2 r^2}{c^2}, \qquad (18)$$
$$C = 2\left(-\frac{GM}{c^2 r^3} + \frac{3\omega^2}{c^2}\right).$$

We have thus calculated by the theory of observable quantities, that:

> The observable space along the Earth's trajectory in the Galaxy is non-holonomic, inhomogeneous, and curved due to the space rotation and/or Newtonian attraction. This should be true for any other planet (or its satellite) as well, or any other body considered within the framework this analysis.

3 Deviation of light in the field of the Galactic rotation

We study how a light ray behaves in a reference body space described by the metric (3). Light moves along isotropic geodesic lines. Such geodesics are trajectories of the parallel transfer of the four-dimensional isotropic wave vector

$$K^\alpha = \frac{\Omega}{c}\frac{dx^\alpha}{d\sigma}, \qquad g_{\alpha\beta}\,K^\alpha K^\beta = 0, \qquad (19)$$

*This is because any linear motion leads to an additional term in the observable metric tensor h_{ik}: see formulae (5) and (6).

where Ω is the proper frequency of the radiation, $d\sigma = h_{ik}\,dx^i dx^k$ is the three-dimensional observable interval*. The equations of geodesic lines in chr.inv.-form are [4, 5]

$$\begin{aligned}&\frac{d\Omega}{d\tau}-\frac{\Omega}{c^2}F_i c^i+\frac{\Omega}{c^2}D_{ik}c^i c^k=0\,,\\&\frac{d(\Omega c^i)}{d\tau}+2\omega(D^i_k+A^{\cdot i}_{k\cdot})c^k-\Omega F^i+\Omega\Delta^i_{kn}c^k c^n=0\,,\end{aligned}\tag{20}$$

where $c^i=\frac{dx^i}{d\tau}$ is the observable chr.inv.-velocity of light (its square is invariant $c_i c^i = h_{ik}c^i c^k = c^2$).

Substituting the chr.inv.-characteristics of the reference space (3) into equations (20), we obtain

$$\frac{1}{\Omega}\frac{d\Omega}{d\tau}-\frac{1}{c^2}\left(\omega^2 r-\frac{GM}{r^2}\right)\frac{dr}{d\tau}=0\,,\tag{21}$$

$$\begin{aligned}&\frac{d}{d\tau}\left(\Omega\frac{dr}{d\tau}\right)-2\Omega\omega r\left(1-\frac{2GM}{c^2 r}+\frac{3\omega^2 r^2}{2c^2}\right)\frac{d\varphi}{d\tau}-\\&-\Omega\left(\omega^2 r-\frac{GM}{r^2}\right)\left(1+\frac{\omega^2 r^2}{c^2}\right)-\frac{2\Omega\omega\mathrm{v}r}{c^2}\frac{d\varphi}{d\tau}\frac{dz}{d\tau}-\\&-\Omega r\left(1-\frac{2GM}{c^2 r}+\frac{2\omega^2 r^2}{c^2}\right)\left(\frac{d\varphi}{d\tau}\right)^2=0\,,\end{aligned}\tag{22}$$

$$\begin{aligned}&\frac{d}{d\tau}\left(\Omega\frac{d\varphi}{d\tau}\right)+\frac{2\Omega\omega}{r}\left(1+\frac{GM}{2c^2 r}+\frac{\omega^2 r^2}{2c^2}\right)\frac{dr}{d\tau}+\\&+\frac{2\omega}{r}\left(1+\frac{\omega^2 r^2}{c^2}\right)\frac{dr}{d\tau}\frac{d\varphi}{d\tau}+\frac{2\Omega\omega\mathrm{v}}{c^2 r}\frac{dr}{d\tau}\frac{dz}{d\tau}=0\,,\end{aligned}\tag{23}$$

$$\frac{d}{d\tau}\left(\Omega\frac{dz}{d\tau}\right)-\frac{2\Omega\omega^2\mathrm{v}r}{c^2}\frac{dr}{d\tau}=0\,.\tag{24}$$

Integrating (21) we obtain the observable proper frequency of the light beam at the moment of observation

$$\Omega=\frac{\Omega_0}{\sqrt{1-\frac{2GM}{c^2 r}-\frac{\omega^2 r^2}{c^2}}}\approx\Omega_0\left(1+\frac{GM}{c^2 r}+\frac{\omega^2 r^2}{2c^2}\right),\tag{25}$$

where Ω_0 is its "initial" proper frequency (in the absence of external affects). We integrate (22)–(24) with the use of (25).

Rewrite (24) as

$$\frac{d}{d\tau}\left(\Omega\frac{dz}{d\tau}\right)=\frac{\Omega\omega^2\mathrm{v}}{c^2}\frac{d}{d\tau}\left(r^2\right),\tag{26}$$

integration of which gives

$$\Omega\frac{dz}{d\tau}=\frac{\Omega\omega^2\mathrm{v}r^2}{c^2}+Q\,,\qquad Q=\mathrm{const},\tag{27}$$

where $\dot z_0=\left(\frac{dz}{d\tau}\right)_0$ is the initial value of $\frac{dz}{d\tau}$, while the integration constant is $Q=\Omega_0\left(\dot z_0-\frac{\omega^2\mathrm{v}r_0^2}{c^2}\right)$.

*So the space-time interval $ds^2=g_{\alpha\beta}\,dx^\alpha dx^\beta$ in chr.inv.-form is $ds^2=c^2d\tau^2-d\sigma^2=0$. Therefore, because $ds^2=0$ along isotropic trajectories by definition, there $d\sigma=c\,d\tau$.

Substituting (27) into (23) and (24) and using Ω from (25), we obtain the system of equations with respect to r and φ,

$$\left.\begin{aligned}&\frac{d}{d\tau}\left(\Omega\frac{d\varphi}{d\tau}\right)+\frac{2\Omega\omega}{r}\left(1+\frac{GM}{2c^2 r}+\frac{\omega^2 r^2}{2c^2}\right)\frac{dr}{d\tau}+\\&+\frac{2\omega}{r}\left(1+\frac{\omega^2 r^2}{c^2}\right)\frac{dr}{d\tau}\frac{d\varphi}{d\tau}+\frac{2\Omega_0\omega\mathrm{v}\dot z_0}{c^2 r}\frac{dr}{d\tau}=0\,,\\&\frac{d}{d\tau}\left(\Omega\frac{dr}{d\tau}\right)-2\Omega\omega r\left(1-\frac{2GM}{c^2 r}+\frac{3\omega^2 r^2}{2c^2}\right)\frac{d\varphi}{d\tau}-\\&-\Omega\left(\omega^2 r-\frac{GM}{r^2}\right)\left(1+\frac{\omega^2 r^2}{c^2}\right)-\frac{2\Omega_0\omega\mathrm{v}\dot z_0 r}{c^2}\frac{d\varphi}{d\tau}-\\&-\Omega r\left(1-\frac{2GM}{c^2 r}+\frac{2\omega^2 r^2}{c^2}\right)\left(\frac{d\varphi}{d\tau}\right)^2=0\,.\end{aligned}\right\}\tag{28}$$

We are looking for an approximate solution to this system. The last term has the dimensionless factor $\frac{\mathrm{v}\dot z_0}{c^2}$. For a light beam, $\dot z_0$ (the initial value of the light velocity along the z-axis) is c. Hence $\frac{\mathrm{v}\dot z_0}{c^2}=\frac{\mathrm{v}}{c}$. At 250 km/sec, attributed to the Earth moving in the Galaxy, $\frac{\mathrm{v}}{c}=8.3\times10^{-4}$. The terms $\frac{GM}{c^2 r}$ and $\frac{\omega^2 r^2}{c^2}$, related to the orbital motion of the Earth, are in order of 10^{-8}. We therefore drop these terms from consideration, so equations (28) become

$$\begin{aligned}&\frac{d}{d\tau}\left(\Omega\frac{dr}{d\tau}\right)-2\Omega\omega r\frac{d\varphi}{d\tau}-\Omega\left(\omega^2 r-\frac{GM_\odot}{r^2}\right)-\\&-\Omega r\left(\frac{d\varphi}{d\tau}\right)^2-\frac{2\Omega_0\omega\mathrm{v}\dot z_0 r}{c^2}\frac{d\varphi}{d\tau}\,,\end{aligned}\tag{29}$$

$$\frac{d}{d\tau}\left(\Omega\frac{d\varphi}{d\tau}\right)+\frac{2\Omega\omega}{r}\frac{dr}{d\tau}+\frac{2\omega}{r}\frac{dr}{d\tau}\frac{d\varphi}{d\tau}+\frac{2\Omega_0\omega\mathrm{v}\dot z_0}{c^2 r}\frac{dr}{d\tau}=0.\tag{30}$$

We rewrite (30) as

$$\ddot\varphi+2(\dot\varphi+\tilde\omega)\frac{\dot r}{r}=0\,,\tag{31}$$

where $\tilde\omega=\omega\left(1+\frac{\mathrm{v}\dot z_0}{c^2}\right)$, $\dot\varphi=\frac{d\varphi}{d\tau}$, $\ddot\varphi=\frac{d^2\varphi}{d\tau^2}$. This is an equation with separable variables, so its first integral is

$$\dot\varphi=\frac{B}{r^2}-\tilde\omega,\qquad B=\mathrm{const}=(\dot\varphi_0+\tilde\omega)r_0^2\,,\tag{32}$$

where $\dot\varphi_0$ and r_0 are the initial values of $\dot\varphi$ and r.

We rewrite (29) as

$$\ddot r-2\tilde\omega r\dot\varphi+\frac{GM}{r^2}-\omega^2 r-r\dot\varphi^2=0\,,\tag{33}$$

where $\dot r=\frac{dr}{d\tau}$, $\ddot r=\frac{d^2r}{d\tau^2}$. In our consideration, $\frac{GM}{r^2}-\omega^2 r$ is zero, so the motion of the Earth around the Sun satisfies the weightlessness condition [9, 10]† — a balance between the

†Each planet, in its orbital motion, should satisfy the *weightlessness condition* $\mathrm{w}=v_i u^i$, where w is the potential of the field attracting the planet to a body around which this planet is orbiting, v_i is the linear velocity of the body's space rotation in this orbit, and $u^i=dx^i/dt$ is the coordinate velocity of the planet in its orbit. The orbital velocity is the same as the space rotation velocity. Hence the weightiness condition can be written as $GM/r=v^2=v_i v^i$ [9, 10].

acting forces of gravity $\frac{GM}{r^2}$ and inertia $\omega^2 r$. Taking this into account, and substituting (32) into (33), we obtain

$$\ddot{r} + \tilde{\omega}^2 r - \frac{B^2}{r^3} = 0\,. \tag{34}$$

We replace the variables as $\dot{r} = p$. So $\ddot{r} = p\frac{dp}{dr}$ and the equation (36) takes the form

$$p\,\frac{dp}{dr} = \frac{B^2}{r^3} - \tilde{\omega}^2 r^2, \tag{35}$$

which can be easily integrated:

$$p^2 = \left(\frac{dr}{d\tau}\right)^2 = -\frac{B^2}{r^2} - \tilde{\omega}^2 r^2 + K\,, \qquad K = \text{const}, \tag{36}$$

where the integration constant is $K = \dot{r}_0^2 + (\dot{\varphi}_0 + \tilde{\omega})^2 r_0^2 + + \tilde{\omega}^2 r_0^2$, so we obtain

$$\frac{dr}{d\tau} = \pm\sqrt{K - \tilde{\omega}^2 r^2 - \frac{B^2}{r^2}}\,. \tag{37}$$

Looking for τ as a function of r, we integrate (37) taking the positive time flow into account (positive values of τ). We obtain

$$\tau = \int_{r_0}^{r} \frac{r dr}{\sqrt{-\tilde{\omega}^2 r^4 + K r^2 - B^2}}\,. \tag{38}$$

Introducing a new variable $u = r^2$ we rewrite (38) as

$$\tau = \frac{1}{2}\int_{u_0}^{u} \frac{du}{\sqrt{-\tilde{\omega}^2 u^2 + K u - B^2}}\,, \tag{39}$$

which integrates to

$$\begin{aligned}\tau = -\frac{1}{2\tilde{\omega}}\Bigg[&\arcsin\left(\frac{-2\tilde{\omega}^2 r^2 + K}{\sqrt{K^2 - 4\tilde{\omega}^2 B^2}}\right) - \\ &- \arcsin\left(\frac{-2\tilde{\omega}^2 r_0^2}{\sqrt{K^2 - 4\tilde{\omega}^2 B^2}}\right)\Bigg]\end{aligned} \tag{40}$$

where

$$\begin{aligned} &K^2 - 4\tilde{\omega}^2 B^2 \equiv Q^2 = \\ &= \left(\dot{r}_0^2 + r_0^2\dot{\varphi}_0^2\right)\left[\dot{r}_0^2 + 4\tilde{\omega}\left(\tilde{\omega} + \dot{\varphi}_0\right) r_0^2 + \dot{\varphi}_0^2 r_0^2\right], \end{aligned} \tag{41}$$

so we obtain r^2 and r

$$r^2 = \frac{Q}{2\tilde{\omega}^2}\sin 2\tilde{\omega}\tau + r_0^2\,, \quad r = \sqrt{\frac{Q}{2\tilde{\omega}^2}\sin 2\tilde{\omega}\tau + r_0^2}\,, \tag{42}$$

where r_0 is the initial displacement in the r-direction.

Substituting (42) into (32) we obtain φ,

$$\begin{aligned}\varphi = &\int_0^{\tau}\left(\frac{B}{r^2} - \tilde{\omega}\right) d\tau = -\tilde{\omega}\tau + \frac{\tilde{\omega} B}{\sqrt{Q^2 - 4\omega^4 r_0^4}} \times \\ &\times \ln\left|\frac{\left(Q + \sqrt{Q^2 - 4\tilde{\omega}^4 r_0^4}\right)\tan\tilde{\omega}\tau + 2\tilde{\omega}^2 r_0^2}{\left(Q - \sqrt{Q^2 - 4\tilde{\omega}^4 r_0^4}\right)\tan\tilde{\omega}\tau + 2\tilde{\omega}^2 r_0^2}\right| + \varphi_0\,,\end{aligned} \tag{43}$$

where φ_0 is the initial displacement in the φ-direction.

Substituting Ω from (25) into (27), and eliminating the terms containing $\frac{GM}{c^2 r}$ and $\frac{\omega^2 r^2}{c^2}$, we obtain the observable velocity of the light beam in the z-direction

$$\dot{z} = \frac{\omega^2 \mathrm{v} r^2}{c^2} + \dot{z}_0 - \frac{\omega^2 \mathrm{v} r_0^2}{c^2}\,, \tag{44}$$

the integration of which gives its observable displacement

$$z = \dot{z}_0\tau + \frac{\omega^2 Q \mathrm{v}}{4\tilde{\omega}^3 c^2}\left(1 - \cos 2\tilde{\omega}\tau\right) + z_0\,, \tag{45}$$

which, taking into account that $\tilde{\omega} = \omega\left(1 + \frac{\mathrm{v}\dot{z}_0}{c^2}\right)$, is

$$z = \dot{z}_0\tau + \frac{\mathrm{v}Q}{4\tilde{\omega}c^2}\left(1 - \cos 2\tilde{\omega}\tau\right)\left(1 - \frac{\mathrm{v}\dot{z}_0}{c^2}\right)^2 + z_0\,. \tag{46}$$

We have obtained solutions for $\dot{r}$, $\dot{\varphi}$, $\dot{z}$ and r, φ, z. We see the galactic velocity of the Earth in only $\dot{z}$ and z.

Let's find corrections to the displacement of the light $\dot{z}$ and its displacement z caused by the motion of the Earth in the rotating and gravitating space of the Galaxy.

As follows from formula (41), Q doesn't include the initial velocity and displacement of the light beam in the z-direction. Besides, $Q = 0$ if $\dot{r}_0 = 0$ and $r_0 = 0$. In a real situation $\dot{r}_0 \neq 0$, because the light beam is emitted from the Earth so r_0 is the distance between the Sun and the Earth. Hence, in our consideration, $Q \neq 0$ always. If $\dot{\varphi}_0 = 0$, the light beam is directed strictly towards the Sun.

We calculate the correction to the light velocity in the r-direction $\Delta\dot{z}_0$ (we mean $\dot{\varphi}_0 = 0, \dot{z}_0 = 0$). Eliminating the term $1 - \frac{\mathrm{v}\dot{z}_0}{c^2}$ we obtain

$$\Delta\dot{z} = \frac{Q\mathrm{v}}{2c^2}\sin 2\tilde{\omega}\tau\,, \qquad Q = \dot{r}_0\sqrt{\dot{r}_0^2 + 4\tilde{\omega}^2 r_0^2}\,. \tag{47}$$

We see that the correction $\Delta\dot{z}_0$ is a periodical function, the frequency of which is twice the angular velocity of the Earth's rotation around the Sun; $2\tilde{\omega} = 4\times 10^{-7}\mathrm{sec}^{-1}$. Because the initial value of the light velocity is $\dot{r}_0 = c$, and also $4\tilde{\omega}^2 r_0^2 \ll c^2$, we obtain the amplitude of the harmonic oscillation

$$\frac{Q\mathrm{v}}{2c^2} = \frac{\dot{r}_0^2}{2c^2}\sqrt{1 + \frac{4\tilde{\omega}^2 r_0^2}{c^2}} \approx \frac{\mathrm{v}}{2}\,, \tag{48}$$

then the correction to the light velocity in the r-direction $\Delta\dot{z}_0$ is,

$$\Delta\dot{z} = \frac{\mathrm{v}}{2}\,\sin 2\tilde{\omega}\tau\, = 4\times 10^{-4}\left(\sin 2\tilde{\omega}\tau\right) c\,. \tag{49}$$

From this resulting "key formula" we have obtained we conclude that:

> The component of the observable vector of the light velocity directed towards the Sun (the r-direction) gains an addition (correction) in the z-direction, because the Earth moves in common with the Sun in the

Galaxy. The obtained correction manifests as a harmonic oscillation added to the world-invariant of the light velocity c. The expected amplitude of the oscillation is $4\times10^{-4}c$, i. e. 120 km/sec; the period $T=\frac{1}{2\tilde{\omega}}$ is half the astronomical year. So the theory predicts an anisotropy of the observable velocity of light due to the inhomogeneity and anisotropy of space, caused by its rotation and the presence of gravitation.

In our statement the anisotropy of the velocity of light manifests in the z-direction. We therefore, in this statement, call the z-direction the *preferred direction*.

We can verify the anisotropy of the velocity of light by experiment. By the theory of observable quantities [4, 5], the invariant c is the length

$$c=\sqrt{h_{ik}\,c^i c^k}=\sqrt{\frac{h_{ik}\,dx^i dx^k}{d\tau}}=\frac{d\sigma}{d\tau} \qquad (50)$$

of the chr.inv.-vector $c^i=\frac{dx^i}{d\tau}$ of the observable light velocity. Let a light beam be directed towards the Sun, i. e. in the r-direction. According to our theory, the Earth's motion in the Galaxy deviates the beam away from the r-axis so that we should observe an additional z-component to the light velocity invariant. Let's set up two pairs of detectors (synchronised clocks) along the r-direction and z-direction in order to measure time intervals during which the light beams travel in these directions. Because the distances $\Delta\sigma$ between the clocks are fixed, and c is constant, the measured time in the z-direction is expected to have a dilation with respect to that measured in the r-direction: by formula (49) the light velocity measured in both directions is expected to be differ by ~120 km/sec at the maximum of the effect.

The most suitable equipment for such an experiment is that used by R. T. Cahill (Flinders University, Australia) in his current experiments on the measurement of the velocity of light in an RF coaxial-cable equipped with a pair of high precision synchronized Rb atomic clocks [11]. This effect probably had a good chance of being detected in similar experiments by D. G. Torr and P. Colen (Utah State University, USA) in the 1980's [12] and, especially, by Roland De Witte (Belgacom Laboratory of Standards, Belgium) in the 1990's [13]. However even De Witte's equipment had a measurement precision a thousand times lower than that currently used by Cahill.

Because the Earth rotates around its own axis we should observe a weak daily variation of this effect. In order to register the complete variation of this value, we should measure it at least during half the astronomical year (one period of its variation).

4 Inhomogeneity and anisotropy of space along the Earth's transit in the Galaxy

We just applied the metric (3) to the Earth's motion in the Galaxy. Following this approach, we can also employ this metric to other preferred directions in the Universe, connected to the motion of another space body, for instance — the motion of our Galaxy in the Local Group of galaxies.

Astronomical observations show that the Sun moves in common with our Galaxy in the Local Group of galaxies at the velocity 700 km/sec.* The metric (3) can take into account this aspect of the Earth's motion as well. In such a case we should expect two weak maximums in the time dilation measured in the above described experimental system during the 24-hour period, when the z-direction coincides with the direction of the apex of the Sun. The amplitude of the variation of the observable light velocity should be 2.8 times the variation caused by the Earth's motion in the Galaxy.

Swedish astronomers in the 1950's discovered that the Local Group of galaxies is a part of an compact "cloud" called the Supercluster of galaxies, consisting of galaxies, small groups of galaxies, and two clouds of galaxies. The Supercluster has a diameter of ~98 million light years, while our Galaxy is located at 62 million light years from the centre. The Supercluster rotates with a period of ~100 billion years in the central area and ~200 billion years at the periphery. As supposed by the Swedes, our Galaxy, located at $\sim2/3$ of the Supercluster's radius, from its centre, rotates around the centre at a velocity of ~700 km/sec. (See Chapter VII, §6 in [14] for the details.)

In any case, in any large scale our metric (3) gives the same result, because any of the spaces is non-holonomic (rotates) around its own centre of gravity. All the spaces are included, one into the other, and cause bizarre spirals in their motions. The greater the number of the space structures taken onto account by our metric (3), the more complicated is the spiral traced out by the Earth observer in the space — the spiral is plaited into other space spirals (the fractal structure of the Universe [15]).

This analysis of our theoretical results, obtained by General Relativity, and the well-known data of observational astronomy leads us to the obvious conclusion:

The main factors forming the observable structure of the space of the Universe are gravitational fields of bulky bodies and their rotations, not the space deformations as previously thought.

Many scientists consider homogeneous isotropic models as models of the real Universe. A homogeneous isotropic space-time is described by Friedmann's metric

$$ds^2=c^2dt^2-R^2\frac{dx^2+dy^2+dz^2}{\left[1+\frac{k}{4}\left(x^2+y^2+z^2\right)\right]^2}\,, \qquad (51)$$

where $R=R(t)$; $k=0,\pm1$. For such a space, the main observable characteristics are $F^i=0$, $A_{ik}=0$, $D_{ik}\neq0$. In other words, such a space can undergo deformation (expansion,

*The direction of this motion is pointed out in the sky as the apex of the Sun. Interestingly, the Sun has a slow drift of 20 km/sec in the same direction as the apex, but within the Galaxy with respect to its plane.

compression, or oscillation), but it is free of rotation and contains no gravitating bodies (fields). So the metric (51) is the necessary and sufficient condition for homogeneity and isotropy. This is a model constructed by an imaginary observer who is located so far away from matter in the real Universe that he sees no such details as stars and galaxies.

In contrast to them, we consider a cosmological model constructed by an Earth observer, who is carried away by all motions of our planet. Zelmanov, the pioneer of inhomogeneous anisotropic relativistic models, pointed out the mathematical conditions of a space's homogeneity and isotropy, expressed with the terms of physically observable characteristics of the space [4]. The conditions of isotropy are

$$F_i = 0\,, \quad A_{ik} = 0\,, \quad \Pi_{ik} = 0\,, \quad \Sigma_{ik} = 0\,, \qquad (52)$$

where $\Pi_{ik} = D_{ik} - \frac{1}{3} D h_{ik}$ and $\Sigma_{ik} = C_{ik} - \frac{1}{3} C h_{ik}$ are the factors of anisotropy of the space deformation and the three-dimensional (observable) curvature. In a space of the metric (3) we have $D_{ik} = 0$, hence there $\Pi_{ik} = 0$. However F_i and A_{ik} are not zero in such a space (see formulae 10 and 11). Besides these there are the non-zero quantities,

$$\begin{aligned} \Sigma_{11} &= -\frac{1}{3}\frac{GM}{c^2 r^3} + \frac{\omega^2}{c^2}\,; \\ \Sigma_{22} &= -\frac{1}{3}\frac{GM}{c^2 r^2} + \frac{\omega^2 r}{c^2}\,; \\ \Sigma_{33} &= \frac{2}{3}\frac{GM}{c^2 r^3} - \frac{2\omega^2}{c^2}\,. \end{aligned} \qquad (53)$$

We see that a space of the metric (3) is anisotropic due to its rotation and gravitation.

The conditions of homogeneity, by Zelmanov [4], are

$$\nabla_j F_i = 0\,, \quad \nabla_j A_{ik} = 0\,, \quad \nabla_j D_{ik} = 0\,, \quad \nabla_j C_{ik} = 0\,. \qquad (54)$$

Calculating the conditions for the metric (3), we obtain

$$\begin{aligned} &\nabla_1 C_{11} = \frac{3GM}{c^2 r^4}\,, \qquad \nabla_1 C_{22} = \frac{3GM}{c^2 r^2}\,, \\ &\nabla_1 F_1 = \omega^2\left(1 + \frac{3\omega^2 r^2}{c^2}\right) + \frac{2GM}{r^3}\left(1 + \frac{3GM}{c^2 r}\right), \\ &\nabla_1 A_{12} = -\omega\left(\frac{2}{r^2} + \frac{\omega^2}{c^2} + \frac{3GM}{c^2 r^3}\right). \end{aligned} \qquad (55)$$

This means, a space of the metric (3) is inhomogeneous due to its rotation and gravitation.

The results we have obtained manifest thus:

> The real space of our Universe, where space bodies move, is inhomogeneous and anisotropic. Moreover, the space inhomogeneity and anisotropy determine the bizarre structure of the Universe which we observe: the preferred directions along which the space bodies move, and the hierarchial distribution of the motions.

5 Conclusions

By means of General Relativity we have shown that the space metric (3) along the Earth's trajectory in the Galaxy, where the Earth follows a complicated spiral traced out by its orbital motion around the Sun and its concomitant motion with the whole solar system around the centre of the Galaxy. We have shown that this metric space is: (a) globally non-holonomic due to its rotation and the presence of gravitation, as manifested by the non-holonomic chr.inv.-tensor A_{ik} (11) calculated in the metric space*; (b) inhomogeneous, because the chr.inv.-Christoffel symbols Δ^k_{ij} indicating inhomogeneity of space, being calculated in the metric space as shown by (17), contain gravitation and space rotation; (c) curved due to gravitation and space rotation, represented in the formulae for the three-dimensional chr.inv.-curvature C_{iklj} calculated in the metric space as shown by (18).

Consequently, in real space there exist "preferred" spatial directions along which space bodies undergo their orbital motions.

We have deduced that the observable velocity of light should be anisotropic in space due to the anisotropy and inhomogeneity of space, caused by the aforementioned factors of gravitation and space rotation, despite the world-invariance of the velocity of light. It has been calculated that two pairs of synchronised clocks should record different values for the speed of light in light beams directed towards the Sun and orthogonal to this direction, at about $4\times10^{-4}\,c$ (0.04% of the measured velocity of light c, i. e. ~ 120 km/sec). This effects should undergo oscillations with a 12-hour period (due to the daily rotation of the Earth) and with a 6-month period (due to the motion of the Earth around the Sun). Equipment most suitable for detecting the effect is that used by R. T. Cahill (Flinders University, Australia) in his current experiment on the measurement of the velocity of light in a one-way RF coaxial-cable equipped with a pair of high precision synchronized Rb atomic clocks.

The predicted anisotropy of the observable velocity of light has been deduced as a direct consequence of the geometrical structure of four-dimensional space-time. Therefore, if the predicted anisotropy is detected by experiment, it will be one more fact in support of Einstein's General Theory of Relativity.

The anisotropy of the observable velocity of light as a consequence of General Relativity was first pointed out by D. Rabounski in the editorial preface to [13], his papers [6, 7], and many private communications with the author, which commenced in Autumn, 2005. He has stated that the anisotropy results from the non-holonomity (rotation) of the

*Gravitation is represented by the mass of the Sun M, while the space rotation is represented by two factors: the angular velocity ω of the solar space rotation in the Earth's orbit (equal to the angular velocity of the Earth's rotation around the Sun), and also the linear velocity v of the rotation of the Sun in common with the whole solar system around the centre in the Galaxy.

local space of a real observer and/or the non-holonomity of the background space of the whole Universe. Moreover, the non-holonomic field of the space background can produce energy, if perturbed by a local rotation or oscillation (as this was theoretically found for stars [6, 7]).

Detailed calculations provided in the present paper show not only that the non-holonomity (rotation) of space is the source of the anisotropy of the observable velocity of light, but also gravitational fields.

This paper will be followed by a series of papers wherein we study the interaction between the fields of the space non-holonomity, and also consider these fields as new sources of energy. This means that we consider open systems. Naturally, given the case of an inhomogeneous anisotropic universe, it is impossible to study it as a closed system since such systems don't physically exist owing to the presence of space non-holonomity and gravitation*. In a subsequent paper we will consider the non-holonomic fields in a space of the metric (3) with the use of Einstein's equations. It is well known that the equations can be applied to a wide variety distributions of matter, even inside atomic nuclei. We can therefore, with the use of the Einstein equations, study the non-holonomic fields and their interactions in any scaled part of the Universe — from atomic nuclei to clusters of galaxies — the problem statement remains the same in all the considerations.

References

1. Crothers S. J. On the general solution to Einstein's vacuum field for the point-mass when $\lambda \neq 0$ and its implications for relativistic cosmology. *Progress in Physics*, 2005, v. 3, 7–18.
2. Crothers S. J. A brief history of black holes. *Progress in Physics*, 2006, v. 2, 54–57.
3. Borissova L. Gravitational waves and gravitational inertial waves in the General Theory of Relativity: a theory and experiments. *Progress in Physics*, 2005, v. 2, 30–62.
4. Zelmanov A. L. Chronometric invariants. Dissertation thesis, 1944. American Research Press, Rehoboth (NM), 2006.
5. Zelmanov A. L. Chronometric invariants and co-moving coordinates in the general relativity theory. *Doklady Acad. Nauk USSR*, 1956, v. 107(6), 815 – 818.
6. Rabounski D. Thomson dispersion of light in stars as a generator of stellar energy. *Progress in Physics*, 2006, v. 4, 3–10.
7. Rabounski D. A source of energy for any kind of star. *Progress in Physics*, 2006, v. 4, 19–23.
8. Schouten J. A., Struik D. J. Einführung in die neuren Methoden der Differentialgeometrie. *Zentralblatt für Mathematik*, 1935, Bd. 11 und Bd. 19.
9. Rabounski D., Borissova L. Particles here and beyond the Mirror. Editorial URSS, Moscow, 2001; arXiv: gr-qc/0304018.
10. Borissova L., Rabounski D. Fields, vacuum, and the mirror Universe. Editorial URSS, Moscow, 2001; CERN, EXT-2003-025.
11. Cahill R. T. A new light-speed anisotropy experiment: absolute motion and gravitational waves detected. *Progress in Physics*, 2006, v. 4, 73–92.
12. Torr D. G., Kolen P. An experiment to measure relative variations in the one-way velocity of light. *Precision Measurements and Fundamental Constants*, Natl. Bur. Stand. (U. S.), Spec. Publ., 1984, v. 617, 675–679.
13. Cahill R. T. The Roland De Witte 1991 experiment (to the memory of Roland De Witte). *Progress in Physics*, 2006, v. 3, 60–65.
14. Vorontsov-Velyaminov B. A. Extragalactic astronomy. Harwood Academic Publishers, N.Y., 1987.
15. Mandelbrot B. The fractal geometry of nature. W. H. Freeman, San Francisco, 1982.
16. Rabounski D. A theory of gravity like electrodynamics. *Progress in Physics*, 2005, v. 2, 15–29.

*According to the Copernican standpoint, the solar system should be a closed system, because that perspective doesn't take into account the fact that the solar system moves around the centre of the Galaxy, which carries it into other, more complicated motions.

Preferred Spatial Directions in the Universe. Part II. Matter Distributed along Orbital Trajectories, and Energy Produced from It

Larissa Borissova
E-mail: lborissova@yahoo.com

Using General Relativity we study the rotating space of an orbiting body (of the Earth in the Galaxy, for example). In such a space Einstein's equations predict that: (1) the space cannot be empty; (2) it abhors a vacuum (i. e. a pure λ-field), and so it must also possess a substantive distribution (e. g. gas, dust, radiations, etc.). In order for Maxwell's equations to satisfy Einstein's equations, it is shown that: (1) a free electromagnetic field along the trajectory of an orbiting body must be present, by means of purely magnetic "standing" waves; (2) electromagnetic fields don't satisfy the Einstein equations in a region of orbiting space bodies if there is no distribution of another substance (e. g. dust, gas or something else). The braking energy of a medium pervading space equals the energy of the space non-holonomic field. The energy transforms into heat and radiations within stars by a stellar energy mechanism due to the background space non-holonomity, so a star takes energy for luminosity from the space during the orbit. Employing this mechanism in an Earth-bound laboratory, we can obtain a new source of energy due to the fact that the Earth orbits in the non-holonomic fields of the space.

1 If a body undergoes orbital motion in a space, the space cannot be empty

This paper extends a study begun in *Preferred Spatial Directions in the Universe: a General Relativity Approach* [1]. We considered a space-time described by the metric*

$$ds^2 = \left(1-\frac{2GM}{c^2r}-\frac{\omega^2r^2}{c^2}\right)c^2dt^2-\frac{2\omega r^2}{c}\,cdt\,d\varphi- \\ -\left(1+\frac{2GM}{c^2r}\right)dr^2-r^2d\varphi^2-\frac{2\omega \mathrm{v} r^2}{c^2}\,d\varphi\,dz-dz^2, \quad (1)$$

where $G = 6.67\times10^{-8}\,\frac{\mathrm{cm}^3}{\mathrm{g}\times\mathrm{sec}^2}$ is Newton's gravitational constant, M is the value of an attracting mass around which a test-body orbits, ω is the cyclic frequency of the orbital motion, v is the linear velocity at which the body, in common with the gravitating mass, moves with respect to the observer and his references.

In fact, this metric describes (in quasi-Newtonian approximation) the space along the path of a body which orbits another body and moves in common with it with respect to the observer's reference frame (which determine his physical reference space), for instance, the motion of the Earth in the Galaxy. So this metric is applicable to bodies orbiting anywhere in the Universe.

Here we study, using Einstein's equations, a space described by the metric (1). This approach gives a possibility of answering this question: does some matter (substance and/or fields) exist along the trajectory of an orbiting body, and what is that matter (if present there)?

*The metric is given in the cylindrical spatial coordinates r, φ, z. See [1] for the reason.

The general covariant Einstein equations are†

$$R_{\alpha\beta}-\frac{1}{2}\,g_{\alpha\beta}\,R=-\kappa\,T_{\alpha\beta}-\lambda\,g_{\alpha\beta}\,, \quad (2)$$

where $R_{\alpha\beta}$ is Ricci's tensor, $g_{\alpha\beta}$ is the fundamental metric tensor, R is the scalar (Riemannian) curvature, $\kappa=\frac{8\pi G}{c^2}=$ $=1.86\times10^{-27}\,\frac{\mathrm{cm}}{\mathrm{g}}$ is Einstein's gravitational constant, $T_{\alpha\beta}$ is the energy-momentum tensor of a distributed matter, λ is the so-called cosmological term that describes non-Newtonian forces of attraction or repulsion‡. A space-time is *empty* if $R_{\alpha\beta}=0$. In this case, $R=0$, $T_{\alpha\beta}=0$, $\lambda=0$, i. e. no substance and no λ-fields. A space-time is pervaded by *vacuum* if $T_{\alpha\beta}=0$ but $\lambda\neq0$ and hence $R_{\alpha\beta}\neq0$.

The Einstein equations can be applied to a wide variety of distributions matter, even inside atomic nuclei. We can therefore, with the use of the Einstein equations, study the distribution of matter in any scaled part of the Universe — from atomic nuclei to clusters of galaxies.

We use the Einstein equations in chronometrically invariant form, i. e. expressed in the terms of physical observed values (chronometric invariants, by A. Zelmanov [3, 4]). In such a form, the general covariant equations (2) are represented by the three sorts of their observable (chronometrically invariant) projections: the projection onto an observer's

†The space-time (four-dimensional) indices are $\alpha,\beta=0,1,2,3$.

‡Depending upon the sign of λ: $\lambda>0$ stands for repulsion, while $\lambda<0$ stands for attraction. The *cosmological term* is also known as the λ-term. The forces described by λ (known as λ-forces) grow in proportional to distance and therefore reveal themselves in full at a "cosmological" distance comparable to the size of the Universe. Because the non-Newtonian gravitational fields (λ-fields) have never been observed, for our Universe in general the numerical value of λ is expected to be $\lambda<10^{-56}\,\mathrm{cm}^{-2}$. Read Chapter 5 in [2] for the details.

time line, the mixed (space-time) projection, and the projection onto the observer's spatial section [3, 4]

$$\frac{{}^*\partial D}{\partial t} + D_{jl}D^{lj} + A_{jl}A^{lj} + {}^*\nabla_j F^j - \frac{1}{c^2}F_jF^j = \\ = -\frac{\kappa}{2}\left(\rho c^2 + U\right) + \widetilde{\lambda}c^2; \tag{3}$$

$${}^*\nabla_j\left(h^{ij}D - D^{ij} - A^{ij}\right) + \frac{2}{c^2}F_jA^{ij} = \kappa J^i; \tag{4}$$

$$\frac{{}^*\partial D_{ik}}{\partial t} - (D_{ij} + A_{ij})\left(D^j_k + A^{\cdot j}_{k\cdot}\right) + DD_{ik} - \\ - D_{ij}D^j_k + 3A_{ij}A^{\cdot j}_{k\cdot} + \frac{1}{2}\left({}^*\nabla_i F_k + {}^*\nabla_k F_i\right) - \\ - \frac{1}{c^2}F_iF_k - c^2C_{ik} = \\ = \frac{\kappa}{2}\left(\rho c^2 h_{ik} + 2U_{ik} - Uh_{ik}\right) + \widetilde{\lambda}c^2h_{ik}, \tag{5}$$

where $\rho = \frac{T_{00}}{g_{00}}$ is the observable density of matter, $J^i = \frac{cT^i_0}{\sqrt{g_{00}}}$ is the vector of the observable density of impulse, $U^{ik} = c^2T^{ik}$ is the tensor of the observable density of the impulse flow (the stress tensor), $U = h_{ik}U^{ik}$. We include $\widetilde{\lambda}$ in the equations because the metric (1) is applicable at any scale, not only the cosmological large scale*.

By the theory of physical observable quantities [3, 4], the quantities D_{ik}, F_i, A_{ik} and C_{ik} are the observable characteristics of the observer's reference space: the chr.inv.-tensor of the rates of the space deformation†

$$D_{ik} = \frac{1}{2}\frac{{}^*\partial h_{ik}}{\partial t}, \tag{6}$$

the chr.inv.-vector of the observable gravitational inertial force

$$F_i = \frac{c^2}{c^2 - \mathrm{w}}\left(\frac{\partial \mathrm{w}}{\partial x^i} - \frac{\partial v_i}{\partial t}\right), \tag{7}$$

the chr.inv.-tensor of the angular velocity of the observable rotation of the space (the space non-holonomity tensor)

$$A_{ik} = \frac{1}{2}\left(\frac{\partial v_k}{\partial x^i} - \frac{\partial v_i}{\partial x^k}\right) + \frac{1}{2c^2}\left(F_iv_k - F_kv_i\right), \tag{8}$$

where $h_{ik} = -g_{ik} + \frac{g_{0i}g_{0k}}{g_{00}} = -g_{ik} + \frac{1}{c^2}v_iv_k$ is the observable spatial chr.inv.-metric tensor, $v_i = -\frac{cg_{0i}}{\sqrt{g_{00}}}$ is the linear velocity of the rotation of the observer's space reference, $\mathrm{w} = c^2\left(1 - \sqrt{g_{00}}\right)$ is the gravitational potential. The quantity $C_{ik} = h^{mn}C_{imkn}$ is built on the tensor of the observable three-dimensional chr.inv.-curvature of the space

$$C_{imkn} = H_{imkn} - \frac{1}{c^2}\left(2A_{mi}D_{nk} + A_{in}D_{mk} + \right. \\ \left. + A_{nm}D_{ik} + A_{mk}D_{in} + A_{ki}D_{mn}\right), \tag{9}$$

which possesses all the properties of the Riemann-Christoffel curvature tensor $R_{\alpha\beta\gamma\delta}$ in the observer's spatial section, and constructed with the use $H_{lkij} = h_{jm}H^{\cdots m}_{lki\cdot}$, where $H^{\cdots m}_{lki\cdot}$ is the chr.inv-tensor similar to Schouten's tensor [5]

$$H^{\cdots m}_{lki\cdot} = \frac{{}^*\partial\Delta^j_{il}}{\partial x^k} - \frac{{}^*\partial\Delta^j_{kl}}{\partial x^i} + \Delta^m_{il}\Delta^j_{km} - \Delta^m_{kl}\Delta^j_{lm}, \tag{10}$$

while Δ^k_{ij} are the observable chr.inv.-Christoffel symbols

$$\Delta^k_{ij} = h^{km}\Delta_{ij,m} = \frac{1}{2}\left(\frac{{}^*\partial h_{im}}{\partial x^j} + \frac{{}^*\partial h_{jm}}{\partial x^i} - \frac{{}^*\partial h_{ij}}{\partial x^m}\right). \tag{11}$$

In the formulae $\frac{{}^*\partial}{\partial x^i} = \frac{\partial}{\partial x^i} - \frac{1}{c^2}\frac{{}^*\partial}{\partial t}$ and $\frac{{}^*\partial}{\partial t} = \frac{1}{\sqrt{g_{00}}}\frac{{}^*\partial}{\partial t}$ are the chr.inv.-spatial derivative and the chr.inv.-time derivative respectively, while ${}^*\nabla_i$ is the spatial chr.inv.-covariant derivative, for instance, the chr.inv.-divergence of a chr.inv.-vector is ${}^*\nabla_i q^i = \frac{{}^*\partial q^i}{\partial x^i} + q^i\frac{{}^*\partial \ln\sqrt{h}}{\partial x^i} = \frac{{}^*\partial q^i}{\partial x^i} + q^i\Delta^j_{ji}$. See [3, 4] or [2] for the details.

We have obtained [1] for the metric (1) the non-zero components of the observable chr.inv.-metric tensor

$$h_{11} = 1 + \frac{2GM}{c^2r}, \qquad h_{22} = r^2\left(1 + \frac{\omega^2r^2}{c^2}\right), \\ h_{23} = \frac{\omega r^2\mathrm{v}}{c^2}, \qquad h_{33} = 1, \\ h^{11} = 1 - \frac{2GM}{c^2r}, \qquad h^{22} = \frac{1 - \frac{\omega^2r^2}{c^2}}{r^2}, \\ h^{23} = -\frac{\omega\mathrm{v}}{c^2}, \qquad h^{33} = 1, \tag{12}$$

nonzero components of F^i and A_{ik}

$$F^1 = \left(\omega^2r - \frac{GM}{r^2}\right)\left(1 + \frac{\omega^2r^2}{c^2}\right), \\ A^{12} = \frac{\omega}{r}\left(1 - \frac{2GM}{c^2r} + \frac{\omega^2r^2}{2c^2}\right), \quad A^{31} = \frac{\omega^2\mathrm{v}r}{c^2}, \tag{13}$$

and non-zero components of C_{ik}

$$C_{11} = -\frac{GM}{c^2r^3} + \frac{3\omega^2}{c^2}, \quad C_{22} = -\frac{GM}{c^2r} + \frac{3\omega^2r^2}{c^2}. \tag{14}$$

Let's substitute the components of F_i, A_{ik}, C_{ik} and the chr.inv.-derivatives into the chr.inv.-Einstein equations (3), (4), and (5). We obtain

$$\omega^2 + \frac{GM}{r^3} + \frac{2\omega^4r^2}{c^2} - \frac{3\omega^2GM}{c^2r} = -\frac{\kappa}{2}\left(\rho c^2 + U\right) + \widetilde{\lambda}c^2; \tag{15}$$

$$\kappa J^1 = 0; \quad \kappa J^2 = \frac{5\omega GM}{c^2r^3}; \quad \kappa J^3 = -\frac{2\omega^2\mathrm{v}}{c^2}; \tag{16}$$

$$\frac{3GM}{r^3} + \frac{6\omega^4r^2}{c^2} - \frac{\omega^2GM}{c^2r} + \frac{6G^2M^2}{c^2r^4} = \\ = \left[\frac{\kappa}{2}\left(\rho c^2 - U\right) + \widetilde{\lambda}c^2\right]\left(1 + \frac{2GM}{c^2r}\right) + \kappa U_{11}; \tag{17}$$

*As probable $\widetilde{\lambda} \sim \frac{1}{R^2}$, where R is the spatial radius of a given region, so the larger the size of a considered region, the smaller is λ. See [2].

†The spatial (three-dimensional) indices are $i, k = 1, 2, 3$.

$$\frac{9\omega^4 r^4}{c^2} - \frac{9\omega^2 GM}{c^2 r} + \frac{2G^2M^2}{c^2 r^2} = \\ = \left[\frac{\kappa}{2}\left(\rho c^2 - U\right) + \widetilde{\lambda}c^2\right] r^2 \left(1 + \frac{\omega^2 r^2}{c^2}\right) + \kappa U_{22}\,; \tag{18}$$

$$\frac{\omega^3 \mathrm{v} r^2}{c^2} - \frac{\omega \mathrm{v} GM}{c^2 r} = \left[\frac{\kappa}{2}\left(\rho c^2 - U\right) + \widetilde{\lambda}c^2\right]\frac{\omega \mathrm{v} r^2}{c^2} + \kappa U_{23}\,; \tag{19}$$

$$\frac{\kappa}{2}\left(\rho c^2 - U\right) + \widetilde{\lambda}c^2 + \kappa U_{33} = 0\,. \tag{20}$$

Equations (15–20) are written for an arbitrary energy-momentum tensor $T_{\alpha\beta}$. As is well known, the left side of the Einstein equations must have a positive sign. We therefore conclude, from the first (scalar) chr.inv.-Einstein equation (15), that the cosmological term $\widetilde{\lambda}$ must be $\widetilde{\lambda} \geqslant 0$. (If $\widetilde{\lambda} > 0$, the non-Newtonian λ-force is the force of repulsion). So, in order to have the metric (1) satisfy the Einstein equations, we can have only the repulsive non-Newtonian forces in the given region described by the metric (1).

We express the right side of the general covariant Einstein equations (2) as the algebraic sum of two tensors

$$\kappa \widetilde{T}_{\alpha\beta} = \kappa T_{\alpha\beta} - \frac{\widetilde{\lambda}}{\kappa} g_{\alpha\beta}\,, \tag{21}$$

where the first tensor describes a substance, while the second describes vacuum (λ-fields). We assume that the given space is permeated by only λ-fields, i. e. $T_{\alpha\beta} = 0$. In such a case the observable components of the energy-momentum tensor of vacuum are

$$\widetilde{\rho} = -\frac{\widetilde{\lambda}}{\kappa}\,, \qquad \widetilde{J}^i = 0\,, \qquad \widetilde{U}^{ik} = \frac{\widetilde{\lambda}c^2}{\kappa}\,. \tag{22}$$

We see that the observable density of vacuum $\widetilde{\rho} = \mathrm{const}$ is $\widetilde{\rho} < 0$, if $\widetilde{\lambda} > 0$ and $\widetilde{J}^i = 0$. So the $\widetilde{\lambda}$-vacuum is a medium with a negative constant density, and also no flows of mass (energy) therein.

We obtain from the the second (vector) chr.inv.-Einstein equation (16): $J^1 = 0$, $J^2 \neq 0$, $J^3 \neq 0$ ($J^3 < 0$), so $J^i \neq 0$ in general. Because $J^i = 0$ in vacuum, we conclude that:

> Any region of space described by the metric specifically along the trajectory of any orbiting body in the Universe cannot be pervaded solely by vacuum, but must also be permeated by another distributed substance.
>
> Orbital motion is the main kind of motion in the Universe. We therefore conclude that the space of the Universe must be non-empty; necessarily filled by a substance (e. g. gas, dust, radiations, etc.). Being a direct deduction from the Einstein equations, this is one more fundamental fact predicted by Einstein's General Theory of Relativity.

Naturally, as astronomical observations in recent decades testify, such substances as gas, dust and radiations are found in any part of that region of the Universe that is accessible by modern astronomical techniques. We therefore aim to describe the medium pervading space, by means of the algebraical sum of two energy-momentum tensors

$$T_{\alpha\beta} = T^{(\mathrm{g})}_{\alpha\beta} + T^{(\mathrm{em})}_{\alpha\beta}\,, \tag{23}$$

where $T^{(\mathrm{em})}_{\alpha\beta}$ is set up for electromagnetic radiations as in [6], while $T^{(\mathrm{g})}_{\alpha\beta}$ describes an ideal liquid or gas

$$T^{(\mathrm{g})}_{\alpha\beta} = \left(\rho_{(\mathrm{g})} - \frac{p}{c^2}\right) b^\alpha b^\beta - \frac{p}{c^2}\, g^{\alpha\beta}, \tag{24}$$

where $\rho_{(\mathrm{g})}$ is the observable density of the medium, p is the pressure within it, while $b^\alpha = \frac{dx^\alpha}{ds}$ is the four-dimensional velocity of the flow of the medium with respect to the reference space (reference body). Gas is a medium in which particles move chaotically with respect to each other, and also with respect to an observer's reference space. So a reference space doesn't accompany to flow of mass (energy) in the gas.

The observable components of $T^{(\mathrm{g})}_{\alpha\beta}$ are

$$\frac{T_{00}}{g_{00}} = \frac{\rho_{(\mathrm{g})} - \frac{p}{c^2}}{1 - \frac{{}^*u^2}{c^2}} - \frac{p}{c^2}\,, \qquad J^i = \frac{\rho_{(\mathrm{g})} - \frac{p}{c^2}}{1 - \frac{{}^*u^2}{c^2}}\, {}^*u^i, \\ U^{ik} = \frac{\left(\rho_{(\mathrm{g})} - \frac{p}{c^2}\right) {}^*u^i {}^*u^k}{1 - \frac{{}^*u^2}{c^2}} + p h^{ik}, \tag{25}$$

while the trace of the stress-tensor U^{ik} is

$$U = \frac{\left(\rho_{(\mathrm{g})} - \frac{p}{c^2}\right) {}^*u^2}{1 - \frac{{}^*u^2}{c^2}} + 3p\,, \tag{26}$$

where ${}^*u^i = \frac{dx^i}{d\tau}$ is the three-dimensional observable velocity of the flow of the medium (${}^*u^2 = {}^*u_i {}^*u^i = h_{ik} {}^*u^i {}^*u^k$).

A reference frame (space) where the flow stream of a mass is $q^i = c^2 J^i \neq 0$, doesn't accompany the medium. As seen from (16) and (25), given the case we are considering, ${}^*u^1 = 0$, while ${}^*u^2 \neq 0$ and ${}^*u^3 \neq 0$. Hence:

> If a body orbits at a radius r in the z-direction, a substantive medium that necessarily pervades the space has motions in the φ and z-directions (in the cylindrical spatial coordinates r, φ, z).

2 Maxwell's equations in a rotating space: a body can orbit only if there is a non-zero interplanetary or interstellar magnetic field along the trajectory

What structure is attributed to an electromagnetic field if the field fills the local space of an orbiting body? As is well known, the energy-momentum tensor of an electromagnetic field has the form [6]

$$T^{(\mathrm{em})}_{\alpha\beta} = \frac{1}{4\pi c^2}\left(-F_{\alpha\sigma}F^{\sigma\cdot}_{\cdot\beta} + \frac{1}{4}\, F_{\sigma\tau}F^{\sigma\tau} g_{\alpha\beta}\right), \tag{27}$$

where $F_{\alpha\beta} = \frac{1}{2}\left(\frac{\partial A_\beta}{\partial x^\alpha} - \frac{\partial A_\alpha}{\partial x^\beta}\right)$ is Maxwell's electromagnetic field tensor, while A^α is the four-dimensional electromagnetic field potential given the observable chr.inv.-projections

$\varphi=\frac{A_0}{\sqrt{g_{00}}}$ and $q^i=A^i$ (the scalar and vector three-dimensional chr.inv-potentials). The observable chr.inv.-components of $T^{(\mathrm{em})}_{\alpha\beta}$ obtained in [2] are

$$\begin{aligned}
&\rho_{(\mathrm{em})}=\frac{E^2+H^{*2}}{8\pi c^2}\,,\quad J^i_{(\mathrm{em})}=\frac{1}{4\pi c}\,\varepsilon^{ikm}E_kH_{*m}\,,\\
&U^{ik}_{(\mathrm{em})}=\rho_{(\mathrm{em})}h^{ik}-\frac{1}{4\pi}\left(E^iE^k+H^{*i}H^{*k}\right),\\
&U_{(\mathrm{em})}=\rho_{(\mathrm{em})}\,,
\end{aligned}\tag{28}$$

where E_i and the H^{*i} are the observable chr.inv.-electric and magnetic field strengths, which are the chr.inv.-projections of the electromagnetic field tensor $F_{\alpha\beta}$ (read Chapter 3 in [2] for the details):

$$E_i=\frac{{}^*\partial\varphi}{\partial x^i}+\frac{1}{c}\frac{{}^*\partial q^i}{\partial t}-\frac{\varphi}{c^2}\,F^i,\tag{29}$$

$$H^{*i}=\frac{1}{2}\,\varepsilon^{imn}H_{mn}=\frac{1}{2}\,\varepsilon^{imn}\left(\frac{{}^*\partial q_m}{\partial x^n}-\frac{{}^*\partial q_n}{\partial x^m}-\frac{2\varphi}{c}A_{mn}\right).\tag{30}$$

We consider electromagnetic fields that fill the space as electromagnetic waves – free fields without the sources that induced them. By the theory of fields, in such an electromagnetic field the electric charge density and the current density vector are zero. In such a case Maxwell's equations have the chr.inv.-form [2]:

$$\left.\begin{aligned}
&{}^*\nabla_iE^i-\frac{2}{c}\,\Omega_mH^{*m}=0\\
&\varepsilon^{ikm}\,{}^*\widetilde{\nabla}_k\left(H_{*m}\sqrt{h}\right)-\frac{1}{c}\frac{{}^*\partial}{\partial t}\left(E^i\sqrt{h}\right)=0
\end{aligned}\right\}\ \mathrm{I}\tag{31}$$

$$\left.\begin{aligned}
&{}^*\nabla_iH^{*i}+\frac{2}{c}\,\Omega_mE^{*m}=0\\
&\varepsilon^{ikm}\,{}^*\widetilde{\nabla}_k\left(E_m\sqrt{h}\right)+\frac{1}{c}\frac{{}^*\partial}{\partial t}\left(H^{*i}\sqrt{h}\right)=0
\end{aligned}\right\}\ \mathrm{II}\tag{32}$$

where $H_i=\frac{1}{2}\,\varepsilon_{imn}H^{mn}$, and ${}^*\widetilde{\nabla}_k={}^*\nabla_k-\frac{1}{c^2}\,F_k$ denotes the chr.inv.-physical divergence.

Because of the ambiguity of the four-dimensional potential A^α, we can choose for $\varphi=0$ [6]. A space wherein the metric (1) is stationary, gives $\frac{{}^*\partial q^i}{\partial t}=0$. Because the components of $g_{\alpha\beta}$ depend solely on $x^1=r$ of the spatial coordinates r, φ, z, the components of the energy-momentum tensor depend only on r. In such a case we obtain, from formulae (29) and (30), $E_i=0$, $H^{*1}=H_{*1}=0$, $H^{*2}=\frac{1}{\sqrt{h}}\frac{\partial q_3}{\partial r}$ and $H^{*3}=-\frac{1}{\sqrt{h}}\frac{\partial q_2}{\partial r}$, so the aforementioned chr.inv.-Maxwell equations take the form

$$\begin{aligned}
&\Omega_mH^{*m}=0\,,\\
&\varepsilon^{ikm}\,{}^*\widetilde{\nabla}_k\left(H_{*m}\sqrt{h}\right)=0\,,\\
&{}^*\nabla_iH^{*i}=0\,.
\end{aligned}\tag{33}$$

We substitute into the first of these equations the values $\Omega_1=0$, $\Omega_2=\frac{\omega^2r\mathrm{v}}{c^2}$ and $\Omega_3=\frac{\omega}{r}\left(1-\frac{2GM}{c^2r}+\frac{\omega^2r^2}{2c^2}\right)$ we have calculated for the metric (1). As a result we obtain a correlation between two components of the electromagnetic field vector chr.inv.-potential q^i, that is

$$q_2'=\frac{\omega\mathrm{v}r^2}{c^2}\,q_3'\,,\tag{34}$$

where the prime denotes the differentiation with respect to r.

With the use of (30) we obtain H_{*2} and H_{*3}

$$H_{*2}=r\left(1-\frac{GM}{c^2r}+\frac{\omega^2r^2}{2c^2}\right)q_3'\,,\quad H_{*3}=0\,,\tag{35}$$

so the second equation of (33) takes the form

$$rq_3''\left(1-\frac{GM}{c^2r}+\frac{\omega^2r^2}{2c^2}\right)+q_3'\left(2-\frac{GM}{c^2r}+\frac{2\omega^2r^2}{c^2}\right)=0,\tag{36}$$

while the third equation of (33) is satisfied identically.

Equation (36) has separable variables, and so can be rewritten as follows

$$\frac{dy}{y}=-\frac{dr}{r}\left(1+\frac{3\omega^2r^2}{2c^2}\right),\tag{37}$$

where $y=q_3'$. Integrating it, we obtain

$$y=q_3'=\frac{K}{r}\,e^{-\frac{3\omega^2r^2}{4c^2}}\approx\frac{K}{r}\left(1-\frac{3\omega^2r^2}{4c^2}\right),\tag{38}$$

where K is a constant of integration. Assuming $r=r_0$ and $y_0=q_{3(0)}$ at the initial moment of time, we determine the constant: $K=y_0\,r_0\left(1+\frac{3\omega^2r_0^2}{4c^2}\right)$. Integrating (38), we have

$$q_3=K\left(\ln r-\frac{3\omega^2r^2}{8c^2}\right)+L\,,\quad L=\mathrm{const}.\tag{39}$$

Determining the integration constant L from the initial conditions, we obtain the final expression for q_3:

$$q_3=K\left[\ln\frac{r}{r_0}-\frac{3\omega^2}{8c^2}\left(r^2-r_0^2\right)\right]+q_3(0)\,,\tag{40}$$

where $q_3(0)$ is the initial value of q_3. Substituting (40) into (34) we obtain the equation

$$q_2'=\frac{\omega\mathrm{v}Kr}{c^2}\,,\tag{41}$$

which is easily integrated to

$$q_2=\frac{\omega\mathrm{v}K}{2c^2}\left(r^2-r_0^2\right).\tag{42}$$

Finally, we calculate the non-zero components of the magnetic strength chr.inv.-vector H^{*i}. Substituting the obtained formulae for q_3' (38) and q_2' (41) into the definition of H^{*i} (30), we obtain

$$\begin{aligned}
&H^{*2}=\frac{1}{\sqrt{h}}H_{31}=q_3'(0)\left(1-\frac{GM}{c^2r}-\frac{\omega^2r^2}{2c^2}+\frac{3\omega^2r_0^2}{4c^2}\right),\\
&H^{*3}=\frac{1}{\sqrt{h}}H_{12}=-\frac{\omega\mathrm{v}r_0}{c^2}\,q_3'(0)\,.
\end{aligned}\tag{43}$$

This is the solution for H^{*i}, the magnetic strength chr. inv.-vector, obtained from the chr.inv.-Maxwell equations in the rotating space of an orbiting body. The solution we have obtained shows that:

> A free electromagnetic field along the trajectory of an orbiting body ($\omega \neq 0$, $\mathrm{v} \neq 0$) cannot be zero, and is represented by purely magnetic "standing" waves (all components of the electric strength are $E^i = 0$).

This fundamental conclusion is easily obtained from the solution (43).

The linear velocity v of the orbiting body (the body moves in the $x^3 = z$-direction) produces effects in only the q_2-component of the three-dimensional observable vector potential (i. e. along the φ-direction).

The solution (43) exists only if the initial value of the derivative with respect to r of the z-component of the three-dimensional observable vector potential is $q_3'(0) \neq 0$.

The z-component $H^{*3} \neq 0$ if the reference body (in common with the observer) moves in the $x^3 = z$-direction at a linear velocity v and, at the same time, rotates orthogonally to it in the $x^2 = \varphi$-direction at an angular velocity ω. The component H^{*3} is positive, if v is negative. So H^{*3} is directed opposite to the motion of the observer (and his reference planet, the Earth for instance). The numerical value of H^{*3} is $\sim 8 \times 10^{-8}$ of H^{*2}. If the reference planet has its orbit "stopped" in the z-direction (a purely theoretical case), only $H^{*2} \neq 0$ is left because it depends on $\frac{GM}{c^2 r}$ and $\frac{\omega^2 r^2}{2c^2}$.

The stationary solution (43) of the chr.inv.-Maxwell equations describes standing magnetic waves in the φ- and z-directions. In such a case, as follows from the condition $E_i = 0$, the Pointing vector (the density of the impulse of the electromagnetic field) is $J^i_{(\mathrm{em})} = 0$ (see formula 28). On the other hand the Einstein equations (15–20) we have obtained for the rotating space of an orbiting body (the same space as that used for the Maxwell equation) have the density of the impulse of matter $J^i \neq 0$ (see formula 16 in the Einstein equations), which should be applicable to any distribution of matter, including electromagnetic fields. This implies that:

> In the rotating space of an orbiting body, electromagnetic fields don't satisfy the Einstein equations if there is no distribution of another substance (dust, gas or something else) in addition to the fields.

As follows from (25) we have obtained in the metric considered, $J^i \neq 0$ for an ideal liquid or gas. So, if an electromagnetic field is added by a gaseous medium (for instance), they can together satisfy the Einstein equations in the rotating space of an orbiting body. We therefore conclude that:

> Interplanetary/interstellar space where space bodies are orbiting, must be necessarily pervaded by electromagnetic fields with a concomitant distribution of substantial matter, such as a gaseous medium, for instance.

We have actually shown that space bodies cannot undergo orbital motion in empty space, i. e. if electromagnetic fields and other substantive media (e. g. dust, gas, etc.) are not present. What a bizarre result!

It should be noted that we have obtained this startling conclusion using no preliminary proposition or hypothesis. This conclusion follows directly from the requirement for Maxwell's equations and Einstein's equations to be both satisfied in the rotating space of an orbiting body. So this is the *actual condition for orbital motion*, according to General Relativity.

3 Preferred spatial directions as a result of the interaction of the space non-holonomity fields

In this section we have to consider three problems arising from the specific space structure we have obtained for orbital motion.

First problem. Refer to the chr.inv.-Einstein equations (15–20) we have obtained in the rotating space of an orbiting body. The most significant terms in the left side of the scalar equation (15) are the first two. They both have a positive sign. Hence the right side of equation (15) must also be positive, i. e. the right side must satisfy the condition,

$$\widetilde{\lambda} c^2 > \frac{\kappa}{2} \left(\rho c^2 + U \right). \qquad (44)$$

Let's apply this condition to a particular case of the orbiting body spaces: the space within the corridor along which the Earth orbits in the Galaxy. As a matter fact, this space is governed by the metric (1). In this space we have, $\omega^2 = 4 \times 10^{-14}\,\mathrm{sec}^{-2}$, $M = M_\odot = 2 \times 10^{33}\,\mathrm{g}$, $r = 15 \times 10^{12}\,\mathrm{cm}$. We obtain, $\omega^2 + \frac{GM}{r^3} \simeq 8 \times 10^{-14}\,\mathrm{sec}^{-2}$. Therefore

$$\widetilde{\lambda} c^2 > 8 \times 10^{-14}\,\mathrm{cm}^{-2}, \qquad \widetilde{\lambda} > 10^{-34}\,\mathrm{cm}^{-2}. \qquad (45)$$

As a result $\widetilde{\lambda} > 10^{-34}\,\mathrm{cm}^{-2}$ numerically equals $\frac{\omega^2}{2c^2}$ — the quantity which was proven in [7] to be the square of the dynamical "magnetic" strength of the field of the space non-holonomity. We therefore conclude that the $\widetilde{\lambda}$-field is connected to the non-holonomity field of the Earth's space.

We note that the Earth's space is non-holonomic due to the effect of a number of factors such as the daily rotation of the Earth, its yearly rotation around the Sun, its common rotation with the solar system around the centre of the Galaxy, etc. Each factor produces a field of non-holonomity, the algebraical sum of which gives the complete field of non-holonomity of the Earth.

Given the problem statement we are considering, the obtained numerical value $\widetilde{\lambda} > 10^{-34}\,\mathrm{cm}^{-2}$ characterizing the non-Newtonian force of repulsion is attributed to the non-holonomity field of the Earth's space which is caused by the Earth's rotation around the Sun. If other problem statements are considered, we can calculate the numerical values of $\widetilde{\lambda}$ characterizing the other factors of the Earth's space non-holonomity. The non-Newtonian forces of repulsion obtained

therein are expected to be directed according to the acting factors (in different directions), so the numerical value of each $\widetilde{\lambda}$ has its own meaning, whilst their sum builds the common non-Newtonian repulsing force acting in the Earth's space.

Second problem. As follows from the scalar Einstein equation (16), the density of the impulse of the distributed matter in the $x^3 = z$-direction

$$J^3 = -\frac{2\omega^2 \mathrm{v}}{\kappa c^2} \tag{46}$$

has a negative numerical value. So the flow of the distributed medium that fills the space is directed opposite to the orbital motion. In other words, according to the theory, the orbiting body should meet a counter-flow by the medium: a "relativistic braking" should be expected in orbital motions. Because the orbiting bodies, e. g. the stars, the planets and the satellites, show no such orbital braking, we propose a mechanism that refurbishes the braking energy of the medium into another sort of energy — heat or radiations, for instance.

This conclusion finds verification in recent theoretical research which, by means of General Relativity, indicates that stars produce energy due to the background space non-holonomity [8, 9]. It is shown in papers [8, 9], that General Relativity, in common with topology, predicts that the most probable configuration of the background space of the Universe is globally non-holonomic. The global anisotropic effect is expected to manifest as the anisotropy of the Cosmic Microwave Background Radiation and the anisotropy of the observable velocity of light. Moreover, if the global non-holonomic background is perturbed by a local rotation or oscillation (local non-holonomic fields), the background field produces energy in order to compensate for the perturbation in it. Such an energy producing mechanism is expected to be operating in stars, in the process of transfer of radiant energy from the central region to the surface, which has verification in the data of observational astrophysics [9].

From the standpoint of our theory herein, the aforementioned mechanism producing stellar energy [8, 9] is due to a number of factors that build the background space non-holonomity field in stars, not only the globally non-holonomic field of the Universe. By our theory, the substantive distribution is also connected to the space non-holonomity so that the braking energy of the medium is related to the space non-holonomity field. So a star, being in orbit in the Galaxy and the group of galaxies, meets the non-holonomity fields produced by the rotations of the Galactic space, the Local Group of galaxies, etc. Then the braking energy of the medium that fills the spaces (the same as for the energy of the space non-holonomic field) transforms into heat and radiations within the star by the stellar energy mechanism as shown in [8, 9]. In other words, a star "absorbs" the energy of the non-holonomity fields of the spaces wherein it is orbiting, then transforms the energy into heat and radiations.

Employing this mechanism in an Earth-bound laboratory, we can obtain a new source of energy due to the fact that the Earth orbits in the non-holonomic fields of the space.

Third problem. A relative variation of the observable velocity of light in the z-direction we have obtained in [1] is

$$\frac{\Delta \dot{z}}{c} = 2 \times 10^{-4} \sin 2\widetilde{\omega}\tau\,, \tag{47}$$

where $\widetilde{\omega} = \omega\left(1 + \frac{\mathrm{v}}{c}\right)$, whilst given an Earth-bound laboratory the space rotation thereof is the sum of the Earth's rotations around the Sun and around the centre of the Galaxy. We see therefore, that we have a relative variation $\frac{\Delta \dot{z}}{c} \neq 0$ of the observable velocity of light only if both $\omega \neq 0$ and $\mathrm{v} \neq 0$. Hence the predicted anisotropy of the observable velocity of light depends on the interaction of two fields of non-holonomity that are represented in the laboratory space (within the framework of the considered problem statement).

The same is true for the flow of matter distributed throughout the space (46): $J^3 \neq 0$ only if both $\omega \neq 0$ and $\mathrm{v} \neq 0$. Thus the energy produced in a star due to the background space non-holonomity should be dependent not only on the absolute value of the non-holonomity (as the sum of all acting non-holonomic fields), but also on the interaction between the non-holonomic fields.

References

1. Borissova L. Preferred spatial directions in the Universe: a General Relativity approach. *Progress in Physics*, 2006, v. 4, 51–58.
2. Borissova L., Rabounski D. Fields, vacuum, and the mirror Universe. Editorial URSS, Moscow, 2001; CERN, EXT-2003-025.
3. Zelmanov A. L. Chronometric invariants. Dissertation thesis, 1944. American Research Press, Rehoboth (NM), 2006.
4. Zelmanov A. L. Chronometric invariants and co-moving coordinates in the general relativity theory. *Doklady Acad. Nauk USSR*, 1956, v. 107(6), 815–818.
5. Schouten J. A., Struik D. J. Einführung in die neuren Methoden der Differentialgeometrie. *Zentralblatt für Mathematik*, 1935, Bd. 11 und Bd. 19.
6. Landau L. D. and Lifshitz E. M. The classical theory of fields. Butterworth–Heinemann, 2003, 428 pages (4th final edition, revised and expanded).
7. Rabounski D. A theory of gravity like electrodynamics. *Progress in Physics*, 2005, v. 2, 15–29.
8. Rabounski D. Thomson dispersion of light in stars as a generator of stellar energy. *Progress in Physics*, 2006, v. 4, 3–10.
9. Rabounski D. A source of energy for any kind of star. *Progress in Physics*, 2006, v. 4, 19–23.

Multi-Spaces and Many Worlds from Conservation Laws

Giuseppe Basini* and Salvatore Capozziello†

*Laboratori Nazionali di Frascati, INFN, Via E. Fermi C.P. 13, I-0044 Frascati (Roma) Italy

‡Dipartimento di Scienze Fisiche, Università di Napoli "Federico II", and INFN, Sez. di Napoli
Complesso Universitario di Monte S. Angelo, Via Cinthia, Edificio N-I-80126 Napoli, Italy

Corresponding author, e-mail: capozziello@na.infn.it

Many Worlds interpretation of Quantum Mechanics can be related to a General Conservation Principle in the framework of the so called Open Quantum Relativity. Specifically, conservation laws in phase space of physical systems (e. g. minisuperspace) give rise to natural selection rules by which it is possible to discriminate among physical and unphysical solutions which, in the specific case of Quantum Cosmology, can be interpreted as physical and unphysical universes. We work out several examples by which the role of conservation laws is prominent in achieving the solutions and their interpretation.

1 Introduction

The issue to achieve a unified field theory cannot overcome to take into account the role and meaning of conservation laws and dynamical symmetries which have always had a fundamental role in physics. From a mathematical viewpoint, their existence allows to "reduce" the dynamics and then to obtain first integrals of motion, which often allow the exact solution of the problem of motion. Noether theorem is a prominent result in this sense, since it establishes a deep link between conservation laws and symmetries. Moreover, conservation laws can play a deep role in the definition of physical theories and, in particular, to define space-times which are of *physical interest*. The underlying philosophy is the fact that the violation of conservation laws (and then the symmetry breaking) could be nothing else but an artificial tool introduced in contemporary physics in order to solve phenomenologically some puzzles and problems, while effective conservation laws are never violated [1]. The absolute validity of conservation laws, instead, allows the solution of a wide variety of phenomena ranging from entanglement of physical systems [2], to the rotation curves of spiral galaxies [4]. Such results do not come from some *a priori* request of the theory, but is derived from the existence of a *General Conservation Law* (in higher dimensional spacetime) where no violation is allowed [5]. This approach naturally leads to a dynamical unification scheme (the so called Open Quantum Relativity [1]) which can be, as a minimal extension, formulated in 5D [6]. In this context, it is worth stressing the deep relations among symmetries and first integrals of motion, conservation laws with the number and dimensionality of configuration spaces. In fact, phenomena, which in standard physics appear as due to symmetry breakings can be encompassed in a multi-space formulation as previously shown by Smarandache [7, 8]. On the other hand, the need of a multi-space formulation of the theory gives rise to a direct application of the "Many Worlds" Interpretation of Quantum Mechanics [9, 10], in the sense that multi-spaces are nothing else but many worlds in the framework of Quantum Cosmology [11]. This is the argument of this paper: we want to show that configuration spaces derived from the request of integrability of the dynamical systems (and then from the presence of conservation laws) are physical universes, (i. e. observable universes) where cosmological parameters can be observed. On the other hand, if conservation laws are not present, in universes which come out in a Many Worlds interpretation are "unphysical" that is, it is not possible to label them by a set of observable cosmological parameters (technically they are "instanton-solutions"). In Sect. 2, we develop mathematical considerations on conservation laws showing how the presence of symmetries allows the integration of the dynamical systems, which means that the phase-space (and general solution) can be "split" in a multi-space of "integrated" components. Sect. 3 is devoted to the discussion of Many Worlds interpretation of Quantum Cosmology and, in particular, to the fact that multi-spaces related to the phase-space of conservation laws can be interpreted as "minisuperspaces" thanks to the Hartle criterion. Many Worlds-solutions from conservation laws are obtained in Sect. 4 by integrating the Wheeler-DeWitt (WDW) equation of Quantum Cosmology. Conclusions are drawn in Sect. 5.

2 Conservation laws and multi-spaces

Before considering multi-spaces and how they can be interpreted as the Many Worlds of Quantum Cosmology, let us discuss the reduction problem of dynamics connected symmetries and conservation laws. Our issue is to show that the total phase-space of a given dynamical system can be split in many subspaces, each of them related to a specific conserved quantity. As a general remark, it is possible to

show that if the Lie derivative of a given geometric quantity (e. g. vector, tensor, differential form) is zero, such a quantity is conserved. This property is *covariant* and specifies the number of dimensions and the nature of configuration space (and then of the phase-space) where the given dynamical system is defined. Furthermore, the existence of conserved quantities always implies a *reduction* of dynamics which means that the order of equations of motion is reduced thanks to the existence of first integrals. Before considering specific systems, let us remind some properties of the Lie derivative and how conservation laws are related to it. Let L_X be the Lie derivative

$$(L_X\omega)\,\xi = \frac{d}{dt}\,\omega\,(g^t_*\,\xi)\,, \tag{1}$$

where ω is a differential form of $\Re^n$ defined on the vector field ξ, g^t_* is the differential of the phase flux $\{g_t\}$ given by the vector field X on a differential manifold $\mathcal{M}$. The discussion can be specified by considering a Lagrangian $\mathcal{L}$ which is a function defined on the tangent space of configurations $T\mathcal{Q} \equiv \{q_i, \dot{q}_i\}$, that is $\mathcal{L} : T\mathcal{Q} \to \Re$. In this case, the vector field X is

$$X = \alpha^i(q)\frac{\partial}{\partial q^i} + \dot{\alpha}^i(q)\,\frac{\partial}{\partial \dot{q}^i}\,, \tag{2}$$

where the dot denotes the derivative with respect to t, and we have

$$L_X\mathcal{L} = X\mathcal{L} = \alpha^i(q)\,\frac{\partial\mathcal{L}}{\partial q^i} + \dot{\alpha}^i(q)\,\frac{\partial\mathcal{L}}{\partial \dot{q}^i}\,. \tag{3}$$

It is important to note that t is simply a parameter which specifies the evolution of the system. The condition

$$L_X\mathcal{L} = 0 \tag{4}$$

implies that the phase flux is conserved along X: this means that a constant of motion exists for $\mathcal{L}$ and a conservation law is associated to the vector X. In fact, by taking into account the Euler-Lagrange equations, it is easy to show that

$$\frac{d}{dt}\left(\alpha^i\,\frac{\partial\mathcal{L}}{\partial\dot{q}^i}\right) = L_X\mathcal{L}\,. \tag{5}$$

If (4) holds, the relation $\Sigma_0 = \alpha^i\,\dfrac{\partial\mathcal{L}}{\partial\dot{q}^i}$ identifies a constant of motion. Alternatively, using a generalized differential for the Lagrangian $\mathcal{L}$, the Cartan one–form, $\theta_{\mathcal{L}} \equiv \dfrac{\partial\mathcal{L}}{\partial\dot{q}^i}\,dq^i$ and defining the inner derivative $i_X\theta_{\mathcal{L}} = \langle\theta_{\mathcal{L}}, X\rangle$, we get

$$i_X\theta_{\mathcal{L}} = \Sigma_0 \tag{6}$$

if, again, condition (4) holds. This representation identifies cyclic variables. Using a point transformation on vector field (2), it is possible to get

$$\tilde{X} = (i_X dQ^k)\,\frac{\partial}{\partial Q^k} + \left[\frac{d}{dt}(i_X dQ^k)\right]\,\frac{\partial}{\partial\dot{Q}^k}\,. \tag{7}$$

From now on, Lagrangians and vector fields transformed by the non–degenerate transformation

$$Q^i = Q^i(q)\,, \qquad \dot{Q}^i(q) = \frac{\partial Q^i}{\partial q^j}\,\dot{q}^j \tag{8}$$

will be denoted by a tilde. If X is a symmetry for the Lagrangian $\mathcal{L}$, also $\tilde{X}$ is a symmetry for the Lagrangian $\tilde{\mathcal{L}}$ giving rise to a conserved quantity, thus it is always possible to choose a coordinate transformation so that

$$i_X dQ^1 = 1\,, \qquad i_X dQ^i = 0\,, \qquad i \neq 1\,, \tag{9}$$

and then

$$\tilde{X} = \frac{\partial}{\partial Q^1}\,, \qquad \frac{\partial\tilde{\mathcal{L}}}{\partial Q^1} = 0\,. \tag{10}$$

It is evident that Q^1 is a cyclic coordinate because dynamics can be reduced. Specifically, the "reduction" is connected to the existence of the second of (10). However, the change of coordinates is not unique and an opportune choice of coordinates is always important. Furthermore, it is possible that more symmetries are existent. In this case more cyclic variables must exist. In general, a reduction procedure by cyclic coordinates can be achieved in three steps: (i) we choose a symmetry and obtain new coordinates as above and after this first reduction, we get a new Lagrangian $\tilde{\mathcal{L}}$ with a cyclic coordinate; (ii) we search for new symmetries in this new space and iterate the reduction technique until it is possible; (iii) the process stops if we select a pure kinetic Lagrangian where all coordinates are cyclic. In such a case, the dynamical system is *completely integrable* and integration can be achieved along every coordinate of configuration space (or every generalized coordinate-conjugate momentum couple of phase space). In this case, the total phase-space is split in subspaces, each one *labelled* by a conserved quantity. Technically, every symmetry selects a constant conjugate momentum since, by the Euler–Lagrange equations we get

$$\frac{\partial\tilde{\mathcal{L}}}{\partial Q^i} = 0 \Longleftrightarrow \frac{\partial\tilde{\mathcal{L}}}{\partial\dot{Q}^i} = \Sigma_i\,, \tag{11}$$

and the existence of a constant conjugate momentum means that a cyclic variable (a symmetry) exists.

However, The Lagrangian $\mathcal{L} = \mathcal{L}(q^i, \dot{q}^j)$ has to be non-degenerate, which means that the Hessian determinant has to be non-zero.

From the Lagrangian formalism, we can pass to the Hamiltonian one through the Legendre transformation

$$\mathcal{H} = \pi_j\dot{q}^j - \mathcal{L}(q^j, \dot{q}^j)\,, \qquad \pi_j = \frac{\partial\mathcal{L}}{\partial\dot{q}^j}\,, \tag{12}$$

defining, respectively, the Hamiltonian function and the conjugate momenta. In the Hamiltonian formalism, the conservation laws are obtained when $\left[\Sigma_j, \mathcal{H}\right] = 0$, $1 \leqslant j \leqslant m$ This is the relation for conserved momenta and, in order to obtain a symmetry, the Hamilton function has to satisfy the relation

$L_\Gamma \mathcal{H} = 0$, where the vector Γ is defined by

$$\Gamma = \dot{q}^i \frac{\partial}{\partial q^i} + \ddot{q}^i \frac{\partial}{\partial \dot{q}^i} . \qquad (13)$$

Let us now go to the specific formalism of Quantum Mechanics which we will use for the following Quantum Cosmology considerations. By the Dirac canonical quantization procedure, we have

$$\pi_j \longrightarrow \hat{\pi}_j = -i\partial_j , \qquad \mathcal{H} \longrightarrow \hat{\mathcal{H}}(q^j, -i\partial_{q^j}) . \qquad (14)$$

If $|\Psi\rangle$ is a *state* of the system (i. e. its wave function), dynamics is given by the Schrödinger eigenvalue equation

$$\hat{\mathcal{H}}|\Psi\rangle = E|\Psi\rangle , \qquad (15)$$

where, obviously, the whole wave-function is given by $|\phi(t,x)\rangle = e^{iEt/\hbar}|\Psi\rangle$. If a symmetry exists, the reduction procedure outlined above can be applied and then, from (11) and (12), we get

$$\begin{aligned} \pi_1 \equiv \frac{\partial \mathcal{L}}{\partial \dot{Q}^1} = i_{X_1}\theta_{\mathcal{L}} &= \Sigma_1 , \\ \pi_2 \equiv \frac{\partial \mathcal{L}}{\partial \dot{Q}^2} = i_{X_2}\theta_{\mathcal{L}} &= \Sigma_2 , \\ \dots \quad \dots & \quad \dots , \end{aligned} \qquad (16)$$

depending on the number of symmetry vectors. After Dirac quantization, we get

$$-i\partial_1|\Psi\rangle = \Sigma_1|\Psi\rangle, \quad -i\partial_2|\Psi\rangle = \Sigma_2|\Psi\rangle, \quad \dots \qquad (17)$$

which are nothing else but translations along the Q^j axis singled out by the corresponding symmetry. Eqs. (17) can be immediately integrated and, being Σ_j real constants, we obtain oscillatory behaviors for $|\Psi\rangle$ in the directions of symmetries, i. e.

$$|\Psi\rangle = \sum_{j=1}^{m} e^{i\Sigma_j Q^j} |\chi(Q^l)\rangle , \qquad m < l \leqslant n , \qquad (18)$$

where m is the number of symmetries, l are the directions where symmetries do not exist and n is the number of dimensions of configuration space. Vice-versa, dynamics given by (15) can be reduced by (17) if, and only if, it is possible to define constant conjugate momenta as in (16), *i.e.* oscillatory behaviors of a subset of solutions $|\Psi\rangle$ exist as a consequence of the fact that symmetries are present in the dynamics. The m symmetries give first integrals of motion. In one and two–dimensional configuration spaces, the existence of a symmetry allows the complete solution of the problem. Therefore, if $m = n$, the problem is completely solvable and a symmetry exists for every variable of configuration space. The reduction procedure of dynamics, connected to the existence of symmetries, allows to select a subset of the general solution of equations of motion, where oscillatory behaviors of the wave functions are found. In other words, symmetries select exact solutions and reduce dynamics. In these cases, the general solution of a dynamical system can be split in a combination of functions each of them depending on a given variable. As a corollary, a Lagrangian (or a Hamiltonian) where only kinetic terms are present gives always rise to a full integrable dynamics. The total phase-space $\mathcal{M}$ of the system, thanks to conservation laws, can be split in the tensor product of phase-spaces (multi-spaces) assigned by conserved momenta, i. e. $\{q_i, \pi_i\} \to \{Q_i, \Sigma_i\}$, and then $\mathcal{M} = \Pi_{i=1}^{n}\{Q_i, \bigotimes \Sigma_i\}$. As we will see, this feature is relevant in minisuperspace Quantum Cosmology.

3 The "many-worlds" interpretation of Quantum Mechanics and the role of conservation laws

The above considerations acquire a fundamental role in Minisuperspace Quantum Cosmology since, as we will see, Conservation Laws give rise to an approach by which it is possible to "select" physical universes. Quantum Cosmology is one of the results of the efforts of last thirty years directed to the quantization of gravity [12]. The aim has been to obtain a scheme in which gravity is treated on the same ground of the other interaction of Nature. Such an approach (not a coherent theory yet) is the *canonical quantization of gravity*. In order to test the theoretical results, Planck's scales, which cannot be reached by the current physics, have to be considered, so the cosmology is the most reasonable area for the application of the observable predictions of quantum gravity. More properly, Quantum Cosmology is the quantization of dynamical systems which are "*universes*". In this context, supposed the Universe as a whole (the ensemble of all the possible universes), it has a quantum mechanical nature and that an observable universe is only a limit concept valid in particular regions of a manifold (*superspace*) composed by all the possible space-like 3-geometries and local configurations of the matter fields. The task of Quantum Cosmology is to relate all the measurable quantities of the observable universe* to the assigned boundary conditions for a wave function in the superspace. This wave function has to be connected to the probability to obtain typical universes (even if, in the standard approach, it is not a proper probability amplitude since a Hilbert space does not exist in the canonical formulation of quantum gravity) [11]. Quantum Cosmology has to solve, in principle, the problem of the initial conditions of the standard cosmology: *i.e.* it should explain the observed universe, specifying the physical meaning of the boundary conditions of the superspace wave function. In other words, the main issue of quantum cosmology is to search for boundary conditions in agreement with the

*An operative definition of "observable universe" could be a universe where cosmological parameters as the Hubble one H_0, the deceleration parameter q_0, the density parameters Ω_M, Ω_Λ, Ω_k and the age t_0 can be inferred by observations [3].

astronomical observations and these conditions have to be contained in the wave function of the universe $|\Psi\rangle$. The dynamical behavior of $|\Psi\rangle$ in the superspace is described by the Wheeler-DeWitt (WDW) equation [12] that is a second order functional differential equation hard to handle, because it has infinite degrees of freedom. Usually attention has been concentrated on finite dimensional models in which the metrics and the matter fields are restricted to particular forms (*minisuperspace models*), like homogeneous and isotropic spacetimes. With these choices, the WDW equation becomes a second order partial differential equation which, possibly, can be exactly integrated. However, by definition, there is no *rest outside of the Universe* in cosmology, so that boundary conditions must be considered as a *fundamental law of physics* [11]. Moreover, not only the conceptual difficulties, but also the mathematical ones, make Quantum Cosmology hard to handle. For example, the superspace of geometrodynamics [13] has infinite degrees of freedom so that it is technically impossible to integrate the full infinite dimensional WDW equation. Besides, a Hilbert space of states describing the universe is not available [12]. Finally, it is not well established how to interpret the solutions of WDW equation in the framework of probability theory. Despite these still unsolved shortcomings, several positive results have been obtained and Quantum Cosmology has become a sort of *paradigm* in theoretical physics researches. For example the infinite-dimensional superspace can be restricted to opportune finite-dimensional configuration spaces called *minisuperspaces*. In this case, the above mathematical difficulties can be avoided and the WDW equation can be integrated. The so called *no boundary condition* by Harte and Hawking [14] and the *tunneling from nothing* by Vilenkin [15] give reasonable laws for initial conditions from which our observable universe could be started. The *Hartle criterion* [11] is an interpretative scheme for the solutions of the WDW equation. Hartle proposed to look for peaks of the wave function of the universe: if it is strongly peaked, we have correlations among the geometrical and matter degrees of freedom; if it is not peaked, correlations are lost. In the first case, the emergence of classical relativistic trajectories (*i.e.* universes) is expected. The analogy to the quantum mechanics is immediate. If we have a potential barrier and a wave function, solution of the Schrödinger equation, we have an oscillatory regime upon and outside the barrier while we have a decreasing exponential behavior under the barrier. The situation is analogous in Quantum Cosmology: now potential barrier has to be replaced by the superpotential $U(h^{ij},\varphi)$, where h^{ij} are the components of the three–metric of geometrodynamics and φ is a generic scalar field describing the matter content. More precisely, the wave function of the universe can be written as

$$\Psi\left[h_{ij}(x),\phi(x)\right]\sim e^{im_P^2 S}\,, \tag{19}$$

where m_p is the Planck mass and

$$S\equiv S_0+m_P^{-2}S_1+\mathrm{O}(m_P^{-4}) \tag{20}$$

is the action which can be expanded. We have to note that there is no normalization factor due to the lack of a probabilistic interpretative full scheme. Inserting S into the WDW equation and equating similar power terms of m_p, one obtains the Hamilton-Jacobi equation for S_0. Similarly, one gets equations for $S_1, S_2\ldots$, which can be solved considering results of previous orders giving rise to the higher order perturbation theory. We need only S_0 to recover the semi-classical limit of Quantum Cosmology [10]. If S_0 is a real number, we get oscillating WKB modes and the Hartle criterion is recovered since $|\Psi\rangle$ is peaked on a phase-space region defined by

$$\pi_{ij}=m_P^2\,\frac{\delta S_0}{\delta h^{ij}}\,,\qquad \pi_\varphi=m_P^2\,\frac{\delta S_0}{\delta\varphi}\,, \tag{21}$$

where π_{ij} and π_φ are classical momenta conjugates to h^{ij} and φ. It is worth stressing, at this point, that such a momenta are nothing else but Conservation Laws. The semi-classical region of superspace, where Ψ has an oscillating structure, is the Lorentz one otherwise it is Euclidean*. In the latter case, we have $S=iI$ and

$$\Psi\sim e^{-m_P^2 I}\,, \tag{22}$$

where I is the action for the Euclidean solutions of classical field equations (*istantons*). This scheme, at least at a semi-classical level, solves the problem of initial conditions. Given an action S_0, Eqs. (21) imply n free parameters (one for each dimension of the configuration space $\mathcal{Q}\equiv\{h^{ij},\varphi\}$) and then n first integrals of motion exactly as in the scheme proposed in the previous section. However the general solution of the field equations involves $2n-1$ parameters (one for each Hamilton equation of motion except the energy constraint). Consequently, the wave function is peaked on a subset of the general solution. In this sense, the boundary conditions on the wave function imply initial conditions for the classical solutions. In other words, the issue is searching for some general method by which selecting such constants of motion related to the emergence of classical trajectories without arbitrarily choosing regions of the phase-space where momenta are conserved. In this sense, there is a deep connection between the conservation laws and the structure of the wave function of the universe. Using the results of the previous section (see Eq. 18), the oscillatory regime, and then the correlation among the variables in the framework of the Hartle criterion, is guaranteed only if conservation laws are present into dynamics. In this context, if conservation laws are absolutely valid, the above *reduction procedure* gives rise to subsets of the infinite dimensional general solution of

*It is important to note that we are using both symbols $|\Psi\rangle$ and Ψ depending on the interpretation which we want to give to the wave function. In the first case, the wave function is considered a "quantum-state", in the second one, it has a semi-classical interpretation.

the WDW equation where oscillating behaviors are recovered. Viceversa, the Hartle criterion is always connected to the presence of a conservation law and then to the emergence of classical trajectories which are *observable universes* where cosmological observations are possible. Then the above result can be given in the following way:

> *In minisuperspace quantum cosmology, the existence of conservation laws yields a reduction procedure of dynamics which allows to find out oscillatory behaviors for the general solution of WDW equation. Viceversa, if a subset of the solution of WDW equation has an oscillatory behavior, conserved momenta have to exist and conservation laws are present. If a conservation law exists for every configuration variable, the dynamical system is completely integrable and the general solution of WDW equation is a superposition of oscillatory behaviors. In other words, conservation laws allow and select observable universes.*

On the other hand, if conservation laws are not valid the WDW multi-space solution give rise to non-observable universes (instanton solutions).

4 Many worlds from conservation laws

In order to give concrete examples of the above results, we can show how, given a generic theory of gravity, it is possible to work out minisuperspace cosmological models where observable universes (classical trajectories) are obtained thanks to the existence of conserved quantities. We shall take into account the most general action in which gravity is nonminimally coupled to a scalar field:

$$\mathcal{A}=\int_{\mathcal{M}} d^4x\sqrt{-g}\left[F(\varphi)R+\frac{1}{2}g^{\mu\nu}\varphi_{;\mu}\varphi_{;\nu}-V(\varphi)+\mathcal{L}_m\right] \quad (23)$$

where the form and the role of $V(\varphi)$ are still general and $\mathcal{L}_m$ represents the standard fluid matter content of the theory. This effective action comes out in the framework of the Open Quantum Relativity [1, 6] a dynamical theory in which, asking for a General Conservation Principle [5], the unification of different interactions is achieved and several shortcomings of modern physics are overcome (see [1] and references therein). The state equation of fluid matter is $p=$ $=(\gamma-1)\rho$ and $1\leqslant\gamma\leqslant 2$ where p and ρ are, respectively, the ordinary pressure and density. Now we have all the ingredients to develop a scalar-tensor gravity quantum cosmology. Using the transformations:

$$\varphi=e^{-\varphi},\quad F(\varphi)=\frac{1}{8}e^{-2\varphi},\quad V(\varphi)=U(\varphi)e^{-2\varphi}, \quad (24)$$

the action (23) can be recast in the form

$$\mathcal{A}=\int d^4x\sqrt{-g}\left\{\exp\left[-2\varphi\right]\left[R+4g^{\mu\nu}\varphi_{;\mu}\varphi_{;\nu}+\right.\right. \\ \left.\left.-U(\varphi)\right]+\mathcal{L}_m\right\}, \quad (25)$$

always using Planck units $8\pi G=c=1$. Let us now take into account a Friedman, Robertson, Walker (FRW) metric $ds^2=dt^2-a^2(t)d\Omega_3^2$, where $d\Omega_3^2$ is the 3–dimensional element of the spacelike manifold. With this assumption, the configuration space is $\mathcal{Q}\equiv\{a,\varphi\}$ and the tangent space is $T\mathcal{Q}\equiv\{a,\dot{a},\varphi,\dot{\varphi}\}$. This is our minisuperspace. Clearly $p=p(a)$ and $\rho=\rho(a)$. Substituting the FRW metric and integrating by parts, the Lagrangian (25) becomes pointlike, that is:

$$\mathcal{L}=\frac{1}{8}a^3e^{-2\varphi}\left[6\left(\frac{\dot{a}}{a}\right)^2-12\dot{\varphi}\left(\frac{\dot{a}}{a}\right)-6\frac{k}{a^2}+\right. \\ \left.+4\dot{\varphi}^2-8U(\varphi)\right]+a^3\mathcal{L}_m\,. \quad (26)$$

At this point, it is worth noting that the scale–factor duality symmetry arises if the transformation of the scale factor of a homogeneous and isotropic space-time metric, $a(t)\to a^{-1}(-t)$, leaves the model invariant, taking into account also the form of the potential U.

Provided the transformations

$$\psi=\varphi-\frac{3}{2}\ln a\,,\qquad Z=\ln a\,, \quad (27)$$

the Lagrangian (26) becomes:

$$\mathcal{L}=e^{-2\psi}\left[4\dot{\psi}^2-3\dot{Z}^2-6ke^{-2Z}-8W\right]+De^{3(1-\gamma)Z} \quad (28)$$

where the potential $W(\psi,Z)$, thanks to the transformations (27), is depending on both the variables of the minisuperspace. In the new variables, the duality invariance has become a parity invariance since Z and $-Z$ are both solutions of dynamics. The emergence of this feature is related to the presence of nonminimal coupling; it allows the fact that several solutions can be extended for $t\to-\infty$ without singularities [3]. Another important consideration is connected to the role of perfect fluid matter. It introduces two further parameters which are D (related to the bulk of matter) and γ (related to the type of matter which can be *e.g.* radiation $\gamma=4/3$ or dust $\gamma=1$). We shall see below that they directly determine the form of cosmological solutions. Two general forms of potential W preserving the duality symmetry

$$W(Z,\psi)=\frac{D}{4}e^{-3\gamma Z}e^{2\psi}\,,\qquad W(Z,\psi)=\Lambda\,, \quad (29)$$

where $\Lambda=$const. These are all the ingredient we need in order to construct our minisuperspace quantum cosmology. Let us start with a simple but extremely didactic example of the above effective action (25) which is

$$\mathcal{A}=\int d^4x\sqrt{-g}\,e^{-2\varphi}\left[R+4(\partial\varphi)^2-\Lambda\right], \quad (30)$$

where $D=k=0$ and $W=\Lambda$. This example is useful to show, as we shall see below, the way in which the full theory

works. The Lagrangian (28) becomes

$$\mathcal{L} = -3e^{-2\psi}\dot{Z}^2 + 4\dot{\psi}^2 e^{-2\psi} - 2\Lambda e^{-2\psi}, \qquad (31)$$

that is cyclic in Z. Due to the considerations in previous section, we have to derive a conserved quantity, relatively to the variable Z, and then an oscillatory behavior for the wave function of the universe Ψ. The Legendre transformation for the conjugate momenta gives

$$\pi_z = \frac{\partial \mathcal{L}}{\partial \dot{Z}} = -6\dot{Z}e^{-2\psi}, \quad \pi_\psi = \frac{\partial \mathcal{L}}{\partial \dot{\psi}} = 8\dot{\psi}e^{-2\psi}, \qquad (32)$$

and the Hamitonian is $\mathcal{H} = \pi_z \dot{Z} + \pi_\psi \dot{\psi} - \mathcal{L}$. From Dirac canonical quantization rules, it is possible to write $\pi_z \to -i\partial_z$ and $\pi_\psi \to -i\partial_\psi$, and then the WDW equation is

$$\left[\frac{1}{12}\,\partial_z^2 - \frac{1}{16}\,\partial_\psi^2 + 2\Lambda e^{-4\psi}\right]\Psi(Z,\psi) = 0\,, \qquad (33)$$

where a simple factor ordering choice is done [11]. This is a second order partial differential equation which can be solved by separation of variables $\Psi(Z,\psi) = A(Z)\,B(\psi)$ from which Eq. (33) can be split into two ordinary differential equations

$$\frac{d^2B(\psi)}{d\psi^2} - \left(32\Lambda e^{-4\psi} + 16E\right)B(\psi) = 0\,, \qquad (34)$$

$$\frac{d^2A(z)}{dz^2} = 12EA(z)\,, \qquad (35)$$

where E is a arbitrary constant. For $E > 0$, the general solution of the WDW equation is

$$\begin{aligned}\Psi(Z,\psi) \propto{}& \exp\left(\pm\sqrt{\frac{3}{2}}Z\right)\times\\ &\times\left[c_0 \mp \frac{1}{8\sqrt{2\Lambda}}\exp\left(\pm 4\sqrt{2\Lambda}\,e^{-2\psi}\right)\right]\times\\ &\times\exp\left[\psi \mp 2\sqrt{2\Lambda}\,e^{-2\psi}\right].\end{aligned} \qquad (36)$$

For $E < 0$, Eq. (35) is a harmonic oscillator whose solutions are $A(Z) \propto \pm\sin(mZ)$ (we have put $|E| = m^2$). In this case the momentum $\pi_z = m$ is a constant of motion. Eq. (34) is solvable in terms of modified Bessel functions and the general solution of Eq. (33) is

$$\Psi(Z,\psi) \propto \pm\sin(mZ)\,K_{\frac{im}{2\Lambda}}\left(\sqrt{2\Lambda}\,e^{-2\psi}\right); \qquad (37)$$

with an evident oscillatory behavior. Finally, in the case $E = 0$, the solution is

$$\Psi(Z,\psi) \propto ZK_0\left(\sqrt{2\Lambda}\,e^{-2\psi}\right), \qquad (38)$$

where K_0 is the modified Bessel function of zero order. The absence of a positive defined scalar product in the superspace prevents the existence of a Hilbert space for the states of the WDW equation; *i. e.* we cannot apply the full probability interpretation to the squared modulus of the wave function of the universe. This is the reason why we have to omit the normalization constants in front of the solutions (36), (37), (38). Various suggestions have been given in literature to interpret Ψ [11], although starting from different points of view, all these different interpretations arrive to the conclusion that, at least in the semiclassical limit, a notion of measure can be introduced considering $|\Psi|^2$. As we said above, the strong peaks of $|\Psi|^2$ (oscillatory behaviors) indicate classical correlations among the dynamical variables, whereas weak variations of $|\Psi|^2$ mean the absence of correlations [11]. In fact the presence of strong amplitude peaks of the wave function seems to be the common indicator of where the classical (in principle observable) universes enucleates in its configuration space. The classical limit of quantum cosmology can be recovered in the oscillation regime with great phase values of Ψ: in this region the wave function is strongly peaked on first integrals of motion related to conservation laws. In the case presented here, the solutions (36), (37), (38) give information on the nature and the properties of classical cosmological behavior: for the *vacuum state*, $E = 0$, we have

$$\Psi \sim \ln a\sqrt{\pi}\,e^{\psi}\exp\left(-\sqrt{2\Lambda}\,e^{-2\psi}\right) \to 0\,, \qquad (39)$$

for $\psi \to -\infty$ and

$$\Psi \sim 2\psi\ln a\,, \qquad (40)$$

for $\psi \to +\infty$. So $|\Psi|^2$ is exponentially small for $\psi \leqslant 0$, while it increases for great ψ. This fact tells us that is most probable a realization of a classical universe for great field configurations (for example see the prescriptions for chaotic inflation where the scalar field has to start with a mass of a few Planck masses [16]). Another feature which emerges from (36) and (37) is the following: as $Z = \ln a$, Ψ can be considered a superposition of states $\Psi(a)$ with states $\Psi(a^{-1})$, that is the wave function of the universe (and also the WDW equation) contains the scale factor duality. Furthermore, using the first integrals of motion (*i.e* the canonical momenta related to conservation laws), we get the classical solutions

$$a(t) = a_0\left[\frac{\cos\lambda\tau + \sin\lambda\tau}{\cos\lambda\tau - \sin\lambda\tau}\right]^{\pm\sqrt{3}/3}, \qquad (41)$$

$$\begin{aligned}\varphi(t) = \frac{1}{4}\ln\left[\frac{\lambda^2}{k\cos^2 2\lambda\tau}\right] \pm\\ \pm\frac{\sqrt{3}}{2}\ln\left|\frac{\cos\lambda\tau + \sin\lambda\tau}{\cos\lambda\tau - \sin\lambda\tau}\right| + \varphi_0\,,\end{aligned} \qquad (42)$$

and

$$a(t) = a_0\exp\left\{\mp\frac{1}{\sqrt{6}}\arctan\left[\frac{1 - 2e^{4\lambda\tau}}{2e^{2\lambda\tau}\sqrt{1 - e^{4\lambda\tau}}}\right]\right\}, \qquad (43)$$

Λ	k	D	γ	*Solution*
$\neq 0$	0	$\neq 0$	1	CT
0	0	$\neq 0$	1	CT
0	± 1	$\neq 0$	4/3	I
$\neq 0$	0	0	$\forall\gamma$	CT
0	$k > 0$	$6k$	$\forall\gamma$	CT and I

Table 1: Main features of the solutions of WDW equation, Classical Trajectories (CT) and Instantons (I), for different values of parameter Λ, k, D, γ.

$$\varphi(t) = \frac{1}{4}\ln\left[\frac{2\lambda^2 e^{4\lambda\tau}}{k\,(1-e^{4\lambda\tau})}\right] \mp \\ \mp \frac{1}{\sqrt{6}}\arctan\left[\frac{1-2e^{4\lambda\tau}}{2e^{2\lambda\tau}\sqrt{1-e^{4\lambda\tau}}}\right] + \varphi_0\,, \tag{44}$$

where $\tau = \pm t$, k is an integration constant and $\lambda^2 = \Lambda/2$. In (41), (42), we have $\Lambda > 0$, in (43), (44) $\Lambda < 0$. These "universes" are "observable" since, starting from these solutions, it is easy to construct all the cosmological parameters H_0, q_0, Ω_Λ, Ω_M and t_0. It is worth stressing that such solutions are found only if conservation laws exists. It is remarkable that the scalar factor duality emerges also for the wave function of the universe in a quantum cosmology context: that is the solutions for a have their dual counterpart a^{-1} in the quantum state described by Ψ. This fact, in the philosophy of quantum cosmology, allows to fix a law for the initial conditions (*e. g.* Vilenkin tunneling from nothing or Hartle-Hawking no-boundary conditions [11]) in which the duality is a property of the configuration space where our classical universe enucleates. This fact gives rise to cosmological solutions which can be consistently defined for $t \to \pm\infty$.

The approach can be directly extended to the Lagrangian (28), from which, by a Legendre transformation and a canonical quantization, we get the WDW equation

$$\left[\frac{1}{2}\,\partial_z^2 - \frac{1}{8}\,\partial_\psi^2 + 3ke^{-2Z-4\psi} + \right. \\ \left. + 4We^{-4\psi} - De^{3(1-\gamma)Z-2\psi}\right]\Psi(Z,\psi) = 0\,, \tag{45}$$

whose solutions can be classified by the potential parameter Λ, the spatial curvature k, the bulk of matter D, and the adiabatic index γ. In the following Table, we give the main features of WDW solutions.

5 Discussion and conclusions

In this paper, we have shown that the reduction procedure of dynamics, related to conservation laws, can give rise to a splitting of the phase-space of a physical system, by which it is possible to achieve the complete solution of dynamics. This result can be applied to Quantum Cosmology, leading to the result that physical many worlds can be related to integrable multi-spaces of the above splitting. From a mathematical viewpoint, the above statement deserves some further discussion. As a first remark the general solution (18) can be interpreted as a superposition of particular solutions (the components in different directions) which result more *solved* (*i.e.* separated in every direction of configuration space) if more symmetries exist. Starting from such a consideration, as a consequence, we can establish a sort of *degree of solvability*, among the components of a given physical system, connected to the number of symmetries: (i) a system is *completely* solvable and separable if a symmetry exists for *every* direction of configuration space (in this case, the system is fully integrable and the relations among its parts can be exactly obtained); (ii) a system is *partially* solved and separated if a symmetry exists for *some* directions of configuration space (in this case, it is not always possible to get a general solution); (iii) a system is *not* separated at all and *no* symmetry exists, i. e. a necessary and sufficient condition to get the general solution does not exist. In other words, we could also obtain the general solution in the last case, but not by a straightforward process of separation of variables induced by the reduction procedure.

A further remark deserves the fact that the eigen-functions of a given operator (in our case the Hamiltonian $\hat{\mathcal{H}}$) define a Hilbert space. The above result works also in this case, so that we can define, for a quantum system whose eigenfunctions are given by a set of commuting Hermitian operators, a *Hilbert Space of General Conservation Laws* (see also [5]). The number of dimensions of such a space is given by the components of superposition (18) while the number of symmetries is given by the oscillatory components. Viceversa, the oscillatory components are *always* related to the number of symmetries in the corresponding Hilbert space. These results can be applied to minisuperspace quantum cosmology. The role of symmetries and conservation laws is prominent to interpret the information contained in the wave function of the universe which is solution of the WDW equation; in fact, the conserved momenta, related to some (or all) of the physical variables defining the minisuperspace, select oscillatory behaviors (*i.e.* strong peaks) in Ψ, which means "correlation" among the physical variables and then classical trajectories whose interpretation is that of "*observable universes*". In this sense, the so called Hartle criterion of quantum cosmology becomes a sufficient and necessary condition to select classical universes among all those which are possible. Working out this approach, we obtain the wave function of the universe Ψ depending on a set of physical parameter which are D, the initial bulk of matter, k, the spatial curvature constant, γ, the adiabatic index of perfect fluid matter, Λ, the parameter of the interaction potential.

The approach allows to recover several classes of interesting cosmological behaviors as De Sitter-like-singularity free solutions, power-law solutions, and pole-like solutions [3].

However, some points have to be considered in the interpretation of the approach. The Hartle criterion works in the context of an Everett-type interpretation of Quantum Cosmology [9, 17] which assumes the idea that the universe branches into a large number of copies of itself whenever a measurement is made. This point of view is the so called *Many Worlds* interpretation of Quantum Cosmology. Such an interpretation is an approach which gives a formulation of quantum mechanics designed to deal with correlations internal to individual, isolated systems. The Hartle criterion gives an operative interpretation of such correlations. In particular, if the wave function is *strongly peaked* in some region of configuration space, the correlations which characterize such a region can be, in principle, observed. On the other hand, if the wave function is *smooth* in some region, the correlations which characterize that region are precluded to the observations (that is, the cosmological parameters as H_0 or Ω_Λ cannot be neither calculated nor observed).

If the wave function is neither peaked nor smooth, no predictions are possible from observations. In conclusion, the analogy with standard quantum mechanics is straightforward. By considering the case in which the individual system consists of a large number of identical subsystems, one can derive, from the above interpretation, the usual probabilistic interpretation of Quantum Mechanics for the subsystems [11, 10]. If a conservation law (or more than one) is present for a given minisuperspace model, then strongly peaked (oscillatory) subsets of the wave function of the universe are found. Viceversa, oscillatory parts of the wave function can be always connected to conserved momenta and then to symmetries.

References

1. Basini G., Capozziello S. *Gen. Relativ. Grav.*, 2005, v. 37, 115.
2. Basini G., Capozziello S. *Europhys. Lett.*, 2003, v. 63, 166.
3. Basini G., Bongiorno F., Capozziello S. *Int. Journ. Mod. Phys.*, 2004, v. D13, 717.
4. Basini G., Bongiorno F., Capozziello S., Ricci M. *Int. Journ. Mod. Phys.*, 2004, v. D13, 359.
5. Basini G., Capozziello S., Longo G. *Phys. Lett.*, 2003, v. 311A, 465.
6. Basini G., Capozziello S. *Gen. Relativ. Grav.*, 2003, v. 35, 2217.
7. Smarandache F. A unifying field in logics: neutrosophic logic. Neutrosophy, neutrosophic set, neutrosophic probability. 3rd edition, American Research Press, Rehoboth, 2003.
8. Mao Linfan. Smarandache multi-space theory. Post-doctoral thesis. Hexis, Phoenix, 2005.
9. Everett H. *Rev. Mod. Phys.*, 1957, v. 29, 454.
10. Halliwell J. J. *Nucl. Phys.*, 1986, v. B266, 228.
11. Hartle J. B. In: *Gravitation in Astrophysics*, Cargese, 1986, eds. B. Carter and J. B. Hartle, Plenum Press, New York, 1986.
12. DeWitt B. S. *Phys. Rev.*, 1967, v. 160, 1113.
13. Misner C. W. *Phys. Rev.*, 1969, v. 186, 1319.
14. Hartle J. B. and Hawking S. W. *Phys. Rev.*, 1983, v. D28, 2960.
15. Vilenkin A. *Phys. Rev.*, 1986, v. D33, 3560.
16. Linde A. D. *Phys. Lett.*, 1982, v. B108, 389.
17. Finkelstein D. *Trans. N. Y. Acad. Sci.*, 1963, v. 25, 621.

SPECIAL REPORT

A New Light-Speed Anisotropy Experiment: Absolute Motion and Gravitational Waves Detected

Reginald T. Cahill

School of Chemistry, Physics and Earth Sciences, Flinders University, Adelaide 5001, Australia
E-mail: Reg.Cahill@flinders.edu.au; http://www.scieng.flinders.edu.au/cpes/people/cahill_r/

Data from a new experiment measuring the anisotropy of the one-way speed of EM waves in a coaxial cable, gives the speed of light as 300,000±400±20km/s in a measured direction RA=5.5±2 hrs, Dec=70±10°S, is shown to be in excellent agreement with the results from seven previous anisotropy experiments, particularly those of Miller (1925/26), and even those of Michelson and Morley (1887). The Miller gas-mode interferometer results, and those from the RF coaxial cable experiments of Torr and Kolen (1983), De Witte (1991) and the new experiment all reveal the presence of gravitational waves, as indicated by the last ± variations above, but of a kind different from those supposedly predicted by General Relativity. Miller repeated the Michelson-Morley 1887 gas-mode interferometer experiment and again detected the anisotropy of the speed of light, primarily in the years 1925/1926 atop Mt.Wilson, California. The understanding of the operation of the Michelson interferometer in gas-mode was only achieved in 2002 and involved a calibration for the interferometer that necessarily involved Special Relativity effects and the refractive index of the gas in the light paths. The results demonstrate the reality of the Fitzgerald-Lorentz contraction as an observer independent relativistic effect. A common misunderstanding is that the anisotropy of the speed of light is necessarily in conflict with Special Relativity and Lorentz symmetry — this is explained. All eight experiments and theory show that we have both anisotropy of the speed of light *and* relativistic effects, and that a dynamical 3-space exists — that absolute motion through that space has been repeatedly observed since 1887. These developments completely change fundamental physics and our understanding of reality. "Modern" vacuum-mode Michelson interferometers, particularly the long baseline terrestrial versions, are, by design flaw, incapable of detecting the anisotropy effect and the gravitational waves.

Contents

1 Introduction

Of fundamental importance to physics is whether the speed of light is the same in all directions, as measured say in a laboratory attached to the Earth. This is what is meant by *light speed anisotropy* in the title of this paper. The prevailing belief system in physics has it that the speed of light is isotropic, that there is no preferred frame of reference, that absolute motion has never been observed, and that 3-space does not, and indeed cannot exist. This is the essence of Einstein's 1905 postulate that the speed of light is independent of the choice of observer. This postulate has determined the course of physics over the last 100 years.

Despite the enormous significance of this postulate there has never been a direct experimental test, that is, in which the one-way travel time of light in vacuum over a set distance has been measured, and repeated for different directions. So how could a science as fundamental and important as physics permit such a key idea to go untested? And what are the consequences for fundamental physics if indeed, as reported herein and elsewhere, that the speed of light is anisotropic, that a dynamical 3-space does exist? This would imply that

if reality is essentially space and matter, with time tracking process and change, then physics has completely missed the existence of that space. If this is the case then this would have to be the biggest blunder ever in the history of science, more so because some physicists have independently detected that anisotropy. While herein we both summarise seven previous detections of the anisotropy and report a new experiment, the implications for fundamental physics have already been substantially worked out. It leads to a new modelling and comprehension of reality known as *Process Physics* [1].

The failure of mainstream physics to understand that the speed of light is anisotropic, that a dynamical 3-space exists, is caused by an ongoing failure to comprehend the operation of the Michelson interferometer, and also by theoretical physicists not understanding that the undisputed successes of special relativity effects, and even Lorentz symmetry, do not imply that the speed of light must be isotropic — this is a mere abuse of logic, as explained later.

The Michelson interferometer is actually a complex instrument. The problem is that the anisotropy of the speed of light affects its actual dimensions and hence its operation: there are actual length contractions of its physical arms. Because the anisotropy of the speed of light is so fundamental it is actually very subtle to design an effective experiment because the sought for effect also affects the instrument in more than one way. This subtlety has been overlooked for some 100 years, until in 2002 the original data was reanalysed using a relativistic theory for the calibration of the interferometer [2].

The new understanding of the operation of the Michelson interferometer is that it can only detect the light speed anisotropy when there is gas in the light paths, as there was in the early experiments. Modern versions have removed the gas and made the instrument totally unable to detect the light speed anisotropy. Even in gas mode the interferometer is a very insensitive device, being 2nd order in v/c and further suppressed in sensitivity by the gas refractive index dependency.

More direct than the Michelson interferometer, but still not a direct measurement, is to measure the one-speed of radio frequency (RF) electromagnetic waves in a coaxial cable, for this permits electronic timing methods. This approach is 1st order in v/c, and independent of the refractive index suppression effect. Nevertheless because it is one-way clocks are required at both ends, as in the Torr and Kolen, and De Witte experiments, and the required length of the coaxial cable was determined, until now, by the stability of atomic clocks over long durations.

The new one-way RF coaxial experiment reported herein utilises a new timing technique that avoids the need for two atomic clocks, by using a very special property of optical fibres, namely that the light speed in optical fibres is isotropic, and is used for transmitting timing information, while in the coaxial cables the RF speed is anisotropic, and is used as the sensor. There is as yet no explanation for this optical fibre effect, but it radically changes the technology for anisotropy experiments, as well and at the same time that of gravitational wave detectors. In the near future all-optical gravitational wave detectors are possible in desk-top instruments. These gravitational waves have very different properties from those supposedly predicted from General Relativity, although that appears to be caused by errors in that derivation.

As for gravitational waves, it has been realised now that they were seen in the Miller, Torr and Kolen, and De Witte experiments, as they are again observed in the new experiment. Most amazing is that these wave effects also appear to be present in the Michelson-Morley fringe shift data from 1887, as the fringe shifts varied from day to day. So Michelson and Morley should have reported that they had discovered absolute motion, a preferred frame, and also wave effects of that frame, that the speed of light has an anisotropy that fluctuated over and above that caused by the rotation of the Earth.

The first and very successful attempt to look for a preferred frame was by Michelson and Morley in 1887. They did in fact detect the expected anisotropy at the level of ± 8 km/s [3], but only according to Michelson's Newtonian calibration theory. However this result has essentially been ignored ever since as they expected to detect an effect of at least ± 30 km/s, which is the orbital speed of the Earth about the Sun. As Miller recognised the basic problem with the Michelson interferometer is that the calibration of the instrument was then clearly not correctly understood, and most likely wrong [4]. Basically Michelson had used Newtonian physics to calibrate his instrument, and of course we now know that that is completely inappropriate as relativistic effects play a critical role as the interferometer is a 2nd order device ($\sim v^2/c^2$ where v is the speed of the device relative to a physical dynamical 3-space*), and so various effects at that order must be taken into account in determining the calibration of the instrument, that is, what light speed anisotropy corresponds to the observed fringe shifts. It was only in 2002 that the calibration of the Michelson interferometer was finally determined by taking account of relativistic effects [2]. One aspect of that was the discovery that only a Michelson interferometer in gas-mode could detect the light anisotropy, as discussed below. As well the interferometer when used in air is nearly a factor of 2000 less sensitive than that according to the inappropriate Newtonian theory. This meant that the Michelson and Morley anisotropy speed variation was now around 330km/s on average, and as high as 400km/s on some days. Miller was aware of this calibration problem, and resorted to a brilliant indirect method, namely to observe the fringe shifts over a period of a year, and to use the effect of the Earth's orbital speed upon the fringe shifts to arrive at

*In Michelson's era the idea was that v was the speed of light relative to an *ether*, which itself filled space. This dualism has proven to be wrong.

a calibration. The Earth's orbital motion was clearly evident in Miller's data, and using this effect he obtained a light speed anisotropy effect of some 200 km/s in a particular direction. However even this method made assumptions which are now known to be invalid, and correcting his earth-effect calibration method we find that it agrees with the new relativistic and gas effects calibration, and both methods now give a speed of near 400 km/s. This also then agrees with the Michelson-Morley results. Major discoveries like that of Miller must be reproduced by different experiments and by different techniques. Most significantly there are in total seven other experiments that confirm this Miller result, with four being gas-mode Michelson interferometers using either air, helium or a He/Ne mixture in the light path, and three experiments that measure variations in the one-way speed of EM waves travelling through a coaxial cable as the orientation of the cable is changed, with the latest being a high precision technique reported herein and in [5, 6]. This method is 1st order in v/c, so it does not require relativistic effects to be taken into account, as discussed later.

As the Michelson interferometer requires a gas to be present in the light path in order to detect the anisotropy it follows that vacuum interferometers, such as those in [7], are simply inappropriate for the task, and it is surprising that some attempts to detect the anisotropy in the speed of light still use vacuum-mode Michelson interferometers, some years after the 2002 discovery of the need for a gas in the light path [2].

Despite the extensive data collected and analysed by Miller after his fastidious testing and refinements to control temperature effects and the like, and most importantly his demonstration that the effects tracked sidereal time and not solar time, the world of physics has, since publication of the results by MIller in 1933, simply ignored this discovery. The most plausible explanation for this situation is the ongoing misunderstanding by many physicists, but certainly not all, that any anisotropy in the speed of light must necessarily by incompatible with Special Relativity (SR), with SR certainly well confirmed experimentally. This is misunderstanding is clarified. In fact Miller's data can now be used to confirm an important aspect of SR. Even so, ignoring the results of a major experiment simply because they challenge a prevailing belief system is not science — ignoring the Miller experiment has stalled physics for some 70 years.

It is clear that the Miller experiment was highly successful and highly significant, and we now know this because the same results have been obtained by later experiments which used *different* experimental techniques. The most significant part of Miller's rigorous experiment was that he showed that the effect tracked sidereal time and not solar time — this is the acid test which shows that the direction of the anisotropy velocity vector is relative to the stars and not to the position of the Sun. This difference is only some 4 minutes per day, but over a year amounts to a huge 24 hours effect, and Miller saw that effect and extensively discussed it in his paper. Similarly De Witte in his extensive 1991 coaxial cable experiment [9] also took data for 178 days to again establish the sidereal time effect: over 178 days this effect amounts to a shift in the phase of the signal through some 12 hours! The sidereal effect has also been established in the new coaxial cable experiment by the author from data spanning some 200 days.

The interpretation that has emerged from the Miller and related discoveries is that space exists, that it is an observable and dynamical system, and that the Special Relativity effects are caused by the absolute motion of quantum systems through that space [1, 25]. This is essentially the Lorentz interpretation of Special Relativity, and then the spacetime is merely a mathematical construct. The new understanding has lead to an explanation of why Lorentz symmetry manifests despite there being a preferred frame, that is, a local frame in which only therein is the speed of light isotropic. A minimal theory for the dynamics of this space has been developed [1, 25] which has resulted in an explanation of numerous phenomena, such as gravity as a quantum effect [25, 8], the so-called "dark matter" effect, the black hole systematics, gravitational light bending, gravitational lensing, and so [21–25].

The Miller data also revealed another major discovery that Miller himself may not have understood, namely that the anisotropy vector actually fluctuates form hour to hour and day to day even when we remove the manifest effect of the Earth's rotation, for Miller may have interpreted this as being caused by imperfections in his experiment. This means that the flow of space past the Earth displays turbulence or a wave effect: basically the Miller data has revealed what we now call *gravitational waves*, although these are different to the waves supposedly predicted by General Relativity. These wave effects were also present in the Torr and Kolen [10] first coaxial cable experiment at Utah University in 1981, and were again manifest in the De Witte data from 1991. Analysis of the De Witte data has shown that these waves have a fractal structure [9]. The Flinders University Gravitational Waves Detector (also a coaxial cable experiment) was constructed to investigate these waves effects. This sees the wave effects detected by Miller, Torr and Kolen, and by De Witte. The plan of this paper is to first outline the modern understanding of how a gas-mode Michelson interferometer actually operates, and the nature, accuracy and significance of the Miller experiment. We also report the other seven experiments that confirm the Miller discoveries, particularly data from the new high-precision gravity wave detector that detects not only a light speed anisotropy but also the wave effects.

2 Special Relativity and the speed of light anisotropy

It is often assumed that the anisotropy of the speed of light is inconsistent with Special Relativity, that only one or the

other can be valid, that they are mutually incompatible. This misunderstanding is very prevalent in the literature of physics, although this conceptual error has been explained [1]. The error is based upon a misunderstanding of how the logic of theoretical physics works, namely the important difference between an *if* statement, and an *if and only if* statement. To see how this confusion has arisen we need to recall the history of Special Relativity (SR). In 1905 Einstein deduced the SR formalism by assuming, in part, that the speed of light is invariant for all relatively moving observers, although most importantly one must ask just how that speed is defined or is to be measured. The SR formalism then predicted numerous effects, which have been extensively confirmed by experiments over the last 100 years. However this Einstein derivation was an *if* statement, and not an *if and only if* statement. For an *if* statement, that *if A then B*, does not imply the truth of A if B is found to be true; only an *if and only if* statement has that property, and Einstein did not construct such an argument. What this means is that the validity of the various SR effects does *not* imply that the speed of light must be isotropic. This is actually implicit in the SR formalism itself, for it permits one to use any particular foliation of the 4-dimensional spacetime into a 3-space and a 1-space (for time). Most importantly it does not forbid that one particular foliation be actual. So to analyse the data from gas-mode interferometer experiments we must use the SR effects, and the fringe shifts reveal the preferred frame, an actual 3-space, by revealing the anisotropic speed of light, as Maxwell and Michelson had originally believed.

For "modern" resonant-cavity Michelson interferometer experiments we predict no rotation-induced fringe shifts, unless operated in gas-mode. Unfortunately in analysing the data from the vacuum-mode experiments the consequent null effect is misinterpreted, as in [7], to imply the absence of a preferred direction, of absolute motion. But it is absolute motion which causes the dynamical effects of length contractions, time dilations and other relativistic effects, in accord with Lorentzian interpretation of relativistic effects.

The detection of absolute motion is not incompatible with Lorentz symmetry; the contrary belief was postulated by Einstein, and has persisted for over 100 years, since 1905. So far the experimental evidence is that absolute motion and Lorentz symmetry are real and valid phenomena; absolute motion is motion presumably relative to some substructure to space, whereas Lorentz symmetry parameterises dynamical effects caused by the motion of systems through that substructure. To check Lorentz symmetry we can use vacuum-mode resonant-cavity interferometers, but using gas within the resonant-cavities would enable these devices to detect absolute motion with great precision. As well there are novel wave phenomena that could also be studied, as discussed herein and in [19, 20].

Motion through the structured space, it is argued, induces actual dynamical time dilations and length contractions in agreement with the Lorentz interpretation of special relativistic effects. Then observers in uniform motion "through" the space will, on measurement of the speed of light using the special but misleading Einstein measurement protocol, obtain always the same numerical value c. To see this explicitly consider how various observers $P, P', \dots$ moving with different speeds through space, measure the speed of light. They each acquire a standard rod and an accompanying standardised clock. That means that these standard rods would agree if they were brought together, and at rest with respect to space they would all have length Δl_0, and similarly for the clocks. Observer P and accompanying rod are both moving at speed v_R relative to space, with the rod longitudinal to that motion. P then measures the time Δt_R, with the clock at end A of the rod, for a light pulse to travel from end A to the other end B and back again to A. The light travels at speed c relative to space. Let the time taken for the light pulse to travel from $A \to B$ be t_{AB} and from $B \to A$ be t_{BA}, as measured by a clock at rest with respect to space*. The length of the rod moving at speed v_R is contracted to

$$\Delta l_R = \Delta l_0 \sqrt{1 - \frac{v_R^2}{c^2}} \,. \tag{1}$$

In moving from A to B the light must travel an extra distance because the end B travels a distance $v_R t_{AB}$ in this time, thus the total distance that must be traversed is

$$c t_{AB} = \Delta l_R + v_R t_{AB} \,, \tag{2}$$

similarly on returning from B to A the light must travel the distance

$$c t_{BA} = \Delta l_R - v_R t_{BA} \,. \tag{3}$$

Hence the total travel time Δt_0 is

$$\Delta t_0 = t_{AB} + t_{BA} = \frac{\Delta l_R}{c - v_R} + \frac{\Delta l_R}{c + v_R} = \tag{4}$$

$$= \frac{2\Delta l_0}{c\sqrt{1 - \frac{v_R^2}{c^2}}} \,. \tag{5}$$

Because of the time dilation effect for the moving clock

$$\Delta t_R = \Delta t_0 \sqrt{1 - \frac{v_R^2}{c^2}} \,. \tag{6}$$

Then for the moving observer the speed of light is defined as the distance the observer believes the light travelled ($2\Delta l_0$) divided by the travel time according to the accompanying clock (Δt_R), namely $2\Delta l_0 / \Delta t_R = 2\Delta l_R / \Delta t_0$, from above, which is thus the same speed as seen by an observer at rest in the space, namely c. So the speed v_R of the observer through space is not revealed by this procedure, and the observer is erroneously led to the conclusion that the speed of light is always c. This follows from two or more

*Not all clocks will behave in this same "ideal" manner.

observers in manifest relative motion all obtaining the same speed c by this procedure. Despite this failure this special effect is actually the basis of the spacetime Einstein measurement protocol. That this protocol is blind to the absolute motion has led to enormous confusion within physics.

To be explicit the Einstein measurement protocol actually inadvertently uses this special effect by using the radar method for assigning historical spacetime coordinates to an event: the observer records the time of emission and reception of radar pulses ($t_r > t_e$) travelling through space, and then retrospectively assigns the time and distance of a distant event B according to (ignoring directional information for simplicity)

$$T_B = \frac{1}{2}\left(t_r + t_e\right), \qquad D_B = \frac{c}{2}\left(t_r - t_e\right), \tag{7}$$

where each observer is now using the same numerical value of c. The event B is then plotted as a point in an individual geometrical construct by each observer, known as a spacetime record, with coordinates (D_B, T_B). This is no different to an historian recording events according to some agreed protocol. Unlike historians, who don't confuse history books with reality, physicists do so. We now show that because of this protocol and the absolute motion dynamical effects, observers will discover on comparing their historical records of the same events that the expression

$$\tau_{AB}^2 = T_{AB}^2 - \frac{1}{c^2}\, D_{AB}^2\,, \tag{8}$$

is an invariant, where $T_{AB} = T_A - T_B$ and $D_{AB} = D_A - D_B$ are the differences in times and distances assigned to events A and B using the Einstein measurement protocol (7), so long as both are sufficiently small compared with the scale of inhomogeneities in the velocity field.

To confirm the invariant nature of the construct in (8) one must pay careful attention to observational times as distinct from protocol times and distances, and this must be done separately for each observer. This can be tedious. We now demonstrate this for the situation illustrated in Fig. 1.

By definition the speed of P' according to P is $v_0' = D_B/T_B$ and so $v_R' = v_0'$, where T_B and D_B are the protocol time and distance for event B for observer P according to (7). Then using (8) P would find that $\left(\tau_{AB}^P\right)^2 = T_B^2 - \frac{1}{c^2} D_B^2$ since both $T_A = 0$ and $D_A = 0$, and whence $\left(\tau_{AB}^P\right)^2 = \left(1 - \frac{v_R'^2}{c^2}\right) T_B^2 = (t_B')^2$ where the last equality follows from the time dilation effect on the P' clock, since t_B' is the time of event B according to that clock. Then T_B is also the time that P' would compute for event B when correcting for the time-dilation effect, as the speed v_R' of P' through space is observable by P'. Then T_B is the "common time" for event B assigned by both observers. For P' we obtain directly, also from (7) and (8), that $\left(\tau_{AB}^{P'}\right)^2 = (T_B')^2 - \frac{1}{c^2}(D_B')^2 = (t_B')^2$, as $D_B' = 0$ and $T_B' = t_B'$. Whence for this situation

$$\left(\tau_{AB}^P\right)^2 = \left(\tau_{AB}^{P'}\right)^2, \tag{9}$$

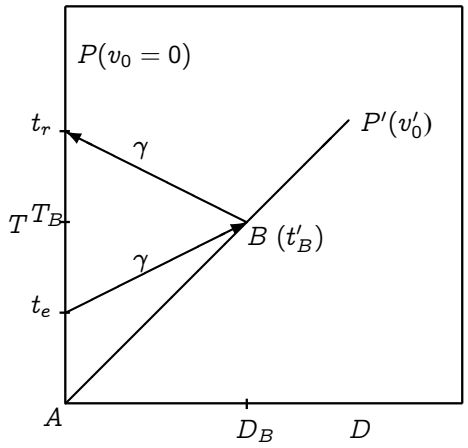

Fig. 1: Here $T - D$ is the spacetime construct (from the Einstein measurement protocol) of a special observer P *at rest* wrt space, so that $v_0 = 0$. Observer P' is moving with speed v_0' as determined by observer P, and therefore with speed $v_R' = v_0'$ wrt space. Two light pulses are shown, each travelling at speed c wrt both P and space. Event A is when the observers pass, and is also used to define zero time for each for convenience.

and so the construction (8) is an invariant.

While so far we have only established the invariance of the construct (8) when one of the observers is at rest in space, it follows that for two observers P' and P'' both in absolute motion it follows that they also agree on the invariance of (8). This is easily seen by using the intermediate step of a stationary observer P:

$$\left(\tau_{AB}^{P'}\right)^2 = \left(\tau_{AB}^{P}\right)^2 = \left(\tau_{AB}^{P''}\right)^2. \tag{10}$$

Hence the protocol and Lorentzian absolute motion effects result in the construction in (8) being indeed an invariant in general. This is a remarkable and subtle result. For Einstein this invariance was a fundamental assumption, but here it is a derived result, but one which is nevertheless deeply misleading. Explicitly indicating small quantities by Δ prefixes, and on comparing records retrospectively, an ensemble of nearby observers agree on the invariant

$$\Delta\tau^2 = \Delta T^2 - \frac{1}{c^2}\,\Delta D^2, \tag{11}$$

for any two nearby events. This implies that their individual patches of spacetime records may be mapped one into the other merely by a change of coordinates, and that collectively the spacetime patches of all may be represented by one pseudo-Riemannian manifold, where the choice of coordinates for this manifold is arbitrary, and we finally arrive at the invariant

$$\Delta\tau^2 = g_{\mu\nu}(x)\,\Delta x^\mu \Delta x^\nu, \tag{12}$$

with $x^\mu = \{D_1, D_2, D_3, T\}$. Eqn. (12) is invariant under the Lorentz transformations

$$x'^\mu = L^\mu{}_\nu\, x^\nu, \tag{13}$$

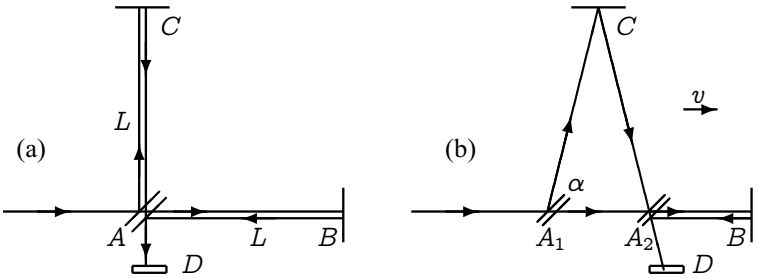

Fig. 2: Schematic diagrams of the Michelson Interferometer, with beamsplitter/mirror at A and mirrors at B and C on arms from A, with the arms of equal length L when at rest. D is a screen or detector. In (a) the interferometer is at rest in space. In (b) the interferometer is moving with speed v relative to space in the direction indicated. Interference fringes are observed at the detector D. If the interferometer is rotated in the plane through 90^o, the roles of arms AC and AB are interchanged, and during the rotation shifts of the fringes are seen in the case of absolute motion, but only if the apparatus operates in a gas. By counting fringe changes the speed v may be determined.

where, for example for relative motion in the x direction, $L^{\mu}{}_{\nu}$ is specified by

$$\begin{aligned} x' &= \frac{x - vt}{\sqrt{1 - v^2/c^2}}\,, \\ y' &= y\,, \\ z' &= z\,, \\ t' &= \frac{t - vx/c^2}{\sqrt{1 - v^2/c^2}}\,. \end{aligned} \tag{14}$$

So absolute motion and special relativity effects, and even Lorentz symmetry, are all compatible: a possible preferred frame is hidden by the Einstein measurement protocol.

So the experimental question is then whether or not a supposed preferred frame actually exists or not — can it be detected experimentally? The answer is that there are now eight such consistent experiments. In Sect. 4.7 we generalise the Dirac equation to take account of the coupling of the spinor to an actual dynamical space. This reveals again that relativistic effects are consistent with a preferred frame — an actual space. Furthermore this leads to the first derivation of gravity from a deeper theory — gravity turns out to be a quantum matter wave effect.

3 Light speed anisotropy experiments

We now consider the various experiments from over more than 100 years that have detected the anisotropy of the speed of light, and so the existence of an actual dynamical space, an observable preferred frame. As well the experiments, it is now understood, showed that this frame is dynamical, it exhibits time-dependent effects, and that these are "gravitational waves".

3.1 Michelson gas-mode interferometer

Let us first consider the new understanding of how the Michelson interferometer works. This brilliant but very subtle device was conceived by Michelson as a means to detect the anisotropy of the speed of light, as was expected towards the end of the 19th century. Michelson used Newtonian physics to develop the theory and hence the calibration for his device. However we now understand that this device detects 2nd order effects in v/c to determine v, and so we must use relativistic effects. However the application and analysis of data from various Michelson interferometer experiments using a relativistic theory only occurred in 2002, some 97 years after the development of Special Relativity by Einstein, and some 115 years after the famous 1887 experiment. As a consequence of the necessity of using relativistic effects it was discovered in 2002 that the gas in the light paths plays a critical role, and that we finally understand how to calibrate the device, and we also discovered, some 76 years after the 1925/26 Miller experiment, what determines the calibration constant that Miller had determined using the Earth's rotation speed about the Sun to set the calibration. This, as we discuss later, has enabled us to now appreciate that gas-mode Michelson interferometer experiments have confirmed the reality of the Fitzgerald-Lorentz length contraction effect: in the usual interpretation of Special Relativity this effect, and others, is usually regarded as an observer dependent effect, an illusion induced by the spacetime. But the experiments are to the contrary showing that the length contraction effect is an actual observer-independent dynamical effect, as Fitzgerald [27] and Lorentz had proposed [28].

The Michelson interferometer compares the change in the difference between travel times, when the device is rotated, for two coherent beams of light that travel in orthogonal directions between mirrors; the changing time difference being indicated by the shift of the interference fringes during the rotation. This effect is caused by the absolute motion of the device through 3-space with speed v, and that the speed of light is relative to that 3-space, and not relative to the apparatus/observer. However to detect the speed of the apparatus through that 3-space gas must be present in the light paths for purely technical reasons. The post relativistic-

effects theory for this device is remarkably simple. The relativistic Fitzgerald-Lorentz contraction effect causes the arm AB parallel to the absolute velocity to be physically contracted to length

$$L_{||} = L\sqrt{1-\frac{v^2}{c^2}}\,. \qquad (15)$$

The time t_{AB} to travel AB is set by $Vt_{AB} = L_{||} + vt_{AB}$, while for BA by $Vt_{BA} = L_{||} - vt_{BA}$, where $V = c/n$ is the speed of light, with n the refractive index of the gas present (we ignore here the Fresnel drag effect for simplicity, an effect caused by the gas also being in absolute motion, see [1]). For the total ABA travel time we then obtain

$$t_{ABA} = t_{AB} + t_{BA} = \frac{2LV}{V^2 - v^2}\sqrt{1-\frac{v^2}{c^2}}\,. \qquad (16)$$

For travel in the AC direction we have, from the Pythagoras theorem for the right-angled triangle in Fig. 1 that $(Vt_{AC})^2 = L^2 + (vt_{AC})^2$ and that $t_{CA} = t_{AC}$. Then for the total ACA travel time

$$t_{ACA} = t_{AC} + t_{CA} = \frac{2L}{\sqrt{V^2 - v^2}}\,. \qquad (17)$$

Then the difference in travel time is

$$\Delta t = \frac{(n^2-1)\,L}{c}\frac{v^2}{c^2} + \mathrm{O}\left(\frac{v^4}{c^4}\right). \qquad (18)$$

after expanding in powers of v/c. This clearly shows that the interferometer can only operate as a detector of absolute motion when not in vacuum ($n = 1$), namely when the light passes through a gas, as in the early experiments (in transparent solids a more complex phenomenon occurs). A more general analysis [1], including Fresnel drag, gives

$$\Delta t = k^2\frac{Lv_P^2}{c^3}\cos\big(2(\theta-\psi)\big)\,, \qquad (19)$$

where $k^2 \approx n(n^2-1)$, while neglect of the relativistic Fitzgerald-Lorentz contraction effect gives $k^2 \approx n^3 \approx 1$ for gases, which is essentially the Newtonian theory that Michelson used.

However the above analysis does not correspond to how the interferometer is actually operated. That analysis does not actually predict fringe shifts for the field of view would be uniformly illuminated, and the observed effect would be a changing level of luminosity rather than fringe shifts. As Miller knew the mirrors must be made slightly non-orthogonal, with the degree of non-orthogonality determining how many fringe shifts were visible in the field of view. Miller experimented with this effect to determine a comfortable number of fringes: not too few and not too many. Hicks [29] developed a theory for this effect — however it is not necessary to be aware of this analysis in using the interferometer: the non-orthogonality reduces the symmetry of the device, and

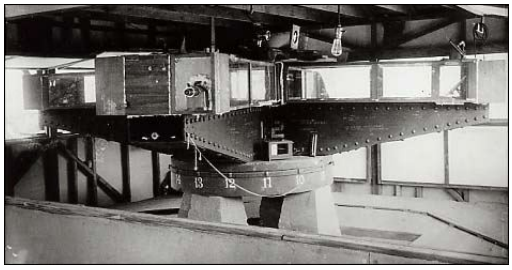

Fig. 3: Miller's interferometer with an effective arm length of $L = 32$ m achieved by multiple reflections. Used by Miller on Mt.Wilson to perform the 1925-1926 observations of absolute motion. The steel arms weighed 1200 kilograms and floated in a tank of 275 kilograms of Mercury. From Case Western Reserve University Archives.

instead of having period of 180° the symmetry now has a period of 360°, so that to (19) we must add the extra term in

$$\Delta t = k^2\frac{Lv_P^2}{c^3}\cos\big(2(\theta-\psi)\big) + a\cos(\theta-\beta)\,. \qquad (20)$$

Miller took this effect into account when analysing his data. The effect is apparent in Fig. 5, and even more so in the Michelson-Morley data in Fig. 4.

The interferometers are operated with the arms horizontal, as shown by Miller's interferometer in Fig. 3. Then in (20) θ is the azimuth of one arm relative to the local meridian, while ψ is the azimuth of the absolute motion velocity projected onto the plane of the interferometer, with projected component v_P. Here the Fitzgerald-Lorentz contraction is a real dynamical effect of absolute motion, unlike the Einstein spacetime view that it is merely a spacetime perspective artifact, and whose magnitude depends on the choice of observer. The instrument is operated by rotating at a rate of one rotation over several minutes, and observing the shift in the fringe pattern through a telescope during the rotation. Then fringe shifts from six (Michelson and Morley) or twenty (Miller) successive rotations are averaged to improve the signal to noise ratio, and the average sidereal time noted, giving the Michelson-Morley data in Fig. 4. or the Miller data like that in Fig. 5. The form in (20) is then fitted to such data by varying the parameters v_P, ψ, a and β, The data from rotations is sufficiently clear, as in Fig. 5, that Miller could easily determine these parameters from a graphical plot.

However Michelson and Morley implicitly assumed the Newtonian value k=1, while Miller used an indirect method to estimate the value of k, as he understood that the Newtonian theory was invalid, but had no other theory for the interferometer. Of course the Einstein postulates, as distinct from Special Relativity, have that absolute motion has no meaning, and so effectively demands that k=0. Using k=1 gives only a nominal value for v_P, being some 8–9 km/s for the Michelson and Morley experiment, and some 10 km/s from Miller; the difference arising from the different latitu-

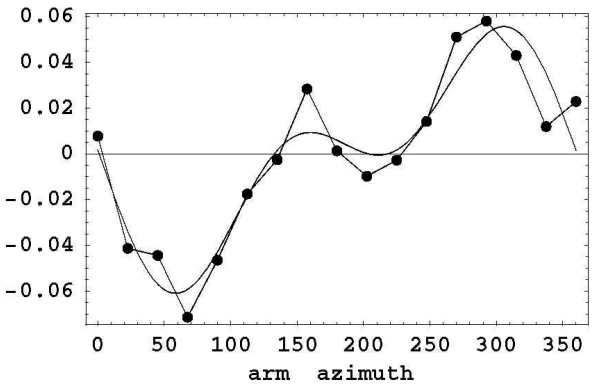

Fig. 4: Example of Michelson-Morley fringe shifts from average of 6 rotations measured every 22.5°, in fractions of a wavelength $\Delta\lambda/\lambda$, vs arm azimuth θ(deg), from Cleveland, Ohio, July 11, 1887 12:00 hrs local time or 7:00 hrs local sidereal time. This shows the quality of the fringe shift data that Michelson and Morley obtained. The curve is the best fit using the form in (20) which includes the Hick's $\cos(\theta-\beta)$ component that is required when the mirrors are not orthognal, and gives $\psi = 140°$, or 40° measured from South, compared to the Miller ψ for August at 7:00 hrs local sidereal time in Fig. 6, and a projected speed of $v_P = 400$ km/s. The Hick's effect is much larger in this data than in the Miller data in Fig. 5.

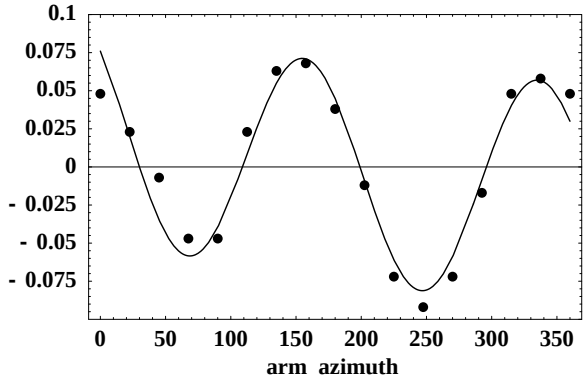

Fig. 5: Typical Miller rotation-induced fringe shifts from average of 20 rotations, measured every 22.5°, in fractions of a wavelength $\Delta\lambda/\lambda$, vs arm azimuth θ(deg), measured clockwise from North, from Cleveland Sept. 29, 1929 16:24 UT; 11:29 hrs average local sidereal time. The curve is the best fit using the form in (20) which includes the Hick's $\cos(\theta-\beta)$ component that is required when the mirrors are not orthognal, and gives $\psi = 158°$, or 22° measured from South, and a projected speed of $v_P = 351$ km/s. This process was repeated some 8,000 times over days throughout 1925/1926 giving, in part, the data in Fig. 6 and Fig. 18.

des of Cleveland and Mt. Wilson, and from Michelson and Morley taking data at limited times. So already Miller knew that his observations were consistent with those of Michelson and Morley, and so the important need for reproducibility was being confirmed.

3.2 Michelson-Morley experiment

The Michelson and Morley air-mode interferometer fringe shift data was based upon a total of only 36 rotations in July 1887, revealing the nominal speed of some 8–9 km/s when analysed using the prevailing but incorrect Newtonian theory which has $k = 1$ in (20), and this value was known to Michelson and Morley. Including the Fitzgerald-Lorentz dynamical contraction effect as well as the effect of the gas present as in (20) we find that $n_{air} = 1.00029$ gives $k^2 = 0.00058$ for air, which explains why the observed fringe shifts were so small. The example in Fig. 4 reveals a speed of 400 km/s with an azimuth of 40° measured from south at 7:00 hrs local sidereal time. The data is clearly very consistent with the expected form in (20). They rejected their own data on the sole but spurious ground that the value of 8 km/s was smaller than the speed of the Earth about the Sun of 30km/s. What their result really showed was that (i) absolute motion had been detected because fringe shifts of the correct form, as in (20), had been detected, and (ii) that the theory giving $k^2 = 1$ was wrong, that Newtonian physics had failed. Michelson and Morley in 1887 should have announced that the speed of light did depend of the direction of travel, that the speed was relative to an actual physical 3-space. However contrary to their own data they concluded that absolute motion had not been detected. This bungle has had enormous implications for fundamental theories of space and time over the last 100 years, and the resulting confusion is only now being finally corrected, albeit with fierce and spurious objections.

3.3 Miller interferometer

It was Miller [4] who saw the flaw in the 1887 paper and realised that the theory for the Michelson interferometer must be wrong. To avoid using that theory Miller introduced the scaling factor k, even though he had no theory for its value. He then used the effect of the changing vector addition of the Earth's orbital velocity and the absolute galactic velocity of the solar system to determine the numerical value of k, because the orbital motion modulated the data, as shown in Fig. 6. By making some 8,000 rotations of the interferometer at Mt. Wilson in 1925/26 Miller determined the first estimate for k and for the absolute linear velocity of the solar system. Fig. 5 shows typical data from averaging the fringe shifts from 20 rotations of the Miller interferometer, performed over a short period of time, and clearly shows the expected form in (20) (only a linear drift caused by temperature effects on the arm lengths has been removed — an effect also removed by Michelson and Morley and also by Miller). In Fig. 5 the fringe shifts during rotation are given as fractions of a wavelength, $\Delta\lambda/\lambda = \Delta t/T$, where Δt is given by (20) and T is the period of the light. Such rotation-induced fringe shifts clearly show that the speed of light is different in different directions. The claim that Michelson interferometers, operating in gas-mode, do not produce fringe shifts under

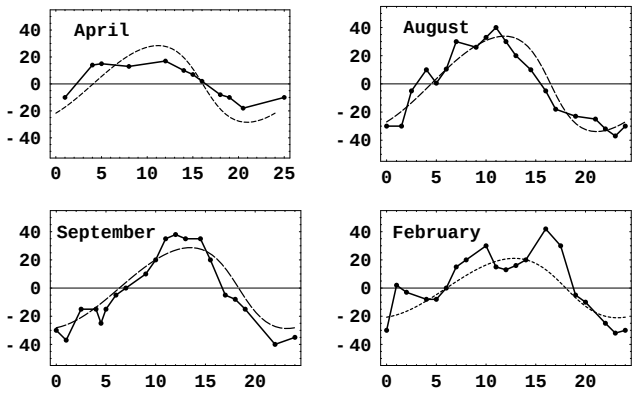

Fig. 6: Miller azimuths ψ, measured from south and plotted against sidereal time in hours, showing both data and best fit of theory giving $v_{cosmic} = 433$ km/s in the direction (RA $= 5.2^{\text{hr}}$, Dec $= -67^\circ$), and using $n = 1.000226$ appropriate for the altitude of Mt. Wilson. The azimuth data gives a clearer signal than the speed data in Fig. 18. The data shows that the time when the azimuth ψ is zero tracks sidereal time, with the zero times being approximately 5 hrs and 17 hrs. However these times correspond to very different local times, for from April to August, for example, there is a shift of 8 hrs in the local time for these crossings. This is an enormous effect. Again this is the acid test for light speed anisotropy experiments when allowing the rotation of the Earth to change the orientation of the apparatus. The zero crossing times are when the velocity vector for absolute motion when projected onto the plane of the interferometer lines up with the local meridian. As well we see variations throughout these composite days with the crossing times changing by as much as ± 3 hrs, The same effect, and perhaps even larger, is seen in the Flinders data in Fig. 15. The above plots also show a distinctive signature, namely the change from month to month. This is caused by the vector addition of the Earth's orbital velocity of 30 km/s, the Sun's spatial in-flow velocity of 42 km/s at the Earth's distance and the cosmic velocity changing over a year. This is the effect that Miller used to calibrate his interferometer. However he did not know of the Sun in-flow component. Only after taking account of that effect does this calibration method agree with the results from the calibration method using Special Relativity, as in (20).

rotation is clearly incorrect. But it is that claim that lead to the continuing belief, within physics, that absolute motion had never been detected, and that the speed of light is invariant. The value of ψ from such rotations together lead to plots like those in Fig. 6, which show ψ from the 1925/1926 Miller [4] interferometer data for four different months of the year, from which the RA $= 5.2$ hr is readily apparent. While the orbital motion of the Earth about the Sun slightly affects the RA in each month, and Miller used this effect do determine the value of k, the new theory of gravity required a reanalysis of the data [1, 19], revealing that the solar system has a large observed galactic velocity of some 420 ± 30 km/s in the direction (RA $= 5.2$ hr, Dec $= -67^\circ$). This is different from the speed of 369 km/s in the direction (RA $= 11.20$ hr, Dec $= -7.22^\circ$) extracted from the Cosmic Microwave Background (CMB) anisotropy, and which describes a motion relative to the distant universe, but not relative to the local 3-space. The Miller velocity is explained by galactic gravitational in-flows [1].

3.4 Other gas-mode Michelson interferometer experiments

Two old interferometer experiments, by Illingworth [11] and Joos [12], used helium, enabling the refractive index effect to be recently confirmed, because for helium, with $n = 1.000036$, we find that $k^2 = 0.00007$. Until the refractive index effect was taken into account the data from the helium-mode experiments appeared to be inconsistent with the data from the air-mode experiments; now they are seen to be consistent [1]. Ironically helium was introduced in place of air to reduce any possible unwanted effects of a gas, but we now understand the essential role of the gas. The data from an interferometer experiment by Jaseja *et al.* [13], using two orthogonal masers with a He-Ne gas mixture, also indicates that they detected absolute motion, but were not aware of that as they used the incorrect Newtonian theory and so considered the fringe shifts to be too small to be real, reminiscent of the same mistake by Michelson and Morley. The Michelson interferometer is a 2nd order device, as the effect of absolute motion is proportional to $(v/c)^2$, as in (20), but 1st order devices are also possible and the coaxial cable experiments described next are in this class. The experimental results and the implications for physics have been extensively reported in [1, 14, 15, 16, 17, 18].

3.5 Coaxial cable speed of EM waves anisotropy experiments

Rather than use light travel time experiments to demonstrate the anisotropy of the speed of light another technique is to measure the one-way speed of radio waves through a coaxial electrical cable. While this not a direct "ideal" technique, as then the complexity of the propagation physics comes into play, it provides not only an independent confirmation of the light anisotropy effect, but also one which takes advantage of modern electronic timing technology.

3.6 Torr-Kolen coaxial cable anisotropy experiment

The first one-way coaxial cable speed-of-propagation experiment was performed at the Utah University in 1981 by Torr and Kolen. This involved two rubidium clocks placed approximately 500 m apart with a 5 MHz radio frequency (RF) signal propagating between the clocks via a buried nitrogen-filled coaxial cable maintained at a constant pressure of 2 psi. Torr and Kolen found that, while the round speed time remained constant within 0.0001% c, as expected from Sect. 2, variations in the one-way travel time were observed. The maximum effect occurred, typically, at the times predicted using the Miller galactic velocity, although

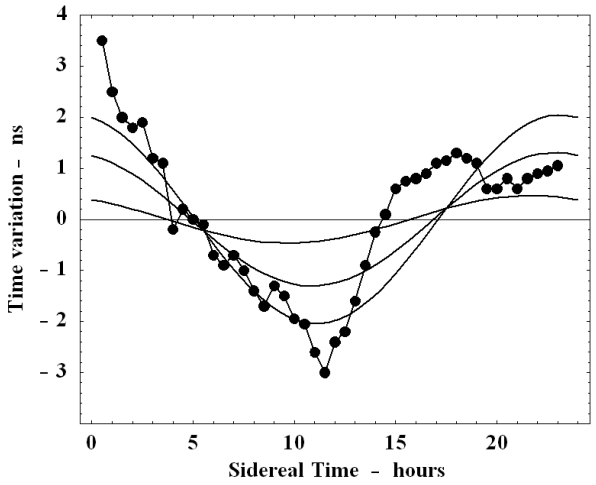

Fig. 7: Data from one day of the Torr-Kolen coaxial cable anisotropy experiment. Smooth curves show variations in travel times when the declination is varied by $\pm 10^\circ$ about the direction ($\mathrm{RA} = 5.2^{\mathrm{hr}}$, $\mathrm{Dec} = -67^\circ$), for a cosmic speed of 433 km/s. Most importantly the dominant feature is consistent with the predicted local sidereal time.

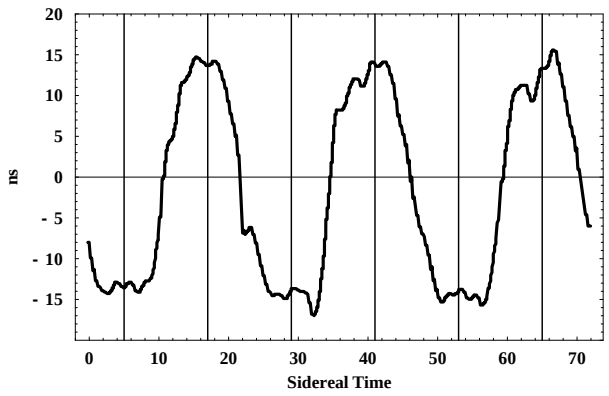

Fig. 8: Variations in twice the one-way travel time, in ns, for an RF signal to travel 1.5 km through a coaxial cable between Rue du Marais and Rue de la Paille, Brussels. An offset has been used such that the average is zero. The cable has a North-South orientation, and the data is $\pm$ difference of the travel times for NS and SN propagation. The sidereal time for maximum effect of ~ 5 hr and ~ 17 hr (indicated by vertical lines) agrees with the direction found by Miller. Plot shows data over 3 sidereal days and is plotted against sidereal time. The fluctuations are evidence of turbulence of gravitational waves.

Torr and Kolen appear to have been unaware of the Miller experiment. As well Torr and Kolen reported fluctuations in both the magnitude, from 1–3 ns, and the time of maximum variations in travel time. These effects are interpreted as arising from the turbulence in the flow of space past the Earth. One day of their data is shown in Fig. 7.

3.7 De Witte coaxial cable anisotropy experiment

During 1991 Roland De Witte performed a most extensive RF coaxial cable travel-time anisotropy experiment, accumulating data over 178 days. His data is in complete agreement with the Michelson-Morley 1887 and Miller 1925/26 interferometer experiments. The Miller and De Witte experiments will eventually be recognised as two of the most significant experiments in physics, for independently and using different experimental techniques they detected essentially the same velocity of absolute motion. But also they detected turbulence in the flow of space past the Earth — none other than gravitational waves. The De Witte experiment was within Belgacom, the Belgium telecommunications company. This organisation had two sets of atomic clocks in two buildings in Brussels separated by 1.5 km and the research project was an investigation of the task of synchronising these two clusters of atomic clocks. To that end 5MHz RF signals were sent in both directions through two buried coaxial cables linking the two clusters. The atomic clocks were caesium beam atomic clocks, and there were three in each cluster: A1, A2 and A3 in one cluster, and B1, B2, and B3 at the other cluster. In that way the stability of the clocks could be established and monitored. One cluster was in a building on Rue du Marais and the second cluster was due south in a building on Rue de la Paille. Digital phase comparators were used to measure changes in times between clocks within the same cluster and also in the one-way propagation times of the RF signals. At both locations the comparison between local clocks, A1-A2 and A1-A3, and between B1-B2, B1-B3, yielded linear phase variations in agreement with the fact that the clocks have not exactly the same frequencies together with a short term and long term phase noise. But between distant clocks A1 toward B1 and B1 toward A1, in addition to the same linear phase variations, there is also an additional clear sinusoidal-like phase undulation with an approximate 24 hr period of the order of 28 ns peak to peak, as shown in Fig. 8. The possible instability of the coaxial lines cannot be responsible for the observed phase effects because these signals are in phase opposition and also because the lines are identical (same place, length, temperature, etc. . .) causing the cancellation of any such instabilities. As well the experiment was performed over 178 days, making it possible to measure with an accuracy of 25 s the period of the phase signal to be the sidereal day (23 hr 56 min).

Changes in propagation times were observed over 178 days from June 3 to November 27, 1991. A sample of the data, plotted against sidereal time for just three days, is shown in Fig. 8. De Witte recognised that the data was evidence of absolute motion but he was unaware of the Miller experiment and did not realise that the Right Ascensions for minimum/maximum propagation time agreed almost exactly with that predicted using the Miller's direction ($\mathrm{RA} = 5.2$ hr, $\mathrm{Dec} = -67^\circ$). In fact De Witte expected that the direction of absolute motion should have been in the CMB direction, but

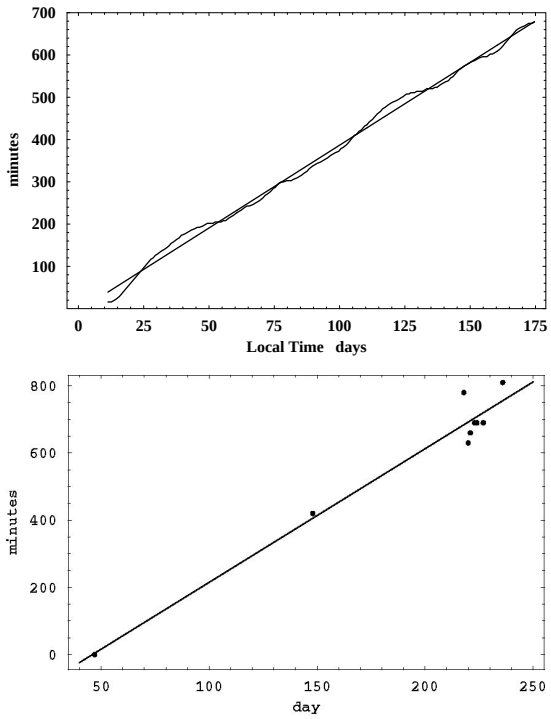

Fig. 9: **Upper:** Plot from the De Witte data of the negative of the drift of the cross-over time between minimum and maximum travel-time variation each day (at $\sim$ 10hr$\pm$1hr ST) versus local solar time for some 180 days. The straight line plot is the least-squares fit to the experimental data, giving an average slope of 3.92 minutes/day. The time difference between a sidereal day and a solar day is 3.93 minutes/day. This demonstrates that the effect is related to sidereal time and not local solar time. **Lower:** Analogous sidereal effect seen in the Flinders experiment. Due to on-going developments the data is not available for all days, but sufficient data is present to indicate a time shift of 3.97 minutes/day. This data also shows greater fluctuations than indicated by the De Witte data, presumably because De Witte used more extensive data averaging.

that would have given the data a totally different sidereal time signature, namely the times for maximum/minimum would have been shifted by 6 hrs. The declination of the velocity observed in this De Witte experiment cannot be determined from the data as only three days of data are available. The De Witte data is analysed in Sect. 4.7 and assuming a declination of 60° S a speed of 430 km/s is obtained, in good agreement with the Miller speed and Michelson-Morley speed. So a different and non-relativistic technique is confirming the results of these older experiments. This is dramatic.

De Witte did however report the sidereal time of the cross-over time, that is in Fig. 8 for all 178 days of data. That showed, as in Fig. 9, that the time variations are correlated with sidereal time and not local solar time. A least-squares best fit of a linear relation to that data gives that the cross-over time is retarded, on average, by 3.92 minutes per solar day. This is to be compared with the fact that a sidereal day

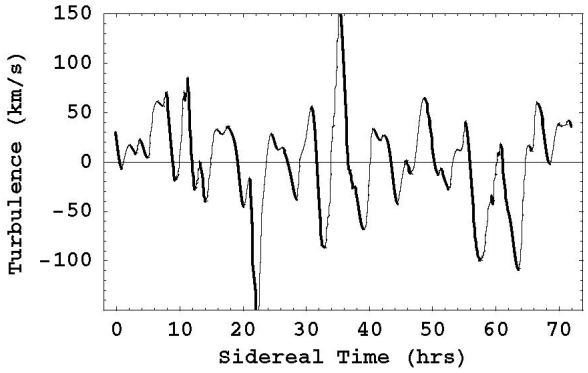

Fig. 10: Shows the speed fluctuations, essentially "gravitational waves" observed by De Witte in 1991 from the measurement of variations in the RF coaxial-cable travel times. This data is obtained from that in Fig. 8 after removal of the dominant effect caused by the rotation of the Earth. Ideally the velocity fluctuations are three-dimensional, but the De Witte experiment had only one arm. This plot is suggestive of a fractal structure to the velocity field. This is confirmed by the power law analysis in [8, 9].

is 3.93 minutes shorter than a solar day. So the effect is certainly galactic and not associated with any daily thermal effects, which in any case would be very small as the cable is buried. Miller had also compared his data against sidereal time and established the same property, namely that the diurnal effects actually tracked sidereal time and not solar time, and that orbital effects were also apparent, with both effects apparent in Fig. 6.

The dominant effect in Fig. 8 is caused by the rotation of the Earth, namely that the orientation of the coaxial cable with respect to the average direction of the flow past the Earth changes as the Earth rotates. This effect may be approximately unfolded from the data leaving the gravitational waves shown in Fig. 10. This is the first evidence that the velocity field describing the flow of space has a complex structure, and is indeed fractal. The fractal structure, i. e. that there is an intrinsic lack of scale to these speed fluctuations, is demonstrated by binning the absolute speeds and counting the number of speeds within each bin, as discussed in [8, 9]. The Miller data also shows evidence of turbulence of the same magnitude. So far the data from three experiments, namely Miller, Torr and Kolen, and De Witte, show turbulence in the flow of space past the Earth. This is what can be called gravitational waves. This can be understood by noting that fluctuations in the velocity field induce ripples in the mathematical construct known as spacetime, as in (32). Such ripples in spacetime are known as gravitational waves.

4 Flinders University gravitational wave detector

In February 2006 first measurements from a gravitational wave detector at Flinders University, Adelaide, were taken. This detector uses a novel timing scheme that overcomes the limitations associated with the two previous coaxial cable

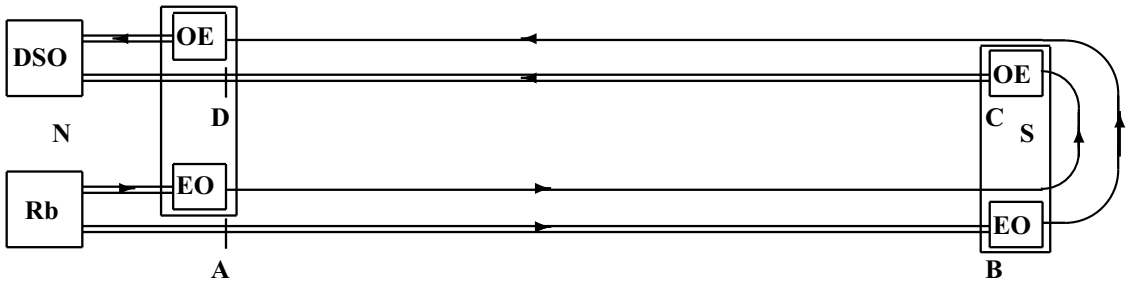

Fig. 11: Schematic layout of the Flinders University Gravitational Wave Detector. Double lines denote coaxial cables, and single lines denote optical fibres. The detector is shown in Fig. 12 and is orientated NS along the local meridian, as indicated by direction D in Fig. 16. Two 10 MHz RF signals come from the Rubidium atomic clock (Rb). The Electrical to Optical converters (EO) use the RF signals to modulate 1.3 μm infrared signals that propagate through the single-mode optical fibres. The Optical to Electrical converters (OE) demodulate that signal and give the two RF signals that finally reach the Digital Storage Oscilloscope (DSO), which measures their phase difference. Pairs of E/O and O/E are grouped into one box. Overall this apparatus measures the *difference* in EM travel time from A to B compared to C to D. All other travel times cancel in principle, though in practice small differences in cable or fibre lengths need to be electronically detected by the looping procedure. The key effects are that the propagation speeds through the coaxial cables and optical fibres respond differently to their absolute motion through space. The special optical fibre propagation effect is discussed in the text. Sections AB and CD each have length 5.0 m. The fibres and coaxial cable are specially manufactured to have negligible variation in travel speed with variation in temperature. The zero-speed calibration point can be measured by looping the arm back onto itself, as shown in Fig. 13, because then the 1st order in v/c effect cancels, and only 2nd order effects remain, and these are much smaller than the noise levels in the system. This detector is equivalent to a one-way speed measurement through a single coaxial cable of length 10 m, with an atomic clock at each end to measure changes in travel times. However for 10 m coaxial cable that would be impractical because of clock drifts. With this set-up the travel times vary by some 25 ps over one day, as shown in Figs.14 and 17. The detector was originally located in the author's office, as shown in Fig. 12, but was later located in an underground laboratory where temperature variations were very slow. The travel time variations over 7 days are shown in Fig. 15.

experiments. The intention in such experiments is simply to measure the one-way travel time of RF waves propagating through the coaxial cable. To that end one would apparently require two very accurate clocks at each end, and associated RF generation and detection electronics.

However the major limitation is that even the best atomic clocks are not sufficiently accurate over even a day to make such measurements to the required accuracy, unless the cables are of order of a kilometre or so in length, and then temperature control becomes a major problem. The issue is that the time variations are of the order of 25 ps per 10 meters of cable. To measure that requires time measurements accurate to, say, 1 ps. But atomic clocks have accuracies over one day of around 100 ps, implying that lengths of around 1 kilometre would be required, in order for the effect to well exceed timing errors. Even then the atomic clocks must be brought together every day to resynchronise them, or use De Witte's method of multiple atomic clocks. However at Flinders University a major breakthrough for this problem was made when it was discovered that unlike coaxial cables, the movement of optical fibres through space does not affect the propagation speed of light through them. This is a very strange effect and at present there is no explanation for it.

4.1 Optical fibre effect

This effect was discovered by Lawrance, Drury and the author, using optical fibres in a Michelson interferometer arrangement, where the effective path length in each arm was 4 metres of fibre. So rather than having light pass through a gas, and being reflected by mirrors, here the light propagates through fibres and, where the mirrors would normally be located, a 180 degree bend in the fibres is formed. The light emerging from the two fibres is directed to a common region on a screen, and the expected fringe shifts were seen. However, and most dramatically, when the whole apparatus was rotated no shift in the fringe shifts was seen, unlike the situation with light passing through a gas as above. This result implied that the travel time in each arm of the fibre was unaffected by the orientation of that arm to the direction of the spatial flow. While no explanation has been developed for this effect, other than the general observation that the propagation speed in optical fibres depends on refractive index profiles and transverse and longitudinal Lorentz contraction effects, as in solids these are coupled by the elastic properties of the solid. Nevertheless this property offered a technological leap forward in the construction of a compact coaxial cable gravitational wave detector. This is because timing information can be sent though the fibres in a way that is not affected by the orientation of the fibres, while the coaxial cables do respond to the anisotropy of the speed of EM radiation in vacuum. Again why they respond in this way is not understood. All we have is that fibres and coaxial cables respond differently. So this offers the opportunity to have a coaxial cable one-way speed measurement set up, but using only one clock, as shown in Fig. 11. Here we have one clock at one end of the coaxial cable, and the arrival time of the RF signal at the other end is used to

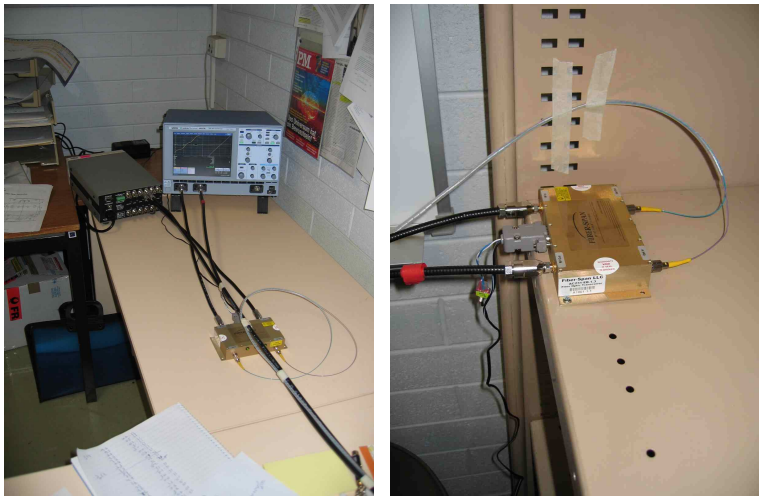

Fig. 12: The Flinders University Gravitational Wave Detector located in the author's office, showing the Rb atomic clock and Digital Storage Oscilloscope (DSO) at the Northern end of the NS 5 m cable run. In the foreground is one Fibre Optic Transceiver. The coaxial cables are black, while the optical fibres are tied together in a white plastic sleeve, except just prior to connecting with the transceiver. The second photograph shows the other transceiver at the Southern end. Most of the data reported herein was taken when the detector was relocated to an isolated underground laboratory with the transceivers resting on a concrete floor for temperature stabilisation.

modulate a light signal that returns to the starting end via an optical fibre. The return travel time is constant, being independent of the orientation of the detector arm, because of this peculiar property of the fibres. In practice one uses two such arrangements, with the RF directions opposing one another. This has two significant advantages, (i) that the effective coaxial cable length of 10 meters is achieved over a distance of just 5 meters, so the device is more easily accommodated in a temperature controlled room, and (ii) temperature variations in that room have a smaller effect than expected because it is only temperature differences between the cables that have any net effect. Indeed with specially constructed phase compensated fibre and coaxial cable, having very low speed-sensitivity to temperature variations, the most temperature sensitive components are the optical fibre transceivers (E/O and O/E in Fig. 11).

Fig. 13: The Flinders University Gravitational Wave Detector showing the cables formed into a loop. This configuration enables the calibration of the detector. The data from such a looping is shown in Fig. 14, but when the detector was relocated to an isolated underground laboratory.

4.2 Experimental components

Rubidium Atomic Clock: Stanford Research System FS725 Rubidium Frequency Standard. Multiple 10MHz RF outputs. Different outputs were used for the two arms of the detector.

Digital Storage Oscilloscope: LeCroy WaveRunner WR6051A 500 MHz 2-channel Digital Storage Oscilloscope (DSO). Jitter Noise Floor 2 ps rms. Clock Accuracy $\leqslant$5 pm. DSO averaging set at 5000, and generating time readings at 440/minute. Further averaged in DSO over 60 seconds, giving stored data stream at one data point/minute. The data was further running-averaged over a 60 minute interval. Connecting the Rb clock directly to the DSO via its two channels showed a long-term accuracy of $\pm$1 ps rms with this setup.

Fibre Optic Transceivers: Fiber-Span AC231-EB-1-3 RF/Fiber Optic Transceiver (O/E and E/O). Is a linear extended band (5–2000 MHz) low noise RF fibre optic transceiver for single mode 1.3 μm fibre optic wireless systems, with independent receiver and transmitter. RF interface is a 50Ω connector and the optical connector is a low reflection FC/APC connector. Temperature dependence of phase delay is not measured yet. The experiment is operated in a uniform temperature room, so that phase delays between the two transceivers cancel to some extent.

Coaxial Cable: Andrews FSJ1-50A Phase Stabilised 50Ω Coaxial Cable. Travel time temperature dependence is 0.026 ps/m/°C. The speed of RF waves in this cable is $c/n = 0.84\,c$, arising from the dielectric having refractive index $n = 1.19$. As well temperature effects cancel because the two coaxial cables are tied together, and so only temperature differences between adjacent regions of the cables can have any effect. If such temperature differences are $<$1°C, then temperature generated timing errors from this source should be $<$0.3 ps for the 10 m.

Optical Fibre: Sumitomo Electric Industries Ind. Ltd Japan Phase Stabilised Optical Fibre (PSOF) — single mode. Uses Liquid Crystal Polymer (LCP) coated single mode optical fibre, with this coating designed to make the travel time temperature dependence $<$0.002 ps/m/°C very small compared

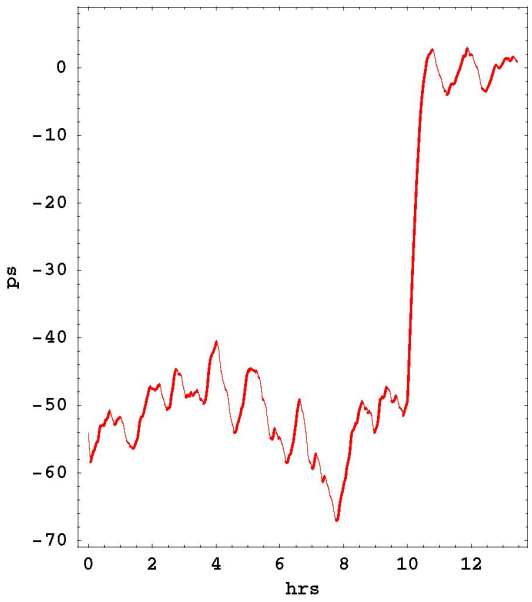

Fig. 14: The detector arm was formed into a loop at approximately 10:00hrs local time. With the system still operating time averaging causes the trace to interpolate during this procedure, as shown. This looping effect is equivalent to having $\mathbf{v} = 0$, which defines the value of $\Delta\tau$. In plotting the times here the zero time is set so that then $\Delta\tau = 0$. Now the detector is calibrated, and the times in this figure are absolute times. The times are the N to S travel time subtracted from the shorter S to N travel time, and hence are negative numbers. This demonstrates that the flow of space past the Earth is essentially from south to north, as shown in Fig. 16. When the arms are straight, as before 10:00hrs we see that on average the two travel times differ by some 55 ps. This looping effect is a critical test for the detector. It clearly shows the effect of absolute motion upon the RF travel times. As well we see Earth rotation, wave and converter noise effects before 10:00hrs, and converter noise and some small signal after 10:00hrs, caused by an imperfect circle. From this data (24) and (25) give $\delta = 72^\circ$ S and $v = 418$ km/s.

to normal fibres (0.07 ps/m/°C). As well temperature effects cancel because the two optical fibres are tied together, and so only temperature differences between adjacent regions of the fibres can have any effect. If such temperature differences are <1°C, then temperature generated timing errors from this source should be <0.02 ps for the 10 m. Now only Furukawa Electric Ind. Ltd Japan manufacturers PSOF.

Photographs of the Flinders detector are shown in Fig. 12. Because of the new timing technology the detector is now small enough to permit the looping of the detector arm as shown in Fig. 13. This enables a key test to be performed as in the loop configuration the signal should disappear, as then the device acts as though it were located at rest in space, because the actual effects of the absolute motion cancel. The striking results from this test are shown in Fig. 14. As well this key test also provides a means of calibrating the detector.

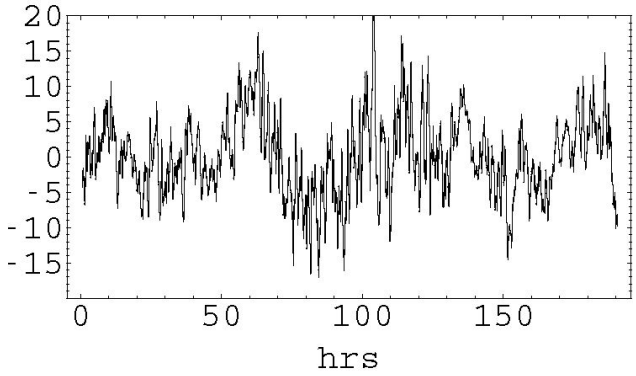

Fig. 15: RF travel time variations in picoseconds (ps) for RF waves to travel through, effectively, 10 meters of coaxial cable orientated in a NS direction. The data is plotted against local Adelaide time for the days August 18–25, 2006. The zero of the travel time variations is arbitrary. The data shows fluctuations identified as earth rotation effect and gravitational waves. These fluctuations exceed those from timing errors in the detector.

4.3 All-optical detector

The unique optical fibre effect permits an even more compact gravitational wave detector. This would be an all-optical system 1st order in v/c device, with light passing through vacuum, or just air, as well as optical fibres. The travel time through the fibres is, as above, unaffected by orientation of the device, while the propagation time through the vacuum is affected by orientation, as the device is moving through the local space.

In this system the relative time differences can be measured using optical interference of the light from the vacuum and fibre components. Then it is easy to see that the vacuum path length needs only be some 5 cm. This makes the construction of a three orthogonal arm even simpler. It would be a cheap bench-top box. In which case many of these devices could be put into operation around the Earth, and in space, to observe the new spatial-flow physics, with special emphasis on correlation studies. These can be used to observe the spatial extent of the fluctuations. As well space-probe based systems could observe special effects in the flow pattern associated with the Earth-Moon system; these effects are caused by the α-dependent dynamics in (26).

4.4 Results from the Flinders detector

Results from the detector are shown in Fig. 15. There the time variations in picoseconds are plotted against local Adelaide time. The times have an arbitrary zero offset. However most significantly we see $\sim$24 hr variations in the travel time, as also seen by De Witte. We also see variations in the times and magnitudes from day to day and within each day. These are the wave effects although as well a component of these is probably also coming from temperature change

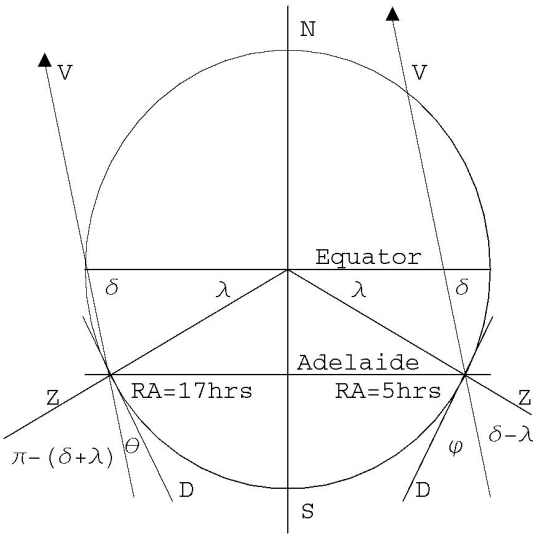

Fig. 16: Profile of Earth, showing NS axis, at Adelaide local sidereal time of RA ≈ 5 hrs (on RHS) and at RA ≈ 17 hrs (on LHS). Adelaide has latitude $\lambda = 38^\circ$ S. Z is the local zenith, and the detector arm has horizontal local NS direction D. The flow of space past the Earth has average velocity $\mathbf{v}$. The average direction, $-\mathbf{v}$, of motion of the Earth through local 3-space has RA ≈ 5 hrs and Declination $\delta \approx 70^\circ$S. The angle of inclination of the detector arm D to the direction $-\mathbf{v}$ is $\phi = \frac{\pi}{2} - \delta + \lambda$ and $\theta = \delta + \lambda - \frac{\pi}{2}$ at these two RA, respectively. As the Earth rotates the inclination angle changes from a minimum of θ to a maximum of ϕ, which causes the dominant "dip" effect in, say, Fig. 17. The gravitational wave effect is the change of direction and magnitude of the flow velocity $\mathbf{v}$, which causes the fluctuations in, say, Fig. 17. The latitude of Mt. Wilson is 34° N, and so its latitude almost mirrors that of Adelaide. This is relevant to the comparison in Fig. 18.

effects in the optical fibre transceivers. In time the instrument will be improved and optimised. But we are certainly seeing the evidence of absolute motion, namely the detection of the velocity field, as well as fluctuations in that velocity. To understand the daily variations we show in Fig. 16 the orientation of the detector arm relative to the Earth rotation axis and the Miller flow direction, at two key local sidereal times. So we now have a very inexpensive gravitational wave detector sufficiently small that even a coaxial-cable three-arm detector could easily be located within a building. Three orthogonal arms permit a complete measurement of the spatial flow velocity. Operating such a device over a year or so will permit the extraction of the Sun in-flow component and the Earth in-flow component, as well as a detailed study of the wave effects.

4.5 Right ascension

The sidereal effect has been well established, as shown in Fig. 9 for both the De Witte and Flinders data. Fig. 6 clearly shows that effect also for the Miller data. None of the other anisotropy experiments took data for a sufficiently long

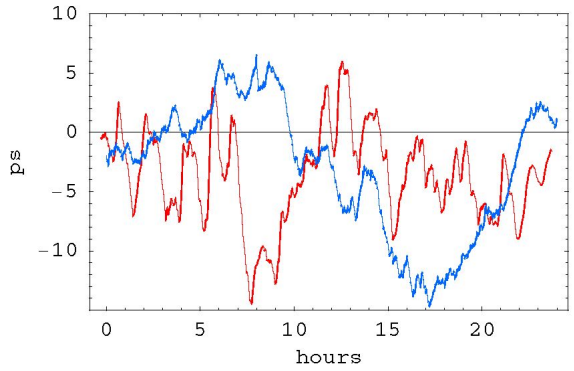

Fig. 17: The superimposed plots show the sidereal time effect. The plot (blue) with the minimum at approximately 17 hrs local Adelaide time is from June 9, 2006, while the plot (red) with the minimum at approximately 8 hrs local time is from August 23, 2006. We see that the minimum has moved forward in time by approximately 9 hrs. The expected shift for this 65 day difference, assuming no wave effects, is 4.3 hrs, but the wave effects shift the RA by some ± 2 hrs on each day as also shown in Fig. 9. This sidereal time shift is a critical test for the confirmation of the detector. Miller also detected variations of that magnitude as shown in Fig. 6. The August 23 data is also shown in Fig. 18, but there plotted against local sidereal time for comparison with the De Witte and Miller data.

enough time to demonstrate this effect, although their results are consistent with the Right Ascension and Declination found by the Miller, De Witte and Flinders experiments. From some 25 days of data in August 2006, the local Adelaide time for the largest travel-time difference is approximately 10 ± 2 hrs. This corresponds to a local sidereal time of 17.5 ± 2 hrs. According to the Miller convention we give the direction of the velocity vector of the Earth's motion through the space, which then has Right Ascension 5.5 ± 2 hrs. This agrees remarkably well with the Miller and De Witte Right Ascension determinations, as discussed above. A one hour change in RA corresponds to a 15° change in direction at the equator. However because the declination, to be determined next, is as large as some 70°, the actual RA variation of ± 2 hrs, corresponds to an angle variation of some $\pm 10^\circ$ at that declination. On occasions there was no discernible unique maximum travel time difference; this happens when the declination is fluctuating near 90°, for then the RA becomes ill-defined.

4.6 Declination and speed

Because the prototype detector has only one arm, rather than the ideal case of three orthogonal arms, to determine the declination and speed we assume here that the flow is uniform and time-independent, and use the changing difference in travel times between the two main coaxial cables. Consider Fig. 11 showing the detector schematic layout and Fig. 16

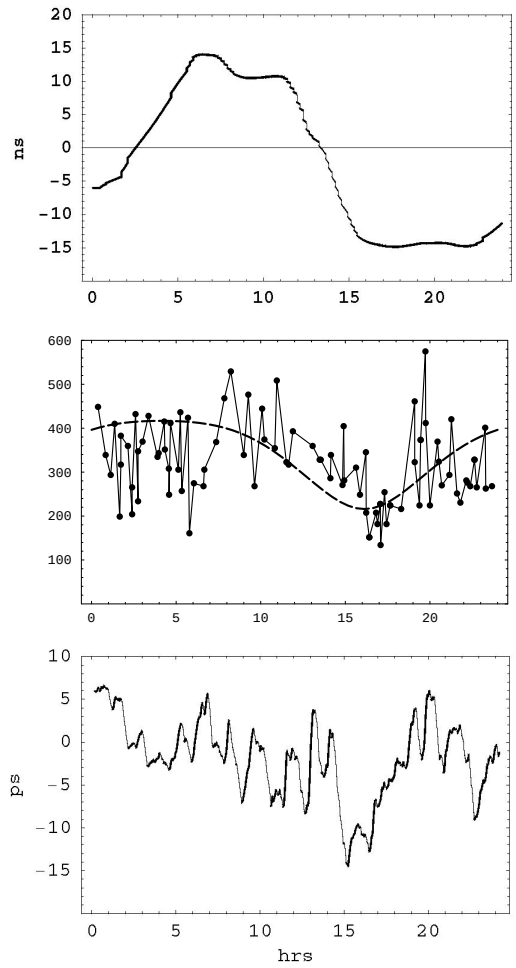

Fig. 18: **Top:** De Witte data, with sign reversed, from the first sidereal day in Fig. 8. This data gives a speed of approximately 430km/s. The data appears to have been averaged over more than 1hr, but still shows wave effects. **Middle:** Absolute projected speeds v_P in the Miller experiment plotted against sidereal time in hours for a composite day collected over a number of days in September 1925. Speed data like this comes from the fits as in Fig. 5 using the Special Relativity calibration in (20). Maximum projected speed is 417 km/s, as given in [3, 20, 9]. The data shows considerable fluctuations. The dashed curve shows the non-fluctuating variation expected over one day as the Earth rotates, causing the projection onto the plane of the interferometer of the velocity of the average direction of the space flow to change. If the data was plotted against solar time the form is shifted by many hours. Note that the min/max occur at approximately 5 hrs and 17 hrs, as also seen by De Witte and the new experiment herein. The corresponding variation of the azimuthal phase ψ from Fig. 5 is shown in Fig. 6. **Bottom:** Data from the new experiment for one sidereal day on approximately August 23. We see similar variation with sidereal time, and also similar wave structure. This data has been averaged over a running 1hr time interval to more closely match the time resolution of the Miller experiment. These fluctuations are believed to be real wave phenomena, predicted by the new theory of space [1]. The new experiment gives a speed of 418 km/s. We see remarkable agreement between all three experiments.

showing the various angles. The travel time in one of the circuits is given by

$$t_1 = \tau_1 + \frac{L_1}{v_c - v\cos(\Phi)} \tag{21}$$

and that in the other arm by

$$t_2 = \tau_1 + \frac{L_1}{v_c + v\cos(\Phi)} \tag{22}$$

where Φ is the angle between the detector direction and the flow velocity $\mathbf{v}$, v_c is the speed of radio frequency (RF) electromagnetic waves in the fibre when $\mathbf{v} = 0$, namely $v_c = c/n$ where n is the refractive index of the dielectric in the coaxial cable, and v is the change in that speed caused by the absolute motion of the coaxial cables through space, when the cable is parallel to $\mathbf{v}$. The factor of $\cos(\Phi)$ is just the projection of $\mathbf{v}$ onto the cable direction. The difference in signs in (21) and (22) arises from the RF waves travelling in opposite directions in the two main coaxial cables. The distance L_1 is the arm length of the coaxial cable from A to B, and L_2 is that from C to D. The constant times τ_1 and τ_2 are travel times arising from the optical fibres, the converters, and the coaxial cable lengths not included in L_1 and L_2, particularly the optical fibre travel times. which is the key to the new detector. The effect of the two shorter coaxial cable sections in each arm are included in τ_1 and τ_2 because the absolute motion effects from these arms is additive, as the RF travels in opposite directions through them, and so only contributes at 2nd order.

Now the experiment involves first the measurement of the difference $\Delta t = t_1 - t_2$, giving

$$\begin{aligned}\Delta t = \tau_1 - \tau_2 + \frac{L_1}{v_c - v\cos(\Phi)} - \frac{L_2}{v_c + v\cos(\Phi)} \approx \\ \approx \Delta\tau + (L_1 + L_2)\cos(\Phi)\,\frac{v}{v_c^2} + \dots\end{aligned} \tag{23}$$

on expanding to lowest order in v/v_c, and where $\Delta\tau \equiv \equiv \tau_1 - \tau_2 + \frac{L_1 - L_2}{v_c}$. Eqn. (23) is the key to the operation of the detector. We see that the effective arm length is $L = L_1 + L_2 = 10$ m. Over time the velocity vector $\mathbf{v}$ changes, caused by the wave effects and also by the Earth's orbital velocity about the Sun changing direction, and as well the Earth rotates on its axis. Both of these effects cause v and the angle Φ to change. However over a period of a day and ignoring wave effects we can assume that v is unchanging. Then we can determine a declination δ and the speed v by (i) measuring the maximum and minimum values of Δt over a day, which occur approximately 12 hours apart, and (ii) determine $\Delta\tau$, which is the time difference when $v = 0$, and this is easily measured by putting the detector arm into a circular loop, as shown in Fig. 13, so that absolute motion effects cancel, at least to 1st order in v/v_c. Now from Fig. 16 we see that the maximum travel time difference Δt_{max} occurs

when $\Phi=\theta=\lambda+\delta-\frac{\pi}{2}$ in (23), and the minimum Δt_{min} when $\Phi=\phi=\lambda-\delta+\frac{\pi}{2}$, 12 hours later. Then the declination δ may be determined by numerically solving the transcendental equation which follows from these two times from (23)

$$\frac{\cos\left(\lambda+\delta-\frac{\pi}{2}\right)}{\cos\left(\lambda-\delta+\frac{\pi}{2}\right)}=\frac{\Delta t_{max}-\Delta\tau}{\Delta t_{min}-\Delta\tau}\,. \tag{24}$$

Subsequently the speed v is obtained from

$$v=\frac{\left(\Delta t_{max}-\Delta t_{min}\right)v_c^2}{L\left(\cos\left(\lambda+\delta-\frac{\pi}{2}\right)-\cos\left(\lambda-\delta+\frac{\pi}{2}\right)\right)}\,. \tag{25}$$

In Fig. 14 we show the travel time variations for September 19, 2006. The detector arm was formed into a loop at approximately 10:00 hrs local time, with the system still operating: time averaging causes the trace to interpolate during this procedure, as shown. This looping effect is equivalent to having $\mathbf{v}=0$, which defines the value of $\Delta\tau$. In plotting the times in Fig. 14 the zero time is set so that then $\Delta\tau=0$. When the arms are straight, as before 10:00 hrs we see that on average the travel times are some 55 ps different: this is because the RF wave travelling S to N is now faster than the RF wave travelling from N to S. The times are negative because the longer S to N time is subtracted from the shorter N to S travel time in the DSO. As well we see the daily variation as the Earth rotates, showing in particular the maximum effect at approximately 8:00 hrs local time (approximately 15hrs sidereal time) as shown for the three experiments in Fig. 18, as well as wave and converter noise. The trace after 10:00 hrs should be flat — but the variations seen are coming from noise effects in the converters as well as some small signal arising from the loop not being formed into a perfect circle. Taking $\Delta t_{max}=-63$ ps and $\Delta t_{min}=-40$ ps from Fig. 14, (24) and (25) give $\delta=72^\circ$ S and $v=418$ km/s. This is in extraordinary agreement with the Miller results for September 1925.

We can also analyse the De Witte data. We have $L=3.0$ km, $v_c=200{,}000$ km/s, from Fig. 8 $\Delta t_{max}-\Delta t_{min}\approx\approx25$ ns, and the latitude of Brussels is $\lambda=51^\circ$ N. There is not sufficient De Witte data to determine the declination of $\mathbf{v}$ on the days when the data was taken. Miller found that the declination varied from approximately 60° S to 80° S, depending on the month. The dates for the De Witte data in Fig. 8 are not known but, for example, a declination of $\delta=60^\circ$ gives $v=430$ km/s.

4.7 Gravity and gravitational waves

We have seen that as well as the effect of the Earth rotation relative to the stars, as previously shown by the data from Michelson-Morley, Illingworth, Joos, Jaseja *el al.*, Torr and Kolen, Miller, and De Witte and the data from the new experiment herein, there is also from the experimental data of Michelson-Morley, Miller, Torr and Kolen, De Witte and from the new experiment, evidence of turbulence in this flow of space past the Earth. This all points to the flow velocity field $\mathbf{v}(\mathbf{r},t)$ having a time dependence over an above that caused simply because observations are taken from the rotating Earth. As we shall now show this turbulence is what is conventionally called "gravitational waves", as already noted [1, 19, 20]. To do this we briefly review the new dynamical theory of 3-space, following [25], although it has been extensively discussed in the related literature. In the limit of zero vorticity for $\mathbf{v}(\mathbf{r},t)$ its dynamics is determined by

$$\nabla\cdot\left(\frac{\partial\mathbf{v}}{\partial t}+(\mathbf{v}\cdot\nabla)\mathbf{v}\right)+ +\frac{\alpha}{8}\left((\mathrm{tr}D)^2-\mathrm{tr}(D^2)\right)=-4\pi G\rho\,, \tag{26}$$

where ρ is the effective matter/energy density, and where

$$D_{ij}=\frac{1}{2}\left(\frac{\partial v_i}{\partial x_j}+\frac{\partial v_j}{\partial x_i}\right). \tag{27}$$

Most significantly data from the bore hole g anomaly and from the systematics of galactic supermassive black hole shows that $\alpha\approx1/137$ is the fine structure constant known from quantum theory [21–24]. Now the Dirac equation uniquely couples to this dynamical 3-space, according to [25]

$$i\hbar\frac{\partial\psi}{\partial t}=-i\hbar\left(c\vec{\alpha}\cdot\nabla+\mathbf{v}\cdot\nabla+\frac{1}{2}\nabla\cdot\mathbf{v}\right)\psi+\beta mc^2\psi \tag{28}$$

where $\vec{\alpha}$ and β are the usual Dirac matrices. We can compute the acceleration of a localised spinor wave packet according to

$$\mathbf{g}\equiv\frac{d^2}{dt^2}\left(\psi(t),\,\mathbf{r}\,\psi(t)\right) \tag{29}$$

With $\mathbf{v}_R=\mathbf{v}_0-\mathbf{v}$ the velocity of the wave packet relative to the local space, as $\mathbf{v}_0$ is the velocity relative to the embedding space*, and we obtain

$$\mathbf{g}=\frac{\partial\mathbf{v}}{\partial t}+(\mathbf{v}\cdot\nabla)\mathbf{v}+(\nabla\times\mathbf{v})\times\mathbf{v}_R-\frac{\mathbf{v}_R}{1-\frac{\mathbf{v}_R^2}{c^2}}\frac{1}{2}\frac{d}{dt}\left(\frac{\mathbf{v}_R^2}{c^2}\right) \tag{30}$$

which gives the acceleration of quantum matter caused by the inhomogeneities and time-dependencies of $\mathbf{v}(\mathbf{r},t)$. It has a term which limits the speed of the wave packet relative to space to be $<c$. Hence we see that the phenomenon of gravity, including the Equivalence Principle, has been derived from a deeper theory. Apart from the vorticity† and relativistic terms in (30) the quantum matter acceleration is the same as that of the structured 3-space [25, 8].

We can now show how this leads to both the spacetime mathematical construct and that the geodesic for matter worldlines in that spacetime is equivalent to trajectories from (30). First we note that (30) may be obtained by extremising the time-dilated elapsed time

$$\tau[\mathbf{r}_0]=\int dt\left(1-\frac{\mathbf{v}_R^2}{c^2}\right)^{1/2} \tag{31}$$

*See [25] for a detailed explanation of the embedding space concept.
†The vorticity term explains the Lense-Thirring effect [30].

with respect to the particle trajectory $\mathbf{r}_0(t)$ [1]. This happens because of the Fermat least-time effect for waves: only along the minimal time trajectory do the quantum waves remain in phase under small variations of the path. This again emphasises that gravity is a quantum wave effect. We now introduce a spacetime mathematical construct according to the metric

$$ds^2 = dt^2 - \frac{\left(d\mathbf{r} - \mathbf{v}\,(\mathbf{r},t)\,dt\right)^2}{c^2} = g_{\mu\nu}dx^\mu dx^\nu . \qquad (32)$$

Then according to this metric the elapsed time in (31) is

$$\tau = \int dt \sqrt{g_{\mu\nu}\frac{dx^\mu}{dt}\frac{dx^\nu}{dt}}\,, \qquad (33)$$

and the minimisation of (33) leads to the geodesics of the spacetime, which are thus equivalent to the trajectories from (31), namely (30). Hence by coupling the Dirac spinor dynamics to the space dynamics we derive the geodesic formalism of General Relativity as a quantum effect, but without reference to the Hilbert-Einstein equations for the induced metric. Indeed in general the metric of this induced spacetime will not satisfy these equations as the dynamical space involves the α-dependent dynamics, and α is missing from GR*.

Hence so far we have reviewed the new theory of gravity as it emerges within the new physics†. In explaining gravity we discover that the Newtonian theory is actually flawed: this happened because the motion of planets in the solar system is too special to have permitted Newtonian to model all aspects of the phenomenon of gravity, including that the fundamental dynamical variable is a velocity field and not an acceleration field.

We now discuss the phenomenon of the so-called "gravitational waves". It may be shown that the metric in (32) satisfies the Hilbert-Einstein GR equations, in "empty" space, but *only* when $\alpha \to 0$:

$$G_{\mu\nu} \equiv R_{\mu\nu} - \frac{1}{2}\,R g_{\mu\nu} = 0\,, \qquad (34)$$

where $G_{\mu\nu}$ is the Einstein tensor, $R_{\mu\nu} = R^{\alpha}_{\mu\alpha\nu}$ and $R = g^{\mu\nu}R_{\mu\nu}$ and $g^{\mu\nu}$ is the matrix inverse of $g_{\mu\nu}$, and the curvature tensor is

$$R^{\rho}_{\mu\sigma\nu} = \Gamma^{\rho}_{\mu\nu,\sigma} - \Gamma^{\rho}_{\mu\sigma,\nu} + \Gamma^{\rho}_{\alpha\sigma}\Gamma^{\alpha}_{\mu\nu} - \Gamma^{\rho}_{\alpha\nu}\Gamma^{\alpha}_{\mu\sigma}, \qquad (35)$$

where $\Gamma^{\alpha}_{\mu\sigma}$ is the affine connection

$$\Gamma^{\alpha}_{\mu\sigma} = \frac{1}{2}\,g^{\alpha\nu}\left(\frac{\partial g_{\nu\mu}}{\partial x^\sigma} + \frac{\partial g_{\nu\sigma}}{\partial x^\mu} - \frac{\partial g_{\mu\sigma}}{\partial x^\nu}\right). \qquad (36)$$

Hence the GR formalism fails on two grounds: (i) it does not include the spatial self-interaction dynamics which has coupling constant α, and (ii) it very effectively obscures the dynamics, for the GR formalism has spuriously introduced the speed of light when it is completely absent from (26), except on the RHS when the matter has speed near that of c relative to the space‡. Now when wave effects are supposedly extracted from (34), by perturbatively expanding about a background metric, the standard derivation supposedly leads to waves with speed c. This derivation must be manifestly incorrect, as the underlying equation (26), even in the limit $\alpha \to 0$, does not even contain c. In fact an analysis of (26) shows that the perturbative wave effects are fluctuations of $\mathbf{v}(\mathbf{r},t)$, and travel at approximately that speed, which in the case of the data reported here is some 400 km/s in the case of earth based detections, i. e. 0.1% of c. These waves also generate gravitational effects, but only because of the α-dependent dynamical effects: when $\alpha \to 0$ we still have wave effects in the velocity field, but that they produce no gravitational acceleration effects upon quantum matter. Of course even in the case of $\alpha \to 0$ the velocity field wave effects are detectable by their effects upon EM radiation, as shown by various gas-mode Michelson interferometer and coaxial cable experiments. Amazingly there is evidence that Michelson-Morley actually detected such gravitational waves as well as the absolute motion effect in 1887, because fluctuations from day to day of their data shows effects similar to those reported by Miller, Torr and Kolen, De Witte, and the new experiment herein. Of course if the Michelson interferometer is operated in vacuum mode it is totally insensitive to absolute motion effects and to the accompanying wave effects, as is the case. This implies that experiments such as the long baseline terrestrial Michelson interferometers are seriously technically flawed as gravitational wave detectors. However as well as the various successful experimental techniques discussed herein for detecting absolute motion and gravitational wave effects a novel technique is that these effects will manifest in the gyroscope precessions observed by the Gravity Probe B satellite experiment [30, 31].

Eqn. (26) determines the dynamical time evolution of the velocity field. However that aspect is more apparent if we write that equation in the integro-differential form

$$\frac{\partial \mathbf{v}}{\partial t} = -\nabla\left(\frac{\mathbf{v}^2}{2}\right) + \\ + G\int d^3r'\,\frac{\rho_{DM}(\mathbf{r}',t) + \rho(\mathbf{r}',t)}{|\mathbf{r}-\mathbf{r}'|^3}(\mathbf{r}-\mathbf{r}') \qquad (37)$$

in which ρ_{DM} is velocity dependent,

$$\rho_{DM}(\mathbf{r},t) \equiv \frac{\alpha}{32\pi G}\left((\mathrm{tr}D)^2 - \mathrm{tr}(D^2)\right), \qquad (38)$$

and is the effective "dark matter" density. This shows several key aspects: (i) there is a local cause for the time de-

*Why the Schwarzschild metric, nevertheless, works is explained in [25].

†Elsewhere it has been shown that this theory of gravity explains the bore hole anomaly, supermassive black hole systematics, the "dark matter" spiral galaxy rotation anomaly effect, as well as the putative successes of GR, including light bending and gravitational lensing.

‡See [1] for a possible generalisation to include vorticity effects and matter related relativistic effects.

pendence from the ∇ term, and (ii) a non-local action-at-a-distance effect from the ρ_{DM} and ρ terms. This is caused by space being essentially a quantum system, so this is better understood as a quantum non-local effect. However (37) raises the question of where the observed wave effects come from? Are they local effects or are they manifestations of distant phenomena? In the latter case we have a new astronomical window on the universe.

5 Conclusions

We now have eight experiments that independently and consistently demonstrated (i) the anisotropy of the speed of light, and where the anisotropy is quite large, namely 300,000 $\pm$420 km/s, depending on the direction of measurement relative to the Milky Way, (ii) that the direction, given by the Right Ascension and Declination, is now known, being established by the Miller, De Witte and Flinders experiments*. The reality of the cosmological meaning of the speed was confirmed by detecting the sidereal time shift over 6 months and more, (iii) that the relativistic Fitzgerald-Lorentz length contraction is a real effect, for otherwise the results from the gas-mode interferometers would have not agreed with those from the coaxial cable experiments, (iv) that Newtonian physics gives the wrong calibration for the Michelson interferometer, which of course is not surprising, (v) that the observed anisotropy means that these eight experiments have detected the existence of a 3-space, (vi) that the motion of that 3-space past the Earth displays wave effects at the level of $\pm$30km/s, as confirmed by three experiments, and possibly present even in the Michelson-Morley data.

The Miller experiment was one of the most significant experiments of the 20th century. It meant that a substructure to reality deeper than spacetime had been revealed, that spacetime was merely a mathematical construct and not an aspect of reality. It meant that the Einstein postulate regarding the invariance of the speed of light was incorrect — in disagreement with experiment, and had been so from the beginning. This meant that the Special Relativity effects required a different explanation, and indeed Lorentz had supplied that some 100 years ago: in this it is the absolute motion of systems through the dynamical 3-space that causes SR effects, and which is diametrically opposite to the Einstein formalism. This has required the generalisation of the Maxwell equations, as first proposed by Hertz in 1888 [26]), the Schrödinger and Dirac equations [25, 8]. This in turn has lead to a derivation of the phenomenon of gravity, namely that it is caused by the refraction of quantum waves by the inhomogeneities and time dependence of the flowing patterns within space. That same data has also revealed the in-flow component of space past the Earth towards the Sun [1], and which also is revealed by the light bending effect observed by light passing close to the Sun's surface [25]. This theory of gravity has in turn lead to an explanation of the so-called "dark matter" effect in spiral galaxies [22], and to the systematics of black hole masses in spherical star systems [25], and to the explanation of the bore hole g anomaly [21, 22, 23]. These effects have permitted the development of the minimal dynamics of the 3-space, leading to the discovery that the parameter that determines the strength of the spatial self-interaction is none other than the fine structure constant, so hinting at a grand unification of space and the quantum theory, along the lines proposed in [1], as an *information theoretic* theory of reality.

These developments demonstrate the enormous significance of the Miller experiment, and the extraordinary degree to which Miller went in testing and refining his interferometer. The author is proud to be extending the Miller discoveries by studying in detail the wave effects that are so apparent in his extensive data set. His work demonstrates the enormous importance of doing novel experiments and doing them well, despite the prevailing prejudices. It was a tragedy and an injustice that Miller was not recognised for his contributions to physics in his own lifetime; but not everyone is as careful and fastidious with detail as he was. He was ignored by the physics community simply because in his era it was believed, as it is now, that absolute motion was incompatible with special relativistic effects, and so it was accepted, without any evidence, that his experiments were wrong. His experiences showed yet again that few in physics actually accept that it is an evidence based science, as Galileo long ago discovered also to his great cost. For more than 70 years this experiment has been ignored, until recently, but even now discussion of this and related experiments attracts hostile reaction from the physics community.

The developments reported herein have enormous significance for fundamental physics — essentially the whole paradigm of 20th century physics collapses. In particular spacetime is now seen to be no more than a mathematical construct, that no such union of space and time was ever mandated by experiment. The putative successes of Special Relativity can be accommodated by the reality of a dynamical 3-space, with time a distinctly different phenomenon. But motion of quantum and even classical electromagnetic fields through that dynamical space explain the SR effects. Lorentz symmetry remains valid, but must be understood as applying only when the space and time coordinates are those arrived at by the Einstein measurement protocol, and which amounts to not making corrections for the effects of absolute motion upon rods and clocks on those measurements. Nevertheless such coordinates may be used so long as we understand that they lead to a confusion of various related effects. To correct the Einstein measurement protocol readings one needs only to have each observer use an absolute motion meter, such as the new compact all-optical devices, as well as a rod and

*Intriguingly this direction is, on average, perpendicular to the plane of the ecliptic. This may be a dynamical consequence of the new theory of space.

clock. The fundamental discovery is that for some 100 years physics has failed to realise that a dynamical 3-space exists — it is observable. This contradicts two previous assumptions about space: Newton asserted that it existed, was unchanging, but not observable, whereas Einstein asserted that 3-space did not exist, could not exist, and so clearly must be unobservable. The minimal dynamics for this 3-space is now known, and it immediately explains such effects as the "dark matter" spiral galaxy rotation anomaly, novel black holes with non-inverse square law gravitational accelerations, which would appear to offer an explanation for the precocious formation of spiral galaxies, the bore hole anomaly and the systematics of supermassive black holes, and so on. Dramatically various pieces of data show that the self-interaction constant for space is the fine structure constant. However unlike SR, GR turns out to be flawed but only because it assumed the correctness of Newtonian gravity. The self-interaction effects for space make that theory invalid even in the non-relativistic regime — the famous universal inverse square law of Newtonian gravity is of limited validity. Uniquely linking the quantum theory of matter with the dynamical space shows that gravity is a quantum matter wave effect, so we can't understand gravity without the quantum theory. As well the dynamics of space is intrinsically non-local, which implies a connectivity of reality that far exceeds any previous notions.

This research is supported by an Australian Research Council Discovery Grant *Development and Study of a New Theory of Gravity*.

Special thanks to Professor Igor Bray (Murdoch Univ.), Professor Warren Lawrance (Flinders Univ.), Luit Koert De Jonge (CERN), Tim Cope (Fiber-Span), Peter Gray (Trio), Bill Drury and Dr Lance McCarthy (Flinders Univ.), Tom Goodey (UK), Shizu Bito (Japan), Pete Brown (Mountain Man Graphics), Dr Tim Eastman (Washington), Dr Dmitri Rabounski (New Mexico) and Stephen Crothers (Australia).

References

1. Cahill R. T. Process Physics: From information theory to quantum space and matter. Nova Science, N.Y., 2005.
2. Cahill R. T. and Kitto K. Michelson-Morley experiments revisited. *Apeiron*, 2003, v. 10(2), 104–117.
3. Michelson A. A. and Morley E. W. *Philos. Mag.*, S. 5, 1887, v. 24, No. 151, 449–463.
4. Miller D. C. *Rev. Mod. Phys.*, 1933, v. 5, 203–242.
5. Cahill R. T. Process Physics and Whitehead: the new science of space and time. Whitehead 2006 Conference, Salzburg, to be pub. in proceedings, 2006.
6. Cahill R. T. Process Physics: self-referential information and experiential reality. *To be pub*.
7. Müller H. *et al.* Modern Michelson-Morley experiment using cryogenic optical resonators. *Phys. Rev. Lett.*, 2003, v. 91(2), 020401-1.
8. Cahill R. T. Dynamical fractal 3-space and the generalised Schrödinger equation: Equivalence Principle and vorticity effects. *Progress in Physics*, 2006, v. 1, 27–34.
9. Cahill R. T. The Roland DeWitte 1991 experiment. *Progress in Physics*, 2006, v. 3, 60–65.
10. Torr D. G. and Kolen P. *Precision Measurements and Fundamental Constants*, ed. by Taylor B. N. and Phillips W. D. Nat. Bur. Stand. (U.S.), Spec. Pub., 1984, v. 617, 675–679.
11. Illingworth K. K. *Phys. Rev.*, 1927, v. 3, 692–696.
12. Joos G. *Ann. der Physik*, 1930, Bd. 7, 385.
13. Jaseja T. S. *et al. Phys. Rev.*, v. A133, 1964, 1221.
14. Cahill R. T. The Michelson and Morley 1887 experiment and the discovery of absolute motion. *Progress in Physics*, 2005, v. 3, 25–29.
15. Cahill R. T. The Michelson and Morley 1887 experiment and the discovery of 3-space and absolute motion. *Australian Physics*, Jan/Feb 2006, v. 46, 196–202.
16. Cahill R. T. The detection of absolute motion: from 1887 to 2005. *NPA Proceedings*, 2005, 12–16.
17. Cahill R. T. The speed of light and the Einstein legacy: 1905-2005. *Infinite Energy*, 2005, v. 10(60), 28–27.
18. Cahill R. T. The Einstein postulates 1905-2005: a critical review of the evidence. In: *Einstein and Poincaré: the Physical Vacuum*, Dvoeglazov V. V. (ed.), Apeiron Publ., 2006.
19. Cahill R. T. Quantum foam, gravity and gravitational waves. arXiv: physics/0312082.
20. Cahill R. T. Absolute motion and gravitational effects. *Apeiron*, 2004, v. 11(1), 53–111.
21. Cahill R. T. Gravity, "dark matter" and the fine structure constant. *Apeiron*, 2005, v. 12(2), 144–177.
22. Cahill R. T. "Dark matter" as a quantum foam in-flow effect. In: *Trends in Dark Matter Research*, ed. J. Val Blain, Nova Science, N.Y., 2005, 96–140.
23. Cahill R. T. 3-Space in-flow theory of gravity: Boreholes, blackholes and the fine structure constant. *Progress in Physics*, 2006, v. 2, 9–16.
24. Cahill R. T. Black holes in elliptical and spiral galaxies and in globular clusters. *Progress in Physics*, 2005, v. 3, 51–56.
25. Cahill R. T. Black holes and quantum theory: the fine structure constant connection. *Progress in Physics*, 2006, v. 4, 44–50.
26. Hertz H. On the fundamental equations of electro-magnetics for bodies in motion. *Wiedemann's Ann.*, 1890, v. 41, 369; Electric waves, collection of scientific papers. Dover, N.Y., 1962.
27. Fitzgerald G. F. *Science*, 1889, v. 13, 420.
28. Lorentz H. A. Electric phenomena in a system moving with any velocity less than that of light. In *The Principle of Relativity*, Dover, N.Y., 1952.
29. Hicks W. M. On the Michelson-Morley experiment relating to the drift of the ether. *Phil. Mag.*, 1902, v. 3, 9–42.
30. Cahill R. T. Novel Gravity Probe B frame-dragging effect. *Progress in Physics*, 2005, v. 3, 30–33.
31. Cahill R. T. Novel Gravity Probe B gravitational wave detection. arXiv: physics/0408097.

Progress in Physics **is an American scientific journal on advanced studies in physics, registered with the Library of Congress (DC, USA): ISSN 1555-5534 (print version) and ISSN 1555-5615 (online version). The journal is peer reviewed and listed in the abstracting and indexing coverage of: Mathematical Reviews of the AMS (USA), DOAJ of Lund University (Sweden), Zentralblatt MATH (Germany), Scientific Commons of the University of St. Gallen (Switzerland), Open-J-Gate (India), Referential Journal of VINITI (Russia), etc.** ***Progress in Physics*** **is an open-access journal published and distributed in accordance with the Budapest Open Initiative: this means that the electronic copies of both full-size version of the journal and the individual papers published therein will always be acessed for reading, download, and copying for any user free of charge. The journal is issued quarterly (four volumes per year).**

Electronic version of this journal:
http://www.ptep-online.com

Postal address for correspondence:

Department of Mathematics and Science
University of New Mexico
200 College Road, Gallup, NM 87301, USA

Printed in the United States of America